ΕΘΝΙΚΟ ΚΑΙ ΚΑΠΟΔΙΣΤΡΙΑΚΟ ΠΑΝΕΠΙΣΤΗΜΙΟ
ΑΘΗΝΩΝ

ΣΧΟΛΗ ΕΠΙΣΤΗΜΩΝ ΥΓΕΙΑΣ

ΙΑΤΡΙΚΗ ΣΧΟΛΗ

ΤΟΜΕΑΣ ΒΑΣΙΚΩΝ ΙΑΤΡΙΚΩΝ ΕΠΙΣΤΗΜΩΝ

ΕΡΓΑΣΤΗΡΙΟ ΒΙΟΛΟΓΙΑΣ

Διευθυντής Καθηγητής Αριστείδης Ηλιόπουλος

ΔΙΔΑΚΤΟΡΙΚΗ ΔΙΑΤΡΙΒΗ

Διερεύνηση του ρόλου της πρωτεΐνης α-συνουκλεΐνης στην παθογένεια της Ατροφίας Πολλαπλών Συστημάτων

Investigation of the role of the protein alpha synuclein on Multiple System Atrophy Pathogenesis

Παναγιώτα Μαυροειδή

Βιολόγος

Αθήνα 2021

«Το έργο συγχρηματοδοτείται από την Ελλάδα και την Ευρωπαϊκή Ένωση (Ευρωπαϊκό Κοινωνικό Ταμείο) μέσω του Επιχειρησιακού Προγράμματος «Ανάπτυξη Ανθρώπινου Δυναμικού, Εκπαίδευση και Διά Βίου Μάθηση», στο πλαίσιο της Πράξης «Ενίσχυση του ανθρώπινου ερευνητικού δυναμικού μέσω της υλοποίησης διδακτορικής έρευνας» (MIS-5000432), που υλοποιεί το Ίδρυμα Κρατικών Υποτροφιών (ΙΚΥ)»

Ευρωπαϊκή Ένωση

Επιχειρησιακό Πρόγραμμα
Ανάπτυξη Ανθρώπινου Δυναμικού,
Εκπαίδευση και Διά Βίου Μάθηση
Με τη συγχρηματοδότηση της Ελλάδας και της Ευρωπαϊκής Ένωσης

ΕΣΠΑ 2014-2020

ΕΘΝΙΚΟ ΚΑΙ ΚΑΠΟΔΙΣΤΡΙΑΚΟ ΠΑΝΕΠΙΣΤΗΜΙΟ ΑΘΗΝΩΝ

ΣΧΟΛΗ ΕΠΙΣΤΗΜΩΝ ΥΓΕΙΑΣ

ΙΑΤΡΙΚΗ ΣΧΟΛΗ

ΤΟΜΕΑΣ ΒΑΣΙΚΩΝ ΙΑΤΡΙΚΩΝ ΕΠΙΣΤΗΜΩΝ

ΕΡΓΑΣΤΗΡΙΟ ΒΙΟΛΟΓΙΑΣ

Διευθυντής Καθηγητής Αριστείδης Ηλιόπουλος

ΔΙΔΑΚΤΟΡΙΚΗ ΔΙΑΤΡΙΒΗ

Διερεύνηση του ρόλου της πρωτεΐνης α-συνουκλεΐνης στην παθογένεια της Ατροφίας Πολλαπλών Συστημάτων

Investigation of the role of the protein alpha synuclein on Multiple System Atrophy Pathogenesis

Παναγιώτα Μαυροειδή

Βιολόγος

Αθήνα 2021

«Το έργο συγχρηματοδοτείται από την Ελλάδα και την Ευρωπαϊκή Ένωση (Ευρωπαϊκό Κοινωνικό Ταμείο) μέσω του Επιχειρησιακού Προγράμματος «Ανάπτυξη Ανθρώπινου Δυναμικού, Εκπαίδευση και Διά Βίου Μάθηση», στο πλαίσιο της Πράξης «Ενίσχυση του ανθρώπινου ερευνητικού δυναμικού μέσω της υλοποίησης διδακτορικής έρευνας» (MIS-5000432), που υλοποιεί το Ίδρυμα Κρατικών Υποτροφιών (ΙΚΥ)»

Ευρωπαϊκή Ένωση

Επιχειρησιακό Πρόγραμμα Ανάπτυξη Ανθρώπινου Δυναμικού, Εκπαίδευση και Διά Βίου Μάθηση

Με τη συγχρηματοδότηση της Ελλάδας και της Ευρωπαϊκής Ένωσης

ΕΣΠΑ 2014-2020

Η παρούσα διδακτορική διατριβή εκπονήθηκε στο Εργαστήριο Βιολογίας της Ιατρικής Σχολής του Εθνικού και Καποδιστριακού Πανεπιστημίου Αθηνών υπό την επίβλεψη της Αναπληρώτριας Καθηγήτριας Μαρίας Ρουμπελάκη. Το πειραματικό μέρος πραγματοποιήθηκε στο Κέντρο Πειραματικής Χειρουργικής και Μεταφραστικής Έρευνας του Ιδρύματος Ιατροβιολογικών Ερευνών της Ακαδημίας Αθηνών (ΙΙΒΕΑΑ) κατά το χρονικό διάστημα Ιούλιος 2017 – Απρίλιος 2021 στο εργαστήριο της Ερευνήτριας Γ' Μαρίας Ξυλούρη.

Ημερομηνία αίτησης υποψηφίου: 26/04/2021

Ημερομηνία ορισμού τριμελούς συμβουλευτικής επιτροπής: 19/07/2017

Ημερομηνία αίτησης αντικατάστασης μέλους της τριμελούς επιτροπής παρακολούθησης της διατριβής (λόγω προαγωγής της εργαστηριακής επιβλέπουσας Ξυλούρη Μαρίας σε Ερευνήτρια Γ'): 16/09/2020 (Α.Π. 2021032768**)**

Ημερομηνία ορισμού θέματος: 29/09/2017 (Α.Π. 1718002981)

Ημερομηνία αίτησης συγγραφής και υποστήριξης της διατριβής στην αγγλική γλώσσα: 28/12/2020 (Α.Π. 63279**)**

Ημερομηνία ορισμού 7μελούς εξεταστικής επιτροπής: 21/05/2021 (Α.Π. 31949)

Ημερομηνία υποστήριξης διδακτορικής διατριβής: 25/06/2021

<u>Τριμελής συμβουλευτική επιτροπή:</u>

1. Δρ. **Ρουμπελάκη Μαρία** (Επιβλέπουσα), Αναπληρώτρια Καθηγήτρια, Ιατρική Σχολή, ΕΚΠΑ
2. Δρ. **Ξυλούρη Μαρία** (<u>Επιστημονική Υπεύθυνη</u>), Ερευνήτρια Γ', ΙΙΒΕΑΑ
3. Δρ. **Στεφανής Λεωνίδας**, Καθηγητής, Ιατρική Σχολή, ΕΚΠΑ και Συνεργαζόμενος Ερευνητής, ΙΙΒΕΑΑ

<u>Μέλη επταμελούς εξεταστικής επιτροπής:</u>

1. Δρ. **Ρουμπελάκη Μαρία** (Επιβλέπουσα), Αναπληρώτρια Καθηγήτρια, Ιατρική Σχολή, ΕΚΠΑ
2. Δρ. **Ξυλούρη Μαρία** (<u>Επιστημονική Υπεύθυνη</u>), Ερευνήτρια Γ', ΙΙΒΕΑΑ
3. Δρ. **Στεφανής Λεωνίδας**, Καθηγητής, Ιατρική Σχολή, ΕΚΠΑ και Συνεργαζόμενος Ερευνητής, ΙΙΒΕΑΑ
4. Δρ. **Καραγωγέως Δόμνα**, Καθηγήτρια, Ιατρική Σχολή, Πανεπιστήμιο Κρήτης
5. Δρ. **Ευθυμιόπουλος Σπύρος**, Καθηγητής, Τμήμα Βιολογίας, ΕΚΠΑ
6. Δρ. **Jensen Poul Henning**, Καθηγητής, Aarhus University, Denmark
7. Δρ. **Πολίτης Παναγιώτης**, Ερευνητής Β', ΙΙΒΕΑΑ

Πρόεδρος της Ιατρικής Σχολής: Καθηγητής Πέτρος Π. Σφηκάκης

Ο ΟΡΚΟΣ ΤΟΥ ΙΠΠΟΚΡΑΤΗ

Ὄμνυμι Ἀπόλλωνα ἰητρὸν, καὶ Ἀσκληπιὸν, καὶ Ὑγείαν, καὶ Πανάκειαν, καὶ θεοὺς πάντας τε καὶ πάσας, ἵστορας ποιεύμενος, ἐπιτελέα ποιήσειν κατὰ δύναμιν καὶ κρίσιν ἐμὴν ὅρκον τόνδε καὶ ξυγγραφὴν τήνδε. Ἡγήσασθαι μὲν τὸν διδάξαντά με τὴν τέχνην ταύτην ἴσα γενέτῃσιν ἐμοῖσι, καὶ βίου κοινώσασθαι, καὶ χρεῶν χρηίζοντι μετάδοσιν ποιήσασθαι, καὶ γένος τὸ ἐξ ωὐτέου ἀδελφοῖς ἴσον ἐπικρινέειν ἄῤῥεσι, καὶ διδάξειν τὴν τέχνην ταύτην, ἢν χρηίζωσι μανθάνειν, ἄνευ μισθοῦ καὶ ξυγγραφῆς, παραγγελίης τε καὶ ἀκροήσιος καὶ τῆς λοιπῆς ἁπάσης μαθήσιος μετάδοσιν ποιήσασθαι υἱοῖσί τε ἐμοῖσι, καὶ τοῖσι τοῦ ἐμὲ διδάξαντος, καὶ μαθηταῖσι συγγεγραμμένοισί τε καὶ ὡρκισμένοις νόμῳ ἰητρικῷ, ἄλλῳ δὲ οὐδενί. Διαιτήμασί τε χρήσομαι ἐπ' ὠφελείῃ καμνόντων κατὰ δύναμιν καὶ κρίσιν ἐμὴν, ἐπὶ δηλήσει δὲ καὶ ἀδικίῃ εἴρξειν. Οὐ δώσω δὲ οὐδὲ φάρμακον οὐδενὶ αἰτηθεὶς θανάσιμον, οὐδὲ ὑφηγήσομαι ξυμβουλίην τοιήνδε. Ὁμοίως δὲ οὐδὲ γυναικὶ πεσσὸν φθόριον δώσω. Ἁγνῶς δὲ καὶ ὁσίως διατηρήσω βίον τὸν ἐμὸν καὶ τέχνην τὴν ἐμήν. Οὐ τεμέω δὲ οὐδὲ μὴν λιθιῶντας, ἐκχωρήσω δὲ ἐργάτῃσιν ἀνδράσι πρήξιος τῆσδε. Ἐς οἰκίας δὲ ὁκόσας ἂν ἐσίω, ἐσελεύσομαι ἐπ' ὠφελείῃ καμνόντων, ἐκτὸς ἐὼν πάσης ἀδικίης ἑκουσίης καὶ φθορίης, τῆς τε ἄλλης καὶ ἀφροδισίων ἔργων ἐπί τε γυναικείων σωμάτων καὶ ἀνδρῴων, ἐλευθέρων τε καὶ δούλων. Ἃ δ' ἂν ἐν θεραπείῃ ἢ ἴδω, ἢ ἀκούσω, ἢ καὶ ἄνευ θεραπηίης κατὰ βίον ἀνθρώπων, ἃ μὴ χρή ποτε ἐκλαλέεσθαι ἔξω, σιγήσομαι, ἄῤῥητα ἡγεύμενος εἶναι τὰ τοιαῦτα. Ὅρκον μὲν οὖν μοι τόνδε ἐπιτελέα ποιέοντι, καὶ μὴ ξυγχέοντι, εἴη ἐπαύρασθαι καὶ βίου καὶ τέχνης δοξαζομένῳ παρὰ πᾶσιν ἀνθρώποις ἐς τὸν αἰεὶ χρόνον. παραβαίνοντι δὲ καὶ ἐπιορκοῦντι, τἀναντία τουτέων.

Απόδοση στα Νέα Ελληνικά

Ορκίζομαι στο θεό Απόλλωνα τον ιατρό και στο θεό Ασκληπιό και στην Υγεία και στην Πανάκεια και επικαλούμενος τη μαρτυρία όλων των θεών ότι θα εκτελέσω κατά τη δύναμη και την κρίση μου τον όρκο αυτόν και τη συμφωνία αυτή. Να θεωρώ τον διδάσκαλό μου της ιατρικής τέχνης ίσο με τους γονείς μου και την κοινωνό του βίου μου. Και όταν χρειάζεται χρήματα να μοιράζομαι μαζί του τα δικά μου. Να θεωρώ την οικογένειά του αδέλφια μου και να τους διδάσκω αυτήν την τέχνη αν θέλουν να την μάθουν χωρίς δίδακτρα ή άλλη συμφωνία. Να μεταδίδω τους κανόνες ηθικής, την προφορική διδασκαλία και όλες τις άλλες ιατρικές γνώσεις στους γιους μου, στους γιους του δασκάλου μου και στους εγγεγραμμένους μαθητές που πήραν τον ιατρικό όρκο, αλλά σε κανέναν άλλο. Θα χρησιμοποιώ τη θεραπεία για να βοηθήσω τους ασθενείς κατά τη δύναμη και την κρίση μου, αλλά ποτέ για να βλάψω ή να αδικήσω. Ούτε θα δίνω θανατηφόρο φάρμακο σε κάποιον που θα μου το ζητήσει, ούτε θα του κάνω μια τέτοια υπόδειξη. Παρομοίως, δεν θα εμπιστευτώ σε έγκυο μέσο που προκαλεί έκτρωση. Θα διατηρώ αγνή και άσπιλη και τη ζωή και την τέχνη μου. Δεν θα χρησιμοποιώ νυστέρι ούτε σε αυτούς που πάσχουν από λιθίαση, αλλά θα παραχωρώ την εργασία αυτή στους ειδικούς της τέχνης. Σε όσα σπίτια πηγαίνω, θα μπαίνω για να βοηθήσω τους ασθενείς και θα απέχω από οποιαδήποτε εσκεμμένη βλάβη και φθορά, και ιδίως από γενετήσιες πράξεις με άνδρες και γυναίκες, ελεύθερους και δούλους. Και όσα τυχόν βλέπω ή ακούω κατά τη διάρκεια της θεραπείας ή και πέρα από τις επαγγελματικές μου ασχολίες στην καθημερινή μου ζωή, αυτά που δεν πρέπει να μαθευτούν παραέξω δεν θα τα κοινοποιώ, θεωρώντας τα θέματα αυτά μυστικά. Αν τηρώ τον όρκο αυτό και δεν τον παραβώ, ας χαίρω πάντοτε υπολήψεως ανάμεσα στους ανθρώπους για τη ζωή και για την τέχνη μου. Αν όμως τον παραβώ και επιορκήσω, ας πάθω τα αντίθετα.

CURRICULUM VITAE

Panagiota Mavroeidi, MSc
Centre for Clinical, Exp. Medicine & Translational Research
Biomedical Research Foundation Academy of Athens (BRFAA)
Soranou Efesiou 4, 11527 Athens, Greece
Tel: 30-210-6597498 or 30-210-6597496, Fax: 30-210-6597545
E-mail: pmavroeidi@bioacademy.gr

BIOGRAPHICAL SKETCH

EDUCATION / TRAINING

2017-2021: Ph.D candidate (Biological Sciences), BRFAA, Greece
2012 – 2015: MSc (Biological Sciences), "Molecular Medicine", Medical School, University of Athens, Greece
2006 – 2012: B.S (Biological Sciences); Department of Biology, University of Athens, Greece

POSITIONS / EMPLOYMENT

2017 – present: PhD candidate, Centre for Clinical, Exp. Medicine & Translational Research, Biomedical Research Foundation Academy of Athens (BRFAA), Greece, PIs: Dr Xilouri M., Dr Roubelakis M., **"*Study of the role of alpha synuclein protein in MSA Pathogenesis*",** Funding Source: Multipe System Atrophy Coalition (2016-2017) and I.K.Y. Scholarship (2018-2021)
2015 – 2017: Research Assistant, Hellenic Pasteur Institute and University of Athens, Greece, PIs: Dr Haralambous S., Dr Efthimiopoulos S., ***"Study of alterations in tau synaptic distribution under conditions of glucose and/or oxygen deprivation"***
2012 – 2015: MSc Student, Medical School, University of Athens, Greece, Supervisor: Dr Efthimiopoulos S., ***"The effect of glucose deprivation on the development of Alzheimer's disease neuropathology"***, Funding Source: ***Aristeia I***

HONORS / AWARDS

September 2017: Award by the Hellenic Society for Neuroscience in memory of the eminent Academician, Neuroscientist and Psychiatrist Costas Stefanis, in the meeting entitled "20 years of alpha- synuclein in Parkinson's Disease & related synucleinopathies: from the bedside to the bench and back to the patient" for the presentation of the work entitled "***Unravelling the mechanism of alpha-synuclein seeding in oligodendrocytes***", Vravrona, Attiki, Greece
April 2018: Scholarship financed by Greece and the European Union (European Social Fund- ESF) through the Operational Programme «Human Resources Development, Education and Lifelong Learning» in the context of the project "Strengthening Human Resources Research Potential via Doctorate Research" (MIS-5000432), implemented by the State Scholarships Foundation (I.K.Y.), for the funding of PhD thesis entitled: **"*Study of the role of alpha synuclein protein in MSA Pathogenesis*",** BRFAA, Athens, Greece
July 2019: **FRM 2019 Travel Grant**, for the participation in the FENS Regional Meeting, Belgrade, Serbia, July 10-13, 2019
September 2019: **Synuclein Meeting Travel Grant,** for the participation in the "Synuclein Meeting 2019: Where we are and where we need to go", Porto, Portugal, September 1-4, 2019

PROFESSIONAL MEMBERSHIPS

Hellenic Society for Neurosciences
Hellenic Society of Biochemistry and Molecular Biology
Hellenic Association for Biological Sciences

PUBLICATIONS IN PEER-REVIEWED JOURNALS

1. Panagiota Mavroeidi, Fedra Arvanitaki, Anastasia-Kuriaki Karakitsou, Markus Zweckstetter, Karin Giller, Stefan Becker, Zachary A. Sorrentino, Benoit I. Giasson, Poul Henning Jensen, Leonidas Stefanis and Maria Xilouri. "***Endogenous Oligodendroglial alpha-Synuclein and TPPP/p25α Orchestrate alpha-Synuclein Pathology in Multiple System Atrophy***", Acta Neuropathol. 2019 Oct;138(4):675.

2. Fouka M, **Mavroeidi P**., Tsaka G, Xilouri M. "***In Search of Effective Treatments Targeting α-Synuclein Toxicity in Synucleinopathies: Pros and Cons.",*** Front Cell Dev Biol. 2020 Sep 4;8:559791

3. Mavroeidi P., Xilouri M. ***"Neurons and Glia Interplay in α-Synucleinopathies",*** Int J Mol Sci. 2021 May 8;22(9):4994

4. Brekk OR, Makridakis M, **Mavroeidi P**, Vlahou A, Xilouri M, Stefanis L. "***Impairment of chaperonemediated autophagy affects neuronal homeostasis through altered expression of DJ-1 and CRMP-2 proteins***.", Mol Cell Neurosci. 2018 Dec 15;95:1-12. doi: 10.1016/j.mcn.2018.12.006.

5. Mavroeidi P., Mavrofrydi O., Pappa E., Panopoulou M., Papazafiri P., Haralambous S., Efthimiopoulos S. (2017) "***Oxygen and glucose deprivation alter synaptic distribution of tau protein***.", J Alzheimers Dis., 60(2):593-604.

6. Divolis G., **Mavroeidi P.,** Mavrofrydi O., Papazafeiri P. (2016) "***Differential effects of calcium on PI3K-Akt and HIF-1α survival pathways.***", Cell Biol Toxicol., 32(5):437-49.

7. Mavrofrydi O., **Mavroeidi P.**, Papazafeiri P. (2016) "***Comparative assessment of HIF-1a and Akt responses in human lung and skin cells exposed to benzo[α]pyrene. Effect of conditioned medium from pre-exposed primary fibroblasts.***", Environ Toxicol., 31(9):1103-12

PUBLICATIONS (submitted/under revision)

1. Panagiota Mavroeidi, Fedra Arvanitaki, Maria Vetsi, Stefan Becker, Dimitrios Vlachakis, Poul Henning Jensen, Leonidas Stefanis and Maria Xilouri, "**Autophagy Mediates the Clearance of Oligodendroglial alpha-Synuclein and TPPP/P25A in Multiple System Atrophy Models",** Autophagy

ORAL PRESENTATIONS IN CONFERENCES

1. Mavroeidi P., Mafrofrydi O., Papazafiri P. "***Investigation of the conditions for the combined activation of***
survival pathways and increased cellular calcium levels in cancer cells," 33rd Annual Scientific Congress of
Greek Association for Biological Sciences 19-21 May 2011, Edessa

2. Panagiota Mavroeidi, Fedra Arvanitaki, Anastasia Kiriaki Karakitsou, Maria Vetsi, Ismini Kloukina, Markus
Zweckstetter, Stefan Becker, Zachary A. Sorrentino, Benoit I. Giasson, Poul Henning Jensen, Leonidas Stefanis
and Maria Xilouri, "***It takes two to tangle: α-synuclein and p25α orchestrate pathology in Multiple System Atrophy***", 28th Meeting of the Hellenic Society for Neuroscience, 4-6 October 2019, Heraklion, Greece

ΕΥΧΑΡΙΣΤΙΕΣ

Ως λόγια που βγαίνουν από την καρδιά μου, αποφάσισα να γράψω αυτές τις ευχαριστίες στην Ελληνική γλώσσα. Τα τέσσερα αυτά τελευταία χρόνια αποτέλεσαν για μένα τόσο μία δοκιμασία αντοχής αλλά και αγάπης προς την επιστήμη μας, όσο και μία πηγή γνώσης και εμπειρίας. Πιστεύω πως βγαίνω πιο δυνατή, όχι μόνο ως Βιολόγος, αλλά ως άνθρωπος που βίωσε στιγμές απόλυτης χαράς και απογοήτευσης, στιγμές κούρασης και ψυχικής ανάτασης, που γνώρισε ποικίλες προσωπικότητες ανθρώπων και μοιράστηκε μαζί τους ανησυχίες και εμπειρίες. Είναι πολλοί αυτοί οι οποίοι συνεισέφεραν στην εκπόνηση της διατριβής αυτής, τόσο πρακτικά, όσο και συναισθηματικά.

Πρώτη απ' όλους θα ήθελα να ευχαριστήσω την Επιστημονική μου Υπεύθυνη, Ξυλούρη Μαρία, Ερευνήτρια Γ΄ του κέντρου Κλινικής, Πειραματικής Χειρουργικής & Μεταφραστικής Έρευνας του Ιδρύματος Ιατροβιολογικών Ερευνών της Ακαδημίας Αθηνών. Την Μαρία την γνωρίζω ήδη από το 2012, όπου επισκέφτηκα το εργαστήριο ως rotator του ΠΜΣ «Μοριακή Ιατρική» και αμέσως την θαύμασα για την δυναμικότητα και τον χαρακτήρα της. Θεωρώ τον εαυτό μου τυχερό που εργάστηκα στο πλάι μίας τόσο δραστήριας ερευνήτριας, η οποία υπήρξε για μένα καθοδηγήτρια και φίλη, με εμπιστεύτηκε από την πρώτη στιγμή και με αγκάλιασε όχι μόνο στη νεοσύστατη ομάδα της, αλλά και στο σπίτι και την οικογένειά της με τα παιδιά της και τον σύζυγό της Σταυρόπουλο Αθανάσιο, τον οποίον επίσης εκτιμώ απεριόριστα. Την ευχαριστώ για όσα έκανε για μένα, αλλά και για όσα συνεχίζει να κάνει.

Θα ήθελα επίσης να ευχαριστήσω και τα άλλα μέλη της τριμελούς συμβουλευτικής επιτροπής μου, την Καθηγήτρια κ. Ρουμπελάκη Μαρία (Ιατρική Σχολή, ΕΚΠΑ), η οποία ήταν η Ακαδημαϊκή Υπεύθυνη αυτής της διατριβής και τον Καθηγητή κ. Στεφανή Λεωνίδα (Ιατρική Σχολή, ΕΚΠΑ), οι οποίοι στάθηκαν στο πλάι μου και ήταν πάντα διαθέσιμοι να με βοηθήσουν και να με συμβουλεύσουν. Επίσης, ευχαριστώ πολύ τα μέλη της επταμελούς εξεταστικής μου επιτροπής, που δέχτηκαν να συμμετάσχουν και με τίμησαν με την παρουσία τους και τις παρατηρήσεις τους σχετικά με τη διατριβή μου: την Καθηγήτρια κ. Καραγωγέως Δόμνα (Ιατρική Σχολή, Κρήτη), τον Καθηγητή κ. Ευθυμιόπουλο Σπύρο (Τμήμα Βιολογίας, ΕΚΠΑ), τον Ερευνητή Β' κ. Πολίτη Παναγιώτη (ΙΙΒΕΑΑ) και τον Καθηγητή κ. Poul Henning Jensen (Aarhus University, Denmark). Είναι άτομα που γνώρισα προσωπικά στην πορεία μου ως φοιτήτρια, άλλους λιγότερο, άλλους περισσότερο και τους θαυμάζω τόσο για το επιστημονικό τους επίπεδο όσο και την ανθρώπινη καλοσύνη τους. Ένα πολύ μεγάλο ευχαριστώ οφείλω και στην Αναπληρώτρια Καθηγήτρια κ. Παπαζαφείρη Παναγιώτα (Τμήμα Βιολογίας, ΕΚΠΑ), η οποία στάθηκε δίπλα μου όλα τα χρόνια της γνωριμίας μας, ήδη από το 2010 όταν με δέχτηκε στην ομάδα της ως προπτυχιακή φοιτήτρια και ήταν η πρώτη που με έμαθε πώς να κινούμαι σε έναν εργαστηριακό χώρο.

Θα ήθελα επίσης να ευχαριστήσω τους συνεργάτες μας Markus Zweckstetter (Max Planck Institute, Germany), Stefan Becker (Max Planck Institute, Germany), Benoit Giasson (University of Florida, USA) και Nadia Stefanova (Medical University Innsbruck, Austria) για την σημαντική τους συμβολή στην εκπόνηση της εργασίας αυτής. Η διατριβή αυτή όμως δεν θα είχε ολοκληρωθεί ποτέ χωρίς την βοήθεια πολύ σημαντικών ανθρώπων στο ΙΙΒΕΑΑ, οι οποίοι μου προσέφεραν τη βοήθειά τους απλόχερα και με χαρά και τους ευγνωμονώ. Πρόκειται για τους: Κλουκίνα Ισμήνη, Ρηγανά Ελένη, Παγκάκη Σταμάτη, Δελή Τάσο, Αλεξάκο Παύλο και Τζανούκο Γιώργο, καθένας τους με έναν ξεχωριστό τρόπο και με φοβερό επαγγελματισμό, με στήριξε στα χρόνια που

κινήθηκα στους χώρους του ΙΙΒΕΑΑ. Φυσικά, οφείλω και ένα μεγάλο ευχαριστώ στον Βλαχάκη Δημήτριο, ο οποίος συνέβαλλε σημαντικά στην ολοκλήρωση της δουλειάς μας.

Η εργαστηριακή ζωή βέβαια δεν θα ήταν εύκολη χωρίς όλους αυτούς τους ανθρώπους, συνεργάτες και φίλους που δημιούργησαν και δημιουργούν ένα τόσο φιλικό και ευχάριστο περιβάλλον. Από όλους αυτούς τους ανθρώπους όμως δεν μπορώ παρά να ξεχωρίσω αυτούς που τρύπωσαν στην καρδιά μου και παρέμειναν εκεί μέχρι και τη στιγμή τούτη, τις: Αρβανιτάκη Φαίδρα, Βέτση Μαρία, Μελαχροινού Κατερίνα, Τσάκα Γρηγορία και Φούκα Μαρία. Χωρίς εσάς η ζωή στο εργαστήριο σίγουρα θα ήταν πολύ πιο δύσκολη, σας ευχαριστώ για την βοήθειά σας και τη φιλία σας…Φυσικά, ήταν σημαντική η παρουσία και η δουλειά και των υπόλοιπων μελών της ομάδας μας, της Βαμβακά-Ιακώβου Αναστασίας και του Δουκουμόπουλου Βαγγέλη, αλλά και των υπολοίπων παιδιών που δούλεψαν μαζί μου κάνοντας την πρακτική τους ή το rotation του master τους. Ευχαριστώ όλα τα μέλη του εργαστηρίου, παλαιότερα και νεότερα, δεν θέλω να αδικήσω κανέναν γιατί όλοι άφησαν το σημάδι τους στο εργαστήριο αυτό. Ιδιαίτερα, θα θυμάμαι πάντα και τις επί παντός επιστητού συζητήσεις στο γραφείο με τον Βεκρέλλη Κώστα, τον ευχαριστώ για τη βοήθεια και την ευχάριστη παρουσία του καθημερινά.

Ευχαριστώ επίσης και τις Κωσταβασίλη Ιωάννα και Τσικίτη Μαίρη, οι οποίες μαζί και με την Κλουκίνα Ισμήνη, δεν μου προσέφεραν μόνο υλικοτεχνική βοήθεια, αλλά και τη φιλία τους και την αγάπη τους. Ένα μεγάλο ευχαριστώ και σε όλους τους φίλους μου, με τους οποίους πορεύτηκα παρέα στα χρόνια των διδακτορικών μας (και όχι μόνο): Διβόλη Γιώργο, Γιαρδόγλου Τότα, Τσιορτού Ποπιάννα, Γκίκα Δημήτρη, Μιχαήλ Άρτεμις, Νίνου Νίκη, Βασιλική Πανταζοπούλου, Κεραμιδιώτου Αθηνά, αλλά και στους φίλους με τους οποίους συνδέομαι με παλιούς εργαστηριακούς δεσμούς, Σαμαρά Αθηνά, Παπαδοπούλου Νάντια, Μαλακτάρη Ελένη και Μπαντούνα Φώτη. Το μεγαλύτερο ευχαριστώ όμως οφείλω στην οικογένειά μου, τους γονείς μου Γεωργία και Δημήτρη, τον αδερφό μου Αντώνη και τον σύζυγό μου Μανώλη Μυγιάκη, οι οποίοι έχουν υπάρξει στήριγμα σε όλες τις στιγμές της ζωής μου και εύχομαι σε όλον τον κόσμο να έχει τέτοιους υπέροχους ανθρώπους στο περιβάλλον του. Η αγάπη μου και η ευγνωμοσύνη μου για εκείνους δεν χωράει σε απλές λέξεις στο χαρτί.

Στην οικογένειά μου…

ABBREVIATIONS

3MA: 3-Methyladenine

ab: antibody

AIF1: Allograft Inflammatory Factor 1

ALP: Autophagy-Lysosome Pathway

AMBRA1: Autophagy And Beclin 1 Regulator 1

ANOVA: Analysis of Variance

AR7: Atypical Retinoid 7

aSyn: alpha-synuclein

ATG: Autophagy related gene

BCAS1: Breast Carcinoma Amplified Sequence 1

BSA: Bovine Serum Albumin

Ci: Curie

CMA: Chaperone-Mediated Autophagy

CMV: Cytomegalovirus

CNS: Central Nervous System

CSF: Cerebrospinal Fluid

CTSD: Cathepsin D

DAT: Dopamine Transporter

DAPI: 4′,6-diamidino-2-phenylindole

DLB: Dementia with Lewy Bodies

DMEM: Dulbecco's Modified Eagle's Medium

Epox: Epoxomicin

ER: Endoplasmic Reticulum

GAPDH: Glyceraldehyde 3-phosphate dehydrogenase

GCase: glucocerebrosidase

GCIs: Glial Cytoplasmic Inclusions

GDNF: Glial Cell Derived Neurotrophic Factor

GFAP: Glial Fibrillary Acidic Protein

GFP: Green Fluorescent Protein

haSyn: human alpha-synuclein

HDAC: Histone Deacetylase

HMW: High Molecular Weight

hrs: hours

HSC70: Heat Shock Cognate 70

HSP70: Heat Shock Protein 70

HSPGs: Heparan Sulfate Proteoglycans

iPSC: induced Pluripotent Stem Cells

KDa: 1000 Da

LAMP1: Lysosomal-Associated Membrane Protein 1

LAMP2A: Lysosome-Associated Membrane Protein 2A

LBs: Lewy Bodies

LC3: Light Chain 3

MAM: Mitochondria-Associated ER Membranes

MBP: Myelin Basic Protein

mcherry: monomeric cherry

miR: micro-RNA (RiboNucleic Acid)

MFI: Mean Fluorescence Intensity

mRFP: monomeric Red Fluorescent Protein

MSA: Multiple System Atrophy

NCIs: Neuronal Cytoplasmic Inclusions

NGS: Normal Goat Serum

NH_4Cl: ammonium chloride

OPCs: Oligodendroglial Progenitor Cells

PBS: Phosphate-Buffered Saline

PC12: Pheochromocytoma cell line

PD: Parkinson's disease

PE: phosphatidylethanolamine

PFFs: Pre-Formed Fibrils

PIs: Protease Inhibitors

PLP: Proteolipid Protein

PTP: Permeability Transition Pore

Rap: Rapamycin

RFP: Red Fluorescent Protein

ROS: Reactive Oxygen Species

RT-PCR: Reverse Transcription Polymerase Chain Reaction

Scr: Scrambled

SDS: Sodium Dodecyl Sulfate

SE: Standard Error

siRNAs: small interfere RNAs

SNARE: soluble N-ethylmaleimide-sensitive factor attachment protein receptor

SQSTM1: Sequestosome 1

SUMO: Small Ubiquitin-like Modifier

taSyn: total alpha-synuclein

TCA: Thrichloroacetic Acid

TEM: Transmission Electron Microscopy

TH: Tyrosine Hydroxylase

TPPP: Tubulin Polymerization Promoting Protein

UCH-L1: Ubiquitin Carboxy-terminal Hydrolase L1

UPS: Ubiquitin-Proteasome System

VAMP2: Vesicle-associated membrane protein 2

VDAC1: Voltage-Dependent Anion Channel 1

VMAT2: Vesicular Monoamine Transporter 2

WT: Wild Type

Περιεχόμενα

ΠΕΡΙΛΗΨΗ

Η Ατροφία Πολλαπλών Συστημάτων αποτελεί μια σπάνια προοδευτική νευροεκφυλιστική νόσο η οποία χαρακτηρίζεται από την παρουσία Γλοιακών Κυτταροπλασματικών Εγκλείστων στα ολιγοδενδροκύτταρα. Τα έγκλειστα αυτά αποτελούνται κυρίως από τη νευρωνική πρωτεΐνη α-συνουκλεΐνη και την ολιγοδενδρογλοιακή φωσφοπρωτεΐνη TPPP/p25α. Ο ακριβής ρόλος των ολιγοδενδρογλοιακών πρωτεϊνών α-συνουκλεΐνη και p25α στο σχηματισμό των Γλοιακών Κυτταροπλασματικών Εγλείστων και τον επακόλουθο νευρωνικό θάνατο, καθώς και οι πρωτεολυτικοί μηχανισμοί που εμπλέκονται στην απομάκρυνση αυτών των πρωτεϊνών υπό φυσιολογικές και παθολογικές συνθήκες, παραμένουν εν πολλοίς άγνωστοι.

Προκειμένου να απαντήσουμε σε αυτά τα ερωτήματα, χρησιμοποιήσαμε τρεις αθανατοποιημένες κυτταρικές σειρές ολιγοδενδροκυττάρων προερχόμενες από εγκέφαλο επίμυος: κύτταρα αγρίου τύπου (OLN-93) με ελάχιστα έως μη-ανιχνεύσιμα επίπεδα ενδογενούς α-συνουκλεΐνης και p25α και ολιγοδενδροκύτταρα που υπερεκφράζουν σταθερά την ανθρώπινη α-συνουκλεΐνη (OLN-AS7) ή την p25α (OLN-p25α). Παράλληλα, χρησιμοποιήθηκαν πρωτογενείς καλλιέργειες διαφοροποιημένων ολιγοδενδροκυττάρων προερχόμενων από αγρίου τύπου (WT-aSyn) μύες και διαγονιδιακούς μύες που στερούνται πλήρως την έκφραση ενδογενούς α-συνουκλεΐνης (KO-aSyn) ή υπερεκφράζουν την ανθρώπινη α-συνουκλεΐνη επιλεκτικά στα ολιγοδενδροκύτταρα (PLP-haSyn). Κυτταρικές σειρές και πρωτογενείς καλλιέργειες επωάστηκαν με προ-σχηματισμένα ινίδια α-συνουκλεΐνης ανθρώπινης προέλευσης ως μοντέλο α-συνουκλεϊνοπάθειας. Αρχικά, διαπιστώθηκε ότι τα ινίδια α-συνουκλεΐνης προσλαμβάνονται γρήγορα από τα ολιγοδενδρογλοιακά κύτταρα και μπορούν να στρατολογήσουν την ενδογενή πρωτεΐνη στο σχηματισμό αδιάλυτων, παθολογικών συσσωματωμάτων.

Η υπερέκφραση των πρωτεϊνών α-συνουκλεΐνη ή/και p25α επιταχύνει τη στρατολόγηση της ενδογενούς α-συνουκλεΐνης και τη δημιουργία παθολογικών διαμορφώσεων αυτής. Στις πρωτογενείς καλλιέργειες ολιγοδενδροκυττάρων οι οποίες επωάστηκαν με ινίδια α-συνουκλεΐνης, παρατηρήθηκε και αποδιοργάνωση του δικτύου των μικροσωληνίσκων και της μυελίνης, προσομοιώνοντας έτσι ένα παθολογικό χαρακτηριστικό της νόσου, το οποίο φαίνεται να εξαρτάται πλήρως από την παρουσία της ενδογενούς α-συνουκλεΐνης.

Επιπρόσθετα, χρησιμοποιώντας απομονωμένες πρωτογενείς καλλιέργειες ολιγοδενδροκυττάρων και νευρώνων, δείξαμε ότι η σχετιζόμενη με την παθολογία φωσφορυλίωση της α-συνουκλεΐνης στο αμινοξικό κατάλοιπο σερίνης 129 εξαρτάται από το πρωτεϊνικό φορτίο α-συνουκλεΐνης και p25α και μπορεί να περιλαμβάνει διαφορετικά «στελέχη» της πρωτεΐνης παρόντα σε ολιγοδενδρογλοιακές και νευρωνικές συνουκλεϊνοπάθειες. Αυτή η υπόθεση υποστηρίχθηκε περαιτέρω από δεδομένα που ελήφθησαν από ανθρώπινο μεταθανάτιο εγκεφαλικό υλικό ασθενών με Ατροφία Πολλαπλών Συστημάτων ή με άνοια με σώματα Lewy, στην οποία τα συσσωματώματα

α-συνουκλεΐνης εντοπίζονται σε νευρώνες. Η σημασία της ενδογενούς α-συνουκλεΐνης στην εκδήλωση παθολογίας επιβεβαιώθηκε περαιτέρω σε *in vivo* πειράματα, όπου η έγχυση ινιδίων α-συνουκλεΐνης στον εγκέφαλο μυών οδήγησε στο σχηματισμό παθολογικών διαμορφώσεων α-συνουκλεΐνης εντός των ολιγοδενδροκυττάρων, οι οποίες συμπεριελάμβαναν την ενδογενή πρωτεΐνη και προκάλεσαν την αποδιοργάνωση του δικτύου μυελίνης σε μύες αγρίου τύπου, αλλά όχι σε μύες οι οποίοι στερούνταν την έκφραση α-συνουκλεΐνης.

Προκειμένου να εξακριβώσουμε τους μηχανισμούς αποικοδόμησης τόσο της ολιγοδενδρογλοιακής α-συνουκλεΐνης όσο και της p25α, πραγματοποιήσαμε αναστολή της οδού αυτοφαγίας-λυσοσώματος με φαρμακολογικά και μοριακά μέσα, καθώς και φαρμακολογική αναστολή του πρωτεασώματος. Τα αποτελέσματά μας υποδεικνύουν ότι οι ενδογενείς ολιγοδενδρογλοιακές πρωτεΐνες α-συνουκλεΐνη και p25α αποικοδομούνται κυρίως από το λυσόσωμα τόσο σε κυτταρικές σειρές όσο και σε πρωτογενείς καλλιέργειες ολιγοδενδροκυττάρων υπό φυσιολογικές συνθήκες. Ταυτόχρονα, αναγνωρίσαμε ένα μοτίβο στην αλληλουχία της p25α το οποίο επιτρέπει την αποτελεσματική αποδόμηση της πρωτεΐνης μέσω της αυτοφαγίας διαμεσολαβούμενης από σαπερόνες σε ένα *in vitro* σύστημα απομονωμένων λυσοσσωμάτων προερχόμενων από εγκέφαλο επίμυος. Χρησιμοποιώντας ινιδιακές μορφές ανθρώπινης α-συνουκλεΐνης, χαρακτηρίσαμε διεξοδικά τη συμβολή του συστήματος αυτοφαγίας-λυσοσώματος στην απομάκρυνση των εξωγενώς προστιθέμενων ινιδίων, αλλά και των επαγόμενων παθολογικών διαμορφώσεων της ενδογενούς ολιγοδενδρογλοιακής α-συνουκλεΐνης. Δείξαμε επίσης ότι η επώαση με ινίδια α-συνουκλεΐνης μειώνει την αυτοφαγική ροή και ότι η πρωτεΐνη p25α ασκεί μια ανασταλτική επίδραση στο μονοπάτι της μακροαυτοφαγίας, ενώ ταυτόχρονα η αυτοφαγία διαμεσολαβούμενη από σαπερόνες ενεργοποιείται ως αντισταθμιστικός μηχανισμός για να απομακρύνει τις παθολογικές μορφές α-συνουκλεΐνης που σχηματίζονται εντός των ολιγοδενδροκυττάρων.

Συμπερασματικά, η παρούσα μελέτη αναδεικνύει το σημαντικό ρόλο που διαδραματίζουν οι ενδογενείς ολιγοδενδρογλοιακές πρωτεΐνες α-συνουκλεΐνη και p25α στο σχηματισμό παθολογικών διαμορφώσεων α-συνουκλεΐνης σε πειραματικά μοντέλα της Ατροφίας Πολλαπλών Συστημάτων. Παράλληλα, αποκαλύπτει τη συμμετοχή της αυτοφαγίας διαμεσολαβούμενης από σαπερόνες και της μακροαυτοφαγίας στη ρύθμιση των επιπέδων τόσο της ενδογενούς ολιγοδενδρογλοιακής α-συνουκλεΐνης όσο και της p25α, σε φυσιολογικές και παθολογικές συνθήκες και προτείνει τη στόχευση αυτών των μονοπατιών ως πιθανούς θεραπευτικούς στόχους για τη νόσο.

ABSTRACT

Multiple System Atrophy is a rare debilitating disease characterized by the presence of distinct glial cytoplasmic inclusions within oligodendrocytes. These inclusions are mainly composed of the neuronal protein alpha-synuclein and the oligodendroglia-specific phosphoprotein TPPP/p25α. The precise role of oligodendroglial alpha-synuclein and p25α in the formation of glial cytoplasmic inclusions and the subsequent neuronal death, as well as the proteolytic mechanisms involved in their turnover in health and disease remains hitherto unclear. To address these questions, we have utilized three immortalized oligodendroglial cell lines originated from rat brain glial cultures: wild-type oligodendrocytes (OLN-93) expressing low to non-detectable levels of the endogenous alpha-synuclein and p25α and cells stably overexpressing human alpha-synuclein (OLN-AS7) or human p25α (OLN-p25α). In parallel, we have used primary cultures of differentiated oligodendroglial cells deriving from wild-type (WT-aSyn) mice or transgenic mice lacking the endogenous alpha-synuclein expression (KO-aSyn) or overexpressing human alpha-synuclein selectively in oligodendrocytes (PLP-haSyn). Both cell lines and primary oligodendrocytes were incubated with human alpha synuclein pre-formed fibrils as a model of alpha-synucleinopathy. Initially, we verified that alpha-synuclein fibrils are readily taken up by oligodendroglial cells and can recruit minute amounts of endogenous alpha-synuclein into the formation of insoluble, highly aggregated, pathological assemblies. The overexpression of human alpha-synuclein or p25α accelerates the recruitment of the endogenous protein and the generation of such aberrant species. In fibril-treated primary oligodendrocytes, the microtubule and myelin networks are disrupted, thus recapitulating a pathological hallmark of Multiple System Atrophy, in a manner totally dependent upon the presence of endogenous alpha-synuclein.

Furthermore, utilizing oligodendroglial and cortical cultures, we demonstrated that the pathology-related phosphorylation of alpha-synuclein at Serine 129 depends on alpha-synuclein and p25α protein load and may involve different alpha-synuclein “strains” present in oligodendroglial and neuronal synucleinopathies. Importantly, this hypothesis was further supported by data obtained from human post-mortem brain material derived from patients with Multiple System Atrophy and dementia with Lewy bodies, where alpha-synuclein accumulates in neurons. Importantly, delivery of alpha-synuclein fibrils into the mouse striatum led to the formation of aberrant alpha-synuclein forms within oligodendroglia, incorporating the endogenous protein, and evoked myelin decompaction in WT-aSyn mice, but not in KO-aSyn mice.

In order to elucidate the degradation mechanisms responsible for the removal of both endogenous oligodendroglial alpha-synuclein and p25α, we pharmacologically and molecularly modulated the autophagy-lysosome pathway and performed pharmacological inhibition of the proteasome. According to our results, both the endogenous oligodendroglial alpha-synuclein and

p25α are degraded mainly by the autophagy-lysosome pathway in oligodendroglial cell lines and murine primary oligodendrocytes under basal conditions. We have also identified a KFERQ-like motif in p25α sequence that enables its effective degradation via chaperone-mediated autophagy in an *in vitro* system of isolated rat brain lysosomes. Utilizing pre-formed alpha-synuclein fibrils as seeds of pathology, we thoroughly characterized the contribution of autophagy-lysosome pathway in the removal of the exogenously added and the seeded oligodendroglial alpha-synuclein pathological assemblies. We have also showed that inoculation with alpha-synuclein fibrils impairs autophagic flux in oligodendrocytes and that p25α exerts an inhibitory effect on macroautophagy, while at the same time chaperone-mediated autophagy is upregulated, probably as a compensatory mechanism, to remove the pathological alpha-synuclein species formed within oligodendrocytes.

Collectively, this line of research highlights the role of endogenous alpha-synuclein and p25α in the formation of pathological aSyn assemblies in experimental models of Multiple System Atrophy. In addition, this study pinpoints the contribution of chaperone-mediated autophagy and macroautophagy in the regulation of oligodendroglial alpha-synuclein and p25α levels, in physiological and pathological conditions and highlights their targeting as a potential therapeutic strategy against Multiple System Atrophy.

I. INTRODUCTION

1. Multiple System Atrophy (MSA)

Multiple system atrophy (MSA) is a fatal neurodegenerative disorder characterized by the progressive loss of the autonomic nervous system, with only symptomatic treatment currently available (Ortiz, Bette et al. 2020). MSA usually occurs after the sixth decade of human life and epidemiological studies indicate a prevalence of 1.9-4.9 per 100,000 people and a frequency of 3 per 100,000 people per year (Bower, Maraganore et al. 1997). The clinical features of the disease are the presence of Parkinsonian symptoms and the development of cerebral ataxia and dysautonomia. Depending on the prevalence of symptoms, two subcategories can be distinguished (Gilman, Low et al. 1999):

a) *MSA-P*: The most common form of MSA, with symptoms similar to Parkinson's Disease (PD), since it is characterized by degeneration of the dopaminergic neurons in the nigrostriatal pathway,

b) *MSA-C*: It is characterized by olivopontocerebellar atrophy with predominant cerebellar features. Interestingly, there is also a mixed type of MSA baring characteristics from both MSA-C and MSA-P types.

Dysautonomy is evident in both types and is expressed via urinary incontinence, respiratory failure, dysarthria, dysphagia and orthostatic hypertension (Gilman, Wenning et al. 2008). Other clinical symptoms that may be associated with MSA are insomnia, REM sleep disturbances, increased reflexes, wheezing, etc. The initial symptoms of the disease may differ between patients, with the symptoms of the autonomic nervous system to usually precede the motor ones (Lipp, Sandroni et al. 2009). Fluorohydrocortisone and anticholinergics are used for the clinical treatment of orthostatic hypotension and urinary dysfunction, respectively (Jessen, Kaduszkiewicz et al. 2010), whereas L-DOPA is used to treat parkinsonian symptoms (Hughes, Colosimo et al. 1992). Unfortunately, the similarities in the clinical manifestations between MSA and PD patients create problems in disease diagnosis. MSA patients have a poor prognosis and the median disease duration from symptom onset to death is 6-9 years (Cao, Zhang et al. 2018; Foubert-Samier, Pavy-Le Traon et al. 2020).

The etiology of MSA still remains unknown; there are studies suggesting that there are no differences in the disease manifestations between male and female patients and that the disease progression is not affected by environmental factors (Stefanova, Bucke et al. 2009). However, the disease initiation has been associated with high exposure of patients to organic solvents, plastic monomers, pesticides and minerals (Vanacore, Bonifati et al. 2001), whereas low education level, daily meat consumption and factory work history seem to increase the risk of MSA. Interestingly,

smoking is negatively associated with the onset of both MSA and PD (Vanacore, Bonifati et al. 2001; Vidal, Vidailhet et al. 2008).

MSA, PD and Dementia with Lewy Bodies (DLB) are collectively termed alpha-synucleinopathies, due to the presence of the neuronal pre-synaptic protein alpha-synuclein (aSyn) within the proteinaceous inclusions formed within neurons or glial cells (Papp, Kahn et al. 1989; Spillantini, Crowther et al. 1998; Jellinger and Lantos 2010). Specifically, in PD and DLB, aSyn accumulates mostly in Lewy bodies (LBs) and Lewy neurites (LNs) in neurons (Spillantini, Schmidt et al. 1997; Spillantini, Crowther et al. 1998), whereas in MSA aSyn deposits mostly within the cytoplasm of oligodendrocytes forming glial cytoplasmic inclusions (GCIs) (Wakabayashi, Hayashi et al. 1998; Wakabayashi, Yoshimoto et al. 1998; Nakamura, Mori et al. 2015) (**Figure 1**). Interestingly, apart from the GCIs present within oligodendrocytes, other inclusions such as neuronal cytoplasmic inclusions (NCIs) have been detected in neuronal cells of MSA brains, mainly composed of aSyn (**Figure 2**) (Papp and Lantos 1992; Takeda, Arai et al. 1997; Yoshida 2007).

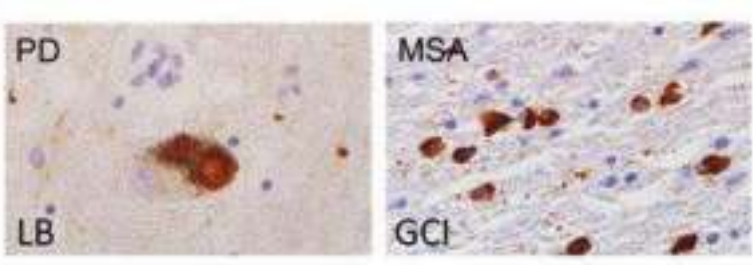

Figure 1: **aSyn aggregations in Parkinson's disease (PD, left) and multiple system atrophy (MSA, right) patients.** LB: Lewy Body, GCI: Glial Cytoplasmic Inclusion. Source: (Peng, Gathagan et al. 2018).

MSA is a typically sporadic neurodegenerative disease (Wenning, Wagner et al. 1993); however there are studies suggesting a family history (Wullner, Abele et al. 2004; Soma, Yabe et al. 2006; Hara, Momose et al. 2007; Wullner, Schmitt et al. 2009; Hohler and Singh 2012; Itoh, Kasai et al. 2014). Several mutations in the *SNCA* gene encoding for aSyn have been linked to PD pathogenesis, such as the A53T, A30P, E46K, H50Q, G51D, A18P and pA29S mutations (Polymeropoulos, Lavedan et al. 1997; Kruger, Kuhn et al. 1998; Zarranz, Alegre et al. 2004; Appel-Cresswell, Vilarino-Guell et al. 2013; Hoffman-Zacharska, Koziorowski et al. 2013; Kiely, Asi et al. 2013; Fares, Ait-Bouziad et al. 2014). However, up-to-date, no hereditable mutations in the coding region of this gene have been identified in MSA cases (Ozawa, Takano et al. 1999). Interestingly, the G51D and A53E mutations in the *SNCA* gene have been proposed as potential links between PD and MSA (Kiely, Asi et al. 2013; Pasanen, Myllykangas et al. 2014). Additionally, in two European populations, four single nucleotide polymorphisms (SNPs) in the *SNCA* gene were associated with increased MSA risk: rs11931074, rs3857059, rs3822086 and

rs3775444 (Al-Chalabi, Durr et al. 2009; Scholz, Houlden et al. 2009). However, the genetic link between *SNCA* and MSA still remains controversial.

MSA risk has been linked with polymorphisms encoding for the *COQ2* enzyme parahydroxybenzoatepolyprenyl transferase, which is implicated in the biosynthetic pathway of coenzyme $Q_{10,}$ part of the mitochondrial electron transport chain. Various *COQ2* variants, such as V393A, L25 V, M128 V, R173H, L402F, A32A and N386I, have been detected in patients with MSA (Collaboration 2013; Chen, Zhao et al. 2015; Wen, Li et al. 2015; Sun, Ohta et al. 2016). In addition, the levels of Q_{10} in the plasma and cerebellum of MSA patients were found decreased in comparison to healthy controls, accompanied by impaired mitochondrial function and increased oxidative stress (Barca, Kleiner et al. 2016; Mitsui, Matsukawa et al. 2016; Schottlaender, Bettencourt et al. 2016). Other genetic links to MSA include the presence of *MAPT* (gene encoding the neuronal tau protein) H_1 haplotype (Vilarino-Guell, Soto-Ortolaza et al. 2011; Labbe, Heckman et al. 2016), *GBA1* mutations (encodes the lysosomal enzyme β- glucocerebrosidase), *LRRK2* variants (Heckman, Schottlaender et al. 2014; Riboldi, Palma et al. 2019), the mitochondrial *CHCHD2* V66 M mutation (Yang, An et al. 2016) and *TNF-α* rs1799964 and *IL-1β* rs16944 polymorphisms (Zhou, Wang et al. 2018).

The accumulation of aSyn within the abnormally expanded cell bodies of oligodendrocytes is the main histophathological hallmark of the disease (Trojanowski and Revesz 2007; Wenning, Stefanova et al. 2008; Jellinger and Lantos 2010). Oligodendrocytes are the myelin-forming cells of the central nervous system (CNS) that together with astrocytes and microglia comprise the brain's glial cells (Bradl and Lassmann 2010). There are two main types of oligodendrocytes, the myelinating and the non-myelinating ones that concentrate in white and grey matter, respectively (Hofmann, Rodriguez-Rodriguez et al. 2017). Many neurodegenerative diseases occur due to either oligodendroglial death or damage to the myelin sheathes they produce, leading to subsequent neuronal demise (Wong, Halliday et al. 2014; Dulamea 2017; Kuhn, Gritti et al. 2019). Mature oligodendrocytes are post-mitotic cells of the CNS responsible for the production of myelin that supports and protects neurons (Wilkins, Majed et al. 2003; Bean 2007; Simons and Nave 2015; Kuhn, Gritti et al. 2019). Oligodendrocytes are involved not only in the neural transmission, but also in the development, maintenance and regeneration of axons (Baumann and Pham-Dinh 2001; Nave and Trapp 2008). The maturation of oligodendrocytes occurs during the development of the CNS and is likely to be influenced by neuronal-derived signals (Richardson, Smith et al. 2000). Adult oligodendrocytes are a heterogeneous population of cells that differs in morphology, maturation, and functional activity (Baumann and Pham-Dinh 2001). Oligodendroglial dysfunction leads to impaired myelin production and consequently to neuronal death in various brain areas (Wong, Halliday et al. 2014; Ettle, Schlachetzki et al. 2016; Dulamea 2017), resulting in autonomic

system failure and loss of muscle movement coordination, which represent the main clinical symptoms of MSA (Mendoza-Velasquez, Flores-Vazquez et al. 2019).

The origin of aSyn in oligodendrocytes of MSA patients remains ambiguous, since it has been proposed that mature oligodendrocytes do not normally express this protein (Djelloul, Holmqvist et al. 2015). Some reports have shown the expression of *SNCA* mRNA in oligodendrocytes, suggesting the presence of the endogenous oligodendrocytic protein (Richter-Landsberg, Gorath et al. 2000; Djelloul, Holmqvist et al. 2015; Kaji, Maki et al. 2018). However, other studies have failed to detect oligodendroglial *SNCA* mRNA expression in the brains of MSA patients (Solano, Miller et al. 2000; Miller, Johnson et al. 2005), or in other studies where *SNCA* mRNA was detected, no differences were observed between controls and MSA patients (Jin, Ishikawa et al. 2008; Asi, Simpson et al. 2014). Moreover, *in vitro* (Kisos, Pukass et al. 2012; Konno, Hasegawa et al. 2012; Ettle, Reiprich et al. 2014; Pukass and Richter-Landsberg 2014; Pukass, Goldbaum et al. 2015; Kaji, Maki et al. 2018) and *in vivo* studies (Rockenstein, Ubhi et al. 2012; Reyes, Rey et al. 2014) demonstrated that exogenous recombinant or neuronally derived aSyn can be taken up by oligodendroglial cell lines, suggesting the neuron-to-glia transfer of aSyn. Recent evidence suggests that the "prion-like" transmission of misfolded aSyn may contribute to MSA disease risk (Woerman, Watts et al. 2018). Yet, little is known regarding the mechanisms underlying the selective transmission of aSyn pathology in oligodendrocytes of MSA brains.

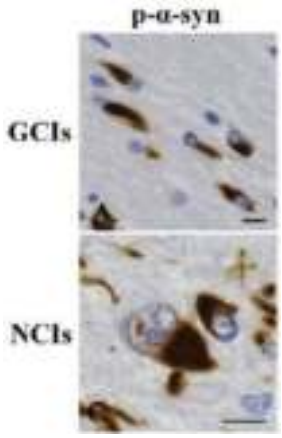

Figure 2: Immunoreactivity of phosphorylated α-synuclein (p-α-syn) in oligodendroglial and neuronal inclusions of Multiple System Atrophy (MSA) brains. GCIs: Glial Cytoplasmic Inclusions, NCIs: Neuronal Cytoplasmic Inclusions. Source: (Miki, Tanji et al. 2018)

GCIs or Papp-Lantos inclusions were first described three decades ago, as multi-shaped oligodendroglial inclusions composed of a 10-nm-sized central core fibrils, positively stained with antibodies against aSyn, surrounded by other aggregated proteins such as αβ-crystallin, ubiquitin, cytoskeletal proteins (Lantos and Papp 1994; Griffin, Hiromura et al. 2004), Hsc70 and Hsp70 chaperones (Kawamoto, Akiguchi et al. 2007) the microtubule-related proteins TPPP/p25α (Tubulin

Polymerization Promoting Protein) and tau (Papp, Kahn et al. 1989; Spillantini, Crowther et al. 1998; Wakabayashi, Yoshimoto et al. 1998; Gai, Pountney et al. 2003; Wenning, Stefanova et al. 2008), cyclin-dependent kinase 5 (Cdk5), LRRK2, parkin, etc. (Griffin, Hiromura et al. 2004; Jellinger and Lantos 2010; Bankston, Li et al. 2013). Comparative analysis of the protein composition of GCIs and LBs revealed that GCIs consist of 11,7% aSyn, 1,9% αβ-crystallin and 2,3% 14-3-3 proteins, whereas LBs are composed of 8.5, 2, and 1.5% respectively (McCormack, Chegeni et al. 2016), thus highlighting the crucial role of aSyn in GCI formation.

2. The neuronal protein alpha-synuclein (aSyn): A chameleon protein

The synuclein family includes α, β and γ synucleins, which share similar structural characteristics and they are encoded in vertebrates by 3 different highly conserved genes (Clayton and George 1998). Alpha-synuclein is a soluble protein, consisting of 140 amino acids, with a molecular weight of about 16 kDa that in humans is encoded by the *SCNA* gene. It is abundant in the CNS and is located in the cytosol of neuronal cells and in presynaptic terminals (Emamzadeh 2016).

Structurally, aSyn is composed of three main regions (Bendor, Logan et al. 2013) (**Figure 3**):

a) The N-terminus, which contains seven repeats of a sequence of 11 amino acids bearing the KTKEGV motif and forming an amphipathic α-helix via which the protein interacts with lipids. This unique repetition pattern is found in all 3 isoforms amongst the different vertebrate species (Busch and Morgan 2012). Interestingly, all mutations associated with PD (A53T, A30P, E46K, G51D and H50Q) are located within this region (Appel-Cresswell, Vilarino-Guell et al. 2013).
b) A hydrophobic region (Non-amyloid-β component, NAC) that participates in aSyn oligomerization (Rodriguez, Ivanova et al. 2015), finally leading to the formation of fibrils similar to those of β-amyloid (Aβ).
c) The C-terminal region that is highly variable in size and sequence and contains a large number of acidic amino acids (Emamzadeh 2016).

3. Physiological role of alpha-synuclein

3a. A role at the synapse

alpha-Synuclein (aSyn) is a small, intrinsically disordered protein that is mainly localized at pre-synaptic terminals (Iwai, Masliah et al. 1995; Withers, George et al. 1997), but is also present in the neuronal somato-dendritic compartment (Andringa, Du et al. 2003), in red blood cells (Barbour, Kling et al. 2008), in the gut and other peripheral tissues (Askanas, Engel et al. 2000; Bottner, Zorenkov et al. 2012; Aldecoa, Navarro-Otano et al. 2015). Although aSyn is highly enriched in presynaptic boutons, it displays a delayed distribution in the terminals, suggesting that it is implicated in later stages of synaptic development, rather than playing a central function role in synapse modulation (Withers, George et al. 1997). Importantly, aSyn is differentially expressed in the various neuronal cell types, being more abundant in excitatory synapses across different brain regions and particularly in central catecholaminergic systems (Li, Henning Jensen et al. 2002). On the contrary, this protein displays a differential expression profile in inhibitory synapses amongst the different areas of the brain, with a particular interest of aSyn presence in striatal GABAergic medium spiny neurons (MSNs) (Taguchi, Watanabe et al. 2016; Taguchi, Watanabe et al. 2019).

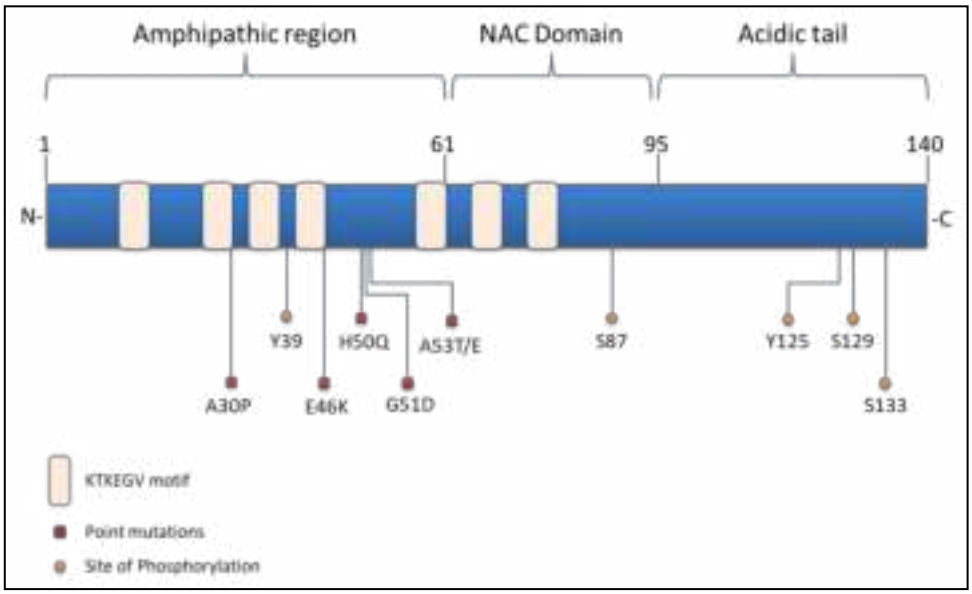

Figure 3: **Structure of alpha-synuclein (aSyn)**. The N-terminal domain of a-synuclein is characterized by the presence of repeated lipid-binding sequences and contains the mutation sites linked with familial PD. The central NAC domain is mainly hydrophobic and favors the aggregation process of the protein. The C-terminal acidic tail carries the majority of a-synuclein phosphorylation sites. Source: (Fouka, Mavroeidi et al. 2020)

The first indication regarding the role of aSyn on neural plasticity arose about 25 years ago, when "synelfin" (synuclein, NACP) expression was found up-regulated during bird song learning (George, Jin et al. 1995). aSyn localization in pre-synaptic boutons is mainly attributed to its tight association with synaptic vesicle membranes (Maroteaux, Campanelli et al. 1988) and its high affinity for the SNARE (soluble N-ethylmaleimide-sensitive factor attachment protein receptor)-complex proteins synaptobrevin-2 (VAMP2), synapsin III and rab3A (Burre, Sharma et al. 2010;

Chen, Wislet-Gendebien et al. 2013; Zaltieri, Grigoletto et al. 2015). It has been proposed that aSyn interacts with VAMP2 and promotes SNARE complex assembly (Burre, Sharma et al. 2010), followed then by its disassembly in order to complete the round of membrane fusion. The crucial role of aSyn assembly with SNARE complex on neuronal survival was further verified by the neuronal dysfunction and impaired survival of triple αβγ-synuclein knockout mice during ageing (Burre, Sharma et al. 2010; Greten-Harrison, Polydoro et al. 2010). Interestingly, aSyn lentiviral overexpression in primary neurons led to enhanced SNARE-complex assembly, further supporting the role of this protein in synaptic activity (Burre, Sharma et al. 2010). The same group later showed that only multimeric membrane-bound, but not the soluble monomeric aSyn, can promote the SNARE complex assembly (Burre, Sharma et al. 2014). It has been also recently suggested that aSyn is involved in synaptic vesicle homeostasis at the pre-synaptic terminal via a Ca^{2+}-dependent mechanism (Lautenschlager, Stephens et al. 2018).

On the contrary, monomeric natively unfolded aSyn at the pre-synaptic terminal is prone to form pathological conformations, thus exerting neurotoxic effects (Burre, Sharma et al. 2015). Another study showed that aSyn is preferably bound to synapsin 1 and VAMP2 when is present in its oligomeric form (Betzer, Movius et al. 2015), highlighting the importance of the conformational state of aSyn for the proper neuronal function. Finally, there are findings supporting the implication of aSyn in synaptic transmission, since it has been found associated with the synaptic vesicle pool, modulating the vesicle mobility, the recycling pool homeostasis and endocytosis (Zhang, Zhang et al. 2008; Scott and Roy 2012; Vargas, Makani et al. 2014).

Moreover, aSyn functions as a molecular chaperone via effective binding to other intracellular proteins. The first indication came with the discovery that aSyn displays structural and functional homology with other molecular chaperones, as the 14-3-3 or small heat shock proteins (Ostrerova, Petrucelli et al. 1999; Kim, Choi et al. 2004). Additional studies revealed that aSyn synergistically acts with the presynaptic cysteine-string protein-alpha (CSPalpha) promoting the assembly of the SNARE complex (Chandra, Gallardo et al. 2005; Burre, Sharma et al. 2010), further validating its chaperoning properties. Biochemical and structural analysis of aSyn strengthened the current indications for its chaperone-like function via the C-terminal region (residues 61-140) (Kim, Paik et al. 2000; Kim, Paik et al. 2002; Park, Jung et al. 2002). However, following studies indicated that the chaperone binding site of aSyn lies within the NAC region (residues 61-95), which interestingly is prone to aggregation and thus highly susceptible to form fibrils (Rekas, Ahn et al. 2012; Srivastava, Raj et al. 2020).

3b. Association with membranes and lipid trafficking

Intracellular aSyn can be found either natively unfolded in a soluble state or membrane-bound forming an alpha-helical or a beta-sheet secondary structure, depending on the solution conditions (Li, Du et al. 2002; Celej, Sarroukh et al. 2012; Burre, Vivona et al. 2013). It has been proposed that there is a bidirectional link between aSyn species formation and membrane remodeling, meaning that not only aSyn structure is affected upon lipid interaction, but also that membrane integrity depends on the presence of different aSyn conformations (Galvagnion, Brown et al. 2016; Chaudhary, Subramaniam et al. 2017; Galvagnion 2017). However, there are controversial results regarding the association of aSyn with membrane lipids and its conformational state, with some studies reporting that membrane-bound aSyn gets protected from aggregation, thus leading to neurotoxicity attenuation (Narayanan and Scarlata 2001; Zhu and Fink 2003; Burre, Sharma et al. 2015), whereas others suggest that interaction of aSyn with membranes triggers its self-association and subsequent aggregation (Cole, Murphy et al. 2002; Lee, Choi et al. 2002; Perni, Galvagnion et al. 2017). Importantly, it has been shown that aSyn PD-related mutations reduce its interaction with membranes, thus further suggesting that aSyn binding on membranes is crucial for its proper functioning (Jensen, Nielsen et al. 1998; Jo, Fuller et al. 2002; Fares, Ait-Bouziad et al. 2014; Ghosh, Sahay et al. 2014; Tsigelny, Sharikov et al. 2015).

A plethora of studies argue that aSyn in its soluble state exists as a monomer (Weinreb, Zhen et al. 1996; Eliezer, Kutluay et al. 2001; Fauvet, Mbefo et al. 2012; Killinger, Melki et al. 2019), whereas others suggest that it occurs physiologically as a tetramer resisting aggregation (Bartels, Choi et al. 2011; Wang, Perovic et al. 2011; Dettmer, Newman et al. 2013). In the presence of lipid membranes, aSyn adopts an alpha helical structure in the N-terminus region that stabilizes the formation of high-order aSyn multimers (Davidson, Jonas et al. 1998; Jo, McLaurin et al. 2000; Eliezer, Kutluay et al. 2001; Burre, Sharma et al. 2014). Interestingly, the membrane curvature seems to affect the structure of aSyn, which can adopt either an elongated or a broken alpha-helix conformation, when bound to a large diameter (~100 nm) or a small, highly curved vesicle, respectively (Chandra, Chen et al. 2003; Jao, Der-Sarkissian et al. 2004; Drescher, Veldhuis et al. 2008; Trexler and Rhoades 2009).

It has been also proposed that aSyn has a role in lipid metabolism, since it participates in fatty acids transportation between the cytosol and membranous compartments (Sharon, Goldberg et al. 2001; Lucke, Gantz et al. 2006) and in lipid and membrane biogenesis organizing and stabilizing the lipid bilayer of membranes and vesicles (Madine, Doig et al. 2006; Adamczyk, Kacprzak et al. 2007). On the other hand, disrupted aSyn expression pattern leads to lipid dysregulation, since both the absence and the overexpression of either wild-type (WT) or mutated aSyn gives rise to

abnormal lipid metabolism (Castagnet, Golovko et al. 2005; Barcelo-Coblijn, Golovko et al. 2007; Ruf, Nubling et al. 2019; Alza, Conde et al. 2021). Finally, several studies have demonstrated that aSyn regulates membrane homeostasis via inhibition of phospholipases activity, such as phospholipase D (Jenco, Rawlingson et al. 1998; Ahn, Rhim et al. 2002; Payton, Perrin et al. 2004; Conde, Alza et al. 2018), however there are controversial results in the literature (Rappley, Gitler et al. 2009).

3c. Dopamine metabolism

Soluble aSyn has been proposed to interact with the dopamine transporter (DAT) and decrease its amount on the plasma membrane, thus regulating the dopamine re-uptake from the synapse and protect neuronal cells from excessive dopamine toxicity (Swant, Goodwin et al. 2011; Butler, Saha et al. 2015). On the other hand, aSyn aggregation triggers DAT recruitment to the plasma membrane that results in massive entry of dopamine and ROS production in neurons (Sidhu, Wersinger et al. 2004). It is obvious that aSyn-mediated modulation of DAT activity is crucial for the proper neuronal functioning via a balanced dopaminergic neurotransmission (**Figure 4**). Moreover, the regulation of dopamine storage is provided by an interaction of aSyn with the vesicular monoamine transporter 2 (VMAT2), which is responsible for the packaging of monoamine transmitters into synaptic vesicles (Danielle Dean E 2008). It has been reported that increased levels of aSyn lead to VMAT2 inhibition and dopamine dysregulation that results in pathological events (Guo, Chen et al. 2008). In addition, aSyn regulates dopamine biosynthesis, via reducing the activity or the phosphorylation status of TH, the rate-limiting enzyme in catecholamine synthesis (Perez, Waymire et al. 2002; Baptista, O'Farrell et al. 2003; Yu, Zuo et al. 2004; Peng, Tehranian et al. 2005; Liu, Jin et al. 2008; Li, Gao et al. 2011). In agreement, enhanced expression or phosphorylation and subsequent aggregation of aSyn alters TH activity and evokes an imbalance in dopamine synthesis (**Figure 4**), thus leading to neurotoxicity (Chu and Kordower 2007; Alerte, Akinfolarin et al. 2008; Lou, Montoya et al. 2010; Wu, Liu et al. 2011). *In vivo* evidence further support the role of aSyn in dopamine metabolism, since the absence of aSyn caused decreased reuptake of dopamine, low levels of tyrosine hydroxylase and DAT in the mouse striatum and reduced number of dopaminergic cells in the substantia nigra of aSyn KO mice (Robertson, Schmidt et al. 2004; Al-Wandi, Ninkina et al. 2010; Chadchankar, Ihalainen et al. 2011).

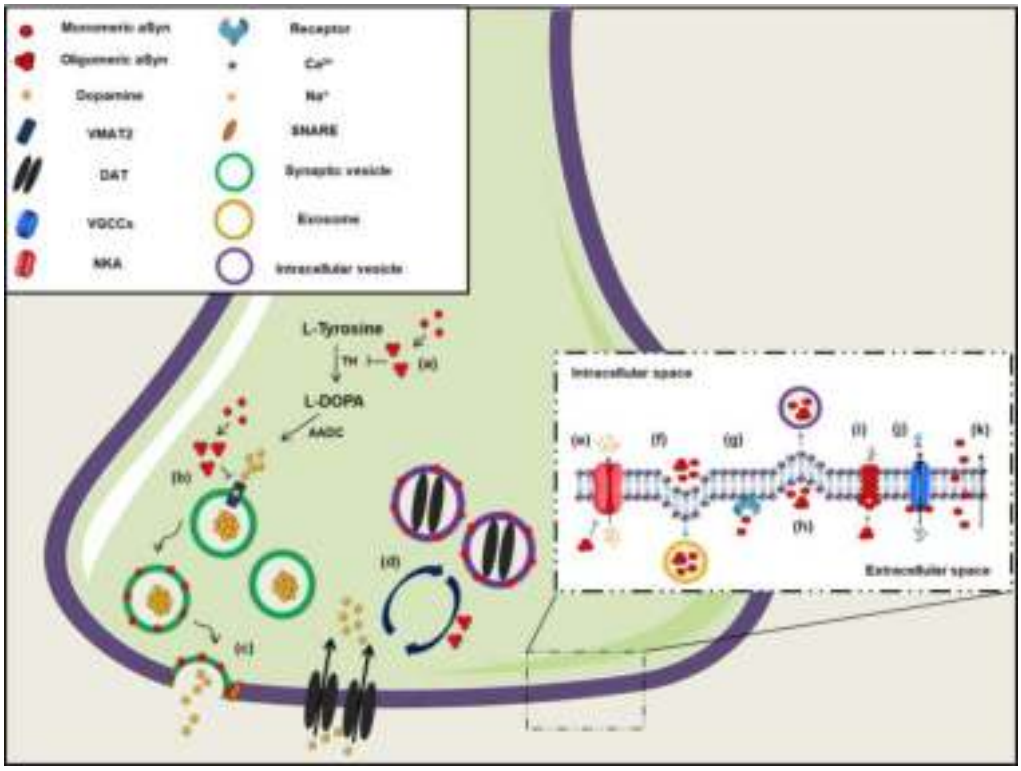

Figure 4: The role of aSyn at the presynaptic terminal.

A schematic representation depicting of aSyn physiological and pathological effects at the synapse: (**a**) aSyn reduces the activity of tyrosine hydroxylase (TH), thus impairing dopamine biosynthesis, (**b**) Increased levels of aSyn inhibit VMAT2, which is responsible for the uptake of monoamines (such as dopamine) into synaptic vesicles, (**c**) aSyn associates with synaptic vesicle membranes and regulates the SNARE-dependent vesicle fusion and neurotransmitter release, (**d**) Soluble aSyn interacts with the dopaminergic transporter DAT and regulates the dopamine re-uptake from the synapse, (**e**) aSyn aggregates interact with Na^+/K^+-ATPase (NKA) preventing the effective pump out of Na^+ ions, (**f**) aSyn is secreted from neuronal cells partly via associating with exosomes, (**g**) Extracellular aSyn interacts with neuronal receptors (i.e. LAG3) for its internalization in neurons or (**h**) it is up-taken via endocytosis, (**i**) PD-linked A30P and A53T mutant aSyn form large membrane pores through which most cations (i.e. Ca^{2+}) can pass non-selectively, (**j**) Extracellular aSyn activates the voltage-gated Ca^{2+} channels (VGCCs), resulting in increased Ca^{2+} influx, (**k**) Monomeric aSyn enters neuronal cells via passive diffusion or direct penetration of their plasma membrane.

4. The role of alpha-synuclein in neuronal pathology

4a. Alpha-synuclein aggregation and post-translational modifications

A central role in the fibril formation and subsequent aggregation of aSyn is thought to be mediated through the NAC region of aSyn, composed of nonpolar side-chains and assembles cross b-structures. Based on that, it has been shown that the deletion of specific residues (74-84) within the core region can abolish aSyn aggregation (Giasson, Murray et al. 2001; Rodriguez, Ivanova et al. 2015). It has been also demonstrated that the endogenous neuronal aSyn and the interaction of

aSyn with lipids plays a central role for aSyn recruitment and subsequent seeding of pathology, as it could behave as a core for the formation of insoluble aggregates (Volpicelli-Daley, Luk et al. 2011; Taguchi, Watanabe et al. 2016; Longhena, Faustini et al. 2017; Killinger, Melki et al. 2019). Apart from point mutations (Narhi, Wood et al. 1999; Pandey, Schmidt et al. 2006; Rutherford, Moore et al. 2014), various post-translational modifications are implicated in aSyn aggregation, the most important of which are phosphorylation, sumoylation, ubiquitination, nitration, N-acetylation, O-GlcNAcylation and truncation.

The phosphorylation of aSyn both at serine and tyrosine residues and particularly at Ser129 is widely considered as an indicator of pathology. However, the effect of Ser129 phosphorylation on aSyn toxicity is still under debate, with the majority of studies suggesting that it accelerates cell toxicity and neurodegeneration (Smith, Margolis et al. 2005; Sugeno, Takeda et al. 2008; Chen, Periquet et al. 2009; Sato, Arawaka et al. 2011; Ma, Hu et al. 2016). On the other hand, many groups have proposed a neuroprotective role of Ser129 phosphorylation since it was reported to drive the conversion of toxic oligomers into less harmful aggregates (Chen and Feany 2005; Azeredo da Silveira, Schneider et al. 2009; Mbefo, Paleologou et al. 2010). Other mechanisms of phosphorylated Ser129 aSyn-mediated neuroprotection include inhibition of its fibrillation (Paleologou, Schmid et al. 2008), upregulation of tyrosine hydrolase (TH) activity (Wu, Liu et al. 2011) or lowering of the protein's membrane-binding affinity (Kuwahara, Tonegawa et al. 2012). Although the 90% of aSyn in LBs is found phosphorylated at Ser129, a significant amount of phosphorylated Ser129 aSyn is also detected in a soluble, rather than in an aggregated state in PD brains (Anderson, Walker et al. 2006). On the contrary, only a small percentage of aSyn is phosphorylated at Ser129 in the brains of healthy controls (Fujiwara, Hasegawa et al. 2002; Sato, Kato et al. 2013; Walker, Lue et al. 2013). In addition, aSyn can be phosphorylated at Ser87, Tyr125, Tyr133 and Tyr136 residues (Paleologou, Oueslati et al. 2010; Xu, Deng et al. 2015; Ganapathy 2017) and these are also implicated in either neurotoxic or neuroprotective events (Chen, Periquet et al. 2009; Paleologou, Oueslati et al. 2010; Lu, Prudent et al. 2011; Fayyad, Erskine et al. 2020).

Moreover, nitrated aSyn is tightly linked to neurodegeneration, as demonstrated by experiments in both cellular and animal models, as well as in patient-derived brains (Giasson, Duda et al. 2000; Danielson, Held et al. 2009; Yu, Xu et al. 2010; McCormack, Mak et al. 2012). It is well-known that aSyn tyrosine nitration is implicated in oxidative damage and disease development (Souza, Peluffo et al. 2008). Four tyrosine residues of aSyn, Tyr39 (within the N-terminus), Tyr125, Tyr133 and Tyr 136 (within the C-terminus) can undergo nitration. Specifically, nitration at Tyr39 has been shown to result in low binding affinity of aSyn on lipid vesicles due to its loss-of-alpha helical conformation status (Hodara, Norris et al. 2004), whereas nitration at Tyr125 seems to play a

crucial role for aSyn dimerization (Takahashi, Yamashita et al. 2002). The linking between two tyrosines has been proposed as a possible mechanism for aSyn oligomer stabilization and its subsequent aggregation into proteinaceous inclusions (10747881). Interestingly, it has been suggested that detection of nitrated aSyn in the human blood serum could potentially serve as a clinical biomarker for PD diagnosis (Fernandez, Garcia-Moreno et al. 2013).

Another post-translational modification of aSyn crucial for its aggregation propensity is ubiquitination, via regulation of the proteasome-dependent protein degradation (Grice and Nathan 2016) and subcellular localization (Pickart and Eddins 2004). Ubiquitinated aSyn has been isolated from LBs and sarkosyl-insoluble fractions derived from synucleinopathy brains (Hasegawa, Fujiwara et al. 2002; Tofaris, Razzaq et al. 2003). C-terminal U-box domain of co-chaperone Hsp70-interacting protein (CHIP), seven in absentia homolog (SIAH) and neuronal precursor cell-expressed, developmentally down-regulated gene 4 (Nedd4) have been identified among the E3 ubiquitin ligases implicated in aSyn ubiquitination (Liani, Eyal et al. 2004; Shin, Klucken et al. 2005; Lee, Wheeler et al. 2008; Rott, Szargel et al. 2008; Kalia, Kalia et al. 2011; Tofaris, Kim et al. 2011). Ubiquitin modification of aSyn has been demonstrated to have differential effects on its accumulation and subsequent aggregation. More precisely, ubiquitination of aSyn at Lys6, Lys12 and Lys21 residues has been shown to moderately inhibit its fibrillation, whereas at Lys10 and Lys23 residues has opposite effects, thus promoting the formation of aSyn inclusions (Meier, Abeywardana et al. 2012). On the other hand, ubiquitination at Lys32, Lys34, Lys43, and Lys96 displays a strong inhibitory effect on aSyn aggregation (Meier, Abeywardana et al. 2012).

Sumoylation is a similar process to ubiquitination, since aSyn is conjugated to small ubiquitin-like modifier (SUMO) at lysine residues. SUMO-1 was found in aSyn-positive inclusions of alpha-synucleinopathy brains or associated with lysosomes of PD animal models (Pountney, Chegini et al. 2005; Weetman, Wong et al. 2013; Wong, Goodwin et al. 2013). It has been also suggested that aSyn sumoylation facilitates its aggregation since it inhibits its degradation (Rott, Szargel et al. 2017). However, controversial studies have proposed a neuroprotective role of aSyn sumoylation, which seems to promote aSyn solubility and thus inhibit its aggregation (Krumova, Meulmeester et al. 2011; Abeywardana and Pratt 2015). Interestingly, another aSyn modification that has been up for debate is its N-terminal acetylation. Although many studies have assigned a neurotoxic role on aSyn N-acetylation, since it has been shown to promote aSyn β-sheet formation and fibrillation (Kang, Moriarty et al. 2012; Iyer, Roeters et al. 2016; Vinueza-Gavilanes, Inigo-Marco et al. 2020), others suggest that either N-acetylated aSyn mediates its physiological binding on synaptic vesicles (Runfola, De Simone et al. 2020), or it acts in a protective manner against aSyn aggregation (Bartels, Kim et al. 2014; Bu, Tong et al. 2017).

O-GlcNAcylation is a biochemical process that involves the attachment of O-linked N-acetylglucosamine to Ser and Thr residues of various proteins, amongst which is aSyn. Murine and human aSyn have been shown to be O-GlcNAcyled in many threonine residues including Thr33, Thr34, Thr54, Thr59, Thr64, Thr72, Thr75, Thr81 and Thr87 (Wang, Park et al. 2009; Wang, Udeshi et al. 2010; Alfaro, Gong et al. 2012; Morris, Knudsen et al. 2015; Wang, Yang et al. 2017). Interestingly, this post-translational modification has repetitively been linked to reduced aSyn aggregation and attenuation of PD-related toxicity (Marotta, Lin et al. 2015; Lewis, Galesic et al. 2017; Zhang, Lei et al. 2017; Levine, Galesic et al. 2019). Finally, aSyn truncation has gained scientific attention, given that C-terminally truncated aSyn has been identified in the inclusions present in PD brains (Baba, Nakajo et al. 1998; Li, West et al. 2005; Kellie, Higgs et al. 2014). Many studies have considered that aSyn truncations have neurotoxic effects due to increased accumulation of misfolded aSyn (Murray, Giasson et al. 2003; Hoyer, Cherny et al. 2004; Tofaris, Garcia Reitbock et al. 2006; Ulusoy, Febbraro et al. 2010; Hall, Yang et al. 2015; Wang, Nguyen et al. 2016; Iyer, Roeters et al. 2017; Ma, Yang et al. 2018; Terada, Suzuki et al. 2018).

4b. Channel formation/Channel interactions

As mentioned above, membrane-bound aSyn adopts an alpha-helical conformation, which facilitates its oligomerization and subsequent aggregation. It has been suggested that aSyn oligomers can form transmembrane channels and pore-like structures that have been linked to pathological events during PD development (Zakharov, Hulleman et al. 2007; Tsigelny, Sharikov et al. 2012; Fantini and Yahi 2013). As a result, vesicles or low-molecular mass molecules may penetrate the cell membrane and in combination with altered cellular ionic homeostasis could potentially lead to cell toxicity and neuronal degeneration (Volles and Lansbury 2002; Quist, Doudevski et al. 2005). Another mechanism for the increased membrane permeability involves the incorporation of aSyn oligomers between the membrane phospholipids, thus leading to the bilayer thinning which thereafter allows the diffusion of small molecules (Stockl, Zijlstra et al. 2013).

A wide range of studies has demonstrated that the ion channels formed by oligomeric aSyn dysregulate cellular ion concentrations and may represent a critical event in the pathogenesis of a-synucleinopathies (Quist, Doudevski et al. 2005). Some PD-linked aSyn mutations, such as E46K and A53T, have been shown to be implicated in the channel formation, whereas other aSyn mutants (i.e. A30P) have displayed low membrane affinity (Zakharov, Hulleman et al. 2007; Di Pasquale, Fantini et al. 2010). However, other groups have shown that A30P and A53T aSyn mutations are responsible for the formation of large membrane pores through which most cations can pass non-selectively (Furukawa, Matsuzaki-Kobayashi et al. 2006). It has been reported that the formation of

such cation-permeable pores could lead either to ion conductivity or to increased calcium (Ca^{2+}) influx and subsequent cell death (Furukawa, Matsuzaki-Kobayashi et al. 2006; Feng, Federoff et al. 2010; Schmidt, Levin et al. 2012; Mironov 2015) (**Figure 4**). Moreover, it is worth-mentioning that upon aSyn cation channel opening, other channels, such as the ATP-dependent potassium channels K (ATP), have been reported to be activated in hippocampal neurons, and this could probably diminish the aSyn-dependent neuronal excitability (Mironov 2015).

Interestingly, it has been shown that aSyn upon binding to plasma membrane aggregates and that this aggregation leads to the redistribution of the α3 subunit of Na^+/K^+-ATPase (NKA). As a result, NKA is no longer able to effectively pump out Na^+ from neurons, thus leading to an intracellular accumulation of Na^+ (Shrivastava, Redeker et al. 2015) (**Figure 4**). Moreover, extracellular aSyn was reported to activate the voltage-gated Ca^{2+} channel Cav2.2 in rat neurons, due to disorganization of lipid rafts in the plasma membrane, resulting in enhanced dopamine release and increased Ca^{2+} influx (Ronzitti, Bucci et al. 2014) (**Figure 4**). Both events may explain the synaptic dysfunction and neuronal vulnerability in PD. Furthermore, it has been proposed that L-type Ca^{2+} channels are implicated in PD development, since administration of L-type Ca^{2+} channel blockers (i.e. isradipine, nimodipine) in animal models and patients with PD, reduced death risk and ameliorated disease manifestations (Chan, Guzman et al. 2007; Ritz, Rhodes et al. 2010; Pasternak, Svanstrom et al. 2012; Singh, Verma et al. 2016). Finally, Liu and his colleagues have proposed that aSyn oligomers inhibit α4β2 Nicotinic Acetylcholine Receptors of Dopaminergic Neurons, thus leading to cholinergic signaling deficits (McGranahan, Patzlaff et al. 2011). In summary, aSyn seems to regulate neuronal toxicity and survival via the formation of channel or pores in the plasma membrane or via its interaction with other channels or receptors crucial for the proper function of neuronal cells.

4c. Interaction of aSyn with mitochondria and ER

Alpha-synuclein displays a remarkable conformational flexibility upon macromolecular interactions and can associate with mitochondrial membranes, thus altering mitochondrial function (Nakamura, Nemani et al. 2011; Robotta, Gerding et al. 2014; Shen, Du et al. 2014). There are reports suggesting that aSyn is a physiological regulator of mitochondrial activity (Ellis, Murphy et al. 2005; Ludtmann, Angelova et al. 2016; Faustini, Marchesan et al. 2019), whereas others support the opposite (Hsu, Sagara et al. 2000; Parihar, Parihar et al. 2008; Hu, Sun et al. 2019). A bidirectional interaction between aSyn aggregation and mitochondrial dysfunction has been implicated in PD pathogenesis. In particular, increased levels of aSyn can lead to mitochondrial

dysfunction (Martin, Pan et al. 2006; Devi, Raghavendran et al. 2008; Bir, Sen et al. 2014; Perfeito, Lazaro et al. 2014; Subramaniam, Vergnes et al. 2014; Di Maio, Barrett et al. 2016), whereas, conversely, impairment of mitochondrial activity may accelerate aSyn pathology (Vila, Vukosavic et al. 2000; Manning-Bog, McCormack et al. 2002; Fornai, Schluter et al. 2005; Radad, Al-Shraim et al. 2019); however the precise underlying mechanisms remain to be elucidated. Both WT and mutant aSyn have been shown to interact with mitochondrial elements, altering both mitochondria morphology and function. Specifically, soluble prefibrillar aSyn oligomers seem to be responsible for complex I dysfunction, loss of membrane potential, disrupted Ca^{2+} homeostasis, enhanced cytochrome c release and ROS production, thus leading to neuronal demise (Devi, Raghavendran et al. 2008; Chinta, Mallajosyula et al. 2010; Loeb, Yakunin et al. 2010; Luth, Stavrovskaya et al. 2014; Paillusson, Gomez-Suaga et al. 2017).

In agreement, experiments in various animal models of a-synucleinopathy have revealed mitochondrial abnormalities, DNA damage, and neuronal degeneration in PD-affected brain regions (Poon, Frasier et al. 2005; Martin, Pan et al. 2006; Chen, Xie et al. 2015). Moreover, *in vitro* and *in vivo* experiments have shown that aSyn inhibits mitochondrial fusion and triggers mitochondrial fragmentation (Kamp, Exner et al. 2010; Nakamura, Nemani et al. 2011). Di Maio and colleagues have proposed that certain post-translationally modified aSyn conformations (soluble oligomers, dopamine-modified, and S129E phosphorylation mimic) lead to impaired mitochondrial function via binding to TOM20 (translocase of the outer membrane receptor) and inhibiting mitochondrial protein import (Di Maio, Barrett et al. 2016) (**Figure 5**).

Nonetheless, there is evidence suggesting an impairment of mitochondrial function upstream of aSyn pathology. Experiments using the pesticides rotenone and paraquat have shown that dysregulation of mitochondrial function leads to nigro-striatal dopaminergic loss and formation of Lewy Body-like inclusions, positively stained with anti-aSyn antibodies and thioflavine S, thus resembling PD features (Betarbet, Sherer et al. 2000; Manning-Bog, McCormack et al. 2002; Nistico, Mehdawy et al. 2011; Tieu 2011; Radad, Al-Shraim et al. 2019). Similarly, incubation of WT aSyn-overexpressing COS-7 cells with mitochondrial inhibitors resulted in the disappearance of the aSyn aggregates formed upon rotenone or oligomycin treatment (Lee, Shin et al. 2002). Interestingly, a plethora of studies utilize the mitochondrial neurotoxin MPTP to induce PD-like pathology in animals, further suggesting that mitochondria impairment is a key player in disease development (Kowall, Hantraye et al. 2000; Vila, Vukosavic et al. 2000; Przedborski, Chen et al. 2001; Fornai, Schluter et al. 2005; Bazzu, Calia et al. 2010; Lee, Oh et al. 2017; Hu, Hu et al. 2020). Genetic studies further support the hypothesis of aSyn accumulation as a secondary event following mitochondrial malfunction. Specifically, mutations in *ATP13A2*, encoding for a lysosomal type 5 P-type ATPase, were shown to result in dysregulation in mitochondrial

depolarization and ATP metabolism leading to mitochondrial fragmentation and subsequent cell death (Grunewald, Arns et al. 2012; Park, Koentjoro et al. 2014).

Apart from its implication in mitochondrial failure, aSyn has been also reported to play a biological role in the association of mitochondria with the endoplasmic reticulum (ER) Ca^{2+} homeostasis. It has been demonstrated that aSyn favors the Ca^{2+} transfer from ER to mitochondria, as a result of the communication the two organelles, probably due to the fact that aSyn can act as a "bridge" via its C terminus (Cali, Ottolini et al. 2012). Later studies further supported the physiological localization of aSyn in mitochondria-associated ER membranes (MAM), stabilizing their interaction, which was perturbed upon aSyn aggregation and its subsequent redistribution (Guardia-Laguarta, Area-Gomez et al. 2014; Guardia-Laguarta, Area-Gomez et al. 2015). Interestingly, the familial PD-linked A53T and A30P aSyn point mutations resulted in their weakened interaction with MAM, which affected MAM function and mitochondrial integrity (Guardia-Laguarta, Area-Gomez et al. 2014).

The association of aSyn with mitochondria was further corroborated by findings indicating interactions between both monomeric and oligomeric aSyn with the Ca^{2+} transporting voltage-dependent anion channel 1 (VDAC1) (Lu, Zhang et al. 2013; Rostovtseva, Gurnev et al. 2015; Hoogerheide, Gurnev et al. 2017; Jacobs, Hoogerheide et al. 2019) (**Figure 5**). Importantly, VDAC1 has been detected on the MAM of ER mediating the communication between the two organelles, regulating Ca^{2+} homeostasis (Shoshan-Barmatz, Zalk et al. 2004; Shoshan-Barmatz and Israelson 2005; De Stefani, Bononi et al. 2012). Moreover, VDAC levels have been found decreased in the nigral neurons of PD brains, where pathological aSyn inclusions had been formed (Chu, Goldman et al. 2014). Additionally, VDAC has been proposed to be a component of the mitochondrial permeability transition pore (PTP), the opening of which has been shown to be affected by aSyn overexpression and oligomerization (Shen, Du et al. 2014; Ludtmann, Angelova et al. 2018). In vivo experiments on transgenic mice overexpressing the human A53T aSyn further supported the role of PTP activity modulation on the mitochondrial dysfunction during PD pathogenesis (Martin, Semenkow et al. 2014).

4d. Unfolded protein response, regulation of ER/Golgi trafficking and Ca^{2+} homeostasis

The ER is a continuous membrane system mainly responsible for the production and processing of lipids and proteins, as well as Ca^{2+} homeostasis. In case of impaired protein folding (ER stress), cells activate a group of signal transduction pathways, known as the unfolded protein response (UPR). It has been previously shown that aSyn overexpression in PD patients leads to

UPR and contributes to the molecular pathogenesis of the disease (Heman-Ackah, Manzano et al. 2017). The ER chaperone glucose regulated protein 78 (GRP78/BIP) has a crucial role on ER stress regulation due to its ability to control the activation of transmembrane ER stress sensors (IRE1, PERK, and ATF6) (Lee 2005). Disassociation of GRP78 from IRE1 and PERK results in stress signaling finally leading to altered ER homeostasis (Wang, Wey et al. 2009). Alpha-synuclein associates with GRP78/BIP under physiological or pathological conditions, thus inducing UPR and leading to dopaminergic cell death (Bellucci, Navarria et al. 2011; Betzer, Movius et al. 2015). Interestingly, Ser129 phosphorylated and aggregated aSyn was found in ER microsomes of A53T transgenic mice and more importantly, administration of the UPR inhibitor salubrinal, effectively attenuated disease manifestations in this PD-mouse model (Colla, Coune et al. 2012; Colla, Jensen et al. 2012). It is worth mentioning that GRP78/BiP levels were found elevated in DLB and PD patient-derived brains in an aSyn burden-dependent manner (Baek, Whitfield et al. 2016). In addition, the protein levels of various ER chaperones were found elevated in a-synucleinopathy models, co-localized with aSyn positive inclusions, suggesting that aggregated aSyn could potentially be implicated in UPR regulation in disease progression (Koch, Smith et al. 1986; Lee 1992; Conn, Gao et al. 2004; Jin, Li et al. 2007; Honjo, Ito et al. 2011; Colla, Coune et al. 2012; Yagi-Utsumi, Satoh et al. 2015; Labrador-Garrido, Cejudo-Guillen et al. 2016).

Proteins synthesized in the ER, are packaged into vesicles and directed to Golgi apparatus for subsequent modifications. One of the first pathological roles attributed to aSyn is the blockade of the vesicular transport from ER to Golgi by antagonizing ER/Golgi SNAREs (Cooper, Gitler et al. 2006; Gitler, Bevis et al. 2008; Thayanidhi, Helm et al. 2010). Towards the same direction, aSyn can also disrupt the intra-Golgi and post-Golgi secretory trafficking, via an abnormal interaction with several Rab-family proteins of the intracellular endocytic pathway (Dalfo, Gomez-Isla et al. 2004; Cooper, Gitler et al. 2006; Gitler, Bevis et al. 2008; Yin, Lopes da Fonseca et al. 2014; Breda, Nugent et al. 2015). In addition, aSyn can also impair the ionic transport and membrane trafficking, resulting in Golgi fragmentation and subsequent cytotoxicity (Gosavi, Lee et al. 2002; Fujita, Ohama et al. 2006; Lee, Khoshaghideh et al. 2006).

Another significant role of aSyn on ER and Golgi function is the regulation of Ca^{2+} homeostasis via its binding on specific channels or pumps localized in these organelles. Specifically, proximity ligation assay (PLA) experiments demonstrated that soluble and insoluble aSyn aggregates, but not monomers, interact with the ER Ca^{2+}-ATPase SERCA, resulting in decreased cytosolic Ca^{2+} that disrupts the physiological cell function and leads to neuronal cell death (Betzer, Lassen et al. 2018) (**Figure 5**). Moreover, administration of the SERCA inhibitor cyclopiazonic acid restored cytosolic Ca^{2+} levels and protected neurons against the aggregated aSyn-dependent cell death (Betzer, Lassen et al. 2018). In agreement to these results, aggregated

aSyn bound on SERCA pump was detected in LBs and GCIs of PD and MSA brains, respectively (Betzer, Lassen et al. 2018). Moreover, PMR1, a Ca^{2+}-transporting ATPase 1 pump regulating the levels of Ca^{2+} and Mn^{+2} ions in the Golgi (Wuytack, Raeymaekers et al. 2003), has been proposed to be a mediator of aSyn-dependent cytotoxicity (**Figure 5**). Specifically, in various PD models (yeast, flies, and nematodes), PMR1 pump has been linked to aSyn pathology via a Ca^{2+}-dependent mechanism, where aSyn accumulation elevated cytosolic Ca^{2+} levels and increased cell death. Interestingly, upon PMR1 deletion, the disease-associated characteristics were abolished, further suggesting the relevance of this pump to aSyn pathology (Buttner, Faes et al. 2013; Nikoletopoulou and Tavernarakis 2018).

4e. Aplha-synuclein in the nucleus

The name aSyn was given to the protein due to its localization in the nucleus and presynatic nerve terminals (Maroteaux, Campanelli et al. 1988). Nuclear aSyn was detected in neurons of various brain regions of rodents and was reported to interact with histones, underlying PD pathology (Mori, Tanji et al. 2002; Goers, Manning-Bog et al. 2003; Yu, Li et al. 2007), even though a single study declares that the nuclear staining of aSyn is attributed to the non-specific signal of some antibodies that probably recognize unknown antigens in neuronal nuclei (Huang, Xu et al. 2011). It has been proposed that aSyn is responsible for epigenetic dysregulation via inhibition of histone acetylation or reduced DNA methylation, thus favoring neuronal degeneration, whereas others suggest that nuclear aSyn regulates cell cycle rate exhibiting cell toxicity (Kontopoulos, Parvin et al. 2006; Desplats, Spencer et al. 2011; Ma, Song et al. 2014) (**Figure 5**). Importantly, histone deacetylase (HDAC) inhibitors attenuated aSyn toxicity and provided neuroprotection in both cell culture and transgenic Drosophila models (Kontopoulos, Parvin et al. 2006; Outeiro, Kontopoulos et al. 2007).

Experiments in SH-SY5Y cells revealed that nuclear translocation of aSyn is regulated by calreticulin and Ca^{2+}, following treatment with retinoic acid and modulates the expression of PD-linked genes such as *ATP13A2* (ATPase cation transporting 13A2) and *PINK1* (PTEN-induced kinase1) (Davidi, Schechter et al. 2020). Interestingly, phosphorylated aSyn at Ser129 was found accumulated in the nucleus of HEK293E-aSyn overexpressing cells and in various brain regions of transgenic (Thy1)-[A30P] aSyn mice (Schell, Hasegawa et al. 2009). Further experiments in H4 cells expressing various aSyn proteins verified that nuclear localization of aSyn depends on its phosphorylation at Ser129 (Pinho, Paiva et al. 2019). The same group supported a role of DNA-binding and gene expression regulation for aSyn providing an insight into the role of modified aSyn

in the nucleus (Pinho, Paiva et al. 2019). Interestingly, other post-translational modifications of aSyn, such as sumoylation, seem to be responsible for the translocation of aSyn from the cytoplasm to the nucleus (Seungjin Ryu 2018). Although the majority of studies support a neurotoxic role for aSyn nuclear localization, some groups proposed that aSyn in the nucleus displays a protective role against DNA damaging, replication stress or impaired nucleocytoplasmic transport (Liu, Lee et al. 2011; Schaser, Osterberg et al. 2019; Chen, Moncalvo et al. 2020).

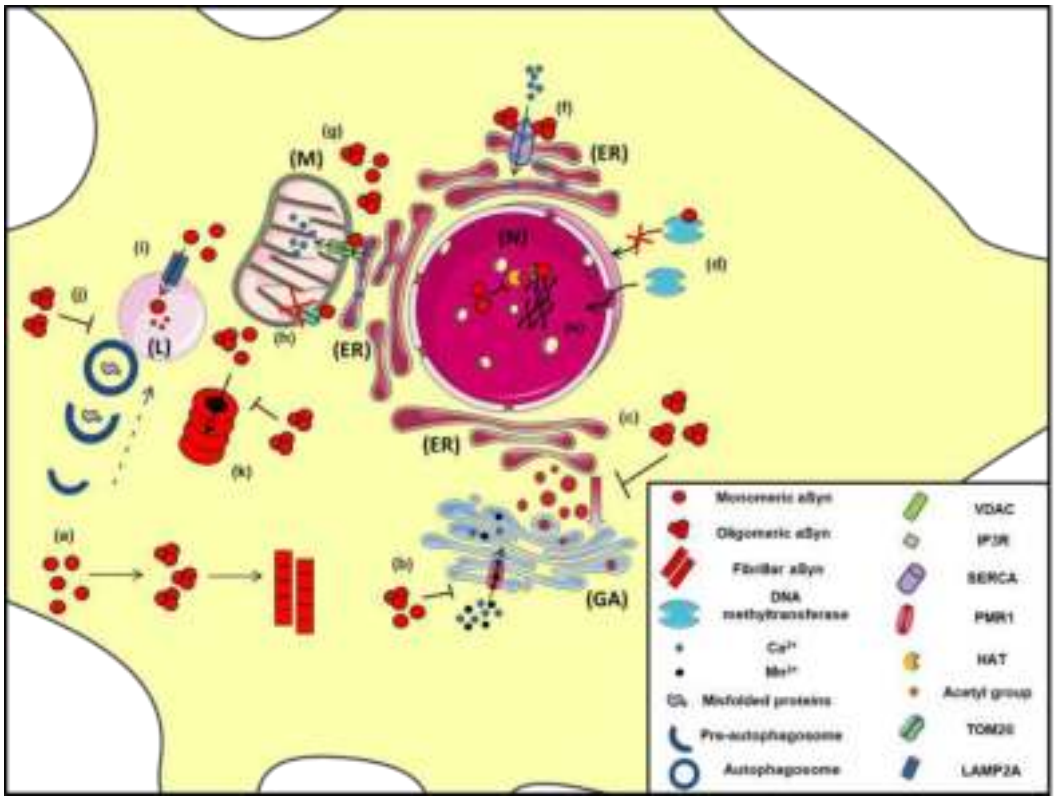

Figure 5: The proposed intracellular effects of various aSyn conformations in neurons.

(**a**) In the cytoplasm of neurons, aSyn monomers form oligomers that can eventually become fibrils, (**b**) Both unfolded and aggregated aSyn impair the function of PMR1 in the Golgi apparatus (GA), resulting in elevated cytosolic Ca^{2+} levels, (**c**) Both WT and mutant A53T aSyn disrupt the vesicular transport from Endoplasmic Reticulum (ER) to Golgi (GA), (**d**) WT aSyn inhibits the transportation of methyltransferases from the cytoplasm to the nucleus (N), (**e**) Inside the nucleus (N), aSyn inhibits histone acetylation, thus interfering in the process of gene transcription, (**f**) In the ER, aSyn aggregates activate the Ca^{2+}-ATPase SERCA, resulting in dysregulated Ca^{2+} homeostasis, (**g**) Both monomeric and oligomeric aSyn interact with Voltage-dependent anion channel 1 (VDAC1) and inositol triphosphate receptors (IP3Rs) and regulates the transmission of Ca^{2+} signals from the ER to mitochondria (M), (**h**) aSyn binds to TOM20, a mitochondrial import receptor subunit, and inhibits normal protein import, (**i**) Normally, monomeric or dimeric forms of aSyn are degraded in the lysosome (L) via Chaperone-Mediated Autophagy (CMA), following their interaction with LAMP2A. However, under pathological conditions, impairment of CMA has been proposed to lead to aSyn accumulation and subsequent cell toxicity, (**j**) Oligomeric aSyn and various misfolded proteins are cleared via macroautophagy, however pathological aSyn has been shown to impair autophagic flux, (**k**) Monomeric and oligomeric aSyn are degraded via the proteasome, however under pathological conditions, increased levels of aSyn or even soluble aSyn oligomers may inhibit proteasomal function, leading to aSyn accumulation and the formation of insoluble aggregates.

4f. Alpha-synuclein in the extracellular space

The first indication that aSyn can be secreted arose from the detection of the protein in human CSF and plasma of PD patients, indicating that aSyn can be released into the extracellular space (Borghi, Marchese et al. 2000; El-Agnaf, Salem et al. 2003), and can exert various deleterious effects on neighboring cells. Further studies supported that aSyn can be secreted from neuronal cells, either via vesicles or exosomes (Lee, Patel et al. 2005; Emmanouilidou, Melachroinou et al. 2010; Danzer, Kranich et al. 2012). Extracellular aSyn has been the subject of intensive research in recent years, mainly due to its propensity to spread from neuron to neuron or other glial cells, as discussed in the following sections. The major hypothesis regarding the onset and spread of aSyn pathology in PD and related synucleinopathies relies in the protein's nucleation propensity that leads to the formation of aberrant aSyn species which then spread to neighboring cells and tissues via various mechanisms.

Furthermore, aSyn has been proposed to act as a "prion-like" protein since it was demonstrated that pathogenic aSyn could transfer from diseased neurons of a PD patient to the healthy transplanted ones, fourteen years after the surgical intervention (Kordower, Chu et al. 2008). Similar results were obtained by other groups in both humans and rats (Li, Englund et al. 2008; Li, Englund et al. 2010; Kordower, Dodiya et al. 2011; Kurowska, Englund et al. 2011). Experiments of PD and DLB patient-derived brain extracts delivered into the brain of mice and non-human primates further validated the transfer of pathological aSyn and the formation of aSyn aggregates within the recipient neurons (Masuda-Suzukake, Nonaka et al. 2013; Recasens, Dehay et al. 2014). Moreover, when Pre-Formed Fibrils (PFFs) were used as seeds in both in vitro and in vivo experiments, the endogenous neuronal aSyn was recruited into the formation of highly insoluble aggregates (Luk, Song et al. 2009; Volpicelli-Daley, Luk et al. 2011; Luk, Kehm et al. 2012; Sacino, Brooks et al. 2014; Paumier, Luk et al. 2015; Abdelmotilib, Maltbie et al. 2017).

Various mechanisms have been proposed for aSyn spread throughout the nervous system, following its release from neurons where it is normally expressed (**Figure 6**). The most important of them include aSyn secretion via vesicles, exosomes or even naked protein (El-Agnaf, Salem et al. 2003; Lee, Patel et al. 2005; El-Agnaf, Salem et al. 2006; Emmanouilidou, Melachroinou et al. 2010; Delenclos, Trendafilova et al. 2017; Fussi, Hollerhage et al. 2018; Gustafsson, Loov et al. 2018), and its uptake from the cells via conventional endocytosis (Sung, Kim et al. 2001; Lee, Suk et al. 2008), passive diffusion (Ahn, Paik et al. 2006), tunneling nanotubes (Abounit, Bousset et al. 2016), membrane penetration (Kayed, Sokolov et al. 2004; Jao, Hegde et al. 2008; Tsigelny, Sharikov et al. 2012) or receptor-mediated internalization (Shrivastava, Redeker et al. 2015; Mao, Ou et al. 2016; Ihse, Yamakado et al. 2017). Once taken-up by recipient cells, the exogenous aSyn has been shown to trigger the endogenous aSyn accumulation via an unknown mechanism (Rey,

Steiner et al. 2016; Karampetsou, Ardah et al. 2017; Karpowicz, Haney et al. 2017; Luna, Decker et al. 2018). However, according to the prevailing hypothesis, upon the cell-internalization of aberrant aSyn conformation (oligomers or fibrils), these serve as a template for the recruitment of the endogenous monomeric aSyn into the formation of insoluble aggregates (Luk, Song et al. 2009; Luk, Kehm et al. 2012; Masuda-Suzukake, Nonaka et al. 2013; Sacino, Brooks et al. 2014; Sacino, Brooks et al. 2014; Volpicelli-Daley, Luk et al. 2014; Wu, Takano et al. 2019). The prevalently unfolded or alpha-helical aSyn is triggered to self-assemble generating fibrils that subsequently deposit as Lewy bodies (Wood, Wypych et al. 1999; Uversky, Li et al. 2001; Chu and Kordower 2015).

Neuron-to-neuron aSyn transmission occurs following both anterograde and retrograde axonal transport or trans-synaptic pathways (Freundt, Maynard et al. 2012; Masuda-Suzukake, Nonaka et al. 2014; Mezias, Rey et al. 2020). Several groups have proposed that dysregulation of axonal transport is implicated in aSyn accumulation at the cell body; however it is not clear whether PD-linked aSyn mutations play a key role in the process per se (Li, Hoffman et al. 2004; Saha, Hill et al. 2004; Lee 2007; Freundt, Maynard et al. 2012; Tang, Das et al. 2012). Notably, aSyn in its oligomeric form has been shown to interfere with microtubules and kinesin motors, thus disrupting the anterograde transport and similar results were obtained in an aSyn overexpressing mouse model for PD, as well as in patients diagnosed with the disease (Chung, Koprich et al. 2009; Chu, Morfini et al. 2012; Prots, Veber et al. 2013). Interestingly, it has been suggested that the variety in a-synucleinopathy phenotypes is attributed to the formation of different aSyn "strains" that display "aggressive" characteristics (Bousset, Pieri et al. 2013; Peng, Gathagan et al. 2018; Holec and Woerman 2020). As a consequence of their disparate structures, these "strains" have discrete biochemical responses along the different brain regions and cell types, thus explaining the various disease manifestations of a-synucleinopathies (Peelaerts, Bousset et al. 2015; Ma, Hu et al. 2016; Candelise, Schmitz et al. 2019; Rey, Bousset et al. 2019; Lau, So et al. 2020; Shahnawaz, Mukherjee et al. 2020).

5. Alpha-synuclein accumulation in oligodendrocytes, propagation and spread of pathology

The origin of aSyn detected in oligodendroglial GCIs still remains enigmatic and there are controversial studies in the literature suggesting either the internalization of neuronally-secreted aSyn by oligodendrocytes or an enhanced expression and decreased degradation of oligodendroglial aSyn (Wakabayashi and Takahashi 2006; Rockenstein, Ubhi et al. 2012; Schwarz, Goldbaum et al. 2012; Asi, Simpson et al. 2014; Reyes, Rey et al. 2014; Djelloul, Holmqvist et al. 2015; Yoon, Ahn et al. 2021). The release of aSyn by neuronal cells, partially bound on vesicles or exosomes is well-

documented (Lee, Patel et al. 2005; Emmanouilidou, Melachroinou et al. 2010; Hansen, Angot et al. 2011; Gustafsson, Loov et al. 2018; Yamada and Iwatsubo 2018) and some studies propose that oligodendrocytes can take-up the neuronally-derived aSyn via dynamin GTPase-, clathrin- and dynasore-dependent mechanisms (Kisos, Pukass et al. 2012; Konno, Hasegawa et al. 2012; Pukass and Richter-Landsberg 2014; Reyes, Rey et al. 2014). The neuron-oligodendrocyte communication can also be mediated via exosomes (Fruhbeis, Frohlich et al. 2013), which are characterized as "Trojan horses" of neurodegeneration (Ghidoni, Benussi et al. 2008) and they could serve as transporters of pathological disease-related proteins, such as aSyn. Moreover, ectopic expression of the endocytosis regulatory proteins Rab5 and Rabaptin-5 in oligodendrocytes of MSA brains may account for the elevated levels of aSyn within oligodendrocytes, probably via enhanced endocytic activity (Nakamura, Kawamoto et al. 2000).

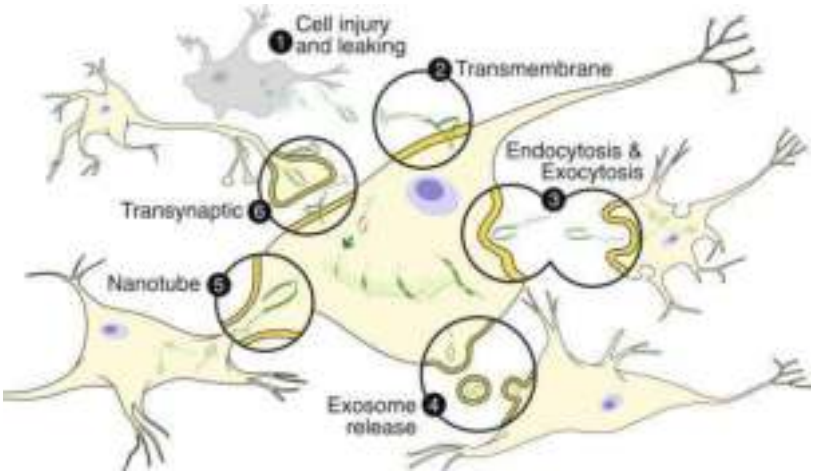

Figure 6: Proposed mechanisms of a-synuclein neuronal transmission.
Alpha synuclein propagates from neurons to neurons via (**1**) leakage from damaged cells, (**2**) membrane penetration, (**3**) conventional exocytosis and endocytosis, (**4**) exosomal binding, (**5**) tunneling nanotubes or (**6**) direct synaptic contact. Source: (Visanji, Brooks et al. 2013).

In vitro and *in vivo* experiments revealed the ability of oligodendrocytes to take up exogenously added recombinant or neuronally-derived aSyn and incorporate it into intracellular GCI-like aggregates (Kisos, Pukass et al. 2012; Konno, Hasegawa et al. 2012; Rockenstein, Ubhi et al. 2012; Pukass and Richter-Landsberg 2014; Reyes, Rey et al. 2014). In a recently published study, mature human oligodendrocytes generated from neural stem cells had the ability to internalize neuronally-derived aSyn and form proteinaceous inclusions, thus further supporting the existing theory for the origin of MSA-related aSyn. Strikingly, it has been shown that once neuronal aSyn is taken up by oligodendrocytes, it accumulates and gains GCI-like characteristics rather determined by the oligodendroglial milieu (Peng, Gathagan et al. 2018). Interestingly, it has been

proposed that aSyn fibrils detected in PD and MSA brains are structurally and biochemically distinct, giving rise to the "strain hypothesis", according to which the generation of the different aSyn conformations present in PD and MSA brains is attributed to events within the environment of different cell types, such as oligodendrocytes and neurons (Bousset, Pieri et al. 2013; Peng, Gathagan et al. 2018; Candelise, Schmitz et al. 2019; Lau, So et al. 2020; Shahnawaz, Mukherjee et al. 2020). Moreover, it has been suggested that the pathological phosphorylation of aSyn at Ser129 is involved in the formation of different aSyn strains present in synucleinopathies (Ma, Hu et al. 2016).

Over the last years, the prion hypothesis has gained a lot of attention regarding the spread of pathological aSyn in the context of both PD and MSA. Specifically, it has been reported that inoculation of transgenic mice overexpressing human A53T aSyn with MSA brain homogenates resulted in CNS dysfunction, whereas, strikingly, the PD brain-derived material did not evoke similar effects (Watts, Giles et al. 2013; Prusiner, Woerman et al. 2015; Woerman, Oehler et al. 2019). Similarly, intrastriatal injections of MSA homogenates in the brains of Tg(SNCA)1Nbm/J mice (knockout for mouse aSyn and overexpressing the human protein) resulted in the detection of hyperphosphosrylated aSyn-positive inclusions in various brain regions (Bernis, Babila et al. 2015). Finally, treatment of HEK293T cells stably expressing fluorescently-tagged aSyn with healthy, PD or MSA brain-derived extracts highlighted that only the MSA-added material was capable of inducing aSyn aggregation (Woerman, Stohr et al. 2015).

There are other possible scenarios that have been proposed to explain aSyn seeding and propagation in MSA brains, based on oligodendrocyte-to-oligodendrocyte communications. Specifically, it is possible that aSyn is taken up by oligodendroglial progenitor cells prior to their maturation, probably impairing the myelination process (Kaji, Maki et al. 2020). Furthermore, another potential mechanism includes aSyn transfer between oligodendrocytes or between oligodendrocytes and other glial cells via tunneling nanotubes or extracellular vesicles (Danzer, Kranich et al. 2012; Abounit, Bousset et al. 2016; Valdinocci, Grant et al. 2018; Guo, Wang et al. 2020). Finally, another scenario suggests that, in MSA pathology, oligodendrocytes adopt unknown cellular uptake mechanisms for aSyn internalization and subsequent propagation (Kaji, Maki et al. 2020); however the precise mechanisms underlying aSyn transfer to oligodendrocytes still remains unknown. The gap junction protein connexin-32 (Cx32) has been also implicated in the uptake of oligomeric aSyn by both neurons and oligodendrocytes (Reyes, Sackmann et al. 2019) and Cx32protein levels were found elevated in animal PD and MSA models, thus suggesting an interaction between Cx32 expression and aSyn cellular uptake (Reyes, Sackmann et al. 2019).

It is interesting to note that oligodendroglial and neuronal aSyn accumulation has been reported to occur in different time points and in particular that aSyn aggregation requires several

months to progress within oligodendrocytes, upon synthetic haSyn-PFFs delivery into the brain of WT mice (Uemura, Uemura et al. 2019). Moreover, *in vitro* aSyn overexpression in oligodendrocytes resulted in delayed maturation of oligodendrocyte progenitor cells and impaired myelin-gene expression and myelination deficits (Ettle, Reiprich et al. 2014; May, Ettle et al. 2014; Ettle, Kerman et al. 2016), whereas in another study aSyn-positive inclusions were mainly detected in BCAS1-expressing (breast carcinoma amplified sequence 1) immature oligodendrocytes of MSA brains (Kaji, Maki et al. 2020). The above observations insinuate that the oligodendroglial maturation and aSyn-aggregate formation are closely linked and may provide information regarding pathogenic events in MSA (**Figure 7**). Several *in vitro* studies have proposed that aSyn aggregation is stimulated by heparin and heparan sulfate (Cohlberg, Li et al. 2002; Ihse, Yamakado et al. 2017; Maiza, Chantepie et al. 2018), linear polysaccharides (glycosaminoglycans) found on the cell membrane and in the extracellular matrix (Iozzo 1998; Medeiros, Mendes et al. 2000). Heparan sulfate has been suggested to mediate aSyn fibril uptake by oligodendrocytes via binding to the plasma membrane (Holmes, DeVos et al. 2013; Ihse, Yamakado et al. 2017), whereas others have proposed that heparin and heparan sulfate proteoglycans (HSPGs) are responsible for aSyn fibrillation (Cohlberg, Li et al. 2002; Lehri-Boufala, Ouidja et al. 2015; Maiza, Chantepie et al. 2018; Hudak, Kusz et al. 2019; Skaanning, Santoro et al. 2020).

Apart from aSyn toxicity *per se*, the overexpression of aSyn in oligodendrocytes can lead to oligodendroglial cell death and subsequent neuronal loss via a plethora of mechanisms. Specifically, aSyn-overexpressing oligodendrocytes are more susceptible to oxidative stress and various cytokine actions (Stefanova, Klimaschewski et al. 2001; Stefanova, Schanda et al. 2003), or display impaired adhesion properties (Tsuboi, Grzesiak et al. 2005). Furthermore, it has been reported that animal MSA models exhibit myelin loss and impaired mitochondrial function, accompanied by severe neurodegeneration in various brain regions (Shults, Rockenstein et al. 2005; Stefanova, Reindl et al. 2005; Yazawa, Giasson et al. 2005; Stefanova, Reindl et al. 2007; Stemberger, Poewe et al. 2010; Kuzdas, Stemberger et al. 2013).

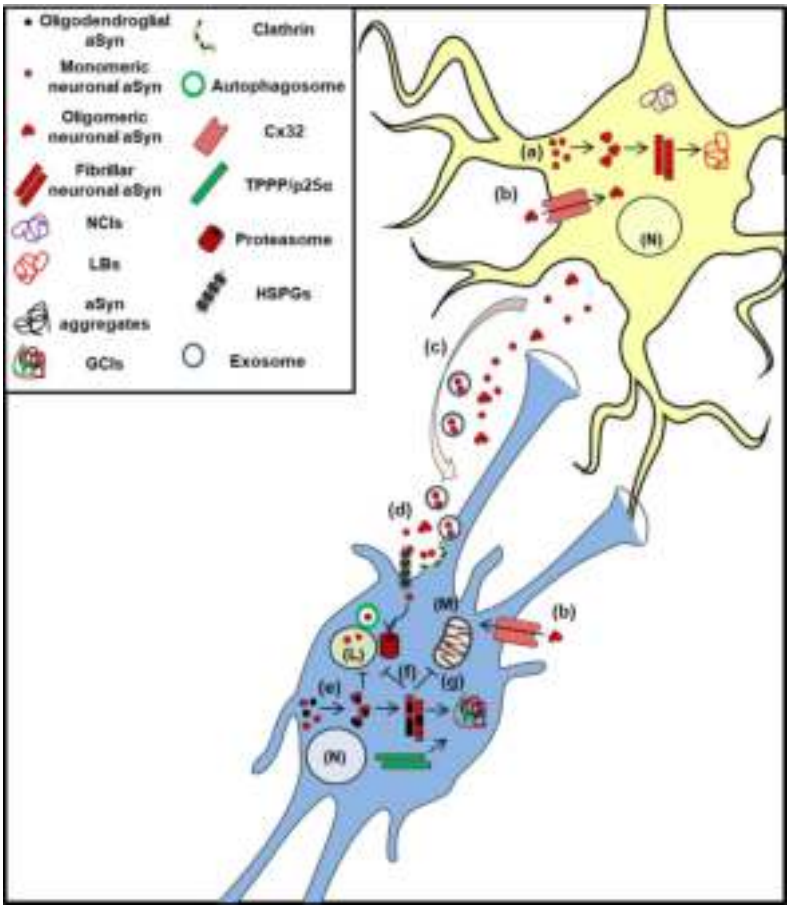

Figure 7: Alpha synuclein in oligodendrocyte-neuron interplay.

(**a**) Neuronal aSyn accumulates to form fibrils that finally deposit in Lewy Bodies (LBs, red) in PD and DLB. Neuronal Cytoplasmic Inclusions (NCIs, purple), composed of aSyn, are also present within neuronal cells in MSA, (**b**) Oligomeric aSyn enters neuronal (yellow) or oligodendroglial (blue) cells via binding to the gap junction protein connexin-32 (Cx32), (**c**) Neurons secrete either free or exosome-bound aSyn which is then transmitted to neighboring cells, such as oligodendrocytes, (**d**) Neuronally-derived aSyn enters oligodendrocytes by clathrin-mediated endocytosis, exosomal transportation, or via binding to Heparan Sulfate ProteoGlycans (HSPGs), (**e**) Inside oligodendrocytes, neuronal aSyn (red) initiates the seeding of the endogenous oligodendroglial aSyn (black) and together with the oligodendroglial-specific TPPP/p25α protein, they lead to the formation of GCIs, (**f**) aSyn aggregates impair the proteolytic machineries of oligodendrocytes [(proteasome and lysosome (**L**)], (**g**) Misfolded aSyn leads to mitochondrial (**M**) dysfunction and subsequent cell toxicity in MSA.

6. Tubulin Polymerization Promoting Protein TPPP/p25α

Beyond aSyn protein, GCIs are rich with the oligodendroglial phosphoprotein TPPP/p25α (or p25α), a brain-specific protein of about 25 kDa, member of the p25 gene family, which is well conserved in vertebrates (Ovadi and Orosz 2009). In humans there are 3 family members: p25α, p25β and p25γ, encoding the respective p25 proteins with 219, 170, and 176 amino acids each. It is an intrinsically disordered protein without a well-defined 3D structure (Orosz, Kovacs et al. 2004;

Zotter, Bodor et al. 2011), however, NMR studies have shown that there are unfolded regions in both the N-terminus (45 amino acids) and at the C-terminus (44 amino acids) surrounding a flexible core (130 amino acids) mainly consisting of 5 α-helixes (DeBonis, Neumann et al. 2015)(http://www.pdb.org/pdb/explore/explore.do?structureId=2JRF). In the healthy brain, p25α is expressed specifically in oligodendrocytes. It has been characterized as a "moonlight protein" due to its ability to perform more than one function inside the cell, as a result of its stereochemical modulation (Olah, Lehotzky et al. 2020). The functions of "moonlight proteins" differ depending on their subcellular localization, cell type expression, oligomeric stage, intracellular interactions with various ligands, etc. As a result, the physiological and pathological role of p25α is not yet well-understood; however there are reports suggesting that its main function is to stabilize the microtubule network (Lehotzky, Tirian et al. 2004).

In addition, p25α regulates microtubules acetylation via its direct association with tubulin deacetylases, such as the histone deacetylase 6 (HDAC6) and NAD^+-dependent deacetylase, sirtuin-2 (SIRT2) (Mangas-Sanjuan, Olah et al. 2015). p25α has been shown to inhibit HDAC6, leading to alterations in the tubulin-HDAC6-p25α complex (Mangas-Sanjuan, Olah et al. 2015). p25α binding to HDAC6 and/or SIRT2 leads to increased tubulin acetylation, thus affecting microtubule stability (Mangas-Sanjuan, Olah et al. 2015). Moreover, under physiological conditions p25α has been proposed to mediate the myelination process and to colocalize with the myelin basic protein (MBP) (Takahashi, Tomizawa et al. 1993; Otzen, Lundvig et al. 2005; Skjoerringe, Lundvig et al. 2006). Recently, p25α has been attributed a role for microtubule nucleation and elongation of the myelin sheath in Golgi outposts (Fu, McAlear et al. 2019).

Similar to aSyn, p25α undergoes post-translational modifications, such as phosphorylation by ERK2 and Cdk 5 (at residues Thr14, Ser18 and Ser160) which inhibits the p25α-depended polymerization of microtubules (Hlavanda, Klement et al. 2007). Furthermore, its phosphorylation by LIM kinase 1 reduces the polymerization potential of the protein (Acevedo, Li et al. 2007), whereas phosphorylation by Rho-associated protein kinase (Rho-associated coiled-coil kinase, ROCK) at residues Ser32, Ser107 and Ser159, does not affect the polymerization function, but inhibits its interaction with HDAC6, eventually leading to increased deacetylase activity (Schofield, Steel et al. 2012). It is obvious though that phosphorylation of p25α in different residues by various kinases plays an important role in regulating the multiple cellular functions of p25α (Schofield, Gamell et al. 2013).

Under pathological conditions, p25α is considered to be re-located from myelin sheaths to the oligodendroglial cell soma and to facilitate aSyn aggregation (Lindersson, Lundvig et al. 2005; Song, Lundvig et al. 2007) (**Figure 8**). *In vitro* experiments utilizing p25α ectopic overexpression in PC12 cells revealed that p25α prevents the fusion of autophagosomes with lysosomes and impairs

aSyn degradation, enhancing its secretion via exophagy (Ejlerskov, Rasmussen et al. 2013). Moreover, concurrent overexpression of p25α and aSyn in OLN-93 rat oligodendroglial cells led to pSer129 aSyn-dependent microtubule retraction from the processes to the perinuclear space, as well as to cytotoxicity and subsequent cell death via activation of the FAS receptor and caspase-8 (Kragh, Lund et al. 2009; Kragh, Fillon et al. 2013). Importantly, the levels of glial cell-derived neurotrophic factor (GDNF) were found significantly decreased in the brains of MBP-haSyn transgenic mice, a mouse model for MSA where human aSyn is specifically overexpressed in oligodendrocytes (Ubhi, Rockenstein et al. 2010). In agreement, similar results were obtained from brain samples of MSA patients, further supporting that oligodendroglial aSyn accumulation is implicated in the dysregulation of neurotrophic support, oxidative stress and neuroinflammation, thus leading to MSA pathogenesis (Ubhi, Rockenstein et al. 2010).

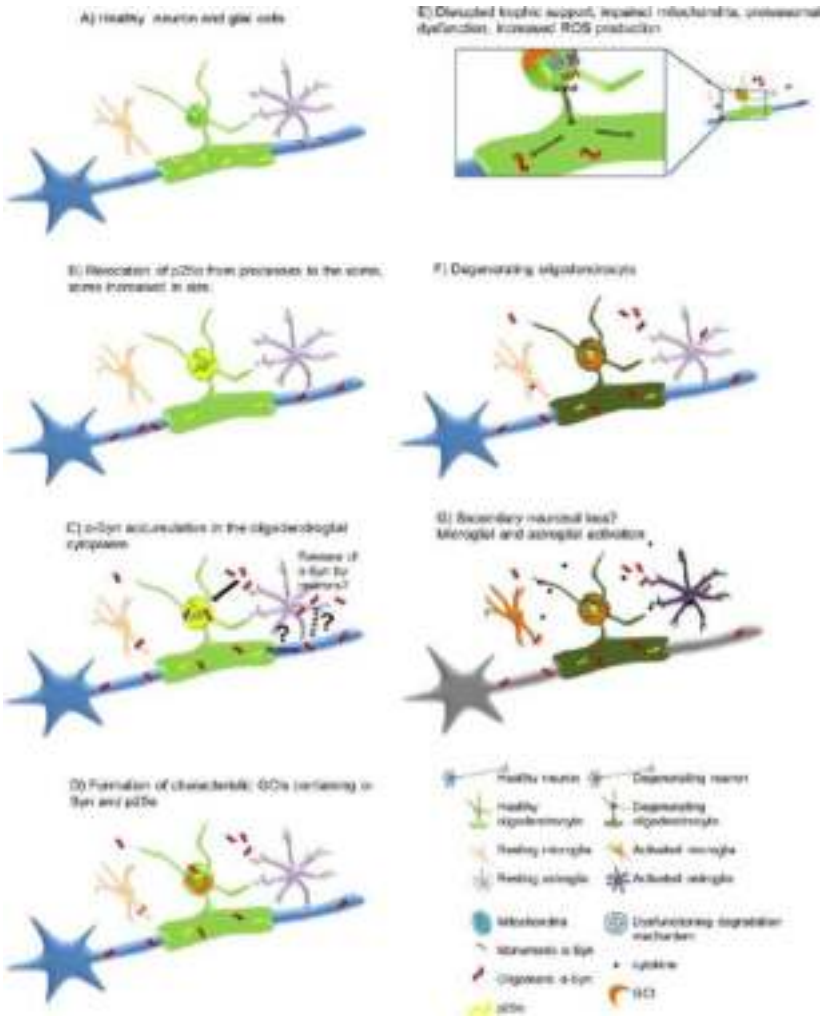

Figure 8: **Prevailing hypothesis of pathological α-synuclein spreading and accumulation underlying neurodegeneration in MSA**. **A**) p25α and monomeric aSyn are normally located in myelin sheaths in presynaptic terminals, respectively, **B**) Relocation of p25α towards the abnormally expanded oligodendroglial cell soma, **C**) The neuronally secreted aSyn is internalized by oligodendrocytes, **D**) Abnormal aSyn accumulation and GCIs formation, **E**) Impaired trophic support, mitochondrial and proteasomal dysfunction and increased ROS production, **F**) Oligodendroglial degeneration, **G**) Secondary neuronal death, microglial and astroglial activation. Source: (Kuzdas-Wood, Stefanova et al. 2014).

According to the prevailing hypothesis regarding the initiation of MSA pathogenesis, it has been proposed that p25α relocates from myelin sheaths to the abnormally expanded oligodendroglial cell soma, triggering aSyn aggregation and finally the formation of GCIs (Stefanova and Wenning 2016) (**Figure 8**). Alpha-synuclein is considered to be internalized by oligodendrocytes following its release from the neighboring neurons and then form toxic aggregates within oligodendrocytes, leading to their degeneration and subsequently to neuronal cell death (Stefanova and Wenning 2016) (**Figure 8**). However, as mentioned above, recent studies have revealed the crucial role of the endogenous oligodendroglial aSyn in the formation of aberrant species (Kaji, Maki et al. 2018), as well as the impact of cellular milieu in the formation of distinct aSyn strains, thus discriminating neuronal from oligodendroglial aSyn pathology (Peng, Gathagan et al. 2018). From the aforementioned data, it is evident that the levels/conformations of both aSyn and p25α proteins are critical to MSA pathogenesis, and the pathways responsible for their clearance may represent potential therapeutic targets for the disease.

7. Intracellular proteolytic machineries

7a. Degradation via the ubiquitin-proteasome system (UPS)

Protein degradation via the ubiquitin-proteasome system (UPS) is mainly responsible for the removal of short half-life nuclear and cytoplasmic proteins. Initially, a 76-residue ubiquitin polypeptide binds to the exposed lysine residues on the surface of the target protein (Glickman and Ciechanover 2002). Ubiquitination is achieved via a 3-step mechanism, catalyzed by: a ubiquitin-activating enzyme (E1), a ubiquitin-conjugating enzyme (E2) and a ubiquitin ligase (E3) (**Figure 9**). Ubiquitin is first activated by an E1 hydrolase and then the E2 enzyme transports it to the E3 ligase, which catalyzes the binding of ubiquitin to the substrate protein, finally forming a multi-ubiquitin chain (Layfield, Tooth et al. 2001; Glickman and Ciechanover 2002; Gallastegui and Groll 2010).

Subsequently, the protein targets are cleaved by the 26S proteasomal complex, and the ubiquitin molecules are released by ubiquitin recycling enzymes, for an additional ubiquitination cycle (Glickman and Ciechanover 2002; Ardley and Robinson 2005). The 26S proteasome complex consists of two protein subunits, the 20S barrel-shaped central subunit, which is the active center of the complex where the protein degradation takes place, and two regulatory 19S subunits that form the cylinder cap (Benaroudj, Zwickl et al. 2003; Crews 2003; Goldberg, Fleming et al. 2003) (**Figure 9**). In case the substrate-proteins are not in a denatured form (such as oligomeric or aggregated proteins) they are degraded via an ubiquitin-independent proteolysis involving

regulatory complexes that lack ATPase activity, such as the PA28 activator (Verhoef, Lindsten et al. 2002; Cascio 2021).

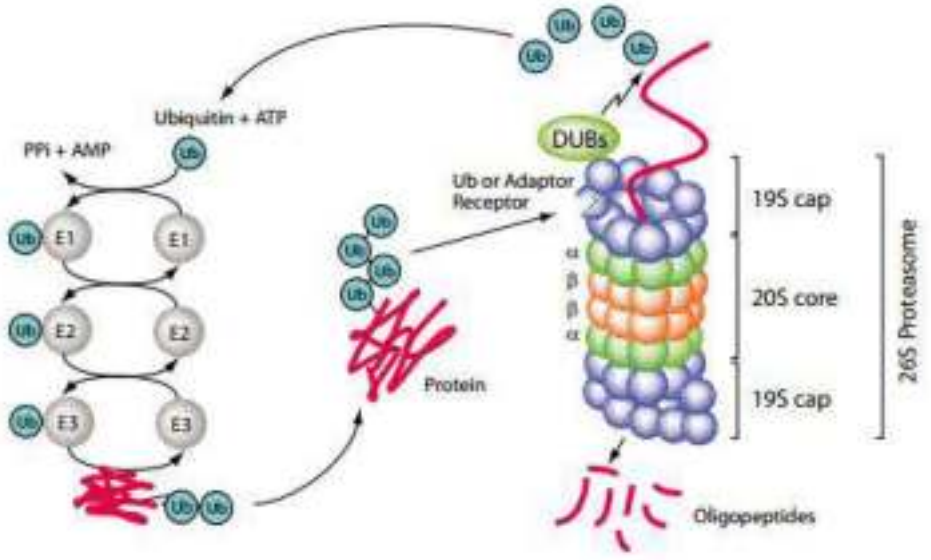

Figure 9: **The ubiquitin-proteasome system (UPS)**

The 26S proteasome complex recognizes polyubiquitinated proteins, which were marked for elimination by the E1, E2 and E3 ubiquitinating enzymes.

Source: https://www.caltagmedsystems.co.uk/information/the-ubiquitin-proteasome-system-2/

7b. Autophagy Lysosome Pathway (ALP)

Autophagy-lysosome pathway (ALP) is a process of protein degradation that delivers cellular components, damaged organelles and protein aggregates to the lysosomes for digestion. The main differences between UPS and ALP degradation lie in the fact that lysosomes are responsible for the degradation of organelles and of proteins with long half-life (Xilouri, Brekk et al. 2013). Lysosomes contain a plethora of proteolytic enzymes, such as proteases, lipases and nucleases that can digest most cellular components. Three different types of autophagy have been identified, depending on the mechanism by which protein substrates are delivered into lysosome for degradation (Klionsky and Emr 2000; Levine and Klionsky 2004): a) microautophagy, b) macroautophagy (MA) and c) chaperone-mediated autophagy (CMA) (**Figure 10**).

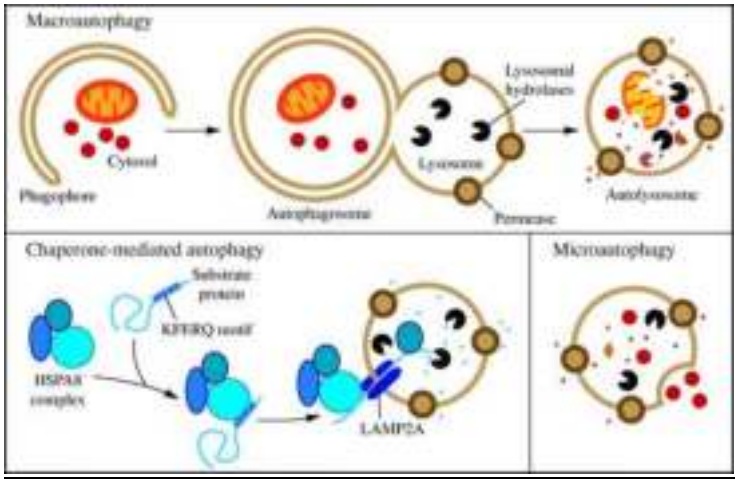

Figure 10: **Three types of autophagy in mammalian cells.**

(Upper panel) Macroautophagy, mediated by *de novo* formed cytosolic double-membrane vesicles, autophagosomes, to transport the protein cargo to the lysosome for degradation, (Lower panel, left) Chaperone-mediated autophagy (CMA), which is responsible for the transport of unfolded proteins, bearing the KFERQ motif, directly across the lysosomal membrane, (Lower panel, right) Microautophagy, which involves the direct uptake of cargo via invagination of the lysosomal membrane. All three autophagic types lead to the digestion of protein cargo and the release of the products back into the cytosol for reuse. Source: (Parzych and Klionsky 2014).

7b (i). Microautophagy

Microautophagy, is a digestion process that involves the direct engulfment of the cytoplasmic cargo via membrane invagination. As a result, the vesicles that are formed enter lysosomes for protein, lipid or organelles digestion (Li, Li et al. 2012; Schuck 2020). Interestingly, three distinct types of microautophagy have been identified in mammalian cells (Oku and Sakai 2018):

a) Type 1 - Microautophagy with Lysosomal Protrusion: Although the precise molecular mechanism remains unknown, this type of microautophagy includes the formation of an "arm-shaped" lysosomal protrusion that wraps around cytoplasmic components (such as organelles) (Sakai and Ogawa 1982).

b) Type 2 - Microautophagy with Lysosomal Invagination: This is a microautophagic invagination process that requires the implication of the small GTPase Rab7 for endosomal incorporation into a specialized organelle named "the apical vacuole". This organelle contains lysosomal enzymes and lysosomal membrane proteins and has been shown to play an important role during mouse embryogenesis (Kawamura, Sun-Wada et al. 2012).

c) Type 3 - Microautophagy with Endosomal Invagination: This is a process for Late Endosomes/MultiVesicular Bodies (LE/MVB) formation via the endosomal sorting complexes required for transport (ESCRT) machinery. The protein cargo is recruited on the endosomal surface via receptors such as Nbr1 and Hsc70 (Sahu, Kaushik et al. 2011).

7b (ii). Macroautophagy

Macroautophagy (MA) is a degradation process mediated by double-membrane vesicles, called autophagosomes (autophagic vacuoles, AVs) (Parzych and Klionsky 2014). These sequestering vesicles are formed *de novo* rather than through membrane budding (Yang and Klionsky 2009). Upon induction of macroautophagy by the ULK1/2 complex, the membrane expands forming the phagophore, which then elongates via the involvement of ATG12–ATG5-ATG16L1 complex, the class III PtdIns3K complex, LC3-II, and ATG9 (Parzych and Klionsky 2014) (**Figure 11**). Interestingly, the induction of autophagy is regulated by the activity of mTOR (mammalian/mechanistic target of rapamycin) or AMPK (AMP activated protein kinase), depending on the nutrient status. Specifically, in case of sufficient nutrient supply, mTOR prevents autophagy induction, whereas under starvation, AMPK triggers the autophagy initiation by inhibiting mTORC1 (Alers, Loffler et al. 2012).

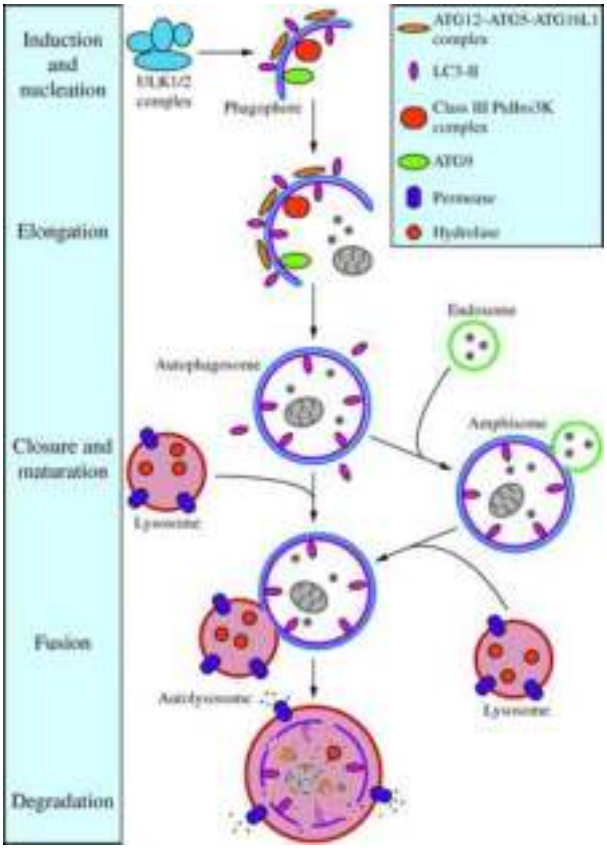

Figure 11: **Steps of mammalian macroautophagy**.

Initially, the ULK1/2 complex triggers the nucleation of the phagophore, followed then by its elongation aided by the ATG12–ATG5-ATG16L1 complex, the class III PtdIns3K complex, LC3-II, and ATG9. Finally, the membrane closes surrounding its cargo to form an autophagosome and LC3-II is cleaved from the outer membrane of this structure. The outer membrane of the autophagosome then fuses with the lysosomal membrane to form an autolysosome. Alternatively, the autophagosome may fuse with an endosome, forming an amphisome, before fusing with the lysosome. In all cases, the contents of the autolysosome are degraded and released back into the cytoplasm for reuse by the cell. Source: (Parzych and Klionsky 2014).

The phagophore expansion is also regulated by the ATG8/LC3 system. For this reason, ATG4 processes ATG8 to reveal a C-terminal glycine (LC3-I) which is then activated by ATG7 (an E1-like enzyme) and transferred to ATG3 (an E2-like enzyme) (Parzych and Klionsky 2014). LC3-I is then conjugated to the lipid phosphatidylethanolamine (PE) via the aid of ATG12–ATG5-ATG16L1 complex (an E3 ligase), to finally form LC3-II (Parzych and Klionsky 2014) (**Figure 12**). Eventually, the membrane closes and then matures before its fusion with the lysosomal membrane, to finally form an autolysosome. Alternatively, the autophagosome may be fused with an endosome, forming an amphisome, before the final fusion with the lysosome (**Figure 12**). In any case, the contents of the vesicles become digested by the lysosomal enzymes and are released to the cytoplasm for reuse (Parzych and Klionsky 2014).

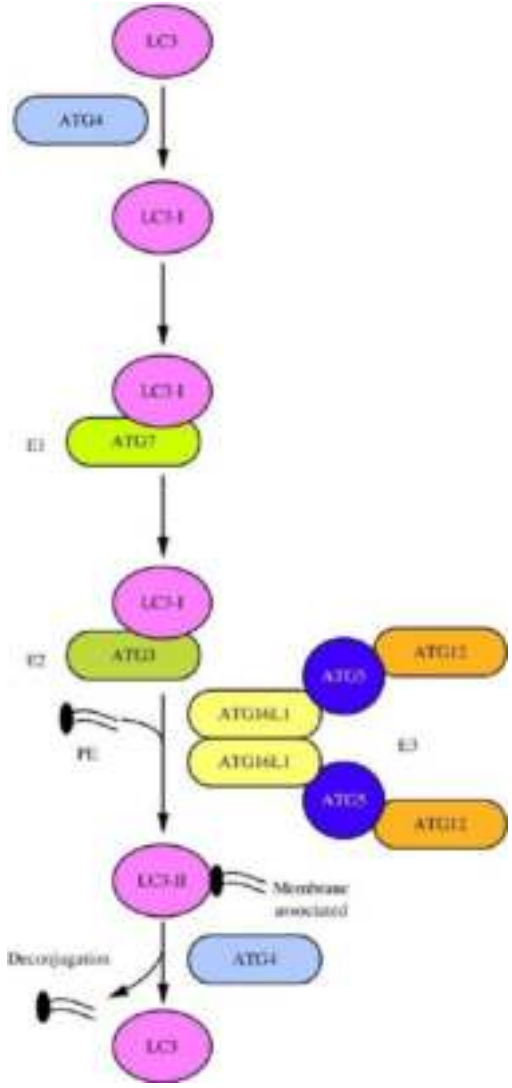

Figure 12: **The LC3 conjugation system**.

ATG4 process LC3 which then reveals a C-terminal glycine (LC3-I). Upon LC3-I activation by ATG7, an E1-like enzyme, it is transferred to the E2-like enzyme ATG3. The ATG12–ATG5-ATG16L1 complex acts as an E3 ligase and conjugates phosphatidylethanolamine (PE) to LC3-I to finally form LC3-II, which can associate with the phagophore. ATG4 can subsequently cleave LC3-II to release LC3 (deconjugation process). Source: (Parzych and Klionsky 2014).

Importantly, the ratio LC3-II/LC3-I is indicative for the autophagosome formation, but not for the autophagic degradation. Since LC3-II is present both on inner and outer autophagosome membranes, it can be degraded itself, especially in cases of prolonged activation of autophagy (Tanida, Minematsu-Ikeguchi et al. 2005). Alternatively, p62 (SQSTM1/sequestosome 1) degradation may also serve as a method for detecting autophagic flux (the macroautophagic degradation activity) (Bjorkoy, Lamark et al. 2005; Bjorkoy, Lamark et al. 2009; Yoshii and Mizushima 2017). p62 is a ubiquitin-binding scaffold protein which interacts with ubiquitinated proteins and has been proposed to link ALP and UPS, since it also serves as a classical receptor of autophagy (selective autophagy) (Liu, Ye et al. 2016). p62 binds LC3 and drives ubiquitinated protein aggregates to degradation via autophagy (Pankiv, Clausen et al. 2007). Apart from being an autophagy adapter, p62 is also an autophagic substrate since it decreases during starvation or accumulates in case of autophagy inhibition (Shvets, Fass et al. 2008; Wu, Jin et al. 2020).

7b (iii). Chaperone-mediated autophagy (CMA)

The CMA pathway is a very selective form of autophagy, responsible for the clearance of proteins that contain the KFERQ signal pentapeptide or other biochemically related motifs and involves the activity of cytosolic chaperones and co-chaperones (Orenstein and Cuervo 2010). All substrates are recognized by the cytosolic Heat sock protein 70 (Hsp70) and the co-chaperone Heat shock cognate protein 70 (Hsc70) and they are transported to the lysosomal membrane (Chiang, Terlecky et al. 1989; Cuervo and Dice 1996; Cuervo, Dice et al. 1997; Agarraberes and Dice 2001; Bandyopadhyay, Kaushik et al. 2008) (**Figure 13**). There, the lysosome associated membrane protein type 2A (LAMP2A) serves as a specific receptor for CMA-substrate proteins, which are then transported to the lysosomal lumen and digested by lysosomal proteases (Saftig and Klumperman 2009) (**Figure 13**).

The activity of the CMA pathway is directly dependent on the levels of LAMP2A in the lysosomal membrane and the presence of Hsc70, located in the lysosomal lumen (Cuervo, Knecht et al. 1995; Agarraberes, Terlecky et al. 1997; Cuervo and Dice 2000). Several studies have proposed that CMA activity increases upon various types of cellular stresses, (Massey, Zhang et al. 2006; Li, Yang et al. 2018; Dash, Aydin et al. 2019; Dong, Aguirre-Hernandez et al. 2020), whereas it decreases with age, mainly due to a reduction in the concentration of the LAMP2A receptor in the lysosomal membrane (Cuervo and Dice 2000). Moreover, enhanced levels of LAMP2A receptor lead to increased CMA activity, thus rendering LAMP2A an effective regulator of CMA (Cuervo and Dice 2000; Zhang and Cuervo 2008). Moreover, impairment of CMA pathway is implicated in

neurodegenerative diseases characterized by the presence of misfolded proteins, such as PD (Cuervo, Stefanis et al. 2004). Specifically, regarding aSyn degradation, it has been shown that PD-linked mutants bind tightly to LAMP2A, thus preventing their own degradation and the transport of other substrate-proteins along the lysosomal membrane, which then accumulate and may cause cell toxicity (Cuervo, Stefanis et al. 2004).

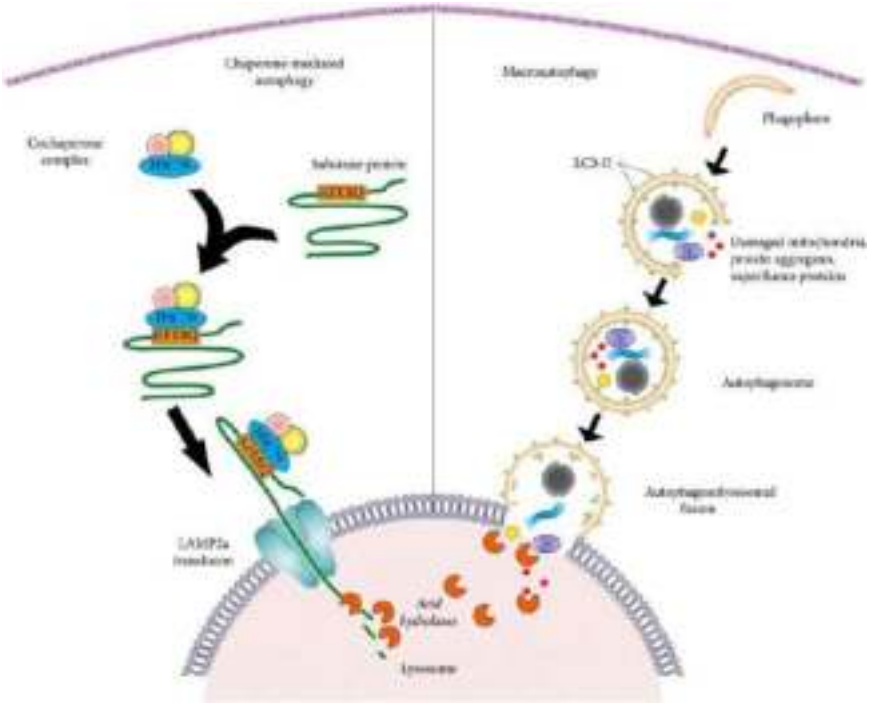

Figure 13: **Schematic representation of macroautophagy and CMA pathways.**
Left: The CMA-targeted proteins bearing the KFERQ recognition sequence are recognized by the HSC70 chaperone protein, which then delivers the substrate to the LAMP2A receptor on the lysosome for degradation. Right: Macroautophagy initiates with the double-membrane vesicle nucleation and its further expansion resulting in the formation of autophagosome. Autophagosomes can engulf misfolded and aggregated proteins or entire organelles. Finally, mature autophagosomes fuse with lysosomes forming autolysosomes, responsible for their cargo digestion. Source: (Ghosh and Pattison 2018).

8. Alpha-synuclein and protein degradation pathways: an intricate interplay

A great wealth of data focuses on the complicated relationship between aSyn degradation and protein degradation pathways. It is well-known that aSyn can be cleared by both the UPS and the ALP (**Figure 14**) in a manner that depends on cell type, tissue and aSyn conformation state (Bennett, Bishop et al. 1999; Webb, Ravikumar et al. 2003; Vogiatzi, Xilouri et al. 2008). Specifically, there are studies demonstrating that aSyn can be degraded by the 26S/20S proteasome both via a ubiquitin-dependent (Rott, Szargel et al. 2011; Haj-Yahya, Fauvet et al. 2013) and a

ubiquitin-independent manner (Tofaris, Layfield et al. 2001; Liu, Corboy et al. 2003). Interestingly, further experiments conducted in PC12, HEK293 and primary mesencephalic cells suggested that pharmacological inhibition of the proteasome does not lead to aSyn accumulation (Rideout, Larsen et al. 2001; Rideout and Stefanis 2002; Vogiatzi, Xilouri et al. 2008), however others have shown that soluble aSyn oligomers, but not monomers, are partially cleared via the 26S proteasome (Emmanouilidou, Stefanis et al. 2010). Importantly, it has been proposed that the UPS is responsible for aSyn removal under normal conditions, while in pathological cases the ALP is recruited to clear the increased aSyn burden (Ebrahimi-Fakhari, Cantuti-Castelvetri et al. 2011).

It has been previously shown that CMA is responsible for the degradation of monomeric or dimeric forms of aSyn via LAMP2A receptor, whereas oligomeric aSyn is cleared mainly via macroautophagy (Cuervo, Stefanis et al. 2004; Vogiatzi, Xilouri et al. 2008; Xilouri, Brekk et al. 2013) (**Figure 14**). Lee and colleagues also suggested that the lysosome is responsible for the removal of oligomeric but not fibrillar aSyn and that lysosomal failure results in aSyn accumulation and aggregation and subsequent cell death (Lee, Khoshaghideh et al. 2004). Moreover, initial *in vivo* evidence suggested that increased aSyn protein levels evoked by paraquat treatment were preferably degraded via CMA in dopaminergic neurons, where the levels of LAMP2A and the lysosomal HSC70, both essential CMA-components, were found elevated (Mak, McCormack et al. 2010). It has been previously shown that boosting CMA function via LAMP2A overexpression in cell lines and primary neuronal cultures and in the rat dopaminergic system mitigated aSyn protein levels and related toxicity (Xilouri, Brekk et al. 2013). Similar neuroprotective effects were obtained upon LAMP2A overexpression in the Drosophila brain (Issa, Sun et al. 2018). On the contrary, LAMP2A silencing led to endogenous aSyn accumulation *in vitro* (Vogiatzi, Xilouri et al. 2008) and *in vivo* (Xilouri, Brekk et al. 2016) and in extensive neurodegeneration of the rat nigrostriatal axis (Xilouri, Brekk et al. 2016). Decreased levels of LAMP2A and HSC70 were reported in the human substantia nigra and amygdala of PD brains (Alvarez-Erviti, Rodriguez-Oroz et al. 2010), whereas, in a subsequent study, LAMP2A was found to be selectively reduced in association with increased aSyn levels, even in the early stages of PD, thus suggesting that dysregulation of CMA-mediated protein degradation occurs prior to substantial aSyn aggregation in PD (Murphy, Gysbers et al. 2015).

However, a bidirectional link between aSyn accumulation and the protein degradation machineries exists and extensive studies have been conducted to elucidate not only the manner of aberrant aSyn degradation in a-synucleinopathies, but also the impact of various aSyn conformations on the proper lysosomal function. It has been proposed that overexpression of A30P and A53T mutants, contrarily to WT aSyn, leads to cell death due to proteasomal inhibition (Tanaka, Engelender et al. 2001). In agreement, Stefanis et al. have provided evidence that

overexpression of mutant aSyn variants results in UPS failure by inhibiting the activity of the 20S/26S proteasome, finally leading to aSyn pathological accumulation (Stefanis, Larsen et al. 2001). On the other hand, other groups have failed to detect alterations in the proteasomal function of PC12 cells or transgenic mice, following overexpression of WT or mutant (A30P, A53T) aSyn (Martin-Clemente, Alvarez-Castelao et al. 2004). Moreover, later studies demonstrated that transient overexpression of WT or mutant aSyn, followed by addition of recombinant aSyn oligomers and fibrils in an osteosarcoma cell line, did not result in any disturbance of the proteasomal function (Zondler, Kostka et al. 2017). Importantly, studies in human post-mortem brains of PD patients also indicate impaired proteasomal function in the substantia nigra (Bentea, Verbruggen et al. 2017), further supporting the crucial role of UPS function in PD pathogenesis.

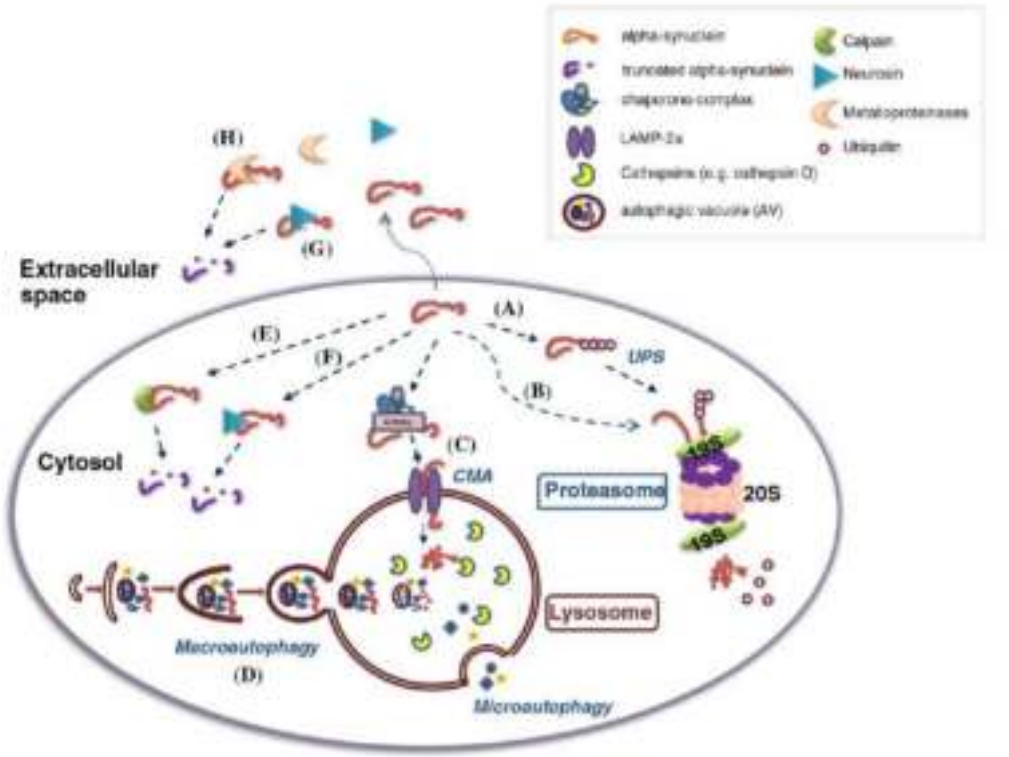

Figure 14: **Proteolytic pathways implicated in alpha-synuclein processing.**

Both ubiquitin-dependent (**A**) and independent (**B**) mechanisms have been proposed to degrade aSyn (wild-type and mutant). Both CMA (**C**) and macroautophagy (**D)** have been proposed to degrade alpha-synuclein, with CMA being responsible for the monomeric wild-type aSyn and macroautophagy being capable of degrading various forms (wild-type, mutant, oligomeric). Besides the proteasome and the lysosome, other proteases such as calpains (**E**) and neurosin (**F**) have been implicated in the cleavage of normal or aggregated forms of intracellular aSyn. Such cleavage may promote the generation of truncated aSyn species with pathogenic significance. Moreover, secreted neurosin (**G**) and metalloproteinases (**H**) have been found to cleave at selective sites extracellular aSyn, generating fragments with increased tendency to aggregate. This figure was modified from Figure 1 in (Xilouri, Brekk et al. 2013).

To this end, *in vitro* and *in vivo* experiments suggested that increased levels of aSyn lead to macroautophagy impairment via its interaction with Rab1a, an event that subsequently results in the autophagosome-formation-related protein Atg9 mislocalization (Winslow, Chen et al. 2010). Similar results were obtained from cells expressing the PD-linked mutation of the retromer protein VPS35, which is involved in autophagy and is implicated in PD pathogenesis (Zavodszky, Seaman et al. 2014). Interestingly, the most well studied PD-linked aSyn mutations, E46K, A30P and A53T, have been shown to promote to ALP dysfunction, via either impairing autophagosome formation or inhibiting the selective removal of damaged mitochondria through mitophagy (Choubey, Safiulina et al. 2011; Yan, Yuan et al. 2014; Lei, Cao et al. 2019). Interestingly, it has been reported that dopamine-modified aSyn inhibits CMA and this could probably shed light into the selective vulnerability of dopaminergic neurons in PD (Martinez-Vicente, Talloczy et al. 2008). Further experiments in human iPSC-derived midbrain dopaminergic neurons revealed that disrupted hydrolase trafficking, due to aSyn overexpression, reduces lysosomal function (Mazzulli, Zunke et al. 2016). Similarly, multiple studies suggest that there is a strong relationship between decreased β-glucocerebrosidase (GCase) activity and aSyn accumulation. In particular, heterozygote mutations in GBA1 gene encoding for GCase represent a major risk factor for PD development with a-synucleinopathy (Osellame, Rahim et al. 2013; Sardi, Clarke et al. 2013; Murphy, Gysbers et al. 2014; Du, Wang et al. 2015; Liu, Chen et al. 2015; Rocha, Smith et al. 2015).

Regarding the hypothesis of impaired aSyn degradation in the context of MSA, both the UPS and the ALP have been proposed to contribute to the accumulation and aggregation of aSyn within oligodendrocytes. The detection of LC3-positive signal or other autophagy-related proteins, such as ubiquitin and p62 in GCIs points a role of the ALP in the pathogenesis of MSA (Mori, Nishie et al. 2005; Terni, Rey et al. 2007; Miki, Mori et al. 2011; Odagiri, Tanji et al. 2012; Schwarz, Goldbaum et al. 2012; Tanji, Odagiri et al. 2013). It has also been suggested that AMBRA1, an upstream protein regulator of autophagy and UCH-L1, a deubiquitylating enzyme, are implicated in neurodegenerative diseases with oligodendroglia pathology (Pukass and Richter-Landsberg 2015; Miki, Tanji et al. 2018). The role of autophagic dysregulation along with mitochondrial impairment in aSyn aggregation was also studied in primary oligodendroglial cultures and in the OLN-t40 oligodendroglial cell line (Pukass, Goldbaum et al. 2015). Moreover, neurosin (kallikrein 6) has been proven an effective serine protease in clearing aSyn from oligodendrocytes both *in vitro* and *in vivo* (Iwata, Maruyama et al. 2003; Spencer, Valera et al. 2015; Kiely, Miners et al. 2019). In addition, treatment of Tg haSyn-PLP mice, a well-established MSA mouse model, with the proteasome inhibitor I for 12 weeks, resulted in enhanced accumulation of both human and endogenous mouse aSyn within the cytoplasm of

oligodendrocytes, thus highlighting the role of UPS in aSyn degradation (Stefanova, Kaufmann et al. 2012).

II. AIM OF THE STUDY

MSA is a debilitating neurodegenerative disorder with poor prognosis and currently unavailable therapy. The accumulation of aSyn and TPPP/p25α proteins within the glial cytoplasmic inclusions (GCIs) represents the key histophathological hallmark of the disease. However, the pathogenic cascade of events underlying the mechanisms of both protein inclusion formation and removal remain hitherto unexplored. The controversial findings regarding the lack of expression of the endogenous aSyn within oligodendrocytes under physiological conditions has turned the spotlight on the neuronal aSyn as the main culprit for the formation of the oligodendroglial GCIs.

The main objectives of the current study is to elucidate the role of the endogenous aSyn and/or p25α in the formation of pathological protein aggregates in MSA-like cellular and animal models and to identify the intracellular proteolytic machineries responsible for the removal of the disease-related oligodendroglial proteins in health and disease. The experimental design of this study includes the inoculation of human pre-formed fibrils (PFFs) of aSyn as seeds, in oligodendroglial cell lines and primary cultures or in the living mouse brain, in order to study the formation of aberrant aSyn species in the absence or presence of aSyn and/or p25α. Moreover, pharmacological and molecular modulation of both UPS and ALP is utilized to uncover the contribution of these degradation machineries in the removal of GCI-like protein aggregates engendered within oligodendrocytes. This line of investigation is expected to shed light on the mechanisms underlying the seeding of aSyn pathology in oligodendrocytes and will aid in the development of potential disease-modifying therapies against MSA and related alpha-synucleinopathies.

III. MATERIALS AND METHODS

1. Cell culture of OLN cell lines

Three different oligodendroglial (OLN) cell lines have been utilized: the immortalized control OLN-93 line originated from primary Wistar rat brain glial cultures (Richter-Landsberg and Heinrich 1996), and the OLN-AS7 and OLN-p25α lines that were generated by transduction of the OLN-93 line with the human wild-type (WT) SNCA or human TPPP/p25α cDNA, respectively. All cells were cultured in Dulbecco's modified Eagle's medium (D6429; Gibco, Invitrogen, Carlsbad, CA, USA) under conditions of 10% fetal bovine serum (10270; Gibco, Invitrogen, Carlsbad, CA, USA), 50 U/mL penicillin, and 50 μg/mL streptomycin. For the selection of OLN-AS7 and OLN-p25α, cells were maintained in 50 μg/mL Zeocin (R25001; Thermo Fisher Scientific, Waltham, MA, USA).

2. Primary oligodendroglial cultures

Briefly, mixed glial cultures were maintained in Dulbecco's modified Eagle's medium supplemented with 10% fetal bovine serum and 1% penicillin/streptomycin for 10–14 days. Loosely attached microglia were removed by shaking for 1 hr (200 rpm, 37°C), followed by additional shaking at 200 rpm for 18 hrs at 37°C for the enrichment of the culture with OPCs. Primary oligodendroglial progenitor cells derived from mixed glial cultures were prepared from P0 to P3 neonatal knockout (KO)-aSyn, wild-type (WT)-aSyn or PLP-human aSyn (haSyn) transgenic mice, as described previously (McCarthy and de Vellis 1980). The cells were then seeded at a density of 80,000 cells/well on poly-D-lysine-coated coverslips in 24-well plates and cultured in SATO medium (Bottenstein and Sato 1979) supplemented with insulin-transferrin-selenium solution (41400045; Gibco, Carlsbad, CA, USA), 1% penicillin/streptomycin, and 1% horse serum (H1138; Sigma-Aldrich, St. Louis, MO, USA). The cells were grown in SATO medium for 4 days prior to the addition of 0.5 μg haSyn PFFs (final concentration: 1 μg/mL culture medium/well) and/or pharmacological inhibitors or enhancers of the protein degradation pathways for 48 hrs in the appropriate concentrations. Subsequently, cells were fixed and preceded for immunofluorescence analysis using antibodies shown in **Table 1**. Differentiation of OPCs to mature oligodendrocytes was verified by labeling the cultures with an anti-MBP antibody (1:200; MCA409S; Bio-Rad, Hercules, CA, USA).

3. Preparation of primary cortical neuron cultures

Cultures of rat (embryonic day 18) cortical neurons were prepared as described previously (Xilouri, Brekk et al. 2013). Briefly, dissociated cells were plated onto poly-D-lysine-coated 24-well dishes at a density of 100,000–120,000 cells/well. The cells were grown in Neurobasal medium (Invitrogen, Carlsbad, CA, USA), supplemented with B27 supplement (Invitrogen, Carlsbad, CA, USA), l-glutamine (0.5 mM), and penicillin/streptomycin (1%) for 5 days prior to the addition of 3 μg haSyn PFFs (final concentration: 3 μg/mL culture medium/well of a 24-well plate).

4. Preparation of haSyn PFFs

HaSyn fibrils were generated as described (Cho, Nodet et al. 2009; Kim, Cho et al. 2009), with several modifications. Shortly, before aggregation, monomeric aSyn in 50 mM HEPES (pH 7.4,) 100 mM NaCl, and 0.02% NaN_3 was centrifuged for 1 hr at 84.000×g. The supernatant was ultra-filtrated (0.2 μm) and adjusted to 0.27 mM. Aggregation was performed for 12 days at 37 °C. Fibrils were collected by ultracentrifugation, washed twice with phosphate-buffered saline (PBS), pH 7.3, at room temperature, and quantified by subtracting the amount of monomeric aSyn protein in the supernatant from the total protein used for aggregation. PFFs were resuspended in PBS (pH 7.3) at a final concentration of 4.5 mg/mL and a working stock solution was prepared at 1 mg/mL. The cells were incubated with 0.5–3 μg non-sonicated haSyn PFFs or PBS as a control for the indicated time points and were either processed for confocal microscopy or lysed and collected for western blot analysis as described below.

5. Sonication of haSyn PFFs

HaSyn PFFs were sonicated using a probe tip sonicator as described previously (Cho, Nodet et al. 2009). Briefly, a working solution of haSyn PFFs was prepared at a final concentration of 0.1 mg/mL and sonicated with 60 pulses at 10% power (total of 30 s, 0.5 s on, 0.5 s off). The cells were incubated with 0.5 μg haSyn PFFs (pre- and post-sonication) or PBS as a control for 48 hrs and processed for confocal microscopy.

6. Pharmacological reagents

The inhibition of the proteasome was achieved with epoxomicin (15 nM) that selectively blocks the chemotrypsin-like activity of the 20S catalytic subunit (Meng, Mohan et al. 1999). For the lysosomal pathway, the inhibitor of phosphatidylinositol-3-kinase, 3-methyladenine (3MA, 10 mM) and the general lysosomal inhibitor NH_4Cl (20 mM) were utilized. Since NH_4Cl is unstable, for the 24 and 48 hrs incubation a renewal of the inhibitor was required every 12 hrs. Induction of

macroautophagy was accomplished with the use of rapamycin (1 μM) that induces the mTOR-dependent macroautophagic pathway (Ballou and Lin 2008) and the RARα antagonist atypical retinoid 7 (AR7, 40 μM) that is reported to activate selectively the CMA pathway (Anguiano, Garner et al. 2013). The reagents were applied for 16-48 hrs and the analysis was performed either by western blotting or with immunocytochemistry.

7. Cell transfections

Transient transfections with haSyn, p25α and/or GFP plasmids or the autophagic flux reporter plasmids were performed with polyethylenimine-PEI (26966; Polysciences, Germany) reagent, and the cells were fixed at the indicated time points using 4% paraformaldehyde (P6148; Sigma-Aldrich, St. Louis, MO, USA) in PBS and processed for immunofluorescence analysis. The autophagic flux of OLN cells upon treatment with haSyn PFFs (or PBS as control) was monitored with the use of RFP/GFP-LC3 (Okerlund, Schneider et al. 2017), and mCherry/GFP-SQSTM1/p62 (Pankiv, Clausen et al. 2007) cDNA plasmids, upon transient transfection with PEI. The RFP/GFP-LC3 plasmid was kindly provided by Dr Craig-Curtis Garner (DZNE, Germany) and the mCherry/GFP-SQSTM1/p62 plasmid by Dr Terje Johansen (University of Tromso, Norway). Cells were cultured in 24-well dishes and PEI with cDNA were diluted in Opti-MEM in a 1:3 ratio. After 4 hrs of incubation, the transfection medium was replaced by fresh DMEM 10% FBS containing either PBS or haSyn PFFs. The lysosomal inhibitor NH_4Cl was used as a positive control for autophagic flux impairment. Forty-eight (48) hours later, cells were fixed using 4% paraformaldehyde (PFA; Sigma-Aldrich, P6148) in PBS and processed for immunofluorescence analysis.

8. Subcellular fractionation and Western immunoblotting

For the biochemical analysis, the cells were plated on 6-well plates at a density of 200,000 cells/well (for treatment up to 96 hrs) or 50,000 cells/well (for treatment up to 10 days). haSyn Pre-Formed Fibrils (PFFs) were added the following day at a final concentration of 1 μg/mL culture medium/well (0.5 μg PFFs) or 3 μg/mL culture medium/well (3 μg PFFs). The cell pellets after being washed with PBS were homogenized in lysis buffers with progressively higher extraction strength. All of them contained protease (Roche, 11836170001) and phosphatase (Roche, 04406837001) inhibitors. Initially, cells were lysed with 1% Triton X-100-containing buffer (150 mM NaCl, 50 mM Tris pH 7.6, 2 mM EDTA), left on ice for 30 min and centrifuged at 13,400 × g for 30 min at 4 °C. The supernatant was collected to obtain the Triton-soluble fraction and the pellet, after 2x washes with PBS, was resuspended in 1% SDS-containing buffer (150 mM NaCl, 50

mM Tris pH 7.6, 2 mM EDTA), sonicated and centrifuged to acquire the SDS-soluble fraction. Finally, the remaining pellet, after 2x washes with PBS, was solubilized in 8 M urea-5% SDS-containing buffer. Primary oligodendroglial cells were lysed using RIPA buffer (150 mM NaCl, 25 mM Tris pH 7.6, 0.5% sodium deoxycholate, 0.1% SDS, 1% NP-40), left on ice for ~ 30 min, and centrifuged at 10,000×g for 15 min at 4 °C. Then, samples of equal protein concentration were processed for western blot analysis utilizing the utilized primary and secondary antibodies shown in **Table 1**. The immunoreactivity for protein band intensity within the linear range of detection was quantified with ImageJ software. All measurements were normalized to β-actin as a loading control.

9. Immunocytochemistry and confocal microscopy

For the immunofluorescence experiments OLN cells were seeded on poly-D-lysine-coated coverslips (P7405; Sigma-Aldrich, St. Louis, MO, USA) in 24-well plates at a density of 10,000 cells/well (for analysis up to 48 hrs) or 1,000 cells/well (for up to 10 days). Mouse primary oligodendrocytes were plated at a density of 80,000 cells/well and differentiated in SATO medium as described above. OLN cell lines and primary oligodendrocytes were treated with haSyn PFFs and/or inhibitors or enhancers of cellular proteolytic pathways at the indicated concentrations and time points. The cells were then fixed with 4% PFA for 40 min, blocked in 10% normal goat serum containing 0.4% Triton X-100 for 1 hr at room temperature, and incubated with primary antibodies overnight at 4 °C. The primary and fluorescent secondary antibodies used are shown in **Table 1**. The dye 4′, 6-diamidine-2′-phenylindole dihydrochloride (DAPI) was utilized for nuclei staining. Images were obtained using a Leica TCS SP5 confocal microscope combined with a dual (tandem) scanner. All confocal images were obtained under equivalent conditions of laser power, pinhole size, gain, and offset settings between the groups.

For the transient transfections with the haSyn, p25α and/or GFP plasmids, quantifications were performed with the Imaris software suite (v7.7.2, Bitplane AG, Zurich, Switzerland), using a static set of parameters to isolate either GFP^+ or $p25\alpha^+$ cell profiles, and then masking the channel containing the human aSyn (LB509 antibody), oxidized/nitrated aSyn (SYN-303 antibody) or the rodent aSyn (D37A6 antibody) signal using said profiles. The masking of the GFP^+ or $p25\alpha^+$ signal was based on fluorescent intensity. ImageJ (v2.0.0) software was used to quantify relative protein levels expressed as mean fluorescence intensity (M.F.I.), area coverage (μm^2) or % area coverage, normalized to the total number of cells/field (the number of DAPI-stained nuclei). M.F.I./cell was used to express the protein levels of interest per cell in the absence of haSyn PFFs, whereas area coverage/cell or % area/cell measurements depicted the levels of the studies proteins following the addition of haSyn PFFs in cells. In the case of primary oligodendroglial cell cultures the area of signal was normalized to the number of TPPP/$p25\alpha^+$ cells (marker for mature oligodendrocytes). To

stain the lectins of the plasma membrane, wheat germ agglutinin (Alexa Fluor™ 488-conjugated; W11261; Thermo Fisher Scientific, Waltham, MA, USA) was added to PFF-treated OLN-93 cells (0.5 μg, 48 hrs) for 10 min at 37°C, prior to fixation for confocal microscopy analysis. For proteinase K treatment, OLN cells were treated with 0.05 μg/mL proteinase-K (AM2542; Thermo Fisher Scientific, Waltham, MA, USA) for 15 min following the addition of 0.5 μg haSyn PFFs for 48 hrs.

10. RNA extraction, cDNA synthesis and real-time PCR

Total RNA was extracted either from OLN-93 cells treated with haSyn PFFs for 2, 12, and 48 hrs (or PBS), or from OLN-AS7 and OLN-p25α cells treated with PBS or epoxomicin (15 nM) or NH_4Cl (20 mM) for 24 or 48 hrs using TRIzol® reagent (Ambion, Thermo Fisher Scientific, Waltham, MA, USA). Following digestion with 1 U/μg DNase I (Promega, Madison, WI, USA) 1 μg total RNA was used to synthesize the first strand cDNA according to the Moloney murine leukemia virus reverse transcription reaction system (Promega, Madison, WI, USA), which subsequently would be the template for the RT-PCR reaction. To this end, duplicates of each sample were analyzed using a Light Cycler 96 (Roche Applied Science, Mannheim, Germany) to determine the levels of rat SNCA (in the case of PFF-treated OLN-93 cells) or human SNCA and TPPP/p25α mRNA (in the case of inhibitors-treated OLN-AS7 and OLN-p25α cells). Rat GAPDH or rat β-actin were used for normalization (reference genes). Primer sequences utilized in the study are shown in **Table 1**. Each cDNA sample was diluted 1:20 before use in the amplification assay. The utilized PCR conditions were 1× buffer (-Mg), 1.5 mm MgCl2, 0.2 mm dNTPs, 0.2 μm primers, template < 500 ng, 2 U Platinum Taq and SYBR Green (Roche, Mannheim, Germany), whereas the PCR cycling conditions were 95°C for 180 s, 95°C for 10 s, 60°C for 15 s, and 72°C for 15 s (45 cycles), and 95°C for 60 s, 65°C for 60 s, 95°C for 10 s, and 37°C for 30 s. for rat SNCA, 95°C for 180 s, 95°C for 10 s, 60°C for 15 s, 72°C for 15 s (45 cycles), 95°C for 60 s, 60°C for 60 s, 95°C for 10 s, 37°C for 30 s for human SNCA and 52°C for 120 s, 95°C for 120 s, 95°C for 15 s, 59°C for 40 s (50 cycles), 95°C for 10 s, 55°C for 60 s, 98°C for 1 s, 37°C for 30 s for human TPPP/p25α. No template samples served as negative controls. Data were analyzed automatically with a threshold set in the linear range of amplification. The cycle number at which any particular sample crossed that threshold (Ct) was used to determine fold difference, whereas the geometric mean of the control gene served as a reference for normalization. Fold difference was calculated with the $2^{-\Delta\Delta Ct}$ method.

11. RNA interference

Small interfering RNAs (siRNAs) targeting the rat *Lamp2a* or the *Atg5* gene were utilized to assess the contribution of CMA or macroautophagy, respectively, in the proteolysis of aSyn and TPPP/p25α in OLN cell lines. In particular, OLN cells were transfected with Lsi1/Lsi2 (*Lamp2a* siRNAs, final concentration 60 nM), *Atg5* si (rn.Ri.Atg5.13.1/2/3 TriFECTa kit DsiRNA, final concentration 10 nM) or scr (the control scrambled siRNA, final concentration 60 nM) in Lipofectamine 2000 (Invitrogen)-containing solution for 72 hrs. The sequences of the scr siRNA or the siRNAs targeting the rat *Lamp2a* are shown in **Table 2**. Analysis was performed with both western blotting and immunocytochemistry.

12. Assessment of survival

Viable cells were quantified by counting the number of intact nuclei in a haemacytometer, after lysing the cells in detergent- containing solution (Rukenstein, Rydel et al. 1991; Farinelli, Greene et al. 1998). This method has been shown to be reproducible and accurate and to correlate well with other methods of assessing cell survival-death (Troy, Stefanis et al. 1997; Stefanis, Park et al. 1999). In more detail, cells were resuspended in a detergent-containing lysis buffer (0.1x PBS, 0.5 % Triton, 2mM $MgCl_2$, 0.013 mM ethyl-hexadecyl-dimethyl-ammonium bromide, 0.28 % glacial acetic acid and 2.82 mM NaCl) and two independent examiners blinded to the identity of the samples counted the number of intact nuclei with the aid of a haemacytometer. Cell counts were performed in triplicate and the results were presented as means ± SE.

13. Intracellular protein degradation assay

OLN cells were cultured to 60-70% confluence in 12-well plates in full DMEM and incubated with 0.5 μg of haSyn PFFs for 48 hrs. Total protein degradation was measured by pulse-chase experiments, by labeling PBS- or PFF-treated OLN cells with [3H] leucine (2 μCi/ml) (Leucine, L-3,4,5, NEN-Perkin Elmer Life Sciences, Belgium) at 37ºC for 24 hrs. The cultures were then extensively washed with medium and returned in complete growth medium containing 2 mM of unlabeled leucine for 6 hrs. This medium containing mainly short-lived proteins was removed and replaced with: fresh medium (DMEM + 0,5% FBS) containing cold leucine (control conditions), medium containing 20 mM NH_4Cl (total lysosomal proteolysis) or medium containing 10 mM 3MA (macroautophagic degradation). The lysosomal degradation that remains unaffected by the use of 3MA was attributed to the CMA pathway, after the assumption that microautophagy can be considered minor (Kaushik and Cuervo 2009).

Aliquots of the medium were taken at 16 hrs after labeling and proteins in the medium were precipitated with 20% thrichloroacetic acid (TCA) for 20 min on ice and centrifuged (10.000 X g, 10 min, 4ºC). Radioactivity in the supernatant (representing degraded proteins) and pellet (representing undegraded proteins) was measured in a liquid scintillation counter (Wallac T414, Perkin Elmer). At the last time point, cells were lysed a mild lysis buffer, containing 0,1 N NaOH and 0,1% sodium deoxycholate. Proteolysis was expressed as the percentage of the initial total acid-precipitable radioactivity (protein) in the cell lysates transformed to acid soluble radioactivity (amino acids and small peptides) in the medium during the incubation (Kaushik and Cuervo 2009).

14. Proteasome Activity Assay

OLN cells were treated with 0.5 μg of haSyn PFFs for 48 hrs and the measurement of the CT-like enzymatic activity was accomplished with the use of the fluorescent properties of the synthetic peptide Suc-LLVY-AMC, as previously described (Emmanouilidou, Stefanis et al. 2010). Suc-LLVY-AMC is a proteasomal substrate that releases a fluorescent molecule (AMC) after cleavage, with emission at 437 nm. The reaction was performed in 5 μg of total protein lysate, with the addition of a resuspension buffer [50 mM Tris-HCl with pH 7.6, 5 mM DTT, 10 mM ATP and 50mM $MgCl_2$] and 100 μM of the fluorogenic substrate, followed by an incubation at 37° for 10 min. Reaction was terminated by addition of 5% SDS and the released fluorescence was calculated with a PerkinElmer LS-55 luminescence spectrophotometer.

15. Isolation of lysosomes

To validate that TPPP/p25α is a CMA substrate, brain lysosomes were isolated from starved Sprague Dawley rats, as previously described (Storrie and Madden 1990; Cuervo, Dice et al. 1997). Tissue was homogenized in 0.25 M sucrose (Applichem, A4734) and the lysosomes were removed from the light mitochondrial fraction using a Nycodenz (Ncd) density gradient after an ultracentrifugation at 141,000 x g for 1 hr. To examine the integrity of the isolated lysosomes, the enzymatic activity of β-hexosaminidase was measured and only when less of 10% of the lysosomes were broken the process could proceed. In our experiments the ability of isolated lysosomes to degrade recombinant TPPP/p25α was explored via western blot analysis using LAMP1, LAMP2A and cathepsin D (CTSD) as lysosomal markers.

16. CMA of recombinant TPPP/p25α by isolated lysosomes

Transport of human recombinant TPPP/p25α into isolated rat brain lysosomes was analyzed using an in vitro system as previously described (Xilouri, Brekk et al. 2016). Briefly, 0.2 μg of

recombinant TPPP/p25α were incubated with freshly isolated rat brain lysosomes in MOPS buffer (10 mM 3-[N-morpholino] propanesulfonic acid, [Sigma-Aldrich, M1254] pH 7.3, 0.3 M sucrose [Applichem, A4734]), in the presence of 0.6 μg recombinant HSPA8/HSC70 (Enzo Life Sciences, AD1-SPP-751-D) for 20 min at 37ºC. Where indicated, lysosomes were pre-incubated with a cocktail of proteinase inhibitors (Roche, 11836153001) for 10 min at 0ºC. A competition assay utilizing 3x (0.6 μg) and 6x (1.2 μg) amount of human recombinant aSyn, a well-established CMA substrate (Cuervo, Stefanis et al. 2004) was also performed to further verify the contribution of CMA to TPPP/p25α proteolysis. At the end of the incubation, lysosomes were collected by centrifugation, washed and subjected to SDS-PAGE and immunoblotted for TPPP/p25α, aSyn, LAMP1, LAMP2A, CTSD and β-actin.

17. Molecular Modelling

The amino acid sequence of the human TPPP/p25α was obtained from the UniProt database (accession no: O94811). Using the Gapped-BLAST through NCBI the homologous human protein with PDB id 2JRF was identified, which was used as template for the homology modelling. The homology modelling of the TPPP/p25α model was carried out using the RCSB entries 2JRF (human) and 1WLM (mouse) as template structures. The sequence alignment between the raw sequence of the all the above revealed more than 87% sequence identity, which allowed conventional homology modelling techniques to be applied. Electrostatic potential surfaces were calculated on grid points per side (65, 65, 65) and the grid fill by solute parameter was set to 80%. The dielectric constants of the solvent and the solute were set to 80.0 and 2.0, respectively. An ionic exclusion radius of 2.0Å, a solvent radius of 1.4Å and a solvent ionic strength of 0.145 M were applied. Amber99 charges and atomic radii were used for this calculation. Energy minimizations were used to remove any residual geometrical strain in each molecular system, using the Charmm27 forcefield as it is implemented into the MOE suite. Molecular systems were then subjected to unrestrained Molecular Dynamics Simulations (MDS) using the MOE suite. MDS took place in a SPC water-solvated, periodic environment. Water molecules were added using the truncated octahedron box extending 7Å from each atom. Molecular systems were neutralized with counter-ions as required. For the purposes of this study all MDS were performed using the NVT ensemble in a canonical environment, at 300 K and a step size equal to 2 femtoseconds for a total 100 nanoseconds simulation time. An NVT ensemble requires that the Number of atoms, Volume and Temperature remain constant throughout the simulation.

18. KFERQ-like motif discovery

The developed scoring methodology in an effort to identify hidden KFERQ-like motifs in TPPP/p25α that reads the primary amino acid sequence both from N' to C' term and vice versa. The methodology is based on the fusion and analysis of amino acid physicochemical and structural properties that resemble the reference properties of the KFERQ motif. We calculated 435 molecular and physicochemical descriptors (dimensions) for each amino acid in an effort to be able to confidently scan the sequence of TPPP/p25α for KFERQ-like motifs. Only the KKRFK pentapeptide was discovered that meets the criteria for a KFERQ-like motif. The acceptable thresholds for each dimension used were calibrated and trained based on the properties of KFERQ and all known and established KREFQ-like motifs. The KFERQ-like motifs included from literature were: KFERQ, RKVEQ, QEKRV, QDLKF, QRFFE, DRIKQ, IRDLQ, QDIRR, QEFVR, QKIIE, DLLRQ, QKDFR, DFRKQ, KDLLQ (Dice 1990). Therefore, the KFERQ likeness of KKRFK was based on an algorithm that has been trained on KFERQ and the 13 established KFERQ-like motifs. Our analysis exploits the dynamic and static information and metrics calculated in an effort to discover patterns and associations among them that will lead to induction of new rules updating the knowledge base and affecting the reasoning process. The combination of the multimodal data collected was used as new knowledge in the form of rules. These rules were exploited to update the reasoning system in order to make adaptive the reasoning processes, i.e., tailored to unique information and characteristics of each motif. Efficient mining of association rules generated a scaled quantification of KFERQ likeness based on 435 physicochemical dimensions. Not only our multimodal methodology on determining KFERQ-likeness, confirms that KKRFK is KFERQ-like based on 435 fused and analyzed physicochemical properties, but we also propose that our approach can be used as a standard of quantification of KFERQ-likeness henceforward.

19. Animals

Eight-week-old male WT C57BL6/C3H (WT-aSyn), C57BL6/JOlaHsd aSyn null (KO-aSyn) (purchased from Harlan Laboratories), or C57BL6 PLP-haSyn transgenic (kindly provided by Dr. Nadia Stefanova, Innsbruck University) mice were housed (6–8 animals/cage) with free access to food and water under a 12-hrs light/dark cycle. All experimental procedures were approved by the Ethics Committee for the Use of Laboratory Animals in the Biomedical Research Foundation of Athens.

20. Surgical procedures

All surgical procedures were performed under general isoflurane (B506; Abbott, Chicago, USA) anesthesia. Eight-week old male WT or KO aSyn mice were placed in a stereotaxic frame (Kopf Instruments, Tujunga, CA, USA) and the right dorsal striatum was targeted using the following coordinates from the bregma: +0.5 mm anteroposterior, −1.6 mm mediolateral, and − 3.4 mm dorsoventral according to the Mouse Brain Atlas (Xiong, Li et al. 2017). A total of 2 μL haSyn PFF solution (final concentration, 2 μg/μL) or PBS was injected unilaterally at a constant flow rate of 0.1 μL/15 s using a pulled glass capillary (diameter, 60–80 mm) attached to a Hamilton syringe with a 22-gauge needle. Following delivery of haSyn PFFs or PBS, the capillary was held in place for 5 min and removed slowly from the brain.

21. Immunohistochemistry and confocal microscopy

At 1 month post-injection, the animals were anesthetized with isoflurane followed by intracardial perfusion with ice-cold PBS and then ice-cold 4% paraformaldehyde solution (n = 4–5 animals/condition/genotype). The brains were removed and post-fixed for 24 hrs in the same preparation of paraformaldehyde and transferred to 15% sucrose for 24 hrs and finally in 30% sucrose until sectioning. The brains were sectioned through the coronal plane at 30 μm increments, and every section throughout the striatum and ventral midbrain was collected. Immunohistochemical staining was carried out in free-floating sections as described previously (Xilouri, Kyratzi et al. 2012) using the primary and secondary antibodies listed in **Table 2**.

22. Transmission electron microscopy (TEM)

22a. Negative staining

Specimens were prepared by adsorbing 5-μLdrops of fibrils (pre- and post-sonication) onto 200 mesh formvar-carbon film-bearing grids (Electron Microscopy Sciences, Hatfield, PA, USA), rinsing with water, and staining with a 2% w/w aqueous uranyl acetate solution for 2 min.

22b. Preparation of cultured cells for EM and immuno-EM

For conventional EM, the cells were fixed for 1 h in 2.5% glutaraldehyde (at 37°C) made up in 0.1M phosphate buffer (pH 7.4). After subsequent buffer washes, the cells were released from the dish by gentle scraping and pelleted at 800 x g for 5 min. The pellets were embedded in 4% low-melting-point agarose in 0.1 M phosphate buffer. After solidification, small cubes were cut and post-fixed with 1% osmium tetroxide for 1 hr on ice. After washing with the above buffer, the

samples were dehydrated in a graded ethanol series and embedded in an Epon/Araldite resin mixture. Ultrathin sections were cut with a DiATOME diamond knife at a thickness of 65 nm on a Leica EM UC7 ultramicrotome (Leica Microsystems, Vienna, Austria), mounted onto 300 mesh copper grids, and stained with uranyl acetate and lead citrate. For immuno-EM, the cells were fixed for 1 h in 3% paraformaldehyde/0.5% glutaraldehyde made up in 0.1 M phosphate buffer and processed as above. Post-embedding double immunogold labeling was performed on thin sections for the detection of human and rodent aSyn. Briefly, the grids were floated on a blocking solution (0.05 M Tris-HCl, pH 7.4, 1% bovine serum albumin [BSA], 0.1% cold water fish gelatin, 5% normal goat serum, 0.1% Tween 20) for 30 min. The grids were then incubated in a mixture of the LB-509 mouse monoclonal antibody (1:100) and D37A6 rabbit monoclonal antibody (1:100) diluted in Tris-HCl/BSA, overnight at 4°C. After several washes with Tris-HCl/BSA, the grids were incubated for 1 hr at room temperature in a mixture of goat anti-mouse IgG conjugated to 10-nm gold particles [1:40] and goat anti-rabbit IgG conjugated to 15-nm gold particles [1:40]. Finally, the grids were counterstained with ethanolic uranyl acetate and lead citrate.

22c. EM for myelin integrity

At 1 month post-injection, haSyn PFF-treated WT- and KO-aSyn mice (n = 4/genotype) were anesthetized and perfused transcardially with 0.1 M PBS (pH 7.2) at 37°C, with a flow rate of 10 mL/min for 5 min and then with a 4% paraformaldehyde/1% glutaraldehyde fixative mixture at the same rate for 15 min. The brain was removed and the ipsilateral striatum was dissected into small pieces and placed in fixative for 1 hr at 4°C. After subsequent buffer washes, the tissue was cut into small pieces and post-fixed in 1% osmium tetroxide/1.5% potassium ferrocyanide for 1 hr on ice to preserve myelin integrity further (Bernis, Babila et al. 2015). This was followed by immersion of the blocks in 2% glutaraldehyde for 1.5 hrs on ice. After washing, the samples were dehydrated and embedded in an Epon/Araldite resin mixture. Ultrathin sections (65 nm) were cut, mounted onto 300 mesh copper grids, and stained with uranyl acetate and lead citrate as above. In all EM procedures, the grids were examined in a Philips 420 transmission electron microscope at an acceleration voltage of 60 kV and photographed with a Megaview G2 CCD camera (Olympus SIS, Münster, Germany) and iTEM image capture software. In order to assess myelin integrity in the PFF-injected mice striatum, we quantified the g ratio (ratio of inner axonal diameter to total outer diameter) and the % of axons with decompacted myelin (Payne, Bartlett et al. 2012). For these quantifications, at least 100 randomly selected myelin sheaths that were cross-sectioned completely without artifacts and could be classified without doubt were counted. Semi-automated analysis of randomly selected myelin sheaths was carried out using a plug-in for ImageJ software as previously described (Cruz-Martinez, Gonzalez-Granero et al. 2016).

23. Autopsy case material

Human brain tissue was obtained through the University of Florida Neuromedicine Human Brain Tissue Bank according to protocols approved by the Institutional Review Board. Post-mortem pathological diagnoses were made according to standard neuropathological criteria (McKeith, Dickson et al. 2005; Trojanowski and Revesz 2007). Cerebellar samples containing GCIs from three MSA cases were studied including the two major pathological subtypes: striatonigral degeneration and olivopontocerebellar atrophy. The cingulate cortex and midbrain containing cortical and brainstem Lewy Bodies (LBs), respectively, from three dementia with Lewy bodies (DLB) cases with concurrent Alzheimer's disease pathology were also utilized.

24. Immunohistochemistry and semi-quantitative scoring

Immunostaining of the sections was performed using standard methods (Duda, Giasson et al. 2000). The sections were rehydrated and subsequent antigen retrieval was performed in a steam bath for 30 min in a 0.2% Tween-20 solution for all antibodies utilized. Non-specific antibody binding was minimized with a 2% fetal bovine serum/0.1 M Tris blocking solution; primary antibodies were diluted in the blocking solution and applied to tissue sections at 4 °C overnight. Biotinylated secondary antibodies (Vector Laboratories, Burlingame, CA, USA) were diluted in the blocking solution and applied to the sections for 1 hr at room temperature. An avidin–biotin complex system (VECTASTAIN ABC Elite Kit; Vector Laboratories, Burlingame, CA, USA) was used to enhance detection of the immunocomplexes, which were visualized using the chromogen 3,3′-diaminobenzidine (DAB Kit; KPL, Gaithersburg, MD, USA). For comparison, all MSA and DLB sections were exposed to DAB for the same amount of time for a given antibody. Tissue sections were counterstained with hematoxylin. All slides were digitally scanned using an Aperio ScanScope CS instrument (40× magnification; Aperio Technologies Inc., Vista, CA, USA), and images of representative areas of pathology were captured using ImageScope software (40×magnifcation; Aperio Technologies, Inc., Vista, CA, USA). Inclusion pathology was observed and assessed qualitatively and confirmed independently by a second observer.

25. Statistical analysis

All statistical analysis was performed utilizing GraphPad Prism 5. To be more specific, differences between or within groups were assessed by unpaired t-test, one-way analysis of variance (ANOVA) with Tukey's post hoc test and two-way ANOVA followed with Bonferroni's correction. Results are displayed as the mean ± standard error (SE), with a p value of < 0.05 defined as statistically significant. Image acquisition and analysis were performed by two independent examiners blinded

to the true identity of the samples. Results are based on the analysis of three independent experiments with at least duplicate samples/condition within each experiment.

26. Tables

Table 1: A table depicting the primary and secondary antibodies used either in western blotting or immunocytochemistry/immunohistochemistry including species reactivity and working dilutions.

Primary antibodies against	Clone	Cat. No.	Working Dilutions		Species Reactivity	Company
			WB	ICC/IHC		
human aSyn	LB-509*	807701	-	1/1000	mouse	Biolegend
	4B12	GTX21904	1/1000	-	mouse	GeneTex
	211	sc-12767	-	1/1000	mouse	Santa Cruz
total aSyn	C20	sc7011R	1/1000	1/1000	rabbit	Santa Cruz
	D10	sc-515879	-	1/1000	mouse	Santa Cruz
	3H2897	sc-69977	-	1/1000	mouse	Santa Cruz
	-	PA5-16738		1/1000	rabbit	Invitrogen
	SYN-1	610786	-	1/1000	mouse	BD Transduction Laboratories
rodent aSyn	D37A6*	4179	1/1000	1/400	rabbit	Cell Signaling
oxidized/nitrated	SYN303	824301	-	1/1000	mouse	Biolegend
aggregated aSyn	MJFR-14-6-4-2	ab209538	-	1/1000	rabbit	Abcam
pSer129 aSyn	EP1536Y	ab51253	1/1000	1/200	rabbit	Abcam
	LS4-2G12		-	1/1000	mouse	
	11A5		-	1/10000	mouse	Imago Pharmaceuticals
p25α			1/1000	1/400	rabbit/rat	
LC3		PM036	1/1000	-	rabbit	MBL
LC3B		NB100-2220	-	1/200	rabbit	Novus
SQSTM1/p62		PM045	1/1000	-	rabbit	MBL
Ubiquitin		Z0458	1/1000	-	rabbit	DAKO
β-actin		TA309077	1/2000	-	mouse	OriGene
Olig-2		AB9610	-	1/500	rabbit	Millipore
O4		MAB1326	-	1/100	mouse	RD Systems
MPB		MCA409S	1/500	1/200	rat	Biorad
α-tubulin		62204	-	1/750	mouse	62204
phospho-Ser404 tau		AP02404PU-N	-	1/1000	rabbit	Acris
GFAP		ab4674	-	1/1500	chicken	Abcam
AIF-1		019-19741	-	1/1000	rabbit	DAKO
Secondary antibodies		**Cat. No.**	**Working Dilutions**		**Species Reactivity**	**Company**
			ICC/IHC			
CF555 red		20033	1/2000		rabbit	Biotium
		20030	1/2000		mouse	Biotium
		20096	1/2000		rat	Biotium
CF488A green		20012	1/2000		rabbit	Biotium
		20010	1/2000		mouse	Biotium
Cy5		115- 175-146	1/400		mouse	Jackson Imm.Affinipure
		111-175-144	1/400		rabbit	Jackson Imm.Affinipure
Dyes		**Cat. No.**	**Working Dilutions**			**Company**
			ICC/IHC			
DAPI		10236276001	1/1000			Signa-Aldrich
Wheat Germ Agglutinin		w11262	1/1000			Thermo Scientific
***working dilutions for EM analysis = 1/100**						

Table 2: A table depicting the sequences of the siRNAs targeting the rat Lamp2a, as well as the rat SNCA, human SNCA, TPPP/p25α rat Gapdh and rat β-actin primer sequences utilized in the RT-PCR.

Target name	**siRNA design**
Rat *Lamp2a* siRNA sense (1) (Lsi1)	CCAUCAUACUGGAUAUGAGdTdT
Rat *Lamp2a* siRNA antisense (1) (Lsi1)	CUCAUAUCCAGUAUGAUGGdTdT
Rat *Lamp2a* siRNA sense (2) (Lsi2)	GGUCUCAAGCGCCAUCAUAdTdT
Rat *Lamp2a* siRNA antisense (2) (Lsi2)	UAUGAUGGCGCUUGAGACCdTdT
Oligo name	**Primer sequence (5´→3´)**
Rat SNCA-Rev	TATCTTTGCTCCACACGGCT
Rat SNCA-For	GCCTTTCACCCCTCTTGCAT
huSNCA-Rev	CACCACACTGTCGTCGAATGG
huSNCA-For	CGCCTTGCCTTCAAGCCTTC
huTPPP/p25α-Rev (1)	CCGGACACATAGCCTGACTC
huTPPP/p25α-For (1)	GGGGTGACGAAAGCCATCTC
huTPPP/p25α-Rev (2)	CGAGATGGCTTTCGTCACCC
huTPPP/p25α-For (2)	AAGTCTTGCCGGACCATCAC
Rat *Gapdh*-Rev	TTCAGCTCTGGGATGACCTT
Rat *Gapdh*-For	TGCCACTCAGAAGACTGTGG
Rat β-actin-Rev	CCACCAATCCACACAGAG
Rat β-actin-For	TGGCTCCTAGCACCATGA

IV. RESULTS

1. **Internalization of haSyn preformed fibrils (PFFs) by oligodendroglial cell lines leads to the formation of Triton-insoluble aSyn species**

In order to assess the uptake and seeding capacity of haSyn PFFs in oligodendroglial cells, we initially utilized the immortalized rat OLN-93 cell line, which expresses very low to non-detectable levels of endogenous aSyn and p25α, and the stable cell lines OLN-AS7 and OLN-p25α, which overexpress human WT-aSyn and p25α, respectively (**Figure 15A**). Stable or transient overexpression of haSyn and p25α in OLN cells was not accompanied by changes in cell viability (**Figure 15B, bottom**). Electron Microscopy was used to monitor fibril morphology and to confirm the presence of fibrils (**Figure 15C**). Treatment of OLN-93 cells with 0.2 and 0.5 μg haSyn PFFs for 48 hrs, led to the dose-dependent accumulation of SDS- and urea-soluble high molecular weight (HMW) aSyn species (**Figure 15D**). The uptake of haSyn PFFs was further verified by staining the lectins of the plasma membrane using wheat germ agglutinin (WGA) (**Figure 15E**).

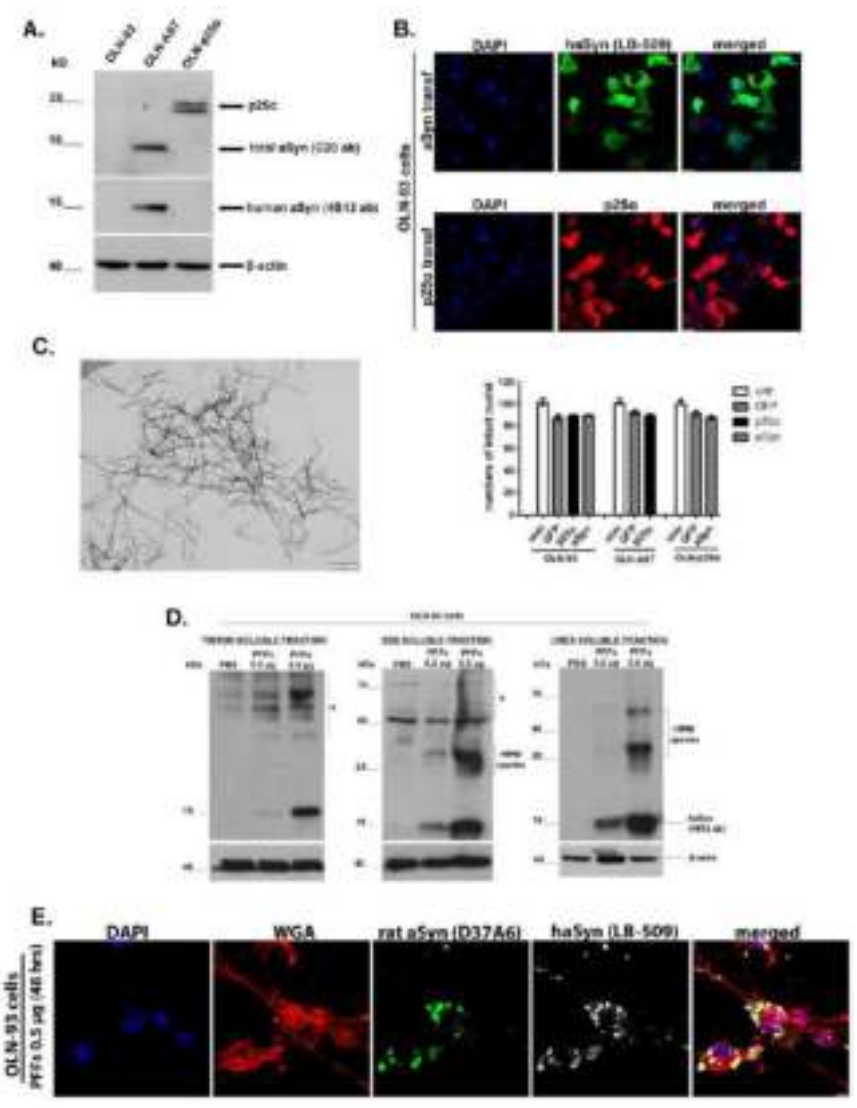

Figure 15: Human aSyn PFFs are taken up by oligodendroglial cell lines and colocalize with endogenous rat aSyn. (**A**) OLN-AS7 and OLN-p25α cells overexpress human aSyn and p25α proteins, respectively. Representative immunoblots for p25α, haSyn (human-specific antibody 4B12), total aSyn (C20 antibody, recognizes endogenous and human aSyn), and β-actin as a loading control in the Triton-soluble fraction. (**B**) (upper rows) Representative immunofluorescence images of OLN-93 cells transfected with haSyn or p25α plasmids for 48 hrs using antibodies against haSyn (green, LB-509 antibody, upper panel) or p25α (red, bottom panel). (bottom row) Quantification of cell viability following transfection of all OLN cell lines with GFP, haSyn of p25α plasmids for 48 hrs. Data are expressed as the mean ± SE of at least three independent experiments with triplicate samples/condition within each experiment. (**C**) Transmission EM image of negative stained haSyn PFF samples confirming the presence of fibrils. Scale bar: 500 nm. (**D**) Biochemical profile of aSyn species formed in OLN-93 cells following the addition of 0.2 and 0.5 μg recombinant haSyn PFFs or PBS as a control at 48 hrs post-addition. Representative immunoblots for both monomeric and HMW species of aSyn (human-specific antibody 4B12) and β-actin as a loading control in Triton-, SDS-, and urea-soluble fractions. Asterisk represents non-specific bands obtained with the human-specific 4B12 antibody (detected also in PBS-treated OLN-93 cells in which no haSyn was present). (**E**) aSyn aggregates, composed of human and endogenous rat aSyn, are located in the perinuclear space and cytoplasm of OLN-93 cells following the addition of 0.5 μg haSyn PFFs for 48 hrs. Representative immunofluorescence images with antibodies against endogenous rat aSyn (green, D37A6 antibody) and haSyn (gray, LB-509). Wheat germ agglutinin was used as a plasma membrane marker (red, WGA) and DAPI as a nuclear marker. Scale bar: 10 μm.

We used 0.5 μg haSyn PFFs in subsequent experiments, and we investigated the solubility and aggregation of internalized PFFs in the OLN cell lines over time (24-96 hrs). The Triton-soluble fraction of all cell lines contained only monomeric aSyn [detected with antibodies against human and total (human+rodent) aSyn] that showed the highest levels at 24 hrs post-addition, which was followed by a time-dependent decrease to baseline levels (PBS-treated cells), evident mostly in the control OLN-93 cells (**Figure 16A and Figure 18A, B**). This could be attributed either to the effective clearance of the formed aSyn species or to the dilution of exogenous aSyn due to cell proliferation.

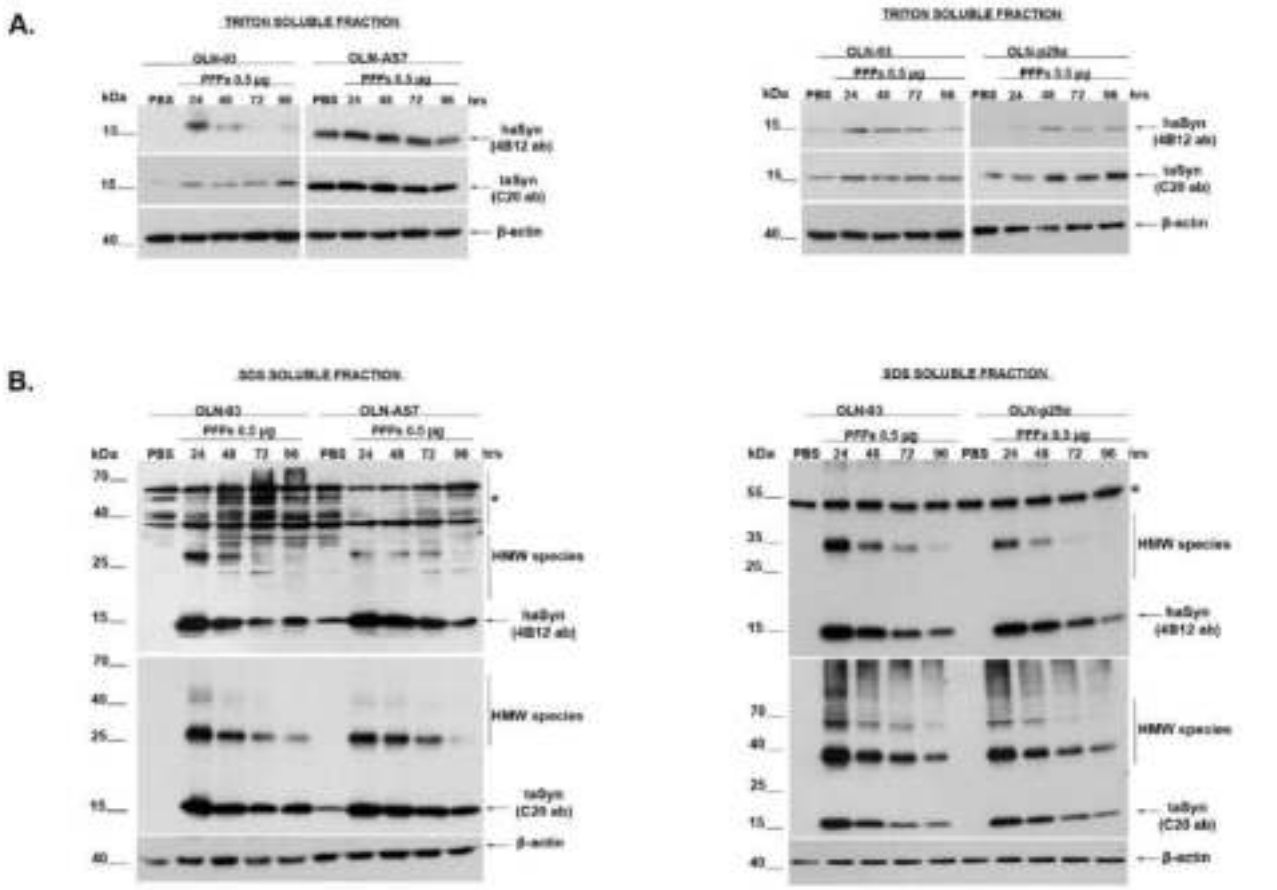

Figure 16: Pre-formed haSyn fibrils are taken up by oligodendroglial cell lines and evoke the formation of Triton-insoluble aSyn species. Representative immunoblots of Triton- and SDS-soluble protein fractions derived from OLN-93, OLN-AS7, and OLN-p25α cells treated with 0.5 μg of haSyn PFFs for various times (24–96 hrs). (**A**) A small fraction of human and total aSyn (detected with 4B12 and C20 antibodies, respectively) is present in the Triton-soluble fraction of OLN-93 and OLN-AS7 (left panel) or OLN-p25α cell lysates (right panel). (**B**) Monomeric and high molecular weight (HMW) aSyn species (human and total) are detected in the SDS-soluble fractions, following the addition of haSyn PFFs, thus representing rather insoluble aSyn species in OLN-93 and OLN-AS7 (left panel) or OLN-p25α cell lysates (right panel). Equal loading was verified by the detection of β-actin levels. Asterisk represents non-specific bands obtained with the human-specific 4B12 antibody (also detected in the PBS-treated OLN-93 or OLN-p25α cells where no human aSyn was present).

Notably, monomeric aSyn levels detected in the Triton-soluble fraction of OLN-AS7 cells remained high over time, possibly due to the stable overexpression of the human protein in these cells, whereas in the OLN-p25α cells both exogenously added human and total aSyn remained at

higher levels than in the OLN-93 cells. HMW-aSyn species were detected mostly in the SDS- and urea- soluble fractions (**Figure 16B, 17A**), thus representing rather insoluble aSyn species. Similar to the Triton-soluble fraction, in the SDS-soluble fraction, the peak levels of monomeric and HMW aSyn were observed at 24 hrs in all cell lines, followed by a gradual decrease over time (48-96 hrs); however, they remained at higher levels than in the PBS-treated cells (**Figure 16B and Figure 18C-F**). Interestingly, in the urea-soluble fraction of OLN-p25α cells, aSyn monomeric and oligomeric forms (both human and total) were relatively resistant to degradation, since their levels remained high compared to control OLN-93 cells, in which their levels decreased over time (**Figure 17A-C**). This could be indicative of a role for p25α in promoting aSyn aggregate formation within oligodendrocytes or in inhibiting the clearance of aSyn aggregates.

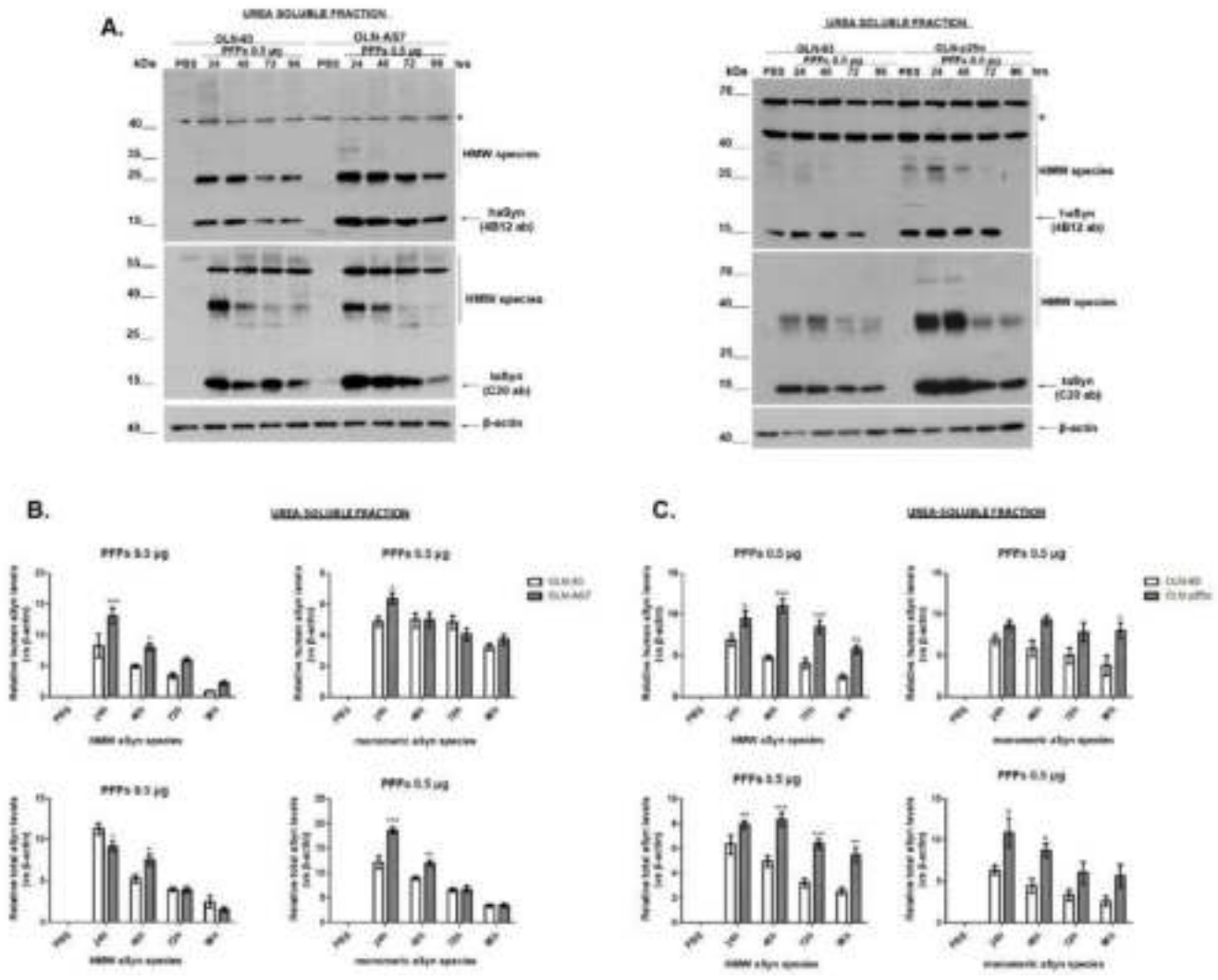

Figure 17: (**A**) **Monomeric and high molecular weight (HMW) aSyn species (human and total) are detected in the urea-soluble fractions, following the addition of haSyn PFFs, thus representing rather insoluble aSyn species in OLN-93 and OLN-AS7 (left panel) or OLN-p25α cell lysates (right panel).** Equal loading was verified by the detection of β-actin levels. Asterisk represents non-specific bands obtained with the human-specific 4B12 antibody (also detected in the PBS-treated OLN-93 or OLN-p25α cells where no human aSyn was present). **B, C** Quantification of monomeric and HMW species of human (upper panels) and total (lower panels) aSyn levels detected in the urea-soluble fraction of OLN-93 and OLN-AS7 cells (**B**) or OLN-93 and OLN-p25α cells (**C**) treated with 0.5 μg PFFs for 24-96 hrs. Data are expressed as the mean±SE of five independent experiments with triplicate samples/condition within each experiment; *p< 0.05; **p< 0.01; ***p<0.001, by two-way ANOVA with Bonferroni's correction, comparing between OLN-93 and OLN-AS7 or OLN-p25α cells treated with haSyn PFFs at all time points.

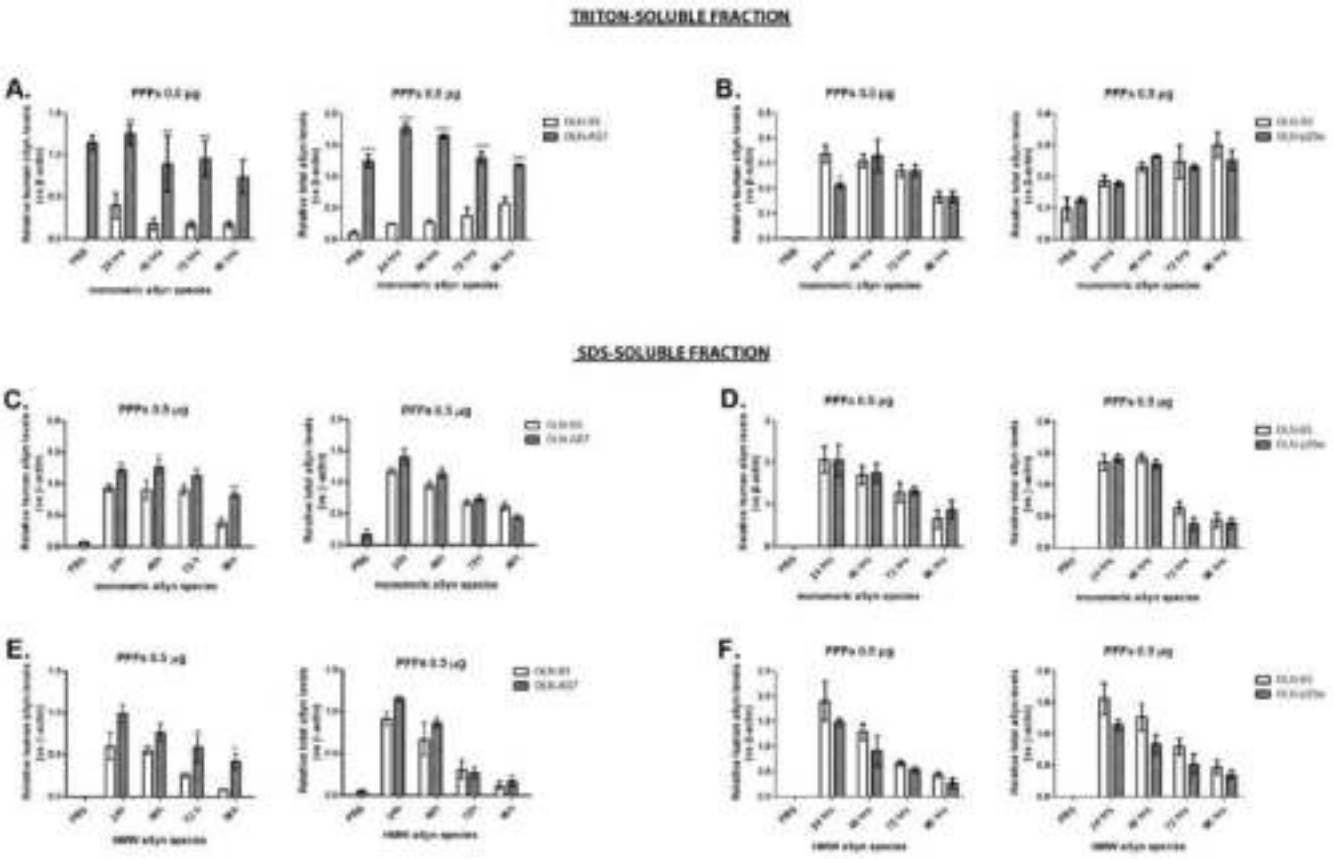

Figure 18: Quantification of relative human and total aSyn levels (monomeric and HMW species) in the Triton- and SDS-soluble fraction of OLN cells treated with 0.5 μg haSyn PFFs. **A, B** Quantification of monomeric human (left panels) and total (right panels) aSyn levels detected in the Triton-soluble fraction of OLN-93 and OLN-AS7 cells (**A**) or OLN-93 and OLN-p25α cells (**B**) treated with 0.5 μg haSyn PFFs (or PBS as a control) for 24-96 hrs. **C-F** Quantification of monomeric (upper panels) and HMW species (bottom panels) of human (left) and total (right) aSyn protein levels detected in the SDS-soluble fraction of OLN-93 and OLN-AS7 cells (**C** and **E**) or OLN-93 and OLN-p25α cells (**D** and **F**) treated with 0.5 μg haSyn PFFs (or PBS as a control) for 24-96 hrs. Data are expressed as the mean ± SE of five independent experiments with triplicate samples/condition within each experiment; *$p < 0.05$; **$p < 0.01$; ***$p < 0.001$, by two-way ANOVA with Bonferroni's correction, comparing between OLN-93 and OLN-AS7 or OLN-p25α cells treated with haSyn PFFs at all time points.

2. Addition of haSyn PFFs to OLN cell lines recruits endogenous rat oligodendroglial aSyn into the formation of highly insoluble aSyn conformations

In order to investigate the ability of haSyn PFFs to act as a template for endogenous oligodendroglial aSyn to form insoluble protein species, we utilized the rodent-specific D37A6 antibody in western blot and confocal microscopy analyses. This antibody does not give any immunofluorescence signal in PBS-treated OLN cells (**Figure 19A and Figure 21**); the addition of 0.5 μg haSyn PFFs, which had no effect on OLN-cell survival as shown in **Figure 22**, was accompanied by the detection of an elevated endogenous aSyn signal, which co-localized with the exogenously added human aSyn, that persisted over time (48 hrs-10 days) and depended, in terms of its intensity, on the exogenously added human material (**Figure 23**). The uptake of haSyn PFFs was further verified by ultrastructural EM analysis, which revealed the presence of filaments in the cell soma of OLN-93 cells treated with haSyn fibrils, which were absent in PBS-treated cells

(**Figure 19B**). Double immuno-EM analysis with nanogold particles of different diameters showed the presence of human and rat aSyn in the formed intracellular filamentous inclusions (**Figure 19B**). Measurement of human or rat endogenous aSyn levels, expressed as % of surface area normalized to the total number of cells/field, revealed no significant differences among the different OLN cells, at 48 hrs and 10 days post-addition of 0.5 μg haSyn PFFs (**Figure 19C**).

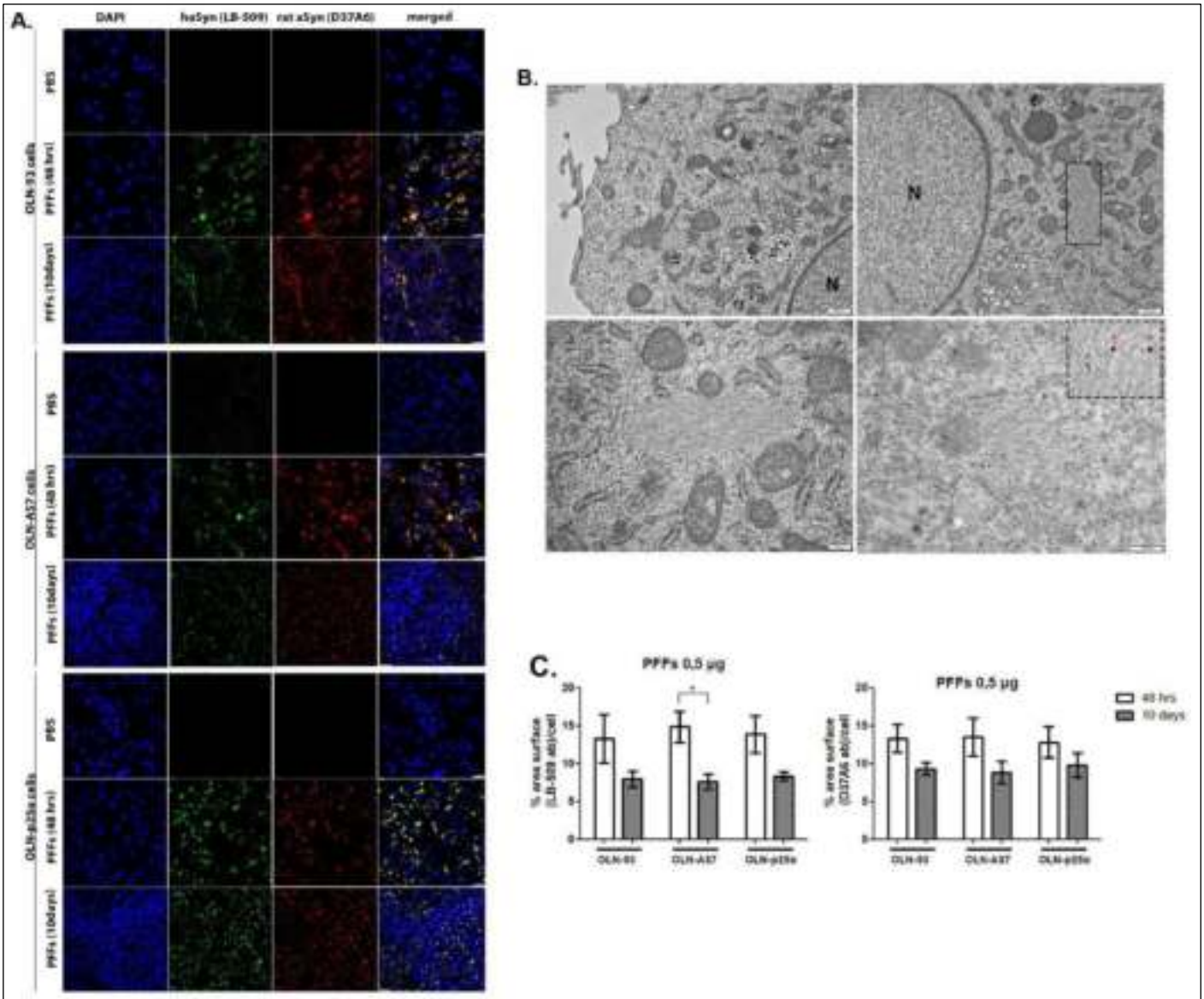

Figure 19: Addition of haSyn PFFs in OLN cell lines leads to the recruitment of endogenous rat oligodendroglial aSyn into highly insoluble aSyn assemblies. (**A**) Representative immunofluorescence images using antibodies against human aSyn (green, LB509 antibody) and endogenous rat aSyn (red, D37A6 antibody) and DAPI staining in OLN cell lines treated with 0.5 μg of haSyn PFFs for 48 hrs and 10 days. Scale bar: 25 μm. (**B**) (Upper panels) ultrastructural transmission EM analysis of PBS-treated (upper left) and haSyn PFFs-treated (upper right) OLN-93 cells showing the presence of filaments (box highlight) in the cell soma near the nucleus of PFF-treated cells (N). (bottom left panel) A higher magnification image of the filaments of PFF-treated cultures is shown. (Box highlight, bottom right panel) double immuno-EM analysis with nanogold particles of different diameters, demonstrating the presence of both human (green asterisk, LB-509, 10 nm) and rodent (red asterisk, D37A6, 15 nm) aSyn in the formed filamentous inclusions in the cell soma of OLN-93 cells. A highpower image of independent PFF-treated cultures is shown in the upper dashed box. Scale bars: 500 nm (upper), 200 nm (bottom) and 100 nm (highlight box). (**C**) Quantification of aSyn levels (human and endogenous rat) measured as % area surface/cell in OLN cell lines following treatment with 0.5 μg PFFs for 48 hrs or 10 days. Data are expressed as the mean±SE of three independent experiments with triplicate samples/condition within each experiment. *p<0.05 by two-way ANOVA with Bonferroni's correction.

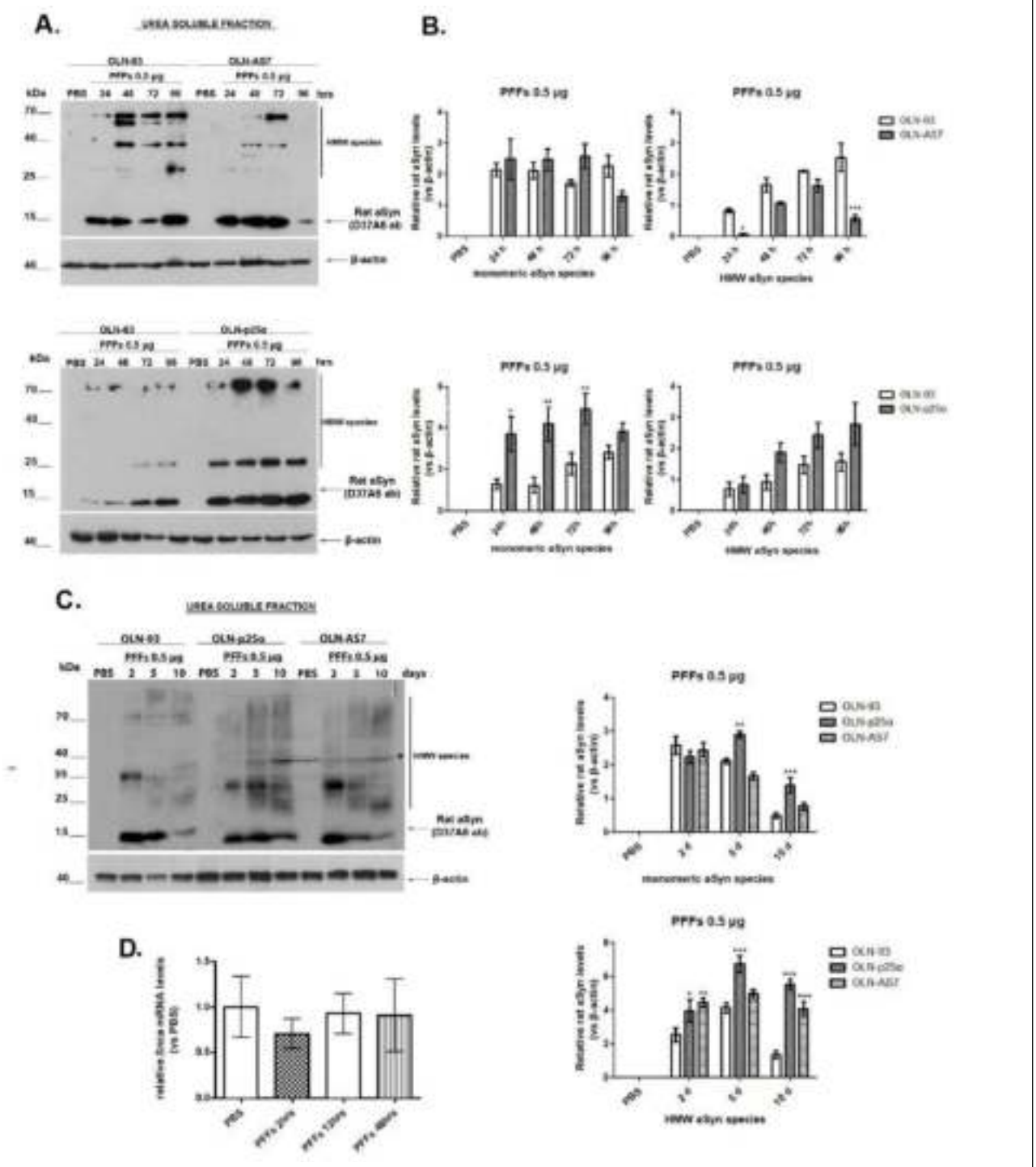

Figure 20: (A) Representative immunoblots demonstrating the presence of endogenous rat aSyn (D37A6 antibody) in the urea-soluble fraction of OLN-93 and OLNAS7 cells (upper panel) or OLN-p25α cells (bottom panel) following treatment with 0.5 μg haSyn PFFs for 24–96 hrs**.** Equal loading was verified by the detection of β-actin levels. (**B**) Quantification of monomeric (left) and HMW species (right) of endogenous rat aSyn levels detected in the urea-soluble fraction of OLN-93 and OLN-AS7 cells (upper row) or OLN-93 and OLN-p25α cells (bottom row) treated with 0.5 μg PFFs for 24–96 h. Data are expressed as the mean ±SE of five independent experiments with triplicate samples/condition within each experiment. *p< 0.05; **p<0.01; ***p<0.001, by two-way ANOVA with Bonferroni's correction. (**C**) (Left panel) representative immunoblots of urea-soluble protein fraction derived from OLN-93, OLN-AS7 and OLN-p25α cells treated with 0.5 μg of haSyn PFFs for 2–10 days. Asterisk represents non-specifc bands obtained with the rodent-specifc D37A6 antibody. (right) Quantification of monomeric (upper row) and HMW species (bottom row) of rat endogenous aSyn detected in the urea-soluble fraction of all OLN cell lines treated with 0.5 μg PFFs for 2–10 days. Data are expressed as the mean ±SE of three independent experiments with triplicate samples/condition within each experiment; *p<0.05; **p<0.01; ***p<0.001, by two-way ANOVA with Bonferroni's correction, comparing between OLN-93 and OLN-AS7 or OLN-p25α cells treated with haSyn PFFs. (**D**) Quantitative real-time PCR reveals unaltered *Snca* levels upon treatment of OLN-93 cells with 0.5 μg haSyn PFFs for 2–48 h. Data are expressed as *Snca* mRNA levels relative to the mRNA levels of β-actin normalized to control-treated cultures (PBS).

Similarly, in the urea-soluble fraction of OLN-p25α cells from 24 hrs to 10 days post-addition of haSyn PFFs, higher levels of monomeric and HMW forms of endogenous rodent aSyn were found compared to OLN-93 and OLN-AS7 cells (**Figure 20A-C**). No rat-specific signal was detected in the Triton- or the SDS-soluble fractions at 24hrs to 10 days post-addition of haSyn PFFs (data not shown). The elevated levels of endogenous aSyn detected following treatment of OLN cells with haSyn PFFs were not attributed to increased transcription of the rat *Snca* gene, encoding endogenous oligodendroglial aSyn, as revealed by quantitative real-time-PCR analysis (**Figure 20D).** The specificity of the D37A6 aSyn antibody to recognize only the rodent protein was validated further by confocal microscopy and western immunoblotting, utilizing human SH-SY5Y dopaminergic cells inducibly overexpressing the WT-aSyn upon the removal of doxycycline (dox) (Vekrellis, Xilouri et al. 2009) and extracts from WT-, KO-, and hA53T-aSyn transgenic mice (**Figure 25A, B**).

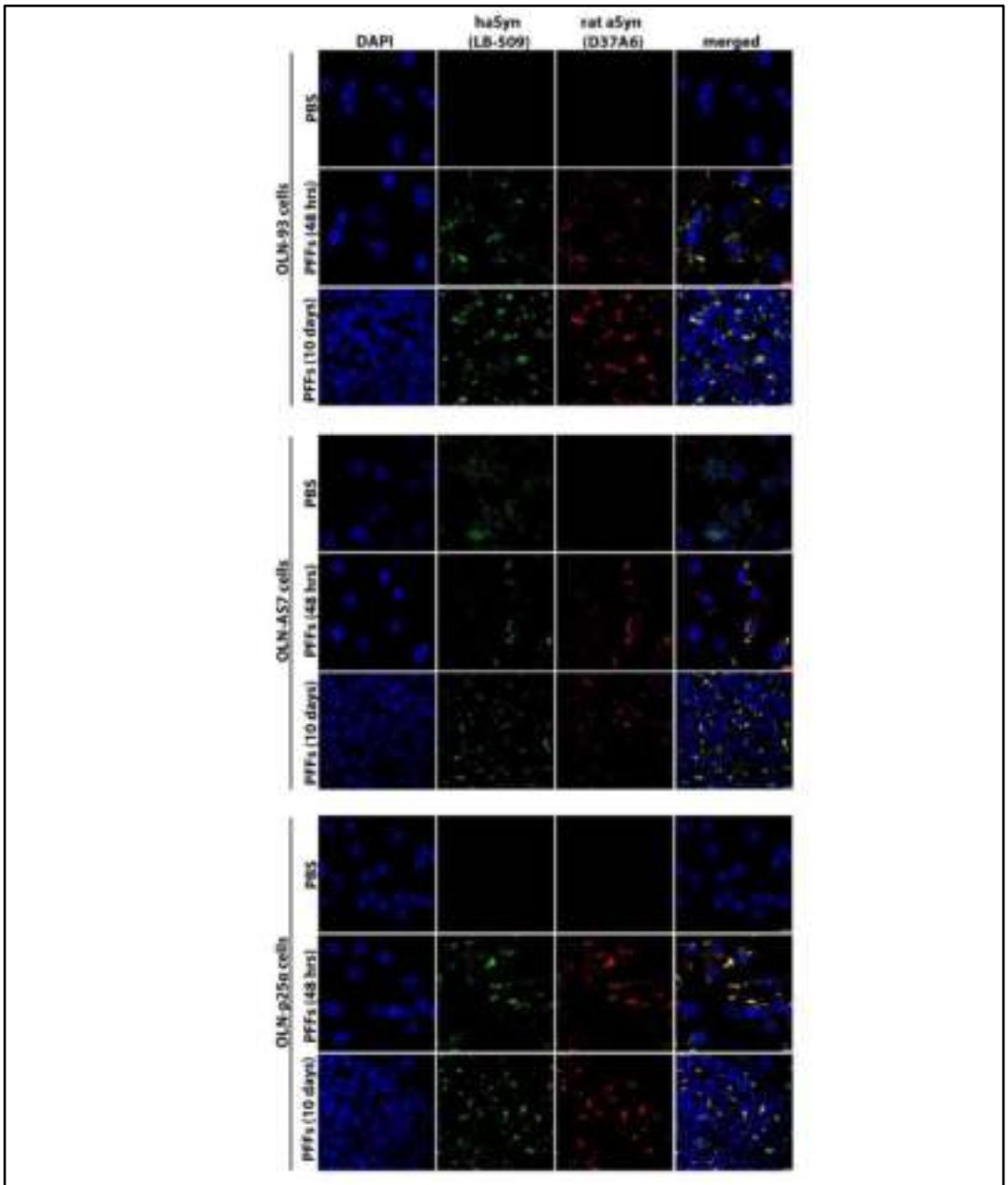

Figure 21: High-power images demonstrating the recruitment of endogenous rat aSyn in all OLN cell lines following the addition of 0.5 μg of haSyn PFFs for 48 hrs and 10 days using antibodies against haSyn (green, LB-509 antibody) and endogenous rat aSyn (red, D37A6 antibody) and DAPI staining. Scale bar: 10 μm.

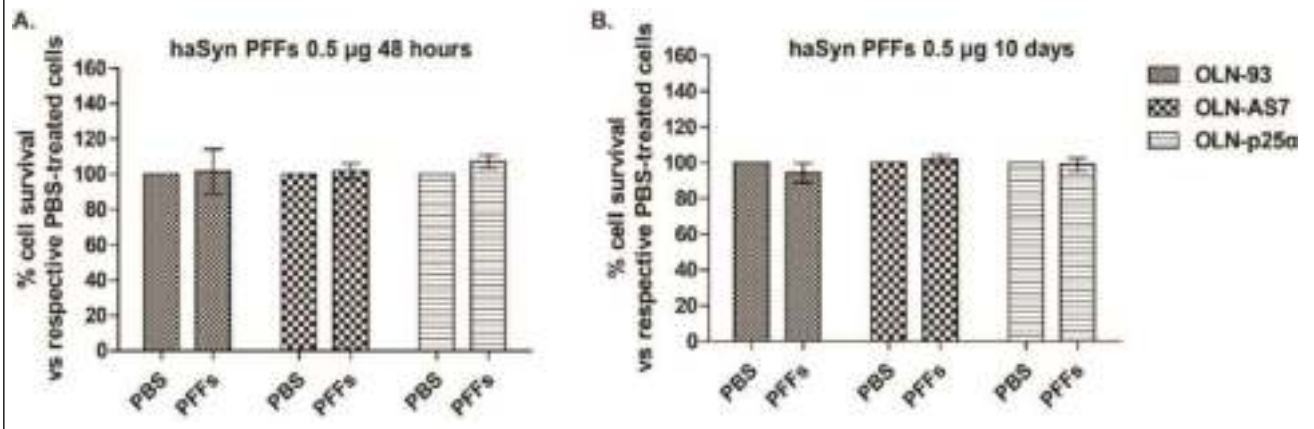

Figure 22: Short-term or prolonged incubation of OLN cells with haSyn PFFs does not affect their survival. Quantification of cell viability following addition of 0.5 µg haSyn PFFs in OLN-93, OLN-AS7 and OLN-p25α cells for 48 hrs (**A**) or 10 days (**B**).

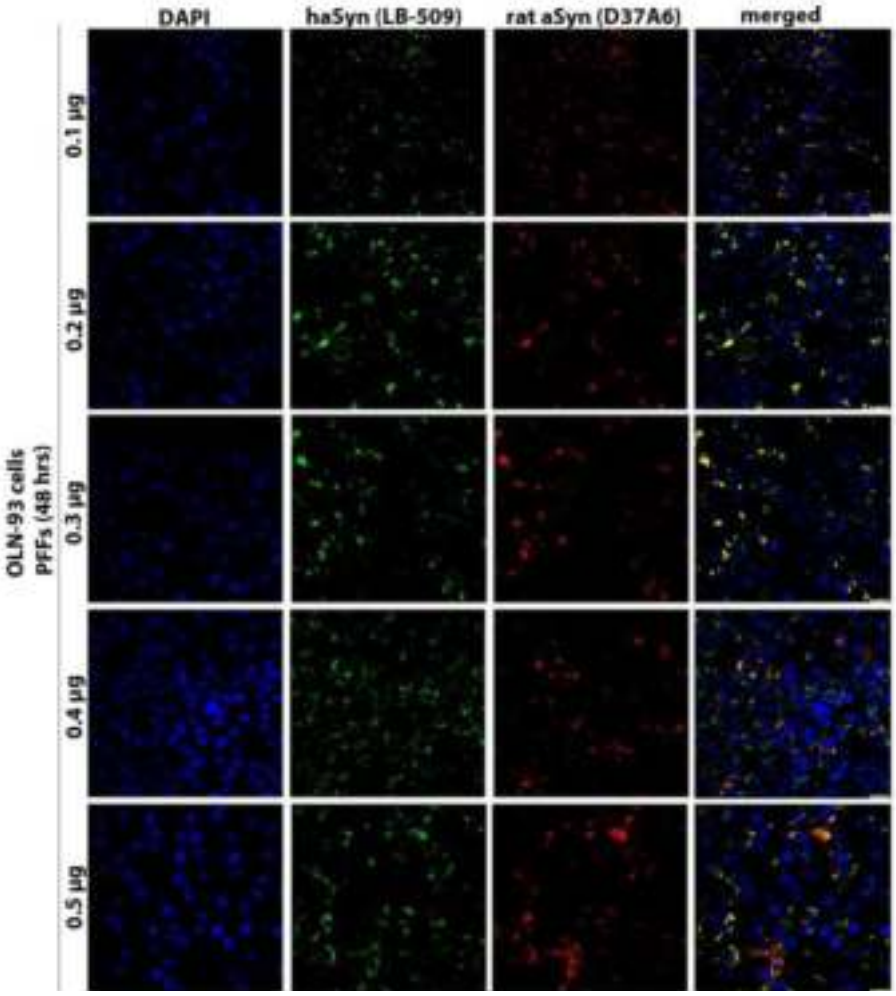

Figure 23: Co-localization of exogenously added haSyn with endogenous rat aSyn following the addition of increasing amounts of haSyn PFFs to OLN-93 cells. The endogenous rat aSyn signal is increased following the incubation of OLN-93 cells even with small amounts of haSyn PFFs (0.1 µg) for 48 hrs. Representative immunofluorescence images with antibodies against haSyn (green, LB-509 antibody) and endogenous rat aSyn (red) and DAPI staining. Scale bar: 25 µm.

In agreement with the immunoblot data (**Figure 17A-C**), OLN-p25α cells retained significantly more proteinase K-resistant human and rodent aSyn species compared to OLN-93 and OLN-AS7 cells (**Figure 24**).

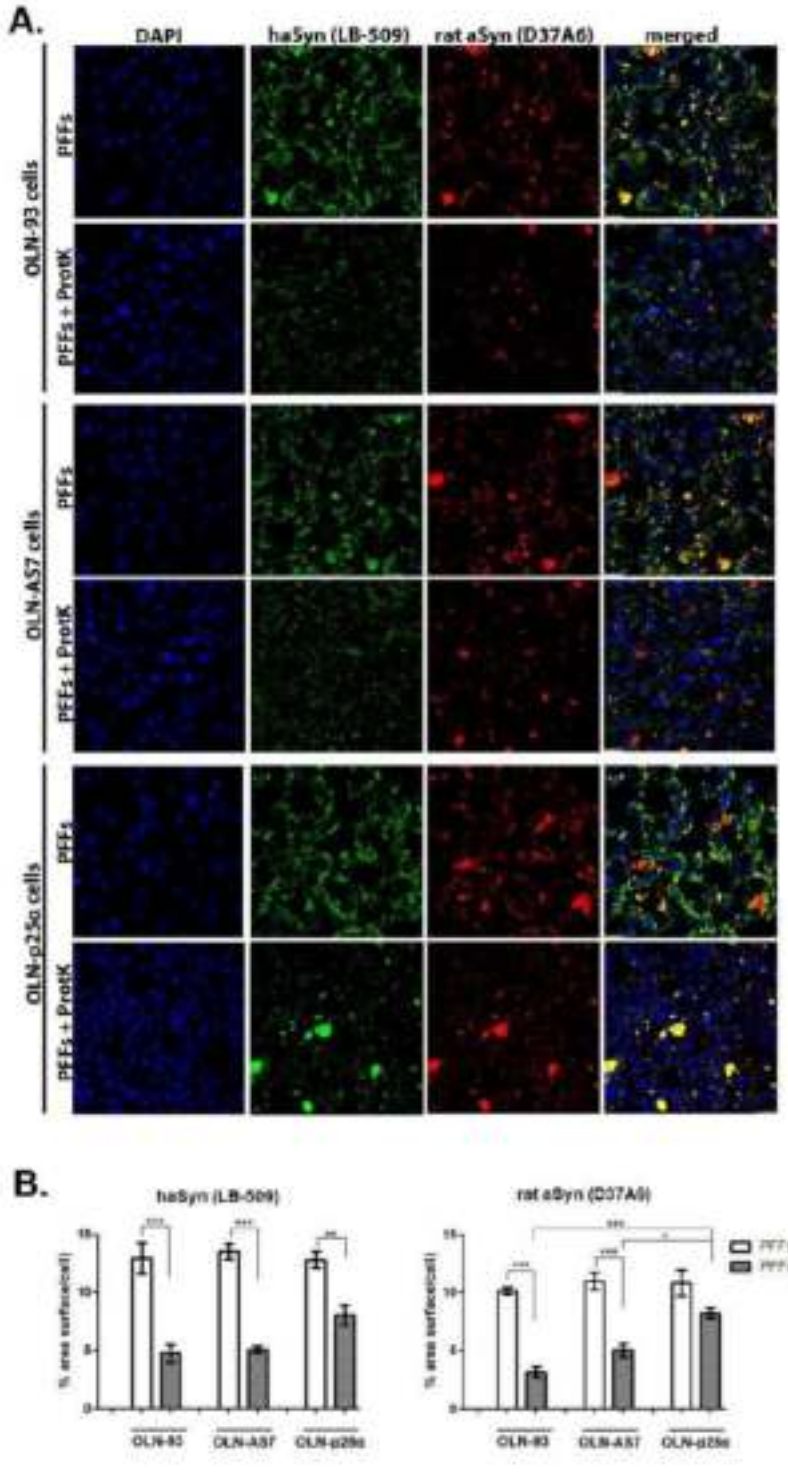

Figure 24: Stable overexpression of p25α promotes the formation of proteinase K-resistant aSyn inclusions formed following the addition of haSyn PFFs. (**A**) Representative immunofluorescence images using antibodies against haSyn (green, LB-509 antibody) and endogenous rat aSyn (red, D37A6 antibody) and DAPI staining in OLN cell lines treated with 0.05 µg/mL proteinase K for 15 min (PFF+ProtK) following the addition of 0.5 µg haSyn PFFs for 48 hrs. Scale bar: 25 µm. (**B**) Quantification of human (left) and endogenous rat (right) aSyn levels measured as % area surface/cell in PFF-treated (0.5 µg for 48 hrs) OLN cell lines without (PFFs) or following proteinase-K (PFF+ProtK) treatment. Data are expressed as the mean ± SE of three independent experiments with triplicate samples/condition within each experiment. *p < 0.05; **p < 0.01; ***p < 0.001 by two-way ANOVA with Bonferroni's correction.

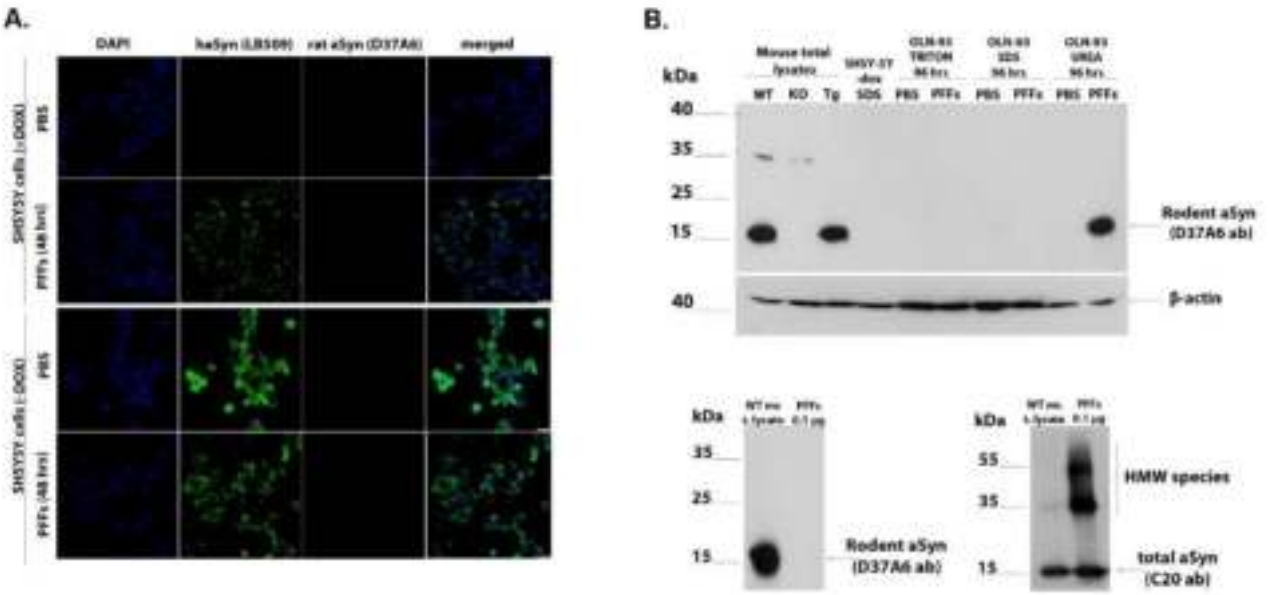

Figure 25: Specificity of the rodent-specific aSyn antibody D37A6. (**A**) Human SH-SY5Y cells inducibly over-expressing human aSyn were treated with 0.5 µg haSyn PFFs for 48hrs. No signal from the rodent-specific aSyn D37A6 antibody was detected. Representative immunofluorescence images with antibodies against haSyn (green, LB-509 antibody) and rodent aSyn (red) and DAPI staining. Scale bar: 25 µm. (**B**) (Upper panel) Representative immunoblots for rodent-specific aSyn and actin in: total brain lysates derived from mice expressing endogenous WT protein (WT-aSyn), mice overexpressing hA53T-aSyn in neurons (hA53T-aSyn), aSyn KO mice (KO-aSyn), SDS-soluble fraction of SH-SY5Y cells pre-treated with haSyn PFFs, and Triton-, SDS-, and urea-soluble fractions of rat OLN-93 cells treated with haSyn PFFs for 96 hrs. (Lower panel) Representative immunoblots for rodent aSyn (D37A6 antibody, left) and total aSyn (C20 antibody, right) in WT-aSyn mouse brain lysate run together with 0.1 µg haSyn PFFs, further confirming the specificity of the D37A6 aSyn antibody to recognize only endogenous rodent aSyn and not exogenously added human fibrils.

3. Overexpression of human aSyn or p25α accelerates the recruitment of the endogenous rat oligodendroglial aSyn and the formation of intracellular oxidized/nitrated aSyn species following the addition of haSyn PFFs

To decipher the impact of human aSyn or p25α overexpression on the seeding of aSyn pathology in OLN cells, we performed time-course analysis from 30 min until 24 hrs post-treatment. Confocal microscopy analysis with antibodies against human and rodent aSyn (LB-509 and D37A6 antibodies, respectively) revealed that haSyn PFFs were taken up effectively by all OLN cell lines within 1 hr, whereas the recruitment of the endogenous rat aSyn represented a later event (**Figure 26**). Interestingly, in control OLN-93 cells, the seeding process was initiated at 12 hrs post-treatment with the haSyn PFFs (**Figure 26A**), whereas in OLN-AS7 and OLN-p25α cells, the endogenous rat aSyn signal was detected earlier, at 2 hrs post-addition (**Figure 26B-C**). Importantly, the recruitment of endogenous rat aSyn evokes a dramatic change in the pattern of haSyn immunostaining and an increase in haSyn immunoreactivity, measured as % area surface/cell, at the onset of seeding (**Figure 26**). This observation suggests a possible role for the seeded rat aSyn in the rapid formation of aSyn aggregates positive for both human and rodent aSyn or in the stabilization of haSyn aggregates, rendering them resistant to degradation.

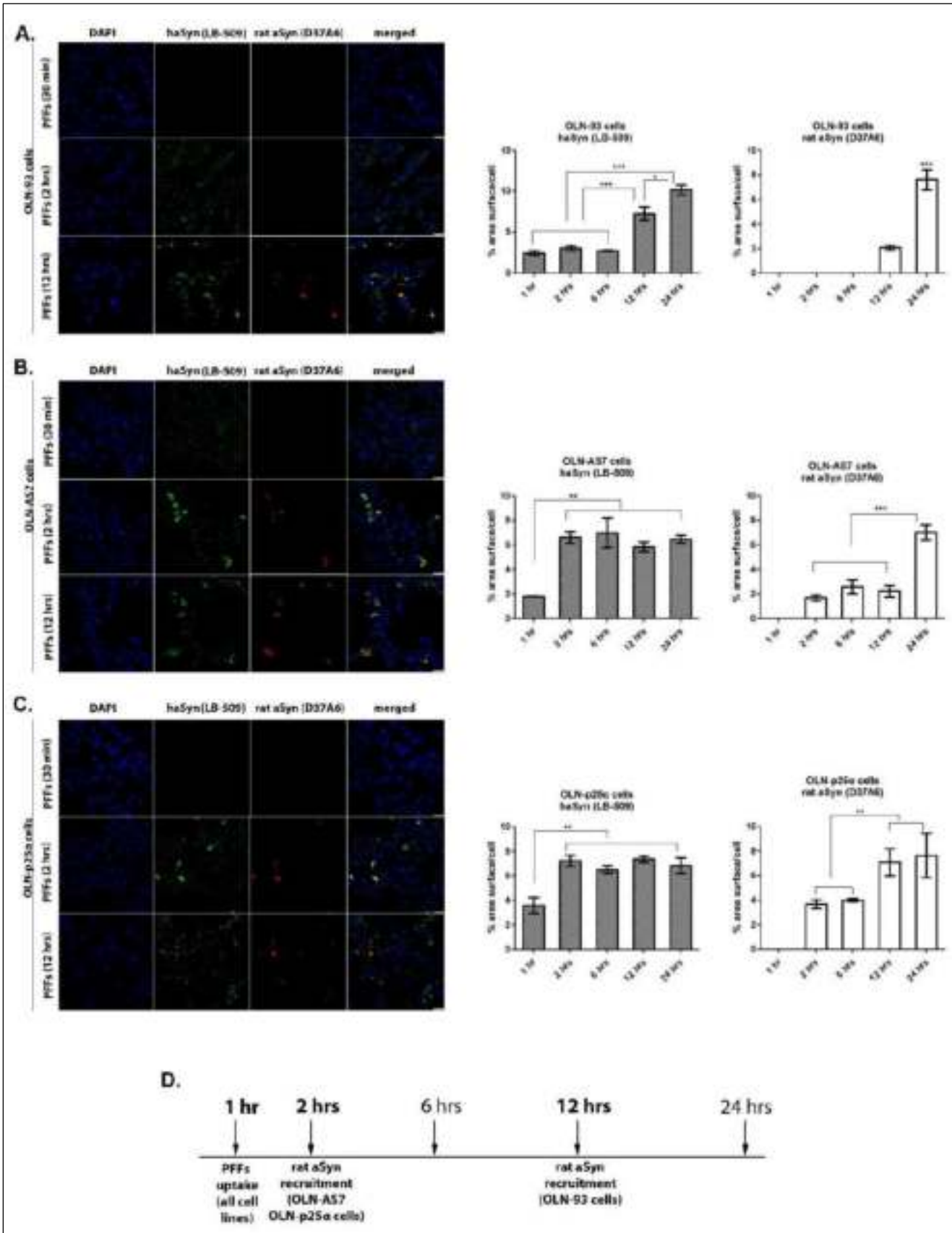

Figure 26: Overexpression of human aSyn or p25α accelerates the recruitment of endogenous rat oligodendroglial aSyn following the addition of haSyn PFFs to OLN cell lines. **A-C** Confocal microscopy with exogenous human-specific and endogenous rat-specific anti-aSyn antibodies reveals the enhanced expression of endogenous rat aSyn at 12 hrs in control OLN-93 cells and at 2 hrs in OLN-AS7 and OLN-p25α cells. (left panels) Representative immunofluorescence images with antibodies against human aSyn (green, LB509 antibody) and rodent aSyn (red) and DAPI staining. Scale bar: 25 μm. (right panels) Quantification of aSyn protein levels (human or endogenous rat aSyn) in OLN-93, OLN-AS7 and OLN-p25α cells measured as % area surface/cell following treatment with 0.5 μg haSyn PFFs for various times (2–12 hrs). Data are expressed as the mean ± SE of three independent experiments with triplicate samples/condition within each experiment; *p<0.05; **p< 0.01; ***p< 0.001, by one-way ANOVA with Tukey's post hoc test. (**D**) A drawing depicting the key time points when the uptake of exogenous haSyn PFFs and the recruitment of endogenous rat aSyn occur in control cells (OLN-93) and cells overexpressing human aSyn (OLN-AS7) or p25α (OLN-p25α).

We next investigated whether excess intracellular aSyn protein load (OLN-AS7 cells) or the presence of p25α (OLN-p25α cells) affects the onset of the appearance of aSyn pathology in oligodendrocytes by assessing the formation of oxidized/nitrated aSyn species over time (30 min – 10 days) with confocal microscopy. Indeed, in OLN-AS7 and OLN-p25α cells, the appearance of oxidized/nitrated aSyn (detected with the SYN303 aSyn antibody) was observed within 8 hrs post-addition of 0.5 μg haSyn PFFs, whereas in the control OLN-93 cells, these pathological species were observed after 20 hrs (**Figures 27 and 28**). Notably, co-staining with the rodent-specific aSyn antibody revealed that endogenous aSyn was a major component of the seeded time-resistant pathological aSyn assemblies. Importantly, the SYN303 aSyn antibody did not recognize exogenously added haSyn PFFs per se, since no signal was observed at 1 hr post-addition, when haSyn PFFs were detected inside the cells (data not shown), further supporting a major role for oligodendroglial aSyn in the seeding of aSyn pathology in OLN cells.

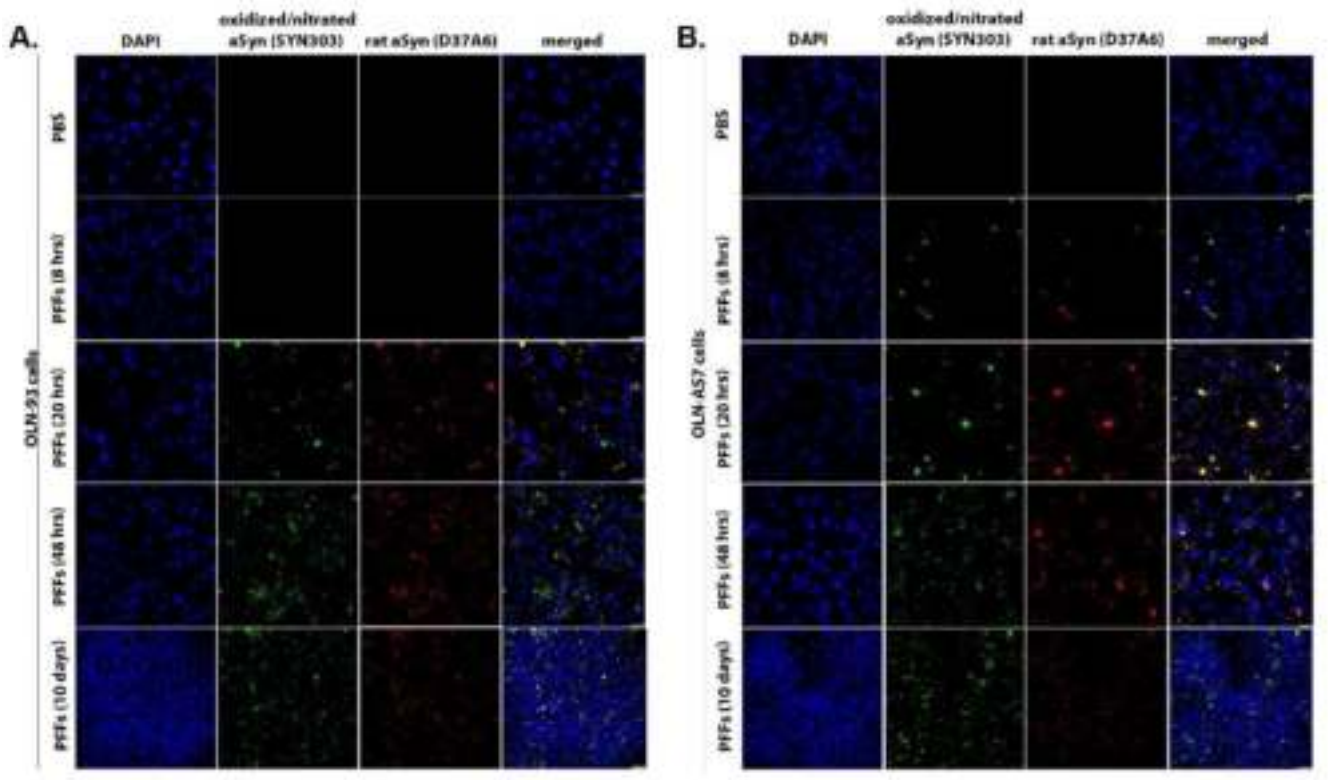

Figure 27: Overexpression of human aSyn facilitates the formation of pathological (oxidized/nitrated) aSyn assemblies following the addition of haSyn PFFs. (**A-B)** In OLN-AS7 cells, the recruitment of endogenous rat aSyn and the formation of pathological aSyn species are detected at 8 hrs, whereas they occur in control OLN-93 cells at 20 hrs post-addition of PFFs. Representative immunofluorescence images of OLN-93 and OLN-AS7 treated with 0.5 μg haSyn PFFs for various times (8–48 hrs and 10 days) using antibodies against oxidized/nitrated aSyn (green, Syn303 antibody) and endogenous rat aSyn (red) and DAPI staining. Scale bar: 25 μm.

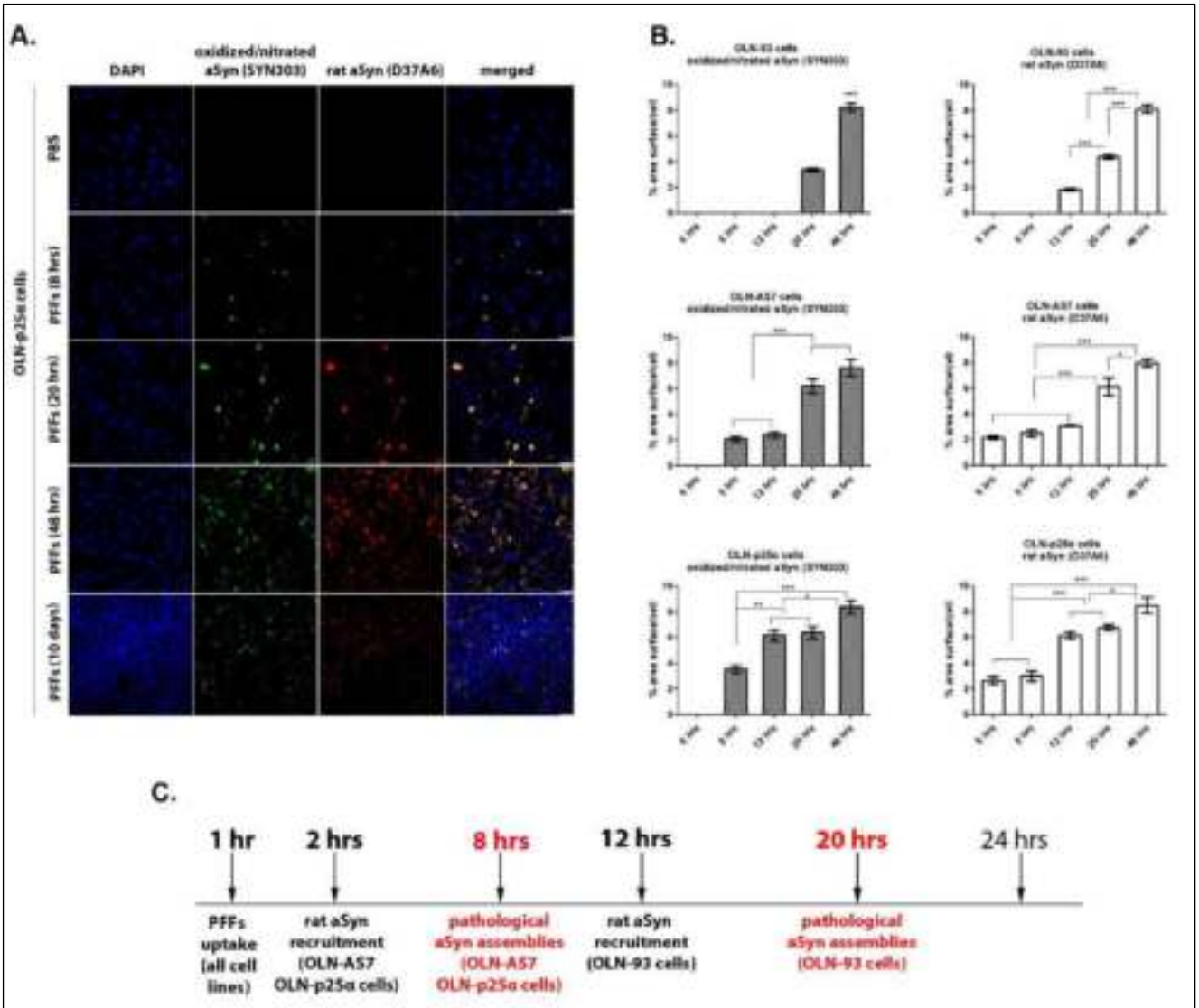

Figure 28: Overexpression of human p25α facilitates the formation of pathological (oxidized/nitrated) aSyn assemblies following the addition of haSyn PFFs. (**A**) In OLN-p25α cells, the recruitment of endogenous rat aSyn and the formation of pathological aSyn species are detected at 8 hrs. Representative immunofluorescence images of OLN-p25α cells treated with 0.5 μg haSyn PFFs for various times (8–48 hrs and 10 days) using antibodies against oxidized/nitrated aSyn (green, Syn303 antibody) and endogenous rat aSyn (red) and DAPI staining. Scale bar: 25 μm. (**B**) Quantification of aSyn protein levels (oxidized/nitrated or endogenous rat aSyn) in OLN-93 (upper row), OLN-AS7 (middle row) and OLN-p25α (bottom row) cells measured as % area surface/ cell following treatment with 0.5 μg haSyn PFFs for various times (6-48 hrs). Data are expressed as the mean±SE of three independent experiments with triplicate samples/condition within each experiment; *p<0.05; **p< 0.01; ***p< 0.001, by one-way ANOVA with Tukey's post hoc test. (**C**) A schema highlighting the time points when the increase in endogenous rat aSyn and the detection of pathological (oxidized/nitrated) aSyn species are observed in the different OLN cell lines.

4. Transient overexpression of human p25α augments the formation of insoluble aberrant aSyn species, consisting of human and endogenous rat protein

In order to validate further the role of p25α in the seeding of aSyn pathology, we used another experimental approach. Specifically, OLN-93 and OLN-AS7 cells were transiently transfected (or co-transfected where indicated) with p25α or/and GFP (as a control) plasmids 6 hrs prior to the addition of 0.5 μg of haSyn PFFs. At 2 days post-transfection, the cells were fixed and processed for confocal microscopy using antibodies against human aSyn (LB-509 antibody, **Figure**

29A), oxidized/nitrated aSyn (SYN303 antibody, **Figure 29B**), or rodent aSyn (D37A6 antibody, **Figure 30A**). The transient overexpression of human p25α increased the accumulation of human (**Figure 29A**) and endogenous rat (**Figure 30A**) aSyn-positive signals and the generation of oxidized/nitrated aSyn species (**Figure 29B**), in OLN-93 and OLN-AS7 cells.

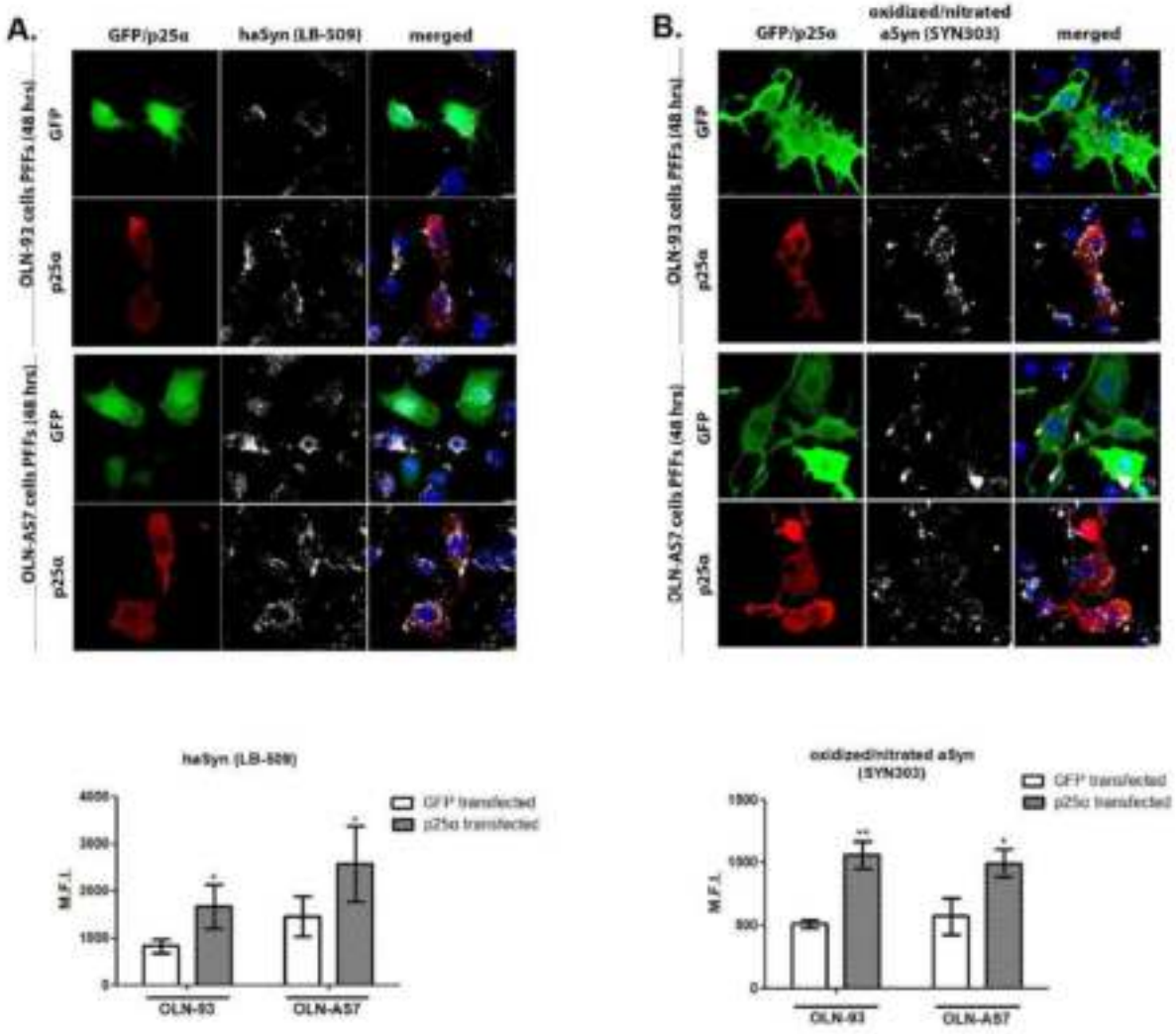

Figure 29: Transient overexpression of human p25α in OLN-93 and OLN-AS7 cells augments the formation of aberrant aSyn species following the addition of haSyn PFFs. (**A-B**, Upper panels) Representative immunofluorescence images of OLN-93 and OLN-AS7 cells transfected with GFP or human p25α plasmids in the presence of haSyn PFFs (48 hrs) using antibodies against: (**A**) haSyn (gray) and (**B**) oxidized/nitrated aSyn (gray). Antibodies against GFP (green) and p25α (red) were used to visualize the transfected cells. Scale bar: 10 μm. (Bottom panels) Quantification of human and oxidized/nitrated aSyn protein levels in OLN-93 and OLN-AS7 cells measured as mean fluorescent intensity in selected GFP (green) or p25α (red) transfected cells, using the image analysis tool Imaris. Data are expressed as the mean±SE of at least three independent experiments with triplicate samples/condition within each experiment; *p<0.05, by Student's unpaired t test.

Additionally, p25α overexpression in OLN-93 cells augmented the formation of monomeric and HMW aSyn species extractable in urea buffer (**Figure 30B**). Such data further support a critical role for p25α in the aggregation of pathological aSyn conformations within oligodendrocytes.

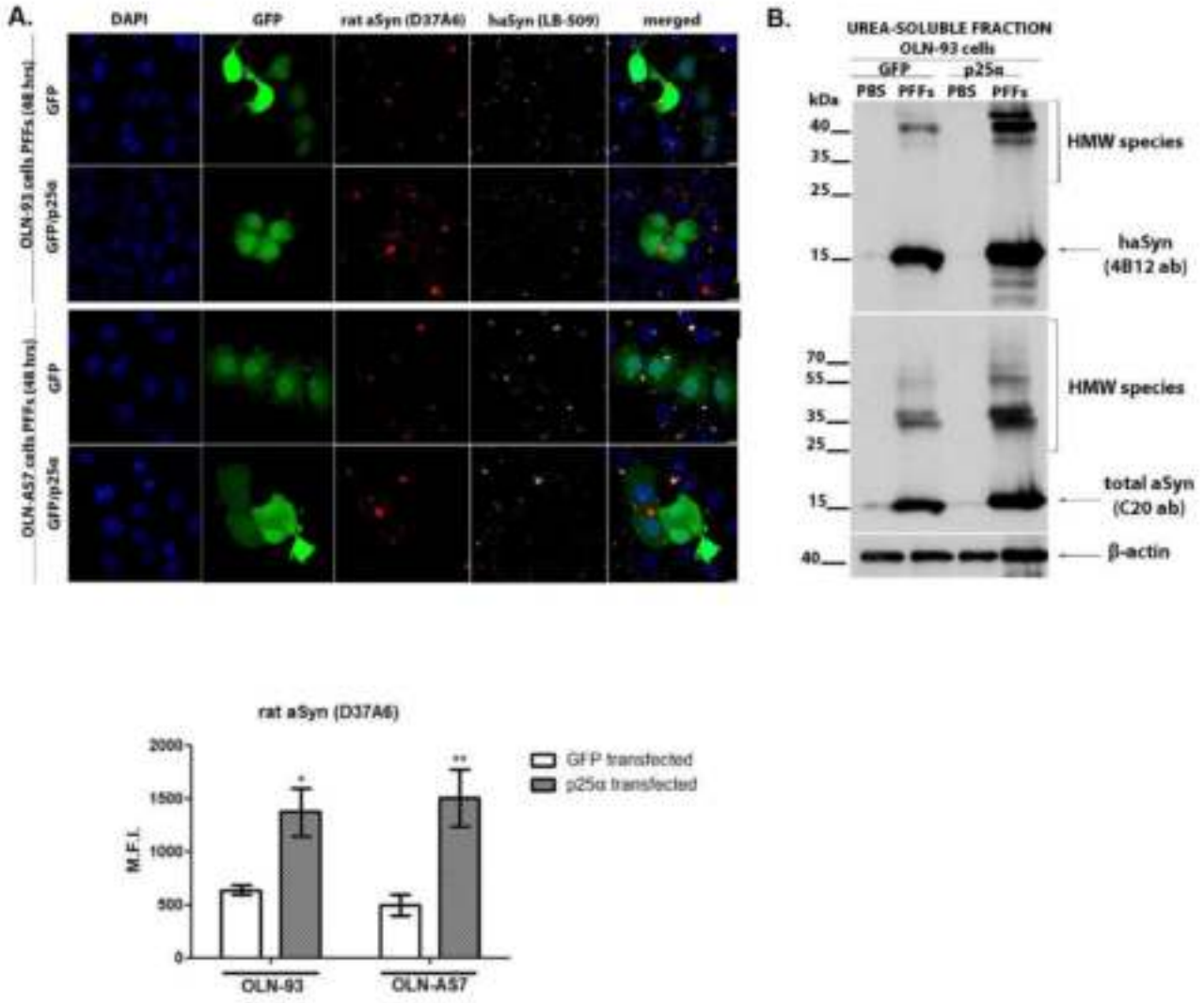

Figure 30: Transient overexpression of human p25α in OLN-93 and OLN-AS7 cells augments the formation of aberrant aSyn species comprised of human and endogenous rat aSyn following the addition of haSyn PFFs. (**A**, Upper panel) Representative immunofluorescence images of OLN-93 and OLN-AS7 cells transfected with GFP or human p25α plasmids in the presence of haSyn PFFs (48 hrs) using antibodies against: haSyn (gray) and endogenous rat aSyn (red). An antibody against GFP (green) was used to visualize the transfected cells. Scale bar: 10 μm. (Bottom panel) Quantification of the endogenous rat aSyn protein levels in OLN-93 and OLN-AS7 cells measured as mean fluorescent intensity in selected GFP or GFP/p25α (green) transfected cells, using the image analysis tool Imaris. Data are expressed as the mean±SE of at least three independent experiments with triplicate samples/condition within each experiment; *p<0.05, by Student's unpaired t test. (**B**) p25α overexpression enhances the accumulation of monomeric and HMW aSyn species following the addition of haSyn PFFs. Representative immunoblots of urea-soluble aSyn species of control OLN-93 cells transfected with GFP or p25α plasmids and treated with 0.5 μg haSyn PFFs for 48 hrs using antibodies against haSyn (4B12 antibody) or total (human +rodent) aSyn (C20 antibody). Equal loading was verified by the detection of β-actin levels.

5. Phosphorylation of aSyn at Ser129 depends on aSyn and p25α protein load and may involve different aSyn aggregate "strains" present in oligodendroglial and neuronal synucleinopathies

Given that the presence of aSyn phosphorylated at Ser129 (pSer129 aSyn) is an indicator of pathology in synucleinopathies, we assessed pSer129 aSyn levels in all OLN cell lines upon treatment with 0.5 or 3 μg haSyn PFFs for 48 hrs and 10 days using a panel of specific pSer129

aSyn antibodies. Importantly, incubation of all OLN cells with 3 μg PFFs resulted in a 20% cell death only in the case of OLN-AS7, probably due to the increased aSyn burden in these cells (**Figure 31**).

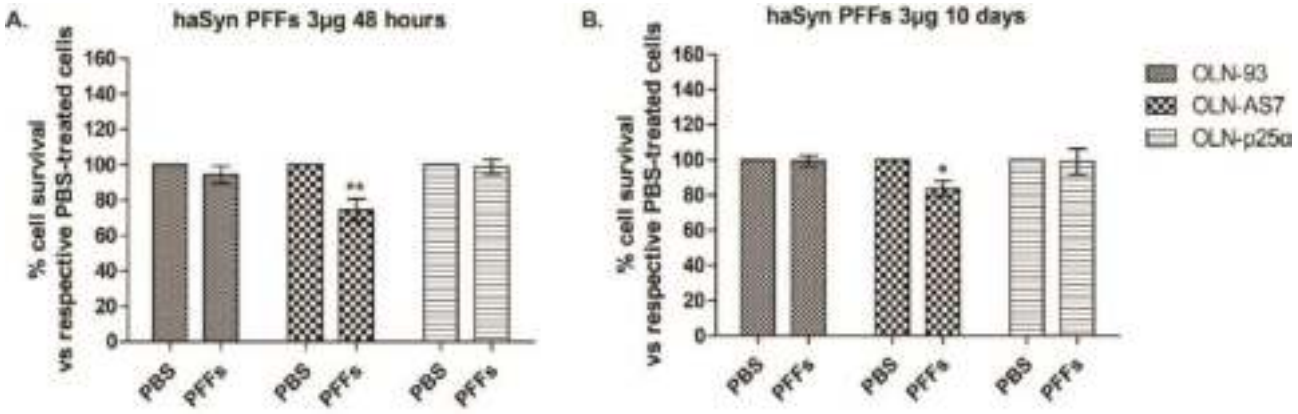

Figure 31: Short-term or prolonged incubation of OLN cells with haSyn PFFs affects only the survival of OLN-AS7 cells, probably due to the increased aSyn protein load. Quantification of cell viability following addition of 3 μg haSyn PFFs in OLN-93, OLN-AS7 and OLN-p25α cells for 48 hrs (**A**) or 10 days (**B**).

Surprisingly, we detected positive pSer129 aSyn signals only in PFFs-treated OLN cells overexpressing human aSyn or p25α (in the presence of 3 μg haSyn PFFs for 10 days) and not in the control OLN-93 cells, using the pSer129 aSyn-specific antibodies 11A5 (**Figure 32A, middle row**) and EP1536Y (**Figure 32A, bottom row**). Conversely, no positive signal was detected in any PFF-OLN-treated cell line using the pSer129 aSyn antibody LS4-2G12 (**Figure 32A, upper row**), which could be attributed to the low affinity of this antibody. Interestingly, no positive pSer129 aSyn signal was detected in the Triton- or SDS-soluble fraction of all PFF-treated OLN cells (**Figure 32B**), whereas pSer129 immunoreactivity was observed only in the urea-soluble fraction of OLN-AS7 cells and to a greater extent in OLN-p25α cells (**Figure 32C**). Most importantly, endogenous rat aSyn co-localized with the 11A5 pSer129 aSyn antibody, suggesting that the seeded oligodendroglial aSyn is phosphorylated, upon the addition of haSyn PFFs (**Figure 32D**).

Strikingly, in PFF-treated primary rat cortical cultures we detected a pSer129 aSyn signal with all antibodies utilized, including the LS4-2G12 antibody that did not give a signal in the OLN seeding model (**Figure 33A**), suggesting that this antibody may recognize distinct pSer129 aSyn assemblies generated specifically in neurons and not in oligodendrocytes. Importantly, this hypothesis was further buttressed by data obtained from human post-mortem brain material derived from patients with neuronal synucleinopathy (DLB) and oligodendroglial synucleinopathy (MSA). As shown in **Figure 33B** and in agreement with our results from PFF-treated primary cortical cultures, all pSer129 antibodies recognized pSer129 aSyn in LBs in the substantia nigra pars compacta (left columns) and cortex (middle columns) of DLB brains to a similar extent. In contrast, and congruent with the data obtained from PFF-treated oligodendroglial cells, LS4-2G12 reactivity for MSA cerebellar GCIs was much weaker than the 11A5 and EP1536Y signals.

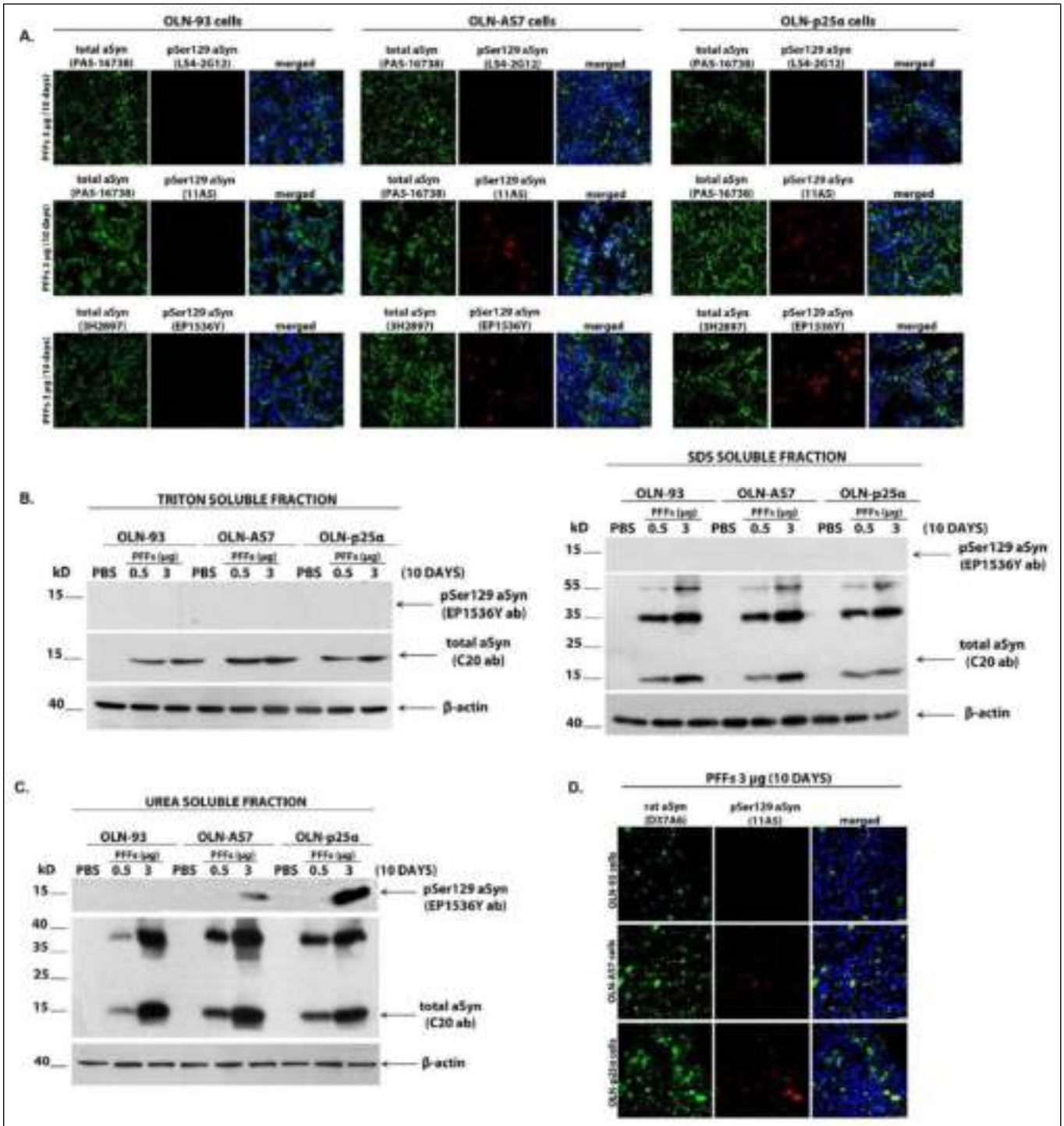

Figure 32: Comparative analysis of pSer129-aSyn phosphorylation in haSyn PFF-treated cultured cells and human post-mortem synucleinopathy brains. (**A**) OLN-93, OLN-AS7 and OLN-p25α cells were treated with 3 μg haSyn PFFs for 10 days and the phosphorylation of aSyn at Ser129 was examined using various pSer129 aSyn-specific antibodies by confocal microscopy. Representative immunofluorescence images with antibodies against total (human +rodent) aSyn (green, PA5-16738 or 3H2897 antibody) and pSer129 aSyn (red, LS4-2G12, 11A5, or EP1536Y antibody) and DAPI staining. Scale bar: 25 μm. (**B, C**) Phosphorylated aSyn at Ser129 (EP1536Y antibody) is detected by immunoblotting only in the urea-soluble fractions of OLN-AS7 and OLN-p25α cells following prolonged incubation with 3 μg PFFs. Representative immunoblots of Triton- and SDS-soluble protein fractions (**B**) or urea-soluble protein fractions (**C**) derived from OLN-93, OLN-AS7 and OLN-p25α cells treated with 0.5 μg or 3 μg of haSyn PFFs for 10 days. (**D**) Endogenous rat aSyn is phosphorylated at Ser129 following prolonged incubation with 3 μg PFFs only in OLN-AS7 and OLN-p25α cells. Representative immunofluorescence images with antibodies against endogenous rat aSyn (green, D37A6 antibody), pSer129 aSyn (red, 11A5 antibody) and DAPI staining. Scale bar: 25 μm.

Finally, the conformation-specific aSyn antibody MJFR-14 recognized better the aberrant aSyn species present in GCIs, compared to LBs (**Figure 33B**), supporting the notion that aSyn generated within oligodendrocytes (MSA) is incorporated into higher order pathological conformations, compared to those generated in neurons (DLB) (Dickson, Liu et al. 1999).

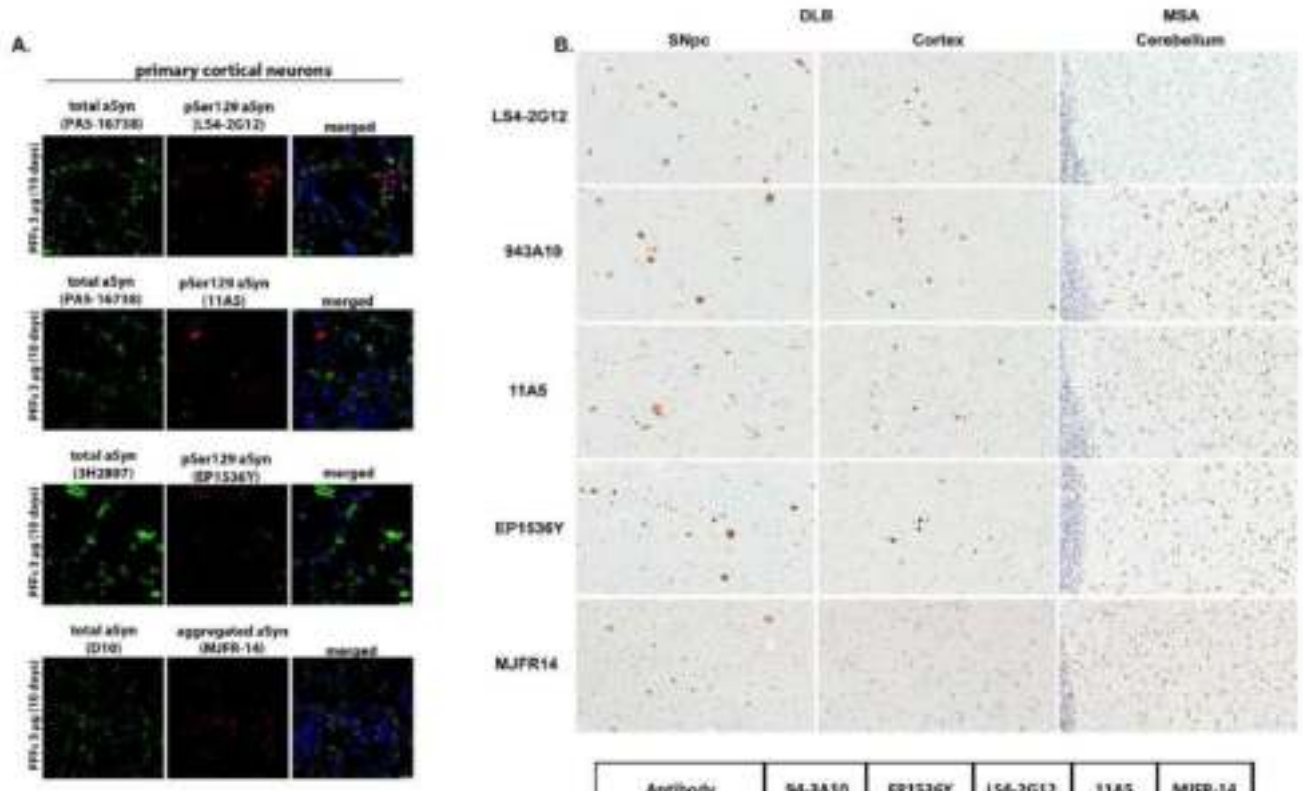

Antibody	94-3A10	EP1536Y	LS4-2G12	11A5	MJFR-14
MSA					
Case 1 Cerebellum	++++	++++	+/-	++++	++++
Case 2 Cerebellum	+++	+++	+/-	+++	+++
Case 3 Cerebellum	++++	+++	+/-	+++	+++
DLB					
Case 4 Cingulate	+++	+++	++	++	+/-
Case 5 Cingulate	++	++	++	++	+/-
Case 6 Cingulate	+++	+++	++	++	+/-
Case 4 Midbrain	+++	+++	+++	+++	+/-
Case 5 Midbrain	+++	+++	+++	+++	+
Case 6 Midbrain	+++	+++	++	++	+

Figure 33: (A) Primary rat cortical neurons were treated with 3 µg haSyn PFFs for 10 days and phosphorylated aSyn, and aggregated aSyn were detected by confocal microscopy. Representative immunofluorescence images with antibodies against total (human+ rodent) aSyn (green, PA5-16738, D10, or 3H2897 antibody), pSer129 aSyn (red, LS4-2G12, 11A5, or EP1536Y antibody), aggregated aSyn (red, MJFR-14 antibody) and DAPI staining. Scale bar: 25 µm. (**B**) (Upper panel) representative DAB-immunostained images using antibodies against phosphorylated (LS4-2G12, 11A5 and EP1536Y antibodies), aggregated aSyn (MJFR-14 antibody) and unmodified aSyn (94-3A10) in human post-mortem brain sections derived from the substantia nigra pars compacta and the cingulate cortex of DLB patients and from the cerebellum of MSA patients. Three confirmed cases of DLB and MSA were utilized for the analysis with similar results, whereby differential reactivity for GCIs vs. LBs was apparent for certain antibodies including LS4-2G12 and MJFR-14. (bottom panel) Immunohistochemical grading of aSyn pathology in different MSA and DLB cases. Glial cytoplasmic inclusions in MSA, cortical LBs in DLB cingulate and brainstem LBs in DLB midbrain were graded using a qualitative assessment of staining intensity and inclusion density by two independent observers. The findings are summarized as (±) rare, (+) mild, (++) moderate, (+++) strong and (++++) severe.

In our cellular systems, the MJFR-14 antibody recognized aggregated aSyn in oligodendrocytes (**Figures 34-35**) and neurons (**Figure 33A**) to a similar extent, a finding that could be explained by the fact that this antibody also recognizes exogenously added haSyn PFFs.

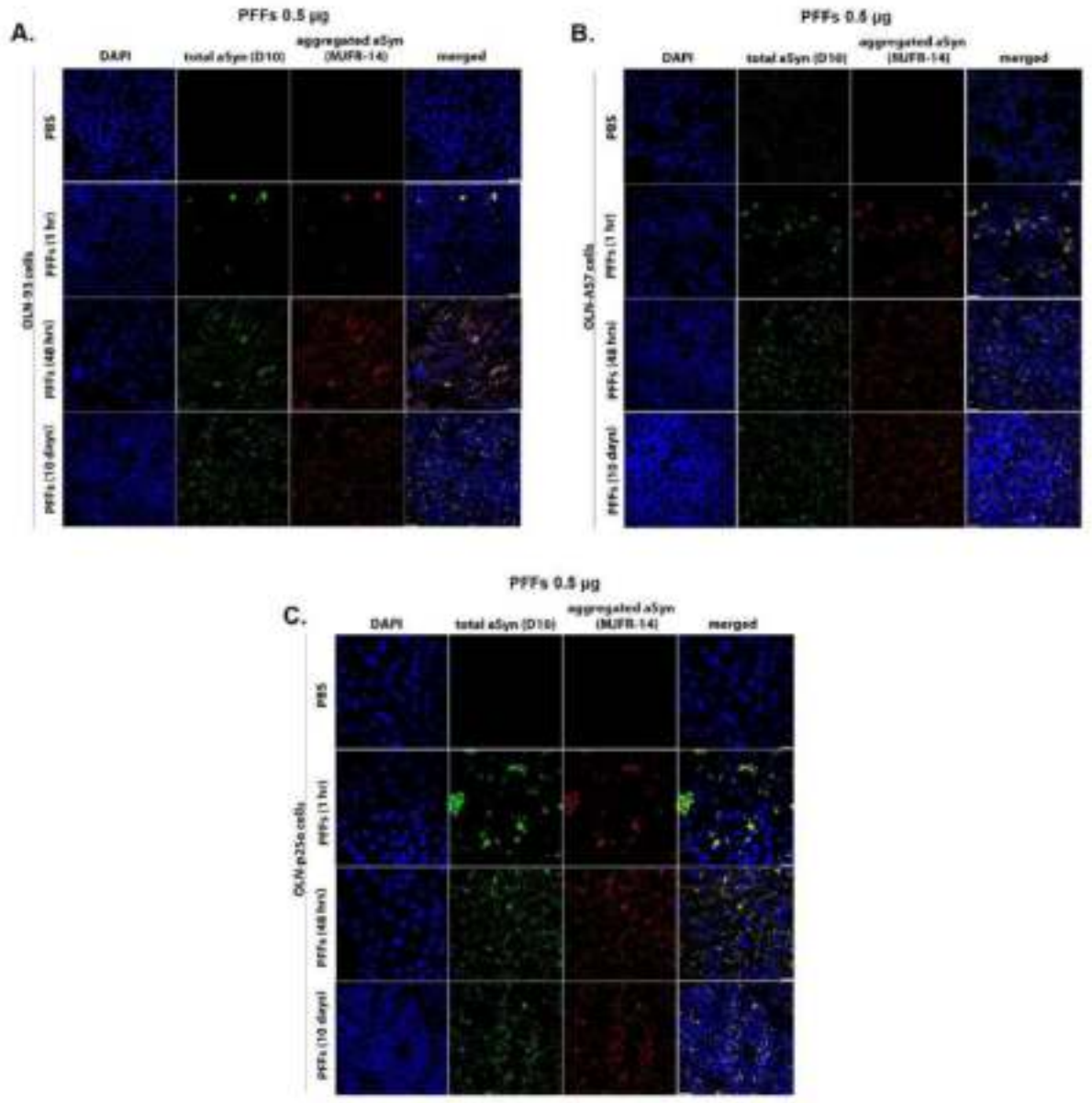

Figure 34: Addition of haSyn PFFs to OLN cells is accompanied by the formation of intracellular insoluble aSyn aggregates, which remain in a fibrillar state even following prolonged incubation with PFFs.

Representative immunofluorescence images depicting the aSyn aggregates in OLN-93 (**A**), OLN-AS7 (**B**), and OLN-p25α cells (**C**) following the addition of 0.5 µg haSyn PFFs at 1 h, 48 hrs and 10 days using antibodies against total (human+rodent) aSyn (green, D10 antibody) and aggregated aSyn (red, MJFR-14 antibody) and DAPI staining. Scale bar: 25 µm.

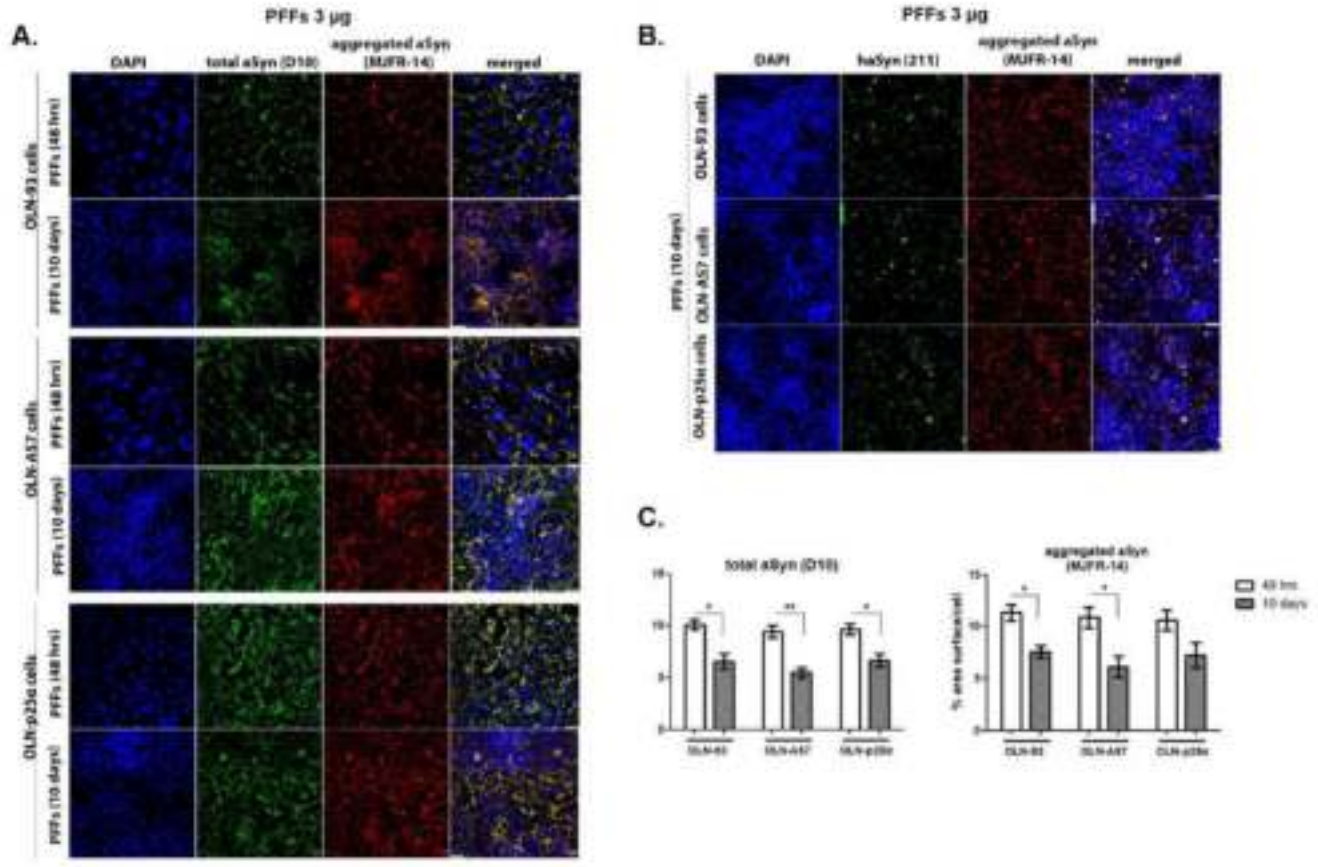

Figure 35: Incubation of OLN cells with 3 µg haSyn PFFs for 48 hrs or 10 days expedites the formation of highly aggregated aSyn forms. (**A**) Representative immunofluorescence images with antibodies against total aSyn (green, D10 antibody) and aggregated aSyn (red, MJFR-14) and DAPI staining. Scale bar: 25 µm. (**B**) Representative immunofluorescence images with antibodies against human aSyn (green, 211 antibody) and aggregated aSyn (red, MJFR-14) and DAPI staining. Scale bar: 25 µm. (**C**) Quantification of total (upper panel) and aggregated (bottom panel) aSyn levels measured as % area surface/cell in OLN cell lines following the addition of 3 µg haSyn PFFs for 48 hrs or 10 days. Data are expressed as the mean ± SE of three independent experiments with triplicate samples/condition within each experiment. *p < 0.05; **p < 0.01 by two-way ANOVA with Bonferroni's correction.

6. Endogenous aSyn is a major component of the seeded pathological aSyn aggregates following the addition of haSyn PFFs

To delineate further the contribution of endogenous oligodendroglial aSyn and p25α in the spread of aSyn pathology, we treated OLN cells with 3 µg PFFs and analyzed aSyn levels at 48 hrs or 10 days (**Figure 36**). With this higher amount of PFFs, over time, the equilibrium of intracellular aSyn protein load in OLN cells shifted toward the seeded endogenous rat protein and notably, this phenomenon was more robust in the presence of human aSyn or p25α (**Figure 36A, B**). Similarly, oxidized/nitrated aSyn conformations were elevated in OLN-AS7 and OLN-p25α cells over time (**Figure 36C, D**). Finally, using the conformation-specific aSyn antibody MJFR-14, which recognizes aggregated conformations exclusively (Lassen, Gregersen et al. 2018), we detected the induction of MJFR-14- positive structures that colocalized from the earliest time point of 1 hr with

structures recognized with a pan-aSyn (human+rodent) antibody (D10); the MJFR-14 antibody showed no reactivity against overexpressed aSyn in the OLN-AS7 cell line (**Figures 34-35**).

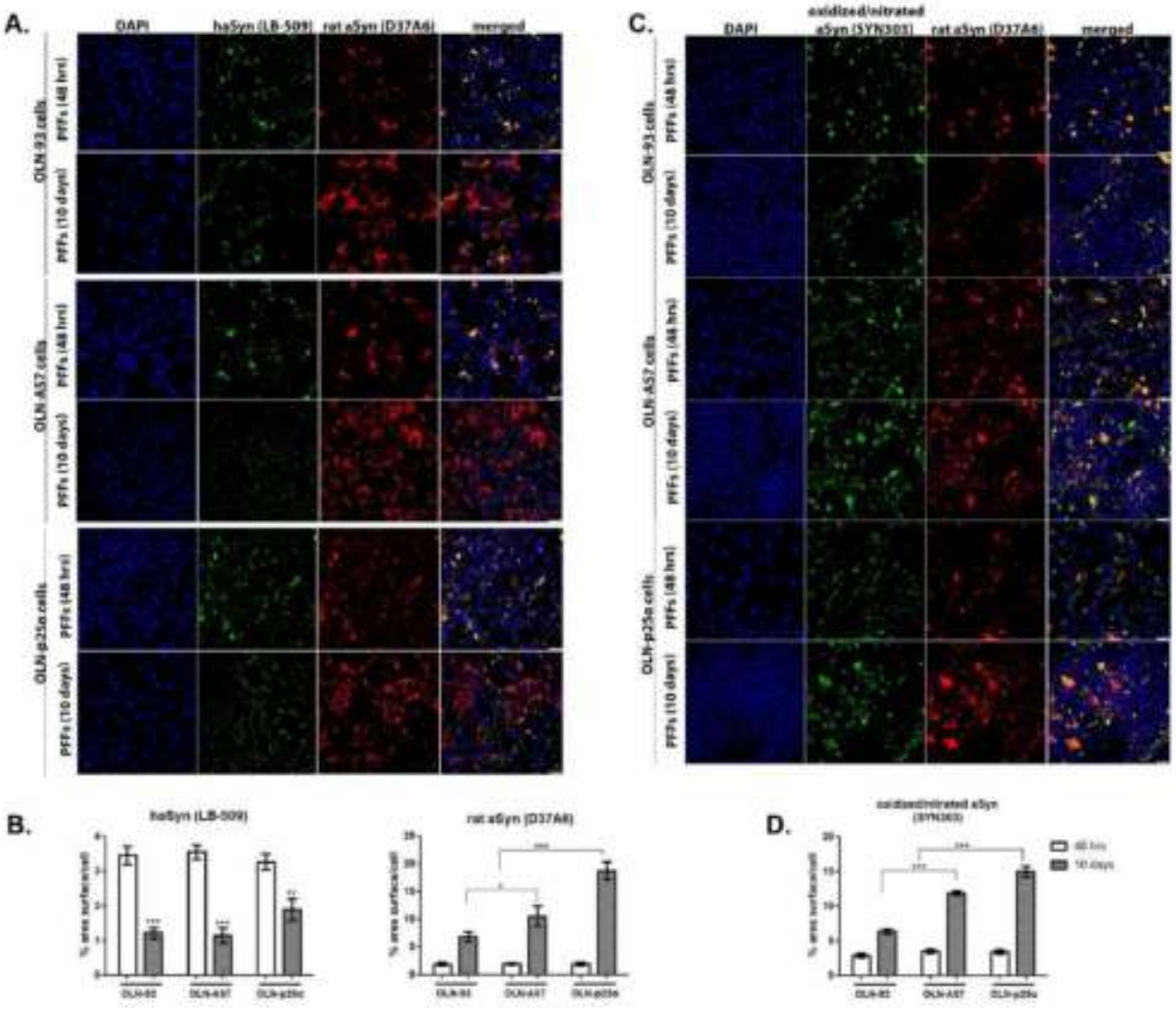

Figure 36: Prolonged incubation of OLN cell lines with high concentrations of haSyn PFFs uncovers the significant contribution of endogenous rat oligodendroglial aSyn to the formation of aberrant aSyn conformations. (**A, B)** Over time, the equilibrium of aSyn protein load shifts toward seeded endogenous rodent aSyn in all cell lines. OLN-93, OLN-AS7 and OLN-p25α cells were incubated with 3 μg human aSyn PFFs for 48 hrs or 10 days, and the recruitment of endogenous rat aSyn was examined by confocal microscopy. (**A**) Representative immunofluorescence images with antibodies against human aSyn (green) and endogenous rat aSyn (red) and DAPI staining. Scale bar: 25 μm. (**B**) Quantification of human and endogenous rat aSyn protein levels measured as % area surface/cell in OLN cell lines following the addition of 3 μg PFFs for 48 hrs or 10 days. Data are expressed as the mean ±SE of at least three independent experiments with triplicate samples/condition within each experiment; *p<0.05; **p<0.01, ***p< 0.001, by two-way ANOVA with Bonferroni's correction. (**C**) The addition of a high concentration of haSyn PFFs (3 μg) leads to the formation of time-resistant pathological (oxidized/nitrated) aSyn species, in which endogenous rat aSyn is the major constituent, as shown using antibodies against oxidized/nitrated aSyn (green) and endogenous rat aSyn (red) and DAPI staining. Scale bar: 25 μm. (**D**) Quantification of oxidized/nitrated aSyn protein levels measured as % area surface/cell in OLN cell lines following the addition of 3 μg PFFs for 48 hrs or 10 days. Data are expressed as the mean ±SE of at least three independent experiments with triplicate samples/condition within each experiment; ***p<0.001, by two-way ANOVA with Bonferroni's correction.

In order to quantitatively estimate the contribution of aSyn and p25α load to the formation and stability of inclusions, we utilized an indirect immunostaining strategy with antibodies against either total aSyn (D10 antibody) or human aSyn (211 antibody) and aggregated aSyn (MJFR-14

antibody), since both the rodent-specific (D37A6) and MJFR-14 antibodies are generated in rabbits (**Figure 37A**).

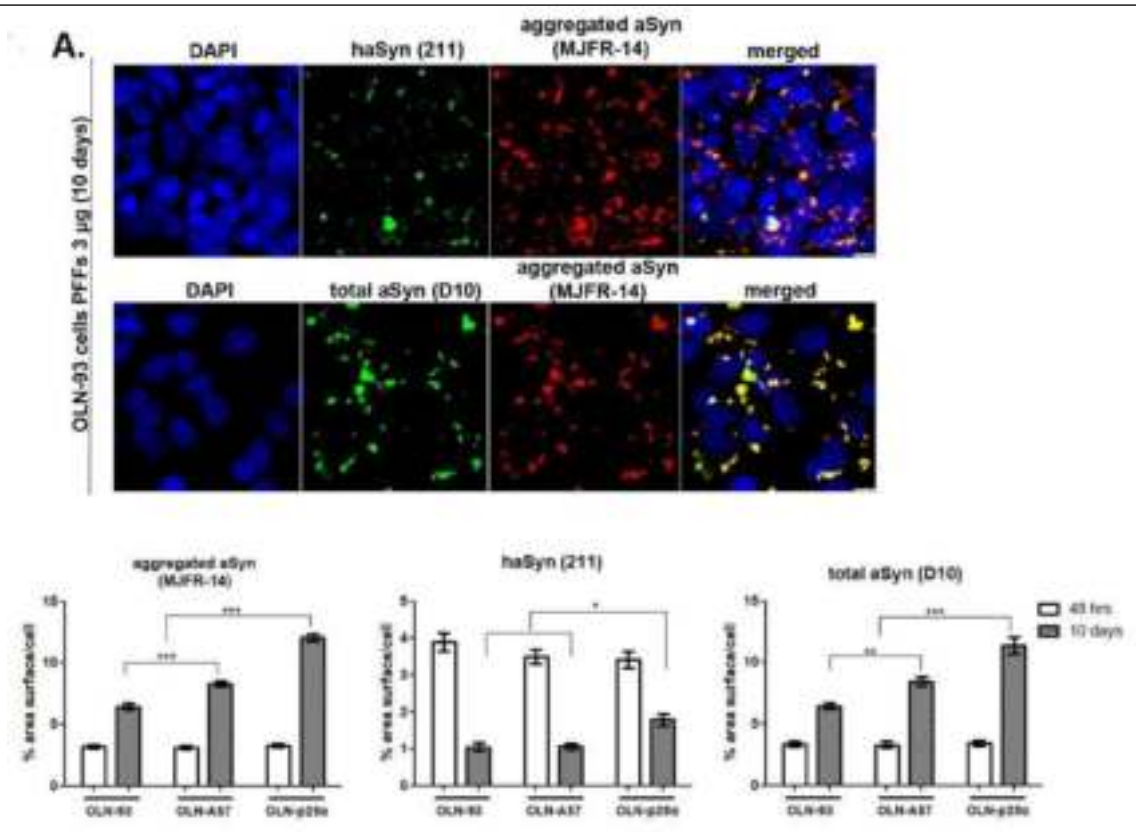

B.

% positive cells (±SD)						
	PFFs 3µg 48 hrs			PFFs 3µg 10 days		
	OLN-93	OLN-AS7	OLN-p25α	OLN-93	OLN-AS7	OLN-p25α
D37A6	88.92 (4.14)	86.41 (1.32)	88.81 (3.31)	91.34 (4.12)	90.85 (3.68)	92.63 (4.59)
LB-509	90.5 (3.45)	86.93 (3.23)	89.06 (3.68)	91.85 (3.67)	90.23 (4.11)	91.88 (3.49)
MJFR-14	91.41 (2.21)	93.88 (1.93)	92.63 (3.28)	90.04 (1.11)	91.8 (1.87)	91.32 (4.24)
SYN303	87.05 (6.32)	86.23 (0.76)	89.96 (3.27)	73.27 (3.87)	81.79 (2.46)	86.91 (2.32)
EP1536Y					13.96 (3.67)	37.99 (12.15)

Figure 37: Incubation of OLN cells with 3 µg PFFs for 48 h or 10 days expedites the formation of aggregated conformations of aSyn. (**A**, upper panel) Representative immunofluorescence images with antibodies against human aSyn (green, 211 antibody, upper panel), total aSyn (human + rodent, green, D10, bottom panel) and aggregated aSyn (red) and DAPI staining in OLN-93 cells. Scale bar: 7.5 µm. (bottom panel) Quantification of aggregated (left), human (middle) and total (human+ rodent) aSyn levels in all OLN cell lines treated with 3 µg haSyn PFFs for 48 h or 10 days, expressed as % area surface/cell verifies the aggregated nature of the generated aSyn assemblies and highlights the contribution of recruited endogenous rat aSyn to the formation of such structures. Data are expressed as the mean±SE of at least three independent experiments with triplicate samples/condition within each experiment; *p<0.05; **p< 0.01; ***p< 0.001 by two-way ANOVA with Bonferroni's correction. (**B**) Quantification of the percentage of positively stained OLN-93, OLNAS7 or OLN-p25α cells treated with 3 µg PFFs for 48 h or 10 days with antibodies against endogenous rat (D37A60), human (LB-509), aggregated (MJFR-14) or pathological aSyn species (oxidized/nitrated aSyn [Syn303] or pSer129-aSyn [EP1536Y]). All data are expressed as the mean± SD of at least three independent experiments with triplicate samples/condition within each experiment.

Total aSyn (human and endogenous rat) and aggregate-aSyn fluorescence signals exhibited a nearly complete co-localization (**Figure 35A and Figure 37A**), whereas staining with the 211 human-specific and MJFR-14 aggregate-specific aSyn antibodies (**Figure 35B and Figure 37A**) revealed partial co-localization, suggesting indirectly that endogenous rat aSyn is a major component of the formed aggregates. Consistent with this idea, MJFR-14-positive immunostaining increased following the addition of PFFs over a period of 10 days, matching the pattern of endogenous rat aSyn, whereas human aSyn-positive structures remained stable or decreased over time, with OLN-p25α cells again exhibiting higher levels of total and aggregated aSyn (**Figure 37A**). Interestingly, the percentage of cells positive for the various aSyn conformations was similar among all OLN cell lines, with the exception of pSer129 aSyn (EP1536Y antibody) (**Figure 37B**), suggesting that the observed differences shown in **Figure 37A** are possibly attributed to the formation of larger aggregates in aSyn- and p25α-expressing cells, compared to OLN-93 cells. Finally, proof-of-concept experiments utilizing sonicated fibrils yielded similar results regarding the seeding of endogenous aSyn and the formation of pathological assemblies (**Figures 38-39**).

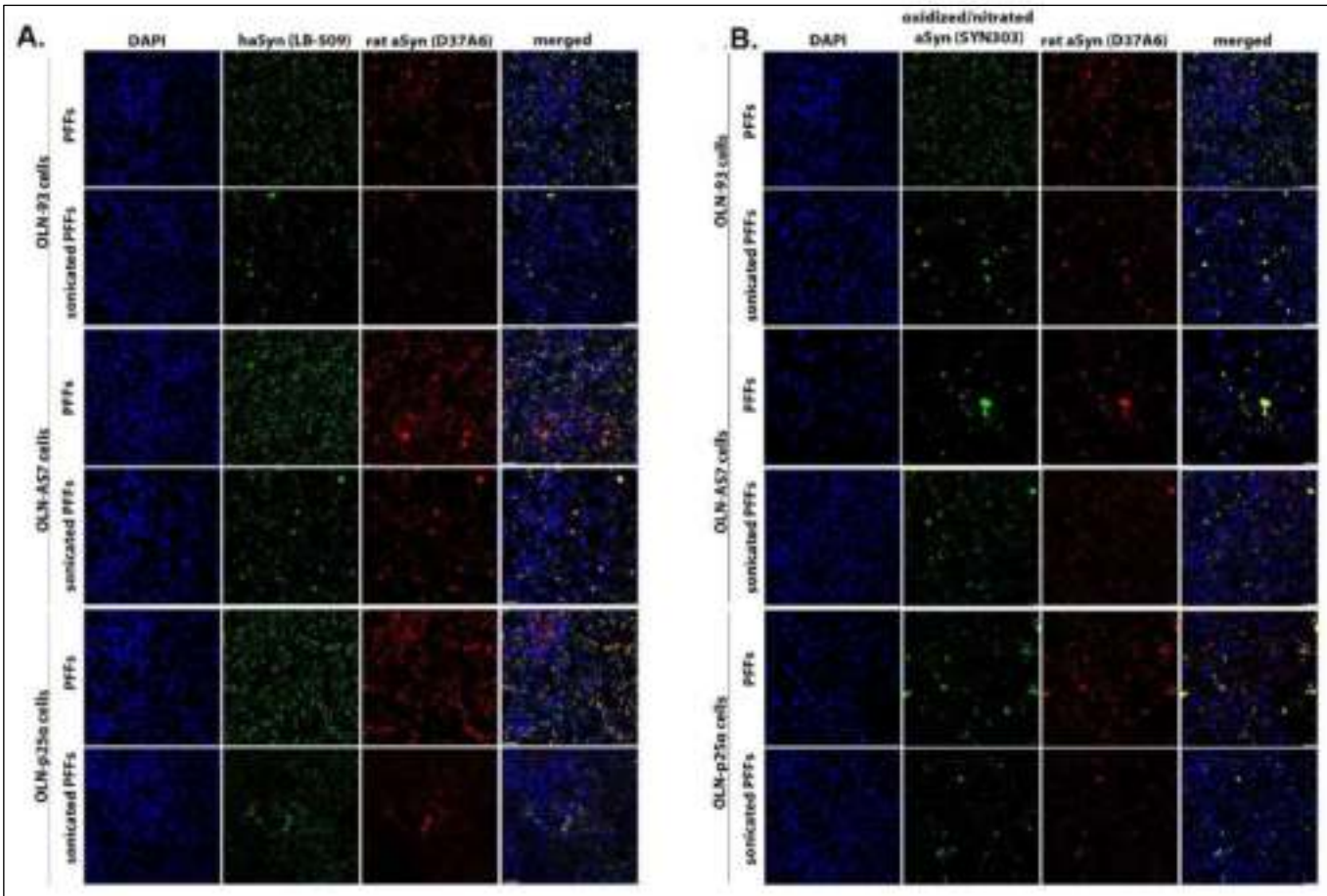

Figure 38: **The addition of sonicated haSyn PFFs leads to the recruitment of endogenous rat aSyn and the formation of pathological aSyn species**. **A-B** Representative immunofluorescence images of all OLN cell lines treated with non-sonicated and sonicated PFFs (0.5 μg for 48 hrs) using antibodies against human aSyn (green, LB-509 antibody), endogenous rat aSyn (red, D37A6 antibody) and oxidized/nitrated aSyn (green, Syn303 antibody) and DAPI staining. Scale bar: 25 μm.

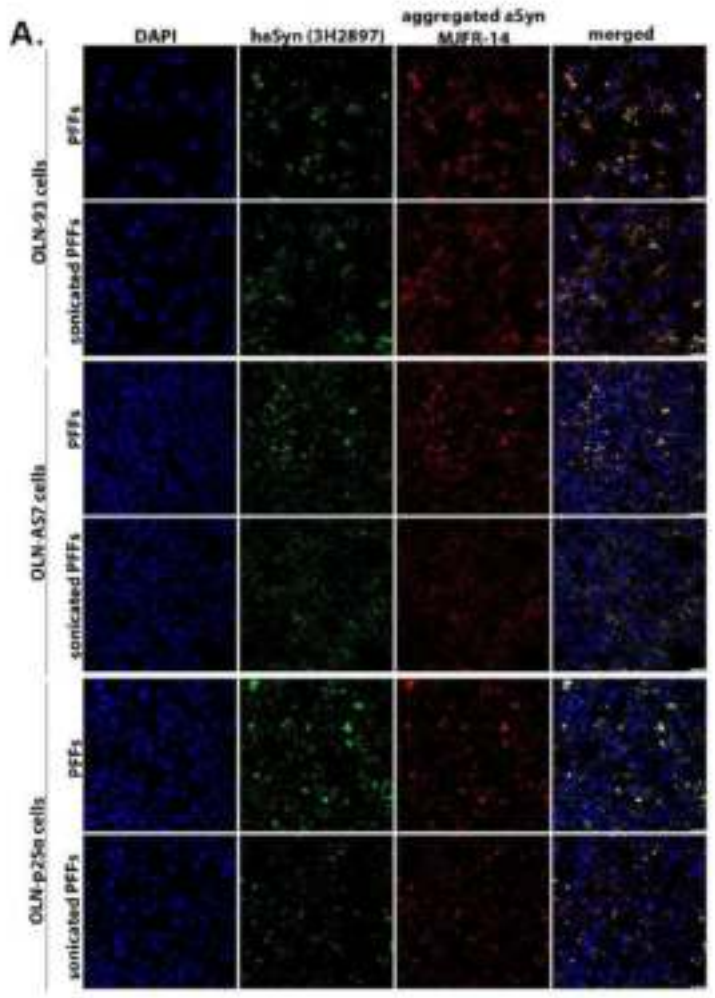

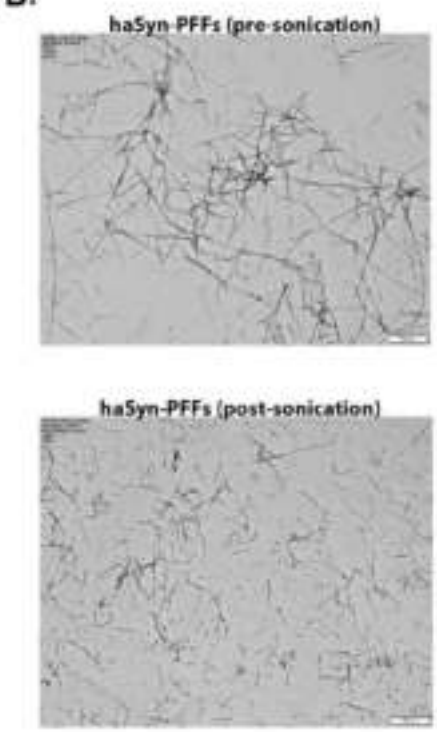

Figure 39: **The addition of sonicated haSyn PFFs leads to the recruitment of endogenous rat aSyn and the formation of pathological aSyn species**. **(A)** Representative immunofluorescence images of all OLN cell lines treated with non-sonicated and sonicated PFFs (0.5 µg for 48 hrs).. Scale bar: 25 µm. (**B**) Transmission EM images of negatively stained haSyn PFF samples pre-sonication (upper) or post-sonication (bottom) confirming the efficient sonication of the fibrils utilized.

7. Endogenous mouse oligodendroglial aSyn is incorporated into pathological aSyn assemblies in primary oligodendrocytes following the addition of haSyn PFFs

To investigate the intracellular processes governing the templating of aSyn pathology in a more physiological cellular setting with properties resembling more closely those of the CNS oligodendrocytes we established a protocol to isolate and cultivate mature oligodendrocytes derived from P0-P3 mouse brains. In order to decipher whether the presence of aSyn, which is small in amount, is a prerequisite for the seeding of exogenous added haSyn, we used primary oligodendrocytes prepared from WT- or KO-aSyn mice. In parallel experiments, we utilized primary cultures from PLP-haSyn mice, a well-established MSA mouse model in which haSyn is overexpressed only in oligodendrocytes, under the PLP promoter (Kahle, Neumann et al. 2002). To differentiate the oligodendroglial progenitor cells into mature, myelin producing (MBP^+) oligodendrocytes, the cells were grown in SATO medium. The enrichment of the cultures with oligodendrocytes was verified utilizing markers for astrocytes (GFAP) and microglia (AIF1/IbaI), as well as markers for the oligodendroglial lineage such as Olig2, O4, and MBP (**Figure 40A, B**).

As observed in the OLN cell lines, the addition of haSyn PFFs (0.5 μg, 48 h) evoked a dramatic increase in the levels of endogenous mouse oligodendroglial aSyn only in the WT-aSyn and PLP-haSyn primary cultures (**Figure 40C**). No fluorescence signal for the rodent-specific D37A6 aSyn antibody was detected in the KO-aSyn cultures or at baseline in the WT-aSyn and PLP-haSyn cultures in the absence of haSyn PFF treatment (**Figures 40C, 41B-C**). The magnitude of the increase was dependent on the endogenous aSyn load, since the rodent-specific aSyn signal was more intense and more compact in the PLP-haSyn oligodendrocytes than in WT-aSyn oligodendrocytes (**Figure 40C**).

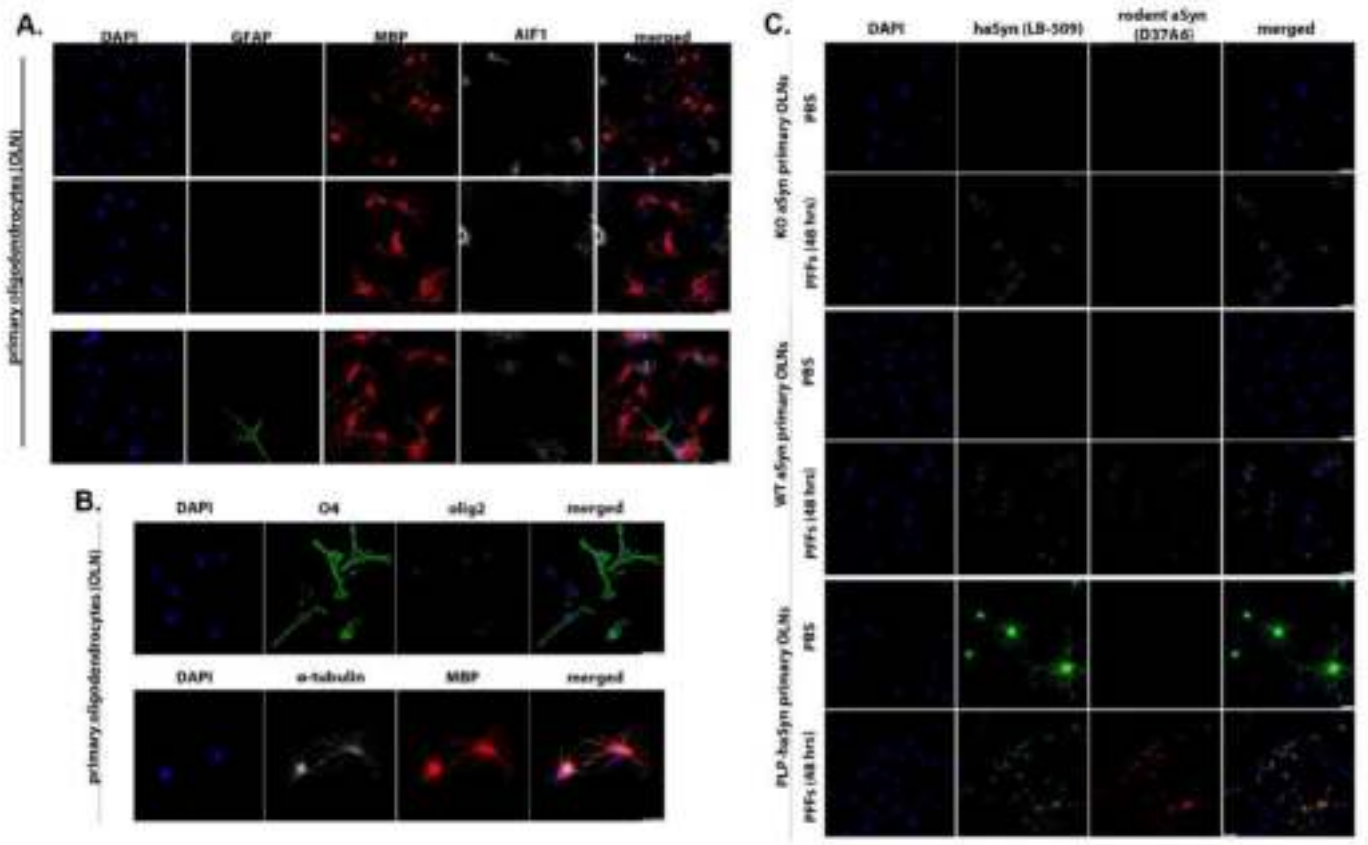

Figure 40: Endogenous mouse oligodendroglial aSyn is incorporated into pathological aSyn assemblies in primary mouse oligodendroglial cultures following the addition of haSyn PFFs. (**A, B**) Mouse primary oligodendroglial cells derived from WT-aSyn pups were grown in SATO medium for 7 days prior to fixation and immunofluorescent analysis. The enrichment of the cultures in mature myelin-producing oligodendrocytes was confirmed with confocal microscopy using antibodies against glial fibrillary acidic protein as an astrocytic marker (green, GFAP), allograft inflammatory factor 1 (gray, AIF1/Iba1) as a marker for microglia and myelin basic protein (red, MBP) as a marker for mature oligodendrocytes (**A**), as well as against the oligodendroglial markers Olig2 (red, AB9610 antibody) and O4 (green, MAB1326 antibody) (**B**). α-Tubulin (gray, 62204 antibody) and DAPI staining were used as cytoskeletal and nuclear markers, respectively. Scale bars: 25 μm (A, upper panels), 50 μm (A, bottom panel) and 10 μm (**B**). (**C**) Confocal microscopy with human-specific (green) and rodent-specific (red) aSyn antibodies identifies the enhanced expression of endogenous mouse aSyn in WT-aSyn and PLP-haSyn oligodendroglial cultures, upon the addition of 0.5 μg haSyn PFFs for 48 h. No rodent-specific signal is detected in KO-aSyn cells.

The formed aSyn species were aggregated, as verified by the strong immunoreactivity of the conformation-specific MJFR-14 antibody, which co-localized completely with the D10 antibody, recognizing the human+rodent protein (**Figure 41A**). Interestingly, the expression pattern of aSyn in the haSyn-PLP cultures changed dramatically from diffuse (in PBS-treated cultures) to strongly

punctated (in PFF-treated cultures), as detected by the LB-509 and D10 antibodies (**Figure 40C, 41A**). Finally, the rodent-specific positive puncta colocalized to a great extent with the oxidized/nitrated aSyn antibody in the WT-aSyn and haSyn-PLP cultures, but not in the KO-aSyn cultures (**Figure 41B-C**), further indicating that the endogenous protein contributes to the formation of such pathological conformations.

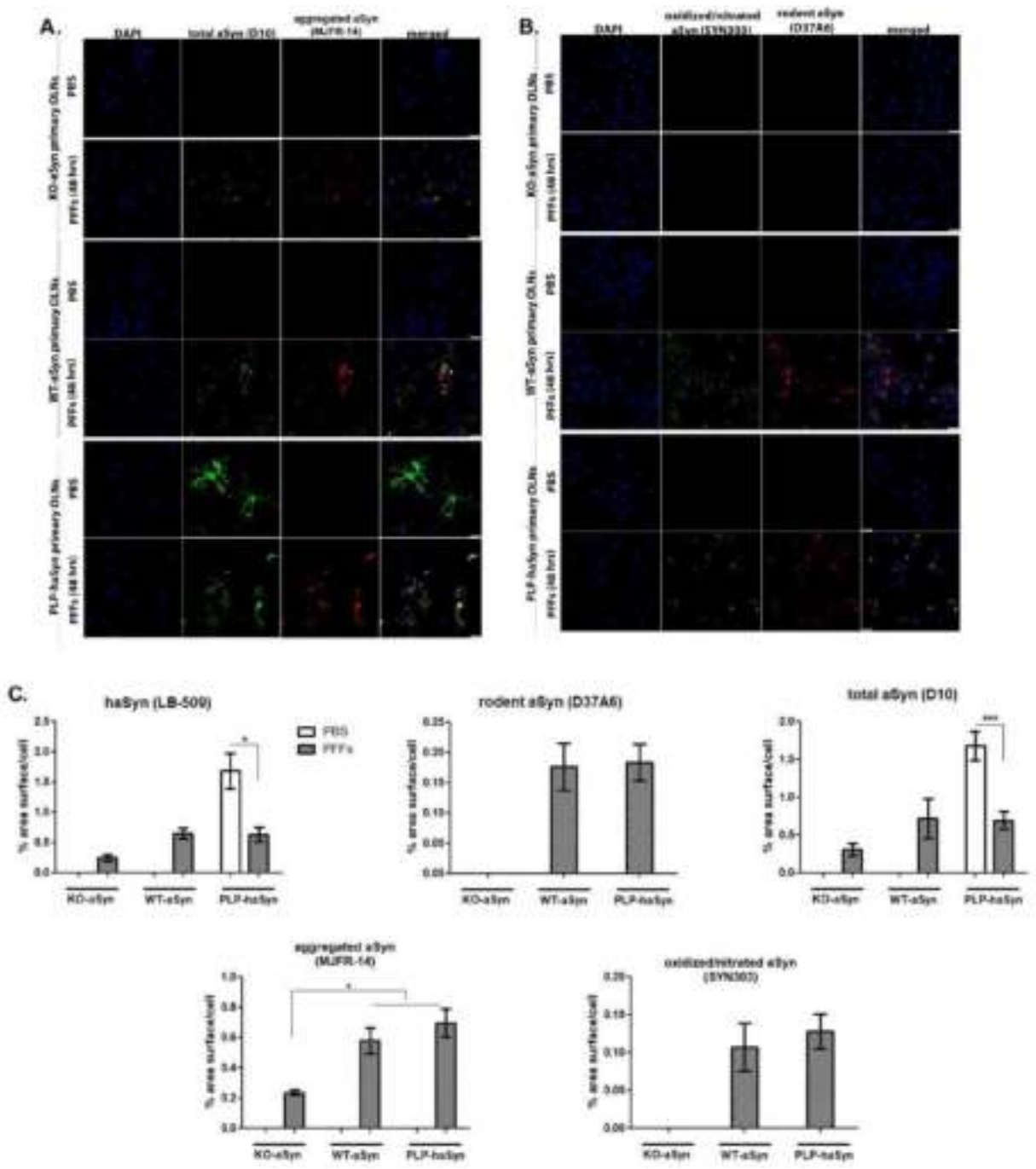

Figure 41: Endogenous mouse oligodendroglial aSyn is incorporated into pathological aSyn assemblies in primary mouse oligodendroglial cultures following the addition of haSyn PFFs. (**A, B)** Both exogenously added human aSyn and endogenous mouse aSyn contribute to the formation of aggregated (**A**) and oxidized/nitrated (**B**) conformations of aSyn in WT-aSyn and PLP-haSyn primary oligodendrocytes incubated with haSyn PFFs. Only exogenously added haSyn PFFs (**A**) and not oxidized/nitrated (**B**) conformations are detected in the KO-aSyn cultures. Representative immunofluorescent images using antibodies against total aSyn (green, D10 antibody) and aggregated aSyn (red) are shown in **A** and against oxidized/nitrated aSyn (green) and endogenous mouse aSyn (red) are shown in **B**. Scale bar: 25 μm. (**C**) Quantification of human, endogenous rodent and total (human and rodent) aSyn protein levels (upper panel) or aggregated and oxidized/nitrated aSyn protein levels (bottom panel) measured as % area surface/cell in KO-aSyn, WT-aSyn or PLP-haSyn mouse primary oligodendroglial cultures following the addition of 0.5 μg PFFs for 48 hrs. Data are expressed as the mean± SE of at least three independent experiments with triplicate samples/condition within each experiment; *p< 0.05; ***p<0.001, by one-way ANOVA with Tukey's post hoc test (to compare between PBS- and PFF-treated cells) or by two-way ANOVA with Bonferroni's correction (to compare between the different PFF-treated cultures).

8. Endogenous oligodendroglial aSyn protein load is closely linked to the redistribution of microtubule-associated proteins upon the addition of haSyn PFFs

Given the close link between aSyn levels and the redistribution p25α in disease pathogenesis, we assessed the expression pattern of p25α in PFF-treated primary mouse oligodendrocytes. As shown in **Figure 42A and 43B**, there was no apparent change in the pattern of p25α expression in PFF-treated KO-aSyn cultures (**Figure 42A, upper rows**), in contrast to WT-aSyn cultures, in which p25α was redistributed from the oligodendroglial processes to the cell body, although no obvious co-localization with haSyn-positive aggregates was observed (**Figure 42A, middle rows**). Remarkably, p25α in the PFF-treated PLP-haSyn oligodendrocytes, beyond its cell body redistribution, accumulated clearly in haSyn-positive cytoplasmic aggregates (**Figure 42A, bottom rows**). This change was related to haSyn PFFs, given that p25α protein levels were similar between the untreated oligodendroglial cultures (**Figures 42A, 43B and 43C**).

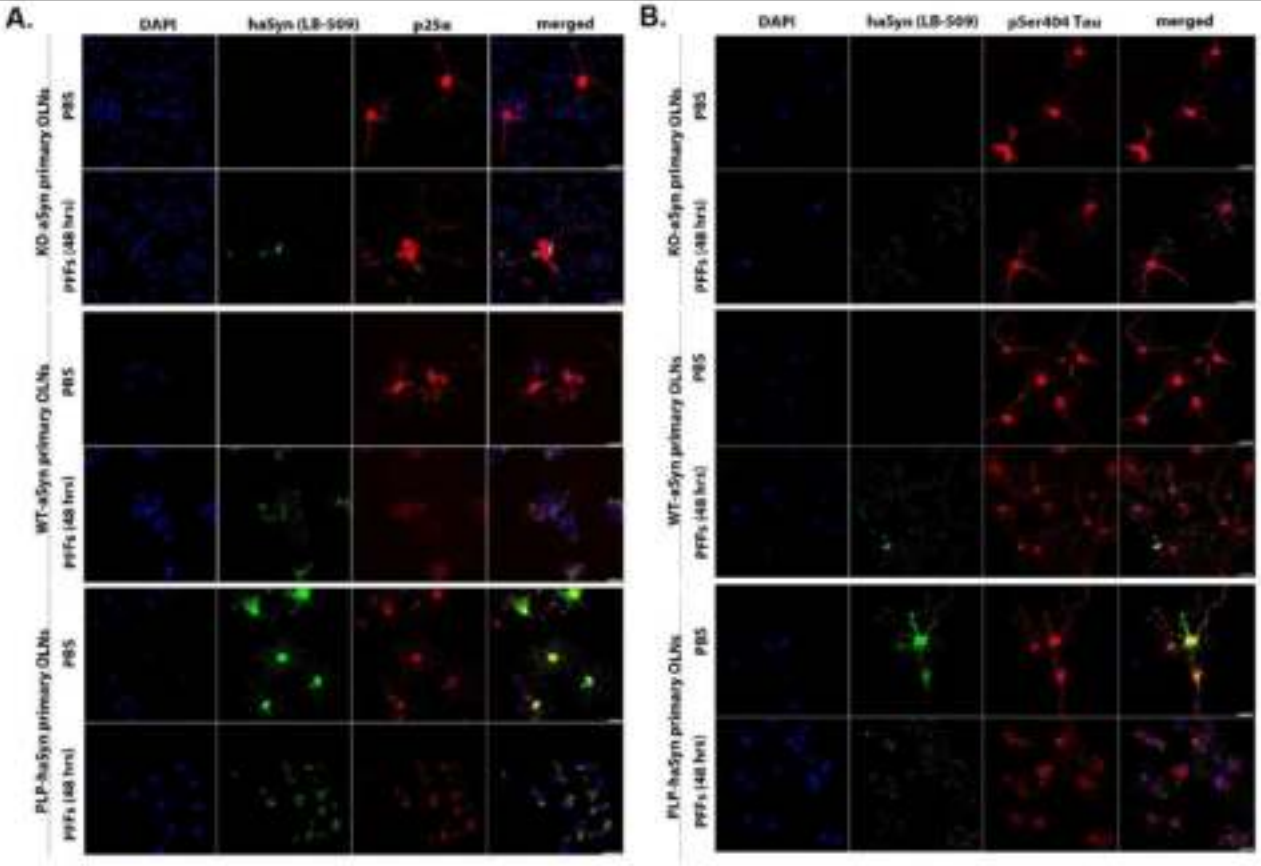

Figure 42: The re-distribution of the microtubule-associated proteins p25α, tau, and MBP in primary oligodendroglial cells depends on endogenous aSyn protein load following the addition of haSyn PFFs. (**A**) p25α redistributes from the oligodendroglial processes to the cell body only in WT-aSyn and in PLP-aSyn cultures and is trapped in aSyn-positive aggregates only in PLP-haSyn oligodendroglial cells (bottom rows), following treatment with haSyn PFFs for 48 hrs. No relocalization of p25α is observed in KO aSyn primary oligodendroglial cultures (upper rows). Representative immunofluorescence images with antibodies against human aSyn (green, LB509), endogenous mouse p25α (red, p25α antibody) and DAPI staining. Scale bar: 25 μm. (**B)** The cellular pattern and distribution of phosphorylated tau at residue Ser404 changes dramatically following the addition of haSyn PFFs in a manner dependent upon the endogenous aSyn protein load. No differences are observed in KO-aSyn cultures treated with haSyn PFFs. Immunofluorescence images with antibodies against human aSyn (green) and pSer404 tau (red, AP01708PU-N antibody) are shown. DAPI is used as a nuclear marker. Scale bar: 25 μm.

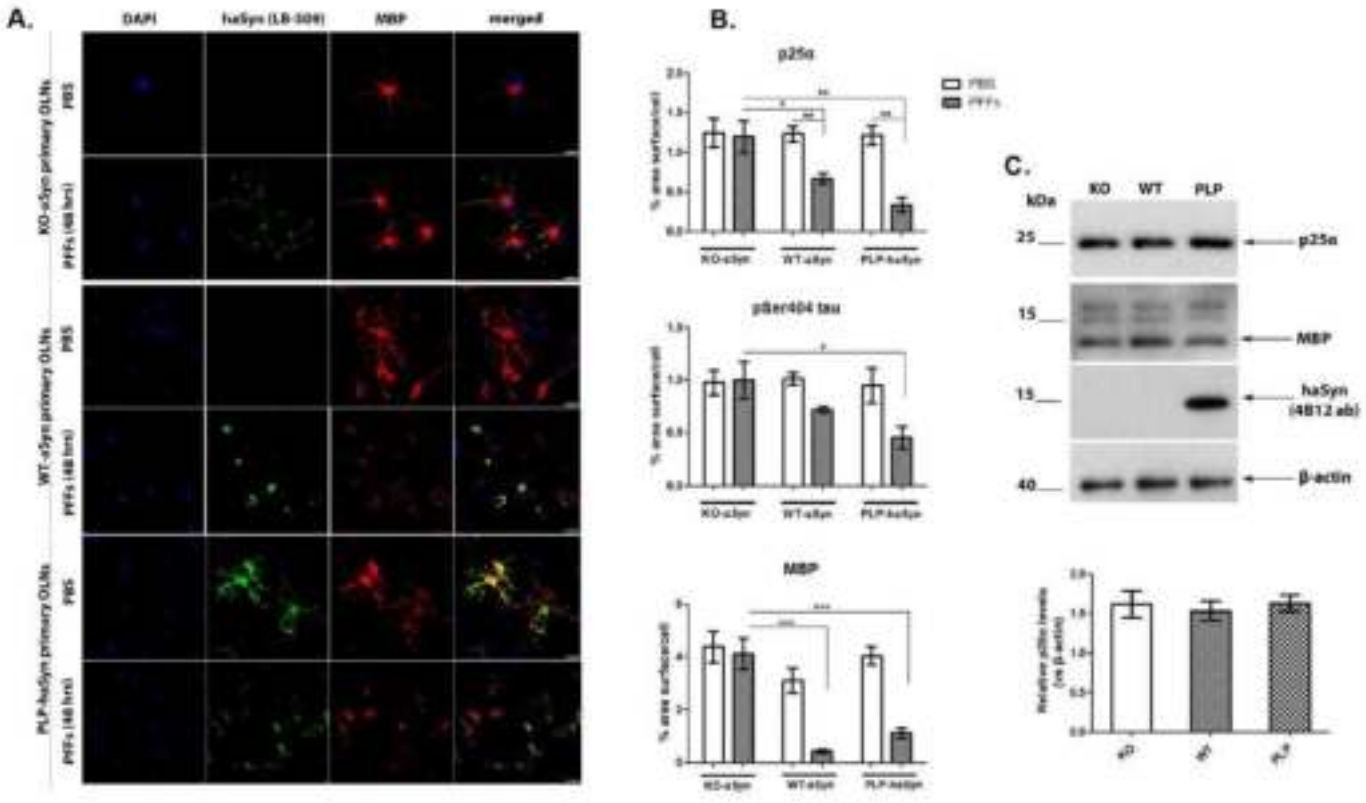

Figure 43: The re-distribution of the microtubule-associated proteins p25α, tau, and MBP in primary oligodendroglial cells depends on endogenous aSyn protein load following the addition of haSyn PFFs. **(A)** The cellular pattern and distribution of MBP changes dramatically following the addition of haSyn PFFs in a manner dependent upon the endogenous aSyn protein load. No differences are observed in KO-aSyn cultures treated with haSyn PFFs, thus highlighting the contribution of the endogenous oligodendroglial aSyn to the dysregulation of myelin. Immunofluorescence images with antibodies against human aSyn (green) and MBP (red) are shown. DAPI is used as a nuclear marker. Scale bar: 25 μm. (**B**) Quantification of p25α (upper row), pSer404 tau (middle row), or MBP protein levels (bottom row) in KO-aSyn, WT-aSyn and PLP-haSyn primary oligodendrocyte cultures treated with 0.5 μg haSyn PFFs for 48 hrs measured as % area surface/cell. Data are expressed as the mean ± SE of three independent experiments with three samples/condition within each experiment; *p< 0.05; **p<0.01; ***p<0.001, by one-way ANOVA with Tukey's post hoc test (to compare between PBS- and PFF-treated cells) or by two-way ANOVA with Bonferroni's correction (to compare between the different PFF-treated cultures). (**C**) No differences are detected in p25α protein levels expressed in KO-aSyn, WT-aSyn, or PLP-haSyn primary oligodendrocytes. (upper panel) Representative immunoblots of p25α, MBP and haSyn (4B12 antibody) protein levels are shown. Equal loading was verified by the detection of β-actin levels. (bottom panel) Quantification of p25α protein levels expressed in all primary oligodendroglial cultures. Data are expressed as the mean ± SE of three independent experiments with triplicate samples/condition within each experiment.

Since p25α is a tubulin polymerization-promoting protein that is involved in the organization of the microtubule network (Tirian, Hlavanda et al. 2003), its re-localization in the presence of haSyn PFFs might also be linked to the altered localization of other microtubule-associated proteins, such as tau, which has also been found to be present in GCIs (Takeda, Arai et al. 1997). To investigate whether the distribution pattern of tau was affected upon the addition of haSyn PFFs, we studied tau phosphorylated at residue Ser404 (pSer404-tau), which is one of the first sites to be hyperphosphorylated leading to the detachment of tau from microtubules, a phenomenon that is closely related to disease pathogenesis in tauopathies (Gustke, Steiner et al. 1992; Alonso, Zaidi et al. 1994; Sun and Gamblin 2009; Mondragon-Rodriguez, Perry et al. 2014). Our data showed that pSer404-tau was redistributed from the processes to the cell soma upon the

addition of haSyn PFFs in a manner dependent on the endogenous aSyn load, since this effect was more evident and robust in PLP-haSyn cultures, whereas the pSer404-tau immunostaining pattern remained unchanged only in the case of KO-aSyn primary oligodendrocytes (**Figures 42B and 43B**). However, pSer404-tau largely failed to be incorporated into haSyn aggregates, even in PLP-haSyn cultures, revealing a different behavior compared to p25α; this may have occurred because this specific phosphorylated form, in contrast to p25α, is unable to bind to microtubules.

Finally, we assessed the impact of exogenously added haSyn PFFs on myelination, which is impaired in MSA brains (Song, Lundvig et al. 2007; Don, Hsiao et al. 2014; Ettle, Kerman et al. 2016). The addition of haSyn PFFs to primary oligodendrocyte precursor cells reportedly leads to the disruption of MBP expression (Kaji, Maki et al. 2018). However, the role of endogenous aSyn in the levels and distribution of MBP remains unknown. In order to investigate whether alterations in the levels of endogenous oligodendroglial aSyn may be linked to alterations in myelin integrity, we assessed haSyn and MBP by confocal microscopy. Our data showed that the presence of endogenous mouse aSyn (in WT-aSyn cultures) or overexpressed human aSyn (in PLP-haSyn cultures) led to a dramatic alteration of MBP immunoreactivity following the addition of haSyn PFFs; in particular, MBP staining was drastically decreased and redistributed from the processes to the cell soma, largely colocalizing with aggregated haSyn (**Figure 43A, B**). On the contrary, KO-aSyn mouse oligodendrocytes did not display any significant changes in MBP levels or distribution (**Figure 43A**), thus indicating a crucial role for seeded oligodendroglial aSyn aggregation in the alterations of MBP.

9. Delivery of haSyn PFFs into the mouse striatum is accompanied by the recruitment of endogenous oligodendroglial protein in MBP+ pathological aggregates and the impairment of myelin integrity

In order to evaluate the seeding capacity of haSyn within oligodendrocytes in vivo, we performed unilateral stereotactic injections of haSyn PFFs (4 μg/brain) (or PBS as a control) into the mouse striatum, to imitate the situation occurring in MSA brains. As shown in **Figure 44A** (bottom panels), the delivery of haSyn PFFs into the mouse striatum seeded the recruitment of endogenous mouse aSyn to form MBP-positive inclusions, which were positive for human and rodent aSyn, detected at 1 month post-injection (**Figure 44A, IPSI, indicated by the asterisks**). The uptake of haSyn PFFs by oligodendrocytes was verified further by co-staining with the p25α antibody (**Figure 44B**), whose specificity for oligodendrocytes in the mouse striatum was confirmed by its complete co-localization with O4 and Olig2 antibodies (**Figure 44C**).

Consistent with the results in the primary oligodendroglial cultures, the MBP-positive signal changed dramatically upon the addition of haSyn PFFs, and MBP^{+} puncta colocalized with the

human (LB-509), rodent (D37A6), total (SYN1) and aggregated aSyn antibodies (**Figures 44A and 45A**). Importantly, such alterations were not observed when a similar amount of haSyn PFFs was injected into the striatum of KO-aSyn mice (**Figure 44A**). Staining with the SYN303 aSyn antibody, which recognizes oxidized/nitrated species, revealed the formation of pathological aggregated aSyn assemblies in MBP^+ oligodendrocytes of the ipsilateral striatum within 1 month of injection (**Figure 45B**). No SYN303 aSyn-positive signal was detected in haSyn PFF-injected KO-aSyn striatum (data not shown), and none of the aforementioned pathological alterations were observed in the ipsilateral striatum of WT-aSyn mice injected with PBS (**Figure 46**).

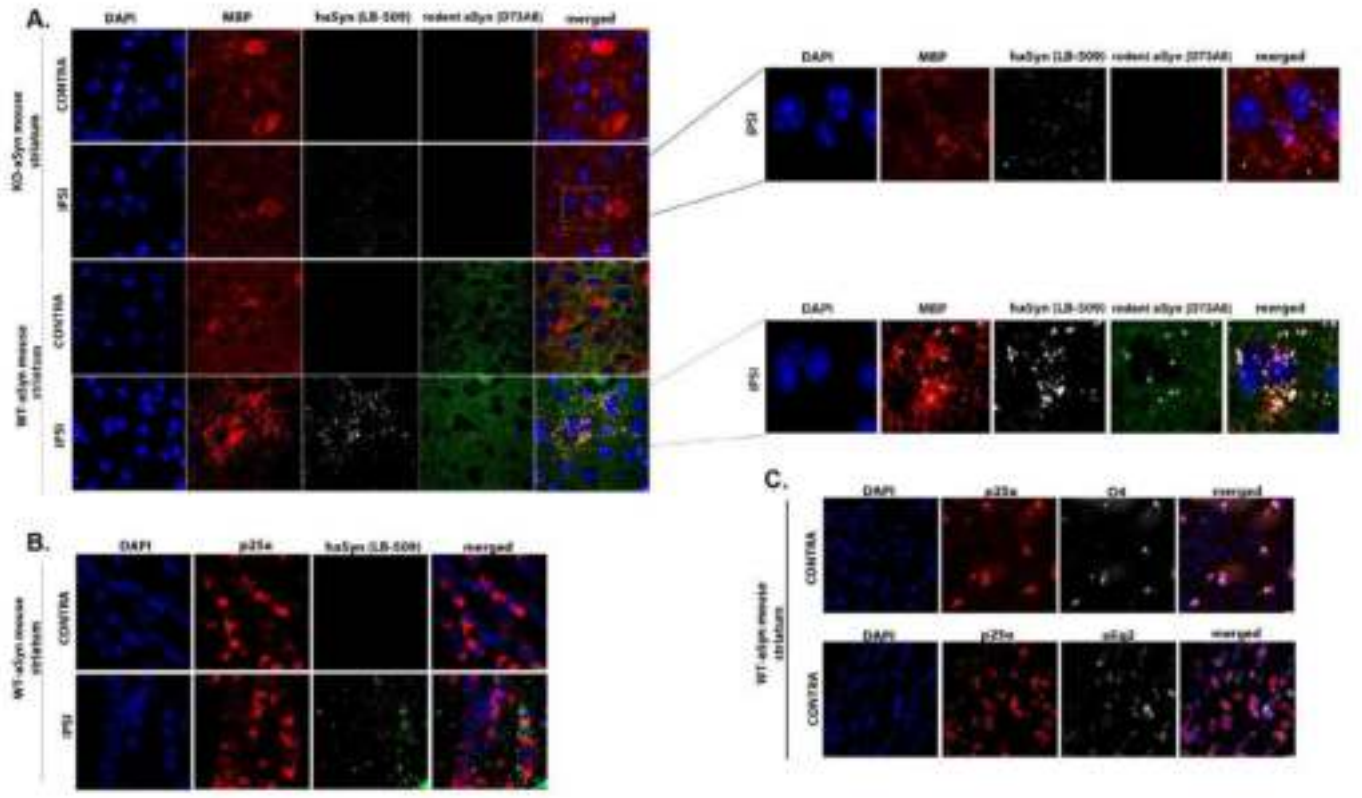

Figure 44: Unilateral delivery of haSyn PFFs (4 µg) into the WT-aSyn mouse striatum results in the recruitment of endogenous mouse oligodendroglial aSyn and the formation of pathological aSyn assemblies. (**A**) Representative immunofluorescence images showing the co-localization (indicated by the asterisks) of exogenously added human aSyn PFFs (gray) with endogenous mouse aSyn (green) in MBP^+ cells (red) in the ipsilateral (IPSI) striatum, but not in the contralateral (CONTRA) striatum, at 1 month post-injection (lower panel). Importantly, no endogenous mouse-specific aSyn signal was detected in the ipsilateral striatum of KO-aSyn mice (upper panel). Scale bar: 10 µm. High-power merged images are shown on the right. (**B**) Human aSyn PFFs are taken up by striatal oligodendrocytes in vivo, as shown by confocal microscopy using antibodies against human aSyn (green, LB-509 antibody) and the oligodendroglial marker p25α (red, p25α antibody). Scale bar: 10 µm. (**C**) The specificity of our home-made p25α antibody to oligodendrocytes was further verified using the O4 (gray, upper panel) and Olig2 (gray, bottom panel) antibodies. Scale bar: 10 µm.

Importantly, ultrastructural EM analysis revealed that haSyn PFFs evoked a clear rearrangement of the myelin sheath in the striatum of WT-aSyn mice, compared to PFF-treated KO-aSyn mice, as depicted by the increased number of axons with a decompacted myelin sheath and axons with myelin vesiculation (**Figure 45 C, D**). Such data support further the aforementioned

results in PFF-treated primary oligodendrocytes (**Figure 43A, B**) and in the PFF-treated ipsilateral WT-aSyn striatum (**Figure 44A and 45A**).

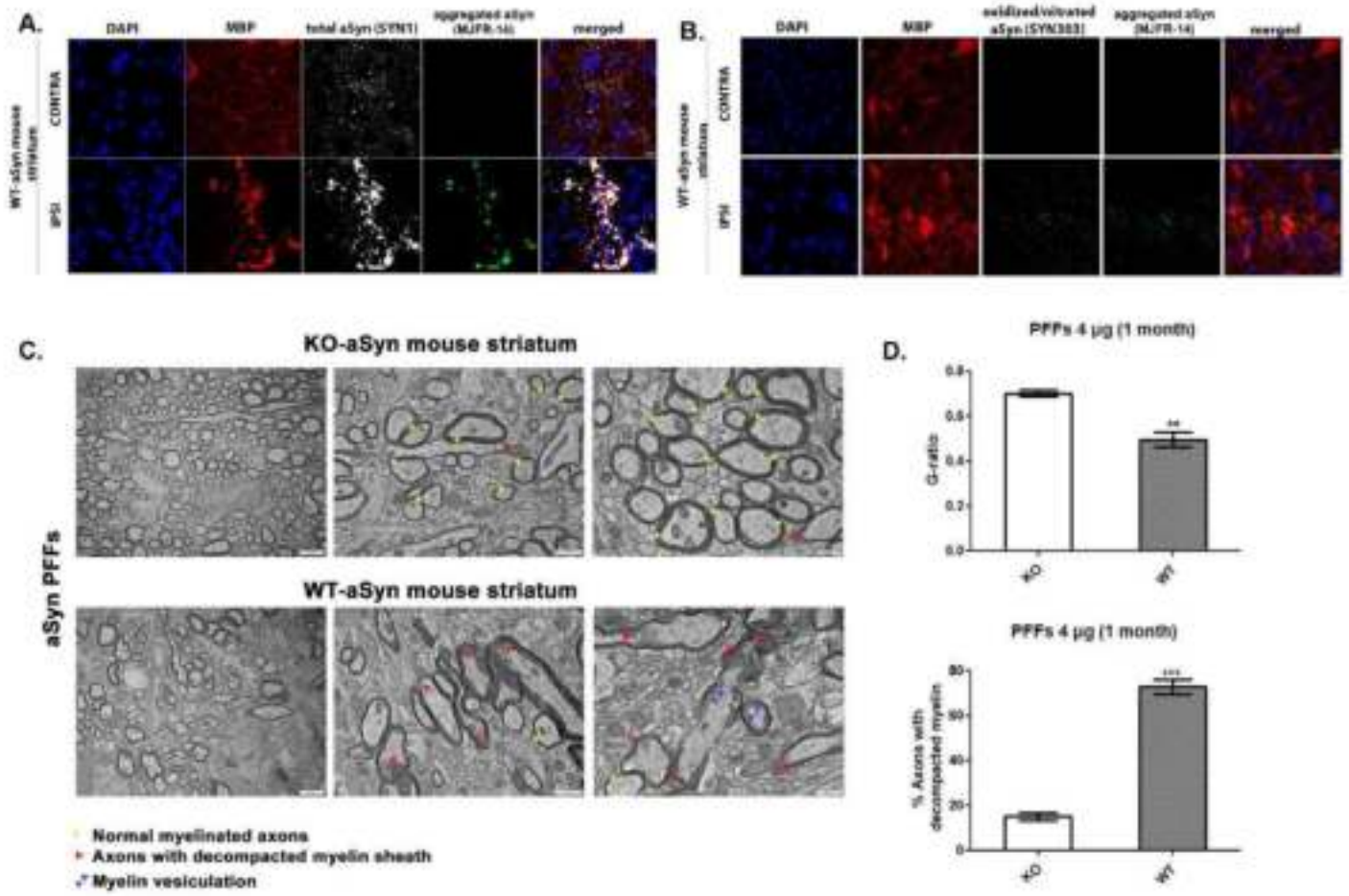

Figure 45: Unilateral delivery of haSyn PFFs (4 µg) into the WT-aSyn mouse striatum results in the recruitment of endogenous mouse oligodendroglial aSyn and the formation of pathological aSyn assemblies. (**A**) MBP redistributes in the PFF-injected striatum and co-localizes with aggregated aSyn conformations. Representative immunofluorescence images for MBP (red), human aSyn (gray, SYN1 antibody), aggregated aSyn (green) and DAPI staining. Scale bar: 10 µm. (**B**) Pathological aSyn assemblies are detected in the ipsilateral striatum of WT-aSyn mice injected with haSyn PFFs at 1 month post-injection, as verified using antibodies against oxidized/nitrated aSyn (gray) and aggregated aSyn (green). Scale bar: 10 µm. (**C**) Ultrastructural transmission EM analysis of haSyn PFF-injected KO-aSyn (upper panel) or WT-aSyn (bottom panel) mouse striatum at 1 month post-injection, revealing myelin sheath decompaction only in WTaSyn neuronal axons (red arrowheads) vs. normal myelinated axons (yellow asterisks). Purple arrowheads point to areas with vesiculated myelin sheaths. Scale bars: 2 µm (left panels), 1 µm (middle panels), and 500 nm (right panels). (**D**) Average myelin g-ratio values (upper row) and quantification of axons with decompacted myelin (bottom row) derived from haSyn PFF-injected KO-aSyn or WT-aSyn mouse striatum. Data are expressed as the mean± SE of n=4 mice per group. **p<0.01; ***p< 0.001 by Student's unpaired t test.

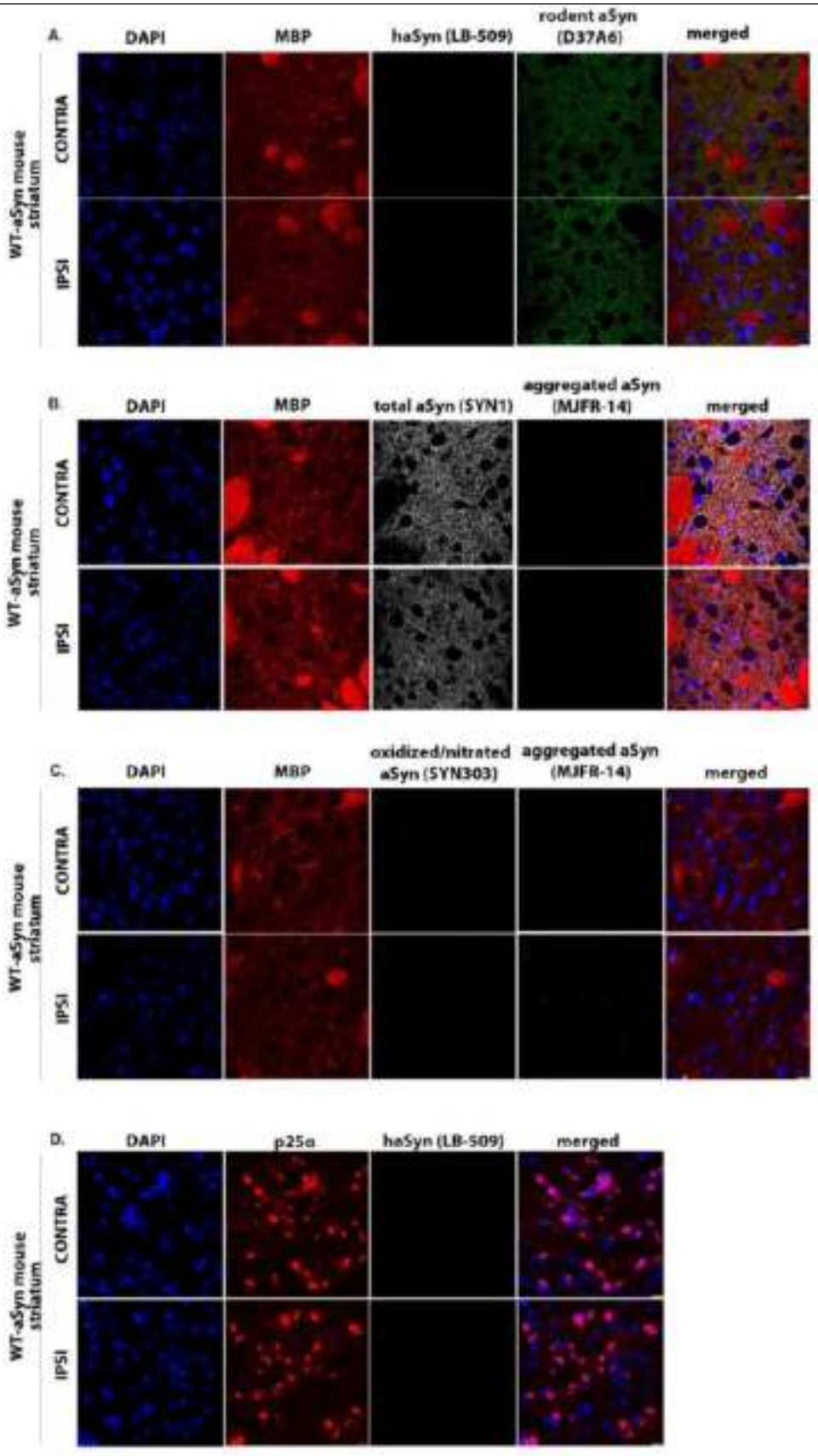

Figure 46: Unilateral intrastriatal delivery of PBS into the mouse WT-aSyn brain is not associated with aSyn-related pathology. (**A-D)** Representative immunofluorescence images with antibodies against haSyn (gray, LB-509 antibody), total aSyn (gray, SYN1 antibody), oxidized/nitrated aSyn (gray, Syn303 antibody), endogenous mouse aSyn (green, D37A6 antibody), aggregated aSyn (green, MJFR-14 antibody), p25α (red, shown in **D**), and MBP (red, shown in **A-C**) and DAPI staining. Scale bar: 10 μm.

10. Both the proteasome and the ALP contributes to the degradation of the endogenous rat oligodendroglial aSyn

Our aforementioned data insinuate that manipulation of the expression of aSyn and/or p25α in oligodendrocytes may provide a rational approach to combat the accumulation of aSyn in GCIs and the progression of MSA. However, the degradation pathways responsible for the clearance of the endogenous oligodendroglial aSyn and p25α in health and disease and the role of ALP manipulation in the context of MSA remained unexplored.

In order to study the degradation pathways responsible for the proteolysis of the endogenous rat oligodendroglial aSyn, we pharmacologically inhibited the lysosome (total and macroautophagy-dependent) and the proteasome, or we performed siRNA-based gene silencing of CMA- and macroautophagy-related genes. Specifically, we utilized the rat oligodendroglial OLN-93, OLN-AS7 and OLN-p25α cell lines, which express very low to non-detectable levels of the endogenous aSyn and we treated cells with 20 mM NH_4Cl (as total lysosomal inhibitor), 10 mM 3MA (as macroautophagy inhibitor) or 15 nM epoxomicin (epox, as proteasomal inhibitor) for 48 hrs. Confocal microscopy analysis revealed that all pharmacological inhibitors significantly increased the oligodendroglial aSyn signal in all lines (expressed as μm^2 area/cell), detected with the rodent-specific D37A6 antibody (**Figure 47A-D**). Moreover, immunoblot analysis further confirmed the notion that the oligodendroglial aSyn is mostly degraded by the lysosome (**Figure 48 A, B**).

In order to dissect the partitioning of CMA and macroautophagy lysosomal pathways in the rodent aSyn degradation under basal conditions, we treated all OLN cell lines with *Lamp2a*-(Lsi1/Lsi2) or *Atg5*- (*Atg5* si) specific siRNAs, targeting the LAMP2A receptor which acts as the rate-limiting step of the pathway or the macroautophagy- ATG5 protein that participates in the formation of the phagophore, which will ultimately become the autophagosome. The efficacy of these siRNAs on LAMP2A or ATG5 downregulation was verified 72 hrs later by confocal microscopy that revealed an almost 3-fold decrease in the respective protein levels as a result of the effective gene silencing (**Figure 49A-D**), measured as M.F.I./cell. *Atg5* siRNA was accompanied by decreased levels of the autophagosome marker LC3B, further verifying the efficient inhibition of macroautophagy (**Figure 49E-F**).

Interestingly, treatment of OLN cells with Lsi1/Lsi2 (**Figure 50**) or *Atg5* (**Figure 51**) siRNAs was accompanied by a significant increase in endogenous rat oligodendroglial aSyn protein levels. It is important to mention that the D37A6 antibody does not produce a specific immunofluorescence signal in control conditions (PBS- or scr siRNA-treated cells, **Figures 47, 50, 51**), whereas in immunoblot analysis, film overexposure enables the detection of the rodent aSyn signal at minute amounts even at basal conditions (**Figure 48**). In all cases, α-tubulin was used as a

cytoskeletal marker, in order to verify the cytoplasmic distribution of the endogenous oligodendroglial aSyn protein.

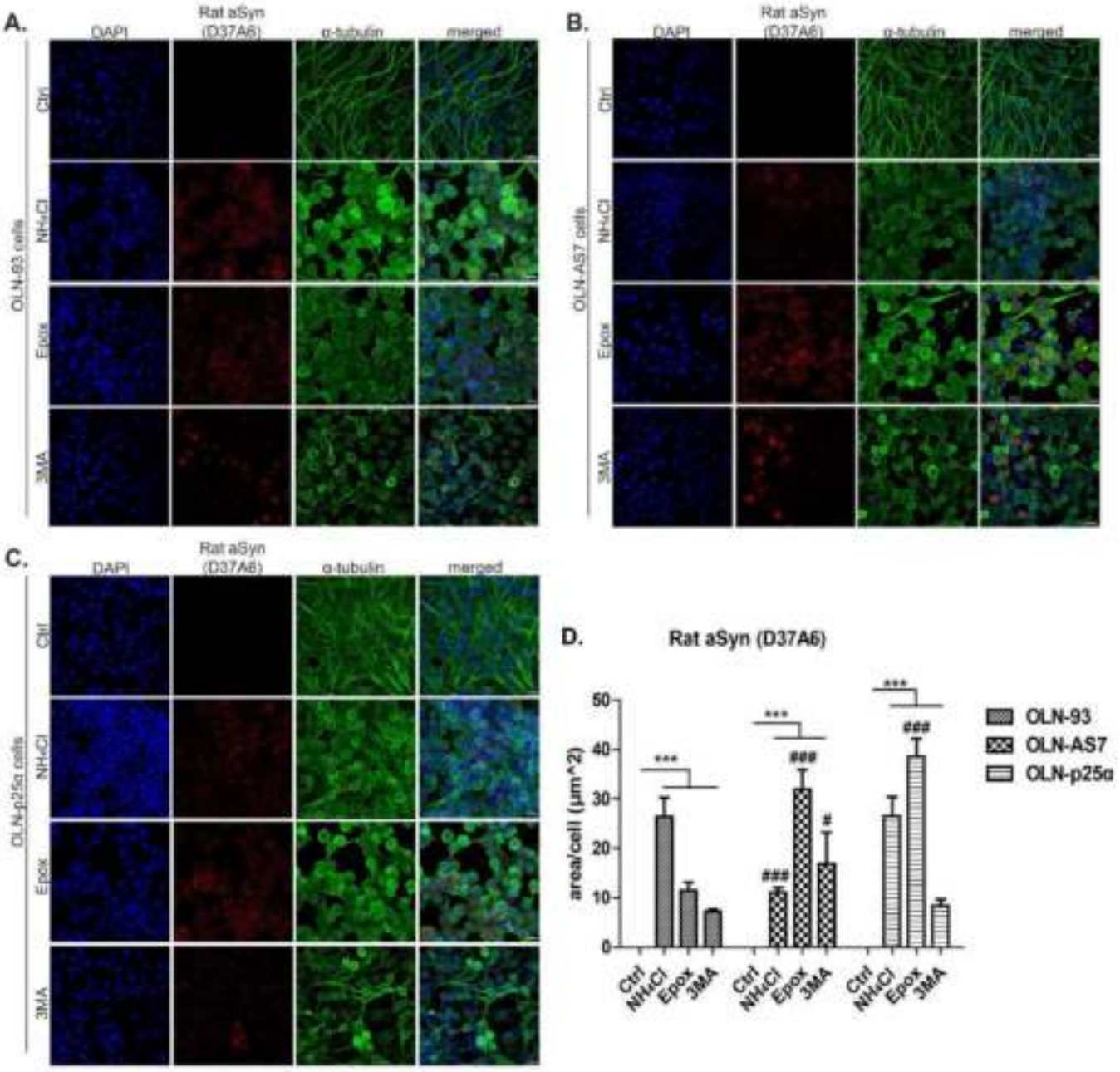

Figure 47: Both autophagy and the proteasome contributes to the degradation of the endogenous rat oligodendroglial aSyn. (**A-C**) Confocal microscopy with endogenous rodent-specific aSyn and α-tubulin antibodies reveals the cytoplasmic accumulation of the endogenous oligodendroglial aSyn in OLN-93 (**A**), OLN-AS7 (**B**) and OLN-p25α cells (**C**) upon treatment with: proteasomal (epoxomicin, 15 nM) or autophagy (NH_4Cl 20 mM, 3MA 10 mM) inhibitors for 48 hrs. Representative immunofluorescence images with antibodies against α-tubulin (green) and rat aSyn (red, D37A6 antibody) and DAPI staining are shown. Scale bar: 25 μm. (**D**) Quantification of the endogenous rat aSyn protein levels in OLN cells measured as μm^2 area surface/cell following treatment with proteasomal (epox) or lysosomal (NH_4Cl, 3MA) inhibitors for 48 hrs. Data are expressed as the mean ± SE of three independent experiments with duplicate samples/condition within each experiment; ***p< 0.001, by one-way ANOVA with Tukey's post hoc test (to compare between inhibitor-treated and untreated cells) or #p<0.05; ###p< 0.001 by two-way ANOVA with Bonferroni's correction (to compare between the different OLN cell lines).

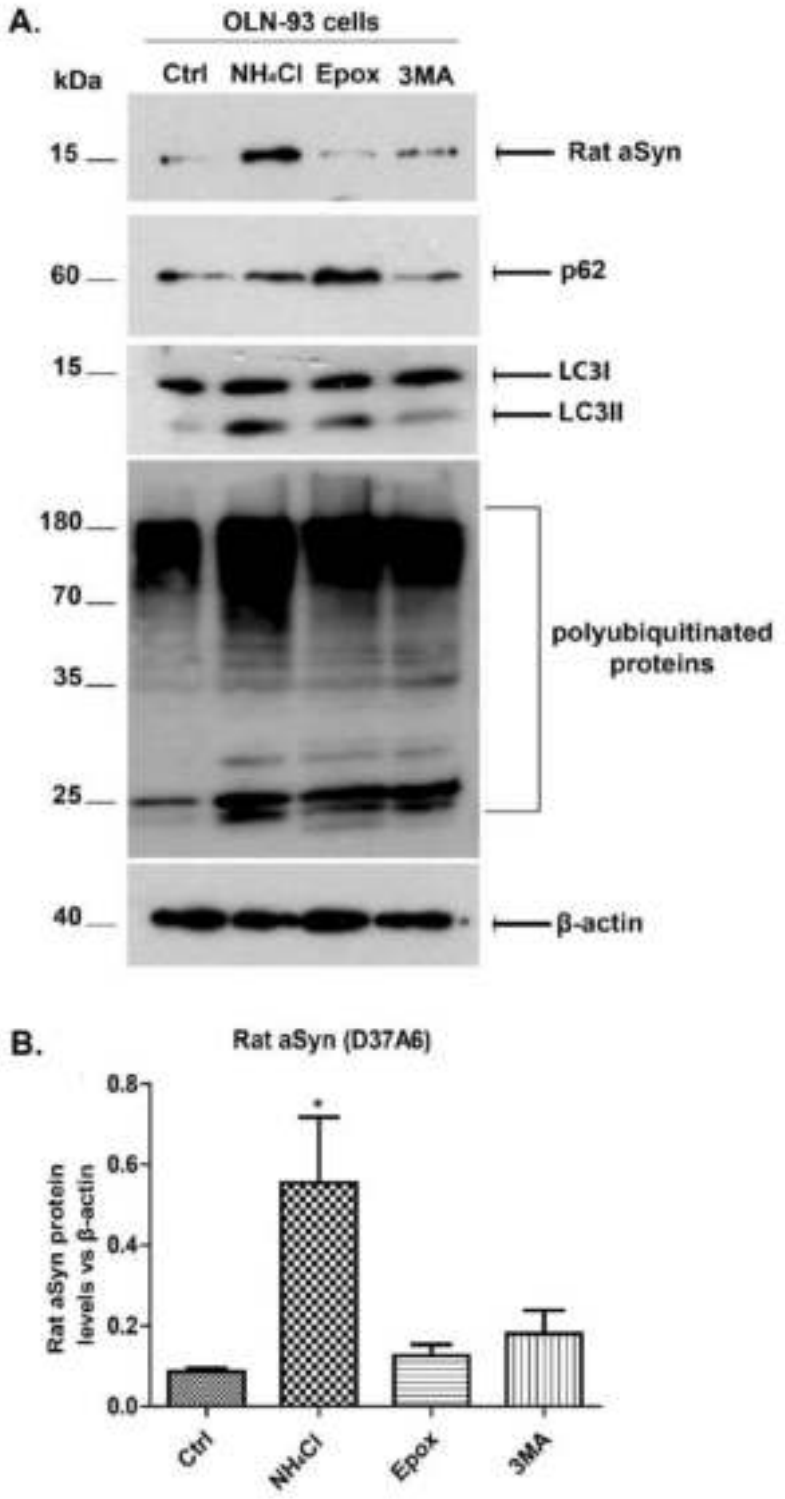

Figure 48: Both autophagy and the proteasome contributes to the degradation of the endogenous rat oligodendroglial aSyn. (**A**) Representative immunoblots for rodent aSyn (D37A6 antibody), poly-ubiquitinated proteins, LC3I & II, and p62 (as macroautophagy markers), and β-actin (as loading control), verifying the increase of endogenous oligodendroglial aSyn protein levels in OLN-93 cells following lysosomal inhibition (NH_4Cl, 48 hrs). (**B**) Quantification of the endogenous rat aSyn protein levels in OLN-93 cells treated with proteasomal (epox) or autophagy (NH_4Cl, 3MA) inhibitors for 48 hrs. Data are expressed as the mean ± SE of three independent experiments with duplicate samples/condition within each experiment; *$p<0.05$, by one-way ANOVA with Tukey's post hoc test.

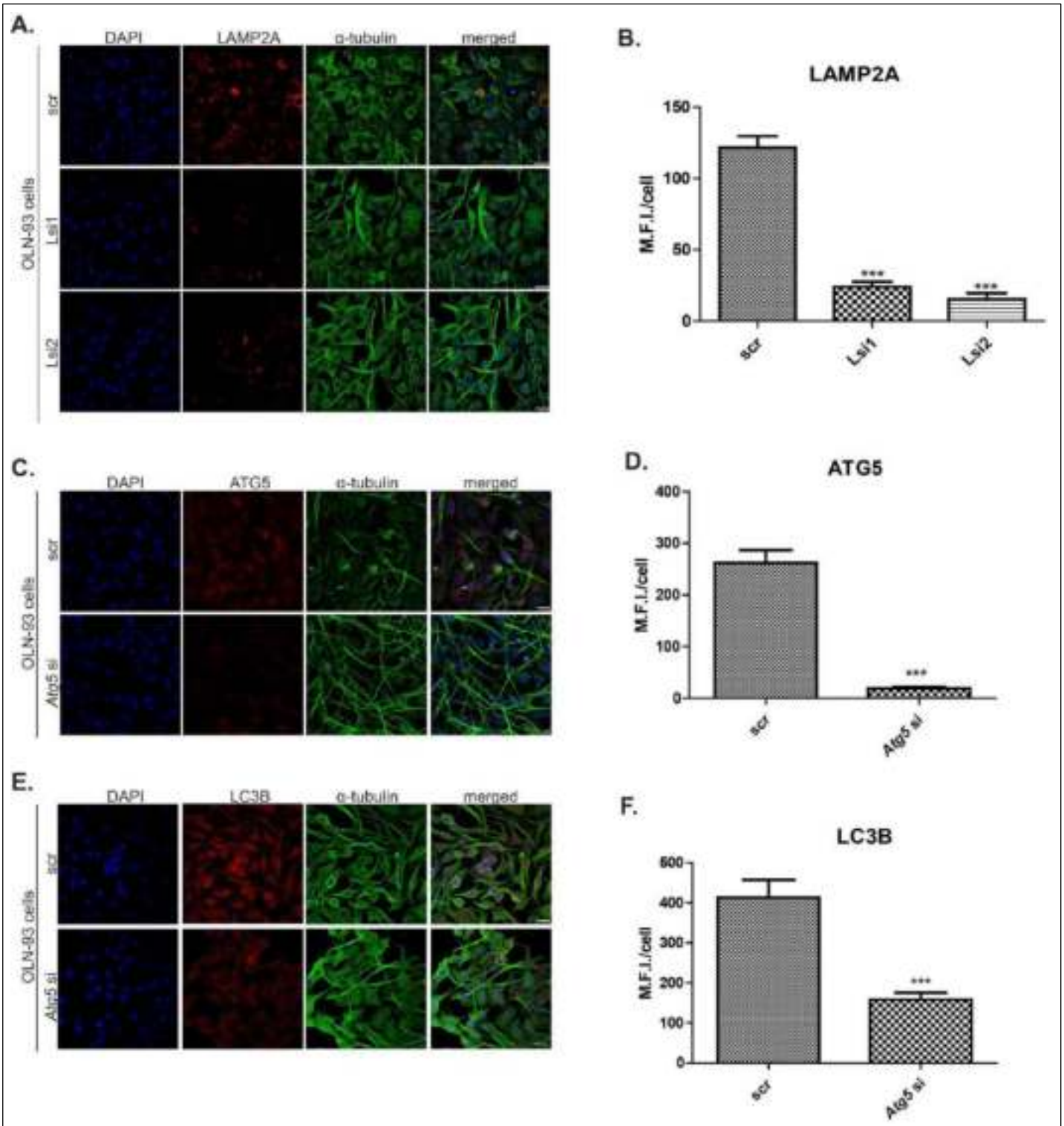

Figure 49: Efficient down-regulation of LAMP2A and ATG5 protein levels by *Lamp2a* and *Atg5* siRNAs, respectively. OLN-93 cells were treated with (**A**) Lsi1/Lsi2 (60 nM) or (**C, E**) *Atg5* si (10 nM) for 72 hrs for *Lamp2a* and *Atg5* silencing, respectively. (**A, C, E**) Representative immunofluorescence images of LAMP2A (A, red) and ATG5 (C, red) proteins verifying the genes' silencing. The reduced expression of the autophagosome marker LC3B (**E**, red) upon *Atg5* siRNA treatment indicates efficient macroautophagy inhibition. A-tubulin is used as cytoskeletal marker (green) and DAPI as nuclear marker. Scale bar: 25 μm. (**B, D, F**) Quantification of LAMP2A (**B**), ATG5 (**D**) and LC3B (**F**) protein levels in OLN-93 cells, measured as M.F.I./cell. Data are expressed as the mean±SE of three independent experiments with duplicate samples/condition within each experiment; ***p< 0.001, by one-way ANOVA with Tukey's post hoc test.

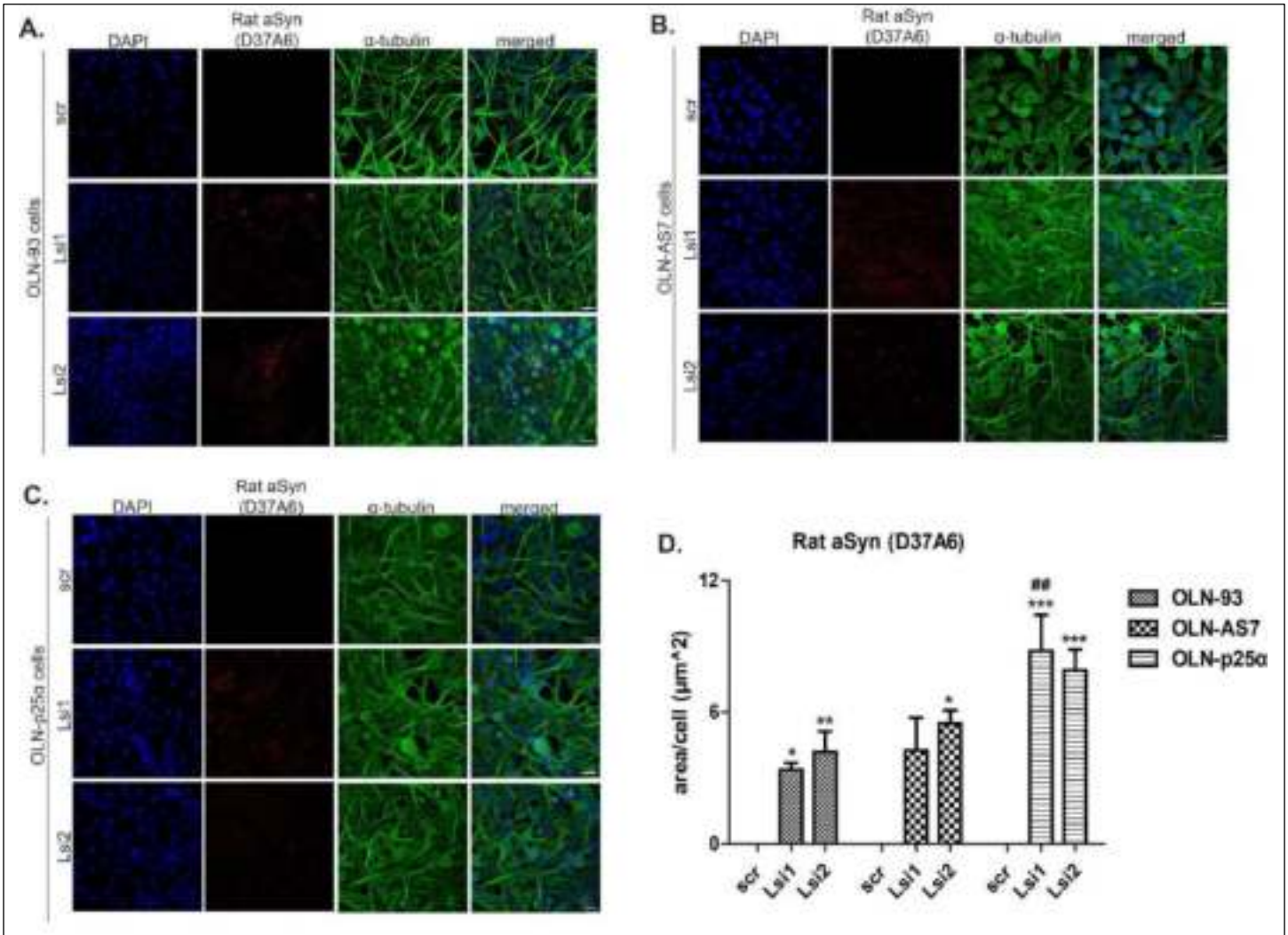

Figure 50: Down-regulation of the CMA-related gene *Lamp2a* leads to the accumulation of the endogenous rat oligodendroglial aSyn. (**A-C**) Representative immunofluorescence images of OLN-93 (**A**), OLN-AS7 (**B**) and OLN-p25α cells (**C**) treated with two different siRNAs targeting the rat Lamp2a receptor (Lsi1/Lsi2, 60 nM) for 72 hrs. Scrambled RNA sequences (scr) were used as negative control. The antibodies utilized were against α-tubulin (green) and rat aSyn (red, D37A6 antibody). DAPI was used as a nuclear marker. Scale bar: 25 μm. (**D**) Quantification of the endogenous rat aSyn protein levels in OLN cells shown in **A-C** measured as μm^2 area surface/cell. Data are expressed as the mean ± SE of three independent experiments with duplicate samples/condition within each experiment; *p<0.05; **<0.01; ***p< 0.001, by one-way ANOVA with Tukey's post hoc test (to compare between siRNA-treated and untreated cells) or ##p< 0.01 by two-way ANOVA with Bonferroni's correction (to compare between the different treated cell cultures).

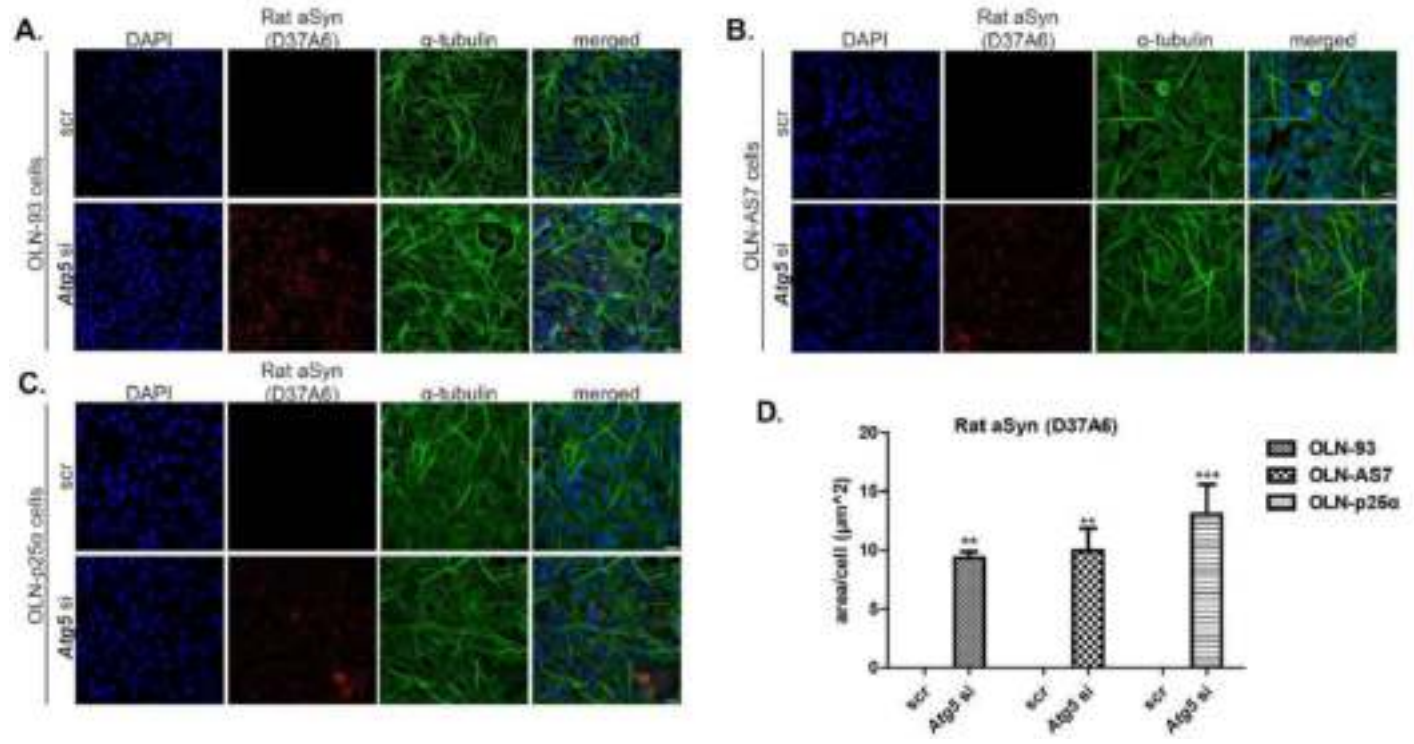

Figure 51: Down-regulation of the macroautophagy-related gene *Atg5* leads to the accumulation of the endogenous rat oligodendroglial aSyn. (**A-C**) Confocal microscopy images depicting the cytoplasmic accumulation of the rodent oligodendroglial aSyn (D37A6 ab, red) in OLN-93 (**A**), OLN-AS7 (**B**) and OLN-p25α cells (**C**) upon treatment with *Atg5*-siRNA (Atg5 si, 10 nM) or scrambled siRNA (scr) for 72 hrs. α-tubulin was used as a cytoskeletal marker and DAPI as a nuclear marker. Scale bar: 25 μm. (**D**) Quantification of the endogenous rat aSyn protein levels in OLN cells shown in **A-D** measured as μm^2 area surface/cell. Data are expressed as the mean ± SE of three independent experiments with duplicate samples/condition within each experiment; **<0.01; ***p< 0.001, by one-way ANOVA with Tukey's post hoc test.

11. The overexpressed human aSyn accumulates upon pharmacological or molecular inhibition of the autophagy-lysosome pathway in OLN-AS7 cells

The degradation of the overexpressed human aSyn was also studied in OLN-AS7 cells, as above. Treatment of rat OLN-AS7 cells with NH_4Cl or 3MA for 48 hrs increased human aSyn protein levels (detected with the human-specific aSyn antibody LB-509) measured as M.F.I./cell, suggesting that this protein is degraded, at least partly, via the ALP (**Figure 52 A, B**). Moreover, the accumulation of human aSyn upon NH_4Cl or 3MA treatment of OLN-AS7 cells for 48 hrs was further verified by immunoblot analysis as shown in **Figure 52 C, D**. In addition, transfection of OLN-AS7 cells with Lsi1/Lsi2 or *Atg5* siRNAs for 72 hrs increased protein levels of human aSyn albeit non-significantly, as detected with confocal microscopy (**Figure 53A, B, E and F)** and immunoblot analysis (**Figure 53 C, D, G and H)**.

Interestingly, proteasomal inhibition (epox, 24 hrs) evoked a robust increase of human *Snca* mRNA levels in OLN-AS7 cells (**Figure 54A**), accompanied by accumulation of human aSyn protein levels (data not shown) due to the epox-mediated non-specific activation of the CMV promoter (which drives the expression of human *Snca* in OLN-AS7 cells), as has been previously

suggested by Biasini et al., 2004 (Biasini, Fioriti et al. 2004). Similar effect has been reported using lactacystin or MG132 (Biasini, Fioriti et al. 2004), rendering difficult the investigation of the role of the proteasome to the degradation of the overexpressed human protein in OLN-AS7 cells. Importantly, treatment of OLN-AS7 cells with NH_4Cl for 24 hrs or 48 hrs did not increase human *Snca* mRNA levels, suggesting that the observed increased protein levels upon lysosomal inhibition was due to impaired degradation (**Figure 54C**).

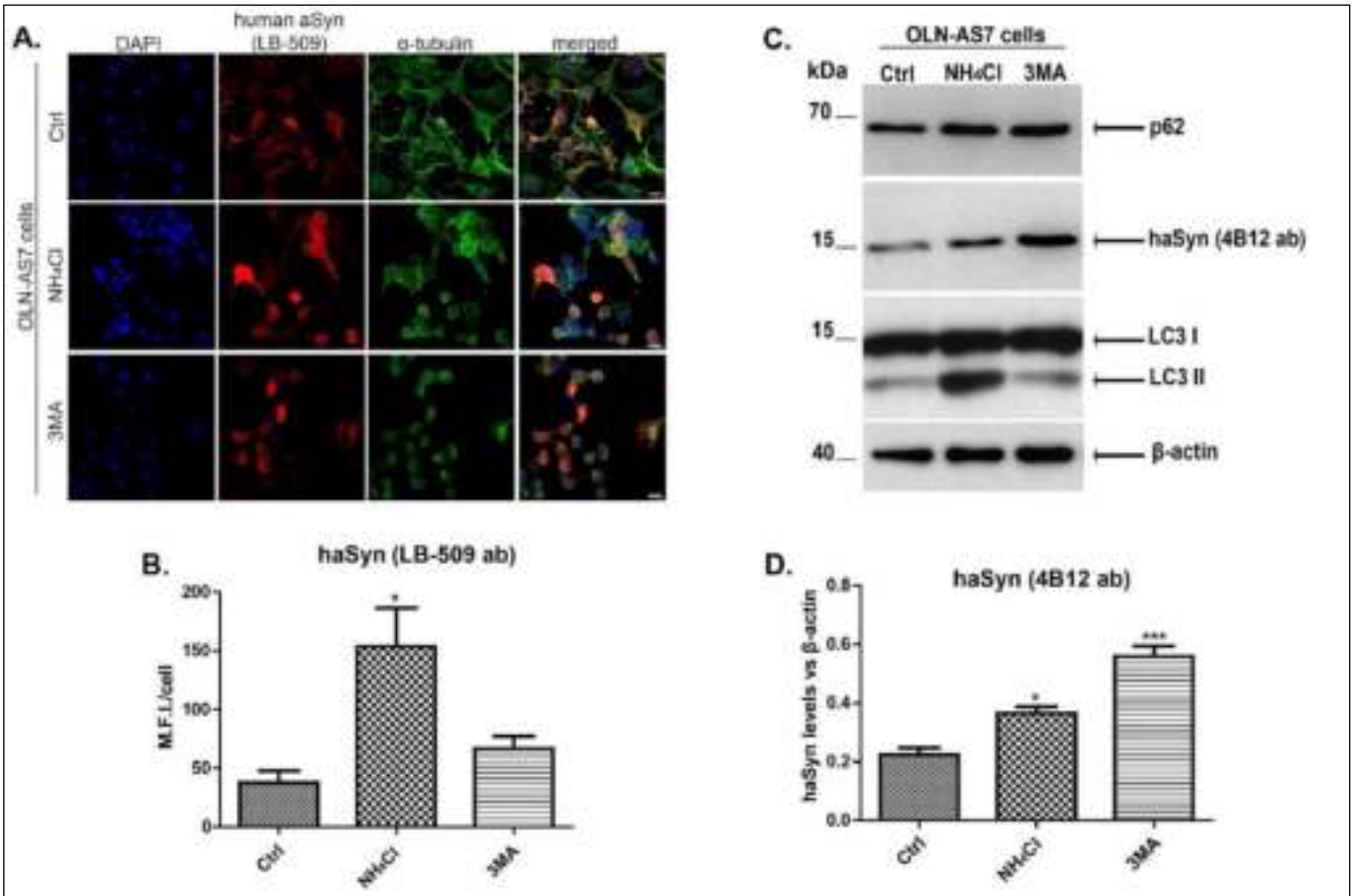

Figure 52: The overexpressed human aSyn accumulates upon pharmacological inhibition of the ALP in OLN-AS7 cells. (**A**) Representative immunofluorescence images of OLN-AS7 cells treated with NH_4Cl (20 mM) or with the macroautophagy inhibitor 3MA (10 mM) using antibodies against human aSyn (red, LB509 antibody) and α-tubulin (green) and DAPI staining. Scale bar: 25 μm. (**B**) Quantification of human aSyn protein levels in OLN-AS7 cells measured as Mean Fluorescence Intensity/cell (M.F.I./cell) following treatment with NH_4Cl, 3MA for 48 hrs. Data are expressed as the mean±SE of three independent experiments with duplicate samples/condition within each experiment; *p<0.05; **p< 0.01, by one-way ANOVA with Tukey's post hoc test. (**C**) Representative immunoblots of human aSyn protein levels (using the human aSyn-specific 4B12 antibody) derived from OLN-AS7 cells following total lysosomal (NH_4Cl) or macroautophagy inhibition (3MA). Antibodies against LC3I & II, and p62 were used as macroautophagy markers and β-actin as loading control. (**D**) Quantification of the human aSyn protein levels in OLN-AS7 cells treated with NH4Cl or 3MA for 48 hrs. Data are expressed as the mean±SE of three independent experiments with duplicate samples/condition within each experiment; *p<0.05; ***p<0.001, by one-way ANOVA with Tukey's post hoc test.

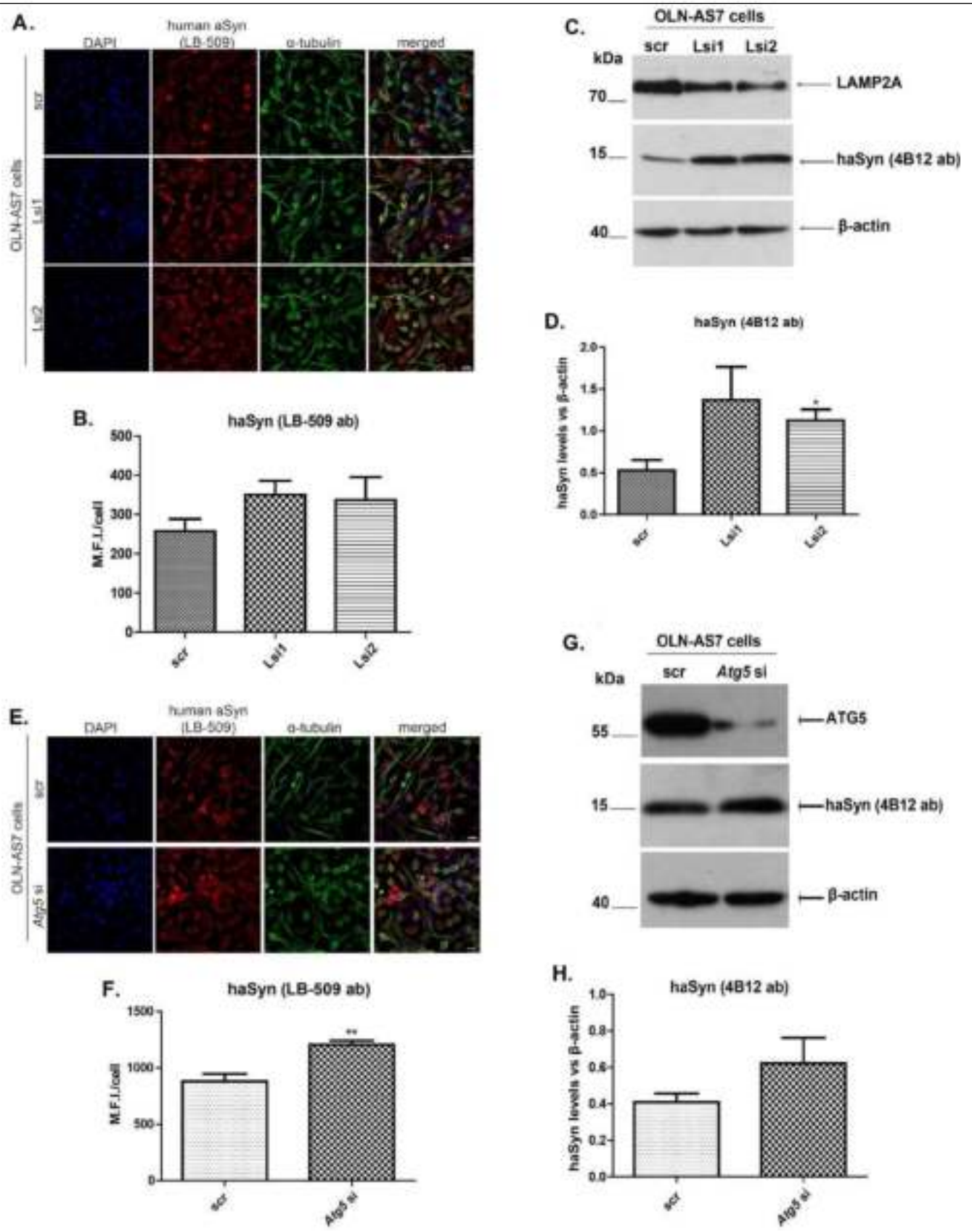

Figure 53: The overexpressed human aSyn accumulates upon molecular inhibition of the ALP in OLN-AS7 cells. (**A, E**) Representative immunofluorescence images of OLN-AS7 cells following siRNA delivery targeting Lamp2a (**A**) or the autophagy-related Atg5 gene (**E**) using antibodies against human aSyn (red, LB509 antibody) and α-tubulin (green) and DAPI staining. Scale bar: 25 μm. (**B, F**) Quantification of human aSyn protein levels in OLN-AS7 cells measured as Mean Fluorescence Intensity/cell (M.F.I./cell) following transfection with Lsi1/Lsi2 (60 nM) (B) or Atg5 si (10 nM) (F) for 72 hrs.

Figure 53 (continued): Scrambled RNA sequences (scr) were used as negative control. Data are expressed as the mean±SE of three independent experiments with duplicate samples/condition within each experiment; *p<0.05; **p< 0.01, by one-way ANOVA with Tukey's post hoc test. (**C, G**) Representative immunoblots of human aSyn protein levels (using the human aSyn-specific 4B12 antibody) derived from OLN-AS7 cells following gene silencing using Lamp2a- (Lsi1/Lsi2) and Atg5-si RNAs, respectively. Gene silencing was verified by the detection of LAMP2A or ATG5 protein levels. Scrambled RNA sequences (scr) were used as negative control. Antibodies against LC3I & II, and SQSTM1 were used as macroautophagy markers and β-actin as loading control. (**D, H**) Quantification of the human aSyn protein levels in OLN-AS7 cells treated with (D) Lsi1/Lsi2 for 72 hrs and (H) Atg5 si for 72 hrs. Data are expressed as the mean±SE of three independent experiments with duplicate samples/condition within each experiment; *p<0.05; ***p<0.001, by one-way ANOVA with Tukey's post hoc test.

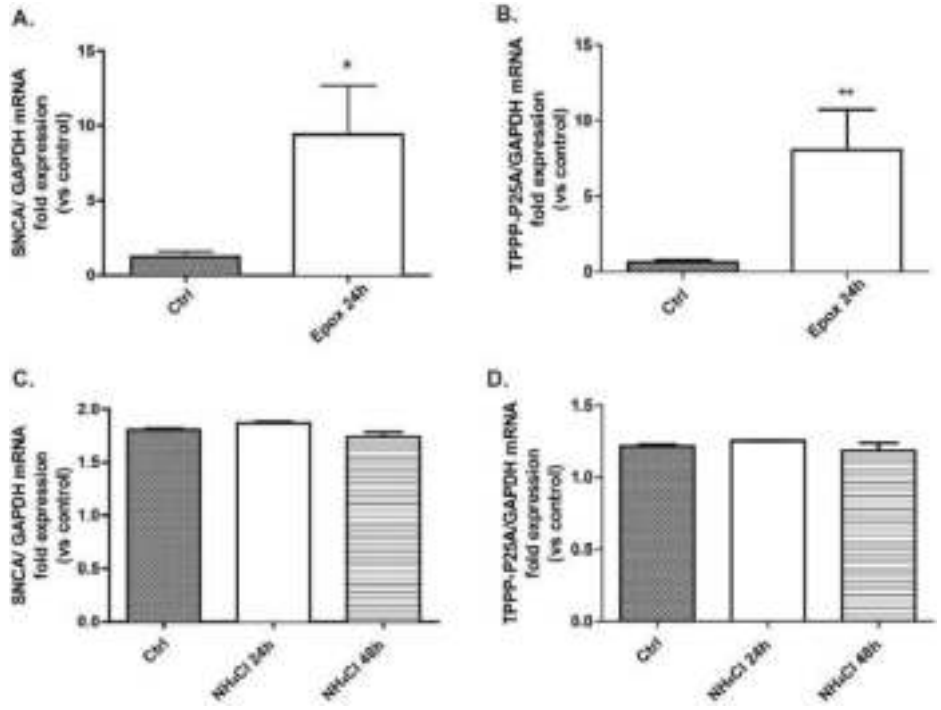

Figure 54: Non-specific CMV-dependent transcriptional up-regulation of human *Snca* and *Tppp/p25α* mRNA by the proteasomal inhibitor epoxomicin. (**A-B**) Expression of *Snca* and *Tppp/p25α* cDNAs is driven by the CMV promoter in OLN-AS7 and OLN-p25α cells, respectively and epoxomicin (epox, 15 nM, 24 hrs) increased the CMV-driven transcription, as assessed by quantitative real-time PCR. (**C-D**) No alterations at the mRNA levels of *Snca* or *Tppp/p25α* were observed when OLN-AS7 and OLN-p25α cells were treated with the total lysosomal inhibitor NH_4Cl (20 mM) for 24 or 48 hrs. Data are expressed as human *Snca* or *Tppp/p25α* mRNA levels relative to the mRNA levels of rat *Gapdh* normalized to control-treated cultures (PBS).

12. The overexpressed human p25α is increased following pharmacological or molecular inhibition of the autophagy-lysosome pathway in OLN-p25α cells

To decipher the role of the ALP on p25α proteolysis, OLN-p25α cells were incubated with 20 mM NH_4Cl or 10 mM 3MA (48 hrs) for total lysosomal or macroautophagy-dependent inhibition, respectively, and protein levels of p25α were assessed by immunofluorescence analysis (as M.F.I./cell) and Western blotting. According to the data presented in **Figure 55** treatment of OLN-p25α cells with these pharmacological inhibitors led to p25α protein accumulation, suggesting

that the lysosome (with macroautophagy contributing to a lesser extent) is responsible, at least partly, for p25α proteolysis under basal conditions.

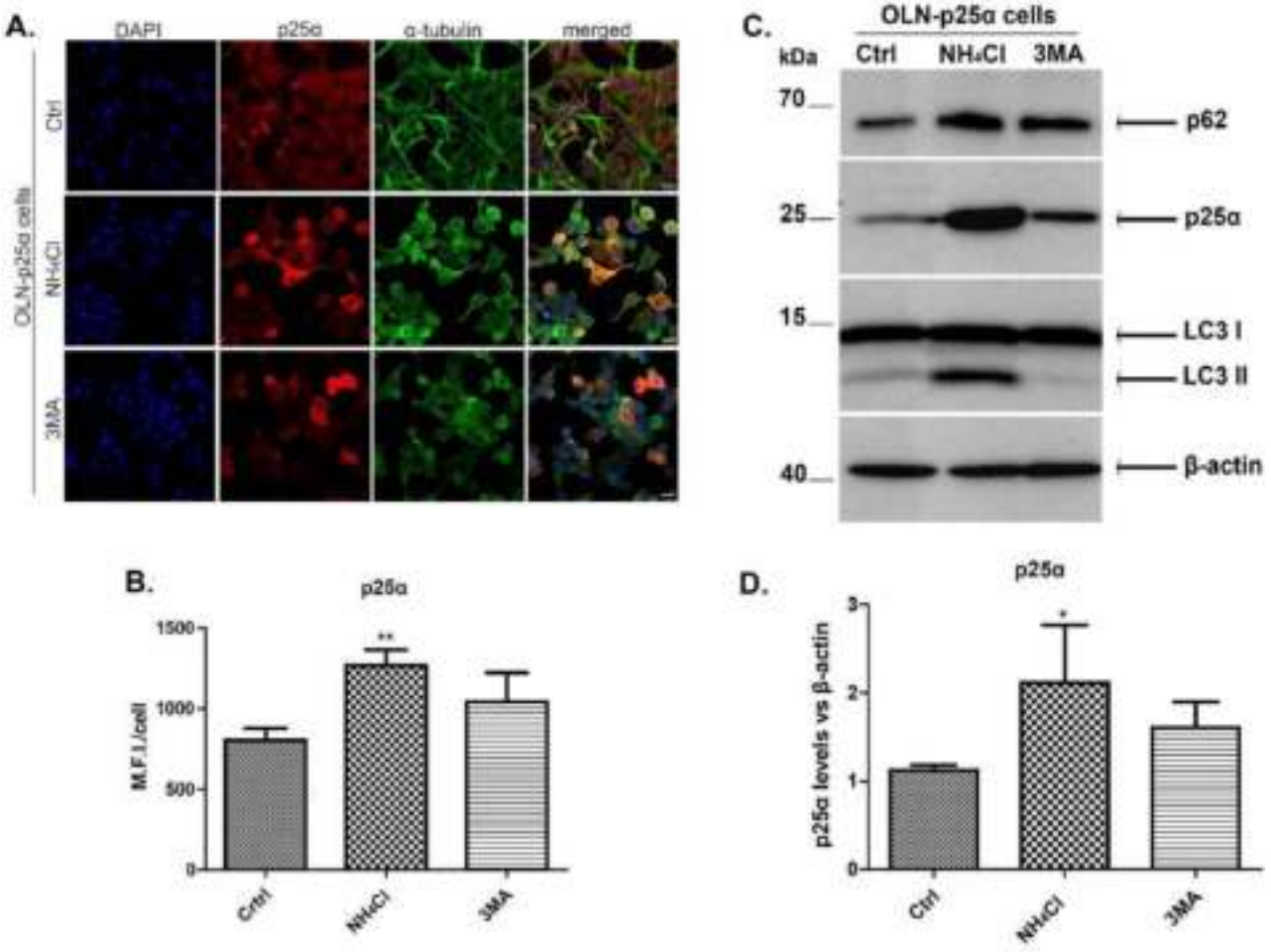

Figure 55: The overexpressed human p25α is increased following pharmacological inhibition of the ALP in OLN-p25α cells. (**A**) Representative immunofluorescence images of OLN-p25α cells showing the increased protein levels of human p25α upon pharmacological inhibition of lysosomal pathways (total, CMA, macroautophagy) using antibodies against human p25α (red) and α-tubulin (green) and DAPI staining. Scale bar: 25 μm. (**B**) Quantification of human p25α protein levels in OLN-p25α cells measured as M.F.I./cell following treatment with NH_4Cl, 3MA for 48 hrs. Data are expressed as the mean±SE of three independent experiments with duplicate samples/condition within each experiment; *p<0.05; **p< 0.01, by one-way ANOVA with Tukey's post hoc test. (**C**) Representative immunoblots of OLN-p25α cell lysates verifying the accumulation of p25α protein levels upon lysosomal inhibition using pharmacological. Antibodies against LC3I & II, and p62 were used as macroautophagy markers and β-actin as a loading control. (**D**) Quantification of the human p25α protein levels in OLN-p25α cells treated with NH4Cl or 3MA for 48 hrs. Data are expressed as the mean±SE of three independent experiments with duplicate samples/condition within each experiment; *p<0.05, by one-way ANOVA with Tukey's post hoc test.

Lamp2a or *Atg5* gene silencing revealed that p25α protein is partially degraded via the CMA and macroautophagy pathways (**Figure 56**), since both manipulations evoked an increase in p25α protein levels with the Lsi2 RNA sequence against rat LAMP2A eliciting a statistically significant accumulation of p25α levels (**Figure 56B, D**). It has to be noted that treatment of all OLN cells with the pharmacological inhibitors NH_4Cl and epox for 48 hrs, had no significant impact on cell survival. However, only in the case of 3MA-treated OLN-AS7 and OLN-p25α cells for 48 hrs, a 20% decrease in cell survival was observed (**Figure 57**). As in OLN-AS7 cells, epoxomicin, but not

NH_4Cl treatment, evoked a non-specific upregulation of human *Tppp/p25α* mRNA levels due the increased CMV-driven promoter gene transcription (see **Figure 54B, D**).

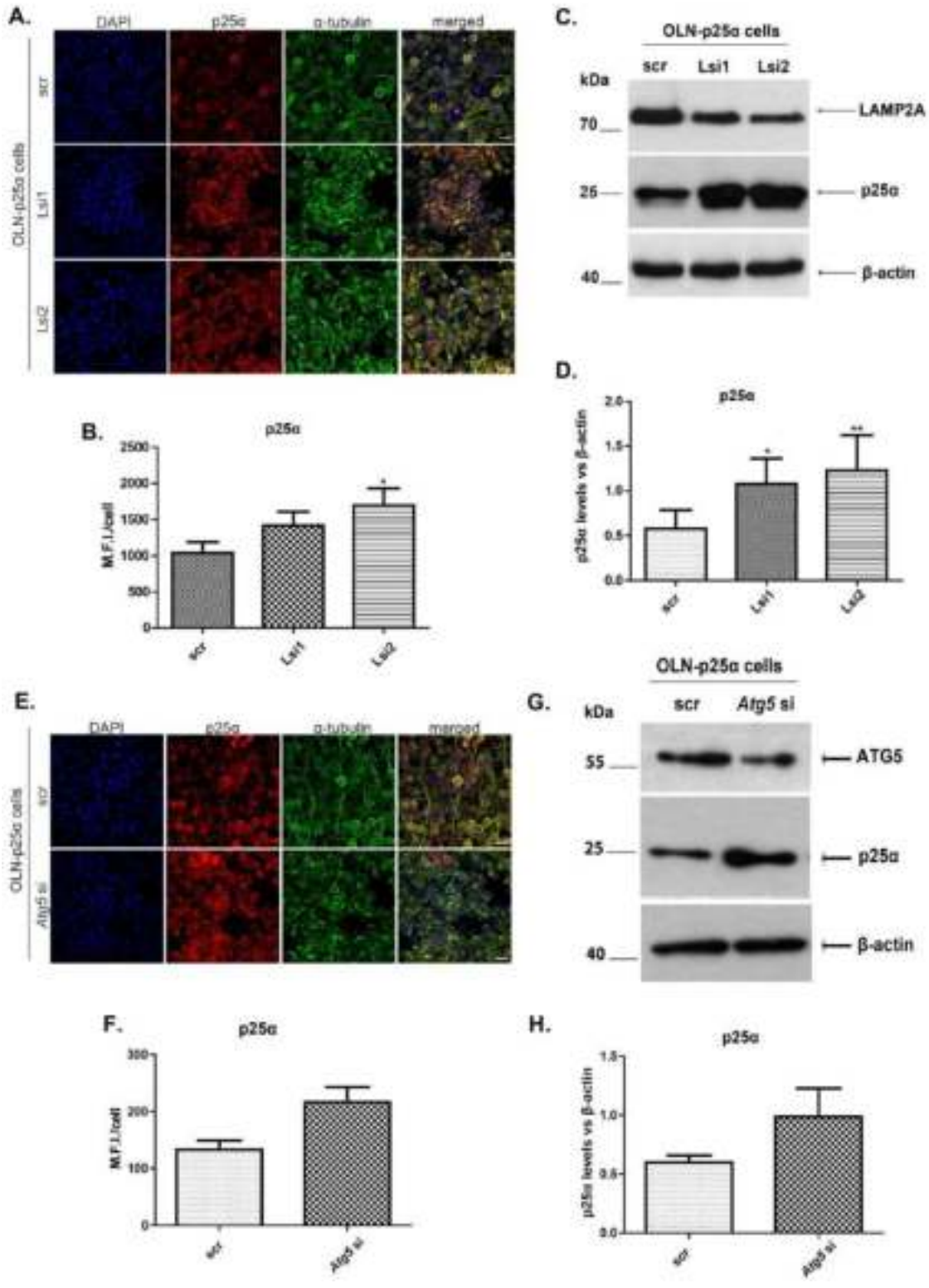

Figure 56: The overexpressed human p25α is increased following molecular inhibition of the ALP in OLN-p25α cells. (**A, E**) Representative immunofluorescence images of OLN-p25α cells showing the increased protein levels of human p25α upon molecular inhibition of lysosomal pathways (total, CMA, macroautophagy) using antibodies against human p25α (red) and α-tubulin (green) and DAPI staining. Scale bar: 25 μm. (**B, F**) Quantification of human p25α protein levels in OLN-p25α cells measured as M.F.I./cell following treatment with *Lamp2a*-or *Atg5*-siRNAs for 72 hrs. Scrambled RNA sequences (scr) were used as negative control.

Figure 56 (continued): Data are expressed as the mean±SE of three independent experiments with duplicate samples/condition within each experiment; *p<0.05; **p< 0.01, by one-way ANOVA with Tukey's post hoc test. (**C, G**) Representative immunoblots of OLN-p25α cell lysates verifying the accumulation of p25α protein levels upon lysosomal inhibition using gene silencing methods. *Lamp2a* and *Atg5* downregulation was verified using antibodies against LAMP2A or ATG5 proteins. Scrambled RNA sequences (scr) were used as negative control. Antibodies against LC3I & II, and p62 were used as macroautophagy markers and β-actin as a loading control. (**D, H**) Quantification of the human p25α protein levels in OLN-p25α cells treated with Lsi1/Lsi2 (60 nM) for 72 hrs and *Atg5* si (10 nM) for 72 hrs. Data are expressed as the mean±SE of three independent experiments with duplicate samples/condition within each experiment; *p<0.05, by one-way ANOVA with Tukey's post hoc test.

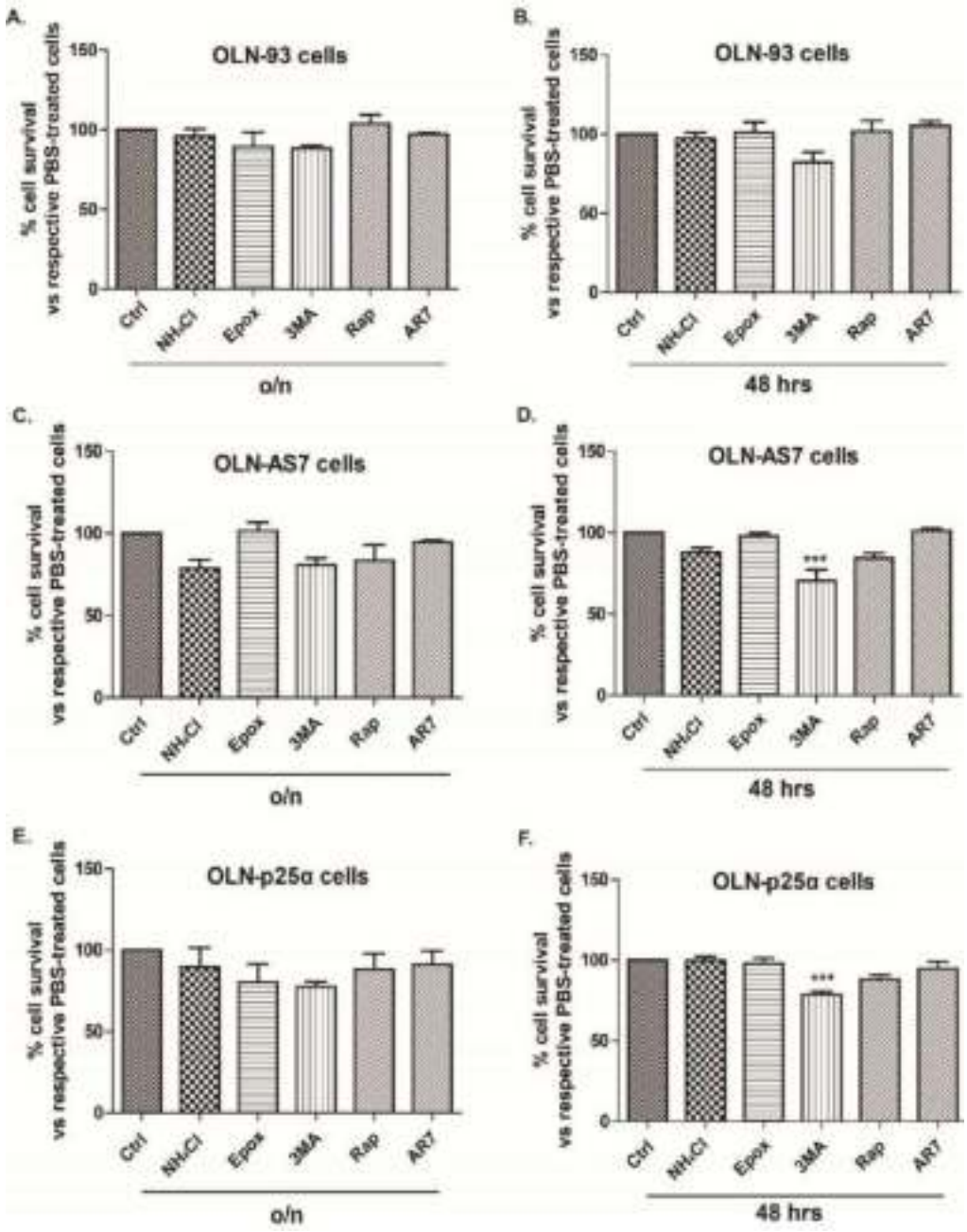

Figure 57: Effects of short-term or prolonged incubation of OLN cells with pharmacological inhibitors/enhancers of degradation pathways on cell survival. Treatment of OLN cells with pharmacological inhibitors (NH_4Cl/20 mM, 3MA/10 mM and epox/15 nM) or enhancers (AR7, 40 μM and rap, 1 μM) for 16 hrs (**A, C, E**) or 48 hrs (**B, D, F**) has no significant impact on cell survival, with the exception of prolonged incubation of OLN-AS7 and OLN-p25α cells with 3MA. Data are expressed as the mean ± SE of at least three independent experiments with triplicate samples/condition within each experiment; ***p< 0.001, by one-way ANOVA with Tukey's post hoc test.

13. The oligodendroglial-specific protein p25α is a putative CMA substrate

In order for a protein to be a CMA substrate, it has to bear a KFERQ-like CMA-targeting motif that guides the delivery of the protein to the level of the lysosomal membrane, where binding with the CMA-specific receptor, LAMP2A, takes place. We therefore examined whether this is the case for p25α, and found that it contains a pentapeptide sequence (KKRFK), consistent with a CMA targeting motif (**Figure 58A**). According to the 3D structure of the rat Cgi-38 protein (PDB id: 1WLM) [homologous of the human p25α (NM_001108461)], the KKRFK is located in a loop, flanked by two adjacent α-helices, both fully exposed to the solvent. **Figure 58A** shows the superposed structures of the human, mouse and the 3D model of the p25α bearing the KKRFK motif.

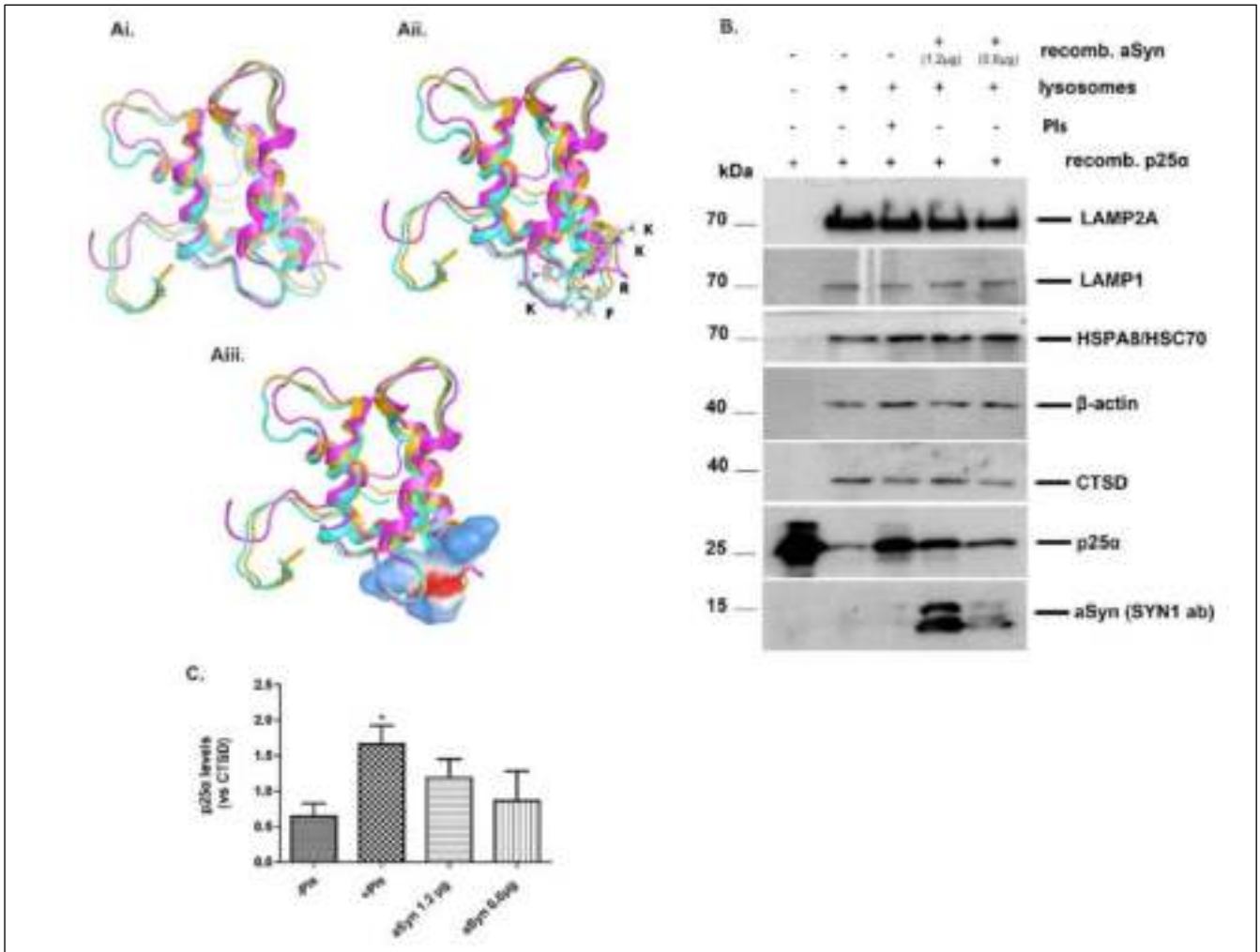

Figure 58: The oligodendroglial-specific protein p25α is a putative CMA substrate, containing a KFERQ-like motif necessary for CMA targeting. (**Ai**) The superposed p25α protein from human (magenta), mouse (orange) and the human model (turquoise), (**Aii**) The superposed X-Ray structures and the model with the KKRFK motif highlighted, (**Aiii**) The KKRFK motif with electrostatic surface. Notice that the KFERQ-like motif region is in a loop, surrounded by two α-helices, fully exposed to the solvent. (**B**) Representative immunoblots of recombinant p25α in vitro degradation via isolated rat brain-derived lysosomes. Lysosomes were incubated with 0.2 μg recombinant human p25α protein in the absence or presence (as negative control) of protease inhibitors (PIs). The addition of increasing amounts of recombinant human monomeric aSyn (0.6 μg or 1.2 μg) reveals the competition of the two proteins (aSyn and p25α) for LAMP2A binding and CMA degradation. Human recombinant HSPA8/HSC70 was used for the substrate translocation to the lysosomes. Lysosomal enrichment was verified by the detection of LAMP2A, LAMP1 and CTSD and equal loading with β-actin and CTSD proteins. (**C**) Quantification of the relative levels of human recombinant p25α protein (versus CTSD levels) in the presence or the absence of PIs or recombinant human monomeric aSyn Data are expressed as the mean±SE of three independent experiments; *p<0.05, by one-way ANOVA with Tukey's post hoc test.

Given that the presence of the CMA motif does not guarantee that the protein is actually degraded via this pathway (Dice 1990), we incubated human recombinant p25α with isolated rat brain lysosomes and assessed the in vitro degradation of the protein, in the presence or absence of Protease Inhibitors (PIs). Under these conditions, we found that purified recombinant p25α added to the incubation medium was translocated into and efficiently degraded by intact brain lysosomes, since lysosomal protease inhibitors increased the levels of the lysosome-associated protein (**Figure 58B-C**). Interestingly, a competition assay utilizing 3x (0.6 μg) and 6x (1.2 μg) amount of human recombinant aSyn, a well-established CMA substrate (Cuervo, Stefanis et al. 2004) effectively inhibited the degradation of p25α by intact lysosomes, in a dose-dependent manner (**Figure 58B-C**). These data, in combination with the increased protein levels of p25α following LAMP2A down-regulation (**Figure 56 A-D**), further confirm that the oligodendroglial p25α is a putative CMA substrate and is degraded via this pathway in OLN cells.

14. Both the exogenously added human aSyn (haSyn PFFs) and the recruited endogenous rat oligodendroglial aSyn are partly degraded via the autophagy-lysosome pathway, without impairing lysosomal function

We subsequently assessed the proteolytic pathways responsible for aSyn and p25α clearance, as well as the role of the overexpressed human aSyn and p25α on the proteasomal and lysosomal function, under conditions of increased aSyn protein burden, thus mimicking the human MSA. To this end, OLN cells were inoculated with 0.5 μg haSyn PFFs for 48 hrs and 16 hrs prior to cell-fixation, lysosomal or proteasomal inhibitors were added to the medium and then fixed cells were stained for immunofluorescence analysis. Epoxomicin was used only for the assessment of the endogenous rodent aSyn degradation, since, as already mentioned, it evokes a CMV-dependent upregulation of the human *Snca* and *Tppp/p25α* mRNA levels (**Figure 54**).

Confocal microscopy analysis revealed that in PFF-treated OLN-93 cells, inhibition of total lysosomal (NH_4Cl) or proteasomal (epox) function leads to a significant increase of both the exogenously added human (green, LB-509 antibody) and the recruited endogenous rodent (red, D37A6 antibody) aSyn **(Figure 59A, D-E)**, measured as μm^2 area/cell. Interestingly, macroautophagy (inhibited by 3MA) seems to participate, albeit to a lesser extent, only in the degradation of haSyn PFFs and not to the seeded rodent aSyn.

Similarly, in PFF-treated OLN-AS7 cells, treatment with epox significantly increased the levels of the recruited endogenous aSyn, whereas total lysosomal inhibition resulted in the accumulation of both rodent and exogenously added fibrillar human aSyn (**Figure 59 B, D-E**). Interestingly, in PFF-treated OLN-p25α cells levels of both rodent and human aSyn did not significantly change upon NH_4Cl or 3MA addition, however when the proteasome was inhibited,

the levels of the endogenous aSyn were found elevated (**Figure 59 C-E**). This could indicate a role of the p25α in the formation of highly insoluble aberrant aSyn species that probably are degradation-resistant and/or impair lysosomal activity. At the same time, p25α protein levels (grey) seem to be slightly, but not significantly, increased upon lysosomal inhibition, which could again presumably be attributed to a potential inhibitory effect on the lysosome due to the concurrent increased aSyn load and p25α overexpression or to a possible degradation of p25α via the proteasome.

To further verify the contribution of the proteasome and the lysosome in the clearance of aberrant aSyn species engendered in the PFF-treated OLN cells, we used fractionated Western immunoblotting; we treated OLN-93 cells with 0.5 μg haSyn PFFs followed by addition of NH_4Cl or epox as above. Cells were collected at 48 hrs and sequentially fractionated using buffers with increasing extraction strength. Immunoblot analysis of the SDS-soluble protein fraction did not reveal any differences in the protein levels of human or total (rodent + human) aSyn upon lysosomal or proteasomal inhibition (data not shown). However, addition of NH_4Cl or epox in PFF-treated OLN-93 cells, led to the detection of increased protein levels (that did not reach statistical significance) of both human (4B12 antibody) and total (SYN1 antibody) monomeric and high molecular weight (HMW) aSyn species in the UREA-soluble fraction (**Figure 60 A-E**).

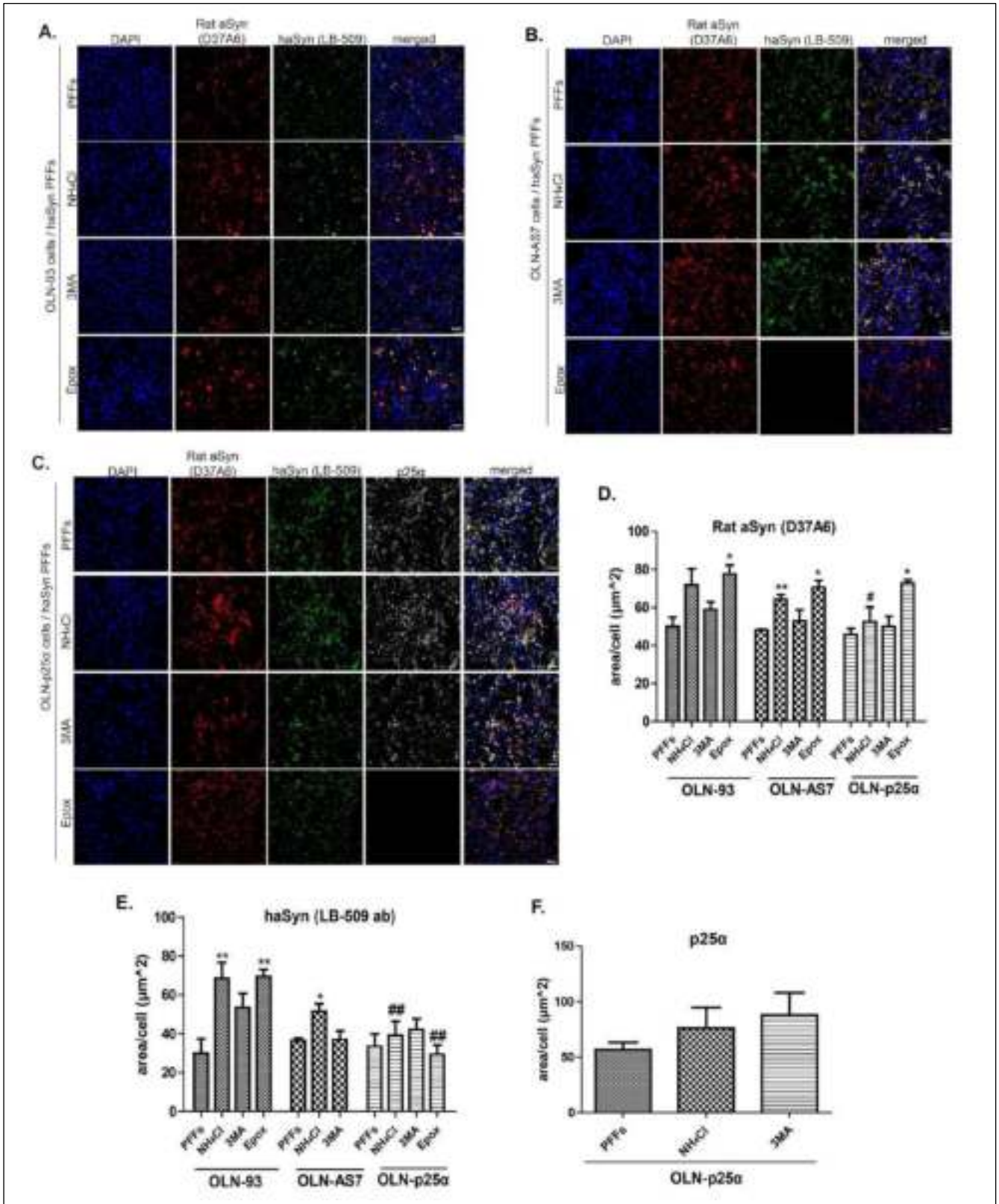

Figure 59: Both the exogenously added human aSyn (haSyn PFFs) and the recruited endogenous rat oligodendroglial aSyn are partly degraded via the ALP. (**A-C**) Representative immunofluorescence images of OLN-93 (**A**), OLN-AS7 (**B**) and OLN-p25α (**C**) cells treated with NH_4Cl (20 mM), 3MA (10 mM) or epoxomicin (epox, 15 nM) for 16 hrs following their incubation with 0.5 µg haSyn PFFs for 32 hrs. (**D-F**) Quantification of the endogenous rodent aSyn (**D**), human aSyn (**E**) or p25α (**F**) protein levels in OLN-93, OLN-AS7 and OLN-p25α cells shown in **A-C** measured as μm^2 area surface/cell. Data are expressed as the mean ± SE of three independent experiments with duplicate samples/condition within each experiment; *p<0.05; **p< 0.01, by one-way ANOVA with Tukey's post hoc test (to compare between inhibitor-treated and untreated cells) or #p<0.05; ##p< 0.01 by two-way ANOVA with Bonferroni's correction (to compare between the different treated cell cultures).

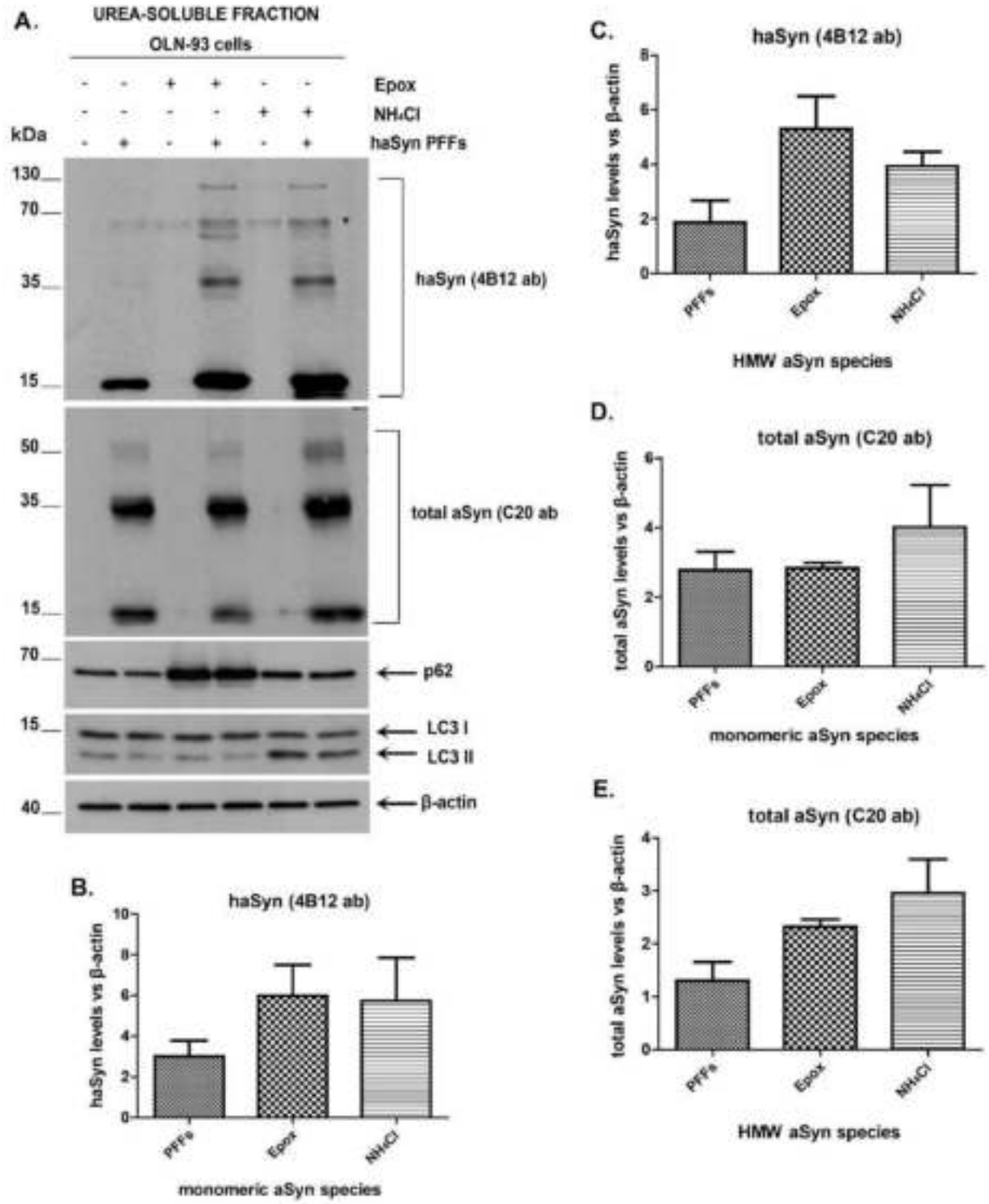

Figure 60: Both the exogenously added human aSyn (haSyn PFFs) and the recruited endogenous rat oligodendroglial aSyn are partly degraded via the ALP. (**A**) Representative immunoblots of the UREA-soluble protein lysates of OLN-93 cells treated with 0.5 μg haSyn PFFs (32 hrs) followed by their incubation with the pharmacological inhibitors epox or NH_4Cl for 16 hrs. Both human (4B12 antibody) and total (endogenous + human) aSyn (C20 antibody) seem to accumulate in the UREA-soluble fraction of OLN-93 cells treated with epox or NH_4Cl following incubation with 0.5 μg haSyn PFFs. Antibodies against LC3I & II, and p62 were used as macroautophagy markers and β-actin as loading control. (**B-E**) Quantification of monomeric and High Molecular Weight (HMW) species of human (**B-C**) and total (**D-E**) aSyn detected in the UREA-soluble fraction of OLN-93 cells treated with 0.5 μg PFFs and epox or NH_4Cl for a total of 48 hrs. Data are expressed as the mean±SE of three independent experiments.

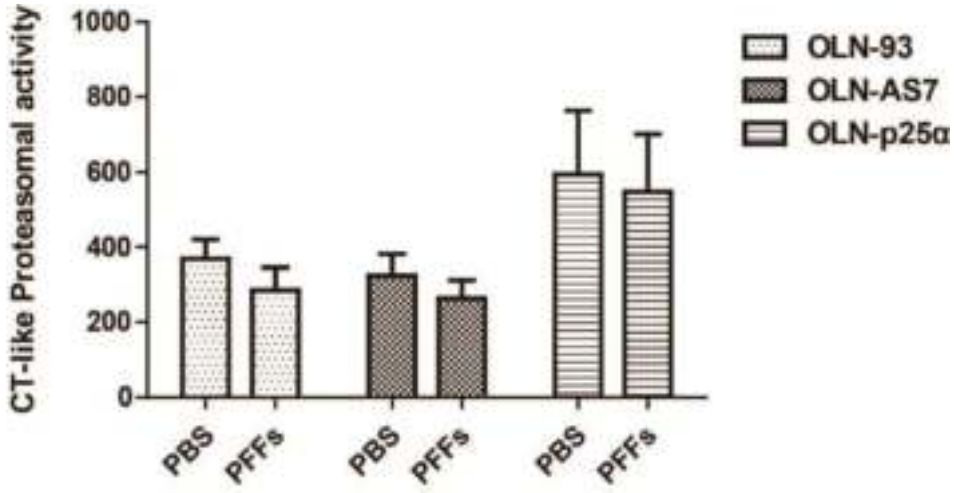

Figure 61: Addition of haSyn PFFs does not affect the chymotrypsin (CT)-like proteasomal activity of OLN cells. CT-like activity of the proteasome was measured in OLN-93, OLN-AS7 and OLN-p25α cells treated with PBS (as control) or 0.5 μg haSyn PFFs for 48 hrs. No significant alterations of the proteasomal activity *in vitro* were detected between PBS- and haSyn PFFs-treated cells. Data are expressed as the mean±SE of three independent experiments with duplicate samples/condition within each experiment.

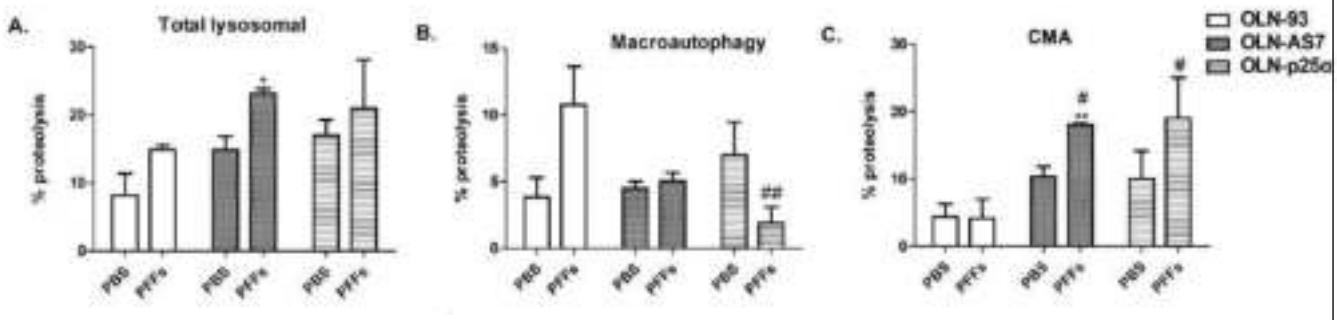

Figure 62: Lysosomal degradation of long-lived proteins is increased in OLN cells upon treatment with 0.5 μg haSyn PFFs for a total of 96 hrs. OLN cells incubated with haSyn PFFs for 48 hrs were labeled with [3H] leucine for another 48 hrs (2 μCi/ml). 16 hrs prior to media collection, cells were treated with or without NH_4Cl (20 mM) or 3MA (10 mM) and degraded proteins were assayed. The rate of total (**A**) (inhibitable by NH_4Cl), macroautophagic (**B**) (inhibitable by 3MA) or CMA-dependent (**C**) long-lived protein degradation in all OLN cells is shown. The increased total lysosomal degradation upon PFF treatment seems to be attributed to the induction of macroautophagy in OLN-93 cells or CMA in OLN-AS7 and OLN-p25α cells. Data are expressed as the mean ± SE of three independent experiments; *p<0.05; **p< 0.01, by one-way ANOVA with Tukey's post hoc test (to compare between PBS- and haSyn PFFs-treated cells) or #p<0.05; ##p< 0.01 by two-way ANOVA with Bonferroni's correction (to compare between the different OLN cells).

Finally, to elucidate the impact of haSyn PFFs on the proteasomal and lysosomal function of all OLN cell lines and the effect, if any, of the overexpressed aSyn or p25α on these proteolytic systems, we measured the CT-like proteasomal activity and the degradation rate of long-lived proteins (total lysosomal, macroautophagy- and CMA- dependent). Strikingly, the CT-like proteasomal activity remained unchanged in all OLN cells upon treatment with 0.5 μg haSyn PFFs for 48 hrs (**Figure 61**).

On the other hand, long-lived protein degradation assay revealed a significant increase of the lysosomal activity upon inoculation of OLN cells with haSyn PFFs, which however varied between the different OLN lines. Specifically, in PFF-treated OLN-93 cells, macroautophagy (3MA-inhibitable) seems to increase in response to the treatment, whereas in PFF-treated OLN-AS7 and OLN-p25α cells, CMA-dependent (NH_4Cl-3MA inhibitable) degradation is significantly enhanced (**Figure 62**). It has to be noted that with this assay we estimate CMA activity by subtracting NH_4Cl-3MA–dependent proteolysis that also contains the contribution of microautophagy, which however is considered to be relative small. Interestingly, the increase of CMA-dependent proteolysis in OLN-p25α cells was accompanied by a significant decrease of macroautophagic activity, thus leading to overall unchanged total lysosomal activity levels, compared to OLN-93 and OLN-AS7 cells. It is important, though, to note that all the above differential responses could also be attributed to clonal variability between the three OLN cell lines.

15. p25α overexpression favors the degradation of both exogenously added (haSyn PFFs) and recruited endogenous oligodendroglial aSyn via CMA and not via macroautophagy

To further elucidate the contribution of macroautophagy and/or CMA in the degradation of rodent aSyn, human aSyn and p25α in the context of MSA, we transfected all OLN cells with Lsi1/Lsi2 (targeting LAMP2A) or *Atg5* (targeting ATG5) siRNAs followed by incubation with 0.5 μg haSyn PFFs for 48 hrs. According to the data presented in **Figures 63-64**, LAMP2A downregulation increased protein levels of the recruited rodent aSyn in all PFF-treated OLN cells; however, the levels of the human aSyn were found elevated only in PFF-treated OLN-p25α cells transfected with Lsi1/Lsi2.

On the other hand, *Atg5* gene silencing led to the accumulation of the rodent and the human aSyn only in PFF-treated OLN-93 and OLN-AS7 cells (**Figure 63A-C, 64B and D**). Moreover, protein levels of p25α were significantly increased upon LAMP2A downregulation, whereas transfection of OLN-p25 cells with *Atg5* si led to a slight accumulation of p25α (**Figures 63C, 64 E and F**). These data, when combined to those presented in **Figure 59A-F** may lead to the hypothesis that under pathological conditions (addition of haSyn PFFs), CMA seems to be the main pathway responsible for the clearance of aSyn (rodent and human) and p25α in OLNp25α cells, whereas both CMA and macroautophagy contribute to the degradation of aSyn (rodent and human) in PFF-treated OLN-93 and OLN-AS7 cells.

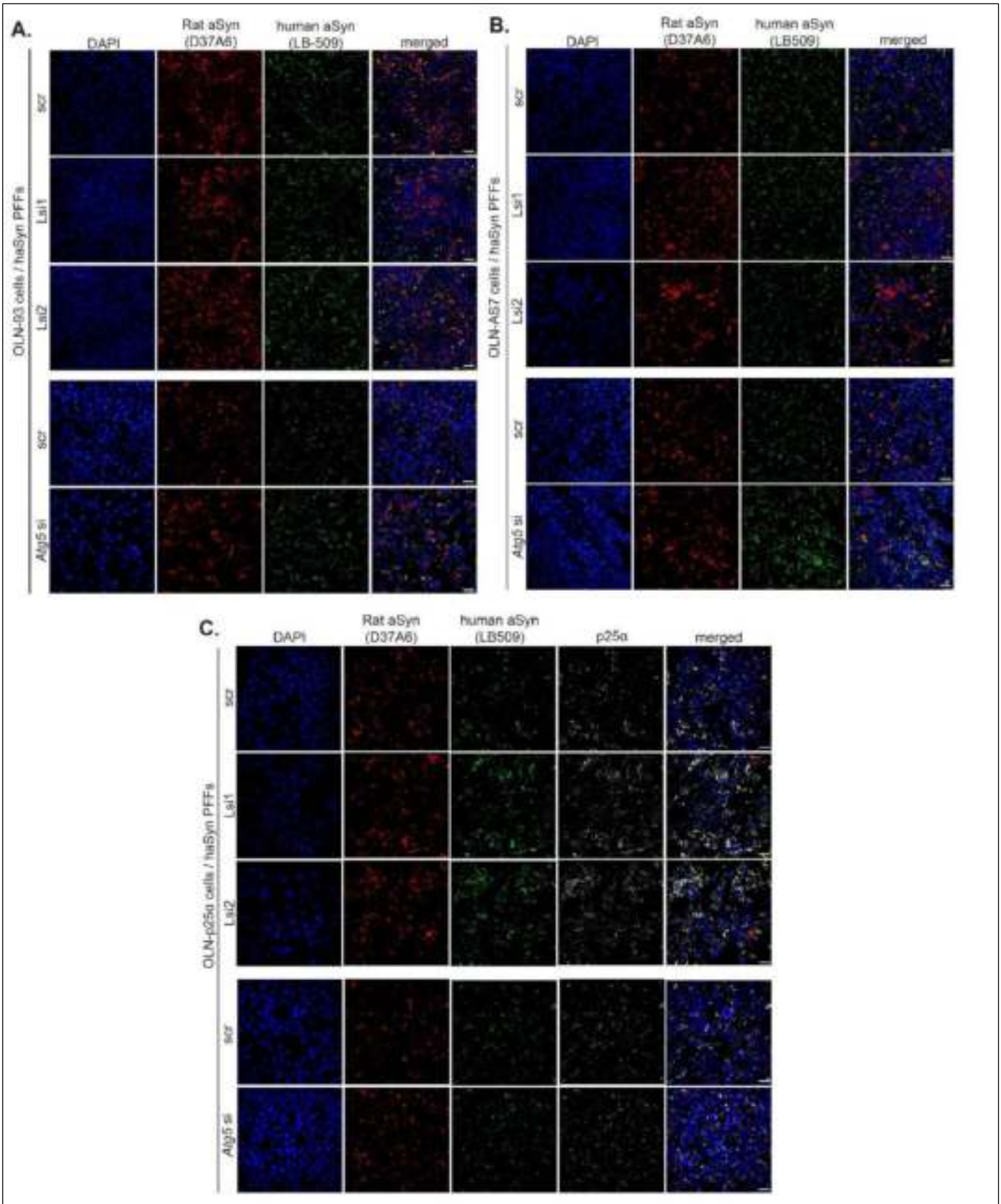

Figure 63: p25α overexpression favors the degradation of both exogenously added (haSyn PFFs) and recruited endogenous oligodendroglial aSyn preferentially via CMA and not via macroautophagy. (**A-C**) Representative immunofluorescence images of OLN-93, OLN-AS7 and OLN-p25α cells incubated with 0.5 µg haSyn PFFs added at 24 hrs following transfection with *Lamp2a*-(Lsi1/Lsi2, 60 nM), *Atg5*-siRNAs (*Atg5* si, 10 nM) or scr siRNA (control) for another 48 hrs, using antibodies against the endogenous rodent aSyn (red, D37A6 antibody), human aSyn (green, LB509 antibody) and p25α (grey) and DAPI staining. Scale bar: 25µm.

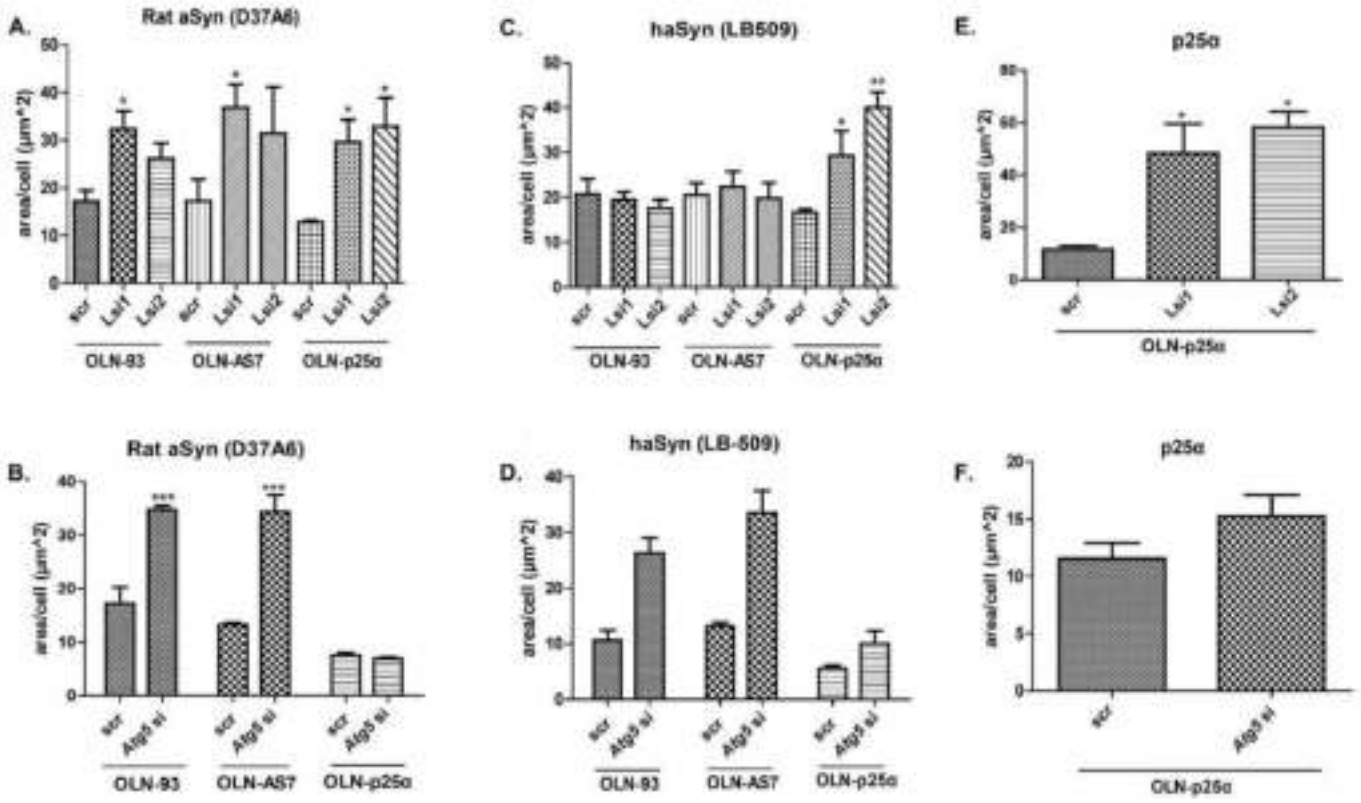

Figure 64: p25α overexpression favors the degradation of both exogenously added (haSyn PFFs) and recruited endogenous oligodendroglial aSyn preferentially via CMA and not via macroautophagy. (**A-F**) Quantification of the endogenous rodent aSyn (**A, B**), human aSyn (**C-D**) or p25α (**E-F**) protein levels in OLN-93, OLN-AS7 and OLN-p25α cells measured as μm^2 area surface/cell. Data are expressed as the mean ± SE of three independent experiments with duplicate samples/condition within each experiment; *p<0.05; **p< 0.01; ***p< 0.001, by one-way ANOVA with Tukey's post hoc test.

16. Addition of haSyn PFFs in OLN cells does not impair autophagosome formation, but seems to interfere with the fusion of autophagosomes with the lysosome

Autophagy is a dynamic process that includes the autophagosome formation, maturation and fusion with lysosomes. In order to measure the autophagic flux in PFF-treated OLN cells we utilized the GFP/RFP-LC3 and GFP/mcherry-SQSTM1 tandem fluorescent-tagged LC3 and SQSTM1/p62, respectively, which allows the dynamic visualization of the formation of autophagosomes and/or autolysosomes.

Specifically, OLN cells were transfected with GFP/RFP-LC3 or GFP/mcherry-SQSTM1/p62 cDNAs and 6 hrs later, 0.5 μg hSyn PFFs were added to the medium for 48 hrs. Based on the fact that the fluorescence of GFP, contrarily to the mRFP or mcherry, is quenched in an acidic environment, autophagy inhibition results in a decrease of red puncta followed by an increase of green puncta, indicative of the low autolysosome formation. Incubation of all OLN cells with 0.5 μg hSyn PFFs for 48 hrs resulted in autophagic flux defects, due to the detection of a lower number of red puncta (in both GFP/RFP-LC3 and GFP/mcherry-p62), as presented in **Figures 65-66**.

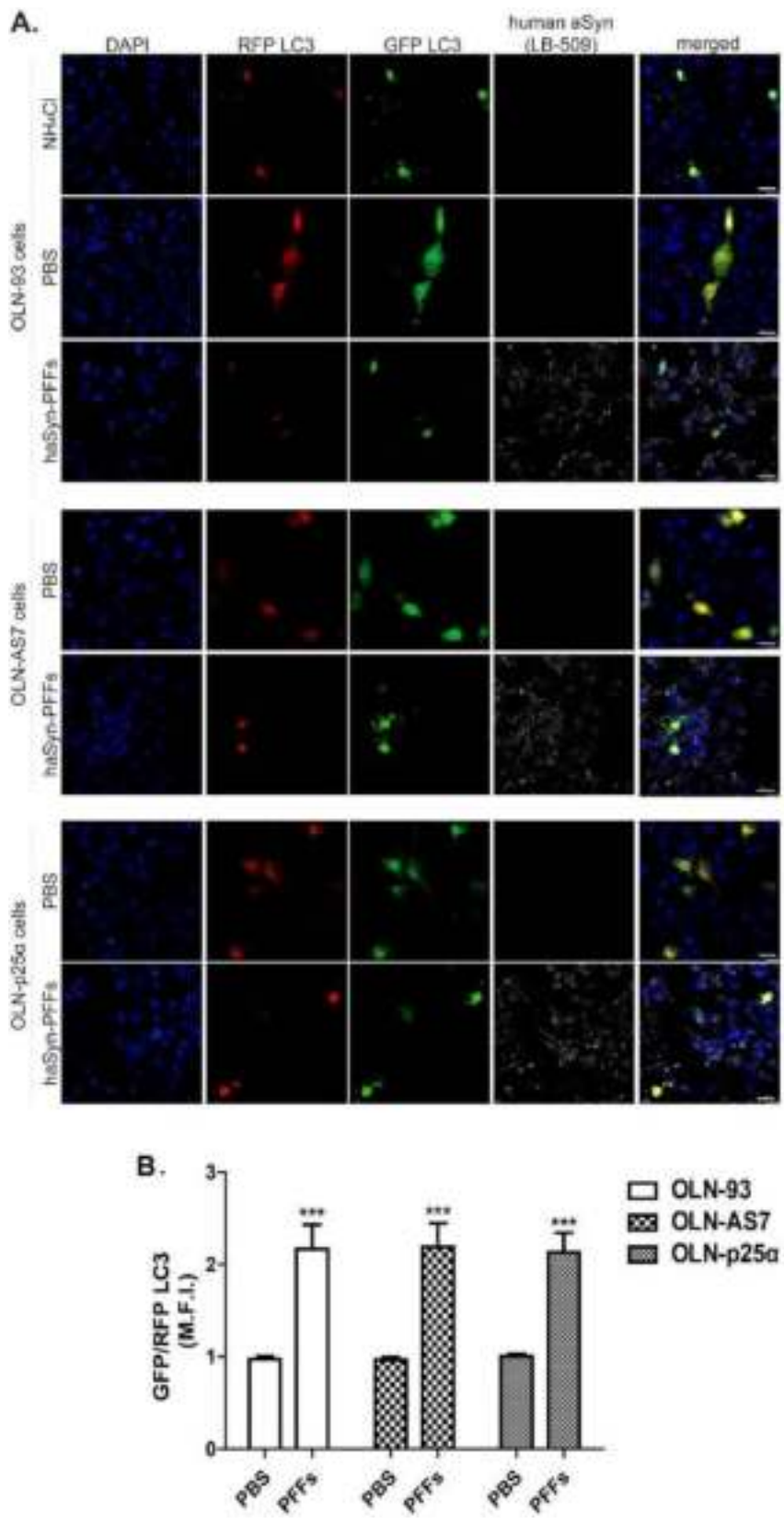

Figure 65: Addition of haSyn PFFs does not impair autophagosome formation, but seems to interfere with the fusion of autophagosomes with the lysosome in all OLN cell lines. (**A**) Representative immunofluorescence images of OLN-93, OLN-AS7 and OLN-p25α cells transfected with GFP/RFP-LC3 construct for 48 hrs. Cells were incubated with PBS (as control) or with 0.5 μg haSyn PFFs 6 hrs post-transfection with the fluorescent constructs and the autophagic flux was assessed via confocal microscopy. Incubation of OLN-93 cells with NH_4Cl (20 mM) for 16 hrs was used as a positive control for the inhibition of lysosomal fusion. DAPI is used as a nuclear marker. Scale bar: 25 μm. (**B**) Calculation of the GFP:RFP fluorescence ratio as an estimation of autophagic flux. The ratio increases when autophagic flux is low, as presented in the graphs. Data are expressed as the mean ± SE of three independent experiments with duplicate samples/condition within each experiment; ***p< 0.001, by one-way ANOVA with Tukey's post hoc test.

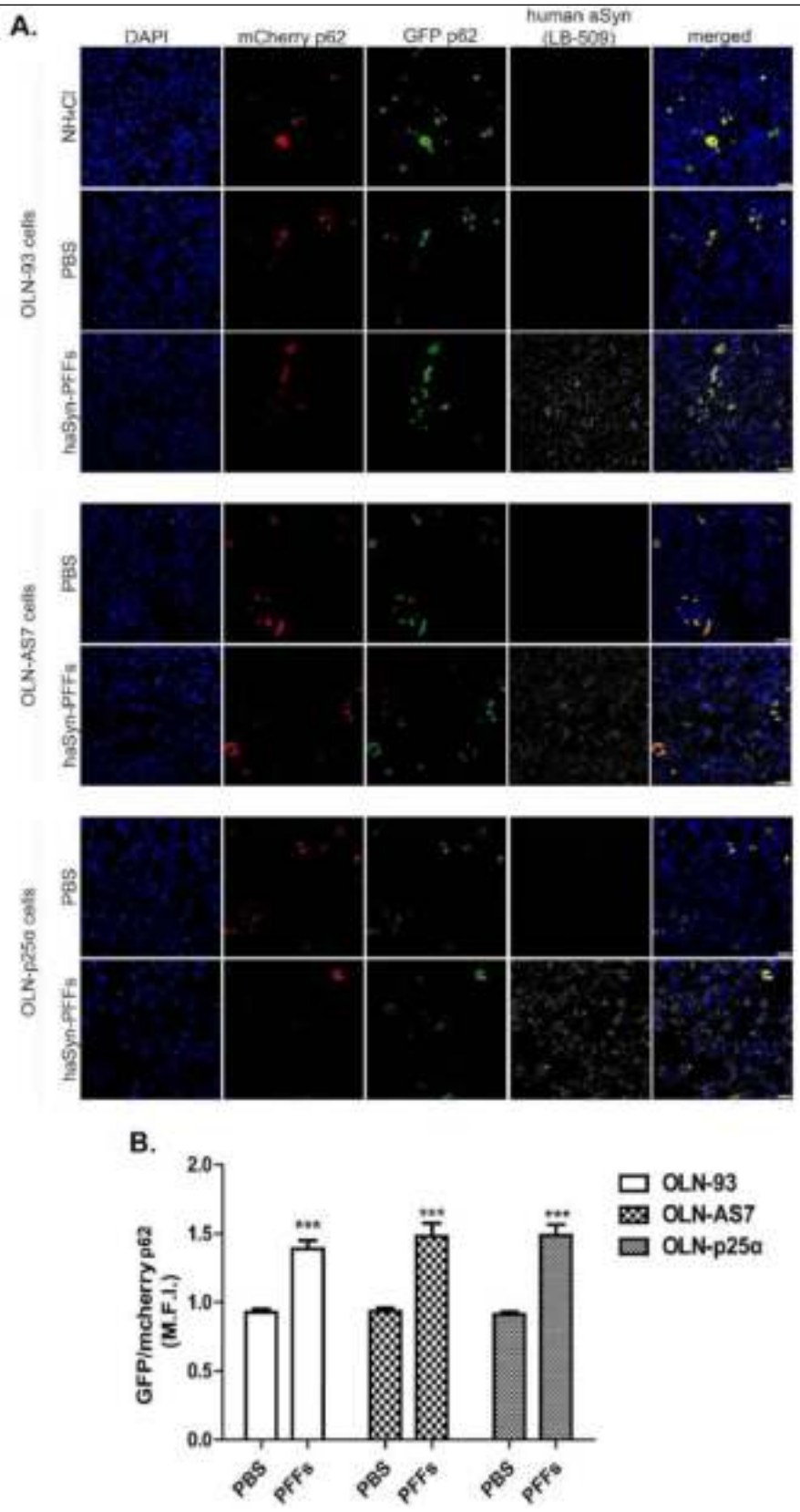

Figure 66: Addition of haSyn PFFs does not impair autophagosome formation, but seems to interfere with the fusion of autophagosomes with the lysosome in all OLN cell lines. (**A**) Representative immunofluorescence images of OLN-93, OLN-AS7 and OLN-p25α cells transfected with GFP/mcherry-p62 construct for 48 hrs. Cells were incubated with PBS (as control) or with 0.5 μg haSyn PFFs 6 hrs post-transfection with the fluorescent constructs and the autophagic flux was assessed via confocal microscopy. Incubation of OLN-93 cells with NH_4Cl (20 mM) for 16 hrs was used as a positive control for the inhibition of lysosomal fusion. DAPI is used as a nuclear marker. Scale bar: 25 μm. (**B**) Calculation of the GFP:mcherry fluorescence ratio as an estimation of autophagic flux. The ratio increases when autophagic flux is low, as presented in the graphs. Data are expressed as the mean ± SE of three independent experiments with duplicate samples/condition within each experiment; ***p< 0.001, by one-way ANOVA with Tukey's post hoc test.

Calculation of GFP:RFP (LC3 cDNA) or GFP:mcherry (SQSTM1/p62 cDNA) ratio is indicative for the autophagic flux process; the ratio increases when autophagic flux is low and decreases when autophagic flux is enhanced. According to our results, autophagic flux was inhibited in all PFF-treated OLN cells, with no differences detected amongst the different cell lines (**Figures 65, 66**).

17. Pharmacological enhancement of CMA (AR7) or macroautophagy (rapamycin) decreases overexpressed human aSyn (OLN-AS7 cells) and p25α (OLN-p25α cells) protein levels under basal conditions

Having established the lysosomal contribution to the clearance of both aSyn and p25α proteins, we investigated the potential therapeutic potential of enhancing macroautophagy (rapamycin, 1 μM) or CMA (AR7, 40 μM), under basal conditions and upon hSyn PFF treatment (see below). We initially verified the induction of CMA activity upon AR7 addition (40 μM, 16 hrs) with confocal microscopy, where we detected increased LAMP2A-positive lysosomes to the perinuclear region of OLN-93 cells, an indirect indicator of increased CMA activity (Kaushik and Cuervo 2009) **(Figure 67A-B)**. Moreover, treatment with AR7 or rapamycin for 16 or 48 hrs did not significantly affect survival of all OLN cells (see **Figure 57**).

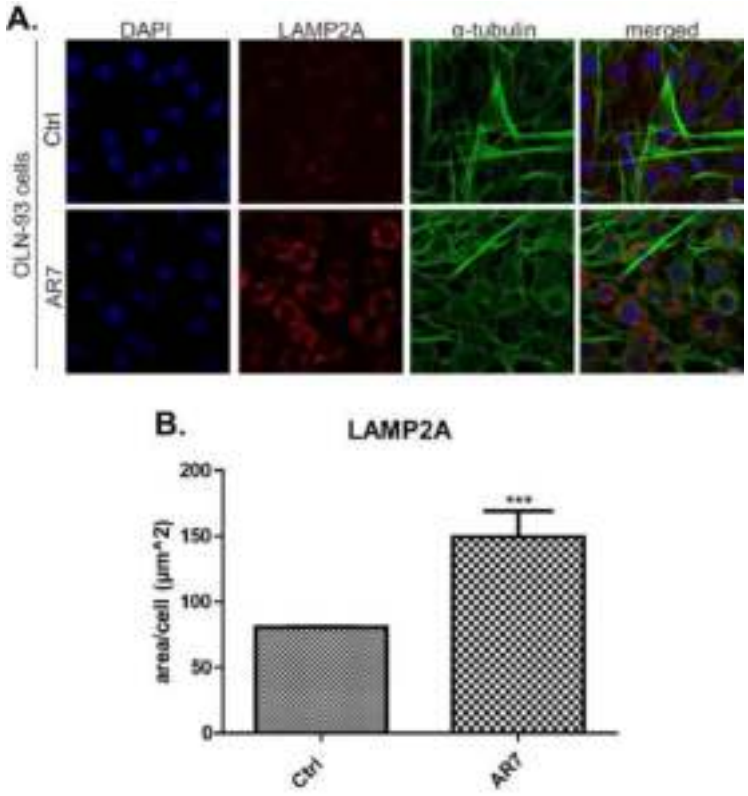

Figure 67: Addition of AR7 in OLN cells evokes the perinuclear re-distribution of the LAMP2A receptor, and by extension enhances the activity of the CMA pathway. (**A**) Representative confocal microscopy images depicting LAMP2A upregulation (red) and increase formation of LAMP2A$^+$ puncta upon treatment of OLN-93 cells with AR7 (40 μM) for 16 hrs. α-tubulin is used as a cytoskeletal marker (green) and DAPI as a nuclear marker. Scale bar: 25 μm. (**B**) Quantification of LAMP2A protein levels, measured as μm^2/cell when OLN-93 cells were treated with AR7 for 16 hrs. Data are expressed as the mean±SE of three independent experiments with duplicate samples/condition within each experiment; ***p< 0.001, by Student's unpaired t test.

Incubation of OLN-AS7 and OLN-p25α cells with both enhancers for 48 hrs under basal conditions led to a significant decrease of human aSyn (human-specific LB-509 or 4B12 antibodies), and p25α levels respectively, verified by both confocal microscopy imaging and analysis (**Figure 68A-D**) and western immunoblotting (**Figure 69A-D**).

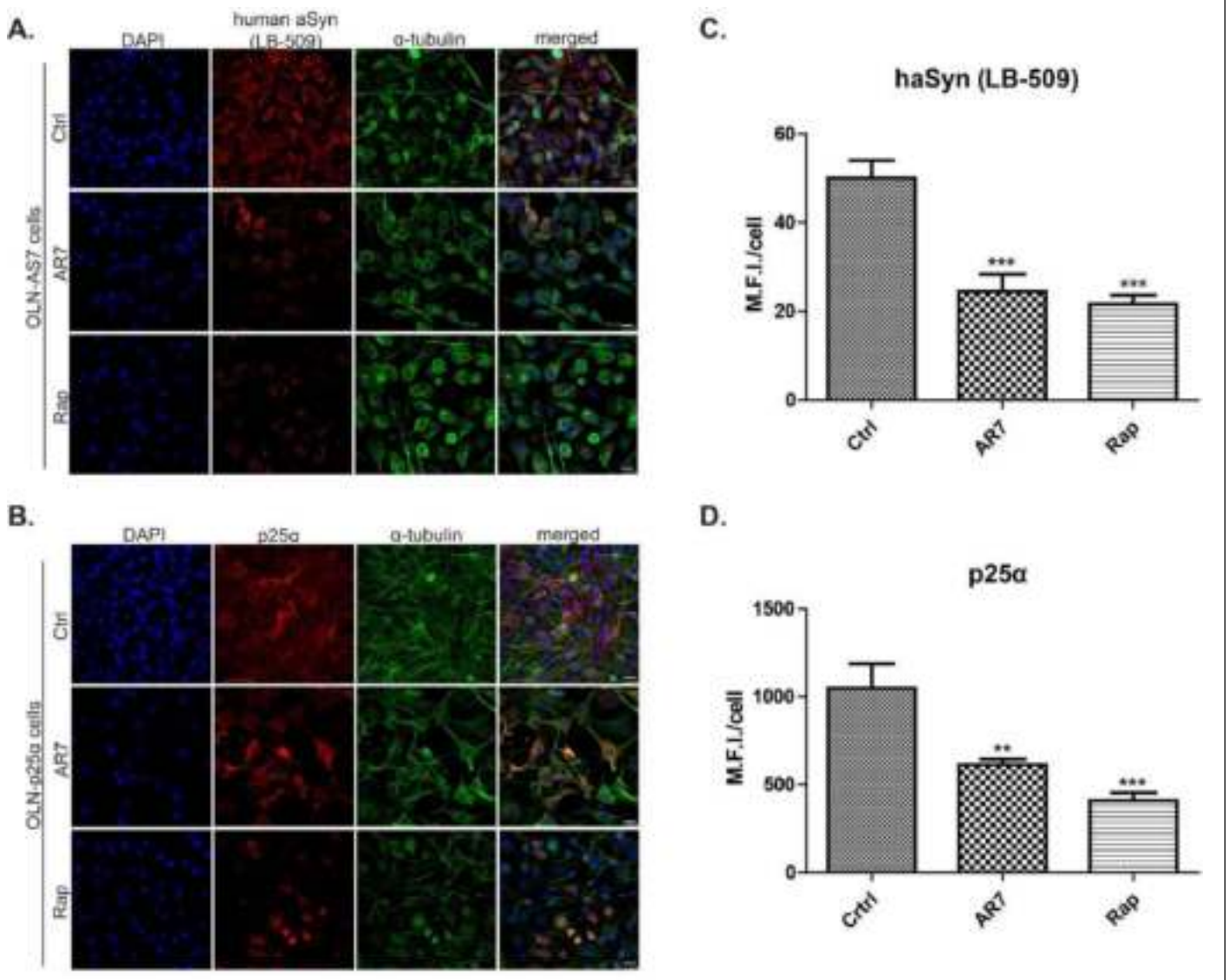

Figure 68: Pharmacological enhancement of CMA (AR7) or macroautophagy (rapamycin) decreases overexpressed human aSyn (OLN-AS7 cells) and p25α (OLN-p25α cells) protein levels under basal conditions. (**A-B**) Confocal microscopy with antibodies against human aSyn (**A**, red, LB-509 antibody) and p25α (**B**, red) reveals the enhanced degradation of these proteins upon treatment of OLN-AS7 and OLN-p25α cells with 40 μM AR7 (CMA enhancer) or 1 μM rapamycin (rap, macroautophagy enhancer) for 48 hrs. α-tubulin is used as a cytoskeletal marker (green) and DAPI as a nuclear marker. Scale bar: 25 μm. (**C-D**) Quantification of human aSyn (**C**) and p25α (**D**) protein levels in OLN-AS7 and OLN-p25α cells respectively, measured as M.F.I./cell following treatment with AR7 or rap for 48 hrs. Data are expressed as the mean±SE of three independent experiments with duplicate samples/condition within each experiment; **p< 0.01; ***p<0.001, by one-way ANOVA with Tukey's post hoc test.

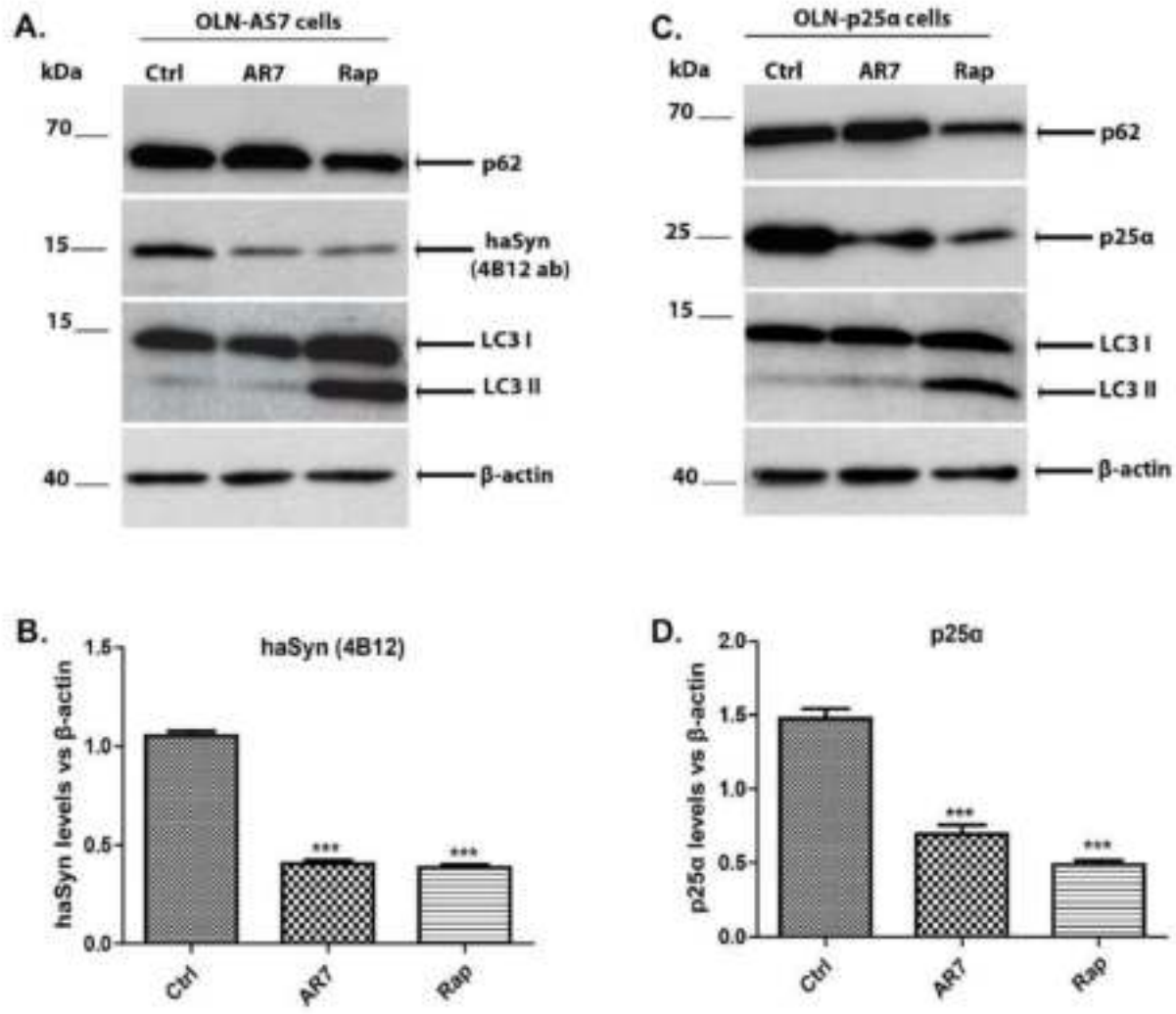

Figure 69: Pharmacological enhancement of CMA (AR7) or macroautophagy (rapamycin) decreases overexpressed human aSyn (OLN-AS7 cells) and p25α (OLN-p25α cells) protein levels under basal conditions. (**A, C**) Representative immunoblots of protein cell lysates derived from OLN-AS7 (**A**) and OLN-p25α cells (**C**) demonstrating the decline of human aSyn (4B12 antibody) and p25α protein levels upon treatment of cells with AR7 or rap for 48 hrs. Antibodies against LC3I & II, and p62 were used as macroautophagy markers and β-actin as loading control. (**B, D**) Quantification of human aSyn (**B**) and p25α (**D**) protein levels vs β-actin in OLN-AS7 and OLN-p25α cells, respectively, treated with AR7 or rap for 48 hrs. Data are expressed as the mean±SE of three independent experiments; ***p<0.001, by one-way ANOVA with Tukey's post hoc test.

18. Pharmacological augmentation of CMA or macroautophagy accelerates the clearance of aberrant aSyn conformations formed upon treatment of OLN cells with haSyn PFFs

To assess the therapeutic potential of macroautophagy or CMA enhancement on the clearance of pathological aSyn assemblies and/or p25α following addition of haSyn PFFs, OLN cells were incubated with 0.5 μg haSyn PFFs for 48 hrs or 10 days. Following PFF-addition and 16 or 48 hrs prior to cell fixation, rapamycin (1 μM) or AR7 (40 μM) were added to the cell medium and then cells were processed for confocal microscopy imaging. Immunofluorescence analysis

revealed that addition of rap or AR7 in all PFF-treated OLN cells evoked a reduction of the endogenous rodent and human haSyn, as well as of the overexpressed p25α (in OLN-p25α cells) protein levels, suggesting that these proteins/conformations can be efficiently cleared via macroautophagy and/or CMA pathways under these conditions **[Figure 70, Figure 73 (Quantifications), Figure 76A-C, Figure 80A-C (Quantifications)].**

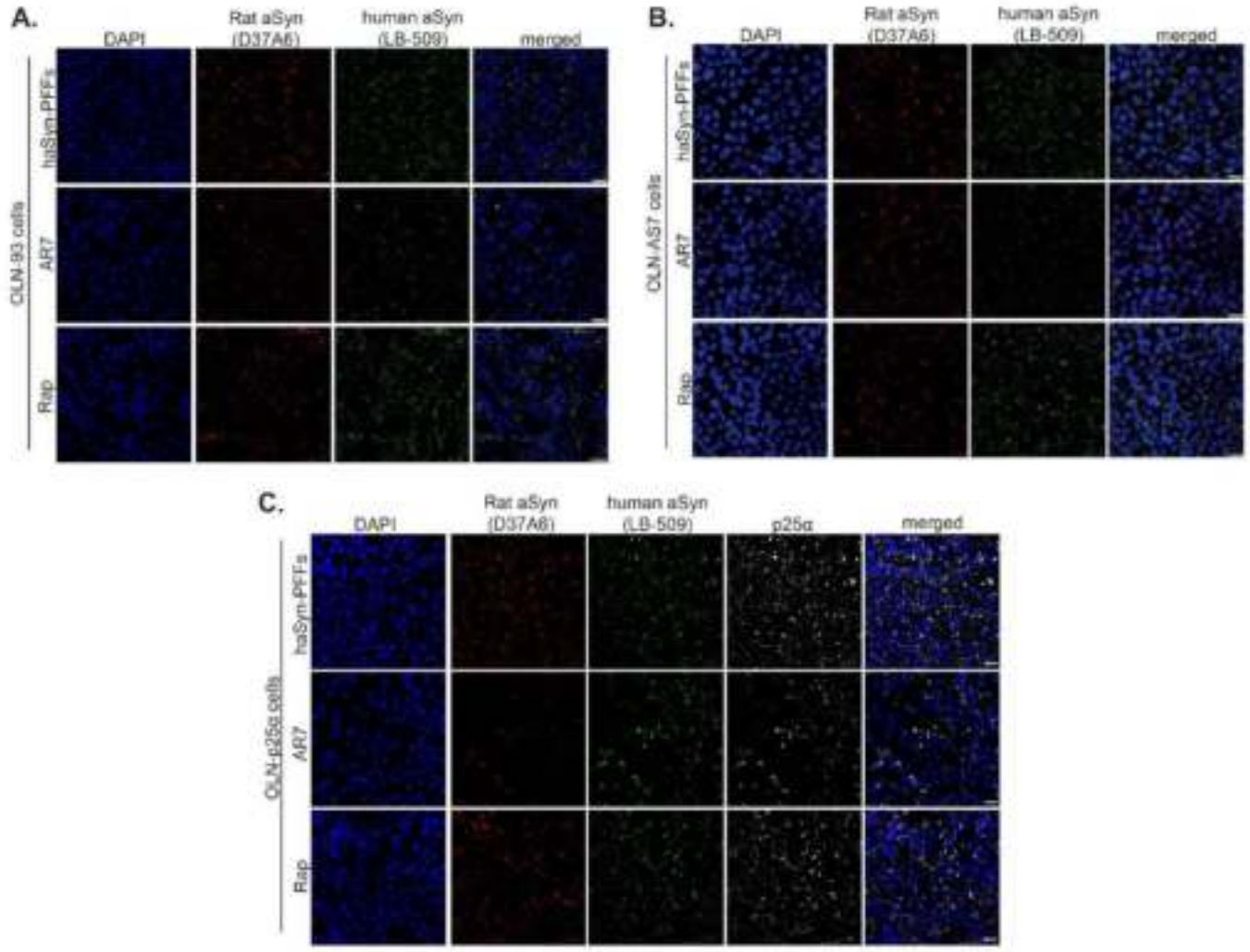

Figure 70: Pharmacological augmentation of CMA or macroautophagy accelerates the clearance of aberrant aSyn conformations formed in PFF-treated oligodendrocytes (48 hrs). (**A-C**) Representative immunofluorescence images using antibodies against the endogenous rodent aSyn (red, D37A6 antibody), the human aSyn (green, LB509 antibody) and p25α (grey) proteins are shown. DAPI is used as nuclear marker. Scale bar: 25 μm.

Moreover, the levels of oxidized/nitrated aSyn seem to be diminished upon induction of macroautophagy with rapamycin in PFF-incubated OLN-93 cells for 48 hrs, whereas in PFF-treated OLN-AS7 and OLN-p25α cells, the levels of oxidized/nitrated aSyn remained unchanged following addition of both rap or AR7 [**Figure 71A-C and Figure73D (Quantifications)**]. CMA induction via AR7 also decreased oxidized/nitrated aSyn species only in OLN-93 cells, although this drop did

not reach statistical significance. On the contrary, upon prolonged incubation of cells with haSyn PFFs and addition of rap or AR7 for 48 hrs, oxidized/nitrated aSyn was effectively degraded upon induction of both lysosomal pathways in all OLN cells **[Figures 77A, 78A, 79A and 80D (Quantifications)]**.

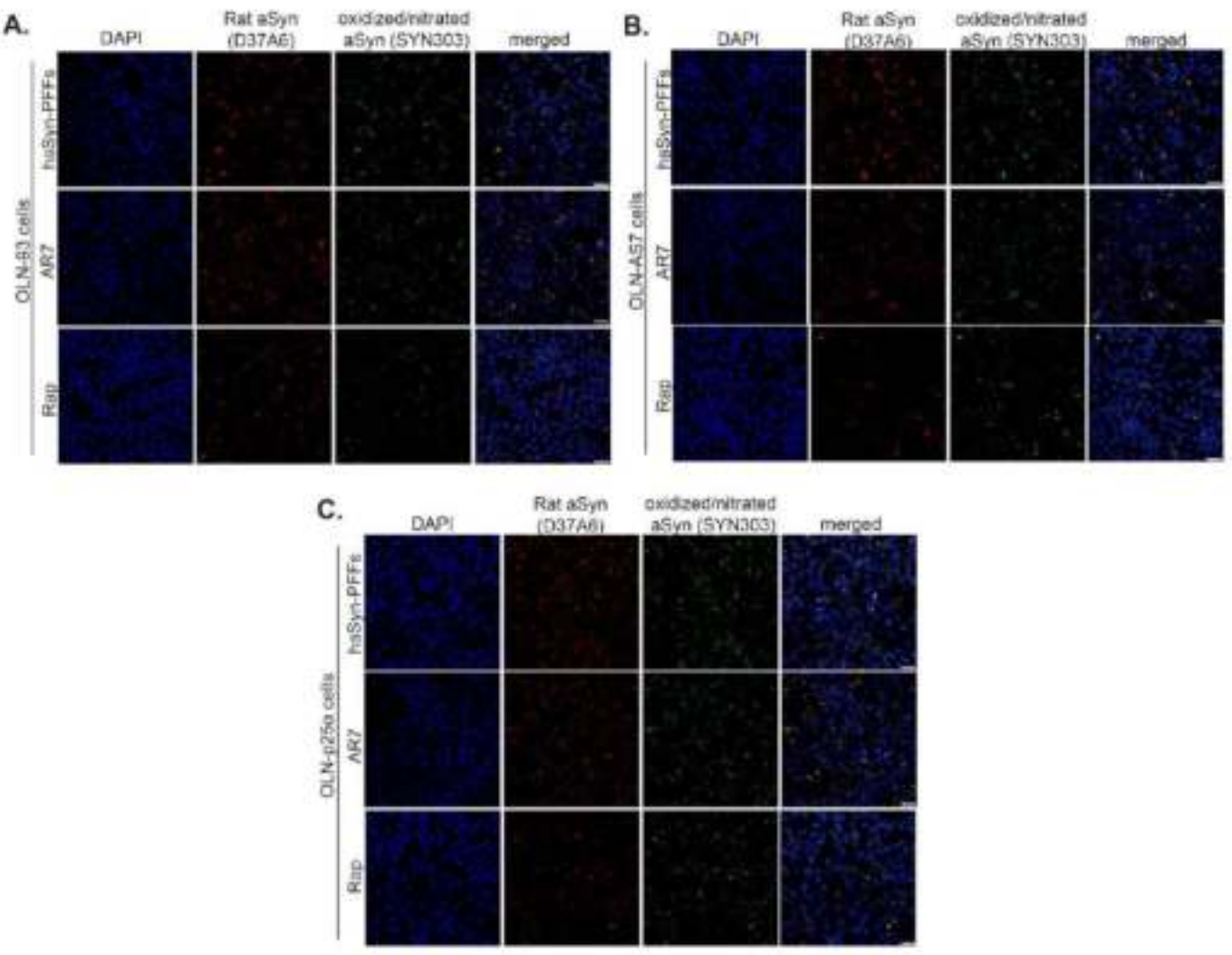

Figure 71: Induction of CMA or macroautophagy leads to effective degradation of pathological aSyn species following short-term treatment of OLN cells with haSyn PFFs. (**A-C**) Representative immunofluorescence images using antibodies against the endogenous rodent aSyn (red, D37A6 antibody) and the oxidized/nitrated aSyn (green, SYN303 antibody) in OLN-93 (**A**), OLN-AS7 (**B**) and OLN-p25α (**C**) cells upon their treatment with 0.5 μg haSyn PFFs for 32 hrs, followed by addition of AR7 or rap for an additional 16 hrs treatment. DAPI staining is used as nuclear marker. Scale bar: 25 μm.

In agreement with the confocal imaging data, we found that the SDS-soluble HMW species of human and total aSyn protein were decreased mainly upon macroautophagy enhancement (addition of 1 μM rap for 16 hrs), although the levels of monomeric aSyn species did not seem to be significantly reduced following incubation of PFF-treated OLN-93 cells either with rap or with AR7 (**Figure 74A-E**).

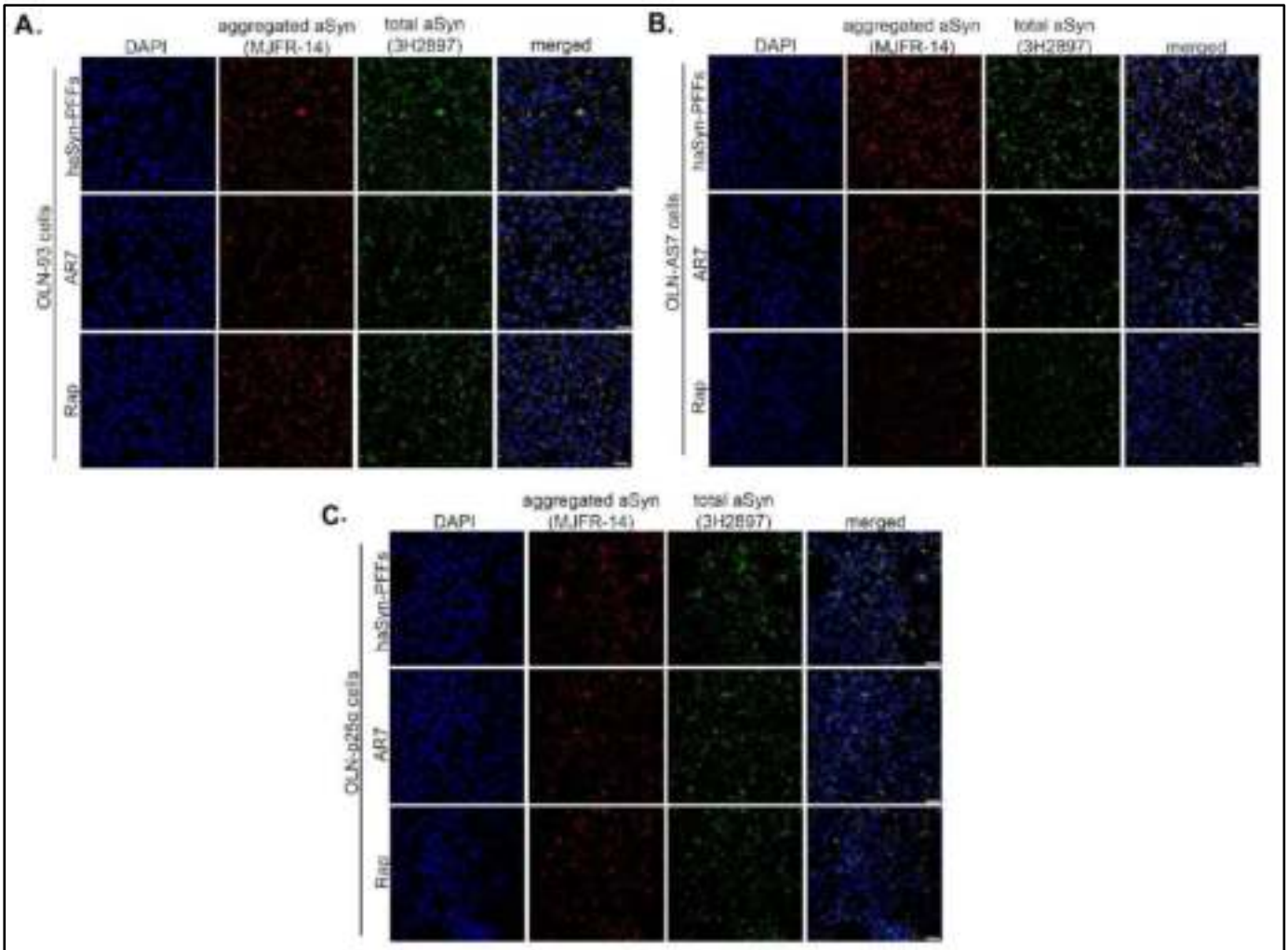

Figure 72: Induction of CMA or macroautophagy leads to effective degradation of pathological aSyn species following short-term treatment of OLN cells with haSyn PFFs. (**A-C**) Representative immunofluorescence images using antibodies against the aggregated aSyn (red, MJFR-14 antibody) and the total (endogenous + human) aSyn (green, 3H2897 antibody) in OLN-93 (**A**), OLN-AS7 (**B**) and OLN-p25α (**C**) cells upon their treatment with 0.5 μg haSyn PFFs for 32 hrs, followed by addition of AR7 or rap for an additional 16 hrs treatment. DAPI staining is used as nuclear marker. Scale bar: 25 μm.

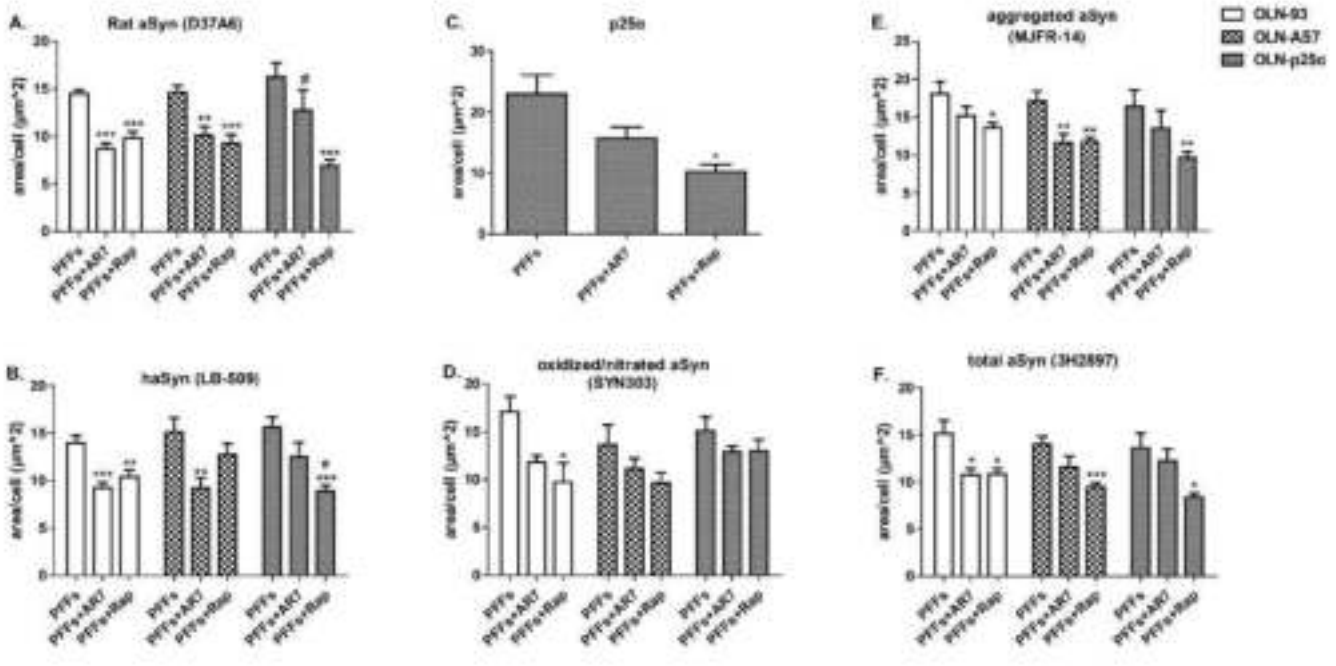

Figure 73: Pharmacological augmentation of CMA or macroautophagy accelerates the clearance of aberrant aSyn conformations formed in PFF-treated oligodendrocytes. (**A-F**) Quantification of the recruited endogenous rodent (**A**), the exogenously added human (**B**) aSyn, the overexpressed human p25α (in OLN-p25α cells) (**C**) and the pathological oxidized/nitrated (**D**), the aggregated (**E**) and the total (rodent + human) (**F**) aSyn protein levels in all OLN cells treated with 40 μM AR7 or 1 μM rap (16 hrs) following the addition of 0.5 μg aSyn PFFs for a total of 48 hrs. Data are expressed as the mean ± SE of three independent experiments with duplicate samples/condition within each experiment; *p<0.05; **p< 0.01; ***p< 0.001, by one-way ANOVA with Tukey's post hoc test (to compare between enhancer-treated and untreated cells) or #p<0.05 by two-way ANOVA with Bonferroni's correction (to compare between the different OLN cell lines).

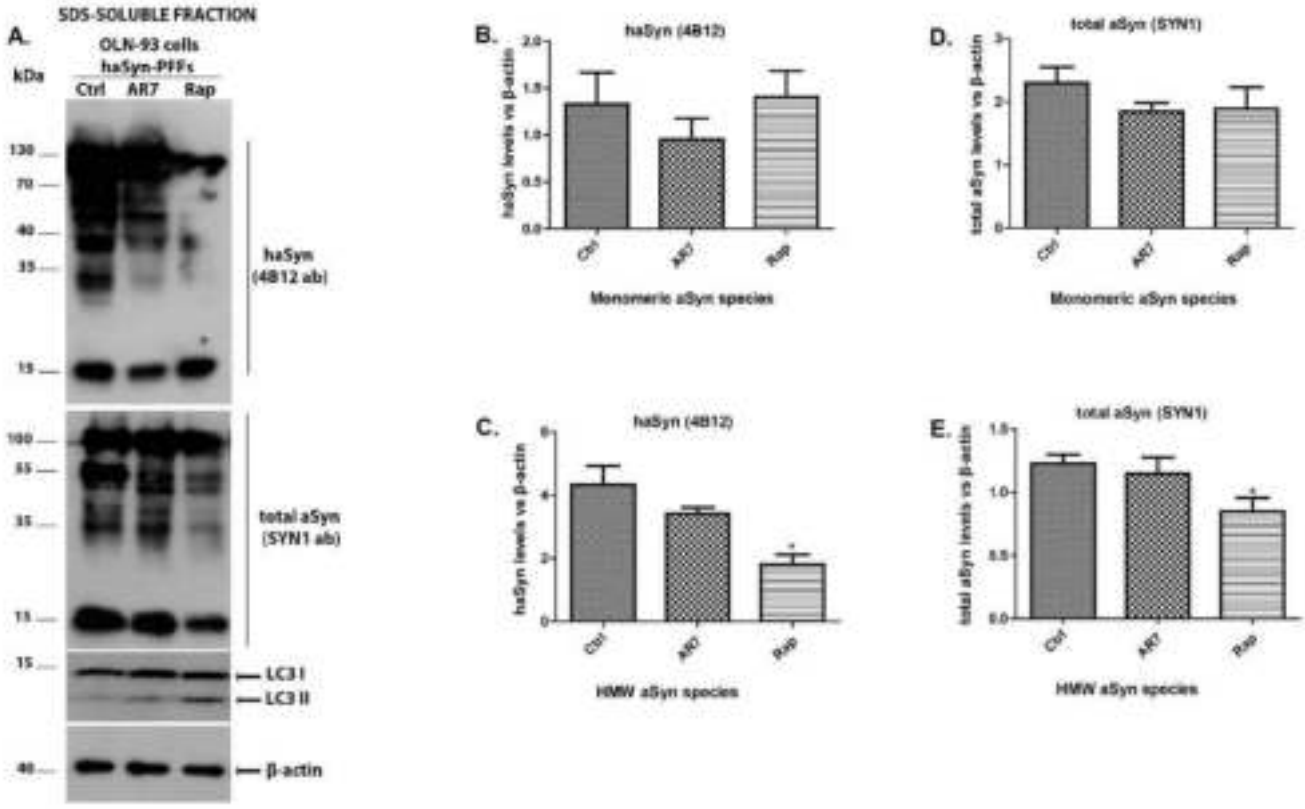

Figure 74: Pharmacological augmentation of CMA or macroautophagy accelerates the clearance of aberrant aSyn conformations formed in PFF-treated oligodendrocytes. (**A**) Representative immunoblots of the SDS-soluble aSyn species of control OLN-93 cells incubated with 0.5 μg haSyn PFFs for 32 hrs followed by addition of AR7 or rap for 16 hrs using antibodies against haSyn (4B12 antibody) or total (rodent + human) aSyn (SYN1 antibody). Equal loading was verified by the detection of β-actin levels. (**B-E**) Quantification of monomeric and HMW species of human (**B** and **C**) and total (rodent + human) (**D** and **E**) aSyn levels detected in the SDS-soluble fraction of OLN-93 treated with 0.5 μg haSyn PFFs for 32 hrs and AR7 or Rap for additionally 16 hrs. Data are expressed as the mean±SE of three independent experiments; *p< 0.05, by one-way ANOVA with Tukey's post hoc test.

Interestingly, the monomeric and HMW aSyn species of the seeded endogenous rodent protein, which are detectable only in the UREA-soluble fraction that contains the most insoluble protein species, seems to be significantly reduced following addition of rap or AR7 in PFF-treated OLN-93 cells (**Figure 75A-C**). Similarly, human and total aSyn protein levels in this UREA-soluble fraction displayed significant reduction upon macroautophagy or CMA enhancement, as presented in **Figure 75 A, D-G**. All the above results suggest that aSyn (endogenous, human, total and pathological species) and p25α can be effectively cleared via the ALP in all conditions tested.

Furthermore, protein levels of aggregated and total aSyn were also decreased upon rap or AR7 (to a lesser extent) treatment in all OLN cells, only following short-term incubation with PFFs, suggesting that under these conditions there is no significant effect of the overexpressed human aSyn or p25α in the clearance of aggregated aSyn species (**Figure 72A-C and Figure 73E-F**). Strikingly, upon long-term incubation of all OLN cells with haSyn PFFs, aggregated and total aSyn could not be effectively cleared only in OLN-p25α cells, thus implying a potential role of the

overexpressed protein in the observed resistance to the degradation of aggregated aSyn assemblies via macroautophagy and CMA [**Figures 77B, 78B, 79B, 80E-F (Quantifications)**].

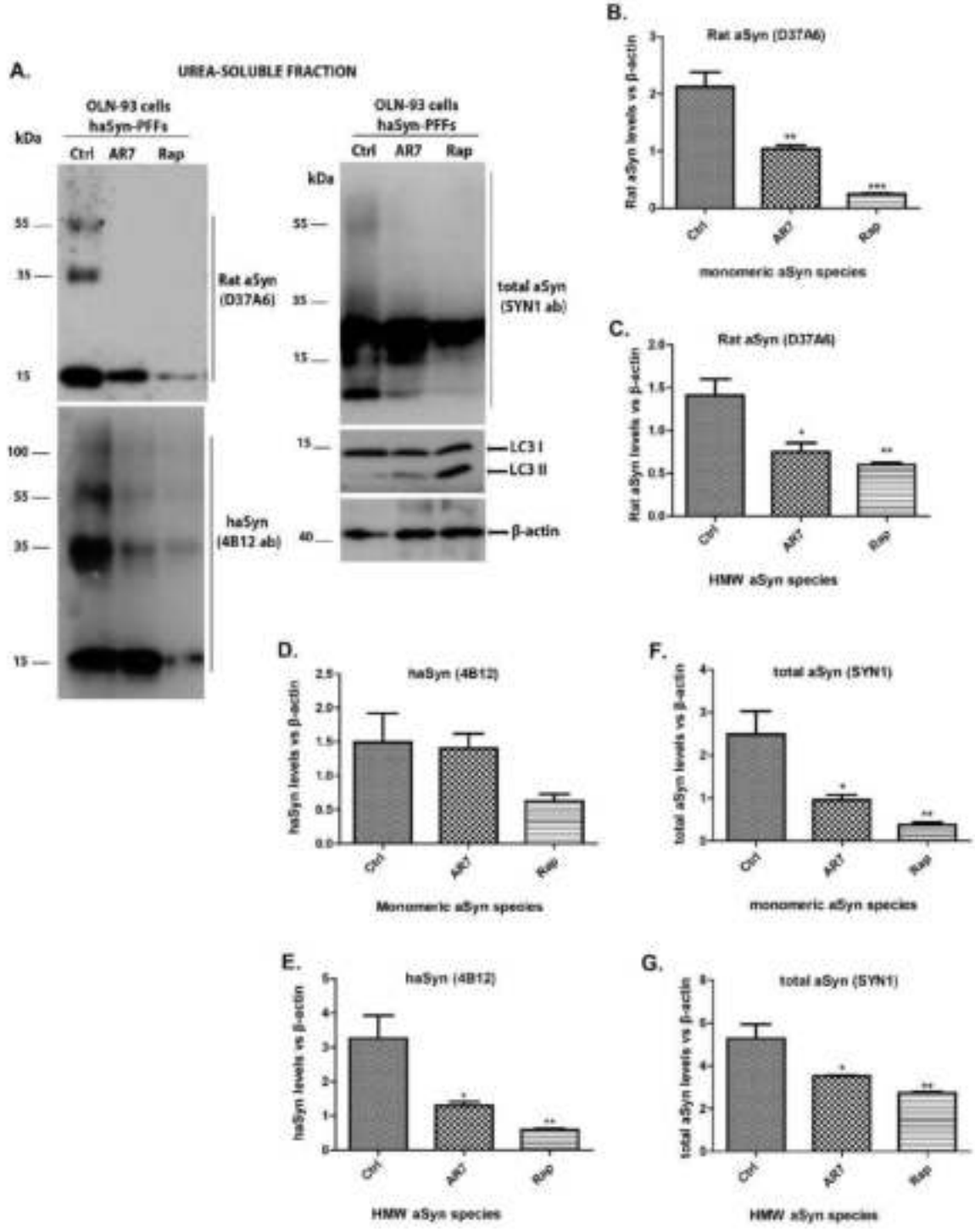

Figure 75: Pharmacological augmentation of CMA or macroautophagy accelerates the clearance of aberrant aSyn conformations formed in PFF-treated oligodendrocytes. (**A**) Representative immunoblots of the UREA-soluble protein fraction derived from OLN-93 cells treated with AR7 or rap following haSyn PFFs addition. Antibodies against rodent aSyn (D37A6 antibody), haSyn (4B12 antibody) or total (rodent + human) aSyn (SYN1 antibody) verified the decrease of the protein levels detected in this fraction upon addition of CMA (AR7) or autophagy (rap) enhancers. β-actin was used as loading control. (**B-G**) Quantification of monomeric and HMW species of rodent (**B** and **C**), human (**D** and **E**) and total (endogenous + human) (**F** and **G**) aSyn levels detected in the UREA-soluble fraction of OLN-93 cells treated with 0.5 μg haSyn PFFs and the autophagy modulators. Data are expressed as the mean±SE of three independent experiments; *p<0.05; **p< 0.01; ***p< 0.001, by one-way ANOVA with Tukey's post hoc test.

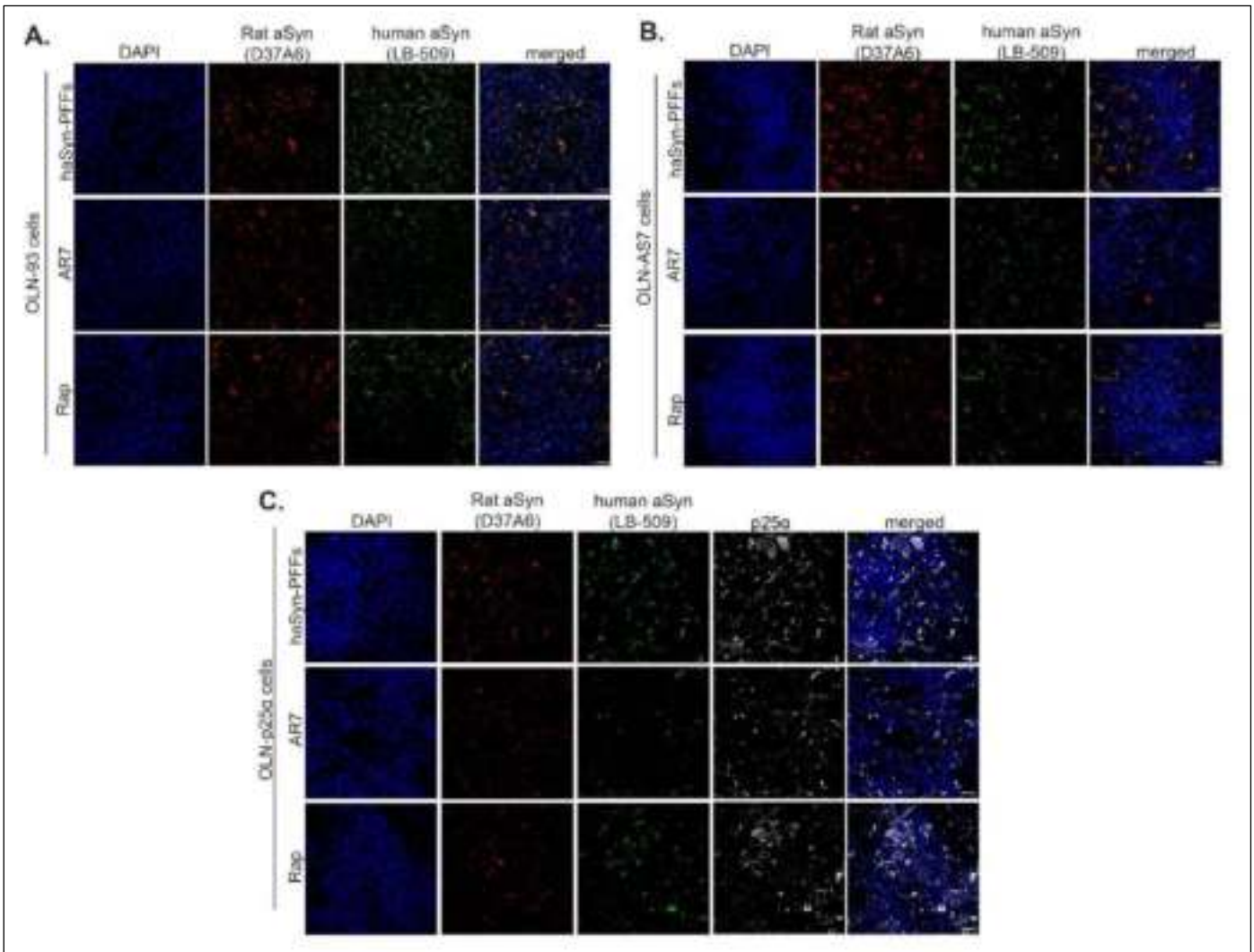

Figure 76: Augmentation of CMA or macroautophagy effectively decreases protein levels of pathological aSyn species and p25α, following prolonged incubation of OLN cells with haSyn PFFs (10 days). OLN cells were incubated with 0.5 μg haSyn PFFs for 8 days followed by addition of AR7 (40 μM) or rap (1 μM) for an additional 48 hrs treatment. (**A-C**) Representative immunofluorescence images using antibodies against the endogenous rodent aSyn (red, D37A6 antibody), the human aSyn (green, LB-509 antibody) and p25α (grey) in all OLN cells are shown. DAPI is used as nuclear marker. Scale bar: 25 μm.

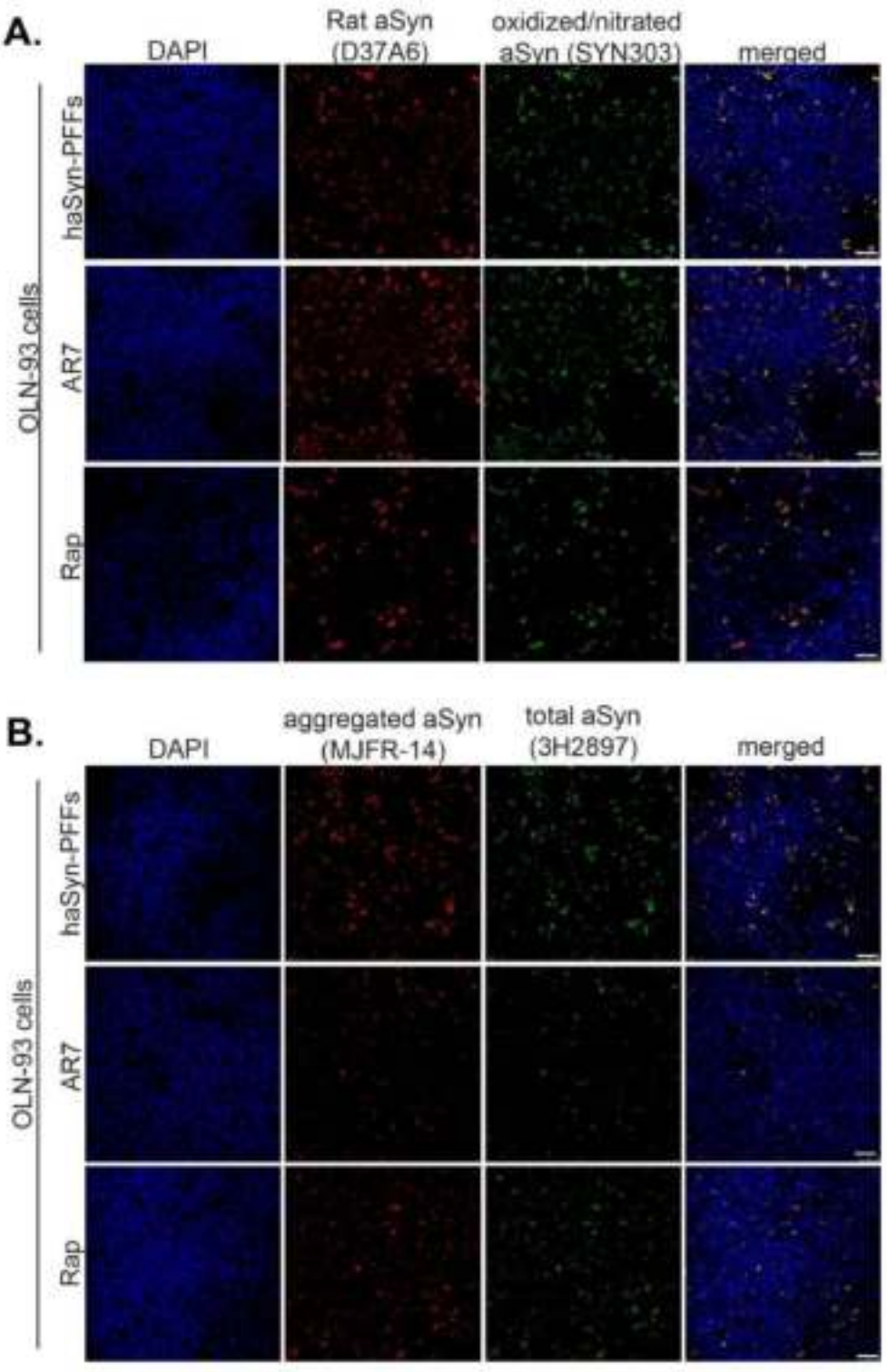

Figure 77: Augmentation of CMA or macroautophagy effectively decreases protein levels of pathological aSyn species and p25α, following prolonged incubation of OLN-93 cells with haSyn PFFs. Representative immunofluorescence images using antibodies against (**A**) the endogenous rodent aSyn (red, D37A6 antibody) and the oxidized/nitrated aSyn (green, SYN303 antibody) and (**B**) against the aggregated aSyn (red, MJFR-14 antibody) and total (rodent + human) aSyn (green, 3H2897 antibody). DAPI is used as nuclear marker. Scale bar: 25 μm

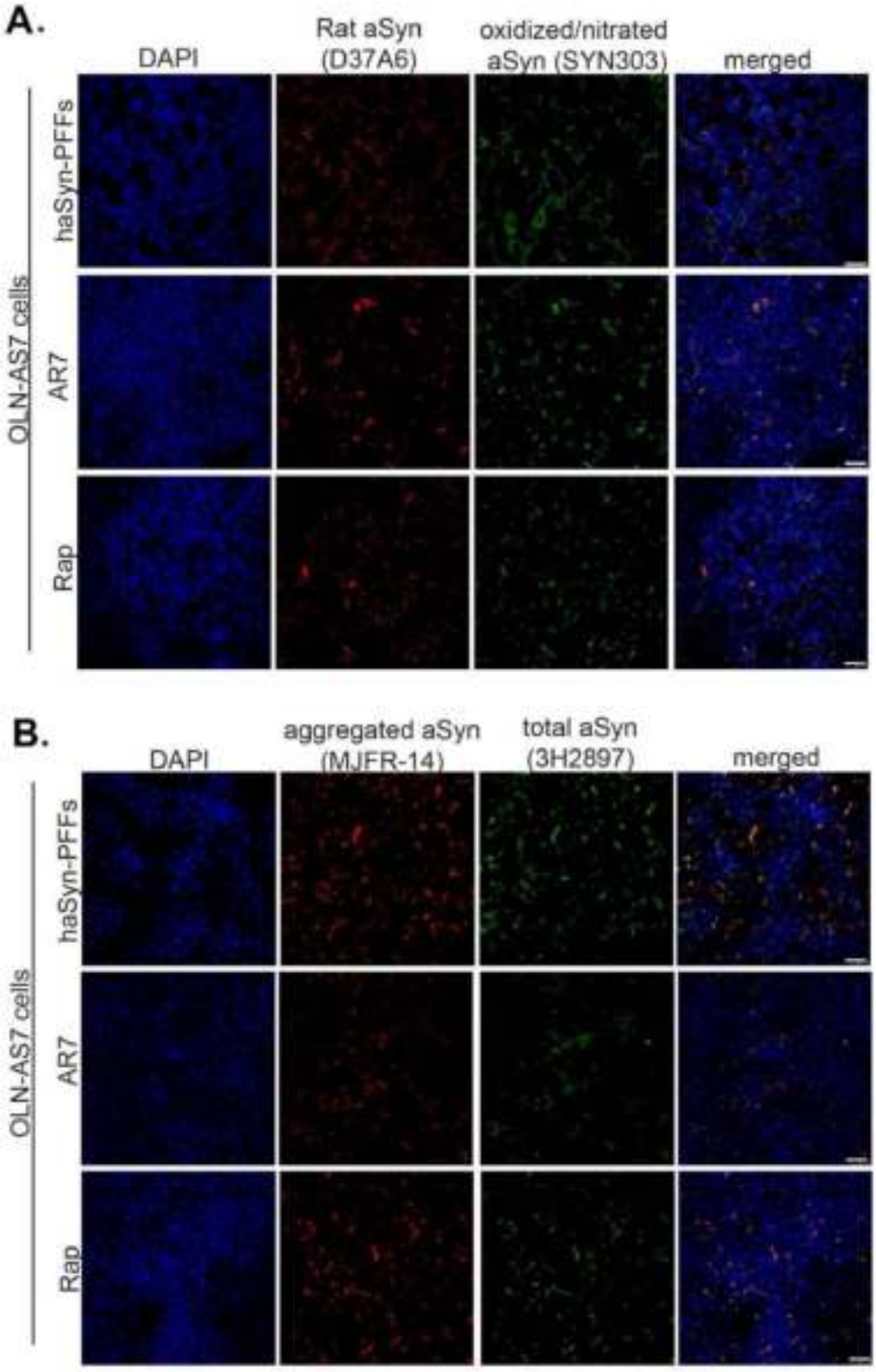

Figure 78: Augmentation of CMA or macroautophagy effectively decreases protein levels of pathological aSyn species and p25α, following prolonged incubation of OLN-AS7 cells with haSyn PFFs. Representative immunofluorescence images using antibodies against (**A**) the endogenous rodent aSyn (red, D37A6 antibody) and the oxidized/nitrated aSyn (green, SYN303 antibody) and (**B**) against the aggregated aSyn (red, MJFR-14 antibody) and total (rodent + human) aSyn (green, 3H2897 antibody). DAPI is used as nuclear marker. Scale bar: 25 μm

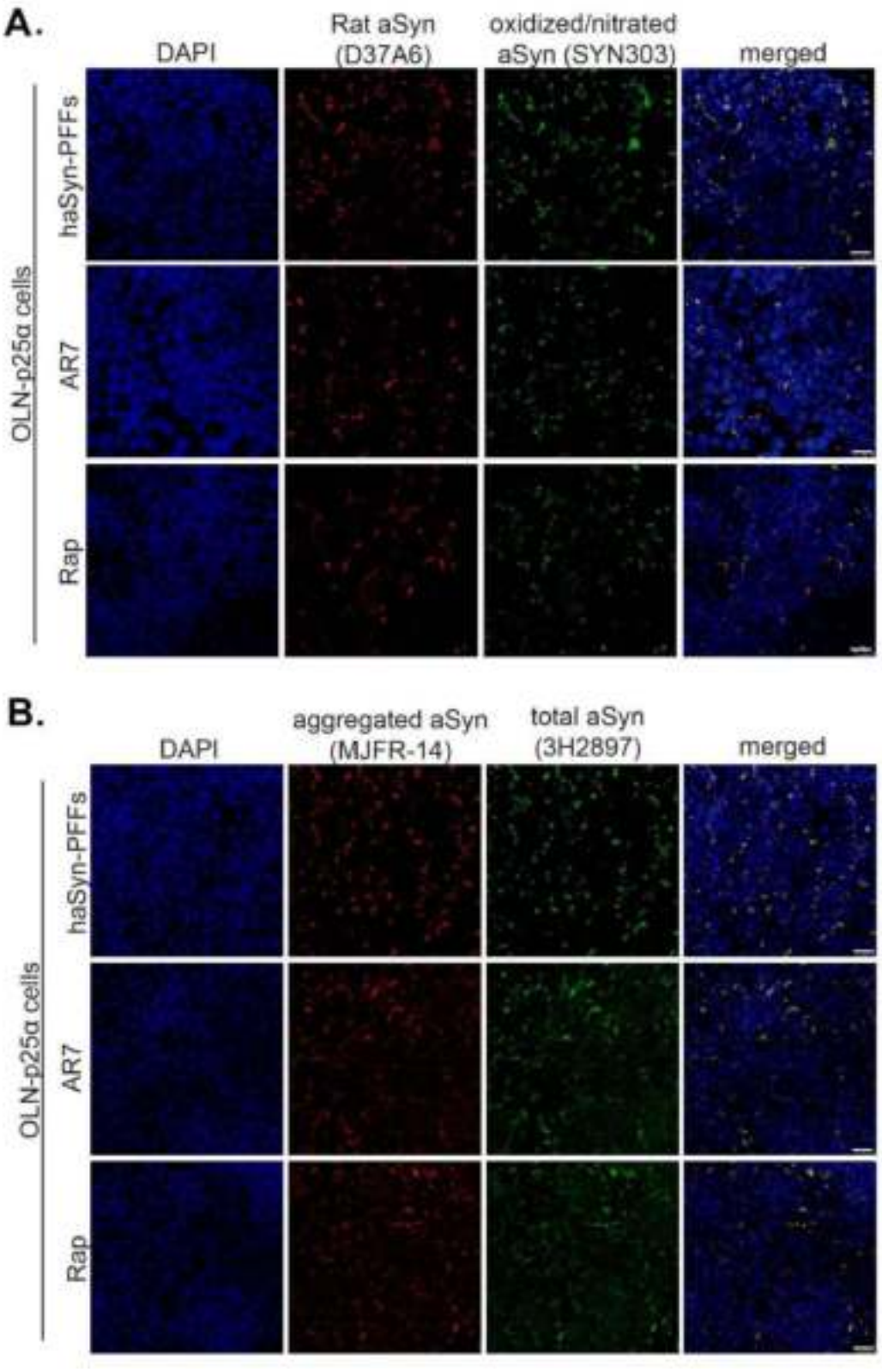

Figure 79: Augmentation of CMA or macroautophagy effectively decreases protein levels of pathological aSyn species and p25α, following prolonged incubation of OLN-p25α cells with haSyn PFFs. Representative immunofluorescence images using antibodies against (**A**) the endogenous rodent aSyn (red, D37A6 antibody) and the oxidized/nitrated aSyn (green, SYN303 antibody) and (**B**) against the aggregated aSyn (red, MJFR-14 antibody) and total (rodent + human) aSyn (green, 3H2897 antibody). DAPI is used as nuclear marker. Scale bar: 25 μm

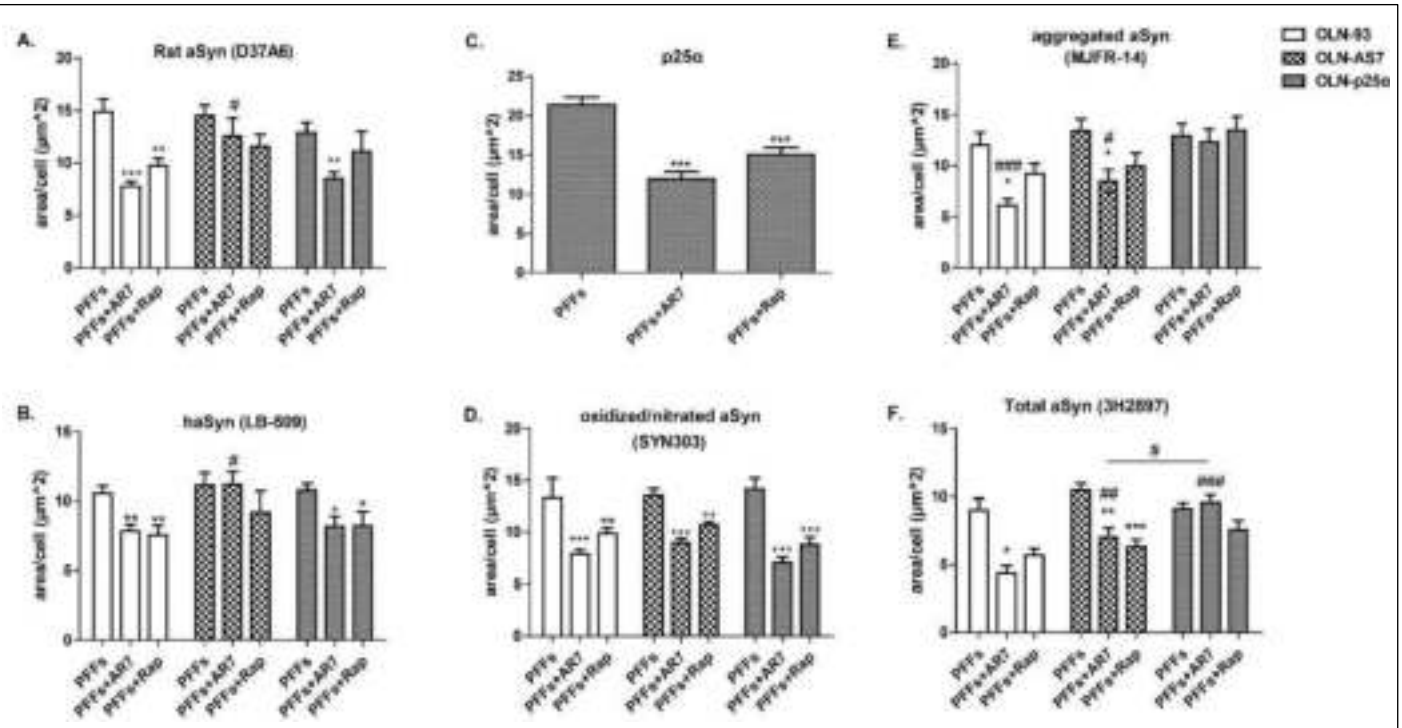

Figure 80: Augmentation of CMA or macroautophagy effectively decreases protein levels of pathological aSyn species and p25α, following prolonged incubation of OLN-p25α cells with haSyn PFFs. (**A-F**) Quantification of the recruited endogenous rodent (**A**), the exogenously added human (**B**) aSyn, the overexpressed human p25α (in OLN-p25α cells) (**C**), the pathological oxidized/nitrated aSyn (**D**), the aggregated (**E**) and the total (**F**) aSyn protein levels in OLN cells shown in A-F. Data are expressed as the mean ± SE of three independent experiments with duplicate samples/condition within each experiment; *p<0.05; **p< 0.01; ***p< 0.001, by one-way ANOVA with Tukey's post hoc test (to compare between enhancer-treated and untreated cells) or #p<0.05; ##p< 0.01; ###p< 0.001 by two-way ANOVA with Bonferroni's correction (to compare between the different OLN cell lines).

19. The MSA-related proteins p25α and aSyn are mainly degraded via the ALP in murine primary oligodendroglial cultures, under physiological and pathological conditions

To delineate the clearance processes responsible for the removal of aSyn and p25α, in health and disease conditions, we cultivated and differentiated primary oligodendrocytes derived from P0 to P3 mouse brains in order to resemble a cellular setting closer to the oligodendrocytes of the central nervous system. To this end, primary oligodendrocytes were cultivated in the presence of PBS (as control) or 0.5 μg haSyn PFFs for 24 hrs, followed by addition of lysosome/macroautophagy (20 mM NH_4Cl, 10 mM 3MA) or proteasome (15 nM epox) inhibitors for an additional 48 hrs. According to the results presented in **Figure 81A-B**, p25α seems to be mainly degraded via the ALP, since its levels were found significantly elevated upon NH_4Cl (both in PBS and PFF-treated cultures) and/or 3MA (PFF-treatment) addition (**Figure 82A-B**).

Furthermore, the endogenous rodent aSyn accumulated when either the lysosome or the proteasome (to a lesser extent) was inhibited (**Figure 82C-D**), whereas the levels of human aSyn were increased upon total lysosomal and macroautophagy impairment (**Figure 82E**). No signal for the endogenous aSyn could be detected in PBS-treated primary oligodendrocytes using the rodent aSyn-specific D73A6 antibody, as shown in **Figure 81A and 82C.**

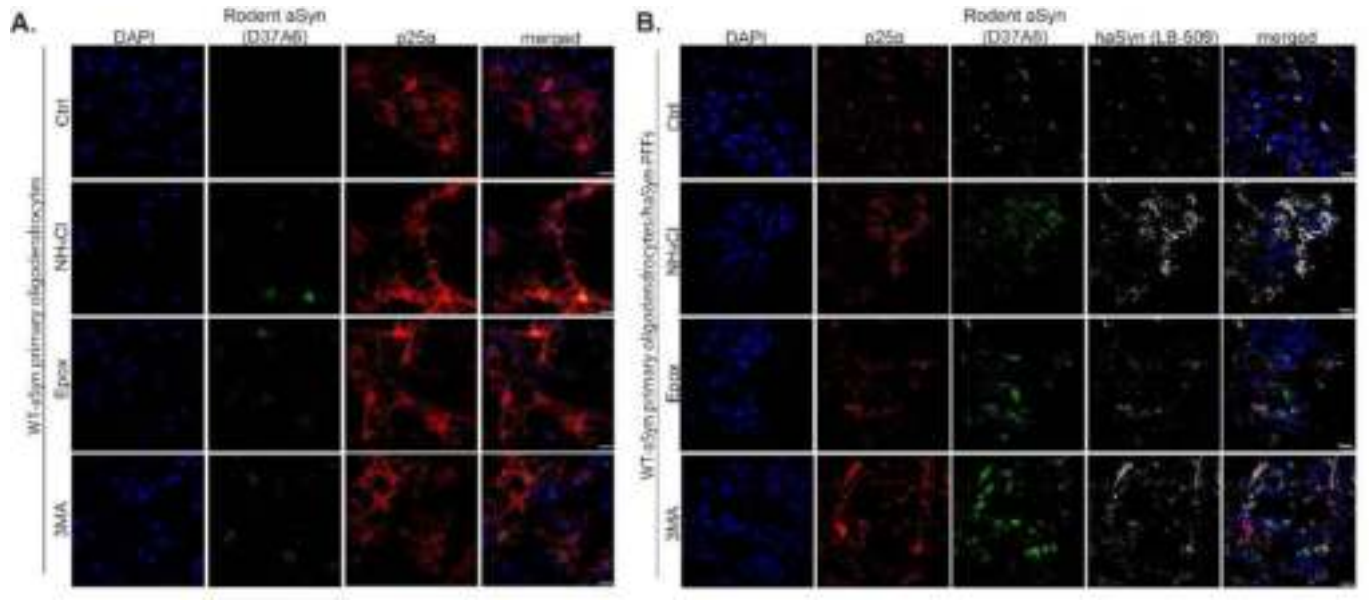

Figure 81: The MSA-related proteins p25α and aSyn are mainly degraded via the ALP in murine primary oligodendroglial cultures, under physiological and pathological conditions. Mouse primary oligodendroglial cultures were incubated with PBS (as control) or haSyn PFFs for 24 hrs followed by their treatment with lysosomal or proteasomal inhibitors for another 48 hrs. (**A-B**) Representative confocal microscopy images depicting the protein levels of p25α (red) upon total lysosomal (NH_4Cl, 20 mM), macroautophagic (3MA, 10 mM) or proteasomal (epox, 15 nM) inhibition (for 48 hrs) in the absence (**A**) or presence (**B**) of 0.5 μg haSyn PFFs for a total of 72 hrs. The recruited endogenous rodent aSyn (green, D37A6 antibody) and the exogenously added haSyn PFFs (grey, LB509 antibody) also seem to be preferentially degraded via the ALP under pathological (**B**, PFFs-treated) conditions. DAPI staining is used as a nuclear marker. Scale bar: 25 μm.

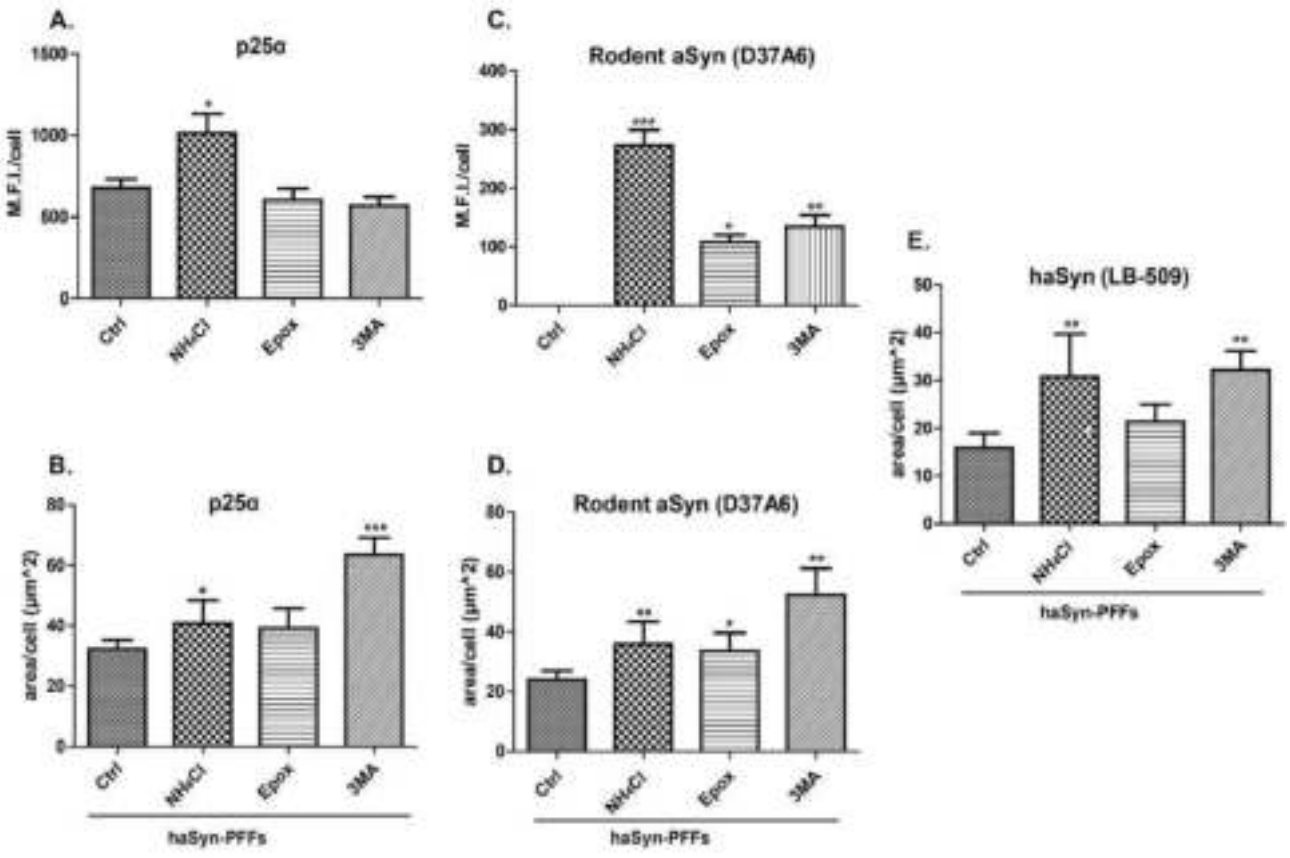

Figure 82: The MSA-related proteins p25α and aSyn are mainly degraded via the ALP in murine primary oligodendroglial cultures, under physiological and pathological conditions. Quantification of p25α (**A-B**), rodent aSyn (**C-D**) and human aSyn (**E**) protein levels in PBS or PFF-treated primary oligodendrocytes, measured as μm^2/cell. Data are expressed as the mean±SE of three independent experiments with duplicate samples/condition within each experiment; *p<0.05; **p< 0.01; ***p< 0.001, by one-way ANOVA with Tukey's post hoc test.

To elucidate further the potential beneficial role of autophagy augmentation in the removal of aSyn and p25α protein levels in primary oligodendrocytes, PBS- or PFF-treated oligodendroglial cultures were incubated with AR7 (40 μM) or rap (1 μM) for 48 hrs **(Figures 83-84).** Confocal microscopy analysis (**Figure 83**) and quantification of aSyn and p25α protein levels revealed that in all conditions tested, incubation with either AR7 or rap led to the effective clearance of p25α (**Figure 84A-B**), the endogenous rodent (**Figure 84C**) and the human aSyn (**Figure 84D**) proteins, thus suggesting that enhancement of macroautophagy or the CMA pathway could potentially mitigate aSyn pathology in MSA and MSA-like conditions.

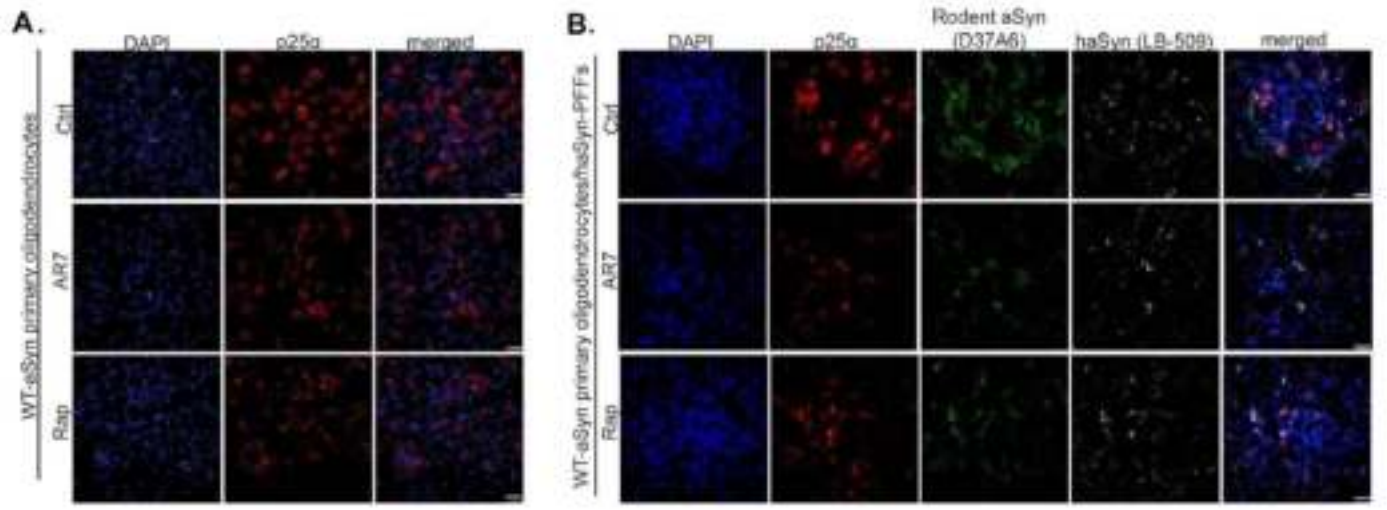

Figure 83: The MSA-related proteins p25α and aSyn are mainly degraded via the ALP in murine primary oligodendroglial cultures, under physiological and pathological conditions. Representative immunofluorescence images of p25α (red), rodent aSyn (green, D37A6 antibody) and haSyn (grey, LB509 antibody) protein levels upon treatment of mouse oligodendrocytes with AR7 (40 μM) or rap (1 μM) for 48 hrs, which were added to cells 24 hrs following addition of PBS, as control, (**A**) or 0.5 μg haSyn PFFs (**B**). DAPI is used as a nuclear marker. Scale bar: 25 μm.

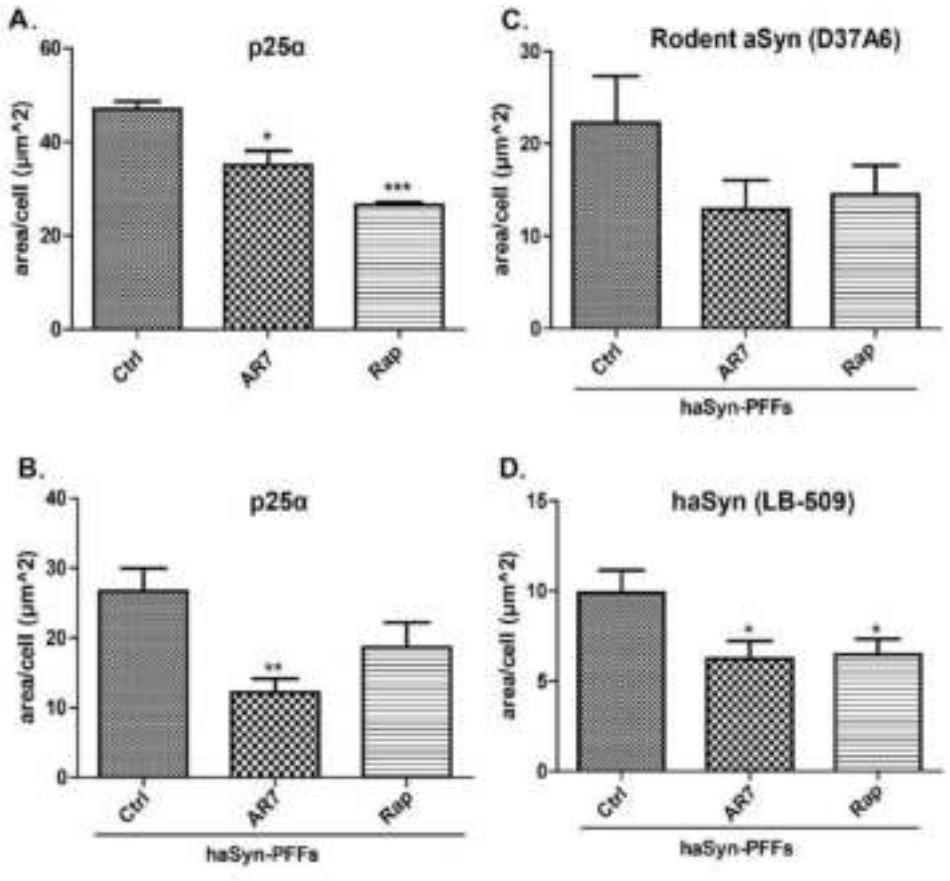

Figure 84: The MSA-related proteins p25α and aSyn are mainly degraded via the ALP in murine primary oligodendroglial cultures, under physiological and pathological conditions. Quantification of p25α (**A, B**), rodent aSyn (**C**) and human aSyn (**D**) protein levels in PBS or PFF-treated primary oligodendrocytes, measured as μm^2/cell. Data are expressed as the mean±SE of three independent experiments with duplicate samples/condition within each experiment; *p<0.05; **p< 0.01; ***p< 0.001, by one-way ANOVA with Tukey's post hoc test.

V. DISCUSSION

The pathological accumulation of abnormally folded aSyn within GSIs found mainly in oligodendrocytes represents the key histopathological hallmark of MSA (Trojanowski and Revesz 2007). Neuronal cytoplasmic and nuclear aSyn inclusions and dystrophic neurites can also be present in MSA brains; however, these lesions appear at a lower frequency than GCIs (Papp and Lantos 1992). The origin of aSyn with oligodendrocytes still remains enigmatic. Even though initial studies suggested that mature oligodendrocytes do not normally express aSyn (Solano, Miller et al. 2000; Ozawa, Okuizumi et al. 2001; Miller, Johnson et al. 2005), subsequent reports proposed that the protein may be expressed in oligodendrocytes, albeit at much lower levels than in neurons (Asi, Simpson et al. 2014; Djelloul, Holmqvist et al. 2015). However, the prevailing hypothesis based mostly on *in vitro* data is that neurons that physiologically express aSyn, release the protein (free or associated with exosomes), which is subsequently taken up by surrounding oligodendrocytes (Kisos, Pukass et al. 2012; Konno, Hasegawa et al. 2012; Rockenstein, Ubhi et al. 2012; Ettle, Reiprich et al. 2014; Pukass and Richter-Landsberg 2014; Reyes, Rey et al. 2014; Pukass, Goldbaum et al. 2015; Kaji, Maki et al. 2018). Furthermore, it has been suggested that p25α, another main component of GCIs, facilitates aSyn aggregation *in vitro* and relocates from the myelin sheath to the oligodendroglial cell soma, prior to aSyn accumulation (Lindersson, Lundvig et al. 2005).

Herein, we assessed the capability of templating the misfolding of endogenous protein, to examine the hypothesis that the prion-like transformation of oligodendroglial aSyn can occur, as has been demonstrated for its neuronal counterpart (Luk, Song et al. 2009; Volpicelli-Daley, Luk et al. 2011; Angot, Steiner et al. 2012; Masuda-Suzukake, Nonaka et al. 2013; Sacino, Thomas et al. 2013). To this end, we first verified that exogenously added haSyn fibrillar seeds are taken up by immortalized oligodendroglial cells and primary oligodendrocytes and can induce the formation of highly insoluble and pathological (aggregated, oxidized/nitrated, and under certain circumstances Ser129 phosphorylated) aSyn assemblies in which the endogenous protein, however minute in amount at baseline, is a central component. The mechanism responsible for the tremendous increase in the expression of endogenous rodent aSyn following PFF addition remains unknown; we have found that the levels of rodent *Snca* mRNA are unchanged in this setting, consistent with the results reported by others in oligodendroglial progenitor cells (Kaji, Maki et al. 2018), suggesting that the stabilization of oligodendrocyte aSyn may be involved.

An upsurge in the expression of endogenous aSyn in haSyn PFF-treated oligodendroglial progenitor cells in culture and the altered expression of proteins associated with neuromodulation and myelination were recently reported (Kaji, Maki et al. 2018). However, the authors of that study failed to find evidence that a similar process occurs in mature, myelin-forming oligodendrocytes. In

contrast, our data clearly demonstrates that the addition of haSyn PFFs to differentiated mouse primary oligodendrocytes induces the seeding of endogenous rodent aSyn, and the dysregulation in myelin, as manifested by the decreased levels and perisomal redistribution of MBP, as well as the colocalization of MBP within aSyn-positive aggregates. This colocalization upon of haSyn PFF administration is similar to what is proposed to occur during the formation of GCIs in human MSA (Wenning, Stefanova et al. 2008). Such a disruption of the myelin sheath is responsible for demyelination, which contributes to disease pathology and clinical manifestations (Matsuo, Akiguchi et al. 1998; Song, Lundvig et al. 2007; Wong, Halliday et al. 2014; Ettle, Kerman et al. 2016). Remarkably, this disruption of myelin was completely prevented in KO-aSyn cultures and in the PFF-injected KO-aSyn striatum, indicating that the presence of endogenous oligodendroglial rat aSyn is a prerequisite for the manifestation of this MSA pathological hallmark. Furthermore, p25α and phospho-tau staining in PFF-treated primary oligodendroglial cultures demonstrated a disruption of the microtubule network that was dependent on the levels of endogenous aSyn. In agreement with our findings, Grigoletto et al. showed an age- and disease-dependent loss of the MBP signal in striatal striosomes accompanied by reduced p25α levels in oligodendrocytes in neuronal synucleinopathy mouse models (Grigoletto, Pukass et al. 2017). They concluded that neuronal aSyn is involved in the regulation and/or maintenance of myelin phospholipids, since aSyn also inhibited the maturation of oligodendrocytes and the formation of membranous sheets *in vitro* (Grigoletto, Pukass et al. 2017).

Even more, our *in vitro* data pinpoint a role for p25α in the prion-like seeding process and aggregation of endogenous oligodendroglial aSyn, illustrating that both the stable and transient overexpression of p25α accelerated the seeding of endogenous aSyn and augmented the formation of pathological aSyn aggregates. p25α reportedly plays a critical role in myelin maturation and relocates early from the myelin sheath to the cytoplasm in MSA (Song, Lundvig et al. 2007). This relocation may impair myelin synthesis and seed aSyn aggregation in oligodendrocytes. Another study also showed that p25α not only relocates from peripheral processes but also from the nucleus to the perinuclear cytoplasm in MSA patients (Ota, Obayashi et al. 2014). The mechanism by which p25α enhances aSyn seeding and aggregation is unclear, and our data suggest that this does not seem to involve necessarily the direct incorporation of p25α into aSyn aggregates, as this occurred only in the case of PLP-haSyn primary oligodendrocytes. Moreover, the absence of p25α redistribution in PFF-treated KO-aSyn cultures suggests that the presence of endogenous oligodendroglial aSyn is a prerequisite for such a phenomenon to occur. Hinting at a possible mechanism, preliminary experiments in our laboratory using OLN-AS7 cells showed that transient p25α overexpression triggered the phosphorylation of aSyn at Ser129 and increased the total levels of aSyn (unpublished observations). Similarly, the co-expression of haSyn and p25α resulted in the

phosphorylation of aggregated, but not monomeric aSyn, in OLN-AS7 cells (Kragh, Lund et al. 2009). Consistent with this idea, in the current work, p25α appeared to stabilize insoluble aSyn conformations. These findings may be applicable more broadly to alpha-synucleinopathies, since p25α is reportedly ectopically expressed in dopaminergic neurons in PD and to be a component of LBs purified from human post-mortem PD brains (Lindersson, Lundvig et al. 2005).

Research over the past few years using recombinant aSyn PFFs and samples from patients with synucleinopathy has provided support to the hypothesis that aSyn may misfold and propagate in a prion-like fashion in MSA patients (Jellinger 2018). The injection of brain homogenates containing aSyn derived from MSA patients into mice triggers the formation of phosphorylated aSyn aggregates and the onset of a neurodegenerative cascade comparable to human MSA pathology (Bernis, Babila et al. 2015; Prusiner, Woerman et al. 2015). Moreover, recent reports have shown that the aSyn pathological conformations found in MSA brains are remarkably stable and resistant to inactivation (Woerman, Kazmi et al. 2018) and that MSA is caused by a unique strain of aSyn assemblies (Melki 2015; Peelaerts, Bousset et al. 2015; Prusiner, Woerman et al. 2015). Supportive of the latter hypothesis are findings showing that pathological aSyn in GCIs and LBs (detected by the Syn303 and Syn7015 fibril-specific antibodies) is conformationally and biologically distinct and that oligodendrocytes, but not neurons, transform misfolded aSyn into a GCI-like strain, highlighting the fact that distinct aSyn strains are generated in different intracellular milieus (Peng, Gathagan et al. 2018). Our comparative analyses of the phosphorylation status of aSyn utilizing different pSer129-specifc antibodies in oligodendroglial cells, primary cortical neurons, and human post-mortem material from DLB and MSA brains, further favor the idea that synucleinopathies are caused by different aSyn strains leading to the detection of distinct, cell-specific, aSyn pathological conformations in each disease (Bousset, Pieri et al. 2013; Melki 2015; Peelaerts, Bousset et al. 2015; Peng, Gathagan et al. 2018; Candelise, Schmitz et al. 2019; Lau, So et al. 2020; Shahnawaz, Mukherjee et al. 2020).

In agreement with our *in vivo* findings, the uptake of haSyn PFFs or GCI-related aSyn derived from MSA patients by oligodendrocytes have been reported (Reyes, Rey et al. 2014; Radford, Rcom-H'cheo-Gauthier et al. 2015). However, other studies have failed to detect exogenous haSyn within oligodendrocytes or other glial cells following inoculation with haSyn PFFs (Paumier, Luk et al. 2015; Rey, Steiner et al. 2016). These contradictory findings may be due to differences in the post-injection time frames when the assessments were performed, since although the uptake of injected aSyn by neurons reportedly occurs within minutes, the intraneuronal signal of internalized proteins begins to decrease at 3 hrs post-injection, probably due to clearance mechanisms (Rey, Petit et al. 2013). Such a scenario may also apply to oligodendrocytes, given that only one *in vivo* study has shown the presence of exogenous aSyn within oligodendrocytes,

assessed at 1 hr post-injection (Reyes, Rey et al. 2014). Our *in vitro* data also demonstrate a decrease of the human protein over time, which, however, may be attributed to clearance mechanisms or to its dilution due to cell proliferation. Another explanation may be that the oligodendroglial uptake of haSyn in the PFF-inoculation models is restricted to near the site of injection, as we have also observed in our model (at least at 1 month post-injection).

Impairment of protein degradation machineries and mitochondrial dysfunction has been also proposed as contributing factor for MSA pathogenesis (Bukhatwa, Zeng et al. 2010; Schwarz, Goldbaum et al. 2012; Stefanova, Kaufmann et al. 2012; Tanji, Odagiri et al. 2013; Monzio Compagnoni, Kleiner et al. 2018; Monzio Compagnoni, Kleiner et al. 2018). In particular, the detection of various aggresome-related proteins and autophagic markers such as p62 and LC3 in GCIs of MSA brains has exposed a crucial role of perturbed proteolysis in the formation of oligodendroglial proteinaceous inclusions (Mori, Nishie et al. 2005; Terni, Rey et al. 2007; Miki, Mori et al. 2011; Chiba, Takei et al. 2012; Makioka, Yamazaki et al. 2012; Odagiri, Tanji et al. 2012; Schwarz, Goldbaum et al. 2012; Tanji, Odagiri et al. 2013; Miki, Tanji et al. 2018; Monzio Compagnoni, Kleiner et al. 2018; Kaji, Maki et al. 2020). A recent comparative study in human post-mortem material from MSA and PD brains concluded that the lysosomal response in relation to aSyn pathology differs between the two synucleinopathies (Puska, Lutz et al. 2018). By systematic comparisons of differently affected neuronal populations in PD, MSA, and non-diseased brains using morphometric immunohistochemistry (cathepsin D), double immunolabelling (cathepsin D/aSyn) laser confocal microscopy, and aSyn immunogold electron microscopy jt has been reported that lysosome-associated aSyn is observed in astroglia and rarely in oligodendroglia and in neurons in MSA, whereas cathepsin D immunoreactivity frequently colocalises with aSyn pre-aggregates in PD nigral neurons (Puska, Lutz et al. 2018).

However, the degradation pathways responsible for the clearance of the endogenous oligodendroglial aSyn and p25α in health and disease and the role of ALP manipulation in the context of MSA remained unexplored. The second arm of our study focused on the degradation pathways responsible for the removal of both oligodendroglial aSyn and p25α, and the impact of fibrillar aSyn on ALP, in an attempt to elucidate the mechanisms responsible for the formation of aSyn-positive aggregates within oligodendrocytes and to identify potential targets for therapy.

Towards this direction, we utilized pharmacological inhibitors or enhancers of the ALP and UPS, or siRNAs targeting autophagy-related genes, under physiological (PBS) or pathological (haSyn PFFs) conditions. According to our results, aSyn (endogenous rodent, overexpressed human and pathology-related conformations) seem to be cleared mainly via CMA and macroautophagy; however to a different magnitude in the various cell lines. A role of macroautophagy in the clearance of aSyn within oligodendrocytes has been previously reported (Schwarz, Goldbaum et al.

2012); however this is the first study demonstrating a role of CMA in the removal of the endogenous and seeded aSyn protein levels and/or aberrant species in oligodendrocytes. This finding contradicts with a prior study that reported a lack of GCI-like formation in oligodendroglia exposed to extracellular soluble/monomeric or fibrillar aSyn concurrently with pharmacological blocking of the fusion of the autophagosome with the lysosome with bafilomycin A1, as well as following genetic knockdown of LC3B (Fellner, Buchinger et al. 2018).

Regarding macroautophagy, it has been previously shown that the endogenously stably overexpressed (OLN-t40 transfected cells) or the exogenously added soluble or pre-aggregated aSyn is mainly removed via macroautophagy in oligodendrocytes and that these aSyn forms do not inhibit the autophagic pathway and flux per se (Pukass, Goldbaum et al. 2015). Moreover, inhibition of the deubiquitylating enzyme Ubiquitin Carboxy-terminal Hydrolase L1 (UCHL1) in oligodendroglial cells was shown to upregulate macroautophagy, thus resulting in the effective removal of aSyn aggregates (Pukass and Richter-Landsberg 2015). Neurosin (kallikrein 6) appears also to be efficient in reducing the levels of aSyn in oligodendrocytes both *in vitro* and *in vivo* (Iwata, Maruyama et al. 2003; Spencer, Valera et al. 2015; Kiely, Miners et al. 2019). Interestingly, treatment of transgenic PLP-haSyn mice, a well-established mouse model for MSA, with the proteasome inhibitor I led to the detection of intracellular aggregates of both human and endogenous murine aSyn, three months after administration of the inhibitor, further supporting the role of the UPS in aSyn clearance (Stefanova, Kaufmann et al. 2012). Furthermore, in agreement with our data showing an impairment of the autophagic flux in PFF-treated OLN cell lines, prior studies also suggested that aggregated aSyn within oligodendrocytes is closely related to autophagy dysregulation (Pukass and Richter-Landsberg 2015; Miki, Tanji et al. 2018). Interestingly, even though with the GFP/RFP-LC3 and GFP/mcherry-SQSTM1 constructs we detect a defect in the autophagic flux upon PFF treatment (**Figure 8**), this was not followed by a statistically significant alteration in the macroautophagic-dependent proteolysis (inhibited by 3MA) in OLN-93 and OLN-AS7 cells (**Figure 6Iii**). A possible explanation for this discrepancy may ascend from the observation that upon PFF treatment we detect a change from a diffuse to a more punctuate pattern, indicative of LC3 II induction and autophagosome formation. If the rate that these autophagosomes are fused with the lysosome is reduced in these cells, then the overall process is as efficient as baseline. In addition, the different time points utilized for the assessment of the autophagic flux (48 hrs) and lysosomal activity (96 hrs) may also account for the observed differences.

In a therapeutic point of view, we investigated the partitioning of CMA and macroautophagy in the clearance of p25α protein in oligodendrocytes, both under physiological and pathological conditions. The contribution of CMA to p25α protein degradation was verified by the identification of the KKRFK pentapeptide motif that meets the criteria for a KFERQ-like motif in p25α amino

acid sequence and its efficient degradation by the *in vitro* system of isolated rat brain lysosomes. In addition, p25α displayed a canonical substrate/pathway relationship, since its levels were increased upon LAMP2A down-regulation, and by extension CMA inhibition, and decreased following induction of the CMA pathway with AR7. Induction of macroautophagy also reduced p25α levels, both in OLN-p25α cells and in primary oligodendrocytes, but less efficiently. Previous studies proposed that p25α is degraded via the proteasome (Lehotzky, Tirian et al. 2004; Lehotzky, Olah et al. 2015); however, our analysis in the epoxomicin-treated primary oligodendrocytes did not yield a statistical contribution of the proteasome in p25α clearance. Due to the non-specific up-regulation of CMV-driven *Tppp/p25α* mRNA by proteasomal inhibitors [as also reported by (Biasini, Fioriti et al. 2004)], the role of the proteasome could not be determined in OLN-p25α cells. Strikingly, the expression of p25α protein (in OLN-p25α cells) seems to hinder the macroautophagic activity (inhibited by 3MA) upon addition of haSyn-PFFs thus favoring the CMA activity, probably as a counterpoise to the proteolytic dysregulation. Likewise, Ejlerskov and et al. have also demonstrated that p25α inhibits the fusion of autophagosomes with the lysosome and leads to the secretion of monomeric and aggregated aSyn via exophagy in PC12 cells (Ejlerskov, Rasmussen et al. 2013).

Finally, the pharmacological CMA- and macroautophagy-specific enhancers AR7 and rapamycin respectively, mitigated the levels of the endogenous and exogenously added aSyn and all its pathological conformations (oxidized/nitrated and aggregated aSyn), together with p25α, both in oligodendroglial cell lines and primary oligodendrocytes. The beneficial effect of macroautophagy induction in the removal of aSyn species in oligodendrocytes has been previously reported. In particular, the geldanamycin analogue 17-AAG [17-(Allylamino)-17-demethoxygeldanamycin] attenuated the formation of aSyn aggregates in OLN-93 cells stably overexpressing the human PD-linked A53T aSyn mutation by stimulating macroautophagy (Riedel, Goldbaum et al. 2010). This effect on macroautophagy induction was also observed in cultured oligodendrocytes derived from the brains of newborn rats (Riedel, Goldbaum et al. 2010). On the other hand, numerous studies have explored the use of various autophagy-enhancing agents in the context of PD pathology, concluding that they exert beneficial effects on neuronal cell survival and accelerate aSyn clearance (Sarkar, Davies et al. 2007; Crews, Spencer et al. 2010; Malagelada, Jin et al. 2010; Wu, Li et al. 2011; Decressac, Mattsson et al. 2013; Perez-Revuelta, Hettich et al. 2014; Sarkar, Chigurupati et al. 2014; Pupyshev, Tikhonova et al. 2019; Pantazopoulou, Brembati et al. 2021). Moreover, the post-translational regulation of autophagy via the use of micro-RNAs (miRs) targeting LAMP2A and HSC70, has been shown to decrease aSyn aggregation in SH-SY5Y cells (Alvarez-Erviti, Seow et al. 2013). Similarly, it has been previously shown that CMA induction via overexpression of the LAMP2A receptor in neuronal cellular and animal synucleinopathy models alleviated aSyn-induced neurotoxic effects (Xilouri, Brekk et al. 2013).

Collectively, our study reveals that the administration of haSyn fibrils to cellular systems, i.e. immortalized oligodendroglial cells and differentiated primary oligodendrocytes, recapitulated critical aspects of MSA pathogenesis, thus representing an attractive model system to study the early events leading to GCI formation. We propose that endogenous aSyn and oligodendroglial phosphoprotein p25α form a dangerous dynamic duo that predisposes oligodendrocytes to accumulate intracellular aSyn aggregates reminiscent of the oligodendroglial inclusions in MSA. Moreover, we show that the endogenous oligodendroglial aSyn and p25α are degraded via the ALP and that conversely, the presence of pathological aSyn (haSyn-PFFs) decreases the autophagic flux of OLN cell lines, albeit without impairing the overall lysosomal activity. The data obtained from cell lines and primary cultures indicate that enhancement of CMA or macroautophagy prevents the accumulation/aggregation of aSyn and/or p25α in rodent MSA-like experimental models, suggesting that ALP manipulation may provide a rationale approach to combat aSyn and p25α accumulation in GCIs. Further validation in pre-clinical models of the disease may pave the way for the use of autophagy modulators or gene-based approaches as therapeutic approaches to attenuate MSA disease progression.

VI. FUTURE PERSPECTIVES

According to our results, the presence of the endogenous oligodendroglial aSyn plays a crucial role in the redistribution of p25α to the cell soma and the formation of $MBP^{+}/aSyn^{+}/p25\alpha^{+}$ aggregates, upon inoculation of oligodendroglial cells with human aSyn seeds. Moreover, the presence of p25α seems to augment the formation of pathological aSyn species in OLN cell lines, suggesting a critical role of p25α in aSyn aggregation following its internalization by oligodendrocytes. Thus, it would be interesting to manipulate the expression of p25α both *in vitro* and *in vivo* and assess the effects in the formation of pathological aSyn aggregates in the context of MSA. To this end, we plan to use a novel adeno-associated viral vector with preferential oligodendrocyte tropism (AAV-Olig001) in order to overexpress or down-regulate (with shRNA) p25α and then study the formation of aSyn assemblies in primary oligodendroglial cell cultures or within the PFF-injected striatum of PLP-haSyn (mouse model for MSA) WT-aSyn and KO-aSyn mice. By this, we expect to detect alterations in the formation of aberrant aSyn species within oligodendrocytes along with the modifications of p25α expression levels.

Moreover, we plan to investigate the transmission of aSyn between oligodendrocytes or from neurons to oligodendrocytes as a possible mechanism of pathological aSyn spread in the context of MSA progression. Exosomes have been proposed as potential mediators for aSyn transfer between neuronal and non-neuronal cells (mostly astrocytes and microglia); however their role in MSA-related aSyn propagation remains yet unexplored. To investigate the hypothesis of an exosomal contribution to MSA pathogenesis, we propose to isolate exosomes from PFF-treated OLN cell lines and apply them in healthy oligodendrocytes in order to verify the ability of pathological aSyn to transmit pathology via exosomes between oligodendrocytes and to trigger the endogenous aSyn accumulation of recipient cells. The findings of the in vitro experiments will be also validated in vivo by inoculating brain exosomes isolated from PLP- or WT-aSyn mouse or human MSA brain (or healthy control brain) unilaterally in the striatum of WT-aSyn mice and assessing the propagation of aSyn pathology at interconnected brain regions. Furthermore, we seek to challenge the hypothesis that in MSA oligodendrocytes uptake aSyn secreted from neurons and that the subsequent accumulation of oligodendroglial aSyn results in reduced myelin production and toxicity to the surrounding neurons. To this end, we will utilize a neuron-oligodendrocyte myelination model system, as well as triple compartment microfluidic chambers (neurons-oligo-neurons) and assess the effects on aSyn seeding and related-toxicity.

Finally, experiments of stereotactic delivery of AAV-Olig001 vectors expressing LAMP2A or Beclin 1 (CMA- and macroautophagy-related proteins respectively) followed by haSyn PFF-injections in the striatum of WT-aSyn mice are expected to corroborate our current results regarding

the role of ALP in aSyn and p25α clearance. All the above experiments aim to uncover potential therapeutic targets that may prevent the accumulation/aggregation of aSyn and/or p25α in oligodendrocytes in an attempt to halt or stop MSA progression.

VII. REFERENCES

Abdelmotilib, H., T. Maltbie, et al. (2017). "alpha-Synuclein fibril-induced inclusion spread in rats and mice correlates with dopaminergic Neurodegeneration." Neurobiol Dis **105**: 84-98.

Abeywardana, T. and M. R. Pratt (2015). "Extent of inhibition of alpha-synuclein aggregation in vitro by SUMOylation is conjugation site- and SUMO isoform-selective." Biochemistry **54**(4): 959-961.

Abounit, S., L. Bousset, et al. (2016). "Tunneling nanotubes spread fibrillar alpha-synuclein by intercellular trafficking of lysosomes." EMBO J **35**(19): 2120-2138.

Acevedo, K., R. Li, et al. (2007). "The phosphorylation of p25/TPPP by LIM kinase 1 inhibits its ability to assemble microtubules." Exp Cell Res **313**(20): 4091-4106.

Adamczyk, A., M. Kacprzak, et al. (2007). "Alpha-synuclein decreases arachidonic acid incorporation into rat striatal synaptoneurosomes." Folia Neuropathol **45**(4): 230-235.

Agarraberes, F. A. and J. F. Dice (2001). "A molecular chaperone complex at the lysosomal membrane is required for protein translocation." J Cell Sci **114**(Pt 13): 2491-2499.

Agarraberes, F. A., S. R. Terlecky, et al. (1997). "An intralysosomal hsp70 is required for a selective pathway of lysosomal protein degradation." J Cell Biol **137**(4): 825-834.

Ahn, B. H., H. Rhim, et al. (2002). "alpha-Synuclein interacts with phospholipase D isozymes and inhibits pervanadate-induced phospholipase D activation in human embryonic kidney-293 cells." J Biol Chem **277**(14): 12334-12342.

Ahn, K. J., S. R. Paik, et al. (2006). "Amino acid sequence motifs and mechanistic features of the membrane translocation of alpha-synuclein." J Neurochem **97**(1): 265-279.

Al-Chalabi, A., A. Durr, et al. (2009). "Genetic variants of the alpha-synuclein gene SNCA are associated with multiple system atrophy." PLoS One **4**(9): e7114.

Al-Wandi, A., N. Ninkina, et al. (2010). "Absence of alpha-synuclein affects dopamine metabolism and synaptic markers in the striatum of aging mice." Neurobiol Aging **31**(5): 796-804.

Aldecoa, I., J. Navarro-Otano, et al. (2015). "Alpha-synuclein immunoreactivity patterns in the enteric nervous system." Neurosci Lett **602**: 145-149.

Alers, S., A. S. Loffler, et al. (2012). "Role of AMPK-mTOR-Ulk1/2 in the regulation of autophagy: cross talk, shortcuts, and feedbacks." Mol Cell Biol **32**(1): 2-11.

Alerte, T. N., A. A. Akinfolarin, et al. (2008). "Alpha-synuclein aggregation alters tyrosine hydroxylase phosphorylation and immunoreactivity: lessons from viral transduction of knockout mice." Neurosci Lett **435**(1): 24-29.

Alfaro, J. F., C. X. Gong, et al. (2012). "Tandem mass spectrometry identifies many mouse brain O-GlcNAcylated proteins including EGF domain-specific O-GlcNAc transferase targets." Proc Natl Acad Sci U S A **109**(19): 7280-7285.

Alonso, A. C., T. Zaidi, et al. (1994). "Role of abnormally phosphorylated tau in the breakdown of microtubules in Alzheimer disease." Proc Natl Acad Sci U S A **91**(12): 5562-5566.

Alvarez-Erviti, L., M. C. Rodriguez-Oroz, et al. (2010). "Chaperone-mediated autophagy markers in Parkinson disease brains." Arch Neurol **67**(12): 1464-1472.

Alvarez-Erviti, L., Y. Seow, et al. (2013). "Influence of microRNA deregulation on chaperone-mediated autophagy and alpha-synuclein pathology in Parkinson's disease." Cell Death Dis **4**: e545.

Alza, N. P., M. A. Conde, et al. (2021). "Neutral lipids as early biomarkers of cellular fate: the case of alpha-synuclein overexpression." Cell Death Dis **12**(1): 52.

Anderson, J. P., D. E. Walker, et al. (2006). "Phosphorylation of Ser-129 is the dominant pathological modification of alpha-synuclein in familial and sporadic Lewy body disease." J Biol Chem **281**(40): 29739-29752.

Andringa, G., F. Du, et al. (2003). "Mapping of rat brain using the Synuclein-1 monoclonal antibody reveals somatodendritic expression of alpha-synuclein in populations of neurons homologous to those vulnerable to Lewy body formation in human synucleopathies." J Neuropathol Exp Neurol **62**(10): 1060-1075.

Angot, E., J. A. Steiner, et al. (2012). "Alpha-synuclein cell-to-cell transfer and seeding in grafted dopaminergic neurons in vivo." PLoS One **7**(6): e39465.

Anguiano, J., T. P. Garner, et al. (2013). "Chemical modulation of chaperone-mediated autophagy by retinoic acid derivatives." Nat Chem Biol **9**(6): 374-382.

Appel-Cresswell, S., C. Vilarino-Guell, et al. (2013). "Alpha-synuclein p.H50Q, a novel pathogenic mutation for Parkinson's disease." Mov Disord **28**(6): 811-813.

Ardley, H. C. and P. A. Robinson (2005). "E3 ubiquitin ligases." Essays Biochem **41**: 15-30.

Asi, Y. T., J. E. Simpson, et al. (2014). "Alpha-synuclein mRNA expression in oligodendrocytes in MSA." Glia **62**(6): 964-970.
Askanas, V., W. K. Engel, et al. (2000). "Novel immunolocalization of alpha-synuclein in human muscle of inclusion-body myositis, regenerating and necrotic muscle fibers, and at neuromuscular junctions." J Neuropathol Exp Neurol **59**(7): 592-598.
Azeredo da Silveira, S., B. L. Schneider, et al. (2009). "Phosphorylation does not prompt, nor prevent, the formation of alpha-synuclein toxic species in a rat model of Parkinson's disease." Hum Mol Genet **18**(5): 872-887.
Baba, M., S. Nakajo, et al. (1998). "Aggregation of alpha-synuclein in Lewy bodies of sporadic Parkinson's disease and dementia with Lewy bodies." Am J Pathol **152**(4): 879-884.
Baek, J. H., D. Whitfield, et al. (2016). "Unfolded protein response is activated in Lewy body dementias." Neuropathol Appl Neurobiol **42**(4): 352-365.
Ballou, L. M. and R. Z. Lin (2008). "Rapamycin and mTOR kinase inhibitors." J Chem Biol **1**(1-4): 27-36.
Bandyopadhyay, U., S. Kaushik, et al. (2008). "The chaperone-mediated autophagy receptor organizes in dynamic protein complexes at the lysosomal membrane." Mol Cell Biol **28**(18): 5747-5763.
Bankston, A. N., W. Li, et al. (2013). "p39, the primary activator for cyclin-dependent kinase 5 (Cdk5) in oligodendroglia, is essential for oligodendroglia differentiation and myelin repair." J Biol Chem **288**(25): 18047-18057.
Baptista, M. J., C. O'Farrell, et al. (2003). "Co-ordinate transcriptional regulation of dopamine synthesis genes by alpha-synuclein in human neuroblastoma cell lines." J Neurochem **85**(4): 957-968.
Barbour, R., K. Kling, et al. (2008). "Red blood cells are the major source of alpha-synuclein in blood." Neurodegener Dis **5**(2): 55-59.
Barca, E., G. Kleiner, et al. (2016). "Decreased Coenzyme Q10 Levels in Multiple System Atrophy Cerebellum." J Neuropathol Exp Neurol **75**(7): 663-672.
Barcelo-Coblijn, G., M. Y. Golovko, et al. (2007). "Brain neutral lipids mass is increased in alpha-synuclein gene-ablated mice." J Neurochem **101**(1): 132-141.
Bartels, T., J. G. Choi, et al. (2011). "alpha-Synuclein occurs physiologically as a helically folded tetramer that resists aggregation." Nature **477**(7362): 107-110.
Bartels, T., N. C. Kim, et al. (2014). "N-alpha-acetylation of alpha-synuclein increases its helical folding propensity, GM1 binding specificity and resistance to aggregation." PLoS One **9**(7): e103727.
Baumann, N. and D. Pham-Dinh (2001). "Biology of oligodendrocyte and myelin in the mammalian central nervous system." Physiol Rev **81**(2): 871-927.
Bazzu, G., G. Calia, et al. (2010). "alpha-Synuclein- and MPTP-generated rodent models of Parkinson's disease and the study of extracellular striatal dopamine dynamics: a microdialysis approach." CNS Neurol Disord Drug Targets **9**(4): 482-490.
Bean, B. P. (2007). "The action potential in mammalian central neurons." Nat Rev Neurosci **8**(6): 451-465.
Bellucci, A., L. Navarria, et al. (2011). "Induction of the unfolded protein response by alpha-synuclein in experimental models of Parkinson's disease." J Neurochem **116**(4): 588-605.
Benaroudj, N., P. Zwickl, et al. (2003). "ATP hydrolysis by the proteasome regulatory complex PAN serves multiple functions in protein degradation." Mol Cell **11**(1): 69-78.
Bendor, J. T., T. P. Logan, et al. (2013). "The function of alpha-synuclein." Neuron **79**(6): 1044-1066.
Bennett, M. C., J. F. Bishop, et al. (1999). "Degradation of alpha-synuclein by proteasome." J Biol Chem **274**(48): 33855-33858.
Bentea, E., L. Verbruggen, et al. (2017). "The Proteasome Inhibition Model of Parkinson's Disease." J Parkinsons Dis **7**(1): 31-63.
Bernis, M. E., J. T. Babila, et al. (2015). "Prion-like propagation of human brain-derived alpha-synuclein in transgenic mice expressing human wild-type alpha-synuclein." Acta Neuropathol Commun **3**: 75.
Betarbet, R., T. B. Sherer, et al. (2000). "Chronic systemic pesticide exposure reproduces features of Parkinson's disease." Nat Neurosci **3**(12): 1301-1306.
Betzer, C., L. B. Lassen, et al. (2018). "Alpha-synuclein aggregates activate calcium pump SERCA leading to calcium dysregulation." EMBO Rep **19**(5).
Betzer, C., A. J. Movius, et al. (2015). "Identification of synaptosomal proteins binding to monomeric and oligomeric alpha-synuclein." PLoS One **10**(2): e0116473.
Biasini, E., L. Fioriti, et al. (2004). "Proteasome inhibition and aggregation in Parkinson's disease: a comparative study in untransfected and transfected cells." J Neurochem **88**(3): 545-553.
Bir, A., O. Sen, et al. (2014). "alpha-Synuclein-induced mitochondrial dysfunction in isolated preparation and intact cells: implications in the pathogenesis of Parkinson's disease." J Neurochem **131**(6): 868-877.

Bjorkoy, G., T. Lamark, et al. (2005). "p62/SQSTM1 forms protein aggregates degraded by autophagy and has a protective effect on huntingtin-induced cell death." J Cell Biol **171**(4): 603-614.
Bjorkoy, G., T. Lamark, et al. (2009). "Monitoring autophagic degradation of p62/SQSTM1." Methods Enzymol **452**: 181-197.
Borghi, R., R. Marchese, et al. (2000). "Full length alpha-synuclein is present in cerebrospinal fluid from Parkinson's disease and normal subjects." Neurosci Lett **287**(1): 65-67.
Bottenstein, J. E. and G. H. Sato (1979). "Growth of a rat neuroblastoma cell line in serum-free supplemented medium." Proc Natl Acad Sci U S A **76**(1): 514-517.
Bottner, M., D. Zorenkov, et al. (2012). "Expression pattern and localization of alpha-synuclein in the human enteric nervous system." Neurobiol Dis **48**(3): 474-480.
Bousset, L., L. Pieri, et al. (2013). "Structural and functional characterization of two alpha-synuclein strains." Nat Commun **4**: 2575.
Bower, J. H., D. M. Maraganore, et al. (1997). "Incidence of progressive supranuclear palsy and multiple system atrophy in Olmsted County, Minnesota, 1976 to 1990." Neurology **49**(5): 1284-1288.
Bradl, M. and H. Lassmann (2010). "Oligodendrocytes: biology and pathology." Acta Neuropathol **119**(1): 37-53.
Breda, C., M. L. Nugent, et al. (2015). "Rab11 modulates alpha-synuclein-mediated defects in synaptic transmission and behaviour." Hum Mol Genet **24**(4): 1077-1091.
Bu, B., X. Tong, et al. (2017). "N-Terminal Acetylation Preserves alpha-Synuclein from Oligomerization by Blocking Intermolecular Hydrogen Bonds." ACS Chem Neurosci **8**(10): 2145-2151.
Bukhatwa, S., B. Y. Zeng, et al. (2010). "A comparison of changes in proteasomal subunit expression in the substantia nigra in Parkinson's disease, multiple system atrophy and progressive supranuclear palsy." Brain Res **1326**: 174-183.
Burre, J., M. Sharma, et al. (2014). "alpha-Synuclein assembles into higher-order multimers upon membrane binding to promote SNARE complex formation." Proc Natl Acad Sci U S A **111**(40): E4274-4283.
Burre, J., M. Sharma, et al. (2015). "Definition of a molecular pathway mediating alpha-synuclein neurotoxicity." J Neurosci **35**(13): 5221-5232.
Burre, J., M. Sharma, et al. (2010). "Alpha-synuclein promotes SNARE-complex assembly in vivo and in vitro." Science **329**(5999): 1663-1667.
Burre, J., S. Vivona, et al. (2013). "Properties of native brain alpha-synuclein." Nature **498**(7453): E4-6; discussion E6-7.
Busch, D. J. and J. R. Morgan (2012). "Synuclein accumulation is associated with cell-specific neuronal death after spinal cord injury." J Comp Neurol **520**(8): 1751-1771.
Butler, B., K. Saha, et al. (2015). "Dopamine Transporter Activity Is Modulated by alpha-Synuclein." J Biol Chem **290**(49): 29542-29554.
Buttner, S., L. Faes, et al. (2013). "The Ca2+/Mn2+ ion-pump PMR1 links elevation of cytosolic Ca(2+) levels to alpha-synuclein toxicity in Parkinson's disease models." Cell Death Differ **20**(3): 465-477.
Cali, T., D. Ottolini, et al. (2012). "alpha-Synuclein controls mitochondrial calcium homeostasis by enhancing endoplasmic reticulum-mitochondria interactions." J Biol Chem **287**(22): 17914-17929.
Candelise, N., M. Schmitz, et al. (2019). "Seeding variability of different alpha synuclein strains in synucleinopathies." Ann Neurol **85**(5): 691-703.
Cao, B., L. Zhang, et al. (2018). "Survival analysis and prognostic nomogram model for multiple system atrophy." Parkinsonism Relat Disord **54**: 68-73.
Cascio, P. (2021). "PA28gamma: New Insights on an Ancient Proteasome Activator." Biomolecules **11**(2).
Castagnet, P. I., M. Y. Golovko, et al. (2005). "Fatty acid incorporation is decreased in astrocytes cultured from alpha-synuclein gene-ablated mice." J Neurochem **94**(3): 839-849.
Celej, M. S., R. Sarroukh, et al. (2012). "Toxic prefibrillar alpha-synuclein amyloid oligomers adopt a distinctive antiparallel beta-sheet structure." Biochem J **443**(3): 719-726.
Chadchankar, H., J. Ihalainen, et al. (2011). "Decreased reuptake of dopamine in the dorsal striatum in the absence of alpha-synuclein." Brain Res **1382**: 37-44.
Chan, C. S., J. N. Guzman, et al. (2007). "'Rejuvenation' protects neurons in mouse models of Parkinson's disease." Nature **447**(7148): 1081-1086.
Chandra, S., X. Chen, et al. (2003). "A broken alpha -helix in folded alpha -Synuclein." J Biol Chem **278**(17): 15313-15318.
Chandra, S., G. Gallardo, et al. (2005). "Alpha-synuclein cooperates with CSPalpha in preventing neurodegeneration." Cell **123**(3): 383-396.
Chaudhary, H., V. Subramaniam, et al. (2017). "Direct Visualization of Model Membrane Remodeling by alpha-Synuclein Fibrillization." Chemphyschem **18**(12): 1620-1626.

Chen, L. and M. B. Feany (2005). "Alpha-synuclein phosphorylation controls neurotoxicity and inclusion formation in a Drosophila model of Parkinson disease." Nat Neurosci **8**(5): 657-663.
Chen, L., M. Periquet, et al. (2009). "Tyrosine and serine phosphorylation of alpha-synuclein have opposing effects on neurotoxicity and soluble oligomer formation." J Clin Invest **119**(11): 3257-3265.
Chen, L., Z. Xie, et al. (2015). "A53T human alpha-synuclein overexpression in transgenic mice induces pervasive mitochondria macroautophagy defects preceding dopamine neuron degeneration." J Neurosci **35**(3): 890-905.
Chen, R. H. C., S. Wislet-Gendebien, et al. (2013). "alpha-Synuclein membrane association is regulated by the Rab3a recycling machinery and presynaptic activity." J Biol Chem **288**(11): 7438-7449.
Chen, V., M. Moncalvo, et al. (2020). "The mechanistic role of alpha-synuclein in the nucleus: impaired nuclear function caused by familial Parkinson's disease SNCA mutations." Hum Mol Genet **29**(18): 3107-3121.
Chen, Y. P., B. Zhao, et al. (2015). "Mutation scanning of the COQ2 gene in ethnic Chinese patients with multiple-system atrophy." Neurobiol Aging **36**(2): 1222 e1227-1211.
Chiang, H. L., S. R. Terlecky, et al. (1989). "A role for a 70-kilodalton heat shock protein in lysosomal degradation of intracellular proteins." Science **246**(4928): 382-385.
Chiba, Y., S. Takei, et al. (2012). "Immunohistochemical localization of aggresomal proteins in glial cytoplasmic inclusions in multiple system atrophy." Neuropathol Appl Neurobiol **38**(6): 559-571.
Chinta, S. J., J. K. Mallajosyula, et al. (2010). "Mitochondrial alpha-synuclein accumulation impairs complex I function in dopaminergic neurons and results in increased mitophagy in vivo." Neurosci Lett **486**(3): 235-239.
Cho, M. K., G. Nodet, et al. (2009). "Structural characterization of alpha-synuclein in an aggregation prone state." Protein Sci **18**(9): 1840-1846.
Choubey, V., D. Safiulina, et al. (2011). "Mutant A53T alpha-synuclein induces neuronal death by increasing mitochondrial autophagy." J Biol Chem **286**(12): 10814-10824.
Chu, Y., J. G. Goldman, et al. (2014). "Abnormal alpha-synuclein reduces nigral voltage-dependent anion channel 1 in sporadic and experimental Parkinson's disease." Neurobiol Dis **69**: 1-14.
Chu, Y. and J. H. Kordower (2007). "Age-associated increases of alpha-synuclein in monkeys and humans are associated with nigrostriatal dopamine depletion: Is this the target for Parkinson's disease?" Neurobiol Dis **25**(1): 134-149.
Chu, Y. and J. H. Kordower (2015). "The prion hypothesis of Parkinson's disease." Curr Neurol Neurosci Rep **15**(5): 28.
Chu, Y., G. A. Morfini, et al. (2012). "Alterations in axonal transport motor proteins in sporadic and experimental Parkinson's disease." Brain **135**(Pt 7): 2058-2073.
Chung, C. Y., J. B. Koprich, et al. (2009). "Dynamic changes in presynaptic and axonal transport proteins combined with striatal neuroinflammation precede dopaminergic neuronal loss in a rat model of AAV alpha-synucleinopathy." J Neurosci **29**(11): 3365-3373.
Clayton, D. F. and J. M. George (1998). "The synucleins: a family of proteins involved in synaptic function, plasticity, neurodegeneration and disease." Trends Neurosci **21**(6): 249-254.
Cohlberg, J. A., J. Li, et al. (2002). "Heparin and other glycosaminoglycans stimulate the formation of amyloid fibrils from alpha-synuclein in vitro." Biochemistry **41**(5): 1502-1511.
Cole, N. B., D. D. Murphy, et al. (2002). "Lipid droplet binding and oligomerization properties of the Parkinson's disease protein alpha-synuclein." J Biol Chem **277**(8): 6344-6352.
Colla, E., P. Coune, et al. (2012). "Endoplasmic reticulum stress is important for the manifestations of alpha-synucleinopathy in vivo." J Neurosci **32**(10): 3306-3320.
Colla, E., P. H. Jensen, et al. (2012). "Accumulation of toxic alpha-synuclein oligomer within endoplasmic reticulum occurs in alpha-synucleinopathy in vivo." J Neurosci **32**(10): 3301-3305.
Collaboration, M. R. (2013). "Mutations in COQ2 in familial and sporadic multiple-system atrophy." N Engl J Med **369**(3): 233-244.
Conde, M. A., N. P. Alza, et al. (2018). "Phospholipase D1 downregulation by alpha-synuclein: Implications for neurodegeneration in Parkinson's disease." Biochim Biophys Acta Mol Cell Biol Lipids **1863**(6): 639-650.
Conn, K. J., W. Gao, et al. (2004). "Identification of the protein disulfide isomerase family member PDIp in experimental Parkinson's disease and Lewy body pathology." Brain Res **1022**(1-2): 164-172.
Cooper, A. A., A. D. Gitler, et al. (2006). "Alpha-synuclein blocks ER-Golgi traffic and Rab1 rescues neuron loss in Parkinson's models." Science **313**(5785): 324-328.
Crews, C. M. (2003). "Feeding the machine: mechanisms of proteasome-catalyzed degradation of ubiquitinated proteins." Curr Opin Chem Biol **7**(5): 534-539.

Crews, L., B. Spencer, et al. (2010). "Selective molecular alterations in the autophagy pathway in patients with Lewy body disease and in models of alpha-synucleinopathy." PLoS One **5**(2): e9313.
Cruz-Martinez, P., S. Gonzalez-Granero, et al. (2016). "Intraventricular injections of mesenchymal stem cells activate endogenous functional remyelination in a chronic demyelinating murine model." Cell Death Dis **7**: e2223.
Cuervo, A. M. and J. F. Dice (1996). "A receptor for the selective uptake and degradation of proteins by lysosomes." Science **273**(5274): 501-503.
Cuervo, A. M. and J. F. Dice (2000). "Age-related decline in chaperone-mediated autophagy." J Biol Chem **275**(40): 31505-31513.
Cuervo, A. M. and J. F. Dice (2000). "Unique properties of lamp2a compared to other lamp2 isoforms." J Cell Sci **113 Pt 24**: 4441-4450.
Cuervo, A. M., J. F. Dice, et al. (1997). "A population of rat liver lysosomes responsible for the selective uptake and degradation of cytosolic proteins." J Biol Chem **272**(9): 5606-5615.
Cuervo, A. M., E. Knecht, et al. (1995). "Activation of a selective pathway of lysosomal proteolysis in rat liver by prolonged starvation." Am J Physiol **269**(5 Pt 1): C1200-1208.
Cuervo, A. M., L. Stefanis, et al. (2004). "Impaired degradation of mutant alpha-synuclein by chaperone-mediated autophagy." Science **305**(5688): 1292-1295.
Dalfo, E., T. Gomez-Isla, et al. (2004). "Abnormal alpha-synuclein interactions with Rab proteins in alpha-synuclein A30P transgenic mice." J Neuropathol Exp Neurol **63**(4): 302-313.
Danielle Dean E, K. R. S., Yingjie Li, Gonzalo E. Torres, Gary W. Miller (2008). "Identification of a novel interaction between α-synuclein and VMAT2." Pharmacology/Experimental Therapeutics: 715.716-715.716.
Danielson, S. R., J. M. Held, et al. (2009). "Preferentially increased nitration of alpha-synuclein at tyrosine-39 in a cellular oxidative model of Parkinson's disease." Anal Chem **81**(18): 7823-7828.
Danzer, K. M., L. R. Kranich, et al. (2012). "Exosomal cell-to-cell transmission of alpha synuclein oligomers." Mol Neurodegener **7**: 42.
Dash, S., Y. Aydin, et al. (2019). "Chaperone-Mediated Autophagy in the Liver: Good or Bad?" Cells **8**(11).
Davidi, D., M. Schechter, et al. (2020). "alpha-Synuclein Translocates to the Nucleus to Activate Retinoic-Acid-Dependent Gene Transcription." iScience **23**(3): 100910.
Davidson, W. S., A. Jonas, et al. (1998). "Stabilization of alpha-synuclein secondary structure upon binding to synthetic membranes." J Biol Chem **273**(16): 9443-9449.
De Stefani, D., A. Bononi, et al. (2012). "VDAC1 selectively transfers apoptotic Ca2+ signals to mitochondria." Cell Death Differ **19**(2): 267-273.
DeBonis, S., E. Neumann, et al. (2015). "Self protein-protein interactions are involved in TPPP/p25 mediated microtubule bundling." Sci Rep **5**: 13242.
Decressac, M., B. Mattsson, et al. (2013). "TFEB-mediated autophagy rescues midbrain dopamine neurons from alpha-synuclein toxicity." Proc Natl Acad Sci U S A **110**(19): E1817-1826.
Delenclos, M., T. Trendafilova, et al. (2017). "Investigation of Endocytic Pathways for the Internalization of Exosome-Associated Oligomeric Alpha-Synuclein." Front Neurosci **11**: 172.
Desplats, P., B. Spencer, et al. (2011). "Alpha-synuclein sequesters Dnmt1 from the nucleus: a novel mechanism for epigenetic alterations in Lewy body diseases." J Biol Chem **286**(11): 9031-9037.
Dettmer, U., A. J. Newman, et al. (2013). "In vivo cross-linking reveals principally oligomeric forms of alpha-synuclein and beta-synuclein in neurons and non-neural cells." J Biol Chem **288**(9): 6371-6385.
Devi, L., V. Raghavendran, et al. (2008). "Mitochondrial import and accumulation of alpha-synuclein impair complex I in human dopaminergic neuronal cultures and Parkinson disease brain." J Biol Chem **283**(14): 9089-9100.
Di Maio, R., P. J. Barrett, et al. (2016). "alpha-Synuclein binds to TOM20 and inhibits mitochondrial protein import in Parkinson's disease." Sci Transl Med **8**(342): 342ra378.
Di Pasquale, E., J. Fantini, et al. (2010). "Altered ion channel formation by the Parkinson's-disease-linked E46K mutant of alpha-synuclein is corrected by GM3 but not by GM1 gangliosides." J Mol Biol **397**(1): 202-218.
Dice, J. F. (1990). "Peptide sequences that target cytosolic proteins for lysosomal proteolysis." Trends Biochem Sci **15**(8): 305-309.
Dickson, D. W., W. Liu, et al. (1999). "Widespread alterations of alpha-synuclein in multiple system atrophy." Am J Pathol **155**(4): 1241-1251.
Djelloul, M., S. Holmqvist, et al. (2015). "Alpha-Synuclein Expression in the Oligodendrocyte Lineage: an In Vitro and In Vivo Study Using Rodent and Human Models." Stem Cell Reports **5**(2): 174-184.

Don, A. S., J. H. Hsiao, et al. (2014). "Altered lipid levels provide evidence for myelin dysfunction in multiple system atrophy." Acta Neuropathol Commun **2**: 150.
Dong, S., C. Aguirre-Hernandez, et al. (2020). "Monitoring spatiotemporal changes in chaperone-mediated autophagy in vivo." Nat Commun **11**(1): 645.
Drescher, M., G. Veldhuis, et al. (2008). "Antiparallel arrangement of the helices of vesicle-bound alpha-synuclein." J Am Chem Soc **130**(25): 7796-7797.
Du, T. T., L. Wang, et al. (2015). "GBA deficiency promotes SNCA/alpha-synuclein accumulation through autophagic inhibition by inactivated PPP2A." Autophagy **11**(10): 1803-1820.
Duda, J. E., B. I. Giasson, et al. (2000). "Immunohistochemical and biochemical studies demonstrate a distinct profile of alpha-synuclein permutations in multiple system atrophy." J Neuropathol Exp Neurol **59**(9): 830-841.
Dulamea, A. O. (2017). "Role of Oligodendrocyte Dysfunction in Demyelination, Remyelination and Neurodegeneration in Multiple Sclerosis." Adv Exp Med Biol **958**: 91-127.
Ebrahimi-Fakhari, D., I. Cantuti-Castelvetri, et al. (2011). "Distinct roles in vivo for the ubiquitin-proteasome system and the autophagy-lysosomal pathway in the degradation of alpha-synuclein." J Neurosci **31**(41): 14508-14520.
Ejlerskov, P., I. Rasmussen, et al. (2013). "Tubulin polymerization-promoting protein (TPPP/p25alpha) promotes unconventional secretion of alpha-synuclein through exophagy by impairing autophagosome-lysosome fusion." J Biol Chem **288**(24): 17313-17335.
El-Agnaf, O. M., S. A. Salem, et al. (2003). "Alpha-synuclein implicated in Parkinson's disease is present in extracellular biological fluids, including human plasma." FASEB J **17**(13): 1945-1947.
El-Agnaf, O. M., S. A. Salem, et al. (2006). "Detection of oligomeric forms of alpha-synuclein protein in human plasma as a potential biomarker for Parkinson's disease." FASEB J **20**(3): 419-425.
Eliezer, D., E. Kutluay, et al. (2001). "Conformational properties of alpha-synuclein in its free and lipid-associated states." J Mol Biol **307**(4): 1061-1073.
Ellis, C. E., E. J. Murphy, et al. (2005). "Mitochondrial lipid abnormality and electron transport chain impairment in mice lacking alpha-synuclein." Mol Cell Biol **25**(22): 10190-10201.
Emamzadeh, F. N. (2016). "Alpha-synuclein structure, functions, and interactions." J Res Med Sci **21**: 29.
Emmanouilidou, E., K. Melachroinou, et al. (2010). "Cell-produced alpha-synuclein is secreted in a calcium-dependent manner by exosomes and impacts neuronal survival." J Neurosci **30**(20): 6838-6851.
Emmanouilidou, E., L. Stefanis, et al. (2010). "Cell-produced alpha-synuclein oligomers are targeted to, and impair, the 26S proteasome." Neurobiol Aging **31**(6): 953-968.
Ettle, B., B. E. Kerman, et al. (2016). "alpha-Synuclein-induced myelination deficit defines a novel interventional target for multiple system atrophy." Acta Neuropathol **132**(1): 59-75.
Ettle, B., S. Reiprich, et al. (2014). "Intracellular alpha-synuclein affects early maturation of primary oligodendrocyte progenitor cells." Mol Cell Neurosci **62**: 68-78.
Ettle, B., J. C. M. Schlachetzki, et al. (2016). "Oligodendroglia and Myelin in Neurodegenerative Diseases: More Than Just Bystanders?" Mol Neurobiol **53**(5): 3046-3062.
Fantini, J. and N. Yahi (2013). "The driving force of alpha-synuclein insertion and amyloid channel formation in the plasma membrane of neural cells: key role of ganglioside- and cholesterol-binding domains." Adv Exp Med Biol **991**: 15-26.
Fares, M. B., N. Ait-Bouziad, et al. (2014). "The novel Parkinson's disease linked mutation G51D attenuates in vitro aggregation and membrane binding of alpha-synuclein, and enhances its secretion and nuclear localization in cells." Hum Mol Genet **23**(17): 4491-4509.
Farinelli, S. E., L. A. Greene, et al. (1998). "Neuroprotective actions of dipyridamole on cultured CNS neurons." J Neurosci **18**(14): 5112-5123.
Faustini, G., E. Marchesan, et al. (2019). "Alpha-Synuclein Preserves Mitochondrial Fusion and Function in Neuronal Cells." Oxid Med Cell Longev **2019**: 4246350.
Fauvet, B., M. K. Mbefo, et al. (2012). "alpha-Synuclein in central nervous system and from erythrocytes, mammalian cells, and Escherichia coli exists predominantly as disordered monomer." J Biol Chem **287**(19): 15345-15364.
Fayyad, M., D. Erskine, et al. (2020). "Investigating the presence of doubly phosphorylated alpha-synuclein at tyrosine 125 and serine 129 in idiopathic Lewy body diseases." Brain Pathol **30**(4): 831-843.
Fellner, L., E. Buchinger, et al. (2018). "Limited effects of dysfunctional macroautophagy on the accumulation of extracellularly derived alpha-synuclein in oligodendroglia: implications for MSA pathogenesis." BMC Neurosci **19**(1): 32.
Feng, L. R., H. J. Federoff, et al. (2010). "Alpha-synuclein mediates alterations in membrane conductance: a potential role for alpha-synuclein oligomers in cell vulnerability." Eur J Neurosci **32**(1): 10-17.

Fernandez, E., J. M. Garcia-Moreno, et al. (2013). "May the evaluation of nitrosative stress through selective increase of 3-nitrotyrosine proteins other than nitroalbumin and dominant tyrosine-125/136 nitrosylation of serum alpha-synuclein serve for diagnosis of sporadic Parkinson's disease?" Antioxid Redox Signal **19**(9): 912-918.
Fornai, F., O. M. Schluter, et al. (2005). "Parkinson-like syndrome induced by continuous MPTP infusion: convergent roles of the ubiquitin-proteasome system and alpha-synuclein." Proc Natl Acad Sci U S A **102**(9): 3413-3418.
Foubert-Samier, A., A. Pavy-Le Traon, et al. (2020). "Disease progression and prognostic factors in multiple system atrophy: A prospective cohort study." Neurobiol Dis **139**: 104813.
Fouka, M., P. Mavroeidi, et al. (2020). "In Search of Effective Treatments Targeting alpha-Synuclein Toxicity in Synucleinopathies: Pros and Cons." Front Cell Dev Biol **8**: 559791.
Freundt, E. C., N. Maynard, et al. (2012). "Neuron-to-neuron transmission of alpha-synuclein fibrils through axonal transport." Ann Neurol **72**(4): 517-524.
Fruhbeis, C., D. Frohlich, et al. (2013). "Neurotransmitter-triggered transfer of exosomes mediates oligodendrocyte-neuron communication." PLoS Biol **11**(7): e1001604.
Fu, M. M., T. S. McAlear, et al. (2019). "The Golgi Outpost Protein TPPP Nucleates Microtubules and Is Critical for Myelination." Cell **179**(1): 132-146 e114.
Fujita, Y., E. Ohama, et al. (2006). "Fragmentation of Golgi apparatus of nigral neurons with alpha-synuclein-positive inclusions in patients with Parkinson's disease." Acta Neuropathol **112**(3): 261-265.
Fujiwara, H., M. Hasegawa, et al. (2002). "alpha-Synuclein is phosphorylated in synucleinopathy lesions." Nat Cell Biol **4**(2): 160-164.
Furukawa, K., M. Matsuzaki-Kobayashi, et al. (2006). "Plasma membrane ion permeability induced by mutant alpha-synuclein contributes to the degeneration of neural cells." J Neurochem **97**(4): 1071-1077.
Fussi, N., M. Hollerhage, et al. (2018). "Exosomal secretion of alpha-synuclein as protective mechanism after upstream blockage of macroautophagy." Cell Death Dis **9**(7): 757.
Gai, W. P., D. L. Pountney, et al. (2003). "alpha-Synuclein fibrils constitute the central core of oligodendroglial inclusion filaments in multiple system atrophy." Exp Neurol **181**(1): 68-78.
Gallastegui, N. and M. Groll (2010). "The 26S proteasome: assembly and function of a destructive machine." Trends Biochem Sci **35**(11): 634-642.
Galvagnion, C. (2017). "The Role of Lipids Interacting with alpha-Synuclein in the Pathogenesis of Parkinson's Disease." J Parkinsons Dis **7**(3): 433-450.
Galvagnion, C., J. W. Brown, et al. (2016). "Chemical properties of lipids strongly affect the kinetics of the membrane-induced aggregation of alpha-synuclein." Proc Natl Acad Sci U S A **113**(26): 7065-7070.
Ganapathy, I. D. a. K. (2017). "Modification of α-Synuclein by Phosphorylation: A Pivotal Event in the Cellular Pathogenesis of Parkinson's Disease." intechopen **Protein Phosphorylation**.
George, J. M., H. Jin, et al. (1995). "Characterization of a novel protein regulated during the critical period for song learning in the zebra finch." Neuron **15**(2): 361-372.
Ghidoni, R., L. Benussi, et al. (2008). "Exosomes: the Trojan horses of neurodegeneration." Med Hypotheses **70**(6): 1226-1227.
Ghosh, D., S. Sahay, et al. (2014). "The newly discovered Parkinson's disease associated Finnish mutation (A53E) attenuates alpha-synuclein aggregation and membrane binding." Biochemistry **53**(41): 6419-6421.
Ghosh, R. and J. S. Pattison (2018). "Macroautophagy and Chaperone-Mediated Autophagy in Heart Failure: The Known and the Unknown." Oxid Med Cell Longev **2018**: 8602041.
Giasson, B. I., J. E. Duda, et al. (2000). "Oxidative damage linked to neurodegeneration by selective alpha-synuclein nitration in synucleinopathy lesions." Science **290**(5493): 985-989.
Giasson, B. I., I. V. Murray, et al. (2001). "A hydrophobic stretch of 12 amino acid residues in the middle of alpha-synuclein is essential for filament assembly." J Biol Chem **276**(4): 2380-2386.
Gilman, S., P. A. Low, et al. (1999). "Consensus statement on the diagnosis of multiple system atrophy." J Neurol Sci **163**(1): 94-98.
Gilman, S., G. K. Wenning, et al. (2008). "Second consensus statement on the diagnosis of multiple system atrophy." Neurology **71**(9): 670-676.
Gitler, A. D., B. J. Bevis, et al. (2008). "The Parkinson's disease protein alpha-synuclein disrupts cellular Rab homeostasis." Proc Natl Acad Sci U S A **105**(1): 145-150.
Glickman, M. H. and A. Ciechanover (2002). "The ubiquitin-proteasome proteolytic pathway: destruction for the sake of construction." Physiol Rev **82**(2): 373-428.

Goers, J., A. B. Manning-Bog, et al. (2003). "Nuclear localization of alpha-synuclein and its interaction with histones." Biochemistry **42**(28): 8465-8471.
Goldberg, M. S., S. M. Fleming, et al. (2003). "Parkin-deficient mice exhibit nigrostriatal deficits but not loss of dopaminergic neurons." J Biol Chem **278**(44): 43628-43635.
Gosavi, N., H. J. Lee, et al. (2002). "Golgi fragmentation occurs in the cells with prefibrillar alpha-synuclein aggregates and precedes the formation of fibrillar inclusion." J Biol Chem **277**(50): 48984-48992.
Greten-Harrison, B., M. Polydoro, et al. (2010). "alphabetagamma-Synuclein triple knockout mice reveal age-dependent neuronal dysfunction." Proc Natl Acad Sci U S A **107**(45): 19573-19578.
Grice, G. L. and J. A. Nathan (2016). "The recognition of ubiquitinated proteins by the proteasome." Cell Mol Life Sci **73**(18): 3497-3506.
Griffin, S. V., K. Hiromura, et al. (2004). "Cyclin-dependent kinase 5 is a regulator of podocyte differentiation, proliferation, and morphology." Am J Pathol **165**(4): 1175-1185.
Grigoletto, J., K. Pukass, et al. (2017). "Higher levels of myelin phospholipids in brains of neuronal alpha-Synuclein transgenic mice precede myelin loss." Acta Neuropathol Commun **5**(1): 37.
Grunewald, A., B. Arns, et al. (2012). "ATP13A2 mutations impair mitochondrial function in fibroblasts from patients with Kufor-Rakeb syndrome." Neurobiol Aging **33**(8): 1843 e1841-1847.
Guardia-Laguarta, C., E. Area-Gomez, et al. (2014). "alpha-Synuclein is localized to mitochondria-associated ER membranes." J Neurosci **34**(1): 249-259.
Guardia-Laguarta, C., E. Area-Gomez, et al. (2015). "A new role for alpha-synuclein in Parkinson's disease: Alteration of ER-mitochondrial communication." Mov Disord **30**(8): 1026-1033.
Guo, J. T., A. Q. Chen, et al. (2008). "Inhibition of vesicular monoamine transporter-2 activity in alpha-synuclein stably transfected SH-SY5Y cells." Cell Mol Neurobiol **28**(1): 35-47.
Guo, M., J. Wang, et al. (2020). "Microglial exosomes facilitate alpha-synuclein transmission in Parkinson's disease." Brain **143**(5): 1476-1497.
Gustafsson, G., C. Loov, et al. (2018). "Secretion and Uptake of alpha-Synuclein Via Extracellular Vesicles in Cultured Cells." Cell Mol Neurobiol **38**(8): 1539-1550.
Gustke, N., B. Steiner, et al. (1992). "The Alzheimer-like phosphorylation of tau protein reduces microtubule binding and involves Ser-Pro and Thr-Pro motifs." FEBS Lett **307**(2): 199-205.
Haj-Yahya, M., B. Fauvet, et al. (2013). "Synthetic polyubiquitinated alpha-Synuclein reveals important insights into the roles of the ubiquitin chain in regulating its pathophysiology." Proc Natl Acad Sci U S A **110**(44): 17726-17731.
Hall, K., S. Yang, et al. (2015). "Behavioural deficits in transgenic mice expressing human truncated (1-120 amino acid) alpha-synuclein." Exp Neurol **264**: 8-13.
Hansen, C., E. Angot, et al. (2011). "alpha-Synuclein propagates from mouse brain to grafted dopaminergic neurons and seeds aggregation in cultured human cells." J Clin Invest **121**(2): 715-725.
Hara, K., Y. Momose, et al. (2007). "Multiplex families with multiple system atrophy." Arch Neurol **64**(4): 545-551.
Hasegawa, M., H. Fujiwara, et al. (2002). "Phosphorylated alpha-synuclein is ubiquitinated in alpha-synucleinopathy lesions." J Biol Chem **277**(50): 49071-49076.
Heckman, M. G., L. Schottlaender, et al. (2014). "LRRK2 exonic variants and risk of multiple system atrophy." Neurology **83**(24): 2256-2261.
Heman-Ackah, S. M., R. Manzano, et al. (2017). "Alpha-synuclein induces the unfolded protein response in Parkinson's disease SNCA triplication iPSC-derived neurons." Hum Mol Genet **26**(22): 4441-4450.
Hlavanda, E., E. Klement, et al. (2007). "Phosphorylation blocks the activity of tubulin polymerization-promoting protein (TPPP): identification of sites targeted by different kinases." J Biol Chem **282**(40): 29531-29539.
Hodara, R., E. H. Norris, et al. (2004). "Functional consequences of alpha-synuclein tyrosine nitration: diminished binding to lipid vesicles and increased fibril formation." J Biol Chem **279**(46): 47746-47753.
Hoffman-Zacharska, D., D. Koziorowski, et al. (2013). "Novel A18T and pA29S substitutions in alpha-synuclein may be associated with sporadic Parkinson's disease." Parkinsonism Relat Disord **19**(11): 1057-1060.
Hofmann, K., R. Rodriguez-Rodriguez, et al. (2017). "Astrocytes and oligodendrocytes in grey and white matter regions of the brain metabolize fatty acids." Sci Rep **7**(1): 10779.
Hohler, A. D. and V. J. Singh (2012). "Probable hereditary multiple system atrophy-autonomic (MSA-A) in a family in the United States." J Clin Neurosci **19**(3): 479-480.
Holec, S. A. M. and A. L. Woerman (2020). "Evidence of distinct alpha-synuclein strains underlying disease heterogeneity." Acta Neuropathol.

Holmes, B. B., S. L. DeVos, et al. (2013). "Heparan sulfate proteoglycans mediate internalization and propagation of specific proteopathic seeds." Proc Natl Acad Sci U S A **110**(33): E3138-3147.
Honjo, Y., H. Ito, et al. (2011). "Protein disulfide isomerase immunopositive glial cytoplasmic inclusions in patients with multiple system atrophy." Int J Neurosci **121**(10): 543-550.
Hoogerheide, D. P., P. A. Gurnev, et al. (2017). "Mechanism of alpha-synuclein translocation through a VDAC nanopore revealed by energy landscape modeling of escape time distributions." Nanoscale **9**(1): 183-192.
Hoyer, W., D. Cherny, et al. (2004). "Impact of the acidic C-terminal region comprising amino acids 109-140 on alpha-synuclein aggregation in vitro." Biochemistry **43**(51): 16233-16242.
Hsu, L. J., Y. Sagara, et al. (2000). "alpha-synuclein promotes mitochondrial deficit and oxidative stress." Am J Pathol **157**(2): 401-410.
Hu, D., X. Sun, et al. (2019). "Alpha-synuclein suppresses mitochondrial protease ClpP to trigger mitochondrial oxidative damage and neurotoxicity." Acta Neuropathol **137**(6): 939-960.
Hu, S., M. Hu, et al. (2020). "Phosphorylation of Tau and alpha-Synuclein Induced Neurodegeneration in MPTP Mouse Model of Parkinson's Disease." Neuropsychiatr Dis Treat **16**: 651-663.
Huang, Z., Z. Xu, et al. (2011). "Determining nuclear localization of alpha-synuclein in mouse brains." Neuroscience **199**: 318-332.
Hudak, A., E. Kusz, et al. (2019). "Contribution of syndecans to cellular uptake and fibrillation of alpha-synuclein and tau." Sci Rep **9**(1): 16543.
Hughes, A. J., C. Colosimo, et al. (1992). "The dopaminergic response in multiple system atrophy." J Neurol Neurosurg Psychiatry **55**(11): 1009-1013.
Ihse, E., H. Yamakado, et al. (2017). "Cellular internalization of alpha-synuclein aggregates by cell surface heparan sulfate depends on aggregate conformation and cell type." Sci Rep **7**(1): 9008.
Iozzo, R. V. (1998). "Matrix proteoglycans: from molecular design to cellular function." Annu Rev Biochem **67**: 609-652.
Issa, A. R., J. Sun, et al. (2018). "The lysosomal membrane protein LAMP2A promotes autophagic flux and prevents SNCA-induced Parkinson disease-like symptoms in the Drosophila brain." Autophagy **14**(11): 1898-1910.
Itoh, K., T. Kasai, et al. (2014). "Definite familial multiple system atrophy with unknown genetics." Neuropathology **34**(3): 309-313.
Iwai, A., E. Masliah, et al. (1995). "The precursor protein of non-A beta component of Alzheimer's disease amyloid is a presynaptic protein of the central nervous system." Neuron **14**(2): 467-475.
Iwata, A., M. Maruyama, et al. (2003). "Alpha-synuclein degradation by serine protease neurosin: implication for pathogenesis of synucleinopathies." Hum Mol Genet **12**(20): 2625-2635.
Iyer, A., S. J. Roeters, et al. (2017). "C-Terminal Truncated alpha-Synuclein Fibrils Contain Strongly Twisted beta-Sheets." J Am Chem Soc **139**(43): 15392-15400.
Iyer, A., S. J. Roeters, et al. (2016). "The Impact of N-terminal Acetylation of alpha-Synuclein on Phospholipid Membrane Binding and Fibril Structure." J Biol Chem **291**(40): 21110-21122.
Jacobs, D., D. P. Hoogerheide, et al. (2019). "Probing Membrane Association of alpha-Synuclein Domains with VDAC Nanopore Reveals Unexpected Binding Pattern." Sci Rep **9**(1): 4580.
Jao, C. C., A. Der-Sarkissian, et al. (2004). "Structure of membrane-bound alpha-synuclein studied by site-directed spin labeling." Proc Natl Acad Sci U S A **101**(22): 8331-8336.
Jao, C. C., B. G. Hegde, et al. (2008). "Structure of membrane-bound alpha-synuclein from site-directed spin labeling and computational refinement." Proc Natl Acad Sci U S A **105**(50): 19666-19671.
Jellinger, K. A. (2018). "Multiple System Atrophy: An Oligodendroglioneural Synucleinopathy1." J Alzheimers Dis **62**(3): 1141-1179.
Jellinger, K. A. and P. L. Lantos (2010). "Papp-Lantos inclusions and the pathogenesis of multiple system atrophy: an update." Acta Neuropathol **119**(6): 657-667.
Jenco, J. M., A. Rawlingson, et al. (1998). "Regulation of phospholipase D2: selective inhibition of mammalian phospholipase D isoenzymes by alpha- and beta-synucleins." Biochemistry **37**(14): 4901-4909.
Jensen, P. H., M. S. Nielsen, et al. (1998). "Binding of alpha-synuclein to brain vesicles is abolished by familial Parkinson's disease mutation." J Biol Chem **273**(41): 26292-26294.
Jessen, F., H. Kaduszkiewicz, et al. (2010). "Anticholinergic drug use and risk for dementia: target for dementia prevention." Eur Arch Psychiatry Clin Neurosci **260 Suppl 2**: S111-115.
Jin, H., K. Ishikawa, et al. (2008). "Analyses of copy number and mRNA expression level of the alpha-synuclein gene in multiple system atrophy." J Med Dent Sci **55**(1): 145-153.

Jin, J., G. J. Li, et al. (2007). "Identification of novel proteins associated with both alpha-synuclein and DJ-1." Mol Cell Proteomics **6**(5): 845-859.
Jo, E., N. Fuller, et al. (2002). "Defective membrane interactions of familial Parkinson's disease mutant A30P alpha-synuclein." J Mol Biol **315**(4): 799-807.
Jo, E., J. McLaurin, et al. (2000). "alpha-Synuclein membrane interactions and lipid specificity." J Biol Chem **275**(44): 34328-34334.
Kahle, P. J., M. Neumann, et al. (2002). "Hyperphosphorylation and insolubility of alpha-synuclein in transgenic mouse oligodendrocytes." EMBO Rep **3**(6): 583-588.
Kaji, S., T. Maki, et al. (2020). "Insights into the pathogenesis of multiple system atrophy: focus on glial cytoplasmic inclusions." Transl Neurodegener **9**: 7.
Kaji, S., T. Maki, et al. (2018). "Pathological Endogenous alpha-Synuclein Accumulation in Oligodendrocyte Precursor Cells Potentially Induces Inclusions in Multiple System Atrophy." Stem Cell Reports **10**(2): 356-365.
Kaji, S., T. Maki, et al. (2020). "BCAS1-positive immature oligodendrocytes are affected by the alpha-synuclein-induced pathology of multiple system atrophy." Acta Neuropathol Commun **8**(1): 120.
Kalia, L. V., S. K. Kalia, et al. (2011). "Ubiquitinylation of alpha-synuclein by carboxyl terminus Hsp70-interacting protein (CHIP) is regulated by Bcl-2-associated athanogene 5 (BAG5)." PLoS One **6**(2): e14695.
Kamp, F., N. Exner, et al. (2010). "Inhibition of mitochondrial fusion by alpha-synuclein is rescued by PINK1, Parkin and DJ-1." EMBO J **29**(20): 3571-3589.
Kang, L., G. M. Moriarty, et al. (2012). "N-terminal acetylation of alpha-synuclein induces increased transient helical propensity and decreased aggregation rates in the intrinsically disordered monomer." Protein Sci **21**(7): 911-917.
Karampetsou, M., M. T. Ardah, et al. (2017). "Phosphorylated exogenous alpha-synuclein fibrils exacerbate pathology and induce neuronal dysfunction in mice." Sci Rep **7**(1): 16533.
Karpowicz, R. J., Jr., C. M. Haney, et al. (2017). "Selective imaging of internalized proteopathic alpha-synuclein seeds in primary neurons reveals mechanistic insight into transmission of synucleinopathies." J Biol Chem **292**(32): 13482-13497.
Kaushik, S. and A. M. Cuervo (2009). "Methods to monitor chaperone-mediated autophagy." Methods Enzymol **452**: 297-324.
Kawamoto, Y., I. Akiguchi, et al. (2007). "Accumulation of Hsc70 and Hsp70 in glial cytoplasmic inclusions in patients with multiple system atrophy." Brain Res **1136**(1): 219-227.
Kawamura, N., G. H. Sun-Wada, et al. (2012). "Delivery of endosomes to lysosomes via microautophagy in the visceral endoderm of mouse embryos." Nat Commun **3**: 1071.
Kayed, R., Y. Sokolov, et al. (2004). "Permeabilization of lipid bilayers is a common conformation-dependent activity of soluble amyloid oligomers in protein misfolding diseases." J Biol Chem **279**(45): 46363-46366.
Kellie, J. F., R. E. Higgs, et al. (2014). "Quantitative measurement of intact alpha-synuclein proteoforms from post-mortem control and Parkinson's disease brain tissue by intact protein mass spectrometry." Sci Rep **4**: 5797.
Kiely, A. P., Y. T. Asi, et al. (2013). "alpha-Synucleinopathy associated with G51D SNCA mutation: a link between Parkinson's disease and multiple system atrophy?" Acta Neuropathol **125**(5): 753-769.
Kiely, A. P., J. S. Miners, et al. (2019). "Exploring the putative role of kallikrein-6, calpain-1 and cathepsin-D in the proteolytic degradation of alpha-synuclein in multiple system atrophy." Neuropathol Appl Neurobiol **45**(4): 347-360.
Killinger, B. A., R. Melki, et al. (2019). "Endogenous alpha-synuclein monomers, oligomers and resulting pathology: let's talk about the lipids in the room." NPJ Parkinsons Dis **5**: 23.
Kim, H. Y., M. K. Cho, et al. (2009). "Structural properties of pore-forming oligomers of alpha-synuclein." J Am Chem Soc **131**(47): 17482-17489.
Kim, T. D., E. Choi, et al. (2004). "Alpha-synuclein has structural and functional similarities to small heat shock proteins." Biochem Biophys Res Commun **324**(4): 1352-1359.
Kim, T. D., S. R. Paik, et al. (2002). "Structural and functional implications of C-terminal regions of alpha-synuclein." Biochemistry **41**(46): 13782-13790.
Kim, T. D., S. R. Paik, et al. (2000). "Structural changes in alpha-synuclein affect its chaperone-like activity in vitro." Protein Sci **9**(12): 2489-2496.
Kisos, H., K. Pukass, et al. (2012). "Increased neuronal alpha-synuclein pathology associates with its accumulation in oligodendrocytes in mice modeling alpha-synucleinopathies." PLoS One **7**(10): e46817.

Klionsky, D. J. and S. D. Emr (2000). "Autophagy as a regulated pathway of cellular degradation." Science **290**(5497): 1717-1721.
Koch, G., M. Smith, et al. (1986). "Endoplasmic reticulum contains a common, abundant calcium-binding glycoprotein, endoplasmin." J Cell Sci **86**: 217-232.
Konno, M., T. Hasegawa, et al. (2012). "Suppression of dynamin GTPase decreases alpha-synuclein uptake by neuronal and oligodendroglial cells: a potent therapeutic target for synucleinopathy." Mol Neurodegener **7**: 38.
Kontopoulos, E., J. D. Parvin, et al. (2006). "Alpha-synuclein acts in the nucleus to inhibit histone acetylation and promote neurotoxicity." Hum Mol Genet **15**(20): 3012-3023.
Kordower, J. H., Y. Chu, et al. (2008). "Lewy body-like pathology in long-term embryonic nigral transplants in Parkinson's disease." Nat Med **14**(5): 504-506.
Kordower, J. H., H. B. Dodiya, et al. (2011). "Transfer of host-derived alpha synuclein to grafted dopaminergic neurons in rat." Neurobiol Dis **43**(3): 552-557.
Kowall, N. W., P. Hantraye, et al. (2000). "MPTP induces alpha-synuclein aggregation in the substantia nigra of baboons." Neuroreport **11**(1): 211-213.
Kragh, C. L., G. Fillon, et al. (2013). "FAS-dependent cell death in alpha-synuclein transgenic oligodendrocyte models of multiple system atrophy." PLoS One **8**(1): e55243.
Kragh, C. L., L. B. Lund, et al. (2009). "Alpha-synuclein aggregation and Ser-129 phosphorylation-dependent cell death in oligodendroglial cells." J Biol Chem **284**(15): 10211-10222.
Kruger, R., W. Kuhn, et al. (1998). "Ala30Pro mutation in the gene encoding alpha-synuclein in Parkinson's disease." Nat Genet **18**(2): 106-108.
Krumova, P., E. Meulmeester, et al. (2011). "Sumoylation inhibits alpha-synuclein aggregation and toxicity." J Cell Biol **194**(1): 49-60.
Kuhn, S., L. Gritti, et al. (2019). "Oligodendrocytes in Development, Myelin Generation and Beyond." Cells **8**(11).
Kurowska, Z., E. Englund, et al. (2011). "Signs of degeneration in 12-22-year old grafts of mesencephalic dopamine neurons in patients with Parkinson's disease." J Parkinsons Dis **1**(1): 83-92.
Kuwahara, T., R. Tonegawa, et al. (2012). "Phosphorylation of alpha-synuclein protein at Ser-129 reduces neuronal dysfunction by lowering its membrane binding property in Caenorhabditis elegans." J Biol Chem **287**(10): 7098-7109.
Kuzdas-Wood, D., N. Stefanova, et al. (2014). "Towards translational therapies for multiple system atrophy." Prog Neurobiol **118**: 19-35.
Kuzdas, D., S. Stemberger, et al. (2013). "Oligodendroglial alpha-synucleinopathy and MSA-like cardiovascular autonomic failure: experimental evidence." Exp Neurol **247**: 531-536.
Labbe, C., M. G. Heckman, et al. (2016). "MAPT haplotype diversity in multiple system atrophy." Parkinsonism Relat Disord **30**: 40-45.
Labrador-Garrido, A., M. Cejudo-Guillen, et al. (2016). "Chaperome screening leads to identification of Grp94/Gp96 and FKBP4/52 as modulators of the alpha-synuclein-elicited immune response." FASEB J **30**(2): 564-577.
Lantos, P. L. and M. I. Papp (1994). "Cellular pathology of multiple system atrophy: a review." J Neurol Neurosurg Psychiatry **57**(2): 129-133.
Lassen, L. B., E. Gregersen, et al. (2018). "ELISA method to detect alpha-synuclein oligomers in cell and animal models." PLoS One **13**(4): e0196056.
Lau, A., R. W. L. So, et al. (2020). "alpha-Synuclein strains target distinct brain regions and cell types." Nat Neurosci **23**(1): 21-31.
Lautenschlager, J., A. D. Stephens, et al. (2018). "C-terminal calcium binding of alpha-synuclein modulates synaptic vesicle interaction." Nat Commun **9**(1): 712.
Layfield, R., D. Tooth, et al. (2001). "Purification of poly-ubiquitinated proteins by S5a-affinity chromatography." Proteomics **1**(6): 773-777.
Lee, A. S. (1992). "Mammalian stress response: induction of the glucose-regulated protein family." Curr Opin Cell Biol **4**(2): 267-273.
Lee, A. S. (2005). "The ER chaperone and signaling regulator GRP78/BiP as a monitor of endoplasmic reticulum stress." Methods **35**(4): 373-381.
Lee, H. J., C. Choi, et al. (2002). "Membrane-bound alpha-synuclein has a high aggregation propensity and the ability to seed the aggregation of the cytosolic form." J Biol Chem **277**(1): 671-678.
Lee, H. J., F. Khoshaghideh, et al. (2006). "Impairment of microtubule-dependent trafficking by overexpression of alpha-synuclein." Eur J Neurosci **24**(11): 3153-3162.

Lee, H. J., F. Khoshaghideh, et al. (2004). "Clearance of alpha-synuclein oligomeric intermediates via the lysosomal degradation pathway." J Neurosci **24**(8): 1888-1896.
Lee, H. J., S. Patel, et al. (2005). "Intravesicular localization and exocytosis of alpha-synuclein and its aggregates." J Neurosci **25**(25): 6016-6024.
Lee, H. J., S. Y. Shin, et al. (2002). "Formation and removal of alpha-synuclein aggregates in cells exposed to mitochondrial inhibitors." J Biol Chem **277**(7): 5411-5417.
Lee, H. J., J. E. Suk, et al. (2008). "Assembly-dependent endocytosis and clearance of extracellular alpha-synuclein." Int J Biochem Cell Biol **40**(9): 1835-1849.
Lee, J. T., T. C. Wheeler, et al. (2008). "Ubiquitination of alpha-synuclein by Siah-1 promotes alpha-synuclein aggregation and apoptotic cell death." Hum Mol Genet **17**(6): 906-917.
Lee, S., S. T. Oh, et al. (2017). "MPTP-induced vulnerability of dopamine neurons in A53T alpha-synuclein overexpressed mice with the potential involvement of DJ-1 downregulation." Korean J Physiol Pharmacol **21**(6): 625-632.
Lee, S. R. M. J. W. M. M. B. J. Q. T. V. M. Y. (2007). "Mechanisms of slow axonal transport of α-synuclein." American Association of Neuropathologists (AANP) **21**(5): A28-A29.
Lehotzky, A., J. Olah, et al. (2015). "Zinc-induced structural changes of the disordered tppp/p25 inhibits its degradation by the proteasome." Biochim Biophys Acta **1852**(1): 83-91.
Lehotzky, A., L. Tirian, et al. (2004). "Dynamic targeting of microtubules by TPPP/p25 affects cell survival." J Cell Sci **117**(Pt 25): 6249-6259.
Lehri-Boufala, S., M. O. Ouidja, et al. (2015). "New roles of glycosaminoglycans in alpha-synuclein aggregation in a cellular model of Parkinson disease." PLoS One **10**(1): e0116641.
Lei, Z., G. Cao, et al. (2019). "A30P mutant alpha-synuclein impairs autophagic flux by inactivating JNK signaling to enhance ZKSCAN3 activity in midbrain dopaminergic neurons." Cell Death Dis **10**(2): 133.
Levine, B. and D. J. Klionsky (2004). "Development by self-digestion: molecular mechanisms and biological functions of autophagy." Dev Cell **6**(4): 463-477.
Levine, P. M., A. Galesic, et al. (2019). "alpha-Synuclein O-GlcNAcylation alters aggregation and toxicity, revealing certain residues as potential inhibitors of Parkinson's disease." Proc Natl Acad Sci U S A **116**(5): 1511-1519.
Lewis, Y. E., A. Galesic, et al. (2017). "O-GlcNAcylation of alpha-Synuclein at Serine 87 Reduces Aggregation without Affecting Membrane Binding." ACS Chem Biol **12**(4): 1020-1027.
Li, H. T., H. N. Du, et al. (2002). "Structural transformation and aggregation of human alpha-synuclein in trifluoroethanol: non-amyloid component sequence is essential and beta-sheet formation is prerequisite to aggregation." Biopolymers **64**(4): 221-226.
Li, J., P. Henning Jensen, et al. (2002). "Differential localization of alpha-, beta- and gamma-synucleins in the rat CNS." Neuroscience **113**(2): 463-478.
Li, J. Y., E. Englund, et al. (2008). "Lewy bodies in grafted neurons in subjects with Parkinson's disease suggest host-to-graft disease propagation." Nat Med **14**(5): 501-503.
Li, J. Y., E. Englund, et al. (2010). "Characterization of Lewy body pathology in 12- and 16-year-old intrastriatal mesencephalic grafts surviving in a patient with Parkinson's disease." Mov Disord **25**(8): 1091-1096.
Li, W., P. N. Hoffman, et al. (2004). "Axonal transport of human alpha-synuclein slows with aging but is not affected by familial Parkinson's disease-linked mutations." J Neurochem **88**(2): 401-410.
Li, W., N. West, et al. (2005). "Aggregation promoting C-terminal truncation of alpha-synuclein is a normal cellular process and is enhanced by the familial Parkinson's disease-linked mutations." Proc Natl Acad Sci U S A **102**(6): 2162-2167.
Li, W., Q. Yang, et al. (2018). "Signaling and induction of chaperone-mediated autophagy by the endoplasmic reticulum under stress conditions." Autophagy **14**(6): 1094-1096.
Li, W. W., J. Li, et al. (2012). "Microautophagy: lesser-known self-eating." Cell Mol Life Sci **69**(7): 1125-1136.
Li, Y. H., N. Gao, et al. (2011). "Alpha-synuclein functions as a negative regulator for expression of tyrosine hydroxylase." Acta Neurol Belg **111**(2): 130-135.
Liani, E., A. Eyal, et al. (2004). "Ubiquitylation of synphilin-1 and alpha-synuclein by SIAH and its presence in cellular inclusions and Lewy bodies imply a role in Parkinson's disease." Proc Natl Acad Sci U S A **101**(15): 5500-5505.
Lindersson, E., D. Lundvig, et al. (2005). "p25alpha Stimulates alpha-synuclein aggregation and is co-localized with aggregated alpha-synuclein in alpha-synucleinopathies." J Biol Chem **280**(7): 5703-5715.

Lipp, A., P. Sandroni, et al. (2009). "Prospective differentiation of multiple system atrophy from Parkinson disease, with and without autonomic failure." Arch Neurol **66**(6): 742-750.
Liu, C. W., M. J. Corboy, et al. (2003). "Endoproteolytic activity of the proteasome." Science **299**(5605): 408-411.
Liu, D., L. Jin, et al. (2008). "Silencing alpha-synuclein gene expression enhances tyrosine hydroxylase activity in MN9D cells." Neurochem Res **33**(7): 1401-1409.
Liu, G., M. Chen, et al. (2015). "Increased oligomerization and phosphorylation of alpha-synuclein are associated with decreased activity of glucocerebrosidase and protein phosphatase 2A in aging monkey brains." Neurobiol Aging **36**(9): 2649-2659.
Liu, W. J., L. Ye, et al. (2016). "p62 links the autophagy pathway and the ubiqutin-proteasome system upon ubiquitinated protein degradation." Cell Mol Biol Lett **21**: 29.
Liu, X., Y. J. Lee, et al. (2011). "Alpha-synuclein functions in the nucleus to protect against hydroxyurea-induced replication stress in yeast." Hum Mol Genet **20**(17): 3401-3414.
Loeb, V., E. Yakunin, et al. (2010). "The transgenic overexpression of alpha-synuclein and not its related pathology associates with complex I inhibition." J Biol Chem **285**(10): 7334-7343.
Longhena, F., G. Faustini, et al. (2017). "The Contribution of alpha-Synuclein Spreading to Parkinson's Disease Synaptopathy." Neural Plast **2017**: 5012129.
Lou, H., S. E. Montoya, et al. (2010). "Serine 129 phosphorylation reduces the ability of alpha-synuclein to regulate tyrosine hydroxylase and protein phosphatase 2A in vitro and in vivo." J Biol Chem **285**(23): 17648-17661.
Lu, L., C. Zhang, et al. (2013). "Voltage-dependent anion channel involved in the alpha-synuclein-induced dopaminergic neuron toxicity in rats." Acta Biochim Biophys Sin (Shanghai) **45**(3): 170-178.
Lu, Y., M. Prudent, et al. (2011). "Phosphorylation of alpha-Synuclein at Y125 and S129 alters its metal binding properties: implications for understanding the role of alpha-Synuclein in the pathogenesis of Parkinson's Disease and related disorders." ACS Chem Neurosci **2**(11): 667-675.
Lucke, C., D. L. Gantz, et al. (2006). "Interactions between fatty acids and alpha-synuclein." J Lipid Res **47**(8): 1714-1724.
Ludtmann, M. H., P. R. Angelova, et al. (2016). "Monomeric Alpha-Synuclein Exerts a Physiological Role on Brain ATP Synthase." J Neurosci **36**(41): 10510-10521.
Ludtmann, M. H. R., P. R. Angelova, et al. (2018). "alpha-synuclein oligomers interact with ATP synthase and open the permeability transition pore in Parkinson's disease." Nat Commun **9**(1): 2293.
Luk, K. C., V. Kehm, et al. (2012). "Pathological alpha-synuclein transmission initiates Parkinson-like neurodegeneration in nontransgenic mice." Science **338**(6109): 949-953.
Luk, K. C., C. Song, et al. (2009). "Exogenous alpha-synuclein fibrils seed the formation of Lewy body-like intracellular inclusions in cultured cells." Proc Natl Acad Sci U S A **106**(47): 20051-20056.
Luna, E., S. C. Decker, et al. (2018). "Differential alpha-synuclein expression contributes to selective vulnerability of hippocampal neuron subpopulations to fibril-induced toxicity." Acta Neuropathol **135**(6): 855-875.
Luth, E. S., I. G. Stavrovskaya, et al. (2014). "Soluble, prefibrillar alpha-synuclein oligomers promote complex I-dependent, Ca2+-induced mitochondrial dysfunction." J Biol Chem **289**(31): 21490-21507.
Ma, K. L., L. K. Song, et al. (2014). "The nuclear accumulation of alpha-synuclein is mediated by importin alpha and promotes neurotoxicity by accelerating the cell cycle." Neuropharmacology **82**: 132-142.
Ma, L., C. Yang, et al. (2018). "C-terminal truncation exacerbates the aggregation and cytotoxicity of alpha-Synuclein: A vicious cycle in Parkinson's disease." Biochim Biophys Acta Mol Basis Dis **1864**(12): 3714-3725.
Ma, M. R., Z. W. Hu, et al. (2016). "Phosphorylation induces distinct alpha-synuclein strain formation." Sci Rep **6**: 37130.
Madine, J., A. J. Doig, et al. (2006). "A study of the regional effects of alpha-synuclein on the organization and stability of phospholipid bilayers." Biochemistry **45**(18): 5783-5792.
Maiza, A., S. Chantepie, et al. (2018). "The role of heparan sulfates in protein aggregation and their potential impact on neurodegeneration." FEBS Lett **592**(23): 3806-3818.
Mak, S. K., A. L. McCormack, et al. (2010). "Lysosomal degradation of alpha-synuclein in vivo." J Biol Chem **285**(18): 13621-13629.
Makioka, K., T. Yamazaki, et al. (2012). "Activation and alteration of lysosomes in multiple system atrophy." Neuroreport **23**(5): 270-276.
Malagelada, C., Z. H. Jin, et al. (2010). "Rapamycin protects against neuron death in in vitro and in vivo models of Parkinson's disease." J Neurosci **30**(3): 1166-1175.

Mangas-Sanjuan, V., J. Olah, et al. (2015). "Tubulin acetylation promoting potency and absorption efficacy of deacetylase inhibitors." Br J Pharmacol **172**(3): 829-840.
Manning-Bog, A. B., A. L. McCormack, et al. (2002). "The herbicide paraquat causes up-regulation and aggregation of alpha-synuclein in mice: paraquat and alpha-synuclein." J Biol Chem **277**(3): 1641-1644.
Mao, X., M. T. Ou, et al. (2016). "Pathological alpha-synuclein transmission initiated by binding lymphocyte-activation gene 3." Science **353**(6307).
Maroteaux, L., J. T. Campanelli, et al. (1988). "Synuclein: a neuron-specific protein localized to the nucleus and presynaptic nerve terminal." J Neurosci **8**(8): 2804-2815.
Marotta, N. P., Y. H. Lin, et al. (2015). "O-GlcNAc modification blocks the aggregation and toxicity of the protein alpha-synuclein associated with Parkinson's disease." Nat Chem **7**(11): 913-920.
Martin-Clemente, B., B. Alvarez-Castelao, et al. (2004). "alpha-Synuclein expression levels do not significantly affect proteasome function and expression in mice and stably transfected PC12 cell lines." J Biol Chem **279**(51): 52984-52990.
Martin, L. J., Y. Pan, et al. (2006). "Parkinson's disease alpha-synuclein transgenic mice develop neuronal mitochondrial degeneration and cell death." J Neurosci **26**(1): 41-50.
Martin, L. J., S. Semenkow, et al. (2014). "Mitochondrial permeability transition pore regulates Parkinson's disease development in mutant alpha-synuclein transgenic mice." Neurobiol Aging **35**(5): 1132-1152.
Martinez-Vicente, M., Z. Talloczy, et al. (2008). "Dopamine-modified alpha-synuclein blocks chaperone-mediated autophagy." J Clin Invest **118**(2): 777-788.
Massey, A. C., C. Zhang, et al. (2006). "Chaperone-mediated autophagy in aging and disease." Curr Top Dev Biol **73**: 205-235.
Masuda-Suzukake, M., T. Nonaka, et al. (2014). "Pathological alpha-synuclein propagates through neural networks." Acta Neuropathol Commun **2**: 88.
Masuda-Suzukake, M., T. Nonaka, et al. (2013). "Prion-like spreading of pathological alpha-synuclein in brain." Brain **136**(Pt 4): 1128-1138.
Matsuo, A., I. Akiguchi, et al. (1998). "Myelin degeneration in multiple system atrophy detected by unique antibodies." Am J Pathol **153**(3): 735-744.
May, V. E., B. Ettle, et al. (2014). "alpha-Synuclein impairs oligodendrocyte progenitor maturation in multiple system atrophy." Neurobiol Aging **35**(10): 2357-2368.
Mazzulli, J. R., F. Zunke, et al. (2016). "alpha-Synuclein-induced lysosomal dysfunction occurs through disruptions in protein trafficking in human midbrain synucleinopathy models." Proc Natl Acad Sci U S A **113**(7): 1931-1936.
Mbefo, M. K., K. E. Paleologou, et al. (2010). "Phosphorylation of synucleins by members of the Polo-like kinase family." J Biol Chem **285**(4): 2807-2822.
McCarthy, K. D. and J. de Vellis (1980). "Preparation of separate astroglial and oligodendroglial cell cultures from rat cerebral tissue." J Cell Biol **85**(3): 890-902.
McCormack, A., N. Chegeni, et al. (2016). "Purification of alpha-synuclein containing inclusions from human post mortem brain tissue." J Neurosci Methods **266**: 141-150.
McCormack, A. L., S. K. Mak, et al. (2012). "Increased alpha-synuclein phosphorylation and nitration in the aging primate substantia nigra." Cell Death Dis **3**: e315.
McGranahan, T. M., N. E. Patzlaff, et al. (2011). "alpha4beta2 nicotinic acetylcholine receptors on dopaminergic neurons mediate nicotine reward and anxiety relief." J Neurosci **31**(30): 10891-10902.
McKeith, I. G., D. W. Dickson, et al. (2005). "Diagnosis and management of dementia with Lewy bodies: third report of the DLB Consortium." Neurology **65**(12): 1863-1872.
Medeiros, G. F., A. Mendes, et al. (2000). "Distribution of sulfated glycosaminoglycans in the animal kingdom: widespread occurrence of heparin-like compounds in invertebrates." Biochim Biophys Acta **1475**(3): 287-294.
Meier, F., T. Abeywardana, et al. (2012). "Semisynthetic, site-specific ubiquitin modification of alpha-synuclein reveals differential effects on aggregation." J Am Chem Soc **134**(12): 5468-5471.
Melki, R. (2015). "Role of Different Alpha-Synuclein Strains in Synucleinopathies, Similarities with other Neurodegenerative Diseases." J Parkinsons Dis **5**(2): 217-227.
Mendoza-Velasquez, J. J., J. F. Flores-Vazquez, et al. (2019). "Autonomic Dysfunction in alpha-Synucleinopathies." Front Neurol **10**: 363.
Meng, L., R. Mohan, et al. (1999). "Epoxomicin, a potent and selective proteasome inhibitor, exhibits in vivo antiinflammatory activity." Proc Natl Acad Sci U S A **96**(18): 10403-10408.

Mezias, C., N. Rey, et al. (2020). "Neural connectivity predicts spreading of alpha-synuclein pathology in fibril-injected mouse models: Involvement of retrograde and anterograde axonal propagation." Neurobiol Dis **134**: 104623.
Miki, Y., F. Mori, et al. (2011). "Accumulation of histone deacetylase 6, an aggresome-related protein, is specific to Lewy bodies and glial cytoplasmic inclusions." Neuropathology **31**(6): 561-568.
Miki, Y., K. Tanji, et al. (2018). "AMBRA1, a novel alpha-synuclein-binding protein, is implicated in the pathogenesis of multiple system atrophy." Brain Pathol **28**(1): 28-42.
Miller, D. W., J. M. Johnson, et al. (2005). "Absence of alpha-synuclein mRNA expression in normal and multiple system atrophy oligodendroglia." J Neural Transm (Vienna) **112**(12): 1613-1624.
Mironov, S. L. (2015). "alpha-Synuclein forms non-selective cation channels and stimulates ATP-sensitive potassium channels in hippocampal neurons." J Physiol **593**(1): 145-159.
Mitsui, J., T. Matsukawa, et al. (2016). "Plasma Coenzyme Q10 Levels in Patients With Multiple System Atrophy." JAMA Neurol **73**(8): 977-980.
Mondragon-Rodriguez, S., G. Perry, et al. (2014). "Phosphorylation of tau protein at sites Ser(396-404) is one of the earliest events in Alzheimer's disease and Down syndrome." Neuropathol Appl Neurobiol **40**(2): 121-135.
Monzio Compagnoni, G., G. Kleiner, et al. (2018). "Mitochondrial dysfunction in fibroblasts of Multiple System Atrophy." Biochim Biophys Acta Mol Basis Dis **1864**(12): 3588-3597.
Monzio Compagnoni, G., G. Kleiner, et al. (2018). "Mitochondrial Dysregulation and Impaired Autophagy in iPSC-Derived Dopaminergic Neurons of Multiple System Atrophy." Stem Cell Reports **11**(5): 1185-1198.
Mori, F., M. Nishie, et al. (2005). "Accumulation of NEDD8 in neuronal and glial inclusions of neurodegenerative disorders." Neuropathol Appl Neurobiol **31**(1): 53-61.
Mori, F., K. Tanji, et al. (2002). "Immunohistochemical comparison of alpha- and beta-synuclein in adult rat central nervous system." Brain Res **941**(1-2): 118-126.
Morris, M., G. M. Knudsen, et al. (2015). "Tau post-translational modifications in wild-type and human amyloid precursor protein transgenic mice." Nat Neurosci **18**(8): 1183-1189.
Murphy, K. E., A. M. Gysbers, et al. (2015). "Lysosomal-associated membrane protein 2 isoforms are differentially affected in early Parkinson's disease." Mov Disord **30**(12): 1639-1647.
Murphy, K. E., A. M. Gysbers, et al. (2014). "Reduced glucocerebrosidase is associated with increased alpha-synuclein in sporadic Parkinson's disease." Brain **137**(Pt 3): 834-848.
Murray, I. V., B. I. Giasson, et al. (2003). "Role of alpha-synuclein carboxy-terminus on fibril formation in vitro." Biochemistry **42**(28): 8530-8540.
Nakamura, K., F. Mori, et al. (2015). "Filamentous aggregations of phosphorylated alpha-synuclein in Schwann cells (Schwann cell cytoplasmic inclusions) in multiple system atrophy." Acta Neuropathol Commun **3**: 29.
Nakamura, K., V. M. Nemani, et al. (2011). "Direct membrane association drives mitochondrial fission by the Parkinson disease-associated protein alpha-synuclein." J Biol Chem **286**(23): 20710-20726.
Nakamura, S., Y. Kawamoto, et al. (2000). "Expression of the endocytosis regulatory proteins Rab5 and Rabaptin-5 in glial cytoplasmic inclusions from brains with multiple system atrophy." Clin Neuropathol **19**(2): 51-56.
Narayanan, V. and S. Scarlata (2001). "Membrane binding and self-association of alpha-synucleins." Biochemistry **40**(33): 9927-9934.
Narhi, L., S. J. Wood, et al. (1999). "Both familial Parkinson's disease mutations accelerate alpha-synuclein aggregation." J Biol Chem **274**(14): 9843-9846.
Nave, K. A. and B. D. Trapp (2008). "Axon-glial signaling and the glial support of axon function." Annu Rev Neurosci **31**: 535-561.
Nikoletopoulou, V. and N. Tavernarakis (2018). "The PMR1 pump in alpha-synuclein toxicity and neurodegeneration." Neurosci Lett **663**: 66-71.
Nistico, R., B. Mehdawy, et al. (2011). "Paraquat- and rotenone-induced models of Parkinson's disease." Int J Immunopathol Pharmacol **24**(2): 313-322.
Odagiri, S., K. Tanji, et al. (2012). "Autophagic adapter protein NBR1 is localized in Lewy bodies and glial cytoplasmic inclusions and is involved in aggregate formation in alpha-synucleinopathy." Acta Neuropathol **124**(2): 173-186.
Okerlund, N. D., K. Schneider, et al. (2017). "Bassoon Controls Presynaptic Autophagy through Atg5." Neuron **93**(4): 897-913 e897.
Oku, M. and Y. Sakai (2018). "Three Distinct Types of Microautophagy Based on Membrane Dynamics and Molecular Machineries." Bioessays **40**(6): e1800008.

Olah, J., A. Lehotzky, et al. (2020). "Microtubule-Associated Proteins with Regulatory Functions by Day and Pathological Potency at Night." Cells **9**(2).
Orenstein, S. J. and A. M. Cuervo (2010). "Chaperone-mediated autophagy: molecular mechanisms and physiological relevance." Semin Cell Dev Biol **21**(7): 719-726.
Orosz, F., G. G. Kovacs, et al. (2004). "TPPP/p25: from unfolded protein to misfolding disease: prediction and experiments." Biol Cell **96**(9): 701-711.
Ortiz, J. F., S. Bette, et al. (2020). "Multiple System Atrophy - Cerebellar Type: Clinical Picture and Treatment of an Often-Overlooked Disorder." Cureus **12**(9): e10741.
Osellame, L. D., A. A. Rahim, et al. (2013). "Mitochondria and quality control defects in a mouse model of Gaucher disease--links to Parkinson's disease." Cell Metab **17**(6): 941-953.
Ostrerova, N., L. Petrucelli, et al. (1999). "alpha-Synuclein shares physical and functional homology with 14-3-3 proteins." J Neurosci **19**(14): 5782-5791.
Ota, K., M. Obayashi, et al. (2014). "Relocation of p25alpha/tubulin polymerization promoting protein from the nucleus to the perinuclear cytoplasm in the oligodendroglia of sporadic and COQ2 mutant multiple system atrophy." Acta Neuropathol Commun **2**: 136.
Otzen, D. E., D. M. Lundvig, et al. (2005). "p25alpha is flexible but natively folded and binds tubulin with oligomeric stoichiometry." Protein Sci **14**(6): 1396-1409.
Outeiro, T. F., E. Kontopoulos, et al. (2007). "Sirtuin 2 inhibitors rescue alpha-synuclein-mediated toxicity in models of Parkinson's disease." Science **317**(5837): 516-519.
Ovadi, J. and F. Orosz (2009). "An unstructured protein with destructive potential: TPPP/p25 in neurodegeneration." Bioessays **31**(6): 676-686.
Ozawa, T., K. Okuizumi, et al. (2001). "Analysis of the expression level of alpha-synuclein mRNA using postmortem brain samples from pathologically confirmed cases of multiple system atrophy." Acta Neuropathol **102**(2): 188-190.
Ozawa, T., H. Takano, et al. (1999). "No mutation in the entire coding region of the alpha-synuclein gene in pathologically confirmed cases of multiple system atrophy." Neurosci Lett **270**(2): 110-112.
Paillusson, S., P. Gomez-Suaga, et al. (2017). "alpha-Synuclein binds to the ER-mitochondria tethering protein VAPB to disrupt Ca(2+) homeostasis and mitochondrial ATP production." Acta Neuropathol **134**(1): 129-149.
Paleologou, K. E., A. Oueslati, et al. (2010). "Phosphorylation at S87 is enhanced in synucleinopathies, inhibits alpha-synuclein oligomerization, and influences synuclein-membrane interactions." J Neurosci **30**(9): 3184-3198.
Paleologou, K. E., A. W. Schmid, et al. (2008). "Phosphorylation at Ser-129 but not the phosphomimics S129E/D inhibits the fibrillation of alpha-synuclein." J Biol Chem **283**(24): 16895-16905.
Pandey, N., R. E. Schmidt, et al. (2006). "The alpha-synuclein mutation E46K promotes aggregation in cultured cells." Exp Neurol **197**(2): 515-520.
Pankiv, S., T. H. Clausen, et al. (2007). "p62/SQSTM1 binds directly to Atg8/LC3 to facilitate degradation of ubiquitinated protein aggregates by autophagy." J Biol Chem **282**(33): 24131-24145.
Pantazopoulou, M., V. Brembati, et al. (2021). "Distinct alpha-Synuclein species induced by seeding are selectively cleared by the Lysosome or the Proteasome in neuronally differentiated SH-SY5Y cells." J Neurochem **156**(6): 880-896.
Papp, M. I., J. E. Kahn, et al. (1989). "Glial cytoplasmic inclusions in the CNS of patients with multiple system atrophy (striatonigral degeneration, olivopontocerebellar atrophy and Shy-Drager syndrome)." J Neurol Sci **94**(1-3): 79-100.
Papp, M. I. and P. L. Lantos (1992). "Accumulation of tubular structures in oligodendroglial and neuronal cells as the basic alteration in multiple system atrophy." J Neurol Sci **107**(2): 172-182.
Parihar, M. S., A. Parihar, et al. (2008). "Mitochondrial association of alpha-synuclein causes oxidative stress." Cell Mol Life Sci **65**(7-8): 1272-1284.
Park, J. S., B. Koentjoro, et al. (2014). "Parkinson's disease-associated human ATP13A2 (PARK9) deficiency causes zinc dyshomeostasis and mitochondrial dysfunction." Hum Mol Genet **23**(11): 2802-2815.
Park, S. M., H. Y. Jung, et al. (2002). "Distinct roles of the N-terminal-binding domain and the C-terminal-solubilizing domain of alpha-synuclein, a molecular chaperone." J Biol Chem **277**(32): 28512-28520.
Parzych, K. R. and D. J. Klionsky (2014). "An overview of autophagy: morphology, mechanism, and regulation." Antioxid Redox Signal **20**(3): 460-473.

Pasanen, P., L. Myllykangas, et al. (2014). "Novel alpha-synuclein mutation A53E associated with atypical multiple system atrophy and Parkinson's disease-type pathology." Neurobiol Aging **35**(9): 2180 e2181-2185.
Pasternak, B., H. Svanstrom, et al. (2012). "Use of calcium channel blockers and Parkinson's disease." Am J Epidemiol **175**(7): 627-635.
Paumier, K. L., K. C. Luk, et al. (2015). "Intrastriatal injection of pre-formed mouse alpha-synuclein fibrils into rats triggers alpha-synuclein pathology and bilateral nigrostriatal degeneration." Neurobiol Dis **82**: 185-199.
Payne, S. C., C. A. Bartlett, et al. (2012). "Myelin sheath decompaction, axon swelling, and functional loss during chronic secondary degeneration in rat optic nerve." Invest Ophthalmol Vis Sci **53**(10): 6093-6101.
Payton, J. E., R. J. Perrin, et al. (2004). "Structural determinants of PLD2 inhibition by alpha-synuclein." J Mol Biol **337**(4): 1001-1009.
Peelaerts, W., L. Bousset, et al. (2015). "alpha-Synuclein strains cause distinct synucleinopathies after local and systemic administration." Nature **522**(7556): 340-344.
Peng, C., R. J. Gathagan, et al. (2018). "Cellular milieu imparts distinct pathological alpha-synuclein strains in alpha-synucleinopathies." Nature **557**(7706): 558-563.
Peng, C., R. J. Gathagan, et al. (2018). "Distinct alpha-Synuclein strains and implications for heterogeneity among alpha-Synucleinopathies." Neurobiol Dis **109**(Pt B): 209-218.
Peng, X., R. Tehranian, et al. (2005). "Alpha-synuclein activation of protein phosphatase 2A reduces tyrosine hydroxylase phosphorylation in dopaminergic cells." J Cell Sci **118**(Pt 15): 3523-3530.
Perez-Revuelta, B. I., M. M. Hettich, et al. (2014). "Metformin lowers Ser-129 phosphorylated alpha-synuclein levels via mTOR-dependent protein phosphatase 2A activation." Cell Death Dis **5**: e1209.
Perez, R. G., J. C. Waymire, et al. (2002). "A role for alpha-synuclein in the regulation of dopamine biosynthesis." J Neurosci **22**(8): 3090-3099.
Perfeito, R., D. F. Lazaro, et al. (2014). "Linking alpha-synuclein phosphorylation to reactive oxygen species formation and mitochondrial dysfunction in SH-SY5Y cells." Mol Cell Neurosci **62**: 51-59.
Perni, M., C. Galvagnion, et al. (2017). "A natural product inhibits the initiation of alpha-synuclein aggregation and suppresses its toxicity." Proc Natl Acad Sci U S A **114**(6): E1009-E1017.
Pickart, C. M. and M. J. Eddins (2004). "Ubiquitin: structures, functions, mechanisms." Biochim Biophys Acta **1695**(1-3): 55-72.
Pinho, R., I. Paiva, et al. (2019). "Nuclear localization and phosphorylation modulate pathological effects of alpha-synuclein." Hum Mol Genet **28**(1): 31-50.
Polymeropoulos, M. H., C. Lavedan, et al. (1997). "Mutation in the alpha-synuclein gene identified in families with Parkinson's disease." Science **276**(5321): 2045-2047.
Poon, H. F., M. Frasier, et al. (2005). "Mitochondrial associated metabolic proteins are selectively oxidized in A30P alpha-synuclein transgenic mice--a model of familial Parkinson's disease." Neurobiol Dis **18**(3): 492-498.
Pountney, D. L., F. Chegini, et al. (2005). "SUMO-1 marks subdomains within glial cytoplasmic inclusions of multiple system atrophy." Neurosci Lett **381**(1-2): 74-79.
Prots, I., V. Veber, et al. (2013). "alpha-Synuclein oligomers impair neuronal microtubule-kinesin interplay." J Biol Chem **288**(30): 21742-21754.
Prusiner, S. B., A. L. Woerman, et al. (2015). "Evidence for alpha-synuclein prions causing multiple system atrophy in humans with parkinsonism." Proc Natl Acad Sci U S A **112**(38): E5308-5317.
Przedborski, S., Q. Chen, et al. (2001). "Oxidative post-translational modifications of alpha-synuclein in the 1-methyl-4-phenyl-1,2,3,6-tetrahydropyridine (MPTP) mouse model of Parkinson's disease." J Neurochem **76**(2): 637-640.
Pukass, K., O. Goldbaum, et al. (2015). "Mitochondrial impairment and oxidative stress compromise autophagosomal degradation of alpha-synuclein in oligodendroglial cells." J Neurochem **135**(1): 194-205.
Pukass, K. and C. Richter-Landsberg (2014). "Oxidative stress promotes uptake, accumulation, and oligomerization of extracellular alpha-synuclein in oligodendrocytes." J Mol Neurosci **52**(3): 339-352.
Pukass, K. and C. Richter-Landsberg (2015). "Inhibition of UCH-L1 in oligodendroglial cells results in microtubule stabilization and prevents alpha-synuclein aggregate formation by activating the autophagic pathway: implications for multiple system atrophy." Front Cell Neurosci **9**: 163.

Pupyshev, A. B., M. A. Tikhonova, et al. (2019). "Therapeutic activation of autophagy by combined treatment with rapamycin and trehalose in a mouse MPTP-induced model of Parkinson's disease." Pharmacol Biochem Behav **177**: 1-11.
Puska, G., M. I. Lutz, et al. (2018). "Lysosomal response in relation to alpha-synuclein pathology differs between Parkinson's disease and multiple system atrophy." Neurobiol Dis **114**: 140-152.
Quist, A., I. Doudevski, et al. (2005). "Amyloid ion channels: a common structural link for protein-misfolding disease." Proc Natl Acad Sci U S A **102**(30): 10427-10432.
Radad, K., M. Al-Shraim, et al. (2019). "Rotenone: from modelling to implication in Parkinson's disease." Folia Neuropathol **57**(4): 317-326.
Radford, R., A. Rcom-H'cheo-Gauthier, et al. (2015). "The degree of astrocyte activation in multiple system atrophy is inversely proportional to the distance to alpha-synuclein inclusions." Mol Cell Neurosci **65**: 68-81.
Rappley, I., A. D. Gitler, et al. (2009). "Evidence that alpha-synuclein does not inhibit phospholipase D." Biochemistry **48**(5): 1077-1083.
Recasens, A., B. Dehay, et al. (2014). "Lewy body extracts from Parkinson disease brains trigger alpha-synuclein pathology and neurodegeneration in mice and monkeys." Ann Neurol **75**(3): 351-362.
Rekas, A., K. J. Ahn, et al. (2012). "The chaperone activity of alpha-synuclein: Utilizing deletion mutants to map its interaction with target proteins." Proteins **80**(5): 1316-1325.
Rey, N. L., L. Bousset, et al. (2019). "alpha-Synuclein conformational strains spread, seed and target neuronal cells differentially after injection into the olfactory bulb." Acta Neuropathol Commun **7**(1): 221.
Rey, N. L., G. H. Petit, et al. (2013). "Transfer of human alpha-synuclein from the olfactory bulb to interconnected brain regions in mice." Acta Neuropathol **126**(4): 555-573.
Rey, N. L., J. A. Steiner, et al. (2016). "Widespread transneuronal propagation of alpha-synucleinopathy triggered in olfactory bulb mimics prodromal Parkinson's disease." J Exp Med **213**(9): 1759-1778.
Reyes, J. F., N. L. Rey, et al. (2014). "Alpha-synuclein transfers from neurons to oligodendrocytes." Glia **62**(3): 387-398.
Reyes, J. F., C. Sackmann, et al. (2019). "Binding of alpha-synuclein oligomers to Cx32 facilitates protein uptake and transfer in neurons and oligodendrocytes." Acta Neuropathol **138**(1): 23-47.
Riboldi, G. M., J. A. Palma, et al. (2019). "Early-onset pathologically proven multiple system atrophy with LRRK2 G2019S mutation." Mov Disord **34**(7): 1080-1082.
Richardson, W. D., H. K. Smith, et al. (2000). "Oligodendrocyte lineage and the motor neuron connection." Glia **29**(2): 136-142.
Richter-Landsberg, C., M. Gorath, et al. (2000). "alpha-synuclein is developmentally expressed in cultured rat brain oligodendrocytes." J Neurosci Res **62**(1): 9-14.
Richter-Landsberg, C. and M. Heinrich (1996). "OLN-93: a new permanent oligodendroglia cell line derived from primary rat brain glial cultures." J Neurosci Res **45**(2): 161-173.
Rideout, H. J., K. E. Larsen, et al. (2001). "Proteasomal inhibition leads to formation of ubiquitin/alpha-synuclein-immunoreactive inclusions in PC12 cells." J Neurochem **78**(4): 899-908.
Rideout, H. J. and L. Stefanis (2002). "Proteasomal inhibition-induced inclusion formation and death in cortical neurons require transcription and ubiquitination." Mol Cell Neurosci **21**(2): 223-238.
Riedel, M., O. Goldbaum, et al. (2010). "17-AAG induces cytoplasmic alpha-synuclein aggregate clearance by induction of autophagy." PLoS One **5**(1): e8753.
Ritz, B., S. L. Rhodes, et al. (2010). "L-type calcium channel blockers and Parkinson disease in Denmark." Ann Neurol **67**(5): 600-606.
Robertson, D. C., O. Schmidt, et al. (2004). "Developmental loss and resistance to MPTP toxicity of dopaminergic neurones in substantia nigra pars compacta of gamma-synuclein, alpha-synuclein and double alpha/gamma-synuclein null mutant mice." J Neurochem **89**(5): 1126-1136.
Robotta, M., H. R. Gerding, et al. (2014). "Alpha-synuclein binds to the inner membrane of mitochondria in an alpha-helical conformation." Chembiochem **15**(17): 2499-2502.
Rocha, E. M., G. A. Smith, et al. (2015). "Sustained Systemic Glucocerebrosidase Inhibition Induces Brain alpha-Synuclein Aggregation, Microglia and Complement C1q Activation in Mice." Antioxid Redox Signal **23**(6): 550-564.
Rockenstein, E., K. Ubhi, et al. (2012). "Neuronal to oligodendroglial alpha-synuclein redistribution in a double transgenic model of multiple system atrophy." Neuroreport **23**(4): 259-264.
Rodriguez, J. A., M. I. Ivanova, et al. (2015). "Structure of the toxic core of alpha-synuclein from invisible crystals." Nature **525**(7570): 486-490.

Ronzitti, G., G. Bucci, et al. (2014). "Exogenous alpha-synuclein decreases raft partitioning of Cav2.2 channels inducing dopamine release." J Neurosci **34**(32): 10603-10615.
Rostovtseva, T. K., P. A. Gurnev, et al. (2015). "alpha-Synuclein Shows High Affinity Interaction with Voltage-dependent Anion Channel, Suggesting Mechanisms of Mitochondrial Regulation and Toxicity in Parkinson Disease." J Biol Chem **290**(30): 18467-18477.
Rott, R., R. Szargel, et al. (2011). "alpha-Synuclein fate is determined by USP9X-regulated monoubiquitination." Proc Natl Acad Sci U S A **108**(46): 18666-18671.
Rott, R., R. Szargel, et al. (2008). "Monoubiquitylation of alpha-synuclein by seven in absentia homolog (SIAH) promotes its aggregation in dopaminergic cells." J Biol Chem **283**(6): 3316-3328.
Rott, R., R. Szargel, et al. (2017). "SUMOylation and ubiquitination reciprocally regulate alpha-synuclein degradation and pathological aggregation." Proc Natl Acad Sci U S A **114**(50): 13176-13181.
Ruf, V. C., G. S. Nubling, et al. (2019). "Different Effects of alpha-Synuclein Mutants on Lipid Binding and Aggregation Detected by Single Molecule Fluorescence Spectroscopy and ThT Fluorescence-Based Measurements." ACS Chem Neurosci **10**(3): 1649-1659.
Rukenstein, A., R. E. Rydel, et al. (1991). "Multiple agents rescue PC12 cells from serum-free cell death by translation- and transcription-independent mechanisms." J Neurosci **11**(8): 2552-2563.
Runfola, M., A. De Simone, et al. (2020). "The N-terminal Acetylation of alpha-Synuclein Changes the Affinity for Lipid Membranes but not the Structural Properties of the Bound State." Sci Rep **10**(1): 204.
Rutherford, N. J., B. D. Moore, et al. (2014). "Divergent effects of the H50Q and G51D SNCA mutations on the aggregation of alpha-synuclein." J Neurochem **131**(6): 859-867.
Sacino, A. N., M. Brooks, et al. (2014). "Brain injection of alpha-synuclein induces multiple proteinopathies, gliosis, and a neuronal injury marker." J Neurosci **34**(37): 12368-12378.
Sacino, A. N., M. Brooks, et al. (2014). "Intramuscular injection of alpha-synuclein induces CNS alpha-synuclein pathology and a rapid-onset motor phenotype in transgenic mice." Proc Natl Acad Sci U S A **111**(29): 10732-10737.
Sacino, A. N., M. A. Thomas, et al. (2013). "Conformational templating of alpha-synuclein aggregates in neuronal-glial cultures." Mol Neurodegener **8**: 17.
Saftig, P. and J. Klumperman (2009). "Lysosome biogenesis and lysosomal membrane proteins: trafficking meets function." Nat Rev Mol Cell Biol **10**(9): 623-635.
Saha, A. R., J. Hill, et al. (2004). "Parkinson's disease alpha-synuclein mutations exhibit defective axonal transport in cultured neurons." J Cell Sci **117**(Pt 7): 1017-1024.
Sahu, R., S. Kaushik, et al. (2011). "Microautophagy of cytosolic proteins by late endosomes." Dev Cell **20**(1): 131-139.
Sakai, M. and K. Ogawa (1982). "Energy-dependent lysosomal wrapping mechanism (LWM) during autophagolysosome formation." Histochemistry **76**(4): 479-488.
Sardi, S. P., J. Clarke, et al. (2013). "Augmenting CNS glucocerebrosidase activity as a therapeutic strategy for parkinsonism and other Gaucher-related synucleinopathies." Proc Natl Acad Sci U S A **110**(9): 3537-3542.
Sarkar, S., S. Chigurupati, et al. (2014). "Neuroprotective effect of the chemical chaperone, trehalose in a chronic MPTP-induced Parkinson's disease mouse model." Neurotoxicology **44**: 250-262.
Sarkar, S., J. E. Davies, et al. (2007). "Trehalose, a novel mTOR-independent autophagy enhancer, accelerates the clearance of mutant huntingtin and alpha-synuclein." J Biol Chem **282**(8): 5641-5652.
Sato, H., S. Arawaka, et al. (2011). "Authentically phosphorylated alpha-synuclein at Ser129 accelerates neurodegeneration in a rat model of familial Parkinson's disease." J Neurosci **31**(46): 16884-16894.
Sato, H., T. Kato, et al. (2013). "The role of Ser129 phosphorylation of alpha-synuclein in neurodegeneration of Parkinson's disease: a review of in vivo models." Rev Neurosci **24**(2): 115-123.
Schaser, A. J., V. R. Osterberg, et al. (2019). "Alpha-synuclein is a DNA binding protein that modulates DNA repair with implications for Lewy body disorders." Sci Rep **9**(1): 10919.
Schell, H., T. Hasegawa, et al. (2009). "Nuclear and neuritic distribution of serine-129 phosphorylated alpha-synuclein in transgenic mice." Neuroscience **160**(4): 796-804.
Schmidt, F., J. Levin, et al. (2012). "Single-channel electrophysiology reveals a distinct and uniform pore complex formed by alpha-synuclein oligomers in lipid membranes." PLoS One **7**(8): e42545.
Schofield, A. V., C. Gamell, et al. (2013). "Tubulin polymerization promoting protein 1 (Tppp1) phosphorylation by Rho-associated coiled-coil kinase (rock) and cyclin-dependent kinase 1 (Cdk1) inhibits microtubule dynamics to increase cell proliferation." J Biol Chem **288**(11): 7907-7917.

Schofield, A. V., R. Steel, et al. (2012). "Rho-associated coiled-coil kinase (ROCK) protein controls microtubule dynamics in a novel signaling pathway that regulates cell migration." J Biol Chem **287**(52): 43620-43629.
Scholz, S. W., H. Houlden, et al. (2009). "SNCA variants are associated with increased risk for multiple system atrophy." Ann Neurol **65**(5): 610-614.
Schottlaender, L. V., C. Bettencourt, et al. (2016). "Coenzyme Q10 Levels Are Decreased in the Cerebellum of Multiple-System Atrophy Patients." PLoS One **11**(2): e0149557.
Schuck, S. (2020). "Microautophagy - distinct molecular mechanisms handle cargoes of many sizes." J Cell Sci **133**(17).
Schwarz, L., O. Goldbaum, et al. (2012). "Involvement of macroautophagy in multiple system atrophy and protein aggregate formation in oligodendrocytes." J Mol Neurosci **47**(2): 256-266.
Scott, D. and S. Roy (2012). "alpha-Synuclein inhibits intersynaptic vesicle mobility and maintains recycling-pool homeostasis." J Neurosci **32**(30): 10129-10135.
Seungjin Ryu, I. B. a. H. L. (2018). "Sumoylated α-synuclein translocates into the nucleus by karyopherin α6." Molecular & Cellular Toxicology **15**: 103-109.
Shahnawaz, M., A. Mukherjee, et al. (2020). "Discriminating alpha-synuclein strains in Parkinson's disease and multiple system atrophy." Nature **578**(7794): 273-277.
Sharon, R., M. S. Goldberg, et al. (2001). "alpha-Synuclein occurs in lipid-rich high molecular weight complexes, binds fatty acids, and shows homology to the fatty acid-binding proteins." Proc Natl Acad Sci U S A **98**(16): 9110-9115.
Shen, J., T. Du, et al. (2014). "alpha-Synuclein amino terminus regulates mitochondrial membrane permeability." Brain Res **1591**: 14-26.
Shin, Y., J. Klucken, et al. (2005). "The co-chaperone carboxyl terminus of Hsp70-interacting protein (CHIP) mediates alpha-synuclein degradation decisions between proteasomal and lysosomal pathways." J Biol Chem **280**(25): 23727-23734.
Shoshan-Barmatz, V. and A. Israelson (2005). "The voltage-dependent anion channel in endoplasmic/sarcoplasmic reticulum: characterization, modulation and possible function." J Membr Biol **204**(2): 57-66.
Shoshan-Barmatz, V., R. Zalk, et al. (2004). "Subcellular localization of VDAC in mitochondria and ER in the cerebellum." Biochim Biophys Acta **1657**(2-3): 105-114.
Shrivastava, A. N., V. Redeker, et al. (2015). "alpha-synuclein assemblies sequester neuronal alpha3-Na+/K+-ATPase and impair Na+ gradient." EMBO J **34**(19): 2408-2423.
Shults, C. W., E. Rockenstein, et al. (2005). "Neurological and neurodegenerative alterations in a transgenic mouse model expressing human alpha-synuclein under oligodendrocyte promoter: implications for multiple system atrophy." J Neurosci **25**(46): 10689-10699.
Shvets, E., E. Fass, et al. (2008). "The N-terminus and Phe52 residue of LC3 recruit p62/SQSTM1 into autophagosomes." J Cell Sci **121**(Pt 16): 2685-2695.
Sidhu, A., C. Wersinger, et al. (2004). "alpha-Synuclein regulation of the dopaminergic transporter: a possible role in the pathogenesis of Parkinson's disease." FEBS Lett **565**(1-3): 1-5.
Simons, M. and K. A. Nave (2015). "Oligodendrocytes: Myelination and Axonal Support." Cold Spring Harb Perspect Biol **8**(1): a020479.
Singh, A., P. Verma, et al. (2016). "Nimodipine, an L-type calcium channel blocker attenuates mitochondrial dysfunctions to protect against 1-methyl-4-phenyl-1,2,3,6-tetrahydropyridine-induced Parkinsonism in mice." Neurochem Int **99**: 221-232.
Skaanning, L. K., A. Santoro, et al. (2020). "The Non-Fibrillating N-Terminal of alpha-Synuclein Binds and Co-Fibrillates with Heparin." Biomolecules **10**(8).
Skjoerringe, T., D. M. Lundvig, et al. (2006). "P25alpha/Tubulin polymerization promoting protein expression by myelinating oligodendrocytes of the developing rat brain." J Neurochem **99**(1): 333-342.
Smith, W. W., R. L. Margolis, et al. (2005). "Alpha-synuclein phosphorylation enhances eosinophilic cytoplasmic inclusion formation in SH-SY5Y cells." J Neurosci **25**(23): 5544-5552.
Solano, S. M., D. W. Miller, et al. (2000). "Expression of alpha-synuclein, parkin, and ubiquitin carboxy-terminal hydrolase L1 mRNA in human brain: genes associated with familial Parkinson's disease." Ann Neurol **47**(2): 201-210.
Soma, H., I. Yabe, et al. (2006). "Heredity in multiple system atrophy." J Neurol Sci **240**(1-2): 107-110.
Song, Y. J., D. M. Lundvig, et al. (2007). "p25alpha relocalizes in oligodendroglia from myelin to cytoplasmic inclusions in multiple system atrophy." Am J Pathol **171**(4): 1291-1303.

Souza, J. M., G. Peluffo, et al. (2008). "Protein tyrosine nitration--functional alteration or just a biomarker?" Free Radic Biol Med **45**(4): 357-366.
Spencer, B., E. Valera, et al. (2015). "A brain-targeted, modified neurosin (kallikrein-6) reduces alpha-synuclein accumulation in a mouse model of multiple system atrophy." Mol Neurodegener **10**: 48.
Spillantini, M. G., R. A. Crowther, et al. (1998). "Filamentous alpha-synuclein inclusions link multiple system atrophy with Parkinson's disease and dementia with Lewy bodies." Neurosci Lett **251**(3): 205-208.
Spillantini, M. G., R. A. Crowther, et al. (1998). "alpha-Synuclein in filamentous inclusions of Lewy bodies from Parkinson's disease and dementia with lewy bodies." Proc Natl Acad Sci U S A **95**(11): 6469-6473.
Spillantini, M. G., M. L. Schmidt, et al. (1997). "Alpha-synuclein in Lewy bodies." Nature **388**(6645): 839-840.
Srivastava, T., R. Raj, et al. (2020). "Fast kinetics of environmentally induced alpha-synuclein aggregation mediated by structural alteration in NAC region and result in structure dependent cytotoxicity." Sci Rep **10**(1): 18412.
Stefanis, L., K. E. Larsen, et al. (2001). "Expression of A53T mutant but not wild-type alpha-synuclein in PC12 cells induces alterations of the ubiquitin-dependent degradation system, loss of dopamine release, and autophagic cell death." J Neurosci **21**(24): 9549-9560.
Stefanis, L., D. S. Park, et al. (1999). "Caspase-dependent and -independent death of camptothecin-treated embryonic cortical neurons." J Neurosci **19**(15): 6235-6247.
Stefanova, N., P. Bucke, et al. (2009). "Multiple system atrophy: an update." Lancet Neurol **8**(12): 1172-1178.
Stefanova, N., W. A. Kaufmann, et al. (2012). "Systemic proteasome inhibition triggers neurodegeneration in a transgenic mouse model expressing human alpha-synuclein under oligodendrocyte promoter: implications for multiple system atrophy." Acta Neuropathol **124**(1): 51-65.
Stefanova, N., L. Klimaschewski, et al. (2001). "Glial cell death induced by overexpression of alpha-synuclein." J Neurosci Res **65**(5): 432-438.
Stefanova, N., M. Reindl, et al. (2005). "Oxidative stress in transgenic mice with oligodendroglial alpha-synuclein overexpression replicates the characteristic neuropathology of multiple system atrophy." Am J Pathol **166**(3): 869-876.
Stefanova, N., M. Reindl, et al. (2007). "Microglial activation mediates neurodegeneration related to oligodendroglial alpha-synucleinopathy: implications for multiple system atrophy." Mov Disord **22**(15): 2196-2203.
Stefanova, N., K. Schanda, et al. (2003). "Tumor necrosis factor-alpha-induced cell death in U373 cells overexpressing alpha-synuclein." J Neurosci Res **73**(3): 334-340.
Stefanova, N. and G. K. Wenning (2016). "Review: Multiple system atrophy: emerging targets for interventional therapies." Neuropathol Appl Neurobiol **42**(1): 20-32.
Stemberger, S., W. Poewe, et al. (2010). "Targeted overexpression of human alpha-synuclein in oligodendroglia induces lesions linked to MSA-like progressive autonomic failure." Exp Neurol **224**(2): 459-464.
Stockl, M. T., N. Zijlstra, et al. (2013). "alpha-Synuclein oligomers: an amyloid pore? Insights into mechanisms of alpha-synuclein oligomer-lipid interactions." Mol Neurobiol **47**(2): 613-621.
Storrie, B. and E. A. Madden (1990). "Isolation of subcellular organelles." Methods Enzymol **182**: 203-225.
Subramaniam, S. R., L. Vergnes, et al. (2014). "Region specific mitochondrial impairment in mice with widespread overexpression of alpha-synuclein." Neurobiol Dis **70**: 204-213.
Sugeno, N., A. Takeda, et al. (2008). "Serine 129 phosphorylation of alpha-synuclein induces unfolded protein response-mediated cell death." J Biol Chem **283**(34): 23179-23188.
Sun, Q. and T. C. Gamblin (2009). "Pseudohyperphosphorylation causing AD-like changes in tau has significant effects on its polymerization." Biochemistry **48**(25): 6002-6011.
Sun, Z., Y. Ohta, et al. (2016). "New susceptible variant of COQ2 gene in Japanese patients with sporadic multiple system atrophy." Neurol Genet **2**(2): e54.
Sung, J. Y., J. Kim, et al. (2001). "Induction of neuronal cell death by Rab5A-dependent endocytosis of alpha-synuclein." J Biol Chem **276**(29): 27441-27448.
Swant, J., J. S. Goodwin, et al. (2011). "alpha-Synuclein stimulates a dopamine transporter-dependent chloride current and modulates the activity of the transporter." J Biol Chem **286**(51): 43933-43943.
Taguchi, K., Y. Watanabe, et al. (2016). "Brain region-dependent differential expression of alpha-synuclein." J Comp Neurol **524**(6): 1236-1258.

Taguchi, K., Y. Watanabe, et al. (2019). "Expression of alpha-synuclein is regulated in a neuronal cell type-dependent manner." Anat Sci Int **94**(1): 11-22.
Takahashi, M., K. Tomizawa, et al. (1993). "A brain-specific protein p25 is localized and associated with oligodendrocytes, neuropil, and fiber-like structures of the CA3 hippocampal region in the rat brain." J Neurochem **60**(1): 228-235.
Takahashi, T., H. Yamashita, et al. (2002). "Tyrosine 125 of alpha-synuclein plays a critical role for dimerization following nitrative stress." Brain Res **938**(1-2): 73-80.
Takeda, A., N. Arai, et al. (1997). "Tau immunoreactivity in glial cytoplasmic inclusions in multiple system atrophy." Neurosci Lett **234**(1): 63-66.
Takeda, A., N. Arai, et al. (1997). "Neuronal inclusions in the dentate fascia in patients with multiple system atrophy." Neurosci Lett **227**(3): 157-160.
Tanaka, Y., S. Engelender, et al. (2001). "Inducible expression of mutant alpha-synuclein decreases proteasome activity and increases sensitivity to mitochondria-dependent apoptosis." Hum Mol Genet **10**(9): 919-926.
Tang, Y., U. Das, et al. (2012). "The slow axonal transport of alpha-synuclein--mechanistic commonalities amongst diverse cytosolic cargoes." Cytoskeleton (Hoboken) **69**(7): 506-513.
Tanida, I., N. Minematsu-Ikeguchi, et al. (2005). "Lysosomal turnover, but not a cellular level, of endogenous LC3 is a marker for autophagy." Autophagy **1**(2): 84-91.
Tanji, K., S. Odagiri, et al. (2013). "Alteration of autophagosomal proteins in the brain of multiple system atrophy." Neurobiol Dis **49**: 190-198.
Terada, M., G. Suzuki, et al. (2018). "The effect of truncation on prion-like properties of alpha-synuclein." J Biol Chem **293**(36): 13910-13920.
Terni, B., M. J. Rey, et al. (2007). "Mutant ubiquitin and p62 immunoreactivity in cases of combined multiple system atrophy and Alzheimer's disease." Acta Neuropathol **113**(4): 403-416.
Thayanidhi, N., J. R. Helm, et al. (2010). "Alpha-synuclein delays endoplasmic reticulum (ER)-to-Golgi transport in mammalian cells by antagonizing ER/Golgi SNAREs." Mol Biol Cell **21**(11): 1850-1863.
Tieu, K. (2011). "A guide to neurotoxic animal models of Parkinson's disease." Cold Spring Harb Perspect Med **1**(1): a009316.
Tirian, L., E. Hlavanda, et al. (2003). "TPPP/p25 promotes tubulin assemblies and blocks mitotic spindle formation." Proc Natl Acad Sci U S A **100**(24): 13976-13981.
Tofaris, G. K., P. Garcia Reitbock, et al. (2006). "Pathological changes in dopaminergic nerve cells of the substantia nigra and olfactory bulb in mice transgenic for truncated human alpha-synuclein(1-120): implications for Lewy body disorders." J Neurosci **26**(15): 3942-3950.
Tofaris, G. K., H. T. Kim, et al. (2011). "Ubiquitin ligase Nedd4 promotes alpha-synuclein degradation by the endosomal-lysosomal pathway." Proc Natl Acad Sci U S A **108**(41): 17004-17009.
Tofaris, G. K., R. Layfield, et al. (2001). "alpha-synuclein metabolism and aggregation is linked to ubiquitin-independent degradation by the proteasome." FEBS Lett **509**(1): 22-26.
Tofaris, G. K., A. Razzaq, et al. (2003). "Ubiquitination of alpha-synuclein in Lewy bodies is a pathological event not associated with impairment of proteasome function." J Biol Chem **278**(45): 44405-44411.
Trexler, A. J. and E. Rhoades (2009). "Alpha-synuclein binds large unilamellar vesicles as an extended helix." Biochemistry **48**(11): 2304-2306.
Trojanowski, J. Q. and T. Revesz (2007). "Proposed neuropathological criteria for the post mortem diagnosis of multiple system atrophy." Neuropathol Appl Neurobiol **33**(6): 615-620.
Troy, C. M., L. Stefanis, et al. (1997). "Nedd2 is required for apoptosis after trophic factor withdrawal, but not superoxide dismutase (SOD1) downregulation, in sympathetic neurons and PC12 cells." J Neurosci **17**(6): 1911-1918.
Tsigelny, I. F., Y. Sharikov, et al. (2015). "Molecular determinants of alpha-synuclein mutants' oligomerization and membrane interactions." ACS Chem Neurosci **6**(3): 403-416.
Tsigelny, I. F., Y. Sharikov, et al. (2012). "Role of alpha-synuclein penetration into the membrane in the mechanisms of oligomer pore formation." FEBS J **279**(6): 1000-1013.
Tsuboi, K., J. J. Grzesiak, et al. (2005). "Alpha-synuclein overexpression in oligodendrocytic cells results in impaired adhesion to fibronectin and cell death." Mol Cell Neurosci **29**(2): 259-268.
Ubhi, K., E. Rockenstein, et al. (2010). "Neurodegeneration in a transgenic mouse model of multiple system atrophy is associated with altered expression of oligodendroglial-derived neurotrophic factors." J Neurosci **30**(18): 6236-6246.

Uemura, N., M. T. Uemura, et al. (2019). "Slow Progressive Accumulation of Oligodendroglial Alpha-Synuclein (alpha-Syn) Pathology in Synthetic alpha-Syn Fibril-Induced Mouse Models of Synucleinopathy." J Neuropathol Exp Neurol **78**(10): 877-890.
Ulusoy, A., F. Febbraro, et al. (2010). "Co-expression of C-terminal truncated alpha-synuclein enhances full-length alpha-synuclein-induced pathology." Eur J Neurosci **32**(3): 409-422.
Uversky, V. N., J. Li, et al. (2001). "Evidence for a partially folded intermediate in alpha-synuclein fibril formation." J Biol Chem **276**(14): 10737-10744.
Valdinocci, D., G. D. Grant, et al. (2018). "Epothilone D inhibits microglia-mediated spread of alpha-synuclein aggregates." Mol Cell Neurosci **89**: 80-94.
Vanacore, N., V. Bonifati, et al. (2001). "Epidemiology of multiple system atrophy. ESGAP Consortium. European Study Group on Atypical Parkinsonisms." Neurol Sci **22**(1): 97-99.
Vargas, K. J., S. Makani, et al. (2014). "Synucleins regulate the kinetics of synaptic vesicle endocytosis." J Neurosci **34**(28): 9364-9376.
Vekrellis, K., M. Xilouri, et al. (2009). "Inducible over-expression of wild type alpha-synuclein in human neuronal cells leads to caspase-dependent non-apoptotic death." J Neurochem **109**(5): 1348-1362.
Verhoef, L. G., K. Lindsten, et al. (2002). "Aggregate formation inhibits proteasomal degradation of polyglutamine proteins." Hum Mol Genet **11**(22): 2689-2700.
Vidal, J. S., M. Vidailhet, et al. (2008). "Risk factors of multiple system atrophy: a case-control study in French patients." Mov Disord **23**(6): 797-803.
Vila, M., S. Vukosavic, et al. (2000). "Alpha-synuclein up-regulation in substantia nigra dopaminergic neurons following administration of the parkinsonian toxin MPTP." J Neurochem **74**(2): 721-729.
Vilarino-Guell, C., A. I. Soto-Ortolaza, et al. (2011). "MAPT H1 haplotype is a risk factor for essential tremor and multiple system atrophy." Neurology **76**(7): 670-672.
Vinueza-Gavilanes, R., I. Inigo-Marco, et al. (2020). "N-terminal acetylation mutants affect alpha-synuclein stability, protein levels and neuronal toxicity." Neurobiol Dis **137**: 104781.
Visanji, N. P., P. L. Brooks, et al. (2013). "The prion hypothesis in Parkinson's disease: Braak to the future." Acta Neuropathol Commun **1**: 2.
Vogiatzi, T., M. Xilouri, et al. (2008). "Wild type alpha-synuclein is degraded by chaperone-mediated autophagy and macroautophagy in neuronal cells." J Biol Chem **283**(35): 23542-23556.
Volles, M. J. and P. T. Lansbury, Jr. (2002). "Vesicle permeabilization by protofibrillar alpha-synuclein is sensitive to Parkinson's disease-linked mutations and occurs by a pore-like mechanism." Biochemistry **41**(14): 4595-4602.
Volpicelli-Daley, L. A., K. C. Luk, et al. (2014). "Addition of exogenous alpha-synuclein preformed fibrils to primary neuronal cultures to seed recruitment of endogenous alpha-synuclein to Lewy body and Lewy neurite-like aggregates." Nat Protoc **9**(9): 2135-2146.
Volpicelli-Daley, L. A., K. C. Luk, et al. (2011). "Exogenous alpha-synuclein fibrils induce Lewy body pathology leading to synaptic dysfunction and neuron death." Neuron **72**(1): 57-71.
Wakabayashi, K., S. Hayashi, et al. (1998). "Accumulation of alpha-synuclein/NACP is a cytopathological feature common to Lewy body disease and multiple system atrophy." Acta Neuropathol **96**(5): 445-452.
Wakabayashi, K. and H. Takahashi (2006). "Cellular pathology in multiple system atrophy." Neuropathology **26**(4): 338-345.
Wakabayashi, K., M. Yoshimoto, et al. (1998). "Alpha-synuclein immunoreactivity in glial cytoplasmic inclusions in multiple system atrophy." Neurosci Lett **249**(2-3): 180-182.
Walker, D. G., L. F. Lue, et al. (2013). "Changes in properties of serine 129 phosphorylated alpha-synuclein with progression of Lewy-type histopathology in human brains." Exp Neurol **240**: 190-204.
Wang, M., S. Wey, et al. (2009). "Role of the unfolded protein response regulator GRP78/BiP in development, cancer, and neurological disorders." Antioxid Redox Signal **11**(9): 2307-2316.
Wang, S., F. Yang, et al. (2017). "Quantitative proteomics identifies altered O-GlcNAcylation of structural, synaptic and memory-associated proteins in Alzheimer's disease." J Pathol **243**(1): 78-88.
Wang, W., L. T. Nguyen, et al. (2016). "Caspase-1 causes truncation and aggregation of the Parkinson's disease-associated protein alpha-synuclein." Proc Natl Acad Sci U S A **113**(34): 9587-9592.
Wang, W., I. Perovic, et al. (2011). "A soluble alpha-synuclein construct forms a dynamic tetramer." Proc Natl Acad Sci U S A **108**(43): 17797-17802.
Wang, Z., K. Park, et al. (2009). "Site-specific GlcNAcylation of human erythrocyte proteins: potential biomarker(s) for diabetes." Diabetes **58**(2): 309-317.

Wang, Z., N. D. Udeshi, et al. (2010). "Enrichment and site mapping of O-linked N-acetylglucosamine by a combination of chemical/enzymatic tagging, photochemical cleavage, and electron transfer dissociation mass spectrometry." Mol Cell Proteomics **9**(1): 153-160.
Watts, J. C., K. Giles, et al. (2013). "Transmission of multiple system atrophy prions to transgenic mice." Proc Natl Acad Sci U S A **110**(48): 19555-19560.
Webb, J. L., B. Ravikumar, et al. (2003). "Alpha-Synuclein is degraded by both autophagy and the proteasome." J Biol Chem **278**(27): 25009-25013.
Weetman, J., M. B. Wong, et al. (2013). "Increased SUMO-1 expression in the unilateral rotenone-lesioned mouse model of Parkinson's disease." Neurosci Lett **544**: 119-124.
Weinreb, P. H., W. Zhen, et al. (1996). "NACP, a protein implicated in Alzheimer's disease and learning, is natively unfolded." Biochemistry **35**(43): 13709-13715.
Wen, X. D., H. F. Li, et al. (2015). "Mutation Analysis of COQ2 in Chinese Patients with Cerebellar Subtype of Multiple System Atrophy." CNS Neurosci Ther **21**(8): 626-630.
Wenning, G. K., N. Stefanova, et al. (2008). "Multiple system atrophy: a primary oligodendrogliopathy." Ann Neurol **64**(3): 239-246.
Wenning, G. K., S. Wagner, et al. (1993). "Multiple system atrophy: sporadic or familial?" Lancet **342**(8872): 681.
Wilkins, A., H. Majed, et al. (2003). "Oligodendrocytes promote neuronal survival and axonal length by distinct intracellular mechanisms: a novel role for oligodendrocyte-derived glial cell line-derived neurotrophic factor." J Neurosci **23**(12): 4967-4974.
Winslow, A. R., C. W. Chen, et al. (2010). "alpha-Synuclein impairs macroautophagy: implications for Parkinson's disease." J Cell Biol **190**(6): 1023-1037.
Withers, G. S., J. M. George, et al. (1997). "Delayed localization of synelfin (synuclein, NACP) to presynaptic terminals in cultured rat hippocampal neurons." Brain Res Dev Brain Res **99**(1): 87-94.
Woerman, A. L., S. A. Kazmi, et al. (2018). "MSA prions exhibit remarkable stability and resistance to inactivation." Acta Neuropathol **135**(1): 49-63.
Woerman, A. L., A. Oehler, et al. (2019). "Multiple system atrophy prions retain strain specificity after serial propagation in two different Tg(SNCA*A53T) mouse lines." Acta Neuropathol **137**(3): 437-454.
Woerman, A. L., J. Stohr, et al. (2015). "Propagation of prions causing synucleinopathies in cultured cells." Proc Natl Acad Sci U S A **112**(35): E4949-4958.
Woerman, A. L., J. C. Watts, et al. (2018). "alpha-Synuclein: Multiple System Atrophy Prions." Cold Spring Harb Perspect Med **8**(7).
Wong, J. H., G. M. Halliday, et al. (2014). "Exploring myelin dysfunction in multiple system atrophy." Exp Neurobiol **23**(4): 337-344.
Wong, M. B., J. Goodwin, et al. (2013). "SUMO-1 is associated with a subset of lysosomes in glial protein aggregate diseases." Neurotox Res **23**(1): 1-21.
Wood, S. J., J. Wypych, et al. (1999). "alpha-synuclein fibrillogenesis is nucleation-dependent. Implications for the pathogenesis of Parkinson's disease." J Biol Chem **274**(28): 19509-19512.
Wu, B., Q. Liu, et al. (2011). "Phosphorylation of alpha-synuclein upregulates tyrosine hydroxylase activity in MN9D cells." Acta Histochem **113**(1): 32-35.
Wu, Q., H. Takano, et al. (2019). "alpha-Synuclein (alphaSyn) Preformed Fibrils Induce Endogenous alphaSyn Aggregation, Compromise Synaptic Activity and Enhance Synapse Loss in Cultured Excitatory Hippocampal Neurons." J Neurosci **39**(26): 5080-5094.
Wu, Y., Y. Jin, et al. (2020). "p62/SQSTM1 accumulation due to degradation inhibition and transcriptional activation plays a critical role in silica nanoparticle-induced airway inflammation via NF-kappaB activation." J Nanobiotechnology **18**(1): 77.
Wu, Y., X. Li, et al. (2011). "Resveratrol-activated AMPK/SIRT1/autophagy in cellular models of Parkinson's disease." Neurosignals **19**(3): 163-174.
Wullner, U., M. Abele, et al. (2004). "Probable multiple system atrophy in a German family." J Neurol Neurosurg Psychiatry **75**(6): 924-925.
Wullner, U., I. Schmitt, et al. (2009). "Definite multiple system atrophy in a German family." J Neurol Neurosurg Psychiatry **80**(4): 449-450.
Wuytack, F., L. Raeymaekers, et al. (2003). "PMR1/SPCA Ca2+ pumps and the role of the Golgi apparatus as a Ca2+ store." Pflugers Arch **446**(2): 148-153.
Xilouri, M., O. R. Brekk, et al. (2013). "Boosting chaperone-mediated autophagy in vivo mitigates alpha-synuclein-induced neurodegeneration." Brain **136**(Pt 7): 2130-2146.
Xilouri, M., O. R. Brekk, et al. (2016). "Impairment of chaperone-mediated autophagy induces dopaminergic neurodegeneration in rats." Autophagy **12**(11): 2230-2247.

Xilouri, M., O. R. Brekk, et al. (2013). "alpha-Synuclein and protein degradation systems: a reciprocal relationship." Mol Neurobiol **47**(2): 537-551.
Xilouri, M., E. Kyratzi, et al. (2012). "Selective neuroprotective effects of the S18Y polymorphic variant of UCH-L1 in the dopaminergic system." Hum Mol Genet **21**(4): 874-889.
Xiong, B., A. Li, et al. (2017). "Precise Cerebral Vascular Atlas in Stereotaxic Coordinates of Whole Mouse Brain." Front Neuroanat **11**: 128.
Xu, Y., Y. Deng, et al. (2015). "The phosphorylation of alpha-synuclein: development and implication for the mechanism and therapy of the Parkinson's disease." J Neurochem **135**(1): 4-18.
Yagi-Utsumi, M., T. Satoh, et al. (2015). "Structural basis of redox-dependent substrate binding of protein disulfide isomerase." Sci Rep **5**: 13909.
Yamada, K. and T. Iwatsubo (2018). "Extracellular alpha-synuclein levels are regulated by neuronal activity." Mol Neurodegener **13**(1): 9.
Yan, J. Q., Y. H. Yuan, et al. (2014). "Overexpression of human E46K mutant alpha-synuclein impairs macroautophagy via inactivation of JNK1-Bcl-2 pathway." Mol Neurobiol **50**(2): 685-701.
Yang, X., R. An, et al. (2016). "Mutational analysis of CHCHD2 in Chinese patients with multiple system atrophy and amyotrophic lateral sclerosis." J Neurol Sci **368**: 389-391.
Yang, Z. and D. J. Klionsky (2009). "An overview of the molecular mechanism of autophagy." Curr Top Microbiol Immunol **335**: 1-32.
Yazawa, I., B. I. Giasson, et al. (2005). "Mouse model of multiple system atrophy alpha-synuclein expression in oligodendrocytes causes glial and neuronal degeneration." Neuron **45**(6): 847-859.
Yin, G., T. Lopes da Fonseca, et al. (2014). "alpha-Synuclein interacts with the switch region of Rab8a in a Ser129 phosphorylation-dependent manner." Neurobiol Dis **70**: 149-161.
Yoon, Y. S., W. J. Ahn, et al. (2021). "Alpha-Synuclein Inclusion Formation in Human Oligodendrocytes." Biomol Ther (Seoul) **29**(1): 83-89.
Yoshida, M. (2007). "Multiple system atrophy: alpha-synuclein and neuronal degeneration." Neuropathology **27**(5): 484-493.
Yoshii, S. R. and N. Mizushima (2017). "Monitoring and Measuring Autophagy." Int J Mol Sci **18**(9).
Yu, S., X. Li, et al. (2007). "Extensive nuclear localization of alpha-synuclein in normal rat brain neurons revealed by a novel monoclonal antibody." Neuroscience **145**(2): 539-555.
Yu, S., X. Zuo, et al. (2004). "Inhibition of tyrosine hydroxylase expression in alpha-synuclein-transfected dopaminergic neuronal cells." Neurosci Lett **367**(1): 34-39.
Yu, Z., X. Xu, et al. (2010). "Nitrated alpha-synuclein induces the loss of dopaminergic neurons in the substantia nigra of rats." PLoS One **5**(4): e9956.
Zakharov, S. D., J. D. Hulleman, et al. (2007). "Helical alpha-synuclein forms highly conductive ion channels." Biochemistry **46**(50): 14369-14379.
Zaltieri, M., J. Grigoletto, et al. (2015). "alpha-synuclein and synapsin III cooperatively regulate synaptic function in dopamine neurons." J Cell Sci **128**(13): 2231-2243.
Zarranz, J. J., J. Alegre, et al. (2004). "The new mutation, E46K, of alpha-synuclein causes Parkinson and Lewy body dementia." Ann Neurol **55**(2): 164-173.
Zavodszky, E., M. N. Seaman, et al. (2014). "Mutation in VPS35 associated with Parkinson's disease impairs WASH complex association and inhibits autophagy." Nat Commun **5**: 3828.
Zhang, C. and A. M. Cuervo (2008). "Restoration of chaperone-mediated autophagy in aging liver improves cellular maintenance and hepatic function." Nat Med **14**(9): 959-965.
Zhang, J., H. Lei, et al. (2017). "Enzymatic O-GlcNAcylation of alpha-synuclein reduces aggregation and increases SDS-resistant soluble oligomers." Neurosci Lett **655**: 90-94.
Zhang, L., C. Zhang, et al. (2008). "Semi-quantitative analysis of alpha-synuclein in subcellular pools of rat brain neurons: an immunogold electron microscopic study using a C-terminal specific monoclonal antibody." Brain Res **1244**: 40-52.
Zhou, X., C. Wang, et al. (2018). "Association of TNF-alpha rs1799964 and IL-1beta rs16944 polymorphisms with multiple system atrophy in Chinese Han population." Int J Neurosci **128**(8): 761-764.
Zhu, M. and A. L. Fink (2003). "Lipid binding inhibits alpha-synuclein fibril formation." J Biol Chem **278**(19): 16873-16877.
Zondler, L., M. Kostka, et al. (2017). "Proteasome impairment by alpha-synuclein." PLoS One **12**(9): e0184040.
Zotter, A., A. Bodor, et al. (2011). "Disordered TPPP/p25 binds GTP and displays Mg2+-dependent GTPase activity." FEBS Lett **585**(5): 803-808.

VIII. APPENDIX

Published work:

1. Endogenous oligodendroglial alpha-synuclein and TPPP/p25α orchestrate alpha-synuclein pathology in experimental multiple system atrophy models.
   Mavroeidi P, Arvanitaki F, Karakitsou AK, Vetsi M, Kloukina I, Zweckstetter M, Giller K, Becker S, Sorrentino ZA, Giasson BI, Jensen PH, Stefanis L, Xilouri M.
   Acta Neuropathol. 2019 Sep;138(3):415-441. doi: 10.1007/s00401-019-02014-y. Epub 2019 Apr 22.

2. In Search of Effective Treatments Targeting α-Synuclein Toxicity in Synucleinopathies: Pros and Cons.
   Fouka M, Mavroeidi P, Tsaka G, Xilouri M.
   Front Cell Dev Biol. 2020 Sep 4;8:559791. doi: 10.3389/fcell.2020.559791. eCollection 2020.

3. Neurons and Glia Interplay in α-Synucleinopathies.
   Mavroeidi P, Xilouri M.
   Int J Mol Sci. 2021 May 8;22(9):4994. doi: 10.3390/ijms22094994.

Submitted-under revisions:

1. Autophagy Mediates the Clearance of Oligodendroglial alpha-Synuclein and TPPP/P25A in Multiple System Atrophy Models
   Panagiota Mavroeidi, Fedra Arvanitaki, Maria Vetsi, Stefan Becker, Dimitrios Vlachakis, Poul Henning Jensen, Leonidas Stefanis and Maria Xilouri
   Autophagy

Participation in international conferences:

1. Panagiota Mavroeidi, Anita Karakitsou, P.H. Jensen, M. Zweckstetter, L. Stefanis and Maria Xilouri, “Unravelling the mechanism of alpha-synuclein seeding in oligodendrocytes”, Interational meeting entitled "20 years of alpha- synuclein in Parkinson's Disease & related synucleinopathies: from the bedside to the bench and back to the patient', Semptember 7th-10th 2017, Mare Nostrum Hotel, Vravrona, Attiki.

2. Panagiota Mavroeidi, Fedra Arvanitaki, Anastasia-Kiriaki Karakitsou, Maria Vetsi, Ismini Kloukina, Markus Zweckstetter, Stefan Becker, Zachary A. Sorrentino, Benoit I. Giasson, Poul Henning Jensen, Leonidas Stefanis and Maria Xilouri, “Endogenous Oligodendroglial alpha-Synuclein and TPPP/p25α Orchestrate alpha-Synuclein Pathology in Multiple System Atrophy”, FENS Regional Meeting, Belgrade, Serbia, July 10-13, 2019

3. Panagiota Mavroeidi, Fedra Arvanitaki, Anastasia-Kiriaki Karakitsou, Maria Vetsi, Ismini Kloukina, Markus Zweckstetter, Stefan Becker, Zachary A. Sorrentino, Benoit I. Giasson, Poul Henning Jensen, Leonidas Stefanis and Maria Xilouri, “Endogenous Oligodendroglial alpha-Synuclein and TPPP/p25α Orchestrate alpha-Synuclein Pathology in Multiple System Atrophy”, "Synuclein Meeting 2019: Where we are and where we need to go", Porto, Portugal, September 1-4, 2019

Acta Neuropathologica
https://doi.org/10.1007/s00401-019-02014-y

ORIGINAL PAPER

Endogenous oligodendroglial alpha-synuclein and TPPP/p25α orchestrate alpha-synuclein pathology in experimental multiple system atrophy models

Panagiota Mavroeidi[1] · Fedra Arvanitaki[1] · Anastasia-Kiriaki Karakitsou[1] · Maria Vetsi[1] · Ismini Kloukina[2] · Markus Zweckstetter[3,4] · Karin Giller[4] · Stefan Becker[4] · Zachary A. Sorrentino[5,6] · Benoit I. Giasson[5,6,7] · Poul Henning Jensen[8] · Leonidas Stefanis[1,9] · Maria Xilouri[1]

Received: 16 December 2018 / Revised: 3 April 2019 / Accepted: 15 April 2019
© Springer-Verlag GmbH Germany, part of Springer Nature 2019

Abstract

Multiple system atrophy (MSA) is characterized by the presence of distinctive glial cytoplasmic inclusions (GCIs) within oligodendrocytes that contain the neuronal protein alpha-synuclein (aSyn) and the oligodendroglia-specific phosphoprotein TPPP/p25α. However, the role of oligodendroglial aSyn and p25α in the formation of aSyn-rich GCIs remains unclear. To address this conundrum, we have applied human aSyn (haSyn) pre-formed fibrils (PFFs) to rat wild-type (WT)-, haSyn-, or p25α-overexpressing oligodendroglial cells and to primary differentiated oligodendrocytes derived from WT, knockout (KO)-aSyn, and PLP-haSyn-transgenic mice. HaSyn PFFs are readily taken up by oligodendroglial cells and can recruit minute amounts of endogenous aSyn into the formation of insoluble, highly aggregated, pathological assemblies. The overexpression of haSyn or p25α accelerates the recruitment of endogenous protein and the generation of such aberrant species. In haSyn PFF-treated primary oligodendrocytes, the microtubule and myelin networks are disrupted, thus recapitulating a pathological hallmark of MSA, in a manner totally dependent upon the seeding of endogenous aSyn. Furthermore, using oligodendroglial and primary cortical cultures, we demonstrated that pathology-related S129 aSyn phosphorylation depends on aSyn and p25α protein load and may involve different aSyn "strains" present in oligodendroglial and neuronal synucleinopathies. Importantly, this hypothesis was further supported by data obtained from human post-mortem brain material derived from patients with MSA and dementia with Lewy bodies. Finally, delivery of haSyn PFFs into the mouse brain led to the formation of aberrant aSyn forms, including the endogenous protein, within oligodendroglia and evoked myelin decompaction in WT mice, but not in KO-aSyn mice. This line of research highlights the role of endogenous aSyn and p25α in the formation of pathological aSyn assemblies in oligodendrocytes and provides in vivo evidence of the contribution of oligodendroglial aSyn in the establishment of aSyn pathology in MSA.

Keywords Alpha-synuclein · Multiple system atrophy · Myelin · Oligodendrocytes · Seeding · Tubulin polymerization promoting protein

Introduction

Multiple system atrophy (MSA) is a fatal, adult-onset, sporadic neurodegenerative disorder of uncertain etiology with no effective treatment [14]. Neuropathologically, MSA is characterized by the accumulation of the neuronal presynaptic protein alpha-synuclein (aSyn) within oligodendrocytes, the myelin-producing cells of the central nervous system, forming glial cytoplasmic inclusions (GCIs), which represent the main histopathological hallmark of MSA [67, 73]. The origin of aSyn in oligodendrocytes of MSA patients is ambiguous, since it has been proposed that mature

Electronic supplementary material The online version of this article (https://doi.org/10.1007/s00401-019-02014-y) contains supplementary material, which is available to authorized users.

✉ Maria Xilouri
mxilouri@bioacademy.gr

Extended author information available on the last page of the article

Published online: 22 April 2019

oligodendrocytes do not normally express this protein [9]. Some reports have shown the expression of *SNCA* (the gene encoding aSyn) mRNA in oligodendrocytes, suggesting the presence of the endogenous oligodendrocytic protein [9, 21, 56]. However, other studies have failed to detect oligodendroglial *SNCA* mRNA expression in the brains of MSA patients [35, 60], or in studies where *SNCA* mRNA was detected, no differences were observed between controls and MSA patients [3, 19]. Moreover, in vitro [13, 21, 23, 24, 48, 49] and in vivo studies [55, 58] demonstrated that exogenous recombinant or neuronally derived aSyn can be taken up by oligodendroglial cell lines, suggesting the neuron-to-glia transfer of aSyn. Recent evidence suggests that the "prion-like" transmission of misfolded aSyn may contribute to MSA disease risk [76]. Yet, little is known regarding the mechanisms underlying the selective transmission of aSyn pathology in oligodendrocytes of MSA brains.

Beyond aSyn, the oligodendroglial-specific phosphoprotein p25α (tubulin polymerization promoting protein, TPPP) is a major component of GCIs and facilitates aSyn aggregation in vitro [18, 25, 28, 61]. Under physiological conditions, p25α interacts with tubulin and myelin basic protein (MBP), thereby facilitating myelination [61]. In MSA, p25α is redistributed from the myelin sheath to the abnormally expanded oligodendroglial cell bodies, an event followed by a reduction of total MBP levels, myelin fragmentation, and accumulation of abnormal aSyn [61]. However, the role of p25α in the transmission and seeding of aSyn pathology has not been addressed.

In the present study, by utilizing pre-formed fibrils (PFFs) of human recombinant aSyn as seeds of pathological aSyn, we show that endogenous oligodendroglial aSyn, which is almost undetectable at baseline, is a major component of the misfolded aSyn assemblies formed in immortalized oligodendroglial cell lines and primary oligodendroglial cultures. More importantly, we demonstrate that endogenous aSyn plays a central role in the impairment of the myelin network in the living mouse brain, further highlighting the contribution of endogenous aSyn to the establishment of the pathology present in MSA brains. Finally, our study supports a central role for p25α in the seeding of misfolded aSyn and in the formation of pathological aSyn conformations, which are considered crucial events underlying the pathology observed in MSA brains.

Methods

Cell culture and treatments

The stable cell line OLN-p25α was established essentially as the OLN-AS7 line [51] by transfecting OLN-93 oligodendroglial cells with a pcDNA3.1 zeo(−)human p25α vector. The parental immortalized OLN-93 cell line (control cells) was derived from primary Wistar rat brain glial cultures [57]. All cells were grown in Dulbecco's modified Eagle's medium (D6429; Gibco, Invitrogen, Carlsbad, CA, USA) supplemented with 10% fetal bovine serum (10,270; Gibco, Invitrogen, Carlsbad, CA, USA), 50 U/mL penicillin, and 50 µg/mL streptomycin. OLN-AS7 and OLN-p25α cells were maintained in 50 µg/mL Zeocin (R25001; Thermo Fisher Scientific, Waltham, MA, USA). The pcDNA3.1 zeo(−) plasmid expressing human p25α was generated as described previously [68]. Primary oligodendroglial progenitor cells derived from mixed glial cultures were prepared from P0 to P3 neonatal knockout (KO)-aSyn, wild-type (WT)-aSyn or PLP-human aSyn (haSyn) transgenic mice, as described previously [32], and cultured in SATO medium [5]. Cultures of rat (embryonic day 18) cortical neurons were prepared as described previously [78] and maintained in Neurobasal medium (Invitrogen, Carlsbad, CA, USA), supplemented with B27 supplement (Invitrogen, Carlsbad, CA, USA), L-glutamine (0.5 mM), and penicillin/streptomycin (1%). A detailed description of the conditions utilized for plating the different cell types, transfections, and treatments are provided in Supplementary Methods (Online Resource 16).

Preparation of haSyn PFFs

HaSyn fibrils were generated as described [6, 22], with several modifications. Shortly, before aggregation, monomeric aSyn in 50 mM HEPES (pH 7.4,) 100 mM NaCl, and 0.02% NaN_3 was centrifuged for 1 h at 84.000×*g*. The supernatant was ultra-filtrated (0.2 µm) and adjusted to 0.27 mM. Aggregation was performed for 12 days at 37 °C. Fibrils were collected by ultracentrifugation, washed twice with phosphate-buffered saline (PBS), pH 7.3, at room temperature, and quantified by subtracting the amount of monomeric aSyn protein in the supernatant from the total protein used for aggregation. PFFs were resuspended in PBS (pH 7.3) at a final concentration of 4.5 mg/mL and a working stock solution was prepared at 1 mg/mL. The cells were incubated with 0.5–3 µg non-sonicated haSyn PFFs (as described above) or PBS as a control for the indicated time points and were either processed for confocal microscopy or lysed and collected for western blot analysis as described below.

Subcellular fractionation and western immunoblotting

OLN cells incubated with haSyn PFFs for various time points were washed twice in ice-cold PBS and sequentially fractionated using buffers with increasing extraction strength, as described in Supplementary Methods (Online Resource 16). Primary oligodendroglial cells were lysed

using RIPA buffer (150 mM NaCl, 25 mM Tris pH 7.6, 0.5% sodium deoxycholate, 0.1% SDS, 1% NP-40), left on ice for ~ 30 min, and centrifuged at 10,000×*g* for 15 min at 4 °C. Western blot analysis of protein extracts was performed as described previously [70] and the antibodies used are shown in Supplementary Table 2 (Online Resource 11). The intensity of each immunoreactive band was estimated by densitometric quantification using ImageJ software.

Immunocytochemistry and confocal microscopy

OLN cell lines and primary mouse oligodendrocyte cultures cultured on poly-D-lysine-coated glass coverslips were treated with haSyn PFFs at the indicated time points. The cells were fixed with 4% paraformaldehyde for 40 min, blocked in 10% normal goat serum containing 0.4% Triton X-100 for 1 h at room temperature, and incubated with primary antibodies overnight at 4 °C. The primary and fluorescent secondary antibodies used are shown in Supplementary Table 2 (Online Resource 11). Images were obtained using a Leica TCS SP5 confocal microscope combined with a dual (tandem) scanner. All confocal images were obtained under equivalent conditions of laser power, pinhole size, gain, and offset settings between the groups. For the transient transfections, quantifications were performed with the Imaris software suite (v7.7.2, Bitplane AG, Zurich, Switzerland), using a static set of parameters to isolate either GFP^+ or $p25\alpha^+$ cell profiles, and then masking the channel containing the human aSyn (LB509 antibody), oxidized/nitrated aSyn (SYN-303 antibody) or the rodent aSyn (D37A6 antibody) signal using said profiles. The masking of the GFP^+ or $p25\alpha^+$ signal was based on fluorescent intensity. ImageJ (v2.0.0) software was used to quantify relative protein levels expressed as mean fluorescence intensity or % area coverage, normalized to the total number of cells/field (the number of DAPI-stained nuclei).

Transmission electron microscopy (EM)

Negative staining

Specimens were prepared by adsorbing 5-µLdrops of fibrils (pre- and post-sonication) onto 200 mesh formvar-carbon film-bearing grids (Electron Microscopy Sciences, Hatfield, PA, USA), rinsing with water, and staining with a 2% w/w aqueous uranyl acetate solution for 2 min.

Preparation of cultured cells for EM and immuno-EM

For conventional EM, the cells were fixed for 1 h at 37 °C in 2.5% glutaraldehyde made up in 0.1 M phosphate buffer (pH 7.4) and processed for EM and immuno-EM as described in Supplementary Methods (Online Resource 16).

EM for myelin integrity

At 1 month post-injection, haSyn PFF-treated WT and KO-aSyn mice ($n = 4$/genotype) were perfused transcardially with 0.1 M PBS (pH 7.2) at 37 °C and then with 4% paraformaldehyde/1% glutaraldehyde. The brain was removed and the ipsilateral striatum was processed for EM analysis as described in Supplementary Methods (Online Resource 16). In all EM procedures, the grids were examined in a Philips 420 transmission electron microscope at an acceleration voltage of 60 kV and photographed with a Megaview G2 CCD camera (Olympus SIS, Münster, Germany) and iTEM image capture software. In order to assess myelin integrity in the PFF-injected mice striatum, we quantified the *g* ratio (ratio of inner axonal diameter to total outer diameter) and the % of axons with decompacted myelin [43]. For these quantifications, at least 100 randomly selected myelin sheaths that were cross-sectioned completely without artifacts and could be classified without doubt were counted. Semi-automated analysis of randomly selected myelin sheaths was carried out using a plug-in for ImageJ software as previously described [7].

RNA extraction, cDNA synthesis and real-time PCR

Total RNA was extracted from OLN-93 cells treated with haSyn PFFs for 2, 12, and 48 h (or PBS) using TRIzol® (Ambion, Thermo Fisher Scientific, Waltham, MA, USA). Following digestion with 1 U/µg DNase I (Promega, Madison, WI, USA), 1 µg total RNA was used for first-strand cDNA synthesis with the Moloney murine leukemia virus reverse transcription system (Promega, Madison, WI, USA) and utilized for real-time PCR, according to the manufacturer's instructions, as described in Supplementary Methods (Online Resource 16).

Autopsy case material

Human brain tissue was obtained through the University of Florida Neuromedicine Human Brain Tissue Bank according to protocols approved by the Institutional Review Board. Post-mortem pathological diagnoses were made according to standard neuropathological criteria [33, 66]. Cerebellar samples containing GCIs from three MSA cases were studied including the two major pathological subtypes: striatonigral degeneration and olivopontocerebellar atrophy (Online Resource 10). The cingulate cortex and midbrain containing cortical and brainstem Lewy Bodies (LBs), respectively, from three dementia with Lewy bodies (DLB) cases with concurrent Alzheimer's disease pathology were also utilized.

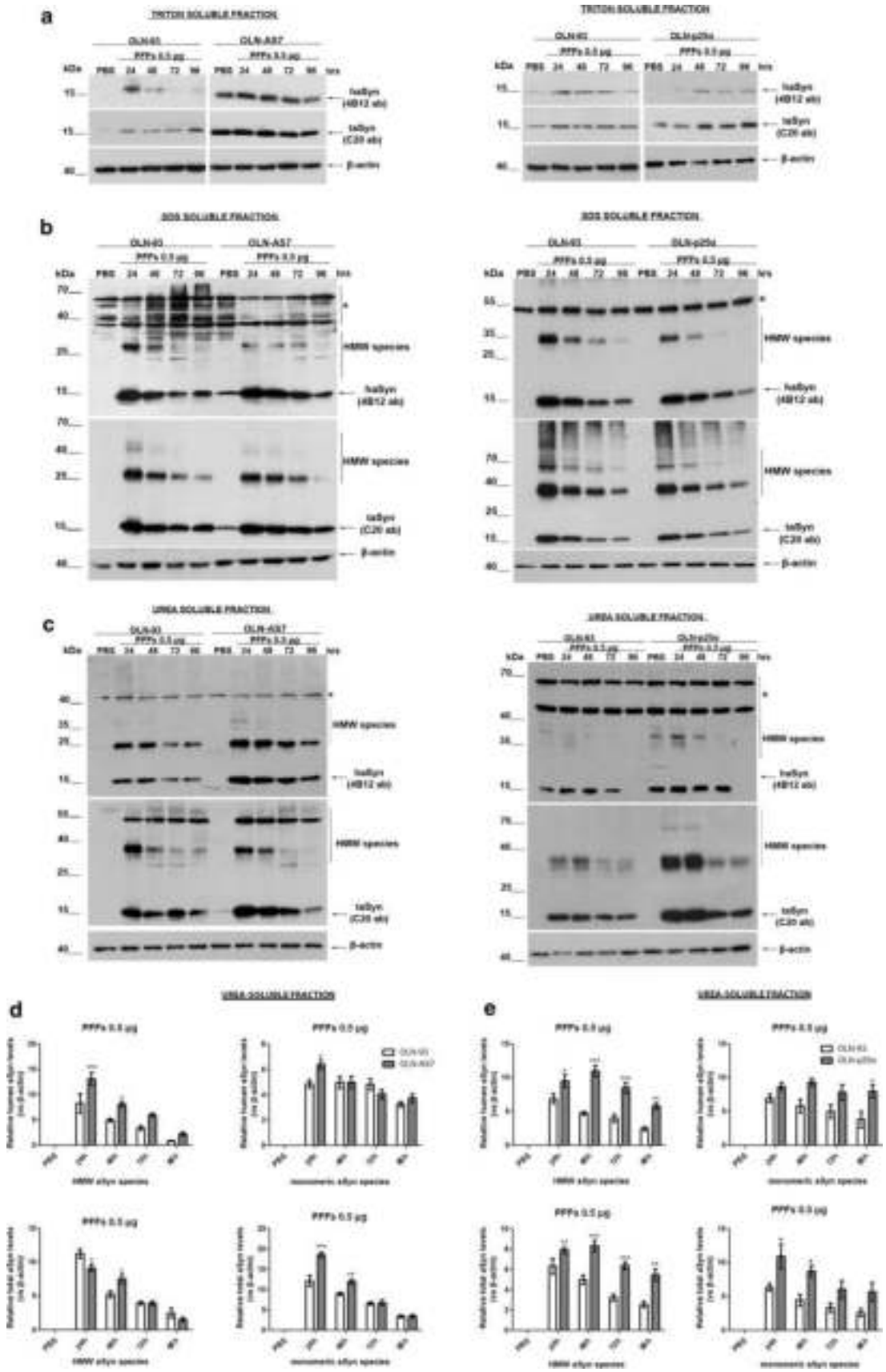
a
TRITON SOLUBLE FRACTION
b
SDS SOLUBLE FRACTION
c
UREA SOLUBLE FRACTION
d
e
HMW species
monomeric

◂**Fig. 1** Pre-formed haSyn fibrils are taken up by oligodendroglial cell lines and evoke the formation of Triton-insoluble aSyn species. Representative immunoblots of Triton-, SDS-, and urea-soluble protein fractions derived from OLN-93, OLN-AS7, and OLN-p25α cells treated with 0.5 μg of haSyn PFFs for various times (24–96 h). **a** A small fraction of human and total aSyn (detected with 4B12 and C20 antibodies, respectively) is present in the Triton-soluble fraction of OLN-93 and OLN-AS7 (left panel) or OLN-p25α cell lysates (right panel). **b**, **c** Monomeric and high molecular weight (HMW) aSyn species (human and total) are mainly detected in the SDS- and urea-soluble fractions, following the addition of haSyn PFFs, thus representing rather insoluble aSyn species in OLN-93 and OLN-AS7 (left panel) or p25α cell lysates (right panel). Equal loading was verified by the detection of β-actin levels. Asterisk represents non-specific bands obtained with the human-specific 4B12 antibody (also detected in the PBS-treated OLN-93 or OLN-p25α cells where no human aSyn was present). **d**, **e** Quantification of monomeric and HMW species of human (upper panels) and total (lower panels) aSyn levels detected in the urea-soluble fraction of OLN-93 and OLN-AS7 cells (**d**) or OLN-93 and OLN-p25α cells (**e**) treated with 0.5 μg PFFs for 24-96 h. Data are expressed as the mean ± SE of five independent experiments with triplicate samples/condition within each experiment; $*p < 0.05$; $**p < 0.01$; $***p < 0.001$, by two-way ANOVA with Bonferroni's correction, comparing between OLN-93 and OLN-AS7 or OLN-p25α cells treated with haSyn PFFs at all time points

Immunohistochemistry and semi-quantitative scoring

Immunostaining of the sections was performed using standard methods [11]. The sections were rehydrated and subsequent antigen retrieval was performed in a steam bath for 30 min in a 0.2% Tween-20 solution for all antibodies utilized. Non-specific antibody binding was minimized with a 2% fetal bovine serum/0.1 M Tris blocking solution; primary antibodies were diluted in the blocking solution and applied to tissue sections at 4 °C overnight. Biotinylated secondary antibodies (Vector Laboratories, Burlingame, CA, USA) were diluted in the blocking solution and applied to the sections for 1 h at room temperature. An avidin–biotin complex system (VECTASTAIN ABC Elite Kit; Vector Laboratories, Burlingame, CA, USA) was used to enhance detection of the immunocomplexes, which were visualized using the chromogen 3,3′-diaminobenzidine (DAB Kit; KPL, Gaithersburg, MD, USA). For comparison, all MSA and DLB sections were exposed to DAB for the same amount of time for a given antibody. Tissue sections were counterstained with hematoxylin. All slides were digitally scanned using an Aperio ScanScope CS instrument (40× magnification; Aperio Technologies Inc., Vista, CA, USA), and images of representative areas of pathology were captured using ImageScope software (40× magnification; Aperio Technologies, Inc., Vista, CA, USA). Inclusion pathology was observed and assessed qualitatively and confirmed independently by a second observer.

Animals

Eight-week-old male WT C57BL6/C3H (WT-aSyn), C57BL6/JOlaHsd aSyn null (KO-aSyn) (purchased from Harlan Laboratories), or C57BL6 PLP-haSyn transgenic (kindly provided by Dr. Nadia Stefanova, Innsbruck University) mice were housed (6–8 animals/cage) with free access to food and water under a 12-h light/dark cycle. All experimental procedures were approved by the Ethics Committee for the Use of Laboratory Animals in the Biomedical Research Foundation of Athens.

Surgical procedures

All surgical procedures were performed under general isoflurane (B506; Abbott, Chicago, USA) anesthesia. Eight-week-old male WT or KO aSyn mice were placed in a stereotaxic frame (Kopf Instruments, Tujunga, CA, USA) and the right dorsal striatum was targeted using the following coordinates from the bregma: +0.5 mm anteroposterior, −1.6 mm mediolateral, and −3.4 mm dorsoventral according to the Mouse Brain Atlas [80]. A total of 2 μL haSyn PFF solution (final concentration, 2 μg/μL) or PBS was injected unilaterally at a constant flow rate of 0.1 μL/15 s using a pulled glass capillary (diameter, 60–80 mm) attached to a Hamilton syringe with a 22-gauge needle. Following delivery of haSyn PFFs or PBS, the capillary was held in place for 5 min and removed slowly from the brain.

Immunohistochemistry and confocal microscopy

At 1 month post-injection, the animals were anesthetized with isoflurane followed by intracardial perfusion with ice-cold PBS and then ice-cold 4% paraformaldehyde solution ($n = 4$–5 animals/condition/genotype). The brains were removed and post-fixed for 24 h in the same preparation of paraformaldehyde and transferred to 15% sucrose for 24 h and finally in 30% sucrose until sectioning. The brains were sectioned through the coronal plane at 30 μm increments, and every section throughout the striatum and ventral midbrain was collected. Immunohistochemical staining was carried out in free-floating sections as described previously [79] using the primary and secondary antibodies described in the Immunocytochemistry and Confocal Microscopy section.

Statistical analysis

The data are shown as the mean ± standard error (SE) of 3 or 5 independent experiments with triplicate samples/condition within each experiment. The mean values ± standard deviation (SD) of each experiment are also provided in Supplementary Table 3 (Online Resource 12). Image

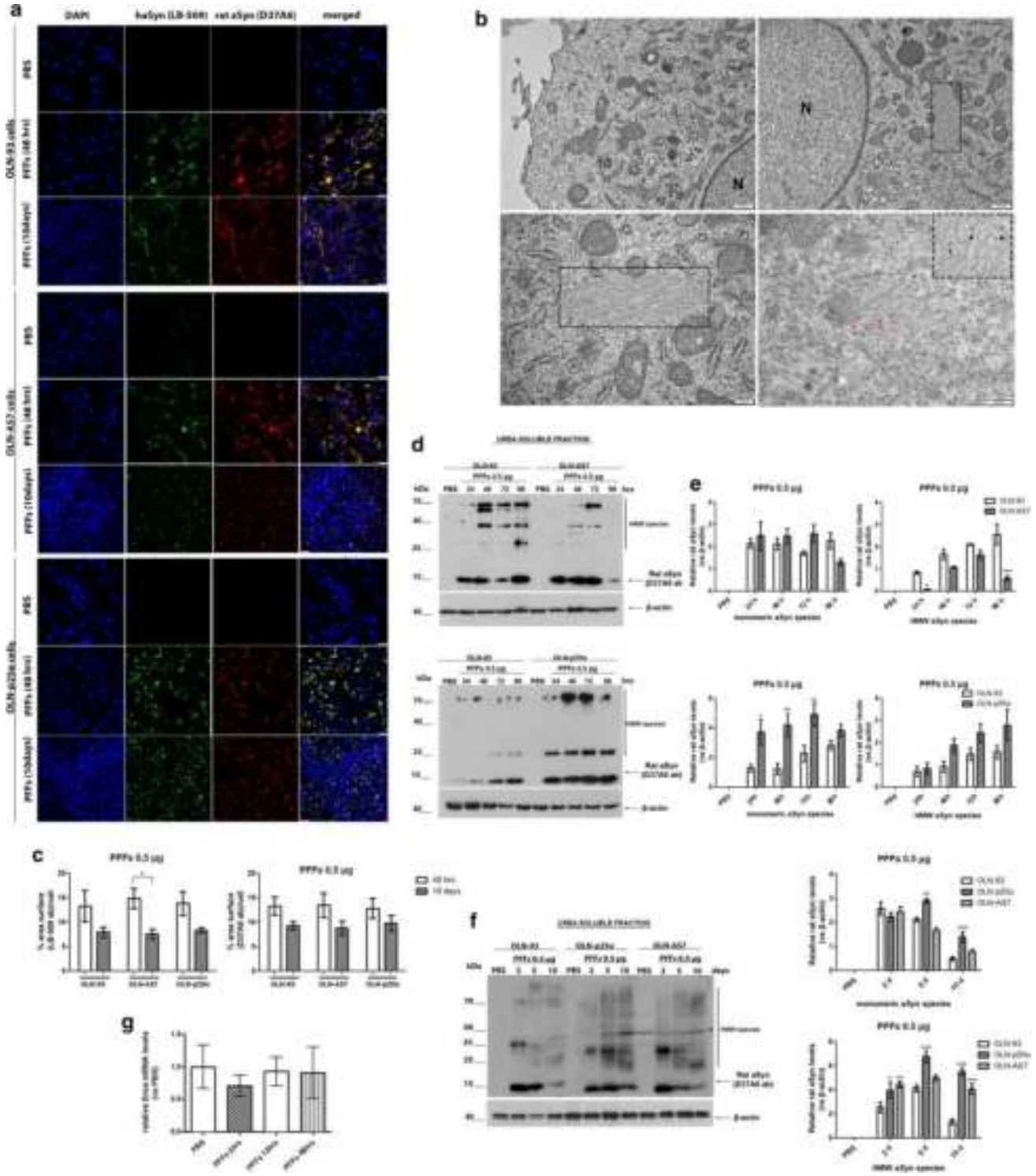

acquisition and analysis were performed by two independent examiners blinded to the true identity of the samples. Statistical analysis was carried out with GraphPad Prism 5 using one-way analysis of variance (ANOVA) with Tukey's post hoc test or two-way ANOVA with Bonferroni's correction. Differences were considered significant for $p < 0.05$.

◂**Fig. 2** Addition of haSyn PFFs in OLN cell lines leads to the recruitment of endogenous rat oligodendroglial aSyn into highly insoluble aSyn assemblies. **a** Representative immunofluorescence images using antibodies against human aSyn (green, LB509 antibody) and endogenous rat aSyn (red, D37A6 antibody) and DAPI staining in OLN cell lines treated with 0.5 µg of haSyn PFFs for 48 h and 10 days. Scale bar: 25 µm. **b** (Upper panels) ultrastructural transmission EM analysis of PBS-treated (upper left) and haSyn PFFs-treated (upper right) OLN-93 cells showing the presence of filaments (box highlight) in the cell soma near the nucleus of PFF-treated cells (N). (bottom left panel) A higher magnification image of the filaments of PFF-treated cultures is shown. (Box highlight, bottom right panel) double immuno-EM analysis with nanogold particles of different diameters, demonstrating the presence of both human (green asterisk, LB-509, 10 nm) and rodent (red asterisk, D37A6, 15 nm) aSyn in the formed filamentous inclusions in the cell soma of OLN-93 cells. A high-power image of independent PFF-treated cultures is shown in the upper dashed box. Scale bars: 500 nm (upper), 200 nm (bottom) and 100 nm (highlight box). **c** Quantification of aSyn levels (human and endogenous rat) measured as % area surface/cell in OLN cell lines following treatment with 0.5 µg PFFs for 48 h or 10 days. Data are expressed as the mean ± SE of three independent experiments with triplicate samples/condition within each experiment. $*p < 0.05$ by two-way ANOVA with Bonferroni's correction. **d** Representative immunoblots demonstrating the presence of endogenous rat aSyn (D37A6 antibody) in the urea-soluble fraction of OLN-93 and OLN-AS7 cells (upper panel) or OLN-p25α cells (bottom panel) following treatment with 0.5 µg haSyn PFFs for 24–96 h. Equal loading was verified by the detection of β-actin levels. **e** Quantification of monomeric (left) and HMW species (right) of endogenous rat aSyn levels detected in the urea-soluble fraction of OLN-93 and OLN-AS7 cells (upper row) or OLN-93 and OLN-p25α cells (bottom row) treated with 0.5 µg PFFs for 24–96 h. Data are expressed as the mean ± SE of five independent experiments with triplicate samples/condition within each experiment. $*p < 0.05$; $**p < 0.01$; $***p < 0.001$, by two-way ANOVA with Bonferroni's correction. **f** (Left panel) representative immunoblots of urea-soluble protein fraction derived from OLN-93, OLN-AS7 and OLN-p25α cells treated with 0.5 µg of haSyn PFFs for 2–10 days. Asterisk represents non-specific bands obtained with the rodent-specific D37A6 antibody. (right) Quantification of monomeric (upper row) and HMW species (bottom row) of rat endogenous aSyn detected in the urea-soluble fraction of all OLN cell lines treated with 0.5 µg PFFs for 2–10 days. Data are expressed as the mean ± SE of three independent experiments with triplicate samples/condition within each experiment; $*p < 0.05$; $**p < 0.01$; $***p < 0.001$, by two-way ANOVA with Bonferroni's correction, comparing between OLN-93 and OLN-AS7 or OLN-p25α cells treated with haSyn PFFs. **g** Quantitative real-time PCR reveals unaltered *Snca* levels upon treatment of OLN-93 cells with 0.5 µg haSyn PFFs for 2–48 h. Data are expressed as *Snca* mRNA levels relative to the mRNA levels of β-actin normalized to control-treated cultures (PBS)

Results

Internalization of haSyn PFFs by oligodendroglial cell lines leads to the formation of Triton-insoluble aSyn species

In order to assess the uptake and seeding capacity of haSyn PFFs in oligodendroglial cells, we initially utilized the immortalized rat OLN-93 cell line, which expresses very low to non-detectable levels of endogenous aSyn and p25α, and the stable cell lines OLN-AS7 and OLN-p25α, which overexpress human WT-aSyn and p25α, respectively (Online Resource 1a). Stable or transient overexpression of haSyn and p25α in OLN cells was not accompanied by changes in cell viability (Online Resource 1b). EM used to monitor fibril morphology and to confirm the presence of fibrils (Online Resource 1c). Treatment of OLN-93 cells with 0.2 and 0.5 µg haSyn PFFs for 48 h, led to the dose-dependent accumulation of SDS- and urea-soluble high molecular weight (HMW) aSyn species (Online Resource 1d). We used 0.5 µg haSyn PFFs in subsequent experiments, and we investigated the solubility and aggregation of internalized PFFs in the OLN cell lines over time (24–96 h). The Triton-soluble fraction of all cell lines contained only monomeric aSyn (detected with antibodies against human and human + rodent aSyn) that showed the highest levels at 24 h post-addition, which was followed by a time-dependent decrease to baseline levels (PBS-treated cells), evident mostly in the control OLN-93 cells (Fig. 1a and Online Resource 2a, b). This could be attributed either to the effective clearance of the formed aSyn species or to the dilution of exogenous aSyn due to cell proliferation. Notably, monomeric aSyn levels detected in the Triton-soluble fraction of OLN-AS7 cells remained high over time, possibly due to the stable overexpression of the human protein in these cells, whereas in the OLN-p25α cells both exogenously added human and total aSyn remained at higher levels than in the OLN-93 cells. HMW-aSyn species were detected mostly in the SDS- and urea- soluble fractions (Fig. 1b, c), thus representing rather insoluble aSyn species. Similar to the Triton-soluble fraction, in the SDS-soluble fraction, the peak levels of monomeric and HMW aSyn were observed at 24 h in all cell lines, followed by a gradual decrease over time (48–96 h); however, they remained at higher levels than in the PBS-treated cells (Fig. 1b and Online Resource 2c–f). Interestingly, in the urea-soluble fraction of OLN-p25α cells, aSyn monomeric and oligomeric forms (both human and total) were relatively resistant to degradation, since their levels remained high compared to control OLN-93 cells, in which their levels decreased over time (Fig. 1c–e). This could be indicative of a role for p25α in promoting aSyn aggregate formation within oligodendrocytes or in inhibiting the clearance of aSyn aggregates.

Addition of haSyn PFFs to OLN cell lines recruits endogenous rat oligodendroglial aSyn into the formation of highly insoluble aSyn conformations

In order to investigate the ability of haSyn PFFs to act as a template for endogenous oligodendroglial aSyn to form insoluble protein species, we utilized the rodent-specific D37A6 antibody in western blot and confocal microscopy analyses.

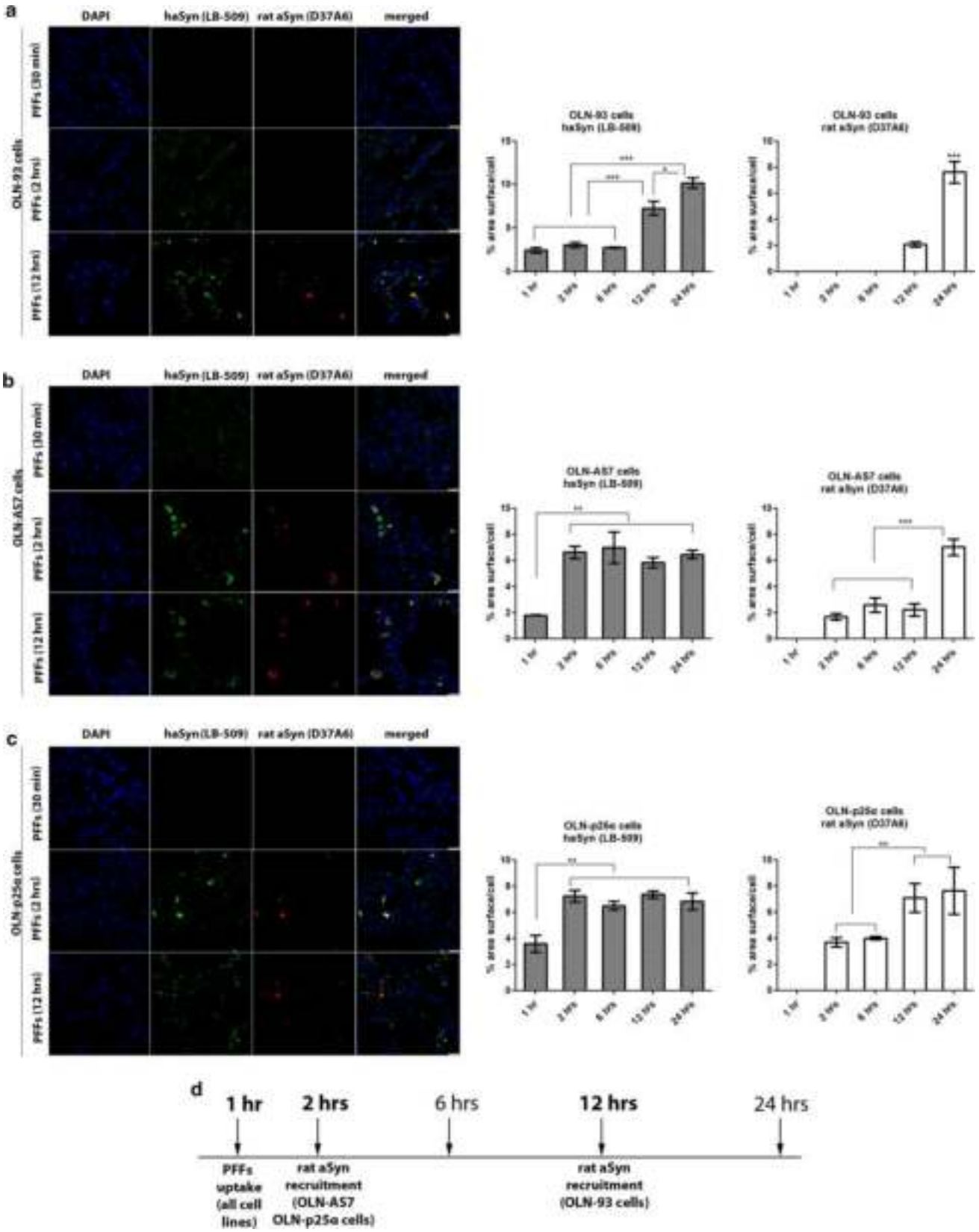
a
DAPI
haSyn (LB-509)
rat aSyn (D37A6)
merged
OLN-93 cells
PFFs (30 min)
PFFs (2 hrs)
PFFs (12 hrs)
OLN-93 cells
haSyn (LB-509)
OLN-93 cells
rat aSyn (D37A6)
% area surface/cell
1 hr
2 hrs
6 hrs
12 hrs
24 hrs
b
DAPI
haSyn (LB-509)
rat aSyn (D37A6)
merged
OLN-AS7 cells
PFFs (30 min)
PFFs (2 hrs)
PFFs (12 hrs)
OLN-AS7 cells
haSyn (LB-509)
OLN-AS7 cells
rat aSyn (D37A6)
% area surface/cell
1 hr
2 hrs
6 hrs
12 hrs
24 hrs
c
DAPI
haSyn (LB-509)
rat aSyn (D37A6)
merged
OLN-p25α cells
PFFs (30 min)
PFFs (2 hrs)
PFFs (12 hrs)
OLN-p25α cells
haSyn (LB-509)
OLN-p25α cells
rat aSyn (D37A6)
% area surface/cell
1 hr
2 hrs
6 hrs
12 hrs
24 hrs
d
1 hr
2 hrs
6 hrs
12 hrs
24 hrs
PFFs uptake (all cell lines)
rat aSyn recruitment (OLN-AS7 OLN-p25α cells)
rat aSyn recruitment (OLN-93 cells)

◂**Fig. 3** Overexpression of human aSyn or p25α accelerates the recruitment of endogenous rat oligodendroglial aSyn following the addition of haSyn PFFs to OLN cell lines. **a–c** Confocal microscopy with exogenous human-specific and endogenous rat-specific anti-aSyn antibodies reveals the enhanced expression of endogenous rat aSyn at 12 h in control OLN-93 cells and at 2 h in OLN-AS7 and OLN-p25α cells. (left panels) Representative immunofluorescence images with antibodies against human aSyn (green, LB509 antibody) and rodent aSyn (red) and DAPI staining. Scale bar: 25 µm. (right panels) Quantification of aSyn protein levels (human or endogenous rat aSyn) in OLN-93, OLN-AS7 and OLN-p25α cells measured as % area surface/cell following treatment with 0.5 µg haSyn PFFs for various times (2–12 h). Data are expressed as the mean ± SE of three independent experiments with triplicate samples/condition within each experiment; $*p < 0.05$; $**p < 0.01$; $***p < 0.001$, by one-way ANOVA with Tukey's post hoc test. **d** A drawing depicting the key time points when the uptake of exogenous haSyn PFFs and the recruitment of endogenous rat aSyn occur in control cells (OLN-93) and cells overexpressing human aSyn (OLN-AS7) or p25α (OLN-p25α)

This antibody does not give any immunofluorescence signal in PBS-treated OLN cells (Fig. 2a and Online Resource 3); the addition of 0.5 µg haSyn PFFs was accompanied by the detection of an elevated endogenous aSyn signal, which co-localized with the exogenously added human aSyn that persisted over time (48 h–10 days) and depended, in terms of its intensity, on the exogenously added human material (Online Resource 4). The uptake of haSyn PFFs was further verified by staining the lectins of the plasma membrane using wheat germ agglutinin (Online Resource 1e and 13) and ultrastructural EM analysis, which revealed the presence of filaments in the cell soma of OLN-93 cells treated with haSyn fibrils, which were absent in PBS-treated cells (Fig. 2b, upper panels). Double immuno-EM analysis with nanogold particles of different diameters, showed the presence of human and rat aSyn in the formed intracellular filamentous inclusions (Fig. 2b, bottom panels). Measurement of human or rat endogenous aSyn levels, expressed as % of surface area normalized to the total number of cells/field, revealed no significant differences among the different OLN cells, at 48 h and 10 days post-addition of 0.5 µg haSyn PFFs (Fig. 2c). However, and in agreement with the immunoblot data (Fig. 1c–e), OLN-p25α cells retained significantly more proteinase K-resistant human and rodent aSyn species compared to OLN-93 and OLN-AS7 cells (Online Resource 5).

Similarly, in the urea-soluble fraction of OLN-p25α cells from 24 h to 10 days post-addition of haSyn PFFs, higher levels of monomeric and HMW forms of endogenous rodent aSyn were found compared to OLN-93 and OLN-AS7 cells (Fig. 2d–f). No rat-specific signal was detected in the Triton- or the SDS-soluble fractions at 24 h–10 days post-addition of haSyn PFFs (data not shown). The elevated levels of endogenous aSyn detected following treatment of OLN cells with haSyn PFFs were not attributed to increased transcription of the rat *Snca* gene, encoding endogenous oligodendroglial aSyn, as revealed by quantitative real-time-PCR analysis (Fig. 2g).

The specificity of the D37A6 aSyn antibody to recognize only the rodent protein was validated further by confocal microscopy and western immunoblotting, utilizing human SH-SY5Y dopaminergic cells inducibly overexpressing the WT-aSyn upon the removal of doxycycline (dox) [69] and extracts from WT-, KO-, and hA53T-aSyn transgenic mice (Online Resource 6 a, b). Importantly, treatment of OLN-93 cells with the proteasomal inhibitor epoxomicin (epox) or the general lysosomal inhibitor NH_4Cl alone or in combination (epox + NH_4Cl) for 48 h revealed an increased aSyn signal upon lysosomal inhibition, as detected with the D37A6 antibody in the absence of haSyn PFFs, further supporting the presence of miniscule amounts of endogenous aSyn in oligodendrocytes that are increased upon inhibition of protein degradation (Online Resource 6c, d).

Overexpression of human aSyn or p25α accelerates the recruitment of the endogenous rat oligodendroglial aSyn and the formation of intracellular oxidized/nitrated aSyn species following the addition of haSyn PFFs

To decipher the impact of human aSyn or p25α overexpression on the seeding of aSyn pathology in OLN cells, we performed time-course analysis from 30 min until 24 h post-treatment. Confocal microscopy analysis with antibodies against human and rodent aSyn (LB509 and D37A6 antibodies, respectively) revealed that haSyn PFFs were taken up effectively by all OLN cell lines within 1 h, whereas the recruitment of the endogenous rat aSyn represented a later event (Fig. 3). Interestingly, in control OLN-93 cells, the seeding process was initiated at 12 h post-treatment with the haSyn PFFs (Fig. 3a), whereas in OLN-AS7 and OLN-p25α cells, the endogenous rat aSyn signal was detected earlier, at 2 h post-addition (Fig. 3b, c). Importantly, the recruitment of endogenous rat aSyn evokes a dramatic change in the pattern of haSyn immunostaining and an increase in haSyn immunoreactivity, measured as % area surface/cell, at the onset of seeding (Fig. 3). This observation suggests a possible role for the seeded rat aSyn in the rapid formation of aSyn aggregates positive for both human + rodent aSyn or in the stabilization of haSyn aggregates, rendering them resistant to degradation.

We next investigated whether excess intracellular aSyn protein load (OLN-AS7 cells) or the presence of p25α (OLN-p25α cells) affects the onset of the appearance of aSyn pathology in oligodendrocytes by assessing the formation of oxidized/nitrated aSyn species over time (30 min–10 days) with confocal microscopy. Indeed, in OLN-AS7 and OLN-p25α cells, the appearance of oxidized/nitrated aSyn (detected with the Syn303 aSyn antibody) was observed

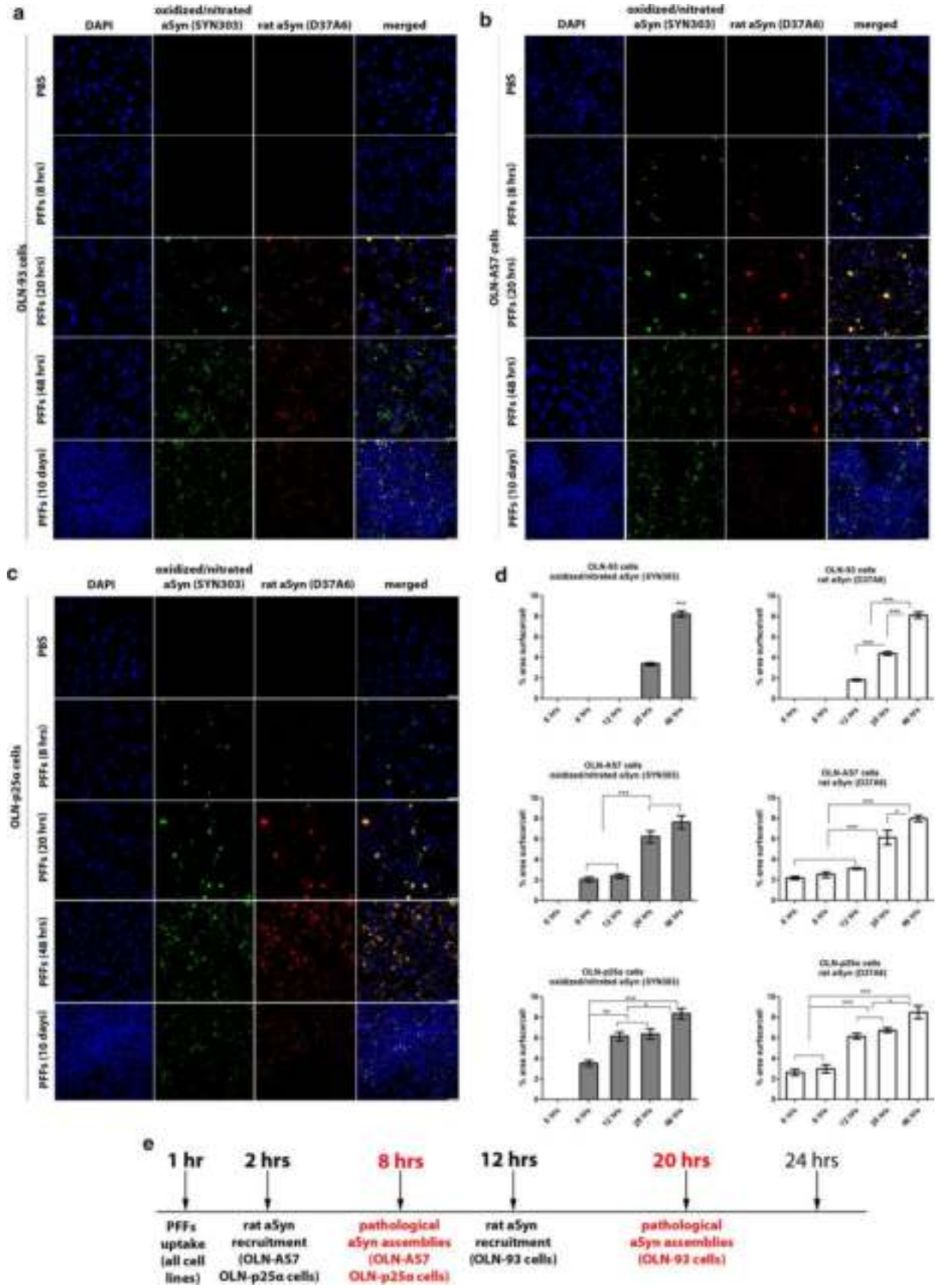
a
DAPI
oxidized/nitrated aSyn (SYN303)
rat aSyn (D37A6)
merged
OLN-93 cells
PBS
PFFs (8 hrs)
PFFs (20 hrs)
PFFs (48 hrs)
PFFs (10 days)
b
DAPI
oxidized/nitrated aSyn (SYN303)
rat aSyn (D37A6)
merged
OLN-A57 cells
PBS
PFFs (8 hrs)
PFFs (20 hrs)
PFFs (48 hrs)
PFFs (10 days)
c
DAPI
oxidized/nitrated aSyn (SYN303)
rat aSyn (D37A6)
merged
OLN-p25α cells
PBS
PFFs (8 hrs)
PFFs (20 hrs)
PFFs (48 hrs)
PFFs (10 days)
d
e
1 hr
2 hrs
8 hrs
12 hrs
20 hrs
24 hrs
PFFs uptake (all cell lines)
rat aSyn recruitment (OLN-A57 OLN-p25α cells)
pathological aSyn assemblies (OLN-A57 OLN-p25α cells)
rat aSyn recruitment (OLN-93 cells)
pathological aSyn assemblies (OLN-93 cells)

◂**Fig. 4** Overexpression of human aSyn or p25α facilitates the formation of pathological (oxidized/nitrated) aSyn assemblies following the addition of haSyn PFFs. **a**–**c** In OLN-AS7 and OLN-p25α cells, the recruitment of endogenous rat aSyn and the formation of pathological aSyn species are detected at 8 h, whereas they occur in control OLN-93 cells at 20 h post-addition of PFFs. Representative immunofluorescence images of OLN-93, OLN-AS7 and OLN-p25α cells treated with 0.5 μg haSyn PFFs for various times (8–48 h and 10 days) using antibodies against oxidized/nitrated aSyn (green, Syn303 antibody) and endogenous rat aSyn (red) and DAPI staining. Scale bar: 25 μm. **d** Quantification of aSyn protein levels (oxidized/nitrated or endogenous rat aSyn) in OLN-93 (upper row), OLN-AS7 (middle row) and OLN-p25α (bottom row) cells measured as % area surface/cell following treatment with 0.5 μg haSyn PFFs for various times (6-48 h). Data are expressed as the mean ± SE of three independent experiments with triplicate samples/condition within each experiment; $*p < 0.05$; $**p < 0.01$; $***p < 0.001$, by one-way ANOVA with Tukey's post hoc test. **e** A schema highlighting the time points when the increase in endogenous rat aSyn and the detection of pathological (oxidized/nitrated) aSyn species are observed in the different OLN cell lines

within 8 h post-addition of 0.5 μg haSyn PFFs, whereas in the control OLN-93 cells, these pathological species were observed after 20 h (Fig. 4). Notably, co-staining with the rodent-specific aSyn antibody revealed that endogenous aSyn was a major component of the seeded time-resistant pathological aSyn assemblies. Importantly, the Syn303 aSyn antibody did not recognize exogenously added haSyn PFFs per se, since no signal was observed at 1 h post-addition, when haSyn PFFs were detected inside the cells (data not shown), further supporting a major role for oligodendroglial aSyn in the seeding of aSyn pathology in OLN cells.

Transient overexpression of human p25α augments the formation of insoluble aberrant aSyn species, consisting of human and endogenous rat protein

In order to validate further the role of p25α in the seeding of aSyn pathology, we used another experimental approach. Specifically, OLN-93 and OLN-AS7 cells were transiently transfected (or co-transfected where indicated) with p25α or/and GFP (as a control) plasmids 6 h prior to the addition of 0.5 μg of haSyn PFFs. At 2 days post-transfection, the cells were fixed and processed for confocal microscopy using antibodies against human aSyn (LB509 antibody, Fig. 5a, left panel), oxidized/nitrated aSyn (Syn303 antibody, Fig. 5b, left panel), or rodent aSyn (D37A6 antibody, Fig. 5c, left panel). The transient overexpression of human p25α increased the accumulation of human (Fig. 5a) and endogenous rat (Fig. 5c) aSyn-positive signals and the generation of oxidized/nitrated aSyn species (Fig. 5b) in OLN-93 and OLN-AS7 cells. Additionally, p25α overexpression in OLN-93 cells augmented the formation of monomeric and HMW aSyn species extractable in urea buffer (Fig. 5d). Such data further support a critical role for p25α in the aggregation of pathological aSyn conformations within oligodendrocytes.

Phosphorylation of aSyn at Ser129 depends on aSyn and p25α protein load and may involve different aSyn aggregate "strains" present in oligodendroglial and neuronal synucleinopathies

Given that the presence of aSyn phosphorylated at Ser129 (pSer129 aSyn) is an indicator of pathology in synucleinopathies, we assessed pSer129 aSyn levels in all OLN cell lines upon treatment with 0.5 or 3 μg haSyn PFFs for 48 h and 10 days using a panel of specific pSer129 aSyn antibodies. Surprisingly, we detected positive pSer129 aSyn signals only in PFFs-treated OLN cells overexpressing human aSyn or p25α (in the presence of 3 μg haSyn PFFs for 10 days) and not in the control OLN-93 cells, using the pSer129 aSyn-specific antibodies 11A5 (Fig. 6a, middle row) and EP1536Y (Fig. 6a, bottom row). Conversely, no positive signal was detected in any PFF-OLN-treated cell line using the pSer129 aSyn antibody LS4-2G12 (Fig. 6a, upper row), which could be attributed to the low affinity of this antibody. Interestingly, no positive pSer129 aSyn signal was detected in the Triton- or SDS-soluble fraction of all PFF-treated OLN cells (Fig. 6b), whereas pSer129 immunoreactivity was observed only in the urea-soluble fraction of OLN-AS7 cells and to a greater extent in OLN-p25α cells (Fig. 6c). Most importantly, endogenous rat aSyn co-localized with the 11A5 pSer129 aSyn antibody, suggesting that the seeded oligodendroglial aSyn is phosphorylated, upon the addition of haSyn PFFs (Fig. 6d).

Strikingly, in PFF-treated primary rat cortical cultures we detected a pSer129 aSyn signal with all antibodies utilized, including the LS4-2G12 antibody that did not give a signal in the OLN seeding model (Fig. 6e), suggesting that this antibody may recognize distinct pSer129 aSyn assemblies generated specifically in neurons and not in oligodendrocytes. Importantly, this hypothesis was further buttressed by data obtained from human post-mortem brain material derived from patients with neuronal synucleinopathy (DLB) and oligodendroglial synucleinopathy (MSA). As shown in Fig. 6f, and in agreement with our results from PFF-treated primary cortical cultures, all pSer129 antibodies recognized pSer129 aSyn in LBs in the substantia nigra pars compacta (left columns) and cortex (middle columns) of DLB brains to a similar extent. In contrast, and congruent with the data obtained from PFF-treated oligodendroglial cells, LS4-2G12 reactivity for MSA cerebellar GCIs was much weaker than the 11A5 and EP1536Y signals. Finally, the conformation-specific aSyn antibody MJFR-14 recognized better the aberrant aSyn species present in GCIs, compared to LBs (Fig. 6f, bottom row), supporting the notion that aSyn generated within oligodendrocytes (MSA) is incorporated into

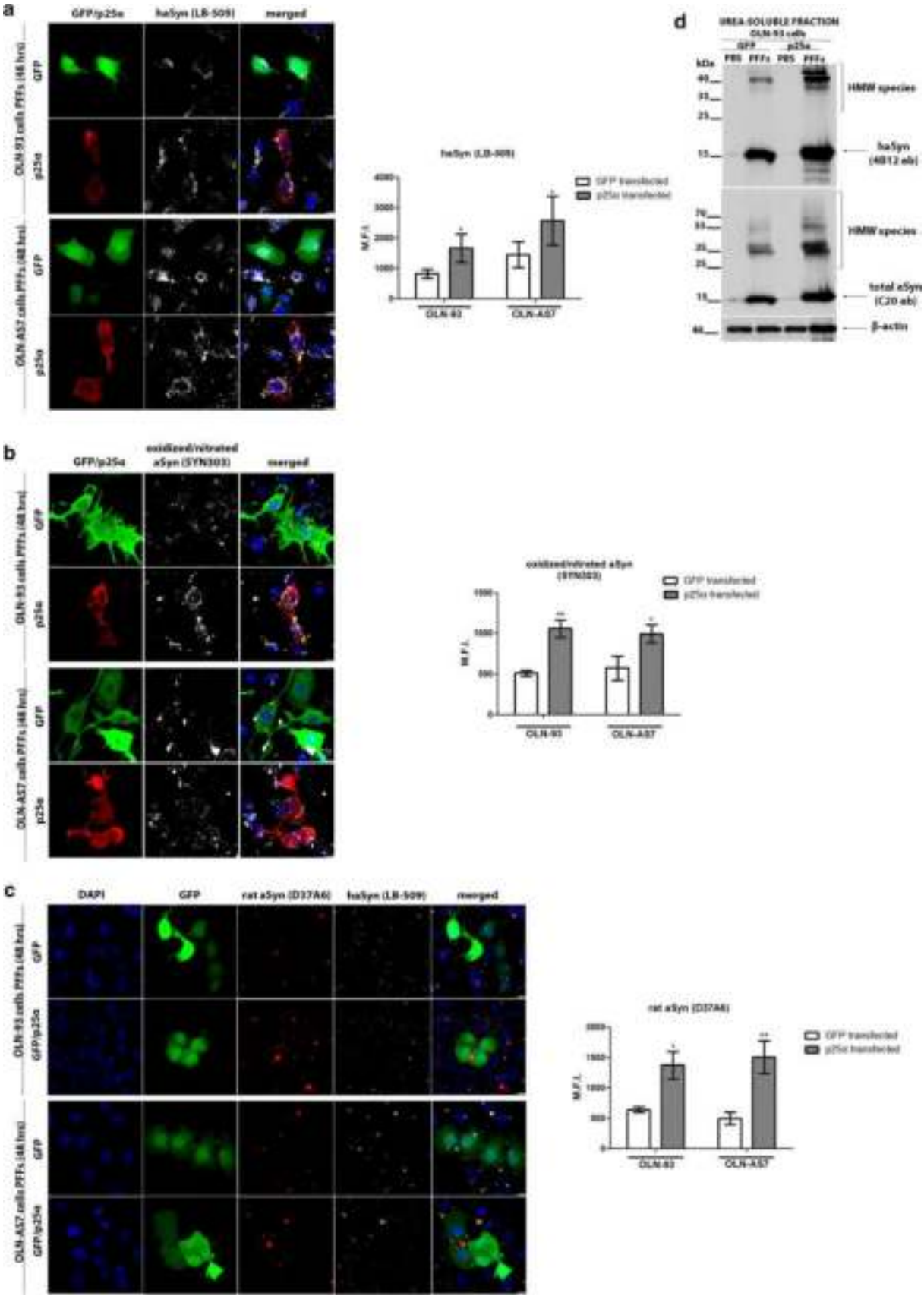
a
GFP/p25α
hαSyn (LB-509)
merged
OLN-93 cells PFFs (48 hrs)
GFP
p25α
OLN-AS7 cells PFFs (48 hrs)
GFP
p25α
hαSyn (LB-509)
M.F.I.
GFP transfected
p25α transfected
OLN-93
OLN-AS7
d
UREA-SOLUBLE FRACTION
OLN-93 cells
GFP
p25α
PBS
PFFs
PBS
PFFs
kDa
HMW species
hαSyn (4B12 ab)
HMW species
total αSyn (C20 ab)
β-actin
b
GFP/p25α
oxidized/nitrated αSyn (SYN303)
merged
OLN-93 cells PFFs (48 hrs)
GFP
p25α
OLN-AS7 cells PFFs (48 hrs)
GFP
p25α
oxidized/nitrated αSyn (SYN303)
M.F.I.
GFP transfected
p25α transfected
OLN-93
OLN-AS7
c
DAPI
GFP
rat αSyn (D37A6)
hαSyn (LB-509)
merged
OLN-93 cells PFFs (48 hrs)
GFP
GFP/p25α
OLN-AS7 cells PFFs (48 hrs)
GFP
GFP/p25α
rat αSyn (D37A6)
M.F.I.
GFP transfected
p25α transfected
OLN-93
OLN-AS7

◂**Fig. 5** Transient overexpression of human p25α in OLN-93 and OLN-AS7 cells augments the formation of aberrant aSyn species comprised of human and endogenous rat aSyn following the addition of haSyn PFFs. **a**–**c** (Left panel) representative immunofluorescence images of OLN-93 and OLN-AS7 cells transfected with GFP or human p25α plasmids in the presence of haSyn PFFs (48 h) using antibodies against: **a** haSyn (gray), **b** oxidized/nitrated aSyn (gray) and **c** rodent aSyn (red). In **a**, **b**, antibodies against GFP (green) and p25α (red) were used to visualize the transfected cells. Scale bar: 10 µm. (Right panel) Quantification of human, oxidized/nitrated, or endogenous rat aSyn protein levels in OLN-93 and OLN-AS7 cells measured as mean fluorescent intensity in selected GFP (green) or p25α (red) transfected cells, using the image analysis tool Imaris (middle panels). Data are expressed as the mean ± SE of at least three independent experiments with triplicate samples/condition within each experiment; $*p < 0.05$, by Student's unpaired *t* test. **d** p25α overexpression enhances the accumulation of monomeric and HMW aSyn species following the addition of haSyn PFFs. Representative immunoblots of urea-soluble aSyn species of control OLN-93 cells transfected with GFP or p25α plasmids and treated with 0.5 µg haSyn PFFs for 48 h using antibodies against haSyn (4B12 antibody) or total (human + rodent) aSyn (C20 antibody). Equal loading was verified by the detection of β-actin levels

higher order pathological conformations, compared to those generated in neurons (DLB) [8]. In our cellular systems, the MJFR-14 antibody recognized aggregated aSyn in oligodendrocytes (Online Resource 7) and neurons (Fig. 6e, bottom row) to a similar extent, a finding that could be explained by the fact that this antibody also recognizes exogenously added haSyn PFFs.

Endogenous aSyn is a major component of the seeded pathological aSyn aggregates following the addition of haSyn PFFs

To delineate further the contribution of endogenous oligodendroglial aSyn and p25α in the spread of aSyn pathology, we treated OLN cells with 3 µg PFFs and analyzed aSyn levels at 48 h or 10 days (Fig. 7). With this higher amount of PFFs, over time, the equilibrium of intracellular aSyn protein load in OLN cells shifted toward the seeded endogenous rat protein and notably, this phenomenon was more robust in the presence of human aSyn or p25α (Fig. 7a, b). Similarly, oxidized/nitrated aSyn conformations were elevated in OLN-AS7 and OLN-p25α cells over time (Fig. 7c, d). Finally, using the conformation-specific aSyn antibody MJFR-14, which recognizes aggregated conformations exclusively [27], we detected the induction of MJFR-14-positive structures that colocalized from the earliest time point of 1 h with structures recognized with a pan-aSyn (human + rodent) antibody (D10); the MJFR-14 antibody showed no reactivity against overexpressed aSyn in the OLN-AS7 cell line (Online Resource 7). In order to quantitatively estimate the contribution of aSyn and p25α load to the formation and stability of inclusions, we utilized an indirect immunostaining strategy with antibodies against either total aSyn (D10 antibody) or human aSyn (211 antibody) and aggregated aSyn (MJFR-14 antibody), since both the rodent-specific (D37A6) and MJFR-14 antibodies are generated in rabbits (Fig. 7e). Total aSyn (human and endogenous rat) and aggregate-aSyn fluorescence signals exhibited a nearly complete co-localization (Fig. 7e and Online Resource 7b), whereas staining with the 211 human-specific and MJFR-14 aggregate-specific aSyn antibodies (Fig. 7e and Online Resource 7c) revealed partial co-localization, suggesting indirectly that endogenous rat aSyn is a major component of the formed aggregates. Consistent with this idea, MJFR-14-positive immunostaining increased following the addition of PFFs over a period of 10 days, matching the pattern of endogenous rat aSyn, whereas human aSyn-positive structures remained stable or decreased over time, with OLN-p25α cells again exhibiting higher levels of total and aggregated aSyn (Fig. 7e). Interestingly, the percentage of cells positive for the various aSyn conformations was similar among all OLN cell lines, with the exception of pSer129 aSyn (EP1536Y antibody) (Fig. 7f), suggesting that the observed differences shown in Fig. 7e are possibly attributed to the formation of larger aggregates in aSyn- and p25α-expressing cells, compared to OLN-93 cells. Finally, proof-of-concept experiments utilizing sonicated fibrils yielded similar results regarding the seeding of endogenous aSyn and the formation of pathological assemblies (Online Resource 8).

Endogenous mouse oligodendroglial aSyn is incorporated into pathological aSyn assemblies in primary oligodendrocytes following the addition of haSyn PFFs

To investigate the intracellular processes governing the templating of aSyn pathology in a more physiological cellular setting with properties resembling more closely those of the oligodendrocytes in the central nervous system, we established a protocol to isolate and cultivate mature oligodendrocytes derived from P0 to P3 mouse brains. In order to decipher whether the presence of aSyn, which is small in amount, is a prerequisite for the seeding of exogenous added haSyn, we used primary oligodendrocytes prepared from WT- or KO-aSyn mice. In parallel experiments, we utilized primary cultures from PLP-haSyn mice, a well-established MSA mouse model in which haSyn is overexpressed only in oligodendrocytes, under the PLP promoter [20]. To differentiate the oligodendroglial progenitor cells into mature, myelin-producing (MBP^+) oligodendrocytes, the cells were grown in SATO medium. The enrichment of the cultures with oligodendrocytes was verified utilizing markers for astrocytes (GFAP) and microglia (AIF1/IbaI), as well as markers for the oligodendroglial lineage such as Olig2, O4, and MBP (Fig. 8a, b). As observed in the OLN cell lines,

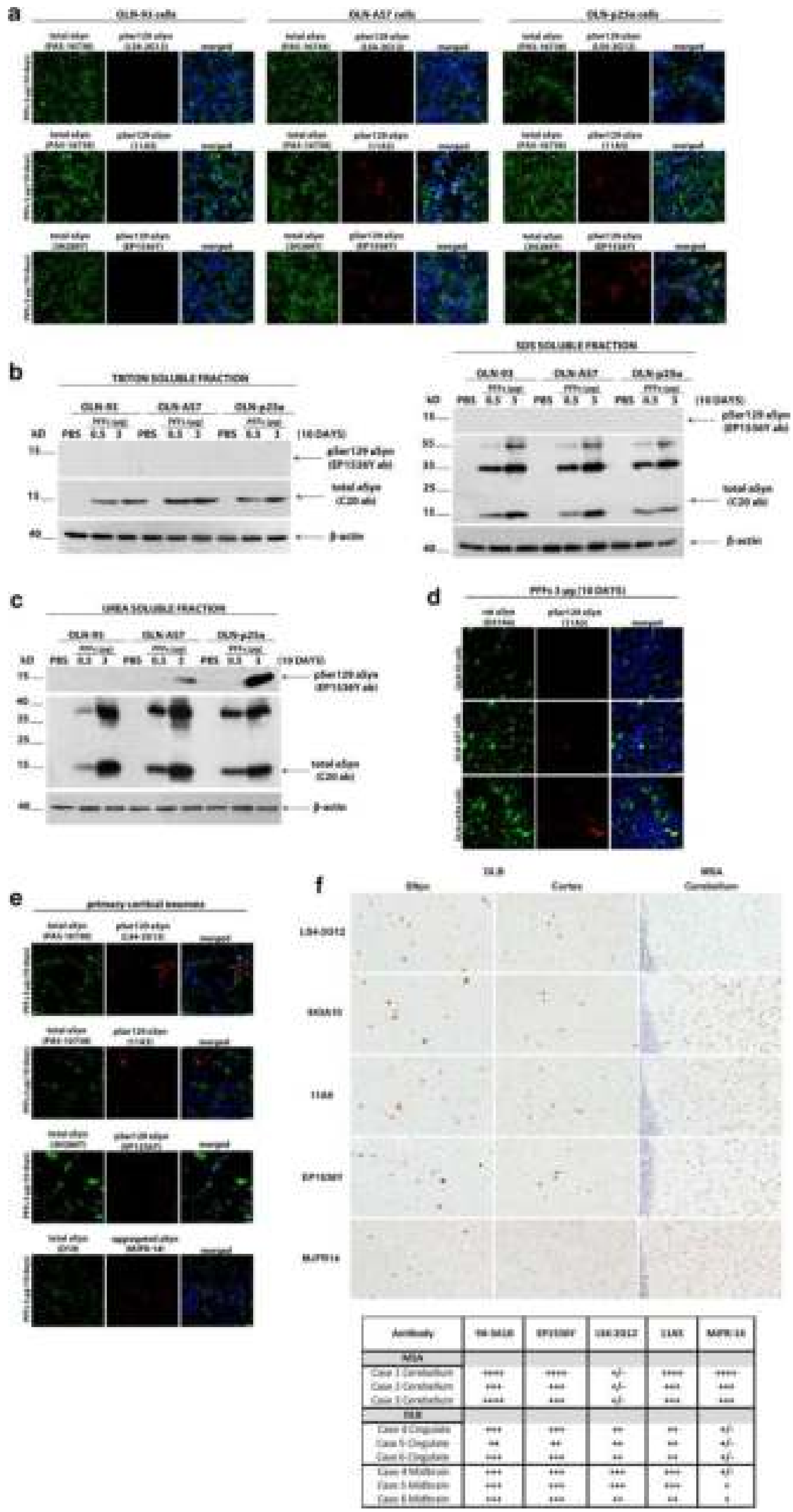
a
b
TRITON SOLUBLE FRACTION
SDS SOLUBLE FRACTION
β-actin
c
UREA SOLUBLE FRACTION
d
e
primary cortical neurons
f
DLB
MSA
Cortex
Cerebellum
Antibody

◂**Fig. 6** Comparative analysis of pSer129-aSyn phosphorylation in haSyn PFF-treated cultured cells and human post-mortem synucleinopathy brains. **a** OLN-93, OLN-AS7 and OLN-p25α cells were treated with 3 μg haSyn PFFs for 10 days and the phosphorylation of aSyn at Ser129 was examined using various pSer129 aSyn-specific antibodies by confocal microscopy. Representative immunofluorescence images with antibodies against total (human + rodent) aSyn (green, PA5-16738 or 3H2897 antibody) and pSer129 aSyn (red, LS4-2G12, 11A5, or EP1536Y antibody) and DAPI staining. Scale bar: 25 μm. **b**, **c** Phosphorylated aSyn at Ser129 (EP1536Y antibody) is detected by immunoblotting only in the urea-soluble fractions of OLN-AS7 and OLN-p25α cells following prolonged incubation with 3 μg PFFs. Representative immunoblots of Triton- and SDS-soluble protein fractions (**b**) or urea-soluble protein fractions (**c**) derived from OLN-93, OLN-AS7 and OLN-p25α cells treated with 0.5 μg or 3 μg of haSyn PFFs for 10 days. **d** Endogenous rat aSyn is phosphorylated at Ser129 following prolonged incubation with 3 μg PFFs only in OLN-AS7 and OLN-p25α cells. Representative immunofluorescence images with antibodies against endogenous rat aSyn (green, D37A6 antibody), pSer129 aSyn (red, 11A5 antibody) and DAPI staining. Scale bar: 25 μm. **e** Primary rat cortical neurons were treated with 3 μg haSyn PFFs for 10 days and phosphorylated aSyn, and aggregated aSyn were detected by confocal microscopy. Representative immunofluorescence images with antibodies against total (human + rodent) aSyn (green, PA5-16738, D10, or 3H2897 antibody), pSer129 aSyn (red, LS4-2G12, 11A5, or EP1536Y antibody), aggregated aSyn (red, MJFR-14 antibody) and DAPI staining. Scale bar: 25 μm. **f** (Upper panel) representative DAB-immunostained images using antibodies against phosphorylated (LS4-2G12, 11A5 and EP1536Y antibodies), aggregated aSyn (MJFR-14 antibody) and unmodified aSyn (94-3A10) in human post-mortem brain sections derived from the substantia nigra pars compacta and the cingulate cortex of DLB patients and from the cerebellum of MSA patients. Three confirmed cases of DLB and MSA were utilized for the analysis with similar results, whereby differential reactivity for GCIs vs. LBs was apparent for certain antibodies including LS4-2G12 and MJFR-14. (bottom panel) Immunohistochemical grading of aSyn pathology in different MSA and DLB cases. Glial cytoplasmic inclusions in MSA, cortical LBs in DLB cingulate and brainstem LBs in DLB midbrain were graded using a qualitative assessment of staining intensity and inclusion density by two independent observers. The findings are summarized as (±) rare, (+) mild, (++) moderate, (+++) strong and (++++) severe

the addition of haSyn PFFs (0.5 μg, 48 h) evoked a dramatic increase in the levels of endogenous mouse oligodendroglial aSyn only in the WT-aSyn and PLP-haSyn primary cultures (Fig. 8c). No fluorescence signal for the rodent-specific D37A6 aSyn antibody was detected in the KO-aSyn cultures or at baseline in the WT-aSyn and PLP-haSyn cultures in the absence of haSyn PFF treatment (Fig. 8c, f). The magnitude of the increase was dependent on the endogenous aSyn load, since the rodent-specific aSyn signal was more intense and more compact in the PLP-haSyn oligodendrocytes than in WT-aSyn oligodendrocytes (Fig. 8c). The formed aSyn species were aggregated, as verified by the strong immunoreactivity of the conformation-specific MJFR-14 antibody, which co-localized completely with the D10 antibody, recognizing the human + rodent protein (Fig. 8d). Interestingly, the expression pattern of aSyn in the haSyn-PLP cultures changed dramatically from diffuse (in PBS-treated cultures) to strongly punctated (in PFF-treated cultures), as detected by the LB509 and D10 antibodies (Fig. 8c, d). Finally, the rodent-specific positive puncta colocalized to a great extent with the oxidized/nitrated aSyn antibody in the WT-aSyn and haSyn-PLP cultures, but not in the KO-aSyn cultures (Fig. 8e, f), further indicating that the endogenous protein contributes to the formation of such pathological conformations.

Endogenous oligodendroglial aSyn protein load is closely linked to the re-distribution of microtubule-associated proteins upon the addition of haSyn PFFs

Given the close link between aSyn levels and the redistribution p25α in disease pathogenesis, we assessed the expression pattern of p25α in PFF-treated primary mouse oligodendrocytes. As shown in Fig. 9a, d, there was no apparent change in the pattern of p25α expression in PFF-treated KO-aSyn cultures (upper rows), in contrast to WT-aSyn cultures, in which p25α was redistributed from the oligodendroglial processes to the cell body, although no obvious co-localization with haSyn-positive aggregates was observed (middle rows). Remarkably, p25α in the PFF-treated PLP-haSyn oligodendrocytes, beyond its cell body redistribution, accumulated clearly in haSyn-positive cytoplasmic aggregates (bottom rows). This change was related to haSyn PFFs, given that p25α protein levels were similar between the untreated oligodendroglial cultures (Fig. 9a, d, e).

Since p25α is a tubulin polymerization-promoting protein that is involved in the organization of the microtubule network [65], its re-localization in the presence of haSyn PFFs might also be linked to the altered localization of other microtubule-associated proteins, such as tau, which has also been found to be present in GCIs [64]. To investigate whether the distribution pattern of tau was affected upon the addition of haSyn PFFs, we studied tau phosphorylated at residue Ser404 (pSer404-tau), which is one of the first sites to be hyperphosphorylated leading to the detachment of tau from microtubules, a phenomenon that is closely related to disease pathogenesis in tauopathies [1, 16, 36, 63]. Our data showed that pSer404-tau was redistributed from the processes to the cell soma upon the addition of haSyn PFFs in a manner dependent on the endogenous aSyn load, since this effect was more evident and robust in PLP-haSyn cultures, whereas the pSer404-tau immunostaining pattern remained unchanged only in the case of KO-aSyn primary oligodendrocytes (Fig. 9b, upper panel and d). However, pSer404-tau largely failed to be incorporated into haSyn aggregates, even in PLP-haSyn cultures, revealing a different behavior compared to p25α; this may have occured because this specific phosphorylated form, in contrast to p25α, is unable to bind to microtubules.

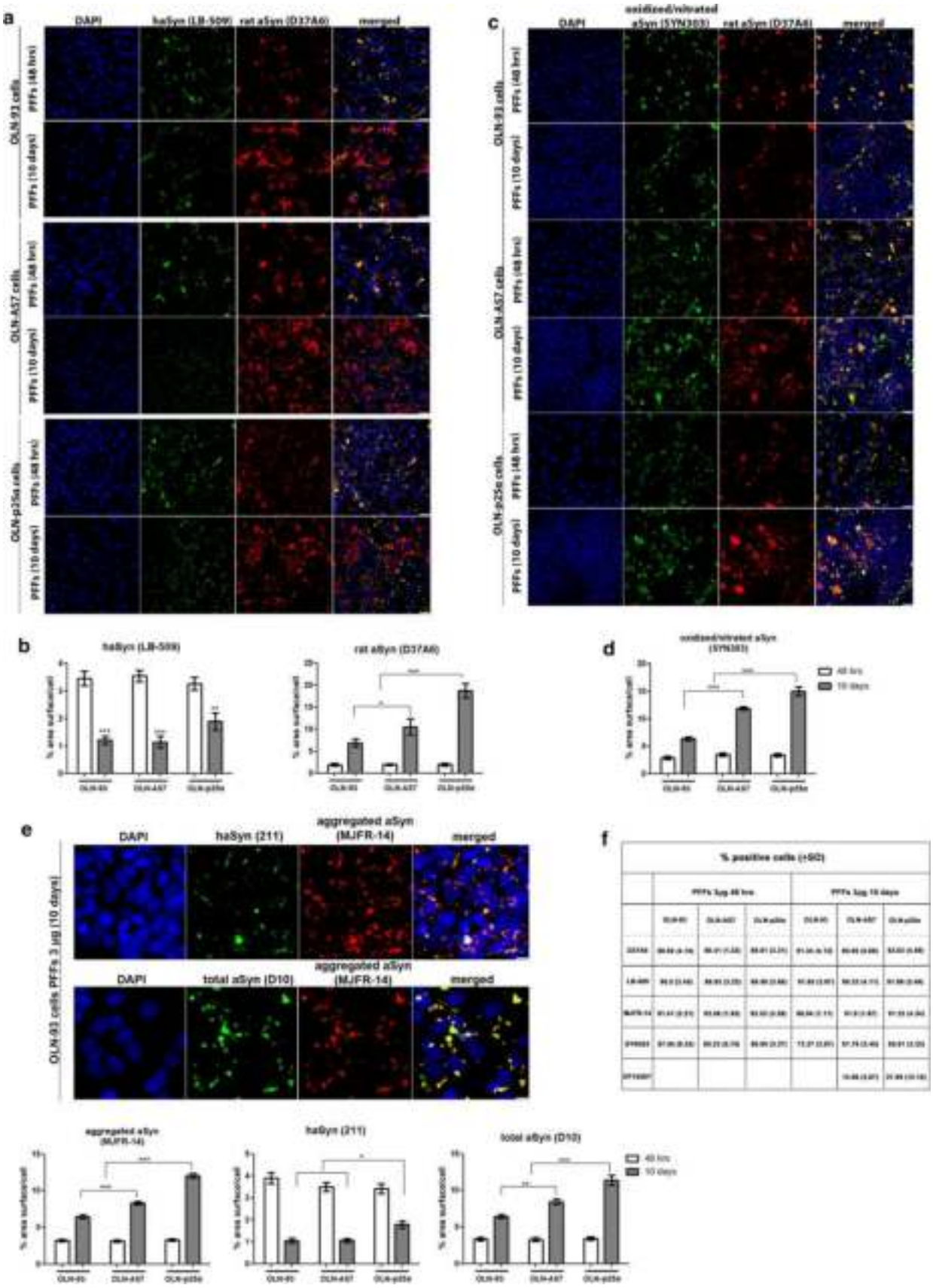
a
DAPI
haSyn (LB-509)
rat aSyn (D37A6)
merged
OLN-93 cells
OLN-AS7 cells
OLN-p25α cells
PFFs (48 hrs)
PFFs (10 days)
c
oxidized/nitrated aSyn (SYN303)
b
haSyn (LB-509)
rat aSyn (D37A6)
% area surface/cell
d
oxidized/nitrated aSyn (SYN303)
48 hrs
10 days
e
DAPI
haSyn (211)
aggregated aSyn (MJFR-14)
merged
OLN-93 cells PFFs 3 µg (10 days)
total aSyn (D10)
f
% positive cells (+SD)
PFFs 1µg 48 hrs
PFFs 1µg 10 days

◂**Fig. 7** Prolonged incubation of OLN cell lines with high concentrations of haSyn PFFs uncovers the significant contribution of endogenous rat oligodendroglial aSyn to the formation of aberrant aSyn conformations. **a**, **b** Over time, the equilibrium of aSyn protein load shifts toward seeded endogenous rodent aSyn in all cell lines. OLN-93, OLN-AS7 and OLN-p25α cells were incubated with 3 µg human aSyn PFFs for 48 h or 10 days, and the recruitment of endogenous rat aSyn was examined by confocal microscopy. **a** Representative immunofluorescence images with antibodies against human aSyn (green) and endogenous rat aSyn (red) and DAPI staining. Scale bar: 25 µm. **b** Quantification of human and endogenous rat aSyn protein levels measured as % area surface/cell in OLN cell lines following the addition of 3 µg PFFs for 48 h or 10 days. Data are expressed as the mean ± SE of at least three independent experiments with triplicate samples/condition within each experiment; $*p < 0.05$; $**p < 0.01$, $***p < 0.001$, by two-way ANOVA with Bonferroni's correction. **c** The addition of a high concentration of haSyn PFFs (3 µg) leads to the formation of time-resistant pathological (oxidized/nitrated) aSyn species, in which endogenous rat aSyn is the major constituent, as shown using antibodies against oxidized/nitrated aSyn (green) and endogenous rat aSyn (red) and DAPI staining. Scale bar: 25 µm. **d** Quantification of oxidized/nitrated aSyn protein levels measured as % area surface/cell in OLN cell lines following the addition of 3 µg PFFs for 48 h or 10 days. Data are expressed as the mean ± SE of at least three independent experiments with triplicate samples/condition within each experiment; $***p < 0.001$, by two-way ANOVA with Bonferroni's correction. **e** (upper panel) Incubation of OLN cells with 3 µg PFFs for 48 h or 10 days expedites the formation of aggregated conformations of aSyn. Representative immunofluorescence images with antibodies against human aSyn (green, 211 antibody, upper panel), total aSyn (human + rodent, green, D10, bottom panel) and aggregated aSyn (red) and DAPI staining in OLN-93 cells. Scale bar: 7.5 µm. (bottom panels) Quantification of aggregated (left), human (middle) and total (human + rodent) aSyn levels in all OLN cell lines treated with 3 µg haSyn PFFs for 48 h or 10 days, expressed as % area surface/cell verifies the aggregated nature of the generated aSyn assemblies and highlights the contribution of recruited endogenous rat aSyn to the formation of such structures. Data are expressed as the mean ± SE of at least three independent experiments with triplicate samples/condition within each experiment; $*p < 0.05$; $**p < 0.01$; $***p < 0.001$ by two-way ANOVA with Bonferroni's correction. **f** Quantification of the percentage of positively stained OLN-93, OLN-AS7 or OLN-p25α cells treated with 3 µg PFFs for 48 h or 10 days with antibodies against endogenous rat (D37A60), human (LB-509), aggregated (MJFR-14) or pathological aSyn species (oxidized/nitrated aSyn [Syn303] or pSer129-aSyn [EP1536Y]). All data are expressed as the mean ± SD of at least three independent experiments with triplicate samples/condition within each experiment

Finally, we assessed the impact of exogenously added haSyn PFFs on myelination, which is impaired in MSA brains [10, 12, 61]. The addition of haSyn PFFs to primary oligodendrocyte precursor cells reportedly leads to the disruption of MBP expression [21]. However, the role of endogenous aSyn in the levels and distribution of MBP remains unknown. In order to investigate whether alterations in the levels of endogenous oligodendroglial aSyn may be linked to alterations in myelin integrity, we assessed haSyn and MBP by confocal microscopy. Our data showed that the presence of endogenous mouse aSyn (in WT-aSyn cultures) or overexpressed human aSyn (in PLP-haSyn cultures) led to a dramatic alteration of MBP immunoreactivity following the addition of haSyn PFFs; in particular, MBP staining was drastically decreased and redistributed from the processes to the cell soma, largely colocalizing with aggregated haSyn (Fig. 9c, d). On the contrary, KO-aSyn mouse oligodendrocytes did not display any significant changes in MBP levels or distribution (Fig. 9c, upper panel), thus indicating a crucial role for seeded oligodendroglial aSyn aggregation in the alterations of MBP.

Delivery of haSyn PFFs into the mouse striatum is accompanied by the recruitment of endogenous oligodendroglial protein in MBP$^+$ pathological aggregates and the impairment of myelin integrity

In order to evaluate the seeding capacity of haSyn within oligodendrocytes in vivo, we performed unilateral stereotactic injections of haSyn PFFs (4 µg/brain) (or PBS as a control) into the mouse striatum, to imitate the situation occurring in MSA brains. As shown in Fig. 10a (bottom panels), the delivery of haSyn PFFs into the mouse striatum seeded the recruitment of endogenous mouse aSyn to form MBP-positive inclusions, which were positive for human and rodent aSyn, detected at 1 month post-injection (Fig. 10a, IPSI, indicated by the asterisks). The uptake of haSyn PFFs by oligodendrocytes was verified further by co-staining with the p25α antibody (Fig. 10b and Online Resource 15), whose specificity for oligodendrocytes in the mouse striatum was confirmed by its complete co-localization with O4 and Olig2 antibodies (Fig. 10c).

Consistent with the results in the primary oligodendroglial cultures, the MBP-positive signal changed dramatically upon the addition of haSyn PFFs, and MBP$^+$ puncta colocalized with the human (LB-509), rodent (D37A6), total (SYN1) and aggregated aSyn antibodies (Fig. 10a, d and Online Resource 14). Importantly, such alterations were not observed when a similar amount of haSyn PFFs was injected into the striatum of KO-aSyn mice (Fig. 10a, upper panels). Staining with the Syn303 aSyn antibody, which recognizes oxidized/nitrated species, revealed the formation of pathological aggregated aSyn assemblies in MBP$^+$ oligodendrocytes of the ipsilateral striatum within 1 month of injection (Fig. 10e). No Syn303 aSyn-positive signal was detected in haSyn PFF-injected KO-aSyn striatum (data not shown), and none of the aforementioned pathological alterations were observed in the ipsilateral striatum of WT-aSyn mice injected with PBS (Online Resource 9). Importantly, ultrastructural EM analysis revealed that haSyn PFFs evoked a clear rearrangement of the myelin sheath in the striatum of WT-aSyn mice, compared to PFF-treated KO-aSyn mice, as depicted by the increased number of axons with a decompacted myelin sheath and axons with myelin vesiculation (Fig. 10f, g). Such data support further the aforementioned results in PFF-treated primary oligodendrocytes (Fig. 9c,

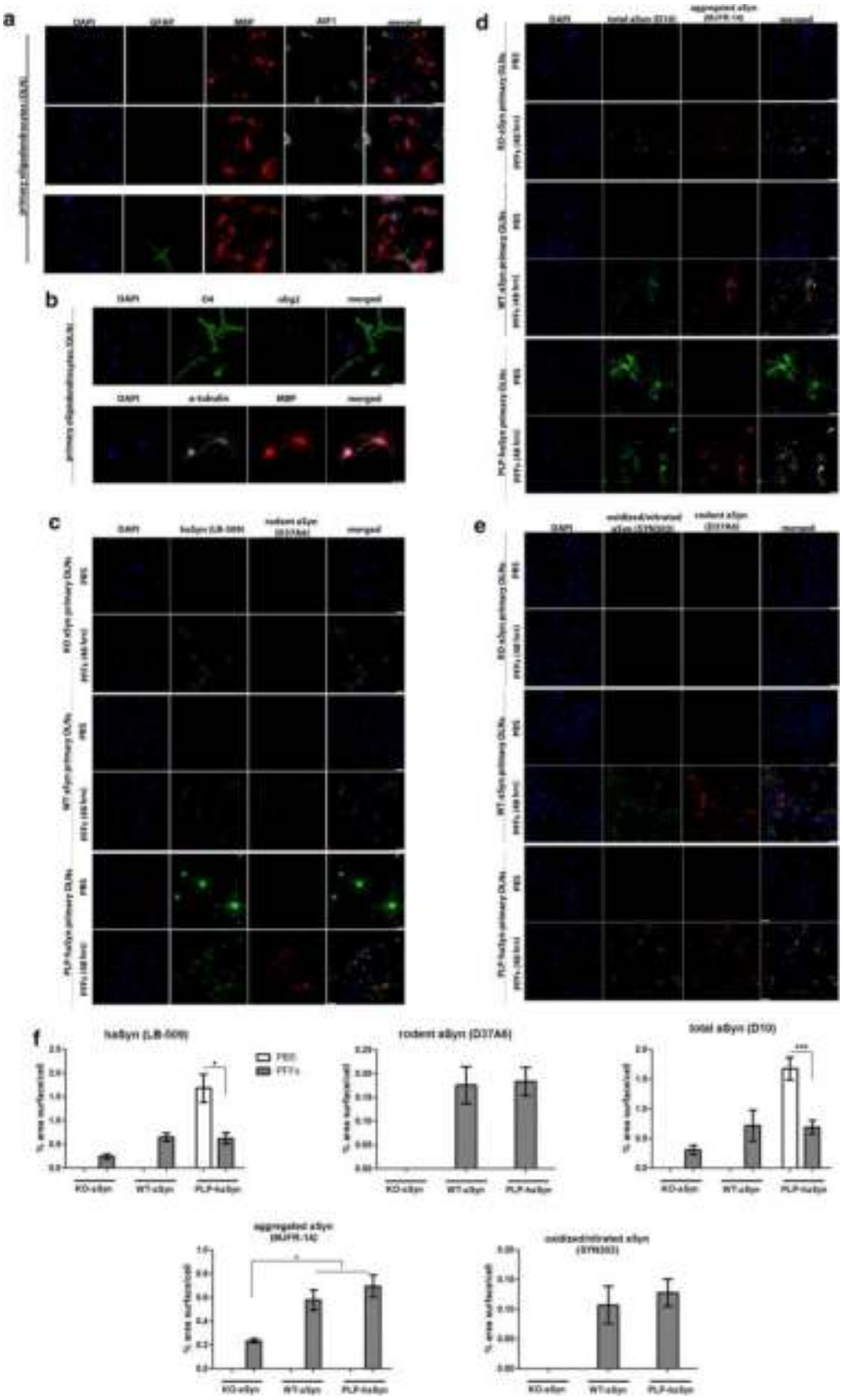
a
DAPI
GFAP
MBP
Aif1
merged
primary oligodendrocytes (OLN)
b
DAPI
O4
olig2
merged
DAPI
α-tubulin
MBP
merged
primary oligodendrocytes (OLN)
c
DAPI
haSyn (LB-509)
rodent aSyn (D37A6)
merged
KO-aSyn primary OLNs
WT-aSyn primary OLNs
PLP-haSyn primary OLNs
PBS
PFFs (48 hrs)
PFFs (168 hrs)
d
DAPI
total aSyn (D10)
aggregated aSyn (MJFR-14)
merged
KO-aSyn primary OLNs
WT-aSyn primary OLNs
PLP-haSyn primary OLNs
PBS
PFFs (48 hrs)
PFFs (168 hrs)
e
DAPI
oxidized/nitrated aSyn (SYN303)
rodent aSyn (D37A6)
merged
KO-aSyn primary OLNs
WT-aSyn primary OLNs
PLP-haSyn primary OLNs
PBS
PFFs (48 hrs)
PFFs (168 hrs)
f
haSyn (LB-509)
rodent aSyn (D37A6)
total aSyn (D10)
PBS
PFFs
% area surface/cell
KO-aSyn
WT-aSyn
PLP-haSyn
aggregated aSyn (MJFR-14)
oxidized/nitrated aSyn (SYN303)

◂**Fig. 8** Endogenous mouse oligodendroglial aSyn is incorporated into pathological aSyn assemblies in primary mouse oligodendroglial cultures following the addition of haSyn PFFs. **a**, **b** Mouse primary oligodendroglial cells derived from WT-aSyn pups were grown in SATO medium for 7 days prior to fixation and immunofluorescent analysis. The enrichment of the cultures in mature myelin-producing oligodendrocytes was confirmed with confocal microscopy using antibodies against glial fibrillary acidic protein as an astrocytic marker (green, GFAP), allograft inflammatory factor 1 (gray, AIF1/IbaI) as a marker for microglia and myelin basic protein (red, MBP) as a marker for mature oligodendrocytes (**a**), as well as against the oligodendroglial markers Olig2 (red, AB9610 antibody) and O4 (green, MAB1326 antibody) (**b**). α-Tubulin (gray, 62204 antibody) and DAPI staining were used as cytoskeletal and nuclear markers, respectively. Scale bars: 25 µm (**a**, upper panels), 50 µm (**a**, bottom panel) and 10 µm (**b**). **c** Confocal microscopy with human-specific (green) and rodent-specific (red) aSyn antibodies identifies the enhanced expression of endogenous mouse aSyn in WT-aSyn and PLP-haSyn oligodendroglial cultures, upon the addition of 0.5 µg haSyn PFFs for 48 h. No rodent-specific signal is detected in KO-aSyn cells. **d**, **e** Both exogenously added human aSyn and endogenous mouse aSyn contribute to the formation of aggregated (**d**) and oxidized/nitrated (**e**) conformations of aSyn in WT-aSyn and PLP-haSyn primary oligodendrocytes incubated with haSyn PFFs. Only exogenously added haSyn PFFs (**d**) and not oxidized/nitrated (**e**) conformations are detected in the KO-aSyn cultures. Representative immunofluorescent images using antibodies against total aSyn (green, D10 antibody) and aggregated aSyn (red) are shown in **d** and against oxidized/nitrated aSyn (green) and endogenous mouse aSyn (red) are shown in **e**. Scale bar: 25 µm. **f** Quantification of human, endogenous rodent and total (human and rodent) aSyn protein levels (upper panel) or aggregated and oxidized/nitrated aSyn protein levels (bottom panel) measured as % area surface/cell in KO-aSyn, WT-aSyn or PLP-haSyn mouse primary oligodendroglial cultures following the addition of 0.5 µg PFFs for 48 h. Data are expressed as the mean ± SE of at least three independent experiments with triplicate samples/condition within each experiment; $*p<0.05$; $***p<0.001$, by one-way ANOVA with Tukey's post hoc test (to compare between PBS- and PFF-treated cells) or by two-way ANOVA with Bonferroni's correction (to compare between the different PFF-treated cultures)

d) and in the PFF-treated ipsilateral WT-aSyn striatum (Fig. 10a, d).

Discussion

Two possible scenarios have been proposed to explain the origin of aSyn in oligodendrocytes and the mechanisms underlying aSyn accumulation in GCIs present in MSA brains: either oligodendrocytes pathologically overexpress aSyn in the context of MSA [3] or they take up neuronally derived protein from their environment [13, 21, 23, 24, 48, 49, 55, 58]. Our results combine these two scenarios by pinpointing the accumulation of endogenous oligodendroglial aSyn as a critical factor for the generation of pathological GCI-like aSyn structures within oligodendrocytes in vitro, triggered by exogenously added human fibrillar aSyn seeds. We also report that the oligodendroglial phosphoprotein p25α plays a pivotal role in the development and progression of aSyn aggregation, by modulating the rate and extent of aSyn seeding and, to some extent, by being incorporated into aSyn-rich pathological assemblies. Notably, the incorporation of endogenous oligodendroglial aSyn in such aberrant inclusions and the impairment of myelin integrity were demonstrated in the PFF-injected mouse brain, thus further highlighting the contribution of the endogenous protein in aSyn pathology in MSA-like models.

MSA, Parkinson's disease (PD), and DLB are collectively termed synucleinopathies [39, 41, 62]. In contrast to PD and DLB, in which aSyn accumulates in neurons that physiologically express the protein, in MSA, the pathological accumulation of abnormally folded aSyn is found mainly in oligodendrocytes [66]. Neuronal cytoplasmic and nuclear aSyn inclusions and dystrophic neurites can also be present in MSA brains; however, these lesions appear at a lower frequency than GCIs [40]. Initial studies suggested that oligodendrocytes do not express aSyn [35, 38, 60], whereas subsequent reports proposed that it may be expressed in oligodendrocytes, albeit at lower levels than in neurons [3, 9]. However, the prevailing hypothesis based mostly on in vitro data is that neurons secrete aSyn, which is subsequently taken up by surrounding oligodendrocytes [13, 21, 23, 24, 48, 49, 55, 58].

Herein, we assessed the capability of templating the misfolding of endogenous protein, to examine the hypothesis that the prion-like transformation of oligodendroglial aSyn can occur, as has been demonstrated for its neuronal counterpart [2, 29, 30, 59, 72]. Our results show that exogenously added haSyn PFFs are taken up by immortalized oligodendroglial cells and primary oligodendrocytes and can induce the formation of highly insoluble and pathological (aggregated, oxidized/nitrated, and under certain circumstances Ser129 phosphorylated) aSyn species in which the endogenous protein, however minute in amount at baseline, is a central component. The mechanism responsible for the tremendous increase in the expression of endogenous rodent aSyn following PFF addition remains unknown; we have found that the levels of rodent *Snca* mRNA are unchanged in this setting, consistent with the results reported by others in oligodendroglial progenitor cells [21], suggesting that the stabilization of oligodendrocyte aSyn may be involved. One possible scenario is that the catabolism of aSyn, most probably through the autophagy pathway as suggested by the accumulation of oligodendroglial aSyn upon lysosomal inhibition, is abrogated by the formation of aberrant aSyn species following the addition of haSyn PFFs.

An upsurge in the expression of endogenous aSyn in haSyn PFF-treated oligodendroglial progenitor cells in culture and the altered expression of proteins associated with neuromodulation and myelination were recently reported [21]. However, the authors of that study failed to find evidence that a similar process occurs in mature,

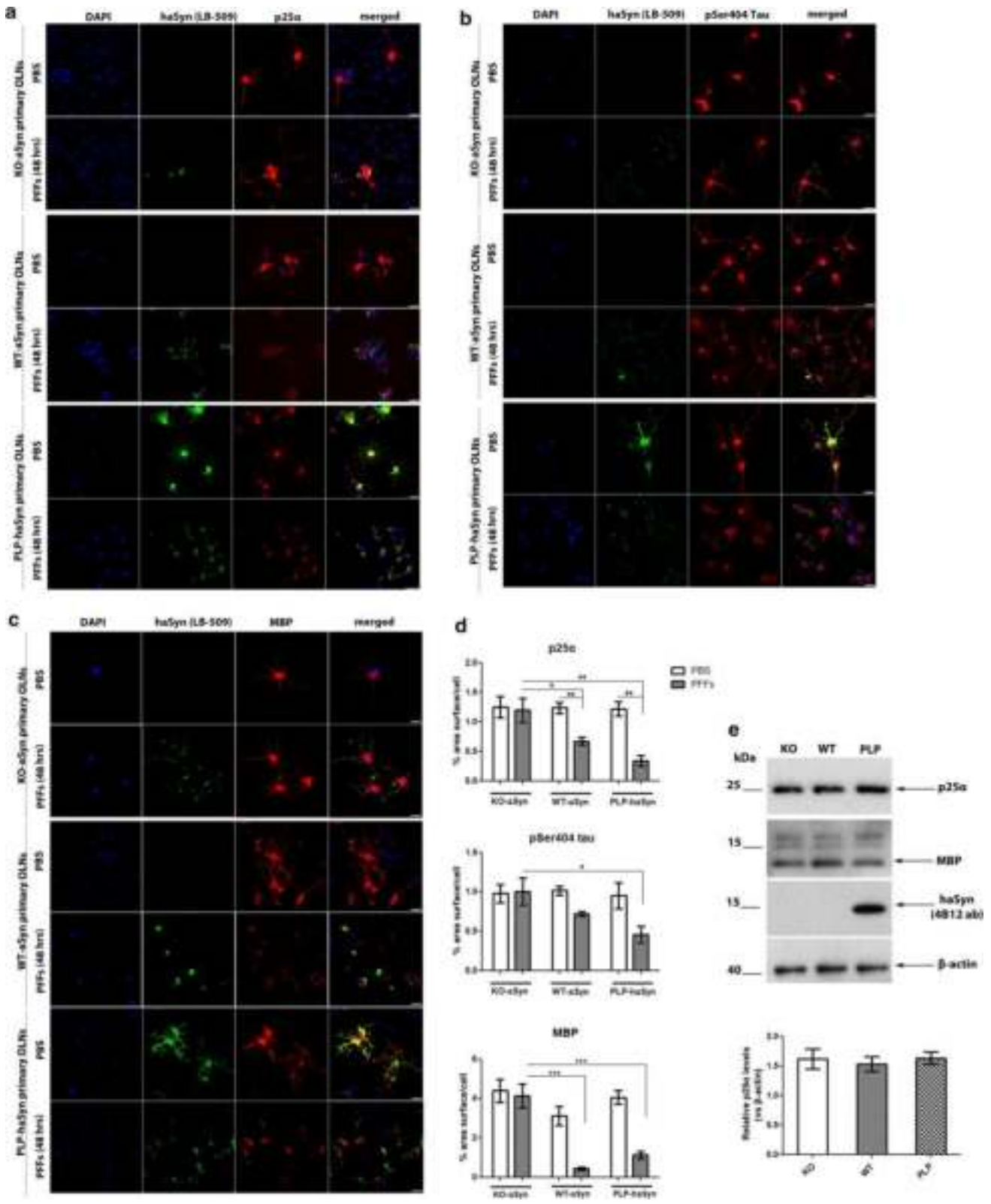

myelin-forming oligodendrocytes. Herein, we show clearly, in contrast to these data, that the addition of haSyn PFFs to mature differentiated mouse primary oligodendrocytes induces the seeding of endogenous rodent aSyn, and the dysregulation in myelin, as manifested by the decreased levels and perisomal redistribution of MBP, as well as the

◂**Fig. 9** The re-distribution of the microtubule-associated proteins p25α, tau, and MBP in primary oligodendroglial cells depends on endogenous aSyn protein load following the addition of haSyn PFFs. **a** p25α redistributes from the oligodendroglial processes to the cell body only in WT-aSyn and in PLP-aSyn cultures and is trapped in aSyn-positive aggregates only in PLP-haSyn oligodendroglial cells (bottom rows), following treatment with haSyn PFFs for 48 h. No relocalization of p25α is observed in KO aSyn primary oligodendroglial cultures (upper rows). Representative immunofluorescence images with antibodies against human aSyn (green, LB509), endogenous mouse p25α (red, p25α antibody) and DAPI staining. Scale bar: 25 µm. **b, c** The cellular pattern and distribution of phosphorylated tau at residue Ser404 and MBP changes dramatically following the addition of haSyn PFFs in a manner dependent upon the endogenous aSyn protein load. No differences are observed in KO-aSyn cultures treated with haSyn PFFs, thus highlighting the contribution of the endogenous oligodendroglial aSyn to the dysregulation of myelin. Immunofluorescence images with antibodies against human aSyn (green) and pSer404 tau (red, AP01708PU-N antibody) are shown in **b** and against human aSyn (green) and MBP (red) are shown in **c**. DAPI is used as a nuclear marker. Scale bar: 25 µm. **d** Quantification of p25α (upper row), pSer404 tau (middle row), or MBP protein levels (bottom row) in KO-aSyn, WT-aSyn and PLP-haSyn primary oligodendrocyte cultures treated with 0.5 µg haSyn PFFs for 48 h measured as % area surface/cell. Data are expressed as the mean ± SE of three independent experiments with three samples/condition within each experiment; $*p < 0.05$; $**p < 0.01$; $***p < 0.001$, by one-way ANOVA with Tukey's post hoc test (to compare between PBS- and PFF-treated cells) or by two-way ANOVA with Bonferroni's correction (to compare between the different PFF-treated cultures). **e** No differences are detected in p25α protein levels expressed in KO-aSyn, WT-aSyn, or PLP-haSyn primary oligodendrocytes. (upper panel) Representative immunoblots of p25α, MBP and haSyn (4B12 antibody) protein levels are shown. Equal loading was verified by the detection of β-actin levels. (bottom panel) Quantification of p25α protein levels expressed in all primary oligodendroglial cultures. Data are expressed as the mean ± SE of three independent experiments with triplicate samples/condition within each experiment

colocalization of MBP within aSyn-positive aggregates. This colocalization upon of haSyn PFF administration is similar to what is proposed to occur during the formation of GCIs in human MSA [74]. Such a disruption of the myelin sheath is responsible for demyelination, which contributes to disease pathology and clinical manifestations [12, 31, 61, 77]. Remarkably, this disruption of myelin was completely prevented in KO-aSyn cultures and in the PFF-injected KO-aSyn striatum, indicating that the presence of endogenous oligodendroglial rat aSyn is necessary for the manifestation of this pathological hallmark of MSA. Furthermore, p25α and phospho-tau staining in PFF-treated cultures demonstrated a disruption of the microtubule network that was dependent on the levels of endogenous aSyn. In agreement with our findings, Grigoletto et al. showed an age- and disease-dependent loss of the MBP signal in striatal striosomes accompanied by reduced p25α levels in oligodendrocytes in neuronal synucleinopathy mouse models [15]. They concluded that neuronal aSyn is involved in the regulation and/or maintenance of myelin phospholipids, since aSyn also inhibited the maturation of oligodendrocytes and the formation of membranous sheets in vitro [15].

Toward the same direction, our in vitro data suggest a role for p25α in the prion-like seeding process and aggregation of endogenous oligodendroglial aSyn, illustrating that both the stable and transient overexpression of p25α accelerated the seeding of endogenous aSyn and augmented the formation of pathological aSyn aggregates. p25α reportedly plays a critical role in myelin maturation and relocates early from the myelin sheath to the cytoplasm in MSA [61]. This relocation may impair myelin synthesis and seed aSyn aggregation in oligodendrocytes. A recent study also showed that p25α not only relocates from peripheral processes but also from the nucleus to the perinuclear cytoplasm in MSA patients [37]. The mechanism by which p25α enhances aSyn seeding and aggregation is unclear, and our data suggest it does not seem to involve necessarily the direct incorporation of p25α into aSyn aggregates, as this occurs only in the case of PLP-haSyn primary oligodendrocytes. Moreover, the absence of p25α redistribution in PFF-treated KO-aSyn cultures suggests that the presence of endogenous oligodendroglial aSyn is a prerequisite for such a phenomenon to occur. Hinting at a possible mechanism, preliminary experiments in our laboratory using OLN-AS7 cells showed that transient p25α overexpression triggered the phosphorylation aSyn at Ser129 and increased the total levels of aSyn (unpublished observations). Similarly, the co-expression of haSyn and p25α results in the phosphorylation of aggregated, but not monomeric aSyn, in OLN-AS7 cells [26]. Consistent with this idea, in the current work, p25α appeared to stabilize insoluble aSyn conformations. These findings may be applicable more broadly to alpha-synucleinopathies, since p25α is reportedly ectopically expressed in dopaminergic neurons in PD and to be a component of LBs purified from human post-mortem PD brains [28].

Research over the past few years using recombinant aSyn PFFs and samples from patients with synucleinopathy has provided support to the hypothesis that aSyn may misfold and propagate in a prion-like fashion in MSA patients [17]. The injection of brain homogenates containing aSyn derived from MSA patients into mice triggers the formation of phosphorylated aSyn aggregates and the onset of a neurodegenerative cascade comparable to human MSA pathology [4, 47]. Moreover, recent reports have shown that the aSyn pathological conformations found in MSA brains are remarkably stable and resistant to inactivation [75] and that MSA is caused by a unique strain of aSyn assemblies [34, 44, 47]. Supportive of the latter hypothesis are findings showing that pathological aSyn in GCIs and LBs (detected by the Syn303 and Syn7015 fibril-specific antibodies) is conformationally and biologically distinct and that oligodendrocytes, but not neurons, transform misfolded aSyn into a GCI-like strain, highlighting

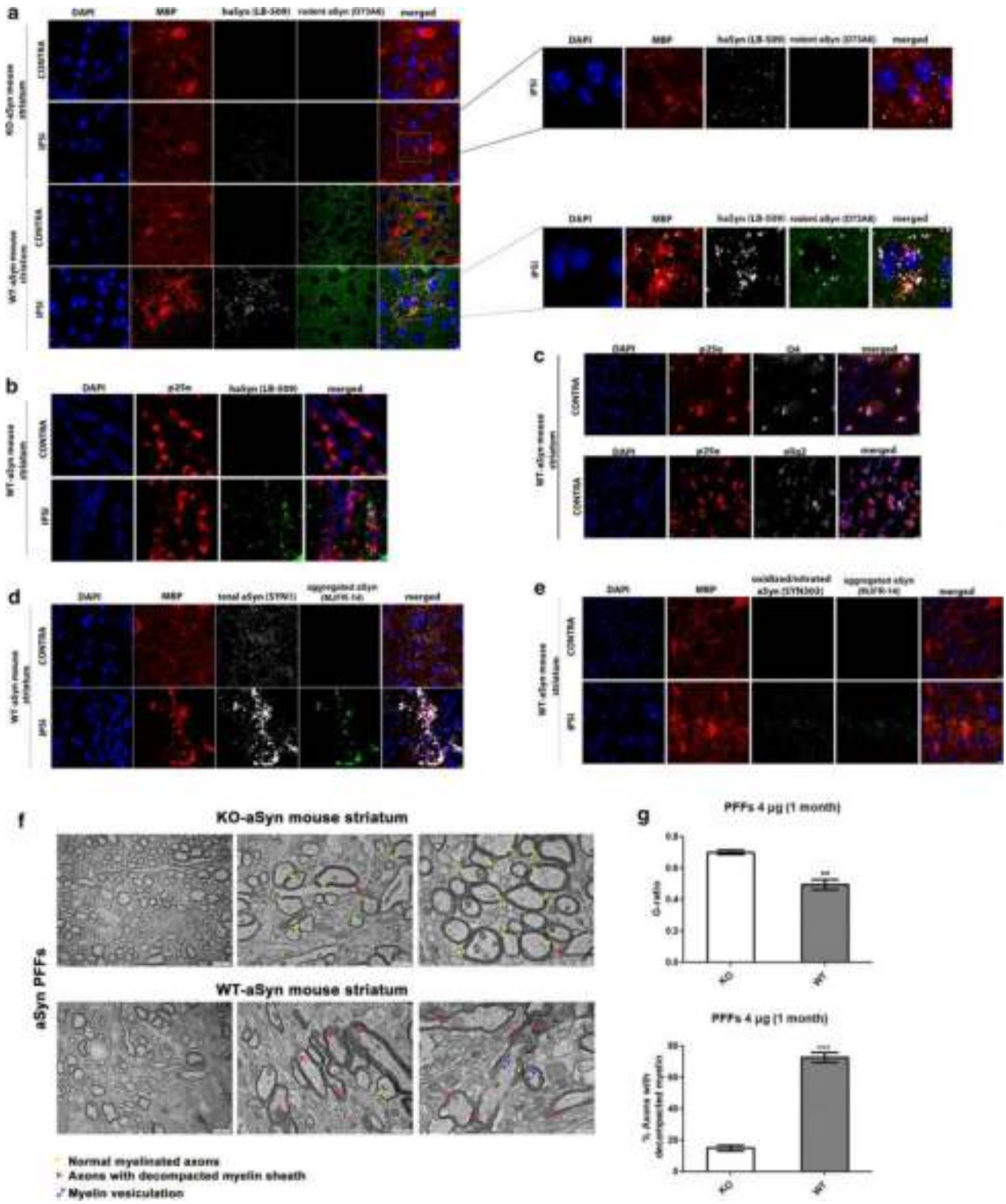

the fact that distinct aSyn strains are generated in different intracellular milieus [45]. Our comparative analyses of the phosphorylation status of aSyn utilizing different pSer129-specific antibodies in oligodendroglial cells, primary cortical neurons, and human post-mortem material from DLB and MSA brains, further favor the idea that synucleinopathies are caused by different aSyn strains leading to the detection of distinct aSyn pathological conformations in each disease, which depend on the intracellular context [34, 44, 45].

◂**Fig. 10** Unilateral delivery of haSyn PFFs (4 µg) into the WT-aSyn mouse striatum results in the recruitment of endogenous mouse oligodendroglial aSyn and the formation of pathological aSyn assemblies. **a** Representative immunofluorescence images showing the co-localization (indicated by the asterisks) of exogenously added human aSyn PFFs (gray) with endogenous mouse aSyn (green) in MBP^+ cells (red) in the ipsilateral (IPSI) striatum, but not in the contralateral (CONTRA) striatum, at 1 month post-injection (lower panel). Importantly, no endogenous mouse-specific aSyn signal was detected in the ipsilateral striatum of KO-aSyn mice (upper panel). Scale bar: 10 µm. High-power merged images are shown on the right. **b** Human aSyn PFFs are taken up by striatal oligodendrocytes in vivo, as shown by confocal microscopy using antibodies against human aSyn (green, LB-509 antibody) and the oligodendroglial marker p25α (red, p25α antibody). Scale bar: 10 µm. **c** The specificity of our home-made p25α antibody to oligodendrocytes was further verified using the O4 (gray, upper panel) and Olig2 (gray, bottom panel) antibodies. Scale bar: 10 µm. **d** MBP redistributes in the PFF-injected striatum and co-localizes with aggregated aSyn conformations. Representative immunofluorescence images for MBP (red), human aSyn (gray, SYN1 antibody), aggregated aSyn (green) and DAPI staining. Scale bar: 10 µm. **e** Pathological aSyn assemblies are detected in the ipsilateral striatum of WT-aSyn mice injected with haSyn PFFs at 1 month post-injection, as verified using antibodies against oxidized/nitrated aSyn (gray) and aggregated aSyn (green). Scale bar: 10 µm. **f** Ultrastructural transmission EM analysis of haSyn PFF-injected KO-aSyn (upper panel) or WT-aSyn (bottom panel) mouse striatum at 1 month post-injection, revealing myelin sheath decompaction only in WT-aSyn neuronal axons (red arrowheads) vs. normal myelinated axons (yellow asterisks). Purple arrowheads point to areas with vesiculated myelin sheaths. Scale bars: 2 µm (left panels), 1 µm (middle panels), and 500 nm (right panels). **g** Average myelin g-ratio values (upper row) and quantification of axons with decompacted myelin (bottom row) derived from haSyn PFF-injected KO-aSyn or WT-aSyn mouse striatum. Data are expressed as the mean ± SE of $n = 4$ mice per group. $^{**}p < 0.01$; $^{***}p < 0.001$ by Student's unpaired *t* test

Along these lines, it is important that we assessed aSyn pathology exclusively within the context of oligodendroglial cell lines, primary mature oligodendrocytes, and even in vivo within defined oligodendroglial cells in situ. Of course the present study has limitations that merit consideration, given that we have utilized uniquely synthetic haSyn PFFs to induce aSyn aggregation, an approach used widely in the field [46, 71, 72]. Another caveat is that we employed human aSyn PFFs, which reportedly induce less severe and widespread pSer129 aSyn pathology following injections in the rat olfactory bulb compared to mouse PFFs [52, 54]; if this is applicable in our in vivo PFF model remains to be addressed. Whether aSyn aggregation and seeding are primary or secondary events in the human MSA disease process and the exact role of p25α in the cascade of events in the context of the human disease are issues that have not yet been elucidated.

In agreement with our in vivo findings, the uptake of haSyn PFFs or GCI-related aSyn derived from MSA patients by oligodendrocytes have been reported [50, 55]. However, other studies have failed to detect exogenous haSyn within oligodendrocytes or other glial cells following inoculation with haSyn PFFs [42, 54]. These contradictory findings may be due to differences in the post-injection time frames when the assessments were performed, since although the uptake of injected aSyn by neurons reportedly occurs within minutes, the intraneuronal signal of internalized proteins begins to decrease at 3 h post-injection, probably due to clearance mechanisms [53]. Such a scenario may also apply to oligodendrocytes, given that only one in vivo study has shown the presence of exogenous aSyn within oligodendrocytes, assessed at 1 h post-injection [55]. Our in vitro data also demonstrate a decrease of the human protein over time, which, however, may be attributed to clearance mechanisms or to its dilution due to cell proliferation. Another explanation may be that the oligodendroglial uptake of haSyn in the PFF-inoculation models is restricted to near the site of injection, as we have also observed in our model (at least at 1 month post-injection).

Collectively, our study reveals that the administration of haSyn fibrils to cellular systems, i.e. immortalized oligodendroglial cells and differentiated primary oligodendrocytes, recapitulated critical aspects of MSA pathogenesis, thus representing an attractive model system to study the early events leading to GCI formation. Herein, we propose that endogenous aSyn and oligodendroglial phosphoprotein p25α form a dangerous dynamic duo that predisposes oligodendrocytes to accumulate intracellular aSyn aggregates reminiscent of the oligodendroglial inclusions in MSA. Finally, the identification of endogenous oligodendroglial aSyn as a major culprit for the development of pathology in vitro and in vivo suggests that manipulation of the expression of aSyn in oligodendrocytes may provide a rationale approach to combat its accumulation in GCIs and the progression of MSA. An alternative strategy may involve lowering p25α levels, as these also correlate with MSA-type pathology.

Acknowledgements The authors would like to thank the BRFAA biological imaging facility for their valuable contribution to confocal imaging and image analysis, George Tzanoukos (M.Sc., Head of the Biomedical Engineering Department, BRFAA) for technical assistance, and the BRFAA Animal Facility. The authors would also like to thank Dr. Nadia Stefanova (Innsbruck University) for providing the C57BL6 PLP-haSyn transgenic mice and Imago Pharmaceuticals for providing the 11A5 antibody. The authors also like to thank Dr. Lee Clough for editing the manuscript. PHJ was supported by the Lundbeck foundation Grant R223-2015-4222 and R248-2016-25. This work was supported by an MSA Coalition grant and a Bodossaki Grant to MX. Partial support was provided by an NIH grant NS1000876 to BG and by the Innovative Medicines Initiative 2 Joint Undertaking under Grant agreement No. 116060 (IMPRiND) to LS. This Joint Undertaking receives support from the European Union's Horizon 2020 research and innovation program and EFPIA. This work was supported by the Swiss State Secretariat for Education, Research and Innovation (SERI) under contract number 17.00038. The opinions expressed and arguments employed herein do not necessarily reflect the official views of these funding bodies.

Author contribution PM carried out the experiments, analyzed and interpreted the data, generated the figures, and participated in the study design, and in writing the manuscript. FA carried out the immunohistochemical analysis of the hPFF-injected mouse brains. AKK performed the initial experiments with the uptake of hPFFs in the OLN cell lines. MV carried out additional experiments required for resubmission. IK performed the EM analysis. MZ, KG, and SB generated the haSyn PFFs. ZS and BG performed immunohistochemical staining and comparative analyses of human brain tissue. PHJ provided the OLN cells, p25α plasmid, and p25α antibody. LS participated in study design, data interpretation, and in writing the manuscript. MX conceived the hypothesis, coordinated and led the study, and participated in study design, data interpretation and in writing the manuscript.

Compliance with ethical standards

Conflict of interest The authors have declared that no conflict of interest exists.

References

1. Alonso AC, Zaidi T, Grundke-Iqbal I, Iqbal K (1994) Role of abnormally phosphorylated tau in the breakdown of microtubules in Alzheimer disease. Proc Natl Acad Sci USA 91:5562–5566
2. Angot E, Steiner JA, Lema Tome CM, Ekstrom P, Mattsson B, Bjorklund A et al (2012) Alpha-synuclein cell-to-cell transfer and seeding in grafted dopaminergic neurons in vivo. PLoS One 7:e39465. https://doi.org/10.1371/journal.pone.0039465
3. Asi YT, Simpson JE, Heath PR, Wharton SB, Lees AJ, Revesz T et al (2014) Alpha-synuclein mRNA expression in oligodendrocytes in MSA. Glia 62:964–970. https://doi.org/10.1002/glia.22653
4. Bernis ME, Babila JT, Breid S, Wusten KA, Wullner U, Tamguney G (2015) Prion-like propagation of human brain-derived alpha-synuclein in transgenic mice expressing human wild-type alpha-synuclein. Acta Neuropathol Commun 3:75. https://doi.org/10.1186/s40478-015-0254-7
5. Bottenstein JE, Sato GH (1979) Growth of a rat neuroblastoma cell line in serum-free supplemented medium. Proc Natl Acad Sci USA 76:514–517
6. Cho MK, Nodet G, Kim HY, Jensen MR, Bernado P, Fernandez CO et al (2009) Structural characterization of alpha-synuclein in an aggregation prone state. Protein Sci 18:1840–1846. https://doi.org/10.1002/pro.194
7. Cruz-Martinez P, Gonzalez-Granero S, Molina-Navarro MM, Pacheco-Torres J, Garcia-Verdugo JM, Geijo-Barrientos E et al (2016) Intraventricular injections of mesenchymal stem cells activate endogenous functional remyelination in a chronic demyelinating murine model. Cell Death Dis 7:e2223. https://doi.org/10.1038/cddis.2016.130
8. Dickson DW, Liu W, Hardy J, Farrer M, Mehta N, Uitti R et al (1999) Widespread alterations of alpha-synuclein in multiple system atrophy. Am J Pathol 155:1241–1251
9. Djelloul M, Holmqvist S, Boza-Serrano A, Azevedo C, Yeung MS, Goldwurm S et al (2015) Alpha-synuclein expression in the oligodendrocyte lineage: an in vitro and in vivo study using rodent and human models. Stem Cell Reports 5:174–184. https://doi.org/10.1016/j.stemcr.2015.07.002
10. Don AS, Hsiao JH, Bleasel JM, Couttas TA, Halliday GM, Kim WS (2014) Altered lipid levels provide evidence for myelin dysfunction in multiple system atrophy. Acta Neuropathol Commun 2:150. https://doi.org/10.1186/s40478-014-0150-6
11. Duda JE, Giasson BI, Gur TL, Montine TJ, Robertson D, Biaggioni I et al (2000) Immunohistochemical and biochemical studies demonstrate a distinct profile of alpha-synuclein permutations in multiple system atrophy. J Neuropathol Exp Neurol 59:830–841
12. Ettle B, Kerman BE, Valera E, Gillmann C, Schlachetzki JC, Reiprich S et al (2016) Alpha-synuclein-induced myelination deficit defines a novel interventional target for multiple system atrophy. Acta Neuropathol 132:59–75. https://doi.org/10.1007/s00401-016-1572-y
13. Ettle B, Reiprich S, Deusser J, Schlachetzki JC, Xiang W, Prots I et al (2014) Intracellular alpha-synuclein affects early maturation of primary oligodendrocyte progenitor cells. Mol Cell Neurosci 62:68–78. https://doi.org/10.1016/j.mcn.2014.06.012
14. Fanciulli A, Wenning GK (2015) Multiple-system atrophy. N Engl J Med 372:249–263. https://doi.org/10.1056/NEJMra1311488
15. Grigoletto J, Pukass K, Gamliel A, Davidi D, Katz-Brull R, Richter-Landsberg C et al (2017) Higher levels of myelin phospholipids in brains of neuronal alpha-synuclein transgenic mice precede myelin loss. Acta Neuropathol Commun 5:37. https://doi.org/10.1186/s40478-017-0439-3
16. Gustke N, Steiner B, Mandelkow EM, Biernat J, Meyer HE, Goedert M et al (1992) The Alzheimer-like phosphorylation of tau protein reduces microtubule binding and involves Ser-Pro and Thr-Pro motifs. FEBS Lett 307:199–205
17. Jellinger KA (2018) Multiple system atrophy: an oligodendroglioneural synucleinopathy1. J Alzheimers Dis 62:1141–1179. https://doi.org/10.3233/JAD-170397
18. Jellinger KA (2006) P25alpha immunoreactivity in multiple system atrophy and Parkinson disease. Acta Neuropathol 112:112. https://doi.org/10.1007/s00401-006-0075-7
19. Jin H, Ishikawa K, Tsunemi T, Ishiguro T, Amino T, Mizusawa H (2008) Analyses of copy number and mRNA expression level of the alpha-synuclein gene in multiple system atrophy. J Med Dent Sci 55:145–153
20. Kahle PJ, Neumann M, Ozmen L, Muller V, Jacobsen H, Spooren W et al (2002) Hyperphosphorylation and insolubility of alpha-synuclein in transgenic mouse oligodendrocytes. EMBO Rep 3:583–588. https://doi.org/10.1093/embo-reports/kvf109
21. Kaji S, Maki T, Kinoshita H, Uemura N, Ayaki T, Kawamoto Y et al (2018) Pathological endogenous alpha-synuclein accumulation in oligodendrocyte precursor cells potentially induces inclusions in multiple system atrophy. Stem Cell Rep 10:356–365. https://doi.org/10.1016/j.stemcr.2017.12.001
22. Kim HY, Cho MK, Kumar A, Maier E, Siebenhaar C, Becker S et al (2009) Structural properties of pore-forming oligomers of alpha-synuclein. J Am Chem Soc 131:17482–17489. https://doi.org/10.1021/ja9077599
23. Kisos H, Pukass K, Ben-Hur T, Richter-Landsberg C, Sharon R (2012) Increased neuronal alpha-synuclein pathology associates with its accumulation in oligodendrocytes in mice modeling alpha-synucleinopathies. PLoS One 7:e46817. https://doi.org/10.1371/journal.pone.0046817
24. Konno M, Hasegawa T, Baba T, Miura E, Sugeno N, Kikuchi A et al (2012) Suppression of dynamin GTPase decreases alpha-synuclein uptake by neuronal and oligodendroglial cells: a potent therapeutic target for synucleinopathy. Mol Neurodegener 7:38. https://doi.org/10.1186/1750-1326-7-38
25. Kovacs GG, Laszlo L, Kovacs J, Jensen PH, Lindersson E, Botond G, Molnar T et al (2004) Natively unfolded tubulin polymerization promoting protein TPPP/p25 is a common marker of alpha-synucleinopathies. Neurobiol Dis 17:155–162. https://doi.org/10.1016/j.nbd.2004.06.006
26. Kragh CL, Lund LB, Febbraro F, Hansen HD, Gai WP, El-Agnaf O et al (2009) Alpha-synuclein aggregation and Ser-129 phosphorylation-dependent cell death in oligodendroglial cells. J Biol

Chem 284:10211–10222. https://doi.org/10.1074/jbc.M809671200
27. Lassen LB, Gregersen E, Isager AK, Betzer C, Kofoed RH, Jensen PH (2018) ELISA method to detect alpha-synuclein oligomers in cell and animal models. PLoS One 13:e0196056. https://doi.org/10.1371/journal.pone.0196056
28. Lindersson E, Lundvig D, Petersen C, Madsen P, Nyengaard JR, Hojrup P et al (2005) p25alpha Stimulates alpha-synuclein aggregation and is co-localized with aggregated alpha-synuclein in alpha-synucleinopathies. J Biol Chem 280:5703–5715. https://doi.org/10.1074/jbc.M410409200
29. Luk KC, Song C, O'Brien P, Stieber A, Branch JR, Brunden KR et al (2009) Exogenous alpha-synuclein fibrils seed the formation of Lewy body-like intracellular inclusions in cultured cells. Proc Natl Acad Sci USA 106:20051–20056. https://doi.org/10.1073/pnas.0908005106
30. Masuda-Suzukake M, Nonaka T, Hosokawa M, Oikawa T, Arai T, Akiyama H et al (2013) Prion-like spreading of pathological alpha-synuclein in brain. Brain 136:1128–1138. https://doi.org/10.1093/brain/awt037
31. Matsuo A, Akiguchi I, Lee GC, McGeer EG, McGeer PL, Kimura J (1998) Myelin degeneration in multiple system atrophy detected by unique antibodies. Am J Pathol 153:735–744. https://doi.org/10.1016/S0002-9440(10)65617-9
32. McCarthy KD, de Vellis J (1980) Preparation of separate astroglial and oligodendroglial cell cultures from rat cerebral tissue. J Cell Biol 85:890–902
33. McKeith IG, Dickson DW, Lowe J, Emre M, O'Brien JT, Feldman H et al (2005) Diagnosis and management of dementia with Lewy bodies: third report of the DLB Consortium. Neurology 65:1863–1872. https://doi.org/10.1212/01.wnl.0000187889.17253.b1
34. Melki R (2015) Role of different alpha-synuclein strains in synucleinopathies, similarities with other neurodegenerative diseases. J Parkinsons Dis 5:217–227. https://doi.org/10.3233/JPD-150543
35. Miller DW, Johnson JM, Solano SM, Hollingsworth ZR, Standaert DG, Young AB (2005) Absence of alpha-synuclein mRNA expression in normal and multiple system atrophy oligodendroglia. J Neural Transm (Vienna) 112:1613–1624. https://doi.org/10.1007/s00702-005-0378-1
36. Mondragon-Rodriguez S, Perry G, Luna-Munoz J, Acevedo-Aquino MC, Williams S (2014) Phosphorylation of tau protein at sites Ser(396-404) is one of the earliest events in Alzheimer's disease and Down syndrome. Neuropathol Appl Neurobiol 40:121–135. https://doi.org/10.1111/nan.12084
37. Ota K, Obayashi M, Ozaki K, Ichinose S, Kakita A, Tada M et al (2014) Relocation of p25alpha/tubulin polymerization promoting protein from the nucleus to the perinuclear cytoplasm in the oligodendroglia of sporadic and COQ2 mutant multiple system atrophy. Acta Neuropathol Commun 2:136. https://doi.org/10.1186/s40478-014-0136-4
38. Ozawa T, Okuizumi K, Ikeuchi T, Wakabayashi K, Takahashi H, Tsuji S (2001) Analysis of the expression level of alpha-synuclein mRNA using postmortem brain samples from pathologically confirmed cases of multiple system atrophy. Acta Neuropathol 102:188–190
39. Papp MI, Kahn JE, Lantos PL (1989) Glial cytoplasmic inclusions in the CNS of patients with multiple system atrophy (striatonigral degeneration, olivopontocerebellar atrophy and Shy-Drager syndrome). J Neurol Sci 94:79–100
40. Papp MI, Lantos PL (1992) Accumulation of tubular structures in oligodendroglial and neuronal cells as the basic alteration in multiple system atrophy. J Neurol Sci 107:172–182
41. Papp MI, Lantos PL (1994) The distribution of oligodendroglial inclusions in multiple system atrophy and its relevance to clinical symptomatology. Brain 117(Pt 2):235–243
42. Paumier KL, Luk KC, Manfredsson FP, Kanaan NM, Lipton JW, Collier TJ et al (2015) Intrastriatal injection of pre-formed mouse alpha-synuclein fibrils into rats triggers alpha-synuclein pathology and bilateral nigrostriatal degeneration. Neurobiol Dis 82:185–199. https://doi.org/10.1016/j.nbd.2015.06.003
43. Payne SC, Bartlett CA, Harvey AR, Dunlop SA, Fitzgerald M (2012) Myelin sheath decompaction, axon swelling, and functional loss during chronic secondary degeneration in rat optic nerve. Invest Ophthalmol Vis Sci 53:6093–6101. https://doi.org/10.1167/iovs.12-10080
44. Peelaerts W, Bousset L, Van der Perren A, Moskalyuk A, Pulizzi R, Giugliano M et al (2015) Alpha-synuclein strains cause distinct synucleinopathies after local and systemic administration. Nature 522:340–344. https://doi.org/10.1038/nature14547
45. Peng C, Gathagan RJ, Covell DJ, Medellin C, Stieber A, Robinson JL et al (2018) Cellular milieu imparts distinct pathological alpha-synuclein strains in alpha-synucleinopathies. Nature 557:558–563. https://doi.org/10.1038/s41586-018-0104-4
46. Polinski NK, Volpicelli-Daley LA, Sortwell CE, Luk KC, Cremades N, Gottler LM et al (2018) Best practices for generating and using alpha-synuclein pre-formed fibrils to model Parkinson's disease in rodents. J Parkinsons Dis 8:303–322. https://doi.org/10.3233/JPD-171248
47. Prusiner SB, Woerman AL, Mordes DA, Watts JC, Rampersaud R, Berry DB et al (2015) Evidence for alpha-synuclein prions causing multiple system atrophy in humans with parkinsonism. Proc Natl Acad Sci USA 112:E5308–E5317. https://doi.org/10.1073/pnas.1514475112
48. Pukass K, Goldbaum O, Richter-Landsberg C (2015) Mitochondrial impairment and oxidative stress compromise autophagosomal degradation of alpha-synuclein in oligodendroglial cells. J Neurochem 135:194–205. https://doi.org/10.1111/jnc.13256
49. Pukass K, Richter-Landsberg C (2014) Oxidative stress promotes uptake, accumulation, and oligomerization of extracellular alpha-synuclein in oligodendrocytes. J Mol Neurosci 52:339–352. https://doi.org/10.1007/s12031-013-0154-x
50. Radford R, Rcom-H'cheo-Gauthier A, Wong MB, Eaton ED, Quilty M, Blizzard C et al (2015) The degree of astrocyte activation in multiple system atrophy is inversely proportional to the distance to alpha-synuclein inclusions. Mol Cell Neurosci 65:68–81. https://doi.org/10.1016/j.mcn.2015.02.015
51. Reimer L, Vesterager LB, Betzer C, Zheng J, Nielsen LD, Kofoed RH et al (2018) Inflammation kinase PKR phosphorylates alpha-synuclein and causes alpha-synuclein-dependent cell death. Neurobiol Dis 115:17–28. https://doi.org/10.1016/j.nbd.2018.03.001
52. Rey NL, George S, Steiner JA, Madaj Z, Luk KC, Trojanowski JQ et al (2018) Spread of aggregates after olfactory bulb injection of alpha-synuclein fibrils is associated with early neuronal loss and is reduced long term. Acta Neuropathol 135:65–83. https://doi.org/10.1007/s00401-017-1792-9
53. Rey NL, Petit GH, Bousset L, Melki R, Brundin P (2013) Transfer of human alpha-synuclein from the olfactory bulb to interconnected brain regions in mice. Acta Neuropathol 126:555–573. https://doi.org/10.1007/s00401-013-1160-3
54. Rey NL, Steiner JA, Maroof N, Luk KC, Madaj Z, Trojanowski JQ et al (2016) Widespread transneuronal propagation of alpha-synucleinopathy triggered in olfactory bulb mimics prodromal Parkinson's disease. J Exp Med 213:1759–1778. https://doi.org/10.1084/jem.20160368
55. Reyes JF, Rey NL, Bousset L, Melki R, Brundin P, Angot E (2014) Alpha-synuclein transfers from neurons to oligodendrocytes. Glia 62:387–398. https://doi.org/10.1002/glia.22611

56. Richter-Landsberg C, Gorath M, Trojanowski JQ, Lee VM (2000) alpha-synuclein is developmentally expressed in cultured rat brain oligodendrocytes. J Neurosci Res 62:9–14. https://doi.org/10.1002/1097-4547(20001001)62:1%3c9:AID-JNR2%3e3.0.CO;2-U
57. Richter-Landsberg C, Heinrich M (1996) OLN-93: a new permanent oligodendroglia cell line derived from primary rat brain glial cultures. J Neurosci Res 45:161–173. https://doi.org/10.1002/(SICI)1097-4547(19960715)45:2%3c161:AID-JNR8%3e3.0.CO;2-8
58. Rockenstein E, Ubhi K, Inglis C, Mante M, Patrick C, Adame A et al (2012) Neuronal to oligodendroglial alpha-synuclein redistribution in a double transgenic model of multiple system atrophy. NeuroReport 23:259–264. https://doi.org/10.1097/WNR.0b013e3283509842
59. Sacino AN, Thomas MA, Ceballos-Diaz C, Cruz PE, Rosario AM, Lewis J et al (2013) Conformational templating of alpha-synuclein aggregates in neuronal-glial cultures. Mol Neurodegener 8:17. https://doi.org/10.1186/1750-1326-8-17
60. Solano SM, Miller DW, Augood SJ, Young AB, Penney JB Jr (2000) Expression of alpha-synuclein, parkin, and ubiquitin carboxy-terminal hydrolase L1 mRNA in human brain: genes associated with familial Parkinson's disease. Ann Neurol 47:201–210
61. Song YJ, Lundvig DM, Huang Y, Gai WP, Blumbergs PC, Hojrup P et al (2007) p25alpha relocalizes in oligodendroglia from myelin to cytoplasmic inclusions in multiple system atrophy. Am J Pathol 171:1291–1303. https://doi.org/10.2353/ajpath.2007.070201
62. Spillantini MG, Crowther RA, Jakes R, Cairns NJ, Lantos PL, Goedert M (1998) Filamentous alpha-synuclein inclusions link multiple system atrophy with Parkinson's disease and dementia with Lewy bodies. Neurosci Lett 251:205–208
63. Sun Q, Gamblin TC (2009) Pseudohyperphosphorylation causing AD-like changes in tau has significant effects on its polymerization. Biochemistry 48:6002–6011. https://doi.org/10.1021/bi900602h
64. Takeda A, Arai N, Komori T, Iseki E, Kato S, Oda M (1997) Tau immunoreactivity in glial cytoplasmic inclusions in multiple system atrophy. Neurosci Lett 234:63–66
65. Tirian L, Hlavanda E, Olah J, Horvath I, Orosz F, Szabo B et al (2003) TPPP/p25 promotes tubulin assemblies and blocks mitotic spindle formation. Proc Natl Acad Sci USA 100:13976–13981. https://doi.org/10.1073/pnas.2436331100
66. Trojanowski JQ, Revesz T (2007) Proposed neuropathological criteria for the post mortem diagnosis of multiple system atrophy. Neuropathol Appl Neurobiol 33:615–620. https://doi.org/10.1111/j.1365-2990.2007.00907.x
67. Tu PH, Galvin JE, Baba M, Giasson B, Tomita T, Leight S et al (1998) Glial cytoplasmic inclusions in white matter oligodendrocytes of multiple system atrophy brains contain insoluble alpha-synuclein. Ann Neurol 44:415–422. https://doi.org/10.1002/ana.410440324
68. Uryu K, Richter-Landsberg C, Welch W, Sun E, Goldbaum O, Norris EH et al (2006) Convergence of heat shock protein 90 with ubiquitin in filamentous alpha-synuclein inclusions of alpha-synucleinopathies. Am J Pathol 168:947–961
69. Vekrellis K, Xilouri M, Emmanouilidou E, Stefanis L (2009) Inducible over-expression of wild type alpha-synuclein in human neuronal cells leads to caspase-dependent non-apoptotic death. J Neurochem 109:1348–1362. https://doi.org/10.1111/j.1471-4159.2009.06054.x
70. Vogiatzi T, Xilouri M, Vekrellis K, Stefanis L (2008) Wild type alpha-synuclein is degraded by chaperone-mediated autophagy and macroautophagy in neuronal cells. J Biol Chem 283:23542–23556. https://doi.org/10.1074/jbc.M801992200
71. Volpicelli-Daley LA, Luk KC, Lee VM (2014) Addition of exogenous alpha-synuclein preformed fibrils to primary neuronal cultures to seed recruitment of endogenous alpha-synuclein to Lewy body and Lewy neurite-like aggregates. Nat Protoc 9:2135–2146. https://doi.org/10.1038/nprot.2014.143
72. Volpicelli-Daley LA, Luk KC, Patel TP, Tanik SA, Riddle DM, Stieber A et al (2011) Exogenous alpha-synuclein fibrils induce Lewy body pathology leading to synaptic dysfunction and neuron death. Neuron 72:57–71. https://doi.org/10.1016/j.neuron.2011.08.033
73. Wakabayashi K, Yoshimoto M, Tsuji S, Takahashi H (1998) Alpha-synuclein immunoreactivity in glial cytoplasmic inclusions in multiple system atrophy. Neurosci Lett 249:180–182
74. Wenning GK, Stefanova N, Jellinger KA, Poewe W, Schlossmacher MG (2008) Multiple system atrophy: a primary oligodendrogliopathy. Ann Neurol 64:239–246. https://doi.org/10.1002/ana.21465
75. Woerman AL, Kazmi SA, Patel S, Freyman Y, Oehler A, Aoyagi A et al (2018) MSA prions exhibit remarkable stability and resistance to inactivation. Acta Neuropathol 135:49–63. https://doi.org/10.1007/s00401-017-1762-2
76. Woerman AL, Watts JC, Aoyagi A, Giles K, Middleton LT, Prusiner SB (2018) Alpha-synuclein: multiple system atrophy prions. Cold Spring Harb Perspect Med. https://doi.org/10.1101/cshperspect.a024588
77. Wong JH, Halliday GM, Kim WS (2014) Exploring myelin dysfunction in multiple system atrophy. Exp Neurobiol 23:337–344. https://doi.org/10.5607/en.2014.23.4.337
78. Xilouri M, Brekk OR, Landeck N, Pitychoutis PM, Papasilekas T, Papadopoulou-Daifoti Z et al (2013) Boosting chaperone-mediated autophagy in vivo mitigates alpha-synuclein-induced neurodegeneration. Brain 136:2130–2146. https://doi.org/10.1093/brain/awt131
79. Xilouri M, Kyratzi E, Pitychoutis PM, Papadopoulou-Daifoti Z, Perier C, Vila M et al (2012) Selective neuroprotective effects of the S18Y polymorphic variant of UCH-L1 in the dopaminergic system. Hum Mol Genet 21:874–889. https://doi.org/10.1093/hmg/ddr521
80. Xiong B, Li A, Lou Y, Chen S, Long B, Peng J et al (2017) Precise cerebral vascular atlas in stereotaxic coordinates of whole mouse brain. Front Neuroanat 11:128. https://doi.org/10.3389/fnana.2017.00128

Publisher's Note Springer Nature remains neutral with regard to jurisdictional claims in published maps and institutional affiliations.

Affiliations

Panagiota Mavroeidi[1] · Fedra Arvanitaki[1] · Anastasia-Kiriaki Karakitsou[1] · Maria Vetsi[1] · Ismini Kloukina[2] · Markus Zweckstetter[3,4] · Karin Giller[4] · Stefan Becker[4] · Zachary A. Sorrentino[5,6] · Benoit I. Giasson[5,6,7] · Poul Henning Jensen[8] · Leonidas Stefanis[1,9] · Maria Xilouri[1]

1 Center of Clinical Research, Experimental Surgery and Translational Research, Biomedical Research Foundation of the Academy of Athens (BRFAA), 4 Soranou Efesiou Street, 11527 Athens, Greece

2 Center of Basic Research, Biomedical Research Foundation of the Academy of Athens, Athens, Greece

3 German Center for Neurodegenerative Diseases (DZNE), Von-Siebold-Str. 3a, 37075 Göttingen, Germany

4 Department for NMR-based Structural Biology, Max Planck Institute for Biophysical Chemistry, Am Faßberg 11, 37077 Göttingen, Germany

5 Department of Neuroscience, University of Florida, Gainesville, FL 32610, USA

6 Center for Translational Research in Neurodegenerative Disease, University of Florida, Gainesville, FL 32610, USA

7 McKnight Brain Institute, University of Florida, Gainesville, FL 32610, USA

8 DANDRITE-Danish Research Institute of Translational Neuroscience and Department of Biomedicine, University of Aarhus, Aarhus C, Denmark

9 1st Department of Neurology, Eginition Hospital, Medical School, National and Kapodistrian University of Athens, Athens, Greece

frontiers in Cell and Developmental Biology

REVIEW
published: 04 September 2020
doi: 10.3389/fcell.2020.559791

In Search of Effective Treatments Targeting α-Synuclein Toxicity in Synucleinopathies: Pros and Cons

*Maria Fouka†, Panagiota Mavroeidi†, Grigoria Tsaka† and Maria Xilouri**

Center of Clinical Research, Experimental Surgery and Translational Research, Biomedical Research Foundation of the Academy of Athens, Athens, Greece

Parkinson's disease (PD), multiple system atrophy (MSA) and Dementia with Lewy bodies (DLB) represent pathologically similar, progressive neurodegenerative disorders characterized by the pathological aggregation of the neuronal protein α-synuclein. PD and DLB are characterized by the abnormal accumulation and aggregation of α-synuclein in proteinaceous inclusions within neurons named Lewy bodies (LBs) and Lewy neurites (LNs), whereas in MSA α-synuclein inclusions are mainly detected within oligodendrocytes named glial cytoplasmic inclusions (GCIs). The presence of pathologically aggregated α-synuclein along with components of the protein degradation machinery, such as ubiquitin and p62, in LBs and GCIs is considered to underlie the pathogenic cascade that eventually leads to the severe neurodegeneration and neuroinflammation that characterizes these diseases. Importantly, α-synuclein is proposed to undergo pathogenic misfolding and oligomerization into higher-order structures, revealing self-templating conformations, and to exert the ability of "*prion-like*" spreading between cells. Therefore, the manner in which the protein is produced, is modified within neural cells and is degraded, represents a major focus of current research efforts in the field. Given that α-synuclein protein load is critical to disease pathogenesis, the identification of means to limit intracellular protein burden and halt α-synuclein propagation represents an obvious therapeutic approach in synucleinopathies. However, up to date the development of effective therapeutic strategies to prevent degeneration in synucleinopathies is limited, due to the lack of knowledge regarding the precise mechanisms underlying the observed pathology. This review critically summarizes the recent developed strategies to counteract α-synuclein toxicity, including those aimed to increase protein degradation, to prevent protein aggregation and cell-to-cell propagation, or to engage antibodies against α-synuclein and discuss open questions and unknowns for future therapeutic approaches.

Keywords: α-synuclein, autophagy, immunotherapy, propagation, protein aggregation, proteasome, synucleinopathies, therapeutics

OPEN ACCESS

Edited by:
Franziska Richter Assencio, University of Veterinary Medicine Hannover, Germany

Reviewed by:
Lisa Fellner, Innsbruck Medical University, Austria
Kelvin C. Luk, University of Pennsylvania, United States

***Correspondence:**
Maria Xilouri
mxilouri@bioacademy.gr

† These authors have contributed equally to this work

Specialty section:
This article was submitted to Molecular Medicine, a section of the journal Frontiers in Cell and Developmental Biology

Received: *07 May 2020*
Accepted: *14 August 2020*
Published: *04 September 2020*

Citation:
Fouka M, Mavroeidi P, Tsaka G and Xilouri M (2020) In Search of Effective Treatments Targeting α-Synuclein Toxicity in Synucleinopathies: Pros and Cons. Front. Cell Dev. Biol. 8:559791. doi: 10.3389/fcell.2020.559791

INTRODUCTION

α-synuclein is a neuronal presynaptic protein, which physiologically regulates neurotransmitter release, whereas its pathological accumulation is the key histopathological hallmark of certain neurodegenerative disorders with similar clinical phenotypes, designated as synucleinopathies (Spillantini and Goedert, 2000). Specifically, in Parkinson's disease (PD) and dementia with Lewy

bodies (DLB), α-synuclein mostly accumulates in Lewy bodies (LBs) and Lewy neurites (LNs) in neurons (Spillantini et al., 1997, 1998), whereas in multiple system atrophy (MSA) α-synuclein deposits mostly within the cytoplasm of oligodendrocytes forming glial cytoplasmic inclusions (GCIs) (Wakabayashi et al., 1998a,b; Nakamura et al., 2015). It is widely accepted that PD, DLB and MSA pathogenesis is the result of complex molecular events and that common pathogenic mechanisms may lead to α-synuclein deposition in these disorders. However, the diversity of α-synuclein pathology observed in α-synucleinopathies is attributed to various events, such as the presence of more than one α-synuclein strain, the intracellular milieu, the interaction of α-synuclein with multiple molecular partners, and the propagation of α-synuclein within different brain regions (Peng et al., 2018b; Longhena et al., 2019). The precise genetic and/or environmental trigger for α-synuclein misfolding still remains unknown; however, genetic mutations, mitochondrial dysfunction, proteolytic systems failure and neuroinflammation have been proposed to facilitate α-synuclein spread in the diseased brain (Polymeropoulos et al., 1997; Bose and Beal, 2016; Rocha et al., 2018). Under physiological conditions, neuronal α-synuclein is found either in the cytosol in a soluble and natively unfolded monomeric or tetrameric form (Weinreb et al., 1996; Bartels et al., 2011; Wang et al., 2011; Fauvet et al., 2012) or in a membrane-bound or vesicle-associated state (Pirc and Ulrih, 2015; Gustafsson et al., 2018; Lautenschlager et al., 2018). On the other hand, pathological α-synuclein in oligomeric, pre-fibrillar and fibrillar form can spread within the diseased brain via various cell-to-cell transmission mechanisms, which are responsible either for its release from neurons or its uptake by neighboring cells. The tendency of α-synuclein to form aggregates lies in the core of its neurotoxic potential and strategies seeking to alleviate the total protein load represent an obvious therapeutic approach.

Current therapeutic approaches for PD and related synucleinopathies can provide only palliative treatment, aiming to control the motor symptoms and delay disease progression. The lack of reliable *in vivo* markers and appropriate animal models to recapitulate the symptoms of these diseases challenge therapy development; however numerous studies have suggested various therapeutic efforts to counteract α-synuclein-related pathology. In the current review, we summarize advances in understanding the pivotal role of α-synuclein in the pathogenesis of synucleinopathies and critically discuss the potential of current therapeutic approaches favoring pathology amelioration with the pros and cons of each strategy.

THE STRUCTURE, FUNCTION AND AGGREGATION OF α-SYNUCLEIN

The synuclein protein was originally identified through several and independent lines of investigation. In 1985, a neuron-specific protein of 143 amino acids (aa) was identified in Torpedo californica cholinergic synaptic vesicles (Maroteaux et al., 1988). Later studies in amyloid plaques from an Alzheimer's disease (AD) brain discovered two unknown peptides, in addition to the major amyloid beta fragment, which were named NAC (non-A beta component of AD amyloid) peptide and its precursor, NACP (Ueda et al., 1993) and identified two proteins of 140 and 134 aa, which were highly expressed in the human brain (Jakes et al., 1994). These results revealed the existence of a new protein family expressed predominantly in presynaptic nerve terminals. The 140 aa protein was named α-synuclein, while the 134 aa protein β-synuclein (Jakes et al., 1994). The third and last protein of the family, γ-synuclein, was found to be highly expressed in ovarian and breast carcinomas (Ji et al., 1997; Bruening et al., 2000).

Structurally, α-synuclein encoded by the *SNCA* gene, lacks a single stable 3D structure in aqueous solutions, transmembrane domain or lipid anchor, concluding that it may behave as a peripheral membrane protein (Weinreb et al., 1996). α-synuclein is composed of three distinct domains namely N-terminal lipid-binding domain, amyloid-binding central region (NAC) and C-terminal binding domain (**Figure 1**). The N-terminal domain is a positively charged lysine-rich region characterized by the presence of a series of seven imperfect amphipathic 11 aa repeats containing a highly conserved KTKEGV hexameric motif, which enable the protein to acquire alpha-helical structure, thus reducing the tendency to form ß-structure and modulating the interactions with membranes (Chandra et al., 2003; Ulmer et al., 2005; Sode et al., 2006). The central NAC region is composed of nonpolar side-chains and assembles cross b-structures, which are involved in fibril formation and aggregation. Based on that, it has been proven that the deletion of specific residues (74–84) within the core region can abolish α-synuclein aggregation (Giasson et al., 2001; Rodriguez et al., 2015). Lastly, the C-terminal domain is a highly acidic tail reported to interact with metals, small molecules, proteins and other α-synuclein domains (Kim et al., 2002; Ly and Julian, 2008).

Even though α-synuclein is considered a natively unfolded, intrinsically disordered amyloid protein, it can adopt an a-helical conformation in the presence of membranes enriched with acidic phospholipid headgroups and high curvature (Davidson et al., 1998; Pirc and Ulrih, 2015) and form fibrillar assembles by converting soluble monomers into β-sheet-like secondary structures. The existence of the protein above a crucial concentration, along with its thermodynamically unstable innate behavior, favors the aggregation and accumulation process, which is closely related to its neurotoxic potential (Ferreon and Deniz, 2007; Afitska et al., 2019). Up to date the native state of α-synuclein remains controversial. Although some studies have reported that α-synuclein purified from human cells is a helically folded dynamic tetramer (Bartels et al., 2011; Wang et al., 2011; Gould et al., 2014) that resists aggregation (Bartels et al., 2011), other studies suggested that α-synuclein exists predominantly as an unfolded monomer (Fauvet et al., 2012). Interestingly, it was suggested that the PD-linked mutations A53T and E46K shift native tetramers to monomers and this underlies the disease initiation (Dettmer et al., 2015). Nonetheless, it is widely accepted that α-synuclein in the cellular milieu exists in various conformations and oligomeric states in a dynamic equilibrium, which can be affected by factors that alter the aggregation process (Cremades et al., 2012). Which particular species of α-synuclein are toxic has been debated, since some consider the amyloid-like insoluble fibrils as the mediators of α-synuclein-induced toxicity

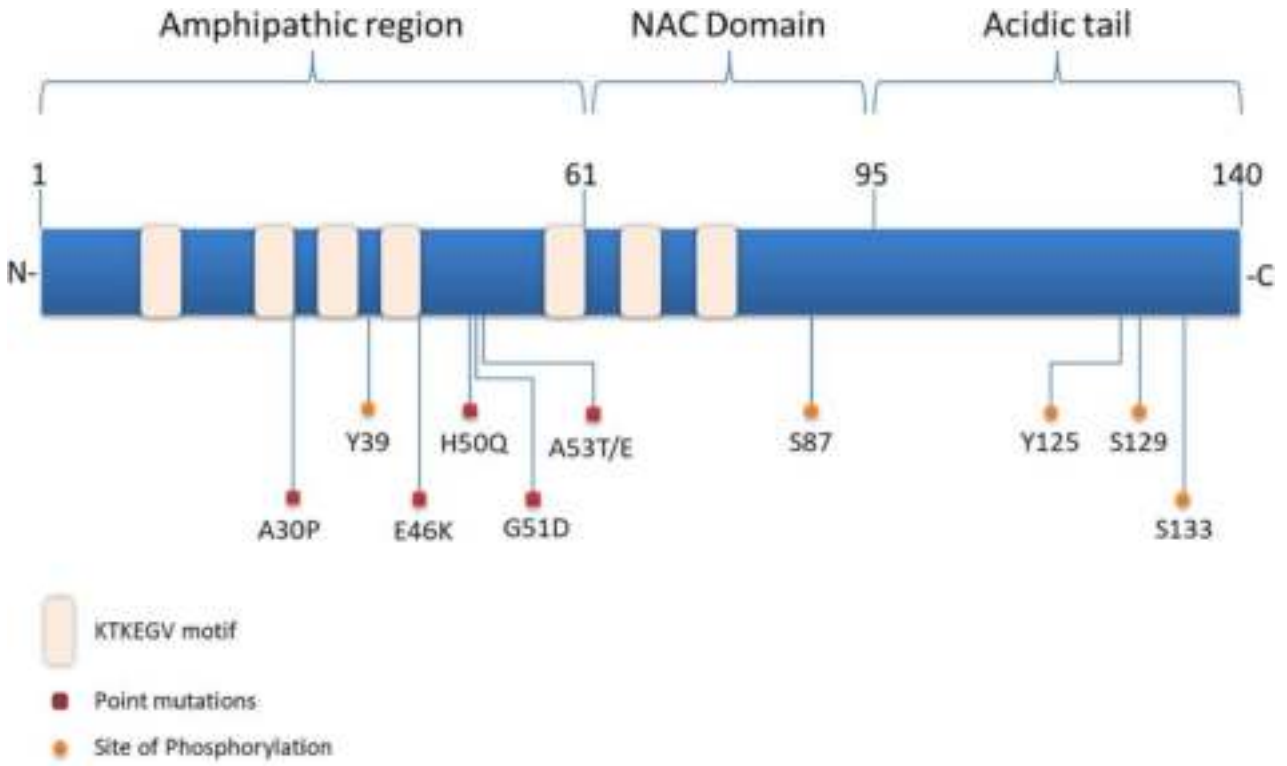

FIGURE 1 | Structure of α-synuclein. The N-terminal domain of α-synuclein is characterized by the presence of repeated lipid-binding sequences and contains the mutation sites linked with familial PD. The central NAC domain is mainly hydrophobic and favors the aggregation process of the protein. The C-terminal acidic tail carries the majority of α-synuclein phosphorylation sites.

(Conway et al., 1998), whereas others suggest that oligomers or protofibrils are the toxic ones (Danzer et al., 2007; Karpinar et al., 2009; Winner et al., 2011).

Slight alterations in the physicochemical features of α-synuclein via post-translational modifications (PTMs), truncations and solution condition modifications could favor the aggregation process (Uversky et al., 2001). Interestingly, the majority of PTMs occur in the acidic tail of the protein (**Figure 1**) and the serine (Ser) and tyrosine phosphorylation are the most extensively studied ones. Experiments utilizing ESI-MS (electrospray ionization mass spectrometry) technology revealed several modifications of α-synuclein in PD brains, such as N- or C-terminal truncations and phosphorylation at Ser129 (Kellie et al., 2014). In healthy brain, only a small proportion of α-synuclein is phosphorylated (Gonzalez et al., 2019), whereas under pathological conditions phosphorylated α-synuclein -mostly at Ser129- is increased in the majority of pathological inclusions, including LBs in PD and DLB, GCIs in MSA and LB-type inclusions of AD (Fujiwara et al., 2002; Saito et al., 2003; Nishie et al., 2004; Waxman et al., 2009). Even though initially phosphorylation of α-synuclein was considered to act prophylactically to protein aggregation, it is now widely accepted that it precedes fibril formation (Shahpasandzadeh et al., 2014; Tenreiro et al., 2014; Oueslati, 2016). Another common phosphorylation site is at Ser87, which is also found to be increased in synucleinopathies (Paleologou et al., 2010). Tyrosine phosphorylation of α-synuclein (Y39) seems to have both prophylactic and harmful effects (Mahul-Mellier et al., 2014; Brahmachari et al., 2016) and phosphorylation at Y125 and Y133 has been suggested to be protective against α-synuclein toxicity (Kleinknecht et al., 2016; El Turk et al., 2018). Beyond phosphorylation, other posttranslational modifications have been shown to affect the aggregation process of α-synuclein, such as nitration, oxidation, acetylation and SUMOylation, but possibly with a protective manner (Krumova et al., 2011; Dikiy and Eliezer, 2014; Vinueza-Gavilanes et al., 2020). Regarding truncation, it is known that truncated forms of α-synuclein account for 10–30% of total protein in patient-derived LB inclusions. In comparison with the full-length protein, C-truncated α-synuclein forms fibrils more rapidly, with distinct coil structures than the linear fibrils formed by the full-length protein. Additionally, α-synuclein can be oxidized through interaction with dopamine, generating dopamine-modified α-synuclein adducts, leading to a decrease in fibril formation and a subsequent increase in protofibril accumulation (Conway et al., 2001), which may enhance toxicity (Norris et al., 2003). Up to date, the physiological or pathological significance of α-synuclein cleavage remains unclear.

The physiological role of α-synuclein is still poorly understood and only its contribution to certain cellular functions is known so far. The presence of α-synuclein in the presynaptic terminals denotes a potential role of the protein in synaptic function

and vesicle trafficking (Jensen et al., 1998). The ability of α-synuclein to promote, as well as to sense, membrane curvature immediately suggested a possible relationship of the protein with the synaptic vesicle cycle. Overexpression of human α-synuclein was found to induce loss of synaptic vesicles and expansion of the plasma membrane through inhibition of both slow and fast vesicle endocytosis (Busch et al., 2014; Xu et al., 2016) and to promote dilation of the fusion pore, thereby accelerating the discharge of cargo (Logan et al., 2017). Importantly, α-synuclein interacts with the soluble N-ethylmaleimide-sensitive factor attachment protein receptor (SNARE) complex, while the loss or overexpression of the protein causes reduction or redistribution of the complex, respectively (Burre et al., 2010, 2014; Garcia-Reitbock et al., 2010) α-synuclein was also reported to promote vesicle clustering through its interaction with vesicle associated membrane protein 2 (VAMP2)/ synaptobrevin-2 and phospholipids (Diao et al., 2013).

Through its predominant role in vesicle trafficking α-synuclein can affect neurotransmitter release and particularly dopamine neurotransmission (Butler et al., 2017), via regulation of dopamine biosynthesis and trafficking of dopamine transporter (DAT), as well as, via modulation of DAT-mediated dopamine efflux (Butler et al., 2017). More specifically, α-synuclein was found to down-regulate indirectly the activity of tyrosine hydroxylase (TH) via inhibition of PP2A phosphatase, thus modulating dopamine production (Peng et al., 2005). However, the main effect of α-synuclein involves the regulation of DAT, where overexpressed α-synuclein enhances its interaction with DAT, altering the ionic conductance of the transporter and influencing the action potential-independent dopamine release, thus resulting in overall decrease of dopamine uptake (Swant et al., 2011; Butler et al., 2015). α-Synuclein also develops physical and functional interactions with other monoamine transporters (MATs), such as NET and SERT. In both cases, α-synuclein has been shown to negatively modulate the cell-surface expression and uptake activity of the transporters in a NAC-domain dependent manner (Wersinger et al., 2006a,b; Jeannotte and Sidhu, 2007). This finding indicates that α-synuclein may exert a homeostatic role, thus supporting that normal MAT expression may depend upon a certain baseline level of α-synuclein–MAT interaction. However, the mechanism by which α-synuclein expression alters MAT distribution should be further investigated. An opposite reported effect of α-synuclein on the dopaminergic pathway is the suppression of apoptosis of dopaminergic neurons (Jin et al., 2011). Supportive of a protective role of α-synuclein at the synapse are also findings showing a cooperative function of the protein with the synaptic vesicle protein cysteine-string protein-alpha (CSPalpha) and SNARE proteins, resulting in protection of nerve terminals against injury (Chandra et al., 2005).

Furthermore, α-synuclein can also act as a molecular chaperone, due to its high homology and interaction with the 14-3-3 proteins and their ligands, such as molecules of the Ras signaling pathway (Xu et al., 2013), thus possibly contributing to neuronal differentiation (Fu et al., 2000). Moreover, α-synuclein is part of a chaperone complex containing the Hsc70/Hsp70 chaperones, participating in the efficient neurotransmitter release (Witt, 2013). The chaperone activity of α-synuclein operates via its N-terminal interaction with the substrate protein, whereas the C-terminal region is responsible for the solubilization of the chaperone complex (Park et al., 2002).

α-SYNUCLEIN AS THE PRIMARY CULPRIT FOR SYNUCLEINOPATHIES

Substantial genetic, neuropathological and biochemical evidence implicates α-synuclein in the pathogenesis of PD and related synucleinopathies. Copy number variations, such as duplication or triplications of the *SNCA* gene encoding for α-synuclein, as well as point mutations and single nucleotide polymorphisms (SNPs) cause PD and DLB or increase the risk of developing the disease (Singleton et al., 2003; Chartier-Harlin et al., 2004; Zarranz et al., 2004; Nalls et al., 2014; Orme et al., 2018). Up to date six missense mutations in the *SNCA* gene are associated with autosomal dominant PD (**Figure 1**): Ala53Thr (A53T), Ala30Pro (A30P), Glu46Lys (E46K), His50Gln (H50Q), Gly51Asp (G51D), and Ala53Glu4 (A53E) (Polymeropoulos et al., 1997; Kruger et al., 1998; Zarranz et al., 2004; Kiely et al., 2013; Proukakis et al., 2013; Pasanen et al., 2014). The PD-linked mutations identified so far are located in the N-terminus of α-synuclein further underscoring the contribution of this region to protein aggregation. Most of them are described to cause early onset PD with rapid disease progression and additional clinical features, such as hallucinations, dementia, pyramidal tract impairment, and autonomic failure. Both mutant A53T and A30P α-synuclein mutations are disordered in dilute solution (like the wild-type protein). However, at higher concentrations, LB-like fibrils and discrete spherical assemblies are formed most rapidly by the A53T mutant (Conway et al., 1998). The A53T mutation has a moderate effect in a small region around the site of mutation, resulting in a local structural tendency for oligomerization (Conway et al., 2000; Bussell and Eliezer, 2001). On the other hand, the A30P mutation is associated with reduced formation of LB inclusions and it seems to promote formation of oligomers, rather than fibrils (Conway et al., 2000; Lazaro et al., 2014). The E46K mutation, through its conformational changes in the monomeric protein enhances the contacts between N- and C-terminus of the protein and promotes fibrillization with an increased tendency to inclusion formation (Fredenburg et al., 2007; Rospigliosi et al., 2009; Lazaro et al., 2014). The H50Q point mutation was discovered at the same year with the G51D and was linked with a late-onset phenotype of PD. H50Q was directly associated with increased α-synuclein aggregation and toxicity (Khalaf et al., 2014). Some of the families harboring these rare mutations have clinical manifestations or neuropathological features of both PD and MSA (Fanciulli and Wenning, 2015; Kiely et al., 2015). In particular, the A53T, A53E and G51D mutations, as well as the *SNCA* gene triplications are associated with a more aggressive MSA-like clinical and pathological phenotype (Kiely et al., 2015).

The genetic link between mutations and copy number variations of the *SNCA* locus and MSA is still controversial, given that common variation in the *SNCA* gene was first identified

as a risk factor for MSA in 2009 (Scholz et al., 2009), but this association was not confirmed in subsequent genome-wide association studies (GWAS) (Chen et al., 2015; Sailer et al., 2016). It is interesting to note that the G51D and A53E α-synuclein mutations seem to play an essential role in the inclusion formation in both neuronal and oligodendroglial cells (Pasanen et al., 2014; Whittaker et al., 2017). During the last decade, GWAS of risk in idiopathic PD revealed that *SNCA* is the major contributor (Satake et al., 2009). However, variability in *LRRK2* (leucine-rich repeat kinase 2), *GAK* (cyclin G-associated kinase) and *MAPT* (microtubule-associated protein tau) has been also implicated, with variants in *SNCA* and *MAPT* found to represent also risk factors for MSA (Scholz et al., 2009; Simon-Sanchez et al., 2009; Vilarino-Guell et al., 2011). Overall, it is apparent that all point mutations of α-synuclein alter its secondary structure, indicating that a single mutation in the *SNCA* gene is adequate for the development of a PD-like phenotype.

α-synuclein is the main component of the proteinaceous inclusions that represent the main histopathological hallmark of synucleinopathies, designated as LBs and LNs in PD and DLB (Spillantini et al., 1997, 1998) and GCIs in MSA (Wakabayashi et al., 1998a,b). Moreover, *in vitro* and *in vivo* overexpression of wild-type or mutant α-synuclein in neurons results in protein aggregation and toxicity, thus leading to phenotypes resembling PD (Giasson et al., 2002; Kirik et al., 2002; Lo Bianco et al., 2002; Vekrellis et al., 2009). Similarly, overexpression of human wild-type α-synuclein in oligodendroglial cell lines (Stefanova et al., 2005; Kragh et al., 2009) or *in vivo* (Kahle et al., 2002; Shults et al., 2005; Yazawa et al., 2005; Stemberger et al., 2010) results in the formation of fibrillar α-synuclein forms, which may cause toxicity in oligodendrocytes and/or in neurons (in the animal models) or increase cell susceptibility to oxidative stress, thus recapitulating many features of MSA. Such data clearly demonstrate that the total protein load and aggregation of α-synuclein is a critical determinant of its neurotoxic potential, giving rise to the "α-synuclein burden hypothesis" which pinpoints a critical role of the protein in idiopathic PD pathogenesis, either through enhanced transcription or through impaired degradation (Vekrellis and Stefanis, 2012). There are conflicting results regarding the mRNA levels of α-synuclein in PD and MSA brains, probably due to the difficulty to maintain a proper RNA integrity in tissues undergone extensive neurodegeneration. Even though the factors controlling *SNCA* transcription *in vivo* remain largely unknown, a number of regulatory transcriptional elements have been identified in neuronal cells, such as the GATA-1 and -2 transcription factors that enhance *SNCA* transcription through binding in the Intron 1 region of *SNCA* gene (Scherzer et al., 2008). Subsequent studies surmised that a signal transduction pathway involving the MAPK 3 and PI3K pathways could be important for controlling *SNCA* transcription (Clough and Stefanis, 2007) and that the transcription factor ZSCAN21 (Zipro1) could play a significant role (Clough et al., 2009; Brenner et al., 2015; Dermentzaki et al., 2016; Lassot et al., 2018). Recently, the CCAAT/enhancer binding protein (C/EBP) δ was identified as a novel repressor of α-synuclein transcription, following its binding to the *SNCA* genomic region in both mice and humans (Valente et al., 2020). Post-transcriptional regulation through microRNAs (Junn et al., 2009; Doxakis, 2010; Surgucheva et al., 2013; Choi D.C.et al., 2018; Kim et al., 2018) or lncRNAs (Lin D.et al., 2018; Elkouris et al., 2019; Zou et al., 2020) has also been reported to alter *SNCA* mRNA levels.

The pathological effects of misfolded α-synuclein involve, amongst others, dysregulation of mitochondrial activity and endoplasmic reticulum (ER)-Golgi trafficking, plasma membrane integrity, synaptic vesicle trafficking and function of the ubiquitin-proteasome (UPS) and the autophagy-lysosome pathway (ALP) (Vekrellis et al., 2011). Overexpression of α-synuclein causes mitochondrial fragmentation (Kamp et al., 2010), event that is associated with an increase in mitochondrial fission rather than a fusion deficiency (Nakamura et al., 2011). Recently, it was reported that α-synuclein is normally localized at mitochondrial-associated membranes, while under pathological conditions α-synuclein dislocates from its sites and affects mitochondrial morphology (Guardia-Laguarta et al., 2014). Another study showed that under pathological conditions and in contrast with the native monomeric α-synuclein, aggregated forms of the protein preferentially bind to mitochondria, leading to mitochondrial dysfunction and cellular respiration limitation (Wang et al., 2019). Moreover, aggregated α-synuclein alters the membrane fusion and fission processes of mitochondria, resulting in fragmentation of the organelle and mitophagy inhibition (Chen and Chan, 2009). This mitochondrial damage is followed by a series of events, such as reactive oxygen species (ROS) production, electron leakage and caspase activation leading eventually to neuronal death (Ganjam et al., 2019). It has also been proposed that ROS production leads to a LRKK2-mediated impairment of endosomal and lysosomal function, resulting in pSer129 α-synuclein accumulation (Di Maio et al., 2018). Since pSer129 α-synuclein is considered an inhibitor of mitochondrial protein import, its aggregation is directly linked to mitochondrial senescence and ROS production, thus creating a positive feedback loop (Di Maio et al., 2018). Along with the mitochondrial dysfunction, α-synuclein aggregation also affects the activity of the ER, inducing protein-folding abnormalities, impaired ER-Golgi transport and calcium leakage, which ultimately lead to further aggregation of the protein (Volles and Lansbury, 2002; Thayanidhi et al., 2010; Colla et al., 2012; Colla, 2019). However, one of the main mechanisms through which α-synuclein causes neurotoxicity is the abnormal interaction of various protein assemblies with membranes, causing membrane disruption, lipid bilayer thinning and vesicle trafficking dysregulation (Hellstrand et al., 2013; Wang and Hay, 2015; Fusco et al., 2017). In the healthy brain, monomeric α-synuclein plays an important role in synaptic function; however, in pathological conditions, α-synuclein aggregation impairs the SNARE complex assembly, through its abnormal interaction with essential proteins for the synaptic vesicle cycle function (Dalfo et al., 2004; Gitler et al., 2008; Choi et al., 2013). It has been also shown that fibrillar α-synuclein may induce synaptic vesicle endocytosis and blockage of vesicle recycling, further contributing to the development of synaptopathy, which characterizes PD and related synucleinopathies (Nemani et al., 2010; Busch et al., 2014; Xu et al., 2016). Formation of

aberrant α-synuclein species has been widely shown to impair the function of the UPS and the ALP pathway, as discussed below. Similar effects are observed in MSA where the pathological accumulation of α-synuclein in oligodendrocytes causes severe disruption of most cellular functions, with the myelination process being a major target of the protein's aberrant effects. The demyelination, along with the reduction of trophic factors, leads to a secondary neuronal cell loss (Shults et al., 2005; Ubhi et al., 2010; Stefanova and Wenning, 2016).

Emerging evidence also suggest that activation of the inflammatory process due to the presence of abnormal α-synuclein species plays a central role in the development of synucleinopathies. Postmortem brain examination, brain imaging and animal studies converged that both the innate and adaptive immune systems are activated in PD contributing to disease progression (Tansey and Romero-Ramos, 2019). Activated microglia, which are considered the most efficient scavengers of extracellular α-synuclein aggregates (Lee et al., 2008b), increase the production of pro-inflammatory cytokines and induce an oxidative stress response (Klegeris et al., 2008; Su et al., 2008; Couch et al., 2011) even in the absence of neuronal loss (Sanchez-Guajardo et al., 2010; Barkholt et al., 2012; Watson et al., 2012). Increased pro-inflammatory mediators such as tumor necrosis factor alpha (TNF-α), interleukin-1-β (IL-1β), interleukin-6 (IL-6) have been shown in the cerebral spinal fluid (CSF) and in the striatum of human PD brains (Mogi et al., 1994a,b; Vawter et al., 1996; Nagatsu et al., 2000), supporting a chronic pro-inflammatory milieu in the brain of PD patients. Apart from α-synuclein mediated activation of microglia in the CNS, a more complex relationship between gut microbial-induced inflammation and α-synuclein expression and aggregation has been proposed to occur in the periphery (Chen S.G.et al., 2016; Choi J.G.et al., 2018). Clinical, epidemiological and animal studies suggest a complex cross-talk between intestinal inflammation and PD pathology initiation and progression (Houser and Tansey, 2017; Chen et al., 2019). Similarly, α-synuclein-evoked microglial activation is commonly detectable in the brains of MSA patients (Ishizawa et al., 2004) and MSA experimental models (Stefanova et al., 2007; Vieira et al., 2015; Monzio Compagnoni and Di Fonzo, 2019). Even though the activation of the inflammatory cascade in synucleinopathies may not represent a primary event but a secondary in response to other phenomena, it definitely contributes to the neuronal degeneration that characterizes these diseases.

α-SYNUCLEIN AND PROTEIN-DEGRADATION PATHWAYS: A COMPLICATED RELATIONSHIP

Unraveling the pathway involved in the degradation of α-synuclein is crucial in understanding the pathogenetic mechanisms underlying its aberrant accumulation in synucleinopathies. Both the UPS and the ALP have been proposed to clear α-synuclein (**Figure 2**); however to a different extent and in a cell-, conformation- and tissue- specific manner (Bennett et al., 1999; Webb et al., 2003; Vogiatzi et al., 2008). Initial studies in purified systems and in neuronal cells, have demonstrated that α-synuclein can undergo both ubiquitin-dependent (Rott et al., 2011; Haj-Yahya et al., 2013) and ubiquitin-independent (Tofaris et al., 2001; Liu et al., 2003) degradation via the 26S/20S proteasome. Additional studies performed in PC12, HEK293 and primary mesencephalic cells failed to detect significant α-synuclein accumulation following pharmacological proteasomal inhibition (Rideout et al., 2001; Rideout and Stefanis, 2002; Vogiatzi et al., 2008). Others have found that only a small proportion of soluble-cell-derived intermediate α-synuclein oligomers, not including monomeric α-synuclein, are targeted to the 26S proteasome for degradation (Emmanouilidou et al., 2010b). In an elegant *in vivo* study it was shown that the UPS is the main degradation pathway for α-synuclein under normal conditions, while with increased α-synuclein burden the ALP is recruited (Ebrahimi-Fakhari et al., 2011). We and others have shown that only the wild-type α-synuclein and not the PD-linked A53T and A30P forms, the phosphorylated or the dopamine-modified α-synuclein, is degraded via the selective process of chaperone-mediated autophagy (CMA) (Cuervo et al., 2004; Martinez-Vicente et al., 2008; Vogiatzi et al., 2008; Mak et al., 2010). CMA can degrade only monomeric or dimeric forms of the protein, whereas macroautophagy is the only process that can clear oligomeric α-synuclein (Xilouri et al., 2013b). Not only mutations but also post-translational modifications such as phosphorylation, sumoylation and ubiquitination may also alter the partitioning of α-synuclein to proteasomal or lysosomal degradation (Xilouri et al., 2016b).

The UPS and the ALP not only degrade α-synuclein but can also be a direct target of the protein's aberrant effects (Xilouri et al., 2016b; Zondler et al., 2017). Initial studies indicated that overexpression of the A30P and A53T mutants make cells more vulnerable to proteasomal inhibition-mediated cell death compared to cells overexpressing the wild-type protein (Tanaka et al., 2001). Additional evidence suggested that overexpression of mutant α-synuclein variants inhibits the activity of the 20S/26S proteasome leading to UPS failure thus, contributing to α-synuclein aggregation (Stefanis et al., 2001), although another study showed that overexpression of wild-type or mutant (A30P, A53T) α-synuclein in PC12 cells or in transgenic mice did not significantly affect proteasomal function (Martin-Clemente et al., 2004). More recently, it was shown that the function of the 20S proteasome was not affected upon administration of recombinant α-synuclein oligomers and fibrils or upon transient expression of wild-type or mutant α-synuclein (Zondler et al., 2017).

Studies in human post-mortem material also indicate that proteasome function is impaired in the substantia nigra of PD patients (Bentea et al., 2017), further cementing a role of a proper UPS function in PD pathogenesis. Beyond the UPS, increased α-synuclein has been reported to impair macroautophagy both *in vitro* and *in vivo* (Winslow et al., 2010), possibly through its interaction with Rab1a, which causes the mislocalization of Atg9, an autophagosome formation-related protein (Winslow et al., 2010). Similarly, Atg9 mislocalization and impaired autophagosome formation has been observed in cells expressing

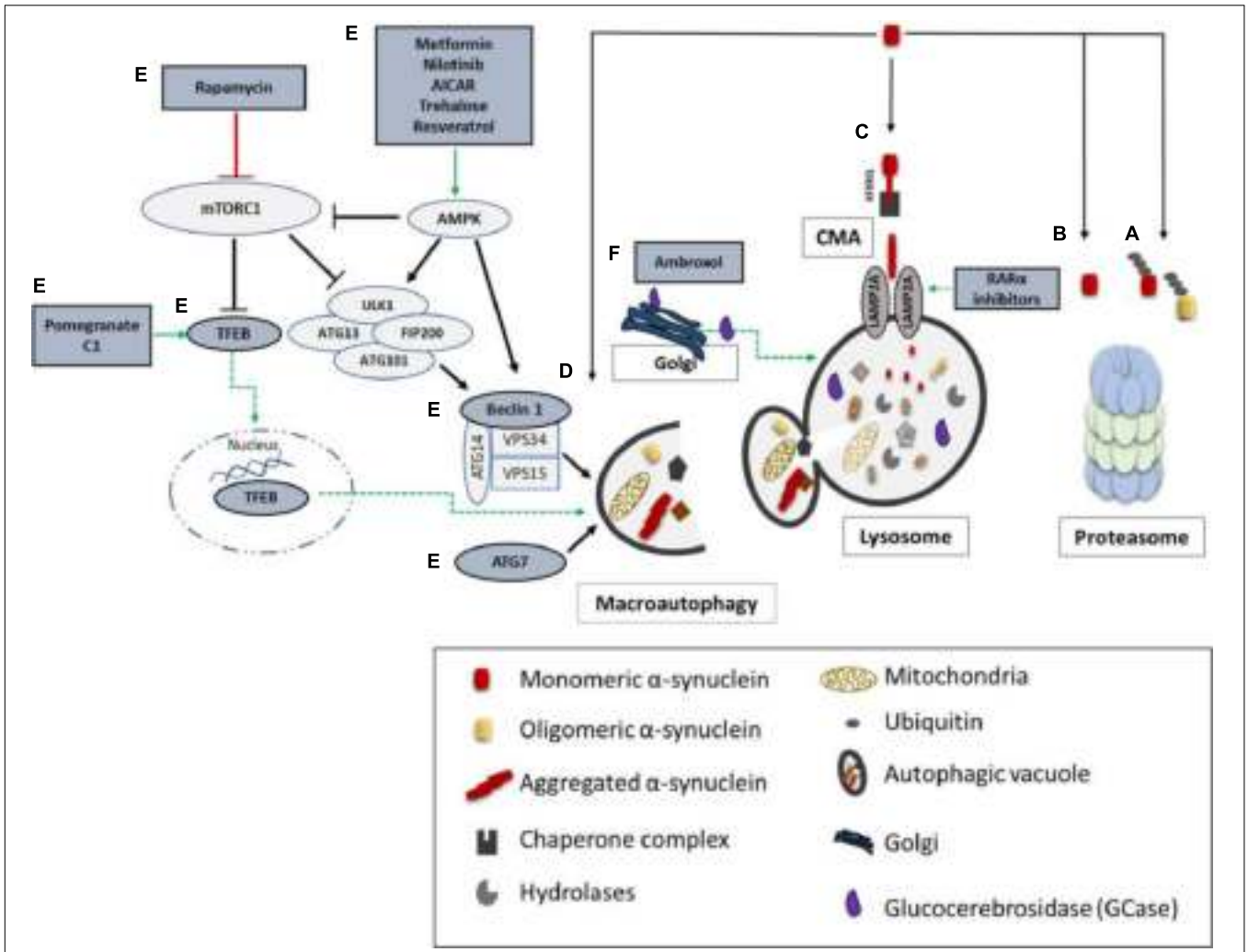

FIGURE 2 | α-synuclein degradation pathways and reported therapeutic approaches to enhance protein clearance. A schematic representation of the main proteolytic pathways implicated in α-synuclein clearance and the proposed targets for potential therapeutic interventions (highlighted in dark grey and green). Wild type and mutant α-synuclein can undergo both ubiquitin-dependent **(A)** and ubiquitin-independent **(B)** degradation via the 20S/26S proteasome. Monomeric wild-type α-synuclein is degraded via CMA, following its binding to the CMA-specific receptor, LAMP2A **(C)**. Molecular upregulation of LAMP2A expression or chemical enhancement of CMA through retinoic acid receptor alpha (RARα) antagonists has been proven successful in alleviating α-synuclein-associated toxicity. Macroautophagy has been also proposed to degrade mutant and aggregated forms of α-synuclein **(D)**. Boosting macroautophagy via mTOR-dependent (rapamycin) or mTOR-independent pharmacological and nutritional modulators (Metformin, Nilotinib, AICAR, Trehalose, Resveratrol, Pomegranate, C1) enhance autophagosome formation, lysosome biogenesis, and lysosome function thus promoting α-synuclein clearance **(E)**. Molecular modulation of macroautophagy via Atg7, Beclin1 or TFEB overexpression is also reported to exert beneficial effects on α-synuclein-related toxicity **(E)**. Lastly, restoration of proper enzymatic activity of GCase has been shown to improve lysosomal function and lessen α-synuclein levels **(F)**.

the PD-linked mutant form of the retromer protein VPS35 (Zavodszky et al., 2014). There is also evidence suggesting that the PD-linked α-synuclein mutations could have a different impact on macroautophagy machinery. In particular, the E46K α-synuclein mutation impairs autophagy at an early stage of autophagosome formation via dysregulation of the JNK1/Bcl2, an mTOR-independent pathway (Yan et al., 2014). Also, the A30P mutant α-synuclein inhibits autophagosome formation via activation of the autophagy transcriptional repressor ZKSCAN3 in a JNK-dependent manner (Lei et al., 2019). Furthermore, the A53T mutation has been shown to dysregulate mitophagy (Choubey et al., 2011), resulting in massive mitochondrial removal accompanied by bioenergetics deficits and neuronal degeneration. However, another study in A53T α-synuclein transgenic mice showed that α-synuclein accumulation leads to activation of the p38 MAPK pathway, which in turn directly phosphorylates Parkin thus inhibiting Parkin-mediated mitophagy (Chen et al., 2018). Several independent studies have proposed that autophagy is controlled by the GTP-ase–p38 MAPK signaling (Obergasteiger et al., 2018), a pathway that may be disturbed in PD. Additionally, mutations in the *GBA1* gene, which encodes for the lysosomal enzyme β-glucocerebrosidase (GCase) and cause Gaucher's disease (GD), are among the most common known genetic risk factors for

PD and DLB (Mata et al., 2008; Clark et al., 2009). Various studies in cell culture and animal models and in human post-mortem material suggest an inverse relationship between α-synuclein accumulation and GCase protein levels and activity where reduced GCase activity coincides with increased levels of α-synuclein (Mazzulli et al., 2011; Osellame et al., 2013; Sardi et al., 2013; Murphy et al., 2014; Du et al., 2015; Liu et al., 2015; Rocha et al., 2015; Chen M.et al., 2016).

The first connection between CMA and PD was established in 2004, where monomeric and dimeric wild-type α-synuclein species were shown to be CMA substrates, whereas the A30P and A53T PD-linked mutant α-synuclein forms bound more tightly to LAMP2A, CMA's specific receptor, but were not up taken and degraded within lysosomes, thus becoming toxic by inhibiting the CMA-mediated degradation of other cytosolic substrate proteins (Cuervo et al., 2004). Subsequently, it was shown that post-translational modifications of wild-type α-synuclein, such as oxidation and nitration of the protein, alter its binding and uptake into lysosomes, while phosphorylation and dopamine-modification almost completely prevents its CMA-dependent degradation (Martinez-Vicente et al., 2008; Xilouri et al., 2009). Reciprocally, CMA inhibition is reported to lead to the formation of detergent-insoluble or high molecular weight oligomeric α-synuclein conformations *in vitro* (Vogiatzi et al., 2008; Xilouri et al., 2009), or to increased intracellular α-synuclein accumulation in nigral neurons *in vivo* (Xilouri et al., 2016b). Furthermore, the protein levels of the two key CMA markers LAMP2A and HSC70, were reported to be decreased in the human substantia nigra and amygdala of PD brains compared to controls (Alvarez-Erviti et al., 2010), while, more recently, decreased protein levels of LAMP2A correlated with increased α-synuclein accumulation were found in PD brain regions harboring α-synuclein pathology (anterior cingulate cortex) and not in other regions that are spared (occipital cortex) (Murphy et al., 2014). Importantly, these decreases correlated directly to CMA activity, since the protein levels of the other two *LAMP2* isoforms (2B and 2C) that do not participate in CMA, were found unaltered between PD and control brains (Murphy et al., 2015). Macroautophagy alterations have also been found in nigral neurons of PD brains (Anglade et al., 1997).

Beyond PD, evidence from human postmortem material from MSA brains suggests the possibility of macroautophagic alterations linked to α-synuclein accumulation in GCIs. More particularly, the detection of SQSTM1/p62 and, in some cases, of LC3 (but not of more mature lysosomal markers) and of the autophagic adaptor protein NBR1 within GCIs together with α-synuclein suggests a possible initial induction of macroautophagy and a subsequent defect in macroautophagy maturation in MSA brains (Chiba et al., 2012; Odagiri et al., 2012; Schwarz et al., 2012; Tanji et al., 2013). In addition, the FBXO27 gene, which encodes a protein associated with ubiquitination and protein degradation, was identified in a recent GWAS as a potential risk factor for MSA (Sailer et al., 2016). These neuropathological studies have also suggested the possibility of impaired proteasomal function as a driving force for GCI formation. Studies in oligodendroglial cells showed that, upon pharmacological proteasomal inhibition, p62 and LC3 accumulate in forming aggregates, in an apparent compensatory response of macroautophagy activation (Schwarz et al., 2012). In addition, dysfunctional macroautophagy evoked through mitochondrial impairment or macroautophagy inhibition resulted in the accumulation of α-synuclein in oligodendroglial cells (Pukass et al., 2015), whereas more recently it was reported that macroautophagy block through genetic or pharmacological inhibition of autophagy was inefficient to increase intracellular accumulation of α-synuclein in oligodendrocytes exposed to monomeric or fibrillar α-synuclein (Fellner et al., 2018). Nonetheless, additional work is needed to elucidate the precise role of UPS and ALP dysfunction in the accumulation of α-synuclein-rich GCIs in MSA brains.

CELL-TO-CELL PROPAGATION OF α-SYNUCLEIN PATHOLOGY IN SYNUCLEINOPATHIES: THE STRAIN HYPOTHESIS

According to Braak staging, Lewy pathology manifested by positive α-synuclein inclusions spreads throughout the brain as PD progresses, primarily affecting the brainstem and olfactory system, thereafter gradually invading the neocortex (Braak et al., 2003). Amongst numerous studies that have tested this hypothesis (Braak et al., 2006; Lebouvier et al., 2010; Pouclet et al., 2012; Grathwohl et al., 2013; Paillusson et al., 2013; Holmqvist et al., 2014), recently it was shown that α-synuclein pre-formed fibrils (PFFs) injected into the duodenal and pyloric muscularis layer evoked a spread of pathologic Ser129 phosphorylated α-synuclein in various brain regions. Interestingly, truncal vagotomy prevented the gut-to-brain transmission of α-synuclein pathology, supporting the Braak hypothesis of a prion-like templating mechanism (Kim et al., 2019). Similarly, a cohort study of vagotomized patients supported that the vagus nerve is involved in the development of PD (Svensson et al., 2015). Recently, α-synuclein inclusions were detected in stomach and heart of a bacterial artificial chromosome (BAC) transgenic rat model injected into the gut wall of the pylorus and duodenum with α-synuclein PFFs. Their findings suggest a secondary anterograde (Dorsal Motor nucleus of the Vagus [DMV]-to-stomach) spreading of α-synuclein pathology, followed by a primary retrograde (duodenum-to-DMV) spreading (Van Den Berge et al., 2019).

However, there are studies presenting controversial results, suggesting that α-synuclein transmission from a peripheral injection site reaches the dorsal nucleus of vagus nerve, but does not further spread in the CNS (Manfredsson et al., 2018; Uemura et al., 2018). The hypothesis of α-synuclein prion-like propagation has gained attention in the recent years, since it has been shown that transplantation of healthy fetal mesencephalic neurons in PD patients led to the formation of LB-like inclusions, indicating the direct transfer of pathogenic α-synuclein from host brain to grafted neurons (Kordower et al., 2008; Li et al., 2008). Similar studies have verified that neurons inside the grafts were positive for LB-like α-synuclein aggregates (Li et al., 2008, 2010;

Kordower et al., 2011; Kurowska et al., 2011). Moreover, inoculation of brain extracts from PD and DLB patients into the striatum and substantia nigra of mice (Masuda-Suzukake et al., 2013) and non-human primates induced α-synuclein aggregation and neurodegeneration (Recasens et al., 2014).

The first clinical evidence to support α-synuclein spread throughout the nervous system was the detection of the protein in human CSF, indicating that α-synuclein can be released into the extracellular space (El-Agnaf et al., 2003). Subsequent studies verified the secretion of α-synuclein from neuronal cells, in part via vesicle- and exosomal-related trafficking (Lee et al., 2005; Emmanouilidou et al., 2010a; Jang et al., 2010; Danzer et al., 2012). On the other hand, conventional endocytosis (Sung et al., 2001; Lee et al., 2008a; Desplats et al., 2009; Hansen et al., 2011; Angot et al., 2012), exosomal transport (Emmanouilidou et al., 2010a; Delenclos et al., 2017), receptor-mediated internalization (Shrivastava et al., 2015; Mao et al., 2016; Ihse et al., 2017), passive diffusion (Ahn et al., 2006), or even direct penetration of the plasma membrane (Kayed et al., 2004; Jao et al., 2008; Lee et al., 2008a; Tsigelny et al., 2012) have been proposed as the main pathways for α-synuclein uptake (**Figure 3**). Amongst the receptors that have been proposed to mediate the uptake of the protein by neurons is the FcγRIIB inhibitory Fc receptor, which has been shown to be responsible for fibrillar α-synuclein cell-to-cell transmission mediated by the FcgRIIB-SHP-1/2 signaling (Choi Y.R.et al., 2018) and the LAG3 receptor reported to interact with fibrillar but not monomeric α-synuclein (Mao et al., 2016). Moreover, heparan sulfate proteoglycans (HSPGs) seem to regulate α-synuclein uptake via macropinocytosis in neurons, whereas GM1 ganglioside is responsible for α-synuclein entry in microglial cells (Park et al., 2009; Holmes et al., 2013). Fibrillar α-synuclein has been shown to interact *in vitro* with HSPGs via specific sequence motifs and thus be effectively endocytosed (Zhang et al., 2020). Recent data revealed that N-linked glycans on the cell surface of neurons interact with acetylated α-synuclein and mediate its internalization and subsequent pathological aggregation (Birol et al., 2019).

It has also been reported that neurons can take up naked α-synuclein following it's binding to specific membrane proteins, which are then partially localized within the lysosomal compartment (Lee et al., 2008a; Karpowicz et al., 2017). Disruption of the lysosomal function has been shown to play an important role in the transmission of α-synuclein pathology and the subsequent neurodegeneration (Xilouri et al., 2016a; Jiang et al., 2017; Klein and Mazzulli, 2018; Minakaki et al., 2018). Importantly, in cases of compromised cell proteolytic machineries, vesicle-associated α-synuclein release seems to be enhanced (Jang et al., 2010; Alvarez-Erviti et al., 2011; Danzer et al., 2012; Lee et al., 2013; Fussi et al., 2018). However, cell-to-cell spread of α-synuclein pathology does not necessarily require cell contacts, since tunneling nanotubes may also represent a possible transmission mechanism (Abounit et al., 2016; **Figure 3**). Exogenous α-synuclein, once taken up by neuronal or glial cells is directed to their cytosol where it recruits the aggregation of the endogenous α-synuclein into the formation of aberrant species, via an up-to-date unknown mechanism (Volpicelli-Daley et al., 2014; Rey et al., 2016; Karampetsou et al., 2017; Karpowicz et al., 2017; Kaji et al., 2018; Luna et al., 2018; Mavroeidi et al., 2019). Many *in vitro* and *in vivo* studies have proposed that exogenously added human α-synuclein PFFs are used as a template and recruit the endogenous soluble monomeric α-synuclein into the formation of insoluble LB-like inclusions (Luk et al., 2009, 2012a; Volpicelli-Daley et al., 2011; Masuda-Suzukake et al., 2013; Sacino et al., 2013a, 2014a,b; Wu et al., 2019). Similar results were obtained *in vivo* when PD brain- or symptomatic α-synuclein transgenic mice-derived homogenates were delivered in the living brains of mice and monkeys (Mougenot et al., 2012; Recasens et al., 2014; Schweighauser et al., 2015).

Two seeding processes have been demonstrated to govern the aggregation of the endogenous α-synuclein: homotypic (or self-seeding) and heterotypic seeding. The term "homotypic seeding" is referred to the sequence-specific templating of α-synuclein that requires the presence of the hydrophobic NAC region (El-Agnaf et al., 1998; Giasson et al., 2001). On the other hand, heterotypic seeding is a process that involves other proteins (such as tau, huntingtin and Aβ) in the initiation of α-synuclein recruitment and fibrillization (Charles et al., 2000; Masliah et al., 2001; Giasson et al., 2003; Pletnikova et al., 2005; Badiola et al., 2011; Tomas-Zapico et al., 2012). Many studies utilizing the α-synuclein PFF-brain inoculation as a PD model, suggest the "connectomic" transmission of pathological α-synuclein from the injection site to various interconnected brain regions (Luk et al., 2012a; Masuda-Suzukake et al., 2013, 2014; Paumier et al., 2015; Peelaerts et al., 2015; Ulusoy et al., 2015; Rey et al., 2016) and that this α-synuclein spread based on the anatomical connections between brain areas (Luk et al., 2012b; Rey et al., 2013, 2016; Peelaerts et al., 2015), party occurs via gap junction channels composed of connexins, formed between adjacent cells (Diaz et al., 2019; Reyes et al., 2019). Finally, a recent study pinpoints 14-3-3 proteins as potential regulators of α-synuclein transmission, proposing that they normally prevent α-synuclein oligomerization and resultant toxicity, whereas 14-3-3 protein dysfunction mediates α-synuclein oligomerization and seeding, that govern PD pathology (Wang et al., 2018). Numerous *in vitro* and *in vivo* studies utilizing α-synuclein PFFs as seeds, have proposed an induction in the endogenous neuronal α-synuclein aggregation, thus favoring the prion-like hypothesis of α-synuclein spread (Luk et al., 2009, 2012a; Volpicelli-Daley et al., 2011; Masuda-Suzukake et al., 2013; Sacino et al., 2014b; Paumier et al., 2015; Peelaerts et al., 2015; Abdelmotilib et al., 2017). Interestingly, not only PFFs but also isolated exosomes from the CSF of PD and DLB patients, containing pathological species of α-synuclein, were able to transfer the disease pathology when applied in human H4 neuroglioma cells (Stuendl et al., 2016).

Beyond PD, the self-propagation of α-synuclein resulting in the formation of insoluble aggregates within the cytoplasm of oligodendrocytes termed MSA also as a prion-like disease. Prusiner et al. originally reported that TgM83$^{+/-}$ mice expressing human A53T α-synuclein when inoculated with MSA, but not PD, brain homogenates developed neurodegeneration, suggesting that a distinct strain of α-synuclein displays prion characteristics during the development of MSA (Watts et al., 2013; Prusiner et al., 2015). Accordingly, treatment of HEK293T cells stably expressing fluorescently-tagged α-synuclein with

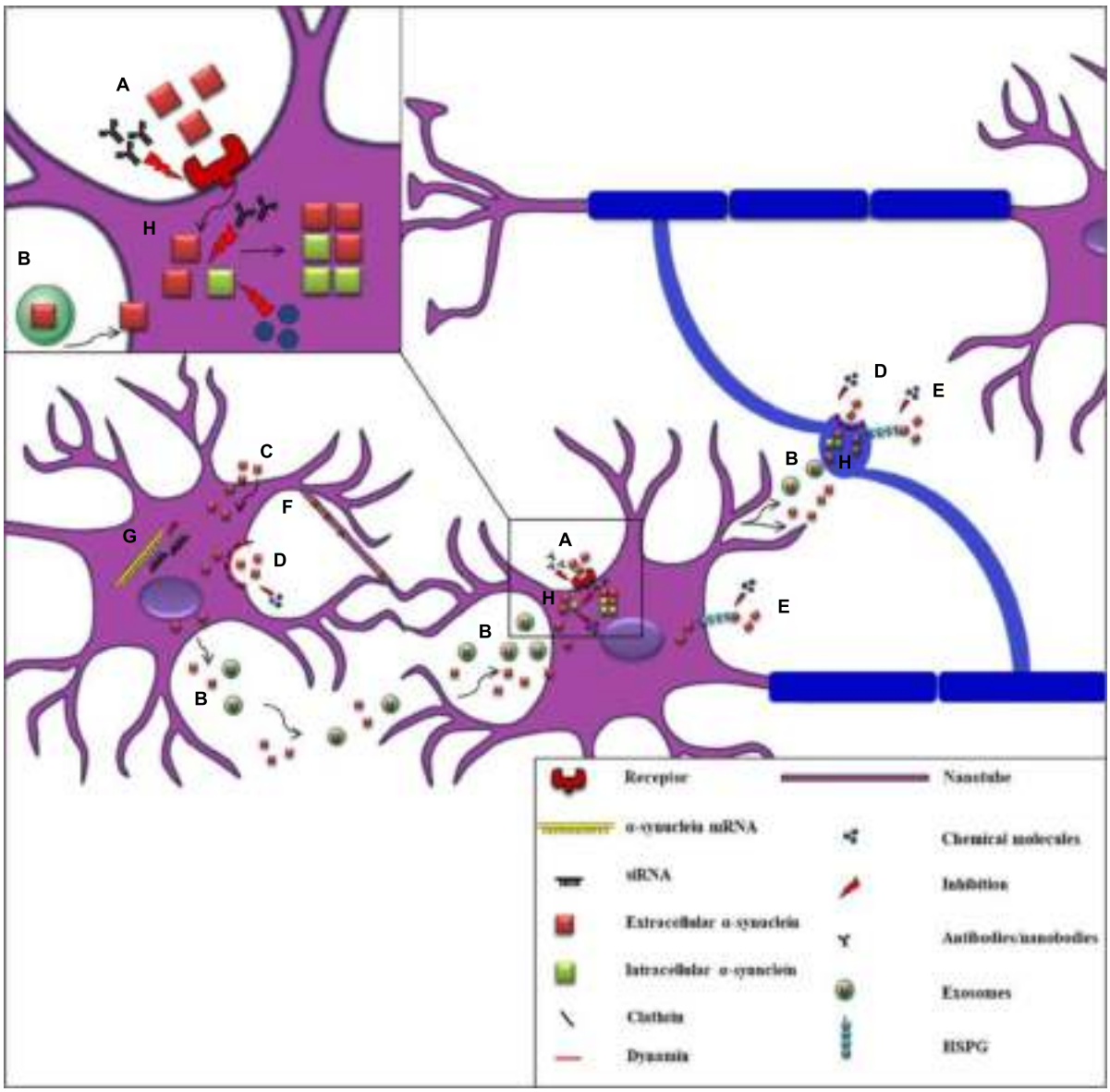

FIGURE 3 | Proposed mechanisms of α-synuclein cell-to-cell propagation and application of candidate therapeutic strategies. A schematic representation of α-synuclein transfer from neurons to neurons (purple) or to oligodendrocytes (blue) via various mechanisms: **(A)** Neuronal receptors (i.e., LAG3) interact with extracellular α-synuclein and mediate its internalization via endocytosis. Antibodies against these receptors effectively inhibit α-synuclein propagation. **(B)** Neuronally-derived, free or exosomal-bound α-synuclein enters neighboring neurons or oligodendrocytes. **(C)** α-synuclein is taken-up by cells via passive diffusion or direct penetration of their plasma membrane. **(D)** Clathrin- or dynamin- mediated endocytosis is responsible for α-synuclein internalization in neurons and oligodendrocytes. Inhibitors targeting these endocytic pathways have been effectively used. **(E)** Heparan Sulfate ProteoGlycans (HSPGs) regulate α-synuclein uptake via macropinocytosis in neurons and oligodendrocytes. Disruption of HSPGs by chemical molecules (heparin or chloral hydrate) inhibits α-synuclein uptake by cells. **(F)** Tunneling nanotubes (thin membranous bridges) have been also proposed as a possible cell-to-cell transmission mechanism of α-synuclein. **(G)** siRNAs (small interfere RNAs) designed against α-synuclein mRNA are used for the reduction of α-synuclein production as an effective therapeutic strategy. **(H)** α-synuclein entrance in neuronal or oligodendroglial cells is followed by its aggregation and the spread of α-synuclein pathology (seeding), finally leading to the formation of aberrant protein species. Various antibodies targeting the NAC or the C-terminal region of α-synuclein and chemical molecules and compounds (i.e., NPT200–11, NPT100-18A, NPT088 etc.) inhibiting α-synuclein aggregation have been used to prevent α-synuclein misfolding.

either healthy-control brain extracts or brain samples derived from PD or MSA patients, revealed that only in the case of MSA-added material, cells developed α-synuclein accumulation (Woerman et al., 2015). The prion-like transmission of α-synuclein pathology was further supported by intrastriatal delivery of MSA homogenates in the brain of human-wild type α-synuclein-expressing mice and detection of pathological α-synuclein aggregates formed in many brain regions (Bernis et al., 2015). Two possible scenarios have been proposed to explain the origin of α-synuclein in oligodendrocytes and the mechanisms

underlying α-synuclein accumulation in GCIs present in MSA brains: either oligodendrocytes pathologically overexpress α-synuclein in the context of MSA (Asi et al., 2014) or they take up neuronally derived protein from their environment (Kisos et al., 2012; Konno et al., 2012; Rockenstein et al., 2012; Ettle et al., 2014; Pukass and Richter-Landsberg, 2014; Reyes et al., 2014; Pukass et al., 2015; Kaji et al., 2018). We have recently suggested that the presence of endogenous oligodendroglial α-synuclein, however minute in amount, is a critical factor for the generation of pathological GCI-like α-synuclein structures within oligodendrocytes and myelin dysregulation evoked by PFF-administration both *in vitro* and *in vivo* (Mavroeidi et al., 2019).

Furthermore, as already mentioned, neuroinflammation is a key mediator of α-synuclein-related toxicity, since microglia and astroglia activation, gliosis and increased secretion of pro-inflammatory factors are often observed in synucleinopathies (Nagatsu and Sawada, 2005; Politis et al., 2012; Tufekci et al., 2012; Fellner and Stefanova, 2013; Kaufman et al., 2013). Many studies focused on α-synuclein transfer between neurons and glial cells (Lee et al., 2010; Sacino et al., 2013b; Reyes et al., 2014). It has been proposed that α-synuclein attracts and activates microglia; however these cells fail to clear α-synuclein, thus leading to an excessive pro-inflammatory response via Toll-like receptor (TLR) and finally to neurodegeneration (Stefanova et al., 2011; Kim et al., 2013; Roodveldt et al., 2013; Tang and Le, 2016). A recent study suggests that the differential activation state of microglial cells plays a crucial role in neuron-to-neuron α-synuclein spread and that IL-4-activated microglia seems to engulf extracellular α-synuclein, thus reducing neuron-to-neuron α-synuclein transmission (George et al., 2019). Others have suggested that pathological α-synuclein spreads through tunneling nanotubes in macrophages and possibly in microglial cells as well (Onfelt et al., 2004). The neuron-to-astrocyte and astrocyte-to-astrocyte transmission of α-synuclein has been shown both in *in vitro* and *ex vivo* experiments, however α-synuclein aggregates are preferably formed within neurons rather than in astrocytes (Lee et al., 2010; Loria et al., 2017). This fact could be attributed to the protective role of astrocytes against α-synuclein aggregation, via enhanced proteolytic processing of exogenously added PFFs (Loria et al., 2017).

Interestingly, it has been proposed that α-synuclein joins into distinct polymorphisms possibly responsible for the variety of disease phenotypes giving rise to the strain hypothesis, underlying the pathogenesis of synucleinopathies. Based on this scenario, the central idea is that α-synuclein fibrils behave as strains with discrete biochemical and structural characteristics, into distinct brain regions and cell types (Cremades et al., 2012; Bousset et al., 2013; Kim et al., 2016; Ma et al., 2016; Pieri et al., 2016; Lau et al., 2020). Supportive of this hypothesis are findings showing that pathological α-synuclein in PD and MSA inclusions is conformationally and biologically distinct and different α-synuclein strains are generated in discrete intracellular milieus (Peng et al., 2018a). We have also shown that the pathology-related S129 α-synuclein phosphorylation in primary cultures and human post-mortem brain material might involve different α-synuclein strains present in oligodendroglial and neuronal synucleinopathies (Mavroeidi et al., 2019).

Most importantly, it is reported that α-synuclein fibrils amplified from the brains (Strohaker et al., 2019) or CSF (Shahnawaz et al., 2020) of PD patients are structurally different than those from MSA, further suggesting that distinct conformational strains of α-synuclein may underlie the different pathology detected in two synucleinopathies. Therefore, it is surmised that based on the diversity of the human strains and via the protein misfolding cyclic amplification (PMCA) technique, we can discriminate between PD and MSA pathology in patient-derived CSF samples with high sensitivity (Shahnawaz et al., 2020). These strains can recruit and seed endogenous α-synuclein, and also propagate by imprinting their unique structural properties on its non-pathogenic counterpart (Bousset et al., 2013; Peelaerts et al., 2015; Mavroeidi et al., 2019). Through their neurotoxic behavior as oligomeric or fibrillar assemblies, α-synuclein strains are the crucial pathogens responsible for the induction of α-synuclein - and tau-specific disease phenotypes (Guo et al., 2013; Peelaerts et al., 2015; Candelise et al., 2019). In addition, it has been recently reported that MSA strains show several similarities with PD strains, but are significantly more potent in inducing motor deficits, nigrostriatal neurodegeneration, α-synuclein pathology, spreading, and inflammation, reflecting the aggressive nature of this disease (Van der Perren et al., 2020). In contrast, DLB-amplified strains displayed very modest neuropathological features.

THERAPEUTIC APPROACHES TO HALT α-SYNUCLEINOPATHY

Unfortunately, up-to-date no disease-modifying therapies exist for α-synucleinopathies only symptomatic therapies to relief motor impairment, including dopamine replacement, deep brain stimulation and pharmacological treatment of non-motor symptoms (Aarsland et al., 2002; Fahn et al., 2004; Ravina et al., 2005; Burn et al., 2006; Okun, 2012). Given the critical role of α-synuclein levels to disease pathogenesis, one obvious approach is to curtail total protein levels, either by reducing protein production or by enhancing protein degradation. Another approach would be to inhibit protein aggregation and misfolding or to alter α-synuclein post-translational modifications such as phosphorylation, which are suggested to affect the aggregation process and the development of toxic species. Targeting the extracellular levels of the protein with antibodies and intervening in the proposed mechanisms of uptake is also an attractive approach, since this may combat α-synuclein propagation and disease progression.

REDUCING α-SYNUCLEIN PRODUCTION

Decreasing the production and the cytoplasmic levels of α-synuclein with the use of RNA interference (RNAi) technology represents an attractive approach for therapy in synucleinopathies (**Figure 3**). Specifically, there are *in vivo* studies showing that delivery of either naked small interfering

RNAs (siRNAs) or lentiviral-mediated RNAi for *SNCA* silencing in the rodent brain, can effectively reduce α-synuclein levels (Sapru et al., 2006; Lewis et al., 2008). Accordingly, similar siRNA delivery in the substantia nigra of squirrel monkeys led to a significant suppression of α-synuclein expression with no toxic effects in the animal physiology (McCormack et al., 2010). Another study also suggested a non-toxic but rather a neuroprotective role of α-synuclein reduction in rats injected with shRNAs against *SNCA* via adeno-associated virus (AAV) (Zharikov et al., 2015).

In vitro and *in vivo* experiments using an amido-bridged nucleic acid (AmNA)-modified antisense oligonucleotide (ASO) resulted in decreased mRNA and protein levels of α-synuclein and improved motor deficits in a PD mouse model (Uehara et al., 2019). In addition, AAV-mediated delivery of an anti- α-synuclein ribozyme (rAAV-SynRz) prevented the death of the nigral dopaminergic neurons in the rat MPTP intoxication model (Hayashita-Kinoh et al., 2006). The rescue of dopaminergic cells loss via gene silencing has also been studied using an AAV harboring a short-hairpin (sh)RNA targeting human *SNCA* in the rat striatum, previously injected with AAV-hSNCA for human α-synuclein overexpression (Khodr et al., 2011). *In vitro* studies from the same group revealed that the miR-30-embedded shRNA silencing vector successfully decreased α-synuclein levels (Han et al., 2011); yet delivery of AAV-mir30-hSNCA in the rat brain did not produce encouraging results towards a potential PD therapy (Khodr et al., 2014).

However, there are controversial studies that present degenerative outcomes following a reduction of α-synuclein levels in the substantia nigra of rats and non-human primates (Gorbatyuk et al., 2010; Kanaan and Manfredsson, 2012; Collier et al., 2016; Teki and Griffiths, 2016; Benskey et al., 2018). siRNA-mediated reduction of α-synuclein has been also shown to regulate dopamine release in SH-SY5Y cells and to be used as a protective mechanism against MPP^+-induced neurotoxicity (Fountaine and Wade-Martins, 2007). Moreover, exosomal-associated siRNA intravenous-delivery targeting α-synuclein mRNA in both wild type and α-synuclein transgenic mice, prevented protein aggregation (Cooper et al., 2014). Additionally, α-synuclein knockdown in the brain of wild-type mice, using siRNAs and an anti-sense oligonucleotide molecule (ASO), did not display any harmful effects on neuronal function (Alarcon-Aris et al., 2018). Finally, beta-2-adrenoreceptor (beta-2AR) ligands were shown to modulate *SNCA* transcription through histone 3 lysine 27 acetylation of *SNCA* promoter and enhancers. Beta-2AR agonists (clenbuterol and salbutamol) when used in various cellular and *in vivo* models, led to the reduction of α-synuclein expression, whereas beta-2AR antagonist propranolol increased *SNCA* transcription and α-synuclein production (Mittal et al., 2017).

ENHANCING α-SYNUCLEIN DEGRADATION

Given the well-recognized role of ALP in α-synuclein degradation (**Figure 2**) the mammalian target of rapamycin (mTOR) has emerged as a therapeutic target for PD. Towards this direction, rapamycin, an inhibitor of mTOR, was shown to reduce α-synuclein accumulation in WT, A30P and A53T α-synuclein-overexpressing PC12 cells (Webb et al., 2003), to attenuate dopaminergic degeneration in neurotoxin-induced (Dehay et al., 2010; Malagelada et al., 2010; Liu et al., 2013) and α-synuclein-overexpressing PD models (Crews et al., 2010) and to improve motor function in A53T α-synuclein transgenic mice (Bai et al., 2015). However, a considerable limitation of rapamycin is that it interferes with numerous other autophagy independent pathways, including immunosuppression (Staats et al., 2013) and that prolonged exposure to rapamycin inhibits mTORC2 (Schreiber et al., 2015), thus leading to the stimulation of other important cellular pathways. To overcome these unwanted side effects, studies focused on TFEB, a down-stream target of mTOR, and showed that TFEB overexpression promoted the clearance of pathologic α-synuclein and restored neurodegeneration in PD animal models (Dehay et al., 2010; Decressac et al., 2013). Similarly, oligodendroglial-targeted TFEB overexpression efficiently prevented α-synuclein accumulation and rescued nigrostriatal neurodegeneration in the PLP-α-synuclein MSA mouse model (Arotcarena et al., 2019).

Moreover, several compounds associated with the activation of the AMP-activated protein kinase (AMPK)-dependent autophagy, such as metformin (Dulovic et al., 2014; Patil et al., 2014; Lu et al., 2016), or nilotinib (Hebron et al., 2013; Karuppagounder et al., 2014; Mahul-Mellier et al., 2014), have been reported to inhibit α-synuclein accumulation and to exert neuroprotection in several PD models. The tyrosine-kinase inhibitor nilotinib -a medication widely used for the treatment of chronic myelogenous leukemia- has now been repurposed for the treatment of PD and a Phase 1 clinical trial in 11 PD and DLB patients showed cognitive and motor improvement following nilotinib administration (NCT02281474). A larger Phase 2 clinic trial including 75 PD patients is currently being conducted with so far promising results (NCT02954978). Comparable findings have been reported upon application of 5-aminoimidazole-4-carboxamide ribonucleotide (AICAR) (a drug used for the treatment of acute lymphoblastic leukemia) in various PD models (Ng et al., 2012; Dulovic et al., 2014). Trehalose, also leads to an AMPK-dependent and mTOR-independent induction of autophagosome biogenesis and has been also shown to exert beneficial effects on cell survival and autophagy-dependent α-synuclein clearance in cellular (Sarkar et al., 2007; Casarejos et al., 2011; Lan et al., 2012) and animal PD models (Sarkar et al., 2014; Tanji et al., 2015; Wu et al., 2015; He et al., 2016). Collectively, given the pleiotropic actions and the limited specificity of these agents for the autophagic process, it's challenging to determine whether the observed beneficial effects are mediated by AMPK activation or are a result of other off-target effects, which limit their potential therapeutic utility in synucleinopathies.

In search of non-chemical methods to modulate autophagy, experimental evidence shows that the natural inducer of autophagy curcumin, counteracted the accumulation of the A53T α-synuclein through down-regulation of the mTOR/p70S6K signaling pathway in SH-SY5Y cells (Pandey et al., 2008;

Jiang et al., 2013) and conferred neuroprotection in rotenone-treated dopaminergic neurons (Satish Bollimpelli and Kondapi, 2015). A curcumin analog, C1, has been recently identified as a novel mTOR-independent activator of TFEB (Song et al., 2016), resulting in enhanced autophagy and increased lysosome biogenesis in the rat brain (Song et al., 2016). Likewise, the natural compound pomegranate has been shown to enhance TFEB activity and activate mTOR-independent autophagy and mitophagy (Tan et al., 2019). The natural plant phenol resveratrol, possibly following the interaction with its direct target SIRT1, was also shown to induce an AMPK-dependent autophagy and exert beneficial effects in several *in vitro* and *in vivo* PD models (Wu Y. et al., 2011; Ferretta et al., 2014; Lin et al., 2014; Guo et al., 2016; Ur Rasheed et al., 2016). A major concern of broad macroautophagy enhancement is the multifunctional role and status of activation in different cell types and tissues and the fact that excessive stimulation of macroautophagy under specific circumstances can exert detrimental effects (Yang et al., 2007; Choi et al., 2010; Xu et al., 2014). We have previously shown that CMA inhibition conferred by aberrant α-synuclein overexpression in neuronal cells resulted to a compensatory induction of macroautophagy and subsequent death, whereas pharmacological and molecular macroautophagy inhibition exerted a protective effect (Xilouri et al., 2009). Furthermore, the activation of mitophagy in primary cortical neurons overexpressing A53T α-synuclein caused mitochondrial destruction and neuronal degeneration that could be rescued by inhibition of macroautophagy (Choubey et al., 2011).

Another promising approach implicates the restoration of proper GCase activity as means to facilitate α-synuclein degradation. *In vivo* studies demonstrated that enhancing GCase activity (either pharmacologically or molecularly) could prevent or diminish formation of toxic α-synuclein species and related toxicity (Sardi et al., 2011, 2013). Enzyme-replacement therapies for GD showed that GCase does not cross the blood-brain barrier (BBB), therefore, recent strategies focused on the development of small-molecule chaperones to correct the folding of GCase, enhance GCase activity and restore lysosomal function to facilitate α-synuclein clearance (Schapira and Gegg, 2013; Blanz and Saftig, 2016). Ambroxol is a drug commonly used as an anti-mucolytic respiratory agent (Malerba and Ragnoli, 2008) and has been shown to restore lysosomal function and reduce oxidative stress in *GBA1* mutant fibroblasts (McNeill et al., 2014; Ambrosi et al., 2015). More recently, ambroxol treatment was found to increase GCase levels, improve autophagy and decrease α-synuclein levels in neural crest stem cell-derived dopaminergic neurons from *GBA1* mutation patients (Yang et al., 2017) and α-synuclein transgenic mice (Migdalska-Richards et al., 2016). The same group reported that oral administration of ambroxol increased GCase activity in the non-human primate brain indicating that ambroxol represents a promising novel disease modifying therapy for the treatment of PD and neuropathic GD (Migdalska-Richards et al., 2017). A phase 2 clinical trial assessing the safety and efficacy of ambroxol to improve motor and cognitive features of PD-GD patients has been recently completed (NCT02914366) (Silveira et al., 2019). Moreover, another clinical trial of PD patients (with or without GBA1 mutations) treated with up to 420 mg/day of ambroxol at 5 intra-dose escalations over the course of 6 months, confirmed the safety, tolerability and CSF penetration of this drug (NCT02941822) (Mullin et al., 2020). Furthermore, treatment with LTI-29, another activator of GCase activity, has been shown to reduce glucosylceramide levels *in vivo*[1] and the safety and tolerability of this therapeutic candidate are being tested in a phase 1 clinical trial in *GBA*-PD patients (NTR6960, EudraCT2017 004086 27). Finally, new glucosylceramide synthase inhibitors capable of crossing the BBB and prevent the substrate buildup in mouse models have arisen as another strategy for intervention (Sardi et al., 2017, 2018). Toward this direction, a phase 1 clinical trial assessing the safety and tolerability of the glycosylsynthase inhibitor Venglustat (GZ/SAR402671) in *GBA*-PD patients has successfully been completed (NCT02906020) and this therapeutic approach is currently into phase 2 (Judith Peterschmitt et al., 2019).

Restoration of CMA activity could also provide therapeutic benefit in synucleinopathies, by not only promoting the clearance of α-synuclein, but also by mitigating its detrimental effects on lysosomal function. To this end, we have shown that overexpression of LAMP2A, CMA's rate-limiting step in human neuroblastoma SH-SY5Y cells, rat primary cortical neurons and nigral dopaminergic neurons *in vivo*, was capable of alleviating α-synuclein-related toxicity (Xilouri et al., 2013a). Similarly, LAMP2A overexpression promoted autophagic flux and prevented α-synuclein-induced PD-like symptoms in the Drosophila brain (Issa et al., 2018). Moreover, pharmacological manipulation of the CMA pathway using AR7, a retinoic acid receptor alpha (RARα) antagonist, in $LRRK2^{R1441G}$ mutant mouse fibroblasts restored the impaired lysosomal function and attenuated the progressive accumulation of both intracellular and extracellular α-synuclein oligomers, surmising that CMA activation could successfully prevent the accumulation of such species (Ho et al., 2020). Based on the findings supporting that pathogenic forms of α-synuclein lead to abnormal LAMP2A binding and disruption of the receptor's assembly (Cuervo et al., 2004; Martinez-Vicente et al., 2008) modulation of LAMP2A dynamics at the lysosomal membrane may also represent a fruitful strategy. CMA activity is regulated by the lysosomal mTORC2/PHLPP1/Akt axis (Arias et al., 2015), suggesting that available drugs acting as inhibitors of mTORC2 or Akt, or as activators of PHLPP1 that can modulate the assembly/disassembly rate of the LAMP2A translocation complex could become attractive targets for selective modulation of CMA.

INHIBITING α-SYNUCLEIN AGGREGATION

Prevention of α-synuclein aggregation and misfolding is a key player in disease confronting (**Figure 3**). The selective specificity of intrabodies/nanobodies allows them to bind to specific regions of different α-synuclein species (monomers, oligomers, fibrils)

[1]https://lti-staging.squarespace.com/our-science/#lti-291

and modulate aggregation, therefore attenuating the disease pathology (Bhatt et al., 2013). The nanobodies VH14*PEST and NbSyn87*PEST target the NAC and the C-terminal regions of α-synuclein, respectively, and have been efficiently used against the formation of pathological pSer129 α-synuclein species following their delivery using viral vectors in the rat substantia nigra (Chatterjee et al., 2018). Three small molecules, NPT200–11, NPT100-18A and NPT088 have been reported as inhibitors of either oligomeric or proteinase K-resistant α-synuclein aggregates, both *in vitro* and *in vivo* (Krishnan et al., 2014; Wrasidlo et al., 2016; Price et al., 2018). Moreover, an emerging number of compounds tested in cellular and mouse models of PD exerted a protective role against α-synuclein pathology. Specifically, polyphenol (-)-epi-gallocatechin-3-gallate (EGCG) is used in both AD and PD cases and acts as an inhibitor of α-synuclein and amyloid beta fibril-maturation, by converting large amyloid fibrils into smaller non-toxic aggregates (Bieschke et al., 2010). Anle138b [3-(1,3-benzodioxol-5-yl)-5-(3-bromophenyl)-1H-pyrazole] is an oligomer modulator shown to prevent the formation of pathological aggregates *in vitro* and *in vivo* of both prion protein PrP(Sc) and α-synuclein (Wagner et al., 2013; Levin et al., 2014). Behavioral and histological analysis of the PLP-α-synuclein transgenic mice treated with anle138b revealed that this aggregation inhibitor effectively attenuated the progression of the MSA-like pathology (Fellner et al., 2016; Heras-Garvin et al., 2019). Interestingly, this compound has gained attention as a promising fluorescent biomarker for the detection of aggregation-related epitopes (Deeg et al., 2015).

CLR01, another aggregation-inhibitor, prevented the formation of β-sheet-rich fibrils and had beneficial effects on the health and survival of a zebrafish model of α-synuclein toxicity (Prabhudesai et al., 2012). Moreover, when PLP- or Thy1-α-synuclein transgenic mice received treatment with CLR01, they displayed amelioration of the α-synuclein-related brain pathology and behavioral deficits (Richter et al., 2017; Herrera-Vaquero et al., 2019). Furthermore, KYP-2047, a prolyl oligopeptidase inhibitor, has also been effectively used against α-synuclein aggregation in both cellular and mouse models of PD (Myohanen et al., 2012), whereas porphyrin phthalocyanine tetrasulfonate, an inhibitor of protein aggregation through binding to vesicle-associated α-synuclein, is suggested to modulate α-synuclein misfolding and toxicity (Fonseca-Ornelas et al., 2014). There are also numerous chemical compounds belonging to polyphenols, phenothiazines, polyene macrolides, porphyrins, rifamycins, Congo red (and its derivatives) and terpenoids, that have been shown to decrease α-synuclein fibrillization (Masuda et al., 2006). Baicalein (flavone), delphinidin (anthocyanidin) and methylthioninium (monoamine oxidase inhibitor) are chemical molecules with inhibitory properties against α-synuclein filament formation (Zhu et al., 2004; Hung et al., 2016; Schwab et al., 2017; Javed et al., 2018) as proposed by *in vitro* and *in vivo* experiments. Similarly, mannitol, catechol-o-methyltransferase inhibitors, cinnamon extract, and ring-fused pyridones have anti-aggregatory properties and provide protection against α-synuclein toxicity (Di Giovanni et al., 2010; Shaltiel-Karyo et al., 2012, 2013; Horvath et al., 2013).

Synthetic peptides are also another therapeutic approach developed for β-sheet structure disruption and inhibition of α-synuclein accumulation (El-Agnaf et al., 2004; Kim et al., 2009; Shaltiel-Karyo et al., 2010). Moreover, the antibiotic rifampicin has been used as a destabilizer of α-synuclein fibrils (Li et al., 2004) and a reduction in monomeric, oligomeric and pathological pSer129 α-synuclein has been reported in a rifampicin-treated transgenic MSA mouse model (Ubhi et al., 2008). Rifampicin has been also tested in a clinical trial where 50 participants received a 12-month treatment with rifampicin (600 mg/day), with however, negative results (Low et al., 2014). Another anti-aggregation therapeutic strategy in the context of MSA would be the inhibition of β-III tubulin and the oligodendroglial-specific phosphoprotein TPPP/p25α, since both proteins are implicated in α-synuclein accumulation (Lindersson et al., 2005; Nakayama et al., 2012; Mavroeidi et al., 2019). Nocodazole, a synthetic tubulin-binding agent that inhibits tubulin polymerization, prevented α-synuclein accumulation in primary neuronal and glial cultures, pinpointing the crucial role of β-III tubulin/α-synuclein interaction in MSA pathogenesis (Nakayama et al., 2012). Unfortunately, up-to-date there are no available p25α inhibitors, although such an approach may exert beneficial effects against MSA.

TARGETING α-SYNUCLEIN POST-TRANSLATIONAL MODIFICATIONS

Taking into account that post-translational modifications of α-synuclein, such as phosphorylation, truncation or oxidation/nitration, are tightly associated with the development of neuropathology (Oueslati et al., 2010; Barrett and Timothy Greenamyre, 2015), modulating these modifications is another viable approach. Although the majority of studies link pSer129-α-synuclein with neuropathology (Smith et al., 2005; Chau et al., 2009; Ma et al., 2016; Grassi et al., 2018), others support that α-synuclein phosphorylation and the subsequent inclusion formation protects cells from toxicity (Chen and Feany, 2005; Paleologou et al., 2008; Wu B.et al., 2011; Kuwahara et al., 2012). Therefore, regulation of the expression and/or activity of kinases and phosphatases responsible for phosphorylation and de-phosphorylation of α-synuclein at Ser129 represent a main target. Specifically, overexpression of G-protein-coupled receptor kinase 6 (GRK6) proposed to phosphorylate α-synuclein via AAVs in the rat substantia nigra, led to extensive degeneration of dopaminergic neurons (Sato et al., 2011). Towards the same direction, mutation of Ser129 to alanine inhibited the G protein-coupled receptor kinase 2 (Gprk2)-mediated phosphorylation of α-synuclein and attenuated α-synuclein toxicity in a PD transgenic fly model (Chen and Feany, 2005). Moreover, *in vitro* and *in vivo* enhancement of α-synuclein de-phosphorylation via the phosphoprotein phosphatase-2A (PP2A) protected neurons against α-synuclein pathology (Lee et al., 2011).

Many studies have also proposed that both C- and N-terminal truncations of α-synuclein facilitate α-synuclein aggregation and misfolding and exhibit pathological properties

(Ulusoy et al., 2010; Hall et al., 2015; Wang et al., 2016; Iyer et al., 2017; Ma et al., 2018; Terada et al., 2018). Monoclonal antibodies against the C-terminal truncation (1H7, 5C1, and 5D12) have been tested in a PD mouse model and the results showed reduced aggregation of α-synuclein and improved neurotoxic and behavioral deficits upon immunotherapy (Games et al., 2014). Other studies focused on calpain targeting by using specific calpain inhibitors *in vivo*, a strategy that resulted in amelioration of α-synuclein pathology (Diepenbroek et al., 2014; Hassen et al., 2018). However, enhancement of calpain activity did not result in the expected exacerbation of α-synuclein pathology (Diepenbroek et al., 2014).

REDUCING UPTAKE AND CELL-TO-CELL TRANSMISSION OF α-SYNUCLEIN

As mentioned above, one proposed mechanism for α-synuclein uptake is endocytosis and inhibiting the protein endocytosis represents another strategy against α-synuclein propagation and spread (**Figure 3**). For example, experiments in α-synuclein-treated cells have shown that deletion of LAG3 or use of antibodies raised against this neuronal receptor effectively inhibits α-synuclein cell-to-cell transfer (Anderson et al., 2016; Mao et al., 2016). Moreover, heparin or chloral hydrate can also act as α-synuclein fibril uptake inhibitors, via disruption of heparan sulphate proteoglycans that normally bind amyloid proteins (Holmes et al., 2013; Karpowicz et al., 2017). Taking into consideration the fact that prion protein (PrPC) is suggested to be implicated in amyloid α-synuclein uptake and neurotoxicity, genetic knockout of PrPC in primary neurons and mice effectively reduced the uptake and aggregation of α-synuclein (Aulic et al., 2017; Ferreira et al., 2017).

Another therapeutic approach to combat α-synuclein cell-to-cell transmission is to target the signaling pathway downstream of the receptor responsible for α-synuclein uptake. For example, the inflammatory response of microglial cells to pathological α-synuclein via TLR signaling can be ameliorated by using TLR4 signaling inhibitors, such as resatorvid (TAK242) (Ii et al., 2006; Kawamoto et al., 2008). In another study, treatment of cells with TAK242 or RSLA (another TLR4 inhibitor) resulted in reduction of TNFα secretion from microglial cells and protection of neuronal cells against α-synuclein neurotoxicity (Hughes et al., 2019). However, when TAK242 was tested in a clinical trial, it failed to reduce serum cytokine levels in patients with severe sepsis and shock or respiratory failure (Rice et al., 2010). Finally, CU-CPT22 (another selective inhibitor for TLR1/2) also reduced TNFα production in primary microglia cells treated with oligomeric α-synuclein and blocked NF-κB nuclear translocation (Daniele et al., 2015). Although most of the existing therapeutic approaches target PD, one of the most promising strategies against MSA is the use of sertraline, a second-generation selective serotonin reuptake inhibitor (SSRI). Sertraline inhibits dynamin 1 and 2 thus blocking the endocytic pathway and it has been shown to inhibit α-synuclein uptake by oligodendrocytes and to prevent pathological α-synuclein spread (Konno et al., 2012). Another SSRI, paroxetine, has already been clinically tested at doses of 30 mg for 2 weeks in 20 patients with MSA and resulted into statistically significant motor improvement (Friess et al., 2006).

IMMUNOTHERAPY

The role of the immune system and neuroinflammation in the pathophysiology of PD and related synucleinopathies, along with the specificity of antigen-antibody binding, render immunotherapy (active and passive) one of the most promising therapeutic approaches (**Figure 4**). The first study of active immunization against α-synuclein utilized full-length α-synuclein vaccination in the PDGF transgenic α-synuclein mice and resulted in decreased α-synuclein accumulation in neuronal cell bodies and synapses (Masliah et al., 2005). Active vaccination of the PDGF and the Thy1 transgenic α-synuclein mice with the PD01A and PD03A vaccines (also known as AFFITOPE) reduced α-synuclein oligomers in axons and synapses, decreased caudo-putamen nucleus degeneration and memory deficits in both mouse models (Mandler et al., 2014). The same results, along with reduced demyelination were observed in an MSA transgenic mouse model (Mandler et al., 2015). Recently, the AFFITOPE was tested and successfully passed into the Phase 1 clinical trial in MSA patients, whereas the clinical trial for PD patients is ongoing[2]. More recently, it was shown that a novel vaccination modality combining an antigen-presenting cell-targeting glucan particle (GP) vaccine delivery system with encapsulated antigen (α-synuclein) plus rapamycin induced both strong anti-α-synuclein antibody titers and neuroprotective T regulatory (Tregs) responses in synucleinopathy models, being more effective than the humoral or cellular immunization alone (Rockenstein et al., 2018). In the same concept, prophylactic vaccinations with full-length recombinant α-synuclein in rats, which subsequent receive AAV-α-synuclein, prevented the accumulation of α-synuclein through the induction of Tregs and microglia activation (Christiansen et al., 2016).

Passive immunization with monoclonal antibodies targeting mostly the C- and N-terminal region of α-synuclein have been also used as means to sequester the extracellular protein, thus inhibiting the propagation of the disease (Masliah et al., 2011; Games et al., 2014; Tran et al., 2014; Shahaduzzaman et al., 2015). The first passive immunotherapy using the PRX002 or 9E4 antibody was tested in 2011, in the PDGF-α-synuclein transgenic mice, and resulted in reduced α-synuclein accumulation in axons and synapses, enhanced lysosomal degradation and improved behavioral and motor defects (Masliah et al., 2011). The promising preclinical results of two antibodies, the PRX002 and the BIIB054 (Weihofen et al., 2019), led to their testing in clinical trials where both of them were found safe and effective in preventing α-synuclein spread. Specifically, PRX002 (PRX002, initially developed by Perrigo, Allegan, MI, United States; patent number US7910333; NCT02157714 and NCT02095171) is a humanized IgG1 monoclonal antibody that resulted in 96.5%

[2]http://sympath-project.eu/wp-content/uploads/PR_AFF009_V1.pdf

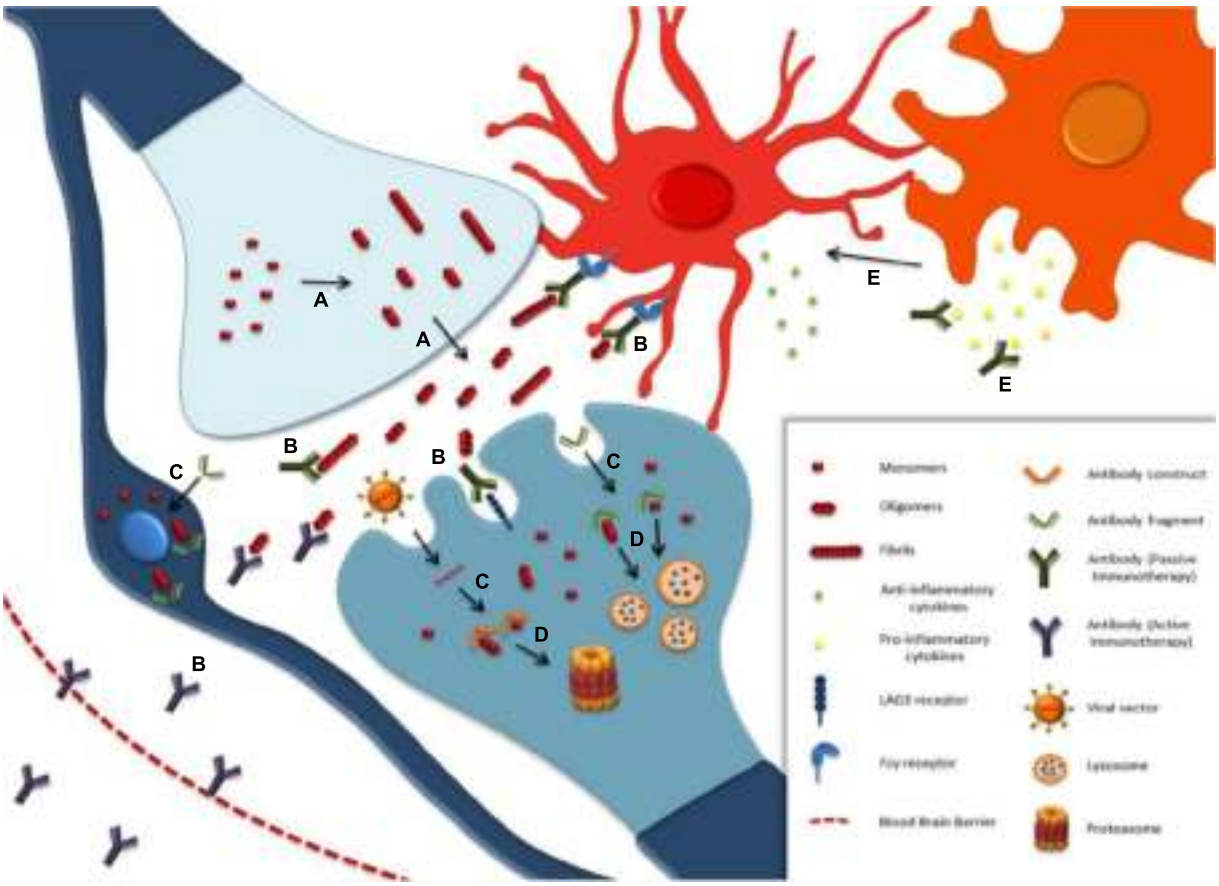

FIGURE 4 | Immunotherapy approaches against α-synuclein. **(A)** Thermodynamically unstable monomers of α-synuclein misfold and aggregate into pathological species. The release of oligomeric and fibrillar α-synuclein into the extracellular space triggers α-synuclein propagation into non-affected cells, microglial activation and neuroinflammation. **(B)** Active or passive immunization mainly aims to lower the extracellular α-synuclein by microglial-mediated degradation and to prevent pathology propagation via antibody binding on receptors facilitating α-synuclein endocytosis. **(C)** The effective targeting of intracellular α-synuclein is achieved by antibody fragments paired with signaling peptides for endocytosis, or viral vector-derived antibody constructs, which are expressed within the cells. **(D)** The engineered intrabodies bind to α-synuclein toxic species and lead them to degradation through proteasomal or autophagic pathways. **(E)** Antibodies against immune system activation is another immunotherapy approach, which aims to reduce pro-inflammatory cytokine release, enhance anti-inflammatory microglial activity and, by that, prevent α-synuclein pathology progression.

decrease of free serum α-synuclein in phase 1a clinical trial (Schenk et al., 2017) and 97% decrease following a single intravenous infusion of the highest dose (60 mg/kg) in phase 1b and these findings prompted the design of an ongoing phase 2 clinical trial (NCT03100149) (Jankovic et al., 2018). BIIB054 (licensed by Biogen) is a fully human-derived monoclonal antibody specifically raised against aggregated and fibrillar α-synuclein that displayed beneficial effects regarding α-synuclein aggregation in the PFF-inoculated PD mouse model (Weihofen et al., 2019). The results from phase 1 clinical trial in PD and healthy patients revealed that BIIB054 is safe and tolerable and have allowed the initiation of phase 2 trial (NCT03318523) (Brys et al., 2019). Finally, other monoclonal antibodies raised against misfolded α-synuclein (Syn211 and Syn303) have been efficiently used *in vivo* and inhibited α-synuclein uptake and pathology transmission (Tran et al., 2014). Other C-terminal targeting α-synuclein antibodies, such as 1H7, 5C1, A1-A6 and ab274 antibodies, were efficiently shown to decrease protein aggregation and exert neuroprotective effects (Bae et al., 2012; Games et al., 2014; Sahin et al., 2017).

The first reported N-terminal targeting antibody, AB1, prevented dopaminergic neuron loss and microgliosis in an AAV-α-synuclein rat model of PD (Shahaduzzaman et al., 2015). Subsequently, the aggregate-selective BIIB054 human α-synuclein antibody was reported to attenuate the spreading of α-synuclein pathology, to rescue motor impairments and to reduce the loss of dopamine transporter density in the nigrostriatal terminals in three different PFF-inoculated mouse models (Weihofen et al., 2019). BIIB054 was originally licensed by Biogen in 2010 and it was first tested in healthy volunteers in 2015. Since then, BIIB054 successfully passed through Phase 1 clinical testing for safety and tolerability and a Phase 2 clinical trial in 311 PD patients is ongoing[3] (Brys et al., 2019). The aggregated forms of α-synuclein are also the target of the monoclonal

[3]https://www.alzforum.org/therapeutics/biib054

antibodies Syn211 and Syn303, with promising reported results in cellular and animal α-synuclein PFF-models (Tran et al., 2014). Antibody targeting of the NAC region is another approach. As such, administration of the NAC32 antibody decreased formation of aberrant species and mitigated α-synuclein-related toxicity by 75% in an A53T mutant α-synuclein neuronal cell line. Importantly, the NAC32 established the prime basis of intrabodies manufacture, and open up new opportunities for intracellular α-synuclein targeting (Lynch et al., 2008). Direct targeting of oligomers is another way to inhibit further the aggregation process and promote the clearance of pathological α-synuclein assemblies. *In vitro* [D5 antibody, (Emadi et al., 2007)] and *in vivo* [Syn-10H antibody, (Emadi et al., 2009)] studies using such oligomer-specific antibodies reported promising anti-aggregation effects. In addition, the D5 antibody paired with the LDL receptor-binding domain of apolipoprotein B resulted in increased penetration of the construct intrabody through the endosomal sorting complex required for transport (ESCRT) and resulted in enhanced α-synuclein oligomer degradation *in vivo* (Spencer et al., 2014). Based on this, the combined administration of a CD5-D5 single-chain antibody prevented astrogliosis, microgliosis and α-synuclein aggregation in a mouse model of MSA (Valera et al., 2017).

Likewise, in the PLP-α-synuclein MSA mouse model, administration of the Rec47 antibody led to enhanced α-synuclein clearance, reduced intracellular seeding of the protein and limited microglial activation (Kallab et al., 2018). Furthermore, the oligomer-specific mAb47 antibody successfully prevented α-synuclein assembly formation in murine co-cultures of astrocytes, oligodendrocytes and neurons and, interestingly, protected astroglia from an oligomeric α-synuclein-mediated mitochondrial dysfunction (Gustafsson et al., 2017). Moreover, MEDI1341, a high affinity α-synuclein antibody that crosses the BBB and binds monomeric and aggregated α-synuclein, prevented cell-to-cell transmission of α-synuclein in PFF-treated neuronal cells and is currently tested in a Phase 1 clinical trial for α-synucleinopathies (ClinicalTrials.gov identifier NCT03272165) (Schofield et al., 2019). A phase 1 clinical study with the monoclonal antibody ABBV-0805 (or BAN0805) that selectively targets oligomeric and protofibrilar forms of α-synuclein has initiated, however no results have been published yet. A variety of antibodies against oligomeric and fibrillar forms of α-synuclein were recently reported. Syn-O1, Syn-O2 and Syn-O4 target oligomers and Syn-F1 and Syn-F2 recognize the fibrillar assemblies. Syn-O1, Syn-O4 and Syn–F1 antibodies limited α-synuclein aggregation with higher efficacy than the other constructs when tested in the PDGF α-synuclein mouse model (El-Agnaf et al., 2017).

Finally, many current immunotherapeutic approaches aim to modulate the immune system imbalance evoked by misfolded α-synuclein accumulation by promoting anti-inflammatory and neuroprotective conditions (Reynolds et al., 2010). Therapies, including administration of the granulocyte macrophage-colony stimulating factor (GM-CSF) and the vasoactive intestinal peptide (VIP), avert the inflammatory role of effector T cells (Teff) by inducing T regulatory cells (Tregs), which are severely diminished in PD patients (Saunders et al., 2012). The GM-CSF stimulating factor, sargramostim, is already in clinical trial phase 1 for PD providing promising results in motor defects improvement (Gendelman et al., 2017). Unfortunately, VIP is rapidly metabolized; hence a VIPR2 agonist, LBT3627, has been designed and used in α-synuclein overexpression rats and MPTP-intoxicated mice with beneficial results (Olson et al., 2015, 2016; Mosley et al., 2019). Therefore, its promising outcome in animal models renders VIP agonist as a therapeutic candidate for clinical testing in the future.

TARGETING THE GUT

α-synuclein spread via the gut-brain axis has gained attention in the last years as a potential therapeutic target against α-synucleinopathies (Holmqvist et al., 2014; Lee et al., 2018; Manfredsson et al., 2018). Many studies have focused on gut microbiota as a regulator of α-synuclein misfolding and transmission towards the brain via the vagus nerve (Sampson et al., 2016; Bhattacharyya et al., 2019; Chiang and Lin, 2019) and results have revealed differences in gut microbiota between PD patients and healthy controls suggesting a role of the gut microbiome in PD pathogenesis (Scheperjans et al., 2015; Unger et al., 2016; Lin A.et al., 2018). To this end, the generation of a germfree α-synuclein PD mouse model resulted in decreased α-synuclein toxicity and neuroinflammation; however when the same mice received gut microbiota from PD patients, they exhibited motor impairment (Sampson et al., 2016). Gastrointestinal dysfunction is connected to PD and several approaches have been developed to alleviate α-synuclein pathological effects, such as therapeutic strategies to stimulate gastric motility (Moore et al., 2018), use of antibiotics and microbiota replacement (Fasano et al., 2015; Felice et al., 2016).

CONCLUDING REMARKS AND FUTURE PERSPECTIVES

Undoubtedly, α-synuclein plays a crucial role in the initiation and progression of the neurodegenerative cascade characterizing PD and related synucleinopathies. Candidate attractive options for therapy aim to reduce protein production or enhance protein degradation, to inhibit protein aggregation and misfolding, to alter α-synuclein post-translational modifications or to target the extracellular levels of the protein with antibodies, thus intervening in the protein uptake and cell-cell propagation mechanisms. All approaches should be handled with caution, since uncontrolled manipulation of the global α-synuclein levels may lead to neurotoxicity, due to the prevailing role of the protein in synaptic neurotransmission. Regarding the degradation strategies, experimental findings surmise that such strategies imply extensive knowledge about dosage and timing of application, a fact that may limit their current therapeutic applicability. Others and we have found that under specific circumstances induction of macroautophagy can have detrimental effects, thus the therapeutic utility of chemical

modulators of macroautophagy or even CMA should be examined with caution given that they may be involved in diverse range of processes. Our experience in regards to CMA enhancement showed that this approach represents a fruitful strategy for synucleinopathies, at least in rodent cellular and animal models. This therapeutic modality is currently being tested in a non-human primate model of α-synucleinopathy and if proven successful it may pave the way for its possible clinical utility for the treatment of PD and related synucleinopathies. In regards to the approaches targeting extracellular α-synuclein, they seem to represent a compelling strategy to slow or halt disease progression, by interfering to the cell-cell transmission mechanisms. However, it still remains to be elucidated whether this transmission involves only the neuronal connectome and, most importantly, which species or strains of the protein are the main culprits for the pathology transmission.

In addition, a growing body of evidence suggests that an underlying cause of the heterogeneity characterizing synucleinopathies is the presence of distinct α-synuclein strains in patient samples. As such, PD- and MSA- derived patient α-synuclein strains exhibit different biophysical/biochemical properties and evoke different responses in cultured cells and animal models. Furthermore, the cellular milieu seems to affect the pathogenetic properties of the engendered strains, suggesting that other co-factors may alter disease initiation and progression. Hence, the aforementioned therapeutic strategies targeting the degradation, modification, secretion and seeding of the distinct strains may result in different outcomes in neurons and oligodendrocytes, raising the possibility of the application of a precision medicine in synucleinopathies in the near future. By utilizing advanced structural biology techniques and cryo-electron microscopy we may attain a better understanding of the clinical heterogeneity amongst α-synucleinopathies, thus offering the opportunity for the future development of strain-specific therapies to halt or delay disease progression.

Collectively, we believe that further research is needed to better understand the precise mechanisms underlying the α-synuclein pathology enigma and to pinpoint the factors that differentiate the pathology observed in synucleinopathies.

AUTHOR CONTRIBUTIONS

MF, PM, and GT wrote the initial draft. MX revised and generated the final version of the manuscript. All authors contributed to the article and approved the submitted version.

FUNDING

Work in Dr. Xilouri's lab is supported by a Michael J. Fox Foundation for Parkinson's research grant (Grant ID 16887). This research is co-financed by Greece and the European Union (European Social Fund – ESF) through the Operational Programme "Human Resources Development, Education and Lifelong Learning" in the context of the project "Strengthening Human Resources Research Potential via Doctorate Research" (MIS-5000432), implemented by the State Scholarships Foundation (IKY).

REFERENCES

Aarsland, D., Laake, K., Larsen, J. P., and Janvin, C. (2002). Donepezil for cognitive impairment in Parkinson's disease: a randomised controlled study. *J. Neurol. Neurosurg. Psychiatry* 72, 708–712. doi: 10.1136/jnnp.72.6.708

Abdelmotilib, H., Maltbie, T., Delic, V., Liu, Z., Hu, X., Fraser, K. B., et al. (2017). alpha-Synuclein fibril-induced inclusion spread in rats and mice correlates with dopaminergic Neurodegeneration. *Neurobiol. Dis.* 105, 84–98. doi: 10.1016/j.nbd.2017.05.014

Abounit, S., Bousset, L., Loria, F., Zhu, S., de Chaumont, F., Pieri, L., et al. (2016). Tunneling nanotubes spread fibrillar alpha-synuclein by intercellular trafficking of lysosomes. *EMBO J.* 35, 2120–2138. doi: 10.15252/embj.201593411

Afitska, K., Fucikova, A., Shvadchak, V. V., and Yushchenko, D. A. (2019). alpha-Synuclein aggregation at low concentrations. *Biochim. Biophys. Acta Proteins Proteom.* 1867, 701–709. doi: 10.1016/j.bbapap.2019.05.003

Ahn, K. J., Paik, S. R., Chung, K. C., and Kim, J. (2006). Amino acid sequence motifs and mechanistic features of the membrane translocation of alpha-synuclein. *J. Neurochem.* 97, 265–279. doi: 10.1111/j.1471-4159.2006.03731.x

Alarcon-Aris, D., Recasens, A., Galofre, M., Carballo-Carbajal, I., Zacchi, N., Ruiz-Bronchal, E., et al. (2018). Selective alpha-synuclein knockdown in monoamine neurons by intranasal oligonucleotide delivery: potential therapy for Parkinson's disease. *Mol. Ther.* 26, 550–567. doi: 10.1016/j.ymthe.2017.11.015

Alvarez-Erviti, L., Rodriguez-Oroz, M. C., Cooper, J. M., Caballero, C., Ferrer, I., Obeso, J. A., et al. (2010). Chaperone-mediated autophagy markers in Parkinson disease brains. *Arch. Neurol.* 67, 1464–1472. doi: 10.1001/archneurol.2010.198

Alvarez-Erviti, L., Seow, Y., Schapira, A. H., Gardiner, C., Sargent, I. L., Wood, M. J., et al. (2011). Lysosomal dysfunction increases exosome-mediated alpha-synuclein release and transmission. *Neurobiol. Dis.* 42, 360–367. doi: 10.1016/j.nbd.2011.01.029

Ambrosi, G., Ghezzi, C., Zangaglia, R., Levandis, G., Pacchetti, C., and Blandini, F. (2015). Ambroxol-induced rescue of defective glucocerebrosidase is associated with increased LIMP-2 and saposin C levels in GBA1 mutant Parkinson's disease cells. *Neurobiol. Dis.* 82, 235–242. doi: 10.1016/j.nbd.2015.06.008

Anderson, A. C., Joller, N., and Kuchroo, V. K. (2016). Lag-3, Tim-3, and TIGIT: co-inhibitory receptors with specialized functions in immune regulation. *Immunity* 44, 989–1004. doi: 10.1016/j.immuni.2016.05.001

Anglade, P., Vyas, S., Javoy-Agid, F., Herrero, M. T., Michel, P. P., Marquez, J., et al. (1997). Apoptosis and autophagy in nigral neurons of patients with Parkinson's disease. *Histol. Histopathol.* 12, 25–31.

Angot, E., Steiner, J. A., Lema Tome, C. M., Ekstrom, P., Mattsson, B., Bjorklund, A., et al. (2012). Alpha-synuclein cell-to-cell transfer and seeding in grafted dopaminergic neurons *in vivo*. *PLoS One* 7:e39465. doi: 10.1371/journal.pone.0039465

Arias, E., Koga, H., Diaz, A., Mocholi, E., Patel, B., and Cuervo, A. M. (2015). Lysosomal mTORC2/PHLPP1/Akt regulate chaperone-mediated autophagy. *Mol. Cell* 59, 270–284. doi: 10.1016/j.molcel.2015.05.030

Arotcarena, M. L., Bourdenx, M., Dutheil, N., Thiolat, M. L., Doudnikoff, E., Dovero, S., et al. (2019). Transcription factor EB overexpression prevents neurodegeneration in experimental synucleinopathies. *JCI Insight* 4:e129719. doi: 10.1172/jci.insight.129719

Asi, Y. T., Simpson, J. E., Heath, P. R., Wharton, S. B., Lees, A. J., Revesz, T., et al. (2014). Alpha-synuclein mRNA expression in oligodendrocytes in MSA. *Glia* 62, 964–970. doi: 10.1002/glia.22653

Aulic, S., Masperone, L., Narkiewicz, J., Isopi, E., Bistaffa, E., Ambrosetti, E., et al. (2017). alpha-Synuclein Amyloids Hijack Prion Protein to Gain Cell Entry,

Facilitate Cell-to-Cell Spreading and Block Prion Replication. *Sci. Rep.* 7:10050. doi: 10.1038/s41598-017-10236-x

Badiola, N., de Oliveira, R. M., Herrera, F., Guardia-Laguarta, C., Goncalves, S. A., Pera, M., et al. (2011). Tau enhances alpha-synuclein aggregation and toxicity in cellular models of synucleinopathy. *PLoS One* 6:e26609. doi: 10.1371/journal.pone.0026609

Bae, E. J., Lee, H. J., Rockenstein, E., Ho, D. H., Park, E. B., Yang, N. Y., et al. (2012). Antibody-aided clearance of extracellular alpha-synuclein prevents cell-to-cell aggregate transmission. *J. Neurosci.* 32, 13454–13469. doi: 10.1523/JNEUROSCI.1292-12.2012

Bai, X., Wey, M. C., Fernandez, E., Hart, M. J., Gelfond, J., Bokov, A. F., et al. (2015). Rapamycin improves motor function, reduces 4-hydroxynonenal adducted protein in brain, and attenuates synaptic injury in a mouse model of synucleinopathy. *Pathobiol. Aging Age Relat. Dis.* 5:28743. doi: 10.3402/pba.v5.28743

Barkholt, P., Sanchez-Guajardo, V., Kirik, D., and Romero-Ramos, M. (2012). Long-term polarization of microglia upon alpha-synuclein overexpression in nonhuman primates. *Neuroscience* 208, 85–96. doi: 10.1016/j.neuroscience.2012.02.004

Barrett, P. J., and Timothy Greenamyre, J. (2015). Post-translational modification of alpha-synuclein in Parkinson's disease. *Brain Res.* 1628(Pt B), 247–253. doi: 10.1016/j.brainres.2015.06.002

Bartels, T., Choi, J. G., and Selkoe, D. J. (2011). alpha-Synuclein occurs physiologically as a helically folded tetramer that resists aggregation. *Nature* 477, 107–110. doi: 10.1038/nature10324

Bennett, M. C., Bishop, J. F., Leng, Y., Chock, P. B., Chase, T. N., and Mouradian, M. M. (1999). Degradation of alpha-synuclein by proteasome. *J. Biol. Chem.* 274, 33855–33858. doi: 10.1074/jbc.274.48.33855

Benskey, M. J., Sellnow, R. C., Sandoval, I. M., Sortwell, C. E., Lipton, J. W., and Manfredsson, F. P. (2018). Silencing alpha synuclein in mature Nigral neurons results in rapid neuroinflammation and subsequent toxicity. *Front. Mol. Neurosci.* 11:36. doi: 10.3389/fnmol.2018.00036

Bentea, E., Verbruggen, L., and Massie, A. (2017). The proteasome inhibition model of Parkinson's disease. *J. Parkinsons Dis.* 7, 31–63. doi: 10.3233/JPD-160921

Bernis, M. E., Babila, J. T., Breid, S., Wusten, K. A., Wullner, U., and Tamguney, G. (2015). Prion-like propagation of human brain-derived alpha-synuclein in transgenic mice expressing human wild-type alpha-synuclein. *Acta Neuropathol. Commun.* 3:75. doi: 10.1186/s40478-015-0254-7

Bhatt, M. A., Messer, A., and Kordower, J. H. (2013). Can intrabodies serve as neuroprotective therapies for Parkinson's disease? Beginning thoughts. *J. Parkinsons Dis.* 3, 581–591. doi: 10.3233/JPD-130252

Bhattacharyya, D., Mohite, G. M., Krishnamoorthy, J., Gayen, N., Mehra, S., Navalkar, A., et al. (2019). Lipopolysaccharide from gut microbiota modulates alpha-synuclein aggregation and alters its biological function. *ACS Chem. Neurosci.* 10, 2229–2236. doi: 10.1021/acschemneuro.8b00733

Bieschke, J., Russ, J., Friedrich, R. P., Ehrnhoefer, D. E., Wobst, H., Neugebauer, K., et al. (2010). EGCG remodels mature alpha-synuclein and amyloid-beta fibrils and reduces cellular toxicity. *Proc. Natl. Acad. Sci. U.S.A.* 107, 7710–7715. doi: 10.1073/pnas.0910723107

Birol, M., Wojcik, S. P., Miranker, A. D., and Rhoades, E. (2019). Identification of N-linked glycans as specific mediators of neuronal uptake of acetylated alpha-Synuclein. *PLoS Biol.* 17:e3000318. doi: 10.1371/journal.pbio.3000318

Blanz, J., and Saftig, P. (2016). Parkinson's disease: acid-glucocerebrosidase activity and alpha-synuclein clearance. *J. Neurochem.* 139(Suppl. 1), 198–215. doi: 10.1111/jnc.13517

Bose, A., and Beal, M. F. (2016). Mitochondrial dysfunction in Parkinson's disease. *J. Neurochem.* 139(Suppl. 1), 216–231. doi: 10.1111/jnc.13731

Bousset, L., Pieri, L., Ruiz-Arlandis, G., Gath, J., Jensen, P. H., Habenstein, B., et al. (2013). Structural and functional characterization of two alpha-synuclein strains. *Nat. Commun.* 4:2575. doi: 10.1038/ncomms3575

Braak, H., de Vos, R. A., Bohl, J., and Del Tredici, K. (2006). Gastric alpha-synuclein immunoreactive inclusions in Meissner's and Auerbach's plexuses in cases staged for Parkinson's disease-related brain pathology. *Neurosci. Lett.* 396, 67–72. doi: 10.1016/j.neulet.2005.11.012

Braak, H., Del Tredici, K., Rub, U., de Vos, R. A., Jansen Steur, E. N., and Braak, E. (2003). Staging of brain pathology related to sporadic Parkinson's disease. *Neurobiol. Aging* 24, 197–211. doi: 10.1016/s0197-4580(02)00065-9

Brahmachari, S., Ge, P., Lee, S. H., Kim, D., Karuppagounder, S. S., Kumar, M., et al. (2016). Activation of tyrosine kinase c-Abl contributes to alpha-synuclein-induced neurodegeneration. *J. Clin. Invest.* 126, 2970–2988. doi: 10.1172/JCI85456

Brenner, S., Wersinger, C., and Gasser, T. (2015). Transcriptional regulation of the alpha-synuclein gene in human brain tissue. *Neurosci. Lett.* 599, 140–145. doi: 10.1016/j.neulet.2015.05.029

Bruening, W., Giasson, B. I., Klein-Szanto, A. J., Lee, V. M., Trojanowski, J. Q., and Godwin, A. K. (2000). Synucleins are expressed in the majority of breast and ovarian carcinomas and in preneoplastic lesions of the ovary. *Cancer* 88, 2154–2163. doi: 10.1002/(sici)1097-0142(20000501)88:9<2154::aid-cncr23>3.0.co;2-9

Brys, M., Fanning, L., Hung, S., Ellenbogen, A., Penner, N., Yang, M., et al. (2019). Randomized phase I clinical trial of anti-alpha-synuclein antibody BIIB054. *Mov. Disord.* 34, 1154–1163. doi: 10.1002/mds.27738

Burn, D., Emre, M., McKeith, I., De Deyn, P. P., Aarsland, D., Hsu, C., et al. (2006). Effects of rivastigmine in patients with and without visual hallucinations in dementia associated with Parkinson's disease. *Mov. Disord.* 21, 1899–1907. doi: 10.1002/mds.21077

Burre, J., Sharma, M., and Sudhof, T. C. (2014). alpha-Synuclein assembles into higher-order multimers upon membrane binding to promote SNARE complex formation. *Proc. Natl. Acad. Sci. U.S.A.* 111, E4274–E4283. doi: 10.1073/pnas.1416598111

Burre, J., Sharma, M., Tsetsenis, T., Buchman, V., Etherton, M. R., and Sudhof, T. C. (2010). Alpha-synuclein promotes SNARE-complex assembly *in vivo* and *in vitro*. *Science* 329, 1663–1667. doi: 10.1126/science.1195227

Busch, D. J., Oliphint, P. A., Walsh, R. B., Banks, S. M., Woods, W. S., George, J. M., et al. (2014). Acute increase of alpha-synuclein inhibits synaptic vesicle recycling evoked during intense stimulation. *Mol. Biol. Cell* 25, 3926–3941. doi: 10.1091/mbc.E14-02-0708

Bussell, R. Jr., and Eliezer, D. (2001). Residual structure and dynamics in Parkinson's disease-associated mutants of alpha-synuclein. *J. Biol. Chem.* 276, 45996–46003. doi: 10.1074/jbc.M106777200

Butler, B., Saha, K., Rana, T., Becker, J. P., Sambo, D., Davari, P., et al. (2015). Dopamine transporter activity is modulated by alpha-Synuclein. *J. Biol. Chem.* 290, 29542–29554. doi: 10.1074/jbc.M115.691592

Butler, B., Sambo, D., and Khoshbouei, H. (2017). Alpha-synuclein modulates dopamine neurotransmission. *J. Chem. Neuroanat.* 83-84, 41–49. doi: 10.1016/j.jchemneu.2016.06.001

Candelise, N., Schmitz, M., Llorens, F., Villar-Pique, A., Cramm, M., Thom, T., et al. (2019). Seeding variability of different alpha synuclein strains in synucleinopathies. *Ann. Neurol.* 85, 691–703. doi: 10.1002/ana.25446

Casarejos, M. J., Solano, R. M., Gomez, A., Perucho, J., de Yebenes, J. G., and Mena, M. A. (2011). The accumulation of neurotoxic proteins, induced by proteasome inhibition, is reverted by trehalose, an enhancer of autophagy, in human neuroblastoma cells. *Neurochem. Int.* 58, 512–520. doi: 10.1016/j.neuint.2011.01.008

Chandra, S., Chen, X., Rizo, J., Jahn, R., and Sudhof, T. C. (2003). A broken alpha -helix in folded alpha -Synuclein. *J. Biol. Chem.* 278, 15313–15318. doi: 10.1074/jbc.M213128200

Chandra, S., Gallardo, G., Fernandez-Chacon, R., Schluter, O. M., and Sudhof, T. C. (2005). Alpha-synuclein cooperates with CSPalpha in preventing neurodegeneration. *Cell* 123, 383–396. doi: 10.1016/j.cell.2005.09.028

Charles, V., Mezey, E., Reddy, P. H., Dehejia, A., Young, T. A., Polymeropoulos, M. H., et al. (2000). Alpha-synuclein immunoreactivity of huntingtin polyglutamine aggregates in striatum and cortex of Huntington's disease patients and transgenic mouse models. *Neurosci. Lett.* 289, 29–32. doi: 10.1016/s0304-3940(00)01247-7

Chartier-Harlin, M. C., Kachergus, J., Roumier, C., Mouroux, V., Douay, X., Lincoln, S., et al. (2004). Alpha-synuclein locus duplication as a cause of familial Parkinson's disease. *Lancet* 364, 1167–1169. doi: 10.1016/S0140-6736(04)17103-1

Chatterjee, D., Bhatt, M., Butler, D., De Genst, E., Dobson, C. M., Messer, A., et al. (2018). Proteasome-targeted nanobodies alleviate pathology and functional decline in an alpha-synuclein-based Parkinson's disease model. *NPJ Parkinsons Dis.* 4:25. doi: 10.1038/s41531-018-0062-4

Chau, K. Y., Ching, H. L., Schapira, A. H., and Cooper, J. M. (2009). Relationship between alpha synuclein phosphorylation, proteasomal inhibition and cell

death: relevance to Parkinson's disease pathogenesis. *J. Neurochem.* 110, 1005–1013. doi: 10.1111/j.1471-4159.2009.06191.x

Chen, H., and Chan, D. C. (2009). Mitochondrial dynamics–fusion, fission, movement, and mitophagy–in neurodegenerative diseases. *Hum. Mol. Genet.* 18, R169–R176. doi: 10.1093/hmg/ddp326

Chen, J., Ren, Y., Gui, C., Zhao, M., Wu, X., Mao, K., et al. (2018). Phosphorylation of Parkin at serine 131 by p38 MAPK promotes mitochondrial dysfunction and neuronal death in mutant A53T alpha-synuclein model of Parkinson's disease. *Cell Death Dis.* 9:700. doi: 10.1038/s41419-018-0722-7

Chen, L., and Feany, M. B. (2005). Alpha-synuclein phosphorylation controls neurotoxicity and inclusion formation in a Drosophila model of Parkinson disease. *Nat. Neurosci.* 8, 657–663. doi: 10.1038/nn1443

Chen, M., Yang, W., Li, X., Wang, P., Yue, F., Yang, H., et al. (2016). Age- and brain region-dependent alpha-synuclein oligomerization is attributed to alterations in intrinsic enzymes regulating alpha-synuclein phosphorylation in aging monkey brains. *Oncotarget* 7, 8466–8480. doi: 10.18632/oncotarget.6445

Chen, Q. Q., Haikal, C., Li, W., and Li, J. Y. (2019). Gut inflammation in association with pathogenesis of Parkinson's disease. *Front. Mol. Neurosci.* 12:218. doi: 10.3389/fnmol.2019.00218

Chen, S. G., Stribinskis, V., Rane, M. J., Demuth, D. R., Gozal, E., Roberts, A. M., et al. (2016). Exposure to the functional bacterial amyloid protein Curli enhances Alpha-synuclein aggregation in aged Fischer 344 Rats and *Caenorhabditis elegans*. *Sci. Rep.* 6:34477. doi: 10.1038/srep34477

Chen, Y., Wei, Q. Q., Ou, R., Cao, B., Chen, X., Zhao, B., et al. (2015). Genetic Variants of SNCA are associated with susceptibility to Parkinson's disease but not amyotrophic lateral sclerosis or multiple system atrophy in a Chinese population. *PLoS One* 10:e0133776. doi: 10.1371/journal.pone.0133776

Chiang, H. L., and Lin, C. H. (2019). Altered gut microbiome and intestinal pathology in Parkinson's disease. *J. Mov. Disord.* 12, 67–83. doi: 10.14802/jmd.18067

Chiba, Y., Takei, S., Kawamura, N., Kawaguchi, Y., Sasaki, K., Hasegawa-Ishii, S., et al. (2012). Immunohistochemical localization of aggresomal proteins in glial cytoplasmic inclusions in multiple system atrophy. *Neuropathol. Appl. Neurobiol.* 38, 559–571. doi: 10.1111/j.1365-2990.2011.01229.x

Choi, B. K., Choi, M. G., Kim, J. Y., Yang, Y., Lai, Y., Kweon, D. H., et al. (2013). Large alpha-synuclein oligomers inhibit neuronal SNARE-mediated vesicle docking. *Proc. Natl. Acad. Sci. U.S.A.* 110, 4087–4092. doi: 10.1073/pnas.1218424110

Choi, D. C., Yoo, M., Kabaria, S., and Junn, E. (2018). MicroRNA-7 facilitates the degradation of alpha-synuclein and its aggregates by promoting autophagy. *Neurosci. Lett.* 678, 118–123. doi: 10.1016/j.neulet.2018.05.009

Choi, J. G., Kim, N., Ju, I. G., Eo, H., Lim, S. M., Jang, S. E., et al. (2018). Oral administration of *Proteus mirabilis* damages dopaminergic neurons and motor functions in mice. *Sci. Rep.* 8:1275. doi: 10.1038/s41598-018-19646-x

Choi, K. C., Kim, S. H., Ha, J. Y., Kim, S. T., and Son, J. H. (2010). A novel mTOR activating protein protects dopamine neurons against oxidative stress by repressing autophagy related cell death. *J. Neurochem.* 112, 366–376. doi: 10.1111/j.1471-4159.2009.06463.x

Choi, Y. R., Cha, S. H., Kang, S. J., Kim, J. B., Jou, I., and Park, S. M. (2018). Prion-like propagation of alpha-synuclein is regulated by the FcgammaRIIB-SHP-1/2 signaling pathway in neurons. *Cell Rep.* 22, 136–148. doi: 10.1016/j.celrep.2017.12.009

Choubey, V., Safiulina, D., Vaarmann, A., Cagalinec, M., Wareski, P., Kuum, M., et al. (2011). Mutant A53T alpha-synuclein induces neuronal death by increasing mitochondrial autophagy. *J. Biol. Chem.* 286, 10814–10824. doi: 10.1074/jbc.M110.132514

Christiansen, J. R., Olesen, M. N., Otzen, D. E., Romero-Ramos, M., and Sanchez-Guajardo, V. (2016). alpha-Synuclein vaccination modulates regulatory T cell activation and microglia in the absence of brain pathology. *J. Neuroinflammation* 13:74. doi: 10.1186/s12974-016-0532-8

Clark, L. N., Kartsaklis, L. A., Wolf Gilbert, R., Dorado, B., Ross, B. M., Kisselev, S., et al. (2009). Association of glucocerebrosidase mutations with dementia with lewy bodies. *Arch. Neurol.* 66, 578–583. doi: 10.1001/archneurol.2009.54

Clough, R. L., Dermentzaki, G., and Stefanis, L. (2009). Functional dissection of the alpha-synuclein promoter: transcriptional regulation by ZSCAN21 and ZNF219. *J. Neurochem.* 110, 1479–1490. doi: 10.1111/j.1471-4159.2009.06250.x

Clough, R. L., and Stefanis, L. (2007). A novel pathway for transcriptional regulation of alpha-synuclein. *FASEB J.* 21, 596–607. doi: 10.1096/fj.06-7111com

Colla, E. (2019). Linking the endoplasmic reticulum to Parkinson's disease and Alpha-Synucleinopathy. *Front. Neurosci.* 13:560. doi: 10.3389/fnins.2019.00560

Colla, E., Coune, P., Liu, Y., Pletnikova, O., Troncoso, J. C., Iwatsubo, T., et al. (2012). Endoplasmic reticulum stress is important for the manifestations of alpha-synucleinopathy *in vivo*. *J. Neurosci.* 32, 3306–3320. doi: 10.1523/JNEUROSCI.5367-11.2012

Collier, T. J., Redmond, D. E. Jr., Steece-Collier, K., Lipton, J. W., and Manfredsson, F. P. (2016). Is Alpha-synuclein loss-of-function a contributor to Parkinsonian pathology? Evidence from Non-human Primates. *Front. Neurosci.* 10:12. doi: 10.3389/fnins.2016.00012

Conway, K. A., Harper, J. D., and Lansbury, P. T. (1998). Accelerated *in vitro* fibril formation by a mutant alpha-synuclein linked to early-onset Parkinson disease. *Nat. Med.* 4, 1318–1320. doi: 10.1038/3311

Conway, K. A., Lee, S. J., Rochet, J. C., Ding, T. T., Williamson, R. E., and Lansbury, P. T. Jr. (2000). Acceleration of oligomerization, not fibrillization, is a shared property of both alpha-synuclein mutations linked to early-onset Parkinson's disease: implications for pathogenesis and therapy. *Proc. Natl. Acad. Sci. U.S.A.* 97, 571–576. doi: 10.1073/pnas.97.2.571

Conway, K. A., Rochet, J. C., Bieganski, R. M., and Lansbury, P. T. Jr. (2001). Kinetic stabilization of the alpha-synuclein protofibril by a dopamine-alpha-synuclein adduct. *Science* 294, 1346–1349. doi: 10.1126/science.1063522

Cooper, J. M., Wiklander, P. B., Nordin, J. Z., Al-Shawi, R., Wood, M. J., Vithlani, M., et al. (2014). Systemic exosomal siRNA delivery reduced alpha-synuclein aggregates in brains of transgenic mice. *Mov. Disord.* 29, 1476–1485. doi: 10.1002/mds.25978

Couch, Y., Alvarez-Erviti, L., Sibson, N. R., Wood, M. J., and Anthony, D. C. (2011). The acute inflammatory response to intranigral alpha-synuclein differs significantly from intranigral lipopolysaccharide and is exacerbated by peripheral inflammation. *J. Neuroinflammation* 8:166. doi: 10.1186/1742-2094-8-166

Cremades, N., Cohen, S. I., Deas, E., Abramov, A. Y., Chen, A. Y., Orte, A., et al. (2012). Direct observation of the interconversion of normal and toxic forms of alpha-synuclein. *Cell* 149, 1048–1059. doi: 10.1016/j.cell.2012.03.037

Crews, L., Spencer, B., Desplats, P., Patrick, C., Paulino, A., Rockenstein, E., et al. (2010). Selective molecular alterations in the autophagy pathway in patients with Lewy body disease and in models of alpha-synucleinopathy. *PLoS One* 5:e9313. doi: 10.1371/journal.pone.0009313

Cuervo, A. M., Stefanis, L., Fredenburg, R., Lansbury, P. T., and Sulzer, D. (2004). Impaired degradation of mutant alpha-synuclein by chaperone-mediated autophagy. *Science* 305, 1292–1295. doi: 10.1126/science.1101738

Dalfo, E., Barrachina, M., Rosa, J. L., Ambrosio, S., and Ferrer, I. (2004). Abnormal alpha-synuclein interactions with rab3a and rabphilin in diffuse Lewy body disease. *Neurobiol. Dis.* 16, 92–97. doi: 10.1016/j.nbd.2004.01.001

Daniele, S. G., Beraud, D., Davenport, C., Cheng, K., Yin, H., and Maguire-Zeiss, K. A. (2015). Activation of MyD88-dependent TLR1/2 signaling by misfolded alpha-synuclein, a protein linked to neurodegenerative disorders. *Sci. Signal.* 8:ra45. doi: 10.1126/scisignal.2005965

Danzer, K. M., Haasen, D., Karow, A. R., Moussaud, S., Habeck, M., Giese, A., et al. (2007). Different species of alpha-synuclein oligomers induce calcium influx and seeding. *J. Neurosci.* 27, 9220–9232. doi: 10.1523/JNEUROSCI.2617-07.2007

Danzer, K. M., Kranich, L. R., Ruf, W. P., Cagsal-Getkin, O., Winslow, A. R., Zhu, L., et al. (2012). Exosomal cell-to-cell transmission of alpha synuclein oligomers. *Mol. Neurodegener.* 7:42. doi: 10.1186/1750-1326-7-42

Davidson, W. S., Jonas, A., Clayton, D. F., and George, J. M. (1998). Stabilization of alpha-synuclein secondary structure upon binding to synthetic membranes. *J. Biol. Chem.* 273, 9443–9449. doi: 10.1074/jbc.273.16.9443

Decressac, M., Mattsson, B., Weikop, P., Lundblad, M., Jakobsson, J., and Bjorklund, A. (2013). TFEB-mediated autophagy rescues midbrain dopamine neurons from alpha-synuclein toxicity. *Proc. Natl. Acad. Sci. U.S.A.* 110, E1817–E1826. doi: 10.1073/pnas.1305623110

Deeg, A. A., Reiner, A. M., Schmidt, F., Schueder, F., Ryazanov, S., Ruf, V. C., et al. (2015). Anle138b and related compounds are aggregation specific fluorescence markers and reveal high affinity binding to alpha-synuclein aggregates. *Biochim. Biophys. Acta* 1850, 1884–1890. doi: 10.1016/j.bbagen.2015.05.021

Dehay, B., Bove, J., Rodriguez-Muela, N., Perier, C., Recasens, A., Boya, P., et al. (2010). Pathogenic lysosomal depletion in Parkinson's disease. *J. Neurosci.* 30, 12535–12544. doi: 10.1523/JNEUROSCI.1920-10.2010

Delenclos, M., Trendafilova, T., Mahesh, D., Baine, A. M., Moussaud, S., Yan, I. K., et al. (2017). Investigation of endocytic pathways for the internalization of exosome-associated oligomeric Alpha-Synuclein. *Front. Neurosci.* 11:172. doi: 10.3389/fnins.2017.00172

Dermentzaki, G., Paschalidis, N., Politis, P. K., and Stefanis, L. (2016). Complex Effects of the ZSCAN21 transcription factor on transcriptional regulation of alpha-synuclein in primary neuronal cultures and *in vivo*. *J. Biol. Chem.* 291, 8756–8772. doi: 10.1074/jbc.M115.704973

Desplats, P., Lee, H. J., Bae, E. J., Patrick, C., Rockenstein, E., Crews, L., et al. (2009). Inclusion formation and neuronal cell death through neuron-to-neuron transmission of alpha-synuclein. *Proc. Natl. Acad. Sci. U.S.A.* 106, 13010–13015. doi: 10.1073/pnas.0903691106

Dettmer, U., Newman, A. J., Soldner, F., Luth, E. S., Kim, N. C., von Saucken, V. E., et al. (2015). Parkinson-causing alpha-synuclein missense mutations shift native tetramers to monomers as a mechanism for disease initiation. *Nat. Commun.* 6:7314. doi: 10.1038/ncomms8314

Di Giovanni, S., Eleuteri, S., Paleologou, K. E., Yin, G., Zweckstetter, M., Carrupt, P. A., et al. (2010). Entacapone and tolcapone, two catechol O-methyltransferase inhibitors, block fibril formation of alpha-synuclein and beta-amyloid and protect against amyloid-induced toxicity. *J. Biol. Chem.* 285, 14941–14954. doi: 10.1074/jbc.M109.080390

Di Maio, R., Hoffman, E. K., Rocha, E. M., Keeney, M. T., Sanders, L. H., De Miranda, B. R., et al. (2018). LRRK2 activation in idiopathic Parkinson's disease. *Sci. Transl. Med.* 10:eaar5429. doi: 10.1126/scitranslmed.aar5429

Diao, J., Burre, J., Vivona, S., Cipriano, D. J., Sharma, M., Kyoung, M., et al. (2013). Native alpha-synuclein induces clustering of synaptic-vesicle mimics via binding to phospholipids and synaptobrevin-2/VAMP2. *eLife* 2:e00592. doi: 10.7554/eLife.00592

Diaz, E. F., Labra, V. C., Alvear, T. F., Mellado, L. A., Inostroza, C. A., Oyarzun, J. E., et al. (2019). Connexin 43 hemichannels and pannexin-1 channels contribute to the alpha-synuclein-induced dysfunction and death of astrocytes. *Glia* 67, 1598–1619. doi: 10.1002/glia.23631

Diepenbroek, M., Casadei, N., Esmer, H., Saido, T. C., Takano, J., Kahle, P. J., et al. (2014). Overexpression of the calpain-specific inhibitor calpastatin reduces human alpha-Synuclein processing, aggregation and synaptic impairment in [A30P]alphaSyn transgenic mice. *Hum. Mol. Genet.* 23, 3975–3989. doi: 10.1093/hmg/ddu112

Dikiy, I., and Eliezer, D. (2014). N-terminal acetylation stabilizes N-terminal helicity in lipid- and micelle-bound alpha-synuclein and increases its affinity for physiological membranes. *J. Biol. Chem.* 289, 3652–3665. doi: 10.1074/jbc.M113.512459

Doxakis, E. (2010). Post-transcriptional regulation of alpha-synuclein expression by mir-7 and mir-153. *J. Biol. Chem.* 285, 12726–12734. doi: 10.1074/jbc.M109.086827

Du, T. T., Wang, L., Duan, C. L., Lu, L. L., Zhang, J. L., Gao, G., et al. (2015). GBA deficiency promotes SNCA/alpha-synuclein accumulation through autophagic inhibition by inactivated PPP2A. *Autophagy* 11, 1803–1820. doi: 10.1080/15548627.2015.1086055

Dulovic, M., Jovanovic, M., Xilouri, M., Stefanis, L., Harhaji-Trajkovic, L., Kravic-Stevovic, T., et al. (2014). The protective role of AMP-activated protein kinase in alpha-synuclein neurotoxicity *in vitro*. *Neurobiol. Dis.* 63, 1–11. doi: 10.1016/j.nbd.2013.11.002

Ebrahimi-Fakhari, D., Cantuti-Castelvetri, I., Fan, Z., Rockenstein, E., Masliah, E., Hyman, B. T., et al. (2011). Distinct roles *in vivo* for the ubiquitin-proteasome system and the autophagy-lysosomal pathway in the degradation of alpha-synuclein. *J. Neurosci.* 31, 14508–14520. doi: 10.1523/JNEUROSCI.1560-11.2011

El Turk, F., De Genst, E., Guilliams, T., Fauvet, B., Hejjaoui, M., Di Trani, J., et al. (2018). Exploring the role of post-translational modifications in regulating alpha-synuclein interactions by studying the effects of phosphorylation on nanobody binding. *Protein Sci.* 27, 1262–1274. doi: 10.1002/pro.3412

El-Agnaf, O., Overk, C., Rockenstein, E., Mante, M., Florio, J., Adame, A., et al. (2017). Differential effects of immunotherapy with antibodies targeting alpha-synuclein oligomers and fibrils in a transgenic model of synucleinopathy. *Neurobiol. Dis.* 104, 85–96. doi: 10.1016/j.nbd.2017.05.002

El-Agnaf, O. M., Jakes, R., Curran, M. D., Middleton, D., Ingenito, R., Bianchi, E., et al. (1998). Aggregates from mutant and wild-type alpha-synuclein proteins and NAC peptide induce apoptotic cell death in human neuroblastoma cells by formation of beta-sheet and amyloid-like filaments. *FEBS Lett.* 440, 71–75. doi: 10.1016/s0014-5793(98)01418-5

El-Agnaf, O. M., Paleologou, K. E., Greer, B., Abogrein, A. M., King, J. E., Salem, S. A., et al. (2004). A strategy for designing inhibitors of alpha-synuclein aggregation and toxicity as a novel treatment for Parkinson's disease and related disorders. *FASEB J.* 18, 1315–1317. doi: 10.1096/fj.03-1346fje

El-Agnaf, O. M., Salem, S. A., Paleologou, K. E., Cooper, L. J., Fullwood, N. J., Gibson, M. J., et al. (2003). Alpha-synuclein implicated in Parkinson's disease is present in extracellular biological fluids, including human plasma. *FASEB J.* 17, 1945–1947. doi: 10.1096/fj.03-0098fje

Elkouris, M., Kouroupi, G., Vourvoukelis, A., Papagiannakis, N., Kaltezioti, V., Matsas, R., et al. (2019). Long non-coding RNAs associated with neurodegeneration-linked genes are reduced in Parkinson's disease patients. *Front. Cell. Neurosci.* 13:58. doi: 10.3389/fncel.2019.00058

Emadi, S., Barkhordarian, H., Wang, M. S., Schulz, P., and Sierks, M. R. (2007). Isolation of a human single chain antibody fragment against oligomeric alpha-synuclein that inhibits aggregation and prevents alpha-synuclein-induced toxicity. *J. Mol. Biol.* 368, 1132–1144. doi: 10.1016/j.jmb.2007.02.089

Emadi, S., Kasturirangan, S., Wang, M. S., Schulz, P., and Sierks, M. R. (2009). Detecting morphologically distinct oligomeric forms of alpha-synuclein. *J. Biol. Chem.* 284, 11048–11058. doi: 10.1074/jbc.M806559200

Emmanouilidou, E., Melachroinou, K., Roumeliotis, T., Garbis, S. D., Ntzouni, M., Margaritis, L. H., et al. (2010a). Cell-produced alpha-synuclein is secreted in a calcium-dependent manner by exosomes and impacts neuronal survival. *J. Neurosci.* 30, 6838–6851. doi: 10.1523/JNEUROSCI.5699-09.2010

Emmanouilidou, E., Stefanis, L., and Vekrellis, K. (2010b). Cell-produced alpha-synuclein oligomers are targeted to, and impair, the 26S proteasome. *Neurobiol. Aging* 31, 953–968. doi: 10.1016/j.neurobiolaging.2008.07.008

Ettle, B., Reiprich, S., Deusser, J., Schlachetzki, J. C., Xiang, W., Prots, I., et al. (2014). Intracellular alpha-synuclein affects early maturation of primary oligodendrocyte progenitor cells. *Mol. Cell. Neurosci.* 62, 68–78. doi: 10.1016/j.mcn.2014.06.012

Fahn, S., Oakes, D., Shoulson, I., Kieburtz, K., Rudolph, A., Lang, A., et al. (2004). Levodopa and the progression of Parkinson's disease. *N. Engl. J. Med.* 351, 2498–2508. doi: 10.1056/NEJMoa033447

Fanciulli, A., and Wenning, G. K. (2015). Multiple-system atrophy. *N. Engl. J. Med.* 372, 249–263. doi: 10.1056/NEJMra1311488

Fasano, A., Visanji, N. P., Liu, L. W., Lang, A. E., and Pfeiffer, R. F. (2015). Gastrointestinal dysfunction in Parkinson's disease. *Parkinsonism Relat. Disord.* 14, 625–639. doi: 10.1016/S1474-4422(15)00007-1

Fauvet, B., Mbefo, M. K., Fares, M. B., Desobry, C., Michael, S., Ardah, M. T., et al. (2012). alpha-Synuclein in central nervous system and from erythrocytes, mammalian cells, and *Escherichia coli* exists predominantly as disordered monomer. *J. Biol. Chem.* 287, 15345–15364. doi: 10.1074/jbc.M111.318949

Felice, V. D., Quigley, E. M., Sullivan, A. M., O'Keeffe, G. W., and O'Mahony, S. M. (2016). Microbiota-gut-brain signalling in Parkinson's disease: implications for non-motor symptoms. *Parkinsonism Relat. Disord.* 27, 1–8. doi: 10.1016/j.parkreldis.2016.03.012

Fellner, L., Buchinger, E., Brueck, D., Irschick, R., Wenning, G. K., and Stefanova, N. (2018). Limited effects of dysfunctional macroautophagy on the accumulation of extracellularly derived alpha-synuclein in oligodendroglia: implications for MSA pathogenesis. *BMC Neurosci.* 19:32. doi: 10.1186/s12868-018-0431-2

Fellner, L., Kuzdas-Wood, D., Levin, J., Ryazanov, S., Leonov, A., Griesinger, C., et al. (2016). Anle138b partly ameliorates motor deficits despite failure of neuroprotection in a model of advanced multiple system atrophy. *Front. Neurosci.* 10:99. doi: 10.3389/fnins.2016.00099

Fellner, L., and Stefanova, N. (2013). The role of glia in alpha-synucleinopathies. *Mol. Neurobiol.* 47, 575–586. doi: 10.1007/s12035-012-8340-3

Ferreira, D. G., Temido-Ferreira, M., Vicente Miranda, H., Batalha, V. L., Coelho, J. E., Szego, E. M., et al. (2017). alpha-synuclein interacts with PrP(C) to induce cognitive impairment through mGluR5 and NMDAR2B. *Nat. Neurosci.* 20, 1569–1579. doi: 10.1038/nn.4648

Ferreon, A. C., and Deniz, A. A. (2007). Alpha-synuclein multistate folding thermodynamics: implications for protein misfolding and aggregation. *Biochemistry* 46, 4499–4509. doi: 10.1021/bi602461y

Ferretta, A., Gaballo, A., Tanzarella, P., Piccoli, C., Capitanio, N., Nico, B., et al. (2014). Effect of resveratrol on mitochondrial function: implications in parkin-associated familiar Parkinson's disease. *Biochim. Biophys. Acta* 1842, 902–915. doi: 10.1016/j.bbadis.2014.02.010

Fonseca-Ornelas, L., Eisbach, S. E., Paulat, M., Giller, K., Fernandez, C. O., Outeiro, T. F., et al. (2014). Small molecule-mediated stabilization of vesicle-associated helical alpha-synuclein inhibits pathogenic misfolding and aggregation. *Nat. Commun.* 5:5857. doi: 10.1038/ncomms6857

Fountaine, T. M., and Wade-Martins, R. (2007). RNA interference-mediated knockdown of alpha-synuclein protects human dopaminergic neuroblastoma cells from MPP(+) toxicity and reduces dopamine transport. *J. Neurosci. Res.* 85, 351–363. doi: 10.1002/jnr.21125

Fredenburg, R. A., Rospigliosi, C., Meray, R. K., Kessler, J. C., Lashuel, H. A., Eliezer, D., et al. (2007). The impact of the E46K mutation on the properties of alpha-synuclein in its monomeric and oligomeric states. *Biochemistry* 46, 7107–7118. doi: 10.1021/bi7000246

Friess, E., Kuempfel, T., Modell, S., Winkelmann, J., Holsboer, F., Ising, M., et al. (2006). Paroxetine treatment improves motor symptoms in patients with multiple system atrophy. *Parkinsonism Relat. Disord.* 12, 432–437. doi: 10.1016/j.parkreldis.2006.04.002

Fu, H., Subramanian, R. R., and Masters, S. C. (2000). 14-3-3 proteins: structure, function, and regulation. *Annu. Rev. Pharmacol. Toxicol.* 40, 617–647. doi: 10.1146/annurev.pharmtox.40.1.617

Fujiwara, H., Hasegawa, M., Dohmae, N., Kawashima, A., Masliah, E., Goldberg, M. S., et al. (2002). alpha-Synuclein is phosphorylated in synucleinopathy lesions. *Nat. Cell Biol.* 4, 160–164. doi: 10.1038/ncb748

Fusco, G., Chen, S. W., Williamson, P. T. F., Cascella, R., Perni, M., Jarvis, J. A., et al. (2017). Structural basis of membrane disruption and cellular toxicity by alpha-synuclein oligomers. *Science* 358, 1440–1443. doi: 10.1126/science.aan6160

Fussi, N., Hollerhage, M., Chakroun, T., Nykanen, N. P., Rosler, T. W., Koeglsperger, T., et al. (2018). Exosomal secretion of alpha-synuclein as protective mechanism after upstream blockage of macroautophagy. *Cell Death Dis.* 9:757. doi: 10.1038/s41419-018-0816-2

Games, D., Valera, E., Spencer, B., Rockenstein, E., Mante, M., Adame, A., et al. (2014). Reducing C-terminal-truncated alpha-synuclein by immunotherapy attenuates neurodegeneration and propagation in Parkinson's disease-like models. *J. Neurosci.* 34, 9441–9454. doi: 10.1523/JNEUROSCI.5314-13.2014

Ganjam, G. K., Bolte, K., Matschke, L. A., Neitemeier, S., Dolga, A. M., Hollerhage, M., et al. (2019). Mitochondrial damage by alpha-synuclein causes cell death in human dopaminergic neurons. *Cell Death Dis.* 10:865. doi: 10.1038/s41419-019-2091-2

Garcia-Reitbock, P., Anichtchik, O., Bellucci, A., Iovino, M., Ballini, C., Fineberg, E., et al. (2010). SNARE protein redistribution and synaptic failure in a transgenic mouse model of Parkinson's disease. *Brain* 133(Pt 7), 2032–2044. doi: 10.1093/brain/awq132

Gendelman, H. E., Zhang, Y., Santamaria, P., Olson, K. E., Schutt, C. R., Bhatti, D., et al. (2017). Evaluation of the safety and immunomodulatory effects of sargramostim in a randomized, double-blind phase 1 clinical Parkinson's disease trial. *NPJ Parkinsons Dis.* 3:10. doi: 10.1038/s41531-017-0013-5

George, S., Rey, N. L., Tyson, T., Esquibel, C., Meyerdirk, L., Schulz, E., et al. (2019). Microglia affect alpha-synuclein cell-to-cell transfer in a mouse model of Parkinson's disease. *Mol. Neurodegener.* 14:34. doi: 10.1186/s13024-019-0335-3

Giasson, B. I., Duda, J. E., Quinn, S. M., Zhang, B., Trojanowski, J. Q., and Lee, V. M. (2002). Neuronal alpha-synucleinopathy with severe movement disorder in mice expressing A53T human alpha-synuclein. *Neuron* 34, 521–533. doi: 10.1016/s0896-6273(02)00682-7

Giasson, B. I., Forman, M. S., Higuchi, M., Golbe, L. I., Graves, C. L., Kotzbauer, P. T., et al. (2003). Initiation and synergistic fibrillization of tau and alpha-synuclein. *Science* 300, 636–640. doi: 10.1126/science.1082324

Giasson, B. I., Murray, I. V., Trojanowski, J. Q., and Lee, V. M. (2001). A hydrophobic stretch of 12 amino acid residues in the middle of alpha-synuclein is essential for filament assembly. *J. Biol. Chem.* 276, 2380–2386. doi: 10.1074/jbc.M008919200

Gitler, A. D., Bevis, B. J., Shorter, J., Strathearn, K. E., Hamamichi, S., Su, L. J., et al. (2008). The Parkinson's disease protein alpha-synuclein disrupts cellular Rab homeostasis. *Proc. Natl. Acad. Sci. U.S.A.* 105, 145–150. doi: 10.1073/pnas.0710685105

Gonzalez, N., Arcos-Lopez, T., Konig, A., Quintanar, L., Menacho Marquez, M., Outeiro, T. F., et al. (2019). Effects of alpha-synuclein post-translational modifications on metal binding. *J. Neurochem.* 150, 507–521. doi: 10.1111/jnc.14721

Gorbatyuk, O. S., Li, S., Nash, K., Gorbatyuk, M., Lewin, A. S., Sullivan, L. F., et al. (2010). *In vivo* RNAi-mediated alpha-synuclein silencing induces nigrostriatal degeneration. *Mol. Ther.* 18, 1450–1457. doi: 10.1038/mt.2010.115

Gould, N., Mor, D. E., Lightfoot, R., Malkus, K., Giasson, B., and Ischiropoulos, H. (2014). Evidence of native alpha-synuclein conformers in the human brain. *J. Biol. Chem.* 289, 7929–7934. doi: 10.1074/jbc.C113.538249

Grassi, D., Howard, S., Zhou, M., Diaz-Perez, N., Urban, N. T., Guerrero-Given, D., et al. (2018). Identification of a highly neurotoxic alpha-synuclein species inducing mitochondrial damage and mitophagy in Parkinson's disease. *Proc. Natl. Acad. Sci. U.S.A.* 115, E2634–E2643. doi: 10.1073/pnas.1713849115

Grathwohl, S. A., Steiner, J. A., Britschgi, M., and Brundin, P. (2013). Mind the gut: secretion of alpha-synuclein by enteric neurons. *J. Neurochem.* 125, 487–490. doi: 10.1111/jnc.12191

Guardia-Laguarta, C., Area-Gomez, E., Rub, C., Liu, Y., Magrane, J., Becker, D., et al. (2014). alpha-Synuclein is localized to mitochondria-associated ER membranes. *J. Neurosci.* 34, 249–259. doi: 10.1523/JNEUROSCI.2507-13.2014

Guo, J. L., Covell, D. J., Daniels, J. P., Iba, M., Stieber, A., Zhang, B., et al. (2013). Distinct alpha-synuclein strains differentially promote tau inclusions in neurons. *Cell* 154, 103–117. doi: 10.1016/j.cell.2013.05.057

Guo, Y. J., Dong, S. Y., Cui, X. X., Feng, Y., Liu, T., Yin, M., et al. (2016). Resveratrol alleviates MPTP-induced motor impairments and pathological changes by autophagic degradation of alpha-synuclein via SIRT1-deacetylated LC3. *Mol. Nutr. Food Res.* 60, 2161–2175. doi: 10.1002/mnfr.201600111

Gustafsson, G., Lindstrom, V., Rostami, J., Nordstrom, E., Lannfelt, L., Bergstrom, J., et al. (2017). Alpha-synuclein oligomer-selective antibodies reduce intracellular accumulation and mitochondrial impairment in alpha-synuclein exposed astrocytes. *J. Neuroinflammation* 14:241. doi: 10.1186/s12974-017-1018-z

Gustafsson, G., Loov, C., Persson, E., Lazaro, D. F., Takeda, S., Bergstrom, J., et al. (2018). Secretion and uptake of alpha-synuclein via extracellular vesicles in cultured cells. *Cell. Mol. Neurobiol.* 38, 1539–1550. doi: 10.1007/s10571-018-0622-5

Haj-Yahya, M., Fauvet, B., Herman-Bachinsky, Y., Hejjaoui, M., Bavikar, S. N., Karthikeyan, S. V., et al. (2013). Synthetic polyubiquitinated alpha-Synuclein reveals important insights into the roles of the ubiquitin chain in regulating its pathophysiology. *Proc. Natl. Acad. Sci. U.S.A.* 110, 17726–17731. doi: 10.1073/pnas.1315654110

Hall, K., Yang, S., Sauchanka, O., Spillantini, M. G., and Anichtchik, O. (2015). Behavioural deficits in transgenic mice expressing human truncated (1-120 amino acid) alpha-synuclein. *Exp. Neurol.* 264, 8–13. doi: 10.1016/j.expneurol.2014.11.003

Han, Y., Khodr, C. E., Sapru, M. K., Pedapati, J., and Bohn, M. C. (2011). A microRNA embedded AAV alpha-synuclein gene silencing vector for dopaminergic neurons. *Brain Res.* 1386, 15–24. doi: 10.1016/j.brainres.2011.02.041

Hansen, C., Angot, E., Bergstrom, A. L., Steiner, J. A., Pieri, L., Paul, G., et al. (2011). alpha-Synuclein propagates from mouse brain to grafted dopaminergic neurons and seeds aggregation in cultured human cells. *J. Clin. Invest.* 121, 715–725. doi: 10.1172/JCI43366

Hassen, G. W., Kesner, L., Stracher, A., Shulman, A., Rockenstein, E., Mante, M., et al. (2018). Effects of novel calpain inhibitors in transgenic animal model of Parkinson's disease/dementia with Lewy bodies. *Sci. Rep.* 8:18083. doi: 10.1038/s41598-018-35729-1

Hayashita-Kinoh, H., Yamada, M., Yokota, T., Mizuno, Y., and Mochizuki, H. (2006). Down-regulation of alpha-synuclein expression can rescue dopaminergic cells from cell death in the substantia nigra of Parkinson's disease rat model. *Biochem. Biophys. Res. Commun.* 341, 1088–1095. doi: 10.1016/j.bbrc.2006.01.057

He, Q., Koprich, J. B., Wang, Y., Yu, W. B., Xiao, B. G., Brotchie, J. M., et al. (2016). Treatment with trehalose prevents behavioral and neurochemical

deficits produced in an AAV alpha-synuclein rat model of Parkinson's disease. *Mol. Neurobiol.* 53, 2258–2268. doi: 10.1007/s12035-015-9173-7

Hebron, M. L., Lonskaya, I., and Moussa, C. E. (2013). Nilotinib reverses loss of dopamine neurons and improves motor behavior via autophagic degradation of alpha-synuclein in Parkinson's disease models. *Hum. Mol. Genet.* 22, 3315–3328. doi: 10.1093/hmg/ddt192

Hellstrand, E., Nowacka, A., Topgaard, D., Linse, S., and Sparr, E. (2013). Membrane lipid co-aggregation with alpha-synuclein fibrils. *PLoS One* 8:e77235. doi: 10.1371/journal.pone.0077235

Heras-Garvin, A., Weckbecker, D., Ryazanov, S., Leonov, A., Griesinger, C., Giese, A., et al. (2019). Anle138b modulates alpha-synuclein oligomerization and prevents motor decline and neurodegeneration in a mouse model of multiple system atrophy. *Mov. Disord.* 34, 255–263. doi: 10.1002/mds.27562

Herrera-Vaquero, M., Bouquio, D., Kallab, M., Biggs, K., Nair, G., Ochoa, J., et al. (2019). The molecular tweezer CLR01 reduces aggregated, pathologic, and seeding-competent alpha-synuclein in experimental multiple system atrophy. *Biochim. Biophys. Acta Mol. Basis Dis.* 1865:165513. doi: 10.1016/j.bbadis.2019.07.007

Ho, P. W., Leung, C. T., Liu, H., Pang, S. Y., Lam, C. S., Xian, J., et al. (2020). Age-dependent accumulation of oligomeric SNCA/alpha-synuclein from impaired degradation in mutant LRRK2 knockin mouse model of Parkinson disease: role for therapeutic activation of chaperone-mediated autophagy (CMA). *Autophagy* 16, 347–370. doi: 10.1080/15548627.2019.1603545

Holmes, B. B., DeVos, S. L., Kfoury, N., Li, M., Jacks, R., Yanamandra, K., et al. (2013). Heparan sulfate proteoglycans mediate internalization and propagation of specific proteopathic seeds. *Proc. Natl. Acad. Sci. U.S.A.* 110, E3138–E3147. doi: 10.1073/pnas.1301440110

Holmqvist, S., Chutna, O., Bousset, L., Aldrin-Kirk, P., Li, W., Bjorklund, T., et al. (2014). Direct evidence of Parkinson pathology spread from the gastrointestinal tract to the brain in rats. *Acta Neuropathol.* 128, 805–820. doi: 10.1007/s00401-014-1343-6

Horvath, I., Sellstedt, M., Weise, C., Nordvall, L. M., Krishna Prasad, G., Olofsson, A., et al. (2013). Modulation of alpha-synuclein fibrillization by ring-fused 2-pyridones: templation and inhibition involve oligomers with different structure. *Arch. Biochem. Biophys.* 532, 84–90. doi: 10.1016/j.abb.2013.01.012

Houser, M. C., and Tansey, M. G. (2017). The gut-brain axis: is intestinal inflammation a silent driver of Parkinson's disease pathogenesis? *NPJ. Parkinsons Dis.* 3:3. doi: 10.1038/s41531-016-0002-0

Hughes, C. D., Choi, M. L., Ryten, M., Hopkins, L., Drews, A., Botia, J. A., et al. (2019). Picomolar concentrations of oligomeric alpha-synuclein sensitizes TLR4 to play an initiating role in Parkinson's disease pathogenesis. *Acta Neuropathol.* 137, 103–120. doi: 10.1007/s00401-018-1907-y

Hung, K. C., Huang, H. J., Wang, Y. T., and Lin, A. M. (2016). Baicalein attenuates alpha-synuclein aggregation, inflammasome activation and autophagy in the MPP(+)-treated nigrostriatal dopaminergic system *in vivo*. *J. Ethnopharmacol.* 194, 522–529. doi: 10.1016/j.jep.2016.10.040

Ihse, E., Yamakado, H., van Wijk, X. M., Lawrence, R., Esko, J. D., and Masliah, E. (2017). Cellular internalization of alpha-synuclein aggregates by cell surface heparan sulfate depends on aggregate conformation and cell type. *Sci. Rep.* 7:9008. doi: 10.1038/s41598-017-08720-5

Ii, M., Matsunaga, N., Hazeki, K., Nakamura, K., Takashima, K., Seya, T., et al. (2006). A novel cyclohexene derivative, ethyl (6R)-6-[N-(2-Chloro-4-fluorophenyl)sulfamoyl]cyclohex-1-ene-1-carboxylate (TAK-242), selectively inhibits toll-like receptor 4-mediated cytokine production through suppression of intracellular signaling. *Mol. Pharmacol.* 69, 1288–1295. doi: 10.1124/mol.105.019695

Ishizawa, K., Komori, T., Sasaki, S., Arai, N., Mizutani, T., and Hirose, T. (2004). Microglial activation parallels system degeneration in multiple system atrophy. *J. Neuropathol. Exp. Neurol.* 63, 43–52. doi: 10.1093/jnen/63.1.43

Issa, A. R., Sun, J., Petitgas, C., Mesquita, A., Dulac, A., Robin, M., et al. (2018). The lysosomal membrane protein LAMP2A promotes autophagic flux and prevents SNCA-induced Parkinson disease-like symptoms in the Drosophila brain. *Autophagy* 14, 1898–1910. doi: 10.1080/15548627.2018.1491489

Iyer, A., Roeters, S. J., Kogan, V., Woutersen, S., Claessens, M., and Subramaniam, V. (2017). C-terminal truncated alpha-synuclein fibrils contain strongly twisted beta-Sheets. *J. Am. Chem. Soc.* 139, 15392–15400. doi: 10.1021/jacs.7b07403

Jakes, R., Spillantini, M. G., and Goedert, M. (1994). Identification of two distinct synucleins from human brain. *FEBS Lett.* 345, 27–32. doi: 10.1016/0014-5793(94)00395-5

Jang, A., Lee, H. J., Suk, J. E., Jung, J. W., Kim, K. P., and Lee, S. J. (2010). Non-classical exocytosis of alpha-synuclein is sensitive to folding states and promoted under stress conditions. *J. Neurochem.* 113, 1263–1274. doi: 10.1111/j.1471-4159.2010.06695.x

Jankovic, J., Goodman, I., Safirstein, B., Marmon, T. K., Schenk, D. B., Koller, M., et al. (2018). Safety and tolerability of multiple ascending doses of PRX002/RG7935, an anti-alpha-synuclein monoclonal antibody, in patients with Parkinson disease: a randomized clinical trial. *JAMA Neurol.* 75, 1206–1214. doi: 10.1001/jamaneurol.2018.1487

Jao, C. C., Hegde, B. G., Chen, J., Haworth, I. S., and Langen, R. (2008). Structure of membrane-bound alpha-synuclein from site-directed spin labeling and computational refinement. *Proc. Natl. Acad. Sci. U.S.A.* 105, 19666–19671. doi: 10.1073/pnas.0807826105

Javed, H., Nagoor Meeran, M. F., Azimullah, S., Adem, A., Sadek, B., and Ojha, S. K. (2018). Plant extracts and phytochemicals targeting alpha-synuclein aggregation in Parkinson's disease models. *Front. Pharmacol.* 9:1555. doi: 10.3389/fphar.2018.01555

Jeannotte, A. M., and Sidhu, A. (2007). Regulation of the norepinephrine transporter by alpha-synuclein-mediated interactions with microtubules. *Eur. J. Neurosci.* 26, 1509–1520. doi: 10.1111/j.1460-9568.2007.05757.x

Jensen, P. H., Nielsen, M. S., Jakes, R., Dotti, C. G., and Goedert, M. (1998). Binding of alpha-synuclein to brain vesicles is abolished by familial Parkinson's disease mutation. *J. Biol. Chem.* 273, 26292–26294. doi: 10.1074/jbc.273.41.26292

Ji, H., Liu, Y. E., Jia, T., Wang, M., Liu, J., Xiao, G., et al. (1997). Identification of a breast cancer-specific gene. BCSG1, by direct differential cDNA sequencing. *Cancer Res.* 57, 759–764.

Jiang, P., Gan, M., Yen, S. H., McLean, P. J., and Dickson, D. W. (2017). Impaired endo-lysosomal membrane integrity accelerates the seeding progression of alpha-synuclein aggregates. *Sci. Rep.* 7:7690. doi: 10.1038/s41598-017-08149-w

Jiang, T. F., Zhang, Y. J., Zhou, H. Y., Wang, H. M., Tian, L. P., Liu, J., et al. (2013). Curcumin ameliorates the neurodegenerative pathology in A53T alpha-synuclein cell model of Parkinson's disease through the downregulation of mTOR/p70S6K signaling and the recovery of macroautophagy. *J. Neuroimmune Pharmacol.* 8, 356–369. doi: 10.1007/s11481-012-9431-7

Jin, H., Kanthasamy, A., Ghosh, A., Yang, Y., Anantharam, V., and Kanthasamy, A. G. (2011). alpha-Synuclein negatively regulates protein kinase Cdelta expression to suppress apoptosis in dopaminergic neurons by reducing p300 histone acetyltransferase activity. *J. Neurosci.* 31, 2035–2051. doi: 10.1523/JNEUROSCI.5634-10.2011

Judith Peterschmitt, M., Gasser, T., Isaacson, S., Kulisevsky, J., Mir, P., Simuni, T., et al. (2019). Safety, tolerability and pharmacokinetics of oral venglustat in Parkinson disease patients with a GBA mutation. *Mol. Genet. Metab.* 126:S117.

Junn, E., Lee, K. W., Jeong, B. S., Chan, T. W., Im, J. Y., and Mouradian, M. M. (2009). Repression of alpha-synuclein expression and toxicity by microRNA-7. *Proc. Natl. Acad. Sci. U.S.A.* 106, 13052–13057. doi: 10.1073/pnas.0906277106

Kahle, P. J., Neumann, M., Ozmen, L., Muller, V., Jacobsen, H., Spooren, W., et al. (2002). Hyperphosphorylation and insolubility of alpha-synuclein in transgenic mouse oligodendrocytes. *EMBO Rep.* 3, 583–588. doi: 10.1093/embo-reports/kvf109

Kaji, S., Maki, T., Kinoshita, H., Uemura, N., Ayaki, T., Kawamoto, Y., et al. (2018). Pathological endogenous alpha-synuclein accumulation in oligodendrocyte precursor cells potentially induces inclusions in multiple system atrophy. *Stem Cell Rep.* 10, 356–365. doi: 10.1016/j.stemcr.2017.12.001

Kallab, M., Herrera-Vaquero, M., Johannesson, M., Eriksson, F., Sigvardson, J., Poewe, W., et al. (2018). Region-specific effects of immunotherapy with antibodies targeting alpha-synuclein in a transgenic model of synucleinopathy. *Front. Neurosci.* 12:452. doi: 10.3389/fnins.2018.00452

Kamp, F., Exner, N., Lutz, A. K., Wender, N., Hegermann, J., Brunner, B., et al. (2010). Inhibition of mitochondrial fusion by alpha-synuclein is rescued by PINK1, Parkin and DJ-1. *EMBO J.* 29, 3571–3589. doi: 10.1038/emboj.2010.223

Kanaan, N. M., and Manfredsson, F. P. (2012). Loss of functional alpha-synuclein: A toxic event in Parkinson's disease? *J. Parkinsons Dis.* 2, 249–267. doi: 10.3233/JPD-012138

Karampetsou, M., Ardah, M. T., Semitekolou, M., Polissidis, A., Samiotaki, M., Kalomoiri, M., et al. (2017). Phosphorylated exogenous alpha-synuclein fibrils

exacerbate pathology and induce neuronal dysfunction in mice. *Sci. Rep.* 7:16533. doi: 10.1038/s41598-017-15813-8

Karpinar, D. P., Balija, M. B., Kugler, S., Opazo, F., Rezaei-Ghaleh, N., Wender, N., et al. (2009). Pre-fibrillar alpha-synuclein variants with impaired beta-structure increase neurotoxicity in Parkinson's disease models. *EMBO J.* 28, 3256–3268. doi: 10.1038/emboj.2009.257

Karpowicz, R. J. Jr., Haney, C. M., Mihaila, T. S., Sandler, R. M., Petersson, E. J., and Lee, V. M. (2017). Selective imaging of internalized proteopathic alpha-synuclein seeds in primary neurons reveals mechanistic insight into transmission of synucleinopathies. *J. Biol. Chem.* 292, 13482–13497. doi: 10.1074/jbc.M117.780296

Karuppagounder, S. S., Brahmachari, S., Lee, Y., Dawson, V. L., Dawson, T. M., and Ko, H. S. (2014). The c-Abl inhibitor, nilotinib, protects dopaminergic neurons in a preclinical animal model of Parkinson's disease. *Sci. Rep.* 4:4874. doi: 10.1038/srep04874

Kaufman, E., Hall, S., Surova, Y., Widner, H., Hansson, O., and Lindqvist, D. (2013). Proinflammatory cytokines are elevated in serum of patients with multiple system atrophy. *PLoS One* 8:e62354. doi: 10.1371/journal.pone.0062354

Kawamoto, T., Ii, M., Kitazaki, T., Iizawa, Y., and Kimura, H. (2008). TAK-242 selectively suppresses Toll-like receptor 4-signaling mediated by the intracellular domain. *Eur. J. Pharmacol.* 584, 40–48. doi: 10.1016/j.ejphar.2008.01.026

Kayed, R., Sokolov, Y., Edmonds, B., McIntire, T. M., Milton, S. C., Hall, J. E., et al. (2004). Permeabilization of lipid bilayers is a common conformation-dependent activity of soluble amyloid oligomers in protein misfolding diseases. *J. Biol. Chem.* 279, 46363–46366. doi: 10.1074/jbc.C400260200

Kellie, J. F., Higgs, R. E., Ryder, J. W., Major, A., Beach, T. G., Adler, C. H., et al. (2014). Quantitative measurement of intact alpha-synuclein proteoforms from post-mortem control and Parkinson's disease brain tissue by intact protein mass spectrometry. *Sci. Rep.* 4:5797. doi: 10.1038/srep05797

Khalaf, O., Fauvet, B., Oueslati, A., Dikiy, I., Mahul-Mellier, A. L., Ruggeri, F. S., et al. (2014). The H50Q mutation enhances alpha-synuclein aggregation, secretion, and toxicity. *J. Biol. Chem.* 289, 21856–21876. doi: 10.1074/jbc.M114.553297

Khodr, C. E., Becerra, A., Han, Y., and Bohn, M. C. (2014). Targeting alpha-synuclein with a microRNA-embedded silencing vector in the rat substantia nigra: positive and negative effects. *Brain Res.* 1550, 47–60. doi: 10.1016/j.brainres.2014.01.010

Khodr, C. E., Sapru, M. K., Pedapati, J., Han, Y., West, N. C., Kells, A. P., et al. (2011). An alpha-synuclein AAV gene silencing vector ameliorates a behavioral deficit in a rat model of Parkinson's disease, but displays toxicity in dopamine neurons. *Brain Res.* 1395, 94–107. doi: 10.1016/j.brainres.2011.04.036

Kiely, A. P., Asi, Y. T., Kara, E., Limousin, P., Ling, H., Lewis, P., et al. (2013). alpha-Synucleinopathy associated with G51D SNCA mutation: a link between Parkinson's disease and multiple system atrophy? *Acta Neuropathol.* 125, 753–769. doi: 10.1007/s00401-013-1096-7

Kiely, A. P., Ling, H., Asi, Y. T., Kara, E., Proukakis, C., Schapira, A. H., et al. (2015). Distinct clinical and neuropathological features of G51D SNCA mutation cases compared with SNCA duplication and H50Q mutation. *Mol. Neurodegener.* 10:41. doi: 10.1186/s13024-015-0038-3

Kim, C., Ho, D. H., Suk, J. E., You, S., Michael, S., Kang, J., et al. (2013). Neuron-released oligomeric alpha-synuclein is an endogenous agonist of TLR2 for paracrine activation of microglia. *Nat. Commun.* 4:1562. doi: 10.1038/ncomms2534

Kim, C., Lv, G., Lee, J. S., Jung, B. C., Masuda-Suzukake, M., Hong, C. S., et al. (2016). Exposure to bacterial endotoxin generates a distinct strain of alpha-synuclein fibril. *Sci. Rep.* 6:30891. doi: 10.1038/srep30891

Kim, S., Kwon, S. H., Kam, T. I., Panicker, N., Karuppagounder, S. S., Lee, S., et al. (2019). Transneuronal propagation of pathologic alpha-synuclein from the gut to the brain models Parkinson's disease. *Neuron* 103, 627–641.e7. doi: 10.1016/j.neuron.2019.05.035

Kim, T., Mehta, S. L., Morris-Blanco, K. C., Chokkalla, A. K., Chelluboina, B., Lopez, M., et al. (2018). The microRNA miR-7a-5p ameliorates ischemic brain damage by repressing alpha-synuclein. *Sci. Signal.* 11:eaat4285. doi: 10.1126/scisignal.aat4285

Kim, T. D., Paik, S. R., and Yang, C. H. (2002). Structural and functional implications of C-terminal regions of alpha-synuclein. *Biochemistry* 41, 13782–13790. doi: 10.1021/bi026284c

Kim, Y. S., Lim, D., Kim, J. Y., Kang, S. J., Kim, Y. H., and Im, H. (2009). beta-Sheet-breaking peptides inhibit the fibrillation of human alpha-synuclein. *Biochem. Biophys. Res. Commun.* 387, 682–687. doi: 10.1016/j.bbrc.2009.07.083

Kirik, D., Rosenblad, C., Burger, C., Lundberg, C., Johansen, T. E., Muzyczka, N., et al. (2002). Parkinson-like neurodegeneration induced by targeted overexpression of alpha-synuclein in the nigrostriatal system. *J. Neurosci.* 22, 2780–2791. doi: 10.1523/jneurosci.22-07-02780.2002

Kisos, H., Pukass, K., Ben-Hur, T., Richter-Landsberg, C., and Sharon, R. (2012). Increased neuronal alpha-synuclein pathology associates with its accumulation in oligodendrocytes in mice modeling alpha-synucleinopathies. *PLoS One* 7:e46817. doi: 10.1371/journal.pone.0046817

Klegeris, A., Pelech, S., Giasson, B. I., Maguire, J., Zhang, H., McGeer, E. G., et al. (2008). Alpha-synuclein activates stress signaling protein kinases in THP-1 cells and microglia. *Neurobiol. Aging* 29, 739–752. doi: 10.1016/j.neurobiolaging.2006.11.013

Klein, A. D., and Mazzulli, J. R. (2018). Is Parkinson's disease a lysosomal disorder? *Brain* 141, 2255–2262. doi: 10.1093/brain/awy147

Kleinknecht, A., Popova, B., Lazaro, D. F., Pinho, R., Valerius, O., Outeiro, T. F., et al. (2016). C-Terminal tyrosine residue modifications modulate the protective phosphorylation of serine 129 of alpha-synuclein in a yeast model of Parkinson's disease. *PLoS Genet.* 12:e1006098. doi: 10.1371/journal.pgen.1006098

Konno, M., Hasegawa, T., Baba, T., Miura, E., Sugeno, N., Kikuchi, A., et al. (2012). Suppression of dynamin GTPase decreases alpha-synuclein uptake by neuronal and oligodendroglial cells: a potent therapeutic target for synucleinopathy. *Mol. Neurodegener.* 7:38. doi: 10.1186/1750-1326-7-38

Kordower, J. H., Chu, Y., Hauser, R. A., Freeman, T. B., and Olanow, C. W. (2008). Lewy body-like pathology in long-term embryonic nigral transplants in Parkinson's disease. *Nat. Med.* 14, 504–506. doi: 10.1038/nm1747

Kordower, J. H., Dodiya, H. B., Kordower, A. M., Terpstra, B., Paumier, K., Madhavan, L., et al. (2011). Transfer of host-derived alpha synuclein to grafted dopaminergic neurons in rat. *Neurobiol. Dis.* 43, 552–557. doi: 10.1016/j.nbd.2011.05.001

Kragh, C. L., Lund, L. B., Febbraro, F., Hansen, H. D., Gai, W. P., El-Agnaf, O., et al. (2009). Alpha-synuclein aggregation and Ser-129 phosphorylation-dependent cell death in oligodendroglial cells. *J. Biol. Chem.* 284, 10211–10222. doi: 10.1074/jbc.M809671200

Krishnan, R., Tsubery, H., Proschitsky, M. Y., Asp, E., Lulu, M., Gilead, S., et al. (2014). A bacteriophage capsid protein provides a general amyloid interaction motif (GAIM) that binds and remodels misfolded protein assemblies. *J. Mol. Biol.* 426, 2500–2519. doi: 10.1016/j.jmb.2014.04.015

Kruger, R., Kuhn, W., Muller, T., Woitalla, D., Graeber, M., Kosel, S., et al. (1998). Ala30Pro mutation in the gene encoding alpha-synuclein in Parkinson's disease. *Nat. Genet.* 18, 106–108. doi: 10.1038/ng0298-106

Krumova, P., Meulmeester, E., Garrido, M., Tirard, M., Hsiao, H. H., Bossis, G., et al. (2011). Sumoylation inhibits alpha-synuclein aggregation and toxicity. *J. Cell Biol.* 194, 49–60. doi: 10.1083/jcb.201010117

Kurowska, Z., Englund, E., Widner, H., Lindvall, O., Li, J. Y., and Brundin, P. (2011). Signs of degeneration in 12-22-year old grafts of mesencephalic dopamine neurons in patients with Parkinson's disease. *J. Parkinsons Dis.* 1, 83–92. doi: 10.3233/JPD-2011-11004

Kuwahara, T., Tonegawa, R., Ito, G., Mitani, S., and Iwatsubo, T. (2012). Phosphorylation of alpha-synuclein protein at Ser-129 reduces neuronal dysfunction by lowering its membrane binding property in *Caenorhabditis elegans*. *J. Biol. Chem.* 287, 7098–7109. doi: 10.1074/jbc.M111.237131

Lan, D. M., Liu, F. T., Zhao, J., Chen, Y., Wu, J. J., Ding, Z. T., et al. (2012). Effect of trehalose on PC12 cells overexpressing wild-type or A53T mutant alpha-synuclein. *Neurochem. Res.* 37, 2025–2032. doi: 10.1007/s11064-012-0823-0

Lassot, I., Mora, S., Lesage, S., Zieba, B. A., Coque, E., Condroyer, C., et al. (2018). The E3 Ubiquitin Ligases TRIM17 and TRIM41 modulate alpha-synuclein expression by regulating ZSCAN21. *Cell Rep.* 25, 2484–2496.e9. doi: 10.1016/j.celrep.2018.11.002

Lau, A., So, R. W. L., Lau, H. H. C., Sang, J. C., Ruiz-Riquelme, A., Fleck, S. C., et al. (2020). alpha-Synuclein strains target distinct brain regions and cell types. *Nat. Neurosci.* 23, 21–31. doi: 10.1038/s41593-019-0541-x

Lautenschlager, J., Stephens, A. D., Fusco, G., Strohl, F., Curry, N., Zacharopoulou, M., et al. (2018). C-terminal calcium binding of alpha-synuclein modulates

synaptic vesicle interaction. *Nat. Commun.* 9:712. doi: 10.1038/s41467-018-03111-4

Lazaro, D. F., Rodrigues, E. F., Langohr, R., Shahpasandzadeh, H., Ribeiro, T., Guerreiro, P., et al. (2014). Systematic comparison of the effects of alpha-synuclein mutations on its oligomerization and aggregation. *PLoS Genet.* 10:e1004741. doi: 10.1371/journal.pgen.1004741

Lebouvier, T., Neunlist, M., Bruley des Varannes, S., Coron, E., Drouard, A., N'Guyen, J. M., et al. (2010). Colonic biopsies to assess the neuropathology of Parkinson's disease and its relationship with symptoms. *PLoS One* 5:e12728. doi: 10.1371/journal.pone.0012728

Lee, H. J., Cho, E. D., Lee, K. W., Kim, J. H., Cho, S. G., and Lee, S. J. (2013). Autophagic failure promotes the exocytosis and intercellular transfer of alpha-synuclein. *Exp. Mol. Med.* 45:e22. doi: 10.1038/emm.2013.45

Lee, H. J., Jung, K. W., Chung, S. J., Hong, S. M., Kim, J., Lee, J. H., et al. (2018). Relation of enteric alpha-synuclein to gastrointestinal dysfunction in patients with Parkinson's Disease and in neurologically intact subjects. *J. Neurogastroenterol. Motil.* 24, 469–478. doi: 10.5056/jnm17141

Lee, H. J., Patel, S., and Lee, S. J. (2005). Intravesicular localization and exocytosis of alpha-synuclein and its aggregates. *J. Neurosci.* 25, 6016–6024. doi: 10.1523/JNEUROSCI.0692-05.2005

Lee, H. J., Suk, J. E., Bae, E. J., Lee, J. H., Paik, S. R., and Lee, S. J. (2008a). Assembly-dependent endocytosis and clearance of extracellular alpha-synuclein. *Int. J. Biochem. Cell Biol.* 40, 1835–1849. doi: 10.1016/j.biocel.2008.01.017

Lee, H. J., Suk, J. E., Bae, E. J., and Lee, S. J. (2008b). Clearance and deposition of extracellular alpha-synuclein aggregates in microglia. *Biochem. Biophys. Res. Commun.* 372, 423–428. doi: 10.1016/j.bbrc.2008.05.045

Lee, H. J., Suk, J. E., Patrick, C., Bae, E. J., Cho, J. H., Rho, S., et al. (2010). Direct transfer of alpha-synuclein from neuron to astroglia causes inflammatory responses in synucleinopathies. *J. Biol. Chem.* 285, 9262–9272. doi: 10.1074/jbc.M109.081125

Lee, K. W., Chen, W., Junn, E., Im, J. Y., Grosso, H., Sonsalla, P. K., et al. (2011). Enhanced phosphatase activity attenuates alpha-synucleinopathy in a mouse model. *J. Neurosci.* 31, 6963–6971. doi: 10.1523/JNEUROSCI.6513-10.2011

Lei, Z., Cao, G., and Wei, G. (2019). A30P mutant alpha-synuclein impairs autophagic flux by inactivating JNK signaling to enhance ZKSCAN3 activity in midbrain dopaminergic neurons. *Cell Death Dis.* 10:133. doi: 10.1038/s41419-019-1364-0

Levin, J., Schmidt, F., Boehm, C., Prix, C., Botzel, K., Ryazanov, S., et al. (2014). The oligomer modulator anle138b inhibits disease progression in a Parkinson mouse model even with treatment started after disease onset. *Acta Neuropathol.* 127, 779–780. doi: 10.1007/s00401-014-1265-3

Lewis, J., Melrose, H., Bumcrot, D., Hope, A., Zehr, C., Lincoln, S., et al. (2008). *In vivo* silencing of alpha-synuclein using naked siRNA. *Mol. Neurodegener.* 3:19. doi: 10.1186/1750-1326-3-19

Li, J., Zhu, M., Rajamani, S., Uversky, V. N., and Fink, A. L. (2004). Rifampicin inhibits alpha-synuclein fibrillation and disaggregates fibrils. *Chem. Biol.* 11, 1513–1521. doi: 10.1016/j.chembiol.2004.08.025

Li, J. Y., Englund, E., Holton, J. L., Soulet, D., Hagell, P., Lees, A. J., et al. (2008). Lewy bodies in grafted neurons in subjects with Parkinson's disease suggest host-to-graft disease propagation. *Nat. Med.* 14, 501–503. doi: 10.1038/nm1746

Li, J. Y., Englund, E., Widner, H., Rehncrona, S., Bjorklund, A., Lindvall, O., et al. (2010). Characterization of Lewy body pathology in 12- and 16-year-old intrastriatal mesencephalic grafts surviving in a patient with Parkinson's disease. *Mov. Disord.* 25, 1091–1096. doi: 10.1002/mds.23012

Lin, A., Zheng, W., He, Y., Tang, W., Wei, X., He, R., et al. (2018). Gut microbiota in patients with Parkinson's disease in southern China. *Parkinsonism Relat. Disord.* 53, 82–88. doi: 10.1016/j.parkreldis.2018.05.007

Lin, D., Liang, Y., Jing, X., Chen, Y., Lei, M., Zeng, Z., et al. (2018). Microarray analysis of an synthetic alpha-synuclein induced cellular model reveals the expression profile of long non-coding RNA in Parkinson's disease. *Brain Res.* 1678, 384–396. doi: 10.1016/j.brainres.2017.11.007

Lin, T. K., Chen, S. D., Chuang, Y. C., Lin, H. Y., Huang, C. R., Chuang, J. H., et al. (2014). Resveratrol partially prevents rotenone-induced neurotoxicity in dopaminergic SH-SY5Y cells through induction of heme oxygenase-1 dependent autophagy. *Int. J. Mol. Sci.* 15, 1625–1646. doi: 10.3390/ijms15011625

Lindersson, E., Lundvig, D., Petersen, C., Madsen, P., Nyengaard, J. R., Hojrup, P., et al. (2005). p25alpha Stimulates alpha-synuclein aggregation and is co-localized with aggregated alpha-synuclein in alpha-synucleinopathies. *J. Biol. Chem.* 280, 5703–5715. doi: 10.1074/jbc.M410409200

Liu, C. W., Corboy, M. J., DeMartino, G. N., and Thomas, P. J. (2003). Endoproteolytic activity of the proteasome. *Science* 299, 408–411. doi: 10.1126/science.1079293

Liu, G., Chen, M., Mi, N., Yang, W., Li, X., Wang, P., et al. (2015). Increased oligomerization and phosphorylation of alpha-synuclein are associated with decreased activity of glucocerebrosidase and protein phosphatase 2A in aging monkey brains. *Neurobiol. Aging* 36, 2649–2659. doi: 10.1016/j.neurobiolaging.2015.06.004

Liu, K., Shi, N., Sun, Y., Zhang, T., and Sun, X. (2013). Therapeutic effects of rapamycin on MPTP-induced Parkinsonism in mice. *Neurochem. Res.* 38, 201–207. doi: 10.1007/s11064-012-0909-8

Lo Bianco, C., Ridet, J. L., Schneider, B. L., Deglon, N., and Aebischer, P. (2002). alpha -Synucleinopathy and selective dopaminergic neuron loss in a rat lentiviral-based model of Parkinson's disease. *Proc. Natl. Acad. Sci. U.S.A.* 99, 10813–10818. doi: 10.1073/pnas.152339799

Logan, T., Bendor, J., Toupin, C., Thorn, K., and Edwards, R. H. (2017). alpha-Synuclein promotes dilation of the exocytotic fusion pore. *Nat. Neurosci.* 20, 681–689. doi: 10.1038/nn.4529

Longhena, F., Faustini, G., Spillantini, M. G., and Bellucci, A. (2019). Living in promiscuity: the multiple partners of Alpha-synuclein at the synapse in physiology and pathology. *Int. J. Mol. Sci.* 20:141. doi: 10.3390/ijms20010141

Loria, F., Vargas, J. Y., Bousset, L., Syan, S., Salles, A., Melki, R., et al. (2017). alpha-Synuclein transfer between neurons and astrocytes indicates that astrocytes play a role in degradation rather than in spreading. *Acta Neuropathol.* 134, 789–808. doi: 10.1007/s00401-017-1746-2

Low, P. A., Robertson, D., Gilman, S., Kaufmann, H., Singer, W., Biaggioni, I., et al. (2014). Efficacy and safety of rifampicin for multiple system atrophy: a randomised, double-blind, placebo-controlled trial. *Parkinsonism Relat. Disord.* 13, 268–275. doi: 10.1016/S1474-4422(13)70301-6

Lu, M., Su, C., Qiao, C., Bian, Y., Ding, J., and Hu, G. (2016). Metformin prevents dopaminergic neuron death in MPTP/P-induced mouse model of Parkinson's disease via autophagy and mitochondrial ROS CLEARANCE. *Int. J. Neuropsychopharmacol.* 19:pyw047. doi: 10.1093/ijnp/pyw047

Luk, K. C., Kehm, V., Carroll, J., Zhang, B., O'Brien, P., Trojanowski, J. Q., et al. (2012a). Pathological alpha-synuclein transmission initiates Parkinson-like neurodegeneration in nontransgenic mice. *Science* 338, 949–953. doi: 10.1126/science.1227157

Luk, K. C., Kehm, V. M., Zhang, B., O'Brien, P., Trojanowski, J. Q., and Lee, V. M. (2012b). Intracerebral inoculation of pathological alpha-synuclein initiates a rapidly progressive neurodegenerative alpha-synucleinopathy in mice. *J. Exp. Med.* 209, 975–986. doi: 10.1084/jem.20112457

Luk, K. C., Song, C., O'Brien, P., Stieber, A., Branch, J. R., Brunden, K. R., et al. (2009). Exogenous alpha-synuclein fibrils seed the formation of Lewy body-like intracellular inclusions in cultured cells. *Proc. Natl. Acad. Sci. U.S.A.* 106, 20051–20056. doi: 10.1073/pnas.0908005106

Luna, E., Decker, S. C., Riddle, D. M., Caputo, A., Zhang, B., Cole, T., et al. (2018). Differential alpha-synuclein expression contributes to selective vulnerability of hippocampal neuron subpopulations to fibril-induced toxicity. *Acta Neuropathol.* 135, 855–875. doi: 10.1007/s00401-018-1829-8

Ly, T., and Julian, R. R. (2008). Protein-metal interactions of calmodulin and alpha-synuclein monitored by selective noncovalent adduct protein probing mass spectrometry. *J. Am. Soc. Mass Spectrom.* 19, 1663–1672. doi: 10.1016/j.jasms.2008.07.006

Lynch, S. M., Zhou, C., and Messer, A. (2008). An scFv intrabody against the nonamyloid component of alpha-synuclein reduces intracellular aggregation and toxicity. *J. Mol. Biol.* 377, 136–147. doi: 10.1016/j.jmb.2007.11.096

Ma, L., Yang, C., Zhang, X., Li, Y., Wang, S., Zheng, L., et al. (2018). C-terminal truncation exacerbates the aggregation and cytotoxicity of alpha-Synuclein: a vicious cycle in Parkinson's disease. *Biochim. Biophys. Acta Mol. Basis Dis.* 1864, 3714–3725. doi: 10.1016/j.bbadis.2018.10.003

Ma, M. R., Hu, Z. W., Zhao, Y. F., Chen, Y. X., and Li, Y. M. (2016). Phosphorylation induces distinct alpha-synuclein strain formation. *Sci. Rep.* 6:37130. doi: 10.1038/srep37130

Mahul-Mellier, A. L., Fauvet, B., Gysbers, A., Dikiy, I., Oueslati, A., Georgeon, S., et al. (2014). c-Abl phosphorylates alpha-synuclein and regulates its degradation: implication for alpha-synuclein clearance and contribution to the pathogenesis of Parkinson's disease. *Hum. Mol. Genet.* 23, 2858–2879. doi: 10.1093/hmg/ddt674

Mak, S. K., McCormack, A. L., Manning-Bog, A. B., Cuervo, A. M., and Di Monte, D. A. (2010). Lysosomal degradation of alpha-synuclein *in vivo*. *J. Biol. Chem.* 285, 13621–13629. doi: 10.1074/jbc.M109.074617

Malagelada, C., Jin, Z. H., Jackson-Lewis, V., Przedborski, S., and Greene, L. A. (2010). Rapamycin protects against neuron death in *in vitro* and *in vivo* models of Parkinson's disease. *J. Neurosci.* 30, 1166–1175. doi: 10.1523/JNEUROSCI.3944-09.2010

Malerba, M., and Ragnoli, B. (2008). Ambroxol in the 21st century: pharmacological and clinical update. *Expert Opin. Drug Metab. Toxicol.* 4, 1119–1129. doi: 10.1517/17425255.4.8.1119

Mandler, M., Valera, E., Rockenstein, E., Mante, M., Weninger, H., Patrick, C., et al. (2015). Active immunization against alpha-synuclein ameliorates the degenerative pathology and prevents demyelination in a model of multiple system atrophy. *Mol. Neurodegener.* 10:10. doi: 10.1186/s13024-015-0008-9

Mandler, M., Valera, E., Rockenstein, E., Weninger, H., Patrick, C., Adame, A., et al. (2014). Next-generation active immunization approach for synucleinopathies: implications for Parkinson's disease clinical trials. *Acta Neuropathol.* 127, 861–879. doi: 10.1007/s00401-014-1256-4

Manfredsson, F. P., Luk, K. C., Benskey, M. J., Gezer, A., Garcia, J., Kuhn, N. C., et al. (2018). Induction of alpha-synuclein pathology in the enteric nervous system of the rat and non-human primate results in gastrointestinal dysmotility and transient CNS pathology. *Neurobiol. Dis.* 112, 106–118. doi: 10.1016/j.nbd.2018.01.008

Mao, X., Ou, M. T., Karuppagounder, S. S., Kam, T. I., Yin, X., Xiong, Y., et al. (2016). Pathological alpha-synuclein transmission initiated by binding lymphocyte-activation gene 3. *Science* 353:aah3374. doi: 10.1126/science.aah3374

Maroteaux, L., Campanelli, J. T., and Scheller, R. H. (1988). Synuclein: a neuron-specific protein localized to the nucleus and presynaptic nerve terminal. *J. Neurosci.* 8, 2804–2815. doi: 10.1523/jneurosci.08-08-02804.1988

Martin-Clemente, B., Alvarez-Castelao, B., Mayo, I., Sierra, A. B., Diaz, V., Milan, M., et al. (2004). alpha-Synuclein expression levels do not significantly affect proteasome function and expression in mice and stably transfected PC12 cell lines. *J. Biol. Chem.* 279, 52984–52990. doi: 10.1074/jbc.M409028200

Martinez-Vicente, M., Talloczy, Z., Kaushik, S., Massey, A. C., Mazzulli, J., Mosharov, E. V., et al. (2008). Dopamine-modified alpha-synuclein blocks chaperone-mediated autophagy. *J. Clin. Invest.* 118, 777–788. doi: 10.1172/JCI32806

Masliah, E., Rockenstein, E., Adame, A., Alford, M., Crews, L., Hashimoto, M., et al. (2005). Effects of alpha-synuclein immunization in a mouse model of Parkinson's disease. *Neuron* 46, 857–868. doi: 10.1016/j.neuron.2005.05.010

Masliah, E., Rockenstein, E., Mante, M., Crews, L., Spencer, B., Adame, A., et al. (2011). Passive immunization reduces behavioral and neuropathological deficits in an alpha-synuclein transgenic model of Lewy body disease. *PLoS One* 6:e19338. doi: 10.1371/journal.pone.0019338

Masliah, E., Rockenstein, E., Veinbergs, I., Sagara, Y., Mallory, M., Hashimoto, M., et al. (2001). beta-amyloid peptides enhance alpha-synuclein accumulation and neuronal deficits in a transgenic mouse model linking Alzheimer's disease and Parkinson's disease. *Proc. Natl. Acad. Sci. U.S.A.* 98, 12245–12250. doi: 10.1073/pnas.211412398

Masuda, M., Suzuki, N., Taniguchi, S., Oikawa, T., Nonaka, T., Iwatsubo, T., et al. (2006). Small molecule inhibitors of alpha-synuclein filament assembly. *Biochemistry* 45, 6085–6094. doi: 10.1021/bi0600749

Masuda-Suzukake, M., Nonaka, T., Hosokawa, M., Kubo, M., Shimozawa, A., Akiyama, H., et al. (2014). Pathological alpha-synuclein propagates through neural networks. *Acta Neuropathol. Commun.* 2:88. doi: 10.1186/s40478-014-0088-8

Masuda-Suzukake, M., Nonaka, T., Hosokawa, M., Oikawa, T., Arai, T., Akiyama, H., et al. (2013). Prion-like spreading of pathological alpha-synuclein in brain. *Brain* 136(Pt 4), 1128–1138. doi: 10.1093/brain/awt037

Mata, I. F., Samii, A., Schneer, S. H., Roberts, J. W., Griffith, A., Leis, B. C., et al. (2008). Glucocerebrosidase gene mutations: a risk factor for Lewy body disorders. *Arch. Neurol.* 65, 379–382. doi: 10.1001/archneurol.2007.68

Mavroeidi, P., Arvanitaki, F., Karakitsou, A. K., Vetsi, M., Kloukina, I., Zweckstetter, M., et al. (2019). Endogenous oligodendroglial alpha-synuclein and TPPP/p25alpha orchestrate alpha-synuclein pathology in experimental multiple system atrophy models. *Acta Neuropathol.* 138, 415–441. doi: 10.1007/s00401-019-02014-y

Mazzulli, J. R., Xu, Y. H., Sun, Y., Knight, A. L., McLean, P. J., Caldwell, G. A., et al. (2011). Gaucher disease glucocerebrosidase and alpha-synuclein form a bidirectional pathogenic loop in synucleinopathies. *Cell* 146, 37–52. doi: 10.1016/j.cell.2011.06.001

McCormack, A. L., Mak, S. K., Henderson, J. M., Bumcrot, D., Farrer, M. J., and Di Monte, D. A. (2010). Alpha-synuclein suppression by targeted small interfering RNA in the primate substantia nigra. *PLoS One* 5:e12122. doi: 10.1371/journal.pone.0012122

McNeill, A., Magalhaes, J., Shen, C., Chau, K. Y., Hughes, D., Mehta, A., et al. (2014). Ambroxol improves lysosomal biochemistry in glucocerebrosidase mutation-linked Parkinson disease cells. *Brain* 137(Pt 5), 1481–1495. doi: 10.1093/brain/awu020

Migdalska-Richards, A., Daly, L., Bezard, E., and Schapira, A. H. (2016). Ambroxol effects in glucocerebrosidase and alpha-synuclein transgenic mice. *Ann. Neurol.* 80, 766–775. doi: 10.1002/ana.24790

Migdalska-Richards, A., Ko, W. K. D., Li, Q., Bezard, E., and Schapira, A. H. V. (2017). Oral ambroxol increases brain glucocerebrosidase activity in a nonhuman primate. *Synapse* 71:e21967. doi: 10.1002/syn.21967

Minakaki, G., Menges, S., Kittel, A., Emmanouilidou, E., Schaeffner, I., Barkovits, K., et al. (2018). Autophagy inhibition promotes SNCA/alpha-synuclein release and transfer via extracellular vesicles with a hybrid autophagosome-exosome-like phenotype. *Autophagy* 14, 98–119. doi: 10.1080/15548627.2017.1395992

Mittal, S., Bjornevik, K., Im, D. S., Flierl, A., Dong, X., Locascio, J. J., et al. (2017). beta2-Adrenoreceptor is a regulator of the alpha-synuclein gene driving risk of Parkinson's disease. *Science* 357, 891–898. doi: 10.1126/science.aaf3934

Mogi, M., Harada, M., Kondo, T., Riederer, P., Inagaki, H., Minami, M., et al. (1994a). Interleukin-1 beta, interleukin-6, epidermal growth factor and transforming growth factor-alpha are elevated in the brain from parkinsonian patients. *Neurosci. Lett.* 180, 147–150. doi: 10.1016/0304-3940(94)90508-8

Mogi, M., Harada, M., Riederer, P., Narabayashi, H., Fujita, K., and Nagatsu, T. (1994b). Tumor necrosis factor-alpha (TNF-alpha) increases both in the brain and in the cerebrospinal fluid from parkinsonian patients. *Neurosci. Lett.* 165, 208–210. doi: 10.1016/0304-3940(94)90746-3

Monzio Compagnoni, G., and Di Fonzo, A. (2019). Understanding the pathogenesis of multiple system atrophy: state of the art and future perspectives. *Acta Neuropathol. Commun.* 7:113. doi: 10.1186/s40478-019-0730-6

Moore, J. S., Gibson, P. R., and Burgell, R. E. (2018). Neuromodulation via interferential electrical stimulation as a novel therapy in gastrointestinal motility disorders. *J. Neurogastroenterol. Motil.* 24, 19–29. doi: 10.5056/jnm17071

Mosley, R. L., Lu, Y., Olson, K. E., Machhi, J., Yan, W., Namminga, K. L., et al. (2019). A synthetic agonist to vasoactive intestinal peptide receptor-2 induces regulatory T cell neuroprotective activities in models of Parkinson's disease. *Front. Cell. Neurosci.* 13:421. doi: 10.3389/fncel.2019.00421

Mougenot, A. L., Nicot, S., Bencsik, A., Morignat, E., Verchere, J., Lakhdar, L., et al. (2012). Prion-like acceleration of a synucleinopathy in a transgenic mouse model. *Neurobiol. Aging* 33, 2225–2228. doi: 10.1016/j.neurobiolaging.2011.06.022

Mullin, S., Smith, L., Lee, K., D'Souza, G., Woodgate, P., Elflein, J., et al. (2020). Ambroxol for the treatment of patients with Parkinson disease with and without glucocerebrosidase gene mutations: a nonrandomized, noncontrolled trial. *JAMA Neurol.* 77, 427–434. doi: 10.1001/jamaneurol.2019.4611

Murphy, K. E., Gysbers, A. M., Abbott, S. K., Spiro, A. S., Furuta, A., Cooper, A., et al. (2015). Lysosomal-associated membrane protein 2 isoforms are differentially affected in early Parkinson's disease. *Mov. Disord.* 30, 1639–1647. doi: 10.1002/mds.26141

Murphy, K. E., Gysbers, A. M., Abbott, S. K., Tayebi, N., Kim, W. S., Sidransky, E., et al. (2014). Reduced glucocerebrosidase is associated with increased alpha-synuclein in sporadic Parkinson's disease. *Brain* 137(Pt 3), 834–848. doi: 10.1093/brain/awt367

Myohanen, T. T., Hannula, M. J., Van Elzen, R., Gerard, M., Van Der Veken, P., Garcia-Horsman, J. A., et al. (2012). A prolyl oligopeptidase inhibitor, KYP-2047, reduces alpha-synuclein protein levels and aggregates in cellular and

animal models of Parkinson's disease. *Br. J. Pharmacol.* 166, 1097–1113. doi: 10.1111/j.1476-5381.2012.01846.x

Nagatsu, T., Mogi, M., Ichinose, H., and Togari, A. (2000). "Cytokines in Parkinson's disease," in *Advances in Research on Neurodegeneration*, eds Y. Mizuno, D. B. Calne, R. Horowski, W. Poewe, P. Riederer, M. B. H. Youdim (Vienna: Springer).

Nagatsu, T., and Sawada, M. (2005). Inflammatory process in Parkinson's disease: role for cytokines. *Curr. Pharm. Des.* 11, 999–1016. doi: 10.2174/1381612053381620

Nakamura, K., Mori, F., Kon, T., Tanji, K., Miki, Y., Tomiyama, M., et al. (2015). Filamentous aggregations of phosphorylated alpha-synuclein in Schwann cells (Schwann cell cytoplasmic inclusions) in multiple system atrophy. *Acta Neuropathol. Commun.* 3:29. doi: 10.1186/s40478-015-0208-0

Nakamura, K., Nemani, V. M., Azarbal, F., Skibinski, G., Levy, J. M., Egami, K., et al. (2011). Direct membrane association drives mitochondrial fission by the Parkinson disease-associated protein alpha-synuclein. *J. Biol. Chem.* 286, 20710–20726. doi: 10.1074/jbc.M110.213538

Nakayama, K., Suzuki, Y., and Yazawa, I. (2012). Binding of neuronal alpha-synuclein to beta-III tubulin and accumulation in a model of multiple system atrophy. *Biochem. Biophys. Res. Commun.* 417, 1170–1175. doi: 10.1016/j.bbrc.2011.12.092

Nalls, M. A., Pankratz, N., Lill, C. M., Do, C. B., Hernandez, D. G., Saad, M., et al. (2014). Large-scale meta-analysis of genome-wide association data identifies six new risk loci for Parkinson's disease. *Nat. Genet.* 46, 989–993. doi: 10.1038/ng.3043

Nemani, V. M., Lu, W., Berge, V., Nakamura, K., Onoa, B., Lee, M. K., et al. (2010). Increased expression of alpha-synuclein reduces neurotransmitter release by inhibiting synaptic vesicle reclustering after endocytosis. *Neuron* 65, 66–79. doi: 10.1016/j.neuron.2009.12.023

Ng, C. H., Guan, M. S., Koh, C., Ouyang, X., Yu, F., Tan, E. K., et al. (2012). AMP kinase activation mitigates dopaminergic dysfunction and mitochondrial abnormalities in Drosophila models of Parkinson's disease. *J. Neurosci.* 32, 14311–14317. doi: 10.1523/JNEUROSCI.0499-12.2012

Nishie, M., Mori, F., Fujiwara, H., Hasegawa, M., Yoshimoto, M., Iwatsubo, T., et al. (2004). Accumulation of phosphorylated alpha-synuclein in the brain and peripheral ganglia of patients with multiple system atrophy. *Acta Neuropathol.* 107, 292–298. doi: 10.1007/s00401-003-0811-1

Norris, E. H., Giasson, B. I., Ischiropoulos, H., and Lee, V. M. (2003). Effects of oxidative and nitrative challenges on alpha-synuclein fibrillogenesis involve distinct mechanisms of protein modifications. *J. Biol. Chem.* 278, 27230–27240. doi: 10.1074/jbc.M212436200

Obergasteiger, J., Frapporti, G., Pramstaller, P. P., Hicks, A. A., and Volta, M. (2018). A new hypothesis for Parkinson's disease pathogenesis: GTPase-p38 MAPK signaling and autophagy as convergence points of etiology and genomics. *Mol. Neurodegener.* 13:40. doi: 10.1186/s13024-018-0273-5

Odagiri, S., Tanji, K., Mori, F., Kakita, A., Takahashi, H., and Wakabayashi, K. (2012). Autophagic adapter protein NBR1 is localized in Lewy bodies and glial cytoplasmic inclusions and is involved in aggregate formation in alpha-synucleinopathy. *Acta Neuropathol.* 124, 173–186. doi: 10.1007/s00401-012-0975-7

Okun, M. S. (2012). Deep-brain stimulation for Parkinson's disease. *N. Engl. J. Med.* 367, 1529–1538. doi: 10.1056/NEJMct1208070

Olson, K. E., Bade, A. N., Schutt, C. R., Dong, J., Shandler, S. J., Boska, M. D., et al. (2016). Manganese-enhanced magnetic resonance imaging for detection of vasoactive intestinal peptide receptor 2 agonist therapy in a model of Parkinson's disease. *Neurotherapeutics* 13, 635–646. doi: 10.1007/s13311-016-0449-z

Olson, K. E., Kosloski-Bilek, L. M., Anderson, K. M., Diggs, B. J., Clark, B. E., Gledhill, J. M., et al. (2015). Selective VIP receptor agonists facilitate immune transformation for dopaminergic neuroprotection in MPTP-intoxicated mice. *J. Neurosci.* 35, 16463–16478. doi: 10.1523/JNEUROSCI.2131-15.2015

Onfelt, B., Nedvetzki, S., Yanagi, K., and Davis, D. M. (2004). Cutting edge: membrane nanotubes connect immune cells. *J. Immunol.* 173, 1511–1513. doi: 10.4049/jimmunol.173.3.1511

Orme, T., Guerreiro, R., and Bras, J. (2018). The genetics of dementia with Lewy bodies: current understanding and future directions. *Curr. Neurol. Neurosci. Rep.* 18:67. doi: 10.1007/s11910-018-0874-y

Osellame, L. D., Rahim, A. A., Hargreaves, I. P., Gegg, M. E., Richard-Londt, A., Brandner, S., et al. (2013). Mitochondria and quality control defects in a mouse model of Gaucher disease–links to Parkinson's disease. *Cell Metab.* 17, 941–953. doi: 10.1016/j.cmet.2013.04.014

Oueslati, A. (2016). Implication of Alpha-synuclein phosphorylation at S129 in synucleinopathies: What have we learned in the last decade? *J. Parkinsons Dis.* 6, 39–51. doi: 10.3233/JPD-160779

Oueslati, A., Fournier, M., and Lashuel, H. A. (2010). Role of post-translational modifications in modulating the structure, function and toxicity of alpha-synuclein: implications for Parkinson's disease pathogenesis and therapies. *Prog. Brain Res.* 183, 115–145. doi: 10.1016/S0079-6123(10)83007-9

Paillusson, S., Clairembault, T., Biraud, M., Neunlist, M., and Derkinderen, P. (2013). Activity-dependent secretion of alpha-synuclein by enteric neurons. *J. Neurochem.* 125, 512–517. doi: 10.1111/jnc.12131

Paleologou, K. E., Oueslati, A., Shakked, G., Rospigliosi, C. C., Kim, H. Y., Lamberto, G. R., et al. (2010). Phosphorylation at S87 is enhanced in synucleinopathies, inhibits alpha-synuclein oligomerization, and influences synuclein-membrane interactions. *J. Neurosci.* 30, 3184–3198. doi: 10.1523/JNEUROSCI.5922-09.2010

Paleologou, K. E., Schmid, A. W., Rospigliosi, C. C., Kim, H. Y., Lamberto, G. R., Fredenburg, R. A., et al. (2008). Phosphorylation at Ser-129 but not the phosphomimics S129E/D inhibits the fibrillation of alpha-synuclein. *J. Biol. Chem.* 283, 16895–16905. doi: 10.1074/jbc.M800747200

Pandey, N., Strider, J., Nolan, W. C., Yan, S. X., and Galvin, J. E. (2008). Curcumin inhibits aggregation of alpha-synuclein. *Acta Neuropathol.* 115, 479–489. doi: 10.1007/s00401-007-0332-4

Park, J. Y., Kim, K. S., Lee, S. B., Ryu, J. S., Chung, K. C., Choo, Y. K., et al. (2009). On the mechanism of internalization of alpha-synuclein into microglia: roles of ganglioside GM1 and lipid raft. *J. Neurochem.* 110, 400–411. doi: 10.1111/j.1471-4159.2009.06150.x

Park, S. M., Jung, H. Y., Kim, T. D., Park, J. H., Yang, C. H., and Kim, J. (2002). Distinct roles of the N-terminal-binding domain and the C-terminal-solubilizing domain of alpha-synuclein, a molecular chaperone. *J. Biol. Chem.* 277, 28512–28520. doi: 10.1074/jbc.M111971200

Pasanen, P., Myllykangas, L., Siitonen, M., Raunio, A., Kaakkola, S., Lyytinen, J., et al. (2014). Novel alpha-synuclein mutation A53E associated with atypical multiple system atrophy and Parkinson's disease-type pathology. *Neurobiol. Aging* 35, 2180.e1–2180.e5. doi: 10.1016/j.neurobiolaging.2014.03.024

Patil, S. P., Jain, P. D., Ghumatkar, P. J., Tambe, R., and Sathaye, S. (2014). Neuroprotective effect of metformin in MPTP-induced Parkinson's disease in mice. *Neuroscience* 277, 747–754. doi: 10.1016/j.neuroscience.2014.07.046

Paumier, K. L., Luk, K. C., Manfredsson, F. P., Kanaan, N. M., Lipton, J. W., Collier, T. J., et al. (2015). Intrastriatal injection of pre-formed mouse alpha-synuclein fibrils into rats triggers alpha-synuclein pathology and bilateral nigrostriatal degeneration. *Neurobiol. Dis.* 82, 185–199. doi: 10.1016/j.nbd.2015.06.003

Peelaerts, W., Bousset, L., Van der Perren, A., Moskalyuk, A., Pulizzi, R., Giugliano, M., et al. (2015). alpha-Synuclein strains cause distinct synucleinopathies after local and systemic administration. *Nature* 522, 340–344. doi: 10.1038/nature14547

Peng, C., Gathagan, R. J., Covell, D. J., Medellin, C., Stieber, A., Robinson, J. L., et al. (2018a). Cellular milieu imparts distinct pathological alpha-synuclein strains in alpha-synucleinopathies. *Nature* 557, 558–563. doi: 10.1038/s41586-018-0104-4

Peng, C., Gathagan, R. J., and Lee, V. M. (2018b). Distinct alpha-Synuclein strains and implications for heterogeneity among alpha-Synucleinopathies. *Neurobiol. Dis.* 109(Pt B), 209–218. doi: 10.1016/j.nbd.2017.07.018

Peng, X., Tehranian, R., Dietrich, P., Stefanis, L., and Perez, R. G. (2005). Alpha-synuclein activation of protein phosphatase 2A reduces tyrosine hydroxylase phosphorylation in dopaminergic cells. *J. Cell Sci.* 118(Pt 15), 3523–3530. doi: 10.1242/jcs.02481

Pieri, L., Madiona, K., and Melki, R. (2016). Structural and functional properties of prefibrillar alpha-synuclein oligomers. *Sci. Rep.* 6:24526. doi: 10.1038/srep24526

Pirc, K., and Ulrih, N. P. (2015). alpha-Synuclein interactions with phospholipid model membranes: key roles for electrostatic interactions and lipid-bilayer structure. *Biochim. Biophys. Acta* 1848(10 Pt A), 2002–2012. doi: 10.1016/j.bbamem.2015.06.021

Pletnikova, O., West, N., Lee, M. K., Rudow, G. L., Skolasky, R. L., Dawson, T. M., et al. (2005). Abeta deposition is associated with enhanced cortical alpha-synuclein lesions in Lewy body diseases. *Neurobiol. Aging* 26, 1183–1192. doi: 10.1016/j.neurobiolaging.2004.10.006

Politis, M., Su, P., and Piccini, P. (2012). Imaging of microglia in patients with neurodegenerative disorders. *Front. Pharmacol.* 3:96. doi: 10.3389/fphar.2012.00096

Polymeropoulos, M. H., Lavedan, C., Leroy, E., Ide, S. E., Dehejia, A., Dutra, A., et al. (1997). Mutation in the alpha-synuclein gene identified in families with Parkinson's disease. *Science* 276, 2045–2047. doi: 10.1126/science.276.5321.2045

Pouclet, H., Lebouvier, T., Coron, E., Des Varannes, S. B., Neunlist, M., and Derkinderen, P. (2012). A comparison between colonic submucosa and mucosa to detect Lewy pathology in Parkinson's disease. *Neurogastroenterol. Motil.* 24, e202–e205. doi: 10.1111/j.1365-2982.2012.01887.x

Prabhudesai, S., Sinha, S., Attar, A., Kotagiri, A., Fitzmaurice, A. G., Lakshmanan, R., et al. (2012). A novel "molecular tweezer" inhibitor of alpha-synuclein neurotoxicity *in vitro* and *in vivo*. *Neurotherapeutics* 9, 464–476. doi: 10.1007/s13311-012-0105-1

Price, D. L., Koike, M. A., Khan, A., Wrasidlo, W., Rockenstein, E., Masliah, E., et al. (2018). The small molecule alpha-synuclein misfolding inhibitor, NPT200-11, produces multiple benefits in an animal model of Parkinson's disease. *Sci. Rep.* 8:16165. doi: 10.1038/s41598-018-34490-9

Proukakis, C., Dudzik, C. G., Brier, T., MacKay, D. S., Cooper, J. M., Millhauser, G. L., et al. (2013). A novel alpha-synuclein missense mutation in Parkinson disease. *Neurology* 80, 1062–1064. doi: 10.1212/WNL.0b013e31828727ba

Prusiner, S. B., Woerman, A. L., Mordes, D. A., Watts, J. C., Rampersaud, R., Berry, D. B., et al. (2015). Evidence for alpha-synuclein prions causing multiple system atrophy in humans with parkinsonism. *Proc. Natl. Acad. Sci. U.S.A.* 112, E5308–E5317. doi: 10.1073/pnas.1514475112

Pukass, K., Goldbaum, O., and Richter-Landsberg, C. (2015). Mitochondrial impairment and oxidative stress compromise autophagosomal degradation of alpha-synuclein in oligodendroglial cells. *J. Neurochem.* 135, 194–205. doi: 10.1111/jnc.13256

Pukass, K., and Richter-Landsberg, C. (2014). Oxidative stress promotes uptake, accumulation, and oligomerization of extracellular alpha-synuclein in oligodendrocytes. *J. Mol. Neurosci.* 52, 339–352. doi: 10.1007/s12031-013-0154-x

Ravina, B., Putt, M., Siderowf, A., Farrar, J. T., Gillespie, M., Crawley, A., et al. (2005). Donepezil for dementia in Parkinson's disease: a randomised, double blind, placebo controlled, crossover study. *J. Neurol. Neurosurg. Psychiatry* 76, 934–939. doi: 10.1136/jnnp.2004.050682

Recasens, A., Dehay, B., Bove, J., Carballo-Carbajal, I., Dovero, S., Perez-Villalba, A., et al. (2014). Lewy body extracts from Parkinson disease brains trigger alpha-synuclein pathology and neurodegeneration in mice and monkeys. *Ann. Neurol.* 75, 351–362. doi: 10.1002/ana.24066

Rey, N. L., Petit, G. H., Bousset, L., Melki, R., and Brundin, P. (2013). Transfer of human alpha-synuclein from the olfactory bulb to interconnected brain regions in mice. *Acta Neuropathol.* 126, 555–573. doi: 10.1007/s00401-013-1160-3

Rey, N. L., Steiner, J. A., Maroof, N., Luk, K. C., Madaj, Z., Trojanowski, J. Q., et al. (2016). Widespread transneuronal propagation of alpha-synucleinopathy triggered in olfactory bulb mimics prodromal Parkinson's disease. *J. Exp. Med.* 213, 1759–1778. doi: 10.1084/jem.20160368

Reyes, J. F., Rey, N. L., Bousset, L., Melki, R., Brundin, P., and Angot, E. (2014). Alpha-synuclein transfers from neurons to oligodendrocytes. *Glia* 62, 387–398. doi: 10.1002/glia.22611

Reyes, J. F., Sackmann, C., Hoffmann, A., Svenningsson, P., Winkler, J., Ingelsson, M., et al. (2019). Binding of alpha-synuclein oligomers to Cx32 facilitates protein uptake and transfer in neurons and oligodendrocytes. *Acta Neuropathol.* 138, 23–47. doi: 10.1007/s00401-019-02007-x

Reynolds, A. D., Stone, D. K., Hutter, J. A., Benner, E. J., Mosley, R. L., and Gendelman, H. E. (2010). Regulatory T cells attenuate Th17 cell-mediated nigrostriatal dopaminergic neurodegeneration in a model of Parkinson's disease. *J. Immunol.* 184, 2261–2271. doi: 10.4049/jimmunol.0901852

Rice, T. W., Wheeler, A. P., Bernard, G. R., Vincent, J. L., Angus, D. C., Aikawa, N., et al. (2010). A randomized, double-blind, placebo-controlled trial of TAK-242 for the treatment of severe sepsis. *Crit. Care Med.* 38, 1685–1694. doi: 10.1097/CCM.0b013e3181e7c5c9

Richter, F., Subramaniam, S. R., Magen, I., Lee, P., Hayes, J., Attar, A., et al. (2017). A molecular Tweezer ameliorates motor deficits in mice overexpressing alpha-Synuclein. *Neurotherapeutics* 14, 1107–1119. doi: 10.1007/s13311-017-0544-9

Rideout, H. J., Larsen, K. E., Sulzer, D., and Stefanis, L. (2001). Proteasomal inhibition leads to formation of ubiquitin/alpha-synuclein-immunoreactive inclusions in PC12 cells. *J. Neurochem.* 78, 899–908. doi: 10.1046/j.1471-4159.2001.00474.x

Rideout, H. J., and Stefanis, L. (2002). Proteasomal inhibition-induced inclusion formation and death in cortical neurons require transcription and ubiquitination. *Mol. Cell. Neurosci.* 21, 223–238. doi: 10.1006/mcne.2002.1173

Rocha, E. M., De Miranda, B., and Sanders, L. H. (2018). Alpha-synuclein: pathology, mitochondrial dysfunction and neuroinflammation in Parkinson's disease. *Neurobiol. Dis.* 109(Pt B), 249–257. doi: 10.1016/j.nbd.2017.04.004

Rocha, E. M., Smith, G. A., Park, E., Cao, H., Graham, A. R., Brown, E., et al. (2015). Sustained systemic glucocerebrosidase inhibition induces brain alpha-synuclein aggregation, microglia and complement C1q activation in Mice. *Antioxid. Redox Signal.* 23, 550–564. doi: 10.1089/ars.2015.6307

Rockenstein, E., Ostroff, G., Dikengil, F., Rus, F., Mante, M., Florio, J., et al. (2018). Combined active humoral and cellular immunization approaches for the treatment of synucleinopathies. *J. Neurosci.* 38, 1000–1014. doi: 10.1523/JNEUROSCI.1170-17.2017

Rockenstein, E., Ubhi, K., Inglis, C., Mante, M., Patrick, C., Adame, A., et al. (2012). Neuronal to oligodendroglial alpha-synuclein redistribution in a double transgenic model of multiple system atrophy. *Neuroreport* 23, 259–264. doi: 10.1097/WNR.0b013e3283509842

Rodriguez, J. A., Ivanova, M. I., Sawaya, M. R., Cascio, D., Reyes, F. E., Shi, D., et al. (2015). Structure of the toxic core of alpha-synuclein from invisible crystals. *Nature* 525, 486–490. doi: 10.1038/nature15368

Roodveldt, C., Labrador-Garrido, A., Gonzalez-Rey, E., Lachaud, C. C., Guilliams, T., Fernandez-Montesinos, R., et al. (2013). Preconditioning of microglia by alpha-synuclein strongly affects the response induced by toll-like receptor (TLR) stimulation. *PLoS One* 8:e79160. doi: 10.1371/journal.pone.0079160

Rospigliosi, C. C., McClendon, S., Schmid, A. W., Ramlall, T. F., Barre, P., Lashuel, H. A., et al. (2009). E46K Parkinson's-linked mutation enhances C-terminal-to-N-terminal contacts in alpha-synuclein. *J. Mol. Biol.* 388, 1022–1032. doi: 10.1016/j.jmb.2009.03.065

Rott, R., Szargel, R., Haskin, J., Bandopadhyay, R., Lees, A. J., Shani, V., et al. (2011). alpha-Synuclein fate is determined by USP9X-regulated monoubiquitination. *Proc. Natl. Acad. Sci. U.S.A.* 108, 18666–18671. doi: 10.1073/pnas.1105725108

Sacino, A. N., Brooks, M., McGarvey, N. H., McKinney, A. B., Thomas, M. A., Levites, Y., et al. (2013a). Induction of CNS alpha-synuclein pathology by fibrillar and non-amyloidogenic recombinant alpha-synuclein. *Acta Neuropathol. Commun.* 1:38. doi: 10.1186/2051-5960-1-38

Sacino, A. N., Brooks, M., McKinney, A. B., Thomas, M. A., Shaw, G., Golde, T. E., et al. (2014a). Brain injection of alpha-synuclein induces multiple proteinopathies, gliosis, and a neuronal injury marker. *J. Neurosci.* 34, 12368–12378. doi: 10.1523/JNEUROSCI.2102-14.2014

Sacino, A. N., Brooks, M., Thomas, M. A., McKinney, A. B., Lee, S., Regenhardt, R. W., et al. (2014b). Intramuscular injection of alpha-synuclein induces CNS alpha-synuclein pathology and a rapid-onset motor phenotype in transgenic mice. *Proc. Natl. Acad. Sci. U.S.A.* 111, 10732–10737. doi: 10.1073/pnas.1321785111

Sacino, A. N., Thomas, M. A., Ceballos-Diaz, C., Cruz, P. E., Rosario, A. M., Lewis, J., et al. (2013b). Conformational templating of alpha-synuclein aggregates in neuronal-glial cultures. *Mol. Neurodegener.* 8:17. doi: 10.1186/1750-1326-8-17

Sahin, C., Lorenzen, N., Lemminger, L., Christiansen, G., Moller, I. M., Vesterager, L. B., et al. (2017). Antibodies against the C-terminus of alpha-synuclein modulate its fibrillation. *Biophys. Chem.* 220, 34–41. doi: 10.1016/j.bpc.2016.11.002

Sailer, A., Scholz, S. W., Nalls, M. A., Schulte, C., Federoff, M., Price, T. R., et al. (2016). A genome-wide association study in multiple system atrophy. *Neurology* 87, 1591–1598. doi: 10.1212/WNL.0000000000003221

Saito, Y., Kawashima, A., Ruberu, N. N., Fujiwara, H., Koyama, S., Sawabe, M., et al. (2003). Accumulation of phosphorylated alpha-synuclein in aging human brain. *J. Neuropathol. Exp. Neurol.* 62, 644–654. doi: 10.1093/jnen/62.6.644

Sampson, T. R., Debelius, J. W., Thron, T., Janssen, S., Shastri, G. G., Ilhan, Z. E., et al. (2016). Gut microbiota regulate motor deficits and neuroinflammation in

a model of Parkinson's disease. *Cell* 167, 1469–1480.e12. doi: 10.1016/j.cell.2016.11.018

Sanchez-Guajardo, V., Febbraro, F., Kirik, D., and Romero-Ramos, M. (2010). Microglia acquire distinct activation profiles depending on the degree of alpha-synuclein neuropathology in a rAAV based model of Parkinson's disease. *PLoS One* 5:e8784. doi: 10.1371/journal.pone.0008784

Sapru, M. K., Yates, J. W., Hogan, S., Jiang, L., Halter, J., and Bohn, M. C. (2006). Silencing of human alpha-synuclein *in vitro* and in rat brain using lentiviral-mediated RNAi. *Exp. Neurol.* 198, 382–390. doi: 10.1016/j.expneurol.2005.12.024

Sardi, S. P., Cedarbaum, J. M., and Brundin, P. (2018). Targeted therapies for Parkinson's disease: from genetics to the clinic. *Mov. Disord.* 33, 684–696. doi: 10.1002/mds.27414

Sardi, S. P., Clarke, J., Kinnecom, C., Tamsett, T. J., Li, L., Stanek, L. M., et al. (2011). CNS expression of glucocerebrosidase corrects alpha-synuclein pathology and memory in a mouse model of Gaucher-related synucleinopathy. *Proc. Natl. Acad. Sci. U.S.A.* 108, 12101–12106. doi: 10.1073/pnas.1108197108

Sardi, S. P., Clarke, J., Viel, C., Chan, M., Tamsett, T. J., Treleaven, C. M., et al. (2013). Augmenting CNS glucocerebrosidase activity as a therapeutic strategy for parkinsonism and other Gaucher-related synucleinopathies. *Proc. Natl. Acad. Sci. U.S.A.* 110, 3537–3542. doi: 10.1073/pnas.1220464110

Sardi, S. P., Viel, C., Clarke, J., Treleaven, C. M., Richards, A. M., Park, H., et al. (2017). Glucosylceramide synthase inhibition alleviates aberrations in synucleinopathy models. *Proc. Natl. Acad. Sci. U.S.A.* 114, 2699–2704. doi: 10.1073/pnas.1616152114

Sarkar, S., Chigurupati, S., Raymick, J., Mann, D., Bowyer, J. F., Schmitt, T., et al. (2014). Neuroprotective effect of the chemical chaperone, trehalose in a chronic MPTP-induced Parkinson's disease mouse model. *Neurotoxicology* 44, 250–262. doi: 10.1016/j.neuro.2014.07.006

Sarkar, S., Davies, J. E., Huang, Z., Tunnacliffe, A., and Rubinsztein, D. C. (2007). Trehalose, a novel mTOR-independent autophagy enhancer, accelerates the clearance of mutant huntingtin and alpha-synuclein. *J. Biol. Chem.* 282, 5641–5652. doi: 10.1074/jbc.M609532200

Satake, W., Nakabayashi, Y., Mizuta, I., Hirota, Y., Ito, C., Kubo, M., et al. (2009). Genome-wide association study identifies common variants at four loci as genetic risk factors for Parkinson's disease. *Nat. Genet.* 41, 1303–1307. doi: 10.1038/ng.485

Satish Bollimpelli, V., and Kondapi, A. K. (2015). Differential sensitivity of immature and mature ventral mesencephalic neurons to rotenone induced neurotoxicity *in vitro*. *Toxicol In Vitro* 30(1 Pt B), 545–551. doi: 10.1016/j.tiv.2015.09.006

Sato, H., Arawaka, S., Hara, S., Fukushima, S., Koga, K., Koyama, S., et al. (2011). Authentically phosphorylated alpha-synuclein at Ser129 accelerates neurodegeneration in a rat model of familial Parkinson's disease. *J. Neurosci.* 31, 16884–16894. doi: 10.1523/JNEUROSCI.3967-11.2011

Saunders, J. A., Estes, K. A., Kosloski, L. M., Allen, H. E., Dempsey, K. M., Torres-Russotto, D. R., et al. (2012). CD4+ regulatory and effector/memory T cell subsets profile motor dysfunction in Parkinson's disease. *J. Neuroimmune Pharmacol.* 7, 927–938. doi: 10.1007/s11481-012-9402-z

Schapira, A. H., and Gegg, M. E. (2013). Glucocerebrosidase in the pathogenesis and treatment of Parkinson disease. *Proc. Natl. Acad. Sci. U.S.A.* 110, 3214–3215. doi: 10.1073/pnas.1300822110

Schenk, D. B., Koller, M., Ness, D. K., Griffith, S. G., Grundman, M., Zago, W., et al. (2017). First-in-human assessment of PRX002, an anti-alpha-synuclein monoclonal antibody, in healthy volunteers. *Mov. Disord.* 32, 211–218. doi: 10.1002/mds.26878

Scheperjans, F., Aho, V., Pereira, P. A., Koskinen, K., Paulin, L., Pekkonen, E., et al. (2015). Gut microbiota are related to Parkinson's disease and clinical phenotype. *Mov. Disord.* 30, 350–358. doi: 10.1002/mds.26069

Scherzer, C. R., Grass, J. A., Liao, Z., Pepivani, I., Zheng, B., Eklund, A. C., et al. (2008). GATA transcription factors directly regulate the Parkinson's disease-linked gene alpha-synuclein. *Proc. Natl. Acad. Sci. U.S.A.* 105, 10907–10912. doi: 10.1073/pnas.0802437105

Schofield, D. J., Irving, L., Calo, L., Bogstedt, A., Rees, G., Nuccitelli, A., et al. (2019). Preclinical development of a high affinity alpha-synuclein antibody, MEDI1341, that can enter the brain, sequester extracellular alpha-synuclein and attenuate alpha-synuclein spreading *in vivo*. *Neurobiol. Dis.* 132:104582. doi: 10.1016/j.nbd.2019.104582

Scholz, S. W., Houlden, H., Schulte, C., Sharma, M., Li, A., Berg, D., et al. (2009). SNCA variants are associated with increased risk for multiple system atrophy. *Ann. Neurol.* 65, 610–614. doi: 10.1002/ana.21685

Schreiber, K. H., Ortiz, D., Academia, E. C., Anies, A. C., Liao, C. Y., and Kennedy, B. K. (2015). Rapamycin-mediated mTORC2 inhibition is determined by the relative expression of FK506-binding proteins. *Aging Cell* 14, 265–273. doi: 10.1111/acel.12313

Schwab, K., Frahm, S., Horsley, D., Rickard, J. E., Melis, V., Goatman, E. A., et al. (2017). A protein aggregation inhibitor, Leuco-Methylthioninium Bis(Hydromethanesulfonate), decreases alpha-synuclein inclusions in a transgenic mouse model of synucleinopathy. *Front. Mol. Neurosci.* 10:447. doi: 10.3389/fnmol.2017.00447

Schwarz, L., Goldbaum, O., Bergmann, M., Probst-Cousin, S., and Richter-Landsberg, C. (2012). Involvement of macroautophagy in multiple system atrophy and protein aggregate formation in oligodendrocytes. *J. Mol. Neurosci.* 47, 256–266. doi: 10.1007/s12031-012-9733-5

Schweighauser, M., Bacioglu, M., Fritschi, S. K., Shimshek, D. R., Kahle, P. J., Eisele, Y. S., et al. (2015). Formaldehyde-fixed brain tissue from spontaneously ill alpha-synuclein transgenic mice induces fatal alpha-synucleinopathy in transgenic hosts. *Acta Neuropathol.* 129, 157–159. doi: 10.1007/s00401-014-1360-5

Shahaduzzaman, M., Nash, K., Hudson, C., Sharif, M., Grimmig, B., Lin, X., et al. (2015). Anti-human alpha-synuclein N-terminal peptide antibody protects against dopaminergic cell death and ameliorates behavioral deficits in an AAV-alpha-synuclein rat model of Parkinson's disease. *PLoS One* 10:e0116841. doi: 10.1371/journal.pone.0116841

Shahnawaz, M., Mukherjee, A., Pritzkow, S., Mendez, N., Rabadia, P., Liu, X., et al. (2020). Discriminating alpha-synuclein strains in Parkinson's disease and multiple system atrophy. *Nature* 578, 273–277. doi: 10.1038/s41586-020-1984-7

Shahpasandzadeh, H., Popova, B., Kleinknecht, A., Fraser, P. E., Outeiro, T. F., and Braus, G. H. (2014). Interplay between sumoylation and phosphorylation for protection against alpha-synuclein inclusions. *J. Biol. Chem.* 289, 31224–31240. doi: 10.1074/jbc.M114.559237

Shaltiel-Karyo, R., Davidi, D., Frenkel-Pinter, M., Ovadia, M., Segal, D., and Gazit, E. (2012). Differential inhibition of alpha-synuclein oligomeric and fibrillar assembly in parkinson's disease model by cinnamon extract. *Biochim. Biophys. Acta* 1820, 1628–1635. doi: 10.1016/j.bbagen.2012.04.021

Shaltiel-Karyo, R., Frenkel-Pinter, M., Egoz-Matia, N., Frydman-Marom, A., Shalev, D. E., Segal, D., et al. (2010). Inhibiting alpha-synuclein oligomerization by stable cell-penetrating beta-synuclein fragments recovers phenotype of Parkinson's disease model flies. *PLoS One* 5:e13863. doi: 10.1371/journal.pone.0013863

Shaltiel-Karyo, R., Frenkel-Pinter, M., Rockenstein, E., Patrick, C., Levy-Sakin, M., Schiller, A., et al. (2013). A blood-brain barrier (BBB) disrupter is also a potent alpha-synuclein (alpha-syn) aggregation inhibitor: a novel dual mechanism of mannitol for the treatment of Parkinson disease (PD). *J. Biol. Chem.* 288, 17579–17588. doi: 10.1074/jbc.M112.434787

Shrivastava, A. N., Redeker, V., Fritz, N., Pieri, L., Almeida, L. G., Spolidoro, M., et al. (2015). alpha-synuclein assemblies sequester neuronal alpha3-Na+/K+-ATPase and impair Na+ gradient. *EMBO J.* 34, 2408–2423. doi: 10.15252/embj.201591397

Shults, C. W., Rockenstein, E., Crews, L., Adame, A., Mante, M., Larrea, G., et al. (2005). Neurological and neurodegenerative alterations in a transgenic mouse model expressing human alpha-synuclein under oligodendrocyte promoter: implications for multiple system atrophy. *J. Neurosci.* 25, 10689–10699. doi: 10.1523/JNEUROSCI.3527-05.2005

Silveira, C. R. A., MacKinley, J., Coleman, K., Li, Z., Finger, E., Bartha, R., et al. (2019). Ambroxol as a novel disease-modifying treatment for Parkinson's disease dementia: protocol for a single-centre, randomized, double-blind, placebo-controlled trial. *BMC Neurol.* 19:20. doi: 10.1186/s12883-019-1252-3

Simon-Sanchez, J., Schulte, C., Bras, J. M., Sharma, M., Gibbs, J. R., Berg, D., et al. (2009). Genome-wide association study reveals genetic risk underlying Parkinson's disease. *Nat. Genet.* 41, 1308–1312. doi: 10.1038/ng.487

Singleton, A. B., Farrer, M., Johnson, J., Singleton, A., Hague, S., Kachergus, J., et al. (2003). alpha-Synuclein locus triplication causes Parkinson's disease. *Science* 302:841. doi: 10.1126/science.1090278

Smith, W. W., Margolis, R. L., Li, X., Troncoso, J. C., Lee, M. K., Dawson, V. L., et al. (2005). Alpha-synuclein phosphorylation enhances eosinophilic cytoplasmic inclusion formation in SH-SY5Y cells. *J. Neurosci.* 25, 5544–5552. doi: 10.1523/JNEUROSCI.0482-05.2005

Sode, K., Ochiai, S., Kobayashi, N., and Usuzaka, E. (2006). Effect of reparation of repeat sequences in the human alpha-synuclein on fibrillation ability. *Int. J. Biol. Sci.* 3, 1–7. doi: 10.7150/ijbs.3.1

Song, J. X., Sun, Y. R., Peluso, I., Zeng, Y., Yu, X., Lu, J. H., et al. (2016). A novel curcumin analog binds to and activates TFEB *in vitro* and *in vivo* independent of MTOR inhibition. *Autophagy* 12, 1372–1389. doi: 10.1080/15548627.2016.1179404

Spencer, B., Emadi, S., Desplats, P., Eleuteri, S., Michael, S., Kosberg, K., et al. (2014). ESCRT-mediated uptake and degradation of brain-targeted alpha-synuclein single chain antibody attenuates neuronal degeneration *in vivo*. *Mol. Ther.* 22, 1753–1767. doi: 10.1038/mt.2014.129

Spillantini, M. G., Crowther, R. A., Jakes, R., Hasegawa, M., and Goedert, M. (1998). alpha-Synuclein in filamentous inclusions of Lewy bodies from Parkinson's disease and dementia with lewy bodies. *Proc. Natl. Acad. Sci. U.S.A.* 95, 6469–6473. doi: 10.1073/pnas.95.11.6469

Spillantini, M. G., and Goedert, M. (2000). The alpha-synucleinopathies: Parkinson's disease, dementia with Lewy bodies, and multiple system atrophy. *Ann. N. Y. Acad. Sci.* 920, 16–27. doi: 10.1111/j.1749-6632.2000.tb06900.x

Spillantini, M. G., Schmidt, M. L., Lee, V. M., Trojanowski, J. Q., Jakes, R., and Goedert, M. (1997). Alpha-synuclein in Lewy bodies. *Nature* 388, 839–840. doi: 10.1038/42166

Staats, K. A., Hernandez, S., Schonefeldt, S., Bento-Abreu, A., Dooley, J., Van Damme, P., et al. (2013). Rapamycin increases survival in ALS mice lacking mature lymphocytes. *Mol. Neurodegener.* 8:31. doi: 10.1186/1750-1326-8-31

Stefanis, L., Larsen, K. E., Rideout, H. J., Sulzer, D., and Greene, L. A. (2001). Expression of A53T mutant but not wild-type alpha-synuclein in PC12 cells induces alterations of the ubiquitin-dependent degradation system, loss of dopamine release, and autophagic cell death. *J. Neurosci.* 21, 9549–9560. doi: 10.1523/jneurosci.21-24-09549.2001

Stefanova, N., Fellner, L., Reindl, M., Masliah, E., Poewe, W., and Wenning, G. K. (2011). Toll-like receptor 4 promotes alpha-synuclein clearance and survival of nigral dopaminergic neurons. *Am. J. Pathol.* 179, 954–963. doi: 10.1016/j.ajpath.2011.04.013

Stefanova, N., Reindl, M., Neumann, M., Kahle, P. J., Poewe, W., and Wenning, G. K. (2007). Microglial activation mediates neurodegeneration related to oligodendroglial alpha-synucleinopathy: implications for multiple system atrophy. *Mov. Disord.* 22, 2196–2203. doi: 10.1002/mds.21671

Stefanova, N., Reindl, M., Poewe, W., and Wenning, G. K. (2005). *In vitro* models of multiple system atrophy. *Mov. Disord.* 20(Suppl. 12), S53–S56. doi: 10.1002/mds.20540

Stefanova, N., and Wenning, G. K. (2016). Review: multiple system atrophy: emerging targets for interventional therapies. *Neuropathol. Appl. Neurobiol.* 42, 20–32. doi: 10.1111/nan.12304

Stemberger, S., Poewe, W., Wenning, G. K., and Stefanova, N. (2010). Targeted overexpression of human alpha-synuclein in oligodendroglia induces lesions linked to MSA-like progressive autonomic failure. *Exp. Neurol.* 224, 459–464. doi: 10.1016/j.expneurol.2010.05.008

Strohaker, T., Jung, B. C., Liou, S. H., Fernandez, C. O., Riedel, D., Becker, S., et al. (2019). Structural heterogeneity of alpha-synuclein fibrils amplified from patient brain extracts. *Nat. Commun.* 10:5535. doi: 10.1038/s41467-019-13564-w

Stuendl, A., Kunadt, M., Kruse, N., Bartels, C., Moebius, W., Danzer, K. M., et al. (2016). Induction of alpha-synuclein aggregate formation by CSF exosomes from patients with Parkinson's disease and dementia with Lewy bodies. *Brain* 139(Pt 2), 481–494. doi: 10.1093/brain/awv346

Su, X., Maguire-Zeiss, K. A., Giuliano, R., Prifti, L., Venkatesh, K., and Federoff, H. J. (2008). Synuclein activates microglia in a model of Parkinson's disease. *Neurobiol. Aging* 29, 1690–1701. doi: 10.1016/j.neurobiolaging.2007.04.006

Sung, J. Y., Kim, J., Paik, S. R., Park, J. H., Ahn, Y. S., and Chung, K. C. (2001). Induction of neuronal cell death by Rab5A-dependent endocytosis of alpha-synuclein. *J. Biol. Chem.* 276, 27441–27448. doi: 10.1074/jbc.M101318200

Surgucheva, I., Gunewardena, S., Rao, H. S., and Surguchov, A. (2013). Cell-specific post-transcriptional regulation of gamma-synuclein gene by micro-RNAs. *PLoS One* 8:e73786. doi: 10.1371/journal.pone.0073786

Svensson, E., Horvath-Puho, E., Thomsen, R. W., Djurhuus, J. C., Pedersen, L., Borghammer, P., et al. (2015). Vagotomy and subsequent risk of Parkinson's disease. *Ann. Neurol.* 78, 522–529. doi: 10.1002/ana.24448

Swant, J., Goodwin, J. S., North, A., Ali, A. A., Gamble-George, J., Chirwa, S., et al. (2011). alpha-Synuclein stimulates a dopamine transporter-dependent chloride current and modulates the activity of the transporter. *J. Biol. Chem.* 286, 43933–43943. doi: 10.1074/jbc.M111.241232

Tan, S., Yu, C. Y., Sim, Z. W., Low, Z. S., Lee, B., See, F., et al. (2019). Pomegranate activates TFEB to promote autophagy-lysosomal fitness and mitophagy. *Sci. Rep.* 9:727. doi: 10.1038/s41598-018-37400-1

Tanaka, Y., Engelender, S., Igarashi, S., Rao, R. K., Wanner, T., Tanzi, R. E., et al. (2001). Inducible expression of mutant alpha-synuclein decreases proteasome activity and increases sensitivity to mitochondria-dependent apoptosis. *Hum. Mol. Genet.* 10, 919–926. doi: 10.1093/hmg/10.9.919

Tang, Y., and Le, W. (2016). Differential roles of M1 and M2 microglia in neurodegenerative diseases. *Mol. Neurobiol.* 53, 1181–1194. doi: 10.1007/s12035-014-9070-5

Tanji, K., Miki, Y., Maruyama, A., Mimura, J., Matsumiya, T., Mori, F., et al. (2015). Trehalose intake induces chaperone molecules along with autophagy in a mouse model of Lewy body disease. *Biochem. Biophys. Res. Commun.* 465, 746–752. doi: 10.1016/j.bbrc.2015.08.076

Tanji, K., Odagiri, S., Maruyama, A., Mori, F., Kakita, A., Takahashi, H., et al. (2013). Alteration of autophagosomal proteins in the brain of multiple system atrophy. *Neurobiol. Dis.* 49, 190–198. doi: 10.1016/j.nbd.2012.08.017

Tansey, M. G., and Romero-Ramos, M. (2019). Immune system responses in Parkinson's disease: early and dynamic. *Eur. J. Neurosci.* 49, 364–383. doi: 10.1111/ejn.14290

Teki, S., and Griffiths, T. D. (2016). Brain bases of working memory for time intervals in rhythmic sequences. *Front. Neurosci.* 10:239. doi: 10.3389/fnins.2016.00239

Tenreiro, S., Reimao-Pinto, M. M., Antas, P., Rino, J., Wawrzycka, D., Macedo, D., et al. (2014). Phosphorylation modulates clearance of alpha-synuclein inclusions in a yeast model of Parkinson's disease. *PLoS Genet.* 10:e1004302. doi: 10.1371/journal.pgen.1004302

Terada, M., Suzuki, G., Nonaka, T., Kametani, F., Tamaoka, A., and Hasegawa, M. (2018). The effect of truncation on prion-like properties of alpha-synuclein. *J. Biol. Chem.* 293, 13910–13920. doi: 10.1074/jbc.RA118.001862

Thayanidhi, N., Helm, J. R., Nycz, D. C., Bentley, M., Liang, Y., and Hay, J. C. (2010). Alpha-synuclein delays endoplasmic reticulum (ER)-to-Golgi transport in mammalian cells by antagonizing ER/Golgi SNAREs. *Mol. Biol. Cell* 21, 1850–1863. doi: 10.1091/mbc.E09-09-0801

Tofaris, G. K., Layfield, R., and Spillantini, M. G. (2001). alpha-synuclein metabolism and aggregation is linked to ubiquitin-independent degradation by the proteasome. *FEBS Lett.* 509, 22–26. doi: 10.1016/s0014-5793(01)03115-5

Tomas-Zapico, C., Diez-Zaera, M., Ferrer, I., Gomez-Ramos, P., Moran, M. A., Miras-Portugal, M. T., et al. (2012). alpha-Synuclein accumulates in huntingtin inclusions but forms independent filaments and its deficiency attenuates early phenotype in a mouse model of Huntington's disease. *Hum. Mol. Genet.* 21, 495–510. doi: 10.1093/hmg/ddr507

Tran, H. T., Chung, C. H., Iba, M., Zhang, B., Trojanowski, J. Q., Luk, K. C., et al. (2014). Alpha-synuclein immunotherapy blocks uptake and templated propagation of misfolded alpha-synuclein and neurodegeneration. *Cell Rep.* 7, 2054–2065. doi: 10.1016/j.celrep.2014.05.033

Tsigelny, I. F., Sharikov, Y., Wrasidlo, W., Gonzalez, T., Desplats, P. A., Crews, L., et al. (2012). Role of alpha-synuclein penetration into the membrane in the mechanisms of oligomer pore formation. *FEBS J.* 279, 1000–1013. doi: 10.1111/j.1742-4658.2012.08489.x

Tufekci, K. U., Meuwissen, R., Genc, S., and Genc, K. (2012). Inflammation in Parkinson's disease. *Adv. Protein Chem. Struct. Biol.* 88, 69–132. doi: 10.1016/B978-0-12-398314-5.00004-0

Ubhi, K., Rockenstein, E., Mante, M., Inglis, C., Adame, A., Patrick, C., et al. (2010). Neurodegeneration in a transgenic mouse model of multiple system atrophy is associated with altered expression of oligodendroglial-derived neurotrophic factors. *J. Neurosci.* 30, 6236–6246. doi: 10.1523/JNEUROSCI.0567-10.2010

Ubhi, K., Rockenstein, E., Mante, M., Patrick, C., Adame, A., Thukral, M., et al. (2008). Rifampicin reduces alpha-synuclein in a transgenic mouse model of multiple system atrophy. *Neuroreport* 19, 1271–1276. doi: 10.1097/WNR.0b013e32830b3661

Ueda, K., Fukushima, H., Masliah, E., Xia, Y., Iwai, A., Yoshimoto, M., et al. (1993). Molecular cloning of cDNA encoding an unrecognized component of amyloid in Alzheimer disease. *Proc. Natl. Acad. Sci. U.S.A.* 90, 11282–11286. doi: 10.1073/pnas.90.23.11282

Uehara, T., Choong, C. J., Nakamori, M., Hayakawa, H., Nishiyama, K., Kasahara, Y., et al. (2019). Amido-bridged nucleic acid (AmNA)-modified antisense oligonucleotides targeting alpha-synuclein as a novel therapy for Parkinson's disease. *Sci. Rep.* 9:7567. doi: 10.1038/s41598-019-43772-9

Uemura, N., Yagi, H., Uemura, M. T., Hatanaka, Y., Yamakado, H., and Takahashi, R. (2018). Inoculation of alpha-synuclein preformed fibrils into the mouse gastrointestinal tract induces Lewy body-like aggregates in the brainstem via the vagus nerve. *Mol. Neurodegener.* 13:21. doi: 10.1186/s13024-018-0257-5

Ulmer, T. S., Bax, A., Cole, N. B., and Nussbaum, R. L. (2005). Structure and dynamics of micelle-bound human alpha-synuclein. *J. Biol. Chem.* 280, 9595–9603. doi: 10.1074/jbc.M411805200

Ulusoy, A., Febbraro, F., Jensen, P. H., Kirik, D., and Romero-Ramos, M. (2010). Co-expression of C-terminal truncated alpha-synuclein enhances full-length alpha-synuclein-induced pathology. *Eur J. Neurosci.* 32, 409–422. doi: 10.1111/j.1460-9568.2010.07284.x

Ulusoy, A., Musgrove, R. E., Rusconi, R., Klinkenberg, M., Helwig, M., Schneider, A., et al. (2015). Neuron-to-neuron alpha-synuclein propagation *in vivo* is independent of neuronal injury. *Acta Neuropathol. Commun.* 3:13. doi: 10.1186/s40478-015-0198-y

Unger, M. M., Spiegel, J., Dillmann, K. U., Grundmann, D., Philippeit, H., Burmann, J., et al. (2016). Short chain fatty acids and gut microbiota differ between patients with Parkinson's disease and age-matched controls. *Parkinsonism Relat. Disord.* 32, 66–72. doi: 10.1016/j.parkreldis.2016.08.019

Ur Rasheed, M. S., Tripathi, M. K., Mishra, A. K., Shukla, S., and Singh, M. P. (2016). Resveratrol protects from toxin-induced parkinsonism: plethora of proofs hitherto petty translational value. *Mol. Neurobiol.* 53, 2751–2760. doi: 10.1007/s12035-015-9124-3

Uversky, V. N., Li, J., and Fink, A. L. (2001). Evidence for a partially folded intermediate in alpha-synuclein fibril formation. *J. Biol. Chem.* 276, 10737–10744. doi: 10.1074/jbc.M010907200

Valente, T., Dentesano, G., Ezquerra, M., Fernandez-Santiago, R., Martinez-Martin, J., Gallastegui, E., et al. (2020). CCAAT/enhancer binding protein delta is a transcriptional repressor of alpha-synuclein. *Cell Death Differ.* 27, 509–524. doi: 10.1038/s41418-019-0368-8

Valera, E., Spencer, B., Fields, J. A., Trinh, I., Adame, A., Mante, M., et al. (2017). Combination of alpha-synuclein immunotherapy with anti-inflammatory treatment in a transgenic mouse model of multiple system atrophy. *Acta Neuropathol. Commun.* 5:2. doi: 10.1186/s40478-016-0409-1

Van Den Berge, N., Ferreira, N., Gram, H., Mikkelsen, T. W., Alstrup, A. K. O., Casadei, N., et al. (2019). Evidence for bidirectional and trans-synaptic parasympathetic and sympathetic propagation of alpha-synuclein in rats. *Acta Neuropathol.* 138, 535–550. doi: 10.1007/s00401-019-02040-w

Van der Perren, A., Gelders, G., Fenyi, A., Bousset, L., Brito, F., Peelaerts, W., et al. (2020). The structural differences between patient-derived alpha-synuclein strains dictate characteristics of Parkinson's disease, multiple system atrophy and dementia with Lewy bodies. *Acta Neuropathol.* 139, 977–1000. doi: 10.1007/s00401-020-02157-3

Vawter, M. P., Dillon-Carter, O., Tourtellotte, W. W., Carvey, P., and Freed, W. J. (1996). TGFbeta1 and TGFbeta2 concentrations are elevated in Parkinson's disease in ventricular cerebrospinal fluid. *Exp. Neurol.* 142, 313–322. doi: 10.1006/exnr.1996.0200

Vekrellis, K., and Stefanis, L. (2012). Targeting intracellular and extracellular alpha-synuclein as a therapeutic strategy in Parkinson's disease and other synucleinopathies. *Expert Opin. Ther. Targets* 16, 421–432. doi: 10.1517/14728222.2012.674111

Vekrellis, K., Xilouri, M., Emmanouilidou, E., Rideout, H. J., and Stefanis, L. (2011). Pathological roles of alpha-synuclein in neurological disorders. *Parkinsonism Relat. Disord.* 10, 1015–1025. doi: 10.1016/S1474-4422(11)70213-7

Vekrellis, K., Xilouri, M., Emmanouilidou, E., and Stefanis, L. (2009). Inducible over-expression of wild type alpha-synuclein in human neuronal cells leads to caspase-dependent non-apoptotic death. *J. Neurochem.* 109, 1348–1362. doi: 10.1111/j.1471-4159.2009.06054.x

Vieira, B. D., Radford, R. A., Chung, R. S., Guillemin, G. J., and Pountney, D. L. (2015). Neuroinflammation in multiple system atrophy: response to and cause of alpha-synuclein aggregation. *Front. Cell. Neurosci.* 9:437. doi: 10.3389/fncel.2015.00437

Vilarino-Guell, C., Soto-Ortolaza, A. I., Rajput, A., Mash, D. C., Papapetropoulos, S., Pahwa, R., et al. (2011). MAPT H1 haplotype is a risk factor for essential tremor and multiple system atrophy. *Neurology* 76, 670–672. doi: 10.1212/WNL.0b013e31820c30c1

Vinueza-Gavilanes, R., Inigo-Marco, I., Larrea, L., Lasa, M., Carte, B., Santamaria, E., et al. (2020). N-terminal acetylation mutants affect alpha-synuclein stability, protein levels and neuronal toxicity. *Neurobiol. Dis.* 137:104781. doi: 10.1016/j.nbd.2020.104781

Vogiatzi, T., Xilouri, M., Vekrellis, K., and Stefanis, L. (2008). Wild type alpha-synuclein is degraded by chaperone-mediated autophagy and macroautophagy in neuronal cells. *J. Biol. Chem.* 283, 23542–23556. doi: 10.1074/jbc.M801992200

Volles, M. J., and Lansbury, P. T. Jr. (2002). Vesicle permeabilization by protofibrillar alpha-synuclein is sensitive to Parkinson's disease-linked mutations and occurs by a pore-like mechanism. *Biochemistry* 41, 4595–4602. doi: 10.1021/bi0121353

Volpicelli-Daley, L. A., Luk, K. C., and Lee, V. M. (2014). Addition of exogenous alpha-synuclein preformed fibrils to primary neuronal cultures to seed recruitment of endogenous alpha-synuclein to Lewy body and Lewy neurite-like aggregates. *Nat. Protoc.* 9, 2135–2146. doi: 10.1038/nprot.2014.143

Volpicelli-Daley, L. A., Luk, K. C., Patel, T. P., Tanik, S. A., Riddle, D. M., Stieber, A., et al. (2011). Exogenous alpha-synuclein fibrils induce Lewy body pathology leading to synaptic dysfunction and neuron death. *Neuron* 72, 57–71. doi: 10.1016/j.neuron.2011.08.033

Wagner, J., Ryazanov, S., Leonov, A., Levin, J., Shi, S., Schmidt, F., et al. (2013). Anle138b: a novel oligomer modulator for disease-modifying therapy of neurodegenerative diseases such as prion and Parkinson's disease. *Acta Neuropathol.* 125, 795–813. doi: 10.1007/s00401-013-1114-9

Wakabayashi, K., Hayashi, S., Kakita, A., Yamada, M., Toyoshima, Y., Yoshimoto, M., et al. (1998a). Accumulation of alpha-synuclein/NACP is a cytopathological feature common to Lewy body disease and multiple system atrophy. *Acta Neuropathol.* 96, 445–452. doi: 10.1007/s004010050918

Wakabayashi, K., Yoshimoto, M., Tsuji, S., and Takahashi, H. (1998b). Alpha-synuclein immunoreactivity in glial cytoplasmic inclusions in multiple system atrophy. *Neurosci. Lett.* 249, 180–182. doi: 10.1016/s0304-3940(98)00407-8

Wang, B., Underwood, R., Kamath, A., Britain, C., McFerrin, M. B., McLean, P. J., et al. (2018). 14-3-3 proteins reduce cell-to-cell transfer and propagation of pathogenic alpha-synuclein. *J. Neurosci.* 38, 8211–8232. doi: 10.1523/JNEUROSCI.1134-18.2018

Wang, T., and Hay, J. C. (2015). Alpha-synuclein toxicity in the early secretory pathway: how it drives neurodegeneration in Parkinsons disease. *Front. Neurosci.* 9:433. doi: 10.3389/fnins.2015.00433

Wang, W., Nguyen, L. T., Burlak, C., Chegini, F., Guo, F., Chataway, T., et al. (2016). Caspase-1 causes truncation and aggregation of the Parkinson's disease-associated protein alpha-synuclein. *Proc. Natl. Acad. Sci. U.S.A.* 113, 9587–9592. doi: 10.1073/pnas.1610099113

Wang, W., Perovic, I., Chittuluru, J., Kaganovich, A., Nguyen, L. T., Liao, J., et al. (2011). A soluble alpha-synuclein construct forms a dynamic tetramer. *Proc. Natl. Acad. Sci. U.S.A.* 108, 17797–17802. doi: 10.1073/pnas.1113260108

Wang, X., Becker, K., Levine, N., Zhang, M., Lieberman, A. P., Moore, D. J., et al. (2019). Pathogenic alpha-synuclein aggregates preferentially bind to mitochondria and affect cellular respiration. *Acta Neuropathol. Commun.* 7:41. doi: 10.1186/s40478-019-0696-4

Watson, M. B., Richter, F., Lee, S. K., Gabby, L., Wu, J., Masliah, E., et al. (2012). Regionally-specific microglial activation in young mice over-expressing human wildtype alpha-synuclein. *Exp. Neurol.* 237, 318–334. doi: 10.1016/j.expneurol.2012.06.025

Watts, J. C., Giles, K., Oehler, A., Middleton, L., Dexter, D. T., Gentleman, S. M., et al. (2013). Transmission of multiple system atrophy prions to transgenic mice. *Proc. Natl. Acad. Sci. U.S.A.* 110, 19555–19560. doi: 10.1073/pnas.1318268110

Waxman, E. A., Mazzulli, J. R., and Giasson, B. I. (2009). Characterization of hydrophobic residue requirements for alpha-synuclein fibrillization. *Biochemistry* 48, 9427–9436. doi: 10.1021/bi900539p

Webb, J. L., Ravikumar, B., Atkins, J., Skepper, J. N., and Rubinsztein, D. C. (2003). Alpha-Synuclein is degraded by both autophagy and the proteasome. *J. Biol. Chem.* 278, 25009–25013. doi: 10.1074/jbc.M300227200

Weihofen, A., Liu, Y., Arndt, J. W., Huy, C., Quan, C., Smith, B. A., et al. (2019). Development of an aggregate-selective, human-derived alpha-synuclein antibody BIIB054 that ameliorates disease phenotypes in Parkinson's disease models. *Neurobiol. Dis.* 124, 276–288. doi: 10.1016/j.nbd.2018.10.016

Weinreb, P. H., Zhen, W., Poon, A. W., Conway, K. A., and Lansbury, P. T. Jr. (1996). NACP, a protein implicated in Alzheimer's disease and learning, is natively unfolded. *Biochemistry* 35, 13709–13715. doi: 10.1021/bi961799n

Wersinger, C., Jeannotte, A., and Sidhu, A. (2006a). Attenuation of the norepinephrine transporter activity and trafficking via interactions with alpha-synuclein. *Eur J. Neurosci.* 24, 3141–3152. doi: 10.1111/j.1460-9568.2006.05181.x

Wersinger, C., Rusnak, M., and Sidhu, A. (2006b). Modulation of the trafficking of the human serotonin transporter by human alpha-synuclein. *Eur. J. Neurosci.* 24, 55–64. doi: 10.1111/j.1460-9568.2006.04900.x

Whittaker, H. T., Qui, Y., Bettencourt, C., and Houlden, H. (2017). Multiple system atrophy: genetic risks and alpha-synuclein mutations. *F1000Res.* 6:2072. doi: 10.12688/f1000research.12193.1

Winner, B., Jappelli, R., Maji, S. K., Desplats, P. A., Boyer, L., Aigner, S., et al. (2011). *In vivo* demonstration that alpha-synuclein oligomers are toxic. *Proc. Natl. Acad. Sci. U.S.A.* 108, 4194–4199. doi: 10.1073/pnas.1100976108

Winslow, A. R., Chen, C. W., Corrochano, S., Acevedo-Arozena, A., Gordon, D. E., Peden, A. A., et al. (2010). alpha-Synuclein impairs macroautophagy: implications for Parkinson's disease. *J. Cell Biol.* 190, 1023–1037. doi: 10.1083/jcb.201003122

Witt, S. N. (2013). Molecular chaperones, alpha-synuclein, and neurodegeneration. *Mol. Neurobiol.* 47, 552–560. doi: 10.1007/s12035-012-8325-2

Woerman, A. L., Stohr, J., Aoyagi, A., Rampersaud, R., Krejciova, Z., Watts, J. C., et al. (2015). Propagation of prions causing synucleinopathies in cultured cells. *Proc. Natl. Acad. Sci. U.S.A.* 112, E4949–E4958. doi: 10.1073/pnas.1513426112

Wrasidlo, W., Tsigelny, I. F., Price, D. L., Dutta, G., Rockenstein, E., Schwarz, T. C., et al. (2016). A de novo compound targeting alpha-synuclein improves deficits in models of Parkinson's disease. *Brain* 139(Pt 12), 3217–3236. doi: 10.1093/brain/aww238

Wu, B., Liu, Q., Duan, C., Li, Y., Yu, S., Chan, P., et al. (2011). Phosphorylation of alpha-synuclein upregulates tyrosine hydroxylase activity in MN9D cells. *Acta Histochem.* 113, 32–35. doi: 10.1016/j.acthis.2009.07.007

Wu, F., Xu, H. D., Guan, J. J., Hou, Y. S., Gu, J. H., Zhen, X. C., et al. (2015). Rotenone impairs autophagic flux and lysosomal functions in Parkinson's disease. *Neuroscience* 284, 900–911. doi: 10.1016/j.neuroscience.2014.11.004

Wu, Q., Takano, H., Riddle, D. M., Trojanowski, J. Q., Coulter, D. A., and Lee, V. M. (2019). alpha-Synuclein (alphaSyn) preformed fibrils induce endogenous alphaSyn aggregation, compromise synaptic activity and enhance synapse loss in cultured excitatory hippocampal neurons. *J. Neurosci.* 39, 5080–5094. doi: 10.1523/JNEUROSCI.0060-19.2019

Wu, Y., Li, X., Zhu, J. X., Xie, W., Le, W., Fan, Z., et al. (2011). Resveratrol-activated AMPK/SIRT1/autophagy in cellular models of Parkinson's disease. *Neurosignals* 19, 163–174. doi: 10.1159/000328516

Xilouri, M., Brekk, O. R., Landeck, N., Pitychoutis, P. M., Papasilekas, T., Papadopoulou-Daifoti, Z., et al. (2013a). Boosting chaperone-mediated autophagy *in vivo* mitigates alpha-synuclein-induced neurodegeneration. *Brain* 136(Pt 7), 2130–2146. doi: 10.1093/brain/awt131

Xilouri, M., Brekk, O. R., Polissidis, A., Chrysanthou-Piterou, M., Kloukina, I., and Stefanis, L. (2016a). Impairment of chaperone-mediated autophagy induces dopaminergic neurodegeneration in rats. *Autophagy* 12, 2230–2247. doi: 10.1080/15548627.2016.1214777

Xilouri, M., Brekk, O. R., and Stefanis, L. (2013b). alpha-Synuclein and protein degradation systems: a reciprocal relationship. *Mol. Neurobiol.* 47, 537–551. doi: 10.1007/s12035-012-8341-2

Xilouri, M., Brekk, O. R., and Stefanis, L. (2016b). Autophagy and alpha-synuclein: relevance to Parkinson's disease and related synucleopathies. *Mov. Disord.* 31, 178–192. doi: 10.1002/mds.26477

Xilouri, M., Vogiatzi, T., Vekrellis, K., Park, D., and Stefanis, L. (2009). Abberant alpha-synuclein confers toxicity to neurons in part through inhibition of chaperone-mediated autophagy. *PLoS One* 4:e5515. doi: 10.1371/journal.pone.0005515

Xu, J., Wu, X. S., Sheng, J., Zhang, Z., Yue, H. Y., Sun, L., et al. (2016). alpha-synuclein mutation inhibits endocytosis at mammalian central nerve terminals. *J. Neurosci.* 36, 4408–4414. doi: 10.1523/JNEUROSCI.3627-15.2016

Xu, Y., Liu, C., Chen, S., Ye, Y., Guo, M., Ren, Q., et al. (2014). Activation of AMPK and inactivation of Akt result in suppression of mTOR-mediated S6K1 and 4E-BP1 pathways leading to neuronal cell death in *in vitro* models of Parkinson's disease. *Cell. Signal.* 26, 1680–1689. doi: 10.1016/j.cellsig.2014.04.009

Xu, Z., Graham, K., Foote, M., Liang, F., Rizkallah, R., Hurt, M., et al. (2013). 14-3-3 protein targets misfolded chaperone-associated proteins to aggresomes. *J. Cell Sci.* 126(Pt 18), 4173–4186. doi: 10.1242/jcs.126102

Yan, J. Q., Yuan, Y. H., Gao, Y. N., Huang, J. Y., Ma, K. L., Gao, Y., et al. (2014). Overexpression of human E46K mutant alpha-synuclein impairs macroautophagy via inactivation of JNK1-Bcl-2 pathway. *Mol. Neurobiol.* 50, 685–701. doi: 10.1007/s12035-014-8738-1

Yang, S. Y., Beavan, M., Chau, K. Y., Taanman, J. W., and Schapira, A. H. V. (2017). A human neural crest stem cell-derived dopaminergic neuronal model recapitulates biochemical abnormalities in GBA1 mutation carriers. *Stem Cell Rep.* 8, 728–742. doi: 10.1016/j.stemcr.2017.01.011

Yang, Y., Fukui, K., Koike, T., and Zheng, X. (2007). Induction of autophagy in neurite degeneration of mouse superior cervical ganglion neurons. *Eur. J. Neurosci.* 26, 2979–2988. doi: 10.1111/j.1460-9568.2007.05914.x

Yazawa, I., Giasson, B. I., Sasaki, R., Zhang, B., Joyce, S., Uryu, K., et al. (2005). Mouse model of multiple system atrophy alpha-synuclein expression in oligodendrocytes causes glial and neuronal degeneration. *Neuron* 45, 847–859. doi: 10.1016/j.neuron.2005.01.032

Zarranz, J. J., Alegre, J., Gomez-Esteban, J. C., Lezcano, E., Ros, R., Ampuero, I., et al. (2004). The new mutation, E46K, of alpha-synuclein causes Parkinson and Lewy body dementia. *Ann. Neurol.* 55, 164–173. doi: 10.1002/ana.10795

Zavodszky, E., Seaman, M. N., Moreau, K., Jimenez-Sanchez, M., Breusegem, S. Y., Harbour, M. E., et al. (2014). Mutation in VPS35 associated with Parkinson's disease impairs WASH complex association and inhibits autophagy. *Nat. Commun.* 5:3828. doi: 10.1038/ncomms4828

Zhang, Q., Xu, Y., Lee, J., Jarnik, M., Wu, X., Bonifacino, J. S., et al. (2020). A myosin-7B-dependent endocytosis pathway mediates cellular entry of alpha-synuclein fibrils and polycation-bearing cargos. *Proc. Natl. Acad. Sci. U.S.A.* 117, 10865–10875. doi: 10.1073/pnas.1918617117

Zharikov, A. D., Cannon, J. R., Tapias, V., Bai, Q., Horowitz, M. P., Shah, V., et al. (2015). shRNA targeting alpha-synuclein prevents neurodegeneration in a Parkinson's disease model. *J. Clin. Invest.* 125, 2721–2735. doi: 10.1172/JCI64502

Zhu, M., Rajamani, S., Kaylor, J., Han, S., Zhou, F., and Fink, A. L. (2004). The flavonoid baicalein inhibits fibrillation of alpha-synuclein and disaggregates existing fibrils. *J. Biol. Chem.* 279, 26846–26857. doi: 10.1074/jbc.M403129200

Zondler, L., Kostka, M., Garidel, P., Heinzelmann, U., Hengerer, B., Mayer, B., et al. (2017). Proteasome impairment by alpha-synuclein. *PLoS One* 12:e0184040. doi: 10.1371/journal.pone.0184040

Zou, J., Guo, Y., Wei, L., Yu, F., Yu, B., and Xu, A. (2020). Long noncoding RNA POU3F3 and alpha-Synuclein in Plasma L1CAM exosomes combined with beta-Glucocerebrosidase activity: potential predictors of Parkinson's disease. *Neurotherapeutics*. doi: 10.1007/s13311-020-00842-5 [Epub ahead of print].

Conflict of Interest: The authors declare that the research was conducted in the absence of any commercial or financial relationships that could be construed as a potential conflict of interest.

Copyright © 2020 Fouka, Mavroeidi, Tsaka and Xilouri. This is an open-access article distributed under the terms of the Creative Commons Attribution License (CC BY). The use, distribution or reproduction in other forums is permitted, provided the original author(s) and the copyright owner(s) are credited and that the original publication in this journal is cited, in accordance with accepted academic practice. No use, distribution or reproduction is permitted which does not comply with these terms.

International Journal of
Molecular Sciences

MDPI

Review

Neurons and Glia Interplay in α-Synucleinopathies

Panagiota Mavroeidi and Maria Xilouri *

Center of Clinical Research, Experimental Surgery and Translational Research, Biomedical Research Foundation of the Academy of Athens, 11527 Athens, Greece; pmavroeidi@bioacademy.gr
* Correspondence: mxilouri@bioacademy.gr; Tel.: +30-2106597498; Fax: +30-2106597545

Abstract: Accumulation of the neuronal presynaptic protein alpha-synuclein within proteinaceous inclusions represents the key histophathological hallmark of a spectrum of neurodegenerative disorders, referred to by the umbrella term a-synucleinopathies. Even though alpha-synuclein is expressed predominantly in neurons, pathological aggregates of the protein are also found in the glial cells of the brain. In Parkinson's disease and dementia with Lewy bodies, alpha-synuclein accumulates mainly in neurons forming the Lewy bodies and Lewy neurites, whereas in multiple system atrophy, the protein aggregates mostly in the glial cytoplasmic inclusions within oligodendrocytes. In addition, astrogliosis and microgliosis are found in the synucleinopathy brains, whereas both astrocytes and microglia internalize alpha-synuclein and contribute to the spread of pathology. The mechanisms underlying the pathological accumulation of alpha-synuclein in glial cells that under physiological conditions express low to non-detectable levels of the protein are an area of intense research. Undoubtedly, the presence of aggregated alpha-synuclein can disrupt glial function in general and can contribute to neurodegeneration through numerous pathways. Herein, we summarize the current knowledge on the role of alpha-synuclein in both neurons and glia, highlighting the contribution of the neuron-glia connectome in the disease initiation and progression, which may represent potential therapeutic target for a-synucleinopathies.

Keywords: aggregation; astrocytes; a-Synuclein; inclusions; microglia; neurons; oligodendroglia; seeding

check for updates

Citation: Mavroeidi, P.; Xilouri, M. Neurons and Glia Interplay in α-Synucleinopathies. *Int. J. Mol. Sci.* **2021**, *22*, 4994. https://doi.org/10.3390/ijms22094994

Academic Editor: Fabio Cavaliere

Received: 6 April 2021
Accepted: 4 May 2021
Published: 8 May 2021

Publisher's Note: MDPI stays neutral with regard to jurisdictional claims in published maps and institutional affiliations.

Copyright: © 2021 by the authors. Licensee MDPI, Basel, Switzerland. This article is an open access article distributed under the terms and conditions of the Creative Commons Attribution (CC BY) license (https://creativecommons.org/licenses/by/4.0/).

1. Introduction

The presynaptic neuronal protein alpha-synuclein (aSyn) under physiological conditions regulates neurotransmitter release and SNARE (soluble N-ethylmaleimide-sensitive factor attachment protein receptor) complex assembly and is considered a chameleon-protein due to its remarkable conformational plasticity [1]. On the other hand, aggregated aSyn is the major component of the proteinaceous inclusions found in the degenerating neurons of Parkinson's disease (PD) and dementia with Lewy bodies (DLB) brains, known as Lewy bodies (LBs) and Lewy neurites (LNs) [2]. Alpha-synuclein also has a strong genetic link to PD pathogenesis, since missense point mutations of the *SNCA* gene encoding for aSyn, *SNCA* gene locus duplications and triplications or gene-enhanced expression are the main causes of familial PD [3–9]. In contrast, multiple system atrophy (MSA), a fatal debilitating neurodegenerative disorder, is characterized by the presence of aggregated aSyn within the glial cytoplasmic inclusions (GCIs) present in the cytoplasm of oligodendrocytes [10–12]. Glial aSyn accumulation is also evident in PD and PD with aSyn-positive deposits reported in astrocytes and oligodendrocytes [13–15]. Contrarily, aSyn-positive inclusions in astrocytes have been also found in MSA [16], but to a lesser extent [14] compared to neuronal and oligodendroglial inclusion pathology.

The clinical and neuropathological heterogeneity in a-synucleinopathies may ascend from the unique properties of the different conformational aSyn strains found in neurons or glia that might contribute to distinct clinical phenotypes [17–20]. Even though the physiological and pathological functions of aSyn in neurons, where the protein is physiologically expressed, are well characterized, the mechanisms underlying the pathological

accumulation of aSyn in the glial cells of the central nervous system (CNS) still necessitates further investigation. Microglia and astroglia have distinct roles in maintaining brain's homeostasis but under stress conditions, such as increased aSyn burden, they can become activated and contribute to disease pathology by triggering neuroinflammatory mechanisms. Reactive astrocytes and microglia have been detected in human post-mortem brains of a-synucleinopathies [13,21–25], further supporting a role of active gliosis in the initiation and progression of the disease. Moreover, all glial cells have been reported to internalize aSyn and a neuron-to-glia transmission is thought to underlie the propagation of aSyn pathology in a-synucleinopathies. In the following sections, we discuss how aSyn affects neuronal and glial function and homeostasis in health and disease.

2. Alpha-Synuclein in Neurons: A Multifaceted Protein

2.1. A Role at the Synapse

alpha-Synuclein (aSyn) is a small, intrinsically disordered protein that is mainly localized at the pre-synaptic terminal [26,27], but is also present in the neuronal somato-dendritic compartment [28], in red blood cells [29], in the gut and other peripheral tissues [30–32]. Although aSyn is highly enriched in presynaptic boutons, it displays a delayed distribution in the terminals, suggesting that it is implicated in later stages of synaptic development, rather than playing a central role in synapse modulation [27]. Importantly, aSyn is differentially expressed in the various neuronal cell types, being more abundant in excitatory synapses across different brain regions and particularly in central catecholaminergic systems [33]. On the contrary, the protein displays a differential expression profile in inhibitory synapses amongst the different brain areas, with a particular interest of aSyn presence in striatal GABAergic medium spiny neurons (MSNs) [34,35].

The first indication regarding the role of aSyn on neural plasticity arose about 25 years ago, when "synelfin" (synuclein, NACP) expression was found up-regulated during bird song learning [36]. The localization of aSyn in pre-synaptic boutons is mainly attributed to its tight association with synaptic vesicle membranes [37] and its high affinity for the SNARE complex proteins synaptobrevin-2 (or Vesicle Associated Membrane Protein 2, VAMP2), synapsin III and rab3A [38–40]. It has been proposed that aSyn interacts with VAMP2 and promotes SNARE complex assembly [38], followed then by its disassembly in order to complete the round of membrane fusion (Figure 1). The crucial role of aSyn assembly with SNARE complex on neuronal survival was further verified by the neuronal dysfunction and impaired survival of triple αβγ-synuclein knockout mice during ageing [38,41]. Interestingly, aSyn lentiviral overexpression in primary neurons led to enhanced SNARE complex assembly, further supporting the role of this protein in synaptic activity [38]. The same group later showed that only multimeric membrane-bound, but not the soluble monomeric aSyn, can promote the SNARE complex assembly [42]. It has been also recently suggested that aSyn is involved in synaptic vesicle homeostasis at the pre-synaptic terminal via a calcium (Ca^{2+})-dependent mechanism [43].

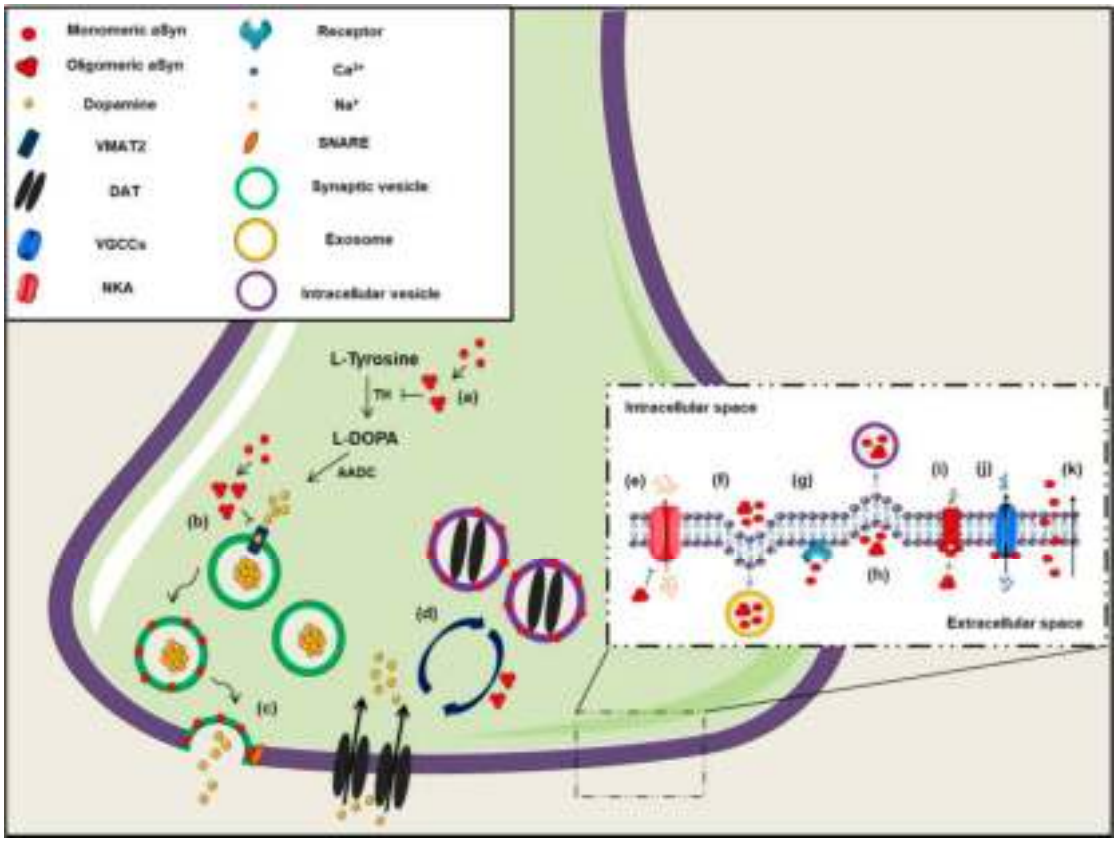

Figure 1. The role of aSyn at the presynaptic terminal. A schematic representation depicting of aSyn physiological and pathological effects at the synapse: (a) aSyn reduces the activity of tyrosine hydroxylase (TH), the enzyme responsible for catalyzing the conversion of L-Tyrosine to L-DOPA, thus impairing dopamine biosynthesis, (b) Increased levels of aSyn inhibit VMAT2, which is responsible for the uptake of monoamines (such as dopamine) into synaptic vesicles, (c) aSyn associates with synaptic vesicle membranes and regulates the SNARE-dependent vesicle fusion and neurotransmitter release, (d) Soluble aSyn interacts with the dopaminergic transporter DAT and decreases its amount on the plasma membrane, thus regulating the dopamine re-uptake from the synapse. However, aSyn aggregates trigger DAT recruitment to the plasma membrane that leads to massive entry of dopamine, (e) aSyn aggregates interact with Na^+/K^+-ATPase (NKA) preventing the effective pump out of Na^+ ions, (f) aSyn is secreted from neuronal cells partly via associating with exosomes, (g) Extracellular aSyn interacts with neuronal receptors (i.e., LAG3) for its internalization in neurons or (h) it is up-taken via endocytosis, (i) PD-linked A30P and A53T mutant aSyn form large membrane pores through which most cations (i.e., Ca^{2+}) can pass non-selectively, (j) Extracellular aSyn activates the voltage-gated Ca^{2+} channels (VGCCs), resulting in increased Ca^{2+} influx, (k) Monomeric aSyn enters neuronal cells via passive diffusion or direct penetration of their plasma membrane.

On the contrary, natively unfolded monomeric aSyn at the pre-synaptic terminal is prone to form pathological conformations, thus exerting neurotoxic effects [44] (Figure 1). It has been additionally suggested that aSyn is preferably bound to synapsin 1 and VAMP2 when the protein is present in its oligomeric form [45], highlighting the importance of the conformational state of aSyn for its proper function. There are also findings supporting the implication of aSyn in synaptic transmission, due to its association with the synaptic vesicle pool, modulating the vesicle mobility, the recycling pool homeostasis and endocytosis [46–48].

Alpha-synuclein can also function as a molecular chaperone via effective binding to other intracellular proteins. The first indication came with the discovery that aSyn displays structural and functional homology with other molecular chaperones, as the 14-3-3 or small heat shock proteins [49,50]. Additional studies revealed that aSyn synergistically acts with the presynaptic cysteine-string protein-alpha (CSPalpha) promoting the assembly of the SNARE complex [38,51], further validating its chaperoning properties. Biochemical and structural analysis of aSyn strengthened the current indications for its chaperone-like

function via its C-terminal region (residues 61-140) [52–54]. However, following studies indicated that the chaperone-binding site of aSyn lies within the non-amyloidal component (NAC) region (residues 61-95), which is prone to aggregation and thus highly susceptible to form fibrils [55,56].

2.2. Association with Membranes and Lipid Trafficking

Intracellular aSyn can be found either natively unfolded in a soluble state or membrane-bound forming an alpha-helical or a beta-sheet secondary structure, depending on the solution conditions [57–59]. It has been proposed that there is a bidirectional link between aSyn species formation and membrane remodeling, meaning that not only aSyn structure is affected upon lipid interaction, but also that membrane integrity depends on the presence of different aSyn conformations [60–62]. However, there are controversial results regarding the association of aSyn with membrane lipids and its conformational state, with some studies reporting that membrane-bound aSyn gets protected from aggregation, thus leading to neurotoxicity attenuation [44,63,64], whereas others suggest that interaction of aSyn with membranes triggers its self-association and subsequent aggregation [65–67]. Importantly, it has been shown that the PD-related aSyn mutations reduce its interaction with membranes, thus further suggesting that aSyn binding on membranes may exert neuroprotective effects [68–72].

A plethora of studies argue that aSyn in its soluble state exists as a monomer [73–76], whereas others suggest that it occurs physiologically as a tetramer resisting aggregation [77–79]. In the presence of lipid membranes, aSyn adopts an alpha helical structure in the N-terminus region that stabilizes the formation of high-order aSyn multimers [42,73,80,81]. Interestingly, the membrane curvature seems to affect the structure of aSyn, which can adopt either an elongated or a broken alpha-helix conformation, when bound to a large diameter (∼100 nm) or a small, highly curved vesicle, respectively [82–85]. It has been also proposed that aSyn has a role in lipid metabolism, since it participates in fatty acids transportation between the cytosol and membranous compartments [86,87] and in lipid and membrane biogenesis organizing and stabilizing the lipid bilayer of membranes and vesicles [88,89]. On the other hand, disrupted aSyn expression pattern leads to lipid dysregulation, since both the absence and the overexpression of either wild-type (WT) or mutated aSyn gives rise to abnormal lipid metabolism [90–93]. Finally, several studies have demonstrated that aSyn regulates membrane homeostasis via inhibition of phospholipases activity, such as phospholipase D [94–97]; however, there are controversial results in the literature [98].

2.3. Aggregation and Post-Translational Modifications

alpha-Synuclein is composed of three distinct domains: the N-terminal lipid-binding domain, the NAC region and the C-terminal binding domain [84,99,100]. A central role in the fibril formation and subsequent aggregation of aSyn is thought to be mediated through the NAC region of the protein composed of nonpolar side-chains and assembles cross b-structures. Based on that, it has been shown that the deletion of specific residues (74-84) within the core region can abolish aSyn aggregation [101,102]. It has been also demonstrated that the endogenous neuronal aSyn and the interaction of aSyn with lipids plays a central role for aSyn recruitment and subsequent seeding of pathology, as it could behave as a core for the formation of insoluble aggregates [35,75,103,104].

Several mutations in the *Snca* gene have been linked to PD pathogenesis, such as the A53T, A30P, E46K, H50Q, G51D, A18P, pA29S and A53E mutations, all located in the N-terminus region [3,5,7,68,105–107]. Most of them are tightly linked to enhanced aSyn aggregation, pathology progression and clinical manifestations in PD. Specifically, A53T and A30P aSyn mutants are natively unfolded, similarly to WT protein. However, at higher concentrations A53T has been shown to accelerate aSyn fibrillization, a critical event in PD pathogenesis [108–110]. On the other hand, A30P promotes aSyn oligomerization rather than fibrillization, thus reducing aggregate formation [109,111]. The E46K mutation

leads to conformational changes of aSyn due to C-terminal to N-terminal contacts in the monomeric protein, resulting in enhanced aSyn accumulation [111–113]. Moreover, the PD-linked H50Q point mutation increases aSyn aggregation propensity and toxicity [114], whereas the G51D mutation has the opposite effects [115]. However, although G51D mutants seem to oligomerize in a slow rate, they form more toxic fibrils, thus suggesting distinct disease mechanisms for the various aSyn mutations [116,117]. Similarly, A53E mutant seems to lead to neuronal toxicity via an aSyn aggregation-independent manner [118]. Strikingly, the G51D and A53E aSyn mutations have been proposed as potential links between PD and MSA [106,119]. However, up-to-date, no hereditable mutations in the coding region of *SNCA* gene have been identified in MSA cases [120]. Apart from point mutations [117,121,122], various post-translational modifications are implicated in aSyn aggregation, the most important of which are phosphorylation, sumoylation, ubiquitination, nitration, N-acetylation, O-GlcNAcylation and truncation.

The phosphorylation of aSyn both at serine and tyrosine residues and particularly at Ser129 is widely considered as an indicator of pathology. However, the effect of Ser129 phosphorylation on aSyn toxicity is still under debate, with the majority of studies suggesting that it accelerates cell toxicity and neurodegeneration [123–127]. Contrarily, others have proposed a neuroprotective role of Ser129 phosphorylation since it was reported to drive the conversion of toxic oligomers into less harmful aggregates [128–130]. Other mechanisms of phosphorylated Ser129 aSyn-mediated neuroprotection include inhibition of its fibrillation [131], upregulation of tyrosine hydroxylase (TH) activity [132] or lowering of the protein's membrane-binding affinity [133]. Although the 90% of aSyn in LBs is found phosphorylated at Ser129, a significant amount of phosphorylated Ser129 aSyn is also detected in a soluble, rather than in an aggregated state in PD brains [134], whereas only a small percentage of aSyn is phosphorylated at Ser129 in the brains of healthy controls [135–137]. In addition, aSyn can be phosphorylated at Ser87, Tyr125, Tyr133 and Tyr136 residues [138,139] and these are also implicated in either neurotoxic or neuroprotective events [127,138,140,141]. Nonetheless, in most in vivo models where aSyn is overexpressed (virally, transgenic or PFF-inoculations) the detection of pSer129 positive aSyn signal is invariably linked to neurotoxicity, indicating a rather neurotoxic and not a neuroprotective role.

Nitrated aSyn is also tightly linked to neurodegeneration, as demonstrated by experiments in both cellular and animal models, as well as in patient-derived brains [142–145], through its implication in oxidative damage and disease development [146]. Four tyrosine residues in aSyn sequence, Tyr39 (within the N-terminus), Tyr125, Tyr133 and Tyr 136 (within the C-terminus) can undergo nitration. Nitration at Tyr39 has been shown to result in low binding affinity of aSyn on lipid vesicles due to its loss-of-alpha helical conformation status [147], whereas nitration at Tyr125 seems to play a crucial role for aSyn dimerization [148]. Moreover, the linking between two tyrosines is considered as a potential mechanism for aSyn oligomer stabilization and its subsequent aggregation into proteinaceous inclusions [149]. In addition, the detection of nitrated aSyn in the human blood serum could potentially serve as a clinical biomarker for PD diagnosis [150].

Another aSyn post-translational modification crucial for its aggregation propensity is ubiquitination, via regulation of the proteasome-dependent protein degradation [151] and the subcellular localization of the protein [152]. Ubiquitinated aSyn has been isolated from LBs and sarkosyl-insoluble fractions derived from synucleinopathy brains [153,154]. CHIP (C-terminal U-box domain of co-chaperone Hsp70-interacting protein), SIAH (seven in absentia homolog) and Nedd4 (neuronal precursor cell-expressed, developmentally down-regulated gene 4) have been identified among the E3 ubiquitin ligases implicated in aSyn ubiquitination [155–160]. Ubiquitin modification has been demonstrated to have differential effects on aSyn accumulation and subsequent aggregation, dependent on the residue being modified. More precisely, ubiquitination at Lys6, Lys12 and Lys21 residues has been shown to moderately inhibit aSyn fibrillation, whereas at Lys10 and

Lys23 residues has been reported to promote the formation of aSyn inclusions [161]. In addition, ubiquitination at Lys32, Lys34, Lys43 and Lys96 inhibits aSyn aggregation [161].

Sumoylation is a similar process to ubiquitination, since aSyn is conjugated to SUMO (small ubiquitin-like modifier) at lysine residues. SUMO-1 was found in aSyn-positive inclusions of a-synucleinopathy brains or associated with lysosomes of PD animal models [162–164]. It has been also suggested that aSyn sumoylation facilitates its aggregation since it inhibits its degradation [165], whereas other studies proposed a neuroprotective role of aSyn sumoylation, which seems to promote aSyn solubility and thus inhibit its aggregation [166,167]. The discrepancy between these data may be attributed to the different lysine residues available for sumoylation being investigated in each study. Another aSyn modification that has been up for debate is its N-terminal acetylation. Although many studies have assigned a neurotoxic role on aSyn N-acetylation, as it has been shown to promote aSyn β-sheet formation and fibrillation [168–170], others suggest that either N-acetylated aSyn mediates its physiological binding on synaptic vesicles [171], or it acts in a protective manner against aSyn aggregation [172,173].

O-GlcNAcylation is a biochemical process that involves the attachment of O-linked N-acetylglucosamine to Ser and Thr residues of various proteins, amongst which is aSyn. Murine and human aSyn have been shown to be O-GlcNAcyled in many threonine residues including Thr33, Thr34, Thr54, Thr59, Thr64, Thr72, Thr75, Thr81 and Thr87 [174–178] and this post-translational modification has repetitively been linked to reduced aSyn aggregation and attenuation of PD-related toxicity [179–182]. Finally, aSyn truncation has gained scientific attention, given that C-terminally truncated aSyn has been identified in the inclusions present in PD brains [183–185]. Many studies have considered that aSyn truncations have neurotoxic effects due to increased accumulation of misfolded aSyn [186–194].

2.4. Channel Formation/Channel Interactions

As mentioned above, membrane-bound aSyn adopts an alpha-helical conformation, which facilitates its oligomerization and subsequent aggregation. It has been suggested that aSyn oligomers can form transmembrane channels and pore-like structures that have been linked to pathological events during PD development (Figure 1) [195–197]. As a result, vesicles or low-molecular mass molecules may penetrate the cell membrane and in combination with altered cellular ionic homeostasis could potentially lead to cell toxicity and neuronal degeneration [198,199]. Another mechanism for the increased membrane permeability involves the incorporation of aSyn oligomers between the membrane phospholipids, thus leading to the bilayer thinning which thereafter allows the diffusion of small molecules [200].

A wide range of studies has demonstrated that the ion channels formed by oligomeric aSyn dysregulate cellular ion concentrations and may represent a critical event in the pathogenesis of a-synucleinopathies [198]. Some PD-linked aSyn mutations, such as E46K and A53T, have been shown to be implicated in the channel formation, whereas other aSyn mutants (i.e., A30P) have displayed low membrane affinity [197,201]. However, other groups have shown that A30P and A53T aSyn mutations are responsible for the formation of large membrane pores through which most cations can pass non-selectively [202]. It has been reported that the formation of such cation-permeable pores could lead either to ion conductivity or to increased Ca^{2+} influx and subsequent cell death [202–205]. Upon aSyn cation channel opening, other channels, such as the ATP-dependent potassium channels K (ATP), have been reported to be activated in hippocampal neurons and this could probably diminish the aSyn-dependent neuronal excitability [205].

Binding of aSyn to the plasma membrane results in the formation of aggregates and this aggregation leads to the redistribution of the α3 subunit of Na^+/K^+-ATPase. As a result, Na^+/K^+-ATPase is no longer able to effectively pump out Na^+ from neurons, thus leading to an intracellular Na^+ accumulation [206]. Furthermore, extracellular aSyn was reported to activate the voltage-gated Ca^{2+} channel Cav2.2 in rat neurons, due to disorga-

nization of lipid rafts in the plasma membrane, resulting in enhanced dopamine release and increased Ca^{2+} influx [207]. Both events may explain the synaptic dysfunction and neuronal vulnerability in PD. L-type Ca^{2+} channels are also implicated in PD development, as administration of L-type Ca^{2+} channel blockers (i.e., isradipine, nimodipine) in animal models and PD patients, reduced death risk and ameliorated disease manifestations [208–211]. Finally, aSyn oligomers can inhibit α4β2 nicotinic acetylcholine receptors of dopaminergic neurons, thus leading to cholinergic signaling deficits [212]. In summary, aSyn seems to regulate neuronal toxicity and survival via the formation of channels or pores in the plasma membrane or via its interaction with other channels or receptors crucial for the proper neuronal activity (Figure 1).

2.5. Dopamine Metabolism

Soluble aSyn has been proposed to interact with the dopamine transporter (DAT) and decrease its amount on the plasma membrane, thus regulating the dopamine re-uptake from the synapse and protect neuronal cells from excessive dopamine toxicity [213,214]. Contrariwise, aSyn aggregation triggers DAT recruitment to the plasma membrane that results in massive entry of dopamine and production of reactive oxygen species (ROS) in neurons [215]. It is obvious that aSyn-mediated modulation of DAT activity is crucial for neuronal functioning via a balanced dopaminergic neurotransmission. Moreover, the regulation of dopamine storage is provided by an interaction of aSyn with the vesicular monoamine transporter 2 (VMAT2), which is responsible for the packaging of monoamine transmitters into synaptic vesicles [216]. It has been reported that increased levels of aSyn lead to VMAT2 inhibition and dopamine dysregulation that results in pathological events [217]. In addition, aSyn regulates dopamine biosynthesis, via reducing the activity or the phosphorylation status of TH, the rate-limiting enzyme in catecholamine synthesis [218–223]. In agreement, enhanced expression or phosphorylation and subsequent aggregation of aSyn alter TH activity and evoke an imbalance in dopamine synthesis, thus leading to neurotoxicity [132,224–226]. In vivo evidence further support the role of aSyn in dopamine metabolism, since the absence of aSyn caused decreased reuptake of dopamine, low levels of TH and DAT in the mouse striatum and reduced number of dopaminergic cells in the substantia nigra of aSyn KO mice [227–229].

2.6. Interaction with Mitochondria and ER

alpha-Synuclein displays a remarkable conformational flexibility upon macromolecular interactions and can associate with mitochondrial membranes, thus altering mitochondrial function [230–232] (Figure 2). There are reports suggesting that aSyn is a physiological regulator of mitochondrial activity [233–235], whereas others support the opposite [236–238]. Such discrepancies could be attributed to the different synuclein models utilized in each study, taking into account that brain homeostasis is a complex process and in vivo studies recapitulate better the interplay between the various brain components, compared to the isolated in vitro cellular setup. A bidirectional interaction between aSyn aggregation and mitochondrial dysfunction has been implicated in PD pathogenesis. In particular, increased levels of aSyn can lead to mitochondrial dysfunction [239–244], whereas, conversely, impairment of mitochondrial activity may accelerate aSyn pathology [245–248]; however, the precise underlying mechanisms remain to be elucidated. Both WT and mutant aSyn have been shown to interact with mitochondrial elements, altering both mitochondria morphology and function. Specifically, soluble pre-fibrillar aSyn oligomers seem to be responsible for complex I dysfunction, loss of membrane potential, disrupted Ca^{2+} homeostasis, enhanced cytochrome c release and ROS production, thus leading to neuronal demise [240,249–252].

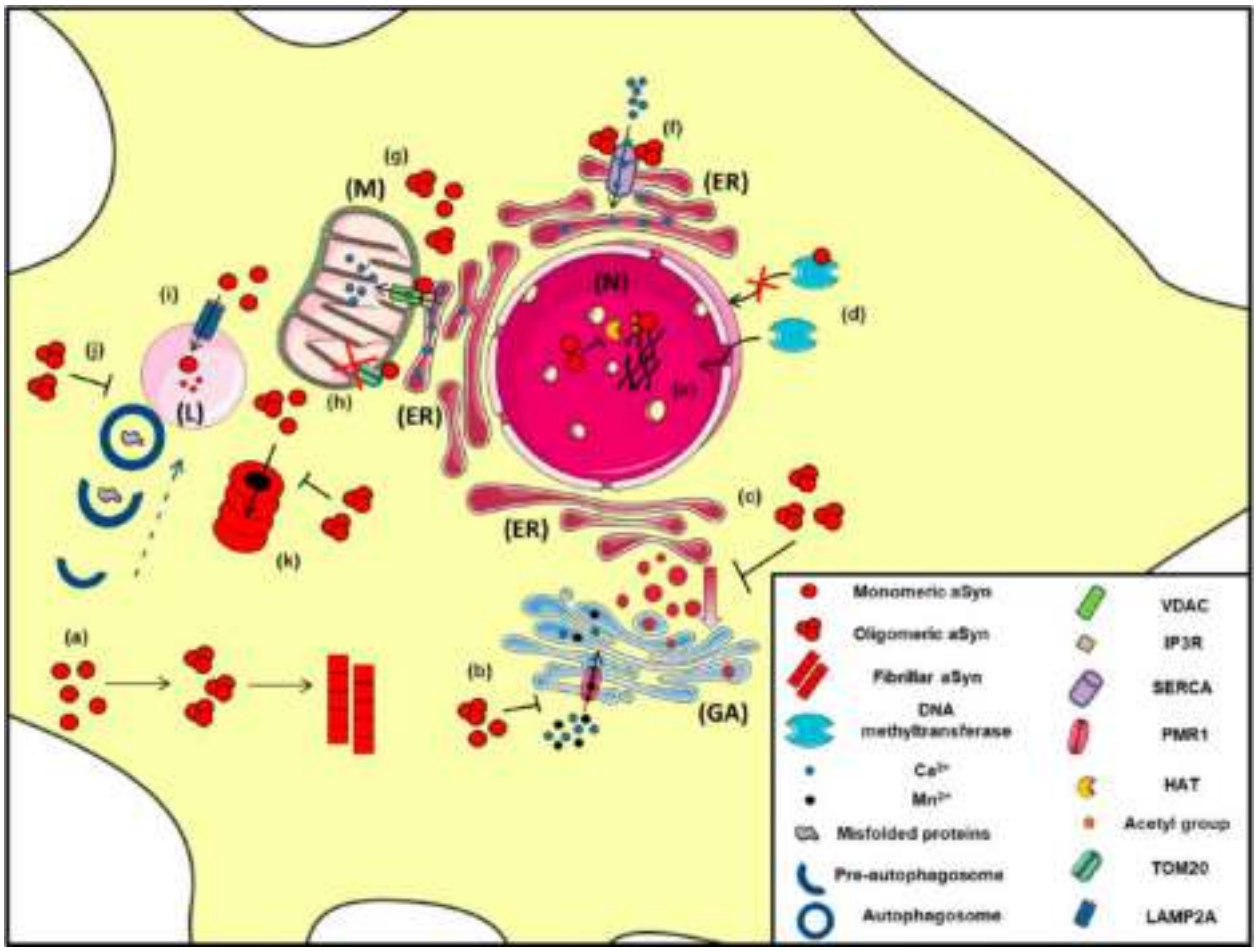

Figure 2. The proposed intracellular effects of various aSyn conformations in neurons. A schematic representation of the aberrant interactions between the various aSyn species with intracellular organelles: (a) In the cytoplasm of neurons, aSyn monomers form oligomers that can eventually become fibrils, (b) Both unfolded and aggregated aSyn impair the function of PMR1, a Ca^{2+}-transporting ATPase pump that regulates Ca^{2+} and Mn^{+2} levels in the Golgi apparatus (GA), resulting in elevated cytosolic Ca^{2+} levels, (c) Both WT and mutant A53T aSyn disrupt the vesicular transport from Endoplasmic Reticulum (ER) to Golgi (GA), (d) WT aSyn inhibits the transportation of methyltransferases from the cytoplasm to the nucleus (N), thus altering DNA methylation of the *SNCA* gene, (e) Inside the nucleus (N), aSyn inhibits histone acetylation via its direct binding to histones or by preventing the action of histone acetyltransferase (HAT) enzymes, thus interfering in the process of gene transcription, (f) In the ER, aSyn aggregates activate the Ca^{2+}-ATPase SERCA, resulting in dysregulated Ca^{2+} homeostasis, (g) Both monomeric and oligomeric aSyn interact with Voltage-dependent anion channel 1 (VDAC1) and inositol triphosphate receptors (IP3Rs), the protein components involved in mitochondrial-associated ER membrane (MAM) and regulates the transmission of Ca^{2+} signals from the ER to mitochondria (M), (h) aSyn binds to TOM20, a mitochondrial import receptor subunit and inhibits normal protein import, (i) Normally, monomeric or dimeric forms of aSyn are degraded in the lysosome (L) via Chaperone Mediated Autophagy (CMA), following their interaction with LAMP2A. However, under pathological conditions, impairment of CMA has been proposed to lead to aSyn accumulation and subsequent cell toxicity, (j) Oligomeric aSyn and various misfolded proteins are cleared via macroautophagy, following the fusion of autophagosomes with the lysosome. Pathological aSyn has been shown to inhibit autophagosome maturation or their fusion with lysosomes, thus impairing autophagic flux, (k) Monomeric and oligomeric aSyn are degraded via the proteasome; however, under pathological conditions, increased levels of aSyn or even soluble aSyn oligomers may inhibit proteasomal function, leading to aSyn accumulation and the formation of insoluble aggregates.

Experiments in various animal models of a-synucleinopathy have revealed mitochondrial abnormalities, DNA damage and neuronal degeneration in PD-affected brain regions [244,253,254]. Moreover, in vitro and in vivo experiments have shown that aSyn inhibits mitochondrial fusion and triggers mitochondrial fragmentation [231,255]. Di Maio and colleagues have proposed that certain post-translationally modified aSyn conformations (soluble oligomers, dopamine-modified and S129E phosphorylation mimic) lead to impaired mitochondrial function via binding to TOM20 (translocase of the outer membrane receptor) and inhibiting mitochondrial protein import [239].

Nonetheless, there is evidence suggesting an impairment of mitochondrial function upstream of aSyn pathology. Experiments using the pesticides rotenone and paraquat have shown that dysregulation of mitochondrial function leads to nigrostriatal dopaminergic loss and formation of LB-like inclusions, positively stained with anti-aSyn antibodies and thioflavine S, thus resembling PD features [246,247,256–258]. Similarly, incubation of WT aSyn-overexpressing COS-7 cells with mitochondrial inhibitors resulted in the disappearance of the aSyn aggregates formed upon rotenone or oligomycin treatment [259]. A plethora of studies that utilize the mitochondrial neurotoxin MPTP to induce PD-like pathology in animals, further suggest that mitochondria impairment is a key player in disease development [245,248,260–264]. Genetic studies further support the hypothesis of aSyn accumulation as a secondary event following mitochondrial malfunction. Specifically, mutations in ATP13A2 (ATPase cation transporting 13A2), encoding for the lysosomal type 5 P-type ATPase, were shown to result in dysregulation in mitochondrial depolarization and ATP metabolism leading to mitochondrial fragmentation and subsequent cell death [265,266].

Apart from its implication in mitochondrial failure, aSyn has been also reported to play a biological role in the association of mitochondria with the endoplasmic reticulum (ER) Ca^{2+} homeostasis. It has been demonstrated that aSyn favors the Ca^{2+} transfer from ER to mitochondria, as a result of the communication the two organelles, probably due to the fact that aSyn can act as a "bridge" via its C terminus [267]. Later studies further supported the physiological localization of aSyn in mitochondria-associated ER membranes (MAM), stabilizing their interaction, which was perturbed upon aSyn aggregation and its subsequent redistribution [268,269]. Interestingly, the familial PD-linked A53T and A30P aSyn point mutations resulted in their weakened interaction with MAM, which affected MAM function and mitochondrial integrity [269].

The association of aSyn with mitochondria was further corroborated by findings indicating interactions between both monomeric and oligomeric aSyn with the Ca^{2+} transporting voltage-dependent anion channel 1 (VDAC1) [270–273]. Importantly, VDAC1 has been detected on the MAM of ER mediating the communication between the two organelles, regulating Ca^{2+} homeostasis [274–276]. Moreover, VDAC levels have been found decreased in nigral neurons of PD brains, where pathological aSyn inclusions had been formed [277]. Additionally, VDAC has been proposed to be a component of the mitochondrial permeability transition pore, the opening of which has been shown to be affected by aSyn overexpression and oligomerization [230,278]. In vivo experiments on transgenic mice overexpressing the human A53T aSyn further supported the role of permeability transition pore activity modulation on the mitochondrial dysfunction during PD pathogenesis [279].

2.7. Unfolded Protein Response, Regulation of ER/Golgi Trafficking and Ca^{2+} Homeostasis

The ER is a continuous membrane system mainly responsible for the production and processing of lipids and proteins, as well as Ca^{2+} homeostasis. In case of impaired protein folding (ER stress), cells activate a group of signal transduction pathways, known as the unfolded protein response (UPR). It has been previously shown that aSyn overexpression in PD patients leads to UPR and contributes to the molecular pathogenesis of the disease [280]. The ER chaperone glucose regulated protein 78 (GRP78/BIP) has a crucial role on ER stress regulation due to its ability to control the activation of transmembrane ER stress sensors

(IRE1, PERK and ATF6) [281]. Disassociation of GRP78 from IRE1 and PERK results in stress signaling, finally leading to altered ER homeostasis [282]. aSyn associates with GRP78/BIP under physiological or pathological conditions, thus inducing UPR and leading to dopaminergic cell death [45,283]. Strikingly, Ser129 phosphorylated and aggregated aSyn was found in ER microsomes of A53T transgenic mice and more importantly, administration of the UPR inhibitor salubrinal, effectively attenuated disease manifestations in this PD-mouse model [284,285]. It is worth mentioning that GRP78/BiP levels were found elevated in DLB and PD brains in an aSyn burden-dependent manner [286]. In addition, the protein levels of various ER chaperones were found elevated in a-synucleinopathy models, co-localized with aSyn positive inclusions, suggesting that aggregated aSyn could potentially be implicated in UPR regulation in disease progression [284,287–293].

Proteins synthesized in the ER, are packaged into vesicles and directed to Golgi apparatus for subsequent modifications. One of the first pathological roles attributed to aSyn is the blockade of the vesicular transport from ER to Golgi by antagonizing ER/Golgi SNAREs [294–296]. Towards the same direction, aSyn can also disrupt the intra-Golgi and post-Golgi secretory trafficking, via an abnormal interaction with several Rab-family proteins of the intracellular endocytic pathway [294,296–299]. Additionally, aSyn can also impair the ionic transport and membrane trafficking, resulting in Golgi fragmentation and subsequent cytotoxicity [300–302].

Another significant role of aSyn on ER and Golgi function is the regulation of Ca^{2+} homeostasis via its binding on specific channels or pumps localized in these organelles (Figure 2). Specifically, proximity ligation assay experiments demonstrated that soluble and insoluble aSyn aggregates, but not monomers, interact with the ER Ca^{2+}-ATPase SERCA, resulting in decreased cytosolic Ca^{2+} that disrupts the physiological cell function and leads to neuronal cell death [303]. Moreover, administration of the SERCA inhibitor cyclopiazonic acid restored cytosolic Ca^{2+} levels and protected neurons against the aggregated aSyn-dependent cell death [303]. In support to these results, aggregated aSyn bound on SERCA pump was detected in LBs and GCIs of PD and MSA brains, respectively [303]. Furthermore, PMR1, a Ca^{2+}-transporting ATPase 1 pump regulating the levels of Ca^{2+} and Mn^{+2} ions in the Golgi [304], has been proposed to be a mediator of aSyn-dependent cytotoxicity. Specifically, in various PD models (yeast, flies and nematodes), PMR1 pump has been linked to aSyn pathology via a Ca^{2+}-dependent mechanism, where aSyn accumulation elevated cytosolic Ca^{2+} levels and increased cell death. Interestingly, upon PMR1 deletion, the disease-associated characteristics were abolished, further suggesting the relevance of this pump to aSyn pathology [305,306].

2.8. a-Synuclein in the Nucleus

The name aSyn was given to the protein due to its localization in the nucleus and presynaptic nerve terminals [37]. Nuclear aSyn was detected in neurons of various brain regions of rodents and was reported to interact with histones, underlying PD pathology [307–309], even though a single study declares that the nuclear staining of aSyn is attributed to the non-specific signal of some antibodies that probably recognize unknown antigens in neuronal nuclei [310]. It has been proposed that aSyn is responsible for epigenetic dysregulation via inhibition of histone acetylation or reduced DNA methylation, thus favoring neuronal degeneration, whereas others suggest that nuclear aSyn regulates cell cycle rate exhibiting cell toxicity [311–313]. Importantly, histone deacetylase (HDAC) inhibitors attenuated aSyn toxicity and provided neuroprotection in both cell culture and transgenic Drosophila models [311,314].

Experiments in SH-SY5Y cells revealed that nuclear translocation of aSyn is regulated by calreticulin and Ca^{2+}, following treatment with retinoic acid and modulates the expression of PD-linked genes such as ATP13A2 and PINK1 (PTEN-induced kinase1) [315]. Interestingly, phosphorylated aSyn at Ser129 was found accumulated in the nucleus of HEK293E-aSyn overexpressing cells and in various brain regions of transgenic (Thy1)-[A30P] aSyn mice [316]. Further experiments in H4 cells expressing various aSyn proteins

verified that nuclear localization of aSyn depends on its phosphorylation at Ser129 [317]. The same group supported a role of DNA-binding and gene expression regulation for aSyn providing an insight into the role of modified aSyn in the nucleus [317]. Furthermore, other post-translational modifications of aSyn, such as sumoylation, seem to be responsible for the translocation of aSyn from the cytoplasm to the nucleus [318]. Although the majority of studies support a neurotoxic role for aSyn nuclear localization, some groups proposed that aSyn in the nucleus displays a protective role against DNA damage, replication stress or impaired nucleo-cytoplasmic transport [319–321]. However, the numerous in vitro and in vivo studies demonstrating a neurotoxic role of nuclear aSyn, in contradiction to the limited number of studies supporting a protective role originated mostly from cell lines or yeast, favors the pathological potential of nuclear aSyn.

2.9. Alpha-Synuclein and Protein Degradation Pathways: An Intricate Interplay

A great wealth of data focuses on the complicated relationship between aSyn clearance and protein degradation pathways (Figure 2). Both the ubiquitin-proteasome system (UPS) and the autophagy lysosome pathway (ALP) are responsible for aSyn degradation in a manner that depends on cell type, tissue and aSyn conformation state [322–324]. Specifically, there are studies demonstrating that aSyn can be degraded by the 26S/20S proteasome via ubiquitin-dependent [325,326] and ubiquitin-independent manner [327,328]. Studies in PC12, HEK293 and primary mesencephalic cells suggested that pharmacological inhibition of the proteasome does not lead to aSyn accumulation [324,329,330]; however, others have shown that soluble aSyn oligomers, but not monomers, are partially cleared via the 26S proteasome [331]. Importantly, it has been proposed that the UPS is responsible for aSyn removal under normal conditions, while in pathological cases the ALP is recruited to clear the increased aSyn burden [332].

Chaperone-mediated autophagy (CMA) is also responsible for the degradation of monomeric or dimeric forms of the protein via the lysosome-associated membrane protein type 2A (LAMP2A), whereas oligomeric aSyn is cleared mainly via macroautophagy [324,333,334]. Lee and colleagues also suggested that the lysosome is responsible for the removal of oligomeric but not fibrillar aSyn and that lysosomal failure results in aSyn accumulation and aggregation and subsequent cell death [335]. Moreover, initial in vivo evidence suggested that increased aSyn protein levels evoked by paraquat treatment were preferably degraded via CMA in dopaminergic neurons, where the levels of LAMP2A and the lysosomal heat shock cognate protein of 70 kDa (HSC70), both essential CMA-components, were found elevated [336]. We have also shown that boosting CMA function via LAMP2A overexpression in cell lines and primary neuronal cultures and in the rat dopaminergic system mitigated aSyn protein levels and related toxicity [337]. Similar neuroprotective effects were obtained upon LAMP2A overexpression in the Drosophila brain [338]. On the contrary, we have also shown that LAMP2A silencing led to endogenous aSyn accumulation in vitro [324] and in vivo [339] and in extensive neurodegeneration of the rat nigrostriatal axis [339]. Decreased levels of LAMP2A and HSC70 were reported in the human substantia nigra and amygdala of PD brains [340], whereas, in a subsequent study, LAMP2A was found to be selectively reduced in association with increased aSyn levels, even in the early stages of PD, thus suggesting a potential dysregulation of CMA-mediated protein degradation prior to substantial aSyn aggregation in PD [341].

However, a bidirectional link between aSyn accumulation and the protein degradation machineries exists and extensive studies have been conducted to elucidate not only the manner of aberrant aSyn degradation in a-synucleinopathies, but also the impact of various aSyn conformations on UPS and ALP function. It has been proposed that overexpression of A30P and A53T mutants, contrarily to WT aSyn, leads to cell death due to proteasomal inhibition [342]. Indeed, overexpression of mutant A53T aSyn resulted in UPS failure by inhibiting the activity of the 20S/26S proteasome, finally leading to aSyn pathological accumulation [343]. Other groups have failed to detect alterations in the proteasomal function of PC12 cells or transgenic mice, following overexpression of WT or mutant (A30P,

A53T) aSyn [344]. Moreover, later studies demonstrated that transient overexpression of WT or mutant aSyn, followed by addition of recombinant aSyn oligomers and fibrils in an osteosarcoma cell line, did not result in any disturbance of the proteasomal function [345]. Importantly, studies in human post-mortem PD brains also suggested impaired proteasomal function in the substantia nigra [346–348], further supporting a role of UPS malfunction in PD pathogenesis. In addition, total rates of protein degradation declines with aging, thus contributing to the pathogenesis of age-related diseases [349]. Even though human post-mortem studies provide valuable information in regards to etiology and/or disease pathogenesis, the data obtained should be treated with caution, given into account the overall decline in the function of multiple systems with aging. For a-synucleinopathies, we believe that the use of tissue from affected and non-affected (in regards to aSyn pathology and neuronal death) brain areas may provide useful information regarding early or late events leading to neurodegeneration.

Increased aSyn protein burden is reported to impair macroautophagy function as well, via its interaction with Rab1a, an event that subsequently results in the autophagosome-formation-related protein Atg9 mislocalization [350]. Similar results were obtained from cells expressing the PD-linked mutation of the retromer protein VPS35, which is involved in autophagy and is implicated in PD pathogenesis [351]. The three most well studied PD-linked aSyn mutations, E46K, A30P and A53T, have been shown to promote ALP dysfunction, via either impairing autophagosome formation or inhibiting the selective removal of damaged mitochondria through mitophagy [352–354]. It has been previously reported that dopamine-modified aSyn inhibits CMA and this could probably shed light into the selective vulnerability of dopaminergic neurons in PD [355]. Further experiments in human iPSC-derived midbrain dopaminergic neurons revealed that disrupted hydrolase trafficking, due to aSyn overexpression, reduces lysosomal function [356]. Similarly, multiple studies suggest that there is a strong relationship between decreased β-glucocerebrosidase (GCase) activity and aSyn accumulation. In particular, heterozygote mutations in *GBA1* gene encoding for β-glucocerebrosidase represent a major risk factor for PD development with a-synucleinopathy [357–362].

2.10. Alpha-Synuclein in the Extracellular Space

The first indication that aSyn can be secreted arose from the detection of the protein in human CSF and plasma of PD patients, indicating that aSyn can be released into the extracellular space [363,364] and can exert various deleterious effects on neighboring cells. Further studies supported that aSyn can be secreted from neuronal cells, either via vesicles or exosomes [365–367]. Extracellular aSyn has been the subject of intensive research in recent years, mainly due to its propensity to spread from neuron to neuron or other glial cells, as discussed in the following sections.

The major hypothesis regarding the onset and spread of aSyn pathology in a-synucleinopathies relies in the protein's nucleation propensity that leads to the formation of aberrant aSyn species, which then spread to neighboring cells and tissues via various mechanisms. Furthermore, aSyn has been proposed to act as a "prion-like" protein since it was demonstrated that pathogenic aSyn could transfer from diseased neurons of a PD patient to the healthy transplanted ones, fourteen years after the surgical intervention [368]. Similar results were obtained by other groups in both humans and rats [369–372]. Experiments of PD and DLB patient-derived brain extracts delivered into the brain of mice and non-human primates further validated the transfer of pathological aSyn and the formation of aSyn aggregates within the recipient neurons [373,374]. Moreover, when Pre-Formed Fibrils (PFFs) were used as seeds in both in vitro and in vivo experiments, the endogenous neuronal aSyn was recruited into the formation of highly insoluble aggregates [104,375–379].

Various mechanisms have been proposed for aSyn spread throughout the nervous system, following its release from neurons where the protein is normally expressed. Candidate mechanisms include aSyn secretion via vesicles, exosomes or even naked protein [364–366,380–383] and its uptake from the cells via conventional endocytosis [384,385], passive diffusion [386], tunneling nanotubes [387], membrane penetration [195,388,389] or receptor-mediated internalization [206,390,391]. Once taken-up by recipient cells, the exogenous aSyn has been shown to trigger the endogenous aSyn accumulation via an unknown mechanism [392–395]. However, according to the prevailing hypothesis, upon the cell-internalization of aberrant aSyn conformations (oligomers or fibrils), these serve as a template for the recruitment of the endogenous monomeric aSyn into the formation of insoluble aggregates [373,375–377,396–398]. The prevalently unfolded or alpha-helical aSyn is triggered to self-assemble generating fibrils that subsequently deposit as Lewy bodies [399–401].

Neuron-to-neuron aSyn transmission occurs following both anterograde and retrograde axonal transport or trans-synaptic pathways [402–404]. Several groups have proposed that dysregulation of axonal transport is implicated in aSyn accumulation at the cell body; however, it is not clear whether PD-linked aSyn mutations play a key role in the process per se [403,405–407]. Notably, aSyn in its oligomeric form has been shown to interfere with microtubules and kinesin motors, thus disrupting the anterograde transport and similar results were obtained in an aSyn overexpressing mouse model for PD, as well as in patients diagnosed with the disease [408–410]. Additionally, it has been suggested that the variety in a-synucleinopathy phenotypes is attributed to the formation of different aSyn "strains" that display "aggressive" characteristics [17,18,411]. As a consequence of their disparate structures, these "strains" have discrete biochemical responses along the different brain regions and cell types, thus explaining the various disease manifestations of a-synucleinopathies [19,20,125,412–414].

3. Glia in the CNS: Scavengers of Extracellular aSyn

3.1. Role in Microglia Function and Dysfunction

Microglial cells are the resident phagocytes of the brain, guarding the CNS homeostasis and performing essential role in health and disease. Specifically, apart from exhibiting immunoreactivity as a response to any changes or inflammatory stimulus, they are responsible for the monitoring and pruning of neuronal synapses [415–419]. Disturbance or loss of brain homeostasis "activates" microglial cells, a term used to describe the changes in their shape, gene expression profile and function during their response [420–423]. A well-regulated immune surveillance of the brain is essential for the proper CNS functioning; however, an excessive and continuous inflammatory response could potentially lead to cellular and tissue damage, tightly linked to the development of various neurodegenerative diseases [424–428]. Enhanced production of pro-inflammatory cytokines, reactive oxygen species (ROS, NO, superoxide) and glutamate has been shown to lead to dopaminergic cell death in PD [429–431].

Indeed, in the diseased brain, microglial cells get activated in two states, M1 and M2, depending on the cytokine signaling pathway involved. The classical pro-inflammatory TNF/IFNγ-mediated activation leads to M1 state, whereas the M2 state is subdivided into the M2a "alternative activation" and the M2c "acquired deactivation" states, acquired following the involvement of anti-inflammatory cytokines IL-4 and IL-13 (for M2a) or IL-10 and TGF-β (for M2c) [432]. It has been proposed that in PD a shift from M2 to M1 phenotype is responsible for disease progression; therefore, the scientific interest has been focused on immunomodulatory therapies promoting the neuroprotective M2 type [433].

3.1.1. Physiological Role of aSyn in Microglia Function

Although aSyn has been primarily characterized as a pre-synaptic neuronal protein, several studies have proposed a physiological role of aSyn in microglial function. Microglial cells from mice lacking aSyn (aSyn -/-) displayed reduced phagocytic activity and

enhanced secretion of pro-inflammatory cytokines, thus suggesting that aSyn modulates the activation phenotype of the brain immune cells and contributes to the clearance of debris present in the local brain microenvironment [434,435]. On the other hand, transient overexpression of WT, A53T or A30P aSyn in BV2 microglial cells led to a distinct pro-inflammatory cytokine profile in combination with impaired phagocytic activity [436]. Additionally, microglia isolated from BAC transgenic mice overexpressing aSyn, exhibited dysregulation of cytokine release and phagocytosis [437]. Data obtained from iPSC-derived macrophages from PD patients harboring the A53T aSyn mutation and aSyn triplication mutations further support the implication of aSyn in the phagocytic capability of these cells [438]. Expression of aSyn in microglia has been also proposed to promote cell migration via the enhanced expression of the cell-surface glycoprotein CD44 and the matrix metalloproteinase membrane-type 1 (MMP-MT1) [439]. However, the presence of various aSyn species in the environment of microglial cells alters their physiology and behavior leading to neuroinflammation and neurodegeneration.

3.1.2. Microgliosis in a-Synucleinopathies

Microgliosis is the reaction of CNS microglial cells to pathogenic insults and their shift from a resting to the active state [440]. Since the first study demonstrating microgliosis in PD brains [25], a plethora of reports highlights an important role of activated microglia in disease pathogenesis in both humans and animal models (reviewed in [441–445]). Microglial activation has been observed in PD brains by in vivo positron emission tomography (PET) imaging studies [446–448], suggesting that microgliosis is an early event that perpetuates during the disease progression. Additional studies have further supported the hypothesis of an early activation of microglia tightly associated to aSyn pathology, in various PD models [192,449–454]. However, other reports suggested that microglia respond differently in the various disease stages, in a manner that depends on the affected brain region and the protein burden of aSyn, indicating the existence of immunological diversity among microglia in the diseased brain [449,450,455].

It has been proposed that the neuron-microglia interaction may contribute to the neuroinflammation that characterizes PD, where neurons expressing aSyn activate microglia, which in turn secrete inflammatory factors surrounding the diseased neurons, thus forming a vicious cycle [456] (Figure 3). Likewise, microgliosis has been also reported in MSA, where aSyn is found aggregated mainly within oligodendrocytes [426,457–459]. This hypothesis for neuron-microglia communication in synucleinopathies is further supported by findings demonstrating an altered expression profile of various cytokines in the brains of PD patients [460]. Moreover, microglial activation has been shown to induce aSyn-mediated neuronal cell death, in both in vitro and in vivo PD models [461–463]. In addition, microglial cells exposed either to cytokines or to PD-derived CSF, displayed alterations in the intracellular aSyn protein levels, suggesting a crucial role of the brain microenvironment for aSyn accumulation in microglia [464,465]. Activated microglia have been also detected in various transgenic animal models overexpressing wild type of mutated aSyn specifically in neurons [192,452–454,466,467]. Experimental PD animal models including the use of the MPTP mouse model or nigral injections of recombinant aSyn fibrils or AAVs overexpressing aSyn are characterized by neuroinflammation followed by a significant degeneration of dopaminergic neurons [449,450,468–470]. Similarly, further results obtained from the rAAV-driven overexpression of aSyn in the mouse substantia nigra show extensive aSyn-mediated microgliosis primarily in the nigrostriatal axis, accompanied by an increase in the production of pro-inflammatory cytokines [410,471,472].

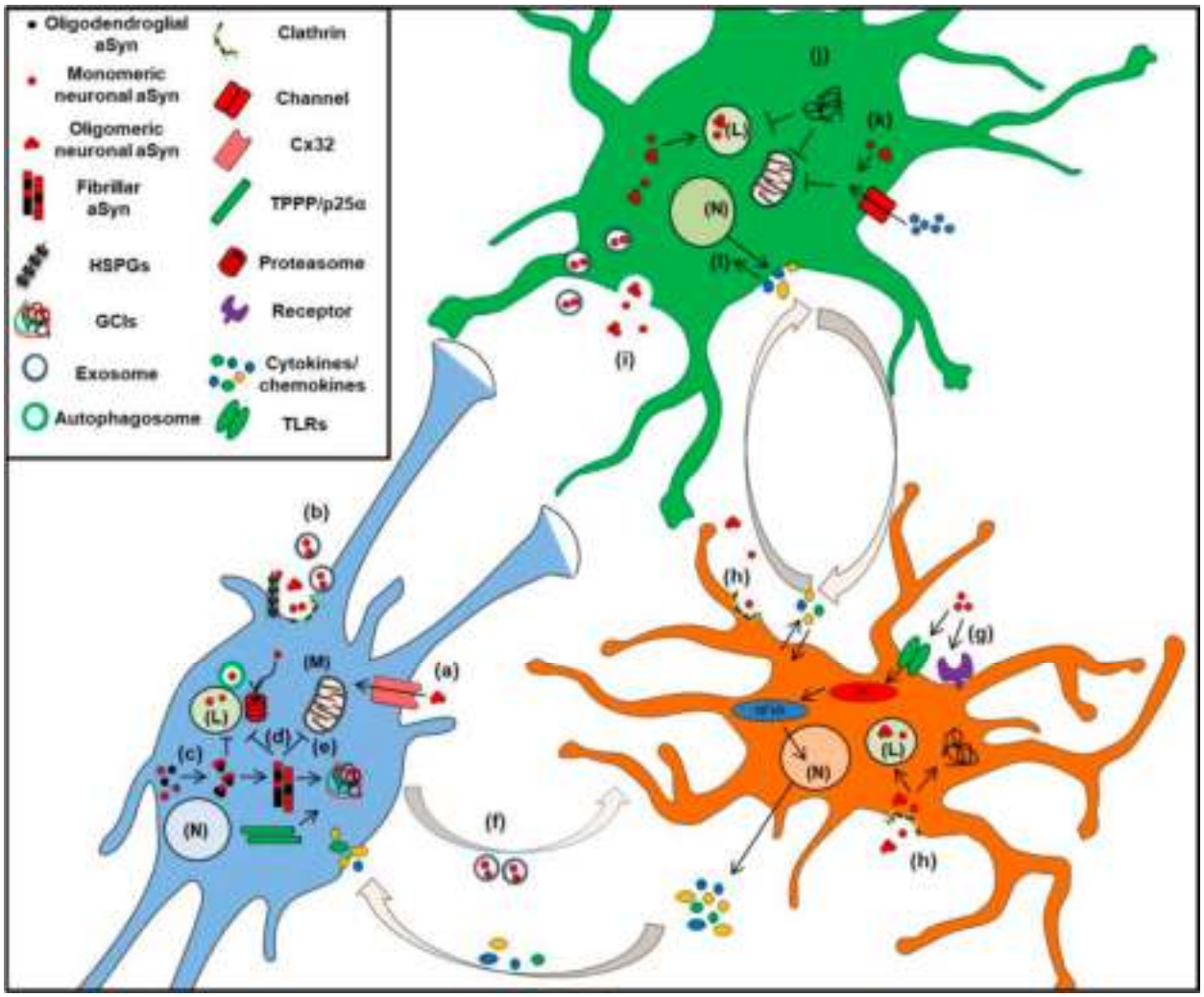

Figure 3. A complicated neuron-glial interrelationship. (a) Oligomeric aSyn enters oligodendrocytes (blue) via binding to the gap junction protein connexin-32 (Cx32), (b) Neuronally-derived aSyn enters oligodendrocytes via clathrin-mediated endocytosis, exosomal transportation, or via binding to Heparan Sulfate ProteoGlycans (HSPGs), (c) Inside oligodendrocytes, neuronal aSyn (red) initiates the seeding of the endogenous oligodendroglial aSyn (black) and together with the oligodendroglial-specific TPPP/p25α protein, they lead to the formation of GCIs, (d) aSyn aggregates impair the proteolytic machineries of oligodendrocytes [(proteasome and lysosome (L)], (e) Misfolded aSyn leads to mitochondrial (M) dysfunction and subsequent cell toxicity in MSA, (f) Oligodendroglial-derived exosomes containing aSyn have been shown to transfer to microglial cells (orange), (g) Extracellular aSyn stimulates TLRs and other receptors (i.e., FcγR, P2X7 etc) to activate microglial transcription factors, such as NFkB, for the production of various pro-inflammatory cytokines (IL1β, TNFa) and chemokines that induce astrocyte (green) reactivity and oligodendroglial damage, (h) Neuronally-secreted aSyn is taken up by microglial cells via clathrin-mediated endocytosis and is then driven to the lysosome (L) for degradation. In pathological conditions, though, it accumulates into aSyn insoluble aggregates, (i) Free or exosome-associated aSyn released by neurons is transmitted to astrocytes via endocytosis and enters the lysosome (L) for its clearance, (j) In disease, aSyn aggregates are formed that lead to lysosomal (L) impairment and mitochondria (M) dysfunction, (k) In astrocytes, aSyn triggers the opening of channels (i.e., Cx43 and Panx1), leading to dysregulation in Ca^{2+} homeostasis and altered mitochondrial morphology, (l) Microglia-secreted cytokines and chemokines activate astrocytes to further produce pro-inflammatory signaling molecules and enhance neurotoxicity.

3.1.3. Activation of Microglia and Clearance of Toxic aSyn Species

Numerous in vitro and in vivo studies have demonstrated that either conditioned medium from aSyn overexpressing cells or aSyn per se (i.e., recombinant monomeric, oligomeric or fibrillar aSyn) robustly activate microglia. In particular, treatment of mi-

croglial cells with non-aggregated aSyn was shown to increase phagocytosis and enhance pro-inflammatory cytokines release, NF-kB nuclear translocation and microglial migration [439,468,473–475], whereas addition of fibrillar aSyn in BV2 cells was reported to reduce their phagocytic activity [474]. In agreement, incubation of human microglial cell lines or primary microglial cells with monomeric aSyn triggered the release of various pro-inflammatory factors [476–479]; however, recently, it has been suggested that monomeric, contrarily to oligomeric aSyn, promotes an anti-inflammatory phenotype of microglia [480]. Other groups have found that aggregated aSyn leads to increased TNFa and ROS production, both related to cell toxicity [456,481–483].

Microglial activation may depend on the aggregation state of aSyn and microglial cells readily take-up fibrillar aSyn and produce pro-inflammatory cytokines [484]. Furthermore, incubation of microglial cells with conditioned media from neuronal cells or with CSF from PD patients resulted in significant secretion of TNFa, IL1β and ROS [465,473,478]. Importantly, it has been shown that PD-related aSyn mutants are more prone to activate microglia when compared to WT protein [463,479,485]. Moreover, elevated levels of CXCL12 chemokine in both postmortem PD brain tissue and in nigral microglia of transgenic A53T mice further support the aSyn-mediated neuroinflammation [486]. Contrariwise, aSyn-evoked microgliosis in some instances leads to the enhanced expression and release of neuroprotective factors, such as BDNF, probably in an attempt for neuronal repair and survival [481]. Notably, studies in microglia of mice lacking aSyn expression have verified the critical role of aSyn in modulating microglial activation [434,435].

aSyn has been proposed to enter microglial cells via a clathrin-mediated endocytosis and leads to neurotoxicity in a Prostaglandin E2 receptor subtype 2 (EP2)-dependent manner [470,487]. Integrin CD11b has been proposed as a mediator of aSyn-induced activation of microglial cells [488–490], whereas other membrane receptors implicated in microglial stimulation in the presence of aSyn are the protease activated receptor 1 (PAR-1), the macrophage antigen 1-receptor (Mac-1), the Fcγ receptors (FcγR), the microglial purinergic receptor P2X7 and the scavenger receptor CD36, as well as the adhesion molecule CD44 and some plasma membrane ion channels [439,463,477,478,483,491–493]. Importantly, Toll-like-receptors 2 and 4 (TLR2 and TLR4) are considered crucial modulators of glial responses in a-synucleinopathies, as well as key players in aSyn phagocytosis. These properties have put them in the spotlight as novel therapeutic modulators of neuroinflammation in neurodegenerative diseases [494–502].

The internalization of aSyn by microglia triggers various immune response-related cascades, including NF-kB, Nrf2, MHCII and inflammasome. Numerous studies have reported activation of NF-kB pathway upon addition of various aSyn conformations in both rodent and human microglial cell lines [468,469,476,478,485,503]. The nuclear translocation of NF-kB is a result of aSyn interaction with TLR that leads to the Myd 88-mediated activation of IkB kinases [504]. Moreover, oligomeric aSyn has been shown to trigger TLR2 signaling in microglial cells via NF-kB and p38 MAPK activation, which has been previously linked to aSyn-related toxicity [469,505]. Another key player in both aSyn pathogenesis and the neuroimmune system is LRRK2 (Leucine-rich repeat kinase 2), constitutively expressed in neurons and glial cells, mutations of which have been characterized as common risk factors for PD. Significantly, manipulation of LRRK2 expression levels in mouse microglial cells has revealed its role in regulating aSyn degradation [506,507].

Furthermore, various studies have proposed that aggregated aSyn results in IL-1β production by reactive microglia, which in turn involves nod-like receptor protein 3 (NLRP3) inflammasome activation [508–510]. Interestingly, the inflammasome related caspase-1 activation is responsible for aSyn truncation and its subsequent pathological accumulation [188]. Apart from the activation of microglial pro-inflammatory transcription factors, such as NFkB, pathological aSyn also affects the antioxidant transcription factor Nrf2 [485,511]. Modifications in the expression levels of Nrf2 have confirmed its role in aSyn clearance and neuronal survival [512–514]. Moreover, since microglial cells act as antigen presenting cells in the brain, it has been proposed that upon aSyn internalization

by microglia, the protein is presented to T-cells via MHCII, which then infiltrate in the CNS and finally lead to neuronal degeneration present in PD and MSA [22,515–520].

Apart from modulating the immune responses in the CNS, microglial cells are the brain's phagocyting cells clearing cellular debris or any toxic insult. Amongst the various threats, extracellular aSyn has been shown to be effectively processed by activated microglia, in some cases via a DJ1-mediated autophagy [474,521–524]. Consistent with these results, experiments utilizing primary cells, have demonstrated that aSyn upon its internalization by microglia is targeted to autophagosomes, thus leading to its degradation [493]. TLR4 also seems to play a crucial role in microglial phagocytosis, since TLR4 (-/-) murine microglial cells exhibit impaired aSyn clearance and enhanced neurotoxicity [494,496]. Furthermore, addition of aSyn fibrils in BV2 and primary microglial cells induces autophagy as a rescue mechanism to restore lysosomal damage [525].

Importantly, aging is another key player in the efficient aSyn clearance, since it has been proposed that microglia and monocytes display reduced phagocytic activity with age [526,527]. Regarding the uptake of aSyn by microglia, it has been reported that ganglioside GM1 and lipid rafts, but not clathrin, caveolae and dynamin, mediate monomeric aSyn internalization, whereas aggregated aSyn enters microglia via clathrin- and calnexin-dependent mechanisms [487,528]. Moreover, microglial uptake of neuronally-derived exosome-associated aSyn via macropinocytosis could potentially account for pathological aSyn spreading [529–531]. Strikingly, apart from the immunomodulating role of microglia in the CNS, it has been also suggested that resting microglia regulates the cell-to-cell transfer of aSyn in vivo [532]. Therefore, further considering the aforementioned involvement of exosomes in the transmission of aSyn pathology, targeting exosome-release from various cell types of the brain could be a potential therapeutic target against disease progression.

3.2. Astrocytes in a-Synucleinopathies

Astrocytes, the star-shaped cells of the brain, are the most abundant glial cells of the CNS, accounting for at least one third of the brain mass. They have a supportive role to neurons, by maintaining osmotic, energetic and structural tissue homeostasis. In particular, it is suggested that astrocytes regulate neurotransmitter removal from the extracellular space, synaptic transmission, myelination, brain energy metabolism and pH homeostasis, ion balance, cholesterol synthesis, blood–brain barrier (BBB) permeability, cerebral blood flow and glymphatic system function [533–543]. It has also been suggested that astrocytes modulate neuronal synaptic activity via a Ca^{2+}-dependent release of transmitters that have a feedback action on neurons, a process known as "gliotransmission" [544–546]. There are two main types of astrocytes in the brain: protoplasmic and fibrous [547]. Protoplasmic astrocytes are highly branched and are mainly located in the gray matter, tightly associated with neuronal cell bodies and synapses [548], whereas fibrous astrocytes have straight and long processes and they are widely distributed in the white matter, contacting nodes of Ranvier [549].

Apart from their crucial role in brain homeostasis and health, astrocytes have been also implicated in the cascade of events underlying neurodegenerative diseases. Specifically, astrocytes in PD brains have been reported to migrate and become reactive and have been classified in two categories depending on their neuroprotective or neurotoxic effects: harmful A1 astrocytes and protective A2 astrocytes [24]. Activated microglial cells induce A1-astrocyte reactivity, leading to neuronal and oligodendroglial cell death and subsequent synaptic impairment [24]. They have been also shown to secrete inflammatory cytokines, partially as a response to the increased aSyn protein load, thus contributing to PD progression and neurodegeneration [550], although there are studies reporting a neuroprotective role of astrocytes in a-synucleinopathies, modulating the levels of accumulated aSyn and protecting neurons against oxidative stress [551,552].

3.2.1. Astrocytes in PD: Friend or Foe?

Up to date, there is little evidence regarding the expression levels [553] and the physiological role of aSyn in astrocytes, such as the implication of aSyn in astrocytic fatty acid

metabolism [90]. It is also suggested that cultured human astrocytes express low levels of aSyn and various inflammatory cytokines or cell stress enhance aSyn production [554,555]. Yet, numerous studies have focused on the role of astrocytes in the modulation of aSyn levels and the regulation of immune responses in neurodegeneration. Interestingly, aSyn-positive inclusions have been detected in astrocytes in various regions of PD and DLB brains [13–15,556–561]. According to the prevailing hypothesis, the accumulated aSyn detected in astrocytes origins from the neighboring diseased neurons, which upon its release is subsequently internalized by astrocytes, probably as a mechanism of clearance and neuroprotection [562] (Figure 3). However, the responses of astrocytes in aSyn-related pathogenesis have been characterized as a "double-edged sword", due to the controversial findings regarding their role in neurotoxicity or neuroprotection [563].

The neuron-to-astrocyte aSyn transmission has been extensively studied and is considered as the prime suspect for the detection of aSyn immunoreactivity within astrocytes in a-synucleinopathies. A seminal study utilizing primary astroglial cultures treated with conditioned media from differentiated SH-SY5Y neuronal cells showed that internalization of neuronally-derived aSyn by astrocytes occurs via endocytosis and results in the formation of proteinase-K resistant aSyn inclusions within astrocytes [550]. Similar results were obtained in transgenic mice overexpressing human aSyn under the neuronal promoter PDGFβ, where aSyn-positive inclusion bodies were observed in both neurons and astrocytes [550]. Furthermore, co-culture of primary astrocytes with SH-SY5Y cells verified the formation of LB-like inclusions positive for aSyn staining [564]. The detection of aSyn within the astrocytic endosomal/lysosomal compartment led to the hypothesis that astrocytes normally internalize neuronally-derived aSyn as a neuroprotective mechanism; however, prolonged exposure to pathological aSyn species may lead to impaired glial lysosomal function and, thus, astrocytic aSyn accumulation [550,565]. In agreement, overexpression of PD-linked aSyn mutants (A30P and A53T) in actrocyte cell lines resulted in impaired autophagic function, mitochondrial failure and cellular apoptosis, thus preventing the astrocyte-mediated neuroprotection [566]. In support to a protective role of astrocytes during PD, it has been reported that neurotrophin-immunoreactive (BDNF and NT-3) astrocytes surrounding degenerating nigral neurons in the brains of idiopathic PD patients may indicate a beneficial role of glial cells against neuronal failure [567]. In addition, elevated levels of the glutathione peroxidase-GPx in astrocytes of the substantia nigra of PD patients, further demonstrates their role against neuropathology [568,569]. Strikingly, overexpression of the Nrf2 transcription factor selectively in astrocytes in the haSyn A53T transgenic mouse model provided protection against aSyn-related toxicity by enhancing its degradation via the ALP [513]. In a recently published study, it was suggested that astrocytes internalize aSyn aggregates and effectively degrade them via proteasomal and autophagic pathways, thus protecting dopaminergic neurons against the aberrant effects of toxic aSyn species [570].

In vitro and ex vivo studies proposed that aSyn can efficiently transmit not only from neurons to astrocytes, but also between astrocytes and translocate to the lysosomes of the recipient cells [571]. However, differently from neurons, astrocytes are able to efficiently degrade fibrillar aSyn, suggesting an active role for these cells in clearing aSyn deposits [571]. It is worth-mentioning that the transfer of aSyn from astrocytes to neurons was reported to a lesser extent, even though another study suggested that aSyn deriving from SNCA-flag tagged PD astrocytes was effectively transferred to the co-cultured surrounding control neurons, which then displayed signs of degeneration [572]. Strikingly, iPSC-derived astrocytes from PD neurons displayed impaired CMA and macroautophagy, which could potentially account for the observed aSyn accumulation, highlighting the implication of astroglial-mediated proteolysis in the spread of aSyn pathology [572]. On the contrary, when astrocytes derived from healthy controls were co-cultured with PD neurons, the former cells absorbed the neuronal aSyn from the medium, thus indicating a potential neuroprotective effect of astrocytes [572].

In another aSyn-overexpressing neuron-astrocyte co-culture, addition of aSyn fibrils led to the formation of aSyn aggregates in both cell types, probably recapitulating the events occurring during PD pathogenesis [573]. It has been also suggested that aSyn enters astrocytes more efficiently than neurons via endocytosis and that aSyn transmission from astroglial to neuronal cells leads to neurotoxicity and cell death [574]. Indeed, the uptake of aSyn by astrocytes has been reported as an early-in-time event, since it was detected in the cytoplasm of the cells within 30 min following aSyn application [574]. The spread of aSyn from neurons to astroglial cells has also been demonstrated in rodent transgenic animal models overexpressing human aSyn in neuronal cells, by the detection of aSyn-positive inclusions within the cytoplasm of these glial cells [575,576]. Furthermore, hippocampal delivery of aSyn fibrils in the brain of M83 A53T Tg mice resulted in the formation of pSer129-positive aSyn inclusions within both astrocytes and microglia, four months post-injection [397],

Various mechanisms have been proposed to underlie aSyn transfer between neurons and astrocytes. For example, it is known that astrocytes, upon oxidative stress, form tunneling nanotubes (TNTs) in order to connect with other non-stressed cells [577]. It has been proposed that various stressors, such as aberrant aSyn, lysosomal dysfunction or mitochondrial failure could trigger TNT formation in astrocytes and enhance aSyn spreading [387,578]. Another mechanism for intercellular communication is via exosomes. Although extensive work has been done regarding the role of exosomes in neuronal aSyn transmission and disease pathology [366,579–582], few studies have proposed a vesicular-mediated transfer of neuroprotective molecules from astrocytes to neurons [583,584] or an exosome-related aSyn spread from neurons to astrocytes [585,586].

Upon aSyn transmission to astrocytes, the latter produce multiple pro-inflammatory cytokines (IL-1α, IL-1β, IL-6, IL-18) and chemokines (CC-, CXC- and CXCL-type) as a response [550,587]. It has been suggested that the pro-inflammatory response of astrocytes to aSyn depends on TLR4 [496,588]. Apart from cytokine release, aSyn leads to Ca^{2+} flux and oxidative stress upon its entry in astroglial cells, presumably leading to neurotoxicity [589–591]. Moreover, in vitro and in vivo experiments have shown that pathological aSyn triggers microglial activation, followed by the induction of reactive A1 astrocytes, finally leading to neurodegeneration [592]. It has been also reported that astrocytes overexpressing hA53T aSyn displayed impaired functions, including glutamate uptake and BBB regulation, resulting in paralysis in transgenic mice [593]. Additionally, aSyn-treated astrocytes have been proposed to produce reduced levels of cholesterol, whereas in parallel they display enhanced GFAP expression, indicative of astrocyte reactivity [594]. Significantly, treatment of astrocytes with various aSyn species (monomeric, oligomeric, fibrillar) induced astrocyte activation and secretion of TNF-α and IL-1β, the expression of which seemed to depend on aSyn species, leading to subsequent non-cell autonomous neuronal degeneration [595]. Other studies revealed that elevated expression levels of myeloperoxidase and enhanced IFN-γ signaling could mediate the astrocytic-activation and inflammation observed in PD brains [21,596–598].

alpha-Synuclein has been reported to trigger the opening of connexin 43 (Cx43) hemichannels and pannexin-1 (Panx1) channels in mouse cortical astrocytes, leading to alterations in $[Ca^{2+}]_i$ levels, production of nitric oxide (NO), enhanced purinergic and glutamatergic signaling, altered mitochondrial morphology and reduced astrocyte survival [599]. Another recently published study suggests that vesicle-associated aSyn, deriving from erythrocytes, effectively crosses the BBB and accumulates within astrocytes, impairing glutamate uptake, probably due to interactions of oligomeric aSyn with excitatory amino acid transporter 2 (EAAT2) [600]. Furthermore, astrocytes overexpressing mutant A35T and A30P aSyn triggered ER stress and damaged the Golgi apparatus, finally leading to apoptotic cell death [601]. Remarkably, co-culture of primary astrocytes overexpressing mutant aSyn with neuronal cells, inhibited neurite outgrowth, probably due to reduced GDNF secretion [601]. Finally, Cy3-labeled aSyn oligomers were internalized by glial cells, primarily astrocytes, which then started to degrade the oligomers via the ALP [602].

In addition to the well-established role of microglia in the activation of astrocytes, astrocytes themselves have been also reported to control microglial activation and microglia-induced neuroinflammation [603,604], thus unraveling an astrocyte-microglia intimate crosstalk (Figure 4). For example, in response to pathological aSyn insult, astrocytes can acquire a pro-inflammatory phenotype that can lead to neuronal death, independent of microglia. Given that astrocytes produce pro-inflammatory cytokines and chemokines as a response to various stimuli, it has been proposed that such astrocytes may mediate the microglial activation detected in aSyn-related brain diseases [605,606]. Various WT or mutant aSyn conformations have been shown to trigger the up-regulation of pro-inflammatory modulators in astrocytes, such as ICAM-1, IL-6 and TNF-α, leading to microglial activation, neuroinflammation and neurotoxic events during PD progression [496,587,607]. Specifically, transgenic mice inducibly overexpressing the PD-related A53T mutant aSyn selectively in astrocytes exhibited reactive astrogliosis accompanied by increased inflammatory responses and microglial activation in brain regions with significant neuronal loss [593]. Moreover, the detection of ICAM-1 positive reactive astrocytes surrounding brain areas with severe neuronal loss in PD brains or in the MPTP mouse PD model, indicates a sustained inflammatory process mainly triggered by astroglial cells, which is responsible for the consequent degeneration of dopaminergic neurons [608]. Finally, similar to the aSyn prion-like mode of action, the neurotoxic reactive astrocyte polarization has been recently proposed to occur during the CNS prion disease, where microglial cells seem to retain a neuroprotective phenotype against the inflammatory astrocytic responses [609]. All the above observations highly cement the contribution of astroglial reactivity in the pathogenesis of PD and related neuronal a-synucleinopathies.

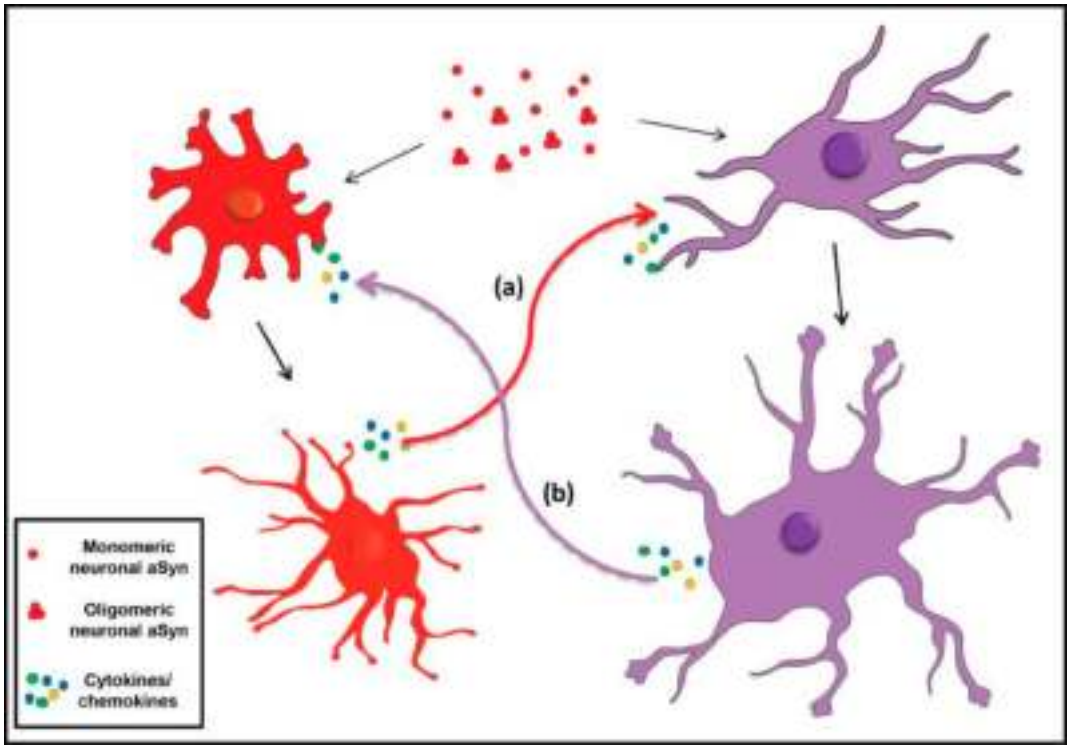

Figure 4. Crosstalk between astrocytes and microglia in a-synucleinopathies. Monomeric or oligomeric aSyn released by neurons is taken-up by astrocytes (purple) and microglia (red), which are then activated and secrete various cytokines or chemokines. (a) According to the prevailing hypothesis, the released pro-inflammatory molecules by microglia trigger the activation of astrocytes (red arrow), leading to excessive inflammation and neurotoxicity. (b) Conversely, aSyn can directly activate astrocytes to secrete pro-inflammatory cytokines or chemokines that recruit and activate microglia (purple arrow) resulting in excessive neuroinflammation.

3.2.2. Implication of astrocytes in MSA pathology

Apart from PD and DLB, astroglial activation is also present in MSA and it seems to play a role in both disease initiation and progression. Extensive astrogliosis has been reported in various brain regions of MSA patients, in some cases accompanied by aSyn-positive inclusions within astrocytes [16,610–613]. In agreement, accumulation of abnormally phosphorylated and aggregated aSyn was present within astrocytes of MSA patients [614]. Interestingly, aSyn-positive doughnut-shaped inclusions were detected in radial processes of Bergmann glia (unipolar protoplasmic astrocytes in the cerebellar cortex) of various a-synucleinopathy brains, including MSA [558]. Although astroglial aSyn accumulation has been demonstrated in the brains of various MSA transgenic mouse models, finally leading to astrogliosis that accompanies neurodegeneration [615–618], Song et al. suggested that subcortical astrocytes in MSA did not display aSyn accumulation, in contrast to PD [14]. However, up-to-date the data on the precise role of astrocytes in MSA are scarce, reinforcing the necessity for further studies to elucidate the contribution of astroglial activation in MSA pathogenesis.

3.3. Alpha-Synuclein in Oligodendrocytes: The Pathologic Hallmark of MSA, A Unique Oligodendrogliopathy

Oligodendrocytes are responsible for the production of myelin [619] that surrounds the neuronal processes, mediates the transmission of electric signals between neurons and provides a neurotrophic support [620–623]. There are two main types of oligodendrocytes, the myelinating and the non-myelinating ones, that concentrate in white and grey matter, respectively [624]. Many neurodegenerative diseases occur due to either oligodendroglial death or damage to the myelin sheathes they produce leading to subsequent neuronal demise [622,625,626]. Oligodendrocytes have been proposed to participate in late PD and DLB progression, rather than in disease initiation [442,627]. This secondary involvement of oligodendrocytes in neuronal a-synucleinopathies was further supported by the detection of aSyn-positive inclusions within non-myelinating oligodendrocytes of PD and DLB brains [15,628], as well as by the presence of complement-activated oligodendrocytes in the diseased brains [629,630]. Moreover, axonal myelination deficits in neurodegenerative diseases also highlight the involvement of oligodendrocytes in neuropathogenetic events [631,632]. Additionally, oligodendroglial cell loss was reported in the striatum of the MPTP-intoxicated mouse PD model, shortly after MPTP administration [633].

On the other hand, the oligodendroglial aSyn inclusions detected in the brains of MSA patients (GCIs) are the main hallmark of the disease and are considered to play a crucial role in the primary events leading to MSA [626]. The involvement of oligodendrocytes in MSA initiation and progression is indisputable, due to the wide distribution of GCIs along the affected brain areas of MSA patients [611,634–637]. Apart from GCIs present within oligodendrocytes, other inclusions, such as neuronal cytoplasmic inclusions (NCIs) have been detected in neuronal somata, axons and nucleus in various brain regions, mainly composed of aSyn [638–640]. GCIs were first described three decades ago, as multi-shaped oligodendroglial inclusions composed of a 10-nm-sized central core fibrils, positively stained with antibodies against aSyn, surrounded by other aggregated proteins such as αβ-crystallin, ubiquitin, cytoskeletal proteins, chaperones and the microtubule-related proteins TPPP/p25α and tau [11,634,641–643]. Comparative analysis of the protein composition of GCIs and LBs revealed that GCIs consist of 11.7% aSyn, 1.9% αβ-crystallin and 2.3% 14-3-3 proteins, whereas LBs are composed of 8.5% aSyn, 2% αβ-crystallin and 1.5% 14-3-3 proteins [644]. It has been also reported that aSyn is a key player in the accumulation of tau and αβ-crystallin within GCIs [645], further highlighting the contribution of aSyn in disease pathogenesis.

Another early hallmark of oligodendroglial pathology in MSA and major component of GCIs is the oligodendroglial-specific phosphoprotein TPPP/p25α, which under physiological conditions has been proposed to mediate the myelination process and colocalize with myelin basic protein (MBP) in normal human brains [646–648]. Under pathological

conditions, TPPP/p25α is considered to re-locate from the myelin sheaths to the abnormally expanded oligodendroglial somata and to trigger aSyn aggregation in vitro [12,649]. In vitro experiments utilizing TPPP/p25α ectopic overexpression in PC12 cells revealed that TPPP/p25α prevents the fusion of autophagosomes with lysosomes and impairs aSyn degradation, enhancing its secretion via exophagy [650]. Moreover, concurrent overexpression of TPPP/p25α and aSyn in OLN-93 rat oligodendroglial cells led to pSer129 aSyn-dependent microtubule retraction from the processes to the perinuclear space, as well as to cytotoxicity and subsequent cell death via activation of the FAS receptor and caspase-8 [651,652]. Recently published work from our lab revealed a crucial role for TPPP/p25α in the recruitment and seeding of oligodendroglial aSyn and in the formation of aberrant aSyn species within oligodendrocytes [653]. Additionally, the levels of glial cell-derived neurotrophic factor (GDNF) were found significantly decreased in the brains of MBP-haSyn transgenic mice, a mouse model for MSA where human aSyn is specifically overexpressed in oligodendrocytes [654]. Similar results were obtained from brain samples of MSA patients, further supporting that oligodendroglial aSyn accumulation is implicated in the dysregulation of neurotrophic support, oxidative stress and neuroinflammation, thus leading to MSA pathogenesis [654].

Alpha-Synuclein Accumulation in Oligodendrocytes, Propagation and Spread of Pathology

The origin of aSyn detected in oligodendroglial GCIs still remains enigmatic and there are controversial studies in the literature suggesting either the internalization of neuronally-secreted aSyn by oligodendrocytes or an enhanced expression and decreased degradation of oligodendroglial aSyn [655–661]. The release of aSyn by neuronal cells, partially bound on vesicles or exosomes is well-documented [365,366,380,662,663] and some studies propose that oligodendrocytes can take-up the neuronally-derived aSyn via dynamin GTPase-, clathrin- and dynasore-dependent mechanisms [658,664–666]. The neuron-oligodendrocyte communication can also be mediated via exosomes [667], which are characterized as "Trojan horses" of neurodegeneration [668] and they could serve as transporters of pathological disease-related proteins, such as aSyn (Figure 3). Moreover, ectopic expression of the endocytosis regulatory proteins Rab5 and Rabaptin-5 in oligodendrocytes of MSA brains may account for the elevated levels of aSyn within oligodendrocytes, probably via enhanced endocytotic activity [669].

In vitro and in vivo experiments revealed the ability of oligodendrocytes to take up exogenously added recombinant or neuronally-derived aSyn and incorporate it into intracellular GCI-like aggregates [658,660,664–666]. In a recently published study, mature human oligodendrocytes generated from neural stem cells had the ability to internalize neuronally-derived aSyn and form proteinaceous inclusions, thus further supporting the existing theory for the origin of MSA-related aSyn. Significantly, it has been shown that once neuronal aSyn is taken up by oligodendrocytes, it accumulates and gains GCI-like characteristics rather determined by the oligodendroglial milieu [17].

Over the last years, the prion hypothesis has gained a lot of attention regarding the spread of pathological aSyn in the context of both PD and MSA. Specifically, it has been reported that inoculation of transgenic mice overexpressing human A53T aSyn with MSA brain homogenates resulted in CNS dysfunction, whereas, strikingly, the PD brain-derived material did not evoke similar effects [670–672]. Similarly, intrastriatal injections of MSA homogenates in the brains of Tg(SNCA)1Nbm/J mice (out for mouse aSyn and overexpressing the human protein) resulted in the detection of hyper-phosphorylated aSyn-positive inclusions in various brain regions [673]. Finally, treatment of HEK293T cells stably expressing fluorescently-tagged aSyn with healthy, PD or MSA brain-derived extracts highlighted that only the MSA-added material was capable of inducing aSyn aggregation [674].

There are other possible scenarios that have been proposed to explain aSyn seeding and propagation in MSA brains, based on oligodendrocyte-to-oligodendrocyte communications. Specifically, it is possible that aSyn is taken up by oligodendroglial progenitor cells

prior to their maturation, probably impairing the myelination process [675]. Finally, another scenario suggests that, in MSA pathology, oligodendrocytes adopt unknown cellular uptake mechanisms for aSyn internalization and subsequent propagation [675]; however, the precise mechanisms underlying aSyn transfer to oligodendrocytes still remains unknown. The gap junction protein connexin-32 (Cx32) has been also implicated in the uptake of oligomeric aSyn by both neurons and oligodendrocytes [676] and Cx32 protein levels were found elevated in animal PD and MSA models, thus suggesting an interaction between Cx32 expression and aSyn cellular uptake [676]. Contrariwise, others and we have suggested that the endogenous aSyn, expressed even at minute amounts, plays a pivotal role in the accumulation of pathological aSyn within oligodendrocytes and the subsequent GCI-like formation [653,677].

It is interesting to note that oligodendroglial and neuronal aSyn accumulation has been reported to occur in different time points and in particular that aSyn aggregation requires several months to progress within oligodendrocytes, upon synthetic haSyn-PFFs delivery into the brain of WT mice [678]. Moreover, in vitro aSyn overexpression in oligodendrocytes resulted in delayed maturation of oligodendrocyte progenitor cells and impaired myelin-gene expression and myelination deficits [679–681], whereas in another study aSyn-positive inclusions were mainly detected in BCAS1-expressing (breast carcinoma amplified sequence 1) immature oligodendrocytes of MSA brains [682]. The above observations insinuate that the oligodendroglial maturation and aSyn-aggregate formation are closely linked and may provide information regarding pathogenic events in MSA.

Regarding the hypothesis of impaired aSyn degradation in the context of MSA, both the UPS and the ALP have been proposed to contribute to the accumulation and aggregation of aSyn within oligodendrocytes. The detection of LC3-positive signal or other autophagy-related proteins, such as ubiquitin and p62 in GCIs points a role of the ALP in MSA pathogenesis [659,683–687]. It has also been suggested that AMBRA1, an upstream protein regulator of autophagy and UCH-L1, a deubiquitylating enzyme, are implicated in neurodegenerative diseases with oligodendroglia pathology [688,689]. The role of autophagic dysregulation along with mitochondrial impairment in aSyn aggregation was also studied in primary oligodendroglial cultures and in the OLN-t40 oligodendroglial cell line [690]. Moreover, neurosin (kallikrein 6) has been proven an effective serine protease in clearing aSyn from oligodendrocytes both in vitro and in vivo [691–693]. In addition, treatment of Tg haSyn-PLP mice, a well-established MSA mouse model, with the proteasome inhibitor I for 12 weeks, resulted in enhanced accumulation of both human and endogenous mouse aSyn within the cytoplasm of oligodendrocytes, thus highlighting the role of UPS in aSyn degradation [694]. Finally, several in vitro studies have proposed that aSyn aggregation is stimulated by heparin and heparan sulfate [391,695,696], linear polysaccharides (glycosaminoglycans) found on the cell membrane and in the extracellular matrix [697,698]. Heparan sulfate has been suggested to mediate aSyn fibril uptake by oligodendrocytes via binding to the plasma membrane [391,699], whereas other have proposed that heparin and heparan sulfate proteoglycans (HSPGs) are responsible for aSyn fibrillation [695,696,700–702].

Apart from aSyn toxicity *per se*, the overexpression of aSyn in oligodendrocytes can lead to oligodendroglial cell death and subsequent neuronal loss via a plethora of mechanisms. Specifically, aSyn-overexpressing oligodendrocytes are more susceptible to oxidative stress and various cytokine actions [591,703], or display impaired adhesion properties [704]. Furthermore, it has been reported that animal MSA models exhibit myelin loss and impaired mitochondrial function, accompanied by severe neurodegeneration in various brain regions [615,617,618,705,706].

4. Conclusions

It has been almost 25 years since the discovery that the Lewy pathology in PD and DLB neurons is immunoreactive for aSyn and, at the same time, neuronal aSyn accumulates in glial inclusions within MSA oligodendrocytes. Even though a plethora of studies focuses on the role of aSyn in neuronal physiology and pathology, increasing amount of data reinforces the contribution of non-cell autonomous neuron-glial interactions in the initiation and progression of a-synucleinopathies. Microglia and astrocytes form the brain's defense system against neurotoxic insults, become activated and release pro-inflammatory factors. However, uncontrolled activation results in chronic microgliosis and astrogliosis that may be detrimental and lead to neurodegeneration. Even more, the deposition of aSyn in oligodendrocytes impairs their myelinating activity and reduces neuronal trophic support, events that eventually result in neuronal demise. Remarkably, neurons, microglia, astrocytes and oligodendrocytes are all able to take up and clear extracellular aSyn; however, glial cells appear to be the most potent scavengers. The endocytosis of various aSyn species might be conformation-sensitive, cell- and receptor-type specific, adding further complexity in disease management.

Undoubtedly, better understanding of the mechanisms mediating the interaction between neurons and glial cells in a-synucleinopathies may provide insights into neuronal dysfunction and death and may uncover novel disease modifying therapies.

Author Contributions: P.M.; writing—original draft preparation, M.X.; writing—review and final editing. Both authors have read and agreed to the published version of the manuscript.

Funding: This research was funded by an MSA UK Trust grant (2019/MX60185), an MSA Coalition grant (2020-05-001) and an MJFF grant (16887).

Institutional Review Board Statement: Not applicable.

Informed Consent Statement: Not applicable.

Data Availability Statement: Not applicable.

Acknowledgments: M.X. is supported by an MSA UK Trust grant (2019/MX60185), an MSA Coalition grant (2020-05-001) and an MJFF grant (16887). This research is co-financed by Greece and the European Union (European Social Fund—ESF) through the Operational Programme «Human Resources Development, Education and Lifelong Learning» in the context of the project "Strengthening Human Resources Research Potential via Doctorate Research" (MIS-5000432), implemented by the State Scholarships Foundation (IKϒ)», awarded to PM.

Conflicts of Interest: The authors declare no conflict of interest.

References

1. Uversky, V.N. A protein-chameleon: Conformational plasticity of alpha-synuclein, a disordered protein involved in neurodegenerative disorders. *J. Biomol. Struct. Dyn.* **2003**, *21*, 211–234. [CrossRef]
2. Spillantini, M.G.; Crowther, R.A.; Jakes, R.; Hasegawa, M.; Goedert, M. alpha-Synuclein in filamentous inclusions of Lewy bodies from Parkinson's disease and dementia with lewy bodies. *Proc. Natl. Acad. Sci. USA* **1998**, *95*, 6469–6473. [CrossRef]
3. Polymeropoulos, M.H.; Lavedan, C.; Leroy, E.; Ide, S.E.; Dehejia, A.; Dutra, A.; Pike, B.; Root, H.; Rubenstein, J.; Boyer, R.; et al. Mutation in the alpha-synuclein gene identified in families with Parkinson's disease. *Science* **1997**, *276*, 2045–2047. [CrossRef] [PubMed]
4. Chartier-Harlin, M.C.; Kachergus, J.; Roumier, C.; Mouroux, V.; Douay, X.; Lincoln, S.; Levecque, C.; Larvor, L.; Andrieux, J.; Hulihan, M.; et al. Alpha-synuclein locus duplication as a cause of familial Parkinson's disease. *Lancet* **2004**, *364*, 1167–1169. [CrossRef]
5. Kruger, R.; Kuhn, W.; Muller, T.; Woitalla, D.; Graeber, M.; Kosel, S.; Przuntek, H.; Epplen, J.T.; Schols, L.; Riess, O. Ala30Pro mutation in the gene encoding alpha-synuclein in Parkinson's disease. *Nat. Genet.* **1998**, *18*, 106–108. [CrossRef] [PubMed]
6. Singleton, A.B.; Farrer, M.; Johnson, J.; Singleton, A.; Hague, S.; Kachergus, J.; Hulihan, M.; Peuralinna, T.; Dutra, A.; Nussbaum, R.; et al. alpha-Synuclein locus triplication causes Parkinson's disease. *Science* **2003**, *302*, 841. [CrossRef] [PubMed]
7. Zarranz, J.J.; Alegre, J.; Gomez-Esteban, J.C.; Lezcano, E.; Ros, R.; Ampuero, I.; Vidal, L.; Hoenicka, J.; Rodriguez, O.; Atares, B.; et al. The new mutation, E46K, of alpha-synuclein causes Parkinson and Lewy body dementia. *Ann. Neurol.* **2004**, *55*, 164–173. [CrossRef]

8. Pals, P.; Lincoln, S.; Manning, J.; Heckman, M.; Skipper, L.; Hulihan, M.; Van den Broeck, M.; De Pooter, T.; Cras, P.; Crook, J.; et al. alpha-Synuclein promoter confers susceptibility to Parkinson's disease. *Ann. Neurol.* **2004**, *56*, 591–595. [CrossRef]
9. Fuchs, J.; Tichopad, A.; Golub, Y.; Munz, M.; Schweitzer, K.J.; Wolf, B.; Berg, D.; Mueller, J.C.; Gasser, T. Genetic variability in the SNCA gene influences alpha-synuclein levels in the blood and brain. *FASEB J.* **2008**, *22*, 1327–1334. [CrossRef]
10. Fanciulli, A.; Stankovic, I.; Krismer, F.; Seppi, K.; Levin, J.; Wenning, G.K. Multiple system atrophy. *Int. Rev. Neurobiol.* **2019**, *149*, 137–192. [CrossRef]
11. Spillantini, M.G.; Crowther, R.A.; Jakes, R.; Cairns, N.J.; Lantos, P.L.; Goedert, M. Filamentous alpha-synuclein inclusions link multiple system atrophy with Parkinson's disease and dementia with Lewy bodies. *Neurosci. Lett.* **1998**, *251*, 205–208. [CrossRef]
12. Song, Y.J.; Lundvig, D.M.; Huang, Y.; Gai, W.P.; Blumbergs, P.C.; Hojrup, P.; Otzen, D.; Halliday, G.M.; Jensen, P.H. p25alpha relocalizes in oligodendroglia from myelin to cytoplasmic inclusions in multiple system atrophy. *Am. J. Pathol.* **2007**, *171*, 1291–1303. [CrossRef] [PubMed]
13. Braak, H.; Sastre, M.; Del Tredici, K. Development of alpha-synuclein immunoreactive astrocytes in the forebrain parallels stages of intraneuronal pathology in sporadic Parkinson's disease. *Acta Neuropathol.* **2007**, *114*, 231–241. [CrossRef] [PubMed]
14. Song, Y.J.; Halliday, G.M.; Holton, J.L.; Lashley, T.; O'Sullivan, S.S.; McCann, H.; Lees, A.J.; Ozawa, T.; Williams, D.R.; Lockhart, P.J.; et al. Degeneration in different parkinsonian syndromes relates to astrocyte type and astrocyte protein expression. *J. Neuropathol. Exp. Neurol.* **2009**, *68*, 1073–1083. [CrossRef]
15. Wakabayashi, K.; Hayashi, S.; Yoshimoto, M.; Kudo, H.; Takahashi, H. NACP/alpha-synuclein-positive filamentous inclusions in astrocytes and oligodendrocytes of Parkinson's disease brains. *Acta Neuropathol.* **2000**, *99*, 14–20. [CrossRef]
16. Wenning, G.K.; Jellinger, K.A. The role of alpha-synuclein in the pathogenesis of multiple system atrophy. *Acta Neuropathol.* **2005**, *109*, 129–140. [CrossRef]
17. Peng, C.; Gathagan, R.J.; Covell, D.J.; Medellin, C.; Stieber, A.; Robinson, J.L.; Zhang, B.; Pitkin, R.M.; Olufemi, M.F.; Luk, K.C.; et al. Cellular milieu imparts distinct pathological alpha-synuclein strains in alpha-synucleinopathies. *Nature* **2018**, *557*, 558–563. [CrossRef]
18. Bousset, L.; Pieri, L.; Ruiz-Arlandis, G.; Gath, J.; Jensen, P.H.; Habenstein, B.; Madiona, K.; Olieric, V.; Bockmann, A.; Meier, B.H.; et al. Structural and functional characterization of two alpha-synuclein strains. *Nat. Commun.* **2013**, *4*, 2575. [CrossRef]
19. Shahnawaz, M.; Mukherjee, A.; Pritzkow, S.; Mendez, N.; Rabadia, P.; Liu, X.; Hu, B.; Schmeichel, A.; Singer, W.; Wu, G.; et al. Discriminating alpha-synuclein strains in Parkinson's disease and multiple system atrophy. *Nature* **2020**, *578*, 273–277. [CrossRef]
20. Candelise, N.; Schmitz, M.; Llorens, F.; Villar-Pique, A.; Cramm, M.; Thom, T.; da Silva Correia, S.M.; da Cunha, J.E.G.; Mobius, W.; Outeiro, T.F.; et al. Seeding variability of different alpha synuclein strains in synucleinopathies. *Ann. Neurol.* **2019**, *85*, 691–703. [CrossRef] [PubMed]
21. Hashioka, S.; Klegeris, A.; Schwab, C.; McGeer, P.L. Interferon-gamma-dependent cytotoxic activation of human astrocytes and astrocytoma cells. *Neurobiol. Aging* **2009**, *30*, 1924–1935. [CrossRef]
22. Imamura, K.; Hishikawa, N.; Sawada, M.; Nagatsu, T.; Yoshida, M.; Hashizume, Y. Distribution of major histocompatibility complex class II-positive microglia and cytokine profile of Parkinson's disease brains. *Acta Neuropathol.* **2003**, *106*, 518–526. [CrossRef] [PubMed]
23. Doorn, K.J.; Moors, T.; Drukarch, B.; van de Berg, W.; Lucassen, P.J.; van Dam, A.M. Microglial phenotypes and toll-like receptor 2 in the substantia nigra and hippocampus of incidental Lewy body disease cases and Parkinson's disease patients. *Acta Neuropathol. Commun.* **2014**, *2*, 90. [CrossRef]
24. Liddelow, S.A.; Guttenplan, K.A.; Clarke, L.E.; Bennett, F.C.; Bohlen, C.J.; Schirmer, L.; Bennett, M.L.; Munch, A.E.; Chung, W.S.; Peterson, T.C.; et al. Neurotoxic reactive astrocytes are induced by activated microglia. *Nature* **2017**, *541*, 481–487. [CrossRef]
25. McGeer, P.L.; Itagaki, S.; Boyes, B.E.; McGeer, E.G. Reactive microglia are positive for HLA-DR in the substantia nigra of Parkinson's and Alzheimer's disease brains. *Neurology* **1988**, *38*, 1285–1291. [CrossRef] [PubMed]
26. Iwai, A.; Masliah, E.; Yoshimoto, M.; Ge, N.; Flanagan, L.; de Silva, H.A.; Kittel, A.; Saitoh, T. The precursor protein of non-A beta component of Alzheimer's disease amyloid is a presynaptic protein of the central nervous system. *Neuron* **1995**, *14*, 467–475. [CrossRef]
27. Withers, G.S.; George, J.M.; Banker, G.A.; Clayton, D.F. Delayed localization of synelfin (synuclein, NACP) to presynaptic terminals in cultured rat hippocampal neurons. *Brain Res. Dev. Brain Res.* **1997**, *99*, 87–94. [CrossRef]
28. Andringa, G.; Du, F.; Chase, T.N.; Bennett, M.C. Mapping of rat brain using the Synuclein-1 monoclonal antibody reveals somatodendritic expression of alpha-synuclein in populations of neurons homologous to those vulnerable to Lewy body formation in human synucleopathies. *J. Neuropathol. Exp. Neurol.* **2003**, *62*, 1060–1075. [CrossRef] [PubMed]
29. Barbour, R.; Kling, K.; Anderson, J.P.; Banducci, K.; Cole, T.; Diep, L.; Fox, M.; Goldstein, J.M.; Soriano, F.; Seubert, P.; et al. Red blood cells are the major source of alpha-synuclein in blood. *Neurodegener. Dis.* **2008**, *5*, 55–59. [CrossRef]
30. Askanas, V.; Engel, W.K.; Alvarez, R.B.; McFerrin, J.; Broccolini, A. Novel immunolocalization of alpha-synuclein in human muscle of inclusion-body myositis, regenerating and necrotic muscle fibers, and at neuromuscular junctions. *J. Neuropathol. Exp. Neurol.* **2000**, *59*, 592–598. [CrossRef]
31. Bottner, M.; Zorenkov, D.; Hellwig, I.; Barrenschee, M.; Harde, J.; Fricke, T.; Deuschl, G.; Egberts, J.H.; Becker, T.; Fritscher-Ravens, A.; et al. Expression pattern and localization of alpha-synuclein in the human enteric nervous system. *Neurobiol. Dis.* **2012**, *48*, 474–480. [CrossRef]

32. Aldecoa, I.; Navarro-Otano, J.; Stefanova, N.; Sprenger, F.S.; Seppi, K.; Poewe, W.; Cuatrecasas, M.; Valldeoriola, F.; Gelpi, E.; Tolosa, E. Alpha-synuclein immunoreactivity patterns in the enteric nervous system. *Neurosci. Lett.* **2015**, *602*, 145–149. [CrossRef]
33. Li, J.; Henning Jensen, P.; Dahlstrom, A. Differential localization of alpha-, beta- and gamma-synucleins in the rat CNS. *Neuroscience* **2002**, *113*, 463–478. [CrossRef]
34. Taguchi, K.; Watanabe, Y.; Tsujimura, A.; Tanaka, M. Expression of alpha-synuclein is regulated in a neuronal cell type-dependent manner. *Anat. Sci. Int.* **2019**, *94*, 11–22. [CrossRef] [PubMed]
35. Taguchi, K.; Watanabe, Y.; Tsujimura, A.; Tanaka, M. Brain region-dependent differential expression of alpha-synuclein. *J. Comp. Neurol.* **2016**, *524*, 1236–1258. [CrossRef] [PubMed]
36. George, J.M.; Jin, H.; Woods, W.S.; Clayton, D.F. Characterization of a novel protein regulated during the critical period for song learning in the zebra finch. *Neuron* **1995**, *15*, 361–372. [CrossRef]
37. Maroteaux, L.; Campanelli, J.T.; Scheller, R.H. Synuclein: A neuron-specific protein localized to the nucleus and presynaptic nerve terminal. *J. Neurosci.* **1988**, *8*, 2804–2815. [CrossRef]
38. Burre, J.; Sharma, M.; Tsetsenis, T.; Buchman, V.; Etherton, M.R.; Sudhof, T.C. Alpha-synuclein promotes SNARE-complex assembly in vivo and in vitro. *Science* **2010**, *329*, 1663–1667. [CrossRef]
39. Zaltieri, M.; Grigoletto, J.; Longhena, F.; Navarria, L.; Favero, G.; Castrezzati, S.; Colivicchi, M.A.; Della Corte, L.; Rezzani, R.; Pizzi, M.; et al. alpha-synuclein and synapsin III cooperatively regulate synaptic function in dopamine neurons. *J. Cell Sci.* **2015**, *128*, 2231–2243. [CrossRef]
40. Chen, R.H.C.; Wislet-Gendebien, S.; Samuel, F.; Visanji, N.P.; Zhang, G.; Marsilio, D.; Langman, T.; Fraser, P.E.; Tandon, A. alpha-Synuclein membrane association is regulated by the Rab3a recycling machinery and presynaptic activity. *J. Biol. Chem.* **2013**, *288*, 7438–7449. [CrossRef]
41. Greten-Harrison, B.; Polydoro, M.; Morimoto-Tomita, M.; Diao, L.; Williams, A.M.; Nie, E.H.; Makani, S.; Tian, N.; Castillo, P.E.; Buchman, V.L.; et al. alphabetagamma-Synuclein triple knockout mice reveal age-dependent neuronal dysfunction. *Proc. Natl. Acad. Sci. USA* **2010**, *107*, 19573–19578. [CrossRef]
42. Burre, J.; Sharma, M.; Sudhof, T.C. alpha-Synuclein assembles into higher-order multimers upon membrane binding to promote SNARE complex formation. *Proc. Natl. Acad. Sci. USA* **2014**, *111*, E4274–E4283. [CrossRef] [PubMed]
43. Lautenschlager, J.; Stephens, A.D.; Fusco, G.; Strohl, F.; Curry, N.; Zacharopoulou, M.; Michel, C.H.; Laine, R.; Nespovitaya, N.; Fantham, M.; et al. C-terminal calcium binding of alpha-synuclein modulates synaptic vesicle interaction. *Nat. Commun.* **2018**, *9*, 712. [CrossRef] [PubMed]
44. Burre, J.; Sharma, M.; Sudhof, T.C. Definition of a molecular pathway mediating alpha-synuclein neurotoxicity. *J. Neurosci.* **2015**, *35*, 5221–5232. [CrossRef] [PubMed]
45. Betzer, C.; Movius, A.J.; Shi, M.; Gai, W.P.; Zhang, J.; Jensen, P.H. Identification of synaptosomal proteins binding to monomeric and oligomeric alpha-synuclein. *PLoS ONE* **2015**, *10*, e0116473. [CrossRef] [PubMed]
46. Scott, D.; Roy, S. alpha-Synuclein inhibits intersynaptic vesicle mobility and maintains recycling-pool homeostasis. *J. Neurosci.* **2012**, *32*, 10129–10135. [CrossRef] [PubMed]
47. Vargas, K.J.; Makani, S.; Davis, T.; Westphal, C.H.; Castillo, P.E.; Chandra, S.S. Synucleins regulate the kinetics of synaptic vesicle endocytosis. *J. Neurosci.* **2014**, *34*, 9364–9376. [CrossRef]
48. Zhang, L.; Zhang, C.; Zhu, Y.; Cai, Q.; Chan, P.; Ueda, K.; Yu, S.; Yang, H. Semi-quantitative analysis of alpha-synuclein in subcellular pools of rat brain neurons: An immunogold electron microscopic study using a C-terminal specific monoclonal antibody. *Brain Res.* **2008**, *1244*, 40–52. [CrossRef] [PubMed]
49. Ostrerova, N.; Petrucelli, L.; Farrer, M.; Mehta, N.; Choi, P.; Hardy, J.; Wolozin, B. alpha-Synuclein shares physical and functional homology with 14-3-3 proteins. *J. Neurosci.* **1999**, *19*, 5782–5791. [CrossRef]
50. Kim, T.D.; Choi, E.; Rhim, H.; Paik, S.R.; Yang, C.H. Alpha-synuclein has structural and functional similarities to small heat shock proteins. *Biochem. Biophys. Res. Commun.* **2004**, *324*, 1352–1359. [CrossRef] [PubMed]
51. Chandra, S.; Gallardo, G.; Fernandez-Chacon, R.; Schluter, O.M.; Sudhof, T.C. Alpha-synuclein cooperates with CSPalpha in preventing neurodegeneration. *Cell* **2005**, *123*, 383–396. [CrossRef]
52. Kim, T.D.; Paik, S.R.; Yang, C.H. Structural and functional implications of C-terminal regions of alpha-synuclein. *Biochemistry* **2002**, *41*, 13782–13790. [CrossRef]
53. Kim, T.D.; Paik, S.R.; Yang, C.H.; Kim, J. Structural changes in alpha-synuclein affect its chaperone-like activity in vitro. *Protein Sci.* **2000**, *9*, 2489–2496. [CrossRef]
54. Park, S.M.; Jung, H.Y.; Kim, T.D.; Park, J.H.; Yang, C.H.; Kim, J. Distinct roles of the N-terminal-binding domain and the C-terminal-solubilizing domain of alpha-synuclein, a molecular chaperone. *J. Biol. Chem.* **2002**, *277*, 28512–28520. [CrossRef] [PubMed]
55. Rekas, A.; Ahn, K.J.; Kim, J.; Carver, J.A. The chaperone activity of alpha-synuclein: Utilizing deletion mutants to map its interaction with target proteins. *Proteins* **2012**, *80*, 1316–1325. [CrossRef]
56. Srivastava, T.; Raj, R.; Dubey, A.; Kumar, D.; Chaturvedi, R.K.; Sharma, S.K.; Priya, S. Fast kinetics of environmentally induced alpha-synuclein aggregation mediated by structural alteration in NAC region and result in structure dependent cytotoxicity. *Sci. Rep.* **2020**, *10*, 18412. [CrossRef] [PubMed]
57. Burre, J.; Vivona, S.; Diao, J.; Sharma, M.; Brunger, A.T.; Sudhof, T.C. Properties of native brain alpha-synuclein. *Nature* **2013**, *498*, E4–E6. [CrossRef]

58. Celej, M.S.; Sarroukh, R.; Goormaghtigh, E.; Fidelio, G.D.; Ruysschaert, J.M.; Raussens, V. Toxic prefibrillar alpha-synuclein amyloid oligomers adopt a distinctive antiparallel beta-sheet structure. *Biochem. J.* **2012**, *443*, 719–726. [CrossRef] [PubMed]
59. Li, H.T.; Du, H.N.; Tang, L.; Hu, J.; Hu, H.Y. Structural transformation and aggregation of human alpha-synuclein in trifluoroethanol: Non-amyloid component sequence is essential and beta-sheet formation is prerequisite to aggregation. *Biopolymers* **2002**, *64*, 221–226. [CrossRef] [PubMed]
60. Chaudhary, H.; Subramaniam, V.; Claessens, M. Direct visualization of model membrane remodeling by alpha-synuclein fibrillization. *ChemPhysChem* **2017**, *18*, 1620–1626. [CrossRef]
61. Galvagnion, C.; Brown, J.W.; Ouberai, M.M.; Flagmeier, P.; Vendruscolo, M.; Buell, A.K.; Sparr, E.; Dobson, C.M. Chemical properties of lipids strongly affect the kinetics of the membrane-induced aggregation of alpha-synuclein. *Proc. Natl. Acad. Sci. USA* **2016**, *113*, 7065–7070. [CrossRef]
62. Galvagnion, C. The Role of Lipids Interacting with alpha-Synuclein in the Pathogenesis of Parkinson's Disease. *J. Parkinsons Dis.* **2017**, *7*, 433–450. [CrossRef] [PubMed]
63. Narayanan, V.; Scarlata, S. Membrane binding and self-association of alpha-synucleins. *Biochemistry* **2001**, *40*, 9927–9934. [CrossRef]
64. Zhu, M.; Fink, A.L. Lipid binding inhibits alpha-synuclein fibril formation. *J. Biol. Chem.* **2003**, *278*, 16873–16877. [CrossRef]
65. Lee, H.J.; Choi, C.; Lee, S.J. Membrane-bound alpha-synuclein has a high aggregation propensity and the ability to seed the aggregation of the cytosolic form. *J. Biol. Chem.* **2002**, *277*, 671–678. [CrossRef] [PubMed]
66. Cole, N.B.; Murphy, D.D.; Grider, T.; Rueter, S.; Brasaemle, D.; Nussbaum, R.L. Lipid droplet binding and oligomerization properties of the Parkinson's disease protein alpha-synuclein. *J. Biol. Chem.* **2002**, *277*, 6344–6352. [CrossRef]
67. Perni, M.; Galvagnion, C.; Maltsev, A.; Meisl, G.; Muller, M.B.; Challa, P.K.; Kirkegaard, J.B.; Flagmeier, P.; Cohen, S.I.; Cascella, R.; et al. A natural product inhibits the initiation of alpha-synuclein aggregation and suppresses its toxicity. *Proc. Natl. Acad. Sci. USA* **2017**, *114*, E1009–E1017. [CrossRef] [PubMed]
68. Fares, M.B.; Ait-Bouziad, N.; Dikiy, I.; Mbefo, M.K.; Jovicic, A.; Kiely, A.; Holton, J.L.; Lee, S.J.; Gitler, A.D.; Eliezer, D.; et al. The novel Parkinson's disease linked mutation G51D attenuates in vitro aggregation and membrane binding of alpha-synuclein, and enhances its secretion and nuclear localization in cells. *Hum. Mol. Genet.* **2014**, *23*, 4491–4509. [CrossRef]
69. Ghosh, D.; Sahay, S.; Ranjan, P.; Salot, S.; Mohite, G.M.; Singh, P.K.; Dwivedi, S.; Carvalho, E.; Banerjee, R.; Kumar, A.; et al. The newly discovered Parkinson's disease associated Finnish mutation (A53E) attenuates alpha-synuclein aggregation and membrane binding. *Biochemistry* **2014**, *53*, 6419–6421. [CrossRef] [PubMed]
70. Jensen, P.H.; Nielsen, M.S.; Jakes, R.; Dotti, C.G.; Goedert, M. Binding of alpha-synuclein to brain vesicles is abolished by familial Parkinson's disease mutation. *J. Biol. Chem.* **1998**, *273*, 26292–26294. [CrossRef]
71. Jo, E.; Fuller, N.; Rand, R.P.; St George-Hyslop, P.; Fraser, P.E. Defective membrane interactions of familial Parkinson's disease mutant A30P alpha-synuclein. *J. Mol. Biol.* **2002**, *315*, 799–807. [CrossRef]
72. Tsigelny, I.F.; Sharikov, Y.; Kouznetsova, V.L.; Greenberg, J.P.; Wrasidlo, W.; Overk, C.; Gonzalez, T.; Trejo, M.; Spencer, B.; Kosberg, K.; et al. Molecular determinants of alpha-synuclein mutants' oligomerization and membrane interactions. *ACS Chem. Neurosci.* **2015**, *6*, 403–416. [CrossRef] [PubMed]
73. Eliezer, D.; Kutluay, E.; Bussell, R., Jr.; Browne, G. Conformational properties of alpha-synuclein in its free and lipid-associated states. *J. Mol. Biol.* **2001**, *307*, 1061–1073. [CrossRef] [PubMed]
74. Weinreb, P.H.; Zhen, W.; Poon, A.W.; Conway, K.A.; Lansbury, P.T., Jr. NACP, a protein implicated in Alzheimer's disease and learning, is natively unfolded. *Biochemistry* **1996**, *35*, 13709–13715. [CrossRef] [PubMed]
75. Killinger, B.A.; Melki, R.; Brundin, P.; Kordower, J.H. Endogenous alpha-synuclein monomers, oligomers and resulting pathology: Let's talk about the lipids in the room. *NPJ Parkinsons Dis.* **2019**, *5*, 23. [CrossRef] [PubMed]
76. Fauvet, B.; Mbefo, M.K.; Fares, M.B.; Desobry, C.; Michael, S.; Ardah, M.T.; Tsika, E.; Coune, P.; Prudent, M.; Lion, N.; et al. alpha-Synuclein in central nervous system and from erythrocytes, mammalian cells, and Escherichia coli exists predominantly as disordered monomer. *J. Biol. Chem.* **2012**, *287*, 15345–15364. [CrossRef]
77. Bartels, T.; Choi, J.G.; Selkoe, D.J. alpha-Synuclein occurs physiologically as a helically folded tetramer that resists aggregation. *Nature* **2011**, *477*, 107–110. [CrossRef] [PubMed]
78. Wang, W.; Perovic, I.; Chittuluru, J.; Kaganovich, A.; Nguyen, L.T.; Liao, J.; Auclair, J.R.; Johnson, D.; Landeru, A.; Simorellis, A.K.; et al. A soluble alpha-synuclein construct forms a dynamic tetramer. *Proc. Natl. Acad. Sci. USA* **2011**, *108*, 17797–17802. [CrossRef]
79. Dettmer, U.; Newman, A.J.; Luth, E.S.; Bartels, T.; Selkoe, D. In vivo cross-linking reveals principally oligomeric forms of alpha-synuclein and beta-synuclein in neurons and non-neural cells. *J. Biol. Chem.* **2013**, *288*, 6371–6385. [CrossRef]
80. Davidson, W.S.; Jonas, A.; Clayton, D.F.; George, J.M. Stabilization of alpha-synuclein secondary structure upon binding to synthetic membranes. *J. Biol. Chem.* **1998**, *273*, 9443–9449. [CrossRef]
81. Jo, E.; McLaurin, J.; Yip, C.M.; St George-Hyslop, P.; Fraser, P.E. Alpha-Synuclein membrane interactions and lipid specificity. *J. Biol. Chem.* **2000**, *275*, 34328–34334. [CrossRef]
82. Trexler, A.J.; Rhoades, E. Alpha-synuclein binds large unilamellar vesicles as an extended helix. *Biochemistry* **2009**, *48*, 2304–2306. [CrossRef] [PubMed]
83. Jao, C.C.; Der-Sarkissian, A.; Chen, J.; Langen, R. Structure of membrane-bound alpha-synuclein studied by site-directed spin labeling. *Proc. Natl. Acad. Sci. USA* **2004**, *101*, 8331–8336. [CrossRef] [PubMed]

84. Chandra, S.; Chen, X.; Rizo, J.; Jahn, R.; Sudhof, T.C. A broken alpha -helix in folded alpha -Synuclein. *J. Biol. Chem.* **2003**, *278*, 15313–15318. [CrossRef]
85. Drescher, M.; Veldhuis, G.; van Rooijen, B.D.; Milikisyants, S.; Subramaniam, V.; Huber, M. Antiparallel arrangement of the helices of vesicle-bound alpha-synuclein. *J. Am. Chem. Soc.* **2008**, *130*, 7796–7797. [CrossRef]
86. Sharon, R.; Goldberg, M.S.; Bar-Josef, I.; Betensky, R.A.; Shen, J.; Selkoe, D.J. alpha-Synuclein occurs in lipid-rich high molecular weight complexes, binds fatty acids, and shows homology to the fatty acid-binding proteins. *Proc. Natl. Acad. Sci. USA* **2001**, *98*, 9110–9115. [CrossRef]
87. Lucke, C.; Gantz, D.L.; Klimtchuk, E.; Hamilton, J.A. Interactions between fatty acids and alpha-synuclein. *J. Lipid Res.* **2006**, *47*, 1714–1724. [CrossRef] [PubMed]
88. Madine, J.; Doig, A.J.; Middleton, D.A. A study of the regional effects of alpha-synuclein on the organization and stability of phospholipid bilayers. *Biochemistry* **2006**, *45*, 5783–5792. [CrossRef]
89. Adamczyk, A.; Kacprzak, M.; Kazmierczak, A. Alpha-synuclein decreases arachidonic acid incorporation into rat striatal synaptoneurosomes. *Folia Neuropathol.* **2007**, *45*, 230–235. [PubMed]
90. Castagnet, P.I.; Golovko, M.Y.; Barcelo-Coblijn, G.C.; Nussbaum, R.L.; Murphy, E.J. Fatty acid incorporation is decreased in astrocytes cultured from alpha-synuclein gene-ablated mice. *J. Neurochem.* **2005**, *94*, 839–849. [CrossRef]
91. Barcelo-Coblijn, G.; Golovko, M.Y.; Weinhofer, I.; Berger, J.; Murphy, E.J. Brain neutral lipids mass is increased in alpha-synuclein gene-ablated mice. *J. Neurochem.* **2007**, *101*, 132–141. [CrossRef]
92. Alza, N.P.; Conde, M.A.; Scodelaro-Bilbao, P.G.; Salvador, G.A. Neutral lipids as early biomarkers of cellular fate: The case of alpha-synuclein overexpression. *Cell Death Dis.* **2021**, *12*, 52. [CrossRef]
93. Ruf, V.C.; Nubling, G.S.; Willikens, S.; Shi, S.; Schmidt, F.; Levin, J.; Botzel, K.; Kamp, F.; Giese, A. Different effects of alpha-synuclein mutants on lipid binding and aggregation detected by single molecule fluorescence spectroscopy and ThT fluorescence-based measurements. *ACS Chem. Neurosci.* **2019**, *10*, 1649–1659. [CrossRef]
94. Conde, M.A.; Alza, N.P.; Iglesias Gonzalez, P.A.; Scodelaro Bilbao, P.G.; Sanchez Campos, S.; Uranga, R.M.; Salvador, G.A. Phospholipase D1 downregulation by alpha-synuclein: Implications for neurodegeneration in Parkinson's disease. *Biochim. Biophys. Acta Mol. Cell Biol. Lipids* **2018**, *1863*, 639–650. [CrossRef]
95. Ahn, B.H.; Rhim, H.; Kim, S.Y.; Sung, Y.M.; Lee, M.Y.; Choi, J.Y.; Wolozin, B.; Chang, J.S.; Lee, Y.H.; Kwon, T.K.; et al. alpha-Synuclein interacts with phospholipase D isozymes and inhibits pervanadate-induced phospholipase D activation in human embryonic kidney-293 cells. *J. Biol. Chem.* **2002**, *277*, 12334–12342. [CrossRef] [PubMed]
96. Jenco, J.M.; Rawlingson, A.; Daniels, B.; Morris, A.J. Regulation of phospholipase D2: Selective inhibition of mammalian phospholipase D isoenzymes by alpha- and beta-synucleins. *Biochemistry* **1998**, *37*, 4901–4909. [CrossRef] [PubMed]
97. Payton, J.E.; Perrin, R.J.; Woods, W.S.; George, J.M. Structural determinants of PLD2 inhibition by alpha-synuclein. *J. Mol. Biol.* **2004**, *337*, 1001–1009. [CrossRef]
98. Rappley, I.; Gitler, A.D.; Selvy, P.E.; LaVoie, M.J.; Levy, B.D.; Brown, H.A.; Lindquist, S.; Selkoe, D.J. Evidence that alpha-synuclein does not inhibit phospholipase D. *Biochemistry* **2009**, *48*, 1077–1083. [CrossRef] [PubMed]
99. Ulmer, T.S.; Bax, A.; Cole, N.B.; Nussbaum, R.L. Structure and dynamics of micelle-bound human alpha-synuclein. *J. Biol. Chem.* **2005**, *280*, 9595–9603. [CrossRef] [PubMed]
100. Sode, K.; Ochiai, S.; Kobayashi, N.; Usuzaka, E. Effect of reparation of repeat sequences in the human alpha-synuclein on fibrillation ability. *Int. J. Biol. Sci.* **2006**, *3*, 1–7. [CrossRef]
101. Giasson, B.I.; Murray, I.V.; Trojanowski, J.Q.; Lee, V.M. A hydrophobic stretch of 12 amino acid residues in the middle of alpha-synuclein is essential for filament assembly. *J. Biol. Chem.* **2001**, *276*, 2380–2386. [CrossRef] [PubMed]
102. Rodriguez, J.A.; Ivanova, M.I.; Sawaya, M.R.; Cascio, D.; Reyes, F.E.; Shi, D.; Sangwan, S.; Guenther, E.L.; Johnson, L.M.; Zhang, M.; et al. Structure of the toxic core of alpha-synuclein from invisible crystals. *Nature* **2015**, *525*, 486–490. [CrossRef] [PubMed]
103. Longhena, F.; Faustini, G.; Missale, C.; Pizzi, M.; Spano, P.; Bellucci, A. The Contribution of alpha-Synuclein Spreading to Parkinson's Disease Synaptopathy. *Neural. Plast.* **2017**, *2017*, 5012129. [CrossRef]
104. Volpicelli-Daley, L.A.; Luk, K.C.; Patel, T.P.; Tanik, S.A.; Riddle, D.M.; Stieber, A.; Meaney, D.F.; Trojanowski, J.Q.; Lee, V.M. Exogenous alpha-synuclein fibrils induce Lewy body pathology leading to synaptic dysfunction and neuron death. *Neuron* **2011**, *72*, 57–71. [CrossRef] [PubMed]
105. Appel-Cresswell, S.; Vilarino-Guell, C.; Encarnacion, M.; Sherman, H.; Yu, I.; Shah, B.; Weir, D.; Thompson, C.; Szu-Tu, C.; Trinh, J.; et al. Alpha-synuclein p.H50Q, a novel pathogenic mutation for Parkinson's disease. *Mov. Disord.* **2013**, *28*, 811–813. [CrossRef]
106. Kiely, A.P.; Asi, Y.T.; Kara, E.; Limousin, P.; Ling, H.; Lewis, P.; Proukakis, C.; Quinn, N.; Lees, A.J.; Hardy, J.; et al. alpha-Synucleinopathy associated with G51D SNCA mutation: A link between Parkinson's disease and multiple system atrophy? *Acta Neuropathol.* **2013**, *125*, 753–769. [CrossRef] [PubMed]
107. Hoffman-Zacharska, D.; Koziorowski, D.; Ross, O.A.; Milewski, M.; Poznanski, J.A.; Jurek, M.; Wszolek, Z.K.; Soto-Ortolaza, A.; Awek, J.A.S.; Janik, P.; et al. Novel A18T and pA29S substitutions in alpha-synuclein may be associated with sporadic Parkinson's disease. *Parkinsonism Relat. Disord.* **2013**, *19*, 1057–1060. [CrossRef]
108. Conway, K.A.; Lee, S.J.; Rochet, J.C.; Ding, T.T.; Williamson, R.E.; Lansbury, P.T., Jr. Acceleration of oligomerization, not fibrillization, is a shared property of both alpha-synuclein mutations linked to early-onset Parkinson's disease: Implications for pathogenesis and therapy. *Proc. Natl. Acad. Sci. USA* **2000**, *97*, 571–576. [CrossRef]

109. Conway, K.A.; Harper, J.D.; Lansbury, P.T. Accelerated in vitro fibril formation by a mutant alpha-synuclein linked to early-onset Parkinson disease. *Nat. Med.* **1998**, *4*, 1318–1320. [CrossRef] [PubMed]
110. Bussell, R., Jr.; Eliezer, D. Residual structure and dynamics in Parkinson's disease-associated mutants of alpha-synuclein. *J. Biol. Chem.* **2001**, *276*, 45996–46003. [CrossRef]
111. Lazaro, D.F.; Rodrigues, E.F.; Langohr, R.; Shahpasandzadeh, H.; Ribeiro, T.; Guerreiro, P.; Gerhardt, E.; Krohnert, K.; Klucken, J.; Pereira, M.D.; et al. Systematic comparison of the effects of alpha-synuclein mutations on its oligomerization and aggregation. *PLoS Genet.* **2014**, *10*, e1004741. [CrossRef]
112. Fredenburg, R.A.; Rospigliosi, C.; Meray, R.K.; Kessler, J.C.; Lashuel, H.A.; Eliezer, D.; Lansbury, P.T., Jr. The impact of the E46K mutation on the properties of alpha-synuclein in its monomeric and oligomeric states. *Biochemistry* **2007**, *46*, 7107–7118. [CrossRef]
113. Rospigliosi, C.C.; McClendon, S.; Schmid, A.W.; Ramlall, T.F.; Barre, P.; Lashuel, H.A.; Eliezer, D. E46K Parkinson's-linked mutation enhances C-terminal-to-N-terminal contacts in alpha-synuclein. *J. Mol. Biol.* **2009**, *388*, 1022–1032. [CrossRef]
114. Khalaf, O.; Fauvet, B.; Oueslati, A.; Dikiy, I.; Mahul-Mellier, A.L.; Ruggeri, F.S.; Mbefo, M.K.; Vercruysse, F.; Dietler, G.; Lee, S.J.; et al. The H50Q mutation enhances alpha-synuclein aggregation, secretion, and toxicity. *J. Biol. Chem.* **2014**, *289*, 21856–21876. [CrossRef]
115. Sanjeev, A.; Mattaparthi, V.S.K. Computational investigation on the effects of H50Q and G51D mutations on the alpha-Synuclein aggregation propensity. *J. Biomol. Struct. Dyn.* **2018**, *36*, 2224–2236. [CrossRef]
116. Lesage, S.; Anheim, M.; Letournel, F.; Bousset, L.; Honore, A.; Rozas, N.; Pieri, L.; Madiona, K.; Durr, A.; Melki, R.; et al. G51D alpha-synuclein mutation causes a novel parkinsonian-pyramidal syndrome. *Ann. Neurol.* **2013**, *73*, 459–471. [CrossRef] [PubMed]
117. Rutherford, N.J.; Moore, B.D.; Golde, T.E.; Giasson, B.I. Divergent effects of the H50Q and G51D SNCA mutations on the aggregation of alpha-synuclein. *J. Neurochem.* **2014**, *131*, 859–867. [CrossRef]
118. Rutherford, N.J.; Giasson, B.I. The A53E alpha-synuclein pathological mutation demonstrates reduced aggregation propensity in vitro and in cell culture. *Neurosci. Lett.* **2015**, *597*, 43–48. [CrossRef] [PubMed]
119. Pasanen, P.; Myllykangas, L.; Siitonen, M.; Raunio, A.; Kaakkola, S.; Lyytinen, J.; Tienari, P.J.; Poyhonen, M.; Paetau, A. Novel alpha-synuclein mutation A53E associated with atypical multiple system atrophy and Parkinson's disease-type pathology. *Neurobiol. Aging* **2014**, *35*, 2180.e1. [CrossRef] [PubMed]
120. Ozawa, T.; Takano, H.; Onodera, O.; Kobayashi, H.; Ikeuchi, T.; Koide, R.; Okuizumi, K.; Shimohata, T.; Wakabayashi, K.; Takahashi, H.; et al. No mutation in the entire coding region of the alpha-synuclein gene in pathologically confirmed cases of multiple system atrophy. *Neurosci. Lett.* **1999**, *270*, 110–112. [CrossRef]
121. Narhi, L.; Wood, S.J.; Steavenson, S.; Jiang, Y.; Wu, G.M.; Anafi, D.; Kaufman, S.A.; Martin, F.; Sitney, K.; Denis, P.; et al. Both familial Parkinson's disease mutations accelerate alpha-synuclein aggregation. *J. Biol. Chem.* **1999**, *274*, 9843–9846. [CrossRef]
122. Pandey, N.; Schmidt, R.E.; Galvin, J.E. The alpha-synuclein mutation E46K promotes aggregation in cultured cells. *Exp. Neurol.* **2006**, *197*, 515–520. [CrossRef] [PubMed]
123. Smith, W.W.; Margolis, R.L.; Li, X.; Troncoso, J.C.; Lee, M.K.; Dawson, V.L.; Dawson, T.M.; Iwatsubo, T.; Ross, C.A. Alpha-synuclein phosphorylation enhances eosinophilic cytoplasmic inclusion formation in SH-SY5Y cells. *J. Neurosci.* **2005**, *25*, 5544–5552. [CrossRef] [PubMed]
124. Sugeno, N.; Takeda, A.; Hasegawa, T.; Kobayashi, M.; Kikuchi, A.; Mori, F.; Wakabayashi, K.; Itoyama, Y. Serine 129 phosphorylation of alpha-synuclein induces unfolded protein response-mediated cell death. *J. Biol. Chem.* **2008**, *283*, 23179–23188. [CrossRef] [PubMed]
125. Ma, M.R.; Hu, Z.W.; Zhao, Y.F.; Chen, Y.X.; Li, Y.M. Phosphorylation induces distinct alpha-synuclein strain formation. *Sci. Rep.* **2016**, *6*, 37130. [CrossRef]
126. Sato, H.; Arawaka, S.; Hara, S.; Fukushima, S.; Koga, K.; Koyama, S.; Kato, T. Authentically phosphorylated alpha-synuclein at Ser129 accelerates neurodegeneration in a rat model of familial Parkinson's disease. *J. Neurosci.* **2011**, *31*, 16884–16894. [CrossRef]
127. Chen, L.; Periquet, M.; Wang, X.; Negro, A.; McLean, P.J.; Hyman, B.T.; Feany, M.B. Tyrosine and serine phosphorylation of alpha-synuclein have opposing effects on neurotoxicity and soluble oligomer formation. *J. Clin. Investig.* **2009**, *119*, 3257–3265. [CrossRef] [PubMed]
128. Azeredo da Silveira, S.; Schneider, B.L.; Cifuentes-Diaz, C.; Sage, D.; Abbas-Terki, T.; Iwatsubo, T.; Unser, M.; Aebischer, P. Phosphorylation does not prompt, nor prevent, the formation of alpha-synuclein toxic species in a rat model of Parkinson's disease. *Hum. Mol. Genet.* **2009**, *18*, 872–887. [CrossRef]
129. Mbefo, M.K.; Paleologou, K.E.; Boucharaba, A.; Oueslati, A.; Schell, H.; Fournier, M.; Olschewski, D.; Yin, G.; Zweckstetter, M.; Masliah, E.; et al. Phosphorylation of synucleins by members of the Polo-like kinase family. *J. Biol. Chem.* **2010**, *285*, 2807–2822. [CrossRef]
130. Chen, L.; Feany, M.B. Alpha-synuclein phosphorylation controls neurotoxicity and inclusion formation in a Drosophila model of Parkinson disease. *Nat. Neurosci.* **2005**, *8*, 657–663. [CrossRef]
131. Paleologou, K.E.; Schmid, A.W.; Rospigliosi, C.C.; Kim, H.Y.; Lamberto, G.R.; Fredenburg, R.A.; Lansbury, P.T., Jr.; Fernandez, C.O.; Eliezer, D.; Zweckstetter, M.; et al. Phosphorylation at Ser-129 but not the phosphomimics S129E/D inhibits the fibrillation of alpha-synuclein. *J. Biol. Chem.* **2008**, *283*, 16895–16905. [CrossRef] [PubMed]

132. Wu, B.; Liu, Q.; Duan, C.; Li, Y.; Yu, S.; Chan, P.; Ueda, K.; Yang, H. Phosphorylation of alpha-synuclein upregulates tyrosine hydroxylase activity in MN9D cells. *Acta Histochem.* **2011**, *113*, 32–35. [CrossRef] [PubMed]
133. Kuwahara, T.; Tonegawa, R.; Ito, G.; Mitani, S.; Iwatsubo, T. Phosphorylation of alpha-synuclein protein at Ser-129 reduces neuronal dysfunction by lowering its membrane binding property in Caenorhabditis elegans. *J. Biol. Chem.* **2012**, *287*, 7098–7109. [CrossRef]
134. Anderson, J.P.; Walker, D.E.; Goldstein, J.M.; de Laat, R.; Banducci, K.; Caccavello, R.J.; Barbour, R.; Huang, J.; Kling, K.; Lee, M.; et al. Phosphorylation of Ser-129 is the dominant pathological modification of alpha-synuclein in familial and sporadic Lewy body disease. *J. Biol. Chem.* **2006**, *281*, 29739–29752. [CrossRef] [PubMed]
135. Fujiwara, H.; Hasegawa, M.; Dohmae, N.; Kawashima, A.; Masliah, E.; Goldberg, M.S.; Shen, J.; Takio, K.; Iwatsubo, T. alpha-Synuclein is phosphorylated in synucleinopathy lesions. *Nat. Cell Biol.* **2002**, *4*, 160–164. [CrossRef] [PubMed]
136. Sato, H.; Kato, T.; Arawaka, S. The role of Ser129 phosphorylation of alpha-synuclein in neurodegeneration of Parkinson's disease: A review of in vivo models. *Rev. Neurosci.* **2013**, *24*, 115–123. [CrossRef]
137. Walker, D.G.; Lue, L.F.; Adler, C.H.; Shill, H.A.; Caviness, J.N.; Sabbagh, M.N.; Akiyama, H.; Serrano, G.E.; Sue, L.I.; Beach, T.G. Changes in properties of serine 129 phosphorylated alpha-synuclein with progression of Lewy-type histopathology in human brains. *Exp. Neurol.* **2013**, *240*, 190–204. [CrossRef]
138. Paleologou, K.E.; Oueslati, A.; Shakked, G.; Rospigliosi, C.C.; Kim, H.Y.; Lamberto, G.R.; Fernandez, C.O.; Schmid, A.; Chegini, F.; Gai, W.P.; et al. Phosphorylation at S87 is enhanced in synucleinopathies, inhibits alpha-synuclein oligomerization, and influences synuclein-membrane interactions. *J. Neurosci.* **2010**, *30*, 3184–3198. [CrossRef]
139. Xu, Y.; Deng, Y.; Qing, H. The phosphorylation of alpha-synuclein: Development and implication for the mechanism and therapy of the Parkinson's disease. *J. Neurochem.* **2015**, *135*, 4–18. [CrossRef]
140. Lu, Y.; Prudent, M.; Fauvet, B.; Lashuel, H.A.; Girault, H.H. Phosphorylation of alpha-Synuclein at Y125 and S129 alters its metal binding properties: Implications for understanding the role of alpha-Synuclein in the pathogenesis of Parkinson's Disease and related disorders. *ACS Chem. Neurosci.* **2011**, *2*, 667–675. [CrossRef]
141. Fayyad, M.; Erskine, D.; Majbour, N.K.; Vaikath, N.N.; Ghanem, S.S.; Sudhakaran, I.P.; Abdesselem, H.; Lamprokostopoulou, A.; Vekrellis, K.; Morris, C.M.; et al. Investigating the presence of doubly phosphorylated alpha-synuclein at tyrosine 125 and serine 129 in idiopathic Lewy body diseases. *Brain Pathol.* **2020**, *30*, 831–843. [CrossRef] [PubMed]
142. Giasson, B.I.; Duda, J.E.; Murray, I.V.; Chen, Q.; Souza, J.M.; Hurtig, H.I.; Ischiropoulos, H.; Trojanowski, J.Q.; Lee, V.M. Oxidative damage linked to neurodegeneration by selective alpha-synuclein nitration in synucleinopathy lesions. *Science* **2000**, *290*, 985–989. [CrossRef] [PubMed]
143. Danielson, S.R.; Held, J.M.; Schilling, B.; Oo, M.; Gibson, B.W.; Andersen, J.K. Preferentially increased nitration of alpha-synuclein at tyrosine-39 in a cellular oxidative model of Parkinson's disease. *Anal. Chem.* **2009**, *81*, 7823–7828. [CrossRef]
144. McCormack, A.L.; Mak, S.K.; Di Monte, D.A. Increased alpha-synuclein phosphorylation and nitration in the aging primate substantia nigra. *Cell Death Dis.* **2012**, *3*, e315. [CrossRef] [PubMed]
145. Yu, Z.; Xu, X.; Xiang, Z.; Zhou, J.; Zhang, Z.; Hu, C.; He, C. Nitrated alpha-synuclein induces the loss of dopaminergic neurons in the substantia nigra of rats. *PLoS ONE* **2010**, *5*, e9956. [CrossRef]
146. Souza, J.M.; Peluffo, G.; Radi, R. Protein tyrosine nitration—Functional alteration or just a biomarker? *Free Radic. Biol. Med.* **2008**, *45*, 357–366. [CrossRef]
147. Hodara, R.; Norris, E.H.; Giasson, B.I.; Mishizen-Eberz, A.J.; Lynch, D.R.; Lee, V.M.; Ischiropoulos, H. Functional consequences of alpha-synuclein tyrosine nitration: Diminished binding to lipid vesicles and increased fibril formation. *J. Biol. Chem.* **2004**, *279*, 47746–47753. [CrossRef] [PubMed]
148. Takahashi, T.; Yamashita, H.; Nakamura, T.; Nagano, Y.; Nakamura, S. Tyrosine 125 of alpha-synuclein plays a critical role for dimerization following nitrative stress. *Brain Res.* **2002**, *938*, 73–80. [CrossRef]
149. Souza, J.M.; Giasson, B.I.; Chen, Q.; Lee, V.M.; Ischiropoulos, H. Dityrosine cross-linking promotes formation of stable alpha -synuclein polymers. Implication of nitrative and oxidative stress in the pathogenesis of neurodegenerative synucleinopathies. *J. Biol. Chem.* **2000**, *275*, 18344–18349. [CrossRef]
150. Fernandez, E.; Garcia-Moreno, J.M.; Martin de Pablos, A.; Chacon, J. May the evaluation of nitrosative stress through selective increase of 3-nitrotyrosine proteins other than nitroalbumin and dominant tyrosine-125/136 nitrosylation of serum alpha-synuclein serve for diagnosis of sporadic Parkinson's disease? *Antioxid. Redox. Signal.* **2013**, *19*, 912–918. [CrossRef]
151. Grice, G.L.; Nathan, J.A. The recognition of ubiquitinated proteins by the proteasome. *Cell Mol. Life Sci.* **2016**, *73*, 3497–3506. [CrossRef]
152. Pickart, C.M.; Eddins, M.J. Ubiquitin: Structures, functions, mechanisms. *Biochim. Biophys. Acta* **2004**, *1695*, 55–72. [CrossRef]
153. Tofaris, G.K.; Razzaq, A.; Ghetti, B.; Lilley, K.S.; Spillantini, M.G. Ubiquitination of alpha-synuclein in Lewy bodies is a pathological event not associated with impairment of proteasome function. *J. Biol. Chem.* **2003**, *278*, 44405–44411. [CrossRef]
154. Hasegawa, M.; Fujiwara, H.; Nonaka, T.; Wakabayashi, K.; Takahashi, H.; Lee, V.M.; Trojanowski, J.Q.; Mann, D.; Iwatsubo, T. Phosphorylated alpha-synuclein is ubiquitinated in alpha-synucleinopathy lesions. *J. Biol. Chem.* **2002**, *277*, 49071–49076. [CrossRef]
155. Liani, E.; Eyal, A.; Avraham, E.; Shemer, R.; Szargel, R.; Berg, D.; Bornemann, A.; Riess, O.; Ross, C.A.; Rott, R.; et al. Ubiquitylation of synphilin-1 and alpha-synuclein by SIAH and its presence in cellular inclusions and Lewy bodies imply a role in Parkinson's disease. *Proc. Natl. Acad. Sci. USA* **2004**, *101*, 5500–5505. [CrossRef]

156. Shin, Y.; Klucken, J.; Patterson, C.; Hyman, B.T.; McLean, P.J. The co-chaperone carboxyl terminus of Hsp70-interacting protein (CHIP) mediates alpha-synuclein degradation decisions between proteasomal and lysosomal pathways. *J. Biol. Chem.* **2005**, *280*, 23727–23734. [CrossRef] [PubMed]
157. Tofaris, G.K.; Kim, H.T.; Hourez, R.; Jung, J.W.; Kim, K.P.; Goldberg, A.L. Ubiquitin ligase Nedd4 promotes alpha-synuclein degradation by the endosomal-lysosomal pathway. *Proc. Natl. Acad. Sci. USA* **2011**, *108*, 17004–17009. [CrossRef] [PubMed]
158. Lee, J.T.; Wheeler, T.C.; Li, L.; Chin, L.S. Ubiquitination of alpha-synuclein by Siah-1 promotes alpha-synuclein aggregation and apoptotic cell death. *Hum. Mol. Genet.* **2008**, *17*, 906–917. [CrossRef] [PubMed]
159. Rott, R.; Szargel, R.; Haskin, J.; Shani, V.; Shainskaya, A.; Manov, I.; Liani, E.; Avraham, E.; Engelender, S. Monoubiquitylation of alpha-synuclein by seven in absentia homolog (SIAH) promotes its aggregation in dopaminergic cells. *J. Biol. Chem.* **2008**, *283*, 3316–3328. [CrossRef]
160. Kalia, L.V.; Kalia, S.K.; Chau, H.; Lozano, A.M.; Hyman, B.T.; McLean, P.J. Ubiquitinylation of alpha-synuclein by carboxyl terminus Hsp70-interacting protein (CHIP) is regulated by Bcl-2-associated athanogene 5 (BAG5). *PLoS ONE* **2011**, *6*, e14695. [CrossRef] [PubMed]
161. Meier, F.; Abeywardana, T.; Dhall, A.; Marotta, N.P.; Varkey, J.; Langen, R.; Chatterjee, C.; Pratt, M.R. Semisynthetic, site-specific ubiquitin modification of alpha-synuclein reveals differential effects on aggregation. *J. Am. Chem. Soc.* **2012**, *134*, 5468–5471. [CrossRef] [PubMed]
162. Weetman, J.; Wong, M.B.; Sharry, S.; Rcom-H'cheo-Gauthier, A.; Gai, W.P.; Meedeniya, A.; Pountney, D.L. Increased SUMO-1 expression in the unilateral rotenone-lesioned mouse model of Parkinson's disease. *Neurosci. Lett.* **2013**, *544*, 119–124. [CrossRef] [PubMed]
163. Wong, M.B.; Goodwin, J.; Norazit, A.; Meedeniya, A.C.; Richter-Landsberg, C.; Gai, W.P.; Pountney, D.L. SUMO-1 is associated with a subset of lysosomes in glial protein aggregate diseases. *Neurotox. Res.* **2013**, *23*, 1–21. [CrossRef]
164. Pountney, D.L.; Chegini, F.; Shen, X.; Blumbergs, P.C.; Gai, W.P. SUMO-1 marks subdomains within glial cytoplasmic inclusions of multiple system atrophy. *Neurosci. Lett.* **2005**, *381*, 74–79. [CrossRef]
165. Rott, R.; Szargel, R.; Shani, V.; Hamza, H.; Savyon, M.; Abd Elghani, F.; Bandopadhyay, R.; Engelender, S. SUMOylation and ubiquitination reciprocally regulate alpha-synuclein degradation and pathological aggregation. *Proc. Natl. Acad. Sci. USA* **2017**, *114*, 13176–13181. [CrossRef]
166. Abeywardana, T.; Pratt, M.R. Extent of inhibition of alpha-synuclein aggregation in vitro by SUMOylation is conjugation site- and SUMO isoform-selective. *Biochemistry* **2015**, *54*, 959–961. [CrossRef] [PubMed]
167. Krumova, P.; Meulmeester, E.; Garrido, M.; Tirard, M.; Hsiao, H.H.; Bossis, G.; Urlaub, H.; Zweckstetter, M.; Kugler, S.; Melchior, F.; et al. Sumoylation inhibits alpha-synuclein aggregation and toxicity. *J. Cell Biol.* **2011**, *194*, 49–60. [CrossRef]
168. Vinueza-Gavilanes, R.; Inigo-Marco, I.; Larrea, L.; Lasa, M.; Carte, B.; Santamaria, E.; Fernandez-Irigoyen, J.; Bugallo, R.; Aragon, T.; Aldabe, R.; et al. N-terminal acetylation mutants affect alpha-synuclein stability, protein levels and neuronal toxicity. *Neurobiol. Dis.* **2020**, *137*, 104781. [CrossRef] [PubMed]
169. Iyer, A.; Roeters, S.J.; Schilderink, N.; Hommersom, B.; Heeren, R.M.; Woutersen, S.; Claessens, M.M.; Subramaniam, V. The impact of N-terminal acetylation of alpha-synuclein on phospholipid membrane binding and fibril structure. *J. Biol. Chem.* **2016**, *291*, 21110–21122. [CrossRef]
170. Kang, L.; Moriarty, G.M.; Woods, L.A.; Ashcroft, A.E.; Radford, S.E.; Baum, J. N-terminal acetylation of alpha-synuclein induces increased transient helical propensity and decreased aggregation rates in the intrinsically disordered monomer. *Protein Sci.* **2012**, *21*, 911–917. [CrossRef]
171. Runfola, M.; De Simone, A.; Vendruscolo, M.; Dobson, C.M.; Fusco, G. The N-terminal acetylation of alpha-synuclein changes the affinity for lipid membranes but not the structural properties of the bound state. *Sci. Rep.* **2020**, *10*, 204. [CrossRef] [PubMed]
172. Bu, B.; Tong, X.; Li, D.; Hu, Y.; He, W.; Zhao, C.; Hu, R.; Li, X.; Shao, Y.; Liu, C.; et al. N-terminal acetylation preserves alpha-synuclein from oligomerization by blocking intermolecular hydrogen bonds. *ACS Chem. Neurosci.* **2017**, *8*, 2145–2151. [CrossRef] [PubMed]
173. Bartels, T.; Kim, N.C.; Luth, E.S.; Selkoe, D.J. N-alpha-acetylation of alpha-synuclein increases its helical folding propensity, GM1 binding specificity and resistance to aggregation. *PLoS ONE* **2014**, *9*, e103727. [CrossRef]
174. Wang, S.; Yang, F.; Petyuk, V.A.; Shukla, A.K.; Monroe, M.E.; Gritsenko, M.A.; Rodland, K.D.; Smith, R.D.; Qian, W.J.; Gong, C.X.; et al. Quantitative proteomics identifies altered O-GlcNAcylation of structural, synaptic and memory-associated proteins in Alzheimer's disease. *J. Pathol.* **2017**, *243*, 78–88. [CrossRef]
175. Alfaro, J.F.; Gong, C.X.; Monroe, M.E.; Aldrich, J.T.; Clauss, T.R.; Purvine, S.O.; Wang, Z.; Camp, D.G., 2nd; Shabanowitz, J.; Stanley, P.; et al. Tandem mass spectrometry identifies many mouse brain O-GlcNAcylated proteins including EGF domain-specific O-GlcNAc transferase targets. *Proc. Natl. Acad. Sci. USA* **2012**, *109*, 7280–7285. [CrossRef] [PubMed]
176. Morris, M.; Knudsen, G.M.; Maeda, S.; Trinidad, J.C.; Ioanoviciu, A.; Burlingame, A.L.; Mucke, L. Tau post-translational modifications in wild-type and human amyloid precursor protein transgenic mice. *Nat. Neurosci.* **2015**, *18*, 1183–1189. [CrossRef] [PubMed]
177. Wang, Z.; Park, K.; Comer, F.; Hsieh-Wilson, L.C.; Saudek, C.D.; Hart, G.W. Site-specific GlcNAcylation of human erythrocyte proteins: Potential biomarker(s) for diabetes. *Diabetes* **2009**, *58*, 309–317. [CrossRef]

178. Wang, Z.; Udeshi, N.D.; O'Malley, M.; Shabanowitz, J.; Hunt, D.F.; Hart, G.W. Enrichment and site mapping of O-linked N-acetylglucosamine by a combination of chemical/enzymatic tagging, photochemical cleavage, and electron transfer dissociation mass spectrometry. *Mol. Cell Proteom.* **2010**, *9*, 153–160. [CrossRef]
179. Zhang, J.; Lei, H.; Chen, Y.; Ma, Y.T.; Jiang, F.; Tan, J.; Zhang, Y.; Li, J.D. Enzymatic O-GlcNAcylation of alpha-synuclein reduces aggregation and increases SDS-resistant soluble oligomers. *Neurosci. Lett.* **2017**, *655*, 90–94. [CrossRef]
180. Levine, P.M.; Galesic, A.; Balana, A.T.; Mahul-Mellier, A.L.; Navarro, M.X.; De Leon, C.A.; Lashuel, H.A.; Pratt, M.R. alpha-Synuclein O-GlcNAcylation alters aggregation and toxicity, revealing certain residues as potential inhibitors of Parkinson's disease. *Proc. Natl. Acad. Sci. USA* **2019**, *116*, 1511–1519. [CrossRef]
181. Lewis, Y.E.; Galesic, A.; Levine, P.M.; De Leon, C.A.; Lamiri, N.; Brennan, C.K.; Pratt, M.R. O-GlcNAcylation of alpha-synuclein at serine 87 reduces aggregation without affecting membrane binding. *ACS Chem. Biol.* **2017**, *12*, 1020–1027. [CrossRef] [PubMed]
182. Marotta, N.P.; Lin, Y.H.; Lewis, Y.E.; Ambroso, M.R.; Zaro, B.W.; Roth, M.T.; Arnold, D.B.; Langen, R.; Pratt, M.R. O-GlcNAc modification blocks the aggregation and toxicity of the protein alpha-synuclein associated with Parkinson's disease. *Nat. Chem.* **2015**, *7*, 913–920. [CrossRef] [PubMed]
183. Li, W.; West, N.; Colla, E.; Pletnikova, O.; Troncoso, J.C.; Marsh, L.; Dawson, T.M.; Jakala, P.; Hartmann, T.; Price, D.L.; et al. Aggregation promoting C-terminal truncation of alpha-synuclein is a normal cellular process and is enhanced by the familial Parkinson's disease-linked mutations. *Proc. Natl. Acad. Sci. USA* **2005**, *102*, 2162–2167. [CrossRef]
184. Kellie, J.F.; Higgs, R.E.; Ryder, J.W.; Major, A.; Beach, T.G.; Adler, C.H.; Merchant, K.; Knierman, M.D. Quantitative measurement of intact alpha-synuclein proteoforms from post-mortem control and Parkinson's disease brain tissue by intact protein mass spectrometry. *Sci. Rep.* **2014**, *4*, 5797. [CrossRef]
185. Baba, M.; Nakajo, S.; Tu, P.H.; Tomita, T.; Nakaya, K.; Lee, V.M.; Trojanowski, J.Q.; Iwatsubo, T. Aggregation of alpha-synuclein in Lewy bodies of sporadic Parkinson's disease and dementia with Lewy bodies. *Am. J. Pathol.* **1998**, *152*, 879–884.
186. Ulusoy, A.; Febbraro, F.; Jensen, P.H.; Kirik, D.; Romero-Ramos, M. Co-expression of C-terminal truncated alpha-synuclein enhances full-length alpha-synuclein-induced pathology. *Eur. J. Neurosci.* **2010**, *32*, 409–422. [CrossRef] [PubMed]
187. Hall, K.; Yang, S.; Sauchanka, O.; Spillantini, M.G.; Anichtchik, O. Behavioural deficits in transgenic mice expressing human truncated (1-120 amino acid) alpha-synuclein. *Exp. Neurol.* **2015**, *264*, 8–13. [CrossRef] [PubMed]
188. Wang, W.; Nguyen, L.T.; Burlak, C.; Chegini, F.; Guo, F.; Chataway, T.; Ju, S.; Fisher, O.S.; Miller, D.W.; Datta, D.; et al. Caspase-1 causes truncation and aggregation of the Parkinson's disease-associated protein alpha-synuclein. *Proc. Natl. Acad. Sci. USA* **2016**, *113*, 9587–9592. [CrossRef]
189. Iyer, A.; Roeters, S.J.; Kogan, V.; Woutersen, S.; Claessens, M.; Subramaniam, V. C-terminal truncated alpha-synuclein fibrils contain strongly twisted beta-sheets. *J. Am. Chem. Soc.* **2017**, *139*, 15392–15400. [CrossRef]
190. Ma, L.; Yang, C.; Zhang, X.; Li, Y.; Wang, S.; Zheng, L.; Huang, K. C-terminal truncation exacerbates the aggregation and cytotoxicity of alpha-Synuclein: A vicious cycle in Parkinson's disease. *Biochim. Biophys. Acta Mol. Basis Dis.* **2018**, *1864*, 3714–3725. [CrossRef] [PubMed]
191. Terada, M.; Suzuki, G.; Nonaka, T.; Kametani, F.; Tamaoka, A.; Hasegawa, M. The effect of truncation on prion-like properties of alpha-synuclein. *J. Biol. Chem.* **2018**, *293*, 13910–13920. [CrossRef] [PubMed]
192. Tofaris, G.K.; Garcia Reitbock, P.; Humby, T.; Lambourne, S.L.; O'Connell, M.; Ghetti, B.; Gossage, H.; Emson, P.C.; Wilkinson, L.S.; Goedert, M.; et al. Pathological changes in dopaminergic nerve cells of the substantia nigra and olfactory bulb in mice transgenic for truncated human alpha-synuclein(1-120): Implications for Lewy body disorders. *J. Neurosci.* **2006**, *26*, 3942–3950. [CrossRef] [PubMed]
193. Hoyer, W.; Cherny, D.; Subramaniam, V.; Jovin, T.M. Impact of the acidic C-terminal region comprising amino acids 109-140 on alpha-synuclein aggregation in vitro. *Biochemistry* **2004**, *43*, 16233–16242. [CrossRef] [PubMed]
194. Murray, I.V.; Giasson, B.I.; Quinn, S.M.; Koppaka, V.; Axelsen, P.H.; Ischiropoulos, H.; Trojanowski, J.Q.; Lee, V.M. Role of alpha-synuclein carboxy-terminus on fibril formation in vitro. *Biochemistry* **2003**, *42*, 8530–8540. [CrossRef] [PubMed]
195. Tsigelny, I.F.; Sharikov, Y.; Wrasidlo, W.; Gonzalez, T.; Desplats, P.A.; Crews, L.; Spencer, B.; Masliah, E. Role of alpha-synuclein penetration into the membrane in the mechanisms of oligomer pore formation. *FEBS J.* **2012**, *279*, 1000–1013. [CrossRef] [PubMed]
196. Fantini, J.; Yahi, N. The driving force of alpha-synuclein insertion and amyloid channel formation in the plasma membrane of neural cells: Key role of ganglioside- and cholesterol-binding domains. *Adv. Exp. Med. Biol.* **2013**, *991*, 15–26. [CrossRef] [PubMed]
197. Zakharov, S.D.; Hulleman, J.D.; Dutseva, E.A.; Antonenko, Y.N.; Rochet, J.C.; Cramer, W.A. Helical alpha-synuclein forms highly conductive ion channels. *Biochemistry* **2007**, *46*, 14369–14379. [CrossRef] [PubMed]
198. Quist, A.; Doudevski, I.; Lin, H.; Azimova, R.; Ng, D.; Frangione, B.; Kagan, B.; Ghiso, J.; Lal, R. Amyloid ion channels: A common structural link for protein-misfolding disease. *Proc. Natl. Acad. Sci. USA* **2005**, *102*, 10427–10432. [CrossRef]
199. Volles, M.J.; Lansbury, P.T., Jr. Vesicle permeabilization by protofibrillar alpha-synuclein is sensitive to Parkinson's disease-linked mutations and occurs by a pore-like mechanism. *Biochemistry* **2002**, *41*, 4595–4602. [CrossRef]
200. Stockl, M.T.; Zijlstra, N.; Subramaniam, V. alpha-Synuclein oligomers: An amyloid pore? Insights into mechanisms of alpha-synuclein oligomer-lipid interactions. *Mol. Neurobiol.* **2013**, *47*, 613–621. [CrossRef]
201. Di Pasquale, E.; Fantini, J.; Chahinian, H.; Maresca, M.; Taieb, N.; Yahi, N. Altered ion channel formation by the Parkinson's-disease-linked E46K mutant of alpha-synuclein is corrected by GM3 but not by GM1 gangliosides. *J. Mol. Biol.* **2010**, *397*, 202–218. [CrossRef] [PubMed]

202. Furukawa, K.; Matsuzaki-Kobayashi, M.; Hasegawa, T.; Kikuchi, A.; Sugeno, N.; Itoyama, Y.; Wang, Y.; Yao, P.J.; Bushlin, I.; Takeda, A. Plasma membrane ion permeability induced by mutant alpha-synuclein contributes to the degeneration of neural cells. *J. Neurochem.* **2006**, *97*, 1071–1077. [CrossRef]
203. Feng, L.R.; Federoff, H.J.; Vicini, S.; Maguire-Zeiss, K.A. Alpha-synuclein mediates alterations in membrane conductance: A potential role for alpha-synuclein oligomers in cell vulnerability. *Eur. J. Neurosci.* **2010**, *32*, 10–17. [CrossRef]
204. Schmidt, F.; Levin, J.; Kamp, F.; Kretzschmar, H.; Giese, A.; Botzel, K. Single-channel electrophysiology reveals a distinct and uniform pore complex formed by alpha-synuclein oligomers in lipid membranes. *PLoS ONE* **2012**, *7*, e42545. [CrossRef]
205. Mironov, S.L. alpha-Synuclein forms non-selective cation channels and stimulates ATP-sensitive potassium channels in hippocampal neurons. *J. Physiol.* **2015**, *593*, 145–159. [CrossRef]
206. Shrivastava, A.N.; Redeker, V.; Fritz, N.; Pieri, L.; Almeida, L.G.; Spolidoro, M.; Liebmann, T.; Bousset, L.; Renner, M.; Lena, C.; et al. Alpha-synuclein assemblies sequester neuronal alpha3-Na+/K+-ATPase and impair Na+ gradient. *EMBO J.* **2015**, *34*, 2408–2423. [CrossRef]
207. Ronzitti, G.; Bucci, G.; Emanuele, M.; Leo, D.; Sotnikova, T.D.; Mus, L.V.; Soubrane, C.H.; Dallas, M.L.; Thalhammer, A.; Cingolani, L.A.; et al. Exogenous alpha-synuclein decreases raft partitioning of Cav2.2 channels inducing dopamine release. *J. Neurosci.* **2014**, *34*, 10603–10615. [CrossRef] [PubMed]
208. Ritz, B.; Rhodes, S.L.; Qian, L.; Schernhammer, E.; Olsen, J.H.; Friis, S. L-type calcium channel blockers and Parkinson disease in Denmark. *Ann. Neurol.* **2010**, *67*, 600–606. [CrossRef] [PubMed]
209. Pasternak, B.; Svanstrom, H.; Nielsen, N.M.; Fugger, L.; Melbye, M.; Hviid, A. Use of calcium channel blockers and Parkinson's disease. *Am. J. Epidemiol.* **2012**, *175*, 627–635. [CrossRef] [PubMed]
210. Chan, C.S.; Guzman, J.N.; Ilijic, E.; Mercer, J.N.; Rick, C.; Tkatch, T.; Meredith, G.E.; Surmeier, D.J. 'Rejuvenation' protects neurons in mouse models of Parkinson's disease. *Nature* **2007**, *447*, 1081–1086. [CrossRef]
211. Singh, A.; Verma, P.; Balaji, G.; Samantaray, S.; Mohanakumar, K.P. Nimodipine, an L-type calcium channel blocker attenuates mitochondrial dysfunctions to protect against 1-methyl-4-phenyl-1,2,3,6-tetrahydropyridine-induced Parkinsonism in mice. *Neurochem. Int.* **2016**, *99*, 221–232. [CrossRef] [PubMed]
212. McGranahan, T.M.; Patzlaff, N.E.; Grady, S.R.; Heinemann, S.F.; Booker, T.K. alpha4beta2 nicotinic acetylcholine receptors on dopaminergic neurons mediate nicotine reward and anxiety relief. *J. Neurosci.* **2011**, *31*, 10891–10902. [CrossRef]
213. Swant, J.; Goodwin, J.S.; North, A.; Ali, A.A.; Gamble-George, J.; Chirwa, S.; Khoshbouei, H. alpha-Synuclein stimulates a dopamine transporter-dependent chloride current and modulates the activity of the transporter. *J. Biol. Chem.* **2011**, *286*, 43933–43943. [CrossRef]
214. Butler, B.; Saha, K.; Rana, T.; Becker, J.P.; Sambo, D.; Davari, P.; Goodwin, J.S.; Khoshbouei, H. Dopamine transporter activity is modulated by alpha-synuclein. *J. Biol. Chem.* **2015**, *290*, 29542–29554. [CrossRef] [PubMed]
215. Sidhu, A.; Wersinger, C.; Vernier, P. alpha-Synuclein regulation of the dopaminergic transporter: A possible role in the pathogenesis of Parkinson's disease. *FEBS Lett.* **2004**, *565*, 1–5. [CrossRef]
216. Dean, E.D.; Li, Y.; Torres, G.E.; Miller, G.W. Identification of a novel interaction between α-synuclein and VMAT2. *FASEB J.* **2008**, *22*, 715.6.
217. Guo, J.T.; Chen, A.Q.; Kong, Q.; Zhu, H.; Ma, C.M.; Qin, C. Inhibition of vesicular monoamine transporter-2 activity in alpha-synuclein stably transfected SH-SY5Y cells. *Cell Mol. Neurobiol.* **2008**, *28*, 35–47. [CrossRef] [PubMed]
218. Perez, R.G.; Waymire, J.C.; Lin, E.; Liu, J.J.; Guo, F.; Zigmond, M.J. A role for alpha-synuclein in the regulation of dopamine biosynthesis. *J. Neurosci.* **2002**, *22*, 3090–3099. [CrossRef]
219. Baptista, M.J.; O'Farrell, C.; Daya, S.; Ahmad, R.; Miller, D.W.; Hardy, J.; Farrer, M.J.; Cookson, M.R. Co-ordinate transcriptional regulation of dopamine synthesis genes by alpha-synuclein in human neuroblastoma cell lines. *J. Neurochem.* **2003**, *85*, 957–968. [CrossRef] [PubMed]
220. Yu, S.; Zuo, X.; Li, Y.; Zhang, C.; Zhou, M.; Zhang, Y.A.; Ueda, K.; Chan, P. Inhibition of tyrosine hydroxylase expression in alpha-synuclein-transfected dopaminergic neuronal cells. *Neurosci. Lett.* **2004**, *367*, 34–39. [CrossRef]
221. Li, Y.H.; Gao, N.; Ye, Y.W.; Li, X.; Yu, S.; Yang, H.; Ueda, K.; Chan, P. Alpha-synuclein functions as a negative regulator for expression of tyrosine hydroxylase. *Acta Neurol. Belg.* **2011**, *111*, 130–135. [PubMed]
222. Liu, D.; Jin, L.; Wang, H.; Zhao, H.; Zhao, C.; Duan, C.; Lu, L.; Wu, B.; Yu, S.; Chan, P.; et al. Silencing alpha-synuclein gene expression enhances tyrosine hydroxylase activity in MN9D cells. *Neurochem. Res.* **2008**, *33*, 1401–1409. [CrossRef]
223. Peng, X.; Tehranian, R.; Dietrich, P.; Stefanis, L.; Perez, R.G. Alpha-synuclein activation of protein phosphatase 2A reduces tyrosine hydroxylase phosphorylation in dopaminergic cells. *J. Cell Sci.* **2005**, *118*, 3523–3530. [CrossRef]
224. Alerte, T.N.; Akinfolarin, A.A.; Friedrich, E.E.; Mader, S.A.; Hong, C.S.; Perez, R.G. Alpha-synuclein aggregation alters tyrosine hydroxylase phosphorylation and immunoreactivity: Lessons from viral transduction of knockout mice. *Neurosci. Lett.* **2008**, *435*, 24–29. [CrossRef]
225. Lou, H.; Montoya, S.E.; Alerte, T.N.; Wang, J.; Wu, J.; Peng, X.; Hong, C.S.; Friedrich, E.E.; Mader, S.A.; Pedersen, C.J.; et al. Serine 129 phosphorylation reduces the ability of alpha-synuclein to regulate tyrosine hydroxylase and protein phosphatase 2A in vitro and in vivo. *J. Biol. Chem.* **2010**, *285*, 17648–17661. [CrossRef] [PubMed]
226. Chu, Y.; Kordower, J.H. Age-associated increases of alpha-synuclein in monkeys and humans are associated with nigrostriatal dopamine depletion: Is this the target for Parkinson's disease? *Neurobiol. Dis.* **2007**, *25*, 134–149. [CrossRef] [PubMed]

227. Chadchankar, H.; Ihalainen, J.; Tanila, H.; Yavich, L. Decreased reuptake of dopamine in the dorsal striatum in the absence of alpha-synuclein. *Brain Res.* **2011**, *1382*, 37–44. [CrossRef]
228. Al-Wandi, A.; Ninkina, N.; Millership, S.; Williamson, S.J.; Jones, P.A.; Buchman, V.L. Absence of alpha-synuclein affects dopamine metabolism and synaptic markers in the striatum of aging mice. *Neurobiol. Aging* **2010**, *31*, 796–804. [CrossRef]
229. Robertson, D.C.; Schmidt, O.; Ninkina, N.; Jones, P.A.; Sharkey, J.; Buchman, V.L. Developmental loss and resistance to MPTP toxicity of dopaminergic neurones in substantia nigra pars compacta of gamma-synuclein, alpha-synuclein and double alpha/gamma-synuclein null mutant mice. *J. Neurochem.* **2004**, *89*, 1126–1136. [CrossRef] [PubMed]
230. Shen, J.; Du, T.; Wang, X.; Duan, C.; Gao, G.; Zhang, J.; Lu, L.; Yang, H. alpha-Synuclein amino terminus regulates mitochondrial membrane permeability. *Brain Res.* **2014**, *1591*, 14–26. [CrossRef] [PubMed]
231. Nakamura, K.; Nemani, V.M.; Azarbal, F.; Skibinski, G.; Levy, J.M.; Egami, K.; Munishkina, L.; Zhang, J.; Gardner, B.; Wakabayashi, J.; et al. Direct membrane association drives mitochondrial fission by the Parkinson disease-associated protein alpha-synuclein. *J. Biol. Chem.* **2011**, *286*, 20710–20726. [CrossRef] [PubMed]
232. Robotta, M.; Gerding, H.R.; Vogel, A.; Hauser, K.; Schildknecht, S.; Karreman, C.; Leist, M.; Subramaniam, V.; Drescher, M. Alpha-synuclein binds to the inner membrane of mitochondria in an alpha-helical conformation. *ChemBioChem* **2014**, *15*, 2499–2502. [CrossRef] [PubMed]
233. Faustini, G.; Marchesan, E.; Zonta, L.; Bono, F.; Bottani, E.; Longhena, F.; Ziviani, E.; Valerio, A.; Bellucci, A. Alpha-synuclein preserves mitochondrial fusion and function in neuronal cells. *Oxid. Med. Cell Longev.* **2019**, *2019*, 4246350. [CrossRef]
234. Ellis, C.E.; Murphy, E.J.; Mitchell, D.C.; Golovko, M.Y.; Scaglia, F.; Barcelo-Coblijn, G.C.; Nussbaum, R.L. Mitochondrial lipid abnormality and electron transport chain impairment in mice lacking alpha-synuclein. *Mol. Cell Biol.* **2005**, *25*, 10190–10201. [CrossRef]
235. Ludtmann, M.H.; Angelova, P.R.; Ninkina, N.N.; Gandhi, S.; Buchman, V.L.; Abramov, A.Y. Monomeric alpha-synuclein exerts a physiological role on brain ATP synthase. *J. Neurosci.* **2016**, *36*, 10510–10521. [CrossRef]
236. Hsu, L.J.; Sagara, Y.; Arroyo, A.; Rockenstein, E.; Sisk, A.; Mallory, M.; Wong, J.; Takenouchi, T.; Hashimoto, M.; Masliah, E. Alpha-synuclein promotes mitochondrial deficit and oxidative stress. *Am. J. Pathol.* **2000**, *157*, 401–410. [CrossRef]
237. Parihar, M.S.; Parihar, A.; Fujita, M.; Hashimoto, M.; Ghafourifar, P. Mitochondrial association of alpha-synuclein causes oxidative stress. *Cell Mol. Life Sci.* **2008**, *65*, 1272–1284. [CrossRef]
238. Hu, D.; Sun, X.; Liao, X.; Zhang, X.; Zarabi, S.; Schimmer, A.; Hong, Y.; Ford, C.; Luo, Y.; Qi, X. Alpha-synuclein suppresses mitochondrial protease ClpP to trigger mitochondrial oxidative damage and neurotoxicity. *Acta Neuropathol.* **2019**, *137*, 939–960. [CrossRef] [PubMed]
239. Di Maio, R.; Barrett, P.J.; Hoffman, E.K.; Barrett, C.W.; Zharikov, A.; Borah, A.; Hu, X.; McCoy, J.; Chu, C.T.; Burton, E.A.; et al. Alpha-synuclein binds to TOM20 and inhibits mitochondrial protein import in Parkinson's disease. *Sci. Transl. Med.* **2016**, *8*, 342ra78. [CrossRef]
240. Devi, L.; Raghavendran, V.; Prabhu, B.M.; Avadhani, N.G.; Anandatheerthavarada, H.K. Mitochondrial import and accumulation of alpha-synuclein impair complex I in human dopaminergic neuronal cultures and Parkinson disease brain. *J. Biol. Chem.* **2008**, *283*, 9089–9100. [CrossRef]
241. Bir, A.; Sen, O.; Anand, S.; Khemka, V.K.; Banerjee, P.; Cappai, R.; Sahoo, A.; Chakrabarti, S. alpha-Synuclein-induced mitochondrial dysfunction in isolated preparation and intact cells: Implications in the pathogenesis of Parkinson's disease. *J. Neurochem.* **2014**, *131*, 868–877. [CrossRef]
242. Perfeito, R.; Lazaro, D.F.; Outeiro, T.F.; Rego, A.C. Linking alpha-synuclein phosphorylation to reactive oxygen species formation and mitochondrial dysfunction in SH-SY5Y cells. *Mol. Cell Neurosci.* **2014**, *62*, 51–59. [CrossRef] [PubMed]
243. Subramaniam, S.R.; Vergnes, L.; Franich, N.R.; Reue, K.; Chesselet, M.F. Region specific mitochondrial impairment in mice with widespread overexpression of alpha-synuclein. *Neurobiol. Dis.* **2014**, *70*, 204–213. [CrossRef] [PubMed]
244. Martin, L.J.; Pan, Y.; Price, A.C.; Sterling, W.; Copeland, N.G.; Jenkins, N.A.; Price, D.L.; Lee, M.K. Parkinson's disease alpha-synuclein transgenic mice develop neuronal mitochondrial degeneration and cell death. *J. Neurosci.* **2006**, *26*, 41–50. [CrossRef]
245. Fornai, F.; Schluter, O.M.; Lenzi, P.; Gesi, M.; Ruffoli, R.; Ferrucci, M.; Lazzeri, G.; Busceti, C.L.; Pontarelli, F.; Battaglia, G.; et al. Parkinson-like syndrome induced by continuous MPTP infusion: Convergent roles of the ubiquitin-proteasome system and alpha-synuclein. *Proc. Natl. Acad. Sci. USA* **2005**, *102*, 3413–3418. [CrossRef]
246. Manning-Bog, A.B.; McCormack, A.L.; Li, J.; Uversky, V.N.; Fink, A.L.; Di Monte, D.A. The herbicide paraquat causes up-regulation and aggregation of alpha-synuclein in mice: Paraquat and alpha-synuclein. *J. Biol. Chem.* **2002**, *277*, 1641–1644. [CrossRef]
247. Radad, K.; Al-Shraim, M.; Al-Emam, A.; Wang, F.; Kranner, B.; Rausch, W.D.; Moldzio, R. Rotenone: From modelling to implication in Parkinson's disease. *Folia Neuropathol.* **2019**, *57*, 317–326. [CrossRef]
248. Vila, M.; Vukosavic, S.; Jackson-Lewis, V.; Neystat, M.; Jakowec, M.; Przedborski, S. Alpha-synuclein up-regulation in substantia nigra dopaminergic neurons following administration of the parkinsonian toxin MPTP. *J. Neurochem.* **2000**, *74*, 721–729. [CrossRef] [PubMed]
249. Chinta, S.J.; Mallajosyula, J.K.; Rane, A.; Andersen, J.K. Mitochondrial alpha-synuclein accumulation impairs complex I function in dopaminergic neurons and results in increased mitophagy in vivo. *Neurosci. Lett.* **2010**, *486*, 235–239. [CrossRef]
250. Loeb, V.; Yakunin, E.; Saada, A.; Sharon, R. The transgenic overexpression of alpha-synuclein and not its related pathology associates with complex I inhibition. *J. Biol. Chem.* **2010**, *285*, 7334–7343. [CrossRef]

251. Luth, E.S.; Stavrovskaya, I.G.; Bartels, T.; Kristal, B.S.; Selkoe, D.J. Soluble, prefibrillar alpha-synuclein oligomers promote complex I-dependent, Ca2+-induced mitochondrial dysfunction. *J. Biol. Chem.* **2014**, *289*, 21490–21507. [CrossRef]
252. Paillusson, S.; Gomez-Suaga, P.; Stoica, R.; Little, D.; Gissen, P.; Devine, M.J.; Noble, W.; Hanger, D.P.; Miller, C.C.J. alpha-Synuclein binds to the ER-mitochondria tethering protein VAPB to disrupt Ca(2+) homeostasis and mitochondrial ATP production. *Acta Neuropathol.* **2017**, *134*, 129–149. [CrossRef] [PubMed]
253. Chen, L.; Xie, Z.; Turkson, S.; Zhuang, X. A53T human alpha-synuclein overexpression in transgenic mice induces pervasive mitochondria macroautophagy defects preceding dopamine neuron degeneration. *J. Neurosci.* **2015**, *35*, 890–905. [CrossRef]
254. Poon, H.F.; Frasier, M.; Shreve, N.; Calabrese, V.; Wolozin, B.; Butterfield, D.A. Mitochondrial associated metabolic proteins are selectively oxidized in A30P alpha-synuclein transgenic mice—A model of familial Parkinson's disease. *Neurobiol. Dis.* **2005**, *18*, 492–498. [CrossRef] [PubMed]
255. Kamp, F.; Exner, N.; Lutz, A.K.; Wender, N.; Hegermann, J.; Brunner, B.; Nuscher, B.; Bartels, T.; Giese, A.; Beyer, K.; et al. Inhibition of mitochondrial fusion by alpha-synuclein is rescued by PINK1, Parkin and DJ-1. *EMBO J.* **2010**, *29*, 3571–3589. [CrossRef]
256. Betarbet, R.; Sherer, T.B.; MacKenzie, G.; Garcia-Osuna, M.; Panov, A.V.; Greenamyre, J.T. Chronic systemic pesticide exposure reproduces features of Parkinson's disease. *Nat. Neurosci.* **2000**, *3*, 1301–1306. [CrossRef]
257. Nistico, R.; Mehdawy, B.; Piccirilli, S.; Mercuri, N. Paraquat- and rotenone-induced models of Parkinson's disease. *Int. J. Immunopathol. Pharmacol.* **2011**, *24*, 313–322. [CrossRef]
258. Tieu, K. A guide to neurotoxic animal models of Parkinson's disease. *Cold Spring Harb. Perspect. Med.* **2011**, *1*, a009316. [CrossRef]
259. Lee, H.J.; Shin, S.Y.; Choi, C.; Lee, Y.H.; Lee, S.J. Formation and removal of alpha-synuclein aggregates in cells exposed to mitochondrial inhibitors. *J. Biol. Chem.* **2002**, *277*, 5411–5417. [CrossRef] [PubMed]
260. Kowall, N.W.; Hantraye, P.; Brouillet, E.; Beal, M.F.; McKee, A.C.; Ferrante, R.J. MPTP induces alpha-synuclein aggregation in the substantia nigra of baboons. *Neuroreport* **2000**, *11*, 211–213. [CrossRef] [PubMed]
261. Przedborski, S.; Chen, Q.; Vila, M.; Giasson, B.I.; Djaldatti, R.; Vukosavic, S.; Souza, J.M.; Jackson-Lewis, V.; Lee, V.M.; Ischiropoulos, H. Oxidative post-translational modifications of alpha-synuclein in the 1-methyl-4-phenyl-1,2,3,6-tetrahydropyridine (MPTP) mouse model of Parkinson's disease. *J. Neurochem.* **2001**, *76*, 637–640. [CrossRef] [PubMed]
262. Hu, S.; Hu, M.; Liu, J.; Zhang, B.; Zhang, Z.; Zhou, F.H.; Wang, L.; Dong, J. Phosphorylation of tau and alpha-synuclein induced neurodegeneration in MPTP mouse model of Parkinson's disease. *Neuropsychiatry Dis. Treat.* **2020**, *16*, 651–663. [CrossRef] [PubMed]
263. Lee, S.; Oh, S.T.; Jeong, H.J.; Pak, S.C.; Park, H.J.; Kim, J.; Cho, H.S.; Jeon, S. MPTP-induced vulnerability of dopamine neurons in A53T alpha-synuclein overexpressed mice with the potential involvement of DJ-1 downregulation. *Korean J. Physiol. Pharmacol.* **2017**, *21*, 625–632. [CrossRef]
264. Bazzu, G.; Calia, G.; Puggioni, G.; Spissu, Y.; Rocchitta, G.; Debetto, P.; Grigoletto, J.; Zusso, M.; Migheli, R.; Serra, P.A.; et al. alpha-Synuclein- and MPTP-generated rodent models of Parkinson's disease and the study of extracellular striatal dopamine dynamics: A microdialysis approach. *CNS Neurol. Disord. Drug Targets* **2010**, *9*, 482–490. [CrossRef]
265. Grunewald, A.; Arns, B.; Seibler, P.; Rakovic, A.; Munchau, A.; Ramirez, A.; Sue, C.M.; Klein, C. ATP13A2 mutations impair mitochondrial function in fibroblasts from patients with Kufor-Rakeb syndrome. *Neurobiol. Aging* **2012**, *33*, 1843.e1. [CrossRef]
266. Park, J.S.; Koentjoro, B.; Veivers, D.; Mackay-Sim, A.; Sue, C.M. Parkinson's disease-associated human ATP13A2 (PARK9) deficiency causes zinc dyshomeostasis and mitochondrial dysfunction. *Hum. Mol. Genet.* **2014**, *23*, 2802–2815. [CrossRef] [PubMed]
267. Cali, T.; Ottolini, D.; Negro, A.; Brini, M. alpha-Synuclein controls mitochondrial calcium homeostasis by enhancing endoplasmic reticulum-mitochondria interactions. *J. Biol. Chem.* **2012**, *287*, 17914–17929. [CrossRef]
268. Guardia-Laguarta, C.; Area-Gomez, E.; Schon, E.A.; Przedborski, S. A new role for alpha-synuclein in Parkinson's disease: Alteration of ER-mitochondrial communication. *Mov. Disord.* **2015**, *30*, 1026–1033. [CrossRef]
269. Guardia-Laguarta, C.; Area-Gomez, E.; Rub, C.; Liu, Y.; Magrane, J.; Becker, D.; Voos, W.; Schon, E.A.; Przedborski, S. alpha-Synuclein is localized to mitochondria-associated ER membranes. *J. Neurosci.* **2014**, *34*, 249–259. [CrossRef] [PubMed]
270. Jacobs, D.; Hoogerheide, D.P.; Rovini, A.; Jiang, Z.; Lee, J.C.; Rostovtseva, T.K.; Bezrukov, S.M. Probing membrane association of alpha-synuclein domains with VDAC nanopore reveals unexpected binding pattern. *Sci. Rep.* **2019**, *9*, 4580. [CrossRef] [PubMed]
271. Rostovtseva, T.K.; Gurnev, P.A.; Protchenko, O.; Hoogerheide, D.P.; Yap, T.L.; Philpott, C.C.; Lee, J.C.; Bezrukov, S.M. Alpha-synuclein shows high affinity interaction with voltage-dependent anion channel, suggesting mechanisms of mitochondrial regulation and toxicity in Parkinson disease. *J. Biol. Chem.* **2015**, *290*, 18467–18477. [CrossRef]
272. Hoogerheide, D.P.; Gurnev, P.A.; Rostovtseva, T.K.; Bezrukov, S.M. Mechanism of alpha-synuclein translocation through a VDAC nanopore revealed by energy landscape modeling of escape time distributions. *Nanoscale* **2017**, *9*, 183–192. [CrossRef]
273. Lu, L.; Zhang, C.; Cai, Q.; Lu, Q.; Duan, C.; Zhu, Y.; Yang, H. Voltage-dependent anion channel involved in the alpha-synuclein-induced dopaminergic neuron toxicity in rats. *Acta Biochim. Biophys. Sin.* **2013**, *45*, 170–178. [CrossRef]
274. Shoshan-Barmatz, V.; Zalk, R.; Gincel, D.; Vardi, N. Subcellular localization of VDAC in mitochondria and ER in the cerebellum. *Biochim. Biophys. Acta* **2004**, *1657*, 105–114. [CrossRef]
275. Shoshan-Barmatz, V.; Israelson, A. The voltage-dependent anion channel in endoplasmic/sarcoplasmic reticulum: Characterization, modulation and possible function. *J. Membr. Biol.* **2005**, *204*, 57–66. [CrossRef] [PubMed]

276. De Stefani, D.; Bononi, A.; Romagnoli, A.; Messina, A.; De Pinto, V.; Pinton, P.; Rizzuto, R. VDAC1 selectively transfers apoptotic Ca2+ signals to mitochondria. *Cell Death Differ.* **2012**, *19*, 267–273. [CrossRef]
277. Chu, Y.; Goldman, J.G.; Kelly, L.; He, Y.; Waliczek, T.; Kordower, J.H. Abnormal alpha-synuclein reduces nigral voltage-dependent anion channel 1 in sporadic and experimental Parkinson's disease. *Neurobiol. Dis.* **2014**, *69*, 1–14. [CrossRef] [PubMed]
278. Ludtmann, M.H.R.; Angelova, P.R.; Horrocks, M.H.; Choi, M.L.; Rodrigues, M.; Baev, A.Y.; Berezhnov, A.V.; Yao, Z.; Little, D.; Banushi, B.; et al. Alpha-synuclein oligomers interact with ATP synthase and open the permeability transition pore in Parkinson's disease. *Nat. Commun.* **2018**, *9*, 2293. [CrossRef] [PubMed]
279. Martin, L.J.; Semenkow, S.; Hanaford, A.; Wong, M. Mitochondrial permeability transition pore regulates Parkinson's disease development in mutant alpha-synuclein transgenic mice. *Neurobiol. Aging* **2014**, *35*, 1132–1152. [CrossRef]
280. Heman-Ackah, S.M.; Manzano, R.; Hoozemans, J.J.M.; Scheper, W.; Flynn, R.; Haerty, W.; Cowley, S.A.; Bassett, A.R.; Wood, M.J.A. Alpha-synuclein induces the unfolded protein response in Parkinson's disease SNCA triplication iPSC-derived neurons. *Hum. Mol. Genet.* **2017**, *26*, 4441–4450. [CrossRef]
281. Lee, A.S. The ER chaperone and signaling regulator GRP78/BiP as a monitor of endoplasmic reticulum stress. *Methods* **2005**, *35*, 373–381. [CrossRef]
282. Wang, M.; Wey, S.; Zhang, Y.; Ye, R.; Lee, A.S. Role of the unfolded protein response regulator GRP78/BiP in development, cancer, and neurological disorders. *Antioxid. Redox. Signal.* **2009**, *11*, 2307–2316. [CrossRef] [PubMed]
283. Bellucci, A.; Navarria, L.; Zaltieri, M.; Falarti, E.; Bodei, S.; Sigala, S.; Battistin, L.; Spillantini, M.; Missale, C.; Spano, P. Induction of the unfolded protein response by alpha-synuclein in experimental models of Parkinson's disease. *J. Neurochem.* **2011**, *116*, 588–605. [CrossRef]
284. Colla, E.; Coune, P.; Liu, Y.; Pletnikova, O.; Troncoso, J.C.; Iwatsubo, T.; Schneider, B.L.; Lee, M.K. Endoplasmic reticulum stress is important for the manifestations of alpha-synucleinopathy in vivo. *J. Neurosci.* **2012**, *32*, 3306–3320. [CrossRef] [PubMed]
285. Colla, E.; Jensen, P.H.; Pletnikova, O.; Troncoso, J.C.; Glabe, C.; Lee, M.K. Accumulation of toxic alpha-synuclein oligomer within endoplasmic reticulum occurs in alpha-synucleinopathy in vivo. *J. Neurosci.* **2012**, *32*, 3301–3305. [CrossRef]
286. Baek, J.H.; Whitfield, D.; Howlett, D.; Francis, P.; Bereczki, E.; Ballard, C.; Hortobagyi, T.; Attems, J.; Aarsland, D. Unfolded protein response is activated in Lewy body dementias. *Neuropathol. Appl. Neurobiol.* **2016**, *42*, 352–365. [CrossRef] [PubMed]
287. Yagi-Utsumi, M.; Satoh, T.; Kato, K. Structural basis of redox-dependent substrate binding of protein disulfide isomerase. *Sci. Rep.* **2015**, *5*, 13909. [CrossRef]
288. Honjo, Y.; Ito, H.; Horibe, T.; Takahashi, R.; Kawakami, K. Protein disulfide isomerase immunopositive glial cytoplasmic inclusions in patients with multiple system atrophy. *Int. J. Neurosci.* **2011**, *121*, 543–550. [CrossRef]
289. Conn, K.J.; Gao, W.; McKee, A.; Lan, M.S.; Ullman, M.D.; Eisenhauer, P.B.; Fine, R.E.; Wells, J.M. Identification of the protein disulfide isomerase family member PDIp in experimental Parkinson's disease and Lewy body pathology. *Brain Res.* **2004**, *1022*, 164–172. [CrossRef]
290. Jin, J.; Li, G.J.; Davis, J.; Zhu, D.; Wang, Y.; Pan, C.; Zhang, J. Identification of novel proteins associated with both alpha-synuclein and DJ-1. *Mol. Cell Proteom.* **2007**, *6*, 845–859. [CrossRef] [PubMed]
291. Koch, G.; Smith, M.; Macer, D.; Webster, P.; Mortara, R. Endoplasmic reticulum contains a common, abundant calcium-binding glycoprotein, endoplasmin. *J. Cell Sci.* **1986**, *86*, 217–232. [CrossRef]
292. Labrador-Garrido, A.; Cejudo-Guillen, M.; Daturpalli, S.; Leal, M.M.; Klippstein, R.; De Genst, E.J.; Villadiego, J.; Toledo-Aral, J.J.; Dobson, C.M.; Jackson, S.E.; et al. Chaperome screening leads to identification of Grp94/Gp96 and FKBP4/52 as modulators of the alpha-synuclein-elicited immune response. *FASEB J.* **2016**, *30*, 564–577. [CrossRef]
293. Lee, A.S. Mammalian stress response: Induction of the glucose-regulated protein family. *Curr. Opin. Cell Biol.* **1992**, *4*, 267–273. [CrossRef]
294. Cooper, A.A.; Gitler, A.D.; Cashikar, A.; Haynes, C.M.; Hill, K.J.; Bhullar, B.; Liu, K.; Xu, K.; Strathearn, K.E.; Liu, F.; et al. Alpha-synuclein blocks ER-Golgi traffic and Rab1 rescues neuron loss in Parkinson's models. *Science* **2006**, *313*, 324–328. [CrossRef]
295. Thayanidhi, N.; Helm, J.R.; Nycz, D.C.; Bentley, M.; Liang, Y.; Hay, J.C. Alpha-synuclein delays endoplasmic reticulum (ER)-to-Golgi transport in mammalian cells by antagonizing ER/Golgi SNAREs. *Mol. Biol. Cell* **2010**, *21*, 1850–1863. [CrossRef] [PubMed]
296. Gitler, A.D.; Bevis, B.J.; Shorter, J.; Strathearn, K.E.; Hamamichi, S.; Su, L.J.; Caldwell, K.A.; Caldwell, G.A.; Rochet, J.C.; McCaffery, J.M.; et al. The Parkinson's disease protein alpha-synuclein disrupts cellular Rab homeostasis. *Proc. Natl. Acad. Sci. USA* **2008**, *105*, 145–150. [CrossRef]
297. Dalfo, E.; Gomez-Isla, T.; Rosa, J.L.; Nieto Bodelon, M.; Cuadrado Tejedor, M.; Barrachina, M.; Ambrosio, S.; Ferrer, I. Abnormal alpha-synuclein interactions with Rab proteins in alpha-synuclein A30P transgenic mice. *J. Neuropathol. Exp. Neurol.* **2004**, *63*, 302–313. [CrossRef] [PubMed]
298. Yin, G.; Lopes da Fonseca, T.; Eisbach, S.E.; Anduaga, A.M.; Breda, C.; Orcellet, M.L.; Szego, E.M.; Guerreiro, P.; Lazaro, D.F.; Braus, G.H.; et al. alpha-Synuclein interacts with the switch region of Rab8a in a Ser129 phosphorylation-dependent manner. *Neurobiol. Dis.* **2014**, *70*, 149–161. [CrossRef] [PubMed]
299. Breda, C.; Nugent, M.L.; Estranero, J.G.; Kyriacou, C.P.; Outeiro, T.F.; Steinert, J.R.; Giorgini, F. Rab11 modulates alpha-synuclein-mediated defects in synaptic transmission and behaviour. *Hum. Mol. Genet.* **2015**, *24*, 1077–1091. [CrossRef]

300. Fujita, Y.; Ohama, E.; Takatama, M.; Al-Sarraj, S.; Okamoto, K. Fragmentation of Golgi apparatus of nigral neurons with alpha-synuclein-positive inclusions in patients with Parkinson's disease. *Acta Neuropathol.* **2006**, *112*, 261–265. [CrossRef] [PubMed]
301. Lee, H.J.; Khoshaghideh, F.; Lee, S.; Lee, S.J. Impairment of microtubule-dependent trafficking by overexpression of alpha-synuclein. *Eur. J. Neurosci.* **2006**, *24*, 3153–3162. [CrossRef]
302. Gosavi, N.; Lee, H.J.; Lee, J.S.; Patel, S.; Lee, S.J. Golgi fragmentation occurs in the cells with prefibrillar alpha-synuclein aggregates and precedes the formation of fibrillar inclusion. *J. Biol. Chem.* **2002**, *277*, 48984–48992. [CrossRef]
303. Betzer, C.; Lassen, L.B.; Olsen, A.; Kofoed, R.H.; Reimer, L.; Gregersen, E.; Zheng, J.; Cali, T.; Gai, W.P.; Chen, T.; et al. Alpha-synuclein aggregates activate calcium pump SERCA leading to calcium dysregulation. *EMBO Rep.* **2018**, *19*. [CrossRef] [PubMed]
304. Wuytack, F.; Raeymaekers, L.; Missiaen, L. PMR1/SPCA Ca2+ pumps and the role of the Golgi apparatus as a Ca2+ store. *Pflugers Arch.* **2003**, *446*, 148–153. [CrossRef]
305. Buttner, S.; Faes, L.; Reichelt, W.N.; Broeskamp, F.; Habernig, L.; Benke, S.; Kourtis, N.; Ruli, D.; Carmona-Gutierrez, D.; Eisenberg, T.; et al. The Ca2+/Mn2+ ion-pump PMR1 links elevation of cytosolic Ca(2+) levels to alpha-synuclein toxicity in Parkinson's disease models. *Cell Death Differ.* **2013**, *20*, 465–477. [CrossRef]
306. Nikoletopoulou, V.; Tavernarakis, N. The PMR1 pump in alpha-synuclein toxicity and neurodegeneration. *Neurosci. Lett.* **2018**, *663*, 66–71. [CrossRef] [PubMed]
307. Goers, J.; Manning-Bog, A.B.; McCormack, A.L.; Millett, I.S.; Doniach, S.; Di Monte, D.A.; Uversky, V.N.; Fink, A.L. Nuclear localization of alpha-synuclein and its interaction with histones. *Biochemistry* **2003**, *42*, 8465–8471. [CrossRef]
308. Mori, F.; Tanji, K.; Yoshimoto, M.; Takahashi, H.; Wakabayashi, K. Immunohistochemical comparison of alpha- and beta-synuclein in adult rat central nervous system. *Brain Res.* **2002**, *941*, 118–126. [CrossRef]
309. Yu, S.; Li, X.; Liu, G.; Han, J.; Zhang, C.; Li, Y.; Xu, S.; Liu, C.; Gao, Y.; Yang, H.; et al. Extensive nuclear localization of alpha-synuclein in normal rat brain neurons revealed by a novel monoclonal antibody. *Neuroscience* **2007**, *145*, 539–555. [CrossRef]
310. Huang, Z.; Xu, Z.; Wu, Y.; Zhou, Y. Determining nuclear localization of alpha-synuclein in synuclein mouse brains. *Neuroscience* **2011**, *199*, 318–332. [CrossRef] [PubMed]
311. Kontopoulos, E.; Parvin, J.D.; Feany, M.B. Alpha-synuclein acts in the nucleus to inhibit histone acetylation and promote neurotoxicity. *Hum. Mol. Genet.* **2006**, *15*, 3012–3023. [CrossRef]
312. Ma, K.L.; Song, L.K.; Yuan, Y.H.; Zhang, Y.; Han, N.; Gao, K.; Chen, N.H. The nuclear accumulation of alpha-synuclein is mediated by importin alpha and promotes neurotoxicity by accelerating the cell cycle. *Neuropharmacology* **2014**, *82*, 132–142. [CrossRef] [PubMed]
313. Desplats, P.; Spencer, B.; Coffee, E.; Patel, P.; Michael, S.; Patrick, C.; Adame, A.; Rockenstein, E.; Masliah, E. Alpha-synuclein sequesters Dnmt1 from the nucleus: A novel mechanism for epigenetic alterations in Lewy body diseases. *J. Biol. Chem.* **2011**, *286*, 9031–9037. [CrossRef]
314. Outeiro, T.F.; Kontopoulos, E.; Altmann, S.M.; Kufareva, I.; Strathearn, K.E.; Amore, A.M.; Volk, C.B.; Maxwell, M.M.; Rochet, J.C.; McLean, P.J.; et al. Sirtuin 2 inhibitors rescue alpha-synuclein-mediated toxicity in models of Parkinson's disease. *Science* **2007**, *317*, 516–519. [CrossRef] [PubMed]
315. Davidi, D.; Schechter, M.; Elhadi, S.A.; Matatov, A.; Nathanson, L.; Sharon, R. Alpha-synuclein translocates to the nucleus to activate retinoic-acid-dependent gene transcription. *iScience* **2020**, *23*, 100910. [CrossRef]
316. Schell, H.; Hasegawa, T.; Neumann, M.; Kahle, P.J. Nuclear and neuritic distribution of serine-129 phosphorylated alpha-synuclein in transgenic mice. *Neuroscience* **2009**, *160*, 796–804. [CrossRef]
317. Pinho, R.; Paiva, I.; Jercic, K.G.; Fonseca-Ornelas, L.; Gerhardt, E.; Fahlbusch, C.; Garcia-Esparcia, P.; Kerimoglu, C.; Pavlou, M.A.S.; Villar-Pique, A.; et al. Nuclear localization and phosphorylation modulate pathological effects of alpha-synuclein. *Hum. Mol. Genet.* **2019**, *28*, 31–50. [CrossRef] [PubMed]
318. Ryu, S.B.I.; Liew, H. Sumoylated α-synuclein translocates into the nucleus by karyopherin α6. *Mol. Cell. Toxicol.* **2019**, *15*, 103–109. [CrossRef]
319. Chen, V.; Moncalvo, M.; Tringali, D.; Tagliafierro, L.; Shriskanda, A.; Ilich, E.; Dong, W.; Kantor, B.; Chiba-Falek, O. The mechanistic role of alpha-synuclein in the nucleus: Impaired nuclear function caused by familial Parkinson's disease SNCA mutations. *Hum. Mol. Genet.* **2020**, *29*, 3107–3121. [CrossRef] [PubMed]
320. Schaser, A.J.; Osterberg, V.R.; Dent, S.E.; Stackhouse, T.L.; Wakeham, C.M.; Boutros, S.W.; Weston, L.J.; Owen, N.; Weissman, T.A.; Luna, E.; et al. Alpha-synuclein is a DNA binding protein that modulates DNA repair with implications for Lewy body disorders. *Sci. Rep.* **2019**, *9*, 10919. [CrossRef]
321. Liu, X.; Lee, Y.J.; Liou, L.C.; Ren, Q.; Zhang, Z.; Wang, S.; Witt, S.N. Alpha-synuclein functions in the nucleus to protect against hydroxyurea-induced replication stress in yeast. *Hum. Mol. Genet.* **2011**, *20*, 3401–3414. [CrossRef] [PubMed]
322. Bennett, M.C.; Bishop, J.F.; Leng, Y.; Chock, P.B.; Chase, T.N.; Mouradian, M.M. Degradation of alpha-synuclein by proteasome. *J. Biol. Chem.* **1999**, *274*, 33855–33858. [CrossRef]
323. Webb, J.L.; Ravikumar, B.; Atkins, J.; Skepper, J.N.; Rubinsztein, D.C. Alpha-synuclein is degraded by both autophagy and the proteasome. *J. Biol. Chem.* **2003**, *278*, 25009–25013. [CrossRef] [PubMed]
324. Vogiatzi, T.; Xilouri, M.; Vekrellis, K.; Stefanis, L. Wild type alpha-synuclein is degraded by chaperone-mediated autophagy and macroautophagy in neuronal cells. *J. Biol. Chem.* **2008**, *283*, 23542–23556. [CrossRef] [PubMed]

325. Rott, R.; Szargel, R.; Haskin, J.; Bandopadhyay, R.; Lees, A.J.; Shani, V.; Engelender, S. alpha-Synuclein fate is determined by USP9X-regulated monoubiquitination. *Proc. Natl. Acad. Sci. USA* **2011**, *108*, 18666–18671. [CrossRef]
326. Haj-Yahya, M.; Fauvet, B.; Herman-Bachinsky, Y.; Hejjaoui, M.; Bavikar, S.N.; Karthikeyan, S.V.; Ciechanover, A.; Lashuel, H.A.; Brik, A. Synthetic polyubiquitinated alpha-Synuclein reveals important insights into the roles of the ubiquitin chain in regulating its pathophysiology. *Proc. Natl. Acad. Sci. USA* **2013**, *110*, 17726–17731. [CrossRef]
327. Tofaris, G.K.; Layfield, R.; Spillantini, M.G. alpha-synuclein metabolism and aggregation is linked to ubiquitin-independent degradation by the proteasome. *FEBS Lett.* **2001**, *509*, 22–26. [CrossRef]
328. Liu, C.W.; Corboy, M.J.; DeMartino, G.N.; Thomas, P.J. Endoproteolytic activity of the proteasome. *Science* **2003**, *299*, 408–411. [CrossRef]
329. Rideout, H.J.; Larsen, K.E.; Sulzer, D.; Stefanis, L. Proteasomal inhibition leads to formation of ubiquitin/alpha-synuclein-immunoreactive inclusions in PC12 cells. *J. Neurochem.* **2001**, *78*, 899–908. [CrossRef]
330. Rideout, H.J.; Stefanis, L. Proteasomal inhibition-induced inclusion formation and death in cortical neurons require transcription and ubiquitination. *Mol. Cell. Neurosci.* **2002**, *21*, 223–238. [CrossRef]
331. Emmanouilidou, E.; Stefanis, L.; Vekrellis, K. Cell-produced alpha-synuclein oligomers are targeted to, and impair, the 26S proteasome. *Neurobiol. Aging* **2010**, *31*, 953–968. [CrossRef] [PubMed]
332. Ebrahimi-Fakhari, D.; Cantuti-Castelvetri, I.; Fan, Z.; Rockenstein, E.; Masliah, E.; Hyman, B.T.; McLean, P.J.; Unni, V.K. Distinct roles in vivo for the ubiquitin-proteasome system and the autophagy-lysosomal pathway in the degradation of alpha-synuclein. *J. Neurosci.* **2011**, *31*, 14508–14520. [CrossRef] [PubMed]
333. Xilouri, M.; Brekk, O.R.; Stefanis, L. alpha-Synuclein and protein degradation systems: A reciprocal relationship. *Mol. Neurobiol.* **2013**, *47*, 537–551. [CrossRef]
334. Cuervo, A.M.; Stefanis, L.; Fredenburg, R.; Lansbury, P.T.; Sulzer, D. Impaired degradation of mutant alpha-synuclein by chaperone-mediated autophagy. *Science* **2004**, *305*, 1292–1295. [CrossRef] [PubMed]
335. Lee, H.J.; Khoshaghideh, F.; Patel, S.; Lee, S.J. Clearance of alpha-synuclein oligomeric intermediates via the lysosomal degradation pathway. *J. Neurosci.* **2004**, *24*, 1888–1896. [CrossRef]
336. Mak, S.K.; McCormack, A.L.; Manning-Bog, A.B.; Cuervo, A.M.; Di Monte, D.A. Lysosomal degradation of alpha-synuclein in vivo. *J. Biol. Chem.* **2010**, *285*, 13621–13629. [CrossRef]
337. Xilouri, M.; Brekk, O.R.; Landeck, N.; Pitychoutis, P.M.; Papasilekas, T.; Papadopoulou-Daifoti, Z.; Kirik, D.; Stefanis, L. Boosting chaperone-mediated autophagy in vivo mitigates alpha-synuclein-induced neurodegeneration. *Brain* **2013**, *136*, 2130–2146. [CrossRef] [PubMed]
338. Issa, A.R.; Sun, J.; Petitgas, C.; Mesquita, A.; Dulac, A.; Robin, M.; Mollereau, B.; Jenny, A.; Cherif-Zahar, B.; Birman, S. The lysosomal membrane protein LAMP2A promotes autophagic flux and prevents SNCA-induced Parkinson disease-like symptoms in the Drosophila brain. *Autophagy* **2018**, *14*, 1898–1910. [CrossRef]
339. Xilouri, M.; Brekk, O.R.; Polissidis, A.; Chrysanthou-Piterou, M.; Kloukina, I.; Stefanis, L. Impairment of chaperone-mediated autophagy induces dopaminergic neurodegeneration in rats. *Autophagy* **2016**, *12*, 2230–2247. [CrossRef]
340. Alvarez-Erviti, L.; Rodriguez-Oroz, M.C.; Cooper, J.M.; Caballero, C.; Ferrer, I.; Obeso, J.A.; Schapira, A.H. Chaperone-mediated autophagy markers in Parkinson disease brains. *Arch. Neurol.* **2010**, *67*, 1464–1472. [CrossRef]
341. Murphy, K.E.; Gysbers, A.M.; Abbott, S.K.; Spiro, A.S.; Furuta, A.; Cooper, A.; Garner, B.; Kabuta, T.; Halliday, G.M. Lysosomal-associated membrane protein 2 isoforms are differentially affected in early Parkinson's disease. *Mov. Disord.* **2015**, *30*, 1639–1647. [CrossRef]
342. Tanaka, Y.; Engelender, S.; Igarashi, S.; Rao, R.K.; Wanner, T.; Tanzi, R.E.; Sawa, A.; Valina, L.D.; Dawson, T.M.; Ross, C.A. Inducible expression of mutant alpha-synuclein decreases proteasome activity and increases sensitivity to mitochondria-dependent apoptosis. *Hum. Mol. Genet.* **2001**, *10*, 919–926. [CrossRef]
343. Stefanis, L.; Larsen, K.E.; Rideout, H.J.; Sulzer, D.; Greene, L.A. Expression of A53T mutant but not wild-type alpha-synuclein in PC12 cells induces alterations of the ubiquitin-dependent degradation system, loss of dopamine release, and autophagic cell death. *J. Neurosci.* **2001**, *21*, 9549–9560. [CrossRef] [PubMed]
344. Martin-Clemente, B.; Alvarez-Castelao, B.; Mayo, I.; Sierra, A.B.; Diaz, V.; Milan, M.; Farinas, I.; Gomez-Isla, T.; Ferrer, I.; Castano, J.G. alpha-Synuclein expression levels do not significantly affect proteasome function and expression in mice and stably transfected PC12 cell lines. *J. Biol. Chem.* **2004**, *279*, 52984–52990. [CrossRef]
345. Zondler, L.; Kostka, M.; Garidel, P.; Heinzelmann, U.; Hengerer, B.; Mayer, B.; Weishaupt, J.H.; Gillardon, F.; Danzer, K.M. Proteasome impairment by alpha-synuclein. *PLoS ONE* **2017**, *12*, e0184040. [CrossRef]
346. Bentea, E.; Verbruggen, L.; Massie, A. The proteasome inhibition model of Parkinson's disease. *J. Parkinsons Dis.* **2017**, *7*, 31–63. [CrossRef] [PubMed]
347. McNaught, K.S.; Jenner, P. Proteasomal function is impaired in substantia nigra in Parkinson's disease. *Neurosci. Lett.* **2001**, *297*, 191–194. [CrossRef]
348. McNaught, K.S.; Belizaire, R.; Isacson, O.; Jenner, P.; Olanow, C.W. Altered proteasomal function in sporadic Parkinson's disease. *Exp. Neurol.* **2003**, *179*, 38–46. [CrossRef] [PubMed]

349. Martinez-Vicente, M.; Sovak, G.; Cuervo, A.M. Protein degradation and aging. *Exp. Gerontol.* **2005**, *40*, 622–633. [CrossRef]
350. Winslow, A.R.; Chen, C.W.; Corrochano, S.; Acevedo-Arozena, A.; Gordon, D.E.; Peden, A.A.; Lichtenberg, M.; Menzies, F.M.; Ravikumar, B.; Imarisio, S.; et al. Alpha-synuclein impairs macroautophagy: Implications for Parkinson's disease. *J. Cell Biol.* **2010**, *190*, 1023–1037. [CrossRef]
351. Zavodszky, E.; Seaman, M.N.; Moreau, K.; Jimenez-Sanchez, M.; Breusegem, S.Y.; Harbour, M.E.; Rubinsztein, D.C. Mutation in VPS35 associated with Parkinson's disease impairs WASH complex association and inhibits autophagy. *Nat. Commun.* **2014**, *5*, 3828. [CrossRef] [PubMed]
352. Yan, J.Q.; Yuan, Y.H.; Gao, Y.N.; Huang, J.Y.; Ma, K.L.; Gao, Y.; Zhang, W.Q.; Guo, X.F.; Chen, N.H. Overexpression of human E46K mutant alpha-synuclein impairs macroautophagy via inactivation of JNK1-Bcl-2 pathway. *Mol. Neurobiol.* **2014**, *50*, 685–701. [CrossRef] [PubMed]
353. Lei, Z.; Cao, G.; Wei, G. A30P mutant alpha-synuclein impairs autophagic flux by inactivating JNK signaling to enhance ZKSCAN3 activity in midbrain dopaminergic neurons. *Cell Death Dis* **2019**, *10*, 133. [CrossRef] [PubMed]
354. Choubey, V.; Safiulina, D.; Vaarmann, A.; Cagalinec, M.; Wareski, P.; Kuum, M.; Zharkovsky, A.; Kaasik, A. Mutant A53T alpha-synuclein induces neuronal death by increasing mitochondrial autophagy. *J. Biol. Chem.* **2011**, *286*, 10814–10824. [CrossRef]
355. Martinez-Vicente, M.; Talloczy, Z.; Kaushik, S.; Massey, A.C.; Mazzulli, J.; Mosharov, E.V.; Hodara, R.; Fredenburg, R.; Wu, D.C.; Follenzi, A.; et al. Dopamine-modified alpha-synuclein blocks chaperone-mediated autophagy. *J. Clin. Investig.* **2008**, *118*, 777–788. [CrossRef]
356. Mazzulli, J.R.; Zunke, F.; Isacson, O.; Studer, L.; Krainc, D. alpha-Synuclein-induced lysosomal dysfunction occurs through disruptions in protein trafficking in human midbrain synucleinopathy models. *Proc. Natl. Acad. Sci. USA* **2016**, *113*, 1931–1936. [CrossRef]
357. Osellame, L.D.; Rahim, A.A.; Hargreaves, I.P.; Gegg, M.E.; Richard-Londt, A.; Brandner, S.; Waddington, S.N.; Schapira, A.H.V.; Duchen, M.R. Mitochondria and quality control defects in a mouse model of Gaucher disease—Links to Parkinson's disease. *Cell Metab.* **2013**, *17*, 941–953. [CrossRef]
358. Sardi, S.P.; Clarke, J.; Viel, C.; Chan, M.; Tamsett, T.J.; Treleaven, C.M.; Bu, J.; Sweet, L.; Passini, M.A.; Dodge, J.C.; et al. Augmenting CNS glucocerebrosidase activity as a therapeutic strategy for parkinsonism and other Gaucher-related synucleinopathies. *Proc. Natl. Acad. Sci. USA* **2013**, *110*, 3537–3542. [CrossRef]
359. Murphy, K.E.; Gysbers, A.M.; Abbott, S.K.; Tayebi, N.; Kim, W.S.; Sidransky, E.; Cooper, A.; Garner, B.; Halliday, G.M. Reduced glucocerebrosidase is associated with increased alpha-synuclein in sporadic Parkinson's disease. *Brain* **2014**, *137*, 834–848. [CrossRef]
360. Du, T.T.; Wang, L.; Duan, C.L.; Lu, L.L.; Zhang, J.L.; Gao, G.; Qiu, X.B.; Wang, X.M.; Yang, H. GBA deficiency promotes SNCA/alpha-synuclein accumulation through autophagic inhibition by inactivated PPP2A. *Autophagy* **2015**, *11*, 1803–1820. [CrossRef]
361. Liu, G.; Chen, M.; Mi, N.; Yang, W.; Li, X.; Wang, P.; Yin, N.; Li, Y.; Yue, F.; Chan, P.; et al. Increased oligomerization and phosphorylation of alpha-synuclein are associated with decreased activity of glucocerebrosidase and protein phosphatase 2A in aging monkey brains. *Neurobiol. Aging* **2015**, *36*, 2649–2659. [CrossRef]
362. Rocha, E.M.; Smith, G.A.; Park, E.; Cao, H.; Graham, A.R.; Brown, E.; McLean, J.R.; Hayes, M.A.; Beagan, J.; Izen, S.C.; et al. Sustained systemic glucocerebrosidase inhibition induces brain alpha-synuclein aggregation, microglia and complement C1q activation in mice. *Antioxid. Redox. Signal.* **2015**, *23*, 550–564. [CrossRef]
363. Borghi, R.; Marchese, R.; Negro, A.; Marinelli, L.; Forloni, G.; Zaccheo, D.; Abbruzzese, G.; Tabaton, M. Full length alpha-synuclein is present in cerebrospinal fluid from Parkinson's disease and normal subjects. *Neurosci. Lett.* **2000**, *287*, 65–67. [CrossRef]
364. El-Agnaf, O.M.; Salem, S.A.; Paleologou, K.E.; Cooper, L.J.; Fullwood, N.J.; Gibson, M.J.; Curran, M.D.; Court, J.A.; Mann, D.M.; Ikeda, S.; et al. Alpha-synuclein implicated in Parkinson's disease is present in extracellular biological fluids, including human plasma. *FASEB J.* **2003**, *17*, 1945–1947. [CrossRef]
365. Lee, H.J.; Patel, S.; Lee, S.J. Intravesicular localization and exocytosis of alpha-synuclein and its aggregates. *J. Neurosci.* **2005**, *25*, 6016–6024. [CrossRef] [PubMed]
366. Emmanouilidou, E.; Melachroinou, K.; Roumeliotis, T.; Garbis, S.D.; Ntzouni, M.; Margaritis, L.H.; Stefanis, L.; Vekrellis, K. Cell-produced alpha-synuclein is secreted in a calcium-dependent manner by exosomes and impacts neuronal survival. *J. Neurosci.* **2010**, *30*, 6838–6851. [CrossRef]
367. Danzer, K.M.; Kranich, L.R.; Ruf, W.P.; Cagsal-Getkin, O.; Winslow, A.R.; Zhu, L.; Vanderburg, C.R.; McLean, P.J. Exosomal cell-to-cell transmission of alpha synuclein oligomers. *Mol. Neurodegener.* **2012**, *7*, 42. [CrossRef]
368. Kordower, J.H.; Chu, Y.; Hauser, R.A.; Freeman, T.B.; Olanow, C.W. Lewy body-like pathology in long-term embryonic nigral transplants in Parkinson's disease. *Nat. Med.* **2008**, *14*, 504–506. [CrossRef] [PubMed]
369. Li, J.Y.; Englund, E.; Holton, J.L.; Soulet, D.; Hagell, P.; Lees, A.J.; Lashley, T.; Quinn, N.P.; Rehncrona, S.; Bjorklund, A.; et al. Lewy bodies in grafted neurons in subjects with Parkinson's disease suggest host-to-graft disease propagation. *Nat. Med.* **2008**, *14*, 501–503. [CrossRef] [PubMed]
370. Li, J.Y.; Englund, E.; Widner, H.; Rehncrona, S.; Bjorklund, A.; Lindvall, O.; Brundin, P. Characterization of Lewy body pathology in 12- and 16-year-old intrastriatal mesencephalic grafts surviving in a patient with Parkinson's disease. *Mov. Disord.* **2010**, *25*, 1091–1096. [CrossRef]

371. Kordower, J.H.; Dodiya, H.B.; Kordower, A.M.; Terpstra, B.; Paumier, K.; Madhavan, L.; Sortwell, C.; Steece-Collier, K.; Collier, T.J. Transfer of host-derived alpha synuclein to grafted dopaminergic neurons in rat. *Neurobiol. Dis.* **2011**, *43*, 552–557. [CrossRef]
372. Kurowska, Z.; Englund, E.; Widner, H.; Lindvall, O.; Li, J.Y.; Brundin, P. Signs of degeneration in 12–22-year old grafts of mesencephalic dopamine neurons in patients with Parkinson's disease. *J. Parkinsons Dis.* **2011**, *1*, 83–92. [CrossRef] [PubMed]
373. Masuda-Suzukake, M.; Nonaka, T.; Hosokawa, M.; Oikawa, T.; Arai, T.; Akiyama, H.; Mann, D.M.; Hasegawa, M. Prion-like spreading of pathological alpha-synuclein in brain. *Brain* **2013**, *136*, 1128–1138. [CrossRef]
374. Recasens, A.; Dehay, B.; Bove, J.; Carballo-Carbajal, I.; Dovero, S.; Perez-Villalba, A.; Fernagut, P.O.; Blesa, J.; Parent, A.; Perier, C.; et al. Lewy body extracts from Parkinson disease brains trigger alpha-synuclein pathology and neurodegeneration in mice and monkeys. *Ann. Neurol.* **2014**, *75*, 351–362. [CrossRef]
375. Luk, K.C.; Kehm, V.; Carroll, J.; Zhang, B.; O'Brien, P.; Trojanowski, J.Q.; Lee, V.M. Pathological alpha-synuclein transmission initiates Parkinson-like neurodegeneration in nontransgenic mice. *Science* **2012**, *338*, 949–953. [CrossRef] [PubMed]
376. Luk, K.C.; Song, C.; O'Brien, P.; Stieber, A.; Branch, J.R.; Brunden, K.R.; Trojanowski, J.Q.; Lee, V.M. Exogenous alpha-synuclein fibrils seed the formation of Lewy body-like intracellular inclusions in cultured cells. *Proc. Natl. Acad. Sci. USA* **2009**, *106*, 20051–20056. [CrossRef]
377. Sacino, A.N.; Brooks, M.; Thomas, M.A.; McKinney, A.B.; Lee, S.; Regenhardt, R.W.; McGarvey, N.H.; Ayers, J.I.; Notterpek, L.; Borchelt, D.R.; et al. Intramuscular injection of alpha-synuclein induces CNS alpha-synuclein pathology and a rapid-onset motor phenotype in transgenic mice. *Proc. Natl. Acad. Sci. USA* **2014**, *111*, 10732–10737. [CrossRef]
378. Paumier, K.L.; Luk, K.C.; Manfredsson, F.P.; Kanaan, N.M.; Lipton, J.W.; Collier, T.J.; Steece-Collier, K.; Kemp, C.J.; Celano, S.; Schulz, E.; et al. Intrastriatal injection of pre-formed mouse alpha-synuclein fibrils into rats triggers alpha-synuclein pathology and bilateral nigrostriatal degeneration. *Neurobiol. Dis.* **2015**, *82*, 185–199. [CrossRef] [PubMed]
379. Abdelmotilib, H.; Maltbie, T.; Delic, V.; Liu, Z.; Hu, X.; Fraser, K.B.; Moehle, M.S.; Stoyka, L.; Anabtawi, N.; Krendelchtchikova, V.; et al. alpha-Synuclein fibril-induced inclusion spread in rats and mice correlates with dopaminergic Neurodegeneration. *Neurobiol. Dis.* **2017**, *105*, 84–98. [CrossRef]
380. Gustafsson, G.; Loov, C.; Persson, E.; Lazaro, D.F.; Takeda, S.; Bergstrom, J.; Erlandsson, A.; Sehlin, D.; Balaj, L.; Gyorgy, B.; et al. Secretion and uptake of alpha-synuclein via extracellular vesicles in cultured cells. *Cell. Mol. Neurobiol.* **2018**, *38*, 1539–1550. [CrossRef]
381. Fussi, N.; Hollerhage, M.; Chakroun, T.; Nykanen, N.P.; Rosler, T.W.; Koeglsperger, T.; Wurst, W.; Behrends, C.; Hoglinger, G.U. Exosomal secretion of alpha-synuclein as protective mechanism after upstream blockage of macroautophagy. *Cell Death Dis.* **2018**, *9*, 757. [CrossRef] [PubMed]
382. El-Agnaf, O.M.; Salem, S.A.; Paleologou, K.E.; Curran, M.D.; Gibson, M.J.; Court, J.A.; Schlossmacher, M.G.; Allsop, D. Detection of oligomeric forms of alpha-synuclein protein in human plasma as a potential biomarker for Parkinson's disease. *FASEB J.* **2006**, *20*, 419–425. [CrossRef]
383. Delenclos, M.; Trendafilova, T.; Mahesh, D.; Baine, A.M.; Moussaud, S.; Yan, I.K.; Patel, T.; McLean, P.J. Investigation of endocytic pathways for the internalization of exosome-associated oligomeric alpha-synuclein. *Front. Neurosci.* **2017**, *11*, 172. [CrossRef] [PubMed]
384. Sung, J.Y.; Kim, J.; Paik, S.R.; Park, J.H.; Ahn, Y.S.; Chung, K.C. Induction of neuronal cell death by Rab5A-dependent endocytosis of alpha-synuclein. *J. Biol. Chem.* **2001**, *276*, 27441–27448. [CrossRef]
385. Lee, H.J.; Suk, J.E.; Bae, E.J.; Lee, J.H.; Paik, S.R.; Lee, S.J. Assembly-dependent endocytosis and clearance of extracellular alpha-synuclein. *Int. J. Biochem. Cell Biol.* **2008**, *40*, 1835–1849. [CrossRef] [PubMed]
386. Ahn, K.J.; Paik, S.R.; Chung, K.C.; Kim, J. Amino acid sequence motifs and mechanistic features of the membrane translocation of alpha-synuclein. *J. Neurochem.* **2006**, *97*, 265–279. [CrossRef] [PubMed]
387. Abounit, S.; Bousset, L.; Loria, F.; Zhu, S.; de Chaumont, F.; Pieri, L.; Olivo-Marin, J.C.; Melki, R.; Zurzolo, C. Tunneling nanotubes spread fibrillar alpha-synuclein by intercellular trafficking of lysosomes. *EMBO J.* **2016**, *35*, 2120–2138. [CrossRef]
388. Kayed, R.; Sokolov, Y.; Edmonds, B.; McIntire, T.M.; Milton, S.C.; Hall, J.E.; Glabe, C.G. Permeabilization of lipid bilayers is a common conformation-dependent activity of soluble amyloid oligomers in protein misfolding diseases. *J. Biol. Chem.* **2004**, *279*, 46363–46366. [CrossRef]
389. Jao, C.C.; Hegde, B.G.; Chen, J.; Haworth, I.S.; Langen, R. Structure of membrane-bound alpha-synuclein from site-directed spin labeling and computational refinement. *Proc. Natl. Acad. Sci. USA* **2008**, *105*, 19666–19671. [CrossRef]
390. Mao, X.; Ou, M.T.; Karuppagounder, S.S.; Kam, T.I.; Yin, X.; Xiong, Y.; Ge, P.; Umanah, G.E.; Brahmachari, S.; Shin, J.H.; et al. Pathological alpha-synuclein transmission initiated by binding lymphocyte-activation gene 3. *Science* **2016**, *353*. [CrossRef] [PubMed]
391. Ihse, E.; Yamakado, H.; van Wijk, X.M.; Lawrence, R.; Esko, J.D.; Masliah, E. Cellular internalization of alpha-synuclein aggregates by cell surface heparan sulfate depends on aggregate conformation and cell type. *Sci. Rep.* **2017**, *7*, 9008. [CrossRef]
392. Rey, N.L.; Steiner, J.A.; Maroof, N.; Luk, K.C.; Madaj, Z.; Trojanowski, J.Q.; Lee, V.M.; Brundin, P. Widespread transneuronal propagation of alpha-synucleinopathy triggered in olfactory bulb mimics prodromal Parkinson's disease. *J. Exp. Med.* **2016**, *213*, 1759–1778. [CrossRef] [PubMed]
393. Karampetsou, M.; Ardah, M.T.; Semitekolou, M.; Polissidis, A.; Samiotaki, M.; Kalomoiri, M.; Majbour, N.; Xanthou, G.; El-Agnaf, O.M.A.; Vekrellis, K. Phosphorylated exogenous alpha-synuclein fibrils exacerbate pathology and induce neuronal dysfunction in mice. *Sci. Rep.* **2017**, *7*, 16533. [CrossRef]

394. Karpowicz, R.J., Jr.; Haney, C.M.; Mihaila, T.S.; Sandler, R.M.; Petersson, E.J.; Lee, V.M. Selective imaging of internalized proteopathic alpha-synuclein seeds in primary neurons reveals mechanistic insight into transmission of synucleinopathies. *J. Biol. Chem.* **2017**, *292*, 13482–13497. [CrossRef] [PubMed]
395. Luna, E.; Decker, S.C.; Riddle, D.M.; Caputo, A.; Zhang, B.; Cole, T.; Caswell, C.; Xie, S.X.; Lee, V.M.Y.; Luk, K.C. Differential alpha-synuclein expression contributes to selective vulnerability of hippocampal neuron subpopulations to fibril-induced toxicity. *Acta Neuropathol.* **2018**, *135*, 855–875. [CrossRef]
396. Volpicelli-Daley, L.A.; Luk, K.C.; Lee, V.M. Addition of exogenous alpha-synuclein preformed fibrils to primary neuronal cultures to seed recruitment of endogenous alpha-synuclein to Lewy body and Lewy neurite-like aggregates. *Nat. Protoc.* **2014**, *9*, 2135–2146. [CrossRef]
397. Sacino, A.N.; Brooks, M.; McKinney, A.B.; Thomas, M.A.; Shaw, G.; Golde, T.E.; Giasson, B.I. Brain injection of alpha-synuclein induces multiple proteinopathies, gliosis, and a neuronal injury marker. *J. Neurosci.* **2014**, *34*, 12368–12378. [CrossRef]
398. Wu, Q.; Takano, H.; Riddle, D.M.; Trojanowski, J.Q.; Coulter, D.A.; Lee, V.M. Alpha-synuclein (alphaSyn) preformed fibrils induce endogenous alphaSyn aggregation, compromise synaptic activity and enhance synapse loss in cultured excitatory hippocampal neurons. *J. Neurosci.* **2019**, *39*, 5080–5094. [CrossRef]
399. Chu, Y.; Kordower, J.H. The prion hypothesis of Parkinson's disease. *Curr. Neurol. Neurosci. Rep.* **2015**, *15*, 28. [CrossRef] [PubMed]
400. Uversky, V.N.; Li, J.; Fink, A.L. Evidence for a partially folded intermediate in alpha-synuclein fibril formation. *J. Biol. Chem.* **2001**, *276*, 10737–10744. [CrossRef]
401. Wood, S.J.; Wypych, J.; Steavenson, S.; Louis, J.C.; Citron, M.; Biere, A.L. alpha-synuclein fibrillogenesis is nucleation-dependent. Implications for the pathogenesis of Parkinson's disease. *J. Biol. Chem.* **1999**, *274*, 19509–19512. [CrossRef]
402. Masuda-Suzukake, M.; Nonaka, T.; Hosokawa, M.; Kubo, M.; Shimozawa, A.; Akiyama, H.; Hasegawa, M. Pathological alpha-synuclein propagates through neural networks. *Acta Neuropathol. Commun.* **2014**, *2*, 88. [CrossRef] [PubMed]
403. Freundt, E.C.; Maynard, N.; Clancy, E.K.; Roy, S.; Bousset, L.; Sourigues, Y.; Covert, M.; Melki, R.; Kirkegaard, K.; Brahic, M. Neuron-to-neuron transmission of alpha-synuclein fibrils through axonal transport. *Ann. Neurol.* **2012**, *72*, 517–524. [CrossRef]
404. Mezias, C.; Rey, N.; Brundin, P.; Raj, A. Neural connectivity predicts spreading of alpha-synuclein pathology in fibril-injected mouse models: Involvement of retrograde and anterograde axonal propagation. *Neurobiol. Dis.* **2020**, *134*, 104623. [CrossRef]
405. Tang, Y.; Das, U.; Scott, D.A.; Roy, S. The slow axonal transport of alpha-synuclein–mechanistic commonalities amongst diverse cytosolic cargoes. *Cytoskeleton* **2012**, *69*, 506–513. [CrossRef] [PubMed]
406. Saha, A.R.; Hill, J.; Utton, M.A.; Asuni, A.A.; Ackerley, S.; Grierson, A.J.; Miller, C.C.; Davies, A.M.; Buchman, V.L.; Anderton, B.H.; et al. Parkinson's disease alpha-synuclein mutations exhibit defective axonal transport in cultured neurons. *J. Cell Sci.* **2004**, *117*, 1017–1024. [CrossRef]
407. Li, W.; Hoffman, P.N.; Stirling, W.; Price, D.L.; Lee, M.K. Axonal transport of human alpha-synuclein slows with aging but is not affected by familial Parkinson's disease-linked mutations. *J. Neurochem.* **2004**, *88*, 401–410. [CrossRef] [PubMed]
408. Prots, I.; Veber, V.; Brey, S.; Campioni, S.; Buder, K.; Riek, R.; Bohm, K.J.; Winner, B. alpha-Synuclein oligomers impair neuronal microtubule-kinesin interplay. *J. Biol. Chem.* **2013**, *288*, 21742–21754. [CrossRef] [PubMed]
409. Chu, Y.; Morfini, G.A.; Langhamer, L.B.; He, Y.; Brady, S.T.; Kordower, J.H. Alterations in axonal transport motor proteins in sporadic and experimental Parkinson's disease. *Brain* **2012**, *135*, 2058–2073. [CrossRef]
410. Chung, C.Y.; Koprich, J.B.; Siddiqi, H.; Isacson, O. Dynamic changes in presynaptic and axonal transport proteins combined with striatal neuroinflammation precede dopaminergic neuronal loss in a rat model of AAV alpha-synucleinopathy. *J. Neurosci.* **2009**, *29*, 3365–3373. [CrossRef] [PubMed]
411. Holec, S.A.M.; Woerman, A.L. Evidence of distinct alpha-synuclein strains underlying disease heterogeneity. *Acta Neuropathol.* **2020**. [CrossRef] [PubMed]
412. Lau, A.; So, R.W.L.; Lau, H.H.C.; Sang, J.C.; Ruiz-Riquelme, A.; Fleck, S.C.; Stuart, E.; Menon, S.; Visanji, N.P.; Meisl, G.; et al. alpha-Synuclein strains target distinct brain regions and cell types. *Nat. Neurosci.* **2020**, *23*, 21–31. [CrossRef]
413. Peelaerts, W.; Bousset, L.; Van der Perren, A.; Moskalyuk, A.; Pulizzi, R.; Giugliano, M.; Van den Haute, C.; Melki, R.; Baekelandt, V. Alpha-synuclein strains cause distinct synucleinopathies after local and systemic administration. *Nature* **2015**, *522*, 340–344. [CrossRef]
414. Rey, N.L.; Bousset, L.; George, S.; Madaj, Z.; Meyerdirk, L.; Schulz, E.; Steiner, J.A.; Melki, R.; Brundin, P. alpha-Synuclein conformational strains spread, seed and target neuronal cells differentially after injection into the olfactory bulb. *Acta Neuropathol. Commun.* **2019**, *7*, 221. [CrossRef]
415. Wake, H.; Fields, R.D. Physiological function of microglia. *Neuron Glia Biol.* **2011**, *7*, 1–3. [CrossRef]
416. Paolicelli, R.C.; Bolasco, G.; Pagani, F.; Maggi, L.; Scianni, M.; Panzanelli, P.; Giustetto, M.; Ferreira, T.A.; Guiducci, E.; Dumas, L.; et al. Synaptic pruning by microglia is necessary for normal brain development. *Science* **2011**, *333*, 1456–1458. [CrossRef]
417. Sierra, A.; Encinas, J.M.; Deudero, J.J.; Chancey, J.H.; Enikolopov, G.; Overstreet-Wadiche, L.S.; Tsirka, S.E.; Maletic-Savatic, M. Microglia shape adult hippocampal neurogenesis through apoptosis-coupled phagocytosis. *Cell Stem Cell* **2010**, *7*, 483–495. [CrossRef]
418. Nimmerjahn, A.; Kirchhoff, F.; Helmchen, F. Resting microglial cells are highly dynamic surveillants of brain parenchyma in vivo. *Science* **2005**, *308*, 1314–1318. [CrossRef] [PubMed]

419. Weinhard, L.; di Bartolomei, G.; Bolasco, G.; Machado, P.; Schieber, N.L.; Neniskyte, U.; Exiga, M.; Vadisiute, A.; Raggioli, A.; Schertel, A.; et al. Microglia remodel synapses by presynaptic trogocytosis and spine head filopodia induction. *Nat. Commun.* **2018**, *9*, 1228. [CrossRef]
420. Colton, C.; Wilcock, D.M. Assessing activation states in microglia. *CNS Neurol. Disord. Drug Targets* **2010**, *9*, 174–191. [CrossRef]
421. Kreutzberg, G.W. Microglia: A sensor for pathological events in the CNS. *Trends Neurosci.* **1996**, *19*, 312–318. [CrossRef]
422. Streit, W.J.; Conde, J.R.; Fendrick, S.E.; Flanary, B.E.; Mariani, C.L. Role of microglia in the central nervous system's immune response. *Neurol. Res.* **2005**, *27*, 685–691. [CrossRef]
423. Van Rossum, D.; Hanisch, U.K. Microglia. *Metab. Brain Dis.* **2004**, *19*, 393–411. [CrossRef] [PubMed]
424. Lecours, C.; Bordeleau, M.; Cantin, L.; Parent, M.; Paolo, T.D.; Tremblay, M.E. Microglial Implication in Parkinson's Disease: Loss of Beneficial Physiological Roles or Gain of Inflammatory Functions? *Front. Cell Neurosci.* **2018**, *12*, 282. [CrossRef]
425. Croisier, E.; Moran, L.B.; Dexter, D.T.; Pearce, R.K.; Graeber, M.B. Microglial inflammation in the parkinsonian substantia nigra: Relationship to alpha-synuclein deposition. *J. Neuroinflamm.* **2005**, *2*, 14. [CrossRef] [PubMed]
426. Vieira, B.D.; Radford, R.A.; Chung, R.S.; Guillemin, G.J.; Pountney, D.L. Neuroinflammation in multiple system atrophy: Response to and cause of alpha-synuclein aggregation. *Front. Cell Neurosci.* **2015**, *9*, 437. [CrossRef]
427. Surendranathan, A.; Su, L.; Mak, E.; Passamonti, L.; Hong, Y.T.; Arnold, R.; Vazquez Rodriguez, P.; Bevan-Jones, W.R.; Brain, S.A.E.; Fryer, T.D.; et al. Early microglial activation and peripheral inflammation in dementia with Lewy bodies. *Brain* **2018**, *141*, 3415–3427. [CrossRef] [PubMed]
428. Mackenzie, I.R. Activated microglia in dementia with Lewy bodies. *Neurology* **2000**, *55*, 132–134. [CrossRef] [PubMed]
429. Mosley, R.L.; Benner, E.J.; Kadiu, I.; Thomas, M.; Boska, M.D.; Hasan, K.; Laurie, C.; Gendelman, H.E. Neuroinflammation, oxidative stress and the pathogenesis of Parkinson's disease. *Clin. Neurosci. Res.* **2006**, *6*, 261–281. [CrossRef]
430. Appel, S.H.; Beers, D.R.; Henkel, J.S. T cell-microglial dialogue in Parkinson's disease and amyotrophic lateral sclerosis: Are we listening? *Trends Immunol.* **2010**, *31*, 7–17. [CrossRef]
431. Peterson, L.J.; Flood, P.M. Oxidative stress and microglial cells in Parkinson's disease. *Mediat. Inflamm.* **2012**, *2012*, 401264. [CrossRef] [PubMed]
432. Tang, Y.; Le, W. Differential roles of M1 and M2 microglia in neurodegenerative diseases. *Mol. Neurobiol.* **2016**, *53*, 1181–1194. [CrossRef]
433. Liu, C.Y.; Wang, X.; Liu, C.; Zhang, H.L. Pharmacological targeting of microglial activation: New therapeutic approach. *Front. Cell Neurosci.* **2019**, *13*, 514. [CrossRef]
434. Austin, S.A.; Floden, A.M.; Murphy, E.J.; Combs, C.K. Alpha-synuclein expression modulates microglial activation phenotype. *J. Neurosci.* **2006**, *26*, 10558–10563. [CrossRef] [PubMed]
435. Austin, S.A.; Rojanathammanee, L.; Golovko, M.Y.; Murphy, E.J.; Combs, C.K. Lack of alpha-synuclein modulates microglial phenotype in vitro. *Neurochem. Res.* **2011**, *36*, 994–1004. [CrossRef]
436. Rojanathammanee, L.; Murphy, E.J.; Combs, C.K. Expression of mutant alpha-synuclein modulates microglial phenotype in vitro. *J. Neuroinflamm.* **2011**, *8*, 44. [CrossRef]
437. Gardai, S.J.; Mao, W.; Schule, B.; Babcock, M.; Schoebel, S.; Lorenzana, C.; Alexander, J.; Kim, S.; Glick, H.; Hilton, K.; et al. Elevated alpha-synuclein impairs innate immune cell function and provides a potential peripheral biomarker for Parkinson's disease. *PLoS ONE* **2013**, *8*, e71634. [CrossRef]
438. Haenseler, W.; Zambon, F.; Lee, H.; Vowles, J.; Rinaldi, F.; Duggal, G.; Houlden, H.; Gwinn, K.; Wray, S.; Luk, K.C.; et al. Excess alpha-synuclein compromises phagocytosis in iPSC-derived macrophages. *Sci. Rep.* **2017**, *7*, 9003. [CrossRef]
439. Kim, S.; Cho, S.H.; Kim, K.Y.; Shin, K.Y.; Kim, H.S.; Park, C.H.; Chang, K.A.; Lee, S.H.; Cho, D.; Suh, Y.H. Alpha-synuclein induces migration of BV-2 microglial cells by up-regulation of CD44 and MT1-MMP. *J. Neurochem.* **2009**, *109*, 1483–1496. [CrossRef]
440. Streit, W.J.; Walter, S.A.; Pennell, N.A. Reactive microgliosis. *Prog. Neurobiol.* **1999**, *57*, 563–581. [CrossRef]
441. Long-Smith, C.M.; Sullivan, A.M.; Nolan, Y.M. The influence of microglia on the pathogenesis of Parkinson's disease. *Prog. Neurobiol.* **2009**, *89*, 277–287. [CrossRef] [PubMed]
442. Halliday, G.M.; Stevens, C.H. Glia: Initiators and progressors of pathology in Parkinson's disease. *Mov. Disord.* **2011**, *26*, 6–17. [CrossRef]
443. De Araujo, F.M.; Cuenca-Bermejo, L.; Fernandez-Villalba, E.; Costa, S.L.; Silva, V.D.A.; Herrero, M.T. Role of microgliosis and NLRP3 inflammasome in Parkinson's disease pathogenesis and therapy. *Cell Mol. Neurobiol.* **2021**. [CrossRef]
444. Jayaram, S.; Krishnamurthy, P.T. Role of microgliosis, oxidative stress and associated neuroinflammation in the pathogenesis of Parkinson's disease: The therapeutic role of Nrf2 activators. *Neurochem. Int.* **2021**, *145*, 105014. [CrossRef]
445. Marinova-Mutafchieva, L.; Sadeghian, M.; Broom, L.; Davis, J.B.; Medhurst, A.D.; Dexter, D.T. Relationship between microglial activation and dopaminergic neuronal loss in the substantia nigra: A time course study in a 6-hydroxydopamine model of Parkinson's disease. *J. Neurochem.* **2009**, *110*, 966–975. [CrossRef]
446. Ouchi, Y.; Yoshikawa, E.; Sekine, Y.; Futatsubashi, M.; Kanno, T.; Ogusu, T.; Torizuka, T. Microglial activation and dopamine terminal loss in early Parkinson's disease. *Ann. Neurol.* **2005**, *57*, 168–175. [CrossRef]
447. Bartels, A.L.; Willemsen, A.T.; Doorduin, J.; de Vries, E.F.; Dierckx, R.A.; Leenders, K.L. [11C]-PK11195 PET: Quantification of neuroinflammation and a monitor of anti-inflammatory treatment in Parkinson's disease? *Parkinsonism Relat. Disord.* **2010**, *16*, 57–59. [CrossRef] [PubMed]

448. Gerhard, A.; Pavese, N.; Hotton, G.; Turkheimer, F.; Es, M.; Hammers, A.; Eggert, K.; Oertel, W.; Banati, R.B.; Brooks, D.J. In vivo imaging of microglial activation with [11C](R)-PK11195 PET in idiopathic Parkinson's disease. *Neurobiol. Dis.* **2006**, *21*, 404–412. [CrossRef]
449. Barkholt, P.; Sanchez-Guajardo, V.; Kirik, D.; Romero-Ramos, M. Long-term polarization of microglia upon alpha-synuclein overexpression in nonhuman primates. *Neuroscience* **2012**, *208*, 85–96. [CrossRef]
450. Sanchez-Guajardo, V.; Febbraro, F.; Kirik, D.; Romero-Ramos, M. Microglia acquire distinct activation profiles depending on the degree of alpha-synuclein neuropathology in a rAAV based model of Parkinson's disease. *PLoS ONE* **2010**, *5*, e8784. [CrossRef] [PubMed]
451. Ginns, E.I.; Mak, S.K.; Ko, N.; Karlgren, J.; Akbarian, S.; Chou, V.P.; Guo, Y.; Lim, A.; Samuelsson, S.; LaMarca, M.L.; et al. Neuroinflammation and alpha-synuclein accumulation in response to glucocerebrosidase deficiency are accompanied by synaptic dysfunction. *Mol. Genet. Metab.* **2014**, *111*, 152–162. [CrossRef]
452. Gomez-Isla, T.; Irizarry, M.C.; Mariash, A.; Cheung, B.; Soto, O.; Schrump, S.; Sondel, J.; Kotilinek, L.; Day, J.; Schwarzschild, M.A.; et al. Motor dysfunction and gliosis with preserved dopaminergic markers in human alpha-synuclein A30P transgenic mice. *Neurobiol. Aging* **2003**, *24*, 245–258. [CrossRef]
453. Emmer, K.L.; Waxman, E.A.; Covy, J.P.; Giasson, B.I. E46K human alpha-synuclein transgenic mice develop Lewy-like and tau pathology associated with age-dependent, detrimental motor impairment. *J. Biol. Chem.* **2011**, *286*, 35104–35118. [CrossRef]
454. Watson, M.B.; Richter, F.; Lee, S.K.; Gabby, L.; Wu, J.; Masliah, E.; Effros, R.B.; Chesselet, M.F. Regionally-specific microglial activation in young mice over-expressing human wildtype alpha-synuclein. *Exp. Neurol.* **2012**, *237*, 318–334. [CrossRef] [PubMed]
455. Garcia-Esparcia, P.; Llorens, F.; Carmona, M.; Ferrer, I. Complex deregulation and expression of cytokines and mediators of the immune response in Parkinson's disease brain is region dependent. *Brain Pathol.* **2014**, *24*, 584–598. [CrossRef]
456. Zhang, W.; Wang, T.; Pei, Z.; Miller, D.S.; Wu, X.; Block, M.L.; Wilson, B.; Zhou, Y.; Hong, J.S.; Zhang, J. Aggregated alpha-synuclein activates microglia: A process leading to disease progression in Parkinson's disease. *FASEB J.* **2005**, *19*, 533–542. [CrossRef] [PubMed]
457. Ishizawa, K.; Komori, T.; Sasaki, S.; Arai, N.; Mizutani, T.; Hirose, T. Microglial activation parallels system degeneration in multiple system atrophy. *J. Neuropathol. Exp. Neurol.* **2004**, *63*, 43–52. [CrossRef]
458. Kubler, D.; Wachter, T.; Cabanel, N.; Su, Z.; Turkheimer, F.E.; Dodel, R.; Brooks, D.J.; Oertel, W.H.; Gerhard, A. Widespread microglial activation in multiple system atrophy. *Mov. Disord.* **2019**, *34*, 564–568. [CrossRef]
459. Harms, A.S.; Kordower, J.H.; Sette, A.; Lindestam Arlehamn, C.S.; Sulzer, D.; Mach, R.H. Inflammation in experimental models of alpha-synucleinopathies. *Mov. Disord.* **2021**, *36*, 37–49. [CrossRef]
460. Hirsch, E.C.; Hunot, S.; Damier, P.; Faucheux, B. Glial cells and inflammation in Parkinson's disease: A role in neurodegeneration? *Ann. Neurol.* **1998**, *44*, S115–S120. [CrossRef]
461. Shavali, S.; Combs, C.K.; Ebadi, M. Reactive macrophages increase oxidative stress and alpha-synuclein nitration during death of dopaminergic neuronal cells in co-culture: Relevance to Parkinson's disease. *Neurochem. Res.* **2006**, *31*, 85–94. [CrossRef] [PubMed]
462. Gao, H.M.; Kotzbauer, P.T.; Uryu, K.; Leight, S.; Trojanowski, J.Q.; Lee, V.M. Neuroinflammation and oxidation/nitration of alpha-synuclein linked to dopaminergic neurodegeneration. *J. Neurosci.* **2008**, *28*, 7687–7698. [CrossRef] [PubMed]
463. Zhang, W.; Dallas, S.; Zhang, D.; Guo, J.P.; Pang, H.; Wilson, B.; Miller, D.S.; Chen, B.; McGeer, P.L.; Hong, J.S.; et al. Microglial PHOX and Mac-1 are essential to the enhanced dopaminergic neurodegeneration elicited by A30P and A53T mutant alpha-synuclein. *Glia* **2007**, *55*, 1178–1188. [CrossRef]
464. Bick, R.J.; Poindexter, B.J.; Kott, M.M.; Liang, Y.A.; Dinh, K.; Kaur, B.; Bick, D.L.; Doursout, M.F.; Schiess, M.C. Cytokines disrupt intracellular patterns of Parkinson's disease-associated proteins alpha-synuclein, tau and ubiquitin in cultured glial cells. *Brain Res.* **2008**, *1217*, 203–212. [CrossRef]
465. Schiess, M.C.; Barnes, J.L.; Ellmore, T.M.; Poindexter, B.J.; Dinh, K.; Bick, R.J. CSF from Parkinson disease patients differentially affects cultured microglia and astrocytes. *BMC Neurosci.* **2010**, *11*, 151. [CrossRef]
466. Lee, M.K.; Stirling, W.; Xu, Y.; Xu, X.; Qui, D.; Mandir, A.S.; Dawson, T.M.; Copeland, N.G.; Jenkins, N.A.; Price, D.L. Human alpha-synuclein-harboring familial Parkinson's disease-linked Ala-53 –> Thr mutation causes neurodegenerative disease with alpha-synuclein aggregation in transgenic mice. *Proc. Natl. Acad. Sci. USA* **2002**, *99*, 8968–8973. [CrossRef]
467. Miller, R.M.; Kiser, G.L.; Kaysser-Kranich, T.; Casaceli, C.; Colla, E.; Lee, M.K.; Palaniappan, C.; Federoff, H.J. Wild-type and mutant alpha-synuclein induce a multi-component gene expression profile consistent with shared pathophysiology in different transgenic mouse models of PD. *Exp. Neurol.* **2007**, *204*, 421–432. [CrossRef]
468. Couch, Y.; Alvarez-Erviti, L.; Sibson, N.R.; Wood, M.J.; Anthony, D.C. The acute inflammatory response to intranigral alpha-synuclein differs significantly from intranigral lipopolysaccharide and is exacerbated by peripheral inflammation. *J. Neuroinflamm.* **2011**, *8*, 166. [CrossRef] [PubMed]
469. Wilms, H.; Rosenstiel, P.; Romero-Ramos, M.; Arlt, A.; Schafer, H.; Seegert, D.; Kahle, P.J.; Odoy, S.; Claasen, J.H.; Holzknecht, C.; et al. Suppression of MAP kinases inhibits microglial activation and attenuates neuronal cell death induced by alpha-synuclein protofibrils. *Int. J. Immunopathol. Pharmacol.* **2009**, *22*, 897–909. [CrossRef]
470. Jin, J.; Shie, F.S.; Liu, J.; Wang, Y.; Davis, J.; Schantz, A.M.; Montine, K.S.; Montine, T.J.; Zhang, J. Prostaglandin E2 receptor subtype 2 (EP2) regulates microglial activation and associated neurotoxicity induced by aggregated alpha-synuclein. *J. Neuroinflamm.* **2007**, *4*, 2. [CrossRef]

471. Theodore, S.; Cao, S.; McLean, P.J.; Standaert, D.G. Targeted overexpression of human alpha-synuclein triggers microglial activation and an adaptive immune response in a mouse model of Parkinson disease. *J. Neuropathol. Exp. Neurol.* **2008**, *67*, 1149–1158. [CrossRef]
472. St Martin, J.L.; Klucken, J.; Outeiro, T.F.; Nguyen, P.; Keller-McGandy, C.; Cantuti-Castelvetri, I.; Grammatopoulos, T.N.; Standaert, D.G.; Hyman, B.T.; McLean, P.J. Dopaminergic neuron loss and up-regulation of chaperone protein mRNA induced by targeted over-expression of alpha-synuclein in mouse substantia nigra. *J. Neurochem.* **2007**, *100*, 1449–1457. [CrossRef]
473. Alvarez-Erviti, L.; Couch, Y.; Richardson, J.; Cooper, J.M.; Wood, M.J. Alpha-synuclein release by neurons activates the inflammatory response in a microglial cell line. *Neurosci. Res.* **2011**, *69*, 337–342. [CrossRef] [PubMed]
474. Park, J.Y.; Paik, S.R.; Jou, I.; Park, S.M. Microglial phagocytosis is enhanced by monomeric alpha-synuclein, not aggregated alpha-synuclein: Implications for Parkinson's disease. *Glia* **2008**, *56*, 1215–1223. [CrossRef] [PubMed]
475. Lee, S.B.; Park, S.M.; Ahn, K.J.; Chung, K.C.; Paik, S.R.; Kim, J. Identification of the amino acid sequence motif of alpha-synuclein responsible for macrophage activation. *Biochem. Biophys. Res. Commun.* **2009**, *381*, 39–43. [CrossRef]
476. Klegeris, A.; Pelech, S.; Giasson, B.I.; Maguire, J.; Zhang, H.; McGeer, E.G.; McGeer, P.L. Alpha-synuclein activates stress signaling protein kinases in THP-1 cells and microglia. *Neurobiol. Aging* **2008**, *29*, 739–752. [CrossRef] [PubMed]
477. Su, X.; Maguire-Zeiss, K.A.; Giuliano, R.; Prifti, L.; Venkatesh, K.; Federoff, H.J. Synuclein activates microglia in a model of Parkinson's disease. *Neurobiol. Aging* **2008**, *29*, 1690–1701. [CrossRef]
478. Lee, E.J.; Woo, M.S.; Moon, P.G.; Baek, M.C.; Choi, I.Y.; Kim, W.K.; Junn, E.; Kim, H.S. Alpha-synuclein activates microglia by inducing the expressions of matrix metalloproteinases and the subsequent activation of protease-activated receptor-1. *J. Immunol.* **2010**, *185*, 615–623. [CrossRef] [PubMed]
479. Roodveldt, C.; Labrador-Garrido, A.; Gonzalez-Rey, E.; Fernandez-Montesinos, R.; Caro, M.; Lachaud, C.C.; Waudby, C.A.; Delgado, M.; Dobson, C.M.; Pozo, D. Glial innate immunity generated by non-aggregated alpha-synuclein in mouse: Differences between wild-type and Parkinson's disease-linked mutants. *PLoS ONE* **2010**, *5*, e13481. [CrossRef] [PubMed]
480. Li, N.; Stewart, T.; Sheng, L.; Shi, M.; Cilento, E.M.; Wu, Y.; Hong, J.S.; Zhang, J. Immunoregulation of microglial polarization: An unrecognized physiological function of alpha-synuclein. *J. Neuroinflamm.* **2020**, *17*, 272. [CrossRef]
481. Reynolds, A.D.; Glanzer, J.G.; Kadiu, I.; Ricardo-Dukelow, M.; Chaudhuri, A.; Ciborowski, P.; Cerny, R.; Gelman, B.; Thomas, M.P.; Mosley, R.L.; et al. Nitrated alpha-synuclein-activated microglial profiling for Parkinson's disease. *J. Neurochem.* **2008**, *104*, 1504–1525. [CrossRef]
482. Beraud, D.; Twomey, M.; Bloom, B.; Mittereder, A.; Ton, V.; Neitzke, K.; Chasovskikh, S.; Mhyre, T.R.; Maguire-Zeiss, K.A. Alpha-synuclein alters toll-like receptor expression. *Front. Neurosci.* **2011**, *5*, 80. [CrossRef]
483. Thomas, M.P.; Chartrand, K.; Reynolds, A.; Vitvitsky, V.; Banerjee, R.; Gendelman, H.E. Ion channel blockade attenuates aggregated alpha synuclein induction of microglial reactive oxygen species: Relevance for the pathogenesis of Parkinson's disease. *J. Neurochem.* **2007**, *100*, 503–519. [CrossRef]
484. Hoffmann, A.; Ettle, B.; Bruno, A.; Kulinich, A.; Hoffmann, A.C.; von Wittgenstein, J.; Winkler, J.; Xiang, W.; Schlachetzki, J.C.M. Alpha-synuclein activates BV2 microglia dependent on its aggregation state. *Biochem. Biophys. Res. Commun.* **2016**, *479*, 881–886. [CrossRef]
485. Hoenen, C.; Gustin, A.; Birck, C.; Kirchmeyer, M.; Beaume, N.; Felten, P.; Grandbarbe, L.; Heuschling, P.; Heurtaux, T. Alpha-synuclein proteins promote pro-inflammatory cascades in microglia: Stronger effects of the A53T mutant. *PLoS ONE* **2016**, *11*, e0162717. [CrossRef] [PubMed]
486. Li, Y.; Niu, M.; Zhao, A.; Kang, W.; Chen, Z.; Luo, N.; Zhou, L.; Zhu, X.; Lu, L.; Liu, J. CXCL12 is involved in alpha-synuclein-triggered neuroinflammation of Parkinson's disease. *J. Neuroinflamm.* **2019**, *16*, 263. [CrossRef] [PubMed]
487. Liu, J.; Zhou, Y.; Wang, Y.; Fong, H.; Murray, T.M.; Zhang, J. Identification of proteins involved in microglial endocytosis of alpha-synuclein. *J. Proteome Res.* **2007**, *6*, 3614–3627. [CrossRef]
488. Hou, L.; Bao, X.; Zang, C.; Yang, H.; Sun, F.; Che, Y.; Wu, X.; Li, S.; Zhang, D.; Wang, Q. Integrin CD11b mediates alpha-synuclein-induced activation of NADPH oxidase through a Rho-dependent pathway. *Redox. Biol.* **2018**, *14*, 600–608. [CrossRef]
489. Hou, L.; Qu, X.; Qiu, X.; Huang, R.; Zhao, X.; Wang, Q. Integrin CD11b mediates locus coeruleus noradrenergic neurodegeneration in a mouse Parkinson's disease model. *J. Neuroinflamm.* **2020**, *17*, 148. [CrossRef] [PubMed]
490. Wang, S.; Chu, C.H.; Stewart, T.; Ginghina, C.; Wang, Y.; Nie, H.; Guo, M.; Wilson, B.; Hong, J.S.; Zhang, J. alpha-Synuclein, a chemoattractant, directs microglial migration via H2O2-dependent Lyn phosphorylation. *Proc. Natl. Acad. Sci. USA* **2015**, *112*, E1926–E1935. [CrossRef] [PubMed]
491. Su, X.; Federoff, H.J.; Maguire-Zeiss, K.A. Mutant alpha-synuclein overexpression mediates early proinflammatory activity. *Neurotox. Res.* **2009**, *16*, 238–254. [CrossRef] [PubMed]
492. Jiang, T.; Hoekstra, J.; Heng, X.; Kang, W.; Ding, J.; Liu, J.; Chen, S.; Zhang, J. P2X7 receptor is critical in alpha-synuclein—Mediated microglial NADPH oxidase activation. *Neurobiol. Aging* **2015**, *36*, 2304–2318. [CrossRef]
493. Cao, S.; Standaert, D.G.; Harms, A.S. The gamma chain subunit of Fc receptors is required for alpha-synuclein-induced pro-inflammatory signaling in microglia. *J. Neuroinflamm.* **2012**, *9*, 259. [CrossRef]
494. Stefanova, N.; Fellner, L.; Reindl, M.; Masliah, E.; Poewe, W.; Wenning, G.K. Toll-like receptor 4 promotes alpha-synuclein clearance and survival of nigral dopaminergic neurons. *Am. J. Pathol.* **2011**, *179*, 954–963. [CrossRef]

495. Venezia, S.; Refolo, V.; Polissidis, A.; Stefanis, L.; Wenning, G.K.; Stefanova, N. Toll-like receptor 4 stimulation with monophosphoryl lipid A ameliorates motor deficits and nigral neurodegeneration triggered by extraneuronal alpha-synucleinopathy. *Mol. Neurodegener.* **2017**, *12*, 52. [CrossRef] [PubMed]
496. Fellner, L.; Irschick, R.; Schanda, K.; Reindl, M.; Klimaschewski, L.; Poewe, W.; Wenning, G.K.; Stefanova, N. Toll-like receptor 4 is required for alpha-synuclein dependent activation of microglia and astroglia. *Glia* **2013**, *61*, 349–360. [CrossRef]
497. Kim, C.; Ho, D.H.; Suk, J.E.; You, S.; Michael, S.; Kang, J.; Joong Lee, S.; Masliah, E.; Hwang, D.; Lee, H.J.; et al. Neuron-released oligomeric alpha-synuclein is an endogenous agonist of TLR2 for paracrine activation of microglia. *Nat. Commun.* **2013**, *4*, 1562. [CrossRef] [PubMed]
498. Dzamko, N.; Gysbers, A.; Perera, G.; Bahar, A.; Shankar, A.; Gao, J.; Fu, Y.; Halliday, G.M. Toll-like receptor 2 is increased in neurons in Parkinson's disease brain and may contribute to alpha-synuclein pathology. *Acta Neuropathol.* **2017**, *133*, 303–319. [CrossRef]
499. Kim, C.; Spencer, B.; Rockenstein, E.; Yamakado, H.; Mante, M.; Adame, A.; Fields, J.A.; Masliah, D.; Iba, M.; Lee, H.J.; et al. Immunotherapy targeting toll-like receptor 2 alleviates neurodegeneration in models of synucleinopathy by modulating alpha-synuclein transmission and neuroinflammation. *Mol. Neurodegener.* **2018**, *13*, 43. [CrossRef]
500. Kwon, S.; Iba, M.; Masliah, E.; Kim, C. Targeting microglial and neuronal toll-like receptor 2 in synucleinopathies. *Exp. Neurobiol.* **2019**, *28*, 547–553. [CrossRef]
501. Caplan, I.F.; Maguire-Zeiss, K.A. Toll-like receptor 2 signaling and current approaches for therapeutic modulation in synucleinopathies. *Front. Pharmacol.* **2018**, *9*, 417. [CrossRef]
502. Roodveldt, C.; Labrador-Garrido, A.; Gonzalez-Rey, E.; Lachaud, C.C.; Guilliams, T.; Fernandez-Montesinos, R.; Benitez-Rondan, A.; Robledo, G.; Hmadcha, A.; Delgado, M.; et al. Preconditioning of microglia by alpha-synuclein strongly affects the response induced by toll-like receptor (TLR) stimulation. *PLoS ONE* **2013**, *8*, e79160. [CrossRef]
503. Reynolds, A.D.; Kadiu, I.; Garg, S.K.; Glanzer, J.G.; Nordgren, T.; Ciborowski, P.; Banerjee, R.; Gendelman, H.E. Nitrated alpha-synuclein and microglial neuroregulatory activities. *J. Neuroimmune Pharmacol.* **2008**, *3*, 59–74. [CrossRef] [PubMed]
504. Daniele, S.G.; Beraud, D.; Davenport, C.; Cheng, K.; Yin, H.; Maguire-Zeiss, K.A. Activation of MyD88-dependent TLR1/2 signaling by misfolded alpha-synuclein, a protein linked to neurodegenerative disorders. *Sci. Signal.* **2015**, *8*, ra45. [CrossRef] [PubMed]
505. Prabhakaran, K.; Chapman, G.D.; Gunasekar, P.G. alpha-Synuclein overexpression enhances manganese-induced neurotoxicity through the NF-kappaB-mediated pathway. *Toxicol. Mech. Methods* **2011**, *21*, 435–443. [CrossRef]
506. Maekawa, T.; Sasaoka, T.; Azuma, S.; Ichikawa, T.; Melrose, H.L.; Farrer, M.J.; Obata, F. Leucine-rich repeat kinase 2 (LRRK2) regulates alpha-synuclein clearance in microglia. *BMC Neurosci.* **2016**, *17*, 77. [CrossRef]
507. Daher, J.P.; Volpicelli-Daley, L.A.; Blackburn, J.P.; Moehle, M.S.; West, A.B. Abrogation of alpha-synuclein-mediated dopaminergic neurodegeneration in LRRK2-deficient rats. *Proc. Natl. Acad. Sci. USA* **2014**, *111*, 9289–9294. [CrossRef] [PubMed]
508. Codolo, G.; Plotegher, N.; Pozzobon, T.; Brucale, M.; Tessari, I.; Bubacco, L.; de Bernard, M. Triggering of inflammasome by aggregated alpha-synuclein, an inflammatory response in synucleinopathies. *PLoS ONE* **2013**, *8*, e55375. [CrossRef] [PubMed]
509. Freeman, D.; Cedillos, R.; Choyke, S.; Lukic, Z.; McGuire, K.; Marvin, S.; Burrage, A.M.; Sudholt, S.; Rana, A.; O'Connor, C.; et al. Alpha-synuclein induces lysosomal rupture and cathepsin dependent reactive oxygen species following endocytosis. *PLoS ONE* **2013**, *8*, e62143. [CrossRef] [PubMed]
510. Zhou, Y.; Lu, M.; Du, R.H.; Qiao, C.; Jiang, C.Y.; Zhang, K.Z.; Ding, J.H.; Hu, G. MicroRNA-7 targets Nod-like receptor protein 3 inflammasome to modulate neuroinflammation in the pathogenesis of Parkinson's disease. *Mol. Neurodegener.* **2016**, *11*, 28. [CrossRef]
511. Beraud, D.; Hathaway, H.A.; Trecki, J.; Chasovskikh, S.; Johnson, D.A.; Johnson, J.A.; Federoff, H.J.; Shimoji, M.; Mhyre, T.R.; Maguire-Zeiss, K.A. Microglial activation and antioxidant responses induced by the Parkinson's disease protein alpha-synuclein. *J. Neuroimmune Pharmacol.* **2013**, *8*, 94–117. [CrossRef] [PubMed]
512. Lastres-Becker, I.; Ulusoy, A.; Innamorato, N.G.; Sahin, G.; Rabano, A.; Kirik, D.; Cuadrado, A. alpha-Synuclein expression and Nrf2 deficiency cooperate to aggravate protein aggregation, neuronal death and inflammation in early-stage Parkinson's disease. *Hum. Mol. Genet.* **2012**, *21*, 3173–3192. [CrossRef]
513. Gan, L.; Vargas, M.R.; Johnson, D.A.; Johnson, J.A. Astrocyte-specific overexpression of Nrf2 delays motor pathology and synuclein aggregation throughout the CNS in the alpha-synuclein mutant (A53T) mouse model. *J. Neurosci.* **2012**, *32*, 17775–17787. [CrossRef] [PubMed]
514. Skibinski, G.; Hwang, V.; Ando, D.M.; Daub, A.; Lee, A.K.; Ravisankar, A.; Modan, S.; Finucane, M.M.; Shaby, B.A.; Finkbeiner, S. Nrf2 mitigates LRRK2- and alpha-synuclein-induced neurodegeneration by modulating proteostasis. *Proc. Natl. Acad. Sci. USA* **2017**, *114*, 1165–1170. [CrossRef]
515. Subbarayan, M.S.; Hudson, C.; Moss, L.D.; Nash, K.R.; Bickford, P.C. T cell infiltration and upregulation of MHCII in microglia leads to accelerated neuronal loss in an alpha-synuclein rat model of Parkinson's disease. *J. Neuroinflamm.* **2020**, *17*, 242. [CrossRef]
516. Harms, A.S.; Cao, S.; Rowse, A.L.; Thome, A.D.; Li, X.; Mangieri, L.R.; Cron, R.Q.; Shacka, J.J.; Raman, C.; Standaert, D.G. MHCII is required for alpha-synuclein-induced activation of microglia, CD4 T cell proliferation, and dopaminergic neurodegeneration. *J. Neurosci.* **2013**, *33*, 9592–9600. [CrossRef]

517. Williams, G.P.; Marmion, D.J.; Schonhoff, A.M.; Jurkuvenaite, A.; Won, W.J.; Standaert, D.G.; Kordower, J.H.; Harms, A.S. T cell infiltration in both human multiple system atrophy and a novel mouse model of the disease. *Acta Neuropathol.* **2020**, *139*, 855–874. [CrossRef]
518. Lindestam Arlehamn, C.S.; Dhanwani, R.; Pham, J.; Kuan, R.; Frazier, A.; Rezende Dutra, J.; Phillips, E.; Mallal, S.; Roederer, M.; Marder, K.S.; et al. Alpha-synuclein-specific T cell reactivity is associated with preclinical and early Parkinson's disease. *Nat. Commun.* **2020**, *11*, 1875. [CrossRef] [PubMed]
519. Sulzer, D.; Alcalay, R.N.; Garretti, F.; Cote, L.; Kanter, E.; Agin-Liebes, J.; Liong, C.; McMurtrey, C.; Hildebrand, W.H.; Mao, X.; et al. T cells from patients with Parkinson's disease recognize alpha-synuclein peptides. *Nature* **2017**, *546*, 656–661. [CrossRef]
520. Jimenez-Ferrer, I.; Backstrom, F.; Duenas-Rey, A.; Jewett, M.; Boza-Serrano, A.; Luk, K.C.; Deierborg, T.; Swanberg, M. The MHC class II transactivator modulates seeded alpha-synuclein pathology and dopaminergic neurodegeneration in an in vivo rat model of Parkinson's disease. *Brain Behav. Immun.* **2021**, *91*, 369–382. [CrossRef]
521. Choi, I.; Zhang, Y.; Seegobin, S.P.; Pruvost, M.; Wang, Q.; Purtell, K.; Zhang, B.; Yue, Z. Microglia clear neuron-released alpha-synuclein via selective autophagy and prevent neurodegeneration. *Nat. Commun.* **2020**, *11*, 1386. [CrossRef]
522. Lee, H.J.; Suk, J.E.; Bae, E.J.; Lee, S.J. Clearance and deposition of extracellular alpha-synuclein aggregates in microglia. *Biochem. Biophys. Res. Commun.* **2008**, *372*, 423–428. [CrossRef]
523. Nash, Y.; Schmukler, E.; Trudler, D.; Pinkas-Kramarski, R.; Frenkel, D. DJ-1 deficiency impairs autophagy and reduces alpha-synuclein phagocytosis by microglia. *J. Neurochem.* **2017**, *143*, 584–594. [CrossRef]
524. Wu, K.C.; Liou, H.H.; Kao, Y.H.; Lee, C.Y.; Lin, C.J. The critical role of Nramp1 in degrading alpha-synuclein oligomers in microglia under iron overload condition. *Neurobiol. Dis.* **2017**, *104*, 61–72. [CrossRef] [PubMed]
525. Bussi, C.; Peralta Ramos, J.M.; Arroyo, D.S.; Gallea, J.I.; Ronchi, P.; Kolovou, A.; Wang, J.M.; Florey, O.; Celej, M.S.; Schwab, Y.; et al. Alpha-synuclein fibrils recruit TBK1 and OPTN to lysosomal damage sites and induce autophagy in microglial cells. *J. Cell Sci.* **2018**, *131*. [CrossRef]
526. Bliederhaeuser, C.; Grozdanov, V.; Speidel, A.; Zondler, L.; Ruf, W.P.; Bayer, H.; Kiechle, M.; Feiler, M.S.; Freischmidt, A.; Brenner, D.; et al. Age-dependent defects of alpha-synuclein oligomer uptake in microglia and monocytes. *Acta Neuropathol.* **2016**, *131*, 379–391. [CrossRef]
527. Scheffold, A.; Holtman, I.R.; Dieni, S.; Brouwer, N.; Katz, S.F.; Jebaraj, B.M.; Kahle, P.J.; Hengerer, B.; Lechel, A.; Stilgenbauer, S.; et al. Telomere shortening leads to an acceleration of synucleinopathy and impaired microglia response in a genetic mouse model. *Acta Neuropathol. Commun.* **2016**, *4*, 87. [CrossRef]
528. Park, J.Y.; Kim, K.S.; Lee, S.B.; Ryu, J.S.; Chung, K.C.; Choo, Y.K.; Jou, I.; Kim, J.; Park, S.M. On the mechanism of internalization of alpha-synuclein into microglia: Roles of ganglioside GM1 and lipid raft. *J. Neurochem.* **2009**, *110*, 400–411. [CrossRef] [PubMed]
529. Fitzner, D.; Schnaars, M.; van Rossum, D.; Krishnamoorthy, G.; Dibaj, P.; Bakhti, M.; Regen, T.; Hanisch, U.K.; Simons, M. Selective transfer of exosomes from oligodendrocytes to microglia by macropinocytosis. *J. Cell Sci.* **2011**, *124*, 447–458. [CrossRef] [PubMed]
530. Chang, C.; Lang, H.; Geng, N.; Wang, J.; Li, N.; Wang, X. Exosomes of BV-2 cells induced by alpha-synuclein: Important mediator of neurodegeneration in PD. *Neurosci. Lett.* **2013**, *548*, 190–195. [CrossRef]
531. Guo, M.; Wang, J.; Zhao, Y.; Feng, Y.; Han, S.; Dong, Q.; Cui, M.; Tieu, K. Microglial exosomes facilitate alpha-synuclein transmission in Parkinson's disease. *Brain* **2020**, *143*, 1476–1497. [CrossRef]
532. George, S.; Rey, N.L.; Tyson, T.; Esquibel, C.; Meyerdirk, L.; Schulz, E.; Pierce, S.; Burmeister, A.R.; Madaj, Z.; Steiner, J.A.; et al. Microglia affect alpha-synuclein cell-to-cell transfer in a mouse model of Parkinson's disease. *Mol. Neurodegener.* **2019**, *14*, 34. [CrossRef] [PubMed]
533. Deitmer, J.W.; Theparambil, S.M.; Ruminot, I.; Noor, S.I.; Becker, H.M. Energy dynamics in the brain: Contributions of astrocytes to metabolism and pH homeostasis. *Front. Neurosci.* **2019**, *13*, 1301. [CrossRef]
534. Dienel, G.A.; Carlson, G.M. Major advances in brain glycogen research: Understanding of the roles of glycogen Have evolved from emergency fuel reserve to dynamic, regulated participant in diverse brain functions. *Adv. Neurobiol.* **2019**, *23*, 1–16. [CrossRef]
535. Halassa, M.M.; Haydon, P.G. Integrated brain circuits: Astrocytic networks modulate neuronal activity and behavior. *Annu. Rev. Physiol.* **2010**, *72*, 335–355. [CrossRef]
536. Haydon, P.G.; Carmignoto, G. Astrocyte control of synaptic transmission and neurovascular coupling. *Physiol. Rev.* **2006**, *86*, 1009–1031. [CrossRef] [PubMed]
537. Kimelberg, H.K.; Nedergaard, M. Functions of astrocytes and their potential as therapeutic targets. *Neurotherapeutics* **2010**, *7*, 338–353. [CrossRef] [PubMed]
538. Seth, P.; Koul, N. Astrocyte, the star avatar: Redefined. *J. Biosci.* **2008**, *33*, 405–421. [CrossRef]
539. Vasile, F.; Dossi, E.; Rouach, N. Human astrocytes: Structure and functions in the healthy brain. *Brain Struct. Funct.* **2017**, *222*, 2017–2029. [CrossRef]
540. Simard, M.; Nedergaard, M. The neurobiology of glia in the context of water and ion homeostasis. *Neuroscience* **2004**, *129*, 877–896. [CrossRef] [PubMed]
541. Mulder, M. Sterols in the central nervous system. *Curr. Opin. Clin. Nutr. Metab. Care* **2009**, *12*, 152–158. [CrossRef]
542. Kiray, H.; Lindsay, S.L.; Hosseinzadeh, S.; Barnett, S.C. The multifaceted role of astrocytes in regulating myelination. *Exp. Neurol.* **2016**, *283*, 541–549. [CrossRef]

543. Traiffort, E.; Kassoussi, A.; Zahaf, A.; Laouarem, Y. Astrocytes and microglia as major players of myelin production in normal and pathological conditions. *Front. Cell. Neurosci.* **2020**, *14*, 79. [CrossRef]
544. Halassa, M.M.; Fellin, T.; Haydon, P.G. The tripartite synapse: Roles for gliotransmission in health and disease. *Trends Mol. Med.* **2007**, *13*, 54–63. [CrossRef]
545. Harada, K.; Kamiya, T.; Tsuboi, T. Gliotransmitter release from astrocytes: Functional, developmental, and pathological implications in the brain. *Front. Neurosci.* **2015**, *9*, 499. [CrossRef] [PubMed]
546. Agulhon, C.; Sun, M.Y.; Murphy, T.; Myers, T.; Lauderdale, K.; Fiacco, T.A. Calcium signaling and gliotransmission in normal vs. reactive astrocytes. *Front. Pharmacol.* **2012**, *3*, 139. [CrossRef]
547. Tabata, H. Diverse subtypes of astrocytes and their development during corticogenesis. *Front. Neurosci.* **2015**, *9*, 114. [CrossRef] [PubMed]
548. Oberheim, N.A.; Takano, T.; Han, X.; He, W.; Lin, J.H.; Wang, F.; Xu, Q.; Wyatt, J.D.; Pilcher, W.; Ojemann, J.G.; et al. Uniquely hominid features of adult human astrocytes. *J. Neurosci.* **2009**, *29*, 3276–3287. [CrossRef] [PubMed]
549. Sofroniew, M.V.; Vinters, H.V. Astrocytes: Biology and pathology. *Acta Neuropathol.* **2010**, *119*, 7–35. [CrossRef]
550. Lee, H.J.; Suk, J.E.; Patrick, C.; Bae, E.J.; Cho, J.H.; Rho, S.; Hwang, D.; Masliah, E.; Lee, S.J. Direct transfer of alpha-synuclein from neuron to astroglia causes inflammatory responses in synucleinopathies. *J. Biol. Chem.* **2010**, *285*, 9262–9272. [CrossRef] [PubMed]
551. Saavedra, A.; Baltazar, G.; Santos, P.; Carvalho, C.M.; Duarte, E.P. Selective injury to dopaminergic neurons up-regulates GDNF in substantia nigra postnatal cell cultures: Role of neuron-glia crosstalk. *Neurobiol. Dis.* **2006**, *23*, 533–542. [CrossRef] [PubMed]
552. Sandhu, J.K.; Gardaneh, M.; Iwasiow, R.; Lanthier, P.; Gangaraju, S.; Ribecco-Lutkiewicz, M.; Tremblay, R.; Kiuchi, K.; Sikorska, M. Astrocyte-secreted GDNF and glutathione antioxidant system protect neurons against 6OHDA cytotoxicity. *Neurobiol. Dis.* **2009**, *33*, 405–414. [CrossRef]
553. Mori, F.; Tanji, K.; Yoshimoto, M.; Takahashi, H.; Wakabayashi, K. Demonstration of alpha-synuclein immunoreactivity in neuronal and glial cytoplasm in normal human brain tissue using proteinase K and formic acid pretreatment. *Exp. Neurol.* **2002**, *176*, 98–104. [CrossRef]
554. Tanji, K.; Imaizumi, T.; Yoshida, H.; Mori, F.; Yoshimoto, M.; Satoh, K.; Wakabayashi, K. Expression of alpha-synuclein in a human glioma cell line and its up-regulation by interleukin-1beta. *Neuroreport* **2001**, *12*, 1909–1912. [CrossRef]
555. Cheng, S.Y.; Trombetta, L.D. The induction of amyloid precursor protein and alpha-synuclein in rat hippocampal astrocytes by diethyldithiocarbamate and copper with or without glutathione. *Toxicol. Lett.* **2004**, *146*, 139–149. [CrossRef]
556. Stevenson, T.J.; Murray, H.C.; Turner, C.; Faull, R.L.M.; Dieriks, B.V.; Curtis, M.A. alpha-synuclein inclusions are abundant in non-neuronal cells in the anterior olfactory nucleus of the Parkinson's disease olfactory bulb. *Sci. Rep.* **2020**, *10*, 6682. [CrossRef] [PubMed]
557. Sorrentino, Z.A.; Giasson, B.I.; Chakrabarty, P. alpha-Synuclein and astrocytes: Tracing the pathways from homeostasis to neurodegeneration in Lewy body disease. *Acta Neuropathol.* **2019**, *138*, 1–21. [CrossRef] [PubMed]
558. Piao, Y.S.; Mori, F.; Hayashi, S.; Tanji, K.; Yoshimoto, M.; Kakita, A.; Wakabayashi, K.; Takahashi, H. Alpha-synuclein pathology affecting Bergmann glia of the cerebellum in patients with alpha-synucleinopathies. *Acta Neuropathol.* **2003**, *105*, 403–409. [CrossRef]
559. Hishikawa, N.; Hashizume, Y.; Yoshida, M.; Sobue, G. Widespread occurrence of argyrophilic glial inclusions in Parkinson's disease. *Neuropathol. Appl. Neurobiol.* **2001**, *27*, 362–372. [CrossRef]
560. Terada, S.; Ishizu, H.; Yokota, O.; Tsuchiya, K.; Nakashima, H.; Ishihara, T.; Fujita, D.; Ueda, K.; Ikeda, K.; Kuroda, S. Glial involvement in diffuse Lewy body disease. *Acta Neuropathol.* **2003**, *105*, 163–169. [CrossRef]
561. Sorrentino, Z.A.; Goodwin, M.S.; Riffe, C.J.; Dhillon, J.S.; Xia, Y.; Gorion, K.M.; Vijayaraghavan, N.; McFarland, K.N.; Golbe, L.I.; Yachnis, A.T.; et al. Unique alpha-synuclein pathology within the amygdala in Lewy body dementia: Implications for disease initiation and progression. *Acta Neuropathol. Commun.* **2019**, *7*, 142. [CrossRef]
562. Booth, H.D.E.; Hirst, W.D.; Wade-Martins, R. The role of astrocyte dysfunction in Parkinson's disease pathogenesis. *Trends Neurosci.* **2017**, *40*, 358–370. [CrossRef]
563. Ding, Z.B.; Song, L.J.; Wang, Q.; Kumar, G.; Yan, Y.Q.; Ma, C.G. Astrocytes: A double-edged sword in neurodegenerative diseases. *Neural. Regen. Res.* **2021**, *16*, 1702–1710. [CrossRef]
564. Ghiglieri, V.; Calabrese, V.; Calabresi, P. Alpha-synuclein: From early synaptic dysfunction to neurodegeneration. *Front. Neurol.* **2018**, *9*, 295. [CrossRef] [PubMed]
565. Sacino, A.N.; Brooks, M.M.; Chakrabarty, P.; Saha, K.; Khoshbouei, H.; Golde, T.E.; Giasson, B.I. Proteolysis of alpha-synuclein fibrils in the lysosomal pathway limits induction of inclusion pathology. *J. Neurochem.* **2017**, *140*, 662–678. [CrossRef]
566. Erustes, A.G.; Stefani, F.Y.; Terashima, J.Y.; Stilhano, R.S.; Monteforte, P.T.; da Silva Pereira, G.J.; Han, S.W.; Calgarotto, A.K.; Hsu, Y.T.; Ureshino, R.P.; et al. Overexpression of alpha-synuclein in an astrocyte cell line promotes autophagy inhibition and apoptosis. *J. Neurosci. Res.* **2018**, *96*, 160–171. [CrossRef] [PubMed]
567. Knott, C.; Stern, G.; Kingsbury, A.; Welcher, A.A.; Wilkin, G.P. Elevated glial brain-derived neurotrophic factor in Parkinson's diseased nigra. *Parkinsonism Relat. Disord.* **2002**, *8*, 329–341. [CrossRef]
568. Damier, P.; Hirsch, E.C.; Zhang, P.; Agid, Y.; Javoy-Agid, F. Glutathione peroxidase, glial cells and Parkinson's disease. *Neuroscience* **1993**, *52*, 1–6. [CrossRef]

569. Mythri, R.B.; Venkateshappa, C.; Harish, G.; Mahadevan, A.; Muthane, U.B.; Yasha, T.C.; Srinivas Bharath, M.M.; Shankar, S.K. Evaluation of markers of oxidative stress, antioxidant function and astrocytic proliferation in the striatum and frontal cortex of Parkinson's disease brains. *Neurochem. Res.* **2011**, *36*, 1452–1463. [CrossRef]
570. Hua, J.; Yin, N.; Xu, S.; Chen, Q.; Tao, T.; Zhang, J.; Ding, J.; Fan, Y.; Hu, G. Enhancing the astrocytic clearance of extracellular alpha-synuclein aggregates by ginkgolides attenuates neural cell injury. *Cell Mol. Neurobiol.* **2019**, *39*, 1017–1028. [CrossRef] [PubMed]
571. Loria, F.; Vargas, J.Y.; Bousset, L.; Syan, S.; Salles, A.; Melki, R.; Zurzolo, C. alpha-Synuclein transfer between neurons and astrocytes indicates that astrocytes play a role in degradation rather than in spreading. *Acta Neuropathol.* **2017**, *134*, 789–808. [CrossRef]
572. Di Domenico, A.; Carola, G.; Calatayud, C.; Pons-Espinal, M.; Munoz, J.P.; Richaud-Patin, Y.; Fernandez-Carasa, I.; Gut, M.; Faella, A.; Parameswaran, J.; et al. Patient-specific iPSC-derived astrocytes contribute to non-cell-autonomous neurodegeneration in Parkinson's disease. *Stem Cell Rep.* **2019**, *12*, 213–229. [CrossRef] [PubMed]
573. Sacino, A.N.; Thomas, M.A.; Ceballos-Diaz, C.; Cruz, P.E.; Rosario, A.M.; Lewis, J.; Giasson, B.I.; Golde, T.E. Conformational templating of alpha-synuclein aggregates in neuronal-glial cultures. *Mol. Neurodegener.* **2013**, *8*, 17. [CrossRef]
574. Cavaliere, F.; Cerf, L.; Dehay, B.; Ramos-Gonzalez, P.; De Giorgi, F.; Bourdenx, M.; Bessede, A.; Obeso, J.A.; Matute, C.; Ichas, F.; et al. In vitro alpha-synuclein neurotoxicity and spreading among neurons and astrocytes using Lewy body extracts from Parkinson disease brains. *Neurobiol. Dis.* **2017**, *103*, 101–112. [CrossRef] [PubMed]
575. Sorrentino, Z.A.; Xia, Y.; Funk, C.; Riffe, C.J.; Rutherford, N.J.; Ceballos Diaz, C.; Sacino, A.N.; Price, N.D.; Golde, T.E.; Giasson, B.I.; et al. Motor neuron loss and neuroinflammation in a model of alpha-synuclein-induced neurodegeneration. *Neurobiol. Dis.* **2018**, *120*, 98–106. [CrossRef]
576. Sorrentino, Z.A.; Brooks, M.M.T.; Hudson, V., 3rd; Rutherford, N.J.; Golde, T.E.; Giasson, B.I.; Chakrabarty, P. Intrastriatal injection of alpha-synuclein can lead to widespread synucleinopathy independent of neuroanatomic connectivity. *Mol. Neurodegener.* **2017**, *12*, 40. [CrossRef]
577. Wang, Y.; Cui, J.; Sun, X.; Zhang, Y. Tunneling-nanotube development in astrocytes depends on p53 activation. *Cell Death Differ.* **2011**, *18*, 732–742. [CrossRef]
578. Rostami, J.; Holmqvist, S.; Lindstrom, V.; Sigvardson, J.; Westermark, G.T.; Ingelsson, M.; Bergstrom, J.; Roybon, L.; Erlandsson, A. Human astrocytes transfer aggregated alpha-synuclein via tunneling nanotubes. *J. Neurosci.* **2017**, *37*, 11835–11853. [CrossRef]
579. Jiang, C.; Hopfner, F.; Katsikoudi, A.; Hein, R.; Catli, C.; Evetts, S.; Huang, Y.; Wang, H.; Ryder, J.W.; Kuhlenbaeumer, G.; et al. Serum neuronal exosomes predict and differentiate Parkinson's disease from atypical parkinsonism. *J. Neurol. Neurosurg. Psychiatry* **2020**, *91*, 720–729. [CrossRef] [PubMed]
580. Karampetsou, M.; Sykioti, V.S.; Leandrou, E.; Melachroinou, K.; Lambiris, A.; Giannelos, A.; Emmanouilidou, E.; Vekrellis, K. Intrastriatal administration of exosome-associated pathological alpha-synuclein is not sufficient by itself to cause pathology transmission. *Front. Neurosci* **2020**, *14*, 246. [CrossRef]
581. Fan, R.Z.; Guo, M.; Luo, S.; Cui, M.; Tieu, K. Exosome release and neuropathology induced by alpha-synuclein: New insights into protective mechanisms of Drp1 inhibition. *Acta Neuropathol. Commun.* **2019**, *7*, 184. [CrossRef]
582. Niu, M.; Li, Y.; Li, G.; Zhou, L.; Luo, N.; Yao, M.; Kang, W.; Liu, J. A longitudinal study on alpha-synuclein in plasma neuronal exosomes as a biomarker for Parkinson's disease development and progression. *Eur. J. Neurol.* **2020**, *27*, 967–974. [CrossRef]
583. Pascua-Maestro, R.; Gonzalez, E.; Lillo, C.; Ganfornina, M.D.; Falcon-Perez, J.M.; Sanchez, D. Extracellular vesicles secreted by astroglial cells transport apolipoprotein D to neurons and mediate neuronal survival upon oxidative stress. *Front. Cell Neurosci.* **2018**, *12*, 526. [CrossRef]
584. Shakespear, N.; Ogura, M.; Yamaki, J.; Homma, Y. Astrocyte-Derived Exosomal microRNA miR-200a-3p Prevents MPP(+)-induced apoptotic cell death through down-regulation of MKK4. *Neurochem. Res.* **2020**, *45*, 1020–1033. [CrossRef] [PubMed]
585. Meng, Y.; Ding, J.; Li, C.; Fan, H.; He, Y.; Qiu, P. Transfer of pathological alpha-synuclein from neurons to astrocytes via exosomes causes inflammatory responses after METH exposure. *Toxicol. Lett.* **2020**, *331*, 188–199. [CrossRef]
586. Ngolab, J.; Trinh, I.; Rockenstein, E.; Mante, M.; Florio, J.; Trejo, M.; Masliah, D.; Adame, A.; Masliah, E.; Rissman, R.A. Brain-derived exosomes from dementia with Lewy bodies propagate alpha-synuclein pathology. *Acta Neuropathol. Commun.* **2017**, *5*, 46. [CrossRef] [PubMed]
587. Klegeris, A.; Giasson, B.I.; Zhang, H.; Maguire, J.; Pelech, S.; McGeer, P.L. Alpha-synuclein and its disease-causing mutants induce ICAM-1 and IL-6 in human astrocytes and astrocytoma cells. *FASEB J.* **2006**, *20*, 2000–2008. [CrossRef] [PubMed]
588. Rannikko, E.H.; Weber, S.S.; Kahle, P.J. Exogenous alpha-synuclein induces toll-like receptor 4 dependent inflammatory responses in astrocytes. *BMC Neurosci.* **2015**, *16*, 57. [CrossRef]
589. Angelova, P.R.; Ludtmann, M.H.; Horrocks, M.H.; Negoda, A.; Cremades, N.; Klenerman, D.; Dobson, C.M.; Wood, N.W.; Pavlov, E.V.; Gandhi, S.; et al. Ca2+ is a key factor in alpha-synuclein-induced neurotoxicity. *J. Cell Sci.* **2016**, *129*, 1792–1801. [CrossRef] [PubMed]
590. Cremades, N.; Cohen, S.I.; Deas, E.; Abramov, A.Y.; Chen, A.Y.; Orte, A.; Sandal, M.; Clarke, R.W.; Dunne, P.; Aprile, F.A.; et al. Direct observation of the interconversion of normal and toxic forms of alpha-synuclein. *Cell* **2012**, *149*, 1048–1059. [CrossRef]
591. Stefanova, N.; Klimaschewski, L.; Poewe, W.; Wenning, G.K.; Reindl, M. Glial cell death induced by overexpression of alpha-synuclein. *J. Neurosci. Res.* **2001**, *65*, 432–438. [CrossRef]

592. Yun, S.P.; Kam, T.I.; Panicker, N.; Kim, S.; Oh, Y.; Park, J.S.; Kwon, S.H.; Park, Y.J.; Karuppagounder, S.S.; Park, H.; et al. Block of A1 astrocyte conversion by microglia is neuroprotective in models of Parkinson's disease. *Nat. Med.* **2018**, *24*, 931–938. [CrossRef]
593. Gu, X.L.; Long, C.X.; Sun, L.; Xie, C.; Lin, X.; Cai, H. Astrocytic expression of Parkinson's disease-related A53T alpha-synuclein causes neurodegeneration in mice. *Mol. Brain* **2010**, *3*, 12. [CrossRef] [PubMed]
594. Koob, A.O.; Paulino, A.D.; Masliah, E. GFAP reactivity, apolipoprotein E redistribution and cholesterol reduction in human astrocytes treated with alpha-synuclein. *Neurosci Lett* **2010**, *469*, 11–14. [CrossRef]
595. Chavarria, C.; Rodriguez-Bottero, S.; Quijano, C.; Cassina, P.; Souza, J.M. Impact of monomeric, oligomeric and fibrillar alpha-synuclein on astrocyte reactivity and toxicity to neurons. *Biochem. J.* **2018**, *475*, 3153–3169. [CrossRef]
596. Choi, D.K.; Pennathur, S.; Perier, C.; Tieu, K.; Teismann, P.; Wu, D.C.; Jackson-Lewis, V.; Vila, M.; Vonsattel, J.P.; Heinecke, J.W.; et al. Ablation of the inflammatory enzyme myeloperoxidase mitigates features of Parkinson's disease in mice. *J. Neurosci.* **2005**, *25*, 6594–6600. [CrossRef] [PubMed]
597. Hashioka, S.; Klegeris, A.; Schwab, C.; Yu, S.; McGeer, P.L. Differential expression of interferon-gamma receptor on human glial cells in vivo and in vitro. *J. Neuroimmunol.* **2010**, *225*, 91–99. [CrossRef]
598. Barcia, C.; Ros, C.M.; Annese, V.; Gomez, A.; Ros-Bernal, F.; Aguado-Yera, D.; Martinez-Pagan, M.E.; de Pablos, V.; Fernandez-Villalba, E.; Herrero, M.T. IFN-gamma signaling, with the synergistic contribution of TNF-alpha, mediates cell specific microglial and astroglial activation in experimental models of Parkinson's disease. *Cell Death Dis.* **2011**, *2*, e142. [CrossRef]
599. Diaz, E.F.; Labra, V.C.; Alvear, T.F.; Mellado, L.A.; Inostroza, C.A.; Oyarzun, J.E.; Salgado, N.; Quintanilla, R.A.; Orellana, J.A. Connexin 43 hemichannels and pannexin-1 channels contribute to the alpha-synuclein-induced dysfunction and death of astrocytes. *Glia* **2019**, *67*, 1598–1619. [CrossRef]
600. Sheng, L.; Stewart, T.; Yang, D.; Thorland, E.; Soltys, D.; Aro, P.; Khrisat, T.; Xie, Z.; Li, N.; Liu, Z.; et al. Erythrocytic alpha-synuclein contained in microvesicles regulates astrocytic glutamate homeostasis: A new perspective on Parkinson's disease pathogenesis. *Acta Neuropathol. Commun.* **2020**, *8*, 102. [CrossRef] [PubMed]
601. Liu, M.; Qin, L.; Wang, L.; Tan, J.; Zhang, H.; Tang, J.; Shen, X.; Tan, L.; Wang, C. alphasynuclein induces apoptosis of astrocytes by causing dysfunction of the endoplasmic reticulumGolgi compartment. *Mol. Med. Rep.* **2018**, *18*, 322–332. [CrossRef]
602. Lindstrom, V.; Gustafsson, G.; Sanders, L.H.; Howlett, E.H.; Sigvardson, J.; Kasrayan, A.; Ingelsson, M.; Bergstrom, J.; Erlandsson, A. Extensive uptake of alpha-synuclein oligomers in astrocytes results in sustained intracellular deposits and mitochondrial damage. *Mol. Cell Neurosci.* **2017**, *82*, 143–156. [CrossRef]
603. Jo, M.; Kim, J.H.; Song, G.J.; Seo, M.; Hwang, E.M.; Suk, K. Astrocytic Orosomucoid-2 Modulates Microglial Activation and Neuroinflammation. *J. Neurosci.* **2017**, *37*, 2878–2894. [CrossRef]
604. Rohl, C.; Sievers, J. Microglia is activated by astrocytes in trimethyltin intoxication. *Toxicol. Appl. Pharmacol.* **2005**, *204*, 36–45. [CrossRef] [PubMed]
605. Lee, H.J.; Kim, C.; Lee, S.J. Alpha-synuclein stimulation of astrocytes: Potential role for neuroinflammation and neuroprotection. *Oxid. Med. Cell Longev.* **2010**, *3*, 283–287. [CrossRef] [PubMed]
606. Farina, C.; Aloisi, F.; Meinl, E. Astrocytes are active players in cerebral innate immunity. *Trends Immunol.* **2007**, *28*, 138–145. [CrossRef] [PubMed]
607. Di Marco Vieira, B.; Radford, R.A.W.; Hayashi, J.; Eaton, E.D.; Greenaway, B.; Jambas, M.; Petcu, E.B.; Chung, R.S.; Pountney, D.L. Extracellular alpha-synuclein promotes a neuroinhibitory secretory phenotype in astrocytes. *Life* **2020**, *10*, 183. [CrossRef]
608. Miklossy, J.; Doudet, D.D.; Schwab, C.; Yu, S.; McGeer, E.G.; McGeer, P.L. Role of ICAM-1 in persisting inflammation in Parkinson disease and MPTP monkeys. *Exp. Neurol.* **2006**, *197*, 275–283. [CrossRef]
609. Barry, M.; Bradford, L.I.M.; David, A.; Hume, C.P.; Neil, A. Mabbott. Complete microglia deficiency accelerates prion disease without enhancing CNS prion accumulation. *Cell Rep.* **2021**. [CrossRef]
610. Watanabe, H.; Saito, Y.; Terao, S.; Ando, T.; Kachi, T.; Mukai, E.; Aiba, I.; Abe, Y.; Tamakoshi, A.; Doyu, M.; et al. Progression and prognosis in multiple system atrophy: An analysis of 230 Japanese patients. *Brain* **2002**, *125*, 1070–1083. [CrossRef]
611. Ozawa, T.; Paviour, D.; Quinn, N.P.; Josephs, K.A.; Sangha, H.; Kilford, L.; Healy, D.G.; Wood, N.W.; Lees, A.J.; Holton, J.L.; et al. The spectrum of pathological involvement of the striatonigral and olivopontocerebellar systems in multiple system atrophy: Clinicopathological correlations. *Brain* **2004**, *127*, 2657–2671. [CrossRef]
612. Jellinger, K.A.; Seppi, K.; Wenning, G.K. Grading of neuropathology in multiple system atrophy: Proposal for a novel scale. *Mov. Disord.* **2005**, *20* (Suppl. S12), S29–S36. [CrossRef]
613. Radford, R.; Rcom-H'cheo-Gauthier, A.; Wong, M.B.; Eaton, E.D.; Quilty, M.; Blizzard, C.; Norazit, A.; Meedeniya, A.; Vickers, J.C.; Gai, W.P.; et al. The degree of astrocyte activation in multiple system atrophy is inversely proportional to the distance to alpha-synuclein inclusions. *Mol. Cell Neurosci.* **2015**, *65*, 68–81. [CrossRef] [PubMed]
614. Nakamura, K.; Mori, F.; Kon, T.; Tanji, K.; Miki, Y.; Tomiyama, M.; Kurotaki, H.; Toyoshima, Y.; Kakita, A.; Takahashi, H.; et al. Accumulation of phosphorylated alpha-synuclein in subpial and periventricular astrocytes in multiple system atrophy of long duration. *Neuropathology* **2016**, *36*, 157–167. [CrossRef] [PubMed]

615. Shults, C.W.; Rockenstein, E.; Crews, L.; Adame, A.; Mante, M.; Larrea, G.; Hashimoto, M.; Song, D.; Iwatsubo, T.; Tsuboi, K.; et al. Neurological and neurodegenerative alterations in a transgenic mouse model expressing human alpha-synuclein under oligodendrocyte promoter: Implications for multiple system atrophy. *J. Neurosci.* **2005**, *25*, 10689–10699. [CrossRef] [PubMed]
616. Valera, E.; Ubhi, K.; Mante, M.; Rockenstein, E.; Masliah, E. Antidepressants reduce neuroinflammatory responses and astroglial alpha-synuclein accumulation in a transgenic mouse model of multiple system atrophy. *Glia* **2014**, *62*, 317–337. [CrossRef] [PubMed]
617. Yazawa, I.; Giasson, B.I.; Sasaki, R.; Zhang, B.; Joyce, S.; Uryu, K.; Trojanowski, J.Q.; Lee, V.M. Mouse model of multiple system atrophy alpha-synuclein expression in oligodendrocytes causes glial and neuronal degeneration. *Neuron* **2005**, *45*, 847–859. [CrossRef] [PubMed]
618. Stefanova, N.; Reindl, M.; Neumann, M.; Haass, C.; Poewe, W.; Kahle, P.J.; Wenning, G.K. Oxidative stress in transgenic mice with oligodendroglial alpha-synuclein overexpression replicates the characteristic neuropathology of multiple system atrophy. *Am. J. Pathol.* **2005**, *166*, 869–876. [CrossRef]
619. Bradl, M.; Lassmann, H. Oligodendrocytes: Biology and pathology. *Acta Neuropathol.* **2010**, *119*, 37–53. [CrossRef]
620. Wilkins, A.; Majed, H.; Layfield, R.; Compston, A.; Chandran, S. Oligodendrocytes promote neuronal survival and axonal length by distinct intracellular mechanisms: A novel role for oligodendrocyte-derived glial cell line-derived neurotrophic factor. *J. Neurosci.* **2003**, *23*, 4967–4974. [CrossRef]
621. Bean, B.P. The action potential in mammalian central neurons. *Nat. Rev. Neurosci.* **2007**, *8*, 451–465. [CrossRef]
622. Kuhn, S.; Gritti, L.; Crooks, D.; Dombrowski, Y. Oligodendrocytes in development, myelin generation and beyond. *Cells* **2019**, *8*, 1424. [CrossRef] [PubMed]
623. Simons, M.; Nave, K.A. Oligodendrocytes: Myelination and axonal support. *Cold Spring Harb. Perspect. Biol.* **2015**, *8*, a020479. [CrossRef] [PubMed]
624. Hofmann, K.; Rodriguez-Rodriguez, R.; Gaebler, A.; Casals, N.; Scheller, A.; Kuerschner, L. Astrocytes and oligodendrocytes in grey and white matter regions of the brain metabolize fatty acids. *Sci. Rep.* **2017**, *7*, 10779. [CrossRef]
625. Dulamea, A.O. Role of oligodendrocyte dysfunction in demyelination, remyelination and neurodegeneration in multiple sclerosis. *Adv. Exp. Med. Biol.* **2017**, *958*, 91–127. [CrossRef]
626. Wong, J.H.; Halliday, G.M.; Kim, W.S. Exploring myelin dysfunction in multiple system atrophy. *Exp. Neurobiol.* **2014**, *23*, 337–344. [CrossRef] [PubMed]
627. Fellner, L.; Jellinger, K.A.; Wenning, G.K.; Stefanova, N. Glial dysfunction in the pathogenesis of alpha-synucleinopathies: Emerging concepts. *Acta Neuropathol.* **2011**, *121*, 675–693. [CrossRef] [PubMed]
628. Campbell, B.C.; McLean, C.A.; Culvenor, J.G.; Gai, W.P.; Blumbergs, P.C.; Jakala, P.; Beyreuther, K.; Masters, C.L.; Li, Q.X. The solubility of alpha-synuclein in multiple system atrophy differs from that of dementia with Lewy bodies and Parkinson's disease. *J. Neurochem.* **2001**, *76*, 87–96. [CrossRef]
629. Yamada, T.; McGeer, P.L.; McGeer, E.G. Lewy bodies in Parkinson's disease are recognized by antibodies to complement proteins. *Acta Neuropathol.* **1992**, *84*, 100–104. [CrossRef]
630. Yamada, T.; McGeer, P.L.; McGeer, E.G. Some immunohistochemical features of argyrophilic grain dementia with normal cortical choline acetyltransferase levels but extensive subcortical pathology and markedly reduced dopamine. *J. Geriatr. Psychiatry Neurol.* **1992**, *5*, 3–13. [CrossRef] [PubMed]
631. Braak, H.; Del Tredici, K. Poor and protracted myelination as a contributory factor to neurodegenerative disorders. *Neurobiol. Aging* **2004**, *25*, 19–23. [CrossRef] [PubMed]
632. Braak, H.; Del Tredici, K. Neuroanatomy and pathology of sporadic Parkinson's disease. *Adv. Anat. Embryol. Cell Biol.* **2009**, *201*, 1–119.
633. Takagi, S.; Hayakawa, N.; Kimoto, H.; Kato, H.; Araki, T. Damage to oligodendrocytes in the striatum after MPTP neurotoxicity in mice. *J. Neural. Transm.* **2007**, *114*, 1553–1557. [CrossRef]
634. Wenning, G.K.; Stefanova, N.; Jellinger, K.A.; Poewe, W.; Schlossmacher, M.G. Multiple system atrophy: A primary oligodendrogliopathy. *Ann. Neurol.* **2008**, *64*, 239–246. [CrossRef] [PubMed]
635. Ozawa, T.; Okuizumi, K.; Ikeuchi, T.; Wakabayashi, K.; Takahashi, H.; Tsuji, S. Analysis of the expression level of alpha-synuclein mRNA using postmortem brain samples from pathologically confirmed cases of multiple system atrophy. *Acta Neuropathol.* **2001**, *102*, 188–190. [CrossRef] [PubMed]
636. Papp, M.I.; Lantos, P.L. The distribution of oligodendroglial inclusions in multiple system atrophy and its relevance to clinical symptomatology. *Brain* **1994**, *117*, 235–243. [CrossRef] [PubMed]
637. Jellinger, K.A.; Lantos, P.L. Papp-Lantos inclusions and the pathogenesis of multiple system atrophy: An update. *Acta Neuropathol.* **2010**, *119*, 657–667. [CrossRef] [PubMed]
638. Papp, M.I.; Lantos, P.L. Accumulation of tubular structures in oligodendroglial and neuronal cells as the basic alteration in multiple system atrophy. *J. Neurol. Sci.* **1992**, *107*, 172–182. [CrossRef]
639. Yoshida, M. Multiple system atrophy: Alpha-synuclein and neuronal degeneration. *Neuropathology* **2007**, *27*, 484–493. [CrossRef]
640. Takeda, A.; Arai, N.; Komori, T.; Kato, S.; Oda, M. Neuronal inclusions in the dentate fascia in patients with multiple system atrophy. *Neurosci. Lett.* **1997**, *227*, 157–160. [CrossRef]
641. Papp, M.I.; Kahn, J.E.; Lantos, P.L. Glial cytoplasmic inclusions in the CNS of patients with multiple system atrophy (striatonigral degeneration, olivopontocerebellar atrophy and Shy-Drager syndrome). *J. Neurol. Sci.* **1989**, *94*, 79–100. [CrossRef]

642. Wakabayashi, K.; Yoshimoto, M.; Tsuji, S.; Takahashi, H. Alpha-synuclein immunoreactivity in glial cytoplasmic inclusions in multiple system atrophy. *Neurosci. Lett.* **1998**, *249*, 180–182. [CrossRef]
643. Gai, W.P.; Pountney, D.L.; Power, J.H.; Li, Q.X.; Culvenor, J.G.; McLean, C.A.; Jensen, P.H.; Blumbergs, P.C. alpha-Synuclein fibrils constitute the central core of oligodendroglial inclusion filaments in multiple system atrophy. *Exp. Neurol.* **2003**, *181*, 68–78. [CrossRef]
644. McCormack, A.; Chegeni, N.; Chegini, F.; Colella, A.; Power, J.; Keating, D.; Chataway, T. Purification of alpha-synuclein containing inclusions from human post mortem brain tissue. *J. Neurosci. Methods* **2016**, *266*, 141–150. [CrossRef] [PubMed]
645. Riedel, M.; Goldbaum, O.; Richter-Landsberg, C. alpha-Synuclein promotes the recruitment of tau to protein inclusions in oligodendroglial cells: Effects of oxidative and proteolytic stress. *J. Mol. Neurosci.* **2009**, *39*, 226–234. [CrossRef]
646. Skjoerringe, T.; Lundvig, D.M.; Jensen, P.H.; Moos, T. P25alpha/Tubulin polymerization promoting protein expression by myelinating oligodendrocytes of the developing rat brain. *J. Neurochem.* **2006**, *99*, 333–342. [CrossRef]
647. Takahashi, M.; Tomizawa, K.; Fujita, S.C.; Sato, K.; Uchida, T.; Imahori, K. A brain-specific protein p25 is localized and associated with oligodendrocytes, neuropil, and fiber-like structures of the CA3 hippocampal region in the rat brain. *J. Neurochem.* **1993**, *60*, 228–235. [CrossRef]
648. Otzen, D.E.; Lundvig, D.M.; Wimmer, R.; Nielsen, L.H.; Pedersen, J.R.; Jensen, P.H. p25alpha is flexible but natively folded and binds tubulin with oligomeric stoichiometry. *Protein Sci.* **2005**, *14*, 1396–1409. [CrossRef]
649. Lindersson, E.; Lundvig, D.; Petersen, C.; Madsen, P.; Nyengaard, J.R.; Hojrup, P.; Moos, T.; Otzen, D.; Gai, W.P.; Blumbergs, P.C.; et al. p25alpha Stimulates alpha-synuclein aggregation and is co-localized with aggregated alpha-synuclein in alpha-synucleinopathies. *J. Biol. Chem.* **2005**, *280*, 5703–5715. [CrossRef] [PubMed]
650. Ejlerskov, P.; Rasmussen, I.; Nielsen, T.T.; Bergstrom, A.L.; Tohyama, Y.; Jensen, P.H.; Vilhardt, F. Tubulin polymerization-promoting protein (TPPP/p25alpha) promotes unconventional secretion of alpha-synuclein through exophagy by impairing autophagosome-lysosome fusion. *J. Biol. Chem.* **2013**, *288*, 17313–17335. [CrossRef] [PubMed]
651. Kragh, C.L.; Fillon, G.; Gysbers, A.; Hansen, H.D.; Neumann, M.; Richter-Landsberg, C.; Haass, C.; Zalc, B.; Lubetzki, C.; Gai, W.P.; et al. FAS-dependent cell death in alpha-synuclein transgenic oligodendrocyte models of multiple system atrophy. *PLoS ONE* **2013**, *8*, e55243. [CrossRef]
652. Kragh, C.L.; Lund, L.B.; Febbraro, F.; Hansen, H.D.; Gai, W.P.; El-Agnaf, O.; Richter-Landsberg, C.; Jensen, P.H. Alpha-synuclein aggregation and Ser-129 phosphorylation-dependent cell death in oligodendroglial cells. *J. Biol. Chem.* **2009**, *284*, 10211–10222. [CrossRef]
653. Mavroeidi, P.; Arvanitaki, F.; Karakitsou, A.K.; Vetsi, M.; Kloukina, I.; Zweckstetter, M.; Giller, K.; Becker, S.; Sorrentino, Z.A.; Giasson, B.I.; et al. Endogenous oligodendroglial alpha-synuclein and TPPP/p25alpha orchestrate alpha-synuclein pathology in experimental multiple system atrophy models. *Acta Neuropathol.* **2019**, *138*, 415–441. [CrossRef] [PubMed]
654. Ubhi, K.; Rockenstein, E.; Mante, M.; Inglis, C.; Adame, A.; Patrick, C.; Whitney, K.; Masliah, E. Neurodegeneration in a transgenic mouse model of multiple system atrophy is associated with altered expression of oligodendroglial-derived neurotrophic factors. *J. Neurosci.* **2010**, *30*, 6236–6246. [CrossRef]
655. Wakabayashi, K.; Takahashi, H. Cellular pathology in multiple system atrophy. *Neuropathology* **2006**, *26*, 338–345. [CrossRef]
656. Djelloul, M.; Holmqvist, S.; Boza-Serrano, A.; Azevedo, C.; Yeung, M.S.; Goldwurm, S.; Frisen, J.; Deierborg, T.; Roybon, L. Alpha-synuclein expression in the oligodendrocyte lineage: An in vitro and in vivo study using rodent and human models. *Stem Cell Rep.* **2015**, *5*, 174–184. [CrossRef]
657. Asi, Y.T.; Simpson, J.E.; Heath, P.R.; Wharton, S.B.; Lees, A.J.; Revesz, T.; Houlden, H.; Holton, J.L. Alpha-synuclein mRNA expression in oligodendrocytes in MSA. *Glia* **2014**, *62*, 964–970. [CrossRef] [PubMed]
658. Reyes, J.F.; Rey, N.L.; Bousset, L.; Melki, R.; Brundin, P.; Angot, E. Alpha-synuclein transfers from neurons to oligodendrocytes. *Glia* **2014**, *62*, 387–398. [CrossRef] [PubMed]
659. Schwarz, L.; Goldbaum, O.; Bergmann, M.; Probst-Cousin, S.; Richter-Landsberg, C. Involvement of macroautophagy in multiple system atrophy and protein aggregate formation in oligodendrocytes. *J. Mol. Neurosci.* **2012**, *47*, 256–266. [CrossRef]
660. Rockenstein, E.; Ubhi, K.; Inglis, C.; Mante, M.; Patrick, C.; Adame, A.; Masliah, E. Neuronal to oligodendroglial alpha-synuclein redistribution in a double transgenic model of multiple system atrophy. *Neuroreport* **2012**, *23*, 259–264. [CrossRef]
661. Yoon, Y.S.; Ahn, W.J.; Ricarte, D.; Ortiz, D.; Shin, C.Y.; Lee, S.J.; Lee, H.J. Alpha-Synuclein Inclusion Formation in Human Oligodendrocytes. *Biomol. Ther.* **2021**, *29*, 83–89. [CrossRef] [PubMed]
662. Hansen, C.; Angot, E.; Bergstrom, A.L.; Steiner, J.A.; Pieri, L.; Paul, G.; Outeiro, T.F.; Melki, R.; Kallunki, P.; Fog, K.; et al. Alpha-synuclein propagates from mouse brain to grafted dopaminergic neurons and seeds aggregation in cultured human cells. *J. Clin. Investig.* **2011**, *121*, 715–725. [CrossRef]
663. Yamada, K.; Iwatsubo, T. Extracellular alpha-synuclein levels are regulated by neuronal activity. *Mol. Neurodegener.* **2018**, *13*, 9. [CrossRef] [PubMed]
664. Kisos, H.; Pukass, K.; Ben-Hur, T.; Richter-Landsberg, C.; Sharon, R. Increased neuronal alpha-synuclein pathology associates with its accumulation in oligodendrocytes in mice modeling alpha-synucleinopathies. *PLoS ONE* **2012**, *7*, e46817. [CrossRef]
665. Konno, M.; Hasegawa, T.; Baba, T.; Miura, E.; Sugeno, N.; Kikuchi, A.; Fiesel, F.C.; Sasaki, T.; Aoki, M.; Itoyama, Y.; et al. Suppression of dynamin GTPase decreases alpha-synuclein uptake by neuronal and oligodendroglial cells: A potent therapeutic target for synucleinopathy. *Mol. Neurodegener.* **2012**, *7*, 38. [CrossRef]

666. Pukass, K.; Richter-Landsberg, C. Oxidative stress promotes uptake, accumulation, and oligomerization of extracellular alpha-synuclein in oligodendrocytes. *J. Mol. Neurosci.* **2014**, *52*, 339–352. [CrossRef] [PubMed]
667. Fruhbeis, C.; Frohlich, D.; Kuo, W.P.; Amphornrat, J.; Thilemann, S.; Saab, A.S.; Kirchhoff, F.; Mobius, W.; Goebbels, S.; Nave, K.A.; et al. Neurotransmitter-triggered transfer of exosomes mediates oligodendrocyte-neuron communication. *PLoS Biol.* **2013**, *11*, e1001604. [CrossRef]
668. Ghidoni, R.; Benussi, L.; Binetti, G. Exosomes: The Trojan horses of neurodegeneration. *Med. Hypotheses* **2008**, *70*, 1226–1227. [CrossRef]
669. Nakamura, S.; Kawamoto, Y.; Nakano, S.; Akiguchi, I. Expression of the endocytosis regulatory proteins Rab5 and Rabaptin-5 in glial cytoplasmic inclusions from brains with multiple system atrophy. *Clin. Neuropathol.* **2000**, *19*, 51–56.
670. Prusiner, S.B.; Woerman, A.L.; Mordes, D.A.; Watts, J.C.; Rampersaud, R.; Berry, D.B.; Patel, S.; Oehler, A.; Lowe, J.K.; Kravitz, S.N.; et al. Evidence for alpha-synuclein prions causing multiple system atrophy in humans with parkinsonism. *Proc. Natl. Acad. Sci. USA* **2015**, *112*, E5308–E5317. [CrossRef]
671. Watts, J.C.; Giles, K.; Oehler, A.; Middleton, L.; Dexter, D.T.; Gentleman, S.M.; DeArmond, S.J.; Prusiner, S.B. Transmission of multiple system atrophy prions to transgenic mice. *Proc. Natl. Acad. Sci. USA* **2013**, *110*, 19555–19560. [CrossRef]
672. Woerman, A.L.; Oehler, A.; Kazmi, S.A.; Lee, J.; Halliday, G.M.; Middleton, L.T.; Gentleman, S.M.; Mordes, D.A.; Spina, S.; Grinberg, L.T.; et al. Multiple system atrophy prions retain strain specificity after serial propagation in two different Tg(SNCA*A53T) mouse lines. *Acta Neuropathol.* **2019**, *137*, 437–454. [CrossRef]
673. Bernis, M.E.; Babila, J.T.; Breid, S.; Wusten, K.A.; Wullner, U.; Tamguney, G. Prion-like propagation of human brain-derived alpha-synuclein in transgenic mice expressing human wild-type alpha-synuclein. *Acta Neuropathol. Commun.* **2015**, *3*, 75. [CrossRef]
674. Woerman, A.L.; Stohr, J.; Aoyagi, A.; Rampersaud, R.; Krejciova, Z.; Watts, J.C.; Ohyama, T.; Patel, S.; Widjaja, K.; Oehler, A.; et al. Propagation of prions causing synucleinopathies in cultured cells. *Proc. Natl. Acad. Sci. USA* **2015**, *112*, E4949–E4958. [CrossRef] [PubMed]
675. Kaji, S.; Maki, T.; Ishimoto, T.; Yamakado, H.; Takahashi, R. Insights into the pathogenesis of multiple system atrophy: Focus on glial cytoplasmic inclusions. *Transl. Neurodegener.* **2020**, *9*, 7. [CrossRef] [PubMed]
676. Reyes, J.F.; Sackmann, C.; Hoffmann, A.; Svenningsson, P.; Winkler, J.; Ingelsson, M.; Hallbeck, M. Binding of alpha-synuclein oligomers to Cx32 facilitates protein uptake and transfer in neurons and oligodendrocytes. *Acta Neuropathol.* **2019**, *138*, 23–47. [CrossRef] [PubMed]
677. Kaji, S.; Maki, T.; Kinoshita, H.; Uemura, N.; Ayaki, T.; Kawamoto, Y.; Furuta, T.; Urushitani, M.; Hasegawa, M.; Kinoshita, Y.; et al. Pathological endogenous alpha-synuclein accumulation in oligodendrocyte precursor cells potentially induces inclusions in multiple system atrophy. *Stem Cell Rep.* **2018**, *10*, 356–365. [CrossRef]
678. Uemura, N.; Uemura, M.T.; Lo, A.; Bassil, F.; Zhang, B.; Luk, K.C.; Lee, V.M.; Takahashi, R.; Trojanowski, J.Q. Slow progressive accumulation of oligodendroglial alpha-synuclein (alpha-Syn) pathology in synthetic alpha-Syn Fibril-Induced Mouse Models of Synucleinopathy. *J. Neuropathol Exp. Neurol* **2019**, *78*, 877–890. [CrossRef]
679. Ettle, B.; Reiprich, S.; Deusser, J.; Schlachetzki, J.C.; Xiang, W.; Prots, I.; Masliah, E.; Winner, B.; Wegner, M.; Winkler, J. Intracellular alpha-synuclein affects early maturation of primary oligodendrocyte progenitor cells. *Mol. Cell Neurosci.* **2014**, *62*, 68–78. [CrossRef]
680. May, V.E.; Ettle, B.; Poehler, A.M.; Nuber, S.; Ubhi, K.; Rockenstein, E.; Winner, B.; Wegner, M.; Masliah, E.; Winkler, J. alpha-Synuclein impairs oligodendrocyte progenitor maturation in multiple system atrophy. *Neurobiol. Aging* **2014**, *35*, 2357–2368. [CrossRef]
681. Ettle, B.; Kerman, B.E.; Valera, E.; Gillmann, C.; Schlachetzki, J.C.; Reiprich, S.; Buttner, C.; Ekici, A.B.; Reis, A.; Wegner, M.; et al. alpha-Synuclein-induced myelination deficit defines a novel interventional target for multiple system atrophy. *Acta Neuropathol.* **2016**, *132*, 59–75. [CrossRef]
682. Kaji, S.; Maki, T.; Ueda, J.; Ishimoto, T.; Inoue, Y.; Yasuda, K.; Sawamura, M.; Hikawa, R.; Ayaki, T.; Yamakado, H.; et al. BCAS1-positive immature oligodendrocytes are affected by the alpha-synuclein-induced pathology of multiple system atrophy. *Acta Neuropathol. Commun.* **2020**, *8*, 120. [CrossRef]
683. Terni, B.; Rey, M.J.; Boluda, S.; Torrejon-Escribano, B.; Sabate, M.P.; Calopa, M.; van Leeuwen, F.W.; Ferrer, I. Mutant ubiquitin and p62 immunoreactivity in cases of combined multiple system atrophy and Alzheimer's disease. *Acta Neuropathol.* **2007**, *113*, 403–416. [CrossRef] [PubMed]
684. Tanji, K.; Odagiri, S.; Maruyama, A.; Mori, F.; Kakita, A.; Takahashi, H.; Wakabayashi, K. Alteration of autophagosomal proteins in the brain of multiple system atrophy. *Neurobiol. Dis.* **2013**, *49*, 190–198. [CrossRef] [PubMed]
685. Odagiri, S.; Tanji, K.; Mori, F.; Kakita, A.; Takahashi, H.; Wakabayashi, K. Autophagic adapter protein NBR1 is localized in Lewy bodies and glial cytoplasmic inclusions and is involved in aggregate formation in alpha-synucleinopathy. *Acta Neuropathol.* **2012**, *124*, 173–186. [CrossRef]
686. Mori, F.; Nishie, M.; Piao, Y.S.; Kito, K.; Kamitani, T.; Takahashi, H.; Wakabayashi, K. Accumulation of NEDD8 in neuronal and glial inclusions of neurodegenerative disorders. *Neuropathol. Appl. Neurobiol.* **2005**, *31*, 53–61. [CrossRef] [PubMed]
687. Miki, Y.; Mori, F.; Tanji, K.; Kakita, A.; Takahashi, H.; Wakabayashi, K. Accumulation of histone deacetylase 6, an aggresome-related protein, is specific to Lewy bodies and glial cytoplasmic inclusions. *Neuropathology* **2011**, *31*, 561–568. [CrossRef]

688. Miki, Y.; Tanji, K.; Mori, F.; Tatara, Y.; Utsumi, J.; Sasaki, H.; Kakita, A.; Takahashi, H.; Fimia, G.M.; Wakabayashi, K. AMBRA1, a novel alpha-synuclein-binding protein, is implicated in the pathogenesis of multiple system atrophy. *Brain Pathol.* **2018**, *28*, 28–42. [CrossRef] [PubMed]
689. Pukass, K.; Richter-Landsberg, C. Inhibition of UCH-L1 in oligodendroglial cells results in microtubule stabilization and prevents alpha-synuclein aggregate formation by activating the autophagic pathway: Implications for multiple system atrophy. *Front. Cell Neurosci.* **2015**, *9*, 163. [CrossRef] [PubMed]
690. Pukass, K.; Goldbaum, O.; Richter-Landsberg, C. Mitochondrial impairment and oxidative stress compromise autophagosomal degradation of alpha-synuclein in oligodendroglial cells. *J. Neurochem.* **2015**, *135*, 194–205. [CrossRef] [PubMed]
691. Spencer, B.; Valera, E.; Rockenstein, E.; Trejo-Morales, M.; Adame, A.; Masliah, E. A brain-targeted, modified neurosin (kallikrein-6) reduces alpha-synuclein accumulation in a mouse model of multiple system atrophy. *Mol. Neurodegener.* **2015**, *10*, 48. [CrossRef]
692. Kiely, A.P.; Miners, J.S.; Courtney, R.; Strand, C.; Love, S.; Holton, J.L. Exploring the putative role of kallikrein-6, calpain-1 and cathepsin-D in the proteolytic degradation of alpha-synuclein in multiple system atrophy. *Neuropathol. Appl. Neurobiol.* **2019**, *45*, 347–360. [CrossRef] [PubMed]
693. Iwata, A.; Maruyama, M.; Akagi, T.; Hashikawa, T.; Kanazawa, I.; Tsuji, S.; Nukina, N. Alpha-synuclein degradation by serine protease neurosin: Implication for pathogenesis of synucleinopathies. *Hum. Mol. Genet.* **2003**, *12*, 2625–2635. [CrossRef] [PubMed]
694. Stefanova, N.; Kaufmann, W.A.; Humpel, C.; Poewe, W.; Wenning, G.K. Systemic proteasome inhibition triggers neurodegeneration in a transgenic mouse model expressing human alpha-synuclein under oligodendrocyte promoter: Implications for multiple system atrophy. *Acta Neuropathol.* **2012**, *124*, 51–65. [CrossRef]
695. Cohlberg, J.A.; Li, J.; Uversky, V.N.; Fink, A.L. Heparin and other glycosaminoglycans stimulate the formation of amyloid fibrils from alpha-synuclein in vitro. *Biochemistry* **2002**, *41*, 1502–1511. [CrossRef] [PubMed]
696. Maiza, A.; Chantepie, S.; Vera, C.; Fifre, A.; Huynh, M.B.; Stettler, O.; Ouidja, M.O.; Papy-Garcia, D. The role of heparan sulfates in protein aggregation and their potential impact on neurodegeneration. *FEBS Lett.* **2018**, *592*, 3806–3818. [CrossRef] [PubMed]
697. Iozzo, R.V. Matrix proteoglycans: From molecular design to cellular function. *Annu. Rev. Biochem.* **1998**, *67*, 609–652. [CrossRef] [PubMed]
698. Medeiros, G.F.; Mendes, A.; Castro, R.A.; Bau, E.C.; Nader, H.B.; Dietrich, C.P. Distribution of sulfated glycosaminoglycans in the animal kingdom: Widespread occurrence of heparin-like compounds in invertebrates. *Biochim. Biophys. Acta* **2000**, *1475*, 287–294. [CrossRef]
699. Holmes, B.B.; DeVos, S.L.; Kfoury, N.; Li, M.; Jacks, R.; Yanamandra, K.; Ouidja, M.O.; Brodsky, F.M.; Marasa, J.; Bagchi, D.P.; et al. Heparan sulfate proteoglycans mediate internalization and propagation of specific proteopathic seeds. *Proc. Natl. Acad. Sci. USA* **2013**, *110*, E3138–E3147. [CrossRef]
700. Skaanning, L.K.; Santoro, A.; Skamris, T.; Martinsen, J.H.; D'Ursi, A.M.; Bucciarelli, S.; Vestergaard, B.; Bugge, K.; Langkilde, A.E.; Kragelund, B.B. The non-fibrillating N-terminal of alpha-synuclein binds and co-fibrillates with heparin. *Biomolecules* **2020**, *10*, 1192. [CrossRef]
701. Hudak, A.; Kusz, E.; Domonkos, I.; Josvay, K.; Kodamullil, A.T.; Szilak, L.; Hofmann-Apitius, M.; Letoha, T. Contribution of syndecans to cellular uptake and fibrillation of alpha-synuclein and tau. *Sci. Rep.* **2019**, *9*, 16543. [CrossRef] [PubMed]
702. Lehri-Boufala, S.; Ouidja, M.O.; Barbier-Chassefiere, V.; Henault, E.; Raisman-Vozari, R.; Garrigue-Antar, L.; Papy-Garcia, D.; Morin, C. New roles of glycosaminoglycans in alpha-synuclein aggregation in a cellular model of Parkinson disease. *PLoS ONE* **2015**, *10*, e0116641. [CrossRef]
703. Stefanova, N.; Schanda, K.; Klimaschewski, L.; Poewe, W.; Wenning, G.K.; Reindl, M. Tumor necrosis factor-alpha-induced cell death in U373 cells overexpressing alpha-synuclein. *J. Neurosci. Res.* **2003**, *73*, 334–340. [CrossRef] [PubMed]
704. Tsuboi, K.; Grzesiak, J.J.; Bouvet, M.; Hashimoto, M.; Masliah, E.; Shults, C.W. Alpha-synuclein overexpression in oligodendrocytic cells results in impaired adhesion to fibronectin and cell death. *Mol. Cell Neurosci.* **2005**, *29*, 259–268. [CrossRef] [PubMed]
705. Kuzdas, D.; Stemberger, S.; Gaburro, S.; Stefanova, N.; Singewald, N.; Wenning, G.K. Oligodendroglial alpha-synucleinopathy and MSA-like cardiovascular autonomic failure: Experimental evidence. *Exp. Neurol.* **2013**, *247*, 531–536. [CrossRef]
706. Stefanova, N.; Reindl, M.; Neumann, M.; Kahle, P.J.; Poewe, W.; Wenning, G.K. Microglial activation mediates neurodegeneration related to oligodendroglial alpha-synucleinopathy: Implications for multiple system atrophy. *Mov. Disord.* **2007**, *22*, 2196–2203. [CrossRef] [PubMed]

Title: Autophagy Mediates the Clearance of Oligodendroglial alpha-Synuclein and TPPP/P25A in Multiple System Atrophy Models

Panagiota Mavroeidi[1], Fedra Arvanitaki[1], Maria Vetsi[1], Stefan Becker[3], Dimitrios Vlachakis[4], Poul Henning Jensen[5], Leonidas Stefanis[1,6] and Maria Xilouri[1 #]

[1]*Center of Clinical Research, Experimental Surgery and Translational Research, Biomedical Research Foundation of the Academy of Athens, Greece*

[2]*Center of Basic Research, Biomedical Research Foundation of the Academy of Athens, Greece*

[3]*Department for NMR-based Structural Biology, Max Planck Institute for Biophysical Chemistry, Am Faßberg 11, 37077 Göttingen, Germany.*

[4]*Genetics and Computational Biology Group, Laboratory of Genetics, Department of Biotechnology, School of Applied Biology and Biotechnology, Agricultural University of Athens, 75 Iera Odos, 11855, Athens, Greece*

[5]*DANDRITE-Danish Research Institute of Translational Neuroscience & Department of Biomedicine, University of Aarhus, Denmark*

[6]*1st Department of Neurology, Eginition Hospital, National and Kapodistrian University of Athens, Medical School, Greece*

Corresponding author

Center of Clinical Research, Experimental Surgery and Translational Research, Biomedical Research Foundation of the Academy of Athens (BRFAA), 4 Soranou Efesiou Street, Athens 11527, Greece

Tel: +30 2106597498; Fax: +30 2106597545; E-mail: mxilouri@bioacademy.gr

Abstract

Accumulation of the neuronal protein alpha-synuclein (SNCA) and of the oligodendroglial phosphoprotein TPPP/P25A within the glial cytoplasmic inclusions (GCIs) represents the key histophathological hallmark of Multiple System Atrophy (MSA). Even though the levels/distribution of both oligodendroglial SNCA and TPPP/P25A proteins are critical for disease pathogenesis, the proteolytic mechanisms involved in their turnover in health and disease remain poorly understood. Herein, by pharmacological and molecular modulation of the autophagy-lysosome pathway (ALP) and pharmacological inhibition of the proteasome we demonstrate that the endogenous oligodendroglial SNCA and TPPP/P25A are degraded mainly by the ALP in murine primary oligodendrocytes and oligodendroglial cell lines under basal conditions. We also identify a KFERQ-like motif in TPPP/P25A sequence that enables its effective degradation via chaperone-mediated autophagy (CMA) in an *in vitro* system of rat brain lysosomes. Furthermore, in a MSA-like setting established by addition of human recombinant SNCA pre-formed fibrils (PFFs) as seeds of pathological SNCA, we thoroughly characterize the contribution of CMA and macroautophagy in particular, in the removal of the exogenously added and the seeded oligodendroglial SNCA pathological assemblies. We also show that PFF treatment impairs autophagic flux and that TPPP/P25A exerts an inhibitory effect on macroautophagy, while at the same time CMA is upregulated to remove the pathological SNCA species formed within oligodendrocytes. Finally, augmentation of CMA or macroautophagy accelerates the removal of the engendered pathological SNCA conformations further suggesting that autophagy targeting may represent a successful approach for the clearance of pathological SNCA and/or TPPP/P25A in the context of MSA.

Keywords: chaperone-mediated autophagy; fibrils; inclusions; macroautophagy; oligodendrocytes; seeding.

Abbreviations

3MA: 3-Methyladenine

ACTB: Actin Beta

ALP: Autophagy-Lysosome Pathway

ATG5: Autophagy related 5

AR7: Atypical Retinoid 7

CMA: Chaperone-Mediated Autophagy

CMV: Cytomegalovirus

CTSD: Cathepsin D

DAPI: 4′,6-diamidino-2-phenylindole

DMEM: Dulbecco's Modified Eagle's Medium

Epox: Epoxomicin

GAPDH: Glyceraldehyde 3-phosphate dehydrogenase

GCIs: Glial Cytoplasmic Inclusions

GFP: Green Fluorescent Protein

HMW: High Molecular Weight

hrs: hours

HSC70: Heat Shock Cognate 70

SNCA: Synuclein Alpha

LAMP1: Lysosomal-Associated Membrane Protein 1

LAMP2A: Lysosome-Associated Membrane Protein 2A

LC3: Light Chain 3

mcherry: monomeric cherry

miR: micro-RNA (RiboNucleic Acid)

MFI: Mean Fluorescence Intensity

mRFP: monomeric Red Fluorescent Protein

MSA: Multiple System Atrophy

OLN: Oligodendrocytes

OPCs: Oligodendroglial Progenitor Cells

PBS: Phosphate-Buffered Saline

PC12: Pheochromocytoma cell line

PD: Parkinson's disease

PFFs: Pre-Formed Fibrils

PIs: Protease Inhibitors

Rap: Rapamycin

RFP: Red Fluorescent Protein

Scr: Scrambled

SDS: Sodium Dodecyl Sulfate

SE: Standard Error

siRNAs: small interfere RNAs

SNCA: Synuclein Alpha

SQSTM1: Sequestosome 1

TPPP: Tubulin Polymerization Promoting Protein

TUBA: Tubulin Alpha

UPS: Ubiquitin-Proteasome System

WT: Wild Type

Introduction

Multiple system atrophy (MSA) is an adult-onset, devastating and relentlessly progressive neurodegenerative disorder of uncertain etiology, mainly characterized by autonomic failure, parkinsonian features and ataxia (1). The neuropathological hallmark of the disease is the presence of glial cytoplasmic inclusions (GCIs) within the cytoplasm of oligodendrocytes. The main components of GCIs are the neuronal protein alpha-synuclein (SNCA) and the oligodendroglial-specific phosphoprotein TPPP/P25A (2-6). The origin of SNCA found in oligodendrocytes still remains enigmatic, taking into account that mature oligodendrocytes do not normally express the protein and there is a controversy regarding the presence of SNCA mRNA in human oligodendrocytes (7-10). Nonetheless, others and we have recently reported that the presence of both the endogenous oligodendroglial SNCA and TPPP/P25A (11-14) is critical for the development and spread of disease pathology.

The identification of endogenous oligodendroglial SNCA as a major culprit for the development of MSA-like pathology (11) suggests that manipulation of the expression of SNCA and/or TPPP/P25A in oligodendrocytes, may provide a rational approach to combat the accumulation of SNCA in GCIs and the progression of MSA. In contrast to the plethora of studies investigating the degradation of neuronal SNCA [reviewed in (15-17)], there is a paucity of data regarding the proteolytic machineries responsible for the clearance of endogenous oligodendroglial SNCA, under physiological and pathological conditions. For TPPP/P25A degradation, two reports showed that proteasomal inhibition resulted in accumulation of the ectopically expressed protein in cell lines (18, 19), whereas no data exist regarding the role of autophagy in TPPP/P25A handling.

Furthermore, dysregulation of both the ubiquitin-proteasome system (UPS) and the autophagy-lysosome pathway (ALP) has been proposed to contribute to the aggregate formation within oligodendrocytes of MSA brains. Specifically, it has been reported that macroautophagy is upregulated during MSA pathogenesis and may participate in the removal of protein aggregates (20). The presence of autophagy-related proteins within GCIs of MSA, such as LC3 and SQSTM1/p62, further supports a potential role of the ALP in disease progression (21-25).

Herein, by utilizing pharmacological inhibitors of both autophagic and proteasomal pathways, or via autophagy-related gene silencing, we provide evidence that the endogenous oligodendroglial SNCA and TPPP/P25A are degraded mainly by the ALP in rat oligodendroglial cell lines and mouse primary oligodendrocytes. Moreover, our data show that TPPP/P25A bears a KFERQ-like motif and is effectively cleared via chaperone-mediated autophagy (CMA) in an *in vitro* system of isolated rat brain lysosomes. Interestingly, by using human recombinant SNCA pre-formed fibrils (PFFs) as seeds of pathological SNCA, we thoroughly characterize the contribution of CMA and macroautophagy in particular, in the removal of the human exogenously added and the seeded rodent oligodendroglial SNCA pathological assemblies. Finally, we demonstrate that upon PFF treatment, autophagic flux is blocked and that TPPP/P25A exerts an inhibitory effect on macroautophagy, while at the same time CMA is upregulated as a compensatory mechanism to effectively remove the pathological SNCA species generated within oligodendrocytes. Most importantly, enhancement of CMA or macroautophagy accelerates the clearance of the engendered pathological SNCA conformations further suggesting that autophagy augmentation may represent a successful approach for the clearance of both SNCA and/or TPPP/P25A in the context of MSA.

Results

Both the proteasome and the ALP contributes to the degradation of the endogenous rat oligodendroglial SNCA

In order to study the degradation pathways responsible for the proteolysis of the endogenous rat oligodendroglial SNCA, we pharmacologically inhibited the lysosome (total and macroautophagy-dependent) and the proteasome, or we performed siRNA-based gene silencing of CMA- and macroautophagy-related genes. Specifically, we utilized the rat oligodendroglial OLN-93 (control), OLN-AS7 (overexpressing human SNCA) and OLN-p25α (overexpressing human TPPP/P25A) cell lines, which express very low to non-detectable levels of the endogenous SNCA and we treated cells with 20 mM NH_4Cl (as total lysosomal inhibitor), 10 mM 3MA (as macroautophagy inhibitor) or 15 nM epoxomicin (epox, as proteasomal inhibitor) for 48 hrs. Confocal microscopy analysis revealed that inhibition of the proteasome or the lysosome increased the oligodendroglial SNCA signal in all lines (expressed as μm^2 area/cell) as detected with the rodent-specific D37A6 antibody (Figure 1A-D), however to a different extent. These data complement recent reported data from our lab (11) supporting both the lysosomal (NH_4Cl- and 3MA-dependent) and the proteasomal contribution to the oligodendroglial SNCA protein turnover. Moreover, immunoblot analysis in the control OLN-93 cells further confirmed the notion that the oligodendroglial SNCA is mostly degraded by the lysosome (Figure 1Ei, ii).

In order to dissect further the partitioning of CMA and macroautophagy lysosomal pathways in the rodent SNCA degradation under basal conditions, we treated all OLN cell lines with *Lamp2a*- (Lsi1/Lsi2) or *Atg5*- (*Atg5* si) specific siRNAs, targeting the LAMP2A receptor which acts as the rate-limiting step of the CMA pathway or the macroautophagy- ATG5 protein that participates in the formation of the phagophore,

which will ultimately become the autophagosome. The efficacy of these siRNAs on LAMP2A or ATG5 gene silencing was verified 72 hrs later by confocal microscopy that revealed an almost 3-fold decrease in the respective protein levels (Supplementary Figure 1A-D), measured as M.F.I./cell. The down-regulation of ATG5 was accompanied by the detection of decreased levels of the autophagosome marker LC3B, further verifying the efficient inhibition of macroautophagy (Supplementary Figure 1E-F). Interestingly, treatment of all OLN cells with Lsi1/Lsi2 or *Atg5* si RNAs significantly increased the protein levels of the endogenous rat oligodendroglial SNCA (Figure 2). It is important to mention that the D37A6 antibody does not produce a specific immunofluorescence signal in control conditions (PBS- or scr si RNA-treated cells, Figure 1 and 2), whereas in immunoblot analysis, film overexposure enables the detection of the rodent SNCA signal at minute amounts even at basal conditions (Figure 1Ei, ii). In all cases, TUBA was used as a cytoskeletal marker, in order to verify the cytoplasmic distribution of the endogenous oligodendroglial SNCA protein.

The overexpressed human SNCA accumulates upon pharmacological or molecular inhibition of the autophagy-lysosome pathway in OLN-AS7 cells

Treatment of rat OLN-AS7 cells with NH_4Cl or 3MA for 48 hrs increased human SNCA protein levels (detected with the human-specific SNCA antibody LB509) measured as M.F.I./cell, suggesting that this protein is degraded, at least partly, via the ALP (Figure 3 Ai, ii). Interestingly, epox treatment of OLN-AS7 cells for 24 hrs evoked a robust increase of human *SNCA* mRNA levels (Supplementary Figure 2A), accompanied by accumulation of human SNCA protein levels (data not shown) due to the epox-mediated non-specific activation of the CMV promoter (which drives the

expression of human SNCA in OLN-AS7 cells), as has been previously suggested by Biasini et al., 2004 (26). Similar effect has been reported using lactacystin or MG132 (26), rendering difficult the investigation of the proteasomal contribution to the degradation of the overexpressed human protein in OLN-AS7 cells. On the contrary, treatment of OLN-AS7 cells with NH_4Cl for 24 hrs or 48 hrs did not alter human SNCA mRNA levels, suggesting that the observed SNCA protein accumulation upon lysosomal inhibition was due to impaired degradation (Supplementary Figure 2C). Moreover, the effect of NH_4Cl or 3MA treatment on human SNCA levels in OLN-AS7 cells was further verified by immunoblot analysis as shown in Figure 3Di, ii. Furthermore, transfection of OLN-AS7 cells with Lsi1/Lsi2 or *Atg5* siRNAs for 72 hrs increased protein levels of human SNCA, as detected with confocal microscopy (Figure 3B-C) and immunoblot analysis (Figure 3E-F). The different human SNCA antibodies utilized for the immunofluorescence (LB509 ab) and the immunoblot (4B12 ab) may account for the differential effects on SNCA levels detected under similar conditions but with different methods.

The overexpressed human TPPP/P25A is increased following pharmacological or molecular inhibition of the autophagy-lysosome pathway in OLN-p25α cells

To decipher the role of the ALP on TPPP/P25A proteolysis, OLN-p25α cells were incubated with 20 mM NH_4Cl or 10 mM 3MA (48 hrs) for total lysosomal or macroautophagy-dependent inhibition, respectively, and protein levels of TPPP/P25A were assessed by immunofluorescence analysis (as M.F.I./cell) and Western blotting. According to the data presented in Figure 4 Ai, ii, treatment of OLN-p25α cells with both inhibitors led to TPPP/P25A protein accumulation, suggesting that the lysosome (with macroautophagy contributing to a lesser extent) is responsible, at least partly,

for TPPP/P25A proteolysis under basal conditions. As in OLN-AS7 cells, epoxomicin, but not NH_4Cl treatment, evoked a non-specific upregulation of human *TPPP/p25α* mRNA levels due to the enhanced CMV-driven promoter gene transcription (Supplementary Figure 2B, D). *Lamp2a* or *Atg5* gene silencing revealed that TPPP/P25A protein is partially degraded via the CMA and macroautophagy pathways (Figure 4B, C, E and F), since both manipulations evoked an increase in TPPP/P25A protein levels with the Lsi2 siRNA sequence against rat LAMP2A eliciting a statistically significant accumulation of TPPP/P25A protein levels (Figure 4Bii, Eii). It has to be noted that treatment of all OLN cells with the pharmacological inhibitors NH_4Cl and epox for 16 or 48 hrs, had no significant impact on cell survival. However, only in the case of 3MA-treated OLN-AS7 and OLN-p25α cells for 48 hrs, a 20% decrease in cell survival was observed (Supplementary Figure 3C-H).

The oligodendroglial-specific protein TPPP/P25A is a putative CMA substrate

In order for a protein to be a CMA substrate, it has to bear a KFERQ-like CMA-targeting motif that guides the delivery of the protein to the level of the lysosomal membrane, where binding with the CMA-specific receptor, LAMP2A, takes place. We therefore examined whether this is the case for TPPP/P25A, and found that it contains a pentapeptide sequence (KKRFK), consistent with a CMA targeting motif. According to the 3D structure of the rat Cgi-38 protein (PDB id: 1WLM) [homologous of the human TPPP/P25A (NM_001108461)], the KKRFK motif is located in a loop, flanked by two adjacent α-helices, both fully exposed to the solvent. The superposed structures of the human, mouse and the 3D model of the TPPP/P25A bearing the KKRFK motif are shown in Figure 5A. Given that the presence of the CMA motif does not guarantee that the protein is actually degraded via this pathway

(27), we incubated human recombinant TPPP/P25A with isolated rat brain lysosomes and assessed the *in vitro* degradation of the protein, in the presence or absence of Protease Inhibitors (PIs). Under these conditions, we found that purified recombinant TPPP/P25A added to the incubation medium was translocated into and efficiently degraded by intact brain lysosomes, since lysosomal protease inhibitors increased the levels of the lysosome-associated protein (Figure 5B-C). Interestingly, a competition assay utilizing 3x (0.6 μg) and 6x (1.2 μg) amount of human recombinant SNCA, a well-established CMA substrate (28) effectively inhibited the degradation of TPPP/P25A by intact lysosomes, in a dose-dependent manner (Figure 5B-C). These data, in combination with the increased protein levels of TPPP/P25A following LAMP2A down-regulation (Figure 4B and E), further confirm that the oligodendroglial TPPP/P25A is a putative CMA substrate and is degraded via this pathway in OLN cells.

Both the exogenously added human SNCA (hSNCA PFFs) and the recruited endogenous rat oligodendroglial SNCA are partly degraded via the autophagy-lysosome pathway, without impairing lysosomal function

We subsequently assessed the proteolytic pathways responsible for SNCA and TPPP/P25A clearance, as well as the role of the overexpressed human SNCA and TPPP/P25A on the proteasomal and lysosomal function, under conditions of increased SNCA protein burden, thus mimicking the human MSA. To this end, OLN cells were inoculated with 1 μg/ml hSNCA PFFs for 48 hrs and 16 hrs prior to cell-fixation, lysosomal or proteasomal inhibitors were added to the medium and then fixed cells were stained for immunofluorescence analysis. Epoxomicin was used only for the assessment of the endogenous rodent SNCA degradation, since, as already mentioned,

it evokes a CMV-dependent upregulation of the human *SNCA* and *TPPP/p25α* mRNA levels (Supplementary Figure 2). We first verified that incubation of all OLN cells with 1 μg/ml hSNCA PFFs for 48 hrs or 10 days does not affect cell survival (Supplementary Figure 3A-B). Confocal microscopy analysis revealed that in PFF-treated OLN-93 cells, inhibition of total lysosomal (NH_4Cl) or proteasomal (epox) function leads to a significant increase of both the exogenously added human (green, LB509 antibody) and the recruited endogenous rodent (red, D37A6 antibody) SNCA (Figure 6A, D-E), measured as μm^2 area/cell. Interestingly, macroautophagy (inhibited by 3MA) seems to participate, albeit to a lesser extent, only in the degradation of hSNCA PFFs and not to the seeded rodent SNCA. However, it should be stressed that if the inhibitors have an effect on the exogenously added human SNCA, this could alter the levels of the endogenous seeded protein through an indirect effect and, vice-versa, alterations in the seeded material may serve to stabilize the human PFFs.

Similarly, in PFF-treated OLN-AS7 cells, treatment with epox significantly increased the levels of the recruited endogenous SNCA, whereas total lysosomal inhibition resulted in the accumulation of both rodent and exogenously added fibrillar human SNCA (Figure 6B, D-E). Interestingly, in PFF-treated OLN-p25α cells levels of both rodent and human SNCA did not significantly change upon NH_4Cl or 3MA addition, however when the proteasome was inhibited, the levels of the endogenous SNCA were found elevated (Figure 6C, D-E). This could indicate a role of the TPPP/P25A in the formation of highly insoluble aberrant SNCA species, as we have previously reported (11) that probably are degradation-resistant and/or impair lysosomal activity. Interestingly, TPPP/P25A protein levels (grey) seem to be slightly, but not significantly, increased upon lysosomal inhibition, which could again presumably be

attributed to a potential inhibitory effect on the lysosome due to the concurrent increased SNCA load and TPPP/P25A overexpression or to a possible degradation of TPPP/P25A via the proteasome.

To further verify the contribution of the proteasome and the lysosome in the clearance of aberrant SNCA species engendered in the PFF-treated OLN cells, we used fractionated Western immunoblotting; we treated OLN-93 cells with 1 μg/ml hSNCA PFFs followed by addition of NH_4Cl or epox as above. Cells were collected at 48 hrs and sequentially fractionated using buffers with increasing extraction strength. Immunoblot analysis of the SDS-soluble protein fraction did not reveal any differences in the protein levels of human or total (rodent + human) SNCA upon lysosomal or proteasomal inhibition (data not shown). However, addition of NH_4Cl or epox in PFF-treated OLN-93 cells, led to the detection of increased protein levels (that did not reach statistical significance) of both human (4B12 antibody) and total (SYN1 antibody) monomeric and high molecular weight (HMW) SNCA species in the UREA-soluble fraction (Figure 6G-H).

Finally, to elucidate the impact of hSNCA PFFs on the proteasomal and lysosomal function of all OLN cell lines and the effect, if any, of the overexpressed SNCA or TPPP/P25A on these proteolytic systems, we measured the CT-like proteasomal activity and the degradation rate of long-lived proteins (total lysosomal, macroautophagy- and CMA- dependent). Strikingly, the CT-like proteasomal activity remained unchanged in all OLN cells upon treatment with 1 μg/ml hSNCA PFFs for 48 hrs (Supplementary Figure 4). On the other hand, long-lived protein degradation assay revealed a significant increase of the lysosomal activity upon inoculation of OLN cells with hSNCA PFFs, which however varied between the different OLN lines. Specifically, in PFF-treated OLN-93 cells, macroautophagy (3MA-inhibitable)

seems to increase in response to the treatment, whereas in PFF-treated OLN-AS7 and OLN-p25α cells, CMA-dependent (NH_4Cl-3MA inhibitable) degradation is significantly enhanced (Figure 6Ii-iii). It has to be noted that with this assay we estimate CMA activity by subtracting NH_4Cl-3MA–dependent proteolysis that also contains the contribution of microautophagy, which however is considered to be relative small. Interestingly, the increase of CMA-dependent proteolysis in OLN-p25α cells was accompanied by a significant decrease of macroautophagic activity, thus leading to overall unchanged total lysosomal activity levels, compared to OLN-93 and OLN-AS7 cells. It is important, though, to note that all the above differential responses could also be attributed to clonal variability between the three OLN cell lines.

TPPP/P25A overexpression favors the degradation of both exogenously added (hSNCA PFFs) and recruited endogenous oligodendroglial SNCA via CMA and not via macroautophagy

To further elucidate the contribution of macroautophagy and/or CMA in the degradation of rodent SNCA, human SNCA and TPPP/P25A in the context of MSA, we transfected all OLN cells with Lsi1/Lsi2 (targeting LAMP2A) or *Atg5* (targeting ATG5) siRNAs followed by incubation with 1 μg/ml hSNCA PFFs for 48 hrs. According to the data shown in Figure 7, LAMP2A downregulation increased protein levels of the recruited rodent SNCA in all PFF-treated OLN cells; however, the levels of the human SNCA were found elevated only in PFF-treated OLN-p25α cells transfected with Lsi1/Lsi2 (Figure 7A-C, Di, Ei). On the other hand, *Atg5* gene silencing led to the accumulation of the rodent and the human SNCA only in PFF-treated OLN-93 and OLN-AS7 cells (Figure 7A-C, Dii, Eii). Moreover, protein levels

of TPPP/P25A were significantly increased upon LAMP2A down-regulation, whereas transfection of OLN-p25 cells with *Atg5* si led to a slight accumulation of TPPP/P25A (Figure 7C, Fi, Fii). These data, when combined to those presented in Figure 6A-F may lead to the hypothesis that under pathological conditions (addition of hSNCA PFFs), CMA seems to be the main pathway responsible for the clearance of SNCA (rodent and human) and TPPP/P25A in OLNp25α cells, whereas both CMA and macroautophagy contribute to the degradation of SNCA (rodent and human) in PFF-treated OLN-93 and OLN-AS7 cells.

Addition of hSNCA PFFs in OLN cells does not impair autophagosome formation, but seems to interfere with the fusion of autophagosomes with the lysosome

Autophagy is a dynamic process that includes the autophagosome formation, maturation and fusion with lysosomes. In order to measure the autophagic flux in PFF-treated OLN cells we utilized the GFP/RFP-LC3 and GFP/mcherry-SQSTM1 tandem fluorescent-tagged LC3 and SQSTM1/p62, respectively, which allows the dynamic visualization of the formation of autophagosomes and/or autolysosomes. Specifically, OLN cells were transfected with GFP/RFP-LC3 or GFP/mcherry-SQSTM1 cDNAs and 6 hrs later, 1 μg/ml hSNCA PFFs were added to the medium for 48 hrs. Based on the fact that the fluorescence of GFP, contrarily to the mRFP or mcherry, is quenched in an acidic environment, autophagy inhibition results in a decrease of red puncta followed by an increase of green puncta, indicative of the low autolysosome formation. Incubation of all OLN cells with hSNCA PFFs impaired autophagic flux, due to the detection of a lower number of red puncta (in both GFP/RFP-LC3 and GFP/mcherry-SQSTM1), as presented in Figure 8A-B.

Calculation of GFP:RFP (LC3 cDNA) or GFP:mcherry (SQSTM1 cDNA) ratio is indicative for the autophagic flux process; the ratio increases when autophagic flux is low and decreases when autophagic flux is enhanced. According to our results, autophagic flux was inhibited in all PFF-treated OLN cells, with no differences detected amongst the different cell lines (Figure 8C-D).

Pharmacological enhancement of CMA (AR7) or macroautophagy (rapamycin) decreases overexpressed human SNCA (OLN-AS7 cells) and TPPP/P25A (OLN-p25α cells) protein levels under basal conditions

Having established the lysosomal contribution to the clearance of both SNCA and TPPP/P25A proteins, we investigated the potential therapeutic potential of enhancing macroautophagy (rapamycin, 1 μM) or CMA (AR7, 40 μM), under basal conditions and upon hSNCA PFF treatment (see below). We initially verified the induction of CMA activity upon AR7 addition (40 μM, 16 hrs) with confocal microscopy, where we detected increased LAMP2A-positive lysosomes to the perinuclear region of OLN-93 cells, an indirect indicator of increased CMA activity (29) (Supplementary Figure 5A-B). Moreover, treatment with AR7 or rapamycin for 16 or 48 hrs did not significantly affect survival of all OLN cells (Supplementary Figure 3C-H). Incubation of OLN-AS7 and OLN-p25α cells with both enhancers for 48 hrs under basal conditions led to a significant decrease of human SNCA (human-specific LB509 or 4B12 antibodies), and TPPP/P25A levels respectively, verified by both confocal microscopy imaging and analysis (Figure 9A-D) and Western immunoblotting (Figure 9E-F).

Pharmacological augmentation of CMA or macroautophagy accelerates the clearance of aberrant SNCA conformations formed upon treatment of OLN cells with hSNCA PFFs

To assess the therapeutic potential of macroautophagy or CMA enhancement on the clearance of pathological SNCA assemblies and/or TPPP/P25A following addition of hSNCA PFFs, OLN cells were incubated with 1 μg/ml hSNCA PFFs for 48 hrs or 10 days. Following PFF-addition and 16 or 48 hrs prior to cell fixation, rapamycin (1 μM) or AR7 (40 μM) were added to the cell medium and then cells were processed for confocal microscopy imaging. Immunofluorescence analysis revealed that addition of rap or AR7 in all PFF-treated OLN cells evoked a reduction of the endogenous seeded rodent and human SNCA, as well as of the overexpressed TPPP/P25A (in OLN-p25α cells) protein levels (in both time points studied), suggesting that these proteins/conformations can be efficiently cleared via macroautophagy and/or CMA pathways (Figure 10A-Ei, Supplementary Figure 7A-C, G-Hi).

Interestingly, at 48 hrs post-PFF treatment the levels of oxidized/nitrated SNCA were significantly decreased upon macroautophagy induction with rapamycin only in OLN-93 cells (Figure 10Eii and Supplementary Figure 6A-C). Likewise, CMA induction via AR7 also decreased oxidized/nitrated SNCA protein species only in OLN-93 cells, although this drop did not reach statistical significance. On the contrary, oxidized/nitrated SNCA protein levels were efficiently removed upon induction of either macroautophagy or CMA in all OLN cells at 10 days post-PFF treatment (Supplementary Figure 7Di, Ei, Fi, Hii). Furthermore, protein levels of aggregated and total SNCA were also decreased upon rap or AR7 (to a lesser extent) treatment in all OLN cells, only following short-term incubation with PFFs, suggesting that under

these conditions there is no significant effect of the overexpressed human SNCA or TPPP/P25A in the clearance of aggregated SNCA species (Supplementary Figure 6D-F and Figure 10Fi-Fii). Strikingly, upon long-term incubation of all OLN cells with hSNCA PFFs, aggregated and total SNCA could not be effectively removed only in OLN-p25α cells, thus implying a potential role of the overexpressed protein in the observed resistance to the degradation of aggregated SNCA assemblies via macroautophagy or CMA (Supplementary Figure 7Dii, Eii, Fii, Ii-Iii).

In agreement with the confocal imaging data, we found that the SDS-soluble HMW species of human and total SNCA protein were decreased mainly upon macroautophagy enhancement (addition of 1 μM rap for 16 hrs), although the levels of monomeric SNCA species did not seem to be significantly reduced following incubation of PFF-treated OLN-93 cells either with rap or with AR7 (Figure 10G-H). Interestingly, the monomeric and HMW SNCA species of the seeded endogenous rodent protein, which are detectable only in the UREA-soluble fraction that contains the most aggregated protein species, were significantly reduced following addition of rap or AR7 in PFF-treated OLN-93 cells (Figure 10I-J). Similarly, human and total SNCA protein levels in this UREA-soluble fraction displayed significant reduction upon macroautophagy or CMA enhancement, as presented in Figure 10I, K, L. All the above results suggest that SNCA (endogenous, human, total and pathological species) and TPPP/P25A can be effectively cleared via the ALP in an MSA cell context.

The MSA-related proteins TPPP/P25A and SNCA are mainly degraded via the ALP in murine primary oligodendroglial cultures, under physiological and pathological conditions

To delineate the clearance processes responsible for the removal of SNCA (endogenous and exogenously added) and TPPP/P25A, in health and disease conditions, we cultivated and differentiated primary oligodendrocytes derived from P0 to P3 mouse brains in order to resemble a cellular setting closer to the oligodendrocytes of the central nervous system. To this end, primary oligodendrocytes were cultivated in the presence of PBS (as control) or 1 μg/ml hSNCA PFFs for 24 hrs, followed by addition of lysosome/macroautophagy (20 mM NH_4Cl, 10 mM 3MA) or proteasome (15 nM epox) inhibitors for an additional 48 hrs. According to the results presented in Figure 11A-C, TPPP/P25A seems to be mainly degraded via the ALP both under baseline and upon PFF-treatment, since its levels were found significantly elevated upon NH_4Cl (both in PBS and PFF-treated cultures) and/or 3MA (PFF-treatment) addition (Figure 11Ci-Cii).

Furthermore, the endogenous rodent SNCA accumulated when either the lysosome or the proteasome (to a lesser extent) was inhibited (Figure 11Di-Dii), whereas the levels of human SNCA were increased upon total lysosomal and macroautophagy impairment (Figure 11E). No signal for the endogenous SNCA could be detected in PBS-treated primary oligodendrocytes using the rodent SNCA-specific D73A6 antibody, as shown in Figure 11A and Di. To elucidate further the potential beneficial role of autophagy augmentation in the removal of SNCA and TPPP/P25A protein levels in primary oligodendrocytes, PBS- or PFF-treated oligodendroglial cultures were incubated with AR7 (40 μM) or rap (1 μM) for 48 hrs. Confocal microscopy analysis and quantification of SNCA and TPPP/P25A protein levels revealed that in all conditions tested, incubation with either AR7 or rap led to the effective clearance of TPPP/P25A (Figure 11Hi, Hii), the endogenous rodent (Figure 11Hiii) and the human SNCA (Figure 11Hiv) proteins, thus suggesting that enhancement of

macroautophagy or the CMA pathway could potentially mitigate SNCA pathology in MSA and MSA-like conditions.

Discussion

Our previous work uncovered the endogenous oligodendroglial SNCA (expressed in minute amounts) and TPPP/P25A as major culprits for the formation of pathological SNCA aggregates in MSA-like experimental models (11). Such data suggest that manipulation of the expression of SNCA and/or TPPP/P25A in oligodendrocytes may provide a rational approach to combat the accumulation of SNCA in GCIs and the progression of MSA. However, the degradation pathways responsible for the clearance of the endogenous oligodendroglial SNCA and TPPP/P25A in health and disease and the role of ALP manipulation in the context of MSA remained unexplored.

Herein, by utilizing naïve (low-undetectable levels of endogenous SNCA and TPPP/P25A) oligodendroglial cell lines, and cells stably overexpressing human SNCA (OLN-AS7) or TPPP/P25A (OLN-p25α) we report that both the ALP and the UPS (to a lesser extent) contribute to the clearance of endogenous oligodendroglial SNCA under basal conditions and upon treatment with hSNCA PFFs. Both CMA and macroautophagy are responsible for the clearance of the various SNCA conformations (rodent endogenous and seeded, human exogenously added, oxidized/nitrated, aggregated) engendered in PFF-treated OLN cell lines, although to a different extent. We also demonstrate that TPPP/P25A bears a CMA-targeting motif and is efficiently cleared via CMA in a cell-free *in vitro* system of isolated brain lysosomes and in the OLN-p25α cells. Finally, we provide proof-of-concept experiments in murine primary oligodendrocytes further corroborating the contribution of the ALP in the efficient

removal of oligodendroglial SNCA and TPPP/P25A both under baseline and following inoculation with hSNCA PFFs as seeds of pathology. Such data suggest that augmentation of CMA or macroautophagy represents an attractive therapeutic approach to counteract the accumulation of SNCA and/or TPPP/P25A in MSA-like conditions.

MSA is characterized by the accumulation of neuronal SNCA and oligodendroglial-specific TPPP/P25A proteins within the cytoplasm of oligodendrocytes, by a hitherto unknown mechanism (2-4, 6). According to the prevailing hypothesis, oligodendrocytes internalize the naturally secreted SNCA from the neighboring neurons, which is subsequently incorporated into pathological aggregates along with other proteins such as TPPP/P25A, ubiquitin, tubulin, HSP70, etc (30-32). The detection of various aggresome-related proteins in GCIs of MSA brains has also exposed a crucial role of perturbed proteolysis in the formation of oligodendroglial proteinaceous inclusions (21, 23-25, 33). Alterations in the levels of autophagic protein markers such as SQSTM1/p62 and LC3 detected in several MSA cases further denote a role of an ALP malfunction in disease pathogenesis (20, 22, 34-36). Likewise, pathological and biochemical analyses using human brain MSA samples revealed that the Autophagy And Beclin 1 Regulator 1 is a component of the pathological inclusions of MSA and upstream proteins of autophagy are impaired in the MSA brain (37). A recent comparative study in human post-mortem material from MSA and PD brains concluded that the lysosomal response in relation to SNCA pathology differs between the two synucleinopathies (38). By systematic comparisons of differently affected neuronal populations in PD, MSA, and non-diseased brains using morphometric immunohistochemistry (cathepsin D), double immunolabelling (cathepsin D/SNCA) laser confocal microscopy, and SNCA immunogold electron

microscopy the authors concluded, amongst others, that lysosome-associated SNCA is observed in astroglia and rarely in oligodendroglia and in neurons in MSA, whereas cathepsin D immunoreactivity frequently colocalises with SNCA pre-aggregates in PD nigral neurons (38).

The role of the oligodendroglial SNCA in the formation of GCIs and the spread of pathology in MSA is still under debate. Our recently published data suggest that the presence of even minute amounts of the endogenous SNCA is a prerequisite for the seeding of SNCA-pathology, the re-distribution of TPPP/P25A and the collapse of the myelin network to occur, in PFF-treated murine oligodendrocytes (11). Thus, the elucidation of the mechanisms governing the degradation of oligodendroglial SNCA and TPPP/P25A may represent an obvious target for therapy in MSA. Towards this direction, we treated oligodendroglial cell lines with pharmacological inhibitors or enhancers of the ALP and UPS, or with siRNAs targeting autophagy-related genes, under physiological (PBS) or pathological (hSNCA PFFs) conditions. According to our results, SNCA (endogenous rodent, overexpressed human and pathology-related conformations) seem to be cleared mainly via CMA and macroautophagy; however to a different magnitude in the various cell lines. A role of macroautophagy in the clearance of SNCA within oligodendrocytes has been previously reported (20); however this is the first study demonstrating a role of CMA in the removal of the endogenous and seeded SNCA protein levels and/or aberrant species in oligodendrocytes. This finding contradicts with a prior study that reported a lack of GCI-like formation in oligodendroglia exposed to extracellular soluble/monomeric or fibrillar SNCA concurrently with pharmacological blocking of the fusion of the autophagosome with the lysosome with bafilomycin A1, as well as following genetic knockdown of LC3B (39).

Regarding macroautophagy, it has been previously shown that the endogenously stably overexpressed (OLN-t40 transfected cells) or the exogenously added soluble or pre-aggregated SNCA is mainly removed via macroautophagy in oligodendrocytes and that these SNCA forms do not inhibit the autophagic pathway and flux per se (40). Moreover, inhibition of the deubiquitylating enzyme Ubiquitin Carboxy-terminal Hydrolase L1 in oligodendroglial cells was shown to upregulate macroautophagy, thus resulting in the effective removal of SNCA aggregates (41). Other proteolytic pathways may also be involved in SNCA clearance in oligodendrocytes. Neurosin (kallikrein 6) appears to be efficient in reducing the levels of SNCA in oligodendrocytes both *in vitro* and *in vivo* (42-44). Interestingly, treatment of transgenic haSyn-PLP mice, a well-established mouse model for MSA, with the proteasome inhibitor I led to the detection of intracellular aggregates of both human and endogenous murine SNCA, three months after administration of the inhibitor, further supporting the role of the UPS in SNCA clearance (45). Furthermore, in agreement with our data showing an impairment of the autophagic flux in PFF-treated OLN cells, prior studies also suggested that aggregated SNCA within oligodendrocytes is closely related to autophagy dysregulation (37, 41). Interestingly, even though with the GFP/RFP-LC3 and GFP/mcherry-SQSTM1 constructs we detect a defect in the autophagic flux upon PFF treatment (Figure 8), this was not followed by a statistically significant alteration in the macroautophagic-dependent proteolysis (inhibited by 3MA) in OLN-93 and OLN-AS7 cells (Figure 6Iii). A possible explanation for this discrepancy may ascend from the observation that upon PFF treatment we detect a change from a diffuse to a more punctuate pattern, indicative of LC3 II induction and autophagosome formation. If the rate that these autophagosomes are fused with the lysosome is reduced in these cells, then the

overall process is as efficient as baseline. In addition, the different time points utilized for the assessment of the autophagic flux (48 hrs) and lysosomal activity (96 hrs) may also account for the observed differences.

The current study highlights for the first time a central role of CMA and macroautophagy in the clearance of TPPP/P25A protein in oligodendrocytes, both under physiological and pathological conditions. The contribution of CMA to TPPP/P25A protein degradation was verified by the identification of the KKRFK pentapeptide motif that meets the criteria for a KFERQ-like motif in TPPP/P25A amino acid sequence and its efficient degradation by the *in vitro* system of isolated rat brain lysosomes. In addition, TPPP/P25A displayed a canonical substrate/pathway relationship, since its levels were increased upon LAMP2A down-regulation and by extension CMA inhibition and decreased following pharmacological induction of the CMA pathway with AR7. Induction of macroautophagy also reduced TPPP/P25A levels, both in OLN-p25α cells and in primary oligodendrocytes, but less efficiently. Previous studies proposed that TPPP/P25A is degraded via the proteasome (18, 19); however, our analysis in the epoxomicin-treated primary oligodendrocytes did not yield a statistical contribution of the proteasome in TPPP/P25A clearance. Due to the non-specific up-regulation of CMV-driven TPPP/P25A mRNA by proteasomal inhibitors [as also reported by (26)], the role of the proteasome could not be determined in OLN-p25α cells. Strikingly, the expression of TPPP/P25A protein (in OLN-p25α cells) seems to hinder the macroautophagic activity (inhibited by 3MA) upon addition of hSNCA-PFFs thus favoring the CMA activity, probably as a counterpoise to the proteolytic dysregulation. Likewise, Ejlerskov and et al. have also demonstrated that TPPP/P25A inhibits the fusion of autophagosomes with the

lysosome and leads to the secretion of monomeric and aggregated SNCA via exophagy in PC12 cells (46).

Finally, the pharmacological CMA- and macroautophagy-specific enhancers AR7 and rapamycin respectively, mitigated the levels of the endogenous and exogenously added SNCA and all its pathological conformations (oxidized/nitrated and aggregated SNCA), together with TPPP/P25A, both in oligodendroglial cell lines and primary oligodendrocytes. The beneficial effect of macroautophagy induction in the removal of SNCA species in oligodendrocytes has been previously reported. In particular, the geldanamycin analogue 17-AAG [17-(Allylamino)-17-demethoxygeldanamycin] attenuated the formation of SNCA aggregates in OLN-93 cells stably overexpressing the human PD-linked A53T SNCA mutation by stimulating macroautophagy (47). This effect on macroautophagy induction was also observed in cultured oligodendrocytes derived from the brains of newborn rats (47). On the other hand, numerous studies have explored the use of various autophagy-enhancing agents in the context of PD pathology, concluding that they exert beneficial effects on neuronal cell survival and accelerate SNCA clearance (48-56). Moreover, the post-translational regulation of autophagy via the use of micro-RNAs (miRs) targeting LAMP2A and HSC70, has been shown to decrease SNCA aggregation in SH-SY5Y cells (57). Similarly, we have previously shown that CMA induction via overexpression of the LAMP2A receptor in neuronal cellular and animal synucleinopathy models alleviated SNCA-induced neurotoxic effects (58).

Collectively, our study reveals that the endogenous oligodendroglial SNCA and TPPP/P25A, the two main GCI-components involved in MSA pathogenesis, are degraded via the ALP and that conversely, the presence of pathological SNCA (hSNCA-PFFs) decreases the autophagic flux of OLN cells, albeit without impairing

the overall lysosomal activity. The data obtained from cell lines and primary cultures indicate that enhancement of CMA or macroautophagy prevents the accumulation/aggregation of SNCA and/or TPPP/P25A in oligodendrocytes. Further validation in pre-clinical models of the disease may pave the way for the use of autophagy modulators or gene-based approaches as therapeutic approaches to halt or attenuate disease progression in human MSA.

Materials and Methods

Cell culture and treatments

Three different oligodendroglial (OLN) cell lines have been utilized: the immortalized control OLN-93 line originated from primary Wistar rat brain glial cultures (59), and the OLN-AS7 and OLN-p25α lines that were generated by transduction of the OLN-93 line with the human wild-type (WT) SNCA or human TPPP/P25A cDNA, respectively. All cells were cultured in Dulbecco's modified Eagle's medium (D6429; Gibco, Invitrogen, Carlsbad, CA, USA) under conditions of 10% fetal bovine serum (10270; Gibco, Invitrogen, Carlsbad, CA, USA), 50 U/mL penicillin, and 50 μg/mL streptomycin. For the selection of OLN-AS7 and OLN-p25α, cells were maintained in 50 μg/mL Zeocin (R25001; Thermo Fisher Scientific, Waltham, MA, USA).

Primary oligodendroglial cultures

Mixed glial cultures generated from P0 to P3 neonatal wild-type (WT) mice were maintained in full DMEM for 10 to 14 days until a monolayer of astrocytes on the bottom and primary oligodendroglial progenitor cells (OPCs) with loosely attached microglia on the top, were apparent. The separation of OPCs was achieved initially with the removal of microglia, by shaking in 200 rpm for 1h in 37°C and then with

continuous shaking under the same conditions for 18 hrs (60). Afterwards, isolated cells were platted on poly-D-lysine-coated coverslips (P7405, Sigma-Aldrich, USA) with a density of 80,000 cells/mm^2 and maintained in SATO medium (61) supplemented with Insulin-Transferrin-Selenium solution (Cat No 41400045, Gibco, Invitrogen, Carlsbad, CA, USA), 1% penicillin/streptomycin and 1% horse serum (H1138; Sigma-Aldrich, St. Louis, MO, USA) for 4 days. Human SNCA PFFs (final concentration 1 μg/mL culture medium/well) were added to TPPP/P25A-positive mature differentiated OLNs for 24 hrs, followed by the addition of either inhibitors or enhancers of the protein degradation pathways for 48 hrs in the appropriate concentrations. Subsequently, cells were fixed and processed for immunofluorescence analysis using antibodies shown in Table 1.

Pharmacological reagents

The inhibition of the proteasome was achieved with epoxomicin (15 nM) that selectively blocks the chemotrypsin-like activity of the 20S catalytic subunit (62). For the lysosomal pathway, the inhibitor of phosphatidylinositol-3-kinase, 3-methyladenine (3MA, 10 mM) and the general lysosomal inhibitor NH_4Cl (20 mM) were utilized. Since NH_4Cl is unstable, for the 24 and 48 hrs incubation a renewal of the inhibitor was required every 12 hrs. Induction of macroautophagy was accomplished with the use of rapamycin (1 μM) that induces the mTOR-dependent macroautophagic pathway (63) and of the CMA pathway with the use of the RARα antagonist AR7 (40 μM) (64). The reagents were applied for 16- 48 hrs and the analysis of their effects was performed either by western blotting or with immunocytochemistry.

Preparation of hSNCA PFFs

Pre-formed human SNCA fibrils (hSNCA PFFs) were generated as previously described (11). PFFs were resuspended in PBS (pH 7.3) to obtain a concentration of 4.5 mg/mL and a working stock solution was prepared with a concentration of 1 mg/mL. In all experiments cells were incubated with 1 μg/ml hSNCA PFFs or PBS as a control for 48 hrs or 10 days and afterwards were either processed for immunocytochemistry and confocal microscopy or lysed and collected for western blot analysis as described below.

Cell transfections

The autophagic flux of OLN cells upon treatment with hSNCA PFFs (or PBS as control) was monitored with the use of RFP/GFP-LC3 (65), and mCherry/GFP-SQSTM1 (66) cDNA plasmids, upon transient transfection with polyethylenimine (PEI, Polysciences, 26966). The RFP/GFP-LC3 plasmid was kindly provided by Dr Craig-Curtis Garner (DZNE, Germany) and the mCherry/GFP-SQSTM1 plasmid by Dr Terje Johansen (University of Tromso, Norway). Cells were cultured in 24-well dishes and PEI with cDNA were diluted in Opti-MEM in a 1:3 ratio. After 4 hrs of incubation, the transfection medium was replaced by fresh DMEM 10% FBS containing either PBS or 1 μg/ml hSNCA PFFs. The lysosomal inhibitor NH_4Cl was used as a positive control for autophagic flux impairment. Forty-eight (48) hours later, cells were fixed using 4% paraformaldehyde (Sigma-Aldrich, P6148) in PBS and processed for immunofluorescence analysis.

RNA interference

Small interfering RNAs (siRNAs) targeting the rat *Lamp2a* or the *Atg5* gene were utilized to assess the contribution of CMA or macroautophagy, respectively, in the proteolysis of SNCA and TPPP/P25A in OLN cell lines. In particular, OLN cells were transfected with Lsi1/Lsi2 (*Lamp2a* siRNAs, final concentration 60 nM), *Atg5* si (rn.Ri.Atg5.13.1/2/3 TriFECTa DsiRNA kit, final concentration 10 nM) or control scrambled siRNA (MISSION siRNA Universal Negative Control #1, SIC001, MERCK, final concentration 60 nM) in Lipofectamine 2000 (Invitrogen)-containing solution for 72 hrs. The siRNAs sequences targeting the rat *Lamp2a* are shown in Table 2. Analysis was performed with both western blotting and immunocytochemistry.

Subcellular fractionation and western immunoblotting

The cell pellets after being washed with PBS were homogenized in lysis buffers with progressively higher extraction strength. All of them contained protease (Roche, 11836170001) and phosphatase (Roche, 04406837001) inhibitors. Initially, cells were lysed with 1% Triton X-100-containing buffer (150 mM NaCl, 50 mM Tris pH 7.6, 2 mM EDTA), left on ice for 30 min and centrifuged at 13,400 × g for 30 min at 4 °C. The supernatant was collected to obtain the Triton-soluble fraction and the pellet, after 2x washes with PBS, was resuspended in 1% SDS-containing buffer (150 mM NaCl, 50 mM Tris pH 7.6, 2 mM EDTA), sonicated and centrifuged to acquire the SDS-soluble fraction. Finally, the remaining pellet, after 2x washes with PBS, was solubilized in 8 M urea-5% SDS-containing buffer. Then, samples of equal protein concentration were processed for western blot analysis utilizing the utilized primary and secondary antibodies shown in Table 1. The immunoreactivity for protein band

intensity within the linear range of detection was quantified with ImageJ software. All measurements were normalized to ACTB as a loading control.

Immunocytochemistry (ICC) and confocal microscopy

Cultured cells in poly-D-lysine-coated glass coverslips were fixed in 4% paraformaldehyde diluted in 1X PBS for 30 min at room temperature. Blocking was conducted utilizing 10% Normal Goat Serum solution containing 0.4% Triton-X for 1 h at room temperature. Afterwards, overnight incubation with primary antibodies at 4ºC was performed followed by incubation with secondary antibodies, in dilutions shown in Table 1. The dye 4′, 6-diamidine-2′-phenylindole dihydrochloride (DAPI) was utilized for nuclei staining. Finally, the stained cells were visualized using a Leica TCS SP5 confocal microscope combined with dual (tandem) scanner. ImageJ (v2.0.0) software was used to quantify relative protein levels expressed as mean fluorescence intensity (M.F.I.) or area coverage (μm^2), normalized to the total number of cells/field (the number of DAPI-stained nuclei). M.F.I./cell or area/cell was used to express the protein levels of interest per cell in the absence or presence of hSNCA PFFs respectively. In the case of primary oligodendroglial cell cultures the area of signal was normalized to the number of TPPP/P25A+ cells (marker for mature oligodendrocytes).

Molecular Modelling

The amino acid sequence of the human TPPP/P25A was obtained from the UniProt database (accession no: O94811). Using the Gapped-BLAST through NCBI the homologous human protein with PDB id 2JRF was identified, which was used as template for the homology modelling. The homology modelling of the TPPP/P25A

model was carried out using the RCSB entries 2JRF (human) and 1WLM (mouse) as template structures. The sequence alignment between the raw sequence of the all the above revealed more than 87% sequence identity, which allowed conventional homology modelling techniques to be applied. Electrostatic potential surfaces were calculated on grid points per side (65, 65, 65) and the grid fill by solute parameter was set to 80%. The dielectric constants of the solvent and the solute were set to 80.0 and 2.0, respectively. An ionic exclusion radius of 2.0Å, a solvent radius of 1.4Å and a solvent ionic strength of 0.145 M were applied. Amber99 charges and atomic radii were used for this calculation. Energy minimizations were used to remove any residual geometrical strain in each molecular system, using the Charmm27 forcefield as it is implemented into the MOE suite. Molecular systems were then subjected to unrestrained Molecular Dynamics Simulations (MDS) using the MOE suite. MDS took place in a SPC water-solvated, periodic environment. Water molecules were added using the truncated octahedron box extending 7Å from each atom. Molecular systems were neutralized with counter-ions as required. For the purposes of this study all MDS were performed using the NVT ensemble in a canonical environment, at 300 K and a step size equal to 2 femtoseconds for a total 100 nanoseconds simulation time. An NVT ensemble requires that the Number of atoms, Volume and Temperature remain constant throughout the simulation.

KFERQ-like motif discovery

The developed scoring methodology in an effort to identify hidden KFERQ-like motifs in TPPP/P25A that reads the primary amino acid sequence both from N' to C' term and vice versa. The methodology is based on the fusion and analysis of amino acid physicochemical and structural properties that resemble the reference properties

of the KFERQ motif. We calculated 435 molecular and physicochemical descriptors (dimensions) for each amino acid in an effort to be able to confidently scan the sequence of TPPP/P25A for KFERQ-like motifs. Only the KKRFK pentapeptide was discovered that meets the criteria for a KFERQ-like motif. The acceptable thresholds for each dimension used were calibrated and trained based on the properties of KFERQ and all known and established KREFQ-like motifs. The KFERQ-like motifs included from literature were: KFERQ, RKVEQ, QEKRV, QDLKF, QRFFE, DRIKQ, IRDLQ, QDIRR, QEFVR, QKIIE, DLLRQ, QKDFR, DFRKQ, KDLLQ (27). Therefore, the KFERQ likeness of KKRFK was based on an algorithm that has been trained on KFERQ and the 13 established KFERQ-like motifs. Our analysis exploits the dynamic and static information and metrics calculated in an effort to discover patterns and associations among them that will lead to induction of new rules updating the knowledge base and affecting the reasoning process. The combination of the multimodal data collected was used as new knowledge in the form of rules. These rules were exploited to update the reasoning system in order to make adaptive the reasoning processes, i.e., tailored to unique information and characteristics of each motif. Efficient mining of association rules generated a scaled quantification of KFERQ likeness based on 435 physicochemical dimensions. Not only our multimodal methodology on determining KFERQ-likeness, confirms that KKRFK is KFERQ-like based on 435 fused and analyzed physicochemical properties, but we also propose that our approach can be used as a standard of quantification of KFERQ-likeness henceforward.

Isolation of lysosomes

To validate that TPPP/P25A is a CMA substrate, brain lysosomes were isolated from starved Sprague Dawley rats, as previously described (67, 68). Tissue was homogenized in 0.25 M sucrose (Applichem, A4734) and the lysosomes were removed from the light mitochondrial fraction using a Nycodenz (Ncd) density gradient after an ultracentrifugation at 141,000 x g for 1 hr. To examine the integrity of the isolated lysosomes, the enzymatic activity of β-hexosaminidase was measured and only when less of 10% of the lysosomes were broken the process could proceed. In our experiments the ability of isolated lysosomes to degrade recombinant TPPP/P25A was explored via western blot analysis using LAMP1, LAMP2A and cathepsin D (CTSD) as lysosomal markers.

CMA of recombinant TPPP/P25A by isolated lysosomes

Transport of human recombinant TPPP/P25A into isolated rat brain lysosomes was analyzed using an *in vitro* system as previously described (69). Briefly, 0.2 μg of recombinant TPPP/P25A were incubated with freshly isolated rat brain lysosomes in MOPS buffer (10 mM 3-[N-morpholino] propanesulfonic acid, [Sigma-Aldrich, M1254] pH 7.3, 0.3 M sucrose [Applichem, A4734]), in the presence of 0.6 μg recombinant HSPA8/HSC70 (Enzo Life Sciences, AD1-SPP-751-D) for 20 min at 37^0C. Where indicated, lysosomes were pre-incubated with a cocktail of proteinase inhibitors (Roche, 11836153001) for 10 min at 0^0C. A competition assay utilizing 3x (0.6 μg) and 6x (1.2 μg) amount of human recombinant SNCA, a well-established CMA substrate (28) was also performed to further verify the contribution of CMA to TPPP/P25A proteolysis. At the end of the incubation, lysosomes were collected by centrifugation, washed and subjected to SDS-PAGE and immunoblotted for TPPP/P25A, SNCA, LAMP1, LAMP2A, CTSD and ACTB.

Intracellular protein degradation assay

OLN cells were cultured to 60-70% confluence in 12-well plates in full DMEM and incubated with 1 μg/ml of hSNCA PFFs for 48 hrs. Total protein degradation was measured by pulse-chase experiments, by labeling PBS- or PFF-treated OLN cells with [^{3}H] leucine (2 μCi/ml) (Leucine, L-3,4,5, NEN-Perkin Elmer Life Sciences, Belgium) at 37ºC for 24 hrs. The cultures were then extensively washed with medium and returned in complete growth medium containing 2 mM of unlabeled leucine for 6 hrs. This medium containing mainly short-lived proteins was removed and replaced with: fresh medium (DMEM + 0,5% FBS) containing cold leucine (*control conditions*), medium containing 20 mM NH_4Cl (*total lysosomal proteolysis*) or medium containing 10 mM 3MA (*macroautophagic degradation*). The lysosomal degradation that remains unaffected by the use of 3MA was attributed to the CMA pathway, after the assumption that microautophagy can be considered minor (29).

Aliquots of the medium were taken at 16 hrs after labeling and proteins in the medium were precipitated with 20% thrichloroacetic acid for 20 min on ice and centrifuged (10.000 X g, 10 min, 4ºC). Radioactivity in the supernatant (representing degraded proteins) and pellet (representing undegraded proteins) was measured in a liquid scintillation counter (Wallac T414, Perkin Elmer). At the last time point, cells were lysed a mild lysis buffer, containing 0,1 N NaOH and 0,1% sodium deoxycholate. Proteolysis was expressed as the percentage of the initial total acid-precipitable radioactivity (protein) in the cell lysates transformed to acid soluble radioactivity (amino acids and small peptides) in the medium during the incubation (29).

Proteasome Activity Assay

OLN cells were treated with 1 μg/ml of hSNCA PFFs for 48 hrs and the measurement of the CT-like enzymatic activity was accomplished with the use of the fluorescent properties of the synthetic peptide Suc-LLVY-AMC, as previously described (70). Suc-LLVY-AMC is a proteasomal substrate that releases a fluorescent molecule (AMC) after cleavage, with emission at 437 nm. The reaction was performed in 5 μg of total protein lysate, with the addition of a resuspension buffer [50 mM Tris-HCl with pH 7.6, 5 mM DTT, 10 mM ATP and 50mM MgCl2] and 100 μM of the fluorogenic substrate, followed by an incubation at 37° for 10 min. Reaction was terminated by addition of 5% SDS and the released fluorescence was calculated with a PerkinElmer LS-55 luminescence spectrophotometer.

Assessment of survival

Viable cells were quantified by counting the number of intact nuclei in a haemacytometer, after lysing the cells in detergent- containing solution (71, 72). This method has been shown to be reproducible and accurate and to correlate well with other methods of assessing cell survival-death (73, 74). In more detail, cells were resuspended in a detergent-containing lysis buffer (0.1x PBS, 0.5 % Triton, 2mM $MgCl_2$, 0.013 mM ethyl-hexadecyl-dimethyl-ammonium bromide, 0.28 % glacial acetic acid and 2.82 mM NaCl) and two independent examiners blinded to the identity of the samples counted the number of intact nuclei with the aid of a haemocytometer. Cell counts were performed in triplicate and the results were presented as means ± SE.

RNA extraction, cDNA synthesis and real-time PCR

Total RNA was extracted from OLN-AS7 and OLN-p25α cells treated with PBS or epoxomicin (15 nM) or NH_4Cl (20 mM) for 24 or 48 hrs using TRIzol® reagent (Ambion, Thermo Fisher Scientific, Waltham, MA, USA). Following digestion with 1 U/μg DNase I (Promega, Madison, WI, USA) 1 μg total RNA was used to synthesize the first strand cDNA according to the Moloney murine leukemia virus reverse transcription reaction system (Promega, Madison, WI, USA), which subsequently would be the template for the RT-PCR reaction. To this end, duplicates of each sample were analyzed using a Light Cycler 96 (Roche Applied Science, Mannheim, Germany) to determine the levels of human *SNCA* and *TPPP/P25A* mRNA and rat *Gapdh* was the reference gene for normalization. Primer sequences utilized in the study are shown in Table 2. Each cDNA sample was diluted 1:20 before use in the amplification assay. The utilized PCR conditions were 1× buffer (-Mg), 1.5 mm $MgCl_2$, 0.2 mm dNTPs, 0.2 μm primers, template < 500 ng, 2 U Platinum *Taq* and SYBR Green (Roche, Mannheim, Germany), whereas the PCR cycling conditions were 95°C for 180 s, 95°C for 10 s, 60°C for 15 s, 72°C for 15 s (45 cycles), 95°C for 60 s, 60°C for 60 s, 95°C for 10 s, 37°C for 30 s for human *SNCA* and 52°C for 120 s, 95°C for 120 s, 95°C for 15 s, 59°C for 40 s (50 cycles), 95°C for 10 s, 55°C for 60 s, 98°C for 1 s, 37°C for 30 s for human *TPPP/P25A*. No template samples served as negative controls. Data were analyzed automatically with a threshold set in the linear range of amplification. The cycle number at which any particular sample crossed that threshold (*Ct*) was used to determine fold difference, whereas the geometric mean of the control gene served as a reference for normalization. Fold difference was calculated with the $2-\Delta\Delta Ct$ method.

Statistical analysis

All statistical analysis was performed utilizing GraphPad Prism 5. To be more specific, differences between or within groups were assessed by unpaired t-test, one-way and two-way analysis of variance (ANOVA) followed by Tukey's post-hoc test and Bonferroni's correction, respectively. Results are displayed as the mean ± standard error (SE), with a p value of < 0.05 defined as statistically significant. Results are based on the analysis of three independent experiments with at least duplicate samples/condition within each experiment.

Acknowledgments

The authors would like to thank the BRFAA biological imaging facility for their valuable contribution to confocal imaging and image analysis, the BRFAA Animal Facility, as well as Grigoria Tsaka, MSc, Anastasia Vamvaka-Iakovou, BSc, Evangelos Doukoumopoulos, BSc and Karin Giller for their technical assistance.

Funding

This work was supported by an MSA UK Trust grant (2019/MX60185), an MSA Coalition grant and a Bodossaki grant to MX. This research is co-financed by Greece and the European Union (European Social Fund- ESF) through the Operational Programme «Human Resources Development, Education and Lifelong Learning» in the context of the project "Strengthening Human Resources Research Potential via Doctorate Research" (MIS-5000432), implemented by the State Scholarships Foundation (IKY)», awarded to PM. The study was for PHJ supported by Lundbeck Foundation grants R223-2015-4222 & R248-2016-2518 for Danish Research Institute of Translational Neuroscience-DANDRITE, Nordic-EMBL Partnership for Molecular

Medicine, Aarhus University, Denmark. Aarhus University. LS has been supported by a GSRT-HFRI grant for Faculty Members & Researchers (HFRI-FM17-3013).

Disclosure statement

No potential conflicts of interest were disclosed.

Tables

Table 1: A table depicting the primary and secondary antibodies used either in western blot or immunocytochemistry including species reactivity and working dilutions.

Primary Antibody against	Clone	Catalog number	Working dilutions (WB)	Working dilutions (ICC)	Species Reactivity	Company
aggregated SNCA	MJFR 14-6-4-2	ab209538	-	1/1000	rabbit	Abcam
human SNCA	LB509	807701	-	1/1000	mouse	Biolegend
	4B12		1/1000	-	mouse	GeneTex
oxidized/ nitrated SNCA	SYN303	824301	-	1/1000	mouse	Biolegend
rodent SNCA	D37A6	4179	1/1000	1/400	rabbit	CellSignaling
total SNCA	C20	sc7011R	1/1000	1/1000	rabbit	Santa Cruz
	SYN1	610786	-	1/1000	mouse	BD Transduction

						Laboratories
TUBA		62004	-	1/750	mouse	62004
ACTB		TA309077	1/2000	-	mouse	OriGene
LC3 LC3B		PM036 NB100-2220	1/1000	- 1/200	rabbit rabbit	MBL Novus
TPPP/P25A			1/1000	1/400	rabbit/rat	
SQSTM1/ p62		PM045	1/1000	-	rabbit	MBL
Ubiquitin		Z0458	1/1000	-	rabbit	DAKO
Secondary antibody		**Catalog number**		**Working dilutions (ICC or WB)**	**Species Reactivity**	**Company**
Goat Anti-Mouse IgG-HRP conjugated		AP124P		1:10000	mouse	Sigma-Aldrich
Goat Anti-Rabbit IgG-HRP conjugated		AP132P		1/10000	rabbit	Sigma-Aldrich
CF555 red		20033		1/2000	rabbit	Biotium
		20030		1/2000	mouse	Biotium
		20096		1/2000	rat	Biotium
CF488A green		20012		1/2000	rabbit	Biotium
		20010		1/2000	mouse	Biotium
Cy5		115-175-146		1/400	mouse	Jackson Imm. Affinipure

		115-175-144		1/400	rabbit	Jackson Imm. Affinipure
Dyes		**Catalog number**		**Working dilutions (ICC)**		**Company**
DAPI		10236276001		1/1000		Sigma- Aldrich

Table 2: A table depicting the sequences of the siRNAs targeting the rat *Lamp2a*, as well as the human *SNCA*, *TPPP/p25α* and rat *Gapdh* primer sequences utilized in the RT-PCR.

Target name	**siRNA design**
Rat *Lamp2a* siRNA sense (1) (Lsi1)	CCAUCAUACUGGAUAUGAGdTdT
Rat *Lamp2a* siRNA antisense (1) (Lsi1)	CUCAUAUCCAGUAUGAUGGdTdT
Rat *Lamp2a* siRNA sense (2) (Lsi2)	GGUCUCAAGCGCCAUCAUAdTdT
Rat *Lamp2a* siRNA antisense (2) (Lsi2)	UAUGAUGGCGCUUGAGACCdTdT
Oligo name	**Primer sequence (5´→3´)**
huSNCA-Rev	CACCACACTGTCGTCGAATGG
huSNCA-For	CGCCTTGCCTTCAAGCCTTC
huTPPP/p25α-Rev (1)	CCGGACACATAGCCTGACTC
huTPPP/p25α-For (1)	GGGGTGACGAAAGCCATCTC
huTPPP/p25α-Rev (2)	CGAGATGGCTTTCGTCACCC
huTPPP/p25α-For (2)	AAGTCTTGCCGGACCATCAC
Rat *Gapdh*-Rev	TTCAGCTCTGGGATGACCTT
Rat *Gapdh*-For	TGCCACTCAGAAGACTGTGG

Figure Legends

Figure 1 Both autophagy and the proteasome contributes to the degradation of the endogenous rat oligodendroglial SNCA. (**A-C**) Confocal microscopy with endogenous rodent-specific SNCA and TUBA antibodies reveals the cytoplasmic accumulation of the endogenous oligodendroglial SNCA in OLN-93 (**A**), OLN-AS7 (**B**) and OLN-p25α cells (**C**) upon treatment with: proteasomal (epoxomicin, 15 nM) or autophagy (NH_4Cl 20 mM, 3MA 10 mM) inhibitors for 48 hrs. Representative immunofluorescence images with antibodies against TUBA (green) and rat SNCA (red, D37A6 antibody) and DAPI staining are shown. Scale bar: 25 μm. (**D**) Quantification of the endogenous rat SNCA protein levels in OLN cells measured as μm^2 area surface/cell following treatment with proteasomal (epox) or lysosomal (NH_4Cl, 3MA) inhibitors for 48 hrs. Data are expressed as the mean ± SE of three independent experiments with duplicate samples/condition within each experiment; ***p< 0.001, by one-way ANOVA with Tukey's post hoc test (to compare between inhibitor-treated and untreated cells) or #p<0.05; ###p< 0.001 by two-way ANOVA with Bonferroni's correction (to compare between the different OLN cell lines). (**Ei**) Representative immunoblots for rodent SNCA (D37A6 antibody), poly-ubiquitinated proteins, LC3I & II, and SQSTM1 (as macroautophagy markers), and ACTB (as loading control), verifying the increase of endogenous oligodendroglial SNCA protein levels in OLN-93 cells following lysosomal inhibition (NH_4Cl, 48 hrs). (**Eii**) Quantification of the endogenous rat SNCA protein levels in OLN-93 cells treated with proteasomal (epox) or autophagy (NH_4Cl, 3MA) inhibitors for 48 hrs. Data are expressed as the mean ± SE of three independent experiments with duplicate samples/condition within each experiment; *p<0.05, by one-way ANOVA with Tukey's post hoc test.

Figure 2 Down-regulation of the CMA- and macroautophagy-related genes, *Lamp2a* and *Atg5* leads to the accumulation of the endogenous rat oligodendroglial SNCA. (**A-C**) Representative immunofluorescence images of OLN-93 (**A**), OLN-AS7 (**B**) and OLN-p25α cells (**C**) treated with two different siRNAs targeting the rat *Lamp2a* receptor (Lsi1/Lsi2, 60 nM) for 72 hrs. Scrambled RNA sequences (scr) were used as negative control. The antibodies utilized were against TUBA (green) and rat SNCA (red, D37A6 antibody). DAPI was used as a nuclear marker. Scale bar: 25 μm. (**D**) Quantification of the endogenous rat SNCA protein levels in OLN cells shown in A-C measured as μm^2 area surface/cell. Data are expressed as the mean ± SE of three independent experiments with duplicate samples/condition within each experiment; *p<0.05; **<0.01; ***p< 0.001, by one-way ANOVA with Tukey's post hoc test (to compare between siRNA-treated and untreated cells) or ##p< 0.01 by two-way ANOVA with Bonferroni's correction (to compare between the different treated cell cultures). (**E-G**) Confocal microscopy images depicting the cytoplasmic accumulation of the rodent oligodendroglial SNCA (D37A6 ab, red) in OLN-93 (**E**), OLN-AS7 (**F**) and OLN-p25α cells (**G**) upon treatment with *Atg5*-siRNA (*Atg5* si, 10 nM) or scrambled siRNA (scr) for 72 hrs. TUBA was used as a cytoskeletal marker and DAPI as a nuclear marker. Scale bar: 25 μm. (**H**) Quantification of the endogenous rat SNCA protein levels in OLN cells shown in E-G measured as μm^2 area surface/cell. Data are expressed as the mean ± SE of three independent experiments with duplicate samples/condition within each experiment; **<0.01; ***p< 0.001, by one-way ANOVA with Tukey's post hoc test.

Figure 3 The overexpressed human SNCA accumulates upon pharmacological or molecular inhibition of the ALP in OLN-AS7 cells. (**A-C**) Representative

immunofluorescence images of OLN-AS7 cells treated with NH_4Cl (20 mM) or with the macroautophagy inhibitor 3MA (10 mM) (**Ai**), or following siRNA delivery targeting *Lamp2a* (**Bi**) or the autophagy-related *Atg5* gene (**Ci**) using antibodies against human SNCA (red, LB509 antibody) and TUBA (green) and DAPI staining. Scale bar: 25 μm. Quantification of human SNCA protein levels in OLN-AS7 cells measured as Mean Fluorescence Intensity/cell (M.F.I./cell) following treatment with NH_4Cl, 3MA for 48 hrs (**Aii**) or transfection with Lsi1/Lsi2 (60 nM) (**Bii**) or *Atg5* si (10 nM) (**Cii**) for 72 hrs. Scrambled RNA sequences (scr) were used as negative control. Data are expressed as the mean±SE of three independent experiments with duplicate samples/condition within each experiment; *p<0.05; **p< 0.01, by one-way ANOVA with Tukey's post hoc test. (**D-F**) Representative immunoblots of human SNCA protein levels (using the human SNCA-specific 4B12 antibody) derived from OLN-AS7 cells following total lysosomal (NH_4Cl) or macroautophagy inhibition (3MA) (**Di**), or CMA-dependent (**Ei**) or macroautophagy-related (**Fi**) gene silencing using *Lamp2a*- (Lsi1/Lsi2) and *Atg5*-si RNAs, respectively. Gene silencing was verified by the detection of LAMP2A or ATG5 protein levels. Scrambled RNA sequences (scr) were used as negative control. Antibodies against LC3I & II, and SQSTM1 were used as macroautophagy markers (**Di**) and ACTB as loading control. Quantification of the human SNCA protein levels in OLN-AS7 cells treated with (**Dii**) NH_4Cl or 3MA for 48 hrs, (**Eii**) Lsi1/Lsi2 for 72 hrs and (**Fii**) *Atg5* si for 72 hrs. Data are expressed as the mean±SE of three independent experiments with duplicate samples/condition within each experiment; *p<0.05; ***p<0.001, by one-way ANOVA with Tukey's post hoc test.

Figure 4 The overexpressed human TPPP/P25A is increased following pharmacological or molecular inhibition of the ALP in OLN-p25α cells. (**A-C**) Representative immunofluorescence images of OLN-p25α cells showing the increased protein levels of human TPPP/P25A upon pharmacological (**Ai**) or molecular (**Bi, Ci**) inhibition of lysosomal pathways (total, CMA, macroautophagy) using antibodies against human TPPP/P25A (red) and TUBA (green) and DAPI staining. Scale bar: 25 μm. Quantification of human TPPP/P25A protein levels in OLN-p25α cells measured as M.F.I./cell following treatment with NH_4Cl, 3MA for 48 hrs (**Aii**) or with *Lamp2a*-or *Atg5*-siRNAs for 72 hrs (**Bii** and **Cii**). Scrambled RNA sequences (scr) were used as negative control. Data are expressed as the mean±SE of three independent experiments with duplicate samples/condition within each experiment; *p<0.05; **p< 0.01, by one-way ANOVA with Tukey's post hoc test. (**D-F**) Representative immunoblots of OLN-p25α cell lysates verifying the accumulation of TPPP/P25A protein levels upon lysosomal inhibition using either pharmacological inhibitors (**Di**) or gene silencing methods (**Ei** and **Fi**). *Lamp2a* and *Atg5* downregulation was verified using antibodies against LAMP2A or ATG5 proteins (**Ei** and **Fi**). Scrambled RNA sequences (scr) were used as negative control. Antibodies against LC3I & II, and SQSTM1 were used as macroautophagy markers (**Di**), and ACTB as a loading control. Quantification of the human TPPP/P25A protein levels in OLN-p25α cells treated with (**Dii**) NH_4Cl or 3MA for 48 hrs, (**Eii**) Lsi1/Lsi2 (60 nM) for 72 hrs and (**Fii**) *Atg5* si (10 nM) for 72 hrs. Data are expressed as the mean±SE of three independent experiments with duplicate samples/condition within each experiment; *p<0.05, by one-way ANOVA with Tukey's post hoc test.

Figure 5 The oligodendroglial-specific protein TPPP/P25A is a putative CMA substrate, containing a KFERQ-like motif necessary for CMA targeting. (A) i) The superposed TPPP/P25A protein from human (magenta), mouse (orange) and the human model (turquoise), ii) The superposed X-Ray structures and the model with the KKRFK motif highlighted, iii) The KKRFK motif with electrostatic surface. Notice that the KFERQ-like motif region is in a loop, surrounded by two α-helices, fully exposed to the solvent. (**B**) Representative immunoblots of recombinant TPPP/P25A *in vitro* degradation via isolated rat brain-derived lysosomes. Lysosomes were incubated with 0.2 μg recombinant human TPPP/P25A protein in the absence or presence (as negative control) of protease inhibitors (PIs). The addition of increasing amounts of recombinant human monomeric SNCA (0.6 μg or 1.2 μg) reveals the competition of the two proteins (SNCA and TPPP/P25A) for LAMP2A binding and CMA degradation. Human recombinant HSPA8/HSC70 was used for the substrate translocation to the lysosomes. Lysosomal enrichment was verified by the detection of LAMP2A, LAMP1 and CTSD and equal loading with ACTB and CTSD proteins. (**C**) Quantification of the relative levels of human recombinant TPPP/P25A protein (versus CTSD levels) in the presence or the absence of PIs or recombinant human monomeric SNCA Data are expressed as the mean±SE of three independent experiments; *$p<0.05$, by one-way ANOVA with Tukey's post hoc test.

Figure 6 Both the exogenously added human SNCA (hSNCA PFFs) and the recruited endogenous rat oligodendroglial SNCA are partly degraded via the ALP, without impairing the total lysosomal activity. (**A-C**) Representative immunofluorescence images of OLN-93 (**A**), OLN-AS7 (**B**) and OLN-p25α (**C**) cells treated with NH_4Cl (20 mM), 3MA (10 mM) or epoxomicin (epox, 15 nM) for 16 hrs following their

incubation with 1 μg/ml hSNCA PFFs for 32 hrs. (**D-F**) Quantification of the endogenous rodent SNCA (**D**), human SNCA (**E**) or TPPP/P25A (**F**) protein levels in OLN-93, OLN-AS7 and OLN-p25α cells shown in A-C measured as μm^2 area surface/cell. Data are expressed as the mean ± SE of three independent experiments with duplicate samples/condition within each experiment; *p<0.05; **p< 0.01, by one-way ANOVA with Tukey's post hoc test (to compare between inhibitor-treated and untreated cells) or #p<0.05; ##p< 0.01 by two-way ANOVA with Bonferroni's correction (to compare between the different treated cell cultures). (**G**) Representative immunoblots of the UREA-soluble protein lysates of OLN-93 cells treated with 1 μg/ml hSNCA PFFs (32 hrs) followed by their incubation with the pharmacological inhibitors epox or NH_4Cl for 16 hrs. Both human (4B12 antibody) and total (endogenous + human) SNCA (C20 antibody) seem to accumulate in the UREA-soluble fraction of OLN-93 cells treated with epox or NH_4Cl following incubation with 1 μg/ml hSNCA PFFs. Antibodies against LC3I & II, and SQSTM1 were used as macroautophagy markers and ACTB as loading control. (**H**) Quantification of monomeric and High Molecular Weight (HMW) species of human (**Hi** and **Hii**) and total (**Hiii** and **Hiv**) SNCA detected in the UREA-soluble fraction of OLN-93 cells treated with 1 μg/ml PFFs and epox or NH_4Cl for a total of 48 hrs. Data are expressed as the mean±SE of three independent experiments. (**I**) Lysosomal degradation of long-lived proteins is increased in OLN cells upon treatment with 1 μg/ml hSNCA PFFs for a total of 96 hrs. OLN cells incubated with hSNCA PFFs for 48 hrs were labeled with [^{3}H] leucine for another 48 hrs (2 μCi/ml). 16 hrs prior to media collection, cells were treated with or without NH_4Cl (20 mM) or 3MA (10 mM) and degraded proteins were assayed. The rate of total (**Ii**) (inhibitable by NH_4Cl), macroautophagic (**Iii**) (inhibitable by 3MA) or CMA-dependent (**Iiii**) long-lived

protein degradation in all OLN cells is shown. The increased total lysosomal degradation upon PFF treatment seems to be attributed to the induction of macroautophagy in OLN-93 cells or CMA in OLN-AS7 and OLN-p25α cells. Data are expressed as the mean ± SE of three independent experiments; *p<0.05; **p< 0.01, by one-way ANOVA with Tukey's post hoc test (to compare between PBS- and hSNCA PFFs-treated cells) or #p<0.05; ##p< 0.01 by two-way ANOVA with Bonferroni's correction (to compare between the different OLN cells).

Figure 7 TPPP/P25A overexpression favors the degradation of both exogenously added (hSNCA PFFs) and recruited endogenous oligodendroglial SNCA preferentially via CMA and not via macroautophagy. (**A-C**) Representative immunofluorescence images of OLN-93, OLN-AS7 and OLN-p25α cells incubated with 1 μg/ml hSNCA PFFs added at 24 hrs following transfection with *Lamp2a*-(Lsi1/Lsi2, 60 nM), *Atg5*-siRNAs (*Atg5* si, 10 nM) or scr siRNA (control) for another 48 hrs, using antibodies against the endogenous rodent SNCA (red, D37A6 antibody), human SNCA (green, LB509 antibody) and TPPP/P25A (grey) and DAPI staining. Scale bar: 25μm. (**D-F**) Quantification of the endogenous rodent SNCA (**Di, Dii**), human SNCA (**Ei-Eii**) or TPPP/P25A (**Fi-Fii**) protein levels in OLN-93, OLN-AS7 and OLN-p25α cells shown in A-C measured as μm^2 area surface/cell. Data are expressed as the mean ± SE of three independent experiments with duplicate samples/condition within each experiment; *p<0.05; **p< 0.01; ***p< 0.001, by one-way ANOVA with Tukey's post hoc test.

Figure 8 Addition of hSNCA PFFs does not impair autophagosome formation, but seems to interfere with the fusion of autophagosomes with the lysosome in all OLN

cell lines. (**A-B**) Representative immunofluorescence images of OLN-93, OLN-AS7 and OLN-p25α cells transfected with GFP/RFP-LC3 (**A**) or GFP/mcherry-SQSTM1 (**B**) constructs for 48 hrs. Cells were incubated with PBS (as control) or with 1 μg/ml hSNCA PFFs 6 hrs post-transfection with the fluorescent constructs and the autophagic flux was assessed via confocal microscopy. Incubation of OLN-93 cells with NH_4Cl (20 mM) for 16 hrs was used as a positive control for the inhibition of lysosomal fusion. DAPI is used as a nuclear marker. Scale bar: 25 μm. (**C-D**) Calculation of the GFP:RFP (in case of LC3 cDNA) or GFP:mcherry (in case of SQSTM1 cDNA) fluorescence ratio as an estimation of autophagic flux. The ratio increases when autophagic flux is low, as presented in the graphs. Data are expressed as the mean ± SE of three independent experiments with duplicate samples/condition within each experiment; ***p< 0.001, by one-way ANOVA with Tukey's post hoc test.

Figure 9 Pharmacological enhancement of CMA (AR7) or macroautophagy (rapamycin) decreases overexpressed human SNCA (OLN-AS7 cells) and TPPP/P25A (OLN-p25α cells) protein levels under basal conditions. (**A-B**) Confocal microscopy with antibodies against human SNCA (**A**, red, LB509 antibody) and TPPP/P25A (**B**, red) reveals the enhanced degradation of these proteins upon treatment of OLN-AS7 and OLN-p25α cells with 40 μM AR7 (CMA enhancer) or 1 μM rapamycin (rap, macroautophagy enhancer) for 48 hrs. TUBA is used as a cytoskeletal marker (green) and DAPI as a nuclear marker. Scale bar: 25 μm. (**C-D**) Quantification of human SNCA (**C**) and TPPP/P25A (**D**) protein levels in OLN-AS7 and OLN-p25α cells respectively, measured as M.F.I./cell following treatment with AR7 or rap for 48 hrs. Data are expressed as the mean±SE of three independent

experiments with duplicate samples/condition within each experiment; **p< 0.01; ***p<0.001, by one-way ANOVA with Tukey's post hoc test. (**Ei, Fi**) Representative immunoblots of protein cell lysates derived from OLN-AS7 (**Ei**) and OLN-p25α cells (**Eii**) demonstrating the decline of human SNCA (4B12 antibody) and TPPP/P25A protein levels upon treatment of cells with AR7 or rap for 48 hrs. Antibodies against LC3I & II, and SQSTM1 were used as macroautophagy markers and ACTB as loading control. (**Eii, Fii**) Quantification of human SNCA (**Eii**) and TPPP/P25A (**Fii**) protein levels vs ACTB in OLN-AS7 and OLN-p25α cells, respectively, treated with AR7 or rap for 48 hrs. Data are expressed as the mean±SE of three independent experiments; ***p<0.001, by one-way ANOVA with Tukey's post hoc test.

Figure 10 Pharmacological augmentation of CMA or macroautophagy accelerates the clearance of aberrant SNCA conformations formed in PFF-treated oligodendrocytes. (**A-C**) Representative immunofluorescence images using antibodies against the endogenous rodent SNCA (red, D37A6 antibody), the human SNCA (green, LB509 antibody) and TPPP/P25A (grey) proteins are shown. DAPI is used as nuclear marker. Scale bar: 25 μm. (**D-F**) Quantification of the recruited endogenous rodent (**Di**), the exogenously added human (**Dii**) SNCA, the overexpressed human TPPP/P25A (in OLN-p25α cells) (**Ei**) and the pathological oxidized/nitrated (**Eii**), the aggregated (**Fi**) and the total (rodent + human) (**Fii**) SNCA protein levels in all OLN cells treated with 40 μM AR7 or 1 μM rap (16 hrs) following the addition of 1 μg/ml hSNCA PFFs for a total of 48 hrs. Data are expressed as the mean ± SE of three independent experiments with duplicate samples/condition within each experiment; *p<0.05; **p< 0.01; ***p< 0.001, by one-way ANOVA with Tukey's post hoc test (to compare between enhancer-treated and untreated cells) or #p<0.05 by two-way ANOVA with

Bonferroni's correction (to compare between the different OLN cell lines). (**G**) Representative immunoblots of the SDS-soluble SNCA species of control OLN-93 cells incubated with 1 μg/ml hSNCA PFFs for 32 hrs followed by addition of AR7 or rap for 16 hrs using antibodies against hSNCA (4B12 antibody) or total (rodent + human) SNCA (SYN1 antibody). Equal loading was verified by the detection of ACTB levels. (**H**) Quantification of monomeric and HMW species of human (**Hi** and **Hii**) and total (rodent + human) (**Hiii** and **Hiv**) SNCA levels detected in the SDS-soluble fraction of OLN-93 treated with 1 μg/ml hSNCA PFFs for 32 hrs and AR7 or Rap for additionally 16 hrs. Data are expressed as the mean±SE of three independent experiments; *p< 0.05, by one-way ANOVA with Tukey's post hoc test. (**I**) Representative immunoblots of the UREA-soluble protein fraction derived from OLN-93 cells treated with AR7 or rap following hSNCA PFFs addition. Antibodies against rodent SNCA (D37A6 antibody), hSNCA (4B12 antibody) or total (rodent + human) SNCA (SYN1 antibody) verified the decrease of the protein levels detected in this fraction upon addition of CMA (AR7) or autophagy (rap) enhancers. ACTB was used as loading control. (**J-L**) Quantification of monomeric and HMW species of rodent (**Ji** and **Jii**), human (**Ki** and **Kii**) and total (endogenous + human) (**Li** and **Lii**) SNCA levels detected in the UREA-soluble fraction of OLN-93 cells treated with 1 μg/ml hSNCA PFFs and the autophagy modulators. Data are expressed as the mean±SE of three independent experiments; *p<0.05; **p< 0.01; ***p< 0.001, by one-way ANOVA with Tukey's post hoc test.

Figure 11 The MSA-related proteins TPPP/P25A and SNCA are mainly degraded via the ALP in murine primary oligodendroglial cultures, under physiological and pathological conditions. Mouse primary oligodendroglial cultures were incubated

with PBS (as control) or hSNCA PFFs for 24 hrs followed by their treatment with lysosomal or proteasomal inhibitors for another 48 hrs. (**A-B**) Representative confocal microscopy images depicting the protein levels of TPPP/P25A (red) upon total lysosomal (NH_4Cl, 20 mM), macroautophagic (3MA, 10 mM) or proteasomal (epox, 15 nM) inhibition (for 48 hrs) in the absence (**A**) or presence (**B**) of 1 μg/ml hSNCA PFFs for a total of 72 hrs. The recruited endogenous rodent SNCA (green, D37A6 antibody) and the exogenously added hSNCA PFFs (grey, LB509 antibody) also seem to be preferentially degraded via the ALP under pathological (**B**, PFFs-treated) conditions. DAPI staining is used as a nuclear marker. Scale bar: 25 μm. (**C**) Quantification of TPPP/P25A (**Ci, Cii**), rodent SNCA (**Di, Dii**) and human SNCA (**E**) protein levels in PBS or PFF-treated primary oligodendrocytes, measured as μm^2/cell. Data are expressed as the mean±SE of three independent experiments with duplicate samples/condition within each experiment; *p<0.05; **p< 0.01; ***p< 0.001, by one-way ANOVA with Tukey's post hoc test. (**F-G**) Representative immunofluorescence images of TPPP/P25A (red), rodent SNCA (green, D37A6 antibody) and hSNCA (grey, LB509 antibody) protein levels upon treatment of mouse oligodendrocytes with AR7 (40 μM) or rap (1 μM) for 48 hrs, which were added to cells 24 hrs following addition of PBS, as control, (**F**) or 1 μg/ml hSNCA PFFs (**G**). DAPI is used as a nuclear marker. Scale bar: 25 μm. (**H**) Quantification of TPPP/P25A (**Hi, Hii**), rodent SNCA (**Hiii**) and human SNCA (**Hiv**) protein levels in PBS or PFF-treated primary oligodendrocytes, measured as μm^2/cell. Data are expressed as the mean±SE of three independent experiments with duplicate samples/condition within each experiment; *p<0.05; **p< 0.01; ***p< 0.001, by one-way ANOVA with Tukey's post hoc test.

A.

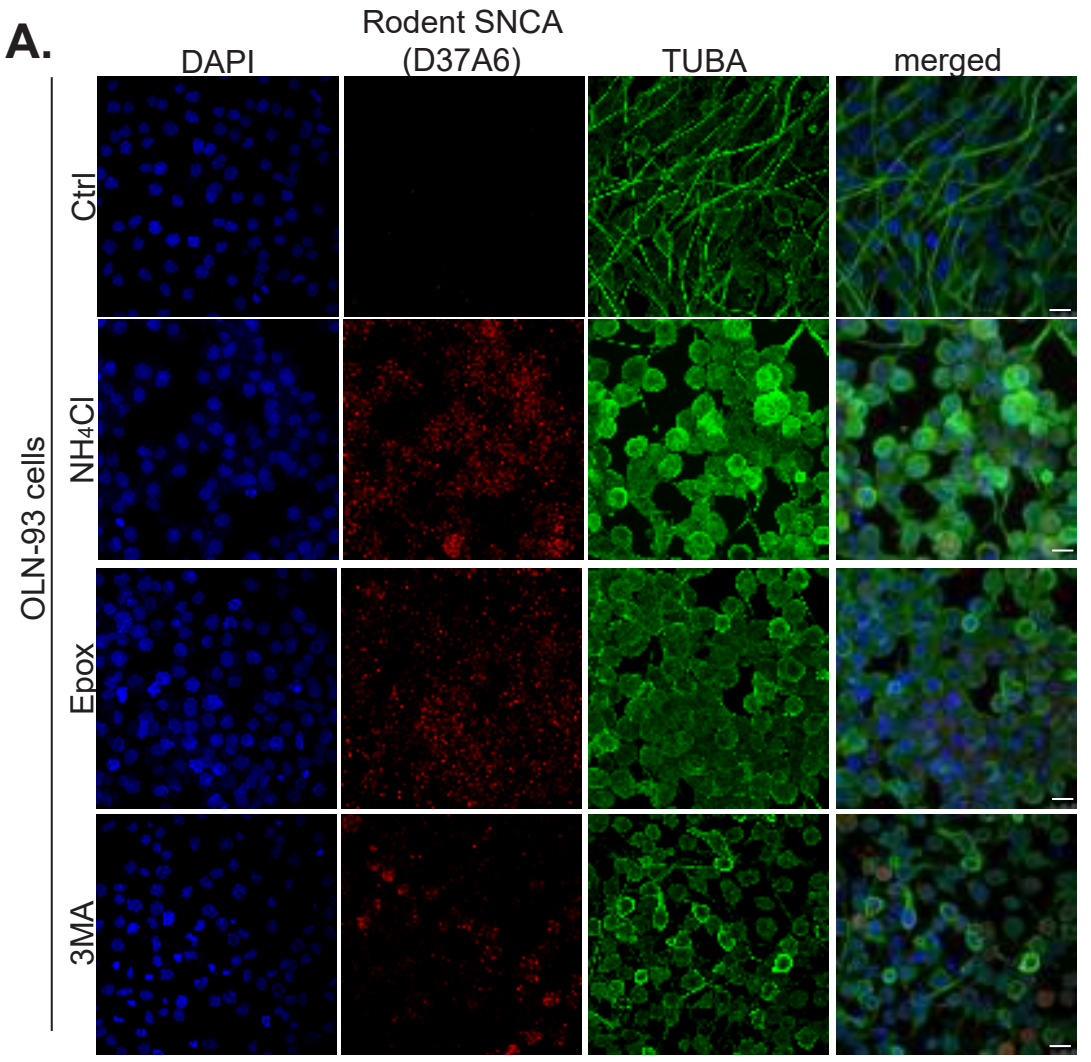
Rodent SNCA (D37A6)
DAPI
TUBA
merged
OLN-93 cells
Ctrl
NH4Cl
Epox
3MA

B.

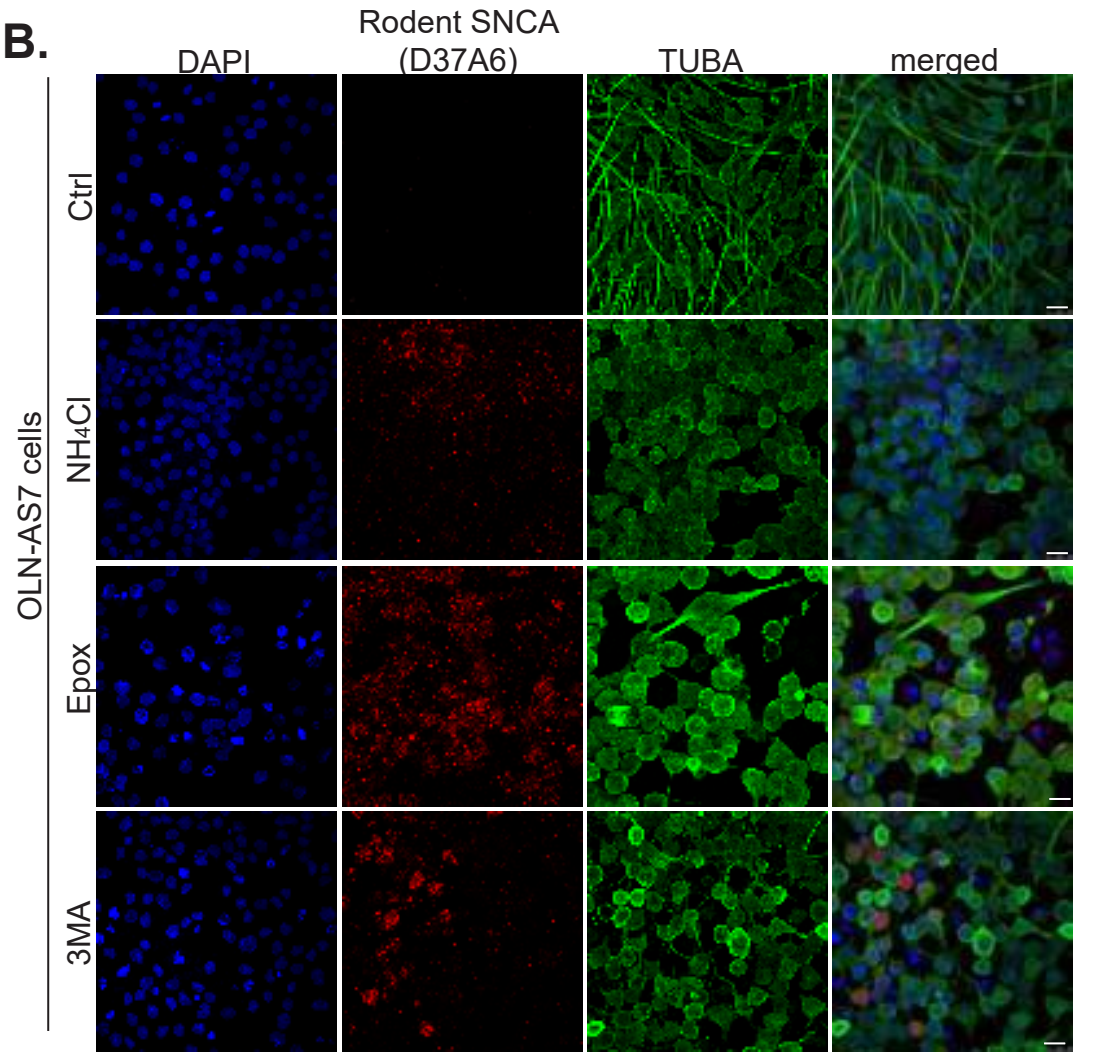
Rodent SNCA (D37A6)
DAPI
TUBA
merged
OLN-AS7 cells
Ctrl
NH4Cl
Epox
3MA

C.

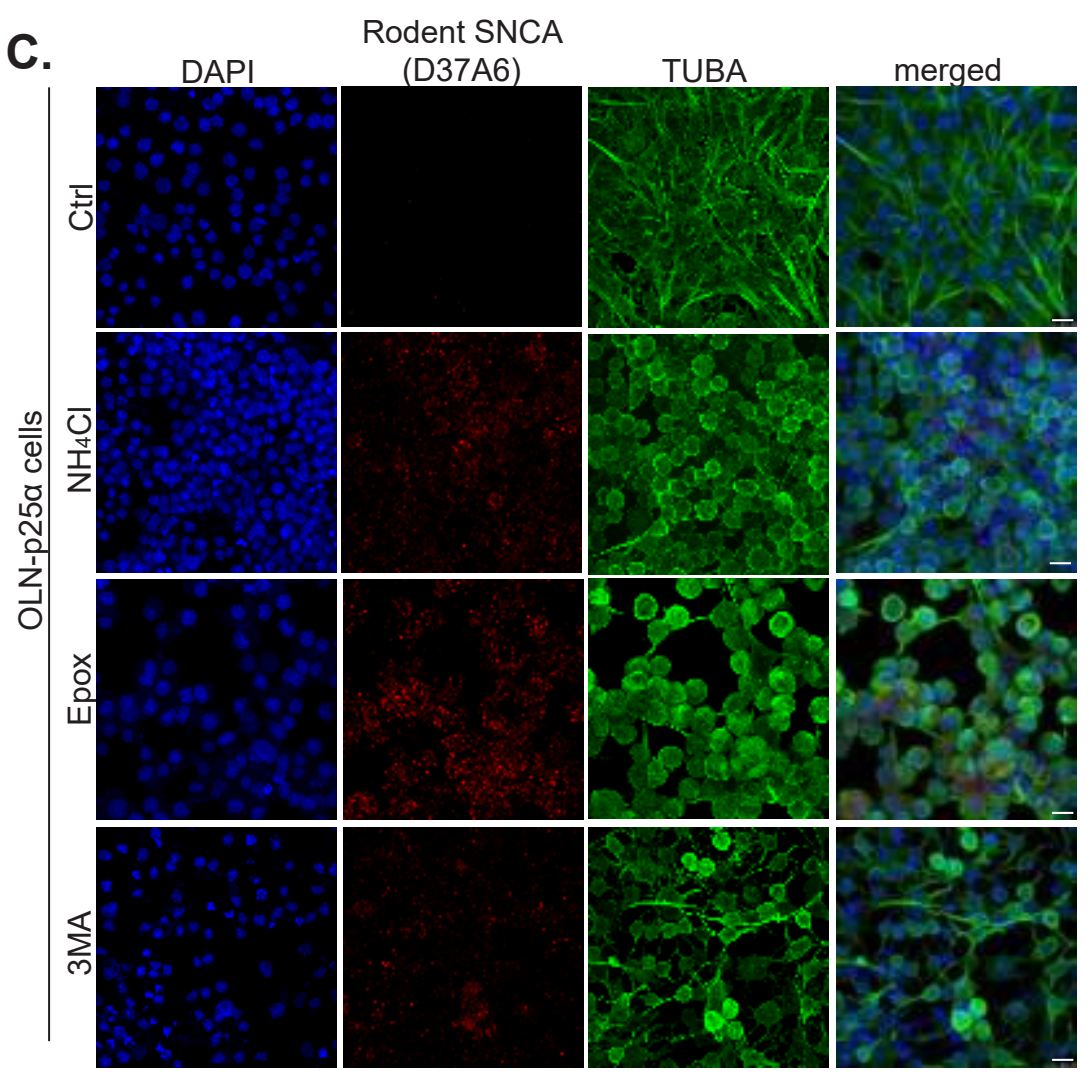
Rodent SNCA (D37A6)
DAPI
TUBA
merged
OLN-p25α cells
Ctrl
NH4Cl
Epox
3MA

Ei.

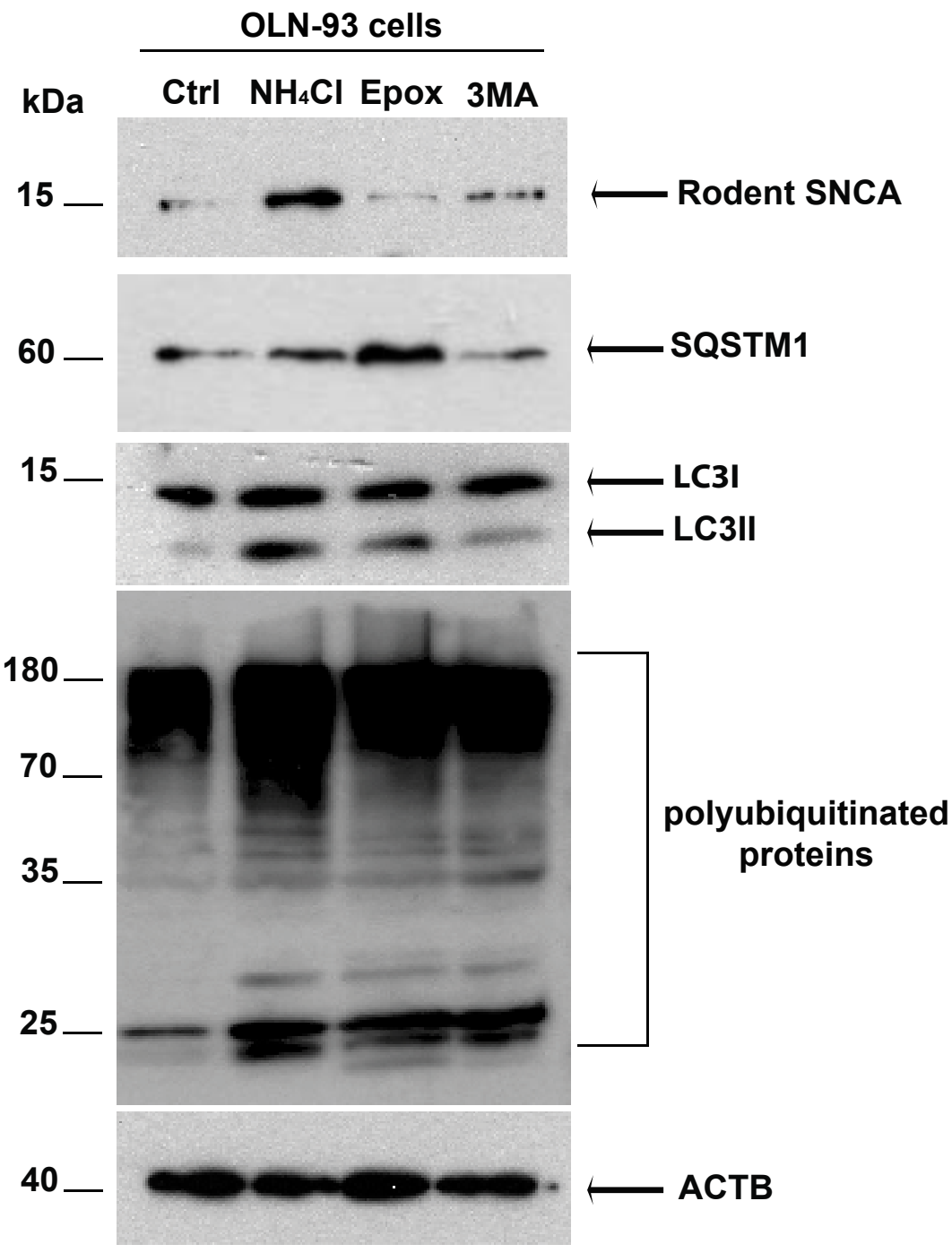
OLN-93 cells
kDa
Ctrl
NH4Cl
Epox
3MA
15
60
15
180
70
35
25
40
Rodent SNCA
SQSTM1
LC3I
LC3II
polyubiquitinated proteins
ACTB

D.

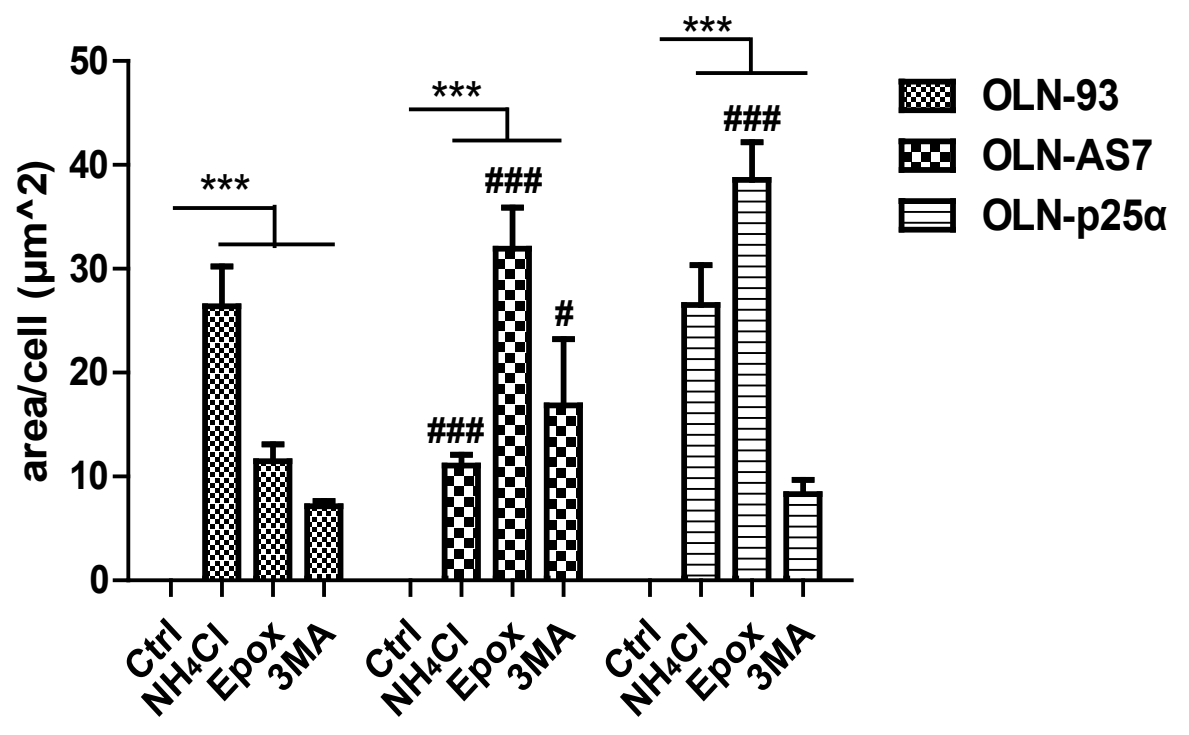
Rodent SNCA (D37A6)
area/cell (μm^2)
50
40
30
20
10
0
***
***
***
###
###
###
#
Ctrl
NH4Cl
Epox
3MA
OLN-93
OLN-AS7
OLN-p25α

Eii.

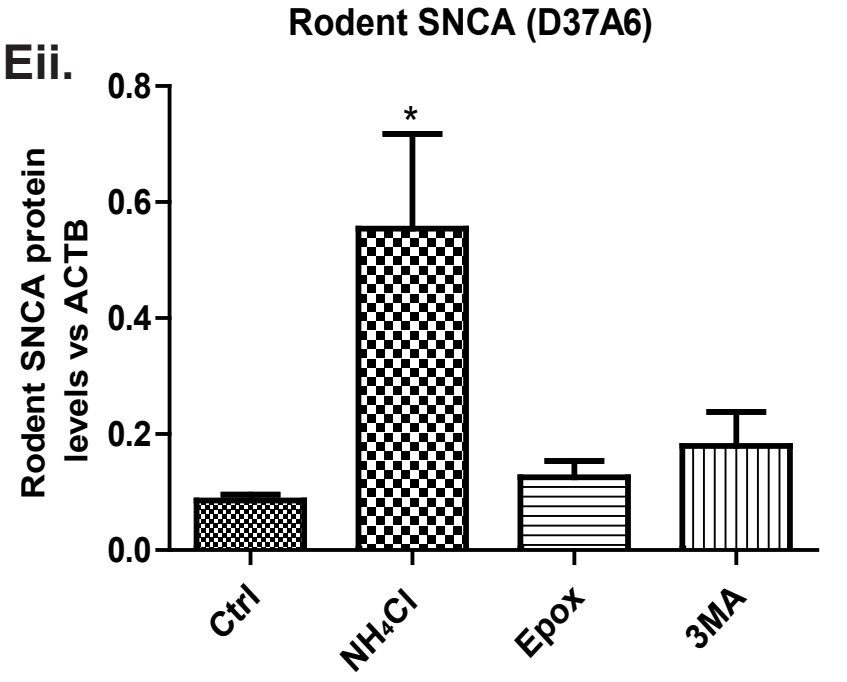
Rodent SNCA (D37A6)
Rodent SNCA protein levels vs ACTB
0.8
0.6
0.4
0.2
0.0
*
Ctrl
NH4Cl
Epox
3MA

A.

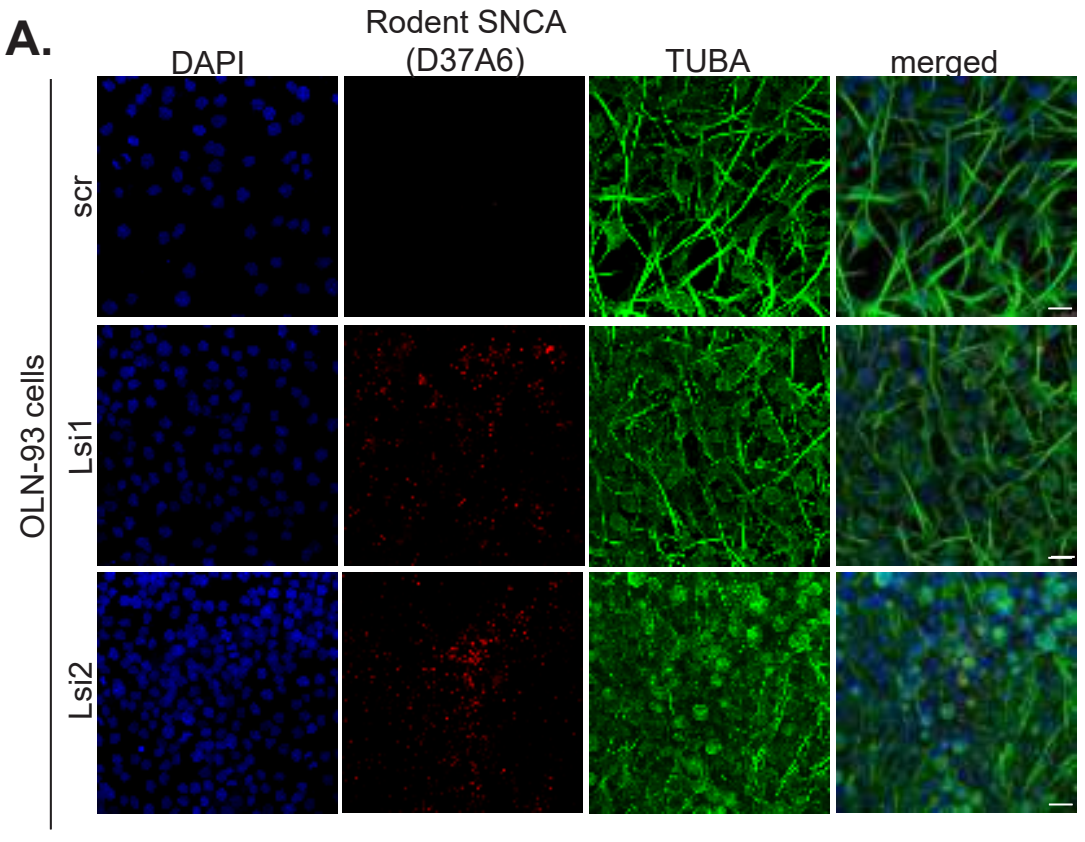
Rodent SNCA (D37A6)
DAPI
TUBA
merged
OLN-93 cells
scr
Lsi1
Lsi2

B.

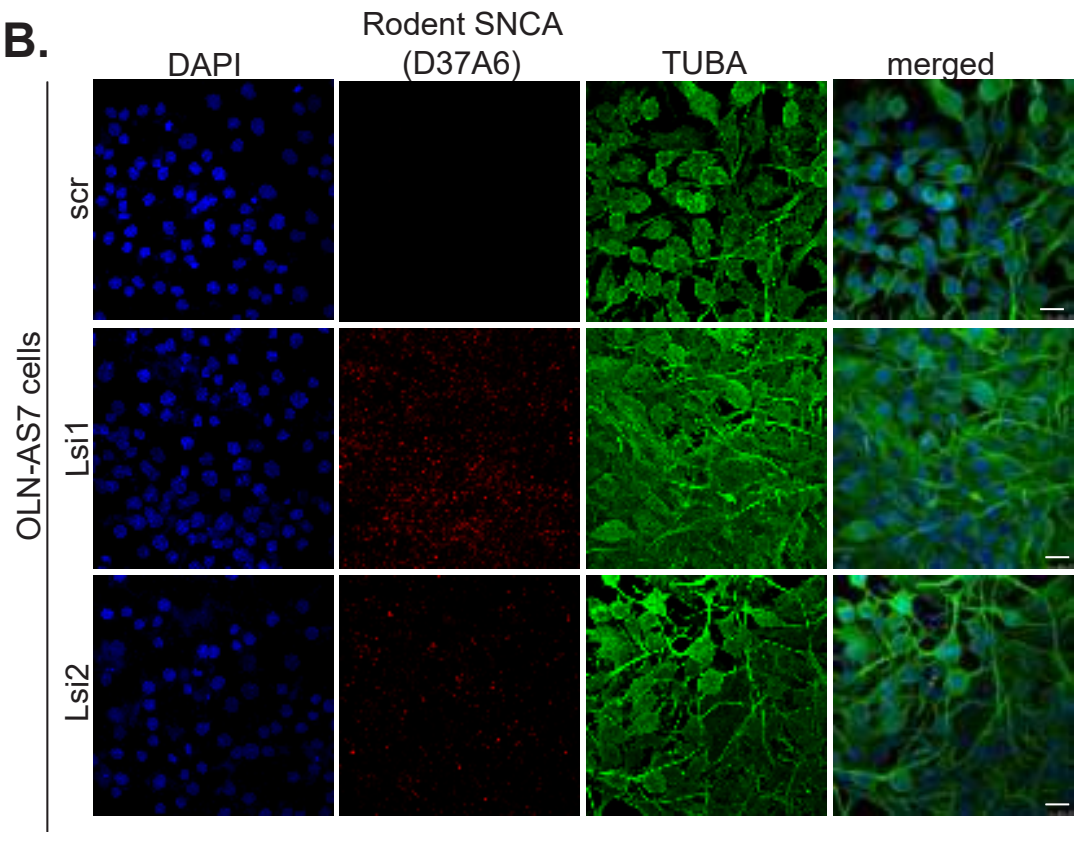
Rodent SNCA (D37A6)
DAPI
TUBA
merged
OLN-AS7 cells
scr
Lsi1
Lsi2

C.

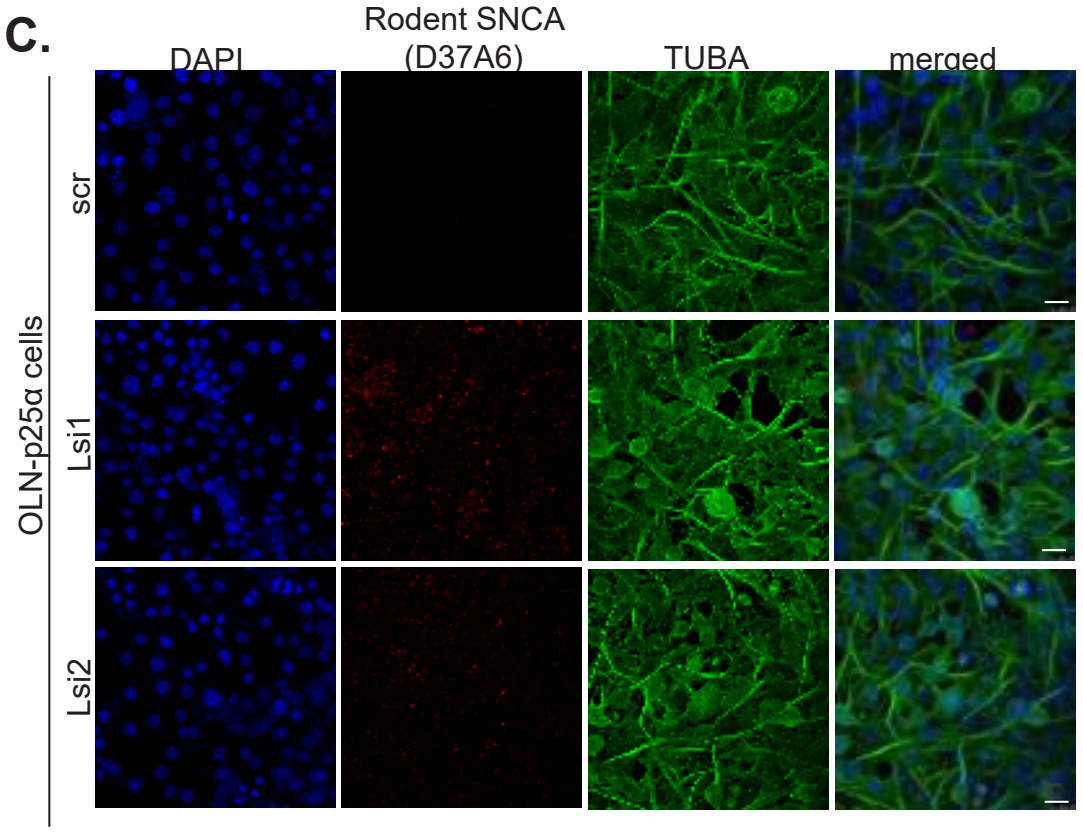
Rodent SNCA (D37A6)
DAPI
TUBA
merged
OLN-p25α cells
scr
Lsi1
Lsi2

D.

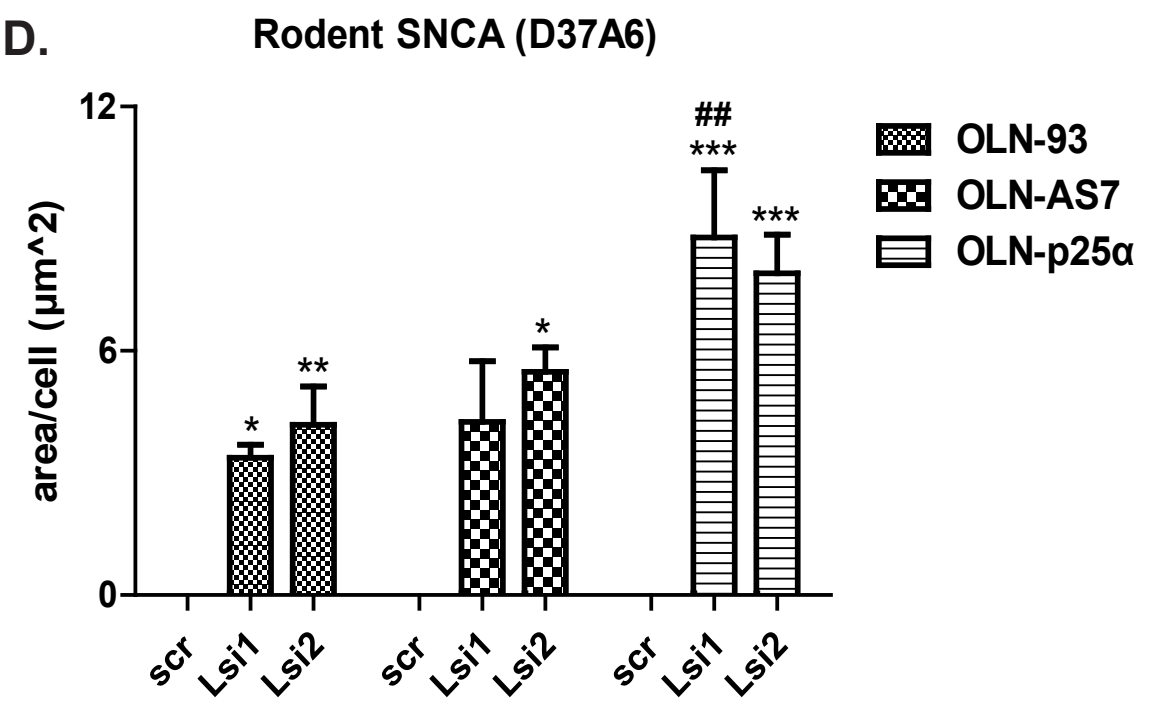
Rodent SNCA (D37A6)
area/cell (μm^2)
12
6
0
*
**
*
##
***
***
scr
Lsi1
Lsi2
scr
Lsi1
Lsi2
scr
Lsi1
Lsi2
OLN-93
OLN-AS7
OLN-p25α

E.

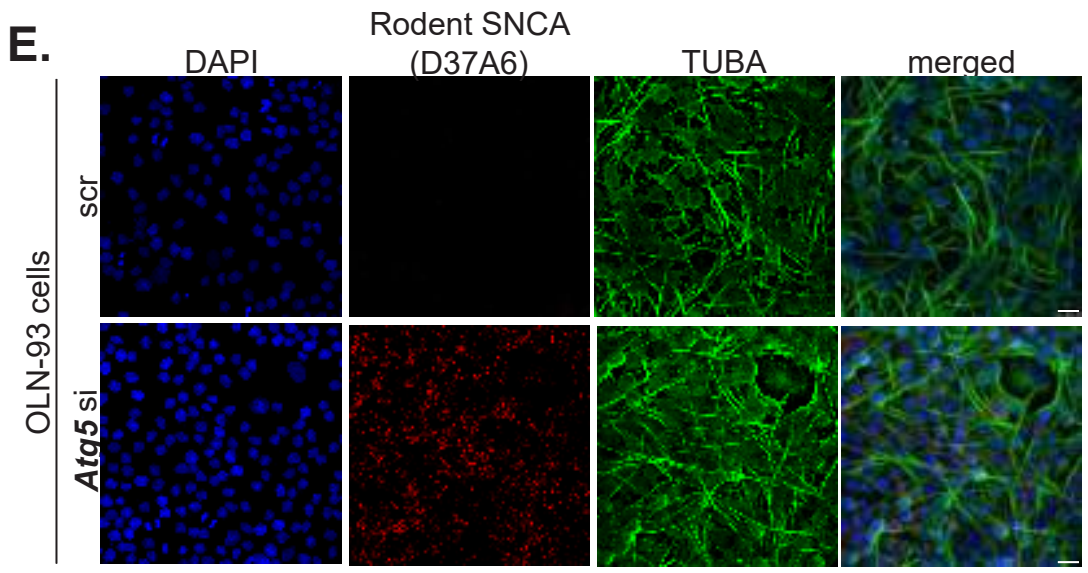
Rodent SNCA (D37A6)
DAPI
TUBA
merged
OLN-93 cells
scr
Atg5 si

F.

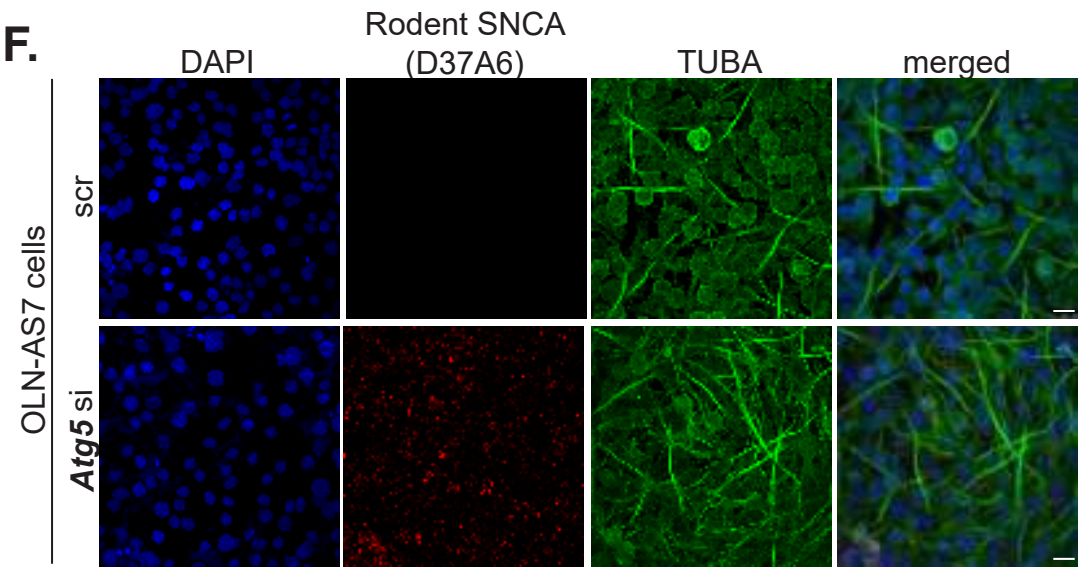
Rodent SNCA (D37A6)
DAPI
TUBA
merged
OLN-AS7 cells
scr
Atg5 si

G.

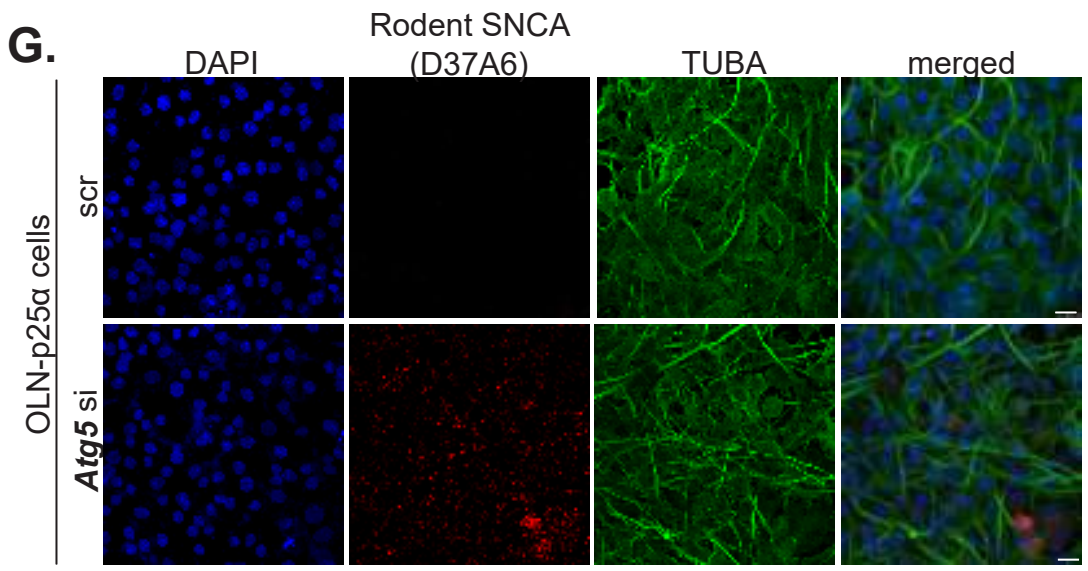
Rodent SNCA (D37A6)
DAPI
TUBA
merged
OLN-p25α cells
scr
Atg5 si

H.

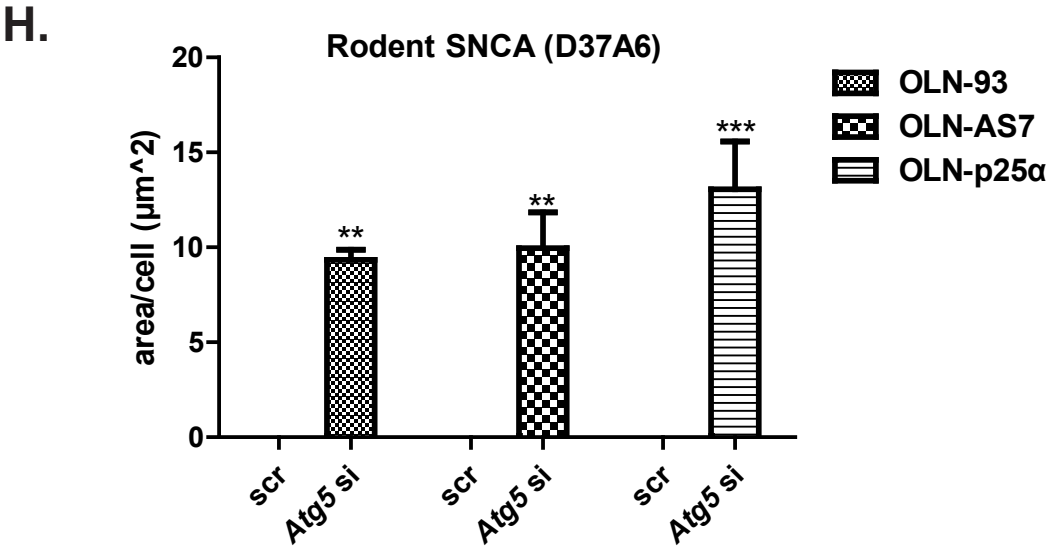
Rodent SNCA (D37A6)
area/cell (μm^2)
20
15
10
5
0
**
**
***
scr
Atg5 si
scr
Atg5 si
scr
Atg5 si
OLN-93
OLN-AS7
OLN-p25α

Ai.

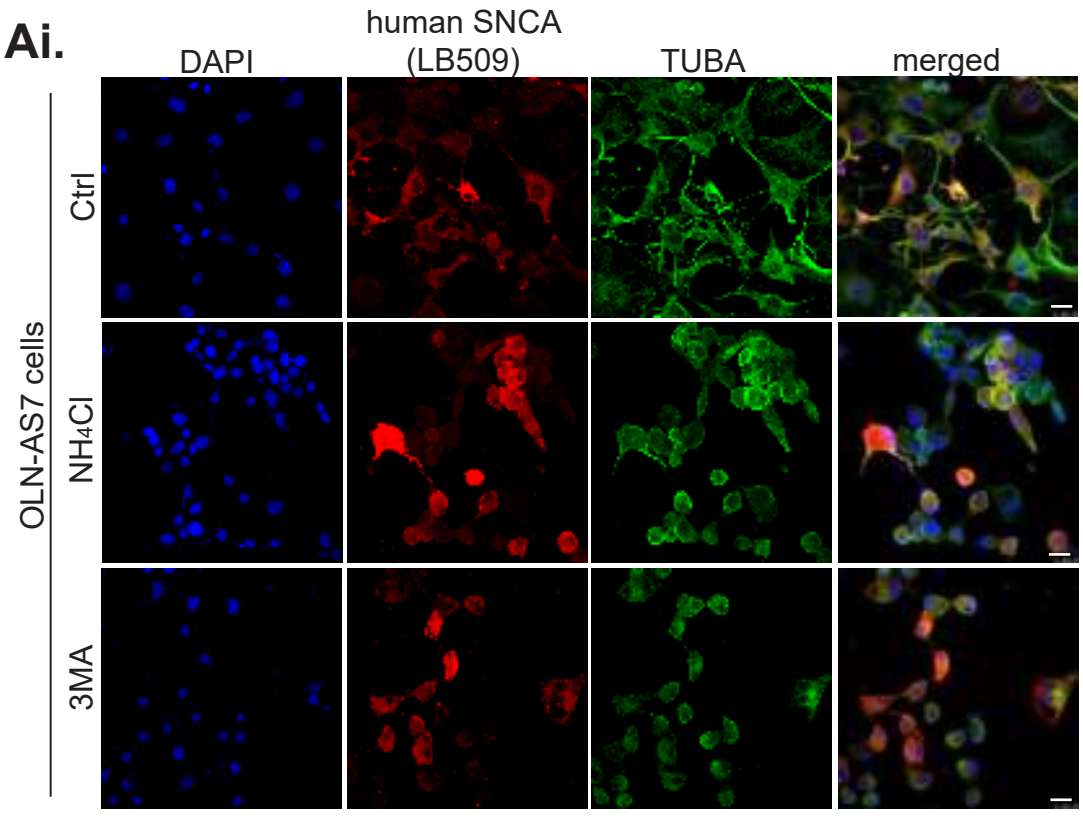

Aii.

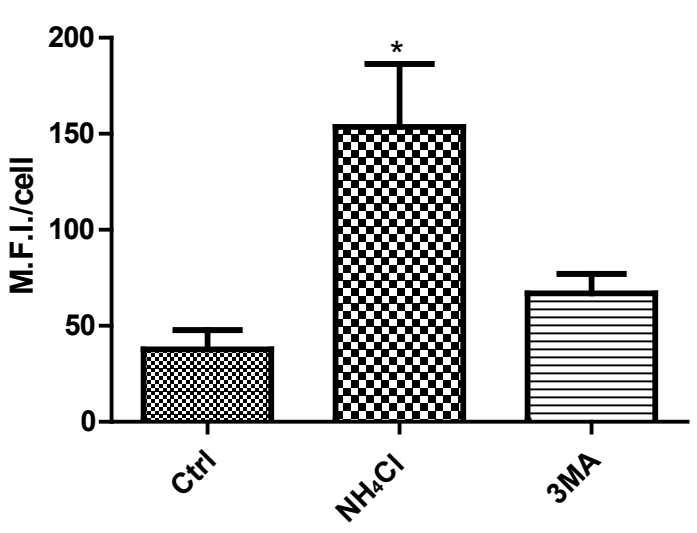

Di.

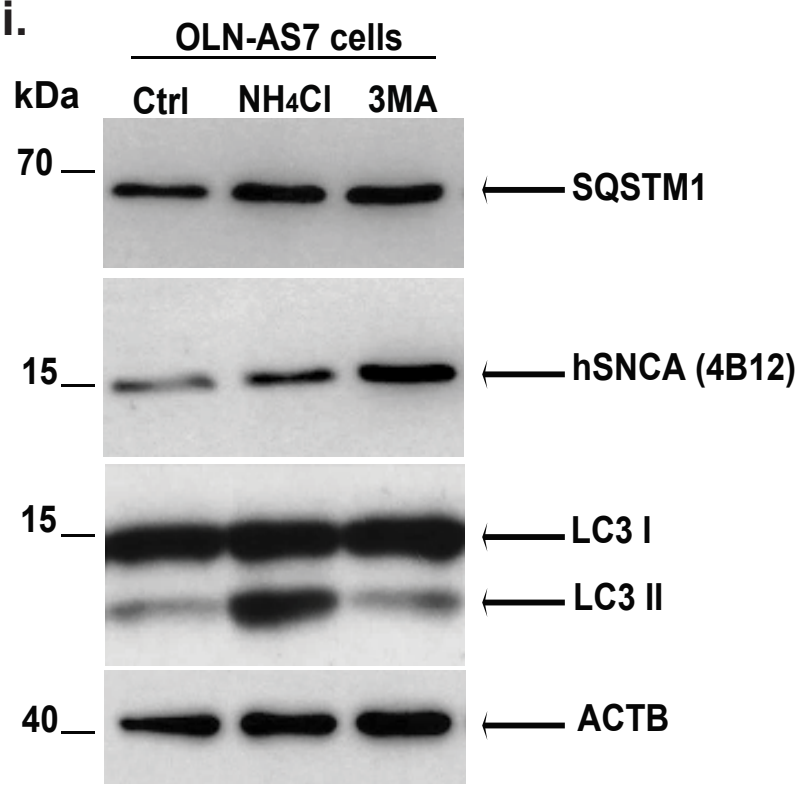

Dii.

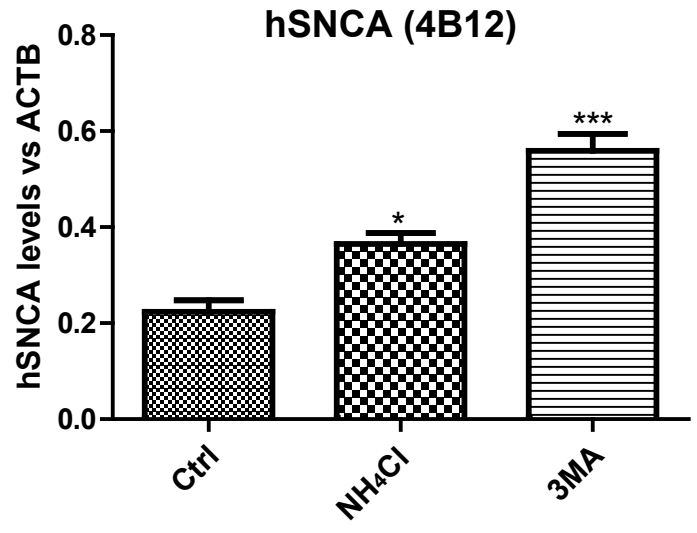

Bi.

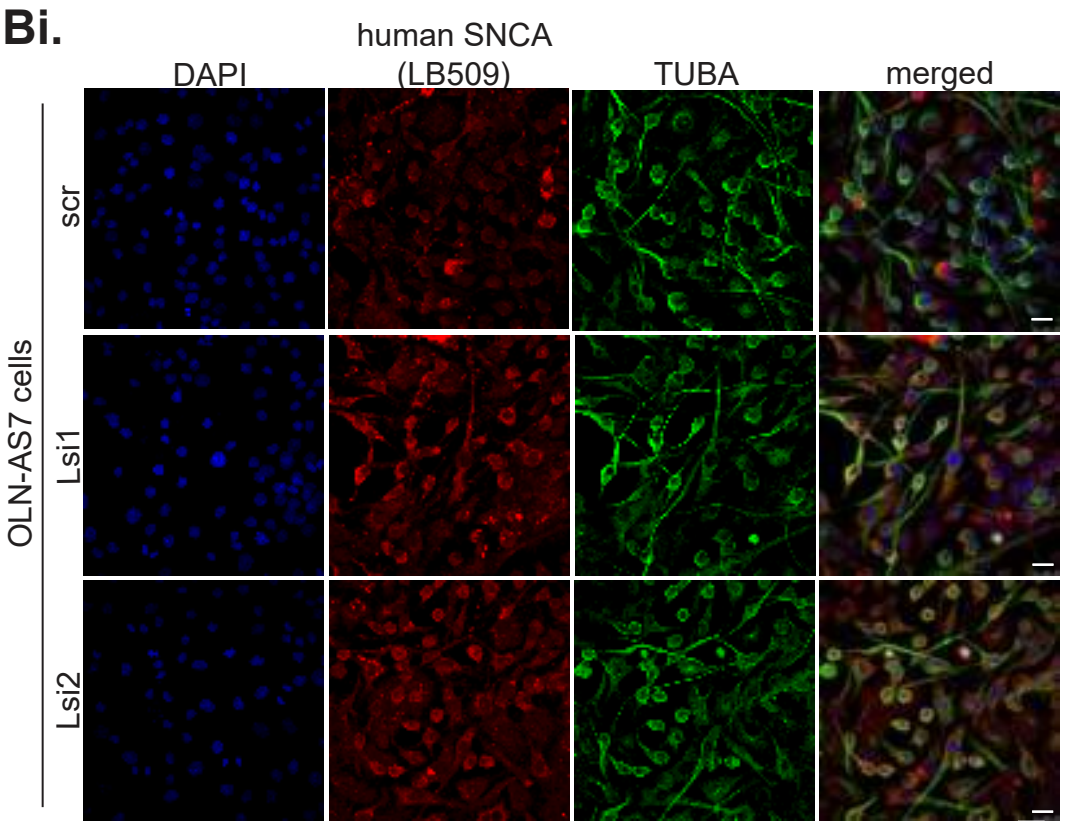

Bii.

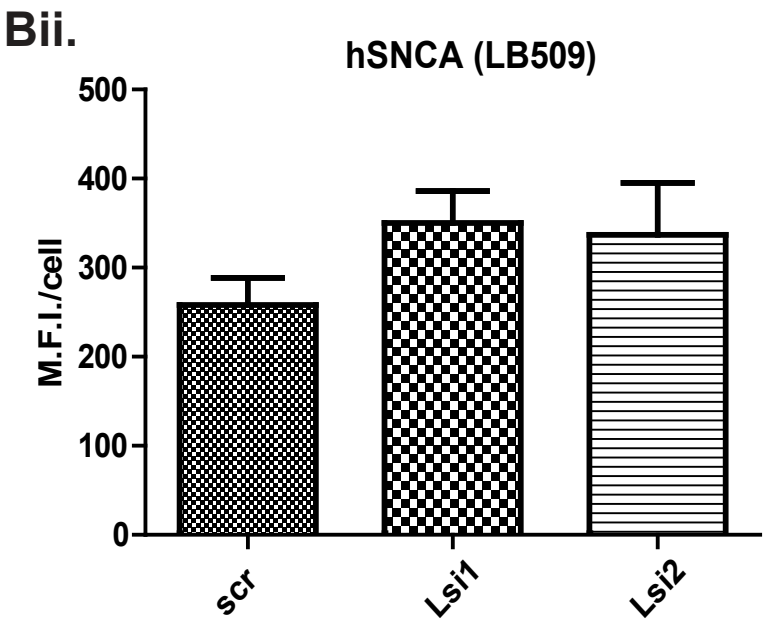

Ei.

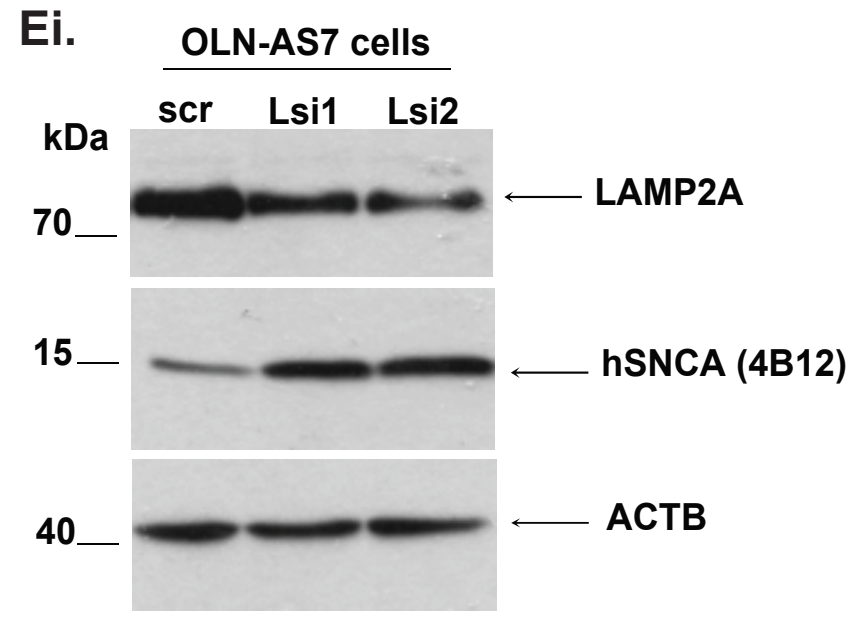

Eii.

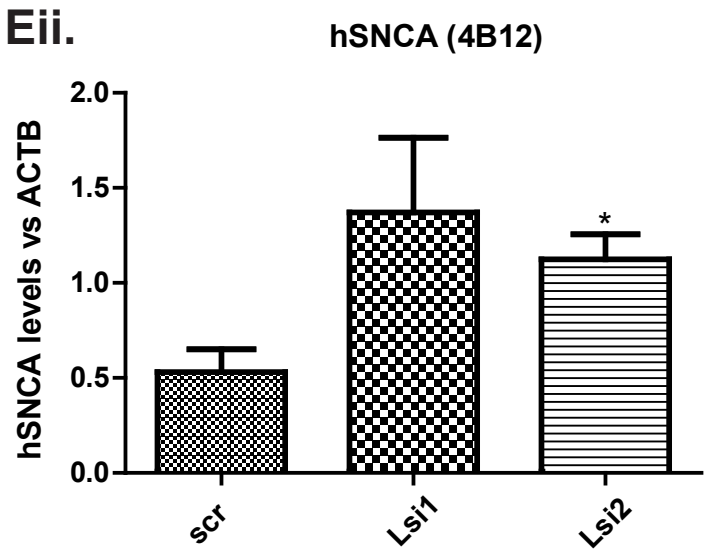

Fi.

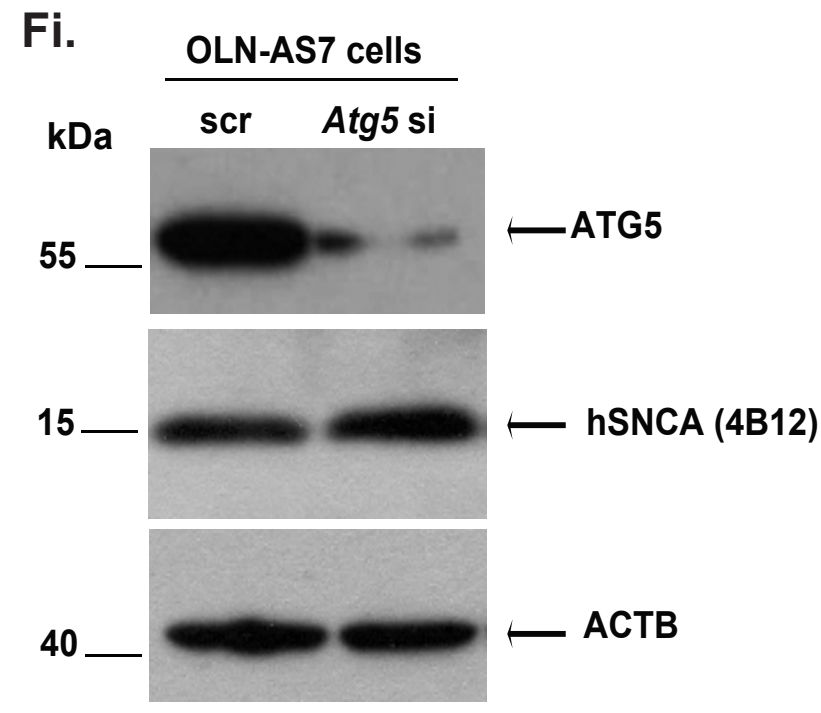

Ci.

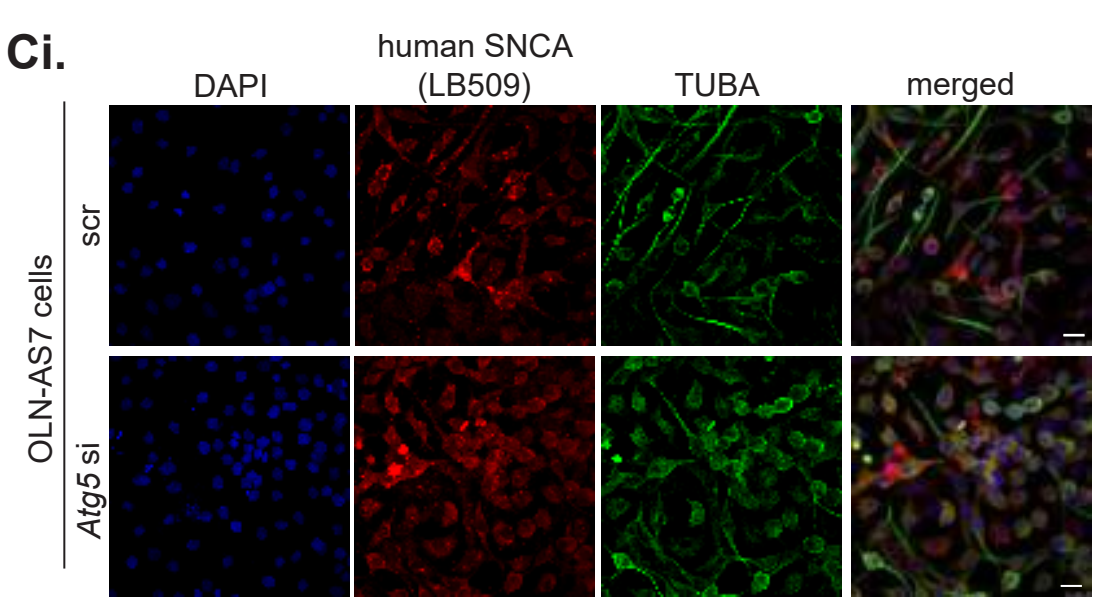

Cii.

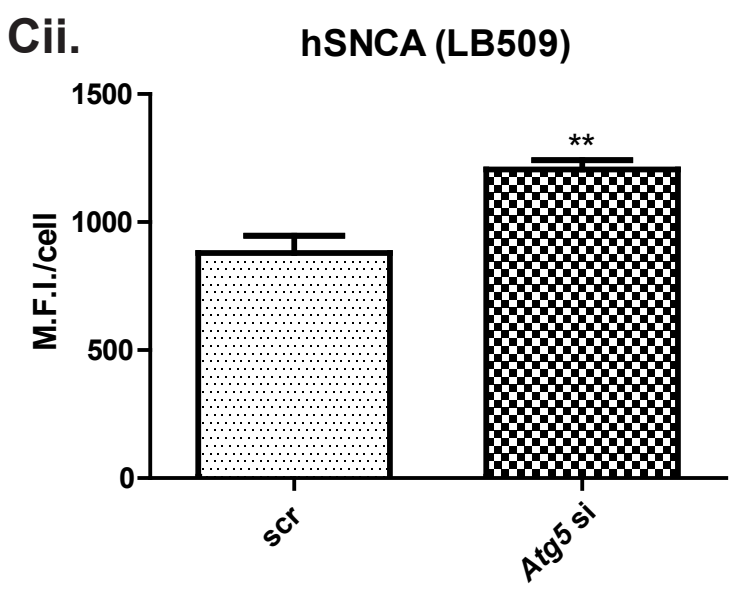

Fii.

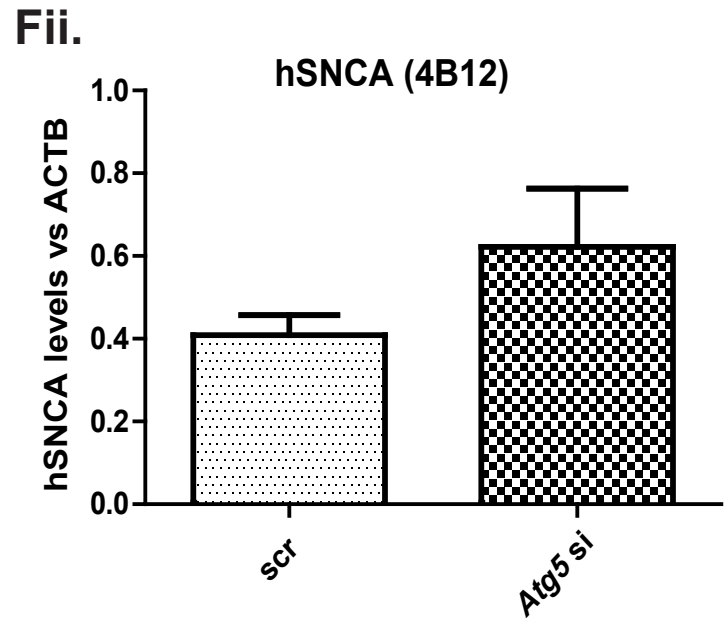

Ai.

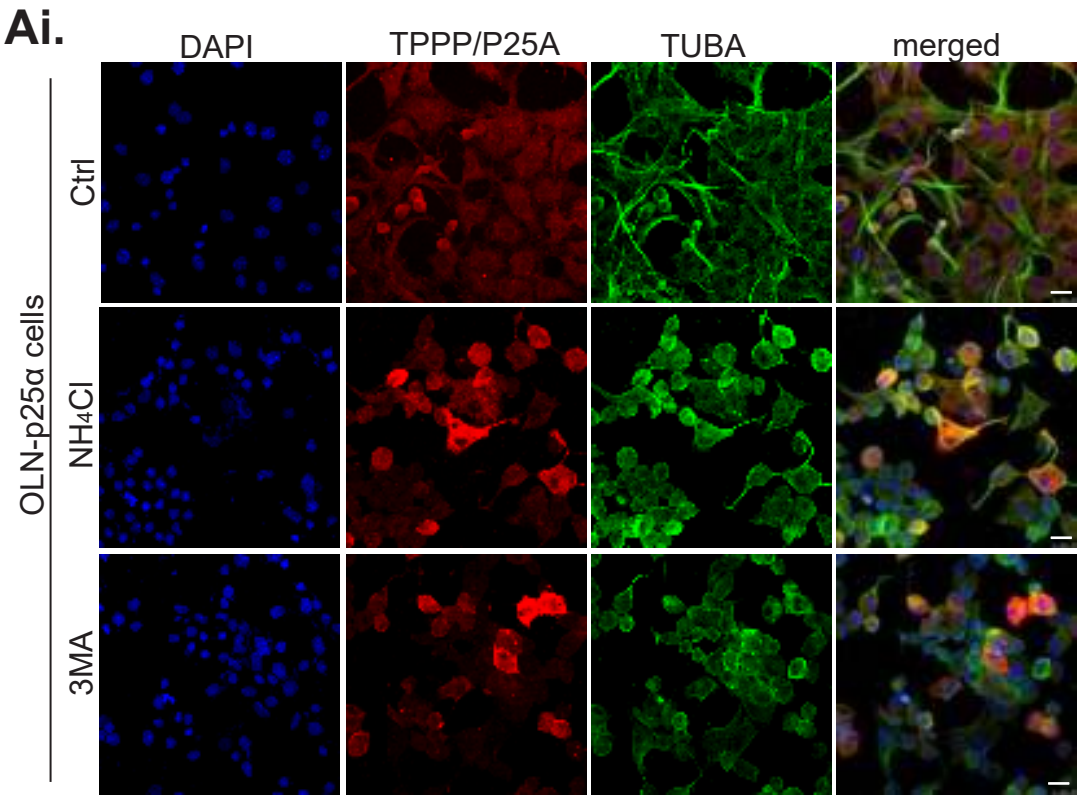

Aii.

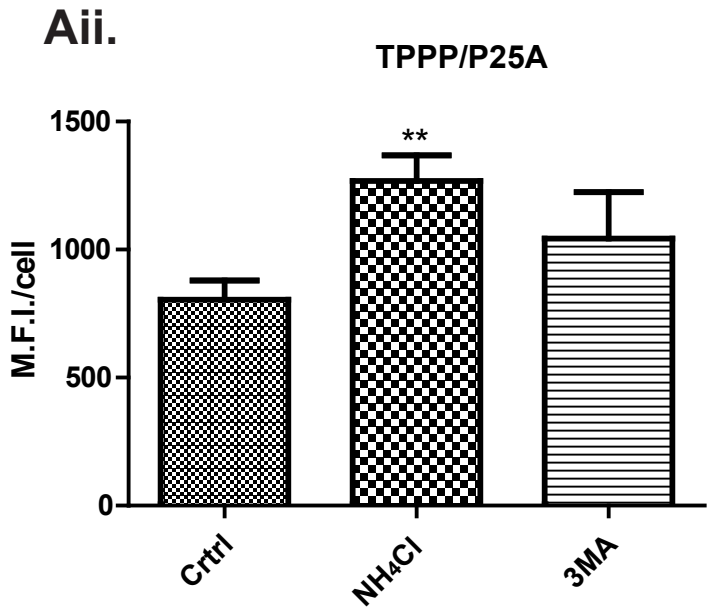

Di.

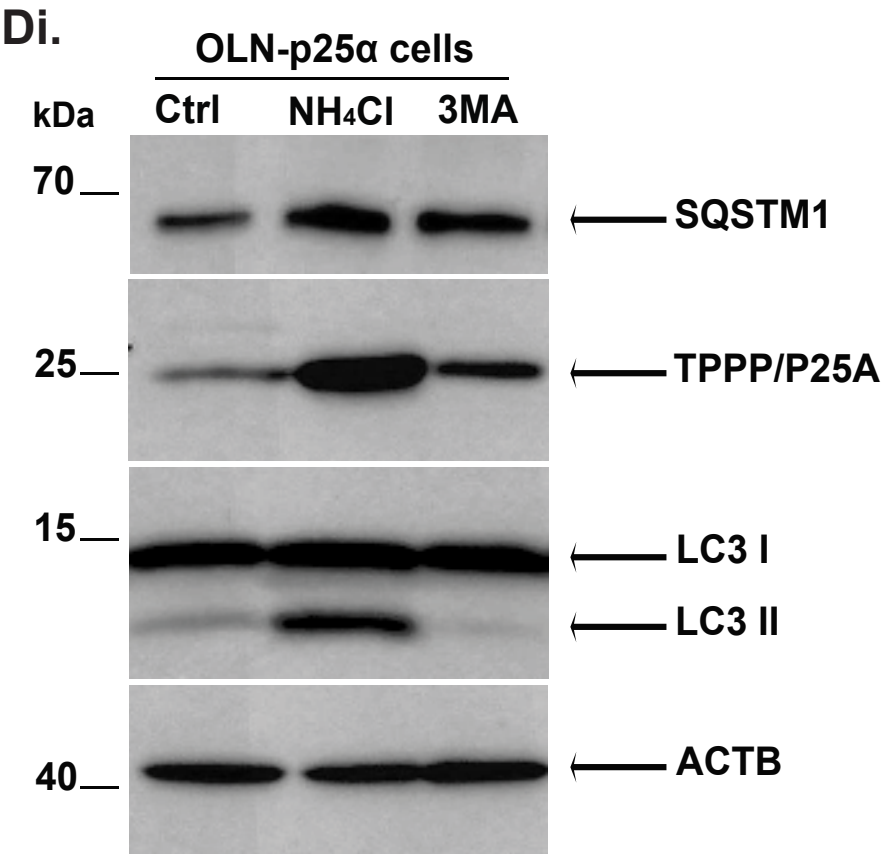

Dii.

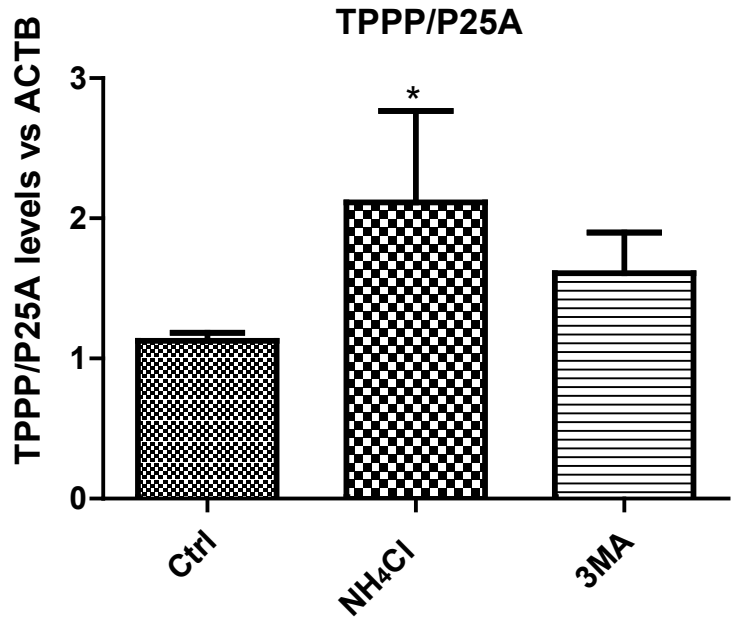

Bi.

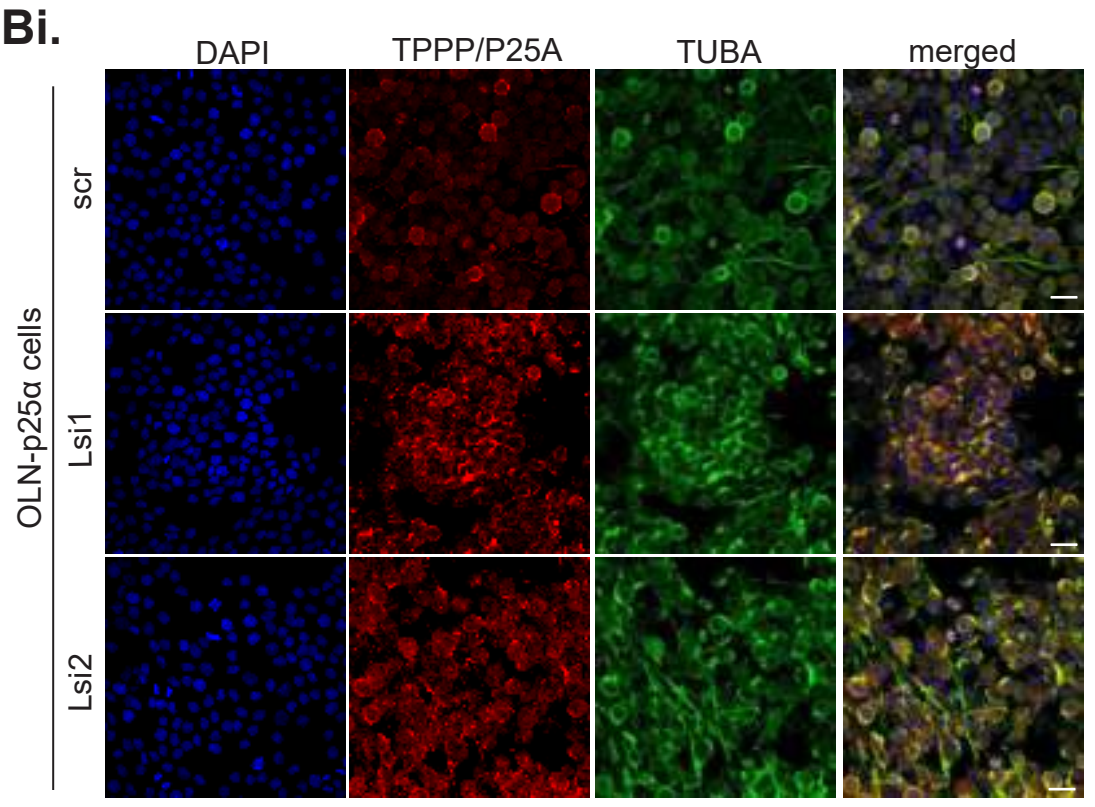

Bii.

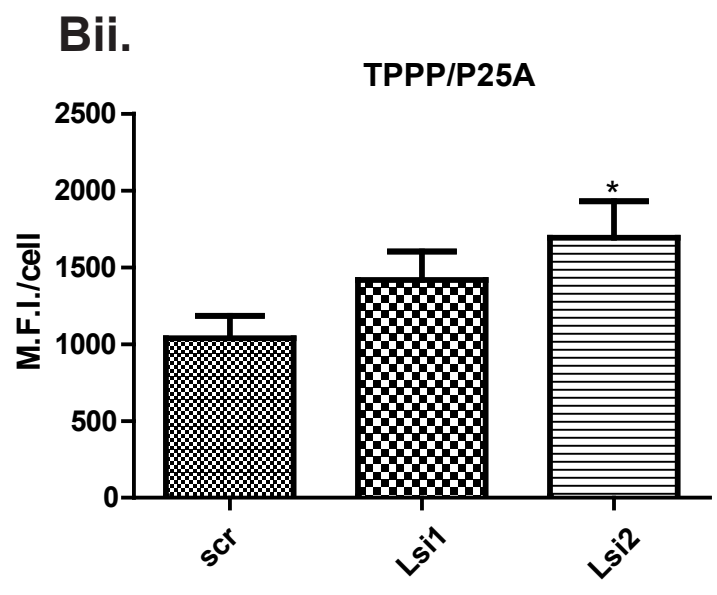

Ei.

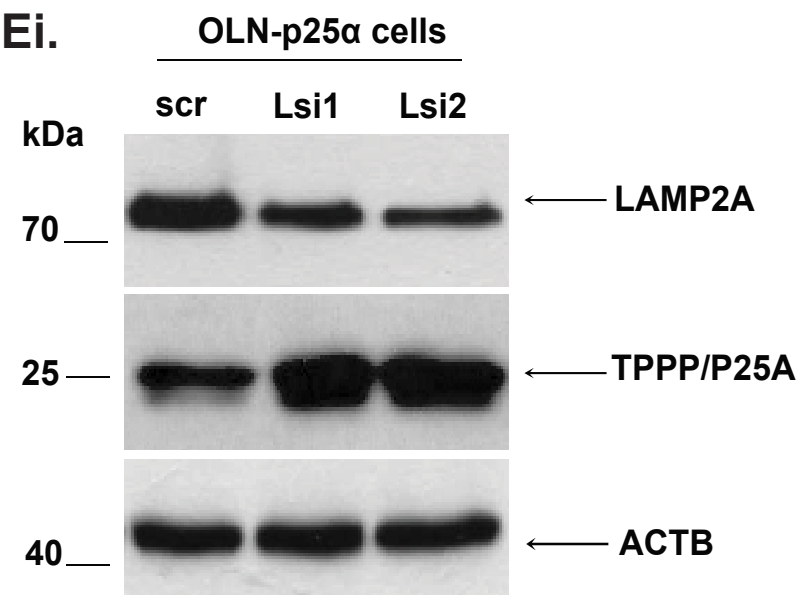

Eii.

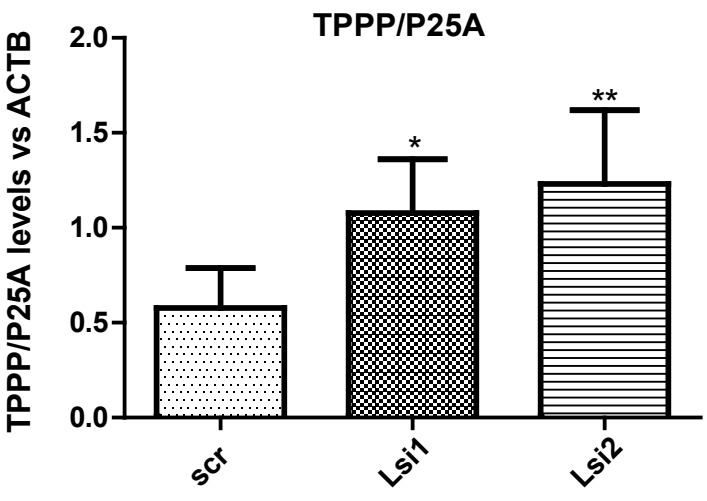

Ci.

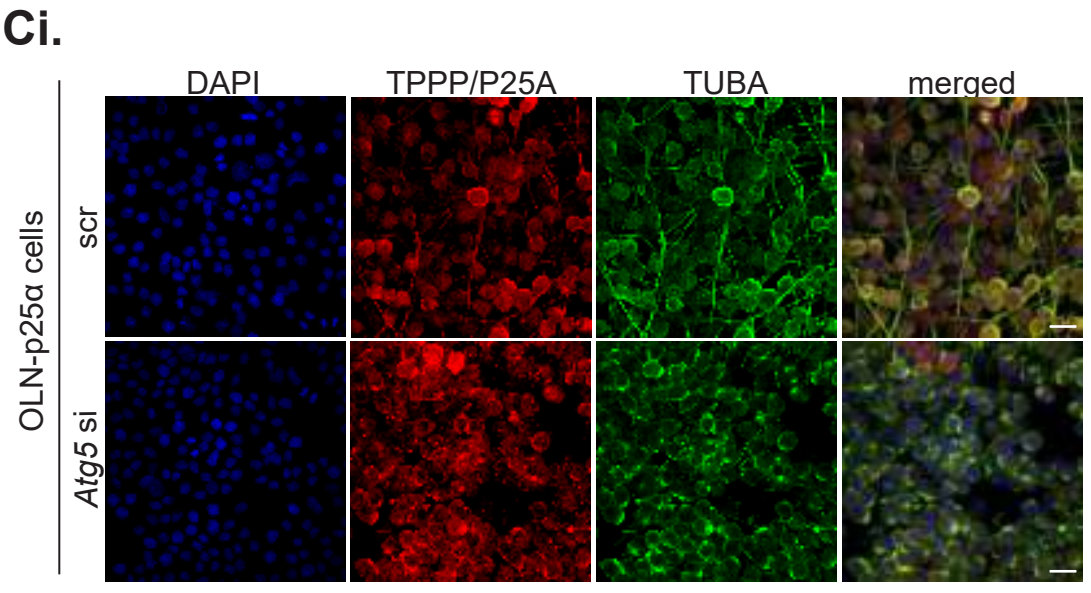

Cii.

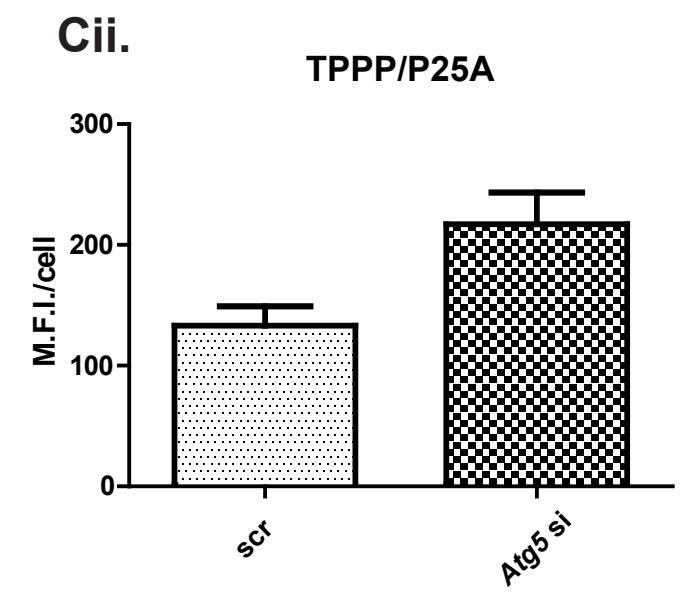

Fi.

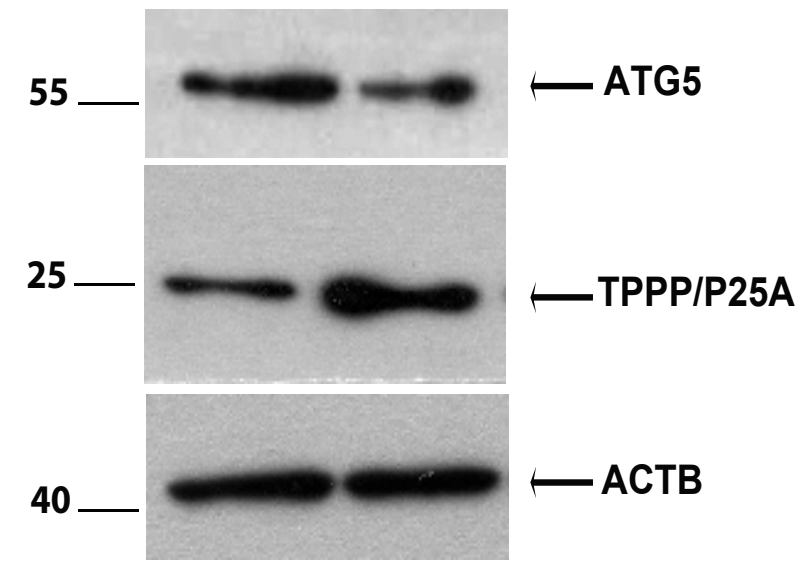

Fii.

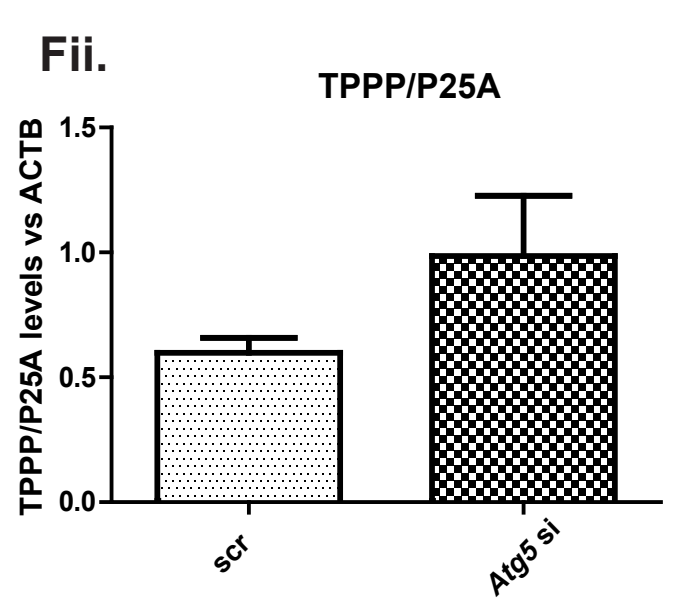

Ai.

Aii.

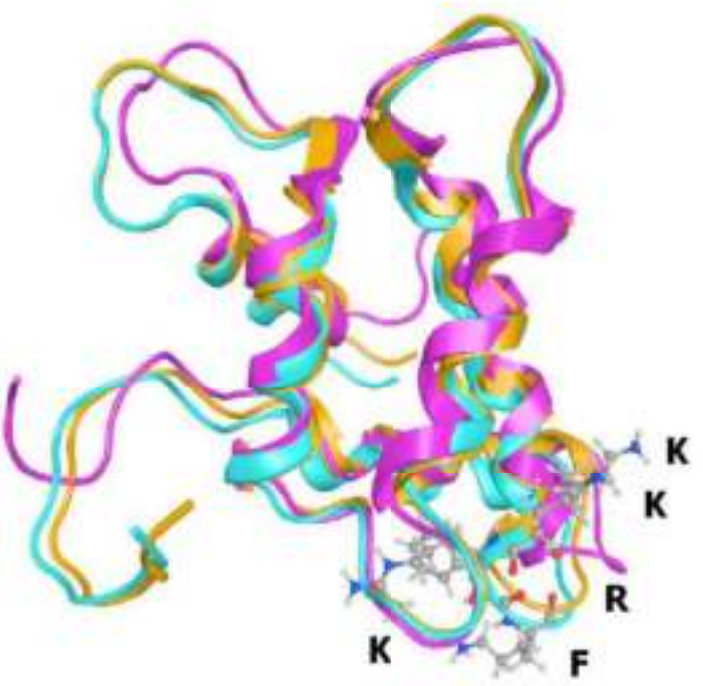

Aiii.

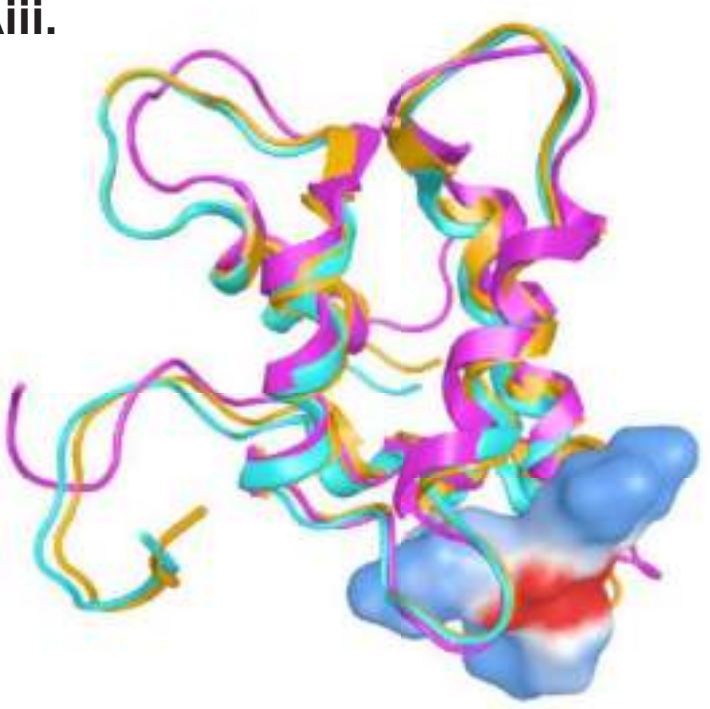

B.

-	-	-	+ (1.2µg)	+ (0.6µg)	recomb. SNCA
-	+	+	+	+	lysosomes
-	-	+	-	-	PIs
+	+	+	+	+	recomb. TPPP/P25A

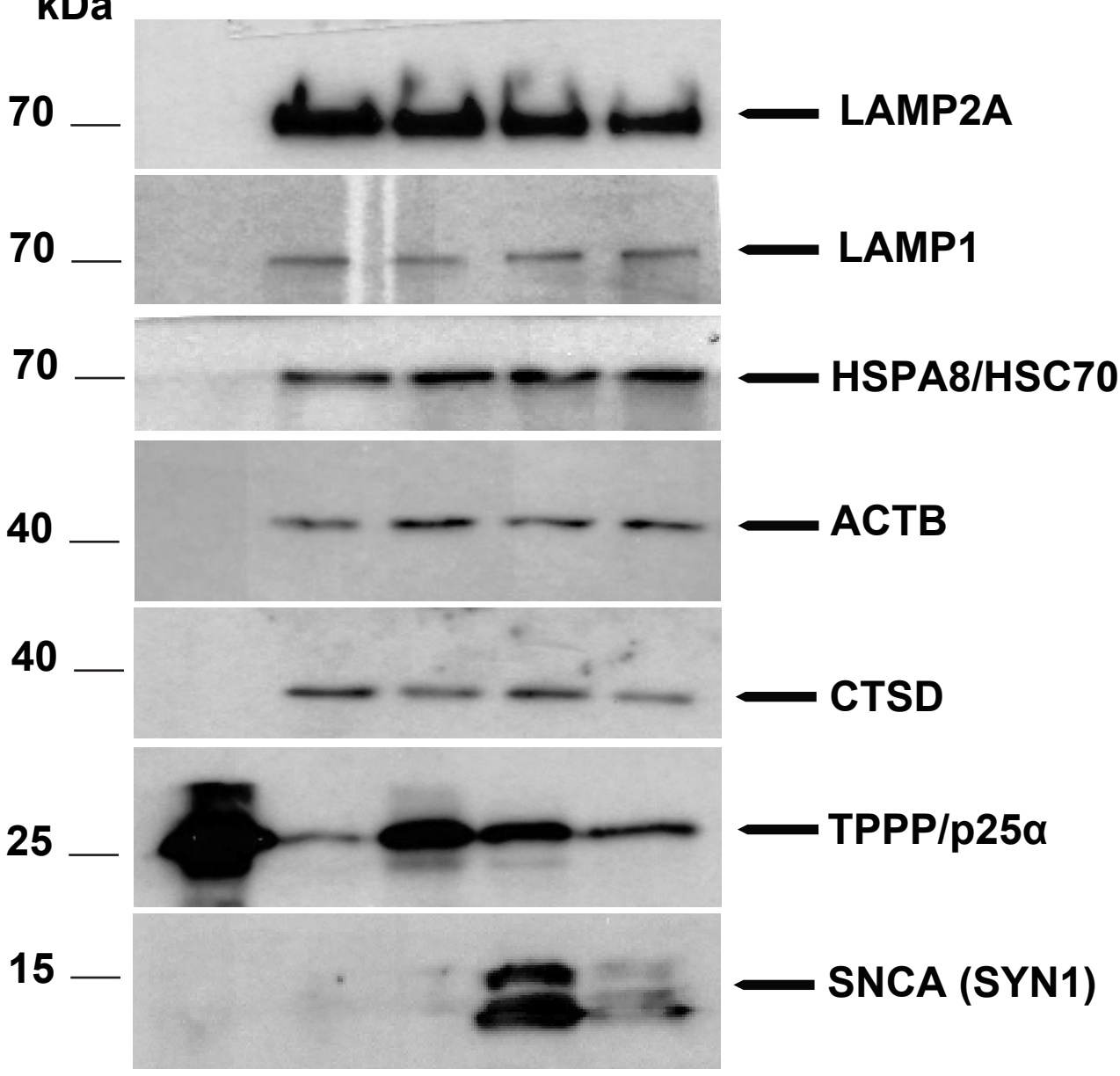

C.

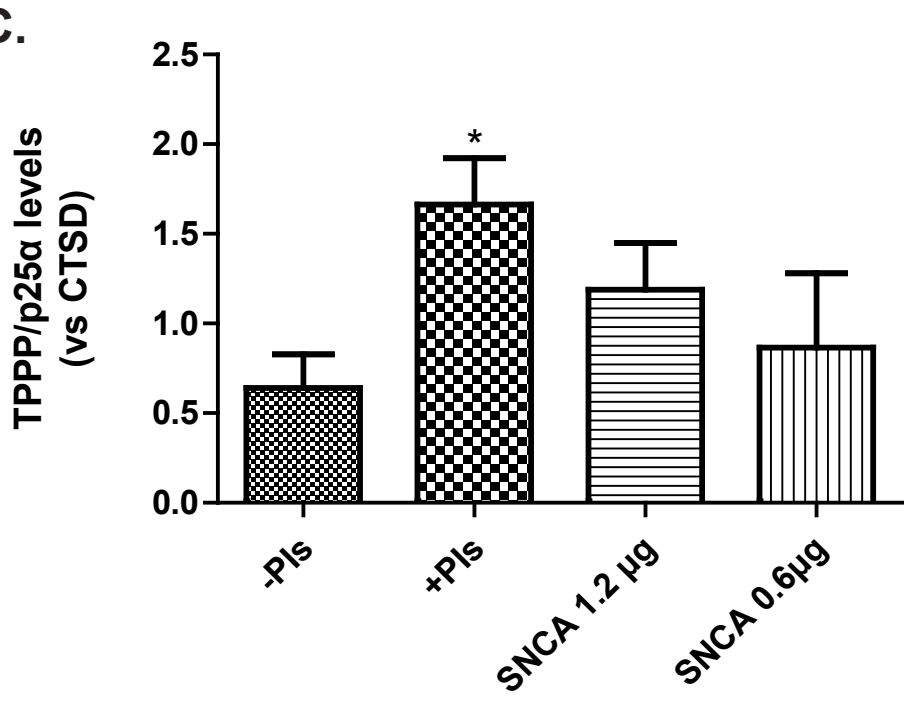

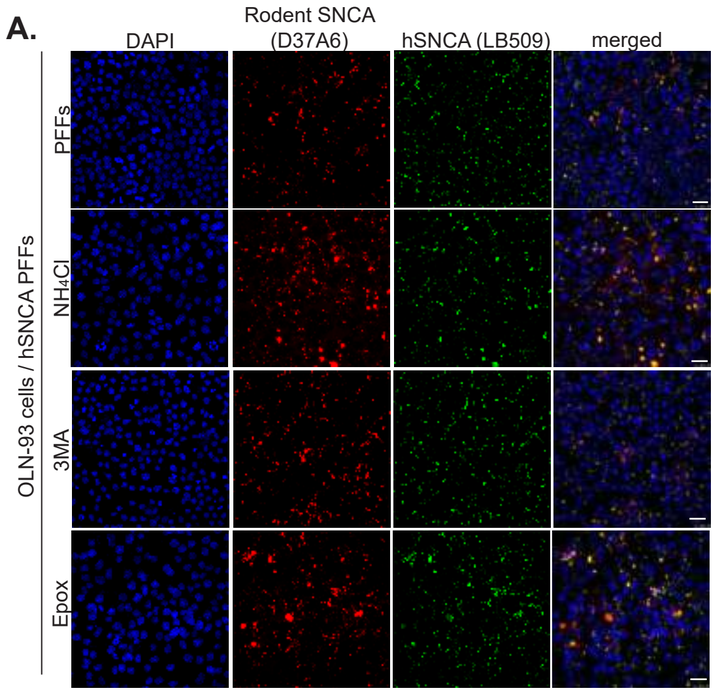
A.
DAPI
Rodent SNCA (D37A6)
hSNCA (LB509)
merged
OLN-93 cells / hSNCA PFFs
PFFs
NH4Cl
3MA
Epox

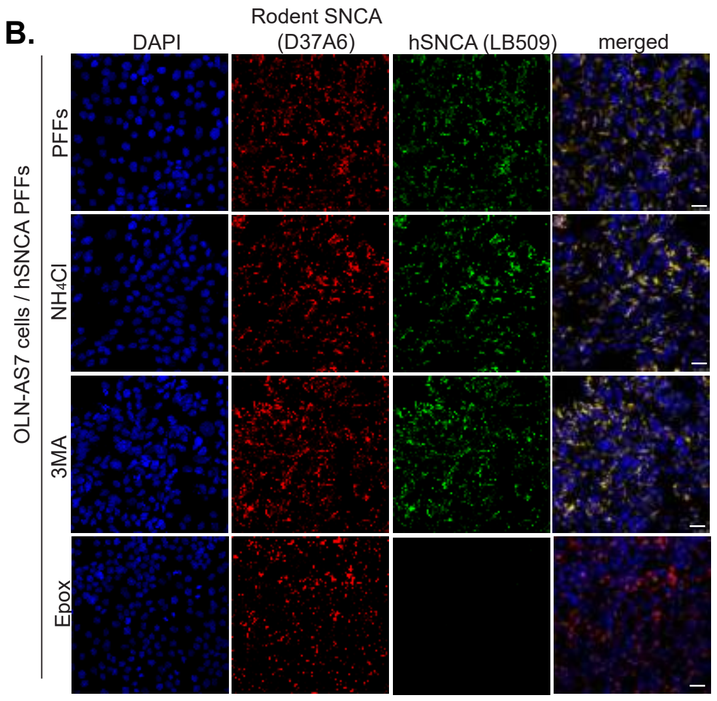
B.
DAPI
Rodent SNCA (D37A6)
hSNCA (LB509)
merged
OLN-AS7 cells / hSNCA PFFs
PFFs
NH4Cl
3MA
Epox

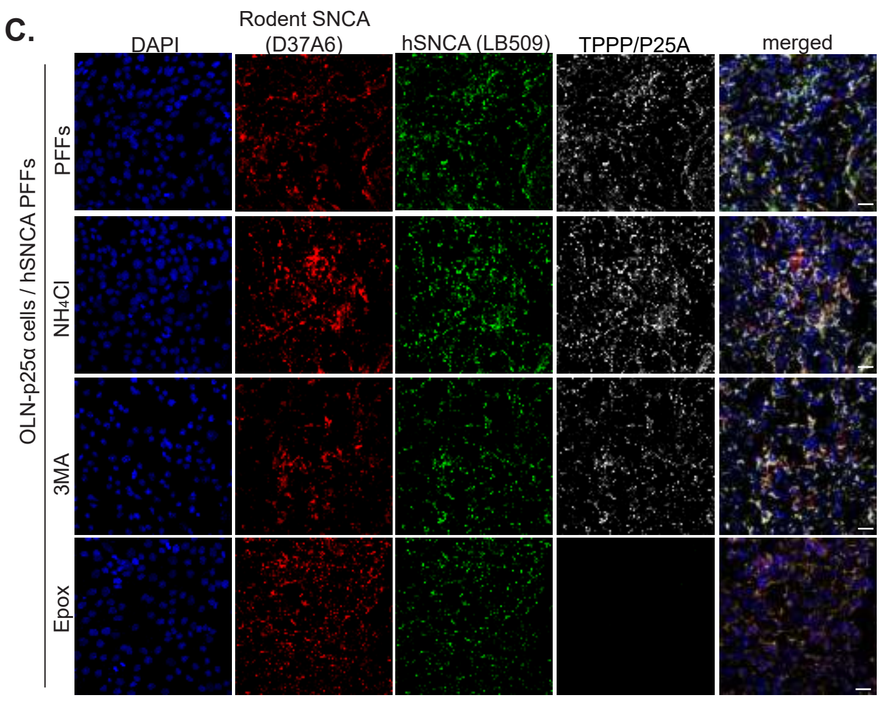
C.
DAPI
Rodent SNCA (D37A6)
hSNCA (LB509)
TPPP/P25A
merged
OLN-p25α cells / hSNCA PFFs
PFFs
NH4Cl
3MA
Epox

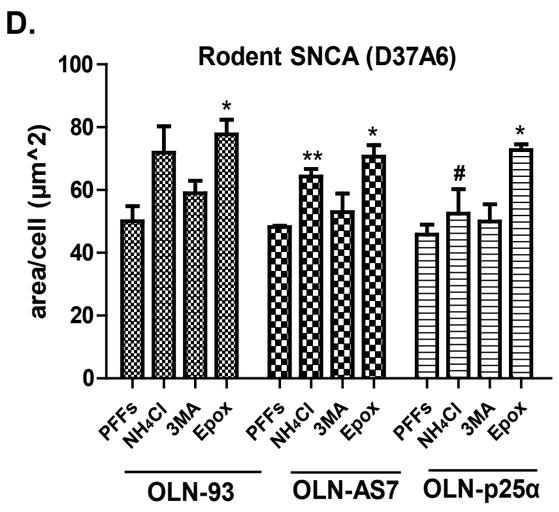
D.
Rodent SNCA (D37A6)
area/cell (µm^2)
PFFs
NH4Cl
3MA
Epox
OLN-93
OLN-AS7
OLN-p25α

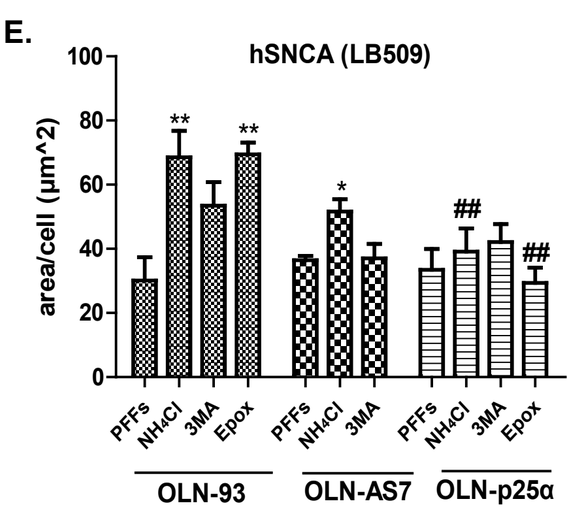
E.
hSNCA (LB509)
area/cell (µm^2)
PFFs
NH4Cl
3MA
Epox
OLN-93
OLN-AS7
OLN-p25α

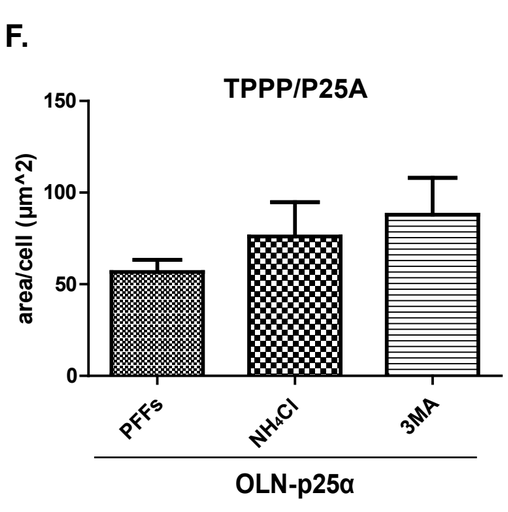
F.
TPPP/P25A
area/cell (µm^2)
PFFs
NH4Cl
3MA
OLN-p25α

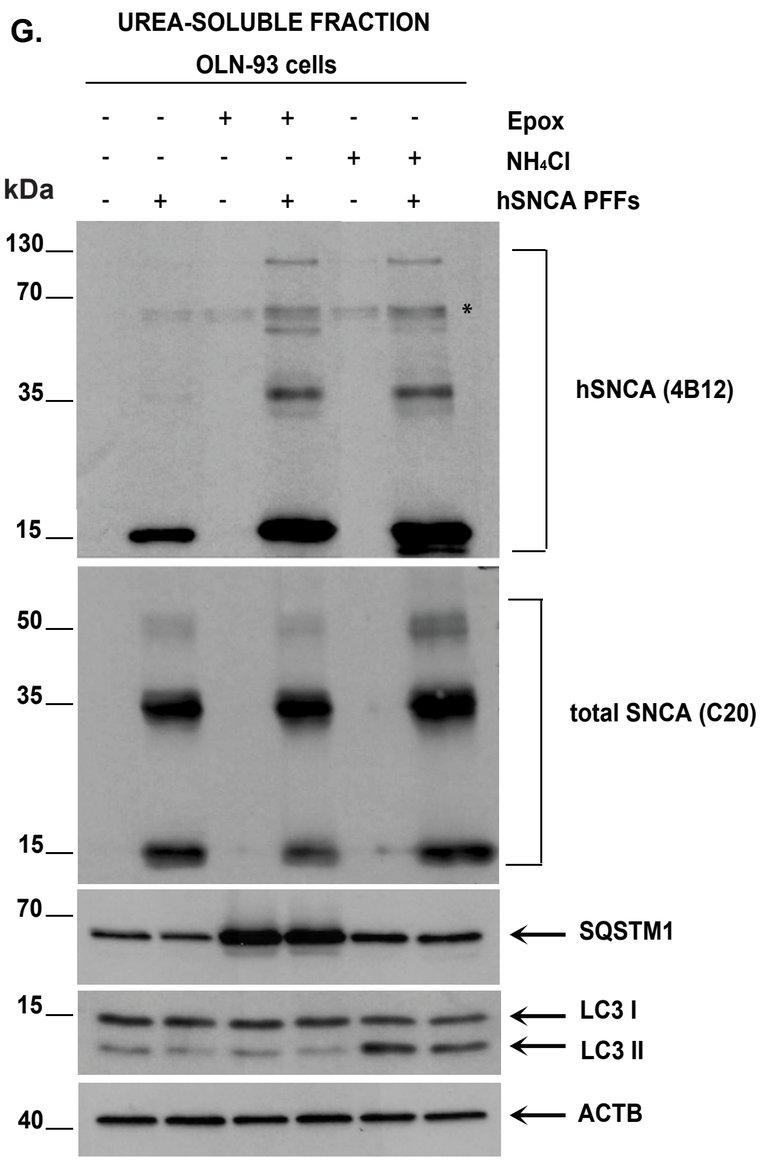
G.
UREA-SOLUBLE FRACTION
OLN-93 cells
Epox
NH4Cl
hSNCA PFFs
kDa
hSNCA (4B12)
total SNCA (C20)
SQSTM1
LC3 I
LC3 II
ACTB

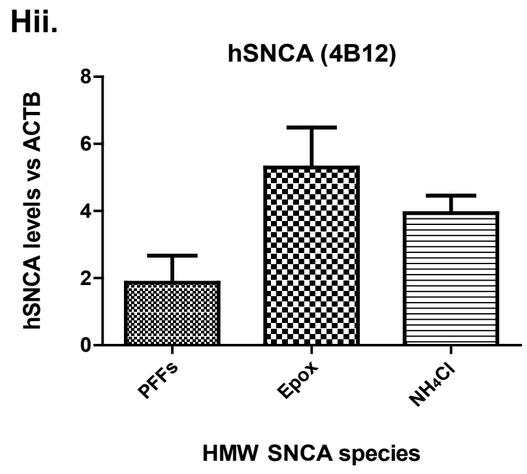
Hii.
hSNCA (4B12)
hSNCA levels vs ACTB
PFFs
Epox
NH4Cl
HMW SNCA species

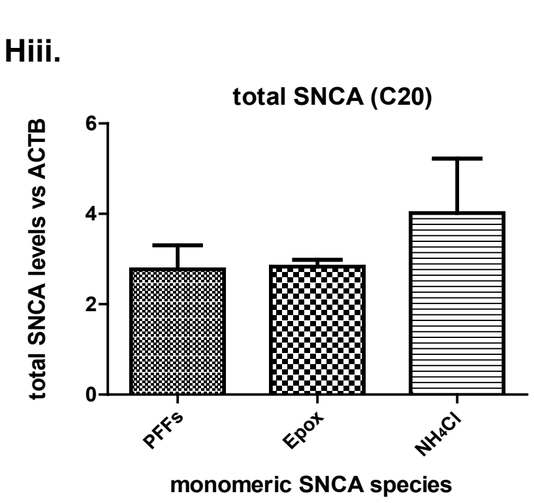
Hiii.
total SNCA (C20)
total SNCA levels vs ACTB
PFFs
Epox
NH4Cl
monomeric SNCA species

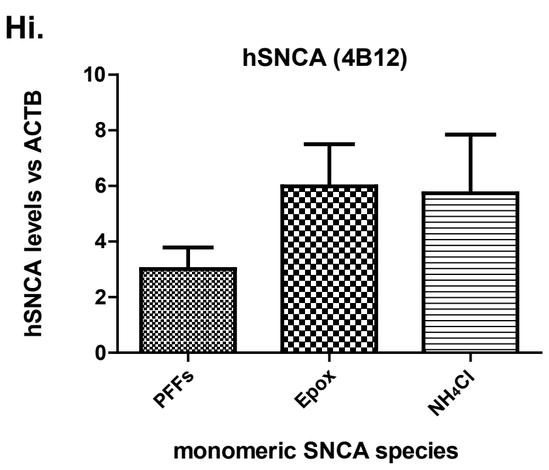
Hi.
hSNCA (4B12)
hSNCA levels vs ACTB
PFFs
Epox
NH4Cl
monomeric SNCA species

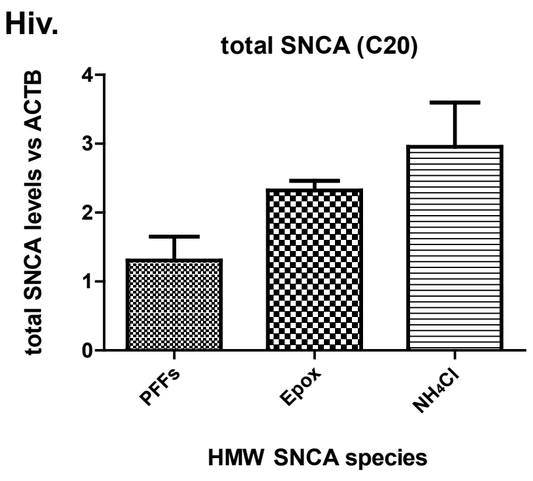
Hiv.
total SNCA (C20)
total SNCA levels vs ACTB
PFFs
Epox
NH4Cl
HMW SNCA species

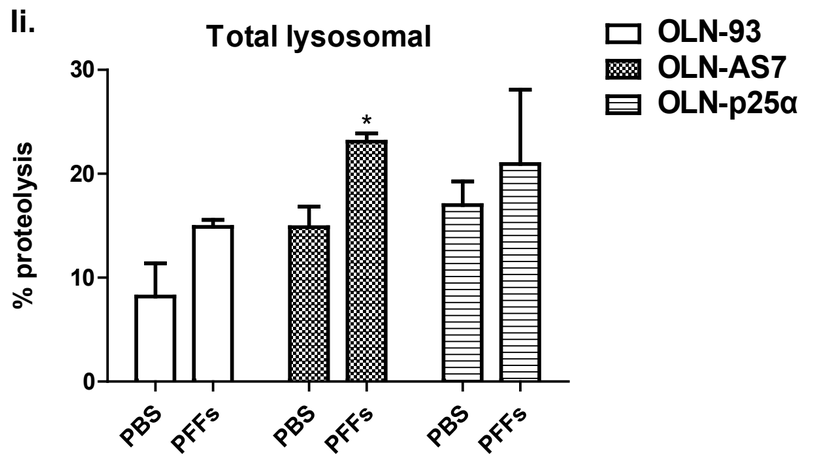
Ii.
Total lysosomal
% proteolysis
PBS
PFFs
OLN-93
OLN-AS7
OLN-p25α

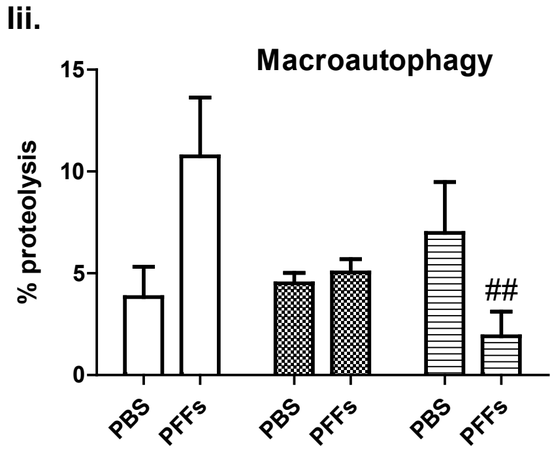
Iii.
Macroautophagy
% proteolysis
PBS
PFFs

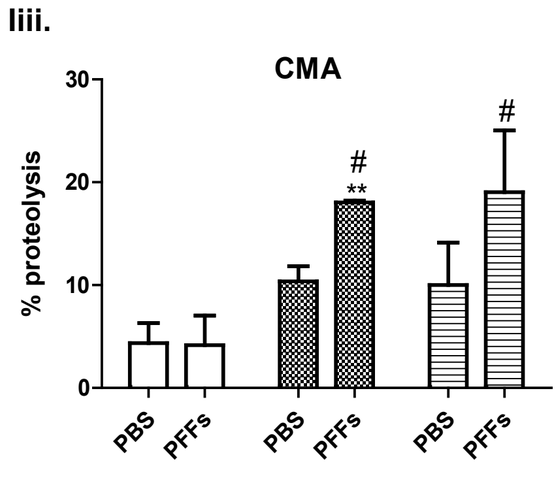
Iiii.
CMA
% proteolysis
PBS
PFFs

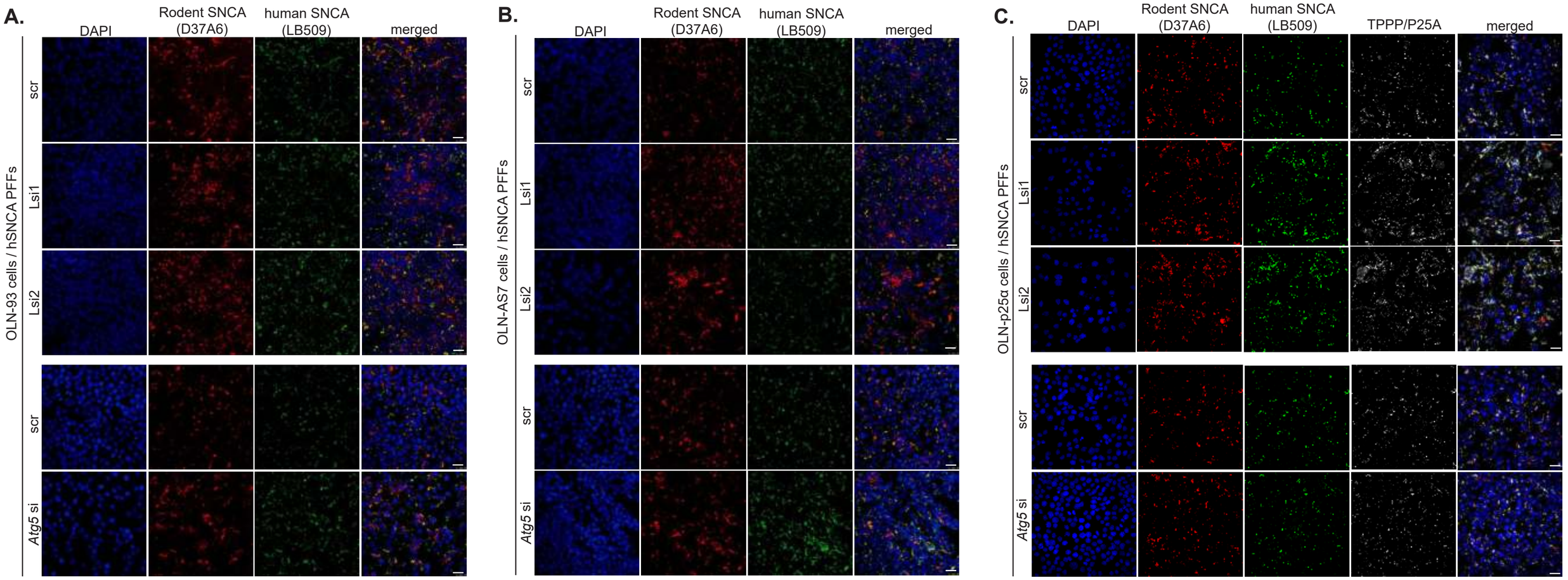
A.
DAPI
Rodent SNCA (D37A6)
human SNCA (LB509)
merged
OLN-93 cells / hSNCA PFFs
scr
Lsi1
Lsi2
scr
Atg5 si
B.
DAPI
Rodent SNCA (D37A6)
human SNCA (LB509)
merged
OLN-AS7 cells / hSNCA PFFs
scr
Lsi1
Lsi2
scr
Atg5 si
C.
DAPI
Rodent SNCA (D37A6)
human SNCA (LB509)
TPPP/P25A
merged
OLN-p25α cells / hSNCA PFFs
scr
Lsi1
Lsi2
scr
Atg5 si

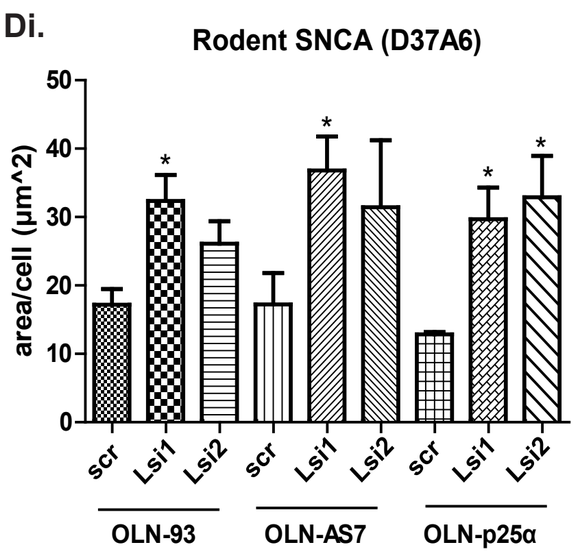
Di.
Rodent SNCA (D37A6)
area/cell (µm^2)
scr
Lsi1
Lsi2
OLN-93
OLN-AS7
OLN-p25α

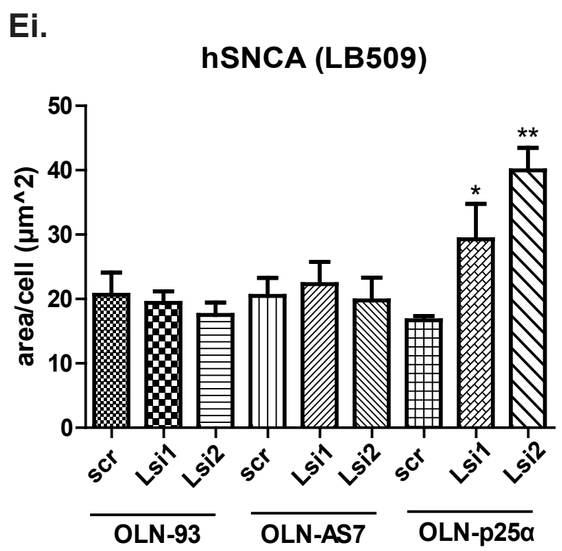
Ei.
hSNCA (LB509)
area/cell (µm^2)
scr
Lsi1
Lsi2
OLN-93
OLN-AS7
OLN-p25α

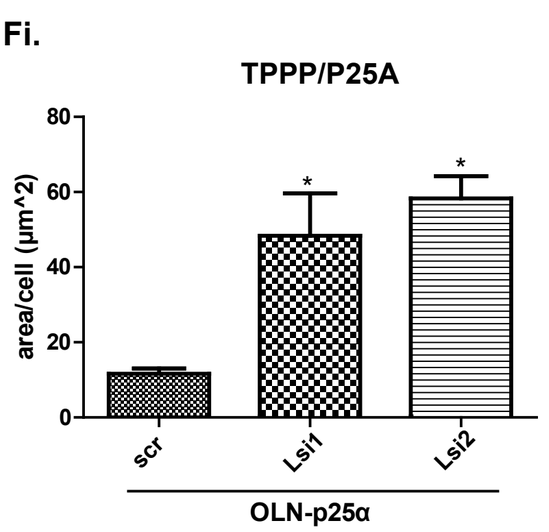
Fi.
TPPP/P25A
area/cell (µm^2)
scr
Lsi1
Lsi2
OLN-p25α

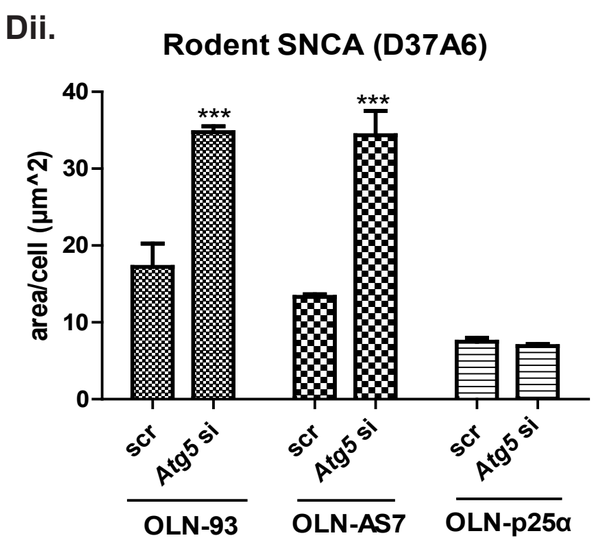
Dii.
Rodent SNCA (D37A6)
area/cell (µm^2)
scr
Atg5 si
OLN-93
OLN-AS7
OLN-p25α

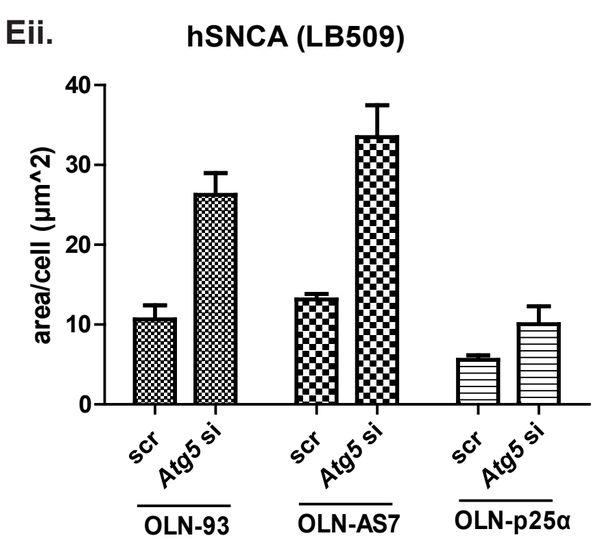
Eii.
hSNCA (LB509)
area/cell (µm^2)
scr
Atg5 si
OLN-93
OLN-AS7
OLN-p25α

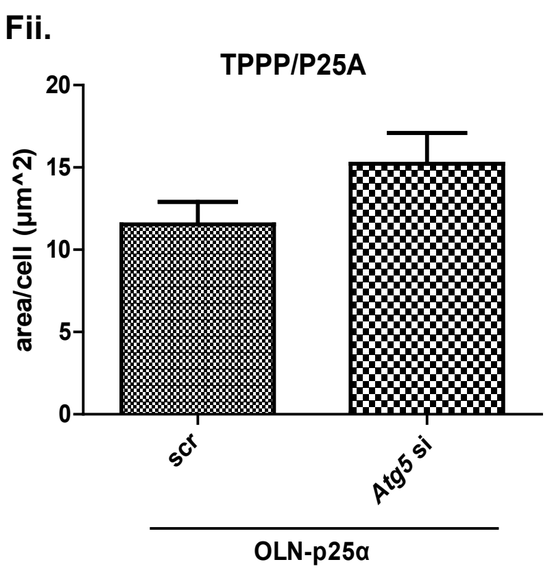
Fii.
TPPP/P25A
area/cell (µm^2)
scr
Atg5 si
OLN-p25α

A.

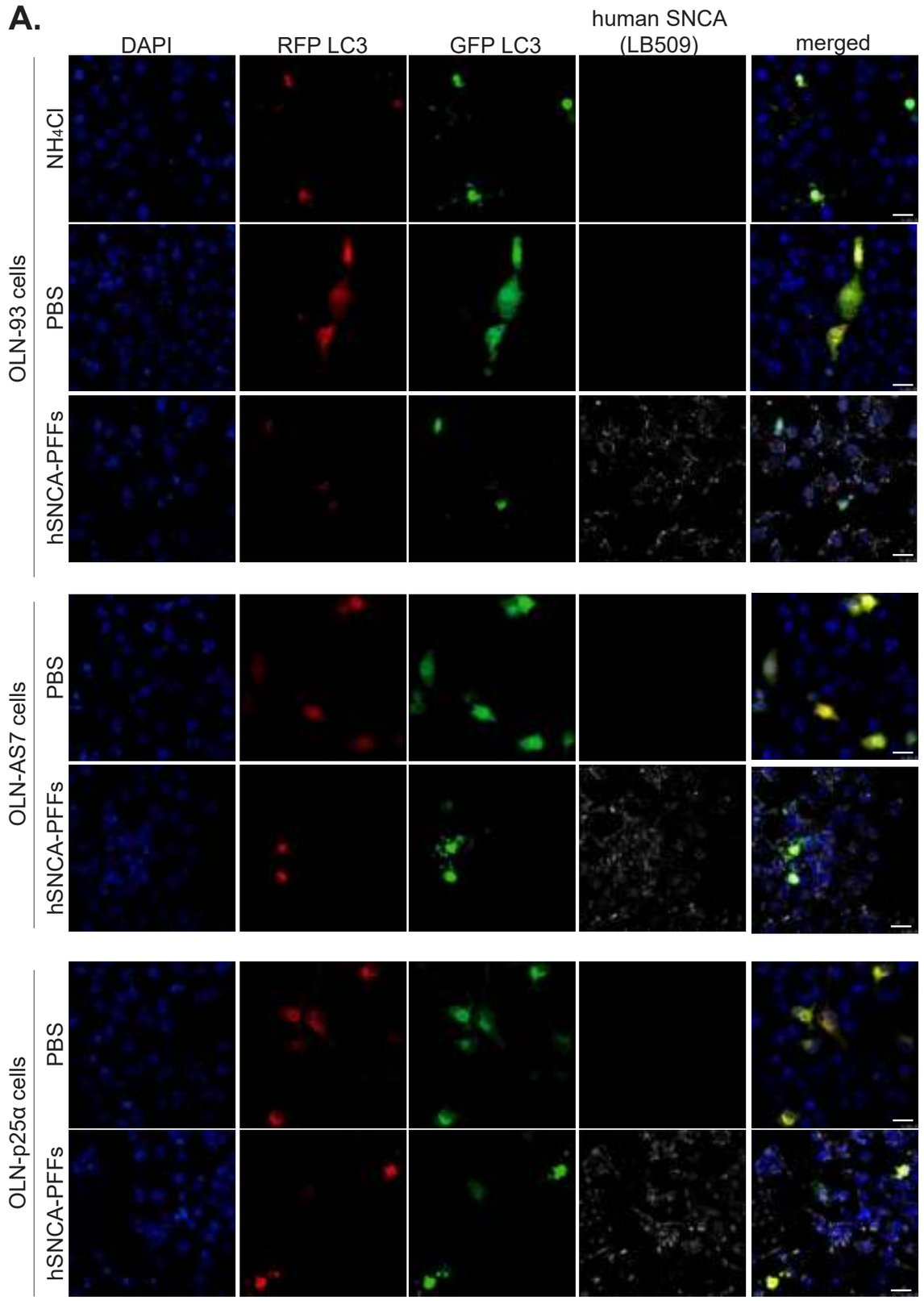
DAPI
RFP LC3
GFP LC3
human SNCA (LB509)
merged
OLN-93 cells
NH4Cl
PBS
hSNCA-PFFs
OLN-AS7 cells
PBS
hSNCA-PFFs
OLN-p25α cells
PBS
hSNCA-PFFs

B.

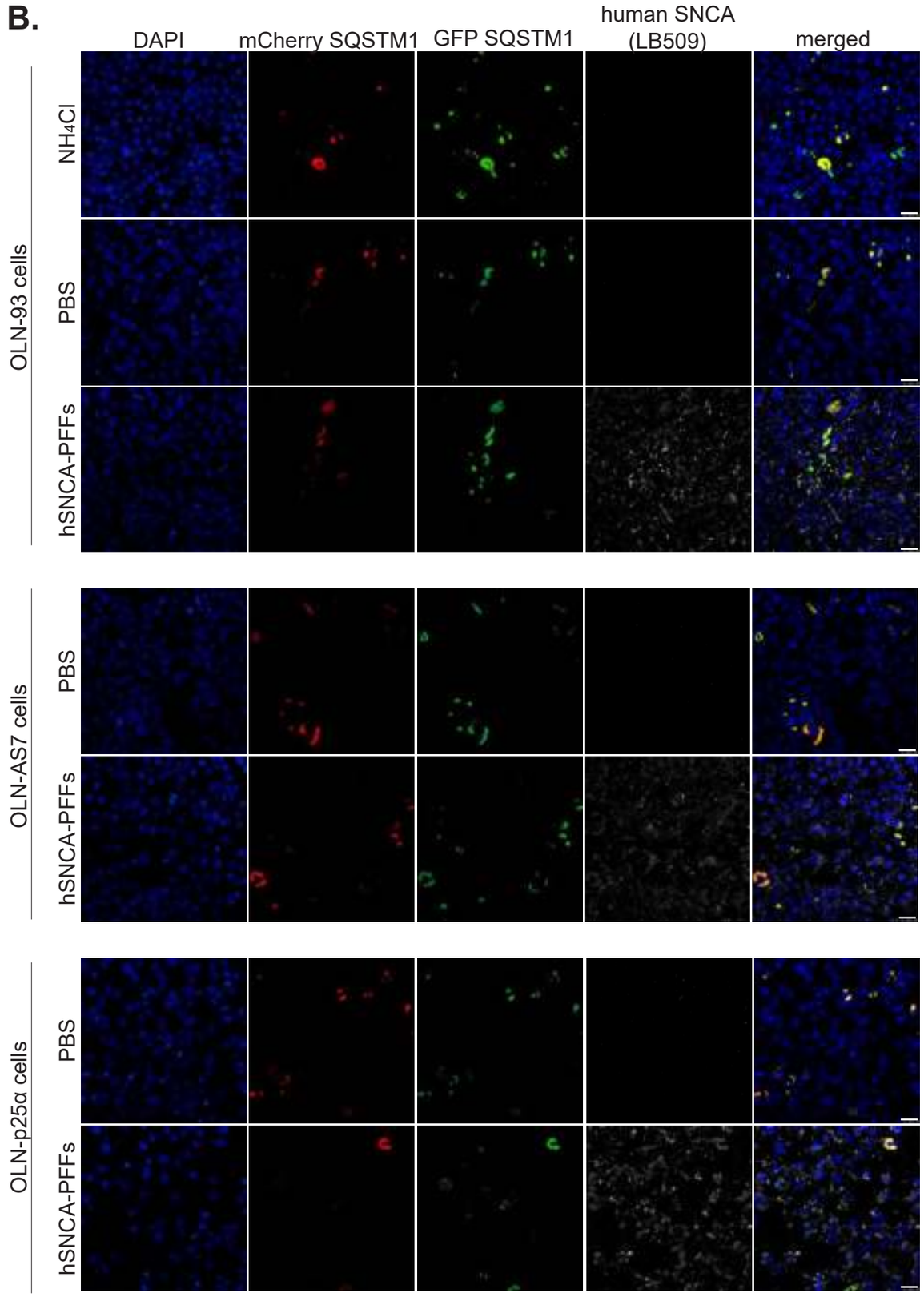
DAPI
mCherry SQSTM1
GFP SQSTM1
human SNCA (LB509)
merged
OLN-93 cells
NH4Cl
PBS
hSNCA-PFFs
OLN-AS7 cells
PBS
hSNCA-PFFs
OLN-p25α cells
PBS
hSNCA-PFFs

C.

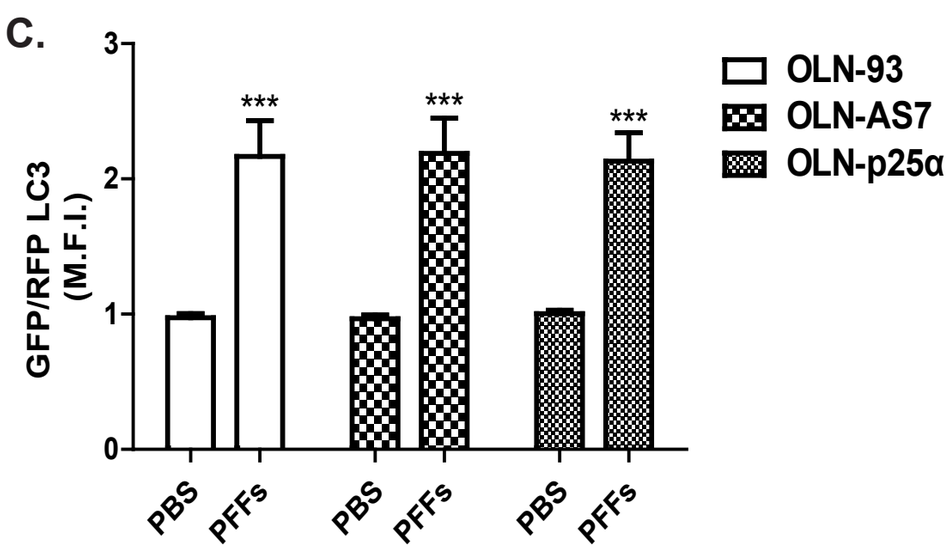
GFP/RFP LC3 (M.F.I.)
3
2
1
0
***
***
***
PBS
PFFs
PBS
PFFs
PBS
PFFs
OLN-93
OLN-AS7
OLN-p25α

D.

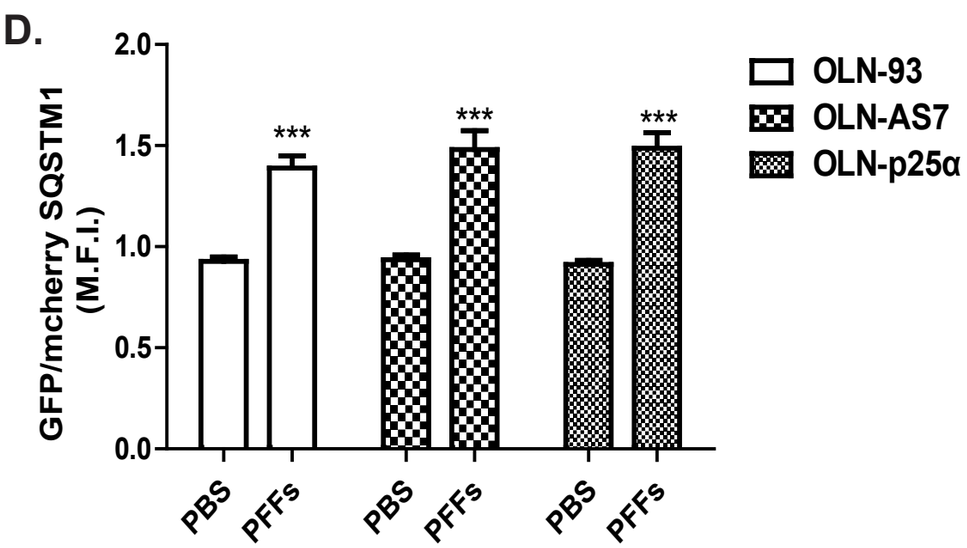
GFP/mcherry SQSTM1 (M.F.I.)
2.0
1.5
1.0
0.5
0.0
***
***
***
PBS
PFFs
PBS
PFFs
PBS
PFFs
OLN-93
OLN-AS7
OLN-p25α

A.

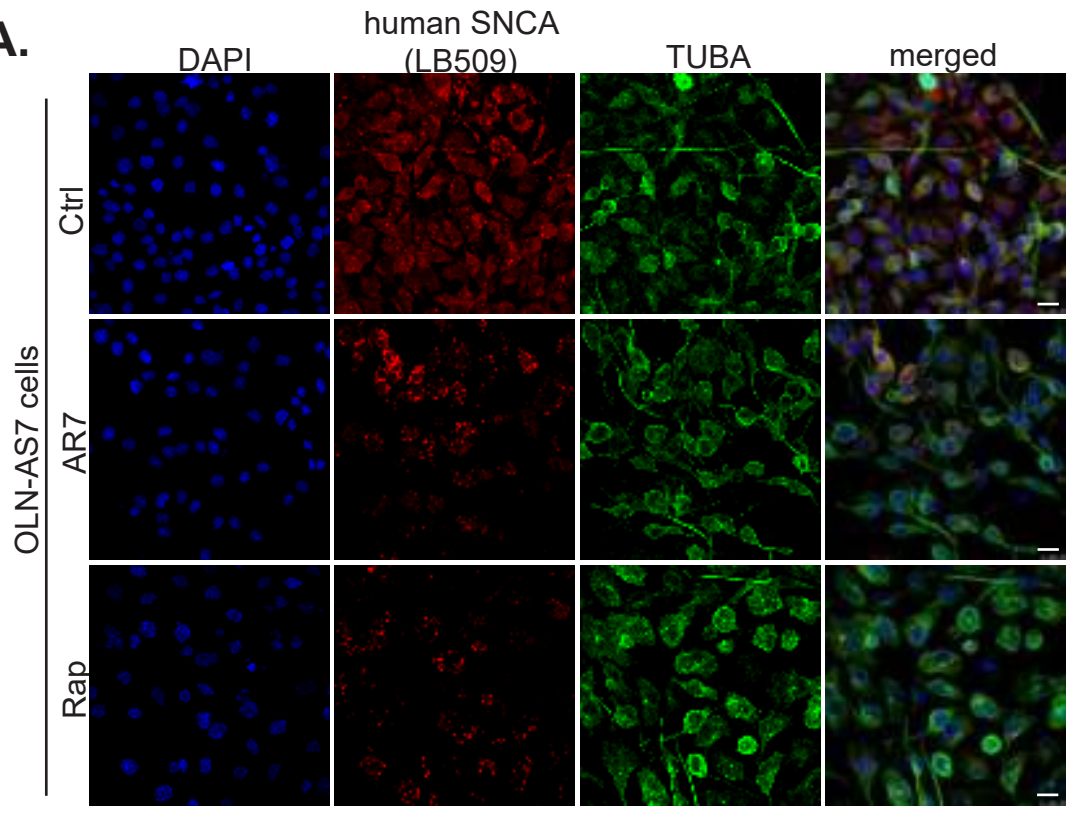

C.

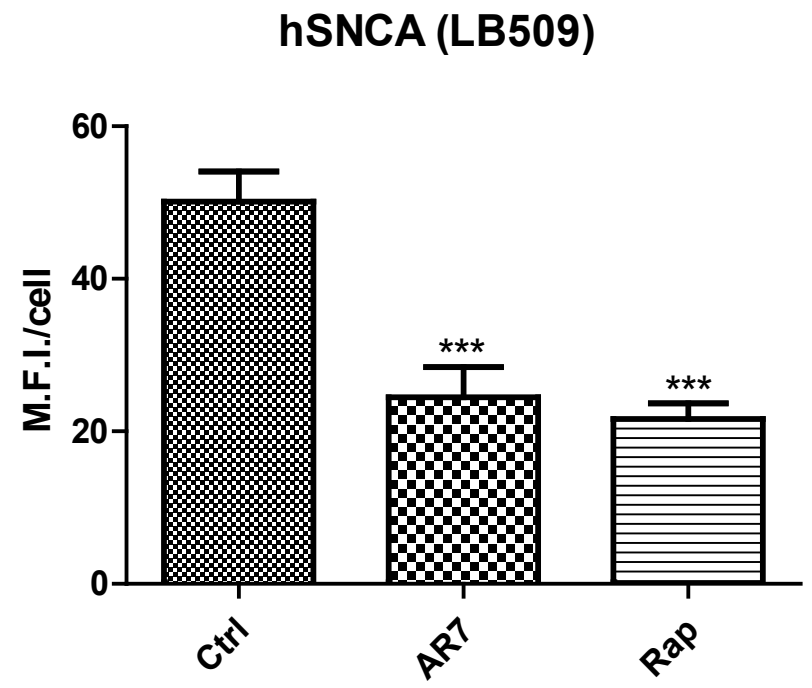

B.

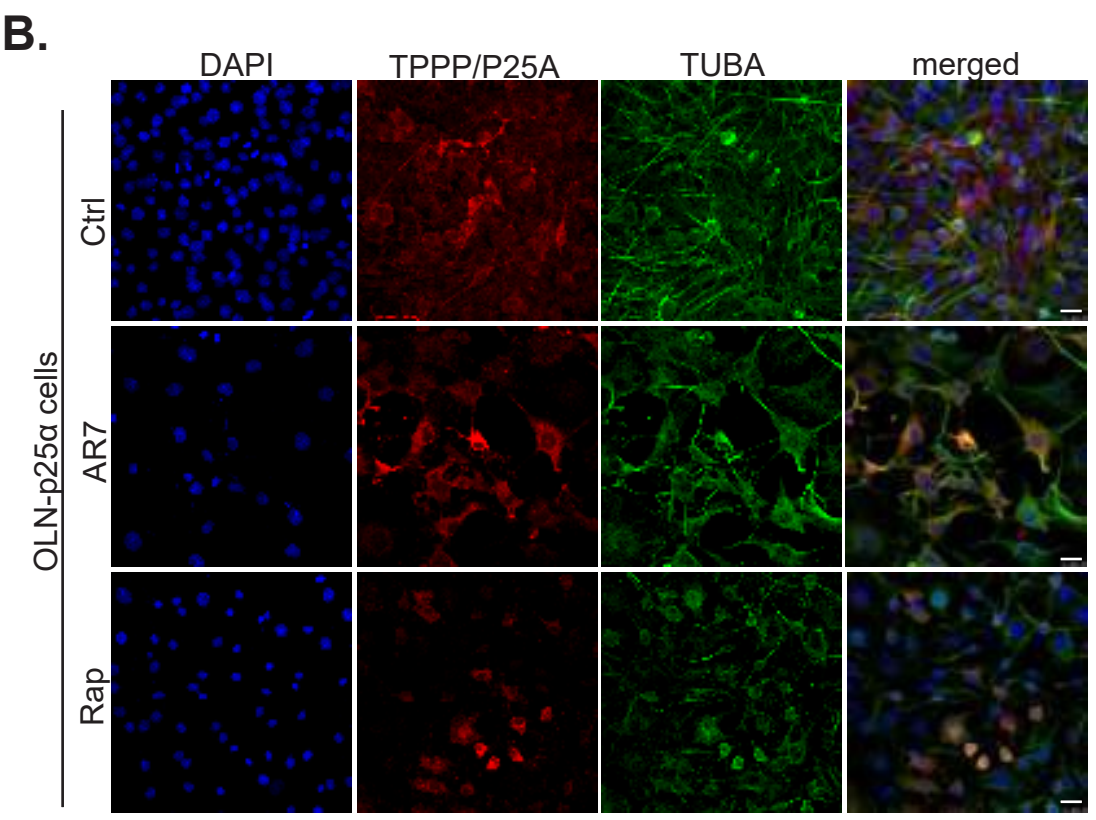

D.

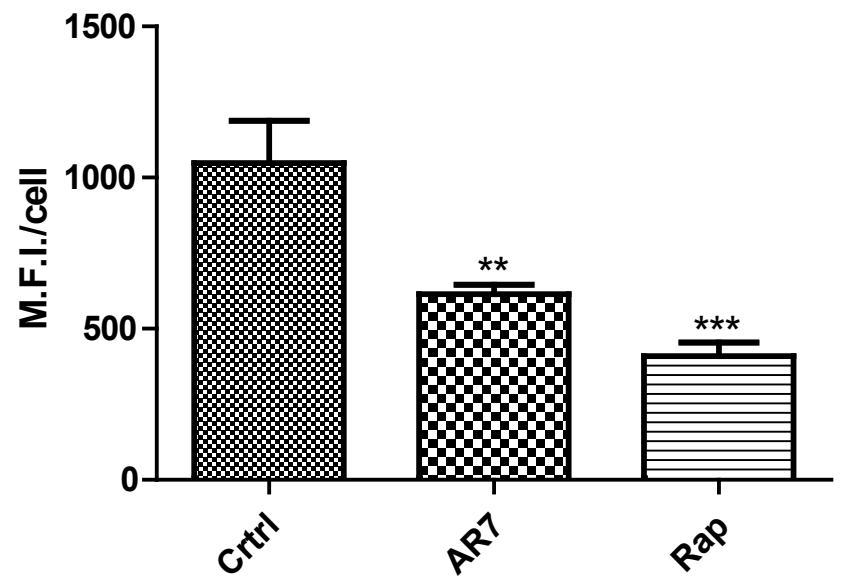

Ei.

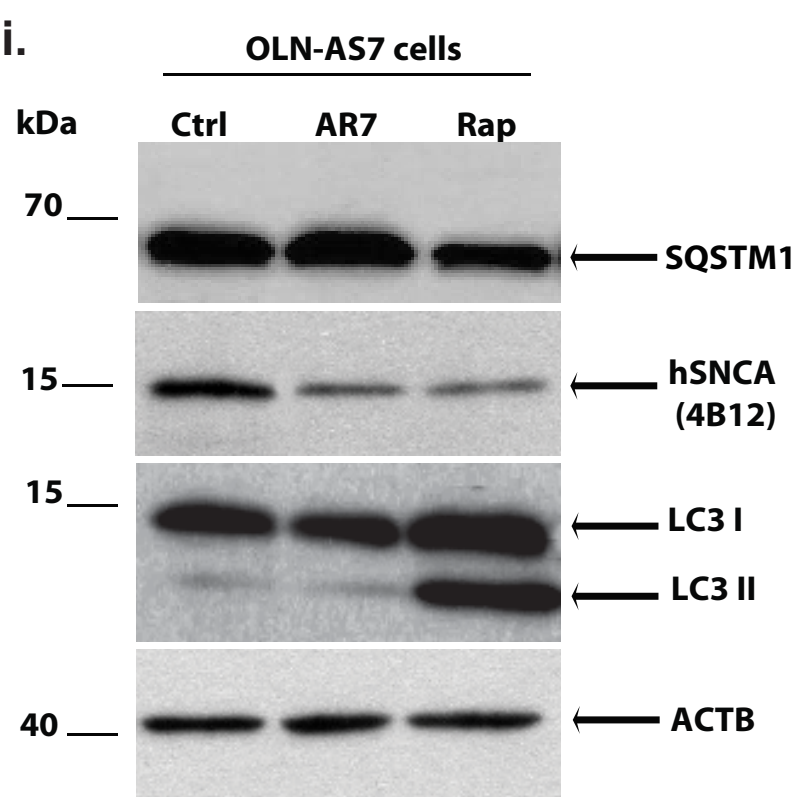

Fi.

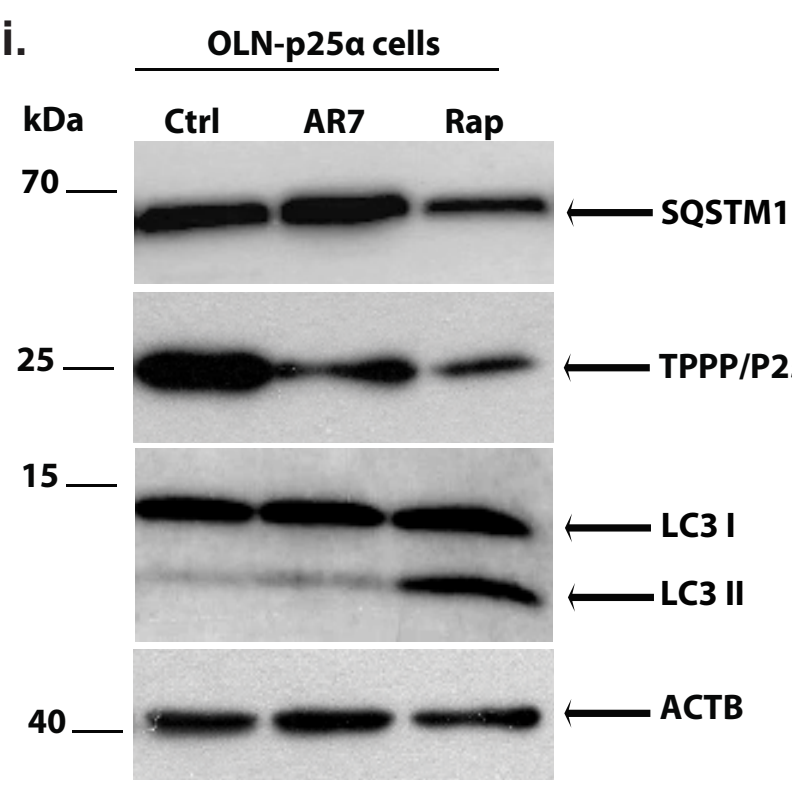

Eii.

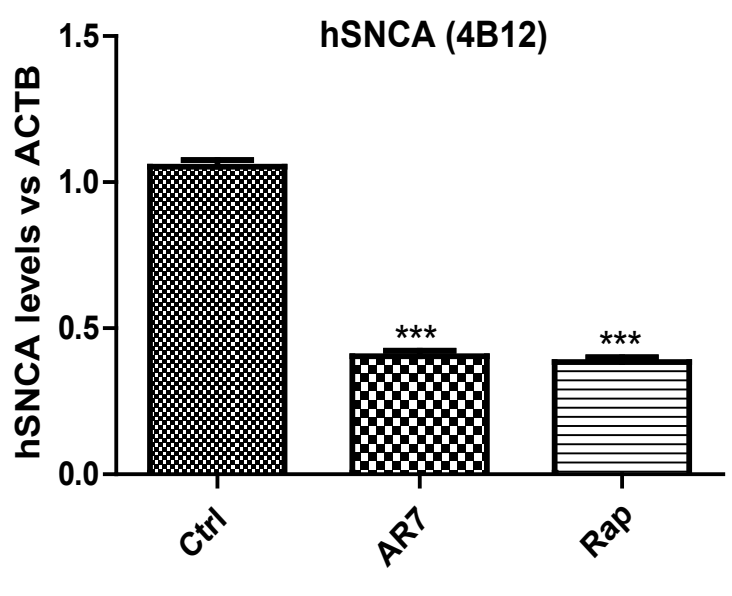

Fii.

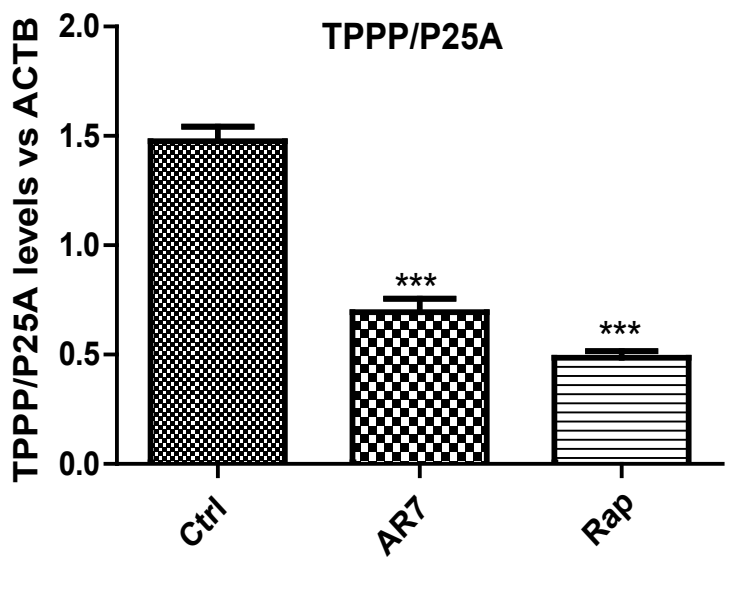

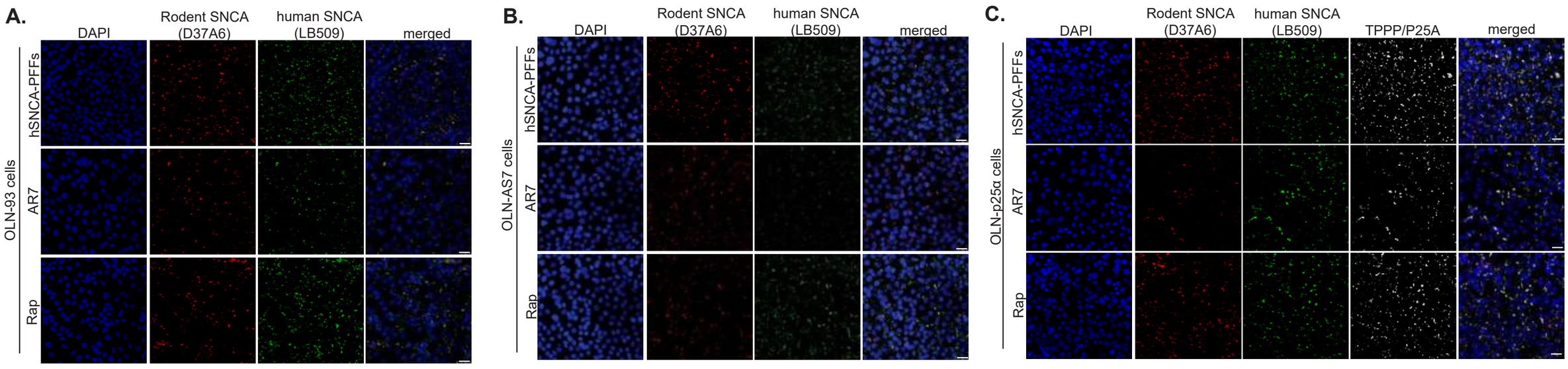
A.
DAPI
Rodent SNCA (D37A6)
human SNCA (LB509)
merged
OLN-93 cells
hSNCA-PFFs
AR7
Rap
B.
OLN-AS7 cells
C.
TPPP/P25A
OLN-p25α cells

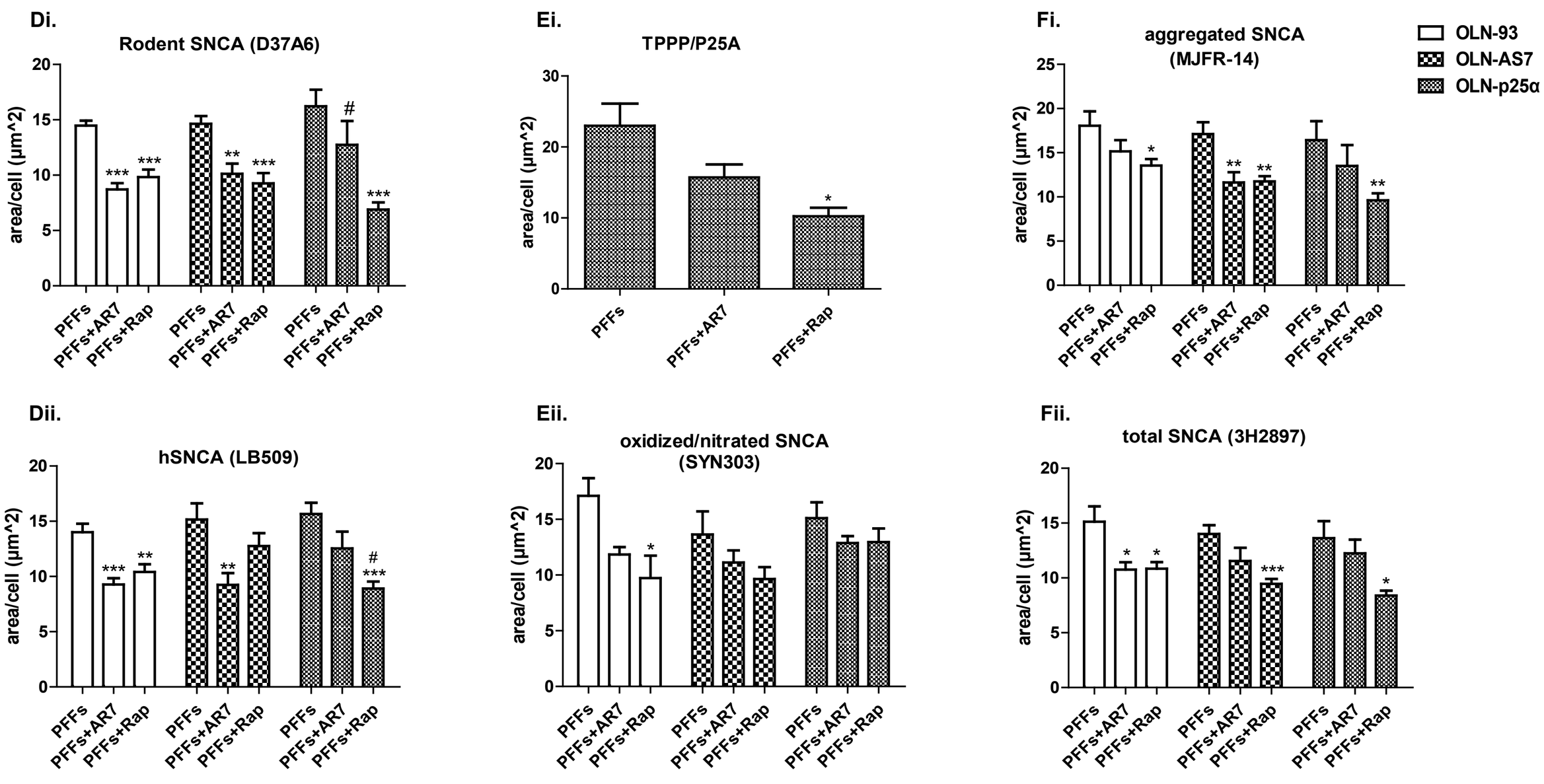
Di.
Rodent SNCA (D37A6)
area/cell (µm^2)
Ei.
TPPP/P25A
Fi.
aggregated SNCA (MJFR-14)
OLN-93
OLN-AS7
OLN-p25α
PFFs
PFFs+AR7
PFFs+Rap
Dii.
hSNCA (LB509)
Eii.
oxidized/nitrated SNCA (SYN303)
Fii.
total SNCA (3H2897)

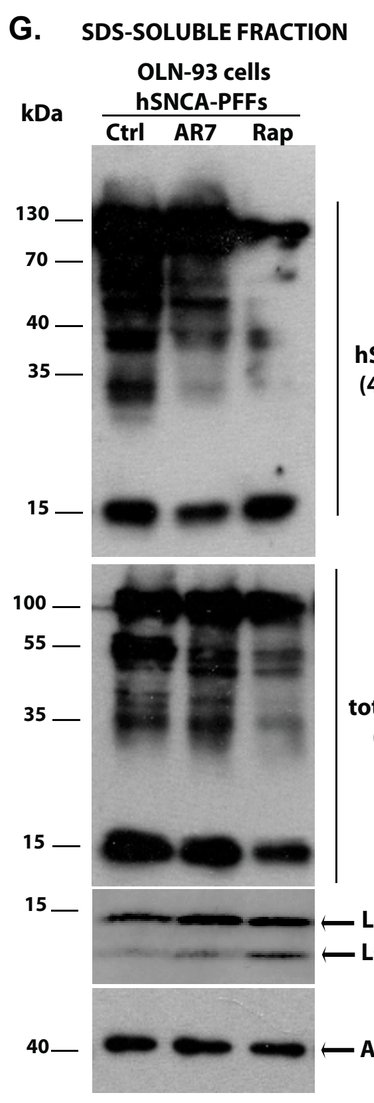
G.
SDS-SOLUBLE FRACTION
OLN-93 cells
hSNCA-PFFs
kDa
Ctrl
AR7
Rap
130
70
40
35
15
hSNCA (4B12)
100
55
35
15
total SNCA (SYN1)
15
LC3 I
LC3 II
40
ACTB

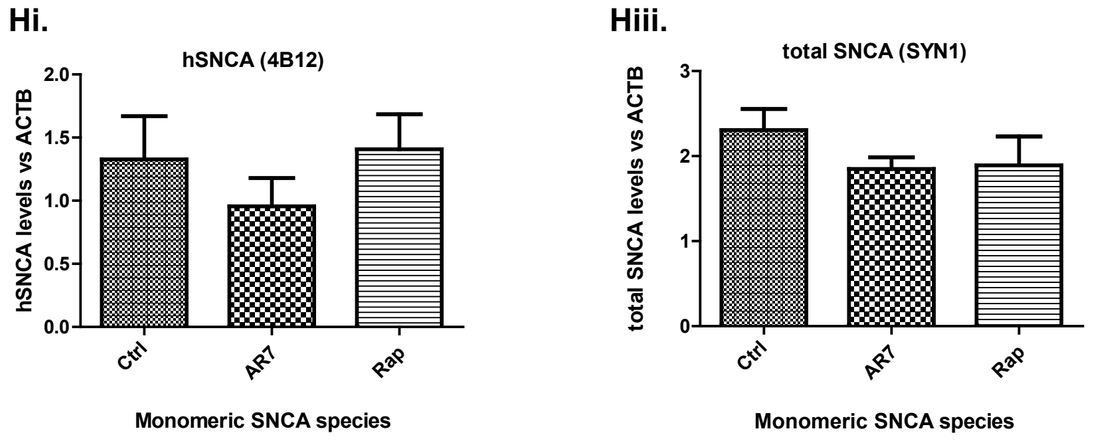
Hi.
hSNCA (4B12)
hSNCA levels vs ACTB
Monomeric SNCA species
Hiii.
total SNCA (SYN1)
total SNCA levels vs ACTB
Hii.
HMW SNCA species
Hiv.
Ctrl
AR7
Rap

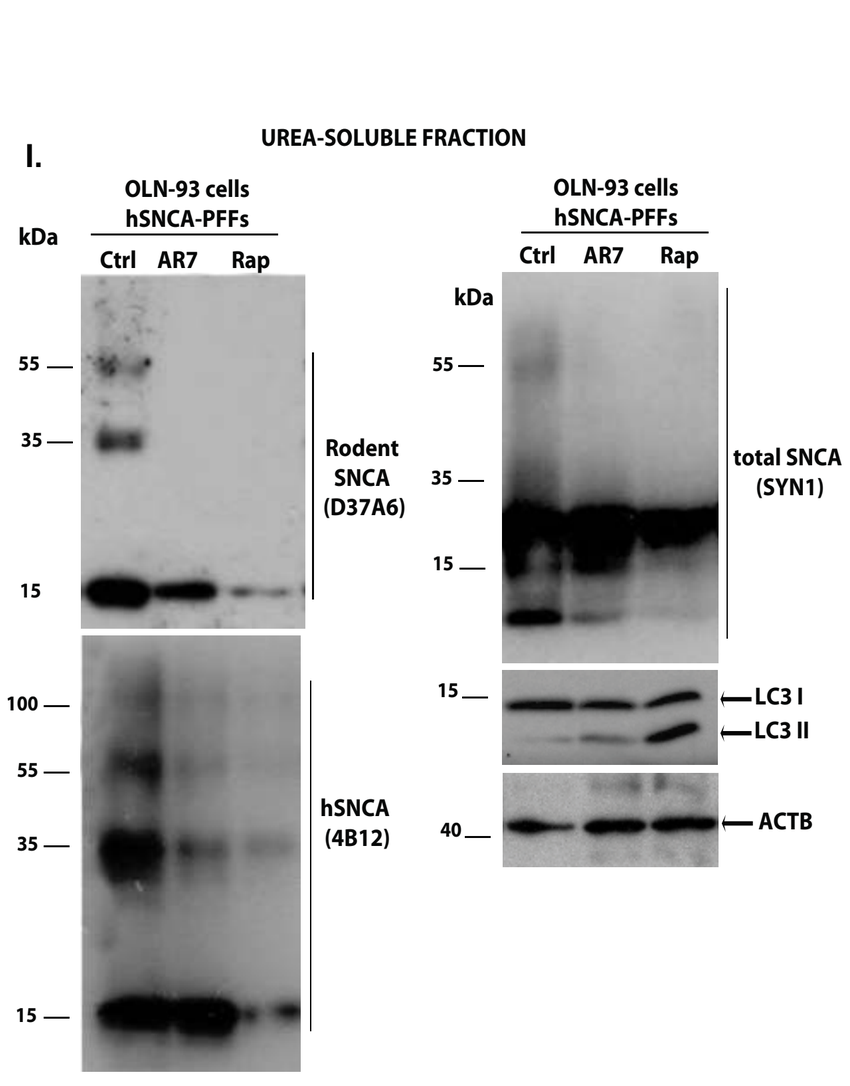
I.
UREA-SOLUBLE FRACTION
OLN-93 cells
hSNCA-PFFs
kDa
Ctrl
AR7
Rap
55
35
15
Rodent SNCA (D37A6)
100
hSNCA (4B12)
total SNCA (SYN1)
LC3 I
LC3 II
40
ACTB

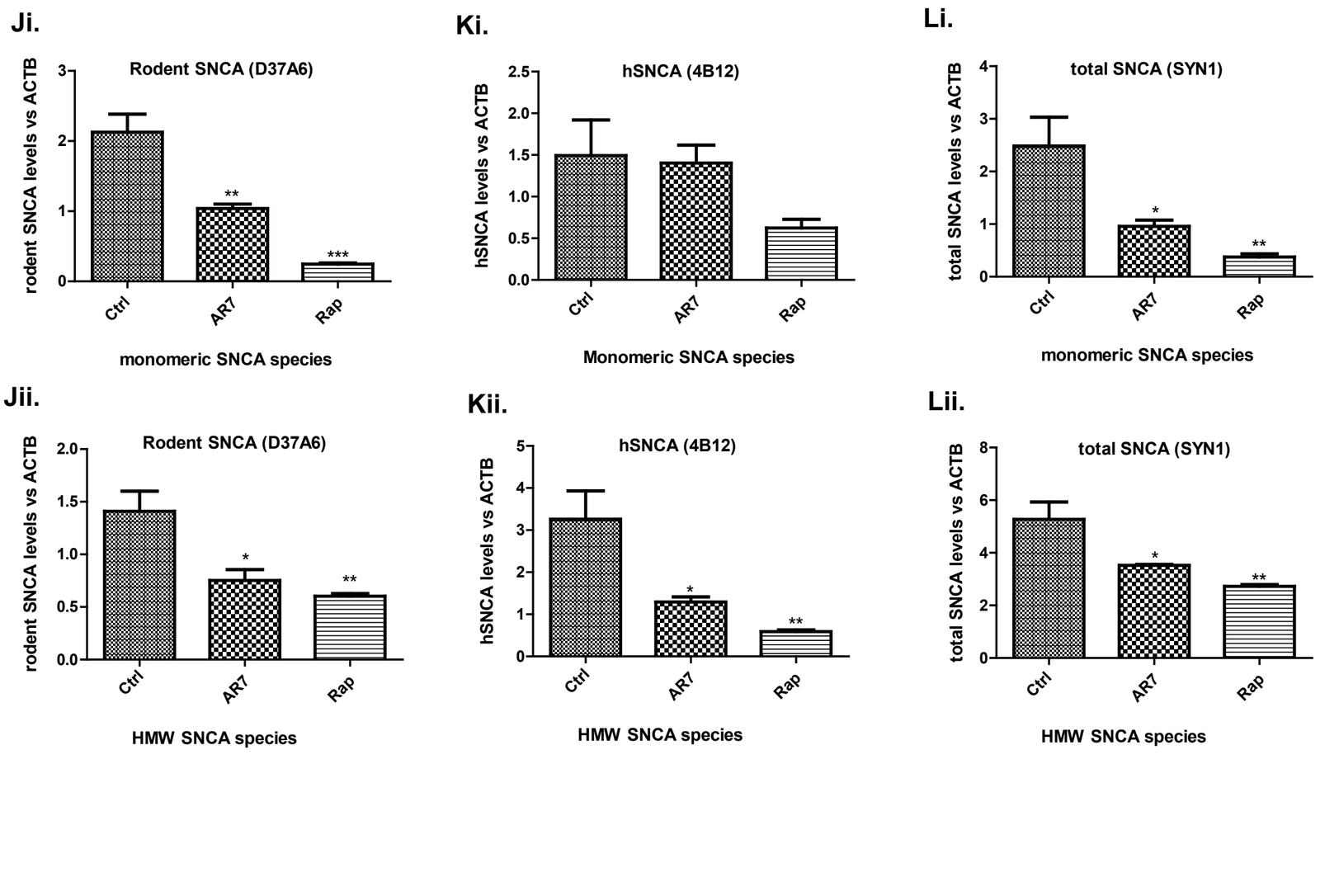
Ji.
Rodent SNCA (D37A6)
rodent SNCA levels vs ACTB
monomeric SNCA species
Ki.
hSNCA (4B12)
hSNCA levels vs ACTB
Monomeric SNCA species
Li.
total SNCA (SYN1)
total SNCA levels vs ACTB
monomeric SNCA species
Jii.
HMW SNCA species
Kii.
Lii.
Ctrl
AR7
Rap

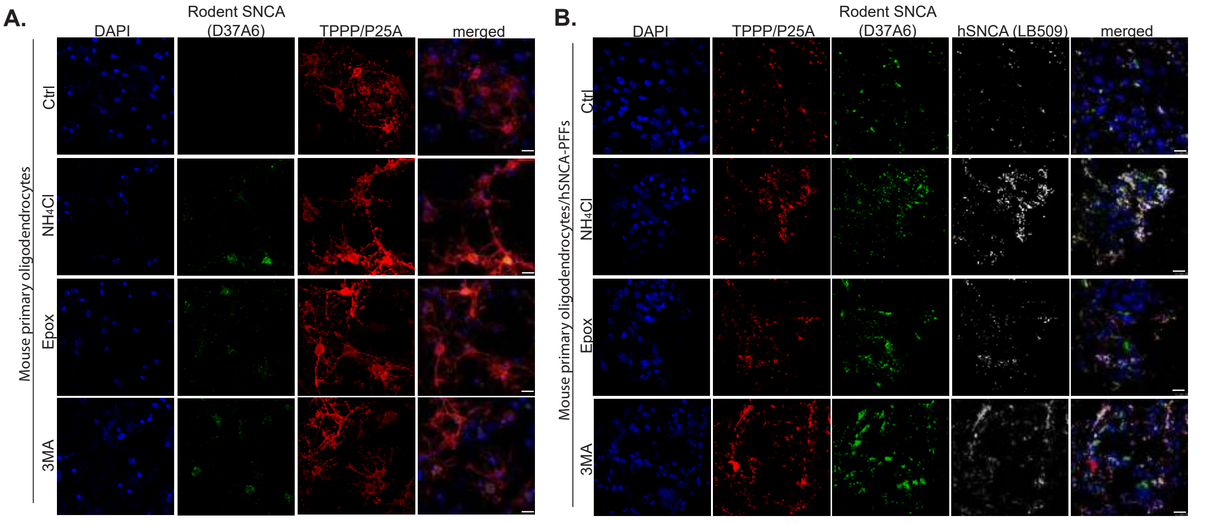
A.
DAPI
Rodent SNCA (D37A6)
TPPP/P25A
merged
Mouse primary oligodendrocytes
Ctrl
NH4Cl
Epox
3MA
B.
DAPI
TPPP/P25A
Rodent SNCA (D37A6)
hSNCA (LB509)
merged
Mouse primary oligodendrocytes/hSNCA-PFFs
Ctrl
NH4Cl
Epox
3MA

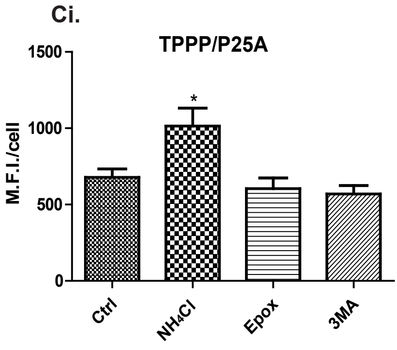
Ci.
TPPP/P25A
M.F.I./cell
1500
1000
500
0
*
Ctrl
NH4Cl
Epox
3MA

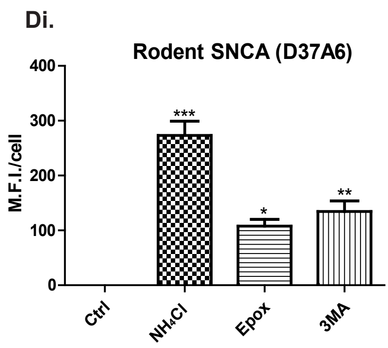
Di.
Rodent SNCA (D37A6)
M.F.I./cell
400
300
200
100
0
***
*
**
Ctrl
NH4Cl
Epox
3MA

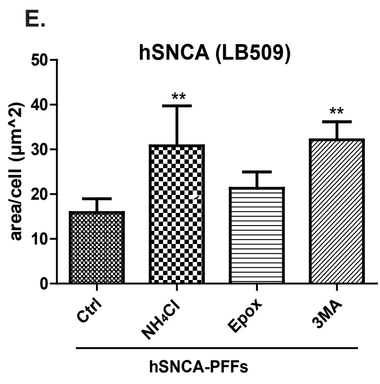
E.
hSNCA (LB509)
area/cell (µm^2)
50
40
30
20
10
0
**
**
Ctrl
NH4Cl
Epox
3MA
hSNCA-PFFs

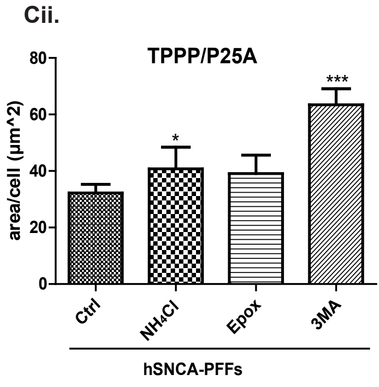
Cii.
TPPP/P25A
area/cell (µm^2)
80
60
40
20
0
*
***
Ctrl
NH4Cl
Epox
3MA
hSNCA-PFFs

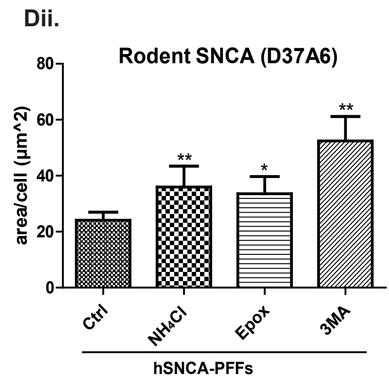
Dii.
Rodent SNCA (D37A6)
area/cell (µm^2)
80
60
40
20
0
**
*
**
Ctrl
NH4Cl
Epox
3MA
hSNCA-PFFs

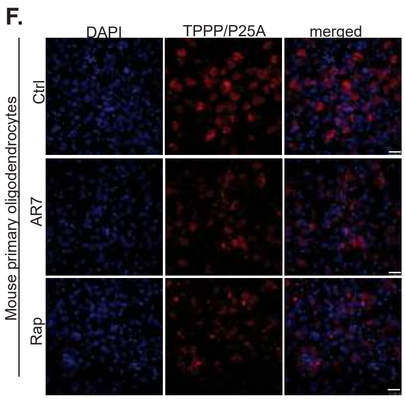
F.
DAPI
TPPP/P25A
merged
Mouse primary oligodendrocytes
Ctrl
AR7
Rap

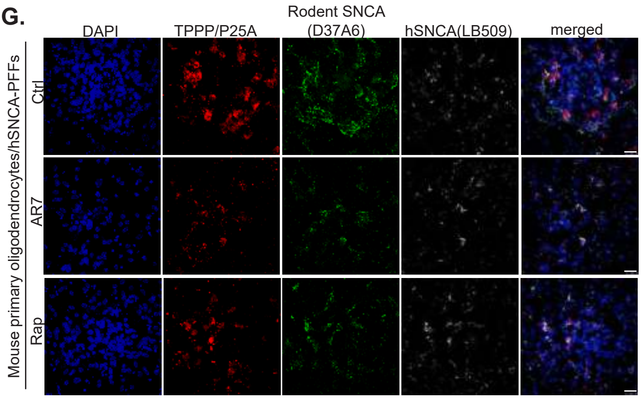
G.
DAPI
TPPP/P25A
Rodent SNCA (D37A6)
hSNCA(LB509)
merged
Mouse primary oligodendrocytes/hSNCA-PFFs
Ctrl
AR7
Rap

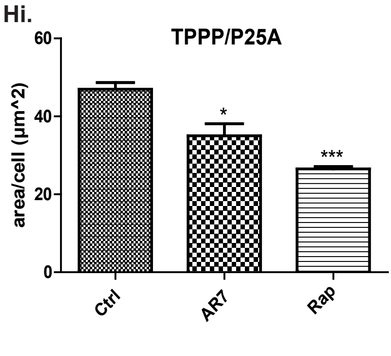
Hi.
TPPP/P25A
area/cell (µm^2)
60
40
20
0
*
***
Ctrl
AR7
Rap

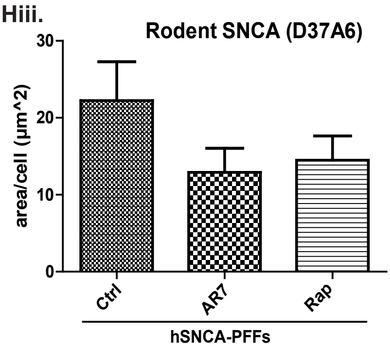
Hiii.
Rodent SNCA (D37A6)
area/cell (µm^2)
30
20
10
0
Ctrl
AR7
Rap
hSNCA-PFFs

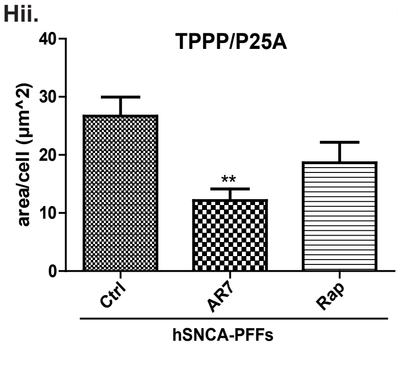
Hii.
TPPP/P25A
area/cell (µm^2)
40
30
20
10
0
**
Ctrl
AR7
Rap
hSNCA-PFFs

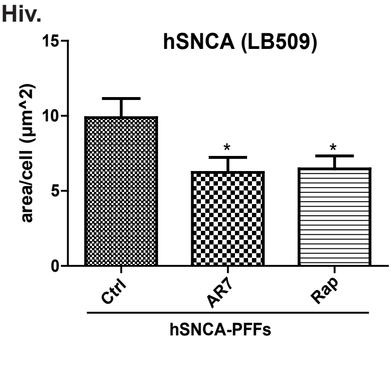
Hiv.
hSNCA (LB509)
area/cell (µm^2)
15
10
5
0
*
*
Ctrl
AR7
Rap
hSNCA-PFFs

A.

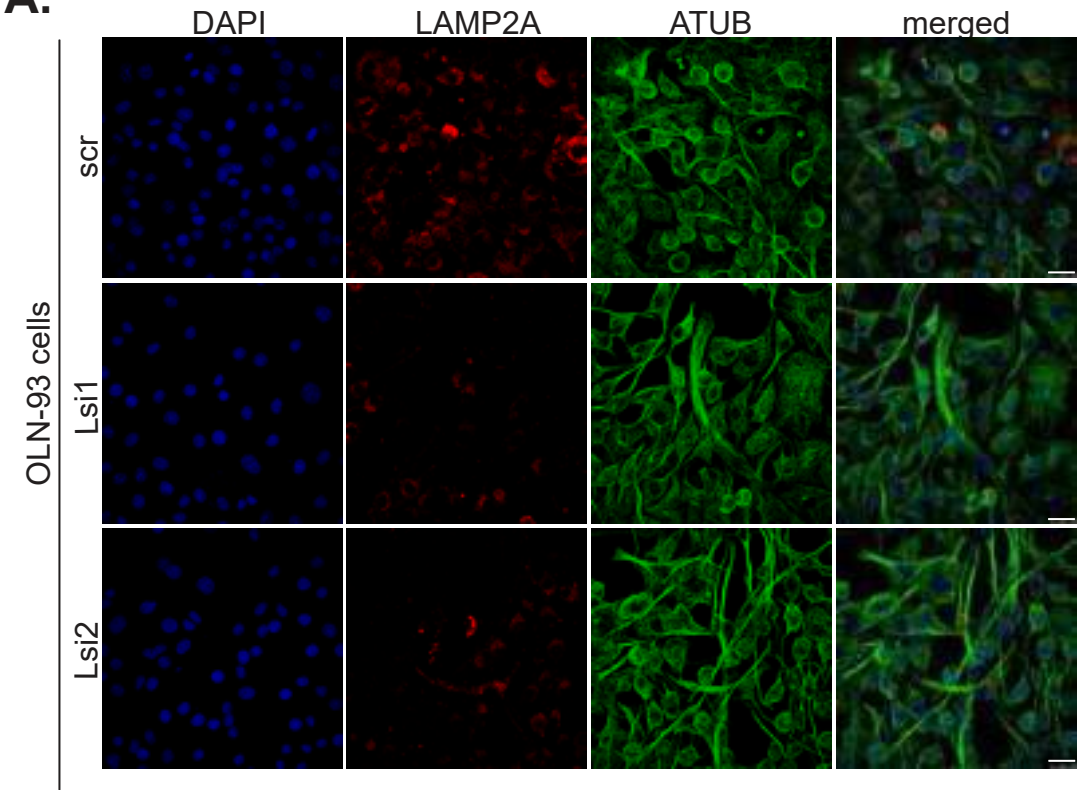
DAPI
LAMP2A
ATUB
merged
OLN-93 cells
scr
Lsi1
Lsi2

B.

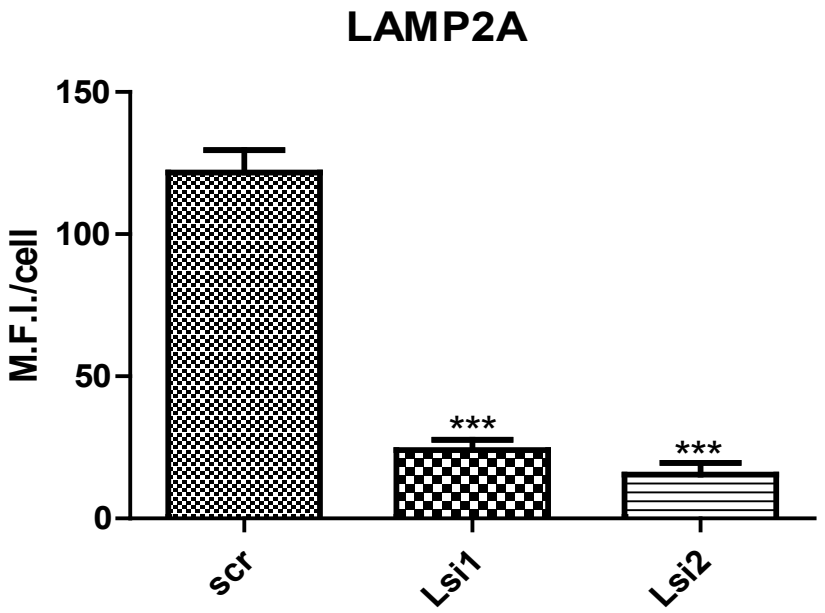
LAMP2A
M.F.I./cell
150
100
50
0
***
***
scr
Lsi1
Lsi2

C.

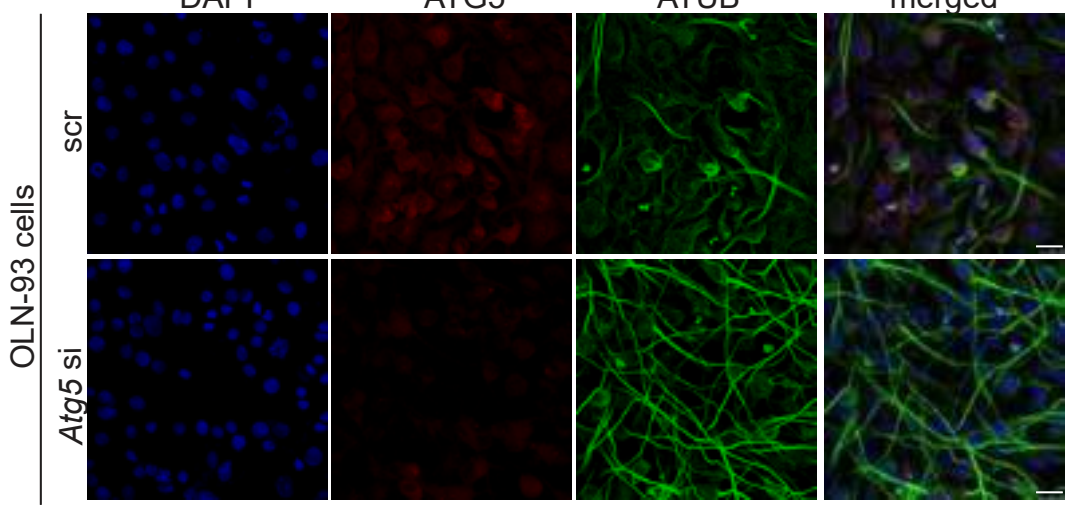
DAPI
ATG5
ATUB
merged
OLN-93 cells
scr
Atg5 si

D.

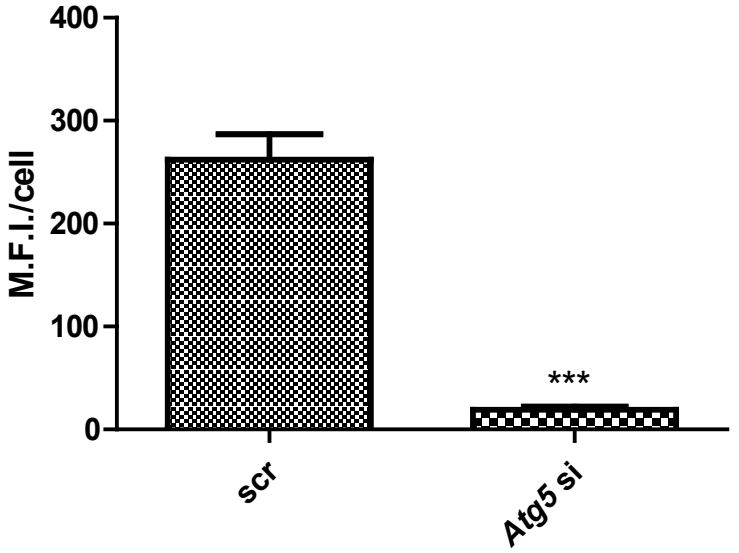
ATG5
M.F.I./cell
400
300
200
100
0
***
scr
Atg5 si

E.

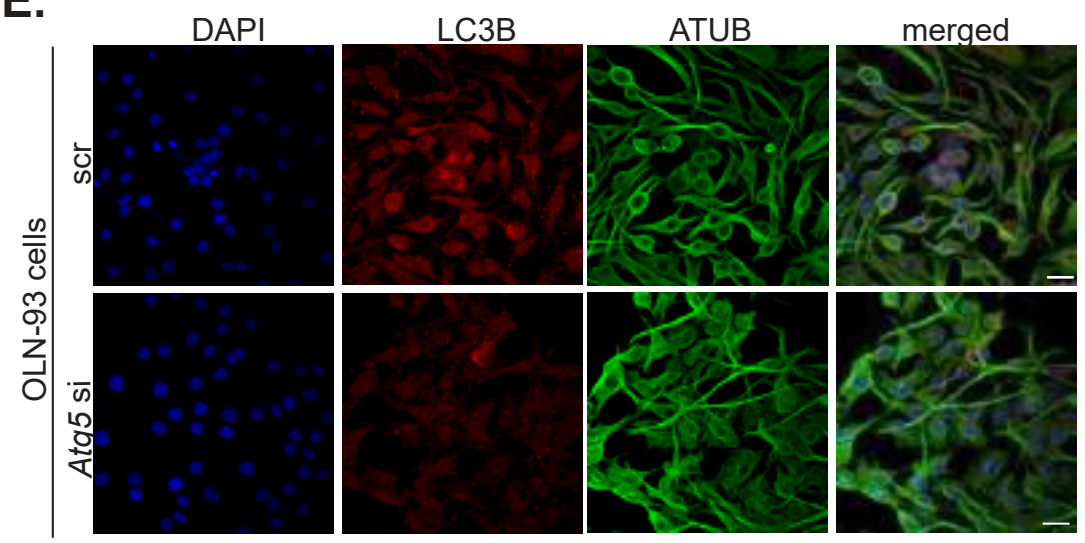
DAPI
LC3B
ATUB
merged
OLN-93 cells
scr
Atg5 si

F.

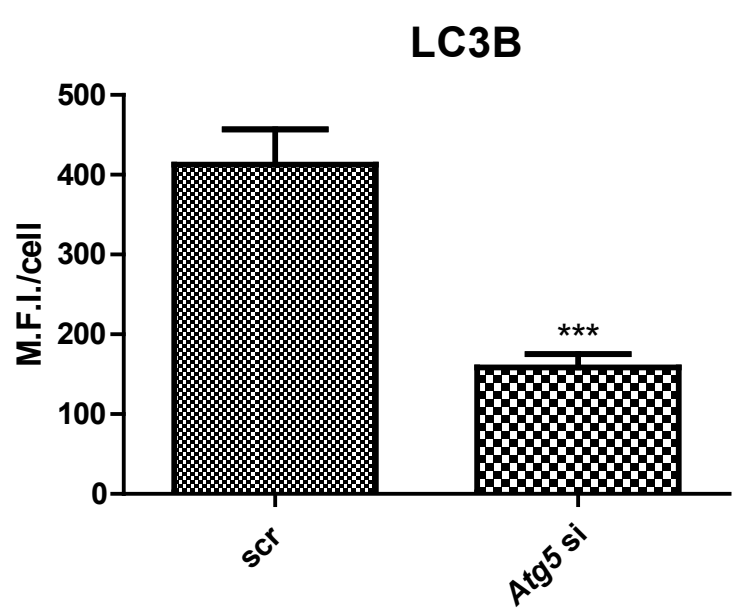
LC3B
M.F.I./cell
500
400
300
200
100
0
***
scr
Atg5 si

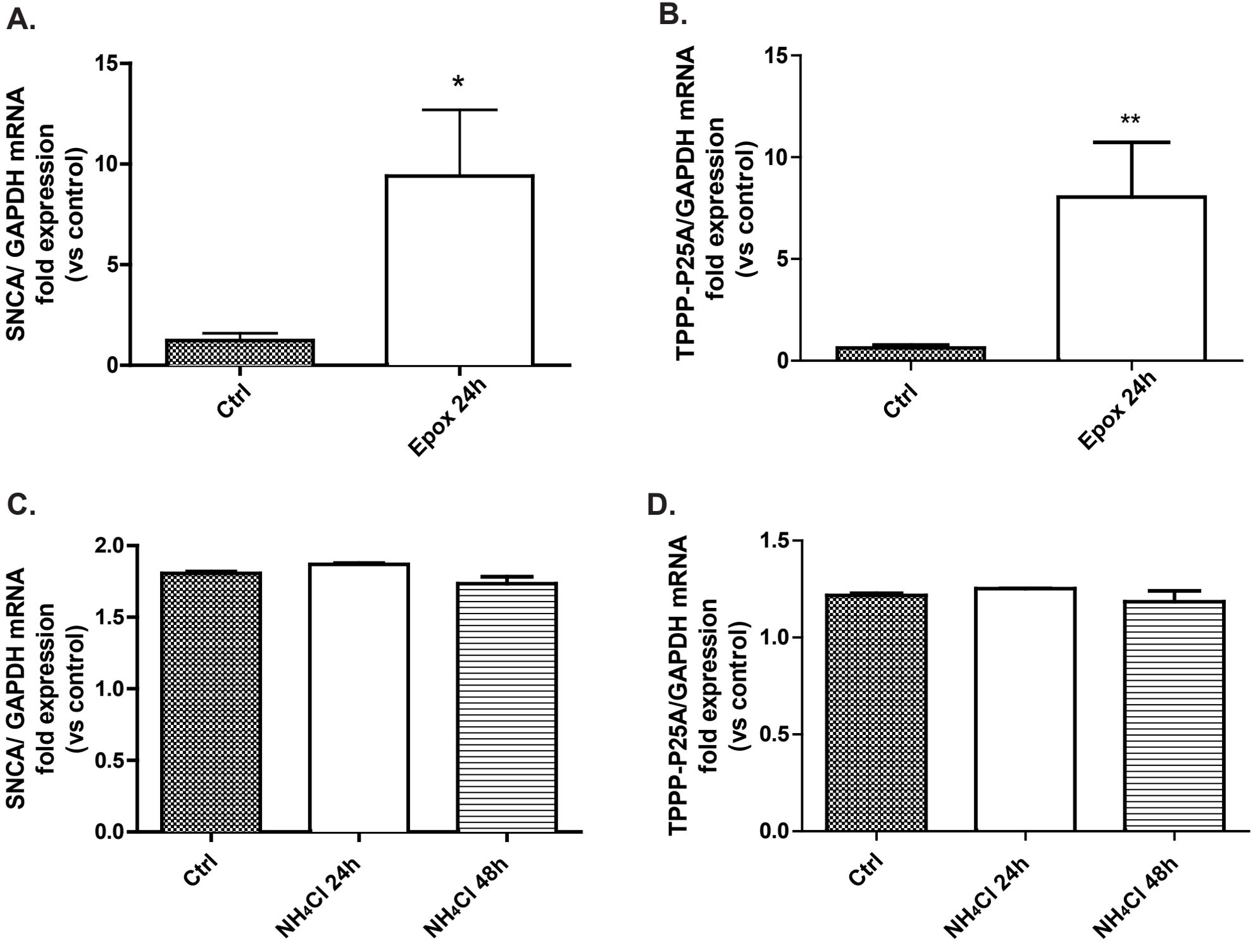
A.
SNCA/ GAPDH mRNA fold expression (vs control)
15
10
5
0
*
Ctrl
Epox 24h
B.
TPPP-P25A/GAPDH mRNA fold expression (vs control)
15
10
5
0
**
Ctrl
Epox 24h
C.
SNCA/ GAPDH mRNA fold expression (vs control)
2.0
1.5
1.0
0.5
0.0
Ctrl
NH4Cl 24h
NH4Cl 48h
D.
TPPP-P25A/GAPDH mRNA fold expression (vs control)
1.5
1.0
0.5
0.0
Ctrl
NH4Cl 24h
NH4Cl 48h

A.

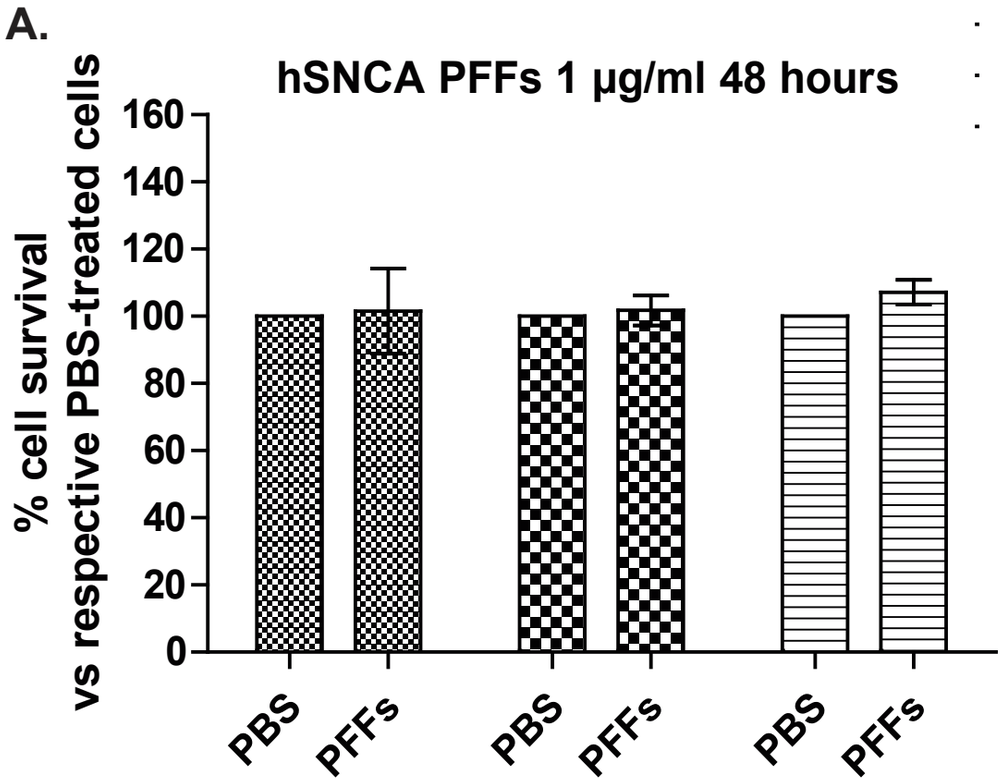
hSNCA PFFs 1 µg/ml 48 hours
% cell survival
vs respective PBS-treated cells
160
140
120
100
80
60
40
20
0
PBS
PFFs
PBS
PFFs
PBS
PFFs

B.

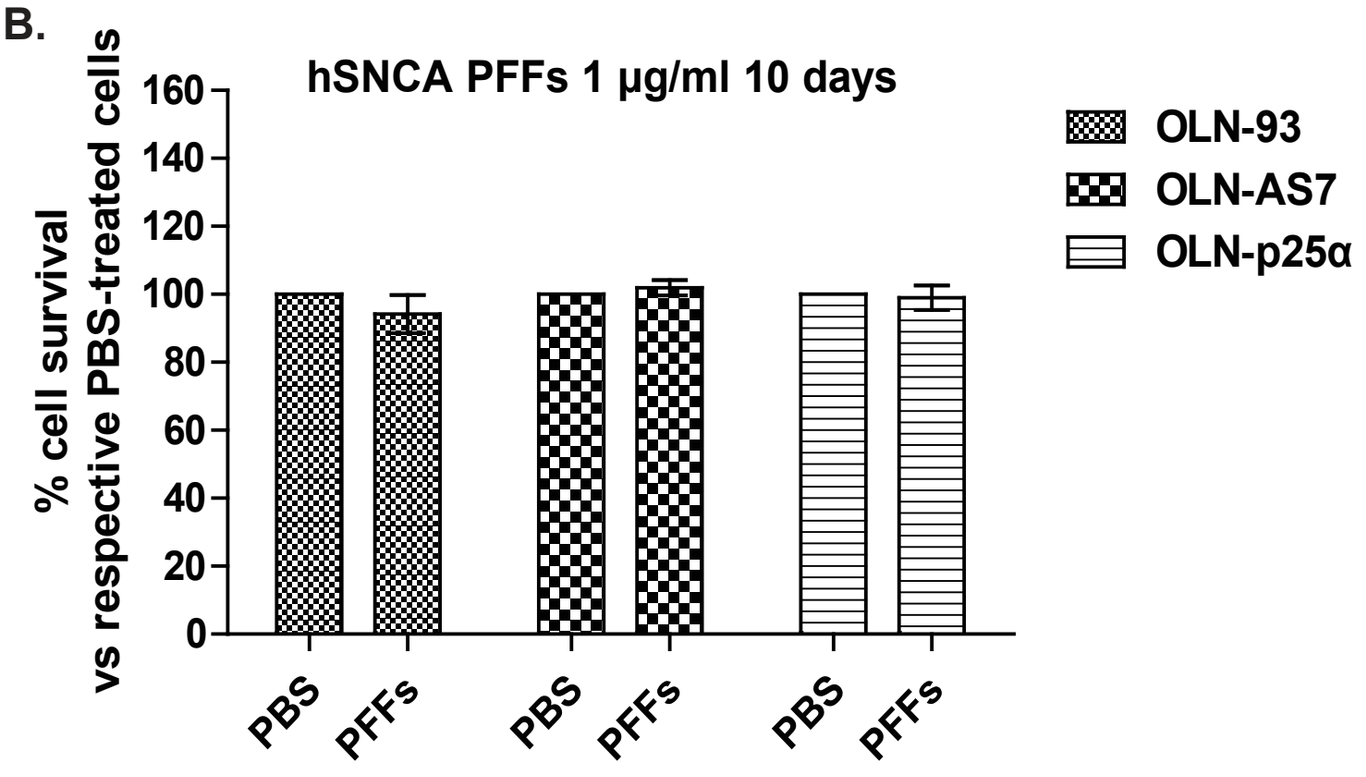
hSNCA PFFs 1 µg/ml 10 days
% cell survival
vs respective PBS-treated cells
160
140
120
100
80
60
40
20
0
PBS
PFFs
PBS
PFFs
PBS
PFFs
OLN-93
OLN-AS7
OLN-p25α

C.

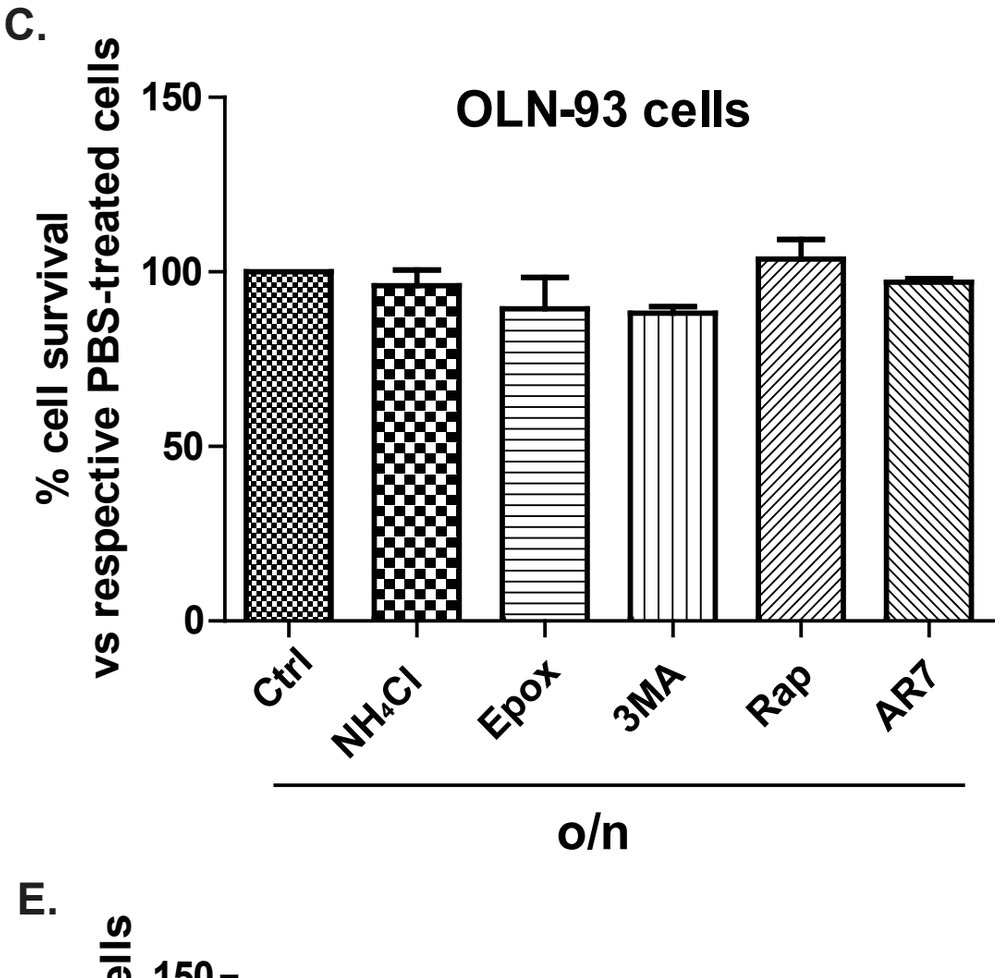
OLN-93 cells
% cell survival
vs respective PBS-treated cells
150
100
50
0
Ctrl
NH4Cl
Epox
3MA
Rap
AR7
o/n

D.

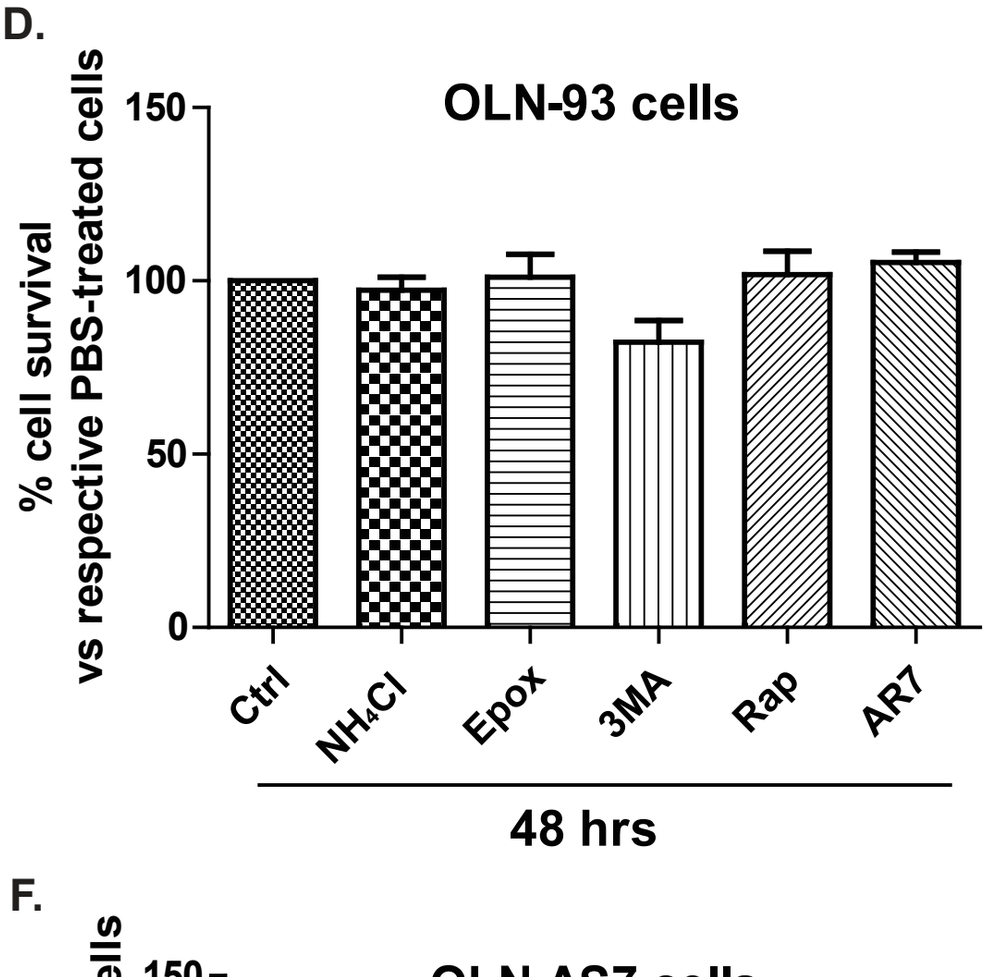
OLN-93 cells
% cell survival
vs respective PBS-treated cells
150
100
50
0
Ctrl
NH4Cl
Epox
3MA
Rap
AR7
48 hrs

E.

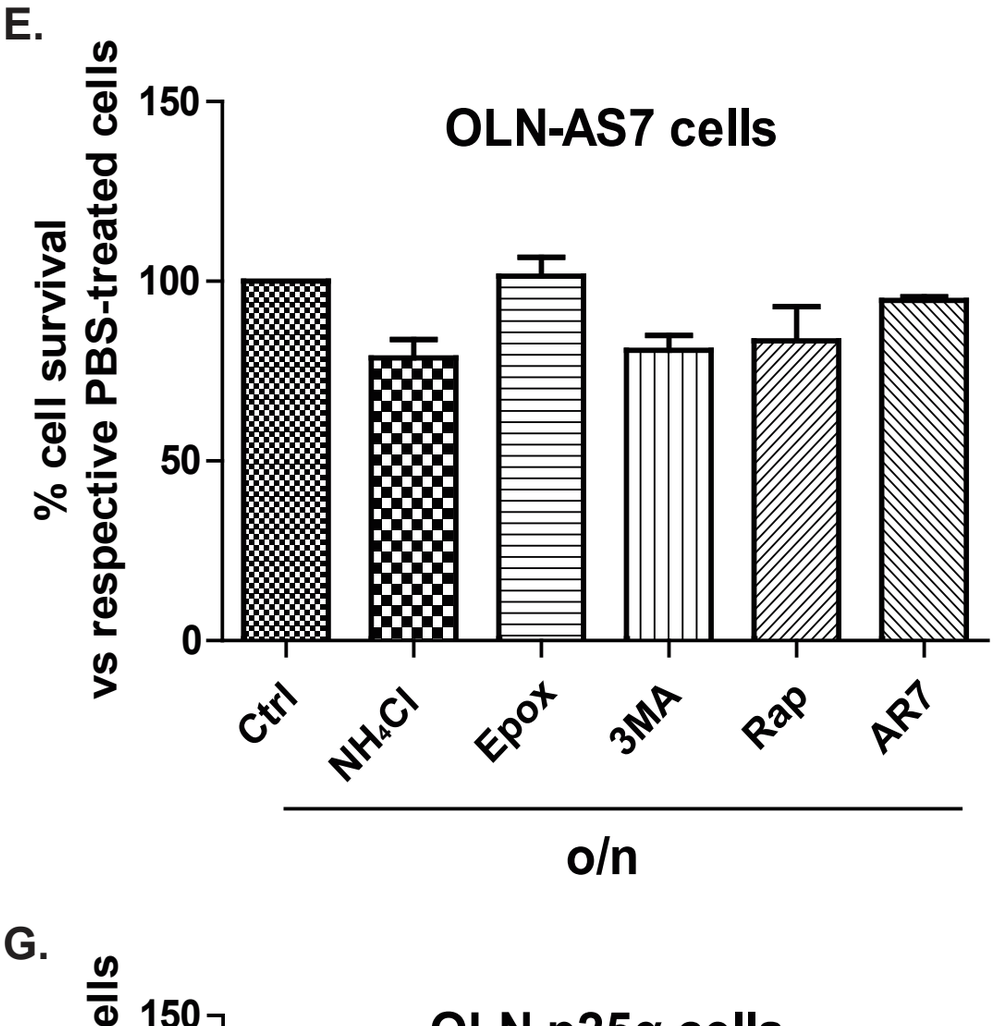
OLN-AS7 cells
% cell survival
vs respective PBS-treated cells
150
100
50
0
Ctrl
NH4Cl
Epox
3MA
Rap
AR7
o/n

F.

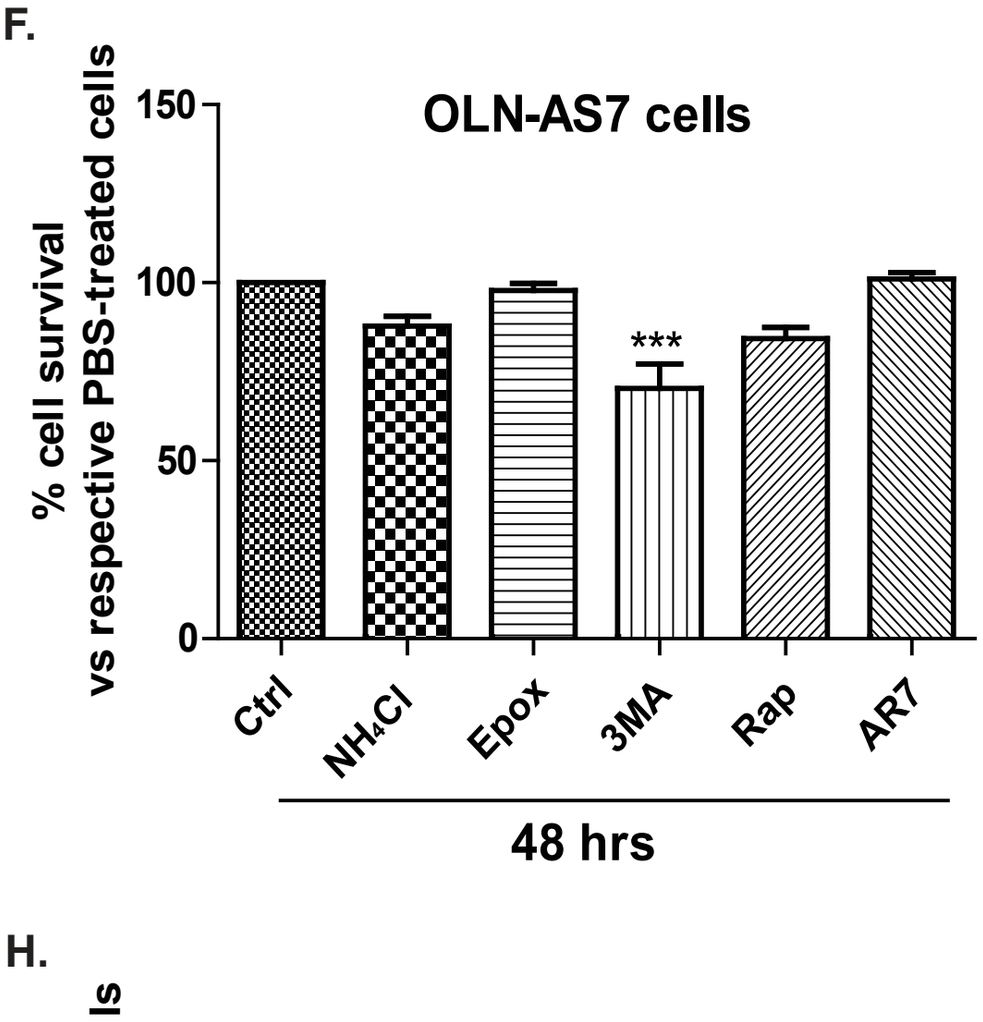
OLN-AS7 cells
% cell survival
vs respective PBS-treated cells
150
100
50
0
***
Ctrl
NH4Cl
Epox
3MA
Rap
AR7
48 hrs

G.

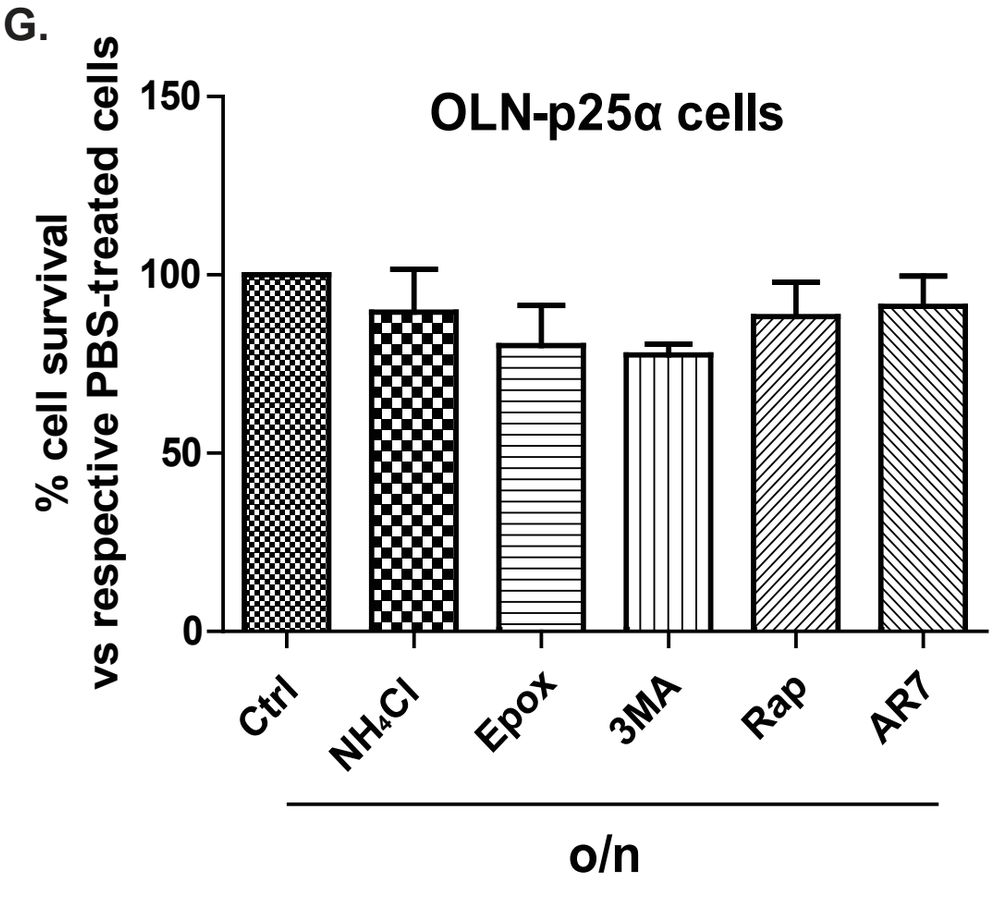
OLN-p25α cells
% cell survival
vs respective PBS-treated cells
150
100
50
0
Ctrl
NH4Cl
Epox
3MA
Rap
AR7
o/n

H.

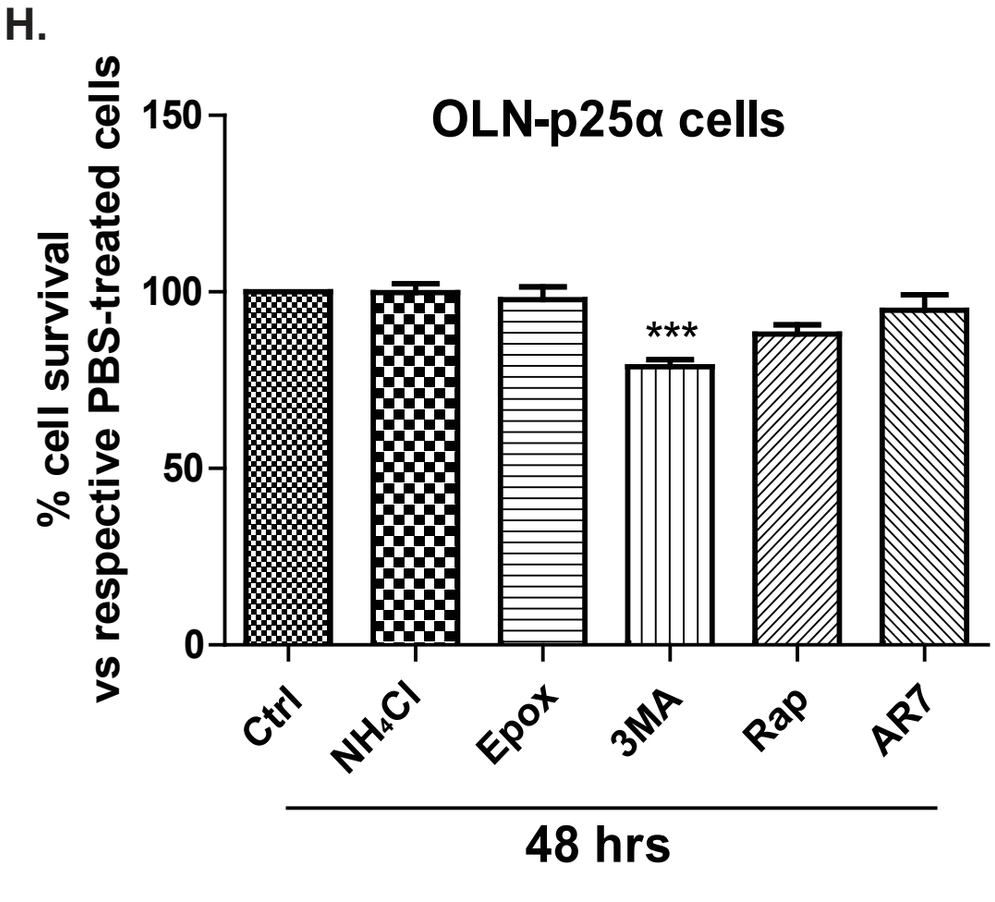
OLN-p25α cells
% cell survival
vs respective PBS-treated cells
150
100
50
0
***
Ctrl
NH4Cl
Epox
3MA
Rap
AR7
48 hrs

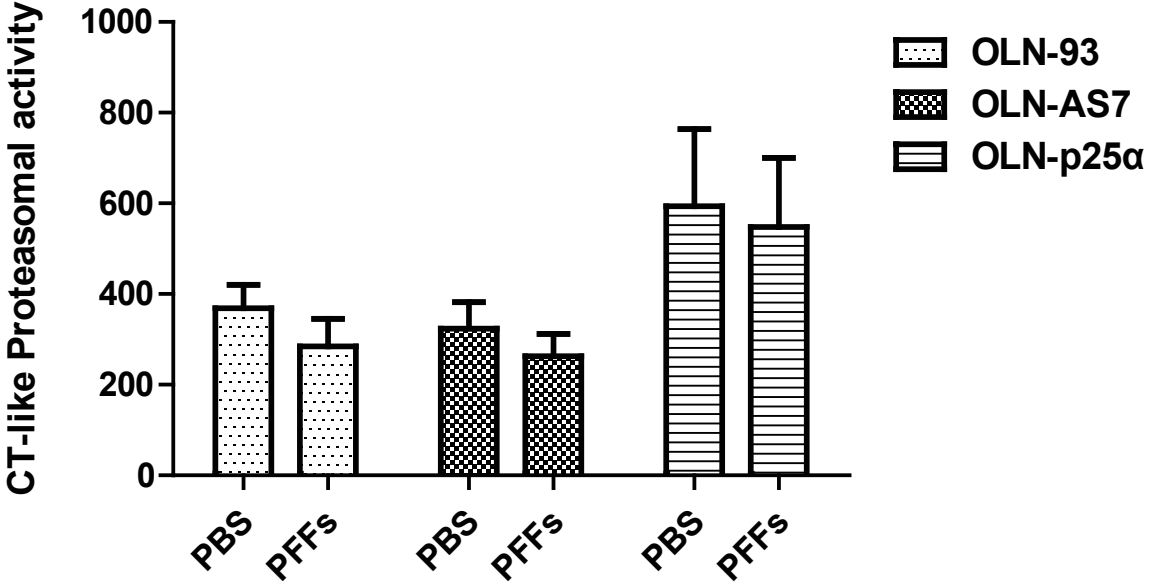
CT-like Proteasomal activity
1000
800
600
400
200
0
PBS
PFFs
PBS
PFFs
PBS
PFFs
OLN-93
OLN-AS7
OLN-p25α

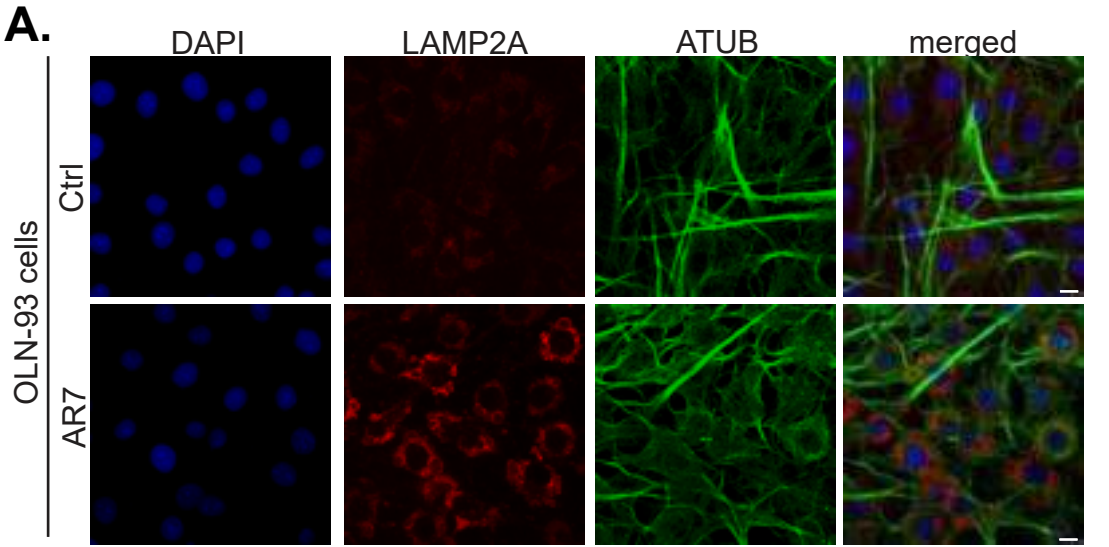
A.
DAPI
LAMP2A
ATUB
merged
OLN-93 cells
Ctrl
AR7

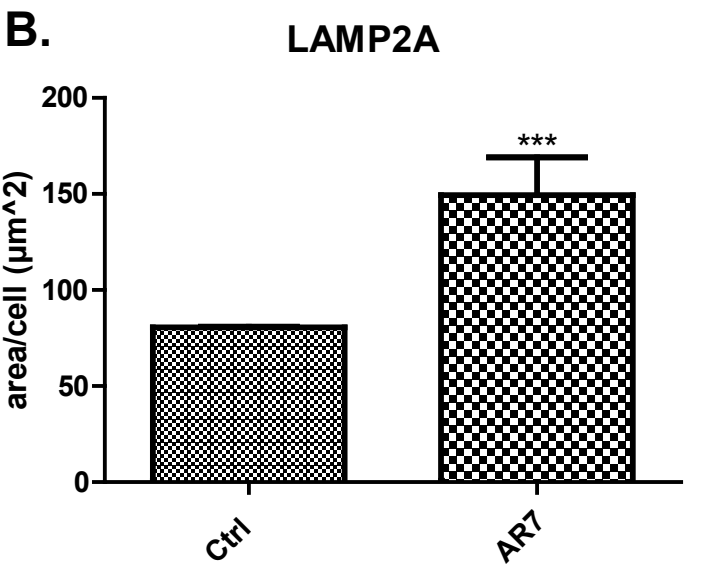
B.
LAMP2A
area/cell (µm^2)
200
150
100
50
0
***
Ctrl
AR7

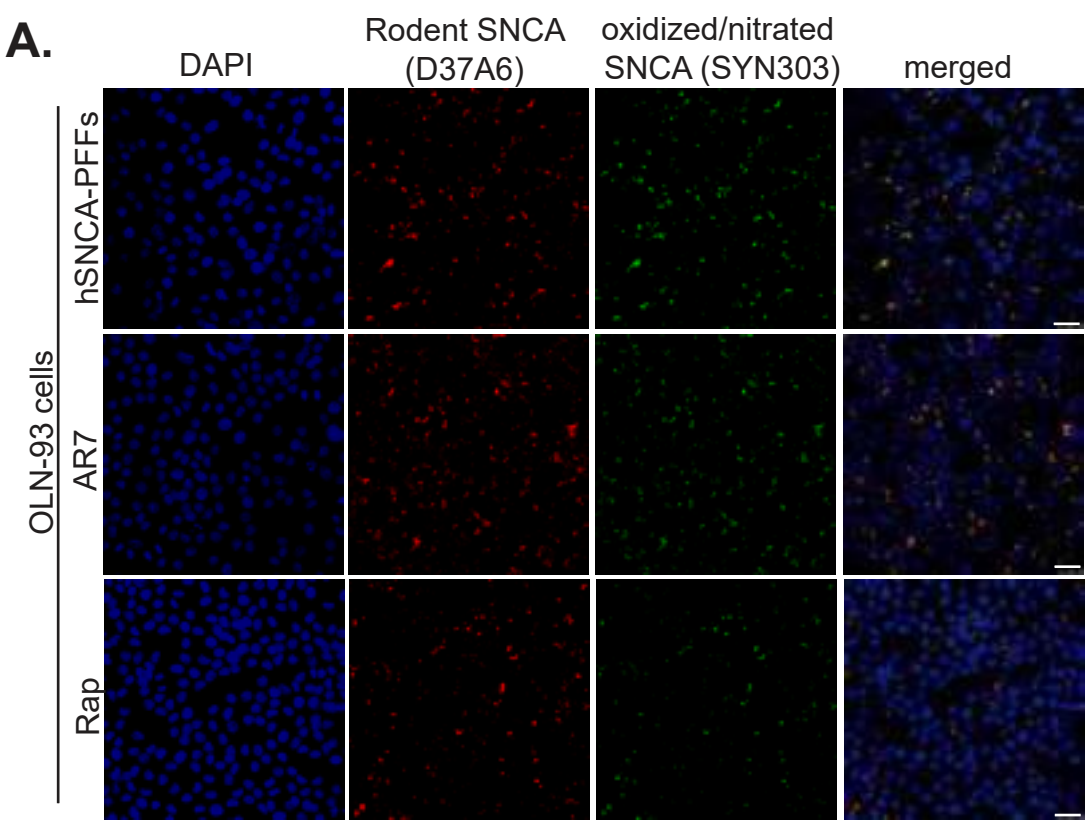
A.
DAPI
Rodent SNCA (D37A6)
oxidized/nitrated SNCA (SYN303)
merged
OLN-93 cells
hSNCA-PFFs
AR7
Rap

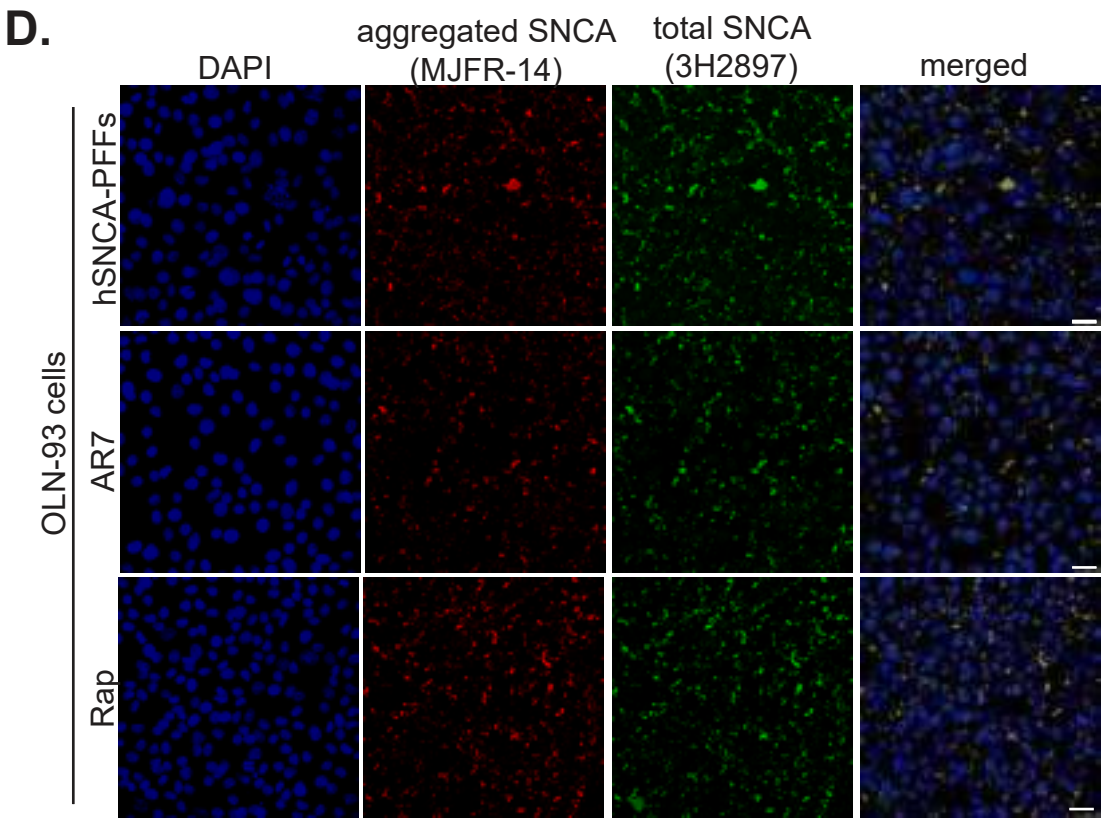
D.
DAPI
aggregated SNCA (MJFR-14)
total SNCA (3H2897)
merged
OLN-93 cells
hSNCA-PFFs
AR7
Rap

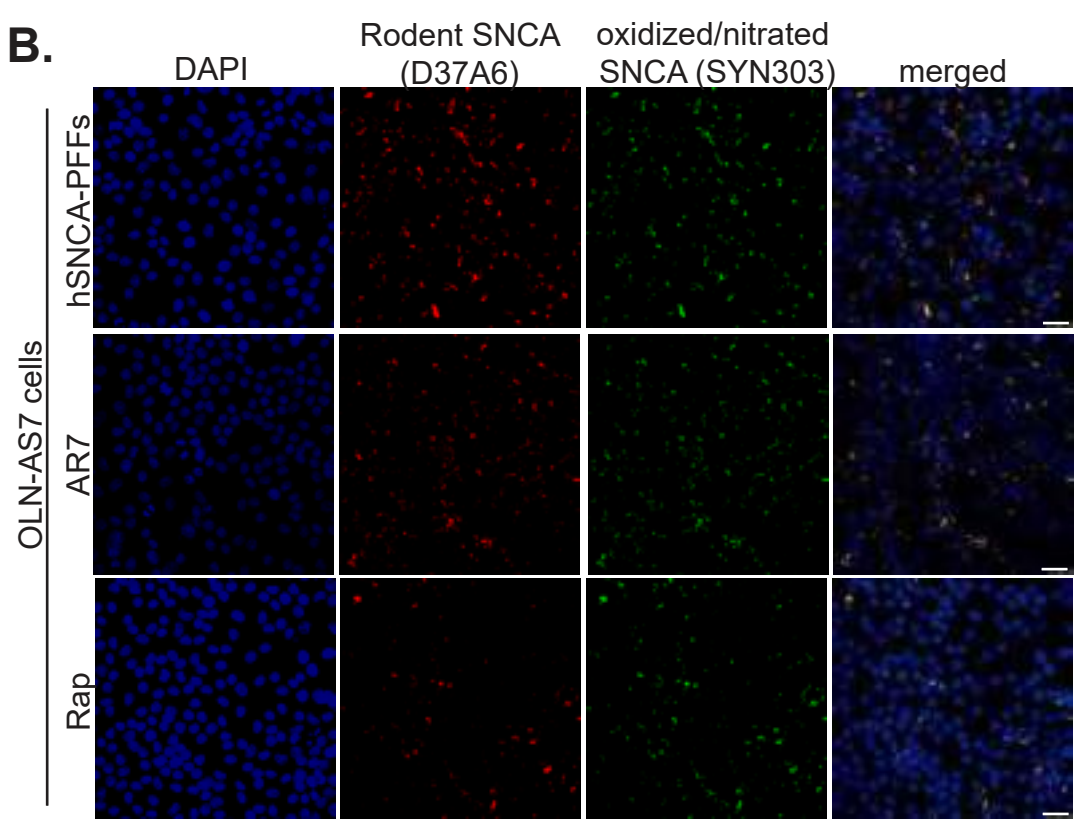
B.
DAPI
Rodent SNCA (D37A6)
oxidized/nitrated SNCA (SYN303)
merged
OLN-AS7 cells
hSNCA-PFFs
AR7
Rap

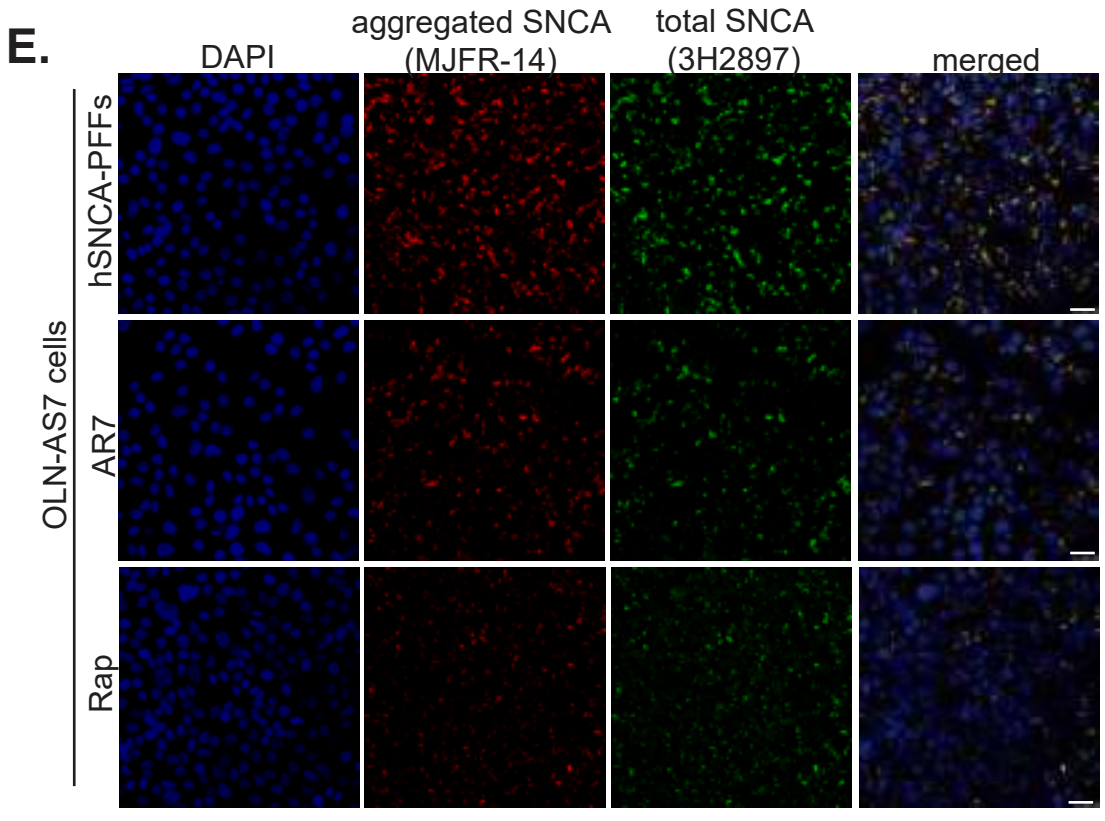
E.
DAPI
aggregated SNCA (MJFR-14)
total SNCA (3H2897)
merged
OLN-AS7 cells
hSNCA-PFFs
AR7
Rap

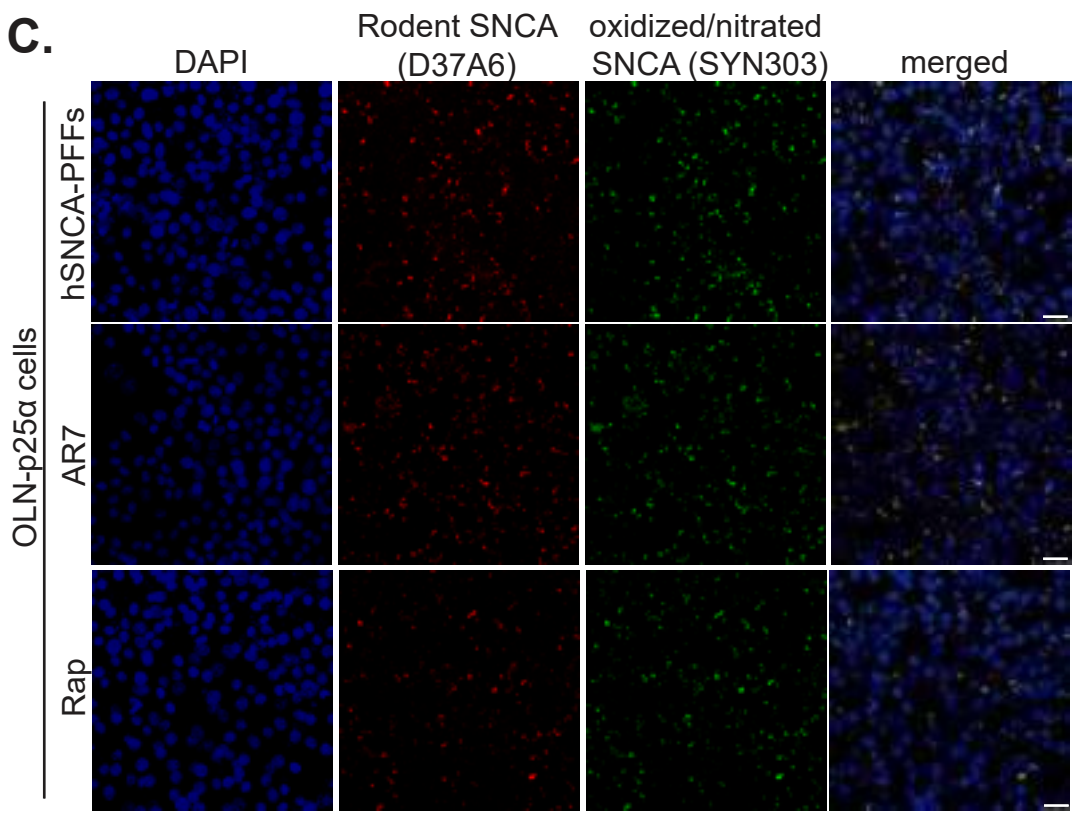
C.
DAPI
Rodent SNCA (D37A6)
oxidized/nitrated SNCA (SYN303)
merged
OLN-p25α cells
hSNCA-PFFs
AR7
Rap

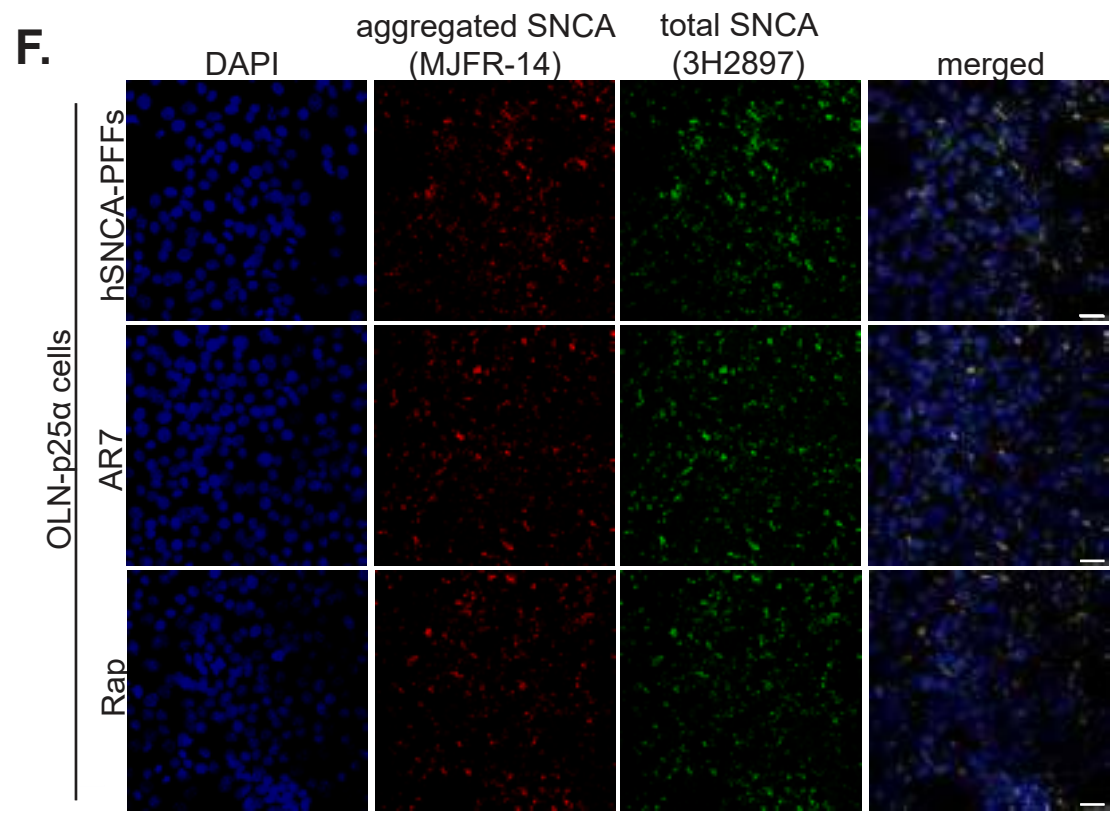
F.
DAPI
aggregated SNCA (MJFR-14)
total SNCA (3H2897)
merged
OLN-p25α cells
hSNCA-PFFs
AR7
Rap

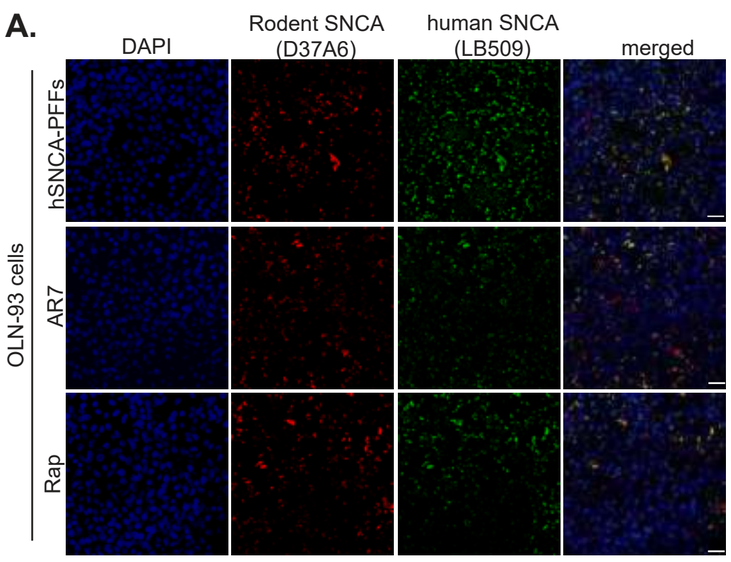
A.
DAPI
Rodent SNCA (D37A6)
human SNCA (LB509)
merged
OLN-93 cells
hSNCA-PFFs
AR7
Rap

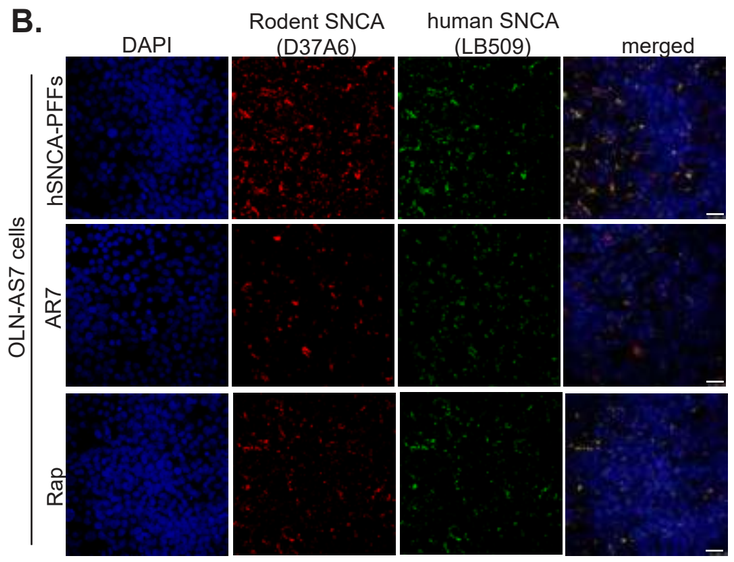
B.
DAPI
Rodent SNCA (D37A6)
human SNCA (LB509)
merged
OLN-AS7 cells
hSNCA-PFFs
AR7
Rap

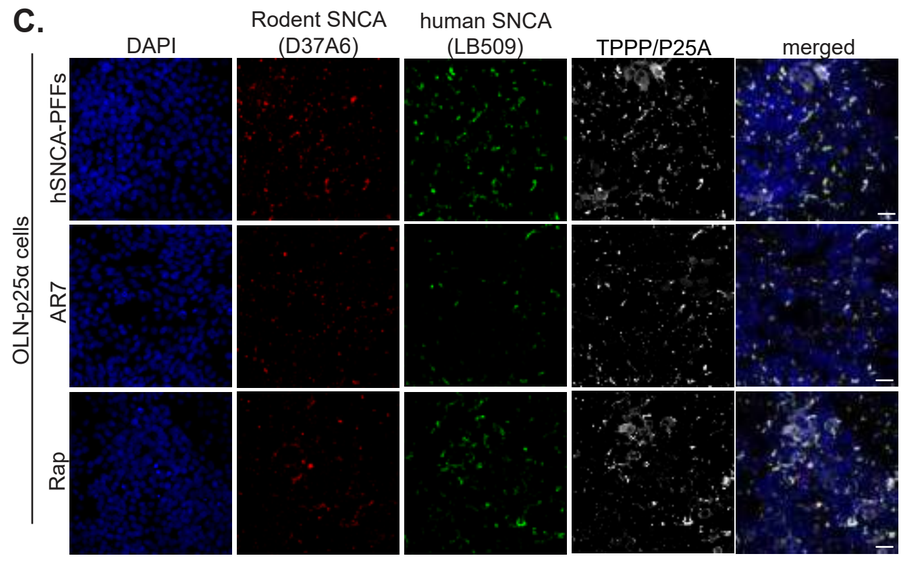
C.
DAPI
Rodent SNCA (D37A6)
human SNCA (LB509)
TPPP/P25A
merged
OLN-p25α cells
hSNCA-PFFs
AR7
Rap

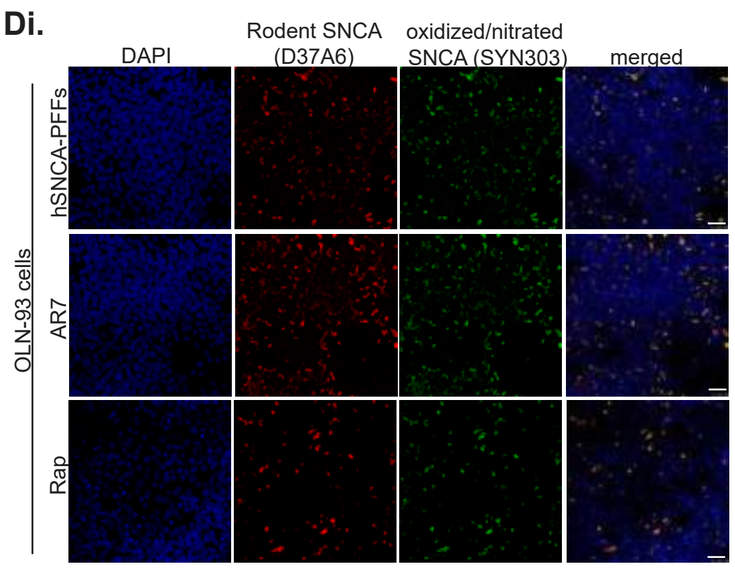
Di.
DAPI
Rodent SNCA (D37A6)
oxidized/nitrated SNCA (SYN303)
merged
OLN-93 cells
hSNCA-PFFs
AR7
Rap

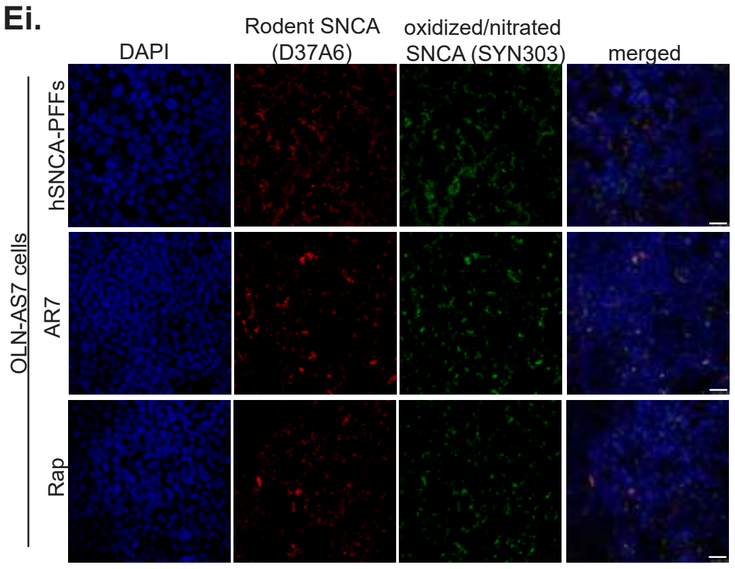
Ei.
DAPI
Rodent SNCA (D37A6)
oxidized/nitrated SNCA (SYN303)
merged
OLN-AS7 cells
hSNCA-PFFs
AR7
Rap

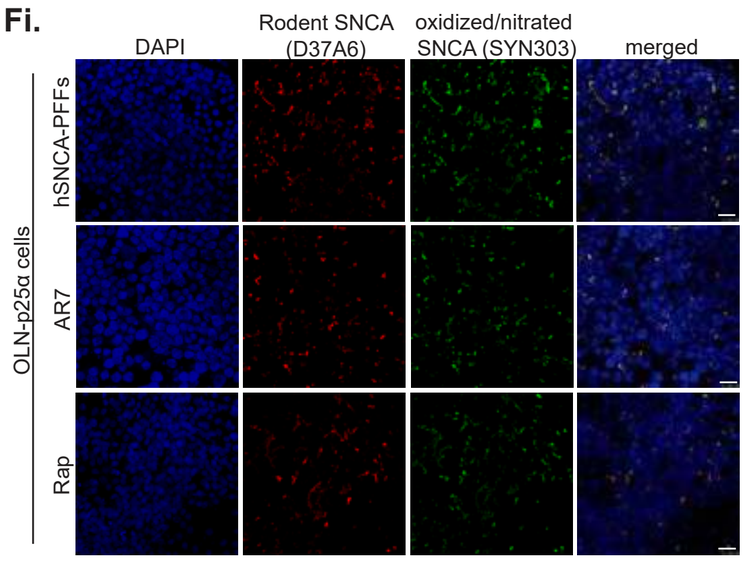
Fi.
DAPI
Rodent SNCA (D37A6)
oxidized/nitrated SNCA (SYN303)
merged
OLN-p25α cells
hSNCA-PFFs
AR7
Rap

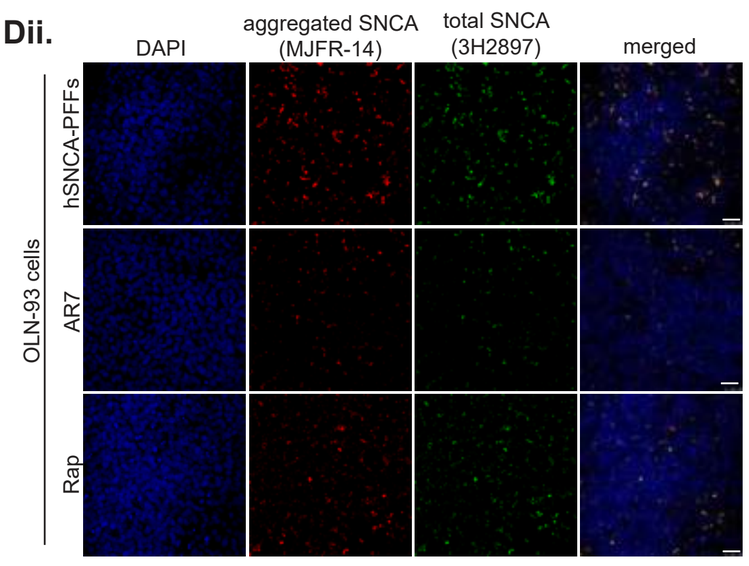
Dii.
DAPI
aggregated SNCA (MJFR-14)
total SNCA (3H2897)
merged
OLN-93 cells
hSNCA-PFFs
AR7
Rap

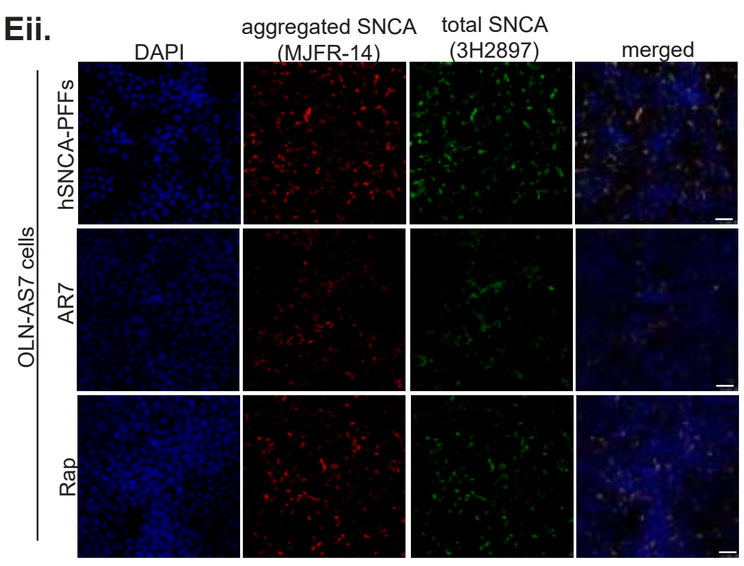
Eii.
DAPI
aggregated SNCA (MJFR-14)
total SNCA (3H2897)
merged
OLN-AS7 cells
hSNCA-PFFs
AR7
Rap

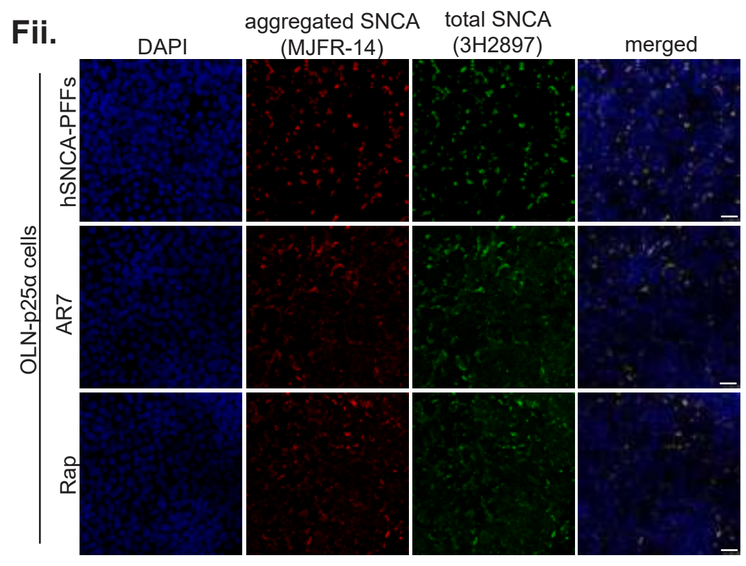
Fii.
DAPI
aggregated SNCA (MJFR-14)
total SNCA (3H2897)
merged
OLN-p25α cells
hSNCA-PFFs
AR7
Rap

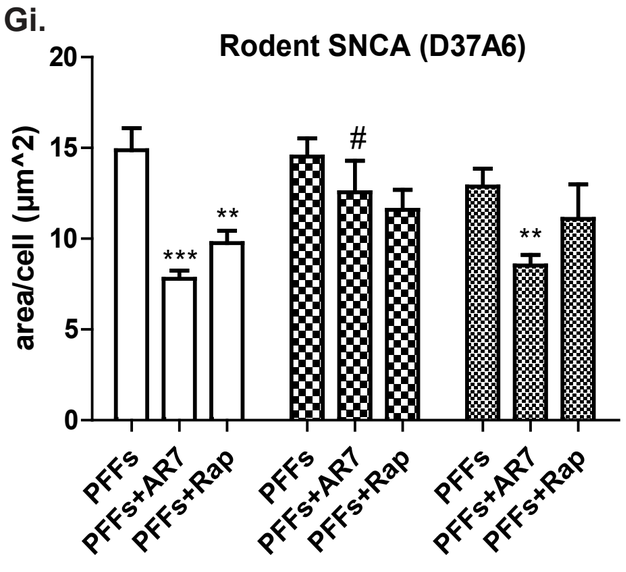
Gi.
Rodent SNCA (D37A6)
area/cell (μm^2)
PFFs
PFFs+AR7
PFFs+Rap

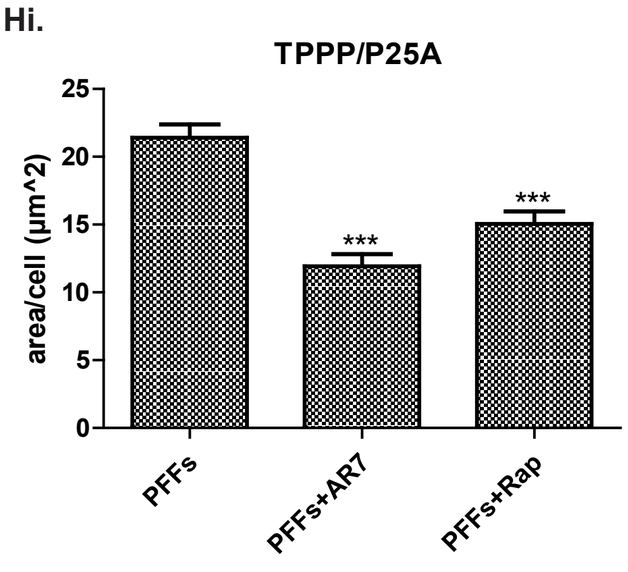
Hi.
TPPP/P25A
area/cell (μm^2)
PFFs
PFFs+AR7
PFFs+Rap

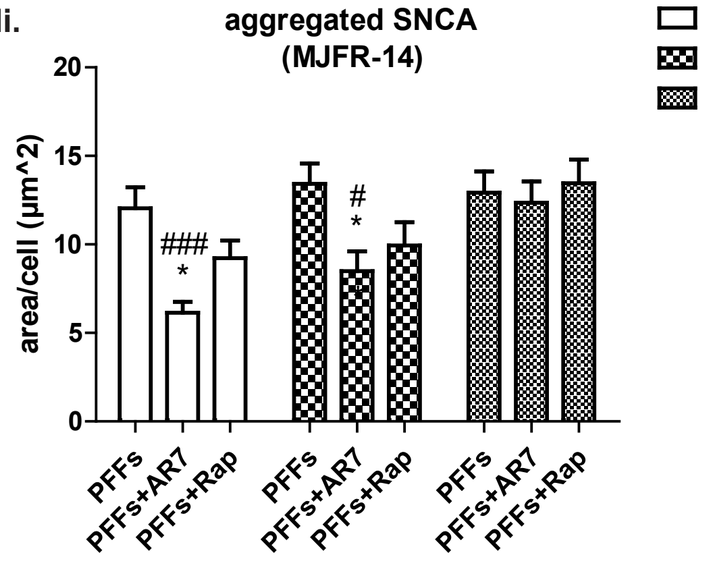
Ii.
aggregated SNCA (MJFR-14)
area/cell (μm^2)
PFFs
PFFs+AR7
PFFs+Rap


OLN-93
OLN-AS7
OLN-p25α

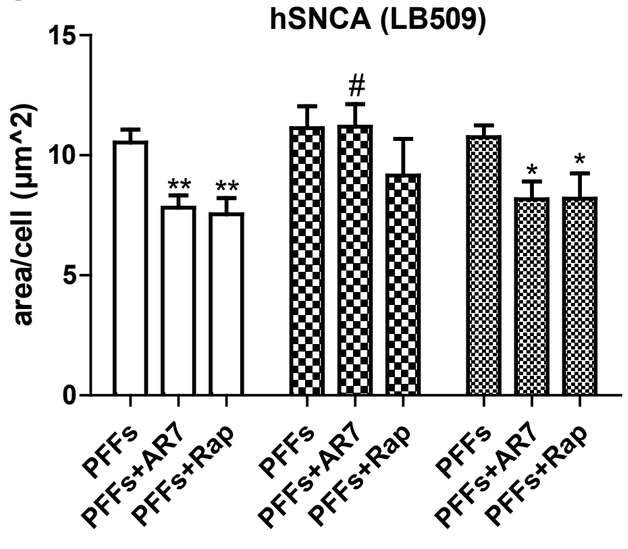
Gii.
hSNCA (LB509)
area/cell (μm^2)
PFFs
PFFs+AR7
PFFs+Rap

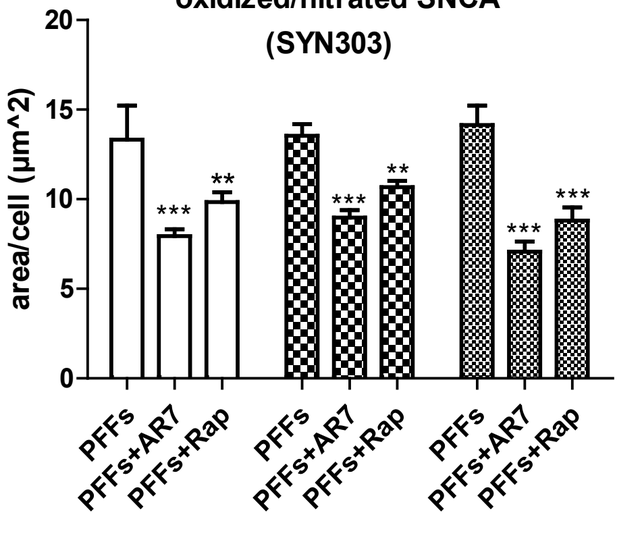
Hii.
oxidized/nitrated SNCA (SYN303)
area/cell (μm^2)
PFFs
PFFs+AR7
PFFs+Rap

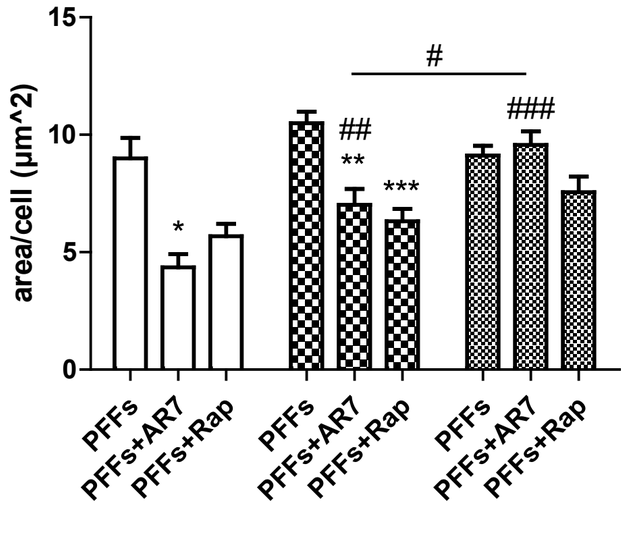
Iii.
Total SNCA (3H2897)
area/cell (μm^2)
PFFs
PFFs+AR7
PFFs+Rap